Jayvadan K. Patel
Yashwant V. Pathak *Editors*

Emerging Technologies for Nanoparticle Manufacturing

Springer

Emerging Technologies for Nanoparticle Manufacturing

Jayvadan K. Patel • Yashwant V. Pathak
Editors

Emerging Technologies for Nanoparticle Manufacturing

Springer

Editors
Jayvadan K. Patel
Nootan Pharmacy College
Sankalchand Patel University
Visnagar, Gujarat, India

Yashwant V. Pathak
Professor and Associate Dean for
Faculty Affairs
Taneja College of Pharmacy
University of South Florida
Tampa, FL, USA

Adjunct Professor, Faculty of Pharmacy
Airlangga University
Surabaya, Indonesia

ISBN 978-3-030-50702-2 ISBN 978-3-030-50703-9 (eBook)
https://doi.org/10.1007/978-3-030-50703-9

Editorial contact: Carolyn Spence
This Springer imprint is published by the registered company Springer Nature Switzerland AG
The registered company address is: Gewerbestrasse 11, 6330 Cham, Switzerland

To the loving memories of my parents Vishnupant and Shalini Pathak and Dr. Keshav Baliram Hedgewar who gave a proper direction, my wife Seema who gave a positive meaning and my son Sarvadaman Pathak who gave a silver lining to my life.

-Yashwant V. Pathak

To my parents Kantilal and Kamuben, my wife Sneha, and my sons Shubh and Labh, without whom this book would not have been possible.

-Jayvadan K. Patel

Foreword

I take great pleasure in writing this foreword to *Emerging Technologies for Nanoparticle Manufacturing*, edited by two experts who are working in this field for many years: Professor Jayvadan K. Patel and Professor Yashwant V. Pathak.

One of the fastest-growing technology in the world is nanotechnology, and it is also considered as the Industrial Revolution of the twenty-first century. Nanotechnology has changed the life of humans. It has not only affected healthcare but also covered a vast majority of applications in various industries. The explosion of communication technology, the digitalization of every aspect of our lives, the changing scenario of global media and social media, and many others, all these can be attributed to the growth of nanotechnology in these sectors.

Several research, development, and manufacturing techniques are used globally to develop better and safer nanomaterials for various applications.

Nanotechnology really changed the critical properties of our day-to-day materials and structures and converted these into smaller and easily manageable and highly useful equipment. The best example is the cell phone and its ability to change the healthcare world so rapidly.

The significant growth of nanotechnology in last two decades can be attributed to the invention of the scanning tunneling microscope (STM) and several other analytical techniques for material characterization as well as carbon nanotubes (CNTs), and fullerenes laid a path toward nanotechnology because atomic- and molecular-level studies could be performed using the STM and nanomaterials. The number of research papers and technical articles and patents related to nanotechnology and nanoproducts has been continuously increasing for nearly two decades. It is growing exponentially with thousands of these being published worldwide.

In a span of one or two decades, it is predicted that the industrial production of nanotechnology will be worth over $1 trillion globally. Thus, this technology will drastically change science, education, manufacturing, and the lifestyles of people around the world, which we are witnessing even today. This will create a significantly increased need for skilled workers in nanotechnology as well as experts in the fields of manufacturing nanoparticles with versatile applications.

This book is edited by Professor Patel and Professor Pathak at a right time when there is a need for creating resources to train such a work force. This book, I believe, will be an excellent reference book for people working in this

area and can serve as a textbook in certain cases at a postgraduate level. It has 27 chapters written by experts in their respective fields and have brought together an excellent scientific knowledge collection for the benefit of the readers.

I must take this opportunity to congratulate not only the two well-known scientists who edited the book but all the authors of the chapters who took arduous efforts to bring this volume for the benefit of students, scientists, and others in the field.

I am sure this book will be very useful and will make a wonderful impression in the scientific community.

Navin Sheth
Vice Chancellor,
Gujarat Technological University,
Ahmedabad, India

Preface

Nanoscience and nanotechnology, nowadays, have become household terms used widely and frequently. In last few decades, they emerged as an interdisciplinary science involving varied field of sciences including, but not restricted to, medicine, pharmacy, chemistry, biology, physics, polymer chemistry, material sciences, and engineering and technology.

Nanotechnology has affected every walk of human life. It has improved and, to some extent, revolutionized many technology and industry sectors: information technology, homeland security, medicine, transportation, energy, food safety, and environmental science, among many others. Described below is a sampling of the rapidly growing list of benefits and applications of nanotechnology.

From being part of a talk by physicist Richard Feynman in the USA on December 29, 1959, to a well-recognized term "Nanotechnology" used by Professor Norio Taniguchi in Japan in early 1961, nanotechnology has come a long way; moreover, with the advances in analytical techniques and material characterization technologies like SEM, TEM, and so on, nanotechnology grew leaps and bound in last two decades, with tens of thousands of papers in different fields of sciences and thousands of patents being given where nanotechnology has changed the field of smaller particles with bigger applications.

Nanoscience and nanotechnology involve the ability to see and to control individual atoms and molecules and very small particles in the nanometer ranges. Everything on Earth is made up of atoms—the food we eat, the clothes we wear, the buildings and houses we live in, and our own bodies. Hence, it will not be an exaggeration if we say the greatest scientist of nanotechnology is none other than Mother Nature.

Although modern nanoscience and nanotechnology concepts are quite new, nanoscale materials were used for centuries. Ayurveda, the Indian system of medicine, has several *Bhasma* formulations that are nanoscale. Traditional Chinese medicine did have some products that could be in the nanoparticle size range. Alternate-sized gold and silver particles created colors in the stained glass windows of medieval churches hundreds of years ago. The artists back then just didn't know that the process they used to create these beautiful works of art actually led to changes in the composition of the materials they were working with.

In medical sciences, nanotechnology is already broadening the medical tools, knowledge, and therapies currently available to clinicians. Nanomedicine, the application of nanotechnology in medicine, draws on the

natural scale of biological phenomena to produce precise solutions for disease prevention, diagnosis, and treatment. Below are some examples of recent advances in this area, including better imaging and diagnostic tools. Below are some examples of recent advances in this area, including better imaging and diagnostic tools, providing newer treatment options for chronic diseases, in regenerative medicine and nano medical robotics and so on.

We have earlier edited several books in the field of nanotechnology and nanoscience to mention a few: *Nano particulate drug delivery systems* (Informa Healthcare, 2007), *Drug delivery nanoparticles formulation and characterization* (Informa Healthcare, 2009), *Advances in Nanotechnology and Applications* (CENTERA, 2008 and 2009), *Bio-interactions of Nanomaterials* (CRC Press, 2015), *Nanobiomaterials for Ophthalmic Drug Delivery* (Springer, 2016), and *Nanotechnology in Nutraceuticals : Production and Consumption* (CRC Press, 2017.

This particular book is devoted to discuss the emerging technologies for nanoparticle manufacturing. This book is divided in to several parts:
Introduction and Biomedical Applications of Nanoparticles: Chapters 1 and 2
Polymeric Nanoparticles: Chapters 3, 4, 5, 6, 7, 8, 9 and 10
Lipid Nanoparticles: Chapters 11, 12, 13, 14, 15, 16 and 17
Metallic Nanoparticles: Chapters 18, 19, 20, 21 and 22
Quality Control of Nanoparticles: Chapter 23
Challenges in Scale-Up Production of Nanoparticles: Chapters 24 and 25
Injectable Nanosystems: Chapter 26
Future Directions and Challenges Ahead: Chapter 27

Most of these chapters are written by a leading group of authors and are very informative and useful to the readers to get a glimpse of emerging technologies for nanoparticle manufacturing.

I am sure this book will be welcomed by the scientific community and we look forward to constructive criticism about the book's contents and topics so that we can improve it in the next editions.

At this stage, we would like to express our sincere thanks to all the lead authors who took enormous efforts to write these chapters with their colleagues and contributed them as part of the reference book for the benefit of readers.

We will be failing if we do not express our sincere thanks to Springer and printer teams who put lot of sincere efforts to get this book in the market.

Our families have contributed to the success of this book by allowing us to work extra hours for it to see the light of day.

Visnagar, Gujarat, India — Jayvadan K. Patel
Tampa, FL, USA — Yashwant V. Pathak

Acknowledgments

I would like to thank Jeffrey, Lavanya, Carolyn, Nicholas, and Deepika, as well as the production teams for their support.

Contents

Part III Lipid Nanoparticles

Part IV Metallic Nanoparticles

Part I

Introduction and Biomedical Applications of Nanoparticles

Introduction to Nanomaterials and Nanotechnology

1

Jayvadan K. Patel, Anita Patel, and Deepak Bhatia

Abstract

Nanotechnology is the innovatory technology of the twenty-first century, and nanoscale materials have created a considerable amount of attention from researchers. It is an emerging interdisciplinary area of research wherever groupings of atoms as well as molecules are handled at the nanometer levels. It can be defined as the systematic study of materials that have properties critically dependent on length scales on the order of nanometers. Such novel and improved properties make nanoscale materials promising candidates to provide the best scientific as well as technological progress in a number of fields in particular communications, electronics, energy, environment, information, biology, pharmacy, health care, and medical care. This chapter first draws attention to the different definitions and classification of nanomaterials based on their origin, chemical composition, materials, and their dimensions. The fundamental properties of matter transform at the nanoscale and the most enhanced and valuable properties of manufactured nanomaterials such as confinement effects, surface effects, mechanical properties, structural properties, thermal properties, optical properties, and magnetic properties are also described. In the last section, we have discussed various methods to fabricate nanomaterials.

Keywords

Nanoscale materials · Size-dependent characteristics · Distinctive properties · Superior performance

1 Introduction

The first technological revolution, at the end of the eighteenth century, has sparked the advancement of industrial research and the attainment of novel materials (Fajardo et al. 2015). At present, the obstacles are the miniaturization of devices as well as instruments; lesser volume, lesser power consumption but superior performance. The progress relies upon searching out novel pleasing materials and the capacity to create minute structures with high accuracy. Though, the growth is not so smooth and effortless. One of the best splendid techniques created to answer such a condition is nanotechnology (Fajardo et al. 2015; Huyen 2011). Recently, the study engaging nanoscale materials has created a considerable

J. K. Patel (✉) · A. Patel
Nootan Pharmacy College, Sankalchand Patel University, Visnagar, Gujarat, India

D. Bhatia
Shenandoah University – ICPH Fairfax, Bernard J. Dunn School of Pharmacy, Fairfax, VA, USA

J. K. Patel, Y. V. Pathak (eds.), *Emerging Technologies for Nanoparticle Manufacturing*,
https://doi.org/10.1007/978-3-030-50703-9_1

amount of attention from researchers. They believe nanotechnology as the innovatory technology of the twenty-first century (The Royal Society 2004).

The word nanotechnology is taken from a Greek word "nano" stands for "dwarf" or "very small," and so it relates to materials of minute size ranges (Nikalje 2015; Rai et al. 2008). The interdisciplinary science of nanotechnology is a talented field wherever groupings of atoms as well as molecules are handled at the nanometer levels. In reality, it is the design of components, materials, devices, and/or systems at near-atomic or molecular levels. Generally, one of the dimensions of nanomaterials is between 1 and 100 nanometers (nm) length in scale. This promising technology implies to the imaging, handling, manufacturing, measuring, modification, modeling, and reduction of matter at nanoscale with characteristic properties, for example, cost-effective, definite, eco-friendly, good strength, lighter, and specific for a variety of purposes (Asmatulu et al. 2010; Taniguchi 1974; Pradeep 2007).

The definition of nanotechnology has been divided into two parts, one is the part about manufacturing at dimensions of 1–100 nm, and the other is about characteristics of materials at the nanoscale that make possible their exploit for novel applications. The size range that holding a great deal of attention is characteristically from 100 nm down to the atomic level, for the reason that it is in this range that materials have fundamentally distinct properties from their bulk counterparts. The most important justifications for this revolutionize in performance are an increased significance of surface as well as the interfacial area (Wardak et al. 2008). At the same time, nanotechnology is a new-fangled paradigm in fundamental thoughts and understanding regarding the physical universe, where the bottom-up approach is the rule and not an exception. In this novel system, one has to imagine in terms of atoms and how they act together to create valuable materials, structures, devices, and systems (Raza and Raza 2013; Rocco 2007; Rocco et al. 2011).

Nanotechnology has been moving from the laboratory surroundings into applications and customer products for quite a while now (Barakat and Jiao 2011). The nanotechnology will create new perspectives for this world and their promises have been noticed to provide the best scientific as well as technological progress in a number of fields in particular communications, electronics, energy, environment, information, health, and medical care (Daryoush and Darvish 2013).

Nanotechnology has also a widespread perspective in the areas of biology, pharmacy, physics, and material science which could merge to contribute to healthcare. Even though the perception of nanotechnology has been investigated in healthcare study for the past three decades, it is still believed to be in the early stage of development as anticipated therapeutic advantages have not been totally understood (Miyazaki and Islam 2007; Sandhiya et al. 2009). Both the educational as well as industrialized groups of people are spending time in addition to money into the development of nanotherapeutics to conquer the superficial challenges and interpret the hypothetically established advantages of nanoparticulate systems into clinical benefits. Although nanotechnology is at its early stages, however, it is expanding quick, opening plentiful perspectives for the logical minds to utilize this enhanced technology for human well-being (Daniel and Astruc 2004).

This chapter addresses to fill up-to-date understanding of manufactured nanomaterials, by providing an extensive review of current progress in the nanotechnology field. It draws attention to the different definitions, classifications, fundamental properties, and synthesis routes of nanomaterials.

2 Nanomaterials

Nanomaterials, previously called by Paul Ehrlich as "Magic Bullets" (Kreuter 2007), are one of the major investigated materials of the century that gave birth to a novel branch of science referred to as nanotechnology (Nasir Khan et al. 2017). Nanomaterials are chemical substances or materials that are created or used at a minute scale. Indeed, the word material speaks about an infinite number of components, jointly showing an averaged statistical performance. As a result, the performance of nanomaterials is affected by specific

interface effects and demonstrates characteristics affected by the size and the restricted number of constituents (Guo et al. 2014).

Nanomaterials are a diverse class of substances that have structural constituents lesser than 100 nm in minimum one dimension. Nanomaterials consist of nanoparticles (NPs), which are particles, with at least two dimensions between about 1 and 100 nm (Klaine et al. 2008). Though, a single globally recognized definition for nanomaterials does not present. Diverse groups have dissimilarities in belief in defining nanomaterials (Boverhof et al. 2015). To be classified as nanomaterials, the material must be less than 100 nm in size in a minimum one direction. The International Organization for Standardization (ISO) has explained nanomaterials as a "material with any external nanoscale dimension or having the internal nanoscale surface structure" (ISO/TS 27687 2008; ISO/TS 80004-1 2010). The US Food and Drug Administration (USFDA) also denote nanomaterials as "materials that have at least one dimension in the range of approximately 1 to 100 nm and exhibit dimension-dependent phenomena". As per the European Union Commission nanomaterials means "a manufactured or natural material that acquires unbound, aggregated or agglomerated particles where external dimensions are between 1-100 nm size ranges," in accordance with Potocnik (2011).

The exploit of different definitions throughout diverse authority's referred to as the most important obstacle to regulatory efforts as it shows the way to legal uncertainty in applying regulatory approaches for indistinguishable nanomaterials. So, the requirement to convince diverging considerations is the main confront in developing a single international definition for nanomaterials.

3 Why Are Nanoscale Materials: So Special and Unique?

Nanoscale materials, which can be either standalone solids or subcomponents in other materials, are smaller than 100 nm in one or more dimensions. Putting this dimension in standpoint, a nanometer (nm) is one-billionth of a meter and one-millionth of a millimeter, approximately four times the diameter of an atom. For our macro-oriented brains, in fact understanding the scale of the nanometer is not easy although real-life comparisons can help give us a good judgment. Such as, the twinkling of an eye is to a year is what a nanometer is to a tool for measuring (Feynman 1960).

Nanoscale materials have a higher surface area to volume ratio in addition to the number of surface atoms as well as their arrangement decides the size and properties of the nanoscale materials (Sarma et al. 2015). Size reduction of materials can bring about an entire range of novel physicochemical features and prosperity of prospective applications (Brechignac et al. 2006). These features very much rely upon size, shape, surface area as well as the structure of elements. Nanoscale materials can be present in single, compound, aggregated, or agglomerated structures with sphere-shaped, cylindrical, and asymmetrical shapes (Kumar and Kumbhat 2016). By the production of nanoscale structures, it is probable to manage the basic properties of materials, for instance, their charge capacity, magnetic properties, melting temperature, and even their color, with no altering the chemical composition of the nanoscale structures'. This will make possible novel, highly efficient materials, and nanotechnologies that were impracticable in the past. The most important benefits of nanomaterials against bulk material consist of a reduction in melting point as well as surface area, an enhancement in dielectric constant in addition to mechanical strength (Maddinedi et al. 2015; Dasgupta et al. 2016; Ranjan et al. 2016; Pulimi and Subramanian 2016). Additionally, the size of nanoscale materials facilitates them to absorb remarkably on to other materials (Dasgupta et al. 2015; Ranjan et al. 2017; Ranjan et al. 2016).

To point up the intrinsic value of influencing matter on such dimensions, Daniel Ratner, Professor of Bioengineering at the University of Washington, suggests a valuable thought experiment. Assume that we have a $3 \times 3 \times 3$ – foot cube of pure gold. If we were to cut in half this cube in all dimensions, we would have eight smaller cubes. These newly formed cubes would

show the similar inherent properties as the original cube of pure gold – each one would still be weighty, glossy, and yellow, with the similar chemical and structural features. If we were to carry on breaking in two until we have cubes dimensions about microns (10^{-6} of a meter), the intrinsic bulk properties of the material would still stay invariable. Also, this is not explicit to gold; the same retains right for ice, steel, plastic, or any pure solid. Though, if we were to get to the nanoscale, quantum effects would start to dominate, and the gold's characteristics, counting its color, intermolecular chemistry, and melting temperature, would alter. These quantum effects had been "averaged out of existence" in the bulk material (Ratner and Ratner 2003; Koo 2016). At the nanoscale, the power of gravity gives van der Waal's forces, surface tension, as well as additional quantum forces.

For differentiation of nanoscale materials from the bulk materials, it is essential to show the distinctive properties of nanoscale materials and their potential effects on science as well as technology. The size of the nanoscale materials has an enormous control on their properties (Fig. 1.1). When a particle is in its bulk state in comparison with its size in its microscale, there is not a large amount of dissimilarity in its properties. On the other hand, when the particle attains a size of smaller than 100 nm, the properties revolutionize notably in comparison with its bulk state. In 1–100 nm, quantum size effects determine the properties of particles, for example, chemical, magnetic, optical, mechanical, electrical, and thermal (Sun 2007; Brust et al. 1994; Daniel and Astruc 2004).

Over the past few decades, the size-dependent properties of gold nanoparticles (AuNPs) have been explicated well (Junk and Riess 2006; Daniel and Astruc 2004). AuNPs demonstrates the size-dependent color. At the nanoscale, the gold particle shows purple color diverse from the bulk, which was yellow-colored. This alteration in color is based on the alteration in their band type from continuous to discrete as a result of confinement effect. These quantum effects in the nanoscale are the fundamental explanations behind the "tunability" of properties. By merely changing the particle size, we can alter the material property of our interest.

Nanoscale structures have extremely higher surface-to-volume ratios as well as aspect ratios, creating them perfect for exploit in polymer nanocomposites. For the past five decades, investigators have been functioning with macrocomposites, for example, filled polymers or a fiber-reinforced polymer matrix composite, in which the length scales of the polymer fillers or the fiber diameters is in micrometer scale. The reinforcement length scale is in micrometers, and the interface of fillers is about to the bulk polymer matrix. For the past two decades, investigators have been finding out nanocomposites, where the length scale of the reinforcement (nanoparticles) is on the nanometer scale. These nanocomposites have ultra-large interfacial area per volume, and the distances between the polymer and filler components are very small.

Before talking about the properties of nanoscale substances, it may be beneficial to explain a case showing the basic effects of the minute size of nanoparticles (Koo 2006). The first and most vital effect of smaller particle size is its vast surface area, and so as to get an idea of the significance of this geometric variable, the surface-over-volume ratio should be discussed. It is assumed that a particle is sphere-shaped, the surface a of one particle with diameter D is $a = \pi D^2$, and the corresponding volume v is $v = \frac{\pi D^3}{6}$. So, the surface/volume ratio is

$$R = \frac{a}{v} = \frac{6}{D} \tag{1.1}$$

This ratio is in inverse proportion to the particle size, and as a result, the surface enlarges with reducing particle size. The same is applicable for the surface per mol A, a quantity that is very important in thermodynamic considerations.

$$A = na = \frac{M}{\left(\delta \pi D^3/6\right)\pi D^2} = \frac{6M}{\delta D} \tag{1.2}$$

In Eq. (1.2), n is the number of particles per mol, M is the molecular weight, and ϱ is the density of the material. Like the surface-over-volume

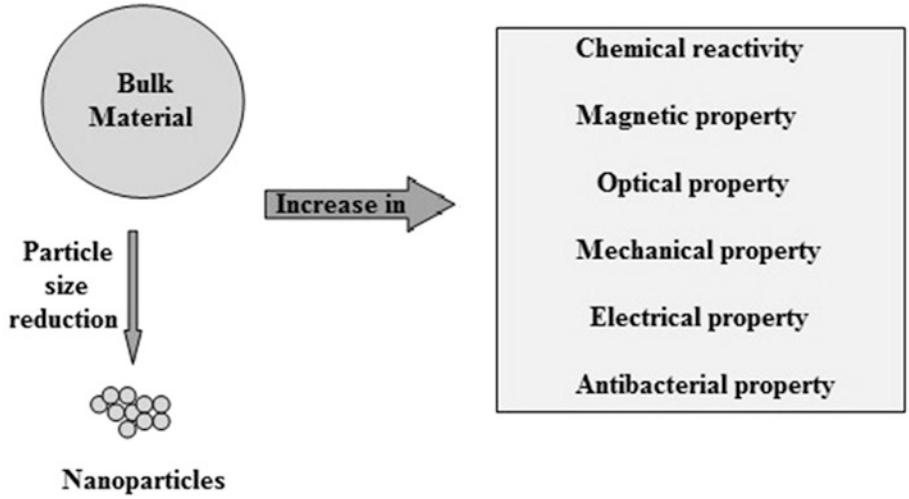

Fig. 1.1 Properties of nanoscale materials

ratio, the area per mol raises in inverse proportion to the diameter of particle. Therefore, larger values of surface area are obtained for particles that are simply a few nanometers in diameter (Koo 2016).

The distinctive properties and superior performance of nanoscale materials are established by their sizes, surface structures, and inter-particle interactions. The role played by particle size is very similar to the role of the particle's chemical composition, adding one more parameter for designing and managing behavior of the particle. To entirely know the impacts of nanoscale materials in nanoscale science and technology, one requires to study why nanoscale materials are so special! (Koo 2016).

The excitation surrounding nanoscale science and technology presents inimitable opportunities to buildup innovatory materials. Nanoscale science and technology is a comparatively young field that includes almost all disciplines of science and engineering. Nanoscale structures are a novel branch of materials study drawing an immense deal of attention due to its impending appliances in chemical catalysis, computing, imaging, material synthesis, medicine, printing, and many other fields (Koo 2016).

On account of all these inimitable behavior and properties, nanoscale materials have greater applications in cosmetics, electronics, and pharmaceutical industries. In addition, they are commonly employed for the advance of health care products and restoration of the polluted environments (Pulimi and Subramanian 2016). Nanoscale materials stand for areas of scientific study and industrialized applications in full expansion (Gaffet 2011). Nanoscale materials in addition play a very important role in drug delivery, imaging, and even in surgical procedure as they have a size range comparable to that of biological molecules for example proteins, receptors, deoxyribonucleic acid (DNA), and ribonucleic acid (RNA) (Gendelman et al. 2015; Pillai 2014; Wang et al. 2013; Wang and Thanou 2010; Torchilin 2005). Nanoparticulate systems are moderately small in size in comparison with cells but are larger than the majority "small molecule" – type drugs, which could get better their residence time in circulation with no risk of clogging the blood vessels, which sequentially can enhance the bioavailability and pharmacokinetic profile of a variety of drugs. Nanoparticles can make use of a natural process called endocytosis to go through cells, which offers a specific benefit in circumstances where normal penetration into cells would be difficult for a particular molecule (Liu et al. 2012). This characteristic is also useful for the targeting of particular organelles within the cells like nuclei with gene knockdown by tiny interfering RNAs (siRNAs) (Torchilin 2011;

Huang et al. 2011a, b; Vander Heiden 2011). Higher surface-area-to-volume ratio is an additional interesting characteristic of nanoparticulate systems, which gives a huge substrate for adherence of definite moieties for active targeting (Moghimi et al. 2005). Surface modification has been done to nanoparticles with specific antibodies or peptides to attain tissue targeting, which lessens the probability of distracted off-target toxicity (Yokoyama 2005; Bae and Park 2011). Consistent with therapeutic and diagnostic requirements, the surface features of nanotherapeutics can be customized with imparting stealth properties to avoid elimination by the reticuloendothelial system, which gets better the circulation time and raises drug concentration at the site of action (Wang and Thanou 2010; Gamucci et al. 2014).

Nanoparticulate technology has opened up new opportunities in the early detection as well as management of different cancers, bio-detection of pathogens, and in the formulation of fluorescent biological labels as they take in both imaging and therapeutic abilities. Nanoparticulate technology is also beneficial in addressing solubility as well as stability problems of poorly soluble drugs and in modifying their pharmacokinetic profiles to get extended plasma half-life. Since the 1980s, the healthcare group of people has met clinical challenges where resistance has developed against antibiotics and chooses other conventional therapeutics. It is feasible that these problems can be tackled with nanoscale materials (Wang et al. 2013; Salata 2004). As of 2014, more than 1800 consumer products containing nanoscale materials are on the market (Vance et al. 2015).

4 Classification of Nanoscale Materials

The manufacturing of traditional products at the nanoscale presently helps and will keep on helping the economic growth of various countries. Till date, a variety of nanoscale products have been documented and lots of other varieties of products are expected to come out in the future. Consequently, the requirement for their categorization has ripened. The first suggestion for nanoscale material classification was specified by Gleiter in 2000 (Gleiter 2000). A nanomaterial is a broad name provided to each kind of material existing at the nanoscale. Several names have been given to these new materials; nanostructured, nanometer-sized, ultrafine-grained, etc. Nanoscale materials can be formed from one or more species of atoms or molecules and can demonstrate a broad range of size-dependent characteristics. In this range of size, nanoscale materials link the gap among tiny molecules and bulk materials in terms of energy states (Johnston and Wilcoxon 2012; Smith and Nie 2010). They can be found naturally or manufactured chemically, mechanically, physically, or biologically with a variety of structures (Saleh 2016). Nanoscale materials can be categorized on the basis of special parameters counting their origin (natural or synthetic); chemical composition; material-based (Carbon-based nanomaterials, Inorganic-based nanomaterials; Organic-based nanomaterials; Composite-based nanomaterials); and on the basis of their dimensions (Saleh and Gupta 2016; Buzea et al. 2007).

4.1 Classification of Nanomaterials Based on Their Origin

Based on their origin, the nanoscale materials can be divided into two categories (Filipponi and Sutherland 2013):

(a) *Natural nanomaterials or nonintentionally made nanomaterials*

These types of materials speak about nanosized materials that belonged naturally to the environment (e.g., proteins, viruses, nanoparticles produced during volcanic eruptions, etc.) or that are formed by individual activity with no plan (e.g., nano-particles produced from diesel combustion). They are formed in nature either by organic species or during human-induced activities. The manufacturing of simulated surfaces with elite micro as well as nanoscale patterns and properties for industrial appliances are easily obtainable from natural origins. Naturally, generated nanomaterials

are present through the Earth's spheres to be precise in the atmosphere, hydrosphere, and lithosphere which are comprised of rocks, soils, magma, or lava at particular stages of evolution and even in the biosphere which covers microorganisms and higher organisms, including humans, apart from anthropogenic activities. Globe is made-up of nanomaterials that are naturally formed and are also present in the oceans, lakes, rivers, groundwater, and hydrothermal vents (Hochella et al. 2015; Sharma et al. 2015; Jordan et al. 2014).

(b) *Synthetic (engineered) nanomaterials or intentionally made nanomaterials*

These types of nanomaterials manufactured with intent by means of a defined production procedure like mechanical grinding, engine exhaust, and smoke or are synthesized by physical, chemical, biological, or hybrid techniques. Synthetic nanomaterials cover up a wide range of materials, counting both inorganic (elemental metals, metal oxides, metal salts, and aluminosilicates) as well as organic (fullerenes, micelle-like amphiphilic polyurethane particles, and dendrimers) materials (Filella 2012). The issue of risk assessment approach has come into existence recently as there is increased manufacturing and succeeding release of engineered nanomaterials in addition to their utilization in consumer products and industrial appliances. This risk assessment approach is very much cooperative in the prediction of the behavior and fate of engineered nanomaterials in different environmental media. The most important confront among engineered nanomaterials is whether existing information is adequate to predict their behavior or if they show a distinctive environment-related performance, diverse from natural nanomaterials. At present, different sources concerned possible applications are employed for the fabrication of engineered nanomaterials (Wagner et al. 2014).

4.2 Classification of Nanomaterials Based on the Chemical Composition

According to their chemical composition, nanomaterials can be categorized as metal-based materials are mainly made-up of metals like silver, gold, and copper. And metal oxide nanomaterials which are made of metal and oxygen, for example, titanium, silica, and alumina (Saleh and Gupta 2016).

4.3 Material-Based Classification

Most recent nanoscale materials can be classified into four material- based categories:

(a) *Carbon-based nanomaterials*

Generally, these carbon-based nanomaterials cover up a wide range of compounds, counting fullerenes (C60), carbon nanotubes (CNTs), carbon nanofibers, carbon black, graphene (Gr), and carbon onions (Filella 2012). For manufacturing these carbon-based nanomaterials different methods are used like laser ablation, arc discharge, and chemical vapor deposition (CVD) (except carbon black) (Kumar and Kumbhat 2016).

(b) *Inorganic-based nanomaterials*

These inorganic-based nanomaterials include metal and metal oxide nanoparticles. These nanomaterials can be synthesized into metals like Au NPs or silver nanoparticles (Ag NPs), metal oxides like titanium dioxide (TiO_2), and Zinc oxide (ZnO) NPs, and semiconductors such as silicon and ceramics (Jeevanandam et al. 2018).

(c) *Organic-based nanomaterials*

Organic-based nanomaterials consist of nanomaterials prepared generally from organic matter, exclusive of carbon-based or inorganic-based nanomaterials. The exploitation of noncovalent interactions for the self-assembly and blueprint of molecules assists to renovate the organic nanomaterials into most wanted structures for instance dendrimers, micelles, liposomes, and polymeric NPs (Jeevanandam et al. 2018).

(d) *Composite-based nanomaterials.*

Composite nanomaterials are multiphase NPs with one phase on the nanoscale dimension that can either join NPs with other NPs or NPs attached with bigger or with bulk-type materials (e.g., hybrid nanofibers) or very complex structures, for example, metalorganic frameworks. The composites may be any combinations of carbon-based, metal-based, or organic-based nanomaterials with any form of metal, or polymer

bulk materials. Nanomaterials are fabricated in diverse morphologies contingent on the essential properties for the desired application (Jeevanandam et al. 2018).

4.4 Classification of Nanomaterials Based on Their Dimensions

Nanomaterials with structural characteristics at the nanoscale can be created in various forms. In 2007, Pokropivny and Skorokhod formed a new idea of classification for nanomaterials which listed the newly developed composites, for example, zero-dimensional (0-D), one-dimensional (1-D), two-dimensional (2-D), and three-dimensional (3-D) nanomaterials shown in Table 1.1 (Pokropivny and Skorokhod 2007). This classification is greatly reliant on the electron association along the dimensions in the nanomaterials. For instance, electrons in 0-D nanomaterials are captured in a dimensionless space while 1-D nanomaterials have electrons that can shift along the *x*-axis, which is less than 100 nm. Similarly, 2D and 3D nanomaterials have electron associations along the *x, y*-axis, and *x*, *y*, *z*-axis in that order. The ability to forecast the properties of nanomaterials decides the classification value of the nanomaterials. The categorization of nanomaterials given by researchers suggested that the features of nanomaterials are ascribing to the particle shape as well as dimensionality, as per the "surface engineering" conception, and thereby class of nanomaterials (Pokropivny and Skorokhod 2007; Tiwari et al. 2012).

In accordance with this conception, nanomaterials can be classified as follows:

(a) *Zero-dimensional (0-D)*

They are crystalline bunches of a few hundred to a few thousand atoms with sizes ranging from 2 to 100 nm (Wani 2015). All the dimensions of the materials present in the nanometer scale are called 0-D nanomaterials. Nanoclusters are forms that are 1 to 100 nm in all space-based dimensions. These are in general sphere-shaped nanostructures, length, breadth, and heights are restricted at a single point. They can be amorphous or crystalline in nature. 0-D nanomaterials play an incredibly vital role in electronics, engineering, and technology. In recent times, the widespread investigation is in development to fabricate nanoparticles for a variety of applications (Cao 2004).

(b) *One-dimensional (1-D)*

The second class of nanoscale materials, subjected as 1-D nanomaterials, is held in reserve for those materials that have nanoscale dimensions that are equal in all but one direction (Balaz 2008). The nanomaterials have one of the dimensions, which are exterior, the nanoscale and are called 1-D-nanomaterials. It has just one parameter whichever length (or) breadth (or) height. These are commonly needle-like nanostructures that include nanotubes, nanowire, nanofibers, and nanorods having a diameter between 1 and 100 nm and a length that could be much larger are classified as 1-D nanostructures. These are also amorphous or crystalline in nature. These nanoscale materials present momentous benefits over bulk or thin-film planar devices (Abdelsalam and Abdelaziz 2014). Nanofibers are to some extent bigger in diameter than the characteristic

Table 1.1 Classification of nanomaterials on the basis of their dimensions

Sr. No.	Class of nanomaterials based on their dimensions	Nature of nanomaterials	Examples of nanomaterials
1	Zero-dimensional (0-D)	Amorphous or crystalline	Single crystalline or polycrystalline nanoparticles
2	One-dimensional (1-D)	Amorphous or crystalline	Nanotubes, nanowires, nanofibers, nanorods
3	Two-dimensional (2-D)	Amorphous or crystalline	Nanofilms, dendrimers, nanolayers, nanotextured surfaces or thin films, nanocoatings, etc.
4	Three-dimensional (3-D)	Crystalline	Quantum dots, fullerenes, nanoparticles, nanocrystals, colloids, nanoshells, nanorings, etc.

nanomaterials definition, though still too small to see to the naked eye. They are generally manufactured by electrospinning technique in the case of inorganic nanofibers or catalytic synthesis method for carbon nanotubes and exhibit size ranges between 50 and 300 nm in diameter. Nanofibers can be aligned biochemically and electrostatically (Kumar and Kumbhat 2016). Nanowires are similar to nanofibers. In these systems, one dimension surpasses by an order of magnitude the other two dimensions, which are in the nano-range (Gubin 2009). Thin films or surface coating also comes under the materials with one dimension in the nanometer scale which have been produced and employed for decades in different areas counting antireflecting coating on sunglasses, chemical and biological sensors, chips of computer memories, electronics, information storage systems, optical devices, and solar cell application. Thin films can be deposited by a range of techniques and can be grown-up controllably at the atomic level (Seshan 2002; Liu et al. 2003).

(c) *Two-dimensional (2-D)*

In this class of nanomaterials, only one dimension is in the nanometer scale, while another two are out of the nanoscale (Gubin 2009). It has simply length and breadth. 2-D nanostructures display plate-like shape (Thomas et al. 2014). The examples of 2-D nanostructures are nanotubes, dendrimers, nanowires, nanofibers, nanofilms, nanolayers, nanotextured surfaces or thin films, and nanocoatings. 2-D nanomaterials can be amorphous or crystalline. They are fabricated from different chemical compositions. They are utilized as a single layer or multilayer structure (Koski and Cui 2013). The properties of 2-D systems are not as much understood and their manufacturing capabilities are less advanced. 2-D systems are applied to structural bulk materials for the purpose of improving the desired properties of the surface, for example, corrosion resistance, wear resistance, friction, and holding the bulk properties of the material unchanged (Koch et al. 2007).

(d) *Three-dimensional (3-D)*

Three-dimensional (3-D) structures are materials having three random dimensions beyond the nanoscale (Saleh and Gupta 2016). It has all parameters of length, breadth, and height. These materials acquire a nanocrystalline nature (Law et al. 2004). These consist of quantum dots or nanocrystals, fullerenes, particles, precipitates, and colloids. A number of 3D systems, for example, natural nanomaterials, metallic oxides, carbon black, TiO_2, and ZnO are widely known, whereas others, for example, dendrimers, fullerenes, and quantum dots portray the maximum confronts in terms of fabrication and understanding of properties. Bulk nanomaterials are composed of multiple arranged nanosized crystals. 3-D nanomaterials include the dispersion of nanoparticles, bundles of nanowires, and nanotubes as well as multinanolayers (Lin et al. 2013; Tiwari et al. 2012).

5 Properties: The Physics at the Nanoscale

In recent times, the material science investigation is paying attention to the discovery of novel materials with new and superior properties and novel synthesis methods to deal with the augmented technological requirement. Nanomaterials are the center of the interest attributable to their remarkable applications and fascinating properties (West and Halas 2003; Sozer and Kokini 2009).

In reality, the fundamental properties of matter transform at the nanoscale and nanomaterials manifested interesting and valuable properties. The physical, as well as chemical properties of nanoparticles can be fairly diverse from those of larger particles of the same substance. They are nearer in size to single atoms and particles over bulk materials, and to clarify their performance, it is essential to make use of quantum mechanics (Kumar and Kumbhat 2016). While nearly all microstructured materials have alike properties to the corresponding bulk materials. This is mostly attributable to the nanometer size of the materials which make them: (a) large fraction of surface atoms; (b) high surface to volume ratio and quantum confinement effects; (c) spatial confinement; (d) reduced imperfections, which do not exist in

the corresponding bulk materials (Roduner 2006). Changed properties can comprise but are not restricted to color, solubility, material strength, electrical conductivity, magnetic performance, mobility, biological activity, and chemical reactivity (Fig. 1.2) (Blackwelder 2007).

Size effects make up a peculiar and attractive aspect of nanomaterials. The effects are taken into consideration by size pertaining to the advancement of chemical, electronic, electromagnetic, spectroscopic, structural, and thermodynamic properties of these predetermined systems with varying sizes (Henry 2008). The properties of a material depend upon the type of motion, its electrons can execute, which relies upon on the gap available for them. Thus, the properties of a material are characterized by an explicit length scale, usually on the nanometer dimension. If the physical size of the substance is lowered under this length scale, its properties transform and turn out to be sensitive to size along with shape. Attributable to our capacity of atom manipulation, we can formulate nanomaterials suitable for specific applications (Sugimoto et al. 2008).

In any matter, the considerable variation of basic electrical and optical properties with decreased size will be seen when the energy spacing between the electronic levels goes beyond the thermal energy. In tiny nanocrystals, the electronic energy levels are not constant as in the bulk but are discrete (limited density of states), on account of the captivity of the electronic gesture function to the physical lengths of the particles. This observable fact is called quantum confinement and consequently, nanocrystals are also referred to as quantum dots (Stucky and Mac Dougall 1990). Furthermore, nanocrystals attain a higher surface area and a great fraction of the atoms in nanocrystals are on its surface. As, this part relies mostly on the size of the particle (30% for a 1 nm crystal, 15% for a 10 nm crystal); it can present go up to size effects in the chemical and physical properties of the nanocrystals.

5.1 Confinement Effect

Quantum size effects are correlated to the "dimensionality" of a system in the nanometer range (Richards and Bonnemann 2005). The quantum effects are an outcome of quantum mechanics and of the particle-wave duplicity. These happen in the case where the size of the system is commensurate with the de Broglie wavelengths of the electrons, phonons, or excitons circulating in them (Naseri and Saion 2012).

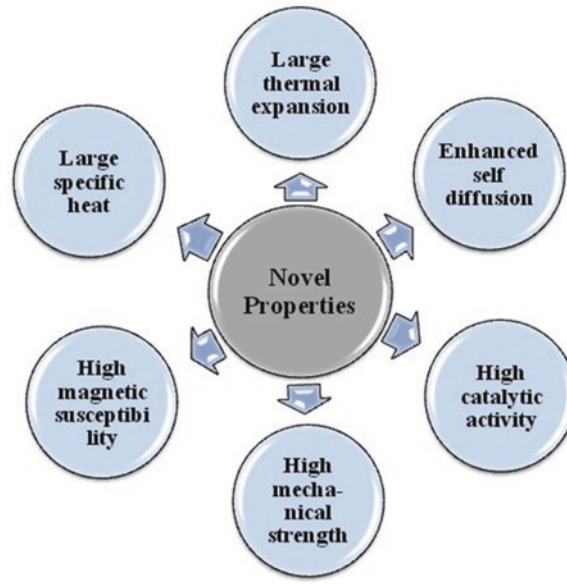

Fig. 1.2 Size-dependent properties

In fact, electrons act at the same time as particles and as waves. Since waves, they travel around the whole space in which they are gratis to move about. The nanograin acts similar to a type of box, in which a definite property may or may not be present. Beneath a particular critical size, characteristics of the property straightforwardly and exactingly rely upon the size of the grain. This is known as the confinement effect (Rezaie et al. 2013). Quantum size effects play a fundamental role in deciding the physical and chemical properties, e.g., charge-transport mechanisms and electronic structure. Optical as well as electron-tunneling spectroscopies are crucial for learning these systems (Roduner 2006; Aznan and Johan 2012).

5.2 Surface Effects

Atoms at surfaces have lesser neighbors than atoms in the bulk. As a consequence of this lesser coordination and unsatisfied bonds, surface atoms are little stabilized compared with bulk atoms (Roduner 2006). If the particle is tiny it has a large fraction of atoms at the surface and the great average binding energy per atom. The surface-to-volume proportion scales with the contrary size, and as a result, there are plentiful properties that comply with the identical scaling law. Edge and corner atoms have even lesser coordination and attach foreign atoms and molecules more strongly. The coordination number is also restricted in small pores (Lokhande and Pathak 2014).

The influence of size reduction is not exclusive of outcomes for the atomic arrangement and the physical properties of substances. In fact, if the structure of the superficial region of a particle is exaggerated over the range of the particle size, a surface layer cannot be specified precisely (De Rogatis et al. 2008). It is acknowledged that the composition or the structure of the crystal is customized at the free surface of the material. The volume of this surface layer turns out to be noteworthy in nanoscale materials. The surface layer of nanomaterials, in that case, can be specified as the outer region where the composition or the structure of the crystal is diverse from those of the particle interior (Wang et al. 2008).

5.3 Mechanical Properties

Nanostructures demonstrate advanced mechanical properties than the bulk materials, for example, mechanical hardness, elastic modulus, tensile stress, fatigue strength, scratch resistance, fracture toughness, etc. (Meyers et al. 2006). The aforementioned augmentation in the mechanical properties of nanomaterial is ascribing to the structural flawlessness of the material. The minute-sized materials acquire free of internal structural deficiencies, for example, dislocations, micro-twins, as well as impurity precipitations. Repeatedly mechanical failure is caused by multiplying imperfections in the nanomaterials, which are more lively and move to the surface, under annealing, purifying the material. This repositioning of defects to the surface departs perfect material structures within the nanomaterials. The exterior surface of nanostructures is very little or free from imperfections than bulk materials. Materials with fewer defects will give out the superior mechanical properties (Eletskii 2007).

In a lot of nanomaterials, hardness is noticed as the most common mechanical property. An actuality of super hard nanocomposites manufactured with borides, carbides, and nitrides (Zhang et al. 2002). Extraordinary production methods were employed to produce such nanocomposites in particular plasma-induced chemical technique and physical vapor deposition technique (Chen et al. 2013; Diserens et al. 1999). The nanomaterials are created containing excellent mechanical properties for impending applications in macro, micro, and nanoscales. Nanocrystalline copper is three times more resistant as compared to usual copper; they are also more flexible (Lu et al. 2004). Carbon nanotubes and nanowires are employed to make high-frequency electromechanical resonators that can be utilized as nanoprobes, or nanotwizzers to control nanomaterials in a nanometer scale (Nguyen et al. 2005; Dequesnes et al. 2002).

Elasticity conception takes up the little, continue, and reversible deformations of isotropic elastic materials (Muskhelishvili 2013). An elastic material exhibits the following three properties: It distorts under stress and comes back to its original shape when the stress withdraws. It is uniform, isotropic, and homogeneously distributed in its occupied volume. Materials are normally not isotropic as they are polycrystalline, with grains having diverse shapes and orientations. Conversely, as the lengths of the materials are very big to correspond to the mean grain, homogeneity, and isotropy hypothesis are occasionally more or less satisfied. Therefore, the elasticity hypothesis is as well employed for polycrystalline materials (Wong et al. 1997; Juve et al. 2010).

5.4 Structural Properties

The reduction in particle size of material results in the transform in interatomic spacing and so, surface and surface energy increase (Sun 2007). The structural alterations are noticed when the particle size reduces predominantly in the nanoscale range. Au NPs can accept a polyhedral shape, for example, cuboctahedral, multiply twinned decahedra (Eguchi et al. 2012). Aforesaid shapes can be explored and understood by the enlargement of crystalline along with a variety of crystallographic directions and energies of different crystallographic planes. Crystalline solid acquires long-range episodic structure of atoms and distinct prototypes. Quasiperiodic crystals do not acquire such long-range episodic structure. A quasiperiodic crystal is an arrangement that is prearranged but not periodic (Yamamoto 1996). The fundamental factor of nanostructured materials is their shape, size, and morphological constitution. The surface morphology of nanostructured materials can be adjusted by means of a chemical agent named surfactant. The morphologies of nanoparticles are adjustable and by scheming them, we can investigate their properties (Ariga et al. 2011).

5.5 Thermal Properties

Several properties of materials can be customized by managing their nanoscale dimensions. Such customized nanostructures can be employed to meet the demands of various applications. The thermodynamics of nanosystem is different from the thermodynamics of macroscopic systems, where the number of particles has a tendency to perpetuity (Labastie and Calvo 2008). Higher surface energy will change monotonically with size and can be taken care of within the structure of thermodynamics (Niepce and Pizzagalli 2008). Among them are the melting and other phase transition temperatures exemplifies the common experimental difference of melting point of gallium nitride spherical nanoparticles aligned with the size of the particles (Antoniammal and Arivuoli 2012). Its physical starting point is the raise of surface energy, the augment of the amplitude of atomic vibrations, and the supplementary surface growth of thermal vibration energy in the consequence (Pokropivny et al. 2007). It has been stated that the specific heat raised with the reduction in particle size, while the melting entropy, as well as enthalpy diminished as the particle size, reduces (Singh et al. 2017).

The exploit of nanofluid to improve the thermal transfer is a hopeful application of the thermal properties of nanomaterials (Murty et al. 2013). Nanofluids are, in general, said to be the solid–liquid composite materials, which contain nanomaterials of size in the range 1–100 nm suspended in a liquid (Obaid et al. 2013). Nanofluids grasp greater than ever interests in both investigate as well as practical appliances because of their very much superior thermal properties in comparison with their base fluids. A great deal of nanomaterials can be employed in nanofluids counting nanoparticles of oxides, nitrides, metals, metal carbides, and nanofibers such as single-wall and multi-wall carbon nanotubes, which can be discrete into different base liquid dependent on the potential applications, for example, water, ethylene glycol, and oils (Gorji and Ranjbar 2017).

The most significant attributes of nanofluids are the momentous increase of thermal conductivity proportionate to liquids exclusive of nanomaterials, which have been proven by numerous investigational works (Keblinski et al. 2005). Nanofluid based devices will facilitate the expansion of real-time, plainly invasive medical diagnostic systems to observe astronaut health and assist in diagnosing and treating sickness (Berger 2012).

As a result, investigators are facing problems for the hypothetical analysis of thermal transport in nanomaterials (Cahill et al. 2003). The thermal properties of nanomaterials can be tailored by numerous factors like the small size of particles, the shape of the particle and huge interface area, etc. Hence, the thermal properties of nanomaterials are fairly diverse in comparison to the bulk materials. As the length of the material lessens to the nanometer range, it is quite similar to the wavelength and means a free path of phonon, which results in the noteworthy transform in phonon transport in the material. As a consequence of the transform in phonon confinement and quantization of phonon transport, thermal properties without human intervention get customized (Balandin 2011).

5.6 Optical Properties

The optical properties are based on electronic structure, an alteration in zone structure results in an alteration in absorption and luminescence spectra. Their distinctiveness such as spectral width and position, and sensitivity to light polarization, rely not only on the inherent properties of the nano-objects (e.g., composition, structure, size, shape) but also on their surroundings (Rezaie et al. 2013).

The diminution of material dimension as well has an effect on the optical properties of the materials. The optical properties powerfully depend upon the size of particles, which are clarified in two ways. One is attributable to the additional confined structure, energy level spacing augmented and a further is concerned to surface plasmon resonance. The optical properties of metallic nanoparticles are measured by the surface plasmon resonance (SPR) phenomenon (Pattnaik 2005). The SPR is resulting from the consistent motion of the conduction band electrons from one surface of the particle to the other, upon communication with an electromagnetic field. The reduction in size beneath the electron mean free path (distance the electron moves between scattering collisions with the lattice centers) brings about intense absorption in the UV-visible range. Optical excitation of the SPR causes the surface plasmon absorption (Homola et al. 1999).

For the semiconducting materials, quantum size consequence is mostly premeditated. Lessening the particle size of semiconducting material, inter-band transition is transferred to the higher frequency, which results in the rise in the bandgap (Schmitt-Rink et al. 1987). The bandgap of semiconducting materials is within a few electron volts, which rises quickly with reducing particle size. Quantum confinement turns out a blue shift in the bandgap (Lin et al. 2005). The optical properties of nanostructured semiconductor powerfully rely upon the particle size. Therefore, the optical properties of such materials are effortlessly adjustable by changing the size of particles. The nanostructured semiconducting materials acquire excellent transporter confinement and energy density states, which assemble it most appropriate and resourceful for laser devices (Huang et al. 2001). When the particle size of metal nanostructures is lesser than the wavelength of incident radiation, a surface plasmon resonance is created. Commencing the above discussion, it is obvious that the optical properties of materials are very much affected by the particle dimension. By changing the dimension of materials in nanometer, we can modify sophisticated optical materials for devices (Sanchez et al. 2011).

5.7 Magnetic Properties

Nanomagnetism is a vibrant and very interesting topic of current solid-state magnetism and nanotechnology (Petracic 2010). It is of foremost scientific attention and high technological

importance. Ferromagnetic nanomaterials encompass prospective benefits over present materials in various appliances in hard magnets, soft magnets, magnetic recording, etc. (Schwarz et al. 2004). It is well recognized, that the coercivity of magnetic substances has an outstanding reliance on their size. Magnetic coercivity rises with the decrease in particle size in the nanometer range going through a highest at the solitary domain size, and afterward reduces one more time for very tiny particles on account of thermal effects and turns into zero at the superparamagnetic particle size. An iron, which is a soft magnetic material with coercivity about 20 Oersted (Oe) at room temperature, could be formed "hard" with a coercivity of 540 Oe (Schwarz et al. 2004). An additional example is the amazing phenomenon of giant magnetoresistance (GMR) of magnetic multilayers that has been developed to enhance the capability of hard discs by over a factor of a hundred in a few years (Mills and Bland 2006).

The magnetic properties are exploited in different appliances like ferrofluids (Hiergeist et al. 1999), and drug delivery (Wu et al. 2011). The magnetic characteristics of the nanoparticles can also be different from those of the related bulk material. Attributable to a smaller size of the particle, the surface area raises and magnetic coupling with neighboring atoms also raises, which leads to the varied magnetic properties.

Ferromagnetism takes place even for the smallest dimensions. The magnetic torques are improved atom-like for clusters with not more than around 100–200 atoms. The magnetic torque diminishes and moves toward the bulk limit, as the size is raised up to 700 atoms, with vibrations probably resulting from surface-induced spin-density waves or structural alterations. Ferromagnetism is referred to a worldwide aspect of nanoparticles of the nonmagnetic oxides (Sundaresan et al. 2006). When the particle size diminishes beneath a definite size, ferromagnetic particles turn out to be unstable. Such instability is as a result of the spontaneous polarization of domains and the adequately elevated surface energy. Owing to this property, ferromagnetic grows to be paramagnetic at the nanometer scale, but it acts in a different way from the conventional paramagnetic and therefore it is named superparamagnetism (Sato et al. 2007).

A bulk ferromagnetic substance generally includes multiple magnetic domains, while nanostructured ferromagnetic substances have minute magnetic nanoparticles and have simply one domain. These domains of different particles are arbitrarily dispersed as a result of thermal fluctuation and develop into aligned in the presence of an externally applied magnetic field (McHenry and Laughlin 2000).

6 Nanomaterials Synthesis Strategies

Nanomaterials fabrication is a tremendous contest and the subject of many kinds of research (Rosei 2004). It is a multidisciplinary domain covering biology, chemistry, engineering, materials science, and physics. The communication among researchers with varied fields will without a doubt give rise to the fabrication of novel materials with customized features. The likelihood of success of nano-manufacturing is dependent on the powerful teamwork among academia and industry with a view to being aware of existing demands and future issues, to develop products straightforwardly transferred into the industrial segment (Charitidis et al. 2014). The production of nanomaterials can adapt solid, liquid, and/or gaseous precursor materials. There are large numbers of production procedures existing to produce different types of nanomaterials organized as buckyballs, clusters, colloids, powders, rods, thin films, tubes, wires, etc. (Chen and Mao 2007; Aruna and Mukasyan 2008). Employing different techniques, synthesized materials can be designed into favorable shapes so that at last, the material can be functional to a definite application. A few of the previously available conventional methods to manufacture diverse types of materials are optimized to acquire novel nanomaterials and a number of new techniques are urbanized (Gilmore et al. 2008; Zhao et al. 2002).

A range of techniques can be utilized for the fabrication of nanoscale materials, but these

techniques are broadly divided into two main classes, i.e., (1) Bottom-up approach and (2) Top-down approach (Wang and Xia 2004) as shown in Fig. 1.3 (Iravani 2011). The manufacturing of nanomaterials by producing things smaller that are by downsizing and by constructing things from smaller building blocks that is by up-scaling. The first approach is referred to as the "top-down" and the second as the "bottom-up" approach (Ozin et al. 2009). These approaches supplementary divide into a variety of subclasses based on the adopted protocols, operation, and reaction condition. Nonetheless, a few writers proposed effective fabrication (computer simulations), as a third approach (Bader et al. 2007).

6.1 Bottom-Up Procedures

This approach is utilized in reverse as nanomaterials are produced from comparatively simple substances; so this approach is also known as building-up approach. Examples of this case are reduction and sedimentation systems. It comprises biochemical production, green production, sol-gel, and spinning (Iravani, 2011).

In this approach, a complex structure is created from small building blocks. These building blocks have precise binding capacities – commonly called molecular recognition properties which permit them to assemble automatically in the proper way. Self-assembly is an indispensable part of bottom-up approaches (Blum et al. 2005).

Bottom-up approaches imitate nature through initiating at the atomic or molecular level and building up via nucleation and/or growth from solid, liquid, or gas precursors as a result of chemical reactions or else physical processes (Dhingra et al. 2010). Colloidal dispersions like microemulsions are an excellent example of the bottom-up conception of nanomaterials manufacturing (Yaya et al. 2012). In general, bottom-up products possess high purity, improved particle size, as well as surface chemistry control. However, the bottom-up concept is in its early stage of development, it guarantees comprehensive alters to up to date techniques of manufacture (Dhingra et al. 2010).

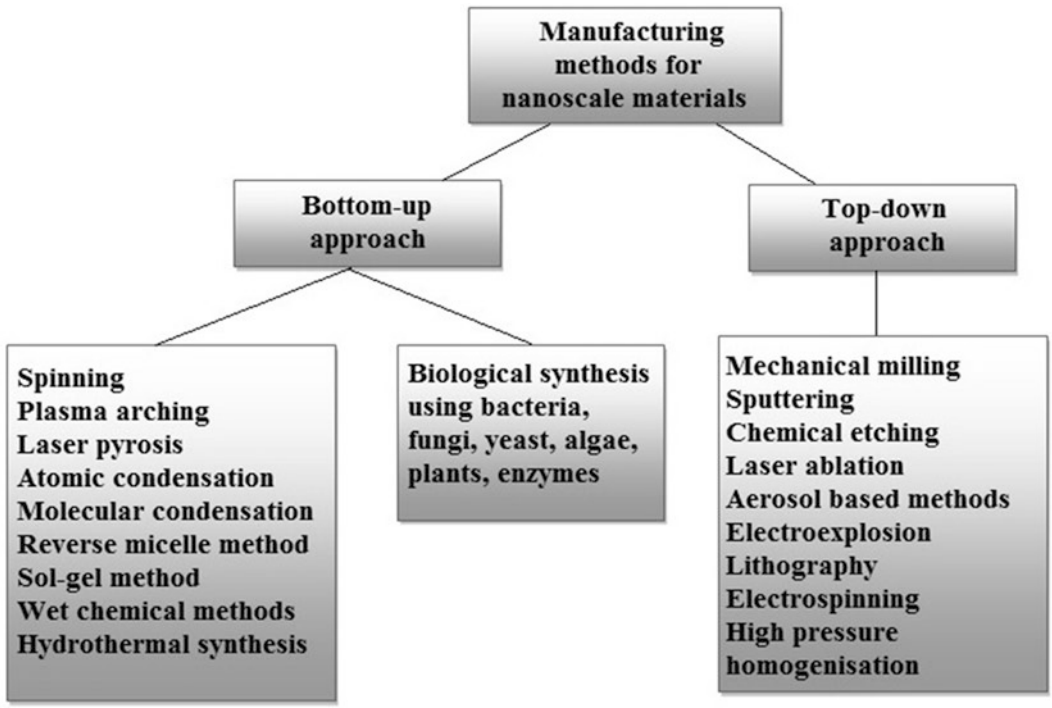

Fig. 1.3 Typical synthesis methods for nanoscale materials

6.2 Top-Down Procedures

The thought of top-down conception is to acquire procedures identified from the macroscopic world and to implement them in a manner that they can be employed for doing a similar thing on a smaller scale. Bulk particles are broken down into smaller and smaller particles. This method is generally carried out on solids or dispersed solids. From prehistoric times, human beings have formed artwork and devices by constructing materials. The characteristic example is the sculpture of stone which is the result of creating 3-D visibly attractive entities from stone. It is a prehistoric work where pieces of irregular natural stone are shaped by the controlled exclusion of stone to present in its most wanted shape (Bashir and Liu 2015).

Briefly, in this conception, a destructive approach is exploited. Starting from the large-sized molecule, which destructed into small-sized units and then these units are transformed into appropriate nanomaterials. Examples of this approach are grinding/milling, physical vapor deposition, and other decomposition techniques (Iravani, 2011).

This method, in general, depends upon physical processes or a combination of physical and/or chemical, electrical, or thermal processes for their manufacturing (Yaya et al. 2012). This is the best established of each and every one form of nanotechnology but it is normally considered that top-down approaches produce a lot more waste (Dhingra et al. 2010).

7 Conclusion

Nanotechnology can be characterized as the understanding, control, and manipulation of materials, having dimensions approximately within the 1–100 nm range, where conventional physics breaks down. Scientists consider nanotechnology as the innovatory technology of the twenty-first century. Nanomaterials refer to natural, incidental, or manufactured materials containing particles in unbound or agglomerated/aggregated states. They are materials with fundamental structural units, particles, fibers, or other essential components smaller than 100 nm in at least one dimension. It has been seen that nanomaterials are diverse from their bulk moieties and cannot be examined as same as bulk or small molecules because of their distinctive properties in nanoscale. The properties of nanomaterials rely upon the composition, chemistry, particle dimension, and interactions with other materials. The manufacturing of nanomaterials is accomplished mostly through two approaches identified as top-down and bottom-up approaches. The first way stands for breaking down the bulk material into smaller and smaller dimensions while the second one is based on consolidating the small clusters. Nanoscience and nanotechnology have the potential to deal with lot of the universal challenges facing society today and improving the quality of life. The appliance of nanotechnology continues to make momentous endowments to inventive and advantageous products across wide areas. In fact, nanotechnology aims to design novel functional smart materials and devices with a broad range of appliances, and it is important to put emphasis on the emergence of new topics like nano energy, nanomedicine, nanoelectronics, nanofood, etc.

References

Abdelsalam HA, Abdelaziz AY. The smart grid state of the art and future trends. Electr Power Compon Syst. 2014;42:306–14.

Antoniammal P, Arivuoli D. Size and shape dependence on melting temperature of gallium nitride nanoparticles. J Nanomater. 2012;2012:415797.

Ariga K, Li M, Richards GJ, Hill JP. Nanoarchitectonics: a conceptual paradigm for design and synthesis of dimension-controlled functional nanomaterials. J Nanosci Nanotechnol. 2011;11:1–13.

Aruna ST, Mukasyan AS. Combustion synthesis and nanomaterials. Curr Opin Solid State Mater Sci. 2008;12:44–50.

Asmatulu R, Asmatulu E, Zhang B. Nanotechnology and nanoethics in engineering education. In: Proceedings of the 2010 Midwest section conference of the American Society for Engineering Education. Lawrence, KS; 2010. p. 1–11.

Aznan NZK, Johan MR. Quantum size effect in ZnO nanoparticles via mechanical milling. J Nanomater. 2012;2012:439010.

Bader SD, Buchanan KS, Chung SH, Guslienko KY, Hoffmann A, Ji Y, et al. Issues in nanomagnetism. Superlattice Microst. 2007;41:72–80.

Bae YH, Park K. Targeted drug delivery to tumors: myths, reality and possibility. J Control Release. 2011;153(3):198–205.

Balandin AA. Thermal properties of graphene and nanostructured carbon materials. Nat Mater. 2011;10:569–81.

Balaz P. Mechanochemistry in nanoscience and minerals engineering. Berlin: Springer; 2008.

Barakat N, Jiao H. Nanotechnology integration to enhance undergraduate engineering education. In: Bernardino J, Quadrado JC, editors. Proceedings of the SEFI annual conference. 1st world engineering education flash week, Lisbon, Portugal; 2011. p. 623–30.

Bashir S, Liu J. Overviews of synthesis of nanomaterials. In: Bashir S, Liu J, editors. Advanced nanomaterials and their applications in renewable energy: Elsevier Science; 2015. p. 51–115.

Berger M. NASA and nanotechnology. 2012. http://www.nanowerk.com. Accessed 10 Oct 2019.

Blackwelder B. Nanotechnology jumps the gun: nanoparticles in consumer products. In: Cameron NM, Mitchell ME, editors. Nanoscale: issues and perspectives for the nano centry. Hoboken: Wiley; 2007. p. 71–82.

Blum AS, Soto CM, Wilson CD, Brower TL, Pollack SK, Schull TL, et al. An engineered virus as a scaffold for three-dimensional self-assembly on the nanoscale. Small. 2005;1:702–6.

Boverhof DR, Bramante CM, Butala JH, Clancy SF, Lafranconi M, West J, et al. Comparative assessment of nanomaterial definitions and safety evaluation considerations. Regul Toxicol Pharmacol. 2015;73(1):137–50.

Brechignac CP, Houdy P, Lahmani M. Nanomaterials and nanochemistry. Berlin/Heidelberg/New York: Springer; 2006.

Brust M, Walker M, Bethell D, Schiffrin DJ, Whyman R. Synthesis of thiolderivatised gold nanoparticles in a two-phase liquid-liquid system. J Chem Soc Chem Commun. 1994;7:801–2.

Buzea C, Pacheco-Blandino I, Robbie K. Nanomaterials and nanoparticles: sources and toxicity. Biointerphases. 2007;2(4):MR17–MR172.

Cahill DG, Ford WK, Goodson KE, Mahan GD, Majumdar A, Maris HJ, et al. Nanoscale thermal transport. J Appl Phys. 2003;93:793–818.

Cao G. Nanostructures and nanomaterials: synthesis, properties and applications. J Am Chem Soc. 2004;126(44):14679.

Charitidis CA, Georgiou P, Koklioti MA, Trompeta AF, Markakis V. Manufacturing nanomaterials: from research to industry. Manuf Rev. 2014;1(11):1–19.

Chen X, Mao SS. Titanium dioxide nanomaterials: synthesis, properties, modifications, and applications. Chem Rev. 2007;107:2891–959.

Chen Z, Dai XJ, Magniez K, Lamb PR, de Celis Leal DR, Fox BL, et al. Improving the mechanical properties of epoxy using multiwalled carbon nanotubes functionalized by a novel plasma treatment. Compos Part A Appl Sci Manuf. 2013;45:145–52.

Daniel MC, Astruc D. Gold nanoparticles: assembly, supramolecular chemistry, Quantumsize related properties and applications towards biology catalysis and nanotechnology. Chem Rev. 2004;104(1):293–346.

Daryoush B, Darvish A. A case study and review of nanotechnology and nanomaterials in green architecture. Res J Environ Earth Sci. 2013;5:78–84.

Dasgupta N, Ranjan S, Mundekkad D, Ramalingam C, Shanker R, Kumar A. Nanotechnology in agro-food: from field to plate. Food Res Int. 2015;69:381–400.

Dasgupta N, Ranjan S, Chakraborty AR, Ramalingam C, Shanker R, Kumar A. Nanoagriculture and water quality management. In: Ranjan S, Dasgupta N, Lichfouste E, editors. Nanoscience in food and agriculture 1, Sustainable agriculture reviews, vol. 20. Cham: Springer; 2016. p. 1–42.

De Rogatis L, Montini T, Gombac V, Cargnell M, Fornasiero P. Stabilized metal nanoparticles embedded into porous oxides: a challenging approach for robust catalysts. In: Prescott WV, Schwartz AI, editors. Nanorods, nanotubes and nanomaterials research progress. New York: Nova Science Publishers; 2008. p. 71–123.

Dequesnes M, Rotkin S, Aluru N. Calculation of pull-in voltages for carbonnanotube-based nanoelectromechanical switches. Nanotechnology. 2002;13(1):120–31.

Dhingra R, Naidu S, Upreti G, Sawhney R. Sustainable nanotechnology: through green methods and life-cycle thinking. Sustainability. 2010;2:3323–38.

Diserens M, Patscheider J, Levy F. Mechanical properties and oxidation resistance of nanocomposite TiN–SiNx physical-vapor-deposited thin films. Surf Coat Technol. 1999;120:158–65.

Eguchi M, Mitsui D, Wu H-L, Sato R, Teranishi T. Simple reductant concentration-dependent shape control of polyhedral gold nanoparticles and their plasmonic properties. Langmuir. 2012;28:9021–6.

Eletskii AV. Mechanical properties of carbon nanostructures and related materials. Phys-Uspekhi. 2007;50:225–61.

Fajardo AR, Pereira AGB, Muniz EC. Hydrogels nanocomposites based on crystals, whiskers and fibrils derived from biopolymers. In: Thakur VK, Thakur MK, editors. Eco-friendly polymer nanocomposites, advanced structured materials. New Delhi: Springer; 2015. p. 43–71.

Feynman RP. There's plenty of room at the bottom. Eng Sci. 1960;23(5):22–36.

Filella M. Nanomaterials. In: Pawliszyn J, editor. Comprehensive sampling and sample preparation, vol. 1. Amsterdam: Academic Press; 2012. p. 109–24.

Filipponi L, Sutherland D. Nanotechnologies: principles, applications, implications and hands-on activities. Directorate-General for Research and Innovation Industrial Technologies (NMP). Luxembourg: European Union; 2013.

Gaffet E. Nanomaterials: a review of the definitions, applications, health effects. How to implement secure development. 2011. https://hal.archives-ouvertes.fr/hal-00598817/file/E.Gaffet-GB.pdf. Accessed 29 Aug 2019.

Gamucci O, Bertero A, Gagliardi M, Bardi G. Biomedical nanoparticles: overview of their surface immune-compatibility. Coatings. 2014;4(1):139–59.

Gendelman HE, Anantharam V, Bronich T, Ghaisas S, Jin H, Kanthasamy AG, et al. Nanoneuromedicines for degenerative, inflammatory, and infectious nervous system diseases. Nanomed Nanotechnol Biol Med. 2015;11(3):751–67.

Gilmore JL, Yi X, Quan L, Kabanov AV. Novel nanomaterials for clinical neuroscience. J Neuroimmune Pharmacol. 2008;3:83–94.

Gleiter H. Nanostructured materials: basic concepts and microstructure. Acta Mater. 2000;48:1–29.

Gorji TB, Ranjbar AA. A review on optical properties and application of nanofluids in direct absorption solar collectors (DASCs). Renew Sust Energ Rev. 2017;72:10–32.

Gubin SP. Magnetic nanoparticles. Weinheim: Wiley; 2009.

Guo D, Xie G, Luo J. Mechanical properties of nanoparticles: basics and applications. J Phys D Appl Phys. 2014;47:1–25.

Henry C. Size effects on structure and morphology of free or supported nanoparticles. In: Brechignac C, Houdy P, Lahmani M, editors. Nanomaterials and nanochemistry. Berlin/Heidelberg: Springer; 2008. p. 3–34.

Hiergeist R, Andra W, Buske N, Hergt R, Hilger I, Richter U, et al. Application of magnetite ferrofluids for hyperthermia. J Magn Magn Mater. 1999;201:420–2.

Hochella MF Jr, Spencer MG, Jones KL. Nanotechnology: nature's gift or scientists' brainchild? Environ Sci Nano. 2015;2(2):114–9.

Homola J, Yee SS, Gauglitz G. Surface plasmon resonance sensors: review. Sensors Actuat B Chem. 1999;54:3–15.

Huang MH, Mao S, Feick H, Yan H, Wu Y, Kind H, et al. Room-temperature ultraviolet nanowire nanolasers. Science. 2001;292:1897–9.

Huang R, Ke W, Han L, Li J, Liu S, Jiang C. Targeted delivery of chlorotoxin-modified DNA loaded nanoparticles to glioma via intravenous administration. Biomaterials. 2011a;32(9):2399–406.

Huang S, Li J, Han L, Liu S, Ma H, Huang R, et al. Dual targeting effect of Angiopep-2- modified, DNA-loaded nanoparticles for glioma. Biomaterials. 2011b;32(28):6832–8.

Huyen D. Carbon nanotubes and semiconducting polymer nanocomposites. In: Yellampalli S, editor. Carbon nanotubes -synthesis, characterization, applications. London: InTech; 2011.

Iravani S. Green synthesis of metal nanoparticles using plants. Green Chem. 2011;13:2638–50.

ISO/TS 27687. Nanotechnologies – terminology and definitions for nanoobjects – nanoparticle, nanofibre, nanoplate. 2008. https://www.iso.org/standard/44278.html. Accessed 25 Jul 2019.

ISO/TS 80004-1. International standardization organization technical standard: nanotechnologies – vocabulary – Part 1: Core terms. International Organization for Standardization, Geneva, Switzerland; 2010. https://www.iso.org/standard/51240.html. Accessed 17 Sep 2019.

Jeevanandam J, Barhoum A, Chan YS, Dufresne A, Danquah MK. Review on nanoparticles and nanostructured materials: history, sources, toxicity and regulations. Beilstein J Nanotechnol. 2018;9:1050–74.

Johnston RL, Wilcoxon JP. Frontiers of nanoscience, vol. 3. Oxford: Elsevier; 2012.

Jordan CC, Kaiser I, Moore VC. 2013 Nanotechnology patent literature review: graphitic carbon-based nanotechnology and energy applications are on the rise. Nanotechnol Law Bus. 2014;11(2):111–25.

Junk A, Riess F. From an idea to a vision: there's plenty of room at the bottom. Am J Phys. 2006;74(9):825–30.

Juve V, Crut A, Maioli P, Pellarin M, Broyer M, Del Fatti N, et al. Probing elasticity at the nanoscale: terahertz acoustic vibration of small metal nanoparticles. Nano Lett. 2010;10:1853–8.

Keblinski P, Eastman JA, Cahill DG. Nanofluids for thermal transport. Mater Today. 2005;8(6):36–44.

Klaine SJ, Alvarez PJJ, Batley GE, Fernandes TE, Hand RD, Lyon DY, et al. Nanoparticles in the environment: behavior, fate, bioavailability and effects. Environ Toxicol Chem. 2008;27(9):1825–51.

Koch CC, Ovidko IA, Seal S, Veprek S. Structural nanocrystalline materials: fundamentals and applications. New York: Cambridge University Press; 2007.

Koo JH. Polymer nanocomposites – processing, characterization, and applications. New York: McGraw-Hill; 2006.

Koo JH. Fundamentals, properties and applications of polymer nanocomposites. New York: Cambridge University Press; 2016. p. 3–17.

Koski KJ, Cui Y. The new skinny in two-dimensional nanomaterials. ACS Nano. 2013;7:3739–43.

Kreuter J. Nanoparticles-a historical perspective. Int J Pharm. 2007;331:1–10.

Kumar N, Kumbhat S. Carbon-based nanomaterials. In: Essentials in nanoscience and nanotechnology. Hoboken: Wiley; 2016. p. 189–236.

Labastie P, Calvo F. Thermodynamics and Solid-liquid transitions. In: Brechignac C, Houdy P, Lahmani M, editors. Nanomaterials and nanochemistry. Berlin/Heidelberg: Springer; 2008. p. 55–87.

Law M, Goldberger J, Yang P. Semiconductor nanowires and nanotubes. Annu Rev Mater Res. 2004;34:83–122.

Lin KF, Cheng HM, Hsu HC, Lin LJ, Hsieh WF. Band gap variation of size-controlled ZnO quantum dots synthesized by sol–gel method. Chem Phys Lett. 2005;409:208–11.

Lin J, Zhang C, Yan Z, Zhu Y, Peng Z, Hauge RH, et al. 3-dimensional graphene carbon nanotube carpet-based microsupercapacitors with high electrochemical performance. Nano Lett. 2013;13:72–8.

Liu H, Li Y, Xiao S, Gan H, Jiu T, Li H, et al. Synthesis of organic one-dimensional nanomaterials by solid-phase reaction. J Am Chem Soc. 2003;125:10794–5.

Liu S, Guo Y, Huang R, Li J, Huang S, Kuang Y, et al. Gene and doxorubicin co-delivery system for targeting therapy of glioma. Biomaterials. 2012;33(19):4907–16.

Lokhande J, Pathak Y. Handbook of metallonutraceuticals. Boca Raton: CRC Press/Taylor & Francis Group; 2014.

Lu L, Shen Y, Chen X, Qian L, Lu K. Ultrahigh strength and high electrical conductivity in copper. Science. 2004;304:422–6.

Maddinedi SB, Mandala BK, Ranjanb S, Dasgupta N. Diastase assisted green synthesis of size controllable gold nanoparticles. RSC Adv. 2015;5:26727–33.

McHenry M, Laughlin D. Nano-scale materials development for future magnetic applications. Acta Mater. 2000;48:223–38.

Meyers MA, Mishra A, Benson DJ. Mechanical properties of nanocrystalline materials. Prog Mater Sci. 2006;51:427–556.

Mills DL, Bland JAC, editors. Nanomagnetism: ultrathin films, multilayers and nanostructures, vol. 1. 1st ed. Amsterdam: Elsevier Science; 2006. p. xi–xiii.

Miyazaki K, Islam N. Nanotechnology systems of innovation – an analysis of industry and academia research activities. Technovation. 2007;27(11):661–75.

Moghimi SM, Hunter AC, Murray JC. Nanomedicine: current status and future prospects. FASEB J. 2005;19(3):311–30.

Murty BS, Shankar P, Raj B, Rath BB, Murday J. Textbook of nanoscience and nanotechnology. Berlin: Springer; 2013.

Muskhelishvili NI. Some basic problems of the mathematical theory of elasticity. Dordrecht: Springer; 2013.

Naseri MG, Saion EB. Crystallization in spinel ferrite nanoparticles. In: Mastai Y, editor. Advances in crystallization processes. Croatia: InTech; 2012. p. 349–80.

Nasir Khan M, Mobin M, Abbas ZK, AlMutairi KA, Siddiqui ZH. Role of nanomaterials in plants under challenging environments. Plant Physiol Biochem. 2017;110:194–209.

Nguyen CV, Ye Q, Meyyappan M. Carbon nanotube tips for scanning probe microscopy: fabrication and high aspect ratio nanometrology. Meas Sci Technol. 2005;16(11):2138–46.

Niepce JC, Pizzagalli L. Structure and phase transitions in nanocrystals. In: Brechignac C, Houdy P, Lahmani M, editors. Nanomaterials and nanochemistry. Berlin/Heidelberg: Springer; 2008. p. 35–54.

Nikalje AP. Nanotechnology and its applications in medicine. Med Chem. 2015;5:81–9.

Obaid HN, Habeeb MA, Rashid FL, Hashim A. Thermal energy storage. Nanofluids J Energy Technol Policy. 2013;3:34–6.

Ozin GA, Arsenault AC, Cademartiri L. Nanochemistry: a chemical approach to nanomaterials. Cambridge: The Royal Society of Chemistry; 2009.

Pattnaik P. Surface plasmon resonance. Appl Biochem Biotechnol. 2005;126:79–92.

Petracic O. Superparamagnetic nanoparticle ensembles. Superlattice Microst. 2010;47:569–78.

Pillai G. Nanomedicines for cancer therapy: an update of FDA approved and those under various stages of development. SOJ Pharm Pharm Sci. 2014;1(2):13–25.

Pokropivny VV, Skorokhod VV. Classification of nanostructures by dimensionality and concept of surface forms engineering in nanomaterial science. Mater Sci Eng C. 2007;27:990–3.

Pokropivny VV, Lohmus R, Hussainova I, Pokropivny A, Vlassov S. Introduction to nanomaterials and nanotechnology. Ukraine: Tartu University Press; 2007. p. 29–40.

Potocnik J. Commission recommendation of 18 October 2011 on the definition of nanomaterials. Off J Eur Communities Legis. 2011;L275:38–40.

Pradeep T. Nano: the essentials – understanding nanoscience and nanotechnology. New Delhi: Tata McGraw-Hill Publishing; 2007. p. 3–15.

Pulimi M, Subramanian S. Nanomaterials for soil fertilisation and contaminant removal. In: Ranjan N, Dasgupta N, Lichfouste E, editors. Nanoscience in food and agriculture 1, Sustainable agriculture reviews, vol. 20. Cham: Springer; 2016. p. 229–46.

Rai M, Yadav A, Gade A. Current trends in phytosynthesis of metal nanoparticles. Crit Rev Biotechnol. 2008;28(4):277–84.

Ranjan S, Nandita D, Bhavapriya R, Ganesh SA, Chidambaram R, Ashutosh K. Microwave irradiation-assisted hybrid chemical approach for titanium dioxide nanoparticle synthesis: microbial and cytotoxicological evaluation. Environ Sci Pollut Res. 2016;23:12287–302.

Ranjan S, Nandita D, Sudandiradoss C, Ramalingam C, Ashutosh K. A novel approach to evaluate titanium dioxide nanoparticle-protein interaction through docking: an insight into the mechanism of action. Proc Natl Acad Sci India Sect B Biol Sci. 2017;87(3):937–43.

Ratner M, Ratner D. Nanotechnology: a gentle introduction to the next big idea. Upper Saddle River: Prentice Hall; 2003. p. 1–18.

Raza H, Raza TZ. Introducing nanoengineering and nanotechnology to the first year students through an interactive seminar course. J Nano Educ. 2013;4:41–6.

Rezaie HR, Shokuhfar A, Arianpour F. Nanocomposite materials from theory to application. In: Andreas OA, Shokuhfar A, editors. New frontiers of nanoparticles and nanocomposite materials. Berlin/Heidelberg: Springer; 2013. p. 171–232.

Richards R, Bonnemann H. Synthetic approaches to metallic nanomaterials. In: CSSR K, Hormes J, Leuschner C, editors. Nanofabrication towards biomedical applications: techniques, tools, applications, and impact. Weinheim: Wiley; 2005. p. 3–32.

Rocco MC. National nanotechnology initiative – past, present, future. In: Goddard WA, Brenner DW, Lyshevski SE, Iafrate GJ, editors. Handbook on nanoscience, engineering and technology. 2nd ed. Boca Raton: Taylor and Francis/CRC Press; 2007. p. 3.1–3.26.

Rocco MC, Mirkin CA, Hersam MC. Nanotechnology research directions for societal needs in 2020: retrospective and outlook. Dordrecht: Springer; 2011.

Roduner E. Size matters: why nanomaterials are different. Chem Soc Rev. 2006;35:583–92.
Rosei F. Nanostructured surfaces: challenges and frontiers in nanotechnology. J Phys Condens Matter. 2004;1:S1373–436.
Royal Society & The Royal Academy of Engineering. Nanoscience and nanotechnologies. 2004. https://royalsociety.org/~/media/Royal_Society_Content/policy/publications/2004/9693.pdf. Accessed 18 Aug 2019.
Salata O. Applications of nanoparticles in biology and medicine. J Nanobiotechnol. 2004;2(3):1–6.
Saleh TA. Nanomaterials for pharmaceuticals determination. Bioenergetics. 2016;5(1):1000226.
Saleh TA, Gupta VK. Nanomaterial and polymer membranes, synthesis, characterization, and applications. Amsterdam: Elsevier; 2016.
Sanchez C, Belleville P, Popall M, Nicole L. Applications of advanced hybrid organic–inorganic nanomaterials: from laboratory to market. Chem Soc Rev. 2011;40:696–753.
Sandhiya S, Dkhar SA, Surendiran A. Emerging trends of nanomedicineean overview. Fundam Clin Pharmacol. 2009;23(3):263–9.
Sarma S, Das R, Brar S, Verma M, Tyagi R, Surampalli R, et al. Fundamental characteristics and their influence on fate and behavior of nanomaterials in environments. In: Brar SK, Verma M, Tyagi RD, Surampalli RY, Zhang TC, editors. Nanomaterials in the environment. 1st ed. Reston: American Society of Civil Engineers; 2015. p. 1–26.
Sato K, Fukushima T, Katayama-Yoshida H. Superparamagnetic blocking phenomena and room-temperature ferromagnetism in wide band-gap dilute magnetic semiconductor (Ga, Mn) N. Jpn J Appl Phys. 2007;46:L682–4.
Schmitt-Rink S, Miller D, Chemla DS. Theory of the linear and nonlinear optical properties of semiconductor microcrystallites. Phys Rev B. 1987;35:8113–25.
Schwarz JA, Contescu CI, Putyera K. Dekker encyclopedia of nanoscience and nanotechnology, vol. 4. Boca Raton: CRC Press; 2004.
Seshan K, editor. Handbook of thin-film deposition processes and techniques-principles, methods, equipment and applications. 2nd ed. Norwich/New York: Noyes/William Andrew Publications; 2002. p. 1–430.
Sharma VK, Filip J, Zboril R, Varma RS. Natural inorganic nanoparticles-formation, fate, and toxicity in the environment. Chem Soc Rev. 2015;44(23):8410–23.
Singh M, Lara S, Tlali S. Effects of size and shape on the specific heat, melting entropy and enthalpy of nanomaterials. J Taibah Univ Sci. 2017;11(6):922–9.
Smith AM, Nie S. Semiconductor nanocrystals: structure, properties, and band gap engineering. Acc Chem Res. 2010;43(2):190–200.
Sozer N, Kokini JL. Nanotechnology and its applications in the food sector. Trends Biotechnol. 2009;27:82–9.
Stucky GD, Mac Dougall JE. Quantum confinement and host/guest chemistry: probing a new dimension. Science. 1990;247:669–78.
Sugimoto Y, Pou P, Custance O, Jelinek P, Abe M, Perez R, et al. Complex patterning by vertical interchange atom manipulation using atomic force microscopy. Science. 2008;322:413–7.
Sun CQ. Size dependence of nanostructures: impact of bond order deficiency. Prog Solid State Chem. 2007;35(1):1–159.
Sundaresan A, Bhargavi R, Rangarajan N, Siddesh U, Rao C. Ferromagnetism as a universal feature of nanoparticles of the otherwise nonmagnetic oxides. Phys Rev B. 2006;74:161306.
Taniguchi T. On the basic concept of nanotechnology. In: Proceedings of the international conference of production engineering, Tokyo, part II. Japan Society of precision Engineering. 1974. p. 18–23.
Thomas S, Rafiei S, Maghsoodlou S. Afzali a foundations of nanotechnology, volume two: nanoelements formation and interaction. New York: Apple Academic Press; 2014.
Tiwari JN, Tiwari RN, Kim KS. Zero-dimensional, one-dimensional, two-dimensional and three-dimensional nanostructured materials for advanced electrochemical energy devices. Prog Mater Sci. 2012;57:724–803.
Torchilin VP. Recent advances with liposomes as pharmaceutical carriers. Nat Rev Drug Discov. 2005;4(2):145–60.
Torchilin V. Tumor delivery of macromolecular drugs based on the EPR effect. Adv Drug Deliv Rev. 2011;63(3):131–5.
Vance ME, Kuiken T, Vejerano EP, McGinnis SP, Hochella MF, Rejeski D, et al. Nanotechnology in the real world: redeveloping the nanomaterial consumer products inventory. Nanotechnology. 2015;6:1769–80.
Vander Heiden MG. Targeting cancer metabolism: a therapeutic window opens. Nat Rev Drug Discov. 2011;10(9):671–84.
Wagner S, Gondikas A, Neubauer E, Hofmann T, von der Kammer F. Spot the difference: engineered and natural nanoparticles in the environment-release, behavior, and fate. Angew Chem Int Ed. 2014;53(46):12398–419.
Wang M, Thanou M. Targeting nanoparticles to cancer. Pharmacol Res. 2010;62(2):90–9.
Wang Y, Xia Y. Bottom-up and top-down approaches to the synthesis of monodispersed spherical colloids of low melting-point metals. NanoLett. 2004;4:2047–50.
Wang B, Xue D, Shi Y, Xue F. Titania 1D nanostructured materials: synthesis, properties and applications. In: Prescott WV, Schwartz AI, editors. Nanorods, nanotubes and nanomaterials research Progress. NewYork: Nova Science Publishers; 2008. p. 163–201.
Wang R, Billone PS, Mullett WM. Nanomedicine in action: an overview of cancer Nanomedicine on the market and in clinical trials. J Nanomater. 2013;2013:629681.

Wani IA. Nanomaterials, novel preparation routes, and characterizations. In: Shah MA, Bhat MA, Davim JP, editors. Nanotechnology applications for improvements in energy efficiency and environmental management, vol. 2015. Hershey: IGI Global Publishers; 2015. p. 1–40.

Wardak A, Gorman ME, Swami N, Deshpande S. Identification of risks in the life cycle of nanotechnology-based products. J Ind Ecol. 2008;12:435–48.

West JL, Halas NJ. Engineered nanomaterials for biophotonics applications: improving sensing, imaging, and therapeutics. Annu Rev Biomed Eng. 2003;5:285–92.

Wong EW, Sheehan PE, Lieber CM. Nanobeam mechanics: elasticity, strength, and toughness of nanorods and nanotubes. Science. 1997;277:1971–5.

Wu H, Liu G, Wang X, Zhang J, Chen Y, Shi J, et al. Solvothermal synthesis of cobalt ferrite nanoparticles loaded on multiwalled carbon nanotubes for magnetic resonance imaging and drug delivery. Acta Biomater. 2011;7:3496–504.

Yamamoto A. Crystallography of quasiperiodic crystals. Acta Crystallogr A Found Crystallogr. 1996;52:509–60.

Yaya A, Agyei-Tuffour B, Dodoo-Arhin D, Nyankson E, Annan E, Konadu DS, et al. Layered nanomaterials- a review. Glob J Eng Des Technol. 2012;1:32–41.

Yokoyama M. Drug targeting with nano-sized carrier systems. J Artif Organs. 2005;8:77–84.

Zhang S, Sun D, Yongqing FU. Superhard nanocomposite coatings: review article. J Mater Sci Technol. 2002;18(6):485–91.

Zhao Y, Li F, Zhang R, Evans DG, Duan X. Preparation of layered doublehydroxide nanomaterials with a uniform crystallite size using a new method involving separate nucleation and aging steps. Chem Mater. 2002;14:4286–91.

2 Biomedical Applications of Nanoparticles

Manish P. Patel and Jayvadan K. Patel

Abstract

During the last decade, biomedical applications of nanoparticles describes the most interesting and investigated applications of nanoparticles, emphasising their therapeutic impact. There have been enormous developments in utilising the power of nanotechnology in various fields including biomedical sciences. The most important biomedical applications of nanoparticles are in disease diagnosis and treatment. Functionalised nanoparticles possess unique properties as contrast agents for dual and even triple modal imaging. The potential of these new generation nanoparticles in targeted drug delivery has revolutionised safe and effective pharmacotherapies for complex diseases. One more step ahead, theranostic nanoparticles are equipped with dual capabilities for disease diagnosis as well as treatment. Specifically, designed nanoparticles have also been utilised to improve the delivery and efficiency of different vaccines, including their application in cancer immunotherapy. This chapter provides an overview of the biomedical applications of nanoparticles and recent advancements in this area on the basis of current research. Progress made in the therapy of severe diseases, such as cancer and difficult infections, is strictly correlated to the scientific progress and technological development in the field of materials science. Nanoparticles have numerous therapeutic applications, starting with the design of new drugs, delivery systems, therapeutic materials, and their contribution to the development of preventive strategies. The chapter highlights the impact of nanoparticles on the therapy of infections, antimicrobial effect, and also anticancer strategies. Nanoparticles are minute particles that produce a major change in the healthcare and biomedical industry. It is not restricted to any field and its presence is observed in every field of biomedicine from diagnosis to treatment to implants to cosmetics.

Keywords

Molecular biology · Biochemistry · Drug targeting · Diagnosis · Cell biology · Biological engineering

M. P. Patel (✉)
Department of Pharmaceutics and Pharmaceutical Technology, L. M. College of Pharmacy, Ahmedabad, India

J. K. Patel
Nootan Pharmacy College, Sankalchand Patel University, Visnagar, Gujarat, India

J. K. Patel, Y. V. Pathak (eds.), *Emerging Technologies for Nanoparticle Manufacturing*,
https://doi.org/10.1007/978-3-030-50703-9_2

1 Introduction

'Nano', when used as prefix to anything, is 'one billionth' fraction, or 10^{-9} of something'. The concept was first described by physicist and Nobel laureate Richard Feynman in his lecture at American Physical Society on December 1959. The lecture was entitled 'There's plenty of room at the bottom'. Over the years, there have been many revolutionary developments across various fields that have supported Feynman's ideas of modifying matter at the atomic scale (Bonelmekki 2017). The research has been continued all these years and will continue for many years to come. The combination of nanotechnology and biotechnology is referred to as nanobiotechnology (Saji et al. 2010). When applied these concepts to improve the medicinal and healthcare of society, it is referred to as biomedicine.

Biomedicine is a branch of medical science that applies biological and physiological principles to clinical practice (Quirke and Gaudillière 2008). It is not restricted within the boundaries of a specific field, but is an amalgamation of numerous fields that are directly or indirectly associated with humans and human health. Some of them are (Wade and Halligan 2004; Engel 1977):

- Molecular biology
- Biochemistry
- Biotechnology
- Biological engineering
- Cell biology
- Cytogenetics, bioinformatics, and gene therapy
- Embryology
- Microbiology, virology, and immunology
- Neuroscience
- Pathology and toxicology, etc.

Nanobiotechnology has proved to be an interesting resource, for revolutionising these biomedical fields in the twenty-first century. It has changed the concept of health. The development in nanobiotechnology has opened the doors for developing newer and modified nanoparticles that shares a property different from its parent compound. This review will highlight the major applications and use of nanoparticles in recent history and its future that will help to improve the biomedical and healthcare system across the globe.

1.1 Applications of Nanoparticles in Biomedical

I. **Molecular Biology**
As per Oxford, molecular biology can be defined as 'the branch of biology that deals with the structure and function of the macromolecules (e.g. proteins and nucleic acids) essential to life'.

1. **Nanoparticles for cell detection and separation:** Outcome of research depends on selection and quality of raw materials and interpretation of data. In molecular biology, it is very important to isolate specified cells from the mixture or group of cells. Based on the efficiency of isolation of a selected cell from complicated mixtures affects the biological research and limits its role for biological applications. Nanoparticle acts as a sensitive tool not only for detection of cells in mixture but also can be used for isolation of those cells. Besides, it is more selective and can be used to detect cells found in trace amounts. This detection of circulating tumour cells (CTCs) is also possible by this technique. It has also been used to successfully capture those circulating tumour cells. Hence, CTCs can be the necessary aid for deeper understanding of the biology of cancer metastasis. It is observed that it acts as a prognostic biomarker for overall survival in cancer patients having metastatic breast, colorectal, and prostate cancer (Wang and Wang 2004).
2. **Nanoparticles for analyte detection:** Detection of biological analyte such as DNA, RNA, and proteins is a tedious and difficult task. Nanoparticle is help-

ful for both qualitative and quantitative analysis of these compounds. Besides, it has a very high level of sensitivity for the same. The advantage of using nanoparticles is that they have a very large surface-area-to-mass ratio, are small in size, and can be modified for study of composition-dependent properties that use surface ligands to detect efficiently and more rapidly.

Mirkin group has successfully developed gold nanoparticles for signal transduction amplification. It uses unique surface chemistry of gold nanoparticles which acts as the biobarcode that detects protein and DNA targets (Wang and Wang 2004).

3. **Subcellular targeting:** Nanoparticles is not only restricted to deliver drugs at cellular levels, but it can also be used for delivering agents to subcellular organelles, which can enlighten us about various molecular processes and pathways that are still unknown. Modern tools for more effective subcellular targeting are being developed for targeted delivery to the cellular organelles such as nucleus, cytosol, endosomes, mitochondria, and lysosomes (Wang and Wang 2004).

II. **Biochemistry**

1. **As catalyst:** Use of substance to increase the rate of reaction without changing its chemical structure is known as catalysis, and use of nanoparticles in catalysis is one of the most widely used applications of nanoparticles. Of them, use of noble metal nanoparticles acts the best, because they have a very high catalytic activity for a large number of chemical reactions. They have a very large surface-area-to-mass ratio, which is responsible for its higher catalytic activity, and so they readily increase the kinetics of reaction. The major advantage of such catalyst is it has been used for development of sensors for rapid detection and they are being used for detection of diseases, moisture, impurities, etc. The most interesting example of such sensor includes glucose nanosensors for detection of diabetes. Other such sensors include choline nanosensors, nicotinamide adenine dinucleotide nanosensors, lactate nanosensors, triglyceride nanosensors, ochratoxin A detectors, urea nanosensors, C-reactive protein detectors, etc. (El Ansary and Faddah 2010).

Similarly, it has been reported that Co_3O_4 is humidity sensitive in the visible wavelength region at room temperature, and so it can be used to detect the maintenance of temperature and humidity levels in air-controlled region (Sun 2006).

2. **Engineered nanoparticles:** Major advantage of nanoparticles is that their properties can be predefined, and based on our requirement, they can be selected. This has led to an attempt to form large varieties of nanoparticles and they are known as engineered nanoparticles. The high production, intense use, and quick disposal of engineered nanoparticles offers interesting developments in biomedical industry. Use of engineered nanoparticles in plant modification and for artificial photosynthesis to improve the yield is already under progress. Development of new metal in nanoparticulate form has been essential to improvise the yield and development of modified crops which can withstand extreme and uncontrolled environment. It has also been helpful to provide essential nutrients to plants required for their growth, improving the quality of crops without degrading the quality of soil (Rico and Chemistry 2015).

III. **Pharmacy**

1. **Drug Targeting** (Fakruddin et al. 2012)**:** Physiology and anatomy of diseased cells differ from normal cells. Drug targeting is possible by utilising these distinct features of diseased tissues. The pathophysiological conditions and anatomical changes of diseased or inflamed tissues can be triggered which offers a great scope for the development of nanoparticles that targets only diseased cells. This helps to increase the concentration of drug in diseased cells compared to normal dose. For example, nanosystems have better transmission and higher retention in tumour cells due to higher vascular permeability and impaired lymphatic drainage in tumours cells. Nanosystems are also quite selective for localised actions in inflamed tissues.

   Nanoparticles can effectively cross blood–brain barrier (meninges) and so can be used for brain targeting and CNS drug delivery. Drug loaded nanoparticles are more selective thereby improving drug efficacy and reducing drug toxicity.

   Nanosystems can also improvise the pharmacokinetics and pharmacodynamics of drug. It is used to mould the final properties of drugs as per the requirement of dosage form. This helps to reduce dose size and frequency, altering the side effects and maintaining the therapeutic efficacy of drug for longer duration within the required therapeutic window.
2. **Diagnosis**

   Current diagnostic methods for most diseases are efficient to identify only after symptoms are visible to medical professionals. Due to this, patient suffers from specific illness for longer time because symptoms appear only after a lag phase. Also, treatment may prove to be lesser effective by the time symptoms have actually appeared. The faster a disease can be detected, the better and more readily it can be cured. Besides, certain life-threatening diseases and disorders can be avoided or minimised by proper understanding of human body and its mechanism. Optimally, diseases should be diagnosed and cured before symptoms even manifest themselves (Fakruddin et al. 2012). This is only possible by improvising the sensitivity and speed of diagnosis.

   Vancomycin, when linked with iron and platinum nanoparticles (also known as FePt-vancomycin nanoparticles), exhibits more selective binding to Gram-negative bacteria at a concentration as low as 15 Cfu per mL. In comparison with luminescence-based assays for bacteria detection (detection limit: 180 cfu mL–1), FePt nanoparticles can detect ten times lower fractions (Sun 2006). Other diagnostics detection of pathogens and diseases/diseased cells includes nucleic acid diagnostics that allows diagnosis at an early symptomless stage of disease progression. This will help for a better and more efficient treatment. Polymerase chain reaction (PCR) and nanotechnology, when combined together, will expand the current options and ensure greater sensitivity and far better efficiency with lower costs. Besides, genetic disorders will be easily identified and cured more readily (Fakruddin et al. 2012). This has been discussed in detail in later part of this review.

   Mesoporous silica nanomaterials can also be used for diagnosis and drug targeting as it offers more loading and faster release of large quantities of biomedical agents (Saji et al. 2010)
3. **Rate-Controlled Drug Delivery** (Chan et al. 2009)

   Use of nanoparticles for controlling the dose, minimising it, and optimising the rate of release of drug, thereby main-

taining the therapeutic dose in the body for longer period of time, helps to improve the efficacy of drug. It is more patient compliant and reduces adverse effects. Several dosage forms in the past and all the present dosages are being designed and developed with the similar intention. Doxil (doxorubicin entrapped in liposomes) was the first FDA-approved liposomal nanodrug formulation in 1995. It is used for the treatment of AIDS associated with Kaposi's sarcoma. It is one such example that has been used in modern day's therapeutics due to its improved activity and is quite successful.

4. **Photoablation Therapy** (Wu et al. 2015)
   A strategy involving the generation of heat by various nanoparticles using outsource energy for treating tumours and cancer has been reported and tested. Such model has been used for treating ovarian cancer and is more effective compared to normal chemotherapies due to reduction in adverse effects. Use of gold nanoparticles to enhance the temperature at targeting sites and destroying the tumour cells gave better and faster results due to their higher conductive properties. Besides, gold nanoparticles readily reach the targeted site and provide a non-invasive route of therapy.
5. **Other Therapeutic Application**

   (a) **Intracellular targeting**: Certain antibiotics fail to diffuse across the cell's lysosomal membrane. This is generally due to the ionic character of antibiotics and neutral extracellular membrane. Lysosomal pH is also responsible for this barrier. This created a need of a drug with greater and better intracellular efficacy which led to development of endocytosable drug carriers such as nanoparticles. Such nanoparticles have higher efficacy. For example, polyhexylcyanoacrylate ampicillin (PIHCA) was effective at a 0.8 mg dose and was more effective in mice compared to 32 mg dose three times a day.

   (b) **Chemotherapy:** Drug entrapped or absorbed in polyalkylcyanoacrylate nanoparticles are more effective in chemotherapy compared to those drugs which are delivered through conventional route. Besides, they have reduced adverse reactions due to lower dose. So far, mitoxantrone in polybutylcyanoacrylate, aclacinomycin in polyisobutylcyanoacrylate, granulocyte colony-stimulating factor in polyalkylcyanoacrylate, acyclovir in polybutylcyanoacrylate, and doxorubicin in polyalkylcyanoacrylate have been tested and passed for their better efficacy.

   (c) **Per oral administration of proteins and peptides:** Proteins and peptides readily undergo proteolytic degradation and, hence, have shorter biological half-life. They have poor absorption due to lack of its ability to cross biological membranes. However, formation of nanoparticles and nanocapsules has helped for successful delivery of enzymes and hormones such as insulin and growth hormone releasing factor.

   (d) **Ocular drug delivery:** Ocular drug delivery is quite problematic due to numerous reasons such as lachrymal drainage, shorter residence time (1–3 min), irritability, sensitive region, sterility, etc. However, this problem has been solved to a certain extent using nanoparticles having biodegradable characteristics. Polymers used for such delivery include albumin, polyester, and polyalkylcyanoacry-

late. These polymers act isotonic to eye, are less irritating, and increase tissue adhesion and residence time of drug.

6. **Other Pharmaceutical Applications** (Fakruddin et al. 2012): It involves drug delivery and gene delivery using liposomes, niosomes, solid liquid nanoparticles, etc. This has been done to modify the properties of molecules and has been quite successful for cardiac therapy, CNS drug delivery, dental care, ophthalmic treatments, orthopaedic applications, etc.

IV. **Cell Biology** (Thimiri Govinda Raj and Khan 2016)
Cell biology revolves around the study of cells and cellular structures. Isolation of cells and cell organelles play an important role for studying the unique features in such a minute structure. For such studies, organelle fractionation plays a major role. The governing factor for organelle fractionation is high yield and high purity. Density-gradient centrifugation (sucrose-based fractionation) is the method generally used for fractionation. This method is based on principle of difference in density for separation. It is further modified based on equilibrium or nonequilibrium centrifugation for organelle separation. Other method used for fractionation involves antibody-based pulldown assay. This assay makes use of magnetic beads that are tagged with antibodies selectively targeting the subcellular compartments. For example, TOM22 antibodies conjugated with magnetic beads are used for isolation of mitochondria. This principle is further modified by post-nanoparticle labelling-based fractionation. Here, organelle-specific antibody conjugated nanoparticles are used to target fractionated subcellular compartment. Such methods improve the yield, purity, and rate of fractionation. Selection of nanoparticles and its designing is based on the cells and cell organelles that are to be isolated.

V. **Embryology** (Remião et al. 2018)
Infertility and subfertility, defined as difficulty to conceive, is a condition that has affected people worldwide. The most revolutionary treatment in this area is assisted reproductive technology (ART) comprising of in vitro embryo production. Nanotechnology can be very useful in the development of non-invasive detection, diagnosis, and minimally invasive treatment of infertility-related disorders. Besides, it also prevents multiple fertilisation which has been a major challenge in current therapy. Also, the use of biosensors mentioned above helps to diagnose faster and more accurately. Gold, silver, carbon, and magnetic nanomaterials are the main materials used to develop new methods of genetic diagnostics. This may help for identification of disease that can develop in future.

VI. **Biological Engineering** (Kundu et al. 2014)
Biomaterials of either natural or synthetic origin are used to fabricate implantable devices, which are carriers for bioactive molecules or substrates to play an important role in tissue regeneration. These bioengineered species show better biocompatibility, flexible mechanical properties and strength, easy scalability, non-toxic products and by-products, etc. Such engineered products are also used as film coating materials on implants that extends its life and prevents wear and tear. Due to their advantageous properties, they may actually be used to develop artificial organs in future.

VII. **Medical Devices** (Harris and Graffagnini 2006)
Nanomaterials are under investigation for modern medical devices. These devices will act as multipurpose devices that will ensure diagnostics along with its routine purposes. Implantable devices such as stents and catheters will be part of these

nanotech-enabled medical devices with an aim to provide convenient real-time diagnosis of disease. Such diagnosis can be done at a clinic rather than at a laboratory. Besides, such implantable devices will cause less irritation and have more improved functionality.

1. **Medical devices in diagnostics**: In the coming years, nanotechnology will enable a shift to preventive medicine and the use of "point of care" diagnostics to quickly identify diseases. Portable diagnostic kits will become available to test whether individuals are genetically predisposed to a specific disease or have the earliest indications of a disease. Nanosphere, Nanomix and Alpha Szensors are a step closer towards such diagnostics. A large number of universities are promoting development of such sensitive sensors for rapid detection of diseases.
2. **Implantable medical devices:** Medical devices such as catheters, stents, and orthopaedic implants are always in risk to get infected with bacteria and microorganisms. Such infections can be responsible for serious illness and may require removal or change of the infected devices. Besides, it requires surgery or other medical procedures that is time consuming and risks patient's life. More than half of all nosocomial infections are caused by implanted medical devices. AcryMed uses silver nanoparticles that prevent formation and accumulation of bacteria. Such bacteria-protecting biofilms on the surface of medical devices are always advantageous.
   Similarly, bone surgeries, such as hip or joint replacements, often use titanium implants. It is quite common that muscle tissue fails to adhere to smooth surface of titanium, which leads to a lack of comfort over a period of time. Altair Nanotechnologies and National Research Council of Canada are working together to develop coating for orthopaedic implants. For this, Altair's nanoscale titanium dioxide is being used as a core material. Coating exhibits improved mechanical properties such as hardness and bond strength when compared with existing implant coatings such as hydroxyapatite. Additionally, these coating shows higher biocompatibility with bone cells that could result in longer lifetime of the implant. Also, Altair is looking forward to sell zirconium oxide nanoparticles for dental applications that can be used as fillings and in prosthetic devices.
   A problem associated with cardiac stents is that they are prone to clog again with fat after they have been implanted. Using stents that can elute drug stored in them in the form of nanoparticles entrapped in polymer is another attempt to solve this problem. Also, nanostructured materials offer opportunities to enhance the surface areas of medical devices to address these problems. Nanotech Catheter Solutions develop catheters and stents using carbon nanotubes ('CNTs'). Matrix of nanotubes might be used to replace polymer-coated stents that provide a non-biodegradable mechanism for slow-continuous release of a drug.
   Nanoparticle-based bioactive coatings are expected to improve mechanical and osteoconductive properties for both dental and orthopaedic implant applications (Saji et al. 2010)

VIII. **Cytogenetics** (Ioannou and Griffin 2010)
Cytogenetics, a branch of genetics, is a study of how chromosomes relate to cell and cell behaviour, particularly during mitosis and meiosis. The recognition of specific chromosomal patterns has widespread applications, and it helps to understand the fundamentals of cell and cell

cycle. Development of cytogenetics in the molecular era has begun after development of FISH *(fluorescent* in situ *hybridisation)*. FISH is a technique that allows to identify direct DNA sequences which are present on chromosomes, and gene mapping is based on this principle. It further facilitates chromosome painting (helps to differentiate chromosomes), advanced diagnostics (identification of chromosomes responsible for disease and disorder), and comparative genomics (for comparison across different species and variation related to them). However, FISH techniques have poor resolution due to use of organic fluorophores. This leads to overlapping of spectra, photo bleaching, etc. These problems have been solved to certain extent using quantum dots. Quantum dots (QDs) are novel inorganic fluorochromes which are nanocrystals made from semiconductor material. They are resistant to photo-bleaching and have narrow excitation and emission wavelengths that can be controlled by particle size. In short, they have the potential for improvising the sensitivity of experiments and are ideal material for FISH analysis and molecular cytogenetics (Ioannou and Griffin 2010).

IX. **Gene Therapy** (Herranz et al. 2012):
Gene theranostics, a newer field that is an amalgamation of nanoparticles, gene therapy, and medical imaging, uses a nanobioconjugate for diagnosis and treatment. The process involves binding of a vector carrying genetic information with a nanoparticle. This nanoparticle provides the signal for imaging. The synthesis of this probe improves the efficiency and quality of gene transduction and imaging contrast. The application of such techniques in biomedicine leads to newer concepts in nanomedicine and theranostics, which can combine diagnosis and therapy in a single probe. Magnetic resonance imaging (MRI) is one of the most sophisticated tools for diagnosis and monitoring of many diseases, which provides excellent anatomical resolution, and multiple physical methods are available to obtain contrast. In addition, the use of molecular probes can improve its sensitivity multiple folds for identifying the genes.
Besides, the success of gene therapy depends on the transgenes to be expressed and the delivery vectors used. Successful gene therapy depends on two important aspects.

(a) Efficient and safe delivery of genes at targeted cells.
(b) Effective monitoring of modified cells or modifying agents by non-invasive imaging techniques. This will allow tracking of gene delivery and gene expression.

The ability of a vector to cross numerous barriers and reaching the targeted site can be improvised by using magnetic nanoparticles and their properties. Besides, bioconjugates of iron and gold have been successfully prepared and utilised in various phases of gene therapy.

X. **Nanobioinformatics** (Maojo and Fritts 2012)**:**
Nanobioinformatics can be defined as application of nanotechnology in modern medicine and computers simultaneously, with an intention to gather information and improvise the overall healthcare system. Various areas where significant research in informatics is applied to nanomedicine that are already underway includes:

- Nanoparticle characterisation
- Modeling and simulation
- Imaging
- Terminologies, ontologies, and standards
- Data integration and exchange
- Systems' interoperability
- Data and text mining for nanomedical research
- Linking nano-information to computerised medical records
- Basic and translational research
- Networks of international researchers, projects, and labs
- Nanoinformatics education
- Ethical issues

In this new context (biomedical or nanomedical), nanoinformatics refers to the use of informatics techniques for analysing and processing information about the structure and physico-chemical characteristics of nanoparticles and nanomaterials, their interaction with their environments, and their applications for nanomedicine.

XI. **Neuroscience** (Silva 2006)
Neuroscience is one of the most complicated fields in biomedical, which is not completely understood yet. However, neuroscience can be simply defined as study that correlates to neurons. The challenges associated with nanotechnology applications in neuroscience are numerous, but the impact it can have on understanding how the nervous system works, how it fails in disease, and how we can intervene at a molecular level is significant. The ability to exploit drugs, small molecules, neurotransmitters, and neural developmental factors offers the potential to tailor technologies to particular applications that may help to treat various CNS disorders. A significant challenge in in vivo applications of nanotechnology is that they are designed to physically interact with neural cells at cellular and subcellular levels, but ultimately aim at engaging functional interactions at a systemic level, which usually involves large groups of interacting neurons and glia. Although technically and conceptually challenging, these types of applications could have a significant impact on clinical neuroscience.

XII. **Microbiology, Virology, and Immunology** (Allahverdiyev and Rafailovich 2011)
The worldwide escalation of bacterial resistance to conventional medical antibiotics is a serious concern for modern medicine. High prevalence of multidrug-resistant bacteria among bacteria-based infections decreases effectiveness of current treatments and causes thousands of deaths. New improvements in present methods and novel strategies are urgently needed to cope with this problem. Owing to their antibacterial activities, metallic nanoparticles represent an effective solution for overcoming bacterial resistance. However, metallic nanoparticles are toxic, which causes restrictions in their use. Recent studies have shown that combining nanoparticles with antibiotics not only reduces the toxicity of both agents towards human cells by decreasing the requirement for high dosages but also enhances their bactericidal properties. Combining antibiotics with nanoparticles also restores their ability to destroy bacteria that have acquired resistance to them. Furthermore, nanoparticles tagged with antibiotics have been shown to increase the concentration of antibiotics at the site of bacterium–antibiotic interaction and to facilitate binding of antibiotics to bacteria. Likewise, combining nanoparticles with antimicrobial peptides and essential oils generates genuine synergy against bacterial resistance.

So, nanotechnology can be a key to avoid growth of resistant microbes and play a major role in immunisation and designing of therapeutic guidelines.

XIII. **Water Treatment** (Amin et al. 2014)**:**
The supply of freshwater is limited all across the globe. It is essential to manage the freshwater, which accounts only 0.5% of total water available across the globe. Also, it is essential to save this freshwater from wasting to ensure a healthy life. Freshwater can be saved by two major ways:

1. Increasing the availability of freshwater
2. Preventing mixture of waste water in this available freshwater

Various methods that involve nanoparticles to attain this are as follows:

1. **Disinfection:** Biological contaminants can be classified into three categories, namely, microorganisms, natural organic matter (NOM), and biological toxins. Contamination from bacteria, protozoans, and viruses is possible in both groundwater and surface water. The toxicity of the standard chlorine chemical disinfection in addition to the carcinogenic and very harmful by-products formation. There are many different types of nanomaterials such as Ag, titanium, and zinc capable of disinfecting waterborne disease-causing microbes. Due to their charge capacity, they possess antibacterial properties. Silver nanoparticles are derived from its salts like silver nitrate and silver chloride, and their effectiveness as biocides is documented in the literature. TiO_2 nanoparticles are among the emerging and most promising photocatalysts for water purification. CNTs (one of nanosorbents) which have been used for removal of biological impurities have received special attention for their excellent capabilities of removing biological contaminants from water. Filtration membranes containing radially aligned CNTs are very effective in removing both bacteria and viruses in very short time due to size exclusion and depth filtration and thus enable such filters to be used as cost-effective and point-of-use water disinfection devices.
2. **Desalination:** Desalination is considered an important alternative for obtaining freshwater source. Nanomaterials are very useful in developing more efficient and cheaper nanostructured and reactive membranes for water/wastewater treatment and desalination such as CNT filters. Nanomaterials offer opportunities to control the cost of desalination and increase its energy efficiency, and among these are CNTs, zeolites, and graphene which are the most effective.

Besides, nanoparticles are also useful in controlling waste management, which includes:

- Infectious waste
- Pathological waste
- Pharmaceutical waste
- Genotoxic waste
- Heavy metals and genotoxic waste

XIV. **Pathology and Toxicology**
Because of increased use of nanotechnology, the risk associated with exposure to nanoparticles, the routes of entry, and the molecular mechanisms of any cytotoxicity need to be well understood. In fact, these tiny particles are able to enter the body through the skin, lungs, or intestinal tract, depositing in several organs and may cause adverse biological reactions by modifying the physiochemical properties of living matter at the nano level. In addition, the toxicity of nanoparticles will also depend

Table 2.1 Nanoparticles in medical developments

Tests using nanoparticles	Used for
Nanosized exosomes	Diagnosis of pancreatic cancer
Nanopore sensors	Identification of viruses
Nanoflares	Diagnosis of cancer cells
Nanowire-based sensor	Diagnosis of prostate cancer
Magnetic nanoparticles	Diagnosis and tumour targeting
Carbon nanotube	Protein indicative oral cancer
Gold nanoparticles	Flu virus
Quantum dots	Diagnosis of cancer cells
Silver nanorods	Separation of viruses and bacteria

on whether they are persistent or cleared from the different organs of entry and whether the host can raise an effective response to sequester or dispose of the particle. Hence, it seems reasonable to evaluate the risk/benefits ratio for the use of nanoparticles in any technological or medical developments Table 2.1.

XV. **Cosmetics** (Prajapati 2011)
Nanoparticles have been identified as a potential next generation cosmetic delivery agent that can provide enhanced skin hydration, bioavailability, stability of the agent, and controlled occlusion. Presence of nanoparticles in cosmetic industry is observed in a wide range of products that includes sunscreens, breast cream, hair care, make-up, moisturising creams, anti-wrinkle cream, toothpaste, face wash and face masks, deodorants and perfumes, lipsticks, blush, eye shadow, nail polish, foundations, after-shave lotions, etc.

2 Conclusion

The current review is a general overview on application of nanoparticles in biomedical and healthcare. Nanoparticles are minute particles that produce a major change in the healthcare and biomedical industry. It is not restricted to any field and its presence is observed in every field of biomedicine from diagnosis to treatment to implants to cosmetics. Besides, it also includes daily needs such as water treatments, pollution control, and waste management. Nanoparticles and fields associated with it are growing at an exponential rate, and this may continue based on its advantages and numerous applications.

Research in the field of nanoparticles promises some great results and its impact will be observed in the years to come. The future of healthcare will be based on the fact of identification of disease in the very early stage and therapies will be more patient compliant. Nanoparticles will provide flexible, modern, and more suitable therapies with minimal adverse effects and maximum therapeutic effects. It will not be restricted to healthcare and will also focus on improvising the overall standard of living. It offers space for cleaner, greener, and safer planet.

The enhanced hardness and strength of nanomaterials in comparison with their coarser counterparts is attractive in making high wear resistance implants. Nanoceramic coatings are attractive in terms of enhancement of mechanical properties (hardness, toughness, friction coefficient, etc.) Carbon nanotubes and nanofibers have been investigated as reinforcement material. The versatility of these fibres suggests that there are a large number of possibilities for future designs that could enhance the efficiency of medical implants.

To sum up, nanoparticles over a much wider space to cover and current knowledge just seems to be the tip of the iceberg. As newer research projects will carry forward, more groundbreaking outcomes can be expected.

References

Allahverdiyev A, Rafailovich M. Coping with antibiotic resistance: combining nanoparticles with antibiotics and other antimicrobial agents. Expert Rev Anti-Infect Ther. 2011;9(11):1035–52.

Amin MT, Alazba AA, Manzoor U. A review of removal of pollutants from water/wastewater using different types of nanomaterials. Adv Mater Sci Eng. 2014;2014:1–25.

Bonelmekki M. An introduction to nanoparticles and nanotechnology. IOP Concise Phys. 2017;2017:1–14.

Chan JM, Zhang L, Yuet KP, Liao G, Rhee J, Langer R, et al. PLGA – Lecithin – PEG Core – shell nanopar-

ticles for controlled drug delivery. Biomaterials. 2009;30(8):1627–34.
El Ansary A, Faddah LM. Nanoparticles as biochemical sensors. Nanotechnol Sci Appl. 2010;3:65–76.
Engel G. The need for a new medical model : a challenge for biomedicine. Sci New Ser. 1977;196(4286):129–36.
Fakruddin M, Hossain Z, Afroz H. Prospects and applications of nanobiotechnology : a medical perspective. J Nanobiotechnol. 2012;10(31):1–8.
Harris DL, Graffagnini MJ. Nanomaterials in medical devices: a snapshot of markets, technologies and companies. Nanotechnol Law Bus. 2006;2007(255):415–22.
Herranz F, Almarza E, Rodríguez I. The application of nanoparticles in gene therapy and magnetic resonance imaging. Natl Inst Health. 2012;74(7):577–91.
Ioannou D, Griffin DK. Nanotechnology and molecular cytogenetics: the future has not yet arrived. Nano Rev. 2010;1(5117):1–14.
Kundu B, Kurland NE, Bano S, Patra C, Engel FB, Yadavalli VK, et al. Silk Proteins for Biomedical Applications : Bioengineering Perspectives. Prog Polym Sci. 2014;39(2):251–67.
Maojo V, Fritts M. Nanoinformatics: developing new computing applications for nanomedicine. Comput Sci Eng. 2012;94(6):521–39.
Prajapati P. Overview on applications of nanoparticles in cosmetics. Asian J Pharm Sci Res. 2011;1(2):40–55.
Quirke V, Gaudillière JP. The era of biomedicine: science, medicine, and public health in Britain and France after the Second World War. Med Hist. 2008;52(4):441–52.
Remião MH, Segatto NV, Pohlmann A, Guterres SS, Seixas FK, Collares T. The potential of nanotechnology in medically assisted reproduction. Perspective. 2018;8:1–9.
Rico CM. Chemistry, biochemistry of nanoparticles, and their role in antioxidant defense system in plants. In: Nanotechnology and plant sciences. Cham: Springer; 2015. p. 1–17.
Saji VS, Choe HC, Yeung KWK. Nanotechnology in biomedical applications : a review. Int J Nano Biomater. 2010;3(2):119–39.
Silva GA. Neuroscience nanotechnology: progress, opportunities and challenges. Nat Rev. 2006;7(1):65–74.
Sun S. Recent advances in chemical synthesis, self-assembly, and applications of FePt nanoparticles. Adv Mater. 2006;18:393–403.
Thimiri Govinda Raj DB, Khan NA. Designer nanoparticle : nanobiotechnology tool for cell biology. Nano Converg. 2016;3(22):1–12.
Wade DT, Halligan PW. Do biomedical models of illness make for good healthcare systems? Br Med J. 2004;329(7479):1398–401.
Wang EC, Wang A. Nanoparticles and their applications in cell and molecular biology. Integr Biol. 2004;6(1):9–26.
Wu C, Yang Y, Hsu Y, Wu T. Nanoparticle-induced intraperitoneal hyperthermia and targeted photoablation in treating ovarian cancer. Oncotarget. 2015;6(29):26861–75.

Part II

Polymeric Nanoparticles

3 Nanocrystallization and Nanoprecipitation Technologies

Vivek P. Patel, Dhara V. Patel, and Jayvadan K. Patel

Abstract

In the last few years, nanoparticles and their applications have dramatically diverted science in the direction of a brand new philosophy. Nanoparticles are building the bridge of scientific knowledge connecting bulk materials to atomic or molecular structures. In the present scenario, nanoparticle research is a very promising branch of scientific research owing to the wide range of potential and promising applications especially in biomedical, optical and electronic fields.

In the current pharmaceutical development pipeline, the poor water solubility of drug candidates remains the biggest challenge. Various processes have been developed to increase the solubility, dissolution velocity and bioavailability of these active ingredients belonging to the biopharmaceutical classification system (BCS) II and IV classifications. Nanocrystal delivery is an emerging technique for overcoming the limitations of drugs that dissolve poorly in water. Nanocrystals are produced in the form of nanosuspensions using top-down (e.g., wet milling) and bottom-up methods (e.g., antisolvent precipitation) in FDA-approved drug products. An ultra cryo-milling technique using liquid nitrogen and dry ice beads has been used as a novel contamination-free process. In the case of the antisolvent precipitation technique, ultrasound and rapid mixing devices have been used as new process intensification techniques. Technological advancements in milling as well as ant solvent precipitation now enable the production of drug nanoparticles on a commercial scale with relative ease.

This chapter provides an updated review of nanocrystal techniques along with marketed product evaluations and a survey of the commercially relevant scientific literature.

Keywords

Nanoparticles · Nanocrystallization · Nanomilling · Antisolvent precipitation

V. P. Patel (✉)
Sun Pharmaceutical Industries Ltd,
Vadodara, Gujarat, India
e-mail: vivek.patel@sunpharma.com

D. V. Patel
Pioneer Pharmacy Degree College,
Vadodara, Gujarat, India

J. K. Patel
Nootan Pharmacy College,
Sankalchand Patel University,
Visnagar, Gujarat, India

J. K. Patel, Y. V. Pathak (eds.), *Emerging Technologies for Nanoparticle Manufacturing*,
https://doi.org/10.1007/978-3-030-50703-9_3

1 Introduction

Nanotechnology is a recent hot topic because of its potential to have an appreciable impact on a number of fields related to biology, chemistry, engineering, as well as medicine.

In the current scenario, approximately 90% of new drug candidates in the development pipeline can have a poor solubility problem that leads to poor dissolution velocity and ultimately variable bioavailability. These new drug candidates belong to biopharmaceutical classification systems (BCS) class II (70%) and class IV (20%). Over the last 10 years, progress in high-throughput screening methods has led to an even higher number of newly discovered drug candidates that have poor water solubility problems (Gigliobianco et al. 2018; Junghanns and Müller 2008; Loftsson and Brewster 2010; Müller and Keck 2012). Given the higher number of poorly bioavailable drug candidates and their non-specific distribution throughout the body may lead to different side effects and may further limit their clinical applications. To overcome the bioavailability issue of drug candidates, appropriate innovative formulation technologies according to the route of administration, e.g., oral and non-oral, need to be adopted (Trapani et al. 2012; Lu et al. 2016a; Keck and Müller 2006).

In the previous era, micronization was used to reduce the particle size and led to an increase in the dissolution velocity of poorly soluble drug candidates. But still, micronization cannot fulfill the needs and satisfy the pharmaceutical requirements to improve the dissolution velocity as well as the bioavailability of drug candidates. The demand for these pharmaceuticals makes the changeover to nanonization. Different and unique innovative nanonization approaches that have emerged to reduce the particle size and improve the dissolution velocity tend to increase the bioavailability of poorly soluble drug candidates for target therapy. These unique innovative technological approaches help to overcome the physicochemical characteristics, including stability issues, that are associated with nanostructures (Jermain et al. 2018).

In this chapter, emerging manufacturing techniques for drug nanoparticles are briefly introduced, followed by a detailed review of the progress of targeted drug delivery. A short introduction with recent advancements in conventional technologies for nanoparticle manufacturing is also included.

2 Definition

The classical definition of "nanocrystals" is crystals with a nanometer size range, typically between a few nanometers and a thousand nanometers and is crystalline in nature. Another characteristic is that they are made up of 100% drug crystals or with a minimal amount of surface stabilizing agents such as surfactant or polymeric carrier stabilizers. Drug nanocrystals, when suspended in dispersion media, are called "nanosuspension." Dispersion media can be either aqueous (e.g., water-based dispersion system) or non-aqueous (e.g., different vegetable oils, polyethylene glycol, polypropylene glycol, and solvents). As per the biopharmaceutical classification systems (BCS), class II drugs are the most prominent candidates for drug nanocrystals, but in some cases class IV drugs may have even more benefits when particle size is decreased.

Nowadays, nanosuspension formulations are used to increase the dissolution velocity and saturation solubility of drug candidates belonging to BCS classes II and IV. Because of the nano-range particles with increased specific surface area, nanosuspensions have unique biological effects. Based on the above-mentioned physicochemical and biological beneficial effects, the US FDA has approved several nanosuspension medications and these are currently marketed well. Owing to the factual information given above, we can say that nanosuspensions are a mature drug delivery system.

"Nanoparticles" are drug-embedded particles in a nanometer size range, but mainly include polymers or lipids, such as polymeric nanoparticles, liposomes, and solid lipid nanoparticles. Nanoparticles can be in either a crystalline or an amorphous physical state, which depends on the

nanoparticle formation technologies. In precipitation techniques, the nanoparticles are generally obtained in an amorphous physical state. Thus, eventually, amorphous drug nanoparticles should not be referred to as nanocrystals (Liu et al. 2012; Peltonen and Hirvonen 2018; Borchard 2015; Gao et al. 2012; Kesisoglou et al. 2007; Liu et al. 2011). Amorphous drug nanoparticles have certain advantages, e.g., it has higher saturation solubility than equally sized nanocrystals. Furthermore, a unique combination of nanometer size range as well as amorphous state is considered ideal for drug candidates to reach the highest saturation solubility. However, to utilize the concept in the pharmaceutical field, it should be equally as important to maintain the amorphous state throughout the shelf-life of product (Hancock and Parks 2000; Gu and Grant 2001).

3 Prominent Attributes

3.1 Surface Area Enlargement

The main idea of nanotechnology is the ratio of surface area to volume. Surface area is increased, whereas the volume remains the same. Moreover, it can be explained as follows: an increase in the particle surface area leads to an increased possibility of having a reaction (with atmosphere or gases or liquid/dissolution solvents around the nanoparticles, etc.). Size reduction via micronization to nanonization (Fig. 3.1) leads to a drastic increase in the surface area and thus the possibility of having a reaction with liquid/dissolution solvents is also increased drastically, or what we call increased dissolution velocity, according to the Noyes–Whitney equation (Eq. 3.1) (Noyes and Whitney 1897).

$$\frac{dC}{dt} = \frac{DS}{Vh}\left(Cs - Cx\right) \tag{3.1}$$

dC/dt, dissolution rate (concentration change as a function of time); *D*, diffusion coefficient; *S*, surface area; *V*, dissolution volume; *h*, diffusion layer thickness; *Cs*, saturation concentration; *C*, concentration at time *t*.

Thus, if considering a particle size reduction from 1 mm (typical particle size for conventional drugs) to 100 nm (typical particle size for drug nanocrystals), then the dissolution velocity is increased 100-fold.

This reflects the fact that the particle size has become an important factor for the determination of dissolution velocity. However, when the dissolution parameter tests are performed under specific dissolution sink conditions, the differences are difficult to identify in numbers between different nanocrystal size fractions; thus, it required a more discriminating dissolution test protocol (Liu et al. 2013).

Therefore, surface area enlargement is the correct way to improve the bioavailability of BCS class II and IV drug candidates where the solubility and dissolution velocity is the rate limiting step. It also seems in most the cases that low dissolution velocity correlates directly with low saturation solubility (Owais et al. 2019; Alshora et al. 2016).

3.2 Increase in Saturation Solubility

Ideally, saturation solubility of drug candidates is dependent on the specific dissolution sink conditions, which include dissolution medium, the concentration of the buffers, pH, and temperature. This is valid up to the micrometer range or above the size of the drug candidates. However, saturation solubility also depends on particle sizes of below approximately 1 μm. Saturation solubility increases with decreasing particle size below 1 μm. Also, according to the Noyes–Whitney equation the dissolution rate dC/dt is proportional to the concentration gradient (Cs − Cx)/h (Cs – saturation solubility, Cx – bulk concentration, h – diffusional distance) and therefore the dissolution velocity is further increased. At the same time, increased saturation solubility also increases the concentration gradient between the gut lumen and the blood, which leads to higher absorption by the passive diffusion mechanism (Fig. 3.2).

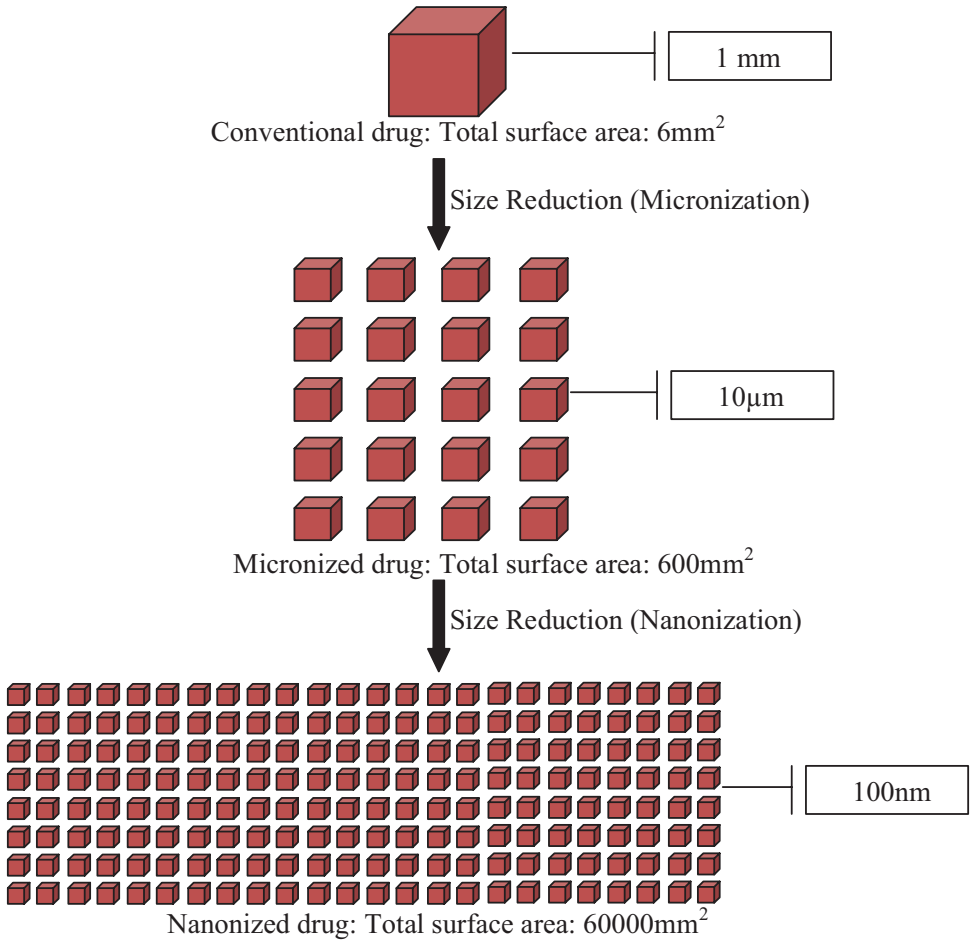

Fig. 3.1 Surface enlargement factor and increase in the number of crystals by size reduction

Generally, the diffusion layer starts to get thinner for particle sizes below approximately 50 µm (Sheng et al. 2007), which furthermore become thinner for particle sizes in the nanometer range and hence enhances the dissolution velocity of nanoparticles compared with microparticles.

According to the Ostwald–Freundlich theory, for particle sizes below approximately 1 µm, the saturation concentration starts to increase. The increasing effect on saturation concentration is more pronounced once the particle size is below 100 nm. Drug saturation solubility is theoretically predicted by the Ostwald–Freundlich equation (Eq. 3.2):

$$S_{\mathrm{NP}} = S_0 \exp\left(\frac{2V_m\gamma}{RTr}\right) \tag{3.2}$$

Where S_{NP} is the solubility of nanoparticles with a radius r, S_0 is the solubility of bulk material, V_m is the molar volume, γ is the interfacial tension, R is the gas constant and T is the temperature.

In his dissertation of 1885, Robert von Helmholtz (son of the German physicist Hermann

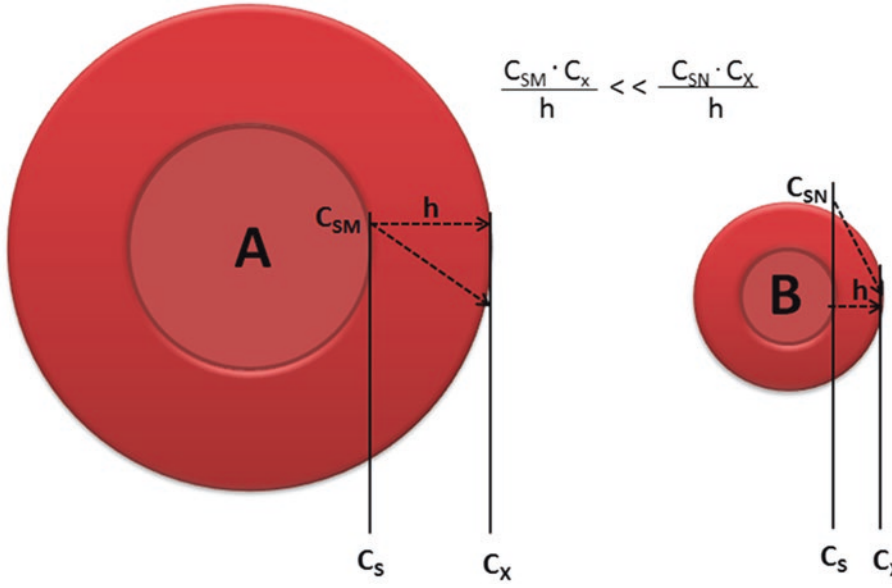

Fig. 3.2 Comparison of (**a**) a microcrystal and (**b**) a nanocrystal and their surface curvature and concentration gradient over the diffusional distance (h). C_s, drug-saturated water at surface (M, microcrystal; N, nanocrystal); C_x, bulk concentration at diffusional distance; h, diffusional distance. $dc/dt \sim (C_s - C_x)/h$

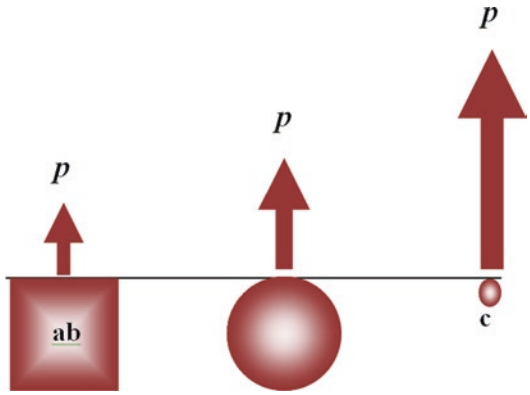

Fig. 3.3 Dissolution pressure (*p*) increased over (**a**) a flat surface, (**b**) a microparticle, and (**c**) a nanoparticle with a high surface curvature

von Helmholtz) achieved the Ostwald–Freundlich equation and explained that Kelvin's equation could be translated into the Ostwald–Freundlich equation (Helmholtz 1886). One aftermath is that small liquid droplets (i.e., particles with more surface curvature or nanoparticles) exhibit a more effective vapor pressure, because the surface is bigger in comparison with the volume. Now, consider that the vapor pressure is equivalent to the dissolution pressure for nanoparticles in liquid; there should be an equilibrium of molecules dissolving and molecules recrystallizing in the state of saturation solubility. This equilibrium can be moved if the dissolution pressure increases, and hence the saturation solubility increases (Fig. 3.3).

The advantageous effect of nanoparticles, the increased dissolution velocity, and the increased saturation concentration all lead to a supersaturated state and ultimately this increases the drug absorption as well as permeation (Brouwers et al. 2007, 2009; Mellaerts et al. 2008).

The biggest challenge faced by scientists during development is to maintain the supersaturated state in vivo until absorption and permeation have taken place, because there is the highest probability of interference via uncontrolled precipitation or crystallization (Peltonen and Hirvonen 2018).

3.3 Crystalline or Amorphous Particle States

Based on the drug delivery applications of drug candidates, crystalline or amorphous particle states are anticipated to prevent or enhance the solubility, dissolution velocity, and pharmacokinetic profile.

The combination of nanometer size and amorphous state of drug candidate is ideal for higher saturation solubility compared with equally sized nanocrystals, but at the same time it is required to be maintained throughout the shelf-life of the product.

Concurrently, the importance of crystalline nanoparticles to the pharmaceutical field can be evaluated by the fact that more than 20 formulations are already on the market and approximately 15–20 are at different stages of clinical trials (Kumar and Burgess 2012).

To calculate the optimal nanosize and crystalline/amorphous state of the drug candidate, keep in mind the following parameters:

- Different administration route (oral, intravenous, intramuscular, pulmonary, ocular, dermal, etc.) (Chen et al. 2014; Fu et al. 2013; Ige et al. 2013; Mauludin et al. 2009; Colombo et al. 2017; Zhai et al. 2014; Vidlářová et al. 2016; Mitri et al. 2011; Muller and Keck 2004; Ganta et al. 2009; Patravale et al. 2004; Shegokar and Singh 2011; Gao et al. 2016; Khan et al. 2013; Liu et al. 2010a, 2018; Yang et al. 2010; Zhao et al. 2011).
- Different pharmaceutical dosage forms (tablets, capsules, suspensions, ointments, etc.) (Baba et al. 2007; Liversidge and Cundy 1995; Merisko-Liversidge et al. 1996; Moschwitzer and Muller 2006; Yang et al. 2017).
- Preservation of physical and chemical stability (Hancock and Parks 2000; Merisko-Liversidge and Liversidge 2011; Trasi and Byrn 2012; Lee 2003; Van Eerdenbrugh et al. 2008).
  - Different lattice arrangements such as short-, long-range order (Kreuter et al. 1995).
  - Glass transition temperature (Tg), X-ray diffraction, birefringence characteristic, melting event, etc.
  - Presence of stabilizers such as polymers, surfactants, and sugars.
- Commanded pharmacokinetics profile.
  - Long circulating and favorable biological properties (Wang et al. 2018; Sharma et al. 2016; Lu et al. 2016b).
  - Potential for passive and active targeting (Huang et al. 2010; Pawar et al. 2014).

4 Production Technologies

Previously, physical and chemical methods were only used to produce nanoparticles. Some of the commonly used physical and chemical methods are solvothermal synthesis, reduction, ion sputtering, and sol gel technique. Basically, there are two main approaches to nanoparticle synthesis; namely, bottom-up approaches and top-down approaches.

Top-down approaches involve the reduction of large particles to the nanometer size range, for example, by milling, whereas bottom-up methods generate nanoparticles by fabricating them from drug molecules in solution, such as by precipitation (Fig. 3.4). Some approaches defined as combined technologies involve the application of two technologies in succession.

Top-down techniques, particularly media milling and high-pressure homogenization, have

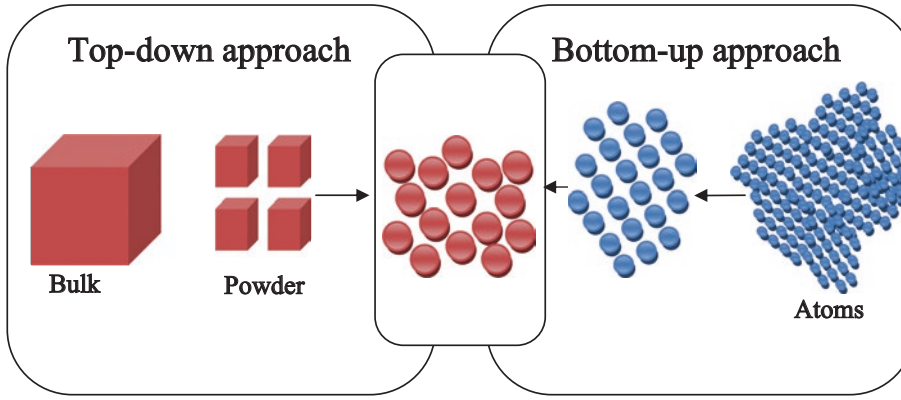

Fig. 3.4 Top-down and bottom-up approaches of nanofabrication

become increasingly recognized by the pharmaceutical industry because it was easy to scale up to a commercial level. Top-down processes are universal techniques for preparing crystalline nanoparticles and have also been accepted by the regulatory authorities (Rabinow 2004).

Bottom-up technologies (i.e., starting from a dissolved molecule, precipitation) were difficult to control the process during scale up. One of the reasons was to remove the solvents and to control the process. The reality was that many poorly soluble drugs were poorly soluble not only in aqueous media but also in organic solvent media (Rawat 2015; Muller et al. 2001).

5 Nanocrystallization and Nanoprecipitation Technologies

Research and development (R&D) and the pharmaceutical industry have to focus their efforts on optimizing scalable processes and formulations, and allow for an appropriate physicochemical and biological stability during the shelf life of the drug product.

6 Media Milling

A milling/grinding chamber, milling media, milling shaft, motor, screen, recirculating chamber, and coolant are the major components of the wet media milling process (Fig. 3.5). The milling chamber can be constructed in a horizontal or a vertical position. In the process, the milling chamber is filled to 70–90% with milling beads sized 0.03–30 mm. The milling beads are made of different materials as needed, such as yttrium-stabilized zirconium oxide, stainless steel, glass alumina, titanium, or certain polymers, such as highly cross-linked polystyrene and methacrylate. Milling/grinding beads are generally available in spherical and cylindrical forms. The milling chamber is filled with slurry containing the drug, water, stabilizers, and surfactants agitated by the motor. The slurry occupies approximately 3–30% (w/v) volume of the milling chamber. The activation of the milling beads occurs by use of an agitator shaft with pegs, disks or smooth-shaped agitating elements. The milling media roll over inside the milling chamber during agitation, generating high energy forces by shearing and impacting large drug crystals to

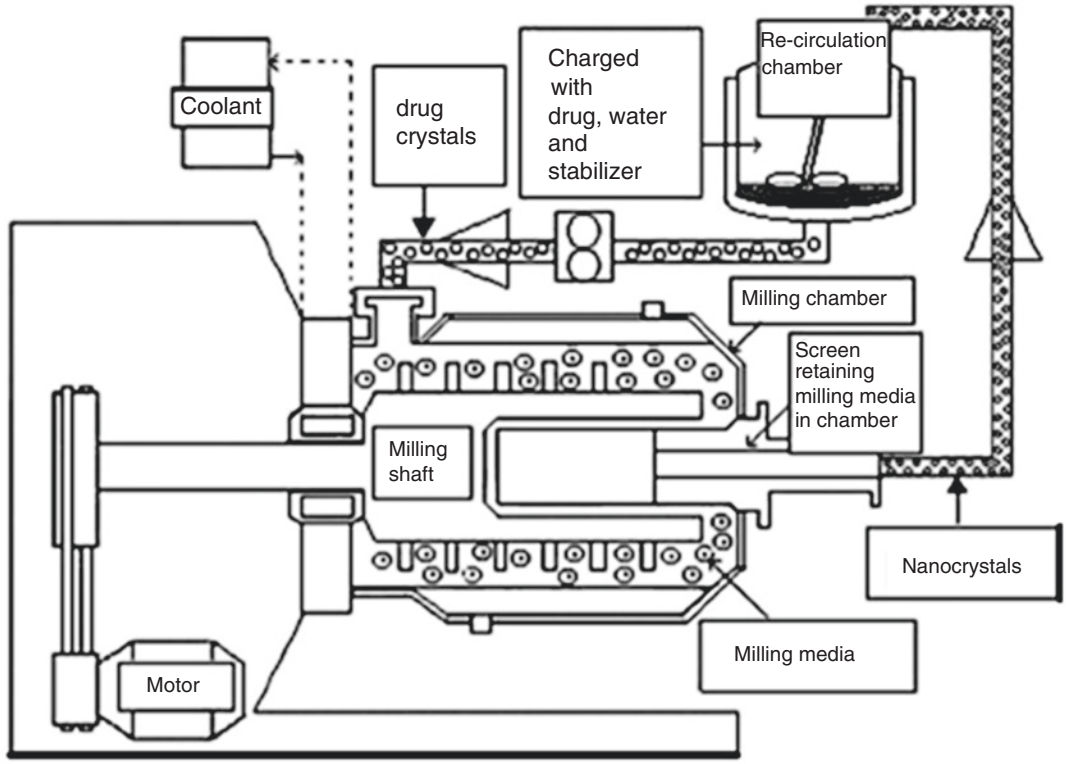

Fig. 3.5 Schematic diagram describing the continuous wet bead milling process with a single chamber

reduce the particle size. Separation of the milling media from the product is done with the help of a screen at the outlet by separation (Yadav et al. 2012; Malamatari et al. 2018; Stenger and Peukert 2003; Kwade 1999). The milling operation can be performed, depending on the production scale and other formulation requirements, either in batch mode (discontinuous mode-single pass processing through one or more mills) (Fig. 3.6) or in recirculation mode (continuous mode-circulation processing with a single vessel). Recirculation is advantageous for reducing costs and milling time.

6.1 Mechanism Involved

- Real comminution: the primary particles are ground during a liquid phase by high shearing, pressure, and impact forces.
- De-agglomeration and dispersing: agglomerates are dispersed by high shearing, pressure, and impact forces. The surface air is removed and the surface of the particle is easily wetted (Fig. 3.7).

The fracturing of a particle can occur when the force exceeds the elastic limit of the particles. Different theories of size reduction are involved (Table 3.1).

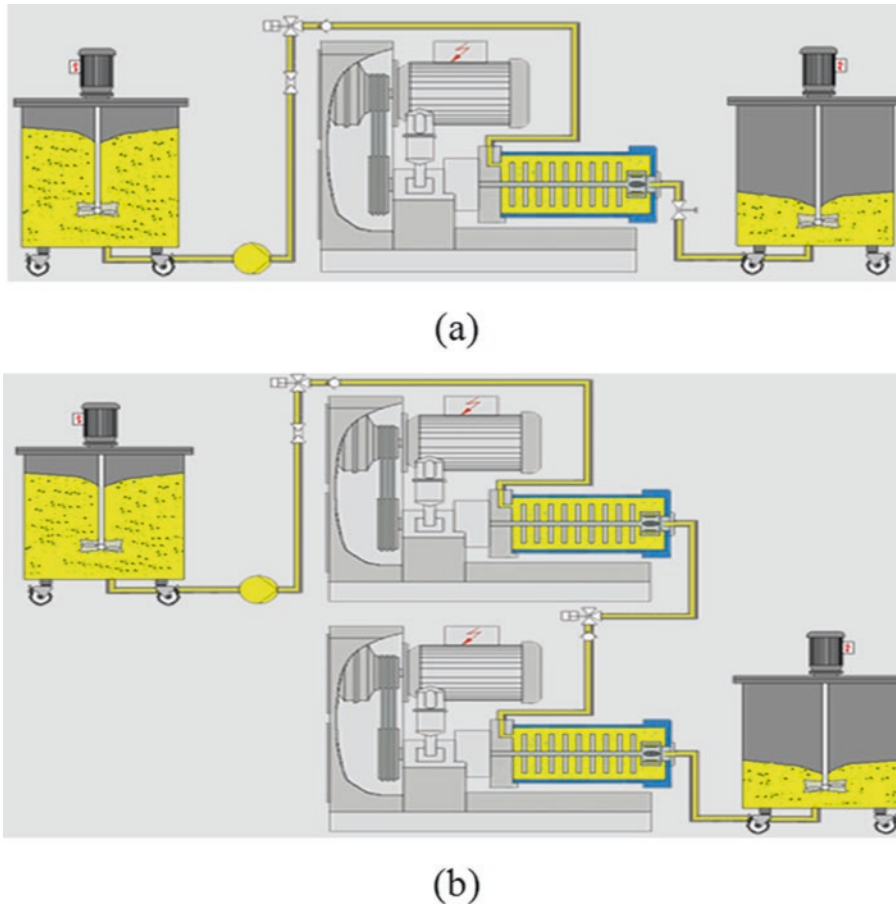

Fig. 3.6 Batch wet bead milling process with (**a**) one or (**b**) more milling chambers

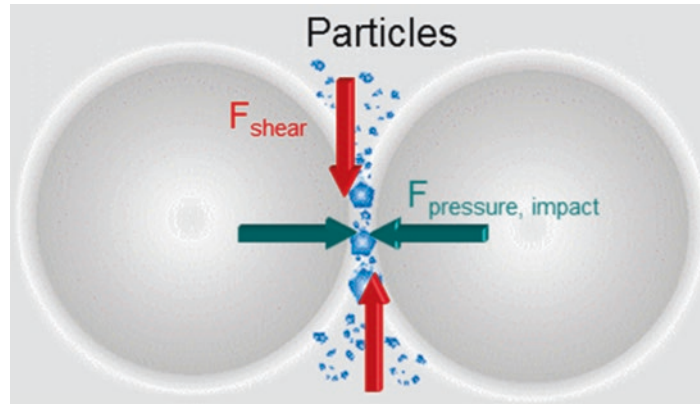

Fig. 3.7 Mechanism involved in the bead milling process

Table 3.1 Different theories of size reduction

Theory	Principle
Griffith theory	The amount of force to be applied, which depends on the length of the crack and the focus of stress at the atomic bond of the apex of the crack
Kick's law	Work required to reduce the size of a given quantity of material is constant for the same reduction ratio regardless of the original size
Rittinger's law	Work useful to reduce particle size is directly proportional to the new particle surface area produced
Bond's law	Work useful to reduce particle size is proportional to the square root of the diameter of the particle produced

6.2 Selection of Bead Size

The bead diameter is limited by its relationship to the particles. The particles should be smaller than the void volume between the grinding beads. Generally, the selection of bead size depends on the following practical rules, which can form the basis of reference points:

- Diameter of the grinding media should be approximately 20–50 times larger than the d_{99} of the particle.
- 1/1,000 diameter value of the selected grinding media is the d_{50} of the final particle size.

Selection of the grinding media depends on the grinding characteristics of the particles, which have to be considered (such as hardness, grain shape, agglomerate/primary grain) to determine the best bead size. Different types of grinding media are available on the market (Table 3.2). Selection of the media type is done based on the criticality of milling process and the formulation requirements. The design of the bead separation system must be suitable for the size of the beads and the feed material size. The screen opening should be from one-third to one-half the diameter of the beads. Thus, overall, the bead milling process depends on the different parameters such as formulation, percentage solids, additives, vehicle, viscosity, mixer speed, flow rate, inlet pressure, outlet temperature, shaft speed, screen size, cooling water temperature and flow, motor power, bead density, bead size, and bead filling.

Currently, pharmaceutical milling machines are designed and built in accordance with the cGMP (Current Good Manufacturing Practices of the Food and Drug Administration), GAMP (Good Automated Manufacturing Practices), GAMP5, ASME BPE (Bioprocessing Equipment Standard of American Society of Mechanical Engineers). UL or CE Electrical components, 21 CFR Part 11 Compliance, FDA (Food and Drug Administration) guidelines or meeting the specifications of other regulatory bodies.

The major disadvantage of this technology includes high energy leading to stability concerns regarding the drugs, contamination from the milling media, and time consumption, as a long-term operation ranging from hours to days is generally required. The long-term operation is dependent on the properties of the drug, the milling media, and the extent of particle size reduction (Gao et al. 2008; Peltonen and Hirvonen 2010). To overcome the above constraints to a certain extent, coolant is circulated to reduce the thermogenic effect. For long-term operation, it is also recommended to use special Yttrium Stabilized Zirconia (YSZ) grinding beads, which have the following special features/advantages:

- Highly cost-effective, low wear, and a long lifetime: YSZ milling/grinding material is the most durable and efficient medium for ball milling of ceramic materials. It reduces operational costs because of its ultra-low wear.
- Relatively high mechanical strength, beads do not break owing to toughness and impact resistance performance.
- High specific gravity, high efficiency, which saves processing time.
- Very smooth and extremely well-polished, even easy to clean, low abrasion to the internal wall of equipment.
- Highly resistant to acids and solvents.
- Because it is virtually contamination free it is an ideal solution for a variety of applications that demand minimal contamination, including, but

Table 3.2 Different types of grinding media

Grinding media type	Density (kg/dm^3)	Minimum diameter d_{min} (mm)	Relative wear rate
Plastic	0.9–2.1	≥ 0.15	+
Glass	2.5	≥ 0.05	0
Quartz sand	2.65	≥ 0.1	−0
Ottawa sand	2.65	≥ 0.2	0 +
Al_2O_3 (99.7%)	3.2	≥ 0.4	0
Al_2O_3 (99.9%)	3.2	≥ 1.0	++
Zirconium silicate	3.7–3.8	≥ 0.2	0 +
Al_2O_3/ZrO_2	4.1	≥ 0.6	+
ZrO_2/Y_2O_3/zirconium silicate	4.6	≥ 0.2	+
ZrO_2/MgO – stabilized	5.5	≥ 0.4	–
ZrO_2/Y_2O_3 – stabilized	6	≥ 0.05	++
ZrO_2/CeO – stabilized	6.1–6.2	≥ 0.4	+
Steel shot	7	≥ 0.1	0
Steel	7.75	≥ 1.0	0 +
Quality increased →			
-- - 0 + ++			

not limited to, nanomaterials, pharmaceuticals, foods, chemicals, batteries, inks, toner, dielectrics, solar cells, semiconductors, aluminum nanoparticles, etc. (Rijesh et al. 2018).

The wet milling approaches of crystalline nanosuspensions in the pharmaceutical industry can also be judged by the fact that more than 20 formulations are already on the market and close to 15 are at different stages of clinical trials (Table 3.3). The modern and sterile wet milling process is a widely adopted processing technology by the pharmaceutical industry for developing different commercial products (Kumar and Burgess 2012; Gulsun et al. 2009; Moschwitzer 2013; Junyaprasert and Morakul 2015). Scaling up with a media mill is possible, but there is a certain limitation in media mill chamber size owing to its weight so that to produce a larger batch size the media mills can be configured in the circulation mode or more milling chambers can be attached. Typically, from a small laboratory scale to a larger production scale can be carried out with different sized chambers from 5 to 15 ml to a few liters, which are commercially available from the Nanomill® system (élan Drug Discovery, King of Prussia, PA, USA), Dynomill (Glen Mills, Clifton, NJ, USA), and Netzsch mills (Netzsch, Exton, PA, USA)).

6.3 Particle Surface Modification

Many orally administered nanosuspensions are modified on the surface using mucoadhesive polymers such as chitosan and carbomer, which can increase the adhesion to the gut wall. The residence time can be increased by improving the adhesiveness of nanocrystals to lumen in the gastrointestinal tract with the addition of mucoadhesive polymers (Thanki et al. 2013; Müller et al. 2001).

In other examples of ophthalmic nanosuspensions, polymers such as carbomer, hydroxypropyl methyl cellulose (HPMC), polyvinylpyrrolidone (PVP), and polyvinyl alcohol (PVA) were used as suspension agents (Bartos et al. 2018).

In many examples, the addition of stabilizers on the particle surface works as physical stabilizers and they may have additional properties such as modifying their bioavailability and pharmaco-

Table 3.3 Examples of FDA-approved nanocrystal products

Drug	Trade name	Dosage form	Manufacturer	Year
Dexamethasone; tobramycin	Tobradex	Ophthalmic suspension	Novartis	1988
Verapamil hydrochloride	Verelan PM®	Capsule	Schwarz Pharma	1998
Brinzolamide	Azopt®	Ophthalmic suspension	Novartis	1998
Dexmethylphenidate hydrochloride	Focalin XR®	Capsule	Novartis	2001
Sirolimus	Rapamune®	Tablet	Wyeth	2000
Tizanidine hydrochloride	Zanaflex®	Capsule	Acorda	2002
Morphine sulfate	Avinza®	Capsule	King Pharma	2002
Methylphenidate hydrochloride	Ritalin LA®	Capsule	Novartis	2002
Diltiazem	Herbesser®	Tablet	Mitsubishi	2002
Aprepitant	Emend®	Capsule	Merck	2003
Dexamethasone; ciprofloxacin	Ciprodex	Ophthalmic suspension	Novartis	2003
Fenofibrate	Tricor®	Tablet	Abbott	2004
Fenofibrate	Triglide®	Tablet	Skye Pharma	2005
Megestrol acetate	Megace® ES	Suspension	Par Pharma	2005
Megestrol acetate	Megace® ES	Oral suspension	PAR Pharmaceuticals	2005
Nepafenac	Nevanac	Ophthalmic suspension	Novartis	2005
Naproxen sodium	Naprelan®	Tablet	Wyeth	2006
Theophylline	Theodur®	Tablet, capsule	Mitsubishi Tanabe Pharma	2008
Paliperidone palmitate	Invega Sustenna®	Monthly intramuscular depot injection	Johnson & Johnson	2009
Nepafenac	Ilevro®	Ophthalmic suspension	Novartis	2012
Aripiprazole	Abilify Maintena kit®	Intramuscular injection	Otsuka Pharmaceutical Co. Ltd.	2014
Paliperidone palmitate	Invega Trinza®	Three-monthly intramuscular depot injection	Johnson & Johnson	2015
Aripiprazole lauroxil	Aristada initio kit®	Intramuscular injection	Alkermes INC	2018

logical activity. For example, albumin, arginine, lecithin, leucin, vitamin E polyethylene glycol succinate (TPGS), and sodium cholic acid provided nanocrystals with additional favorable biological properties.

Coating the nanocrystals with surfactants was done to allow barrier crossing and access to treating brain diseases by modifying the permeation at the blood–brain barrier (BBB). For example, atovaquone was safely and effectively used against *T. gondii* in vitro to treat toxoplasmic encephalitis, but the oral micronized solution showed poor bioavailability. In vivo studies confirmed the capacity of nanosuspensions coated with sodium dodecyl sulfate to cross the blood–brain barrier and permit the treatment of toxoplasmic encephalitis and other cerebral diseases (Shubar et al. 2011).

7 Cryo-Milling

7.1 Definition

Cryo-milling is a technique that involves high-energy ball milling performed in liquid nitrogen at cryogenic temperatures. Because of the intense ball milling at these temperatures, the size of the original powder is reduced to the nanoscale level in a relatively shorter time. Furthermore, the cryo-milling process is capable of producing nanocrystalline materials with enhanced thermal stability of particles. Thus, among the different mechanical processes, such as inert gas condensation, electrode position, rapid solidification, and sputtering, cryo-milling represents a new and effective technique for the production of nano-sized powders (Birringer et al. 1984; Back et al. 2005).

7.2 Ultra Cryo-Milling

An ultra cryo-milling technique uses liquid nitrogen and dry ice as beads. Liquid nitrogen is used as a dispersing solvent instead of water and dry ice was used as a milling medium instead of zirconia beads. The crystals are pulverized by collision with the dry ice beads at cryogenic temperatures. Because dry ice beads and liquid nitrogen spontaneously sublimate and vaporize under ambient conditions, both materials can be easily removed after the milling process, resulting in no residual solvent or bead material remnants in the milled product. Even if beads are broken or eroded during the milling process, there is no concern about contamination. The milled material is easily and efficiently recovered because the separation process from the beads is not necessary. Thus, it is also called a contamination-free cryo-milling technique. It is also advantageous that the dried products are directly available owing to spontaneous vaporization of liquid nitrogen so that a drying process is not required after the process. Thus, this approach encompasses the advantages of both dry and wet milling.

It has been reported that the milling efficiency is much higher than with dry milling using jet milling because dispersing the medium would actively disturb the coaggregation between the milled particles. In contrast, it has also been reported that the milling efficiency is slower compared with the zirconia beads at cryogenic temperatures, suggesting that dry ice is an inferior milling material to zirconia in liquid nitrogen under cryogenic conditions. The mechanism of wet media milling has been reported as the collision between the beads and the vessel wall. The milling efficiency is mainly dependent on collision energy. Heavy zirconia bead density (6.0 g/cm^3) would likely provide a higher collision energy to the particles than a light dry ice bead density (1.56 g/cm^3). In addition, zirconia beads have a more uniform size, a smoother surface, and a more rigid body than dry ice beads; thus, effective milling power would result from collision between heavier, similar-sized, and smooth-surfaced beads (Uemoto et al. 2018) (Table 3.4).

8 Solvent–Antisolvent Precipitation

Antisolvent precipitation is a bottom-up method, and produces fine particles by starting at the atomic level. This method gives better control over particle properties such as size, morphology, and crystallinity, compared with top-down methods. Antisolvent precipitation is the most attractive method of all the bottom-up methods. Antisolvent precipitation techniques provide a more convenient procedure at room temperatures and atmospheric pressure with no specific requirement of expensive equipment, and is at the same time easily scalable compared with other bottom-up methods (Dua et al. 2015).

8.1 Fundamental Principle of Antisolvent Precipitation Techniques

Antisolvent precipitation techniques proceed in steps of mixing of the solution and antisolvent, the generation of supersaturation, nucleation, and growth by coagulation and condensation, followed by agglomeration in the case of uncontrolled growth (Fig. 3.8).

The precipitation driving force is speedy and eminent supersaturation. The crucial crystal properties, such as size, morphology, and purity are significantly dependent on the rate, magnitude, and uniformity of supersaturation that generated during the process of crystallization (Mullin and Nyvlt 1971; Jones and Mullin 1974).

One component of the crystals' supersaturation (S) in liquids is defined in Eq. (3.3):

$$S = \frac{C}{C*} \tag{3.3}$$

where C is the actual drug concentration in the solution (mol/l) and $C*$ is the drug equilibrium solubility (mol/l) in a mixture of organic solvent and antisolvent.

It has been frequently observed that a higher degree of supersaturation typically results in lower Gibbs free energy and leads to higher nucleation rates (Dirksen and Ring 1991; Sugimoto 2003; Cushing et al. 2004).

Table 3.4 Examples obtained from the scientific literature on the use of cryo-milling for the production of drug nanoparticles

Drug	Observations	Equipment	References
Phenytoin	Novel ultra cryo-milling micronization technique using dry ice beads and liquid nitrogen	Wet milling machine (RMB-04, Aimex, Tokyo, Japan)	Sugimoto et al. (2012a, b)
Griseofulvin	Continued mode of attrition with milling time	Cryogenic impact mill (Spex CertiPrep 6750, Metuchen, NJ, USA)	Otte and Carvajal (2011)
Ketoconazole	Continued milling caused apparent particle growth		
Furosemide	Solid state amorphization and chemical decomposition	Cryogenic impact mill (Spex CertiPrep 6750)	Adrjanowicz et al. (2011)
Indomethacin	Dissolution rate depended on the milling time	Oscillatory ball mill (Mixer Mill MM301, Retsch, Haan, Germany)	Karmwar et al. (2011, 2012), Botker et al. (2011)
Phenytoin, ibuprofen, salbutamol sulfate	No change in crystal form and amorphization after milling	Wet milling machine (RMB-04, Aimex)	Niwa et al. (2010)
Glibenclamide	Transformation from crystalline to amorphous state without chemical decomposition	Cryogenic freezer/mill (Spex SamplePrep 6770)	Wojnarowska et al. (2010)
Ranitidine hydrochloride	Ranitidine hydrochloride polymorph forms 1 and 2 could be fully converted to the amorphous form	Oscillatory ball mill (Mixer Mill MM301, Retsch)	Chieng et al. (2008)
Carbamazepine	Higher amorphization with cryogenic co-grinding than with room temperature co-grinding	Cryogenic impact mill (Spex CertiPrep 6750)	Jayasankar et al. (2006)
Whole inactivated influenza virus	Dry powder influenza vaccine successfully formulated	Micro-ball mill (SPEX CertiPrep 3117)	Garmise et al. (2006)
Indomethacin polymorphs and solvates	Amorphous materials obtained after milling possessed similar Tg, but significant differences in their physical stability	Cryogenic impact mill (Spex CertiPrep 6750)	Crowley and Zografi (2002)

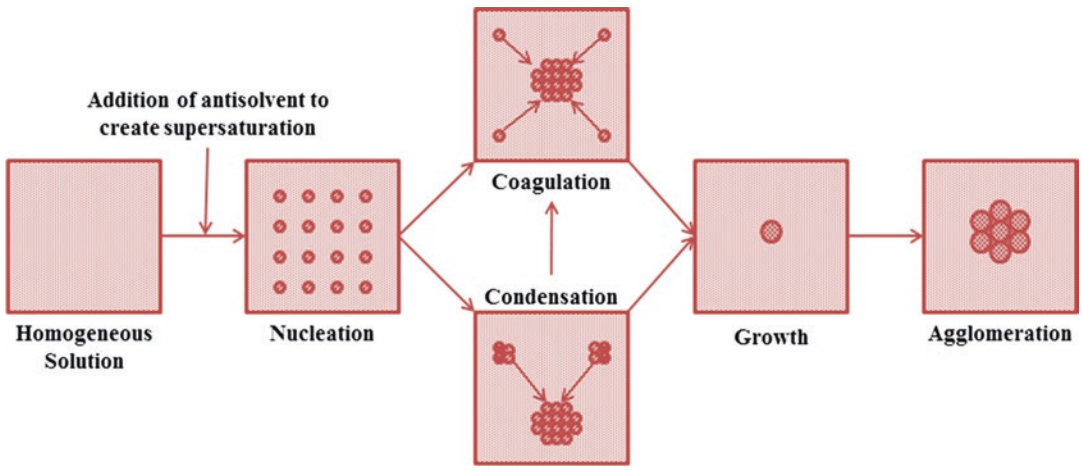

Fig. 3.8 The particle precipitation process

$$B^0 \propto \exp\left(\frac{\Delta Gcr}{kT}\right) \tag{3.4}$$

where B^0 is the nucleation rate, k is Boltzmann's constant, ΔGcr is the critical free energy, and T is the absolute temperature.

There are two mechanisms of "primary" nucleation, homogeneous and heterogeneous nucleation. In homogenous nucleation, the new solid phase generation is in the absence of foreign particles and surrounding surfaces. While in heterogeneous nucleation, the existing foreign particles promote nucleation (Söhnel and Garside 1992). In contrast, "secondary nucleation" is started by existing native crystals through mechanical abrasion or through thermodynamic effects.

The free energy for homogeneous nucleation is given in Eq. (3.5):

$$\Delta Gcr = \frac{16\pi\gamma_{sl}^3\upsilon^2}{3(kT)^2\left(\ln(1+s)\right)^2} \tag{3.5}$$

Thus, after combining Eqs. (3.4) and (3.5), the rate of homogeneous nucleation in the solution is derived by (Eq. 3.6)

$$B^0 = A_{\text{hom}} \exp\left(-\frac{16\pi\gamma_{sl}^3\upsilon^2}{3k^3T^3\left(\ln(1+s)\right)^2}\right) \tag{3.6}$$

where B^0 is the nucleation rate, A_{hom} is the pre-exponential factor, γ_{sl} is the interfacial tension at the solid–liquid interface, υ is the molar volume, and T is the temperature. Nucleation rates are primarily dependent on supersaturation and interfacial energy (γ), and the order of magnitude of A_{hom} typically varies from 10^{32} to 10^{36}. Furthermore, A_{hom} is dependent on the attachment mechanism of the solute on the growing particle surface, i.e., either interface transfer control or volume diffusion control (Johnson 2003; LaMer and Dinegar 1950; Guo et al. 2005; Matteucci et al. 2006; Dalvi and Dave 2010). Table 3.5 summarizes the various examples of drugs obtained from the scientific literature on the use of the antisolvent precipitation technique.

To obtain nanoparticles with a narrow size distribution, the following parameters should be kept in mind:

- Create a high degree of super saturation
- Uniform spatial concentration distributions in solutions
- Negligible growth of all crystals

There are two important parameters. One is the meta stable zone, the range of concentration where no crystallization is observed within a given time. It also called the energy barrier for particle precipitation from saturated solution. In order to achieve higher nucleation rates, a meta stable zone width should be shorter. Another parameter is the induction time. The induction time is the time elapsed between suspension of supersaturation and the appearance of detectable crystals (Granberg et al. 2001; Dixit and Zukoski 2002; Lyczko et al. 2002; Barrett and Glennon 2002; Omar et al. 2006; Schöll et al. 2007; Lindenberg and Mazzotti 2009; Kelly and Rodr'guez-Hornedo 2009; Mahajan and Kirwan 1993; Kim and Mersmann 2001; Chen et al. 2000; Dalvi and Dave 2009).

The nucleation and growth of particles occur simultaneously and both compete for consumption of supersaturation. Once nucleation occurs, the particles grow by condensation (τ_{cond}) and by coagulation (τ_{coag}). Condensation competes with nucleation by decreasing supersaturation. Coagulation can reduce the rate of condensation by reducing the total number of particles and the surface area (Thybo et al. 2008; Sun 2002; Jones 2002).

Once the particles grow, they also start to agglomerate because the process depends on the population density. Further agglomeration also depends on the Brownian motion of nanoparticles. It has been reported that at higher temperatures, the Brownian motion increases and results in a further increase in the growth rates of crystals. While at lower temperatures, the smaller crystals and the larger population density with higher surface energy cause agglomeration (Lince et al. 2008).

Table 3.5 Examples of various drug nanoparticles by antisolvent precipitation

Drug	Water solubility (mg/ml)	Nucleation type/model	Particle size (nm)	References
Alpha ketoglutarate	–	–	110	Sultana et al. (2011)
Ascorbyl palmitate	0.34	Classical theory of homogeneous nucleation	780	Beck et al. (2010)
Atropine sulfate	2.2	–	100–600	Ali et al. (2009a)
Atorvastatin calcium	0.12	–	240	Zhang et al. (2009a)
Beclomethasone dipropionate	0.049	Classical theory of homogeneous nucleation	440	
Bicalutamide	0.005	Classical theory of nucleation with some modification	115	Lindfors et al. (2008)
β-Carotene	–	Primary nucleation	100	Zhu et al. (2007)
β-Carotene and C_{12}-Au	–	–	103	Gindy et al. (2008a)
Cefuroxime axetil	0.145	Primary nucleation	80	Dhumal et al. (2008a)
Cefradine	21.3	Homogeneous nucleation	300	Zhong et al. (2005)
Curcumin	0.00019	Nonclassical pathway	30–50	He et al. (2010, 2011)
Danazol	0.238	Homogeneous nucleation	364	Zhao et al. (2007)
Danazol	0.238	Homogeneous nucleation	190	Zhao et al. (2009)
Diatrizoic acid	0.39	–	136	El-Gendy et al. (2010)
Docetaxel	0.000025	–	180	Cheng et al. (2007a)
Felodipine	0.356	–	60	Lindfors et al. (2007)
Fenofibrate	0.25	Classical theory of homogeneous nucleation	882	Meng et al. (2009)
Hydrocortisone	0.32	–	80	Ali et al. (2009b)
Ibuprofen	0.049	Classical theory of homogeneous nucleation	702	Dalvi and Dave (2010)
Insulin	–	–	200	Klingler et al. (2009)
Itraconazole	Insoluble	Homogeneous primary nucleation	300	Matteucci et al. (2006, 2008)
Maleimide	–	–	85	Gindy et al. (2008b)
Megestrol acetate	0.002	Classical theory of homogeneous nucleation	208	Zhang et al. (2009b)
Nitrendipine	0.19	Classical theory of homogeneous nucleation	209	Xia et al. (2010)
Norfloxacin	0.264	–	170	Panagiotou et al. (2009)
Odanacatib	–	Classical theory of homogeneous nucleation	350	Kumar et al. (2009a)
Paclitaxel	0.277	–	100	Pattekari et al. (2011)
PLGA and PLA	–	–	84–168	Bilati et al. (2005)
PLGA-PEG and PLGA-lipid	–	–	70–80	Valencia et al. (2010)
Progesterone	0.00881	–	267	Salem (2010)

(continued)

Table 3.5 (continued)

Drug	Water solubility (mg/ml)	Nucleation type/model	Particle size (nm)	References
Roxithromycin	0.0000189	Classical theory of homogeneous nucleation	–	Guo (2005)
Salbutamol sulfate	0.003	Classical theory of homogeneous nucleation	100	Hu et al. (2008)
Salmeterol xinafoate	0.11	Classical theory of homogeneous nucleation	254	Murnane et al. (2008)
Sirolimus	0.086	Classical theory of homogeneous nucleation	863	Gandhi and Murthy (2010)
Spironolactone	0.022	A spherical cluster was formed first, followed by rearrangement of the spheres into ordered nanocrystals	330	Dong et al. (2011), Erdemir et al. 2009)
Theophylline	5	–	290	Salem et al. (2011a)

PEG poly(ethylene glycol), P*LGA* poly(lactide-coglycolide), *PLA* polylactic acid

Particle engineering requires the fine-tuning of different variables such as meta stable zone width, induction time, interfacial surface energy, and supersaturation, to obtain the desired particle characteristics. However, fine tuning and control of these variables require prior observations and in situ measurements. Several methods have been reported for the detection and measurement of nucleation and growth kinetics so far and are summarized in Table 3.6.

8.2 Step-Up Antisolvent Precipitation Process

8.2.1 Mixing

Mixing generates supersaturation followed by nucleation and growth in a step-up antisolvent precipitation process. There are two main time scales, mixing time (τ_{mix}) and the precipitation or induction time ($\tau_{precipitation}$), both of which are associated with the process of particle formation. Mixing time (τ_{mix}) comprises the time required for macro mixing, meso mixing, and micro mixing. Mixing that occurs on a crystallizer scale is called macro mixing. Meso mixing is also known as turbulent mixing and it consists of the large-scale mass transfer of a solution. Molecular diffusion and engulfment of different solvent composition regions below the Kolmogorov micro scale is called micro mixing (Johnson and Prud'homme 2003a, b; Gradl et al. 2006; Shekunov et al. 2001; Baldyga et al. 1997). $\tau_{precipitation}$ is composed of nucleation time ($\tau_{nucleation}$) and growth time (τ_{growth}). The Damköhler number (Da), dimensionless is the ratio of τ_{mix} to $\tau_{precipitation}$. Thus, when Da is greater than 1, the mixing process is slower than the precipitation process, supersaturation is accomplished at a slower rate, and the metastable zone is crossed very slowly. This leads to particle growth and the formation of large crystals. On the other hand, when Da is less than 1, τ_{mix} is reduced compared with $\tau_{precipitation}$, the solution is mixed uniformly at the micro level, where supersaturation is accomplished rapidly and nucleation takes place swiftly. The mixing process is faster than the precipitation step and controls overall particle formation. In a situation where supersaturation is highly accomplished, then the meta stable zone is crossed quickly, and nucleation dominates in the precipitation process. This leads to a large number of nuclei and the precipitation of nanoparticles with a narrower size distribution.

Currently, two approaches have been reportedly used for increasing the mixing rate; namely, the high jet velocity mixing device and ultrasound precipitation (Muntó et al. 2005; Zhao et al. 2007; Beck et al. 2010).

8.2.2 Mixing Devices

There are various mixing device designs reported, such as a static mixer, high gravity precipitation, a confined impinging jet, a multi-inlet vortex

Table 3.6 Methods for the detection and measurement of nucleation and growth kinetics

Purpose	Characterization techniques	References
Nucleation and growth kinetics	ATR-FTIR	Schöll et al. (2007)
	FBRM	Barrett and Glennon (2002, Schöll et al. (2007)
	Laminar flow diffusion chamber	Dong et al. (2011)
	Raman spectroscopy	Ali et al. (2011)
	Microscopic analysis	Zhu et al. (2010b)
Metastable zone width	FBRM	Barrett and Glennon (2002)
	Saturation temperature measurement	Lyczko et al. (2002)
	Visual appearance	Liu et al. (2010b)
Induction time	FBRM	Barrett and Glennon (2002), Lindenberg and Mazzotti (2009)
	ATR-FTIR	Schöll et al. (2007), Lindenberg and Mazzotti (2009)
	Visual appearance	Omar et al. (2006)
	Laser scattering method	Zhi et al. (2011)
	Conductivity measurement	Lyczko et al. (2002)
	Lasentec PVM	Omar et al. (2006)
	SEM	Teychene and Biscans (2008)
Interfacial energy	Theoretical correlation by Mersmann and Bennema	Teychene and Biscans (2008)
	Contact angle measurement using KVS CAM 200 equipped with a CCD camera	
	Contact angle measurement using Young equation	Granberg et al. (2001)
	Using tensiometer: (Krüss processor tensiometer K12, Wilhelmy plate method)	

(continued)

Table 3.6 (continued)

ATR-FTIR attenuated total reflection-Fourier transform infrared spectroscopy, *CCD* charge-coupled device, *FBRM* focused beam reflectance measurement, *PVM* particle vision and measurement, *SEM* scanning electron microscopy

mixer (MIVM), a Y-shaped micro channel reactor, and a T-mixer.

Mixing devices facilitate the process and intensify nanoparticle formation by reducing the diffusion length between drugs containing a solvent and those containing an antisolvent. Mixing devices help to achieve mixing time by milli- to microseconds. In some mixer designs, additional ultrasound as an external energy can help in rapid mixing to achieve higher supersaturation in a very short time.

A *static mixer* consists of a series of motionless identical elements with a specific structure of mixing elements. The mixing elements are able to redistribute fluid in the radial and tangential directions to realize rapid and homogeneous mixing. Many of the research groups reported the use of static mixing for antisolvent precipitation of drug nanoparticles, as summarized in Table 3.7 (Gassmann et al. 1994; Douroumis and Fahr 2006; Douroumis et al. 2008; Dong et al. 2010; Hu et al. 2011).

High gravity antisolvent precipitation (HGAP), where, under the high gravity, the rotating packed bed disseminates or breaks up the fluids into very fine droplets. The rate of mass transfer is higher in a rotating packed bed than in a conventional reactor. The particle size decreases as the rotating speed is increased. The use of HGAP in the production of fine particles of danazol, cefuroxime axetil, salbutamol sulfate, and cefradine has been reported (Hu et al. 2008; Zhao et al. 2009; Chiou et al. 2007; Zhong et al. 2005; Chen et al. 2006).

A *multi-inlet vortex mixer* has been reported for many organic and inorganic compounds via flash nanoprecipitation, as summarized in Table 3.7, where the mixing rate is too rapid and requires less time compared with nucleation and drug particle growth time. The flow rate can be adjustable with the entry of solvent and antisolvent into the mixer in such a way that different levels of supersatura-

Table 3.7 Summary of mixing devices used for the antisolvent precipitation technique

Process	Drug	Particle size (nm)	References
Static mixer	Betamethasone valerate-17	250	Douroumis and Fahr (2006)
	Oxcarbazepine	970	
	Spironolactone	500	Dong et al. (2010)
	Fenofibrate	328	Hu et al. (2011)
HGRP	Benzoic acid by reacting sodium benzoate and HCl	10	Chen et al. (2004)
	Cefradine	300	Zhong et al. (2005)
	Competitive boric acid, iodate, and iodide reaction	–	Yang et al. (2005)
	Cefuroxime axetil	305	Chen et al. (2006)
	Danazol	190	Zhao et al. (2009)
CIJ	Competitive Bourne reactions	–	Johnson and Prud'homme (2003a)
	β-Carotene	100	Johnson and Prud'homme (2003b)
	Cyclosporine A	18–700	Chiou et al. (2008)
	Competitive iodide–iodate model reaction	300	Hu et al. (2008)
	Poly-ε-caprolactone and poly(methoxypolyethyleneglycol cyanoacrylate-co-hexadecyl cyanoacrylate)	150	Lince et al. (2011)
Impinging device	Spironolactone	302	Dong et al. (2011)
Multi-inlet vortex mixer	Competitive Bourne reactions	–	Liu et al. (2008)
	β-Carotene and C_{12}-Au	103	Gindy et al. (2008a)
	Maleimide	85	Gindy et al. (2008c)
	β-Carotene	100	Zhu et al. (2010a)
Mixing tee with ultrasound	Itraconazole	145	Cheng et al. (2009)
	Odanacatib	350	
YMCR	Danazol	364	Zhao et al. (2007)
	Hydrocortisone	295	Ali et al. (2011)
	Atorvastatin calcium	480	Zhang et al. (2010)
	Cefuroxime axetil	350	Wang et al. (2010)
Microporous tube-in-tube microchannel reactor	Cefuroxime axetil	400	Zhu et al. (2010b)
T-shaped microchannel	Curcumin	190	(Liu et al. 2010b)
T-mixer with ultrasound	Ascorbyl palmitate	780	Beck et al. (2010)
	Itraconazole	347	
Ultrasound with batch reactor	Cefuroxime axetil	80	Dhumal et al. (2008b)
	Ibuprofen	702	Verma et al. (2009)
	Curcumin	60	Zheng et al. (2010)
	Diatrizoic acid	136	El-Gendy et al. (2010)
	Nitrendipine	209	Xia et al. (2010)
	Sirolimus	863	Gandhi and Murthy (2010)

CIJ confined impinging jet, *HGRP* high-gravity reactive precipitation, *YMCR* Y-shaped microfluidic reactor

tion can be achievable. An adjustable facility can help to control the adsorption of the stabilizer, particle growth, and the size of the nanoparticles. Based on the literature, it has been observed that the end fluid phase, which contains mostly antisolvent and a smaller amount of organic solvent in the

end solution helps to reduce the extent of Ostwald ripening of particle suspensions (Liu et al. 2007, 2008; Gindy et al. 2008c, d; Kumar et al. 2009b; Zhu et al. 2010a; Cheng et al. 2009).

A *confined impinging jet (CIJ)* is reported for the nanoparticle production of several drugs via the antisolvent precipitation technique. The high velocity jet of fluid facilitates the rapid mixing, ensuring a shorter mixing time than precipitation. The CIJ reactor chamber's geometry, size, and ratio of chamber diameter to jet diameter impact the mixing performance. This high mixing efficiency assists in achieving high supersaturation and high nucleation results in uniform fine nanoparticle precipitation. Furthermore, fast stabilizer distribution on the newly formed surfaces of the nanoparticles via adjustment of the precipitation kinetics of the stabilizer and the drug results in very fine and uniformly stabilized drug nanoparticles (Mahajan and Kirwan 1996; Chiou et al. 2008).

Microchannel reactor technology (MRT) provides a high level of velocity and energy dissipation compared with a conventional reactor. Microreactor mixing is mainly operated by molecular diffusion. Moreover, fine control of supersaturation can be achieved by proper selection of stream ratios. MRT is a continuous process and scalable to enable handling of flow rates of a few liters per minute. There are different shaped micro channel reactors reported in the literature. Y-shaped mixers have been used for the precipitation of danazol, hydrocortisone, atorvastatin calcium, and cefuroxime axetil nanoparticles. Similarly, the reported T-mixers remove the issues of proper alignment of nozzles associated with impinging jets. T-mixers are also used in combination with ultrasound in antisolvent precipitations such as fenofibrate, itraconazole, griseofulvin, ascorbyl palmitate, and sulfamethoxazole. Ultrasound used in the mixing zone helps to improve mixing and generates high supersaturation, resulting in controlled growth of fine and uniform nanoparticles (Ehrfeld et al. 1999; Panagiotou et al. 2009; Wang et al. 2010; Zhang et al. 2010; Wong et al. 2004).

Microporous tube-in-tube microchannel reactors (MTMCR) have provided effective micro mixing and high throughput capacities. It has been reported for use in continuous nanoparticle production of amorphous cefuroxime axetil (Wang et al. 2009).

9 Role of Stabilizer in Antisolvent Precipitation Techniques

The role of a stabilizer to make a protective layer on the particle surface during antisolvent precipitation leads to controlled growth and agglomeration. It can be added in either the solvent or the antisolvent phase. There are two main mechanisms of thermodynamic stabilization involved, i.e., steric stabilization and electrostatic repulsion. A list of stabilizers used in the stabilization of nanoparticles during antisolvent precipitation techniques is given in Table 3.8.

10 Future Perspectives

The potential of nanocrystals for different applications needed to be investigated in detail. Nanocrystals will combine with implantable sustained release drug delivery systems to attain a higher local concentration. Future perspective studies on novel unique approaches to manufacturing nanocrystals and related products have a huge market. The use of emerging nanocrystal technology is expected to increase in the future, with exploration of different routes of administrations (i.e., oral, parenteral, pulmonary, ocular, and dermal) to enhance

Table 3.8 Summary of stabilizers for the stabilization of nanoparticles precipitated by antisolvent precipitation techniques

Drug	Stabilizer	Particle size (nm)	References
Ascorbyl palmitate	PEG (4000)	780	Beck et al. (2010)
Alpha ketoglutarate	Lutrol F68 and PVA	110	Sultana et al. (2011)
AC	HPMC	240	Zhang et al. (2009a)
AZ68	PVP and SDS, Miglyol	152	Sigfridsson et al. (2007)
β-Carotene and C12-Au	Poly(ethylene glycol-block-caprolactone) PEG-b-PCL	103	Gindy et al. (2008a)
β-Carotene	Polycaprolactone	100	Zhu et al. (2007)
	PS-b-PEO	100	Liu et al. (2007)
	PEI and chitosan	60	Zhu et al. (2010a)
	PEG-b-PLGA + poly(acrylic) acid	140	Kelly and Rodr'guez-Hornedo (2009)
Bicalutamide	Lactose	330	Li et al. (2011)
	PVP	115	Lindfors et al. (2008)
Curcumin	PLGA–PEG and Pluronic F-68	81	Anand et al. (2010)
	PS and BSA	60–100	Yen et al. (2010)
	Polyvinyl pyrrolidone	142	
Cytarabine	PLGA	125	Yadav and Sawant (2010)
Docetaxel	PLGA-b-PEG	70	Cheng et al. (2007b)
Fenofibrate	PEG (4000)	882	Beck et al. (2010)
	SDS and HPMC E3	318	Hu et al. (2011)
Hydrocortisone	HPMC, SLS, PVP	80	Ali et al. (2009b)
	HPMC, PVP, Tween 80	295	Chiou et al. (2008)
Itraconazole	Poloxamer 407	300	Matteucci et al. (2006)
	HPMC	300	Matteucci et al. (2008)
	HPMC	279	Chen et al. (2008)
	Polystyrene-block-polyethylene oxide	145	Kumar et al. (2009a)
	PEG (4000)	347	Beck et al. (2010)
Megestrol acetate	PVP and SDS	208	Granberg et al. (2001)
Nitrendipine	PVA	209	Dua et al. (2015)
Odanacatib	Polystyrene-block-polyethylene oxide	350	Kumar et al. (2009a)
Paclitaxel	l-Leucine (Leu) and polyvinylpyrrolidone (PVP K90)	299	El-Gendy et al. (2010)
	Chitosan and alginic acid	100	Pattekari et al. (2011)
Progesterone	Stearic acid	267	Salem (2010)
Sirolimus	Tween-80	863	Gandhi and Murthy (2010)
Spironolactone	HPMC	231	Dong et al. (2009)
	HPMC and SDS	500	Dong et al. (2010)
	HPMC and SDS	330	Zhao et al. (2007)
Theophylline	Stearic acid	290	Salem et al. (2011b)

AC atorvastatin calcium, *BSA* bovine serum albumin, *HPMC* hydroxypropyl methylcellulose, *PEG* poly(ethylene glycol), *PEG-b-PLGA* poly-(ethylene glycol)-b-poly(lactide-coglycolide), *PEI*, poly(ethylene imine), *PLGA* poly(lactide-coglycolide), *PS* protamine sulfate, *PS-b-PEO* poly(styrene)-b-poly(ethylene oxide), *PVA* polyvinyl alcohol, *PVP* polyvinylpyrrolidone, *SDS* sodium dodecyl sulfate

the bioavailability of nutraceuticals or cosmetics products as well as pharmaceutical products.

References

Adrjanowicz K, Kaminski K, Grzybowska K, Hawelek L, Paluch M, Gruszka I, Zakowiecki D, Sawicki W, Lepek P, Kamysz W, Guzik L. Effect of cryogrinding on chemical stability of the sparingly water-soluble drug furosemide. Pharm Res. 2011;28(12):3220–36.

Ali R, Jain G, Iqbal Z, Talegaonkar S, Pandit P, Sule S, Malhotra G, Khar R, Bhatnagar A, Ahmad F. Development and clinical trial of nano-atropine sulfate dry powder inhaler as a novel organophosphorous poisoning antidote. Nanomedicine. 2009a;5:55–63.

Ali H, York P, Blagden N. Preparation of hydrocortisone nanosuspension through a bottom-up nanoprecipitation technique using microfluidic reactors. Int J Pharm. 2009b;375:107–13.

Ali H, York P, Ali A, Blagden N. Hydrocortisone nanosuspensions for ophthalmic delivery: a comparative study between microfluidic nanoprecipitation and wet milling. J Control Release. 2011;149:175–81.

Alshora DH, Ibrahim MA, Alanazi FK. Chapter 6 – nanotechnology from particle size reduction to enhancing aqueous solubility. In: Surface chemistry of nanobiomaterials: applications of nanobiomaterials, vol. 3. Cambridge, MA: Elsevier; 2016. p. 163–91.

Anand P, Nair H, Sung B, Kunnumakkara A, Yadav V, Tekmal R, Aggarwal B. Design of curcumin-loaded PLGA nanoparticles formulation with enhanced cellular uptake, and increased bioactivity in vitro and superior bioavailability in vivo. Biochem Pharmacol. 2010;79:330–8.

Baba K, Pudavar HE, Roy I, Ohulchanskyy TY, Chen Y, Pandey RK, Prasad PN. New method for delivering a hydrophobic drug for photodynamic therapy using pure nanocrystal form of the drug. Mol Pharm. 2007;4:289–97.

Back SH, Lee GH, Kang S. Effect of cryomilling on particle size and microstrain in a WC-Co alloy. Mater Trans. 2005;46(1):105–10.

Baldyga J, Bourne J, Hearn S. Interaction between chemical reactions and mixing on various scales. Chem Eng Sci. 1997;52:457–66.

Barrett P, Glennon B. Characterizing the metastable zone width and solubility curve using Lasentec FBRM and PVM. Chem Eng Res Des. 2002;80:799–805.

Bartos C, Jójárt-Laczkovich O, Katona G, Budai-Szűcs M, Ambrus R, Bocsik A, Gróf I, Anna Deli M, Szabó-Révész P. Optimization of a combined wet milling process in order to produce poly(vinyl alcohol) stabilized nanosuspension. Drug Des Devel Ther. 2018;12:1567–80.

Beck C, Dalvi S, Dave R. Controlled liquid antisolvent precipitation using a rapid mixing device. Chem Eng Sci. 2010;65:5669–75.

Bilati U, Allémann E, Doelker E. Development of a nanoprecipitation method intended for the entrapment of hydrophilic drugs into nanoparticles. Eur J Pharm Sci. 2005;24:67–75.

Birringer R, Gleiter H, Klein HP, Marquardt P. Nanocrystalline materials – an approach to a novel solid structure with gas-like disorder? Phys Lett A. 1984;102(8):365–9.

Borchard G. Drug nanocrystals. In: Crommelin D, de Vlieger J, editors. Non-biological complex drugs, AAPS advances in the pharmaceutical sciences series, vol. 20. Cham: Springer; 2015. p. 171–89.

Botker JP, Karmwar P, Strachan CJ, Cornett C, Tian F, Zujovic Z, Rantanen J, Rades T. Assessment of crystalline disorder in cryo-milled samples of indomethacin using atomic pair-wise distribution functions. Int J Pharm. 2011;417(1–2):112–9.

Brouwers J, Tack J, Augustijns P. In vitro behavior of a phosphate ester prodrug of amprenavir in human intestinal fluids and in the Caco-2 system: illustration of intraluminal supersaturation. Int J Pharm. 2007;336:302–9.

Brouwers J, Brewster ME, Augustijns P. Supersaturating drug delivery systems: the answer to solubility-limited oral bioavailability? J Pharm Sci. 2009;98:2549–72.

Chen J, Wang Y, Guo F, Wang X, Zheng C. Synthesis of nanoparticles with novel technology: high-gravity reactive precipitation. Ind Eng Chem Res. 2000;39:948–54.

Chen J, Zhou M, Shao L, Wang Y, Yun J, Chew N, Chan H. Feasibility of preparing nanodrugs by high-gravity reactive precipitation. Int J Pharm. 2004;269:267–74.

Chen J, Zhang J, Shen Z, Zhong J, Yun J. Preparation and characterization of amorphous cefuroxime axetil drug nanoparticles with novel technology: high-gravity antisolvent precipitation. Ind Eng Chem Res. 2006;45:8723–7.

Chen W, Gu B, Wang H, Pan J, Lu W, Hou H. Development and evaluation of novel itraconazole-loaded intravenous nanoparticles. Int J Pharm. 2008;362:133–40.

Chen L, Wang Y, Zhang J, Hao L, Guo H, Lou H, Zhang D. Bexarotene nanocrystal – oral and parenteral formulation development, characterization and pharmacokinetic evaluation. Eur J Pharm Biopharm. 2014;87:160–9.

Cheng J, Teply B, Sherifi I, Sung J, Luther G, Gu F, Levy-Nissenbaum E, Radovic-Moreno A, Langer R, Farokhzad O. Formulation of functionalized PLGA-PEG nanoparticles for in vivo targeted drug delivery. Biomaterials. 2007a;28:869–76.

Cheng J, Teply B, Sherifi I, Sung J, Luther G, Gu F, Nissenbaum E, Radovic-Moreno A, Langer R, Farokhzad O. Formulation of functionalized PLGA-PEG nanoparticles for in vivo targeted drug delivery. Biomaterials. 2007b;28:869–76.

Cheng J, Olsen M, Fox R. A microscale multi-inlet vortex nanoprecipitation reactor: turbulence measurement and simulation. App Phys Lett. 2009;94:204104.

Chieng N, Rades T, Saville D. Formation and physical stability of the amorphous phase of ranitidine hydrochloride polymorphs prepared by cryo-milling. Eur J Pharm Biopharm. 2008;68(3):771–80.

Chiou H, Li L, Hu T, Chan H, Chen J, Yun J. Production of salbutamol sulfate for inhalation by high-gravity controlled antisolvent precipitation. Int J Pharm. 2007;331:93–8.

Chiou H, Chan H, Heng D, Prud'homme R, Raper J. A novel production method for inhalable cyclosporine A powders by confined liquid impinging jet precipitation. J Aerosol Sci. 2008;39:500–9.

Colombo M, Staufenbiel S, Rühl E, Bodmeier R. In situ determination of the saturation solubility of nanocrystals of poorly soluble drugs for dermal application. Int J Pharm. 2017;521:156–66.

Crowley KJ, Zografi G. Cryogenic grinding of indomethacin polymorphs and solvates: assessment of amorphous phase formation and amorphous phase physical stability. J Pharm Sci. 2002;91(2):492–507.

Cushing B, Kolesnichenko V, O'Connor C. Recent advances in the liquid-phase syntheses of inorganic nanoparticles. Chem Rev. 2004;104:3893–946.

Dalvi S, Dave R. Analysis of nucleation kinetics of poorly water-soluble drugs in presence of ultrasound and hydroxypropyl methyl cellulose during antisolvent precipitation. Int J Pharm. 2010;387:172–9.

Dalvi SV, Dave RN. Controlling particle size of a poorly water-soluble drug using ultrasound and stabilizers in antisolvent precipitation. Ind Eng Chem Res. 2009;48:7581–93.

Dhumal R, Biradar S, Yamamura S, Paradkar A, York P. Preparation of amorphous cefuroxime axetil nanoparticles by sonoprecipitation for enhancement of bioavailability. Eur J Pharma Biopharma. 2008a;70:109–15.

Dhumal R, Biradar S, Yamamura S, Paradkar A, York P. Preparation of amorphous cefuroxime axetil nanoparticles by sonoprecipitation for enhancement of bioavailability. Eur J Pharm Biopharm. 2008b;70:109–15.

Dirksen J, Ring T. Fundamentals of crystallization: kinetic effects on particle size distributions and morphology. Chem Eng Sci. 1991;46:2389–427.

Dixit N, Zukoski C. Nucleation rates and induction times during colloidal crystallization: links between models and experiments. Phys Rev. 2002;66:051602.

Dong Y, Ng W, Shen S, Kim S, Tan R. Preparation and characterization of spironolactone nanoparticles by antisolvent precipitation. Int J Pharm. 2009;375:84–8.

Dong Y, Ng W, Hu J, Shen S, Tan R. A continuous and highly effective static mixing process for antisolvent precipitation of nanoparticles of poorly water-soluble drugs. Int J Pharm. 2010;386:256–61.

Dong Y, Ng W, Shen S, Kim S, Tan R. Controlled antisolvent precipitation of spironolactone nanoparticles by impingement mixing. Int J Pharm. 2011;410:175–9.

Douroumis D, Fahr A. Nano- and micro-particulate formulations of poorly water-soluble drugs by using a novel optimized technique. Eur J Pharm Biopharm. 2006;63:173–5.

Douroumis D, Scheler S, Fahr A. Using a modified Shepards method for optimization of a nanoparticulate cyclosporine a formulation prepared by a static mixer technique. J Pharm Sci. 2008;97:919–30.

Dua J, Lib X, Zhaoc H, Zhoua Y, Wanga L, Tiana S, Wanga Y. Nanosuspensions of poorly water-soluble drugs prepared by bottom-up technologies. Int J Pharm. 2015;495:738–49.

Ehrfeld W, Golbig K, Hessel V, Löwe H, Richter T. Characterization of mixing in micromixers by a test reaction: single mixing units and mixer arrays. Ind Eng Chem Res. 1999;38:1075–82.

El-Gendy N, Aillon K, Berkland C. Dry powdered aerosols of diatrizoic acid nanoparticle agglomerates as a lung contrast agent. Int J Pharm. 2010;391:305–12.

Erdemir D, Lee A, Myerson A. Nucleation of crystals from solution: classical and two-step models. Acc Chem Res. 2009;42:621–9.

Fu Q, Sun J, Ai X, Zhang P, Li M, Wang Y, Liu X, Sun Y, Sui X, Sun L. Nimodipine nanocrystals for oral bioavailability improvement: role of mesenteric lymph transport in the oral absorption. Int J Pharm. 2013;448:290–7.

Gandhi P, Murthy Z. Solubility and crystal size of sirolimus in different organic solvents. J Chem Eng Data. 2010;55:5050–4.

Ganta S, Paxton JW, Baguley BC, Garg S. Formulation and pharmacokinetic evaluation of an asulacrine nanocrystalline suspension for intravenous delivery. Int J Pharm. 2009;367:179–86.

Gao L, Zhang D, Chen M. Drug nanocrystals for the formulation of poorly soluble drugs and its application as a potential drug delivery system. J Nanopart Res. 2008;10:845–62.

Gao L, Liu GY, Ma JL, Wang XQ, Zhou L, Li X. Drug nanocrystals: in vivo performances. J Control Release. 2012;30:307–24.

Gao W, Chen Y, Thompson DH, Park K, Li T. Impact of surfactant treatment of paclitaxel nanocrystals on biodistribution and tumor accumulation in tumor-bearing mice. J Control Release. 2016;237:168–76.

Garmise RJ, Mar K, Crowder TM, Hwang R, Ferriter M, Huang J, Mikszta JA, Sullivan VJ, Hickey AJ. Formulation of a dry powder influenza vaccine for nasal delivery. AAPS Pharm Sci Tech. 2006;7(1):E131–7.

Gassmann P, List M, Schweitzer A, Sucker H. Hydrosols: alternatives for the parenteral application of poorly water soluble drugs. Eur J Pharm Biopharm. 1994;40:64–72.

Gigliobianco MS, Casadidio C, Censi R, Martino PD. Nanocrystals of poorly soluble drugs: drug bioavailability and physiochemical stability. Pharmaceutics. 2018;10(134):1–29.

Gindy M, Panagiotopoulos A, Prud'homme R. Composite block copolymer stabilized nanoparticles: simultaneous encapsulation of organic actives and inorganic nanostructures. Langmuir. 2008a;24:83–90.

Gindy M, Ji S, Hoye T, Panagiotopoulos A, Prud'homme R. Preparation of poly(ethylene glycol) protected nanoparticles with variable bioconjugate ligand density. Biomacromolecules. 2008b;9:2705–11.

Gindy M, Hoye S, Panagiotopoulos A, Prud'homme R. Preparation of poly(ethylene glycol) protected nanoparticles with variable bioconjugate ligand density. Biomacromolecules. 2008c;9:2705–11.

Gradl J, Schwarzer H, Schwertfirm F, Manhart M, Peukert W. Precipitation of nanoparticles in a T-mixer: coupling the particle population dynamics with hydrodynamics through direct numerical simulation. Chem Eng Process. 2006;45:908–16.

Granberg R, Ducreux C, Gracin S, Rasmuson A. Primary nucleation of paracetamol in acetone–water mixtures. Chem Eng Sci. 2001;56:2305–13.

Gu CH, Grant DJ. Estimating the relative stability of polymorphs and hydrates from heats of solution and solubility data. J Pharm Sci. 2001;90(9):1277–87.

Gulsun T, Gursoy RN, Levent O. Nanocrystal technology for oral delivery of poorly water-soluble drugs. FARAD J Pharm Sci. 2009;34:55–65.

Guo Z, Zhang M, Li H, Wang J, Kougoulos E. Effect of ultrasound on anti-solvent crystallization process. J Cryst Growth. 2005;273:555–63.

Hancock BC, Parks M. What is the true solubility advantage for amorphous pharmaceuticals? Pharm Res. 2000;17(4):397–404.

He Y, Huang Y, Cheng Y. Structure evolution of curcumin nanoprecipitation from a micromixer. Cryst Growth Des. 2010;10:1021–4.

He Y, Huang Y, Wang W, Cheng Y. Integrating micromixer precipitation and electrospray drying toward continuous production of drug nanoparticles. Chem Eng J. 2011;168:931–7.

Helmholtz RV. Untersuchungen über Dämpfe und Nebel, besonders über solche von Lösungen (Investigations of vapors and mists, and especially of such things from solutions). Ann Phys. 1886;263(4):508–43.

Hu T, Chiou H, Chan H, Chen J, Yun J. Preparation of inhalable salbutamol sulphate using reactive high gravity controlled precipitation. J Pharm Sci. 2008;97:944–9.

Hu J, Ng W, Dong Y, Shen S, Tan R. Continuous and scalable process for water-redispersible nanoformulation of poorly aqueous soluble APIs by antisolvent precipitation and spray-drying. Int J Pharm. 2011;404:198–204.

Huang X, Peng X, Wang Y, Wang Y, Shin DM, El-Sayed MA, Nie S. A reexamination of active and passive tumor targeting by using rod-shaped gold nanocrystals and covalently conjugated peptide ligands. ACS Nano. 2010;4:5887–96.

Ige PP, Baria RK, Gattani SG. Fabrication of fenofibrate nanocrystals by probe sonication method for enhancement of dissolution rate and oral bioavailability. Colloids Surf B Biointerfaces. 2013;108:366–73.

Jayasankar A, Somwangthanaroj A, Shao ZJ, Rodríguez-Hornedo N. Cocrystal formation during cogrinding and storage is mediated by amorphous phase. Pharm Res. 2006;23(10):2381–92.

Jermain SV, Brough C, Williams RO. Amorphous solid dispersions and nanocrystal technologies for poorly water-soluble drug delivery-an update. Int J Pharm. 2018;535:379–92.

Johnson B. Flash Nanoprecipitation of organic actives via confined micromixing and block copolymer stabilization. Princeton: Princeton University; 2003.

Johnson B, Prud'homme R. Chemical processing and micromixing in confined impinging jets. AICHE J. 2003a;49:2264–82.

Johnson B, Prud'homme R. Flash nanoprecipitation of organic actives and block copolymers using a confined impinging jets mixer. Aust J Chem. 2003b;56:1021–4.

Jones A. Crystallization process systems. Oxford/Boston: Butterworth-Heinemann; 2002.

Jones A, Mullin J. Programmed cooling crystallization of potassium sulphate solutions. Chem Eng Sci. 1974;29:105–18.

Junghanns J-UA, Müller RH. Nanocrystal technology, drug delivery and clinical applications. Int J Nanomed. 2008;3(3):295–310.

Junyaprasert VB, Morakul B. Nanocrystals for enhancement of oral bioavailability of poorly water-soluble drugs. Asian J Pharm Sci. 2015;10(1):13–23.

Karmwar P, Graeser K, Gordon KC, Strachan CJ, Rades T. Investigation of properties and recrystallisation behaviour of amorphous indomethacin samples prepared by different methods. Int J Pharm. 2011;417(1–2):94–100.

Karmwar P, Graeser K, Gordon KC, Strachan CJ, Rades T. Effect of different preparation methods on the dissolution behaviour of amorphous indomethacin. Eur J Pharm Biopharm. 2012;80(2):459–64.

Keck CM, Müller RH. Drug nanocrystals of poorly soluble drugs produced by high pressure homogenization. Eur J Pharm Biopharm. 2006;62:3–16.

Kelly R, Rodr'guez-Hornedo N. Solvent effects on the crystallization and preferential nucleation of carbamazepine anhydrous polymorphs: a molecular recognition perspective. Org Process Res Dev. 2009;13:1291–300.

Kesisoglou F, Panmai S, Wu Y. Nanosizing – oral formulation development and biopharmaceutical evaluation. Adv Drug Deliv Res. 2007;59:631–44.

Khan MS, Vishakante GD, Bathool A. Development and characterization of pilocarpine loaded Eudragit nanosuspensions for ocular drug delivery. J Biomed Nanotechnol. 2013;9:124–31.

Kim K, Mersmann A. Estimation of metastable zone width in different nucleation processes. Chem Eng Sci. 2001;56:2315–24.

Klingler C, Müller B, Steckel H. Insulin-micro- and nanoparticles for pulmonary delivery. Int J Pharm. 2009;377:173–9.

Kreuter J, Alyautdin RN, Kharkevich DA, et al. Passage of peptides through the blood – brain barrier with colloidal polymer particles nanoparticles. Brain Res. 1995;6741:171–4.

Kumar S, Burgess DJ. Nanosuspensions. In: Wright JC, Burgess DJ, editors. Long acting injections and implants. New York: Springer; 2012. p. 239–61.

Kumar V, Wang L, Riebe M, Tung H, Prud'homme R. Formulation and stability of itraconazole and odanacatib nanoparticles: governing physical parameters. Mol Pharm. 2009a;6:1118–24.

Kumar V, Hong S, Maciag A, Saavedra J, Adamson D, Prud'homme R, Keefer L, Chakrapani H. Stabilization of the nitric oxide (NO) prodrugs and anticancer leads, PABA/NO and double JS-K, through incorporation into PEG-protected nanoparticles. Mol Pharm. 2009b;7:291–8.

Kwade A. Wet comminution in stirred media mills – research and its practical application. Powder Technol. 1999;105:14–20.

LaMer V, Dinegar R. Theory, production and mechanism of formation of monodispersed hydrosols. J Am Chem Soc. 1950;72:4847–54.

Lee J. Drug nano- and microparticles processed into solid dosage forms: physical properties. J Pharm Sci. 2003;92(10):2057–68.

Li C, Le Y, Chen J. Formation of bicalutamide nanodispersion for dissolution rate enhancement. Int J Pharm. 2011;404:257–63.

Lince F, Marchisio D, Barresi A. Strategies to control the particle size distribution of poly-[epsilon]-caprolactone nanoparticles for pharmaceutical applications. J Colloid Interface Sci. 2008;322:505–15.

Lince F, Marchisio D, Barresi A. A comparative study for nanoparticle production with passive mixers via solvent-displacement: use of CFD models for optimization and design. Chem Eng Process. 2011;50:356–68.

Lindenberg C, Mazzotti M. Effect of temperature on the nucleation kinetics of [alpha] l-glutamic acid. J Cryst Grow. 2009;311:1178–84.

Lindfors L, Skantze P, Skantze U, Westergren J, Olsson U. Amorphous drug nanosuspensions. 3. Particle dissolution and crystal growth. Langmuir. 2007;23:9866–74.

Lindfors L, Forssén S, Westergren J, Olsson U. Nucleation and crystal growth in supersaturated solutions of a model drug. J Colloid Interface Sci. 2008;325:404–13.

Liu Y, Kathan K, Saad W, Prud'homme R. Ostwald ripening of beta-carotene nanoparticles. Phys Rev Lett. 2007;98:036102.

Liu Y, Cheng C, Prud'homme R, Fox R. Mixing in a multi-inlet vortex mixer (MIVM) for flash nanoprecipitation. Chem Eng Sci. 2008;63:2829–42.

Liu Y, Huang L, Liu F. Paclitaxel nanocrystals for overcoming multidrug resistance in cancer. Mol Pharm. 2010a;7:863–9.

Liu Z, Huang Y, Jin Y, Cheng Y. Mixing intensification by chaotic advection inside droplets for controlled nanoparticle preparation. Microfluid Nanofluid. 2010b;9:773–86.

Liu P, Rong X, Laru J, Van Veen B, Kiesvaara J, Laaksonen T, Peltonen L. Nanosuspensions of poorly soluble drugs: preparation and development by wet milling. Int J Pharm. 2011;411:215–22.

Liu Y, Xie P, Zhang D, Zhang Q. A mini review of nanosuspensions development. J Drug Target. 2012;20(3):209–23.

Liu P, De Wolf O, Laru J, Heikkilä T, Van Veen B, Kiesvaara J, Hirvonen J, Peltonen L, Laaksonen T. Dissolution studies of poorly soluble drug nanosuspensions in non-sink conditions. AAPS PharmSciTech. 2013;14:748–56.

Liu T, Han M, Tian F, Cun D, Rantanen J, Yang M. Budesonide nanocrystal-loaded hyaluronic acid microparticles for inhalation: in vitro and in vivo evaluation. Carbohydr Polym. 2018;181:1143–52.

Liversidge GG, Cundy KC. Particle size reduction for improvement of oral bioavailability of hydrophobic drugs. I. Absolute oral bioavailability of nanocrystalline danazol in beagle dogs. Int J Pharm. 1995;125:91–7.

Loftsson T, Brewster ME. Pharmaceutical applications of cyclodextrins: basic science and product development. J Pharm Pharmacol. 2010;62:1607–21.

Lu Y, Ye L, Wu W. Injected nanocrystals for targeted drug delivery. Acta Pharm Sin B. 2016a;6(2):106–13.

Lu Y, Li Y, Wu W. Injected nanocrystals for targeted drug delivery. Acta Pharm Sin B. 2016b;6:106–13.

Lyczko N, Espitalier F, Louisnard O, Schwartzentruber J. Effect of ultrasound on the induction time and the metastable zone widths of potassium sulphate. Chem Eng J. 2002;86:233–41.

Mahajan A, Kirwan D. Rapid precipitation of biochemical. J Phys D Appl Phys. 1993;26:176–80.

Mahajan A, Kirwan D. Micromixing effects in a two-impinging-jets precipitator. AICHE J. 1996;42:1801–14.

Malamatari M, Taylor MG, Malamataris S, Douroumis D, Kachrimanis K. Pharmaceutical nanocrystals: production by wet milling and applications. Drug Discov Today. 2018;00(00):1–14.

Matteucci M, Hotze M, Johnston K, Williams R. Drug nanoparticles by antisolvent precipitation: mixing energy versus surfactant stabilization. Langmuir. 2006;22:8951–9.

Matteucci M, Paguio J, Miller M, Williams R III, Johnston K. Flocculated amorphous nanoparticles for highly supersaturated solutions. Pharm Res. 2008;25:2477–87.

Mauludin R, Müller RH, Keck CM. Development of an oral rutin nanocrystal formulation. Int J Pharm. 2009;370:202–9.

Mellaerts R, Mols R, Kayaert P, Annaert P, Van Humbeeck J, Van den Mooter G, Martens JA, Augustijns P. Ordered mesoporous silica induces pH-independent supersaturation of the basic low solubility compound itraconazole resulting in enhances transepithelial transport. Int J Pharm. 2008;357:169–79.

Meng X, Chen Y, Chowdhury S, Yang D, Mitra S. Stabilizing dispersions of hydrophobic drug molecules using cellulose ethers during anti-solvent synthesis of micro-particulates. Colloids Surf B Biointerfaces. 2009;70:7–14.

Merisko-Liversidge E, Liversidge GG. Nanosizing for oral and parenteral drug delivery: a perspective on formulating poorly-water soluble compounds using wet media milling technology. Adv Drug Deliv Rev. 2011;63:427–40.

Merisko-Liversidge E, Sarpotdar P, Bruno J, Hajj S, Wei L, Peltier N, Rake J, Shaw J, Pugh S, Polin L. Formulation and antitumor activity evaluation of nanocrystalline suspensions of poorly soluble anticancer drugs. Pharm Res. 1996;13:272–8.

Mitri K, Shegokar R, Gohla S, Anselmi C, Müller RH. Lutein nanocrystals as antioxidant formulation for oral and dermal delivery. Int J Pharm. 2011;420:141–6.

Moschwitzer JP. Drug nanocrystals in the commercial pharmaceutical development process. Int J Pharm. 2013;453(1):142–56.

Moschwitzer J, Muller RH. Spray coated pellets as carrier system for mucoadhesive drug nanocrystals. Eur J Pharm Biopharm. 2006;62:282–7.

Muller RH, Keck CM. Challenges and solutions for the delivery of biotech drugs – a review of drug nanocrystal technology and lipid nanoparticles. J Biotechnol. 2004;113:151–70.

Müller RH, Keck CM. Twenty years of drug nanocrystals: where are we, and where do we go? Eur J Pharm Biopharm. 2012;80:1–3.

Muller RH, Jacobs C, Kayser O. Nanosuspensions as particulate drug formulations in therapy. Rationale for development and what we can expect for the future. Adv Drug Deliv Rev. 2001;47:3–19.

Müller RH, Jacobs C, Kayser O. Nanosuspensions as particulate drug formulations in therapy: rationale for development and what we can expect for the future. Adv Drug Deliv Rev. 2001;47:3–19.

Mullin J, Nyvlt J. Programmed cooling of batch crystallizers. Chem Eng Sci. 1971;26:369–77.

Muntó M, Sala S, Cano M, Gimeno M, Ventosa N, Veciana J. New technologies for the preparation of micro- and nanostructured materials with potential applications in drug delivery and clinical diagnostics. Contrib Sci. 2005;3:11–8.

Murnane D, Marriott C, Martin G. Developing an environmentally benign process for the production of microparticles: amphiphilic crystallization. Eur J Pharm Biopharm. 2008;69:72–82.

Niwa T, Nakanishi Y, Danjo K. One-step preparation of pharmaceutical nanocrystals using ultra cryomilling technique in liquid nitrogen. Eur J Pharm Sci. 2010;41(1):78–85.

Noyes A, Whitney W. The rate of solution of solid substances in their own solutions. J Am Chem Soc. 1897;19:930–4.

Omar W, Mohnicke M, Ulrich J. Determination of the solid liquid interfacial energy and thereby the critical nucleus size of paracetamol in different solvents. Cryst Res Technol. 2006;41:337–43.

Otte A, Carvajal MT. Assessment of milling-induced disorder of two pharmaceutical compounds. J Pharm Sci. 2011;100:1793–804.

Owais M, Zia Q, Jamal F, Zubair S. Nanocrystal based therapeutics: scope and potential application in health sciences. Nanomed Nanotechnol J. 2019;2(1):122.

Panagiotou T, Mesite S, Fisher R. Production of norfloxacin nanosuspensions using microfluidics reaction technology through solvent/antisolvent crystallization. Ind Eng Chem Res. 2009;48:1761–71.

Patravale V, Date AA, Kulkarni R. Nanosuspensions: a promising drug delivery strategy. J Pharm Pharmacol. 2004;56:827–40.

Pattekari P, Zheng Z, Zhang X, Levchenko T, Torchilin V, Lvov Y. Top-down and bottom-up approaches in production of aqueous nanocolloids of low solubility drug paclitaxel. Phys Chem Chem Phys. 2011;13:9014–9.

Pawar VK, Singh Y, Meher JG, Gupta S, Chourasia MK. Engineered nanocrystal technology: in-vivo fate, targeting and applications in drug delivery. J Control Release. 2014;183:51–66.

Peltonen L, Hirvonen J. Pharmaceutical nanocrystals by nanomilling: critical process parameters, particle fracturing and stabilization methods. J Pharm Pharmacol. 2010;62:1569–79.

Peltonen L, Hirvonen J. Drug nanocrystals – versatile option for formulation of poorly soluble materials. Int J Pharm. 2018;537(1–2):73–83.

Stenger F, Peukert W. The role of particle interactions on suspension rheology – application to submicron grinding in stirred ball mills. Chem Eng Technol. 2003;26:177–83.

Rabinow BE. Nanosuspensions in drug delivery. Nat Rev Drug Discov. 2004;3:785–96.

Rawat RS. Dense plasma focus – from alternative fusion source to versatile high energy density plasma source for plasma nanotechnology. J Phys Conf Ser. 2015;591:012021.

Rijesh M, Deepak A, Dev K, Surendranathan AO, Sreekanth MS. Effect of milling time on production of aluminium nanoparticle by high energy ball milling. Int J Mech Eng Technol. 2018;9(8):646–52.

Salem H. Sustained-release progesterone nanosuspension following intramuscular injection in ovariectomized rats. Int J Nanomedicine. 2010;5:943–54.

Salem H, Abdelrahim M, Eid K, Sharaf M. Nanosized rods agglomerates as a new approach for formulation of a dry powder inhaler. Int J Nanomed. 2011a;6:311–20.

Salem H, Abdelrahim M, Eid K, Sharaf M. Nanosized rods agglomerates as a new approach for formulation of a dry powder inhaler. Int J Nanomedicine. 2011b;6:311–20.

Schöll J, Lindenberg C, Vicum L, Mazzotti M, Brozio J. Antisolvent precipitation of PDI 747: kinetics of particle formation and growth. Cryst Growth Des. 2007;7:1653–61.

Sharma S, Singh J, Verma A, Teja V, Shukla RP, Singh S, Sharma V, Konwar R, Mishra P. Hyaluronic acid anchored paclitaxel nanocrystals improves chemotherapeutic efficacy and inhibits lung metastasis in tumor-bearing rat model. RSC Adv. 2016;6:73083–95.

Shegokar R, Singh KK. Surface modified nevirapine nanosuspensions for viral reservoir targeting: in vitro and in vivo evaluation. Int J Pharm. 2011;421:341–52.

Shekunov B, Baldyga J, York P. Particle formation by mixing with supercritical antisolvent at high Reynolds numbers. Chem Eng Sci. 2001;56:2421–33.

Sheng JJ, Sirois PJ, Dressman JB, Amidon GL. Particle diffusional layer thickness in a USP dissolution apparatus II: a combined function of particle size and paddle speed. J Pharm Sci. 2007;97:4815–29.

Shubar HM, Lachenmaier S, Heimesaat MM, Lohman U, Mauludin R, Mueller RH, Fitzner R, Borner K, Liesenfeld O. SDS-coated atovaquone nanosuspensions show improved therapeutic efficacy against experimental acquired and reactivated toxoplasmosis by improving passage of gastrointestinal and blood-brain barriers. J Drug Target. 2011;19:114–24.

Sigfridsson K, Forssén S, Holländer P, Skantze U, Verdier J. A formulation comparison, using a solution and different nanosuspensions of a poorly soluble compound. Eur J Pharm Biopharm. 2007;67:540–7.

Söhnel O, Garside J. Precipitation: basic principles and industrial applications. Boston: Butterworth-Heinemann; 1992.

Sugimoto T. Formation of monodispersed nano- and micro-particles controlled in size, shape, and internal structure. Chem Eng Tech. 2003;26:313–21.

Sugimoto S, Niwa T, Nakanishi Y, Danjoa K. Development of a novel ultra cryo-milling technique for a poorly water-soluble drug using dry ice beads and liquid nitrogen. Int J Pharm. 2012a;426:162–9.

Sugimoto S, Niwa T, Nakanishi Y, Danjoa K. Novel ultra-cryo milling and co-grinding technique in liquid nitrogen to produce dissolution-enhanced nanoparticles for poorly water-soluble drugs. Chem Pharm Bull. 2012b;60:325–33.

Sultana S, Talegaonkar S, Ali R, Mittal G, Bhatnagar A, Ahmad F. Formulation development and optimization of alpha ketoglutarate nanoparticles for cyanide poisoning. Powder Technol. 2011;211:1–9.

Sun Y. Supercritical fluid technology in materials science and engineering: syntheses, properties, and applications. New York: Marcel Dekker; 2002.

Teychene S, Biscans B. Nucleation kinetics of polymorphs: induction period and interfacial energy measurements. Cryst Growth Des. 2008;8:1133–9.

Thanki K, Gangwal RP, Sangamwar AT, Jain S. Oral delivery of anticancer drugs: challenges and opportunities. J Control Release. 2013;170:15–40.

Thybo P, Hovgaard L, Lindeløv J, Brask A, Andersen S. Scaling up the spray drying process from pilot to production scale using an atomized droplet size criterion. Pharm Res. 2008;25:1610–20.

Trapani G, Denora N, Trapani A, Laquintana V. Recent advances in ligand targeted therapy. J Drug Target. 2012;20:1–22.

Trasi NS, Byrn SR. Mechanically induced amorphization of drugs: a study of the thermal behavior of cryomilled compounds. AAPS PharmSciTech. 2012;13:772–84.

Uemoto Y, Toda S, Adachi A, Kondo K, Niwa T. Ultra cryo-milling with liquid nitrogen and dry ice beads: characterization of dry ice as milling beads for application to various drug compounds. Chem Pharm Bull. 2018;66(8):794–804.

Valencia P, Basto P, Zhang L, Rhee M, Langer R, Farokhzad O, Karnik R. Single-step assembly of homogenous lipid-polymeric and lipid-quantum dot nanoparticles enabled by microfluidic rapid mixing. ACS Nano. 2010;4:1671–9.

Van Eerdenbrugh B, Froyen L, Van Humbeeck J, Martens JA, Augustijns P, Van den Mooter G. Drying of crystalline drug nanosuspensions the importance of surface hydrophobicity on dissolution behavior upon redispersion. Eur J Pharm Sci. 2008;35(1):127–35.

Verma S, Gokhale R, Burgess D. A comparative study of top-down and bottom-up approaches for the preparation of micro/nanosuspensions. Int J Pharm. 2009;380:216–22.

Vidlářová L, Romero GB, Hanuš J, Štěpánek F, Müller RH. Nanocrystals for dermal penetration enhancement – effect of concentration and underlying mechanisms using curcumin as model. Eur J Pharm Biopharm. 2016;104:216–25.

Wang Q, Wang J, Yu W, Shao L, Chen G, Chen J. Investigation of micromixing efficiency in a novel high-throughput microporous tube-in-tube microchannel reactor. Ind Eng Chem Res. 2009;48:5004–9.

Wang J, Zhang Q, Zhou Y, Shao L, Chen J. Microfluidic synthesis of amorphous cefuroxime axetil nanoparticles with size-dependent and enhanced dissolution rate. Chem Eng J. 2010;162:844–51.

Wang T, Qi J, Ding N, Dong X, Zhao W, Lu Y, Wang C, Wu W. Tracking translocation of self-discriminating curcumin hybrid nanocrystals following intravenous delivery. In J Pharm. 2018;546:10–9.

Wojnarowska Z, Grzybowska K, Adrjanowicz K, Kaminski K, Paluch M, Hawelek L, Wrzalik R, Dulski M, Sawicki W, Mazgalski J, Tukalska A, Bieg T. Study of the amorphous glibenclamide drug: analysis of the molecular dynamics of quenched and cryomilled material. Mol Pharm. 2010;7(5):1692–707.

Wong S, Ward M, Wharton C. Micro T-mixer as a rapid mixing micromixer. Sensors Actuators B Chem. 2004;100:359–79.

Xia D, Quan P, Piao H, Piao H, Sun S, Yin Y, Cui F. Preparation of stable nitrendipine nanosuspensions using the precipitation–ultrasonication method for enhancement of dissolution and oral bioavailability. Eur J Pharm Sci. 2010;40:325–34.

Yadav K, Sawant K. Modified nanoprecipitation method for preparation of cytarabine-loaded PLGA nanoparticles. AAPS PharmSciTech. 2010;11:1456–65.

Yadav TP, Yadav RM, Singh DP. Mechanical milling: a top down approach for the synthesis of nanomaterials and nanocomposites. Nanosci Nanotechnol. 2012;2(3):22–48.

Yang H, Chu G, Zhang J, Shen Z, Chen J. Micromixing efficiency in a rotating packed bed: experiments and simulation. Ind Eng Chem Res. 2005;44:7730–7.

Yang W, Johnston KP, Williams RO III. Comparison of bioavailability of amorphous versus crystalline itraconazole nanoparticles via pulmonary administration in rats. Eur J Pharm Biopharm. 2010;75:33–41.

Yang C, Gao S, Dagnæs-Hansen F, Jakobsen M, Kjems J. Impact of peg chain length on the physical properties and bioactivity of PEGylated chitosan/siRNA nanoparticles in vitro and in vivo. ACS Appl Mater Interfaces. 2017;9:12203–16.

Yen F, Wu T, Tzeng C, Lin L, Lin C. Curcumin nanoparticles improve the physicochemical properties of curcumin and effectively enhance its antioxidant and antihepatoma activities. J Agric Food Chem. 2010;58:7376–82.

Zhai X, Lademann J, Keck CM, Müller RH. Dermal nanocrystals from medium soluble actives–physical stability and stability affecting parameters. Eur J Pharm Biopharm. 2014;88:85–91.

Zhang H, Wang J, Zhang Z, Le Y, Shen Z, Chen J. Micronization of atorvastatin calcium by antisolvent precipitation process. Int J Pharm. 2009a;374:106–13.

Zhang Z, Shen Z, Wang J, Zhao H, Chen J, Yun J. Nanonization of megestrol acetate by liquid precipitation. Ind Eng Chem Res. 2009b;48:8493–9.

Zhang H, Wang J, Shao L, Chen J. Microfluidic fabrication of monodispersed pharmaceutical colloidal spheres of atorvastatin calcium with tunable sizes. Ind Eng Chem Res. 2010;49:4156–61.

Zhao H, Wang J, Wang Q, Chen J, Yun J. Controlled liquid antisolvent precipitation of hydrophobic pharmaceutical nanoparticles in a microchannel reactor. Ind Eng Chem Res. 2007;46:8229–35.

Zhao H, Wang J, Zhang H, Shen Z, Yun J, Chen J. Facile preparation of danazol nanoparticles by high-gravity anti-solvent precipitation (HGAP) method. Chin J Chem Eng. 2009;17:318–23.

Zhao R, Hollis CP, Zhang H, Sun L, Gemeinhart RA, Li T. Hybrid nanocrystals: achieving concurrent therapeutic and bioimaging functionalities toward solid tumors. Mol Pharm. 2011;8:1985–91.

Zheng Z, Zhang X, Carbo D, Clark C, Nathan C, Lvov Y. Sonication-assisted synthesis of polyelectrolyte-coated curcumin nanoparticles. Langmuir. 2010;26:7679–81.

Zhi M, Wang Y, Wang J. Determining the primary nucleation and growth mechanism of cloxacillin sodium in methanol-butyl acetate system. J Cryst Grow. 2011;314:213–9.

Zhong J, Shen Z, Yang Y, Chen J. Preparation and characterization of uniform nanosized cephradine by combination of reactive precipitation and liquid anti-solvent precipitation under high gravity environment. Int J Pharm. 2005;301:286–93.

Zhu Z, Anacker J, Ji S, Hoye T, Macosko C, Prud'homme R. Formation of block copolymer-protected nanoparticles via reactive impingement mixing. Langmuir. 2007;23:10499–504.

Zhu Z, Margulis-Goshen K, Magdassi S, Talmon Y, Macosko C. Polyelectrolyte stabilized drug nanoparticles via flash nanoprecipitation: a model study with L-carotene. J Pharm Sci. 2010a;99:4295–306.

Zhu W, Wang J, Shao L, Zhang H, Zhang Q, Chen J. Liquid antisolvent preparation of amorphous cefuroxime axetil nanoparticles in a tube-in-tube microchannel reactor. Int J Pharm. 2010b;395:260–5.

Microfluidics Technology for Nanoparticles and Equipment

4

Salwa and Lalit Kumar

Abstract

"Microfluidics" is a generalized term denoting both, the science studying the conduct of fluids (gases and liquids) through microchannels and the manufacturing technology of micro miniature devices containing chambers and tunnels through which fluids flow or are confined to flow. Advancement in the field of nanotechnology has emphasized on the use of microfluidics due to several benefits associated with this technology in comparison to conventional techniques of nanoparticle fabrication. Microfluidic reactors have offered a vast range of advantages including better controllability and uniformity of nanoparticle characteristics. Potential applications of nanoparticles have made them an undeniable tool in the field of pharmaceuticals. Though nanoparticles are foreseen to overcome the challenges in effective delivery of therapeutic agents, the drawbacks associated with traditional preparation techniques has resulted in slow translation from research to clinical applications. Production of nanoparticles in commercial scale is an existing active challenge which could be overcome by the exciting opportunities of microfluidic technology to develop easy, safe and cost-effective drug delivery systems with good reproducibility. This chapter encompasses an overview of microfluidics technology in the production of nanoparticles and the use of micro devices as tools for investigation.

Keywords

Microfluidics · Nanoparticles · Micro-mixers · Reactor · Microparticles · Microfluidic technology · Microdevices, etc.

1 Introduction

A revolutionary novel approach has been promised by the superior properties of nanoparticles which will have a major influence in wide variety of novel applications. Nanotechnology field is booming its development with manufacturing of nanostructured materials being the sparkling topic of research. "Microfluidics" is a generalized term denoting both, the science studying the conduct of fluids (gases and liquids) through micro channels and the manufacturing technology of micro miniature devices containing chambers and tunnels through which fluids flow or are confined to flow. Microfluidics is rapidly emerging as a breakthrough technology with its key attributes being processing of fluids (from 10^{-9} to

Salwa · Lalit Kumar (✉)
Department of Pharmaceutics, Manipal College of Pharmaceutical Sciences, Manipal Academy of Higher Education, Udupi, Karnataka, India
e-mail: lalit.kumar@manipal.edu

J. K. Patel, Y. V. Pathak (eds.), *Emerging Technologies for Nanoparticle Manufacturing*,
https://doi.org/10.1007/978-3-030-50703-9_4

10^{-18} L) in conduits with dimensions of tens to hundreds of microns and multidisciplinary nature of the physical principles and of the manufacture of the devices being used. The development and success of new applications has shown the value of the technology since its inception. The early applications of microfluidic devices were prompted by their capability to utilize lesser volumes of samples and reagents, perform analyses in a short period of time due to short diffusion distances and attain high level of compactness due to system unification (Vladisavljević et al. 2013). Microfluidics can provide an effective way of controlling mixing, saving sample consumption, achieving consistent particle size and producing materials with new structures and functions (Edel et al. 2002).

Due to challenges in the commercialization of this technology, microfluidics is not being widely used, yet despite compelling advantages, it seems that this technology has many promising advantages. Microfluidics is also known to be a medium for chemical and biomedical applications called Lab-on-a-Chip (LOC) or micro total analysis systems (μTAS) (Sackmann et al. 2014). Microfluidic device allows for single unit operation or incorporates multiple unit operations. Flow inside microfluidic devices is almost always laminar which denotes that mixing usually takes place by molecular diffusion enabling complete mixing within seconds or minutes unlike conventional flask-based systems which could take days (Janasek et al. 2006). Advantages of microfluidics include enabling of complete mixing, significant reduction in the volumes of sample and reagents, cost saving on reagents and less waste production (Tarn and Pamme 2014). Development of LOC devices has strongly motivated the microfluidic research, and it is anticipated to bring breakthrough transformation in the field of biology and chemistry. Microfluidic devices are microsystems that are capable of integrating the entire laboratory into one chip because of the convergence of microfluidic channels and active or passive elements, namely, valves, mixers, filters and so on. The ability of microfluidic devices to manipulate small amounts of fluids is where their major advantage lies, contributing to the likelihood of very limited sample analysis and thus making most of the bioanalysis less invasive and practical in unspecialized point of care centres. Further, microfluidic proceedings render a positive environmental impact by reducing the usage of reagents and allow highly automated measurements (Bragheri et al. 2020).

Microfluidic devices have enabled "sample in-report out" capability with shorter analysis time being performed on a single device including all the aspects of an analysis process, from sampling to detection (Gubala et al. 2011) (Fig. 4.1). Due to benefits achieved from the precise management and handling of biological particles and

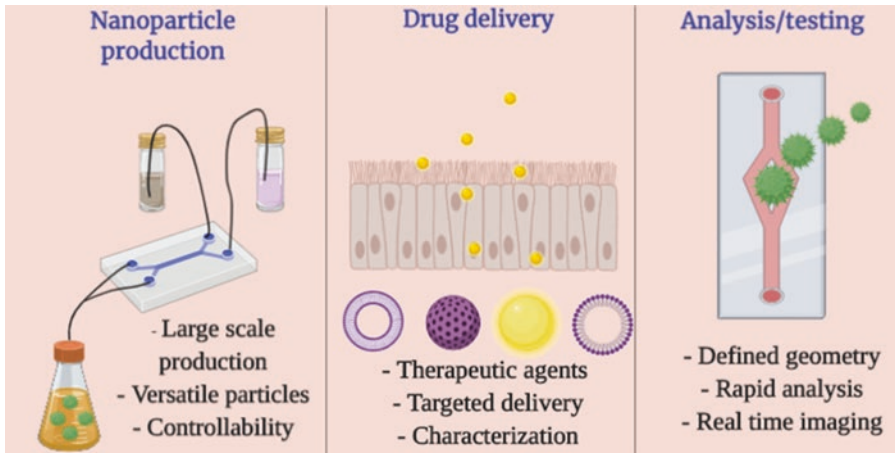

Fig. 4.1 Applications of microfluidic technology

their neighbouring microenvironment, this interesting technique has substantial advantages over traditional macroscale systems (e.g., centrifuge, flow cytometry etc.).

The merits of microfluidics include but are not confined to

(i) smaller sample size and volume of reagents,
(ii) rapid processing of specimens,
(iii) extreme sensitivity,
(iv) inexpensive,
(v) increased portability and
(vi) well integrated and automated capacity to decrease human interference and error (Bhagat et al. 2010; Zhang et al. 2016a, b, c).

Although in the nascent stage, microfluidics has found its applications in diverse fields ranging from biology to information technology (Fig. 4.1). Because of the need for more effective analytical methods such as gas chromatography (GC), high-performance liquid chromatography (HPLC) and capillary electrophoresis, the original application source for microfluidics technology started in chemical analysis, creating a true revolution. Such techniques have been used in conjunction with high-power lasers to enhance the sensitivity and resolution of optical detection instruments while utilizing smaller quantity of samples at low molecular concentrations. Possession of chemical and biological weapons by the countries at the end of Cold War led to the origin of (prompted) second branch of microfluidics resulting in the development of effective and portable detection systems using microfluidic devices. In 1980s, genomics research explosion in the field of molecular biology led to third impact on microfluidics development. And the last contribution came from microelectronics.

2 Principle Foundation

Microfluidics involves developing structures where it is possible to use small amount of fluids. At microscale, fluids behave differently including surface tension and patterns of energy dissipation. Microfluidic systems are not miniaturized versions of their macroscale counterparts as most of the physical characteristics, including surface-to-volume ratio and mass transfer dependent on diffusion, do not increase proportionally from macro to micro domains. Omnipresence of laminar flow due to chief position of viscous forces is one the peculiar characteristic represented by the microfluidic systems. Flow of liquids is usually categorized into *laminar and turbulent*. For the laminar flow systems, currents of the fluid will stream in parallel under constant environmental conditions and the velocity does not change over time at any point within. It allows mass transfer solely in the flow direction by convection, and a mixture is obtained only by molecular diffusion. But the turbulent flow is characterized by space and time changes in vortex formation and flow. From the physical perspective, the two mechanisms vary with regard to the relative significance of viscous forces (friction by the channel walls) and inertial forces (fluid momentum) and are measured by the Reynold's number. Reynolds number is low in micro channels with 10–500 nm diameter. This results in laminar flow without any turbulence and the mixture of fluids is influenced by diffusion. The viscosity effect is dominated over the inertial effects at low Reynolds number and complete laminar flow is produced.

Reynolds number (Re) is calculated using the below formula:

$$\mathrm{Re} = \frac{\text{Intertial Forces}}{\text{Viscous Forces}} = \frac{V_S D}{\mu}$$

Where, V_s = characteristic velocity of the fluid, D = diameter of the conduct through which the fluid passes or characteristic length and μ = dynamic viscosity of the fluid.

3 Mixing

Micromixer architecture is usually designed to reduce the direction of mixing and augment the surface area of touch. Depending on the process used to achieve microscale mixing, micromixers are classified into two categories: passive or active.

3.1 Active Micromixers

External source of energy is used in active micromixers and also in fluid pumping power to produce time-dependent disturbances of the stream field and speed up the mixing mechanism (Yaralioglu et al. 2004). Based on the external forces used, micromixers are categorized as pressure field driven, acoustic (ultrasound) driven, temperature induced or magneto hydrodynamic. Compared to passive micromixers, active micromixers generally have lower mixing efficiency. The implementation of such systems in commercial applications is minimal due to the need for integration of the system with peripheral devices (actuators for external power source) and the tedious and costly manufacturing techniques. Therefore, usage of external sources of energy (in the form of ultrasonic waves) could lead to creation of high temperature gradients that could seriously harm the bio actives. For the above reasons, active mixers do not seem to be a sensible choice for the application of microfluidics in medical, chemical and biological applications (Nguyen and Wu 2004).

3.2 Passive Micromixers

Passive micromixers solely rely on fluid pumping power, and they use different channel designs so as to reorganize the fluid flow so as to decrease the diffusion length and increase the contact surface area. Compared to active micromixers, associated cost effectiveness and flexible manufacturing routes made the passive micromixers to be reported as first microfluidic device. With more advanced LOC devices, they can be easily integrated. The mixing time can be minimized by separating the fluid flow by sequential or parallel lamination, hydrodynamically concentrating fluid flows, adding gas or liquid bubbles into the stream or improving messy advection by using ribs and groves installed over the walls of the channel.

4 Microfluidic Reactors: Features for the Manufacture of Nanoparticles

Microfluidic reactors provide interchangeable design having the ability to increase the number of modules that can be tailored to different system requirements. Microfluidic technology provides the opportunity to synthesize nanomaterials at the stage of use. This removes the need for hazardous materials to be processed and transported and allows the handling of nanoparticles that are susceptible to ageing or phase change, depending on localized conditions or are not economically viable for mass manufacturing. Scaling up of the fabrication by “numbering up” (arrangement of parallel microreactors) allows for a combination of capital investment and market growth, lowering the risk of investment, that is worthwhile in developing fields like nanotechnology. Microfluidic reactors are continuous flow chemical synthesis reactors that usually contain a network of diminutive flow streams below the range of millimetres. The channel grid is patterned to increase the efficiency of the nanoparticle towards appropriate shape, composition or size distribution of the desired reaction. Microfluidic reactors have progressed from basic tubing to advanced and dynamic devices incorporating converging management of controlling parameters and techniques for in situ characterization in a chip.

A number of features make microfluidic reactors particularly attractive compared to conventional macroscale reactors in the manufacture and scrutinization of nanomaterials. Many of these attributes are derived from the microchannel’s specific flow characteristics in the microchannel and the microfluidic domain in general, such as the ubiquity of the fairly inevitable laminar flow and a larger volume-to-surface ratio.

The nanomaterial processing implications and benefits of these properties are briefly described as follows:

- Under continuous flow conditions, efficient and controllable mixing occurs leading to the

formation of a homogeneous environment for the reaction to take place.
- Greater and effective regulation of temperature and transfer of heat.
- *In situ* tracking of the progression of nanoparticle production by a resolution dependent on residence time.
- Temporal reaction regulation by adding reagent during the reaction phase at exact time intervals.
- Monitor nanoparticles characteristics by monitoring the process kinetics.
- High throughput testing of different formulations by adjusting the system parameters on-line.
- Post synthesis integration of processes and measurement systems on a platform of single technology.
- By increasing the number of microreactors, there is possibility to extend the process.

Previously mentioned array of features shows considerable potential of microfluidics to translate current traditional batch technology into continuous microfluidic process for the development of nanoparticles. Various researchers have focused in this direction and made significant advances; however, this technology is yet at the stage of infancy and more work needs to be carried out so as to prove the effectiveness of microfluidic technology over the traditional batch method.

5 Design of the Reactor

Conventional batch techniques lack meticulous control upon the mixing rate and level of supersaturation, resulting in unregulated processes of nucleation and development, leading to poor control over the ultimate characteristics of particles. Steady transfer of heat/mass can significantly enhance the controllability of these properties, which in return determines the physico-chemical characteristics of the nanomaterials prepared. In this regard, microscale reactors could bestow homogeneous, efficient (by fraction to hundreds of milliseconds) and replicable mixing conditions, reflecting a means of obtaining nanoparticles with outstanding structural properties theoretically. Microscale mixers are distinguished by greater surface-to-volume ratio, which provides the opportunity to increase mass and heat transmission compared to traditional mass mixing units. This results in a drastically reduced mixing period relative to the nucleation and growth kinetics, which opens up the opportunity of exerting control over them. Microreactors for nanomaterial development can be divided in two groups with regard to the mixing method and the features of the device: segmented flow microreactors and continuous flow.

Advantages of microfluidic technology (Park et al. 2010; Wang et al. 2011; Capretto et al. 2013; Zhao 2013) are as follows:

1. Reagent consumption in minute quantities, about 10^2–10^3 times lesser than conventional techniques, thus solving economic and safety issues.
2. Larger surface area provides improved mass and heat transfer.
3. Provides precise control over flow.
4. Continuous flow processes.
5. Reduced mixing time.
6. Reproducibility.
7. Consumption of less power.
8. Rapid production of libraries of various materials by altering fluid phase composition and flow rate.
9. Produces particles with a co-efficient of variation of<5% and higher efficiency of encapsulation.
10. Due to integration and low power consumption, miniaturization allows portability and on spot analysis.
11. Microfluidic chip parallelization allows for high-performance and multiple analyses at a time.
12. Rapid evaluation and quick response owing to shorter diffusion path.
13. Rapid testing of nanoparticles in various phases of clinical development.

Disadvantages (Khan et al. 2015) are as follows:

1. New technology, not yet fully understood.
2. At microscale, surface forces such as surface tension, van der Waals, electrical and

roughness of the surface dominate, making these reactions more complex than the macroscale.

3. Emulsification is a time-consuming technique and the production is small, with microfluidic emulsion droplets forming at tens to hundreds of microliters/minute (small production rate of nanoparticles).

6 Fabrication of Microfluidic Devices

The need of higher extent of integration in microfluidic devices opens up opportunities for modern fabrication technologies with the potential to miniaturize many core fluidic components aiming to improve the compactness of these devices and their functionalities (Bragheri et al. 2020). A broad spectrum of materials is used by different processes for the manufacture of microfluidic devices. During the initial development of microfluidics, silicon and glass materials were used for the manufacture of devices via photolithography and wet etching methods. Today, though these materials (Table 4.1) are still used, they have been replaced by polymer material due to their amenability to mass fabrication (Tarn and Pamme 2014). However, research lab now-a-days employ a flexible elastomer material, poly(dimethylsiloxane) (PDMS), that is better suited for rapid prototyping. Paper microfluidic devices are being developed recently (Li et al. 2012). Fabrication typically follows the mechanism of assembling channels on the surface of a solid substrate, before drilling or punching entry holes into the substratum, and eventually binding them to another plate in order to seal the channels. Solutions are allowed to be introduced by connecting tubing or reservoirs to the access holes (Tarn and Pamme 2014).

The fabrication technique of microfluidic reactors has been derived from microelectronic technology. The following processes can be characterized conservatively as soft lithographic microfabrication processes that can vary significantly based on the final product: cover design and manufacturing, mould creation, moulding and demoulding, punching and bonding of PDMS. Most of the moulds are generally designed using photolithography on a silicon wafer substratum using UV curable polyepoxide resin negative photoresist called U-8. Blueprints of micropatterned mould designs were initially done in computer aided design (CAD) for use as negative photomasks on transparent films. After figuring the silicon wafer with the required designs, PDMS that is not crosslinked is gushed into the mould, healed and demoulded. The demolished PDMS substrates are later punched to make input and output ports for any media reservoir, hydrogel seed ports, actuation chambers, and other characteristics that can be incorporated in a model.

Glass has been the most common product in most reagents and solvents since it is chemically inert. Glass visibility allows microchannel visual inspection in the manufacture of nanostructures. It is well known to detect a fouling system and manufacturing procedures. Glass has low thermal

Table 4.1 Materials used in fabrication of microfluidic moulds

Fabrication material	Advantages	Disadvantages
PDMS	Inexpensive material, easily mouldable into channels, produces micrometre-sized features with high fidelity, low permeability to water, easy usage and optically transparent	Upon contact with organic solvents, acids or bases, swelling and degradation will take place; hydrophobic, surface absorption of small molecules and preparation in clean rooms is required
Silicon	Stable at higher temperatures and chemically inert, readily available	Expensive, fragile and opaque to UV and visible light
Glass (borosilicate, quartz, crown white, soda lime glass)	Inexpensive, optically transparent, efficient heat dissipation, chemically inert, rigid, resistant to high temperatures and can be easily modified	Difficult to fabricate, preparation in clean rooms is required sometimes

conductivity which restricts the features that require good transfer of heat. Because methods developed for the production of semiconductor chips can be used to generate a variety of 3D configurations. Silicon has also found extensive usage in the manufacture of microreactors. In contrast to glass, silicon and oxidized silicon are chemically resistant to several reagents and solvents that provide excellent heat transfer capabilities for silicon-based reactors. Exothermic reactions requiring rapid removal of heat and also the reactions requiring extremely high or low temperatures are benefitted from the microreactors made of silicon. There is no doubt that the technology of silicon is by far the most modern technology in production. Lithographic structuring and consequent etching (wet and dry etching) enable designs to be sculpted with great precision into micron range wafers. Inoxidable steel is the standard material for process chemistry, and the reactors based on stainless steel chips were produced, including modular systems such as micromixers and heat exchangers. Microreactors of stainless steel are usually made using traditional machining, electroforming, electro-discharge (EDM) and laser ablation. Measurements of such reactor systems are usually bigger than that of glass or silicon reactors since the determination of the production methods is less precise than that used in glass or silicon. Steel-based flow chips are particularly beneficial for operations including high heat loads and hazardous chemicals, except for synthesis processes involving strong acids, because of the better chemical stability and thermal resistivity of stainless steel. Microflow systems based on polymers, produced from polymers such as PDMS, are cheaper and simple to manufacture. The vast range of plastic products, showing a broader range of characteristics, deals with a void in micro-system manufacturing. It is quite simple to reproduce chips, but most of the solvents used to synthesize nonaqueous nanoparticles are incompatible with these polymers showing minimal mechanical strength and poor thermal conductivity. Therefore, the employment of these reactors is often limited at atmospheric pressure and mild temperatures to aqueous wet-chemistry methods. Their manufacture follows the common technique of soft lithography, in which a negative photoresist is being used to construct a master chip, preceded by casting of the silicon elastomer on this mould and further healing. The PDMS coating is stripped off to close the channels and applied to a glass slide. Some popular replication technologies, like hot embossing and microinjection moulding, are available. In polymer-based chips, some new polymers were applied to overcome the PDMS drawbacks.

7 Microfluidic Devices: Types

The two most widely used devices for production of nanoparticles are as follows:

(a) *Microchannel-based devices* – These are the devices that integrate multiple functions and are made using various materials such as glass, silicon, stainless steel, metals and polymers by various micro-manufacturing processes such as micromachining, micromilling, lithography and mould duplication. In this device, minimization of interfacial area will result in spontaneous droplet formation, and therefore when flow rate of oil phase is kept within certain range, the droplet size will only be dependent on the microchannel geometry (Martins et al. 2018). These devices are costly and time-consuming to produce, but they are uncomplicated to operate and can also be combined to obtain higher yields.

(b) *Microcapillary-based devices* – They are made of readily available commercially cheap parts, but they are highly efficient as devices based on microchannels (Khan et al. 2013). It is possible to manufacture and operate these systems under vigorous chemical conditions in very less time. Capillary-based devices represent the simplest design configuration in the order of microns consisting primarily of silica, steel or polymer capillary tubes. They are used in the simplest function to control tiny scale flows in the preliminary test. Generally used for the fabrication of metal nanoparticles with increased output of nanoparticles through rapid and

precise temperature control. In the development of metal and semiconductor nanocrystals, ease of manufacture and operation, use of robust materials that can resist higher temperature has gained attention on the capillary devices. Sometimes lining up the capillaries and placing them in parallel becomes very difficult and they also suffer from lumen blockage, chemical adhesion to the channel surface and high polydispersity of the product. In certain situations, these drawbacks are faced with the use of coaxial tube reactors or segmented flows, wherein two immiscible laminar flow liquids result in the formation of reactant solution droplets that avoid contact with the reactor walls of the reacting stage.

8 Formulation of Nano Drug Delivery System Using Microfluidics

Approaches of diverse variety have been reported to fabricate microscale and nanoscale particles. Currently, substantial concentration is being given to development of organic nanocarriers particularly in pharmaceuticals unlike past where tremendous interest of scientists was to develop inorganic nanocarriers. Though nanoparticles are foreseen to repress the challenges in effective delivery of therapeutics, the drawbacks associated with traditional preparation techniques has resulted in slow translation from research to clinical applications. In such scenario, microfluidic technology has taken a front seat as an advanced approach in the development of drug delivery systems with better physico-chemical properties and reproducibility. Potential applications of nanoparticles have made them an undeniable tool in the field of pharmaceuticals. Pharmaceutical researchers have begun to realize the important attributes that microfluidic technique has bestowed on nanocarriers. Microfluidic synthesis has been suggested to be predominant in comparison to benchtop techniques for producing better quality, monodisperse particles because of the capability to retain precise control of all solution variables which includes concentration of the reactant, temperature and time of reagent addition. Nanotechnology in medicine, especially for drug delivery, is spreading rapidly. The drug delivery method for nanoparticles is the science and technology of a nano-meter scale (10–1000 nm), comprising of two major ingredients, one of which is an active pharmaceutical ingredient and another is an excipient required for the development of such systems. There has already been extensive testing of nanostructures such as liposomes, lipid nanocarriers, conjugated polymers, dendrimers, magnetic nanoparticles, nanoparticles made from inorganic materials like silicon and carbon. They have unique physical, optical and electronic characteristics. In the nucleus of nanoparticles, nano drug carriers encapsulate and adsorb the drug on their surface. Pure drug nanoparticles dispersed as nanocrystals or amorphous precipitates were also identified.

Processing techniques for nanoparticles include dialysis, solvent evaporation, nanoprecipitation, emulsification/solvent diffusion and supercritical fluid technology. Depending on the application of the material, the selection of the preparation method must be adjusted to achieve the properties of interest. Nanoparticles produced in conventional equipment using the aforementioned technologies are deficit of control over mixing, nucleation and growth phenomena which ultimately lead to end products with a large particle size distribution that is a major disadvantage (Zhao et al. 2011; Khan et al. 2015). More recently, a narrow distribution synthesis of nanoparticles has been reported using microfluidics in which the hydrodynamic flow is exclusively laminar with a Reynold number not exceeding 20 allowing regulated and reproducible fluid flow properties. This removes unregulated physicomechanical and chemical instability linked to large-scale structures. In addition, stream relative flow rates and preformed polymers or monomers are modified to form nanoparticles of different regulated sizes and size distributions.

Nanoparticle drug delivery is quite challenging because of quality control check during

fabrication, batch-to-batch product dissimilarity and non-reproducible test results. There is a pressing need to develop stable, reproducible, high throughput and cost-effective methods for the preparation of nanoparticles. In this context, microfluidic engineering has emerged as a powerful tool in the high throughput, managed and direct material preparation for various applications (Zhang et al. 2016a, b, c). Microfluidic reaction system offers clear advantage over bulk synthesis, most notably in their ability to fine tune the physical and chemical compositions of the final product.

The use of nanoparticles for therapeutics and diagnostics has a significant promise in the treatment of major diseases. Nonetheless, the transition of nanoparticles from bench to bedside has progressed at a slower pace due to the difficulty of generating accurate batch-to-batch nanoparticles, the lack of rapid testing, the lack of ability to obtain physiologically pertinent test results in traditional pre-screening platforms in vitro (Kim and Langer 2015) and higher production costs. Through solving some of these problems, microfluidic technologies offer a way to accelerate the clinical translation of nanoparticles (Khan et al. 2015). Latest developments in microfluidics have allowed a young generation of nanoparticle production and delivery techniques and demonstrated the scope for enhanced explanatory power of preclinical nanoparticle research in the biomimetic microfluidic system.

8.1 Pure Drug Nanoparticles

More recently, the focus of different researchers has moved to active pharmaceutical ingredient nanoparticles due to their significant effect in improving the therapeutic efficacy of different drugs. There are preparations for both amorphous and crystalline nanoparticles, but more focus has been paid to the latter. Pharmaceutical nanocrystals consist of active pharmaceutical ingredient (API), which is often prepared in an aqueous solution with a stabilizer. Approximately 40% of newly developed APIs suffer from poor water solubility and due to their lower level of dissolution, bioavailability will be limited (Zhao et al. 2007). While there are many techniques available to improve solubility and bioavailability, the reduction of particle size has appeared as a flexible method (Merisko-Liversidge et al. 2003). When manufactured in bulk, small particles suffer from a high polydispersity index, while the microfluidic approach allows the processing of dispersed nanoparticles, both amorphous and crystalline.

8.1.1 Crystalline Drug Nanoparticles

Dev et al. prepared crystalline drug nanoparticles in a vigorous micromixing environment, produced by means of a rapidly rotating surface consisting of a 6 cm diameter hollow thin cylinder with a length of 30 cm rotating at a speed of 2000 rpm (Dev et al. 2011). Meloxicam nanoparticles were prepared by maintaining all the process parameters constant except for speed of rotations which resulted in 20–200 nm size range. Nanoparticles prepared with higher speed have a uniform morphology with smaller size due to reduced fluid density, which ultimately influences local supersaturation and obtains ultrafine crystalline nanoparticles. Meloxicam nanoparticles when coated with polymer (poloxamer 188) were found to be more stable, spherical in shape and uniform with smooth surface. Differential scanning calorimetry (DSC) and X-ray diffraction (XRD) can be used to prove the crystalline structure of the product nanoparticles. Enhancement level of meloxicam nanoparticles dissolution has been documented compared to micronized drug that may be due to nanosizing, normal size and increased specific surface area. The dissolution frequency depends on the regularity and form of the particles. Dissolution profile decreases for particles of the same size as the rate of brittleness and irregularity increases (Mosharraf and Nyström 1995). Oral bioavailability of danazol increased from 5.1% to 82.3% due to the level of increased speed of dissolution and solubility of saturation leading to rapid and full dissolution, which is an important factor in drug absorption (Liversidge and Gundy 1995). Zhao et al. prepared danazol nanoparticles of crystalline from using a Y-shaped microchannel

reactor by liquid antisolvent (AS) precipitation (LASP) method without any additives and recorded 100% dissolution of nanoparticles in 5 min compared to 35% of raw danazol particles. The team also investigated the influence on particle size of the antisolvent/solvent ratio (AS/S, i.e. deionized water/ethanol) and reported that small particle sizes were achieved by increasing the AS/S ratio from 5 to 40. This may be attributed to an immediate rise in the danazol solution's super-saturation level and a decrease in the solute concentration on the formed crystal layer (Zhao et al. 2007).

8.2 Amorphous Drug Nanoparticles

Amorphous nanoparticles have an aberrant shape which can be broken into parts of the heart and outer shell. The core part is similar to the amorphous bulk part and due to large structural defects the shell is more porous (Vo and Ganguli, 2012). Wang et al. prepared volume controlled nanoparticles of amorphous cefuroxime axetil (CFA) by precipitation AS using a Y junction microchannel reactor. The mixture of acetone and isopropyl ether was used respectively as solvent and CFA AS. Reduction in particle size was accomplished by decreasing temperature, CFA concentration and CFA solution flow rate in acetone or by rising the rate of flow of AS. SEM images of the prepared nanoparticles seemed more consistent and monodispersed than amorphous CFA microparticles obtained from spray drying. XRD and DSC studies further confirmed the amorphous nature of CFA nanoparticles. Amorphous existence of CFA nanoparticles has resulted in an increase in the dissolution profile relative to raw crystalline CFA and industrial amorphous CFA due to amorphous composition, uniform particle size and lower nanoparticles surface area (Wang et al. 2010). Zhang et al. performed similar studies and were able to prepare LASP CFA drug nanoparticles using T-junction microchannels of stainless steel (Zhang et al. 2011). Smaller particles with wide and uniform particle size distribution were obtained by choosing the CFA solution as the injection step. Better dissolution of nanoparticles was also observed compared to raw crystalline, which dissolved during dissolution studies to only about 55% (Zhang et al. 2011). Zhao et al. prepared danazol nanoparticles of crystalline form using a Y-shaped microchannel reactor. Control of process parameters like size of the micropore and annular channel played an influential role in tuning particle size. Reduction of pore size resulted in reduced particle size with tapered distribution due to increased micromixing of solvent and AS together with greater interface pressure between dispersed and continuous phases. Reduction in annular length resulted in smaller particle size with wide distribution due to an increase in continuous phase velocity with narrow channels resulting in enhanced micro-mixing (Zhu et al. 2010). Zhang et al. produced monodispersed amorphous colloidal spheres of atorvastatin calcium (AC), using a LASP process in the Y-shaped microfluidic reactor showing 80% dissolution in 10 mins in comparison to 45% by marketed AC. This result was attributed due to monodispersity, small particle size, amorphous nature and larger surface area (Zhang et al. 2010).

8.3 API Loaded Nanoparticles Generated Using Microfluidic Technology

Since a decade, a real explosion has taken place in the development of microfluidic-mediated preparation of nanoparticles. Microfluidic tools have proved to be an interesting solution for accurate control of the physico-chemical properties of the generated dispersion. Nanoparticle fabrication by conventional methods is widely associated with non-standard, multiple step methods such as nanoprecipitation and emulsification-based process of solvent evaporation (Ahn et al. 2018). Nanoprecipitation leads to the formation of nanoparticles from a colloidal suspension between the two aqueous solvent phases by drop-wise addition of drug dissolved in a solvent into another solvent under agitation. It is possible to obtain desired characteristics of the synthesized particles by regulating the agitation speed and fall rate. Method based on emulsifica-

tion includes the creation of nanoparticles by mixing and diluting emulsions that is formed at the interface of two solvent surfaces. Particle size may be regulated by turbulence in this process. The conventional method of preparing nanoparticles results in polydisperse distributions and variations from batch to batch, thereby requiring an extra step to homogenize the prepared nanoparticles.

Enhancement in the therapeutic effect and reduction of drug toxicity along with improved absorption of poorly soluble and unstable drugs can be achieved by effective drug delivery carriers (Ahn et al. 2018). The quality and manageability of a drug release profile are key factors in accomplishing a drug delivery system that relies on physico-chemical characteristics such as volume, shape and composition. For example, smaller-diameter nanoparticles (less than 10 nm) can be filtered through the pores of the kidney's glomerular membrane (Wilmer et al. 2016), whereas bigger particles are readily identified by the body's immune system (Champion et al. 2007). Recent advancement in microfluidics offers a wide range of potentiality to handle very low sample quantities and allow scalable manufacture of variable volume, shape and surface composition nanoparticles to encourage the efficacy of drug delivery, release profile and removal at the time of treatment (Kim and Langer 2015). It can also provide accurately regulated effective and reproducible scale-up manufacturing.

9 Microfluidic and Bulk Technologies: Comparison (Jahn et al. 2007)

The flow conditions correction provides a method to alter the average size and volume distributions of nanoparticles. During the injection process, agitation is crucial in the macroscale system to promote rapid mixing and narrow distributions of particle size. Microfluidic system which facilitates continuous particle creation (Fig. 4.2) avoids disassembly and assembly processes that are often needed in conventional bulk technologies and enables dynamic flow control and mixing parameters to customize particles to your needs. Microfluidic systems have the potential to become a mainstream technology that enables formulations of particles with unparalleled homogeneity and fine critical control over the critical process parameters that are difficult to achieve in bulk techniques (Jahn et al. 2007). Conventional techniques essentially rely on large volume mixing and end up suffering from impoverished reproducibility from batch to batch and hardships to enforce quick screening and optimize nanomaterial characteristics. In this context, microfluidic technology has proved the ability to generate nanoparticles in a manageable and replicable manner, giving the aforementioned problems a possible solution.

Unique features that notably make microfluidics an appealing technique for the production of nanoparticles include

(i) controllable and efficient mixing resulting in homogenous reaction environment.
(ii) efficient temperature control and heat transfer.
(iii) in situ monitoring possibility during the production stage.
(iv) tuning the nanomaterial characteristics by controlling kinetics of the process.
(v) post synthesis processes and measurement systems can be integrated on a single technology platform.
(vi) rapid optimization and high throughput screening on nanoparticles biological activity.

10 Microfluidics: Nanoparticles Drug Delivery

Physico-chemical properties of the nanoparticles are strongly affected by the characteristics of size, shape and crystal structure. A superior control over the process parameters is desirable in the production of nanoparticles so as to fabricate material of desired features. In this context, microfluidic reactors that allow accurate fluid and fluid interface control and manipulation offer potential benefits for nanoparticles processing. Material yield, size distribution and reduction of

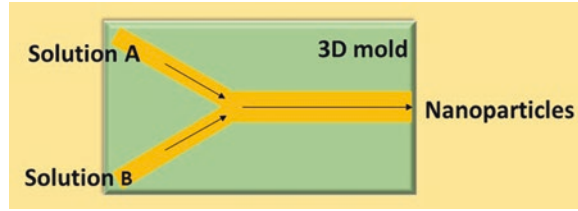

Fig. 4.2 Process of nanoparticle production using microfluidics

unwanted by material formation can be dramatically improved by allowing quick and uniform heat and mass transfer due to small size and resulting high surface-to-volume ratio. In addition, solvent reuse possibilities and advanced isolation techniques are likely to offer cost-effective and environmental friendly nanoparticles processing techniques (Chang et al. 2008).

Microfluidic technology is lending a very helping hand in drug delivery. The conventional method of synthesis of nanoparticles involves controlling the inertial and viscous effect of mass transport in fluids, both associated with nonlinearities that lead to instability, such as turbulence (Björnmalm et al. 2014). Nevertheless, inertial effect in microfluidics is negligible, allowing for the synthesis of nanoparticles in a very regulated and repeatable manner that was challenging to accomplish in traditional production processes. Several microfluidic methods which can be used to prepare nanoparticles are discussed below:

10.1 Flow Focusing Method

When mixing and diffusion regulated reactions are needed, hydrodynamic focusing is a sturdy tool for microfluidics. Hydrodynamic focusing is created while the fluids with varying speeds are added side by side. Most ordinary way of conducting hydrodynamic focusing is by using three inlet microfluidics where side fluids are filled with the core stream containing the value specimens. Microfluidics has the ability to quickly combine reagents that provide a homogeneous reaction environment and accurately add reagents during the phase of reaction (Mello and Mello 2004). This method allowed the synthesis of drug encapsulated nanoparticles using PLGA-PEG with a given size, low polydispersity index, slower release and high drug loading (Valencia et al. 2010). An intractable single layer along with three simultaneous inlets for the vertical focusing was proposed for 3D hydrodynamic fluid focusing accompanied by traditional horizontal focusing flow (Karnik et al. 2008). This design made it possible to separate the polymer that was precipitated on the channel walls, which was being the major difficulty for concentrating on 2D flow. Flow focusing microfluidics also prepared liposomes employing a central flow stream ethanol solution containing lipid being filled by two side streams of aqueous solution (Jahn et al. 2007). It is possible to modify the size of nanoparticles by adjusting the volumetric flow rate ratio between the side and the central streams when a narrow sheet focuses on the lipid channel. Danilo D. Lasic's proposed theory states that the lipids that are solubilized in an organic solvent will turn into the structure of phospholipid fragment (BPF) of the intermediate bilayer (Lasic 1988). Lipid solubility is decreased and instability in the boundary layer of BPFs is caused by continuous diffusion across ethanol and water solutions, causing lipid bending and closure and ultimately leading to lipid vesicles formation (Lasic 1988). T-shaped microfluidics was used by Jahn et al., who first documented the preparation of liposomes using this technology, to prepare liposomes in the range of 100–300 nm (Jahn et al. 2004). Increased flow rate ratio and shear stress resulted in smaller vesicle size being formed. A recent study developed microfluidic architecture for the mass manufacturing of liposomes in view of this technology's future industrial translation (Carugo et al. 2016). Also well illustrated was the function of lipid formulation, lipid concentration, residual amount of solvent, production method and drug charging. Simple to produce and run, hydrodynamic flow concentrating systems are

efficient in preparing particles having uniform size distribution.

10.2 Micro-vortices Method

Microfluidics operating at greater Reynolds number (almost 1100) can be used by guided micro-vortices to produce nanoparticles. By adjusting the inlet pressure, dynamic 3D chemical profiles are regulated with a single 2D microfluidics in which micro-vortices are playing an important role in generating adjustable 3D designs in microfluidics (Kim et al. 2011). This impetus led to the development of hybrid nanoparticles of lipid and polymer at the intersection of three inlets by symmetric micro-vortices. Productivity increased by 1000 times using the method of micro-vortices compared to the synthesis of nanoparticles based on diffusive mixing. Micro-vortices method was evolved to address the limitations of moderate diffusive mixing. Air bubbles can cause serious problems as micro-vortices work under the number and pressure of relatively high Reynolds.

10.3 Chaotic Flow Method

Under normal circumstances, turbulence use may be prevented by traditional microchannels in laminar flow, but flow disrupting patterns (e.g., herringbone mixers) may be utilized to actively blend fluids inside a stream. Chaotic advection is one of the methods to increase blending efficiency using geometric designs to bring about transversal flow of materials stretching and folding fluid volume across a microchannel's cross-sectional area. The staggered herringbone mixer uses an assembly of "herringbone mixer" to cause vigorous mixing inside the continuous flow on one or more surfaces of a microchannel (Stroock et al. 2002). It has been noted for its fabrication simplicity and effectiveness. Fluid will be reallocated throughout the whole cross-section of the channel, drastically decreasing Taylor dispersion and ultimately ending up in an almost even distribution of residence time. Recently, lipid nanoparticles were fabricated using herringbone mixers and further, effect of lipid concentration and mixing performance on particle size was established (Maeki et al. 2015; Maeki et al. 2017). The herringbone mixer increases the surface area exponentially amongst two fluids with the path length covered, culminating in quicker mixing by diffusion at an equal flow rate ratio compared to the hydrodynamic flow focusing process. Adding additional array of herringbone increases the performance of mixing with the quality of particle synthesis.

10.4 Droplets Method

One of the favoured methods for nanoparticle synthesis is droplet-based microfluidics which is having the potential of generating extremely reproducible and homogeneous particles. The current approach regulates discrete fluid volumes with laminar flow regimes in an immiscible state. Microfluidics ability to produce separate droplets is grasped to produce nanoparticles that are supported by efficiently controlled interfaces and rate of flow. A multi-step synthesis method for nanoparticles was described using droplet-based microfluidics in the millisecond timescale (Shestopalov et al. 2004). Two streams of aqueous solutions were brought together in a shorter segment, allowing a laminar flow to be produced side by side. In addition, a multiple step synthesis of cadmium sulphide or cadmium selenide core shell particles was used with this droplet-based process. Hui et al. suggested single step preparation of polymeric Janus nanoparticles by this method (Xie et al. 2012). Two molecules for co-delivery with different physico-chemical properties are rapidly synthesized and incorporated in Janus particles using microfluidic device implemented with side by side capillaries. Therefore, droplet microfluidics is one of the best methods for multi-functional carriers of drug with size tunability and drug release profile. Low production yield and complex protocol for droplet fabrication are the main challenges of this method.

10.5 Other Methods

Flow lithography is a technique in photolithography where a template for generating nanoparticles is projected directly into a photocurable polymer. This method can generate particles of different shapes, which are easier to operate due to the simpler nature of the flow. However, this method is limited to drug molecules that are not photosensitive, unable to synthesize sub-micron sized particles and unfit for high-performance manufacturing.

Photo-resistant materials are not suitable for this technique where bio-compatibility and functionalization of the nanoparticles is necessary. It requires cumbersome multiple step alignment and defence techniques which are not easy to execute.

Stop flow lithography (SFL), a flow stream of an oligomer, is halted before polymerizing, thereby providing a better resolution over synthesized nanoparticles in the flow (Dendukuri et al. 2007). Encoded particles for biomolecule analysis use this method. Major challenge of SFL is to increase cell viability for various biomedical applications because of cell damaging UV light and unfavourable pre-polymer.

11 Microfluidics: Nanoparticles Characterization

The most essential characteristics of nanoparticles that need to be described before interacting with in vivo systems are particle size, shape, surface charge, drug loading efficiency and stability. Characterization methods have a major impact on medical translation chances. One of the biggest barriers is the failure to confirm in vivo drug safety.

11.1 Characterization of Particle Size and Morphology

The generic feature of nanoparticles and crucial determinant of biodistribution and retention in targeted tissues is particle size. Most commonly, particle size is determined by Dynamic light scattering (DLS) technique which measures size of the particles in suspension (Instruments M. 2012).

11.2 Charge Characterization

Microfluidics has authorized the advancement of high throughput tools that are able to characterize certain features of nanoparticles such as effective size and charge on the surface of the particles. An analyser of nanoparticles has been developed that combines a simple microfluidic layout with a high electrical reading (Fraikin et al. 2011). The analyser has two elements: a microfluidic channel which guides the analyte's pressure-driven flow through the electrical sensor, specifically designed to maximize measurement bandwidth, and the sensor itself that consists of two voltage bias electrodes and a single optically lithographed read electrode embedded in the microchannel. This analyser allows for rapid electronic detection and volumetric analysis of nanoparticles that are not labelled in a multi-component mixture of 500,000 particles/second, including viruses suspended in salt and blood plasma. It is potentially handy in broader scope of applications due to its low cost, scalable fabrication method and simple readout electronics. Among other nanoparticles, metallic nanoparticles can be differentiated by the characteristic spectral dependence of the resonance activity of the surface plasmon (SPR). It also provides additional local environment data and anisotropy shape. Interferometric techniques can distinguish single dielectric nanoparticles, which has inspired Mitra et al. to improve real-time identification of sub-100 nm polystyrene particles, viruses and larger proteins which move through a microfluidic channel on the basis of their polarizability (Mitra et al. 2010). It is possible to determine the length, concentration and surface charge of the nanoparticles at the same time (Kozak et al. 2012). The approaches that change the size of adjustable pore sensors provide a superior comprehension of nanoparticles basic features and characterization of their features by means of high throughput.

11.3 Characterization of Drug Loading and Drug Release

Drug release pattern is a key component in the application of nanoparticles and is linked straightaway to the stability and pharmacological effect of the drug. Drug release rate generally relies on solubility of the drug, surface-bound or adsorbed drug desorption, nanoparticle matrix diffusion of the drug, nanoparticle matrix erosion or degradation, and erosion/diffusion system combination. The nanoparticles drug loading ability is characterized as the quantity of drug bound by carrier mass and is generally determined by UV-Visible spectroscopy, high-performance liquid chromatography (HPLC) and gel filtration. Because of its increased sensitivity, decreased consumption of sample and the capability to perform multiple measurements, microfluidic-based liquid chromatography has gained significant awareness these days. Microfluidic-based LC is made up of pumps, ports for injection, columns and detectors. To create a microfluidic HPLC chip, polyimide films are laminated with laser ablated channels and port (Yin et al. 2005). In a single device, an enrichment column, a separation column and a nano-electron spray tip are incorporated into an HPLC chip in order to decrease the delay and dead volumes among the components as well as the volume of after separation. Gao et al. (2012) established an advanced, mass spectrometry (MS) detection microfluidic platform for high-performance drug screening: highly sensitive chips from MS/LC. The bulkiness of supplementary components such as power supply or pump can pose both on-chip miniaturization and integration problems as well as the detector.

12 Microfluidics: Nanoparticle Evaluation

Drug delivery systems should be non-toxic, biodegradable, safe to deliver to the appropriate site of target and should have more therapeutic effect on pure API. Through static tissue culture plates, the drug delivery process is conventionally tested, but sadly, this avoids the significant effects of 3D, flowing environments and other mechanical and biochemical environmental conditions. Microfluidic techniques have now shown promise for closely imitating microenvironments in physiology. Existing cell culture systems have failed to recapitulate the pathology of human organ stage, so pre-clinical drug candidate studies rely entirely on costly and highly variable animal models. It illustrates the need for better models to replicate cells, tissues and organs structure and functions. The incorporation of cellular in vitro methods on chips enables real-time scanning, microscopic analysis, cell function and assessment of behaviour.

A variety of microfluidic devices and techniques have been developed over the past few decades, and their introduction has led to a revolution in life science. Scientists around the world have drawn attention to the use of microfluidic devices for organ-on-a-chip, protein and DNA analysis, drug discovery and drug delivery, cell segregation and analysis, and diagnosis. Microfluidic devices provide less costly sample consumption, faster molecular diffusion due to shorter microchannel size, good reaction time control, greater volume to volume ratio and greater efficiency of separation. The use of microfluidic devices in diagnostics, organ on a chip biomolecular analysis, cell analysis and synthesis of nanomaterial has been extended due to the exceptional characteristics (Maeki et al. 2018).

13 Production of Nanoparticles Using Microfluidic Devices

13.1 Lipid Nanoparticles (LNPs)

The platform of microfluidics has allowed the researchers to control the problems of fabricating size-controlled lipid nanoparticles (Table 4.2). Principle involved in the formation of LNPs using microfluidics remains same as that of conventional methods. The thin film hydration, organic solvent injection, detergent extraction and reverse phase evaporation are commonly used in conventional methods of pre-

Table 4.2 Applications of microfluidic technology

Applications	References
Emulsion	Okushima et al. (2004)
Microgel	De Geest et al. (2005)
Calcium alginate gel microparticles	Liu et al. (2006)
Colloid filled hydrogel granules	Shepherd et al. (2006)
Liposome	Jahn (2007)
Mesoporous silica particles	Carroll (2008)
Alginate micro and nanoparticles	Rondeau and Cooper-White (2008)
Temperature sensitive liposome-hydrogel hybrid nanoparticles	Hong et al. (2010)
Spherical and non-spherical fat particles	Kim and Vanapalli (2013)
Polyelectrolyte particles	Watanabe et al. (2014)

paring LNPs. Microfluidic-based LNP processing productively makes use of fluid dynamics, surface or interface, and microfluidic system design and generates wider particle size range with improved particle size distribution compared to conventional methods. LNP preparation using capillary-based device involves the introduction of lipid dissolved in organic solvent and aqueous solution into the microfluidic device. Flow rate, flow rate ratio, mixing frequency and lipid concentration are parameters that are critical in controlling particle size. In chip-based device, lipid stream is stressed by the aqueous solution flow which leads to the formation of liquid-liquid interface LNPs due to dilution of the organic solvent. As the organic solvent is being condensed by molecular diffusion and the lipid molecules dissolved in the organic solution begin to form LNPs, the polarity of the solution increases at the liquid-liquid interface. Shorter microfluidics diffusion length enables solvent dilution to be faster and more homogeneous than traditional batchwise reactors. First reported microfluidic-based LNP preparation device was a flat microchannel manufactured by chemical etching or standard photolithographic technique. Capillary array device and chaotic mixing device can be utilized to prepare LNPs to improve size controllability.

13.2 Polymeric Nanoparticles

Treatment of multiple diseases with core shell nanoparticles can be improved in terms of therapeutic efficacy and side effects (Hans and Lowman 2002). Biocompatible and biodegradable nanoparticles made up of polylactic acid-polyethylene glycol (PLA-PEG) have received tremendous attention as they promise to combine various useful features such as encapsulation of high quantities of drugs, controlled release of drugs with adjustable release profiles and specific targeting of receptors (Xiao et al. 2010; Wilkosz et al. 2018). The simple and rapid technology used to prepare polymeric nanoparticles is the bulk nanoprecipitation by solvent exchange. But in this method, phase mixing occurs slowly and unregulated in favour of creating hetero-sized nano-colloids due to uneven polymer distribution, resulting in inadequate batch-to-batch consistency. Improving the reproducibility and controllability of the synthesis of nanoparticles is crucial as in vivo quality depends heavily on their physico-chemical properties. Microfluidics provides a precise controlled environment for the processing of polymeric nanoparticles with better defined properties and excellent batch-to-batch reliability (Valencia et al. 2012, 2013). Nanoprecipitation provides minimal possibilities for downscaling and upscaling, and microfluidics can overcome these limitations, making the technology highly useful for high-performance testing during the development of new nanomedicines and for clinical applications requiring sufficient quantities of uniform properties of nanoparticles (Lim et al. 2014). Microfluidics is therefore considered an ideal platform for optimizing the size distribution of polymeric nanoparticles with multi-components. Abstiens and Goepferich prepared polymeric nanoparticles using specific PLA-PEG to PLGA ratios and demonstrated that microfluidics is a valuable technology for the reproducible and scalable processing of nanoparticles with precisely

adjustable particle characteristics (Abstiens and Goepferich 2019).

13.3 Theranostic Nanoparticles

One of the major challenges in nanomedicine presently is the production of nanoplatforms that are able to target, treat, image, diagnose and track the progress of disease at the very same time. A novel nanohybrid composed of AcDEX nanoparticles which encapsulated dextranylated PSi (DPSi) and dextranylated gold nanoparticles (DAu NPs) for liver regeneration and acute liver failure was easily synthesized by microfluidic mixing in a co-flow capillary microtubule. Single step co-encapsulation of both NPs was achieved by modulating the surface properties of nanoparticles and composition of organic phase (Liu et al. 2018). PEGylated crosslinked hyaluronic acid NPs were produced successfully by nanoprecipitation in microfluidics in a one-step manner. The NPs formed were loaded with a model dye (ATTO633 or ATTO488) and a gadolinium-based magnetic resonance imaging contrast agent (Gd-DTPA) for multimodal imaging. Furthermore, the results obtained from certain studies prove that the system can be ultimately used to encapsulate drugs and thereby represent a very attractive platform for theranostics (Russo et al. 2017).

14 Microfluidic Tools for Nanoparticles Investigation

14.1 Organ-on-a-Chip

The organ on chips is in fact designed to absolutely recreate the natural physiology and mechanical forces that cells are subjected to experience in the human body. The structure, function and physiology of living tissue in vivo are typically not adequately recapitulated by traditional 2D monolayer cell culture system. Microfluidic technologies can restore the organ's multicellular structures, tissue interfaces, physico-chemical microenvironments and vascular perfusion by implementing "Organ-on-a-chip". Organ-on-a-chip software provides organ flexibility that is not feasible with traditional high-resolution 2D and 3D culture techniques, real-time image analysis and in vitro research, inclusive of biochemical, metabolic and genetic processes of living cells (Bhatia and Ingber 2014). It is a technology in which the cultivated organ cells are joined together on a small plastic plate. Liquids will flow to and from the cells through the tiny channels of the chip. With the utilization of advanced equipment, researchers can perform all sorts of measurements, such as cell activity, inflammation reactions and therapeutic response of the medicines. Many individual organs have been built on chips to date, including lung-on-a-chip, blood vessel-on-a-chip, blood brain-on-a-chip, tumour-on-a-chip, liver-on-a-chip and heart-on-a-chip, and these are about the size of an AA battery. The chips are lined with human cells and their tiny fluidic channels reproduce blood and/or air flows in the human body. Chips are allowed to recreate breathing motions or undergo muscle contractions due to their flexibility. It should be particularly valuable in the context of drug delivery and production for the investigation of molecular mechanisms of action, toxicity and efficacy testing and detection of the biomarker. Chip transparency enables the researchers to see the functionality, behaviour and reaction of the organ at cellular and molecular levels (Ahn et al. 2018) (Fig. 4.3).

14.2 Blood Vessel-on-a-Chip

The scientists from Duke University were successful in generating human blood vessels on a chip. These vessels not only can deliver nutrients and oxygen into the tissue but also can contract and dilate just like blood vessels in the human body helping in regulation of body temperature and metabolism. The major purpose of the nanocarriers in the field of medicine is to convey nano drugs safely and reliably to the target site. Hence, the particles should be designed appropriately

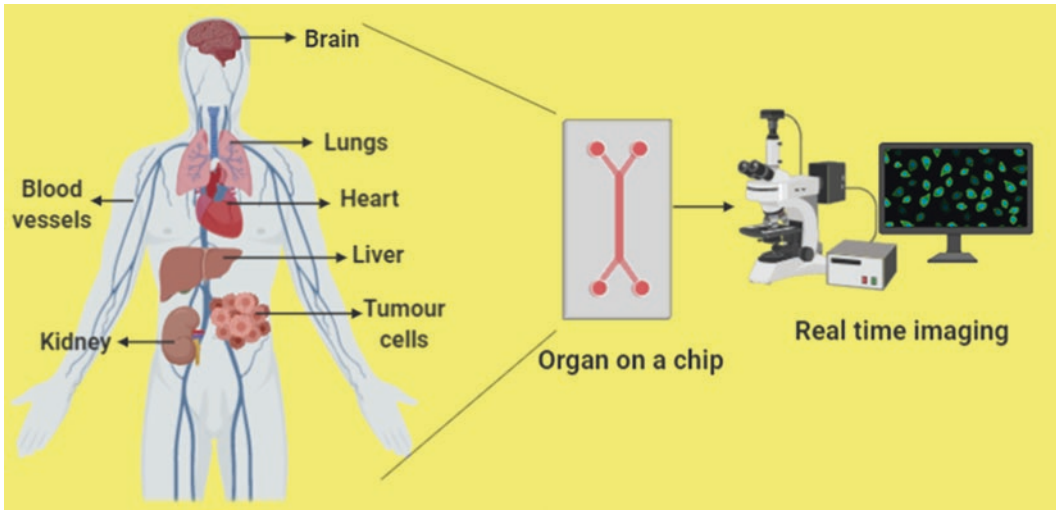

Fig. 4.3 Nanoparticle investigation tools using microfluidic technology

according to the factors such as load and target site, along with the consideration of their microcirculatory pathways as most of the nanoparticles are intravenously injected and pass through the blood vessels (Gupta et al. 2016). Synthetic microvascular network (SMN), an in vitro system, has been widely adopted in early research using microfluidic platform on drug delivery systems focusing upon the consequences of distinctive vessel anatomical characteristics, even without the cultivation of vascular endothelial cells. This method observed particle motion in real time, based on the particle size and shape, and also demonstrated that the structure of a blood vessel facilitates particle aggregation (Doshi et al. 2010). It is now expected that microfluidic in vitro models will furnish awareness into hemodynamics in microcirculation of the nanoparticles by imitating dynamic flow conditions in physiologically applicable microenvironments (Rathod et al. 2017). In addition, hemorheology is another factor in consideration in assessing the efficiency rate of nanoparticle delivery. It demonstrated how the inter connection between these cells and the nanoparticles can influence the collection of delivery systems after the introduction of blood cells in a microfluidic assay. Interaction amongst the particles and the red blood cells has been influenced by differences in nanoparticles particle size or surface chemistry (Namdee et al. 2013). Thanks to microfluidics, several scientists were able to perform quick and cost-effective tests to determine the impact of shear stress on endothelium aggregation or cytotoxicity. Selective permeability is one of the key features of the microvascular system that can be regulated in a microfluidic model in vitro. To research the translocation of nanoparticles across the endothelium, in vitro assay to test permeability of the vessel is therefore required. The evolution of in vitro vascular system has taken an enormous leap over a decade with the use of microfluidic and microfabrication technologies. Because of the high dependency of pharmacokinetics on morphology and physiology of the vessel, microfluidic technology may prove to be a perfect platform for evaluating the concealed mechanisms that will donate to the contribution of a high-performance drug delivery device.

14.3 Blood Brain Barrier-on-a-Chip

Blood-brain barrier (BBB) is a sophisticated vascular network of central nervous system (CNS) inherently equipped for the defence of bloodstream toxic substance and brain homeostasis maintenance. It restricts the passage of molecules from the brain vasculature into the brain via its

high transendothelial electrical resistance and low paracellular and transcellular permeability. It is being considered as a major obstacle in the therapeutic development for CNS disorders, making it is a biggest confrontation to pharmaceuticals to model drugs and their delivery system to achieve ample level of penetration across BBB. Most of the studies are being carried out on cell cultures and animal models which fail to completely recapitulate the human BBB properties. Microfluidic-based blood brain barrier-on-a-chip is therefore an effective tool for researching the brain's physiological structure and the barrier system's molecular mechanism. As many new chip systems are currently being evolved and falling into the focus of pharmaceuticals, they should be designed for the testing of nanomedicines targeted targeted to CNS. Microfluidic BBB holds great potential in disease modelling, drug discovery, neurotoxicity screening and personalized medicine applications.

14.4 Tumour-on-a-Chip

Albeit enormous efforts to cure cancer, it remains one of the leading causes of death. Better understanding of the tumour microenvironment as well as effective means to screen lead molecules of the drug can be achieved using sophisticated technologies which include emerging tumour-on-a-chip technology. These micro devices allow well controlled microscopic studies of interaction among tumour cells, immune cells and the cells present in the tumour microenvironment, of which simple tissue cultures and animal models are not amenable to do. Drug delivery by tumour-on-a-chip focuses on cancer nanomedicine's effectiveness and toxicity. Microfluidics have distinct benefits over traditional macro cell cultures by enabling accurate regulation of physiological signals such as hydrostatic pressure, shear stress, oxygen and nutritional gradient to reproduce tumour microenvironments.

Microfluidic testing of nanoparticles can be grouped into two categories:

(i) using spheroids formed by co-culturing single cells or multicellular cells, and
(ii) mimicking tumour microenvironment by culturing cells incorporating of biological barrier as well as cancer cells in microchannels embedding a three-dimensional extracellular matrix (Xu et al. 2014).

The microfluidics system permits cancer cells to grow in steady location in the same area. In addition, in the same spheroid, it can also track the drug reaction over time. It is not only possible to trap cells inside small droplets, but it is also possible to administer reagents using less volumes, about 1000 times smaller than those being utilized in classical assays. Degree of accumulation must be measured according to environmental conditions. Studies including cut-off pore size, pressure of the interstitial fluid and microstructure of the tumour tissue were conducted to investigate the efficiency of delivery of nanoparticles under tumour microenvironmental variation. The results suggest that tumour-microenvironment-on-chip can imitate complicated tumour transportation as well as provide particular information on nanoparticles transportation behaviour. Nanoparticles layout for site-specific drug delivery takes into consideration the tumour microenvironment's complex interaction with nanoparticles. To quantitatively classify response of the drug and resistance to types of cancer cells, it is important to examine the mechanism of cell-type-specific drug transport. The experimental models and the theoretical models developed allow for quantitative investigation of pathways for the delivery of drugs to the cells and resistance of the drug. Few experimental framework offers an extremely pertinent microenvironment of the cells for testing different types of drug response to cancer, as it offers manageable 3D extracellular environments under oxygenation. The tumour's microenvironment has distinctive features like leakage and divergence of endothelial tumour cells in the vascular system, inadequate perfusion, lower pH and strong interstitial pressure and microenvironmental interaction among different cells. Nanoparticles could be a fantastic tool for making a dramatic advancement for this microenvironment. Several types of nanoparticle carriers can target the tumour's vascular endothelium

having different porosity and pore size. The device has significant potential in activities such as cell/cell-drug interaction studies and accelerated testing of cancer drug therapies (Tang et al. 2017). A secret to tumour overcoming is the development of a microfluidic device for rapid synthesis of combinations and optimization of nanoparticles. The emerging microfluidic system is a device that can theoretically speed up nanoparticles discovery and translation into the clinics. The microenvironment of the tumour includes a number of interactions between different components (cancer, fibroblast, immune cell, endothelial cell). To sum up, the microfluidic platform for drug screening for tumour microenvironment in individual patients can be maximized when combined with nanoparticles. The development of nanoparticles that reflect tumour microenvironment enables the rapid and patient-specific evaluation of cancer nano drugs and contributes to the development of precision medicine.

14.5 Lung-on-a-Chip

Lungs are the critical respiratory organs that connect the circulatory system with the outside as a gas exchange interface. As far as gross anatomy is concerned, the lung has a complex hierarchical system of branching pathways in which the large trachea becomes gradually smaller bronchi and bronchioles networks and finally ends up in alveolar sacs that are closed. The alveolar pockets, surrounded by comprehensive capillary networks, serve as the main functional communication system between blood and inhaled gases and promote exchange of oxygen, carbon dioxide and other toxic substances. Drugs absorbed through the lungs can be systemically delivered directly through the circulatory system, a process used as a significant conduit of rapidly acting drug delivery. Unfettered access to the blood circulatory system also provides a framework for distributing payloads which would otherwise be metabolized by first-pass metabolism and digestive processes which include oral administration enabling protein to deliver valuable loads like those of insulin and hGH at higher levels of bioavailability. Pharmacological inhalers can come in different forms, ranging from basic small molecule gases such as nitrous oxide to vaporized liquids such as chloroform and nicotine, to dry aerosolized powders such as insulin and fluticasone propionate (Patton et al. 2004). With the rise of science of nanoparticles, efforts to integrate nanodrug carriers and other medicinal activities arose as a popular research. A number of forms and materials of nanoparticles comprising chitosan, cerium oxide, silica, PLGA, alginate, silver and CNT have been tested as possible drug and biological carriers with mixed results. In the situations of insulin contained in chitosan nanoparticles and elcatonin contained in chitosan-treated PLGA nanoparticles, qualitative decreases in blood glucose and calcium levels from the respective carriers were reported in in vivo models. Traditional inorganic, non-biodegradable nanoproduct carriers such as gold, silica and cerium oxide have shown cytotoxicity and detrimental effects in both traditional 2D in vitro and in vivo experiments, but shortcomings in traditional methodologies have created significant difficulties in achieving meaningful information. Due to the branching design of the lung and the lengthy paths that medicines need to travel to enter the alveoli, successful execution is hard to manage and prone to lower yield, and verification of practical successful delivery conditions with traditional in vitro 2D cultures is daunting in vivo and impractical (Van Midwoud et al. 2011). The difficulty in imitating both macroscale tissue structures and histological roles of the cells in traditional 2D in vitro systems and also the resource strength of using in vivo rodent models resulted in a significant need for an in vivo as in vitro microfluidic device that is able to bridge the gap between in vitro and realistic economic implementation. The lung-on-a-chip was unveiled by the researchers of Wyss Institute in 2010, designing a lung alveolar tissue template consisting of primary tissue cultures and adding mechanical extending features to form the foundation for a range of mechano transductive and histological layering requirements. The toxicity of silica nanoparticles was monitored using this

process. Recently, lung-on-a-chip has been used to explicate patterns of human lung cancer (non-small cell lung cancer) development and invasion. This study suggested that regional microenvironmental indications produced by cells comprising the epithelial and endothelial tissues of the lung, as well as mechanical respiratory motions, could have a significant impact on the growth of human lung cancer in vitro. Most specifically, without breathing movements, tumour cells are immune to anti-cancer drugs (rociletinib). Due to the highly centralized existence of pulmonary morphology and the crucial role of macroscale tissue organization in the mechanical function of the lung, the lung-on-a-chip model has technical and operational obstacles to address if it is to completely imitate macroscopic lung function in a physiologically applicable manner to aerosolized delivery methods. Technical problems on a chip platform are largely limited to imitating some operational features of an individual with highly localized tissue groups, like alveoli and broader air channels, and the feasibility of the cells. So far, the enlightening windshield offered by workable culture times is inadequate to quantify extensive observations of post-nanoparticles beyond the weeks. Ultimately, further progress in research into in vitro lung nanoparticles requires both the means of evaluating the connections of examined particles with the macroscale functionality of lung tissues and would considerably benefit from the means of investigating medium to permanent particle consequences.

14.6 Liver-on-a-Chip

The liver is a vital organ with several distinctive roles, which includes promoting other systemic metabolism processes. For many fundamental reasons resulting from higher degree of metabolic activity, the liver is particularly important in the context of pharmaceutical research. The liver acts as a functional hub for metabolism of all the medications administered orally as a first pass metabolic test. Based on liver interactions, orally administered drug dosage forms can be made entirely inactive from liver-dependent first-pass metabolism, even before it circulates in the blood. Pharmaceutical products that enter systemic circulation are screened and filtered by the liver as a part of the circulatory system, either through non-oral alternate routes of administration or via the initial first pass. Kupffer cells bound to liver act as a portion of the mononuclear phagocyte system (MPS), that behaves as a macrophage immune reaction which appears to sequestrate and aggregate about 30–99% of circulating nanoparticles, and may lead to higher hepatotoxicity (Zhang et al. 2016a, b, c). Because of the higher extent of liver metabolic reactions with pharmacologically active drugs, hepatotoxicity significantly contributes to the failure of drug trials. Not surprisingly, hepatotoxicity assays are in high demand. There are many distinct models of microfluidic hepatic tissue, each exchanging different levels of simplicity and ease of use in return for more biologically relevant information such as conditions of in vivo regulation. For example, a research integrated a multi cell line tissue model of Caco-2/TH29-MTX intestinal co-culture model and HepG2/C3A liver co-culture model to measure the penetrating ability via intestinal cell line co-culture tissues into the tissues of the liver cell line and to examine the extent and consequences of nanoparticles accumulation on cell tissue viability and cell junction condition. To undertake a three-dimensional tissue structure hepatotoxicity assay for qualitative viability screening, Bhise et al. established a bioprinted spheroid bioreactor system of hepG2/C3A co-cultures (Bhise et al. 2016). The usage of cell lines such as HepG2 and C3A instead of primary cells and ex vivo surgically removed tissue cultures poses obvious concerns about data reliability, but the use of primary and ex vivo tissue cultures comes at the expense of a significantly increased level of cultivation complexity and a much reduced sustainable cultivation period. In addition, surgically removed rat liver ex vivo and intestinal tissue slice chip successfully integrated and preserved the processes of metabolism, levels and inter tissue connections in vivo for the intestinal portion up to 8 h and 24 h for the liver subunit. Several

methods for addressing nanoparticles hepatotoxicity included bypassing the full absorption of liver nanoparticles by modifying the nanoparticles' surface to attach to red blood cells. In in vivo models, attempts have been made to minimize the absorption of nanoparticles by Kupffer cells by modifying substrates of nanoparticles and surface therapies, dosage profiles and concurrent drugs with varying degrees of success suggesting the potential for future research and standardization. Although existing liver on a chip system is definitely an upgrade in terms of in vivo as the arrangement of polarized endothelial membranes over past 2D hepatocyte monocultures, new platform-built 3D structures still need to shape functional multiple layer hepatic tissues like those seen in the hepatic lobule. To determine the accessibility of nanoparticles to the liver as a whole, tissue structure is important as a hypothetical nanoparticle would have to penetrate the hepatic lobule into the sinusoid with endothelial lining and Kupffer cells through the circulatory vasculature before reaching hepatic cells. Since the first pass metabolic operation of the liver, such as MPS facilitated by the Kupffer cell, is also extremely tissue dependent, continued work is required to design nanoparticles and bioavailability with any level of precision. In almost all, hepatic metabolic and viability testing for nanoparticles delivery would enormously benefit the improvement of in vivo engineered tissues such as in vitro and also the use of primary cells.

14.7 Kidney-on-a-Chip

A huge number of kidney-on-a-chip systems are made up of renal cells incorporated in the ECM interface or membranes positioned beside perfusable microchannels which can provide nutrients, waste removal and stream stimulation. Classically, in vitro studies are performed on plastic tissue culture plates under static conditions. Nevertheless, in vivo epithelial cells of the renal proximal tubule are subjected to persistent fluid shear pressure of the lumen. 3D microfluidic renal models developed in the ECM were more drug-induced toxicity tolerant and best suited to chronic toxicity regulation compared to 2D counterparts due to microfluidics (DesRochers et al. 2013). Kidney-on-a-chip allows high resolution, real-time molecular imaging in an in vitro process, which is a significant advantage in delving deeper into the drug delivery mechanism. Jang et al. suggested on-a-chip renal proximal tubule that can accurately predict the toxicity that the drug may produce in humans. The on-a-chip kidney proximal tubule consists of an apical channel isolated from a bottom reservoir by an ECM coated porous membrane where epithelial cells of human proximal tubule are grown in the presence of apical fluid shear pressure After the administration of cisplatin by injecting into the interstitial pocket of the device, the proximal tubular cells demonstrated increase in cell injury in both static and dynamic conditions. Nevertheless, cisplatin weakened proximal tubule cells that were grown in the presence of flow, recovered to a much larger extent than cells in static condition. The kidneys are one amongst the key sites because of their glomerular filtration for the degradation of chemicals and drugs among the tissues of concern in systemic toxicity reactions. Analysis of drug delivery using kidney-on-a-chip can provide valuable insight into the exploration of mechanisms of the cellular system for forecasting kidney toxicity and drug clearance in vitro.

14.8 Heart-on-a-Chip

Heart is one of the organs closely linked with drug cytotoxicity, and so a proper in vitro drug test model is in great demand in the pharmaceutical industry. Most cardiac tissue engineering cases have been formed using innovative biomaterials such as coiled fibre scaffolds integrated with gold nanoparticles (Fleischer et al. 2014), carbon nanotube incorporated hydrogel sheets or tri-layered elastomeric scaffolds. In addition, lab-on-a-chip technology has come up with the development of models for high-performance pharmacological studies that reflect physiological characteristics. A cantilever system called

muscle thin films (MTF) for quantitative heart autonomous contractility analysis is one of the initial heart-on-a-chip designs. The cardiomyocyte and matrix synchronization of the system were determined and aligned with the heart function. In addition, different heart-on-a-chip models used human cardiac cells or iPSC-based 3D bioprinting technology (Zhang et al. 2015) to imitate the physiology or microenvironment of the cardiac system. All of the above-mentioned models primarily aimed at applying high throughput and high content drug testing, and these implementations have already been shown for small molecule drugs already on the market. They showed specific cardiophysiological reactions to every stimulus of the drug, changes in the contraction speed or orientation, suggesting that the models were appropriate for research.

15 Companies Working on Microfluidic Technology

The market of microfluidic-based devices is growing enormously since 2014 due to increasing demand and miniaturizing of microfluidic chips. The market value is expected to increase in the future. Several innovative companies are well established and few are emerging to explore the field to showcase the commercial benefits of microfluidic technologies (Table 4.3). Applications range from biology to electronics, tissue engineering to organ-on-a-chip, food safety to polymer synthesis, cancer research to nanotechnology and the list goes on.

Table 4.3 Companies working on microfluidic technology

Company name	Products/services
Advanced liquid logic	Lab-on-a-chip microfluidic devices
Affymetrix	Parallel genetic arrays
Caliper life sciences	Microfluidics, liquid handling, etc.
Daktari diagnostics	Point-of-care diagnostics
Micronics	In vitro diagnostics
1CellBio, Inc.	Single cell genomics analysis
1Drop diagnostics	Point of care diagnostic devices
Achira labs	Lab-on-a-chip platform
Arborsense Inc.	Wearable alcohol monitoring technology

16 Future Developments

A vast range of applications of microfluidics have now outstretched the point because of which it is possible to perform individual and multiple integrated processes. Bringing such a technology into commercial devices that can be easily used by the non-specialist, systemization of microfluidic components, allowing intuitive handling and operation by unskilled end users are the major concerns of future developments. Multinational companies are now heavily investing in microfluidic devices for commercialization of these systems. Many smaller companies being spun out of university activities are also working in this direction. Using microfluidics to produce, classify and test drug delivery systems for nanoparticles may boost controllability and reproducibility as well as preclinical studies performance.

Developing new nanoparticles for drug delivery has turned out to be an interdisciplinary project at the junction of biology, engineering, medicine, chemistry and materials sciences. Such technologies would allow highly reproducible particles to be robustly supplied to the whole developmental activity and thus rise their chances of victorious clinical transitions. A perfect drug delivery system with high payload capacity and active targeting is biodegradable, biocompatible, robust and easier to fabricate. Microfluidic production process has the ability to solve most of the inefficiencies and bottlenecks during scaling up and batch variance controls that are associated with conventional bulk synthesis. Hence, for the successful transfer of nanoparticles for drug delivery from the laboratory to the hospital, microfluidic technology for the development of drug delivery particles is required. The manufacture of microfluidic drug delivery particles has greatly increased the tunability of combining precursor reagents, simplifying the flexible integration of therapeutic molecules, imaging agents and targeting ligands into a multi-functional multi-component device. In microfluidic particle

synthesis, designing a scalable system that upholds those physico-chemical properties is a major challenge. As computational fluid dynamics enables simulation of mixing flow patterns or nanoparticle formation, it can be applied in a broader range of manufacturing and drug delivery strategies. For instance, as mentioned above, microfluidic modules are required to be well designed in order to avoid secondary flows in parallelization creation (toward industrial scale), that can lead to certain issues in the main streams of bulk flow. Computational fluid dynamics is a precious tool in scale-up production to automate these complex processes.

In addition, presence of air bubbles is the most recurring problem associated with microfluidics.

Due to the dimensions of the tube that are in microscale, it can be very difficult to remove air bubbles and can also prove harmful to the experimental studies. Within microfluidic devices, the origin of air bubbles can be at the beginning of the test or due to fluid filling, porous materials, leakage and the dissolved gas. Nevertheless, unintentional disruption because of the creation of air bubbles in microfluidic devices must be sorted out, as this along with the increasing the hydraulic resistance inside the flow, also results in inefficient manufacture and characterization of the drug delivery system. The important feature of microfluidics in the application of drug delivery systems is the capability to test drug delivery nanoparticles using organ-on-a-chip technology. The microfluidic systems can combine tissue-like 3D cell culture and stem cell engineering for drug testing. Co-culturing multiple types of cell inside well-arranged microenvironments can likely reconstitute various functional organ like tissues that can provide real-time biologically pertinent test data. Such models can overcome conventional systems and allow more complicated and practical microenvironments to be reconstituted. Developments in practical models could be made by integrating ever more sophisticated microenvironmental control processes at the price of added difficulty. Complexity raises a multitude of issues that need to be resolved if the advantages of preparing advanced and constant reconstituted tissues are required to outweigh the price linked with complexity related functional problems of the model process and additional potential variables in the interpretation of tests. It is possible to observe difficulties inherent in the relationship complexity between traditional 2D cell culture assays and microfluidic 3D tissue culture platforms. The platforms of microfluidic tissue cultivation are a leap further from in vivo as microenvironmental 2D cell culture and are capable to pattern multiple types of cells into heterogeneous, polarized tissues that mimic physiologically identical within vivo counterparts. The microfluidic tissue culture systems have the ability to deliver more physiologically related tissue and cellular responses in vivo as advanced platforms in comparison to those developed from 2D macrofluidic chips, with the expense of raised costs and difficulties linked with the design and operation of microfluidic tools. Microfluidic systems, made up of microchannels, chambers and other micropatterned structures, require more energy, time and exclusive infrastructure than simple 2D devices to manufacture.

Generally, the costs of production and problems rise directly with complexity. Additionally, relatively higher number of tissue cultures performing techniques inducing microphysiological environment over 2D cell culture creates increased technological and skill requirements in order to use tissue culture platforms skilfully. While 2D microtiter and plant cultures are commonly used as basic assays to evaluate simple quantitative or qualitative attributes like individual cell viability by standardized and simple to understand, multiplexable reporting processes, results of the experiment from the tissue culture platform can involve analysis of physiological responses across a much more complicated tissue level across a wide range of possible multiscalable morphological reactions. The integration of many designed variables and environmental changes combines the microfluidic tissue culture platforms input and output into a dramatic rise in degrees of freedom relative to simple 2D cultures. Higher degrees of freedom in 3D tissue cultivation convert into more difficulties in the design and execution of managed protocols along

with added levels of complexity in results of the experiment; 3D tissue cultivation techniques and quantification metrics of tests are low structured and specified in practice in comparison to 2D alternatives. Increase in complexity will eventually turn into indistinguishable exacerbations of microfluidics production, use and understanding summons. As they are now, microfluidic systems still face some obstacles that need to be addressed before large-scale industrial-scale deployment. Mass production problems and compliance with high throughput testing are some of the key features discussed by adoption-enhancing initiatives. Soft lithography, which was originally developed as a means of quicker prototyping, is ideal for pilot-scale microfabrication, with low initial investment per design to produce a limited number of moulds. Though soft lithography allows a new usable microfluidic model to be developed using PDMS within the time span of 24 h of drafting, the technique uses frangible silicon wafer moulds and PDMS casting steps that is laboriously bottlenecked resulting in the restriction of the scaling up of high throughput manufacturing.

Many industrial and educational undertakings such as Emulate, MIMETAS and Curiochips have sought relatively more upscalable production techniques like those of injection moulding and 3D printing for the production of microfluidic systems to address the inefficiencies in soft lithographic microfabrication on a larger scale. The integration of large-scale production methods into the manufacturing of microfluidic chips is an important step in ensuring that demands on a commercial scale can be provided. Technology attempts to increase manufacturing capacity has allowed a higher level of quality control and standardization of the factors for better compliance with the productivity. Most traditionally manufactured microfluidic PDMS systems are punched manually or in a device-specific configuration, creating distinct shape factors and input/output ports that can differ considerably even within devices of the same type. The implementation of standardized, mass production friendly prototypes developed in large, consistent lots allows automatic management through the current infrastructure of HTS microtiter plate. Although educational microfluidic tissue system work focusses on extremely sophisticated models for greater in vivo fidelity such as reconstitution, industrial application innovation has concentrated on streamlining models for versatile systems which are more user-friendly and applicable to a broader spectrum of tissues. While the simplification approach compromises with the aspects of practical tissue production, a compromise between lower yet still significant levels of realism and higher usability for a broader customer base can be influential for industrial adoption. While organ-on-a-chip technology is still under its developmental stage, it would definitely carry on to grow in the near future to provide microenvironments that are physiologically/pathologically important to test multifunctional particles of drug delivery.

Further investigations are needed in order to understand the effects of lipid nanoparticles (LNPs) size on stability, in vivo kinetics and performance of nano drug delivery systems. Nonetheless, recognizing the impact of the size of nanocarriers will furnish essential information for the scientists to build next-generation nanomedicines and to elucidate the relationship between diseases and the extracellular vesicles (EVs). LNP development which is on-demand assures newer applications of microfluidic system for better performance and loss-less testing of LNP-based pharmaceutical candidate compounds and tailor-made medicines. Furthermore, microfluidic systems can combine pre- and post-treatment functions into LNP production and expand production through numbering or parallelization of devices. Microfluidic systems have necessary features for commercial applications to build next-generation LNP-based nanomedicines. We foresee microfluidic technologies to become a new benchmark for both the generation and separation of LNP from EVs. New microfluidic platforms will be built to extend the utility of the development of microfluidic nanoparticles. Breakthroughs in nanomedicine mandated the need to establish methods for producing more robust and manageable nanoparticles. Classical approaches rely primarily on high

volume mixing and end up suffering from low batch-to-batch reproducibility and problems in implementing rapid evaluation and nanomaterial properties optimization. In this context, it has been demonstrated the ability of continuous flow microfluidic reactors to produce micro and nanoparticles in a manageable and reproducible fashion that provides a potential solution to the above-mentioned problems. Relatively little has been achieved for the development of organic nanomaterials compared to intensive research at the intersection of inorganic nanoparticles and microfluidics. Considering its high potential in nanomedicine, the use of microfluidic reactors has been increasing in the production of various nanostructured drug delivery systems. It has been found that the fluid dynamic environment in microfluidic areas has significant implications for nanomaterials.

Notably, unique properties that make microfluidics an attractive technique for nanomaterial processing, include:

(i) effective and manageable mixing resulting in a homogeneous reaction environment;
(ii) effective temperature regulation and heat transfer;
(iii) in situ monitoring of nanomaterial production processes and
(iv) possibility of modifying nanomaterial attributes.

Such properties were used by different researchers to generate different categories of nanomaterials, namely drug nanoparticles, niosomes, polymeric micelles, liposomes, polymerosomes and hybrid nanoparticles. Given the breathing operation and the very promising results so far, the field of microfluidic processing of nanomaterials is still at its early stage. Therefore, microfluidic reactors can become a standard manufacturing method to formulate nanomedicine delivery systems with incredible degree of controllability and homogeneity. In order to advance this technology, different aspects should be discussed in the future. The comparatively low nanomaterial output speed is one of the most important drawbacks of microfluidic devices. This is attributable to the small size of the functioning channels and the related technical constraint of feasible mass flow rate due to increased microchannel pressure drop with increased rate of flow.

Lately, several strategies have been proposed to address this particular issue, demonstrating the production of nanoparticles up to 3 g per h. It was found that they rely on new micromixer designs in which either micro-vortices, multi-lamination or jet-impact strategies were used to achieve high production rates without compromising mixing controllability. Further scientists are expected to try to solve this problem in the future, as it is representing one of the key problems that hinders the usage of microfluidic devices in commercial environments. Increased system output is often accomplished by parallelizing functional units individually. Nonetheless, maintaining equal physical conditions within each system is often challenging, leading to lower control over the characteristics of NPs at some point. Increased production volume should therefore be followed by products of better quality. Soft lithography techniques are feasible to be used in this respect to generate microchannel architectures with precisely regulated dimensional properties, permitting increased microchannel parallelization with precise flow field prognosis within each microfluidic device segment.

A group of researchers recently developed a multiple layered system with three layers of PDMS and a glass slide for high throughput polymeric NP processing. System design included a tree shaped structure with N100 output channels through which MPEG–PLGA solution in acetonitrile was hydrodynamically oriented. In addition, the microfluidic system was designed to allow self-assembly of nanoparticle outside PDMS tube, thereby circumventing probability of fouling over the channel walls. Nanoparticles with an average diameter of 50–200 nm were obtained, distinguished by remarkably smaller distribution of size in comparison to batch processing. Specifically, NP production speed was increased in comparison to the previous studies (polymer flow rate 0.5–2.0 mL/h) and is a positive step towards bulk manufacturing of nanoparticles. In line measuring systems, microfluidic reactors are also ideal for adding data on the

characteristics of the nanomaterials generated on time. Such information could then be used to monitor the functioning of the system and thus act quickly to avoid or mitigate the effects of any undesired deviation on the nanomaterial batch. As already seen, this data could be incorporated into a command system to produce intrinsic suggestions to automatically adjust the reaction conditions in order to preserve important nanomaterial properties. Furthermore, line measurement devices will provide timely information on the properties of the nanomaterial generated, reducing the amount of time required during optimization and screening phase. Nevertheless, given the fascinating applications of in-line measurement systems, only minimal research has been dedicated to this field, so new studies are likely to tackle this issue in the near future. In general, the techniques developed often suffer from nanoparticle specificity and low sensitivity rendering them inappropriate for comprehensive nanoparticle characterization and performance testing on a large scale. Tarabella et al., reported promising advances in a recent study to overcome these limitations. Authors have developed a microfluidic-based organic electrochemical transistor (OET) capable of sensing and monitoring liposomal structures in real time. It has been shown that the micro device is an effective and sensitive detection system with the lowest detection limit of 10–7 mg/mL falling in the range needed for drug loading and drug delivery applications. The difficulties faced in handling nanometre-sized bodies are also one of the biggest challenges in the area of nanoparticle studies and their physico-chemical characterization. However, challenges remain as such to achieve higher level control and effective communication with analytical and detector systems.

Electrophoresis is the most commonly used method in this area, despite its contactless nature, and recent research has demonstrated its ability to control nanoparticles in a continuous flow configuration. Contactless manipulation approaches are generally favoured to mechanical manipulation that could theoretically jeopardize nanoparticle credibility. However, the latter is typically easier to incorporate, and it does not allow the external energy sources to be implemented. Recent developments in the area of mechanical regulation of nanoparticles have been reported in a research by Wang et al. For multi-scale "smooth" filtration of a liposome suspension, researchers produced ciliated micropillars. Cilia comprised of porous nanowires of silicon that bound the liposomes suspended and could then be dissolved in phosphate buffer saline to retrieve the entangled specimen. Notably, liposomes were whole after the device was operated. The minimal requirement in terms of reagent use is another important feature of microfluidic reactors. It could provide a forum for quick optimization and high throughput testing of biological activity of nanomaterials, along with the likelihood of system variation of process parameters, including concentration of reactants and content. A move towards this framework was recently introduced using a continuous flow model. However, given that rapidly increasing interest and technological advances in droplet microfluidics for testing applications, the pairing of microreactor technology and droplet-based testing systems may be evident in the future. For the assessment of biological efficiency of nanoparticles, the design of systems having the ability of imitating the dynamic behavioural stream environment is important. Recently, Kusunose et al. reported a micro-flow chamber based on PDMS to investigate liposome binding to a monolayer of endothelial cells subject to physiologically relevant liquid shear pressure in the range 2.4–8.6 dyn/cm^2.

This system can be used to test the efficiency of nanoparticles for drug delivery applications as a substitute to rodent models. Notably, communication mechanisms between nanoparticles and cells and the cellular processes controlling the delivery of intracellular drugs remain unknown to a greater extent. Recent research by Sahay et al. has opened up interesting new perspectives into the mechanisms of cellular absorption of short-interfering RNA (siRNA) loaded in nanoparticles generated by microfluidic technology. Authors have shown that the performance of take-up could be increased by developing delivery carriers to avoid recycling pathways (i.e. endocytosis). This has been demonstrated

recently by various authors besides nanoparticles. In this regard, it is important to note that achievable rapid mixing in microfluidics provides a way to "lock" the formed nanoparticle in non-equilibrium structure and crystal frameworks with the goal of creating non-conventional shapes of nanomaterials. Research into this path has recently been published with positive results, but with scant information on the underlying governing structures. Wang and his colleagues have lately examined the function of both chemical and fluidic conditions in the morphology of self-assemblies of co-polymers developed using a two-phase gas-liquid segmented microreactor. Researchers outlined unusual properties of microfluidic growth compared to macroscale synthesis. It represents a very exciting research area that could open up a potential highway that is not limited to nanomedicine alone. In addition, it should be noted that only a few studies examined the encapsulation of nanoparticles involved in a microfluidic process or associated mechanisms of governance. In reality, this is crucial for the development of new therapeutic approaches and as the recent scientific studies indicate, it is expected to be the subject of potential investigations. In this regard, Majedi et al. used a T-shape 2D HFF system to generate hydrophobically altered chitosan nanoparticles containing hydrophobic anticancer drug (i.e. paclitaxel). Researchers examined the impact of operating parameters on charging performance and studied kinetics of drug release from NPs.

The need for more post-processing steps to acquire specimens appropriate for in-vivo and in-vitro testing following microfluidic nanomaterial development is yet another critical problem that needs to be addressed ahead. These include, for example, purification by dialysis of the reaction mixture from toxic solvent and isolation of the particles from the reaction product. Also, an interesting area of upcoming research is the development and construction of vesicles to be used as prototypes of physiological systems. Microfluidics can be a strong tool for creating cellular models with dimensional control and integration subcellular structures. A recent study by Mijajlovic et al. performed a synthesis of 1-palmitoyl-2-oleoyl-sn-glycero-3-phosphocholine (POPC) vesicles using 2D HFF method. Since the moment POPC is one of the basic components of the cellular membrane, the formed vesicles can find its application in the modelling of cells or organelles. A research by Kamiya et al. recently documented the development of vesicles of cell size that encapsulate tiny vesicles through multiple step pulsed jetting. The developed "vesicles in a vesicle" may reflect an artificial cell template to be used in biological process analysis, like intracellular vesicle traffic. In summary, regardless of the fact that the usage of microfluidic reactor for the production of nanomaterial is not yet a commercially active technology, experimentation over the past few decades has shown that the microfluidics can promote the development of nanomaterials for the purpose of drug delivery, providing a new technique for improving and modifying their characteristics. Due to the fast development of nanomedicine and microfluidics branches, the extension of expertise at their convergence is expected to provide amazing new ways to customize nanomaterials characteristics through regulated microfluidic precipitation in the future.

17 Conclusion

Need for the development of more robust and controllable procedures has been dictated by the advancements in the field of nanomedicine for the production of nanoparticles. Nanoparticles formulation using microfluidic chips is currently a very active field of research. Despite the fact that use of microfluidic technology for nanoparticle production has not matured yet, the research carried out previously established that microfluidics could facilitate the production of nanoparticles for drug delivery purposes.

In summary, this technology allows microfluidics to generate nanoparticles for the delivery of the drugs in a manageable, replicable and high throughput manner, and also to characterize and validate the quality of particles under reconstituted 3D microenvironmental conditions that are physiologically important. Microfluidics may

imitate the features of human organs and may allow researchers to anticipate the safety and efficacy of pharmacological drug molecules before entering into clinical phase trials. Furthermore, organ-on-a-chip devices can use microfabrication, miniaturization and guided engineering techniques to spatiotemporally manipulate 3D extracellular environments. The use of microfluidics in drug delivery experiments of nanoparticles will appear to be a crucial element in accelerating pre-clinical step-by-step development, thereby minimizing the time and resources necessary to launch medicines. In the past two decades, microfluidics has gained a great deal of interest from the scientific community. This technique has been widely regarded and applied in a short span of time in several fields of science such as chemistry, chemical engineering, material science, medicine, biology and so on. The fundamentals of fluid flow in systems with incredibly small distinctive dimensions (generally hundreds of microns) have been explained by now and thanks to the efforts of many scientists. This has been valuable for the successful development of drug-loaded micro and nanocarriers and permits the development of a complete set of systems for the manufacturing of such materials. Microfluidic tools have therefore been used to generate a broad spectrum of microcarriers (microspheres, microgels, microcapsules, core-shell particles, Janus particles, microfibers, etc.) and nanocarriers (polymeric nanoparticles, solid-lipid nanoparticles, nano-emulsions, drug conjugates, Janus nanoparticles, etc.), wherein different active pharmaceutical ingredients are packed for local, systemic or targeted delivery. It should be noted that a single unit can also be used with minor modifications to quickly build a wide range of charged carriers. It has been shown that carriers generated from microfluidic systems have better length, better encapsulation efficiency, better linking of targeting agents onto the appropriate nanocarriers and are essentially more efficient in in vitro and in vivo tests than those developed in traditional equivalent macro-systems.

Since microfluidic systems use very limited amount of materials and resources for the manufacture of nanocarriers, they are extremely ideal for

(i) those interested in researching and developing new systems for delivery;
(ii) those associated with costly or minimal amounts of available components and
(iii) those concerned with carcinogenic materials, thus saving materials and time.

Given all these benefits, such micro devices are associated with some disadvantages as below:

(i) clean room facilities may be required for the manufacturing of these devices and the process can also be time consuming;
(ii) clogging of channels is the major problem and the model and material of the system needs to be selected with utmost care depending on the nature of the application and
(iii) such devices are generally not yet appropriate for commercial applications.

Therefore, it is highly appreciable to fabricate new microfluidic tools for large scale manufacturing or to depend on the so-called numbering method that comprises of parallelizing many same kind micro devices. Microfluidics is still in its infancy in the area of medical applications. Hence, hardships are being faced in figuring out the exact area in which this particular technique will prosper in future. As a guess, prospective healthcare environments can be foreseen. One possible area that scientists and pharmaceutical industries are likely to focus on in the future is guided polymer carriers with the ability to transport protein and anticancer drugs. Amongst the most interesting carrier anatomy is the Janus system that can store and distribute two different drugs at the same time.

Microfluidic 3D cancer models therefore have the capability to effectively recognize cancer drug targets compared to conventional rodent models that lacks the capability to mimic human physiology and functions. Last but not least, as it would be very simple, cheap and easy to use, this method is ready to take the diagnostic point of care to a newer level. Instead of waiting for results from the standard medical laboratory diagnostic test, this would allow healthcare professionals to easily detect and classify on-site

treatment. Therefore, the combination of microfluidics and the medical profession is setting a newer paradigm of safe, reliable, quick, simple and minimal cost testing/diagnostic tools and medications.

References

Abstiens K, Goepferich AM. Microfluidic manufacturing improves polydispersity of multicomponent polymeric nanoparticles. J Drug Deliv Sci Technol. 2019;49:433–9.

Ahn J, Ko J, Lee S, Yu J, Kim Y, Jeon NL. Microfluidics in nanoparticle drug delivery; from synthesis to pre-clinical screening. Adv Drug Deliv Rev. 2018;128:29–53.

Bhagat AAS, Bow H, Hou HW, Tan SJ, Han J, Lim CT. Microfluidics for cell separation. Med Biol Eng Comput. 2010;48(10):999–1014.

Bhatia SN, Ingber DE. Microfluidic organs-on-chips. Nat Biotechnol. 2014;32(8):760.

Bhise NS, Manoharan V, Massa S, Tamayol A, Ghaderi M, Miscuglio M, Lang Q, ZhangYS SSR, Calzone G, Annabi N. A liver-on-a-chip platform with bioprinted hepatic spheroids. Biofabrication. 2016;8(1):014101.

Björnmalm M, Yan Y, Caruso F. Engineering and evaluating drug delivery particles in microfluidic devices. J Control Release. 2014;190:139–49.

Bragheri F, Vazquez RM, Osellame R. Microfluidics. In: Three-dimensional microfabrication using two-photon polymerization: William Andrew Publishing; 2020. p. 493–526.

Capretto L, Carugo D, Mazzitelli S, Nastruzzi C, Zhang X. Microfluidic and lab-on-a-chip preparation routes for organic nanoparticles and vesicular systems for nanomedicine applications. Adv Drug Deliv Rev. 2013;65(11–12):1496–532.

Carroll NJ, Rathod SB, Derbins E, Mendez S, Weitz DA, Petsey DN. Droplet-based microfluidics for emulsion and solvent evaporation synthesis of monodisperse mesoporous silica microspheres. Langmuir. 2008;24(3):658–661.

Carugo D, Bottaro E, Owen J, Stride E, Nastruzzi C. Liposome production by microfluidics: potential and limiting factors. Sci Rep. 2016;6:25876.

Champion JA, Katare YK, Mitragotri S. Particle shape: a new design parameter for micro-and nanoscale drug delivery carriers. J Control Release. 2007;121(1–2):3–9.

Chang CH, Paul BK, Remcho VT, Atre S, Hutchison JE. Synthesis and post-processing of nanomaterials using microreaction technology. J Nanoparticle Res. 2008;10(6):965–80.

De Geest BG, Urbanski JP, Thorsen T, Demeester J, De Smedt SC. Synthesis of monodisperse biodegradable microgels in microfluidic devices. Langmuir. 2005;21(23):10275–10279.

Dendukuri D, Gu SS, Pregibon DC, Hatton TA, Doyle PS. Stop-flow lithography in a microfluidic device. Lab Chip. 2007;7(7):818–88.

DesRochers TM, Suter L, Roth A, Kaplan DL. Bioengineered 3D human kidney tissue, a platform for the determination of nephrotoxicity. PLoS One. 2013;8(3):59219.

Dev S, Iyer KS, Raston CL. Nanosized drug formulations under microfluidic continuous flow. Lab Chip. 2011;11(19):3214–7.

Doshi N, Prabhakarpandian B, Rea-Ramsey A, Pant K, Sundaram S, Mitragotri S. Flow and adhesion of drug carriers in blood vessels depend on their shape: a study using model synthetic microvascular networks. J Control Release. 2010;146(2):196–200.

Edel JB, Fort R, demello JC, demello AJ. Microfluidic routes to the controlled production of nanoparticles. Chem Commun. 2002;10:1136–7.

Fleischer S, Shevach M, Feiner R, Dvir T. Coiled fiber scaffolds embedded with gold nanoparticles improve the performance of engineered cardiac tissues. Nanoscale. 2014;6(16):9410–4.

Fraikin JL, Teesalu T, McKenney CM, Ruoslahti E, Cleland AN. A high-throughput label-free nanoparticle analyser. Nat Nanotechnol. 2011;6(5):308.

Gao D, Li H, Wang N, Lin JM. Evaluation of the absorption of methotrexate on cells and its cytotoxicity assay by using an integrated microfluidic device coupled to a mass spectrometer. Anal Chem. 2012;84(21):9230–7.

Gubala V, Harris LF, Ricco AJ, Tan MX, Williams DE. Point of care diagnostics: status and future. Anal Chem. 2011;84(2):487–515.

Gupta N, Liu JR, Patel B, Solomon DE, Vaidya B, Gupta V. Microfluidics-based 3D cell culture models: utility in novel drug discovery and delivery research. Bioeng Transl Med. 2016;1(1):63–81.

Hans ML, Lowman AM. Biodegradable nanoparticles for drug delivery and targeting. Curr Opin Solid State Mater Sci. 2002;6(4):319–27.

Hong JS, Stavis SM, DePaoli Lacerda SH, Locascio LE, Raghavan SR, Gaitan M. Microfluidic directed self-assembly of liposome-hydrogel hybrid nanoparticles. Langmuir. 2010;26(13):1581–88.

Instruments M. Dynamic light scattering: an introduction in 30 minutes. Technical Note Malvern. 2012. MRK656–01, 1.

Jahn A, Vreeland WN, Gaitan M, Locascio LE. Controlled vesicle self-assembly in microfluidic channels with hydrodynamic focusing. J Am Chem Soc. 2004;126(9):2674–5.

Jahn A, Vreeland WN, DeVoe DL, Locascio LE, Gaitan M. Microfluidic directed formation of liposomes of controlled size. Langmuir. 2007;23(11):6289–93.

Janasek D, Franzke J, Manz A. Scaling and the design of miniaturized chemical-analysis systems. Nature. 2006;442(7101):374.

Karnik R, Gu F, Basto P, Cannizzaro C, Dean L, Kyei-Manu W, Langer R, Farokhzad OC. Microfluidic platform for controlled synthesis of polymeric nanoparticles. Nano Lett. 2008;8(9):2906–12.

Khan IU, Serra CA, Anton N, Vandamme T. Microfluidics: a focus on improved cancer targeted drug delivery systems. J Control Release. 2013;72(3):1065–74.

Khan IU, Serra CA, Anton N, Vandamme TF. Production of nanoparticle drug delivery systems with microfluidics tools. Expert Opin Drug Deliv. 2015;12(4):547–62.

Kim J, Vanapalli SA. Microfluidic production of spherical and nonspherical fat particles by thermal quenching of crystallizable oils. Langmuir. 2013;29(39):12307–12316.

Kim Y, Langer R. Microfluidics in nanomedicine. Rev Cell Biol Mol Med. 2015;1(2):127–52.

Kim Y, Joshi SD, Davidson LA, LeDuc PR, Messner WC. Dynamic control of 3D chemical profiles with a single 2D microfluidic platform. Lab Chip. 2011;11(13):2182–8.

Kozak D, Anderson W, Vogel R, Chen S, Antaw F, Trau M. Simultaneous size and ζ-potential measurements of individual nanoparticles in dispersion using size-tunable pore sensors. ACS Nano. 2012;6(8):6990–7.

Lasic DD. The mechanism of vesicle formation. Biochem J. 1988;56(1):1.

Li X, Ballerini DR and Shen W. A perspective on paper-based microfluidics: Current status and future trends. Biomicrofluidics. 2012;6:011301.

Lim JM, Bertrand N, Valencia PM, Rhee M, Langer R, Jon S, Farokhzad OC, Karnik R. Parallel microfluidic synthesis of size-tunable polymeric nanoparticles using 3D flow focusing towards *in vivo* study. Nanomed Nanotechnol. 2014;10(2):401–9.

Liu Z, Li Y, Li W, Xiao C, Liu D, Dong C, Zhang M, Mäkilä E, Kemell M, Salonen J, Hirvonen JT. Multifunctional nanohybrid based on porous silicon nanoparticles, gold nanoparticles, and acetalated dextran for liver regeneration and acute liver failure theranostics. Adv Mater. 2018;30(24):1703393.

Liu K, Ding HJ, Liu J, Chen Y, Zha XZ. Shape-controlled production of biodegradable calcium alginate microparticles using a novel microfluidic device. Langmuir. 2006;22(22):9453–57.

Liversidge GG, Cundy KC. Particle size reduction for improvement of oral bioavailability of hydrophobic drugs: I. absolute oral bioavailability of nanocrystalline danazol in beagle dogs. Int J Pharm. 1995;125(1):91–7.

Maeki M, Saito T, Sato Y, Yasui T, Kaji N, Ishida A, Tani H, Baba Y, Harashima H, Tokeshi M. A strategy for synthesis of lipid nanoparticles using microfluidic devices with a mixer structure. RSC Adv. 2015;5(57):46181–5.

Maeki M, Fujishima Y, Sato Y, Yasui T, Kaji N, Ishida A, Tani H, Baba Y, Harashima H, Tokeshi M. Understanding the formation mechanism of lipid nanoparticles in microfluidic devices with chaotic micromixers. PLoS One. 2017;12(11):0187962.

Maeki M, Kimura N, Sato Y, Harashima H, Tokeshi M. Advances in microfluidics for lipid nanoparticles and extracellular vesicles and applications in drug delivery systems. Adv Drug Deliv Rev. 2018;128:84–100.

Martins JP, Torrieri G, Santos HA. The importance of microfluidics for the preparation of nanoparticles as advanced drug delivery systems. Expert Opin Drug Deliv. 2018;15(5):469–79.

Mello JD, Mello AD. Focus Microscale reactors: nanoscale products. Lab Chip. 2004;4(2):11N–5N.

Merisko-Liversidge E, Liversidge GG, Cooper ER. Nanosizing: a formulation approach for poorly-water-soluble compounds. Eur J Pharm Sci. 2003;18(2):113–20.

Mitra A, Deutsch B, Ignatovich F, Dykes C, Novotny L. Nano-optofluidic detection of single viruses and nanoparticles. ACS Nano. 2010;4(3):1305–12.

Mosharraf M, Nyström C. The effect of particle size and shape on the surface specific dissolution rate of microsized practically insoluble drugs. Int J Pharm. 1995;122(1–2):35–47.

Namdee K, Thompson AJ, Charoenphol P, Eniola-Adefeso O. Margination propensity of vascular-targeted spheres from blood flow in a microfluidic model of human microvessels. Langmuir. 2013;29(8):2530–5.

Nguyen NT, Wu Z. Micromixers-a review. J Micromech Microeng. 2004;15(2):R1.

Okushima S, Nisisako T, Torii T, Higuchi T. Controlled production of monodisperse double emulsions by two-step droplet breakup in microfluidic devices. Langmuir. 2004;20(23):9905–9908.

Park JI, Saffari A, Kumar S, Günther A, Kumacheva E. Microfluidic synthesis of polymer and inorganic particulate materials. Annu Rev Mater Res. 2010;40:415–43.

Patton JS, Fishburn CS, Weers JG. The lungs as a portal of entry for systemic drug delivery. Proc Am Thorac Soc. 2004;1(4):338–44.

Rathod ML, Ahn J, Jeon NL, Lee J. Hybrid polymer microfluidic platform to mimic varying vascular compliance and topology. Lab Chip. 2017;17(14):2508–16.

Rondeau E, Cooper-White JJ. Bipolymer microparticle and nanoparticle formation within a microfluidic device. Langmuir. 2008;24(13):6937–6945.

Russo M, Grimaldi AM, Bevilacqua P, Tammaro O, Netti PA, Torino E. PEGylated crosslinked hyaluronic acid nanoparticles designed through a microfluidic platform for nanomedicine. Nanomedicine. 2017;12(18):2211–22.

Shepherd RF, Conrad JC, Rhodes SK, Link DR, Marquez M, Weitz DA, Lewis JA. Microfluidic assembly of homogeneous and janus colloid-filled hydrogel granules. Langmuir. 2006;22(21):8618–22.

Sackmann EK, Fulton AL, Beebe DJ. The present and future role of microfluidics in biomedical research. Nature. 2014;507(7491):181.

Shestopalov I, Tice JD, Ismagilov RF. Multi-step synthesis of nanoparticles performed on millisecond time

scale in a microfluidic droplet-based system. Lab Chip. 2004;4(4):316–21.
Stroock AD, Dertinger SK, Ajdari A, Mezić I, Stone HA, Whitesides GM. Chaotic mixer for microchannels. Science. 2002;295(5555):647–51.
Tang Y, Soroush F, Sheffield JB, Wang B, Prabhakarpandian B, Kiani MF. A biomimetic microfluidic tumor microenvironment platform mimicking the EPR effect for rapid screening of drug delivery systems. Sci Rep. 2017;7(1):9359.
Tarn MD, Pamme N. Microfluidics. Reference module in chemistry, molecular sciences and chemical engineering. 2014. p. 1–7.
Valencia PM, Basto PA, Zhang L, Rhee M, Langer R, Farokhzad OCand Karnik R. Single-step assembly of homogenous lipid-polymeric and lipid-quantum dot nanoparticles enabled by microfluidic rapid mixing. ACS Nano. 2010;4(3):1671–9.
Valencia PM, Farokhzad OC, Karnik R, Langer R. Microfluidic technologies for accelerating the clinical translation of nanoparticles. Nat Nanotechnol. 2012;7(10):623.
Valencia PM, Pridgen EM, Rhee M, Langer R, Farokhzad OC, Karnik R. Microfluidic platform for combinatorial synthesis and optimization of targeted nanoparticles for cancer therapy. ACS Nano. 2013;7(12):10671–80.
Vo VH, Ganguli D. Amorphous nanoparticles – experiments and computer simulations. Phys Rep. 2012;518(3):81–140.
Van Midwoud PM, Verpoorte E, Groothuis GM. Microfluidic devices for *in vitro* studies on liver drug metabolism and toxicity. Integr Biol. 2011;3(5):509–21.
Vladisavljević GT, Khalid N, Neves MA, Kuroiwa T, Nakajima M, Uemura K, Ichikawa S, Kobayashi I. Industrial lab-on-a-chip: design, applications and scale-up for drug discovery and delivery. Adv Drug Deliv Rev. 2013;65(11–12):1626–63.
Wang JX, Zhang QX, Zhou Y, Shao L, Chen JF. Microfluidic synthesis of amorphous cefuroxime axetil nanoparticles with size-dependent and enhanced dissolution rate. Chem Eng J. 2010;162(2):844–51.
Wang JT, Wang J, Han JJ. Fabrication of advanced particles and particle-based materials assisted by droplet-based microfluidics. Small. 2011;7(13):1728–54.
Watanabe T, G. Lopez C, Douglas JF, Ono T, Cabral JT. Microfluidic approach to the formation of internally porous polymer particles by solvent extraction. Langmuir. 2014;30(9):2470–79
Wilkosz N, Łazarski G, Kovacik L, Gargas P, Nowakowska M, Jamróz D, Kepczynski M. Molecular insight into drug-loading capacity of PEG–PLGA nanoparticles for itraconazole. J Phys Chem B. 2018;122(28):7080–90.
Wilmer MJ, Ng CP, Lanz HL, Vulto P, Suter-Dick L, Masereeuw R. Kidney-on-a-chip technology for drug-induced nephrotoxicity screening. Trends Biotechnol. 2016;34(2):156–70.
Xiao RZ, Zeng ZW, Zhou GL, Wang JJ, Li FZ, Wang AM. Recent advances in PEG–PLA block copolymer nanoparticles. Int J Nanomedicine. 2010;5:1057.
Xie H, She ZG, Wang S, Sharma G, Smith JW. One-step fabrication of polymeric Janus nanoparticles for drug delivery. Langmuir. 2012;28(9):4459–63.
Xu X, Farach-Carson MC, Jia X. Three-dimensional *in vitro* tumor models for cancer research and drug evaluation. Biotechnol Adv. 2014;32(7):1256–68.
Yaralioglu GG, Wygant IO, Marentis TC, Khuri-Yakub BT. Ultrasonic mixing in microfluidic channels using integrated transducers. Anal Chem. 2004;76(13):3694–8.
Yin H, Killeen K, Brennen R, Sobek D, Werlich M, van de Goor T. Microfluidic chip for peptide analysis with an integrated HPLC column, sample enrichment column, and nanoelectrospray tip. Anal Chem. 2005;77(2):527–33.
Zhang HX, Wang JX, Shao L, Chen JF. Microfluidic fabrication of monodispersed pharmaceutical colloidal spheres of atorvastatin calcium with tunable sizes. Ind Eng Chem Res. 2010;9(9):4156–61.
Zhang QX, Xu LM, Zhou Y, Wang JX, Chen JF. Preparation of drug nanoparticles using a T-junction microchannel system. Ind Eng Chem Res. 2011;50(24):13805–12.
Zhang YS, Aleman J, Arneri A, Bersini S, Piraino F, Shin SR, Dokmeci MR, Khademhosseini A. From cardiac tissue engineering to heart-on-a-chip: beating challenges. Biomed Mater. 2015;10(3):034006.
Zhang J, Yan S, Yuan D, Alici G, Nguyen NT, Warkiani ME, Li W. Fundamentals and applications of inertial microfluidics: a review. Lab Chip. 2016a;16(1):10–34.
Zhang J, Yan S, Yuan D, Alici G, Nguyen NT, Warkiani ME, Li W. Fundamentals and applications of inertial microfluidics: a review. Lab Chip. 2016b;16(1):10–34.
Zhang YN, Poon W, Tavares AJ, McGilvray ID, Chan WC. Nanoparticle-liver interactions: cellular uptake and hepatobiliary elimination. J Control Release. 2016c;240:332–48.
Zhao CX. Multiphase flow microfluidics for the production of single or multiple emulsions for drug delivery. Adv Drug Deliv Rev. 2013;65(11–12):1420–46.
Zhao H, Wang JX, Wang QA, Chen JF, Yun J. Controlled liquid antisolvent precipitation of hydrophobic pharmaceutical nanoparticles in a microchannel reactor. Ind Eng Chem Res. 2007;46(24):8229–35.
Zhao CX, He L, Qiao SZ, Middelberg AP. Nanoparticle synthesis in microreactors. Chem Eng Sci. 2011;66(7):1463–79.
Zhu WZ, Wang JX, Shao L, Zhang HX, Zhang QX, Chen JF. Liquid antisolvent preparation of amorphous cefuroxime axetil nanoparticles in a tube-in-tube microchannel reactor. Int J Pharm. 2010;395(1–2):260–5.

Production of Nanocomposites via Extrusion Techniques

5

Komal Parmar, Jayvadan K. Patel, and Deepak Bhatia

Abstract

Nanomaterials have always attracted the world with their innumerable and fascinating properties. Incorporation of nanoparticles in the nano matrix makes the nanocomposite which further shows amelioration in the basic characteristics of the material. The present chapter reviews the extrusion method employed in the fabrication of various types of nanocomposites including polymer matrix and metal matrix systems.

Keywords

Nanocomposites, · Polymer matrix · Matrix systems · Extrusion

1 Introduction

Dimensions of the particle play an important role in the physico-chemical properties of the matter. Nano-scale dimensions may lead to change in the properties of the material which can thereby prove to be beneficial in wide areas of science such as biomedical science (Ramos et al. 2017), electronics (Kamyshny and Magdassi 2019), optics (Ren et al. 2019), electrochemistry (Rassaei et al. 2011) and food science (Singh et al. 2017). Nanocomposites are the heterogeneous material of one or more nanoparticles embedded in a matrix. Depending on the composition of matrix, nanocomposites are classified into three types, viz., Ceramic-based nanocomposites, metal-based nanocomposites and polymer-based nanocomposites (Fig. 5.1). Their properties are determined by composition, structure and interfacial interactions of the materials. Ceramic-based nanocomposites are fabricated by various methods including polymer precursor process (Yu et al. 2019; Lu et al. 2016), sintering method (Wen et al. 2018; Kuznetsova et al. 2018). Metal matrix nanocomposites are processed by techniques namely spray pyrolysis (Zheng et al. 2017; Zhao et al. 2012), rapid solidification (Sobhani et al. 2013; Nayak et al. 2012), vapor phase synthesis (Muflikhun et al. 2019; Vucaj et al. 2014), electrodeposition method (Beltowska-Lehman et al. 2018; Birlik et al. 2016), sol-gel method (Famojuro et al. 2013; Sui

K. Parmar (✉)
ROFEL, Shri G.M. Bilakhia College of Pharmacy, Vapi, Gujarat, India

J. K. Patel
Nootan Pharmacy College, Sankalchand Patel University, Visnagar, Gujarat, India

D. Bhatia
Shenandoah University – ICPH Fairfax, Bernard J. Dunn School of Pharmacy, Fairfax, VA, USA

J. K. Patel, Y. V. Pathak (eds.), *Emerging Technologies for Nanoparticle Manufacturing*,
https://doi.org/10.1007/978-3-030-50703-9_5

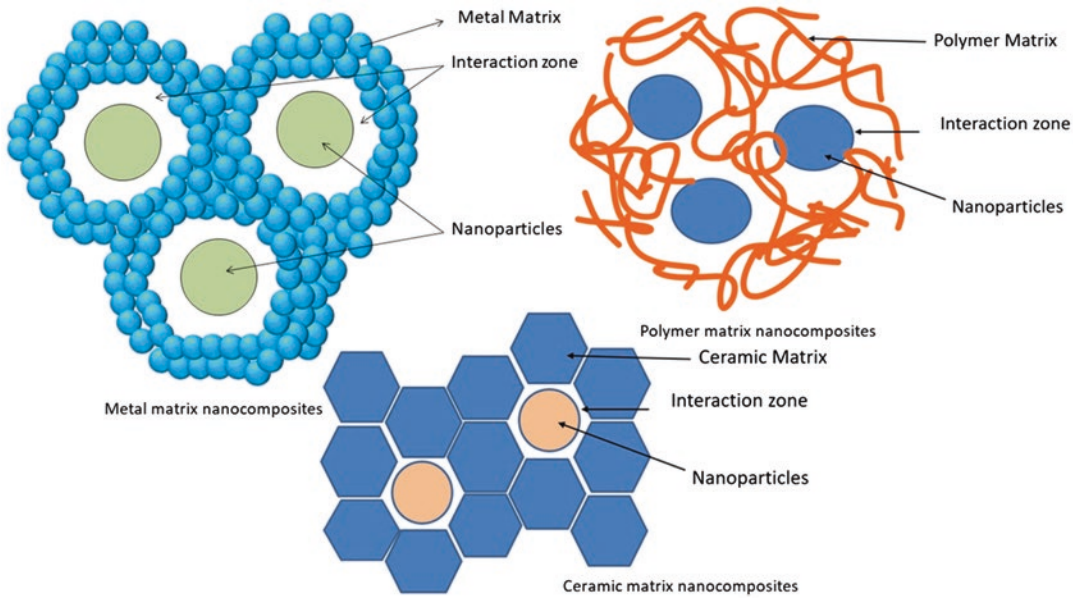

Fig. 5.1 Various types of nanocomposites

and Charpentier 2012), pressure infiltration process (Hu et al. 2016; Itskos et al. 2011) and co-precipitation method (Sahu et al. 2018; Das and Sirvasatava 2016). Polymer based nanocomposites can be prepared by various simple and complex techniques such as sol-gel method (Yadav and Jeevanandam 2015; Ansari et al. 2018), *in situ* polymerization method (Wang et al. 2015; O'Neill et al. 2017), solution mixing method (Zeng et al. 2011; Son and Park 2018), melt mixing method (Shimpi et al. 2017; Agarwal et al. 2019), *in situ* intercalative polymerization (Pavlacky and Webster 2015; Xu et al. 2016) and electrospinning method (Amini et al. 2018; Asokan et al. 2010).

Over the past few decades, extrusion technique is investigated by the research scholars in the preparation of nano range materials, viz. liposomes (Ong et al. 2016), solid lipid nanoparticles (Patil et al. 2015), gold nanoparticles (Khongkow et al. 2019), nanoemulsions (Alliod et al. 2018) and nanofiber (Wang et al. 2014). Extrusion is a simple, continuous technique in which the materials are passed through a membrane filter consisting of definite size pores which thereby results into multiparticulate system ranging from micron to nano size (Fig. 5.2).The process entails nanoporous membranes as template for production of nanomaterials, and the physical parameters of the nanopores govern the size, shape and structure of the fabricated nanomaterials. Materials are extruded through the membranes either in the molten state or in the solid state.

2 Polymeric Nanocomposites by Extrusion Method

Polymer nanocomposites are fabricated by embedding nanoparticles in polymer matrix. These nanocomposites possess high interfacial surface area between polymer matrix and the embedded nanoparticles. Generally, inorganic materials are mixed with the organic part (polymers) which then exhibits unique characteristics with improved barrier properties (Fu et al. 2019; Crosby and Lee 2007). Improved properties include resistance to temperature (Haruna and Wen 2019), enhanced mechanical properties (Liu et al. 2019), resistance to ionizing radiation (Borjanovic et al. 2012), improved optoelectronic properties (Mitra et al. 2013), improved dielectric properties (Deshmukh et al. 2017) and resistance to flame (Gao et al. 2014).

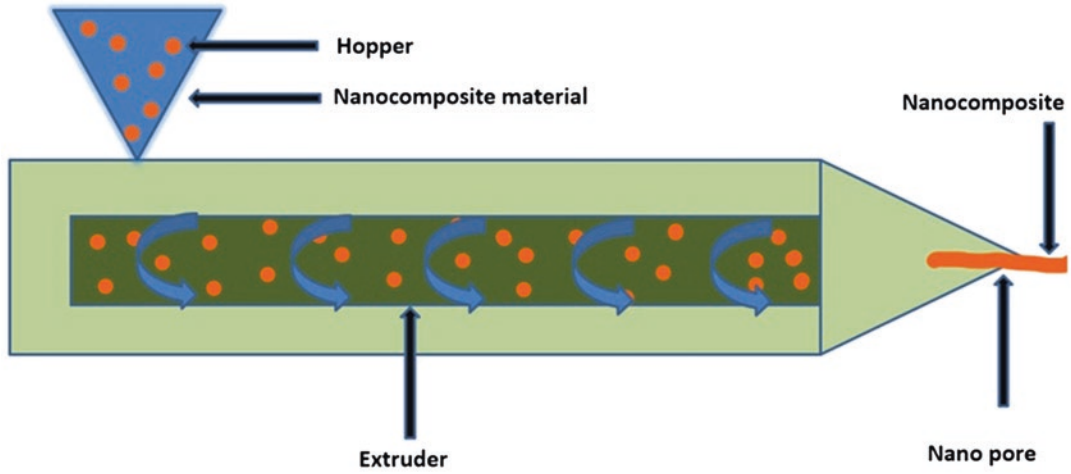

Fig. 5.2 Schematic diagram of extrusion process

Extrusion method is widely exploited in fabrication of polymeric nanocomposites by employing few modifications such as ultrasound and water assisted extrusion. Melt extrusion is the common method utilized in the synthesis of polymeric nanocomposites. In melt extrusion technique, the molten material is passed through the nozzle of extruder to transform into material of definite shape. In some process, the polymer is fed into the nozzle in solid state and is melted inside the extruder, thereby leaving the extruder in a definite form. Here in, the extruder acts as a pump forcing the polymer through the system and fabricating the nanomaterials. Typical extruder consists of part for feeding the polymer, a portion for melting and plasticizing the polymer, a pumping and pressurizing system. Screw extruders are most important among the other extruders because of its ability to continuously convert the feed material into final product. The feed material is forced through the rotating screw force in the barrel and moved forward in the die where the material is melted. Further, the molten material is forced through the orifice and fabricated into definite shape. Thus, the whole process is divided into several steps including feeding, melting of the material, mixing, conveying and flowing through the die under pressure (Stankovic et al. 2015). Depending on the design of extruder, there may be one or two screws, where twin screw extruder has gained more popularity due to its better mixing capacity. Twin extruder utilizes two interconnected screws which allow possibility of number of configurations throughout the process. These screws can rotate in clockwise (corotating) or anticlockwise (counter rotating) manner. Friction produced between the screws and the barrel produces a driving force for the content to reach the orifice (Patil et al. 2016). Figure 5.3 demonstrates the schematic representation of extrusion process in twin extruder. The extrudate obtained at the end is cooled by air, water or by contact with cold surface. To maximize the degree of crystallinity of the extrudate made up of semi-crystalline polymers, cooling rate is to be controlled. With rapid cooling rate, small crystals will be obtained and annealing will result into additional growth of crystals (Eldridge and Mount 2011). Various factors affect the quality of the product fabricated from the extrusion process such as viscosity of the polymer, viscosity of polymer due to change in shear rate and temperature, elasticity of the polymeric material, ambient temperature, relative humidity and moisture of the feed (Taubner and Shishoo 2001).

Polymers used in hot melt extrusion process require thermal stability and ability to mix on a molecular level (Kolter et al. 2012). Polymers can be either biodegradable or non-biodegradable. Generally, the polymers are low molecular weight materials with free volume between the polymer chains. This lowers the melting point or the glass

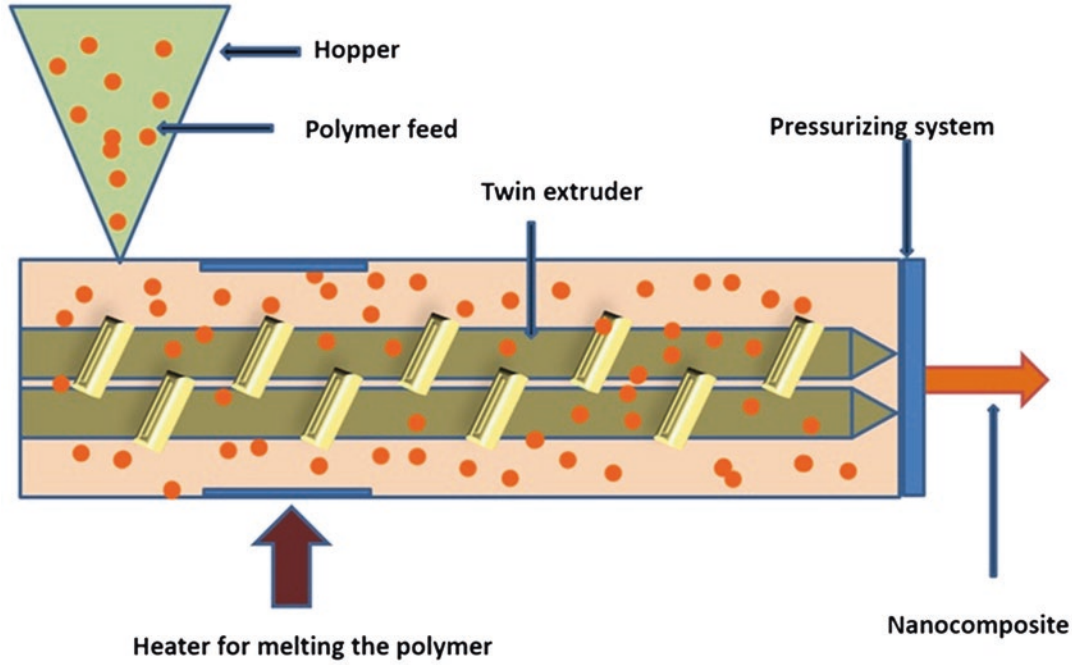

Fig. 5.3 Schematic diagram of a twin extruder for nanocomposite fabrication

transition temperature of the polymer, thereby improving the elasticity of the polymeric composition. Commonly used polymers include polyethylene glycol, polypropylene glycol, aliphatic esters, polyurethanes, polyvinyl lactam polymers and cellulose derivatives. Table 5.1 demonstrates list of polymeric systems prepared by extrusion technique.

Ultrasound-assisted melt extrusion for the fabrication of nanocomposites has shown a growing interest in the last decade. A schematic representation of ultrasound assisted hot melt extrusion technique is demonstrated in Fig. 5.4. Various research study reported the fabrication of polymeric nanocomposites by ultrasound-assisted melt extrusion technique. In a study reported by Isayev and co-workers, a novel method using ultrasound assisted twin screw extrusion process for the constant distribution of multi walled carbon nanotubes in a polymer matrix for the production of nanocomposites. Results demonstrated moderate improvement in the mechanical properties after ultrasonic treatment (Isayev et al. 2009). In another such similar work was reported, wherein polypropylene/multi walled carbon nanotubes were prepared using ultra sound assisted melt extrusion process. Prepared nanocomposites showed more flexibility characteristics than its counterpart fabricated without ultrasound treatment (Mata-Padilla et al. 2015). Liang and co-investigators fabricated ultrahigh molecular weight polyethylene/organic montmorillonite nanocomposites using ultrasound deformation which led to superior tensile strength of the final product (Liang et al. 2017). Other authors reported polycaprolactone/hydroxyapatite nanocomposite prepared using ultrasound-assisted melt blending. The technique led to better dispersion of needle-shaped hydroxyapatite (Akhbar et al. 2017). In another similar study, Nylon 6/Cu Nanocomposites were produced by an ultrasound-assisted extrusion process. Mechanical properties of the final product were significantly improved for 0.1% concentration nanocomposite (Sierra-Avila et al. 2018).

Water assisted extrusion is another modification combined with melt extrusion of polymeric materials. It was first reported with fabrication of polyamide/untreated clay nanocomposites by wherein the polymer and clay are melted and

Table 5.1 Various polymeric systems fabricated by extrusion technique

Polymer used	Polymeric system	Authors
Poly lactic acid, Poly butylene succinate	Nanobiocomposite	Monika et al. (2018)
Polyethylene glycol	Nanocomposite	Campbell et al. (2008)
Polyvinyl pyrrolidone	Polymeric matrix	Gupta et al. (2014)
Polyurethane	Nanocomposite	Wohlleben et al. (2013)
Ethylene-vinyl acetate copolymer	Nanocomposite	Zhang and Sundararaj (2004)
Polyacrylic acid	Nanocomposite	Shen et al. (2011)
Polyethylene oxide	Polymeric matrix	Healy et al. (2018)
Polysaccharide	Nanocomposite	Pereda et al. (2014)
Hydroxy propyl methyl cellulose	Nanocomposite	Azad et al. (2019)
Polypropylene	Nanocomposite	Cabello-Alvarado et al. (2019)
Polystyrene	Clay nanocomposite	Luecha and Magaraphan (2019)

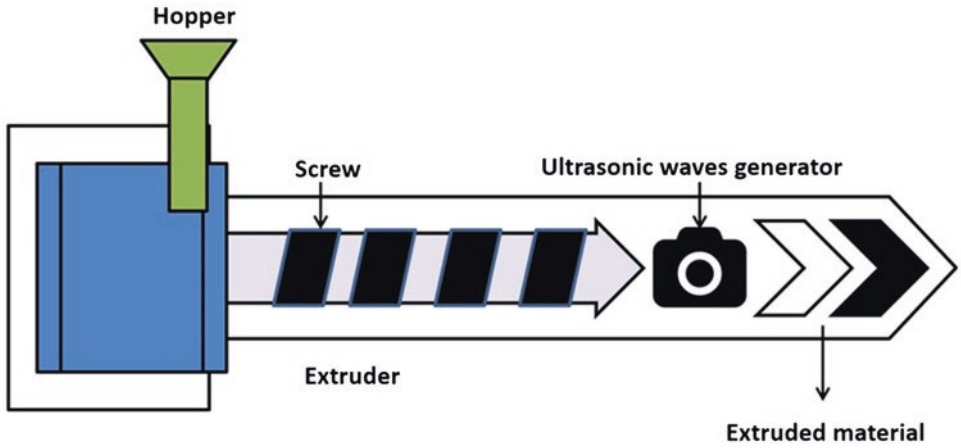

Fig. 5.4 Schematic representation of ultrasound assisted extrusion process

mixed with water in the extruder. Water injection system and degassing system are utilized to introduce at high pressure and temperature and then removed by the later respectively (Korbee and Van Geneen 1999). A schematic representation of water assisted extrusion process is shown in Fig. 5.5. Since then various research work employing fabrication of polymer/clay nanocomposites by water assisted extrusion process are reported. Polypropylene/halloysite nanotube nanocomposites were prepared using water assisted extrusion technique. Researchers reported dynamic improvement in linear viscoelastic properties and storage modulus of the prepared nanocomposites (Lecouvet et al. 2011). Similar work was reported in which polypropylene/clay nanocomposites were fabricated using water assisted extrusion process at high shear stress. Thermal, rheological and tensile properties were found to be improved in the prepared nanocomposites (Lee et al. 2015). In other such study, poly(lactic acid)/halloysite nanocomposites were synthesized by means of water assisted technique. Study revealed improvement in thermomechanical and flame-retardant properties of the nanocomposites. Also, results concluded that water acted as a barrier which prevented polymer degradation during the extrusion process (Stoclet et al. 2014). Charlon and his co-workers demonstrated use of water assisted extrusion process for the preparation of poly[(butylene succinate)-co-(butylene adipate)]-montmorillonite nanocomposites. The treatment enhanced the dispersion and exfoliation levels of montomorillonite and improved the barrier properties of the nanocomposites (Charlon et al. 2016). In another research

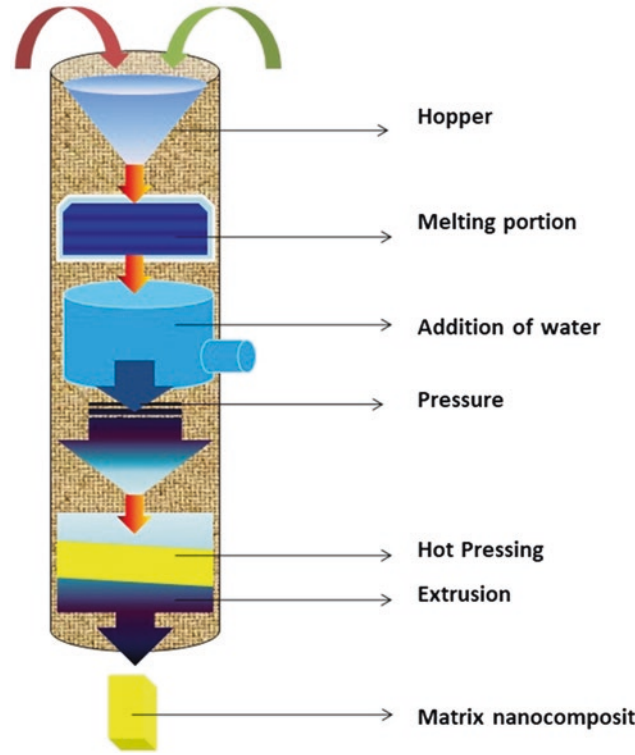

Fig. 5.5 Schematic representation of water assisted melt extrusion process

work, bio-based polyethylene terephthalate glycol-modified/clay nanocomposites were synthesized using the water-assisted extrusion process. Results demonstrated improved rheological and tensile properties of the prepared nanocomposites (Lee and Lee 2018).

3 Metal Matrix Nanocomposites Prepared by Extrusion Method

Metal matrix nanocomposites are comprised up of two parts: one consists of metal as matrix and the other is a strengthening agent. Mostly used strengthening agents are ceramic, carbon nanotubes and Aluminium oxide. Various researchers have reported extrusion technique for the synthesis of metal matrix nanocomposites. In one such work, aluminium metal nanocomposites were prepared by A356 aluminum metal matrix nanocomposites by melt extrusion method. Carbon nanotubes and Al_2O_3 were used as reinforcing agents. Preparation of hybrid metal matrix nanocomposites of A356 aluminum demonstrated two times more resistance against deformation than that of the original metal material (Kim et al. 2014). In another study, aluminium metal matrix nanocomposites were fabricated using microwave sintering and hot extrusion process. Silicon carbide was employed as reinforcing material. Structural and thermal properties were studied and demonstrated a significant improvement in compressive and tensile strength of the aluminium metal matrix nanocomposites with the addition of silicon carbide (Reddy et al. 2017). Nano-sized Si_3N_4/Al composites were synthesized using a powder metallurgy technique including microwave sintering method and hot extrusion treatment. Results revealed enhancement of compressive and tensile strength of aluminium nanocomposites with presence of Si_3N_4 (Matli et al. 2017). In another investigation, researchers demonstrated increase in mechanical properties of metal alloy matrix nanocomposites. Nano-TiB_2 particles reinforced Al–Zn–Mg–Cu alloys matrix composites were fabricated by extrusion process. The high strength of 687 MPa

and ductility of 14.8% were achieved in the resultant hybrid nanocomposites (Liu et al. 2018). Dong and co-workers studied influence of extrusion temperature varying from 480 to 560 °C on the microstructure and mechanical properties of SiCnw/2024Al nanocomposite. Results showed better properties of the hybrid nanocomposites synthesized at extrusion temperature higher than 520 °C. This employment of higher temperature led to densification of the nanocomposite and improvement in the mechanical strength. Highest strength and elastic modulus measure were found to be 709.4 MPa and 109.8 GPa, respectively.

4 Conclusion

Extrusion technique is undoubtedly gearing in efficiency in production of various types of nanocomposites with wide range of applications. Various investigators have already reported metal and polymer matrix nanocomposites fabricated by extrusion treatment. It is the simplest of all methods for the preparation of nanocomposites. Nanocomposites prepared by this method have proved to be mechanically strong and gained enhanced properties. Extrusion technique has been and will be the efficient technique for the synthesis of nanocomposites.

References

Agarwal K, Prasad M, Katiyar M, Kumar R, Prasad NE. Preparation and characterization of $Ni_{0.5}Zn_{0.5}Fe_2O_4$ + polyurethane nanocomposites using melt mixing method. Silicon. 2019;11(2):1035–45.

Akhbar S, Subuki I, Sharudin RW, Ismail MH. Morphology of polycaprolactone/needle-shapedhydroxyapatite (PCL/HAN) nanocomposite blends usingultrasound assisted melt blending. IOP Conf Ser Mater Sci Eng. 2017;213:012025. https://doi.org/10.1088/1757-899X/213/1/012025.

Alliod O, Valour JP, Urbaniak S, Fessi H, Dupin D, Charcosset C. Preparation of oil-in-water nanoemulsions at large-scale using premix membrane emulsification and Shirasu Porous Glass (SPG) membranes. Colloids Surf A Physicochem Eng Asp. 2018;557:76–84.

Amini M, Haddadi SA, Ghaderi S, Ahmad Ramazani SA, Ansarizadeh MH. Preparation and characterization of PVDF/Starch nanocomposite nanofibers using electrospinning method. Mater Today Proc. 2018;5(7):15613–9.

Ansari F, Sobhani A, Salavati-Niasari M. Simple sol-gel synthesis and characterization of new $CoTiO_3$/$CoFe_2O_4$ nanocomposite by using liquid glucose, maltose and starch as fuel, capping and reducing agents. J Colloid Interface Sci. 2018;514:723–32.

Asokan K, Park JY, Choi SW, Kim SS. Nanocomposite ZnO–SnO2 nanofibers synthesized by electrospinning method. Nanoscale Res Lett. 2010;5:747.

Azad MOK, Kim WW, Jin CW, Kang WS, Park CH, Cho DH. Development of a polymer-mediated soybean nanocomposite by hot melt extrusion to improve its functionality and antioxidant properties. Foods. 2019;8(2):41. https://doi.org/10.3390/foods8020041.

Beltowska-Lehman E, Bigos A, Indyka P, Chojnacka A, Drewienkiewicz A, Zimowski S, Kot M, Szczerba MJ. Optimisation of the electrodeposition process of Ni-W/ZrO_2 nanocomposites. J Electroanal Chem. 2018;813:39–51.

Birlik I, Azem NFA, Toparli M, Celik E, Delice TK, Yildirim S, Bardakcioglu O, Dikici T. Preparation and characterization of Ni–TiO_2 nanocomposite coatings produced by electrodeposition technique. Front Mater. 2016; https://doi.org/10.3389/fmats.2016.00046.

Borjanovic V, Bistricic L, Mikac L, McGuire GE, Zamboni I, Jaksic M, Shenderova O. Polymer nanocomposites with improved resistance to ionizing radiation. J Vac Sci Technol B Microelectron Nanometer Struct. 2012;30(4):1803. https://doi.org/10.1116/1.4724310.

Cabello-Alvarado C, Reyes-Rodríguez P, Andrade-Guel M, Cadenas-Pliego G, Pérez-Alvarez M, Cruz-Delgado VJ, Melo-López L, Quiñones-Jurado ZV, Ávila-Orta CA. Melt-mixed thermoplastic nanocomposite containing carbon nanotubes and titanium dioxide for flame retardancy applications. Polymers. 2019;11(7):1204. https://doi.org/10.3390/polym11071204.

Campbell K, Craig DQ, McNally T. Poly(ethylene glycol) layered silicate nanocomposites for retarded drug release prepared by hot-melt extrusion. Int J Pharm. 2008;363(1-2):126–31.

Charlon S, Follain N, Dargent E, Soulestin J, Sclavons M, Marais S. Poly[(butylene succinate)-co-(butylene adipate)]-montmorillonite nanocomposites prepared by water-assisted extrusion: role of the dispersion level and of the structure-microstructure on the enhanced barrier properties. J Phys Chem C. 2016;120(24):13234–48.

Crosby AJ, Lee JY. Polymer nanocomposites: the "nano" effect on mechanical properties. Polym Rev. 2007;47(2):217–29.

Das S, Sirvasatava VC. Synthesis and characterization of ZnO–MgO nanocomposite by co-precipitation method. Smart Sci. 2016;4(4):190–5.

Deshmukh K, Ahamed MB, Sadasivuni KK, Ponnamma D, Deshmukh RR, Trimukhe AM, Pasha SKK, Polu AR, AlMaadeed MA, Chidambaram K. Solution-

processed white graphene-reinforced ferroelectric polymer nanocomposites with improved thermal conductivity and dielectric properties for electronic encapsulation. J Polym Res. 2017;24:27. https://doi.org/10.1007/s10965-017-1189-4.

Eldridge M, Mount I. Extrusion processes. In: Applied plastics engineering handbook. Boston: Elsevier; 2011. p. 227–66.

Famojuro AT, Ojo IAO, Egharevba GO, Maaza MA. Sol-gel/hydrothermal synthesis of mixed metal oxide of Titanium and zinc (tio2 /zno) nanocomposites through direct chemical method. IFE J Sci. 2013;15(2):321–9.

Fu S, Sun Z, Huang P, Li Y, Hu N. Some basic aspects of polymer nanocomposites: a critical review. Nano Mater Sci. 2019;1(1):2–30.

Gao Y, Wu J, Wang Q, Wilkie CA, O'Hare D. Flame retardant polymer/layered double hydroxide nanocomposites. J Mater Chem A. 2014;2(29):10996–1016.

Gupta SS, Meena A, Parikh T, Serajuddin ATM. Investigation of thermal and viscoelastic properties of polymers relevant to hot melt extrusion – I: Polyvinylpyrrolidone and related polymers. J Excipients Food Chem. 2014;5(1):32–45.

Haruna MA, Wen D. Stabilization of polymer nanocomposites in high-temperature and high-salinity brines. ACS Omega. 2019;4(7):11631–41.

Healy AV, Waldron C, Geever LM, Devine DM, Lyons JG. Degradable nanocomposites for fused filament fabrication applications. J Manuf Mater Process. 2018;2:29. https://doi.org/10.3390/jmmp2020029.

Hu L, O'Neil M, Erturun V, Benitez R, Proust G, Karaman I, Radovic M. High-performance metal/carbide composites with far-from-equilibrium compositions and controlled microstructures. Sci Rep. 2016;6:35523. https://doi.org/10.1038/srep35523.

Isayev AI, Kumar R, Lewis TM. Ultrasound assisted twin screw extrusion of polymer–nanocomposites containing carbon nanotubes. Polymer. 2009;50(1):250–60.

Itskos G, Rohatgi PK, Moutsatsou A, Vasilatos C, Defow JD, Koukouzas N. Synthesis and characterization of ZnO–MgO nanocomposite by Co-precipitation method. In: World of Coal Ash (WOCA) conference-May 9-12, 2011, Denver, CO, USA. http://www.flyash.info/

Kamyshny A, Magdassi S. Conductive nanomaterials for 2D and 3D printed flexible electronics. Chem Soc Rev. 2019;48(6):1712–40.

Khongkow M, Yata T, Boonrungsiman S, Ruktanonchai UR, Graham D, Namdee K. Surface modification of gold nanoparticles with neuron-targeted exosome for enhanced blood–brain barrier penetration. Sci Rep. 2019;9:8278. https://doi.org/10.1038/s41598-019-44569-6.

Kim HH, Babu JSS, Kang CG. Hot extrusion of A356 aluminium metal matrix composite with carbon nanotube/Al_2O_3 hybrid reinforcement. Metall Mater Trans A. 2014;45(5):2636–45.

Kolter K, Karl M, Gryckze A. Hot-melt extrusion with basf pharma polymers. Extrusion compendium (2nd revised and enlarged edition). 2012; ISBN 978-3-00-039415-39417.

Korbee RA, Van Geneen AA. Process for the preparation of a polyamidenanocomposite composition. WO; 1999. p. 029767.

Kuznetsova E, Peretyagin P, Smirnov A, Solis W, Torrecillas R. Near-net shapes Al2O3–SiCw Ceramic nanocomposites produced by hybrid spark plasma sintering. In: Anisimov K, et al., editors. Proceedings of the scientific-practical conference "research and development – 2016". Cham: Springer; 2018.

Lecouvet B, Sclavons M, Bourbigot S, Devaux J, Bailly C. Water-assisted extrusion as a novel processing route to prepare polypropylene/halloysite nanotube nanocomposites: structure and properties. Polymer. 2011;52:4284–95.

Lee N, Lee S. Water-assisted extrusion of bio-based PETG/clay nanocomposites. Korea-Aust Rheol J. 2018;30(1):47–53.

Lee S, Yoo J, Lee JW. Water-assisted extrusion of polypropylene/clay nanocomposites in high shear condition. J Ind Eng Chem. 2015;31:317–22.

Liang W, Xiaochun Y, Guangjian H, Yanhong F, Jinping Q. Ultrasound-assisted melt mixing for the preparation of UHMWPE/OMMT nanocomposites. J Thermoplast Compos Mater. 2017;31(6):784–802.

Liu J, Chen Z, Zhang F, Ji G, Wang M, Ma Y, Ji V, Zhong S, Wu Y, Wang H. Simultaneously increasing strength and ductility of nanoparticles reinforced Al composites via accumulative orthogonal extrusion process. Mater Res Lett. 2018;6(8):406–12.

Liu M, Younes H, Hong H, Peterson GP. Polymer nanocomposites with improved mechanical and thermal properties by magnetically aligned carbon nanotubes. Polymer. 2019;166:81–7.

Lu Y, Chen F, An P, Ye L, Qiu W, Zhao T. Polymer precursor synthesis of TaC–SiC ultrahigh temperature ceramic nanocomposites. RSC Adv. 2016;6(91):88770–99776.

Luecha W, Magaraphan R. Fabrication of nanoclay gel composite: a novel nanoclay masterbatch approach to nanocomposite preparation via melt extrusion process. Polym Compos. 2019;40(7):2751–67.

Mata-Padilla JM, Avila-Orta CA, Medellın-Rodrıguez FJ, Hernandez-Hernandez E, Jimenez-Barrera RM, Cruz-Delgado VJ, Valdez-Garza J, Solıs-Rosales SG, Torres-Martınez A, Lozano-Estrada M, Castro EDB. Structural and morphological studies on the deformation behavior of polypropylene/multi-walled carbon nanotubes nanocomposites prepared through ultrasound-assisted melt extrusion process. J Polym Sci B Polym Phys. 2015;53:475–91.

Matli PR, Ubaid F, Shakoor RA, Parande G, Manakari V, Yusuf M, Mohamed AMA, Gupta M. Improved properties of Al–Si3N4 nanocomposites fabricated through a microwave sintering and hot extrusion process. RSC Adv. 2017;7(55):34401–10.

Mitra S, Cook S, Svrcek V, Blackley RA, Zhou W, Kovac J, Cvelbar U, Mariotti D. Improved optoelectronic properties of silicon nanocrystals/polymer nanocom-

posites by microplasma-induced liquid chemistry. J Phys Chem C. 2013;117(44):23198–207.
Monika AKP, Bhasney SM, Bhagabati P, Katiyar V. Effect of dicumyl peroxide on a Poly(lactic acid) (PLA)/Poly(butylenesuccinate) (PBS)/functionalized chitosan-based nanobiocomposite for packaging: a reactive extrusion study. ACS Omega. 2018;3:13298–312.
Muflikhun MA, Frommelt MC, Farman M, Chua AY, Santos GNC. Structures, mechanical properties and antibacterial activity of Ag/TiO_2 nanocomposite materials synthesized via HVPG technique for coating application. Heliyon. 2019;5(4):e01475.
Nayak SS, Kim DH, Pabi SK, Murty BS. Nanocomposites of aluminium alloys by rapid solidification processing. Trans Indian Inst Metals. 2012;65(6):647–51.
O'Neill A, Archer E, McIlhagger A, Lemoine P, Dixon D. Polymer nanocomposites: *In situ* polymerization of polyamide 6 in the presence of graphene oxide. Polym Compos. 2017;38(3):528–37.
Ong SG, Chitneni M, Lee KS, Ming LC, Yuen KH. Evaluation of extrusion technique for nanosizing liposomes. Pharmaceutics. 2016;8(4):36. https://doi.org/10.3390/pharmaceutics8040036.
Patil H, Feng X, Ye X, Majumdar S, Repka MA. Continuous production of fenofibrate solid lipid nanoparticles by hot-melt extrusion technology: a systematic study based on a quality by design approach. AAPS J. 2015;17(1):194–205.
Patil H, Tiwari RV, Repka MA. Hot-melt extrusion: from theory to application in pharmaceutical formulation. AAPS PharmSciTech. 2016;17(1):20–42.
Pavlacky E, Webster DC. An *in situ* intercalative polymerization method for preparing UV curable clay–polymer nanocomposites. J Appl Polym Sci. 2015;132(39):42601. https://doi.org/10.1002/app.42601.
Pereda M, El Kissi N, Dufresne A. Extrusion of polysaccharide nanocrystal reinforced polymer nanocomposites through compatibilization with poly(ethylene oxide). ACS Appl Mater Interfaces. 2014;6(12):9365–75.
Ramos AP, Cruz MAE, Tovani CB, Ciancaglini P. Biomedical applications of nanotechnology. Biophys Rev. 2017;9(2):79–89.
Rassaei L, Marken F, Silanpaa M, Amiri M, Cirtiu CM, Silanpaa M. Nanoparticles in electrochemical sensors for environmental monitoring. TrAC Trends Anal Chem. 2011;30(11):1704–15.
Reddy MP, Shakoor RA, Parande G, Manakari V, Ubaid F, Mohamed AMA, Gupta M. Enhanced performance of nano-sized SiC reinforced Al metal matrixnanocomposites synthesized through microwave sintering and hotextrusion techniques. Prog Nat Sci Mater Int. 2017;27:606–14.
Ren W, Lin G, Clarke C, Zhou J, Jin D. Optical nanomaterials and enabling technologies for high-security-level anticounterfeiting. Adv Mater. 2019; https://doi.org/10.1002/adma.201901430.
Sahu S, Sahu UK, Patel RK. Synthesis of thorium–ethanolamine nanocomposite by the co-precipitation method and its application for Cr(vi) removal. New J Chem. 2018;42(7):5556–69.
Shen D, Fang L, Chen X, Tang Y. Structure and properties of polyacrylic acid modified hydroxyapatite/liquid crystal polymer composite. J Reinf Plast Compos. 2011;30(13):1155–63.
Shimpi N, Shirole S, Mishra S. Polypropylene/nTiO2 nanocomposites using melt mixing and its investigation on mechanical and thermal properties. Polym Compos. 2017;38(7):1273–9.
Sierra-Avila R, Perez-Alvarez M, Valdez-Garza J, Avila-Orta CA, Jimenez-Regalado EJ, Mata-Padilla JM, Soto-Castruita E, Cadenas-Pliego G. Synthesis and thermomechanical characterization of nylon 6/Cu nanocomposites produced by an ultrasound-assisted extrusion method. Adv Mater Sci Eng. 2018;2018:4792735. https://doi.org/10.1155/2018/4792735.
Singh T, Shukla S, Kumar P, Wahla V, Bajpai VK, Rather IA. Application of nanotechnology in food science: perception and overview. Front Microbiol. 2017;8:1501. https://doi.org/10.3389/fmicb.2017.01501.
Sobhani M, Arabi H, Mirhabibi AR. TEM characterization and properties of Cu-1 wt.% Tib_2nanocomposite prepared by rapid solidification and subsequent heat treatment. J Nanostruct. 2013;2:519–26.
Son YR, Park SJ. Green preparation and characterization of graphene oxide/carbon nanotubes-loaded carboxymethyl cellulose nanocomposites. Sci Rep. 2018;8:17601. https://doi.org/10.1038/s41598-018-35984-2.
Stankovic M, Frijlink HW, Hinrichs WLJ. Polymeric formulations for drug release prepared by hot melt extrusion: application and characterization. Drug Discov Today. 2015;20(7):812–23.
Stoclet G, Sclavons M, Lecouvet B, Devaux J, Van Velthem P, Boborodea A, Bourbigot S, SallemIdrissi N. Elaboration of poly(lactic acid)/halloysite nanocomposites by means of water assisted extrusion: structure, mechanical properties and fire performance. RSC Adv. 2014;101(4):57553–63.
Sui R, Charpentier P. Synthesis of metal oxide nanostructures by direct sol–gel chemistry in supercritical fluids. Chem Rev. 2012;112(6):3057–82.
Taubner V, Shishoo R. Influence of processing parameters on the degradation of poly(L-lactide) during extrusion. J Appl Polym Sci. 2001;79:2128–35.
Vucaj N, Quinn MDJ, Baechler C, Notley SM, Cottis P, Hojati-Talemi P, Fabretto MV, Wallace GG, Murphy PJ, Evans DR. Vapor phase synthesis of conducting polymer nanocomposites incorporating 2D nanoparticles. Chem Mater. 2014;26(14):4207–13.
Wang J, Langhe D, Ponting M, Wnek GE, Korley LTJ, Baer E. Manufacturing of polymer continuous nanofibers using a novel co-extrusion and multiplication technique. Polymer. 2014;55(2):673–85.
Wang X, Kalali EN, Wang DY. An in situ polymerization approach for functionalized MoS2/nylon-6 nanocomposites with enhanced mechanical properties and thermal stability. J Mater Chem A. 2015;3(47):24112–20.

Wen Q, Yu Z, Xu Y, Lu Y, Fasel C, Morita K, Guillon O, Buntkowsky G, Ionescu E, Riedel R. SiC/HfyTa1−yCxN1−x/C ceramic nanocomposites with HfyTa1−yCxN1−x-carbon core–shell nanostructure and the influence of the carbon-shell thickness on electrical properties. J Mater Chem C. 2018;6(4):855–64.

Wohlleben W, Meier MW, Vogel S, Landsiedel R, Cox G, Hirth S, Tomovic Z. Elastic CNT–polyurethane nanocomposite: synthesis, performance and assessment of fragments released during use. Nanoscale. 2013;5:369–80.

Xu T, Liao MT, Han W. Polyacrylamide/metakaolinite nanocomposites by in-situ intercalative polymerization. Part Sci Technol. 2016;34(5):602–7.

Yadav SK, Jeevanandam P. Synthesis of PbS–Al2O3 nanocomposites by sol–gel process and studies on their optical properties. Opt Mater. 2015;46:209–15.

Yu Z, Lv X, Lai S, Yang L, Lei W, Luan X, Riedel R. ZrC–ZrB_2–SiC ceramic nanocomposites derived from a novel single-source precursor with high ceramic yield. J Adv Ceram. 2019;8(1):112–20.

Zeng XF, Kong XR, Ge JL, Liu HT, Gao C, Shen ZG, Chen JF. Effective solution mixing method to fabricate highly transparent and optical functional organic–inorganic nanocomposite film. Ind Eng Chem Res. 2011;50(6):3253–8.

Zhang F, Sundararaj U. Nanocomposites of ethylene-vinyl acetate copolymer (EVA) and organoclay prepared by twin-screw melt extrusion. Polym Compos. 2004;25(5):535–42.

Zhao C, Krall A, Zhao H, Zhang Q, Li Y. Ultrasonic spray pyrolysis synthesis of Ag/TiO2 nanocomposite photocatalysts for simultaneous H2 production and CO2 reduction. Int J Hydrog Energy. 2012;37(13):9967–76.

Zheng J, Calvillo L, Valero-Vidal C, Marega C, Sekar P, Shuang S, Girardi L, Agnoli S, Rizzi GA, Granozzi G. Ag-Vanadates/GO nanocomposites by aerosol-assisted spray pyrolysis: preparation and structural and electrochemical characterization of a versatile material. ACS Omega. 2017;2(6):2792–802.

6 The Use of Supercritical Fluid Technologies for Nanoparticle Production

Jayvadan K. Patel, Deepak Bhatia, Yashwant V. Pathak, and Anita Patel

Abstract

One of the most important challenges that pharmaceutical companies are presently facing is low bioavailability of drug, which is generally a result of poor aqueous drug solubility/dissolution rates; this may restrict the therapeutic efficiency of marketed drugs. The bioavailability of pharmaceuticals' existing in a solid formulation strongly relies on the size, particle size distribution, and morphology of the particles. In recent years, the major approaches that have been put into practice to overcome poor drug solubility/dissolution rates are drug particle size reduction (i.e., micronization/nanonization). Numerous particle engineering techniques have been applied for this purpose, including spray-drying, freeze-drying, liquid anti-solvent crystallization or milling processes. These technologies present numerous drawbacks, for example, the difficulty of controlling particle size and particle size distribution, product degradation due to mechanical or thermal stresses, or the contamination of the particles with organic solvents or other toxic substances. Therefore, different alternative precipitation techniques are being explored. In recent years pharmaceutical processing using supercritical fluids, for the precipitation of pharmaceuticals and natural substances, has attracted great attention from the pharmaceutical industry. This is mostly attributable to the some well-known beneficial technological features of this method, as well as to other increasingly important subjects for the pharmaceutical industry, namely, their "green" sustainable, safe, and "environmentally friendly" intrinsic characteristics.

Keywords

Supercritical fluid · Particle formation · Nanoparticles · Environmentally friendly

1 Introduction

The bioavailability of pharmaceuticals existing in a solid formulation strongly relies on the size, particle size distribution, and morphology of the particles. The particle precipitation into micro/nanoparticles has been an active research area for decades (Chattopadhyay and Gupta 2001a;

J. K. Patel · A. Patel (✉)
Nootan Pharmacy College, Sankalchand Patel University, Visnagar, Gujarat, India

D. Bhatia
Bernard J. Dunn School of Pharmacy, Shenandoah University – ICPH Fairfax, Fairfax, VA, USA

Y. V. Pathak
College of Pharmacy, University of South Florida Health, Tampa, FL, USA

J. K. Patel, Y. V. Pathak (eds.), *Emerging Technologies for Nanoparticle Manufacturing*,
https://doi.org/10.1007/978-3-030-50703-9_6

Kalogiannis et al. 2005; Rehman et al. 2001; Velaga et al. 2002; Yeo and Lee 2004). The greatest prerequisite in the appliance of nanomaterials is its size along with morphology control which decides the potential application of the nanoparticles, as their properties differ notably with size. Because of this, there is an increasing interest in the development of well-organized micronization/nanonization technologies. Micro- and nanoparticles can be obtained by a variety of techniques. Conventional techniques counting spray drying, freeze-drying, solute recrystallization, interfacial polymerization, and milling processes present numerous problems such as excessive use of solvent, degradation of the product due to mechanical or thermal stresses, structural changes, formulation instability, low drug loading efficiency, and, mainly, broad particle size distribution (He et al. 2004; Chen et al. 2011). In some cases, the processing of particle formation is extended to achieve uniform size distribution by subsequent milling and sieving, which often give rise to the damage of sensitive biomolecules because of high shear forces (Ginty et al. 2005, 2006).

In addition, the majority of these processes usually depend on the use of a large number of organic solvents, which cause product damage, toxicity, inflammability, and biocompatibility problems, among others (Pasquali and Bettini 2008). Therefore these processes for particle formation may not be worthwhile. For this reason, different alternative precipitation methods are being explored (Martin and Cocero 2008). However, the application of supercritical fluids (SCFs) is an attractive alternative for this particle formation because it removes these drawbacks.

In the last few years, the supercritical fluid (SCF) technology has gained tremendous attention from investigators over the established pharmaceutical manufacturing strategies because of the environmentally benignant nature and economically promising character of SCFs (Kompella and Koushik 2001; Bałdyga et al. 2010; Chen et al. 2017). SCF technology has been commonly utilized for a variety of applications, for instance chromatography, extraction, material processing, and reaction. A most significant feature of particle formation from the SCF technique is the ability of manufacturing solids with unique morphology and small size.

The appliance of supercritical fluids (SCFs) for the precipitation of pharmaceuticals and natural substances has gained remarkable interest attributable to the extraordinary properties of these fluids (Bertucco and Vetter 2001). These SCFs have unique properties such as liquid-like density, gas-like viscosity, and larger diffusivities than those of typical liquids, resulting in higher mass transfer rate. These make them excellent solvents for various industrial developments. Additionally, by altering the experimental conditions like temperature and pressure, its solvent power, as well as selectivity, can be modified (Montes et al. 2019).

In the past few decades, this high-pressure technology has been commonly implemented for acquiring products because of the environmentally friendly nature and economically hopeful nature of SCFs (Hauthal 2001). In several SCF precipitation techniques, the need for organic solvents is totally eliminated, whereas in others a small quantity of organic solvent is employed, which can be totally removed from the product because of the high solubility of these solvents in SCF, as a result circumventing the contamination of the product (Shariati and Peters 2003; Jung and Perrut 2001; Reverchon 1999). SCFs take benefit of the benign solvents, that is, CO_2 and water, to avoid the issues associated with the traditional strategies for precipitation of drug either alone or in combination with the biodegradable polymers (Kalani and Yunus 2011). For that reason, these SCFs act as an effectual replacement for organic solvents in producing pharmaceutical products (Hauthal 2001; Ginty et al. 2005). More frequently, SCFs as harmless solvents present substantial attention in pharmaceutical manufacturing processes due to their solvating power in sorting out the components and significant alterations in their physicochemical properties beyond the critical point (Kankala et al. 2017). Furthermore, additional advantages of SCFs consist of solubilizing ability and simplicity of recycling, among others. By modifying the critical pressure and temperature, the physical properties

of SCFs specifically density, viscosity, solvency, and diffusivity that exist amid both liquid and gas can be simply changed during the processing of solutes (Pasquali and Bettini 2008; Kalani and Yunus 2011; Wu and Li 2008; Davies et al. 2008). In this context, SCFs such as water and solvents like acetone, CO_2/ethanol mixture, chlorodifluoromethane, diethyl ether, nitrous oxide, propane, and trifluoromethane are operated at their equivalent supercritical conditions (Kankala et al. 2017; Davies et al. 2008; Reverchon and Adami 2006; Byrappa et al. 2008; Hakuta et al. 2003; Meziani et al. 2002; Warwick et al. 2002; Krober and Teipel 2002). The distinguishing characteristics of these SCFs, counting the critical parameters and other features, for instance, solubility, have been previously reported elsewhere (Perry 1997).

In all the SCFs existing, supercritical CO_2 (SC-CO_2) has greater focus from investigators because of its broad adaptableness, safety, cost-efficiency, and demanding gentle conditions for operation (temperature 304 K/31.1 °C and pressure 7.38 MPa/73.8 bar) under ambient conditions (Kankala et al. 2017). In addition, it ought to be distinguished that SC-CO_2 is accepted as safe and sound by the US Food and Drug Administration in pharmaceutical production as it is harmless, nonreactive, nontoxic, nonpolluting, and nonflammable (Djerafi et al. 2015; Kalani and Yunus 2011; Kankala et al. 2017). Moreover, it presents numerous benefits which are greatly favorable for particle manufacturing, for example, low cohesive energy density, low polarizability per unit volume, and higher volatility, among others (Davies et al. 2008). Furthermore, the distinctive physical properties of SC-CO_2, like density, diffusivity solvency, and viscosity, can be operated beyond its critical point by setting the temperature and pressure (Kankala et al. 2017). Growing demand for particle manufacturing of different active pharmaceutical ingredients (APIs) and study on their crystalline morphologies along with the target of solving the drawbacks of presently existing conventional techniques specifically particle damage as well as detriment of bioactivity by strong shear forces, different particle size distribution, and others have acquired great consideration of investigators to the SCF technology (Tomasko et al. 2003; Chen et al. 2011). Though the knowledge of implementing SCF for particle fabrication is still in their early years (46) (Huang et al. 2005). Numerous papers have been published in relation to the appliances of SCF on the fabrication of nanomaterials (Jung and Perrut 2001; Reverchon and Adami 2006; Martin and Cocero 2008).

2 Supercritical Fluid Technology

SCF technology is in exploit since the late nineteenth century as a means to know the natural mineralization, the actual momentum for this technique as a tool to handle a considerable number of materials started in the 1980s. With the discovery of Green Chemistry in the early 1990s, there was a rush in the acceptance of SCF technology. Green Chemistry is vital due to SCFs, mainly SC-CO_2, and, to a more limited degree, SC-H_2O is noticed as environment friendly more satisfactory substitute for the petroleum-based solvents, which are at present employed in the world's chemical industries (DeSimone 2002). The undesirable effects of the residual solvents from both processing and environmental point of view have been acknowledged. Therefore, the intermediary processing methods for pharmaceutical products have restricted applications compared to the alternate methods of material processing like SCF technique. In the last decade SCF technology has observed a decisive growth in its application for manufacturing a choice of materials. SCF technology substitutes organic solvents in several chemical processes, counting chemical manufacturing, food processing like decaffeination of coffee beans, extraction, nanoparticle production, particles coating, polymer processing, recycling, waste treatment, etc. (Markocic et al. 2013; Wang and Chang 2015; Habulin et al. 2007; Skerget et al. 2011; Knez and Weidner 2003). Especially for the nanomaterial manufacturing for the advanced drug delivery and for drug formulation systems, SCF technique comes out as an option to the majority of the present techniques (Palakodaty et al. 2002).

Contrary to the traditional particle fabrication techniques such as freeze-drying, spray-drying, and precipitation, where a large particle is initially produced and after that comminuted to the preferred size, SCF technique entails growing the particles in a controlled manner to achieve the desired morphology. The adverse effects instigating from the energy imparted to the system to achieve size reduction can thus be avoided (McHugh and Krukonis 1994; Cabanas and Poliakoff 2001). The particles once produced need not experience additional processing or handling and this characteristic putting SCF technology flexible to fabricate biomolecules and other sensitive molecules in their inhabitant pure state (Hamidreza et al. 2016; Chattopadhyay and Gupta 2002a). These techniques are rooted in a simple theory in which a drug and a polymer are co-precipitated together by means of the anti-solvent (non-solvent) properties of SC-CO_2, since the majority polymers and drugs are not appropriate in SC-CO_2. This process, however, is expected to be successful when polymer and drug molecules are able to form a solid solution. SCF technologies produce nanoparticles with solvent levels below 25 ppm. The advancements in SCF technology have promoted the manufacturing of new pharmaceuticals from small molecular drugs to biological macromolecules, for example, peptides, proteins, and nucleic acids (Tservistas et al. 2001). These growths have given birth to a new discipline, viz., pharmaceutical materials science, which deals with physical principles ordinary in materials science to confront in such areas as drug delivery, manufacture, and processing of nanoparticle systems for exploit in pharmaceutical applications (Elliot and Hancook 2006).

The benefits of SCF technology, for instance, are (i) quick one-step processing; (ii) mild operating temperature that has made SCFs an attractive technology particularly for heat-sensitive materials; (iii) facilitating the particle size to be reduced to such a great extent, which can be employed for aerosol drug delivery systems (Erkey 2009). The solubility of poorly water-soluble drugs can be improved, devoid of heating the substance, only with the aid of micronization induced by SC-CO_2 (Lin and Jang 2008); (iv) SCF technology has the potential to replace the use of organic solvents that have been commonly used in the production of solid composite lipid/drug nanoparticles (Thote and Gupta 2005; Chattopadhyay et al. 2007).

The elevated pressure needed, higher maintenance cost, and prerequisite of the accessories/auxiliary types of equipment restrict the utilization of SCF technology for most of the pharmaceuticals. Thus, it gives the impression that this method cannot totally replace traditional methods as it is not appropriate for the processing of all pharmaceuticals (Girotra et al. 2013).

3 Supercritical Fluids

"Supercritical" is a condition of a substance beyond its critical temperature (TC) and critical pressure (PC). A substance in its supercritical condition is characterized as supercritical fluid (SCF). The critical point stands for the highest temperature and pressure at which the substance can be present as a vapor and liquid in equilibrium (Sheth et al. 2012). At this condition, the fluid has inimitable properties, where it does not condense or evaporate to form a liquid or gas. A characteristic pressure-temperature phase diagram is shown in Fig. 6.1.

In the supercritical phase, there is no phase boundary amid the gas and the liquid phase. Briefly, it can act as if it is a liquid or a gas, but is actually neither (Sheth et al. 2012). The properties of SCF are in between that of liquid and gas. This Janus-faced nature of SCFs takes place from the reality that the liquid and gaseous phases join together and turn into identical at the critical point (Matsubara et al. 2010; Pinkston et al. 2004; Li and Hsieh 2008). The density of an SCF is similar to that of liquids, whereas its diffusivity and viscosity are similar to those of gases, as can be seen from Table 6.1. Additionally, the surface tension of an SCF is zero (Ollanketo et al. 2001). The "law of corresponding states" as given by van der Waals suggests that compounds act likewise below the same values of the reduced variables. This enables important comparison of

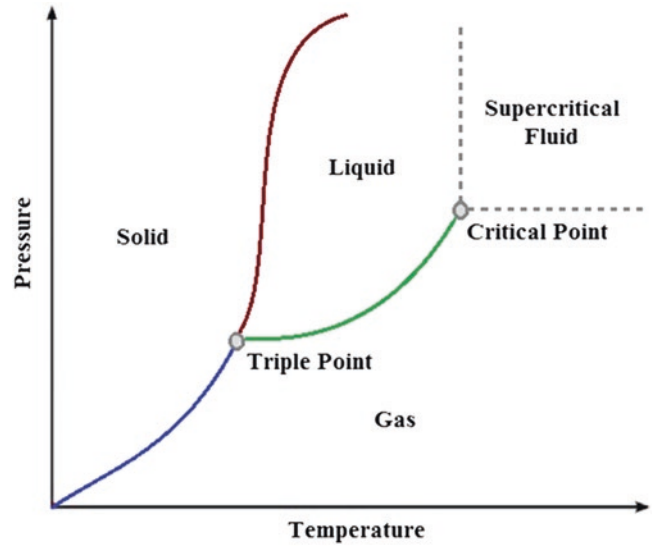

Fig. 6.1 Pressure-temperature phase diagram

Table 6.1 Characteristic magnitudes of thermophysical properties (Smith 1999)

Fluid	Density (Kg/m^3)	Viscosity (cp)	Diffusion coefficient (cm^2/s)
Gas	1	10^{-2}	10^{-1}
SCF	300–800	0.03–0.1	10^{-4}
Liquid	10^3	1	10^{-5}

different compounds under a variety of situations; however differences can be considerable in close proximity to the critical point (Saito 2013).

The densities of a substance in its supercritical region are either similar or near to that of the same substance in its liquid phase. This feature permits SCF to improve the solubility of poorly soluble drugs greater than the gaseous state could. The liquid-like density makes possible the strong solvent power of SCFs for a variety of solutes. The most fascinating features of SCFs are that their physical properties are very susceptible to temperature and pressure and there exists density inhomogeneity in the critical state. In a supercritical state, the density of the solvent around the solute can be much higher than that of the bulk, especially in the critical state of supercritical solvents, which is frequently described as a clustering (Yamini and Bahramifar 2000; Housaindokht and Bozorgmehr 2008; Knez et al. 2014; Ramsey et al. 2009; Sovilj et al. 2011; Yang and Zhong 2005). In contrast, the diffusivity and viscosity of SCFs are near to that of gas; which facilitates fast mass transfer or else diffusion of SCFs into materials as compared to that of the liquid states (Sheth et al. 2012).

Not each and every feature of SCFs are in between those of liquids and gases; properties like compressibility as well as heat capacity are notably elevated close to the critical stage than they are in liquids or gases. Though the properties of a substance may alter significantly with pressure in close proximity to the critical point, the majority of them display no discontinuity (Sovilj et al. 2011; Yang and Zhong 2005; Munshi and Bhaduri 2009; Dong et al. 2013; Cooper 2000). The alterations set up steadily, more willingly than with a sudden onset, when the situations move toward the critical point. SCFs are very much compressible, predominantly close to the critical point and their density, and therefore the solvation power can be cautiously regulated by little alterations in temperature and/or pressure (Yasuji et al. 2008; Mishima 2008). Even though these distinctive and balancing physical properties permit the progress of well-organized and adaptable methods, the SCFs are not worldwide "super-solvents." Handfuls of drug substances are displaying solubility in SCFs with no addition of a co-solvent.

Though every gas possibly will achieve supercritical state beyond their critical stage, for sev-

eral, tremendously higher pressure, as well as temperatures, might be necessary which may not be appropriate for pharmaceuticals. One must also consider the safety and affordability in addition to mild processing conditions, when choosing the SCF; for example, Xenon and Sulfur hexafluoride (when sufficiently purified) have low critical values, but remain too expensive for commercial use. Gases like nitrous oxide or ethane also has low critical values but they are able to produce explosive mixtures and are thus dangerous to handle. Trifluoromethane, a chemically inert and nonflammable compound, has low critical temperature and pressure and also low toxicity. Additionally, trifluoromethane has strong lasting dipole moments (1.56 D), which aid the solubilization of pharmaceutical materials. On the other hand, carbon dioxide (CO_2) is the most favored SCF for the treating of heat-sensitive pharmaceuticals like biologicals. It has a low critical temperature (31.2 °C) and pressure (73.8 bars) and is nonhazardous, nonflammable, and environmentally harmless (Sheth et al. 2012).

The most commonly employed SCF is supercritical CO_2 (SC-CO_2), which is economical and nonpolluting and whose critical parameters are easy to be achieved in industrial equipment. Regardless of the issues over the greenhouse consequence of CO_2, it can be measured as an environmentally affable substitute to available organic solvents, in view of the fact that the CO_2 utilized in this method is already recycled and so the net load on the environment is unaffected (Byrappa et al. 2008). Though in last few years, not only the materials handling is being carried out with SC-CO_2, but also alcohols, ammonia, light hydrocarbons, and water have been suggested, along with the others, for nanomaterials manufacturing at supercritical states (Markocic et al. 2013; Wang and Chang 2015).

4 Supercritical Processes for Nanoparticles Manufacturing

SCFs have been suggested as a medium to manufacture nanomaterials. SCF precipitation processes can be categorized according to the function of the SCFs in the method. In fact, SCFs have been intended as solvents, solutes, anti-solvents, and reaction media. SCF can take action as a solvent, as in the rapid expansion of supercritical solutions (RESS) technique (Martin and Cocero 2008; Gosselin et al. 2003). It can act as a solute, as in the precipitation from gas-saturated solution (PGSS) technique (Fraile et al. 2013; Martin and Cocero 2008), and as an anti-solvent, in the supercritical anti-solvent (SAS) (Bertucco et al. 1996; Sacchetin et al. 2016) and gaseous anti-solvent (GAS) techniques (Yeo et al. 1993). It can act as a propeller, in the supercritical assisted atomization (SAA) technique (Martin and Cocero 2008; Reverchon 2002; Shen et al. 2014). It can also act as a reagent (Beckman 2004) and others like aerosol solvent extraction system (ASES) (Hakuta et al. 2003), precipitation with compressed anti-solvent (PCA) (Falk et al. 1997), supercritical anti-solvent with enhanced mass transfer (SAS-EM) (Chattopadhyay and Gupta 2002a), solution-enhanced dispersion by supercritical fluids (SEDS) (Chen et al. 2012a), and suspension-enhanced dispersion by supercritical fluids (SpEDS) (Chen et al. 2012b). Regardless of the variation in the actions, SCF behaves as a re-precipitation aid for quick, homogenous, as well as smooth nucleation of solutes (drug and/or polymer) in each and every above-mentioned technique proposed for particle manufacturing. Furthermore, the operating effectiveness of these techniques entirely depends upon the choice of a proper solvent and fine adjustment of the critical factors (Vemavarapu et al. 2005).

4.1 Particles from Gas-Saturated Solutions (PGSS)

Lots of drugs are either polar or exhibit higher molecular weights. It is not easy to solubilize these materials in CO_2, which is a nonpolar solvent, still in a supercritical situation excluding the help of a co-solvent. Conversely, SC-CO_2 has the aptitude to penetrate into organic substances, like polymers. When SC-CO_2 penetrates into the polymer, it decreases the melting point and reduces its viscosity. These aspects are made

exploit of in the PGSS technique (Sheth et al. 2012). The SCF is employed as a solute in the PGSS method (Kerc et al. 1999).

In the PGSS operations, the physical mixture of the drug and the polymer are initially subjected to SCF. It entails the melting of the substance to be treated, which afterward dissolves in SCF under pressure. In subsequent melting, the additional introduction of the SC-CO_2 dissolves the mixture further and viscosity diminishes. This solution is, after that, atomized by the use of a nozzle and a pressure regulating valve into a receiver. Because of quick depressurization, the dissolved SCF gets away, as a result, the development of composite microparticles (Mishima 2008). For the reason that the solubility of compressed gases in liquids and solids such as polymers are generally elevated, and much greater than the solubility of such liquids and solids in the compressed gas state, the method exists in solubilizing SC-CO_2 in melted or liquid-suspended materials, leading to a named gas-saturated solution/suspension that is again expanded through a nozzle with the development of solid particles or droplets. The materials subjected do not require solubility in SC-CO_2, which is the most important benefit of this technique. This method can be employed with suspensions of active substrates in a polymer or other carrier substance which leads composite microspheres (Jung and Perrut 2001; Date and Patravale 2004; Palakodaty et al. 2002; Byrappa et al. 2008). This procedure is intended for fabricating particles of materials that absorb SCFs at higher concentrations like polyethylene, polyester, polyethylene glycol, poly (vinylpyrrolidone) (PVP), and polylactic acid (Sheth et al. 2012). This strategy is beneficial than other SCF processes because it requires a small amount of SCF (Hakuta et al. 2003; Kerc et al. 1999).

Figure 6.2 shows the fundamental apparatus employed in the PGSS processing of materials. The PGSS can be applicable to process inorganic powders to pharmaceutical compounds. Low handling cost and wide range of products that can be processed like liquid droplets or solid particles is the straightforwardness of this technique, which unlock wide opportunities for the development of PGSS system, not only for high-value substances but also possibly for merchandise, despite limits related to the complexity to observe particle size. A number of pharmaceuticals, for example albuterol sulfate, calcium antagonist drugs, cromolyn sodium, DL-alanine, glucose, glutathione, nifedipine, tobramycin, etc., and in addition lots of inorganic and organic compounds such as glycerides, metal oxides, plastic additives, pigments, phosphors, spinels, etc. have been urbanized with the PGSS technique (Jung and Perrut 2001; Date and Patravale 2004; Palakodaty et al. 2002; Byrappa et al. 2008).

The benefits of the PGSS technique are similar to those of the RESS technique; it can be carried out without employing organic solvents and it generally needed low pressures as well as consumption of gas as compared to the RESS technique. The segregation of the ingredients when they move across the pressure drop is one of the major problems of the conventional PGSS technique. Particles of the drug and the polymer are produced independently, but the polymer microparticles comprising the drug could not be achieved. PGSS has been customized to conquer the agglomeration and nonuniform particle size distribution issues. Researchers suggested a system to defeat the separation difficulty, by an arrangement of two separate mixing compartments in the apparatus. In the first compartment, the drug and the polymer are mixed to homogeneity; let them melt in SC-CO_2. This melt was then moved from the first compartment to the second one, where it was mixed with additional SCF, resulting in an extra fall in the viscosity of the melt. The mixture was at last sprayed and further expansion took place, resulting in the formation of uniform size of microparticles of the polymer-drug mix (Shekunov et al. 2006; Sheth et al. 2012).

4.2 Rapid Expansion of Supercritical Solutions (RESS)

The RESS technique is schematically illustrated in Fig. 6.3. This technique is employed when the

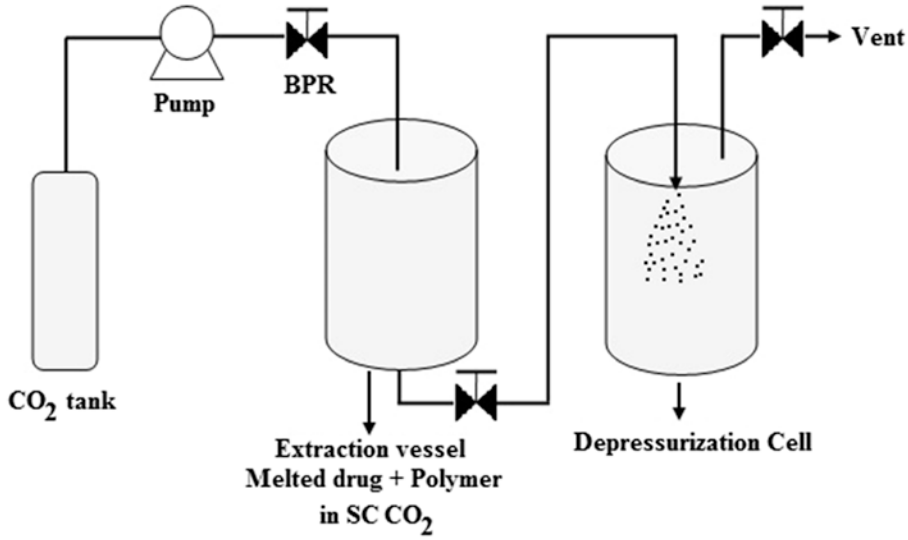

Fig. 6.2 Schematic representation of equipment set up for PGSS process (Sheth et al. 2012)

solute like polymer, drug, or drug-polymer matrix freely dissolves in the SCF.

The RESS technique is accomplished by means of the saturation of the SCF with a drug or drug-polymer matrix, followed by depressurization of the solution by passing through a heated nozzle into a low-pressure vessel that creates quick nucleation of the drug or drug-polymer in the form of incredibly smaller particles that are collected from the gaseous stream. The morphology of the obtained solid material, amorphous or crystalline, depends upon the chemical constitution of the substance and on the RESS parameters like impact distance of the jet against a surface, temperature, pressure drop, nozzle geometry, etc. (Jung and Perrut 2001). The very quick discharge of the solute in the gaseous state is supposed to give surety of the fabrication of nanoparticles. This technique is most appealing because of the absence of organic solvents.

In designing this technique, the solubility of the substance plays a vital role in particle fabrication and processing as the majority of the pharmaceutical materials, for example, drugs, high molecular weight proteins, and polymers are polar in nature. In a few cases, little quantities of organic solvents are needed to get better the affinity of polar drug molecules (Mishima 2008). RESS technique is the simpler and an effectual technique in the SCF technology, but it is restricted in its appliance owing to its comparatively higher cost and poor solubility of polymers in non-polar SC-CO_2. To tackle this problem, high amounts of SC-CO_2 are favored at an industrial scale (Chen et al. 2011). Furthermore, the progressions in the RESS technique have been developed to beat certain drawbacks. A fascinating variant of the RESS technique is the rapid expansion of a supercritical solution into a liquid solvent (RESOLV) that is comprised of atomizing the supercritical solution into a liquid. Processing in this way, it should be feasible to reduce particle growth in the precipitator chamber, as a consequence enhancing the RESS technique performance. In addition, through interaction with the nucleating solid particles as well as the materials present in the liquid medium, a chemical reaction step can also be included. These types of alterations in the procedure reduce particle agglomeration in the expansion jet (Dalvi et al. 2013).

From the hypothetical point of analysis, the budding aspects of RESS are very fascinating, although the outcomes have not been predominantly in high quality in some cases. It is in many cases problematic to control the particle size of the precipitates. At some stage in the expansion step, the particles fuse in the supersonic free jet

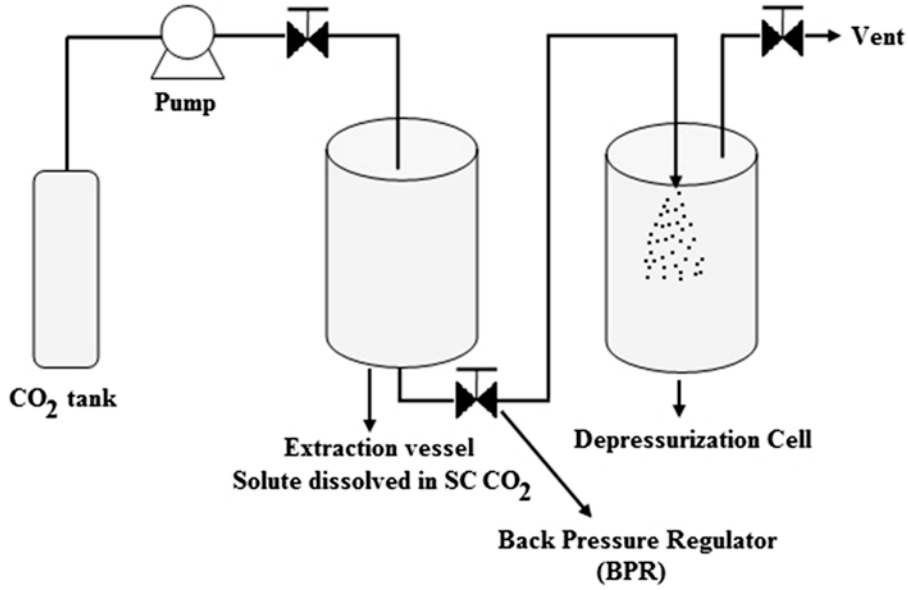

Fig. 6.3 Schematic representation of the RESS process (Jung and Perrut 2001; Montes et al. 2011)

generated in the precipitation chamber, and, so, in several cases, needlelike particles have been achieved. The generation of tilting needles can be elucidated by the existence of electrostatic charges on the surface of the particles, provoked by the rapid relative motion among the particles and the gas contained in the expansion vessel (Reverchon et al. 1995).

For the production of nanoparticles, RESOLV configuration has been confirmed to be more successful, as the liquid that gets the expanding jet can inhibit the particle growth. To shield particles from agglomeration, a little quantity of stabilizing agent is added in the liquid.

The main drawback of RESS and RESOLV techniques is that both techniques are applicable only to those products which have a moderate solubility in the chosen SCF. Regrettably, a lot of solid materials with high molecular weight and polar bonds are a good candidate for fabrication of nanoparticles, displaying extremely low or negligible solubility in SC-CO_2, and show a decreased solubility in lots of other substances which can be good candidates as SCF (Reverchon and Adami 2006). RESOLV technique has also the issue of the recovery of particles from the liquid solution employed to get better the performance of process: in this configuration, the technique is no more solventless (Reverchon and Adami 2006). A further modification of the RESOLV process consists of the use of water in SC-CO_2 (w/c) microemulsion used as a modified supercritical solvent to dissolve $AgNO_3$ (Sun et al. 2001).

One more modified technique is the rapid expansion of a supercritical solution with solid co-solvent (RESS-SC), which results in nanoparticles. In processing, the additional co-solvent enhances the solubility of the APIs to a larger degree by circumventing superficial exposure among particles, which augments the surface area of contact to SCF, and ultimately, lyophilization can eliminate the co-solvent (Thakur and Gupta 2005). In spite of its progressions, RESS still has some restraints that are improved on by the changed SCF actions as anti-solvent in the reaction chamber.

4.3 Gas Anti-solvent Processes (GAS)

Gas anti-solvent (GAS) technique has been urbanized with the intention to attain nanoparti-

cles of the hydrophobic materials which cannot be developed by the RESS technique because of their poor solubility in SCFs. The starting point of the GAS technique is derived from the fact that when a solution is expanded satisfactorily by a gas, the liquid state is no longer a choice of solvent for the solute and nucleation takes place. For instance, a GAS was employed to decrease the lower critical solution temperature of polymeric solutions to concentrate polymers (McHugh and Guckes 1985; Seckner et al. 1988). The solute to be undergoing micronization is present in a liquid solution; the SCF must be totally miscible with the liquid solvent, while the solute must be insoluble in the SCF. As a consequence, the liquid solution along with SCF brings the generation of a solution, causing supersaturation and precipitation of the solute. The generation of the liquid mix is incredibly quick caused by the improved mass transfer rates that distinguish SCFs, and accordingly, nanoparticles could be formed (Byrappa et al. 2008).

This method is most widely used for polymers as they are generally insoluble in SCFs. Saturation of the polar solvent, comprising a dissolved substrate, with SC-CO_2, in this manner diminishing the solvent power of a polar solvent, resulting in the precipitation of the substrate is the fundamental theory of this system (Dehghani and Foster 2003). A ternary system consisting of polymer, liquid organic solvent, and gas as anti-solvent is employed in this method. The polymer first dissolved in a chosen organic solvent and then the gas is permitted to pass from a closed vessel. With the increase in pressure, the concentration of the gas so employed increases in the chamber and the polymer is precipitated out. As soon as the solvent is introduced in the method, phase separation among liquid-solid and liquid-liquid took place because they are shifted to higher temperatures (Jung and Perrut 2001). The quick expansion of SCFs through the nozzle of the vessel happens which is after that followed by a fall in temperature and pressure. The size of the particle produced by this technique mostly relies on the diameter of the nozzle and its length (Girotra et al. 2013).

The GAS technique has been fruitfully used for the formation of insulin in poly-l-lactide (PLLA) nanoparticles. The method produces nanoparticles with high encapsulation efficiency as well as high yield of nanoparticles of with the size range of 400–600 nm and preservation of greater than 80% of the insulin hypoglycemic activity and was as well capable of getting rid of extensive utilization of organic solvent (Elvassore et al. 2001).

4.4 Supercritical Anti-solvent Processes (SAS)

The SAS technique is intended for the compounds that have poor solubility in SCF. In this technique, organic solvents like acetone, dichloromethane (DCM), and dimethyl sulfoxide (DMSO) are used to dissolve the materials, and SCF act as a non-solvent to solute/API (Kalani and Yunus 2011). Briefly, in the SAS, the solute undergoing a micronization process is present in the liquid solution, and the SCF must be completely miscible with the liquid solvent, while the solute is ought to be insoluble in the SCF at the process arrangements. As a result, exposing the liquid solution with the SCF brings about the generation of a solution, forming supersaturation and subsequent precipitation of the solute. Because of the improved mass transfer rates, the formation of the liquid mix is very rapid that differentiates SCFs, and, accordingly, nanoparticles could be developed (Kalani and Yunus 2011). The SAS technique has been utilized by a number of researchers for the production of nanoparticles by using different process conditions, but the most important variations have relied upon the manner by which the process brings about, in a batch or a semicontinuous means (Reverchon 1999). In a batch operation (GAS), the precipitation chamber is first charged with a known quantity of the liquid solution, and, after that, the supercritical anti-solvent is introduced until the ultimate pressure is achieved. While in the semicontinuous operation (SAS), the liquid solutions, as well as the supercritical anti-solvent, are constantly added to the precipitation chamber in co-current or counter-

current manner. The liquid solution injection device as well plays a significant role (Dehghani and Foster 2003). The injector is specially planned to turn out liquid jet breakup and the creation of small-sized droplets to create a greater mass transfer surface among the liquid and the gaseous state. High-pressure vapor-liquid equilibria (VLEs) and mass transfer amid the liquid and the SCF, in addition, play a significant action in SAS. Predominantly, VLEs of the ternary system solute-solvent-SC anti-solvent and the location of the working point in SAS processing with regard to these VLEs can be influential for the victory of the procedure. The development of a single supercritical region is the key footstep for the winning fabrication of nanoparticles (Reverchon et al. 2003). At the last stage of the precipitation process, the washing step with pure supercritical anti-solvent is as well essential to circumvent the condensation of the liquid medium that otherwise showers on the precipitate transforming its distinctiveness. As a rule, SC-CO_2 has been employed in this technique.

As the injection of the liquid solution is appropriately carried out, the boundaries of the SAS process are in the complexity of guessing VLE adjustments brought by the existence of solute on the binary liquid-SCF system. Extremely multifaceted phase behaviors can be developed. In the simpler situation, the change of the mixture critical point (MCP) in direction to the higher pressures can be found. In the condition of more raise in the MCP pressure, incredibly high pressures will be needed to attain a single-phase system and the successful manufacturing of nanoparticles achieved (Reverchon and De Marco 2004).

The production of extremely larger crystals is found in certain situations which are in relation to SAS precipitation from a liquid-rich phase because of an alteration of the shape and the degree of the miscibility gap (Reverchon 1999). When two phases are concurrently present, a variety of morphologies can be achieved that can be depending upon the precipitation from a liquid-rich state (crystals) and the SCF-rich state (amorphous particles); the comparative amounts of precipitates are correlated to the partition factor of the solute among the two phases.

The product of the SAS technique is completely related to the order of the introduction of solvent, SCF, and other substrates. Furthermore, parameters like the chemical composition of solute as well as an organic solvent, temperature, and pressure are essential to be optimized. SAS has achieved superior drug loading capacity as compared to that of the RESS technique, facilitating the production of fine particles (Mishima 2008). Latest progressions in SAS micronization methods consist of expanded liquid anti-solvent (ELS) (Prosapio et al. 2016) and the supercritical assisted injection in a liquid anti-solvent (SAILA) techniques (Campardelli et al. 2012); conversely, profound analysis on these techniques so far remains to be reported. The ELS is processed with SCF and an organic solvent at expanding liquidity states (Prosapio et al. 2016). SCF-assisted extraction of emulsions (SFEE) is another tailored SAS method (Della et al. 2010).

4.5 Aerosol Solvent Extraction System (ASES)

In ASES, formation of particles takes place at a higher anti-solvent-to-solvent proportion following spraying the drug/polymer solution into SCF through an atomization device. The mass transfer of SCF relies upon atomization efficiency, whereas mass transfer of solvent depends on the dispersing as well as the mixing of organic solvent and SCF. For loading high quantities of drugs, ASES is not an appropriate technique attributable to their more affinity for organic solvent, which finally decreases the loading quantity in the polymer following organic solvent extraction process (Mishima 2008).

This technique is very much related to the SAS technique. In the ASES, the solution is sprayed via an atomization nozzle as fine droplets into compressed CO_2 (Bleich et al. 1993). The dissolution of the SCF into the liquid droplets is achieved by expansion of large volume, and, as a result, there is a drop in the liquid solvent power, inducing a sharp increase in the supersaturation in the liquid mix, and resulting into the generation of uniform-sized micro/

nanoparticles. Briefly, the SCF is introduced to the top of the high-pressure chamber through a high-pressure pump. The material to be micronized in a solution form is added into the high-pressure chamber by means of a nozzle as soon as the system achieves a steady state. The liquid has to be introduced at a higher pressure than the chamber operating pressure to get tiny liquid droplets and the particles are brought together at the base of the chamber (Byrappa et al. 2008). The fluid mixture (SCF and the solvent) exits the vessel and flows to a depressurization tank where the pressure-temperature conditions allow gas-liquid separation. The pumping of the liquid has to be discontinued once the gathering of enough amounts of micro/nanoparticles and pure SCF goes on to run through the chamber to eliminate leftover solvent from the micro/nanoparticles (Byrappa et al. 2008; Hakuta et al. 2003).

The fundamental working theory of this system is the extraction characteristics of the SCFs. First, the drug and the polymer are dissolved into an organic solvent and then this solvent is atomized into the SC-CO_2. The organic solvent is chosen in a manner ensuring that it is soluble in SC-CO_2. The solvent is afterward extracted resulting into the development of micro/nanoparticles (Girotra et al. 2013).

In addition, a minor modification of the ASES technique is referred to as the precipitation with a compressed anti-solvent (PCA) technique, which successfully manufactures micro/nanoparticles with a narrow size distribution. This progression has been documented as a single-step method specially processed to precipitate proteins (Shoyele and Cawthorne 2006).

4.6 Supercritical Anti-solvent with Enhanced Mass Transfer (SAS-EM)

SAS-EM is a sophisticated SAS technique specifically designed to defeat the existing drawbacks of the SAS technique (Chattopadhyay and Gupta 2002a). In the SAS-EM technique, a vibrating ultrasonic processor has been employed for atomizing the solution jet into micro-droplets. Because of this modification, the working method produces higher turbulence, which ultimately improves the mixing process and consequently the mass transfer rate and forms smaller-sized particles (Langer and Vacanti 1993).

4.7 Solution-Enhanced Dispersion by Supercritical Fluids (SEDS)

One more up-gradation of the SAS technique is the SEDS technique which is particularly designed for single as well as binary compounds. In the SEDS technique, a specially designed coaxial nozzle has been utilized, which comprises two channels for a single compound and three channels for binary compounds.

The SEDS method is carried out at a lesser drying time in addition to improved mass transfer rates, which diminish the ASES procedure restraints. In a characteristic SEDS technique, the dispersed materials are atomized through a specifically designed co-axial nozzle for the control of the particle morphology (Mishima 2008). The fundamental theory is rooted in dispersing an aqueous solution, which comprises the biomaterials, along with SC-CO_2 and a polar organic solvent in a three-channeled coaxial nozzle. Moreover, the SC-CO_2 is employed to take out the aqueous part of the product. The organic solvent is acting as a precipitating agent as well as a modifier, making possible the non-polar CO_2 to eliminate the water (Tservistas et al. 2001; Young et al. 1999). The dispersion in the jet at the nozzle exit allows the quick development of small-sized dry micro/nanoparticles (Byrappa et al. 2008). The mass transfer rate of SCF into the sprayed droplet decides the particle generation by the solvent transfer rate into the SCF stage. The higher the mass transfer rate facilitating, the quicker the nucleation, resulting into smaller particle sizes with not as much agglomeration (Shoyele and Cawthorne 2006).

In fact, a polymer processing with organic solvents is very easy to get with the SEDS technique owing to solubility issues. In addition, the continuous SEDS procedure has prolonged the shelf life of polymeric substances. In this method,

water-soluble materials can as well be dealt with by means of introducing organic solvent via a co-axial three-compartment nozzle (Palakodaty et al. 1998). Identical to GAS, even SEDS has been comprehensively utilized for the micro/nanoparticles fabrication of a wide variety of organics, biopolymers, composites, etc. (Byrappa et al. 2008; Girotra et al. 2013).

4.8 Suspension-Enhanced Dispersion by Supercritical Fluids (SpEDS Process)

The SEDS technique has been specially modified into SpEDS technique to conquer its processing damage problems (Chen et al. 2012b). The operation of both techniques is mostly identical, except that SpEDS has an auxiliary injector arrangement for efficiently pumping the loaded suspension (Chen et al. 2012b). The SpEDS technique is specifically planned to achieve core-shell structured micro/nanoparticles with high drug encapsulation efficiency as well as longer sustained drug release features in contrast to other SCF-assisted co-precipitation techniques (Chen et al. 2012a, c).

4.9 Supercritical Assisted Atomization (SAA)

Supercritical assisted atomization (SAA) is the latest technique (Reverchon 2002) in which the SCF acts as an atomizing medium. The technique is anchored in the solubilization of SC-CO_2 in the liquid solution produced by the solvent and the solid solute, followed by atomization of resulting solution using a thin wall nozzle. When SAA technique is accurately performed, two atomization procedures come to pass: the first one is the formation of primary droplets at the outlet of the nozzle by means of pneumatic atomization; the second one obliterates these droplets with the quick discharge of CO_2 from the interior of the droplet known as decompressive atomization. Amorphous or crystalline particles have been formed, on the basis of the process temperatures as well as the chemical structures of the solid solute. By utilizing SAA technique, investigators have prepared polymethylmethacrylate nanoparticles using acetone as a solvent. In this method, they used 10 mg/mL polymethylmethacrylate in acetone, and they employed a mixing temperature 80 °C and a mixing pressure of 76 bar and produced nanoparticles with a mean diameter of 120 nm (Reverchon and Spada 2004). The major problem of this technique is that the smallest particles formed relay on the dimensions of the smallest droplets produced (one droplet-one particle method). These dimensions are related to the standard parameters that regulate droplet dimensions at some stage in atomization: surface tension, viscosity, and amount of SCF dissolved in the liquid.

5 Application of SCF for Production of Nanoparticles

Zinc acetate nanoparticles, a catalyst precursor, have been prepared by the SAS technique. Nanoparticles formed showing particle size in a range of 30–50 nm at the best processing temperature-pressure conditions (Reverchon et al. 1999). Chattopadhyay and Gupta produced fullerene (C60) nanoparticles from a solution of toluene. They have performed experiments in a SAS batch mode (injection in static SCF) and fullerene nanoparticles as small as 29–63 nm were achieved operating at different conditions (Chattopadhyay and Gupta 2000).

Reverchon and coworkers have been processed dextran, a bio-polymer using DMSO. The nanoparticles formed have a spherical morphology and a mean particle size ranging between 125 and 150 nm (Reverchon et al. 2000). Chattopadhyay and Gupta (2001b, 2002b) produced griseofulvin (antifungal, antibiotic) particles as low as 130 nm and lysozyme (enzyme) particles of about 190 nm using SAS-EM technique.

β-sitosterol nanoparticles of about 200 nm mean diameter have been prepared by Turk and coworkers using the RESS technique. They tested

the method in SC-CO_2 at different pre-expansion temperatures as well as pressures and found that for β-sitosterol the alteration of pre-expansion conditions does not lead to substantial differences in the diameters of nanoparticles. They also employed this technique for the manufacturing of griseofulvin nanoparticles using supercritical CHF_3 (Turk et al. 2002).

Snavely et al. (2002) developed insulin nanoparticles using the SAS technique with the aid of an ultrasonic nozzle. They achieved powder consisting of physical aggregates of 50 nm spherical particles forming cobweb-like and sponge-like structures that can be de-agglomerated in smaller components. The development of cobweb structures has been described by other researchers and is most likely attributable to the impact, and the accidental coalescence of the nanoparticles of some polymers has also been formed. Nanometric lysozyme particles with the smallest mean diameter of 180 nm were also developed by Muhrer and Mazzotti (2003) using the GAS technique.

Cyclosporine nanoparticles have been developed by the rapid expansion from supercritical to aqueous solutions (RESAS) technique, and the effect of different stabilizes like nonionic surfactants, e.g. Tween 80, Pluronic F127, Myrtj 52, and phospholipid-based surfactant on the particle size, is also compared. Among all the nonionic surfactant, Tween 80 generates smaller particle sizes that range from 660 to 970 nm, while phospholipid-based surfactant generates cyclosporine nanoparticles with size that ranges between 200 and 300 nm, which is smaller than particles generated by Tween 80 at the same concentration of the surfactant and drug/surfactant ratio. This outcome is due to the aggregation of a large quantity of surfactant for phospholipid vesicle than that for micelle. In addition, the favored curvature of the surfactant is more encouraging for vesicle than micelle as the boundary with water is little curved for vesicle as compared to micelle. Also, vesicles are comparatively stable, so the enlargement of the drug particles by collision/coagulation is diminished (Young et al. 2003).

Sane et al. (2003) developed fluorinated tetraphenyl porphyrin spherical, agglomerated nanoparticles with mean particle sizes from 60 to 80 nm, at various pre-expansion temperatures using RESS technique. Pestov and coworkers have also employed the RESS technique for the production of solvent-free and photoreactive nanoparticles of 2, 5-distyrylpyrazine (DSP) monomer. They precipitated DSP from $CHClF_2$ and they have also observed greater photoreactivity in the solid state as compared to micro-scale crystals (Pestov et al., 2003).

Using the RESS technique, Varshosaz et al. (2009) produced amorphous cefuroxime axetil nanoparticles. They studied the effect of formulation parameters, like the nozzle temperature (varying between 50 and 70 °C) and the extraction column temperatures (varying between 60 and 90 °C), on the particle size as well as morphology. Amorphous nanoparticles showing the mean size of 159 nm were achieved with 60 °C nozzle temperature and 90 °C column temperature. They also observed that when the temperatures of the nozzle as well as the extraction column were reduced to 50 °C and 75 °C, correspondingly, and the particle size was raised to 465 nm.

Pure naproxen nanoparticles were produced and naproxen nanoparticles coated with polylactic acid using the RESS technique. The researchers confirmed that the coating of polylactic acid stabilized the naproxen nanoparticles towards aggregation as well as coagulation (Gadermann et al. 2009).

Amoxicillin nanoparticles were developed by the SAS technique using N-methyl pyrrolidone and CO_2 as solvent and anti-solvent, respectively, and the effect of primary drug concentration, the flow rate of drug solution, temperature, and pressure and nozzle diameter on particle size as well as size distribution have been studied. Investigators found that if the initial drug concentration increased, it results in bigger particle sizes with a wide particle size distribution. The outcome is that the higher the condensation rate from the higher drug concentration, the higher the super-saturation from higher drug concentration. Greater flow rate results in smaller particle

sizes because of a greater degree of mixing. Spherical nanoparticles of amoxicillin with a mean size diameter of 216–505 nm were achieved by the SAS technique (Montes et al. 2010).

Digitoxin nanoparticles were formulated by the RESS technique, and the effects of processing parameters, for example flow rate, distance of spray, and pre-expansion temperature on the particle size, were studied. It was observed that the particle size of digitoxin particles reduces with the raise of flow rate as well as spray distance. In the earlier case, the residence time of droplets within the nozzle and in the expansion vessel is reduced by raising the flow rate. This reduces growth time for particle and resultant in smaller particle sizes. The latter case is the ensuing of two opposing phenomena. First, as the spraying distance is small, the residence time of droplets inside the expansion vessel lessens resulting in smaller particle sizes. In the contrary, small spraying distance leads to the coalescence of droplets because of lessening angles amid droplets. Conversely, particle size rises by raising the pre-expansion temperature. In every circumstance, the particle size of digitoxin was reduced from 0.2–8 μm to 68–458 nm (Atila et al. 2010).

5-Fluorouracil (5-FU) nanoparticles were formulated using the SAS technique to improve the physical characteristics of 5-FU to administer it directly to the respiratory tract. Different mixtures of methanol with dichloromethane, acetone, or ethanol were utilized for particle fabrication, and their effects on the physical characteristics of the final products were investigated. The experimental conditions for pressure in the range of 100 and 150 bars, a temperature of 40 °C, and a flow rate of 1 mL/min were kept. Regardless of variations in size, the particles did not differ in their morphology. The obtained nanoparticles were of a regular shape, somewhat spherical, and showed smooth surface, while the automatically milled particles exhibited less uniformity, showed surface irregularities and a wide particle size distribution, and appeared clustered. 5-FU nanoparticles prepared from methanol-dichloromethane 50:50 had a mean particle size of 248 nm (Kalantarian et al. 2010).

Raloxifene nanoparticles were formulated by the RESS technique, and the effect of extraction temperature, extraction pressure, and spray distance on the formation were investigated. It was observed that by raising extraction pressure from 10 to 18 MPa as well as spray distance from 5 to 10 cm, the particle size reduced. On the other hand, by raising extraction temperature from 40 to 60 °C, the particle size turned out to be smaller; however, a further raise in temperature to 80 °C reduces the particle size. The latter case can be clarified by the fact that higher temperature brings about a higher degree of supersaturation because the solubility increases at the elevated temperature. And this high level of supersaturation enhances the number of nuclei creation, which sequentially raises the likelihood of a collision and subsequently larger particle production. Raloxifene nanoparticles of 14.11 nm were achieved at the best possible condition of 50 °C temperature, 17.7 MPa extraction pressure, and 10 cm spraying distance (Keshavarz et al. 2012).

Beclometasone dipropionate nanoparticles were developed using the RESS technique, employing CO_2 as a supercritical solvent. A full factorial two-level design was used so as to evaluate the processing parameters counting the pre-expansion temperature, extraction pressure, and fraction of co-solvent on the particle size and particle size distribution of beclometasone dipropionate nanoparticles. The mean sizes of beclometasone dipropionate nanoparticles were found in between 64.1 and 294 nm. Analysis of Variance (ANOVA) demonstrated that the extraction pressure was the most significant parameter and a high extraction pressure also plays a significant role for the development of small-sized particles, whereas increasing the pre-expansion temperature and weight fraction of co-solvent displays an increase in particle size. The RESS technique demonstrated as a talented process for the fabrication of beclometasone dipropionate nanoparticles that may well result in the enhancement of the drug's physicochemical characteristics (Mohsen et al. 2015).

Cefquinome nanoparticles were prepared by using the SAS technique. By orthogonal experimentations, it was established that the concentra-

tion of the solution was the most important feature in this technique, followed by the feeding speed of solution, precipitation pressure, and precipitation temperature. For the moment, the best possible processing conditions of preparing cefquinome nanoparticles were 100 mg/mL concentration of the solution, 1.5 mL/min solution flow speed, 13Mpa processing pressure, and processing temperature 33 °C. A confirmatory trial was performed under this situation. It was observed that the look of particles was flakes and the mean diameter of particles processed was 710 nm. Furthermore, univariate analysis was carried out to study the influence of the decree of individual factors on particle size. Outcomes confirmed that the mean diameter enlarged with an increase in the concentration of the solution, however, lowered with an increase in the feeding speed of the solution. The consequence of both precipitation pressure as well as temperature on the mean diameter was comprehensive. When these two parameters increased, the mean diameter might show an extreme point. The SAS technique for preparing cefquinome nanoparticles grasps significant insinuations for the enhancement of the effectiveness of cefquinome and the growth of pharmaceutical developments (Xiao et al. 2015).

Spherical-shaped polycaprolactone nanoparticles were fruitfully produced by SCF extraction of emulsions. The competence of the SC-CO_2 extraction was studied and related to that of solvent extraction at atmospheric pressure. The investigations have been done on the effects of operating parameters like the concentration of polymer (0.6–10% w/w in acetone), the concentration of surfactant (0.07 and 0.14% w/w), and polymer-to-surfactant weight ratio (1:1–16:1 w/w) on the surface morphology as well as particle size. Spherical polycaprolactone nanoparticles with average particle sizes between 190 and 350 nm were developed that mostly rely on the polymer concentration, which was the most significant parameter where an increase in the particle size was directly compared to total polymer concentration in the product. Polycaprolactone nanoparticles were characterized by dynamic light scattering technique and scanning electron microscopy technique. The results showed that SCF extraction of emulsions can be useful for the formulation of polycaprolactone nanoparticles without aggregation and in a relatively small period of just 1 h (Ajiboye et al. 2018).

6 Summary and Future Perspective

The nanoparticles for drug delivery manufactured using different SCFs present controllable particle size and high degrees of diffusivity in both drugs and synthetic polymers. The SCF technique has given a clean environmentally pleasant nanoparticle manufacturing technique as a substitute to the customary technique. SCF technique will aid to deal with the industry's challenges to hit upon quicker, faster, and more cost-effective techniques to grow novel drug nanoparticles for sustained and controlled delivery without being affected by the harsh operating environments. The production manufacturing of nanoparticles with precise physicochemical characteristics is a major problem in the pharmaceutical industry. The problems one should deal with for victorious nanoparticle manufacturing is to opt for a successful SCF technique relating to temperature, pressure, mass transfer, and type of solvent utilized and phase behavior. Application of SCF technique to manufacture nanoparticles for drug delivery along with small particle size, improved flexibility, and enhanced rate of dissolution with SC-CO_2 proposes a significant role for this technology in future drug delivery appliances and takes new prototypes in healthcare and getting better human health. A great number of SCF-based techniques are urbanized in current years. There is still potential to progress the available SCF techniques by improving processing conditions like physical and chemical parameters. Moreover, lots of new techniques can be urbanized by accepting the features of SCFs, the nature of the solute, and their interaction. For sure, SCF techniques are superior techniques over available and traditional techniques like milling/crushing for size reduction, soxhlet extraction, spray coating, impregnation by soak-

ing, etc. Still, extensive investigation is required to put together it in realistic and at an industrial level. Hence, the overall perspective is very optimistic for future applications, and the healthiness of the future generation can be guaranteed with the help of the SCF technique. In this sense, nanoparticles manufacturing with SCF technology might see thrilling perspectives.

References

Ajiboye AL, Trivedi V, Mitchell JC. Preparation of polycaprolactone nanoparticles via supercritical carbon dioxide extraction of emulsions. Drug Deliv Transl Res. 2018;8:1790–6.

Atila C, Yildiz N, Caliml A. Particle size design of digitoxin in supercritical fluids. J Supercrit Fluids. 2010;51:404–11.

Bałdyga J, Kubicki D, Shekunov BY, Smith KB. Mixing effects on particle formation in supercritical fluids. Chem Eng Res Des. 2010;88:1131–41.

Beckman EJ. Supercritical and near-critical CO_2 in green chemical synthesis and processing. J Supercrit Fluids. 2004;28:121–91.

Bertucco A, Vetter G, editors. High pressure process technology: fundamentals and applications, industrial chemistry library, vol. 9. 1st ed. Amsterdam: Elsevier; 2001.

Bertucco A, Pallado P, Benedetti L. Formation of biocompatible polymer microspheres for controlled drug delivery by a supercritical anti-solvent technique. Process Technol Proc. 1996;12:217–22.

Bleich J, Muller BW, Wabmus W. Aerosol solvent extraction system: a new microparticle production technique. Int J Pharm. 1993;97:111–7.

Byrappa K, Ohara S, Adschiri T. Nanoparticle's synthesis using supercritical fluid technology – towards biomedical applications. Adv Drug Deliv Rev. 2008;60:299–327.

Cabanas A, Poliakoff M. The continuous hydrothermal synthesis of nano-particulate ferrites in near critical and supercritical water. J Mater Chem. 2001;11:1408–16.

Campardelli R, Adami R, Della Porta G, Reverchon E. Nanoparticle precipitation by supercritical assisted injection in a liquid anti-solvent. Chem Eng J. 2012;192:246–51.

Chattopadhyay P, Gupta RB. Supercritical CO_2-based production of fullerene nanoparticles. Ind Eng Chem Res. 2000;39:2281–9.

Chattopadhyay P, Gupta RB. Production of antibiotic nanoparticles using supercritical CO_2 as anti-solvent with enhanced mass transfer. Ind Eng Chem Res. 2001a;40:3530–9.

Chattopadhyay P, Gupta RB. Production of griseofulvin nanoparticles using supercritical CO_2 anti-solvent with enhanced mass transfer. Int J Pharm. 2001b;228:19–31.

Chattopadhyay P, Gupta RB. Supercritical CO_2 based production of magnetically responsive micro- and nanoparticles for drug targeting. Ind Eng Chem Res. 2002a;41:6049–58.

Chattopadhyay P, Gupta RB. Protein nanoparticles formation by supercritical anti-solvent with enhanced mass transfer. AICHE J. 2002b;48:235–44.

Chattopadhyay P, Shekunov BY, Yim D, Cipolla D, Boyd B, Farr S. Production of solid lipid nanoparticle suspensions using supercritical fluid extraction of emulsions (SFEE) for pulmonary delivery using the AERx system. Adv Drug Deliv Rev. 2007;59:444–53.

Chen AZ, Zhao Z, Wang SB, Li Y, Zhao C, Liu YG. A continuous RESS process to prepare PLA–PEG–PLA microparticles. J Supercrit Fluids. 2011;59:92–7.

Chen AZ, Wang GY, Wang SB, Feng JG, Liu YG, Kang YQ. Preparation of poly-(methyl vinyl ether-co-maleic anhydride) nanoparticles by solution-enhanced dispersion by supercritical CO_2. Materials. 2012a;5:1841–52.

Chen AZ, Wang GY, Wang SB, Li L, Liu YG, Zhao C. Formation of methotrexate-PLLA-PEG-PLLA composite microspheres by microencapsulation through a process of suspension-enhanced dispersion by supercritical CO_2. Int J Nanomedicine. 2012b;7:3013–22.

Chen AZ, Li L, Wang SB, Lin XF, Liu YG, Zhao C, et al. Study of Fe_3O_4-PLLA-PEG-PLLA magnetic microspheres based on supercritical CO_2: preparation, physicochemical characterization, and drug loading investigation. J Supercrit Fluids. 2012c;67:139–48.

Chen BQ, Kankala RK, Chen AZ, Yang DZ, Cheng DZ, Jiang XX, et al. Investigation of silk fibroin nanoparticle-decorated poly(l-lactic acid) composite scaffolds for osteoblast growth and differentiation. Int J Nanomedicine. 2017;12:1877–90.

Cooper AI. Polymer synthesis and processing using supercritical carbon dioxide. J Mater Chem. 2000;10:207–14.

Dalvi SV, Azad MA, Dave R. Precipitation and stabilization of ultrafine particles of Fenofibrate in aqueous suspension by RESOLV. Powder Technol. 2013;236:75–84.

Date AA, Patravale VB. Current strategies for engineering drug nanoparticles. Curr Opin Colloid Interface Sci. 2004;9:222–35.

Davies OR, Lewis AL, Whitaker MJ, Tai H, Shakesheff KM, Howdle SM. Applications of supercritical CO_2 in the fabrication of polymer systems for drug delivery and tissue engineering. Adv Drug Deliv Rev. 2008;60:373–87.

Dehghani F, Foster NR. Dense gas anti-solvent processes for pharmaceutical formulation. Curr Opin Solid State Mater Sci. 2003;7:363–9.

Della PG, Falco N, Reverchon E. NSAID drugs release from injectable microspheres produced by supercritical fluid emulsion extraction. J Pharm Sci. 2010;99:1484–99.

DeSimone JM. Practical approaches to green solvents. Science. 2002;297:799–803.
Djerafi R, Masmoudi Y, Crampon C, Meniai A, Badens E. Supercritical anti-solvent precipitation of ethyl cellulose. J Supercrit Fluids. 2015;105:92–8.
Dong Z, Li Y, Lin M, Li M. A study of the mechanism of enhancing oil recovery using supercritical carbon dioxide microemulsions. Pet Sci. 2013;10:91–6.
Elliot J, Hancook B. Pharmaceutical materials science: an active new frontier in materials research. MRS Bull. 2006;31:869–71.
Elvassore N, Bertucco A, Caliceti P. Production of insulin-loaded poly(ethylene glycol)/poly(l-lactide) (PEG/PLA) nanoparticles by gas anti-solvent techniques. J Pharm Sci. 2001;90:1628–36.
Erkey C. Preparation of metallic supported nanoparticles and films using supercritical fluid deposition. J Supercrit Fluids. 2009;47:517–22.
Falk R, Randolph TW, Meyer JD, Kelly RM, Manning MC. Controlled release of ionic compounds from poly (L-lactide) microspheres produced by precipitation with a compressed anti-solvent. J Control Release. 1997;44:77–85.
Fraile M, Martin A, Deodato D, Rodriguez-Rojo S, Nogueira ID, Simplicio AL, et al. Production of new hybrid systems for drug delivery by PGSS (particles from gas saturated solutions) process. J Supercrit Fluids. 2013;81:226–35.
Gadermann M, Kular S, Al-Marzouqi A, Signorell R. Formation of naproxen/polylactic acid nanoparticles by pulsed rapid expansion of supercritical solutions. Phys Chem Chem Phys. 2009;11:7861–8.
Ginty PJ, Whitaker MJ, Shakesheff KM, Howdle SM. Drug delivery goes supercritical. Mater Today. 2005;8:42–8.
Ginty PJ, Howard D, Rose FRAJ, Whitaker MJ, Barry JJA, Tighe P, et al. Mammalian cell survival and processing in supercritical CO_2. Proc Natl Acad Sci. 2006;103:7426–31.
Girotra P, Singh SK, Nagpal K. Supercritical fluid technology: a promising approach in pharmaceutical research. Pharm Dev Technol. 2013;18:22–38.
Gosselin PM, Thibert R, Preda M, McMullen JN. Polymorphic properties of micronized carbamazepine produced by RESS. Int J Pharm. 2003;252:225–33.
Habulin M, Primozic M, Knez Z. Supercritical fluids as solvents for enzymatic reactions. Acta Chim Slov. 2007;54:667–77.
Hakuta Y, Hayashi H, Arai K. Fine particle formation using supercritical fluids. Curr Opin Solid State Mater Sci. 2003;7:341–51.
Hamidreza AB, Reza BS, Mahdi CS, Mahdi DY, Fatemeh EF, Hassan FH. Nanotechnology and supercritical fluids. J Fundam Appl Sci. 2016;8:839–59.
Hauthal WH. Advances with supercritical fluids. Chemosphere. 2001;43:123–35.
He WZ, Suo QL, Jiang ZH, Shan A, Hong HL. Precipitation of ephedrine by SEDS process using a specially designed prefilming atomizer. J Supercrit Fluids. 2004;31:101–10.
Housaindokht MR, Bozorgmehr MR. Calculation of solubility of methimazole, phenazopyridine and propranolol in supercritical carbon dioxide. J Supercrit Fluids. 2008;43:390–7.
Huang Z, Sun GB, Chiew YC, Kawi S. Formation of ultrafine aspirin particles through rapid expansion of supercritical solutions (RESS). Powder Technol. 2005;160:127–34.
Jung J, Perrut M. Particle design using supercritical fluids: literature and patent survey. J Supercrit Fluids. 2001;20:179–219.
Kalani M, Yunus R. Application of supercritical antisolvent method in drug encapsulation: a review. Int J Nanomedicine. 2011;6:1429–42.
Kalantarian P, Najafabadi AR, Haririan I, Vatanara A, Yamini Y, Darabi M, et al. Preparation of 5-fluorouracil nanoparticles by supercritical antisolvents for pulmonary delivery. Int J Nanomedicine. 2010;5:763–70.
Kalogiannis CG, Pavlidou E, Panayiotou CG. Production of amoxicillin microparticles by supercritical anti-solvent precipitation. Ind Eng Chem Res. 2005;44:9339–46.
Kankala RK, Zhang YS, Wang SB, Lee CH, Chen AZ. Supercritical fluid technology: an emphasis on drug delivery and related biomedical applications. Adv Healthc Mater. 2017;6:1700433.
Kerc J, Srcic S, Knez Z, Sencar-Bozic P. Micronization of drugs using supercritical carbon dioxide. Int J Pharm. 1999;182:33–9.
Keshavarz A, Karimi-Sabet J, Fattahi A, Golzary AA, Rafiee-Tehrani M, Dorkoosh FA. Preparation and characterization of raloxifene nanoparticles using Rapid Expansion of Supercritical Solution (RESS). J Supercrit Fluids. 2012;63:169–79.
Knez Z, Weidner E. Particle's formation and particle design using supercritical fluids. Curr Opin Solid State Mater. 2003;7:353–61.
Knez Z, Markocic E, Leitgeb M, Primozic M, Hrncic MK, Skerget M. Industrial applications of supercritical fluids: a review. Energy. 2014;77:235–43.
Kompella UB, Koushik K. Preparation of drug delivery systems using supercritical fluid technology. Crit Rev Ther Drug Carrier Syst. 2001;18:173–99.
Krober H, Teipel U. Materials processing with supercritical anti-solvent precipitation: process parameters and morphology of tartaric acid. J Supercrit Fluids. 2002;22:229–35.
Langer R, Vacanti JP. Tissue engineering. Science. 1993;260:920–6.
Li F, Hsieh Y. Supercritical fluid chromatography-mass spectrometry for chemical analysis. J Sep Sci. 2008;31:1231–7.
Lin YC, Jang SM. Formation of micro-size drug particles with supercritical fluids. J Biotechnol. 2008;136S:S144–6.
Markocic E, Kramberger B, Bennekom JGV, Heeres HJ, Vos J, Knez Z. Glycerol reforming in supercriti-

cal water; a short review. Renew Sust Energ Rev. 2013;8:23–40.
Martin A, Cocero MJ. Micronization processes with supercritical fluids: fundamentals and mechanisms. Adv Drug Deliv Rev. 2008;60:339–50.
Matsubara A, Fukusaki E, Bamba T. Metabolite analysis by supercritical fluid chromatography. Bioanalysis. 2010;2:27–34.
McHugh MA, Guckes TL. Separating polymer solutions with supercritical Fluids. Macromolecules. 1985;18:674–80.
McHugh MA, Krukonis VJ. Supercritical fluid extraction: principles and practice. 2nd ed. Boston: Butterworth-Heinemann; 1994. p. 1–144.
Meziani MJ, Rollins HW, Allard LF, Sun YP. Protein-protected nanoparticles from rapid expansion of supercritical solution into aqueous solution. J Phys Chem B. 2002;106:11178–82.
Mishima K. Biodegradable particle formation for drug and gene delivery using supercritical fluid and dense gas. Adv Drug Deliv Rev. 2008;60:411–32.
Mohsen H, Alireza V, Reza Z. Formation and characterization of beclomethasone dipropionate nanoparticles using rapid expansion of supercritical solution. Adv Pharm Bull. 2015;5:343–9.
Montes A, Tenorio A, Gordillo MD, Pereyra C, Ossa EJM. Screening design of experiment applied to supercritical anti-solvent precipitation of amoxicillin: Exploring new miscible conditions. J Supercrit Fluids. 2010;51:399–403.
Montes A, Gordillo MD, Pereyra C, Martinez EJ. Particles formation using supercritical fluids. In: Nakajima H, editor. Mass transfer – advanced aspects. Europe: InTech Open; 2011. p. 461–80.
Montes A, Pereyra C, de la Ossa EJM. Mean aspects controlling supercritical CO_2 precipitation processes. In: Alfredo I, editor. Heat and mass transfer – advances in science and technology applications. London: Intech Open; 2019. p. 1–15.
Muhrer G, Mazzotti M. Precipitation of lysozyme nanoparticles from dimethyl sulfoxide using carbon dioxide as anti-solvent. Biotechnol Prog. 2003;19:549–56.
Munshi P, Bhaduri S. Supercritical CO_2: a twenty-first century solvent for the chemical industry. Curr Sci India. 2009;97:63–72.
Ollanketo M, Hartonen K, Riekkola M, Holm Y, Hiltunen R. Supercritical carbon dioxide extraction of lycopene in tomato skins. Eur Food Res Technol. 2001;212:561–5.
Palakodaty S, York P, Pritchard J. Supercritical fluid processing of materials from aqueous solutions: the application of SEDS to lactose as a model substance. Pharm Res. 1998;15:1835–43.
Palakodaty S, Sloan R, Kordikowski A. Pharmaceutical and biological materials processing with supercritical fluids. In: Sun YP, editor. Supercritical fluid technology in materials science and engineering. New York: Marcel Dekker Inc.; 2002. p. 439–90.
Pasquali I, Bettini R. Are pharmaceutics really going supercritical? Int J Pharm. 2008;364:176–87.
Perry RH. Perry's chemical engineers' handbook. 7th ed. New York: McGraw-Hill; 1997.
Pestov D, Levit N, Kessick R, Tepper G. Photosensitive 2,5- distyrylpyrazine particles produced from rapid expansion of supercritical solutions. Polymer. 2003;44:3177–83.
Pinkston JD, Stanton DT, Wen D. Elution and preliminary structure retention modeling of polar and ionic substances in supercritical fluid chromatography using volatile ammonium salts as mobile phase additives. J Sep Sci. 2004;27:115–23.
Prosapio V, Reverchon E, De Marco I. Polymers ultrafine particles for drug delivery systems precipitated by supercritical carbon dioxide+ organic solvent mixtures. Powder Technol. 2016;292:140–8.
Ramsey E, Sun Q, Zhang Z, Zhang C, Gou W. Mini-review: green sustainable processes using supercritical fluid carbon dioxide. J Environ Sci. 2009;21:720–6.
Rehman M, Shekunov BY, York P, Colthorpe P. Solubility and precipitation of nicotinic acid in supercritical carbon dioxide. J Pharm Sci. 2001;90:1570–82.
Reverchon E. Supercritical anti-solvent precipitation of micro- and nano-particles. J Supercrit Fluids. 1999;15:1–21.
Reverchon E. Supercritical-assisted atomization to produce micro and/or nanoparticles of controlled size and distribution. Ind Eng Chem Res. 2002;41:2405–11.
Reverchon E, Adami R. Nanomaterials and supercritical fluids. J Supercrit Fluids. 2006;37:1–22.
Reverchon E, De Marco I. Supercritical anti-solvent micronization of Cefonicid: thermodynamic interpretation of results. J Supercrit Fluids. 2004;31:207–15.
Reverchon E, Spada A. Crystalline microparticles of controlled size produced by supercritical-assisted atomization. Ind Eng Chem Res. 2004;43:1460–5.
Reverchon E, Porta GD, Taddeo R, Pallado P, Stassi A. Solubility and micronization of griseofulvin in supercritical CHF_3. Ind Eng Chem Res. 1995;34:4087–91.
Reverchon E, Porta GD, Sannino D, Ciambelli P. Supercritical anti-solvent precipitation of nanoparticles of a zinc oxide precursor. Powder Technol. 1999;102:127–34.
Reverchon E, Porta GD, De Rosa I, Subra P, Letourneur D. Supercritical anti-solvent micronization of some biopolymers. J Supercrit Fluids. 2000;18:239–45.
Reverchon E, Caputo G, De Marco I. Role of phase behavior and atomization in the supercritical anti-solvent precipitation. Ind Eng Chem Res. 2003;42:6406–14.
Sacchetin PSC, Setti RF, Vieira e Rosa P de T, Moraes AM. Properties of PLA/PCL particles as vehicles for oral delivery of the androgen hormone 17α-methyltestosterone. Mater Sci Eng C. 2016;58:870–81.
Saito M. History of supercritical fluid chromatography: Instrumental development. J Bioeng. 2013;115:590–9.
Sane A, Taylor S, Sun YP, Thies MC. RESS for the preparation of fluorinated porphyrin nanoparticles. Chem Commun. 2003;21:2720–1.

Seckner AJ, McClellan AK, McHugh MA. High pressure solution behavior of the polymer-toluene-ethane system. AICHE J. 1988;34:9–14.

Shariati A, Peters CJ. Recent developments in particle design using supercritical fluids. Curr Opin Solid State Mater Sci. 2003;7:371–83.

Shekunov BY, Chattopadhyay P, Seitzinger JS. Method and apparatus for enhanced size reduction of particles using liquefaction of materials. US Patent 6,986,846, January 17, 2006. Accessed 20 Sept 2019.

Shen YB, Du Z, Wang Q, Guan YX, Yao SJ. Preparation of chitosan microparticles with diverse molecular weights using supercritical fluid assisted atomization introduced by hydrodynamic cavitation mixer. Powder Technol. 2014;254:416–24.

Sheth P, Sandhu H, Singhal D, Malick W, Shah N, Kislalioglu MS. Nanoparticles in the pharmaceutical industry and the use of supercritical fluid technologies for nanoparticle production. Curr Drug Deliv. 2012;9:269–84.

Shoyele SA, Cawthorne S. Particle engineering techniques for inhaled biopharmaceuticals. Adv Drug Deliv Rev. 2006;58:1009–29.

Skerget M, Knez Z, Hrncic MK. Solubility of solids in sub- and supercritical fluids: a review. J Chem Eng Data. 2011;56:694–719.

Smith RM. Supercritical fluid in separation science the dreams, the reality and the future. J Chromatogr A. 1999;856:83–115.

Snavely WK, Subramaniam B, Rajewski RA, Defelippis MR. Micronization of insulin from halogenated alcohol solution using supercritical carbon dioxide as an anti-solvent. J Pharm Sci. 2002;91:2026–39.

Sovilj MN, Nikolovski BG, Spasojevic MD. Critical review of supercritical fluid extraction of selected spice plant materials. Maced J Chem Chem Eng. 2011;30:197–220.

Sun YP, Atorngitjawat P, Meziani MJ. Preparation of silver nanoparticles via rapid expansion of water in carbon dioxide microemulsion into reductant solution. Langmuir. 2001;17:5707–10.

Thakur R, Gupta RB. Rapid expansion of supercritical solution with solid co solvent (RESS-SC) process: formation of griseofulvin nanoparticles. Ind Eng Chem Res. 2005;44:7380–7.

Thote AJ, Gupta RB. Formation of nanoparticles of a hydrophilic drug using supercritical carbon dioxide and microencapsulation for sustained release. Nanomedicine. 2005;1:85–90.

Tomasko DL, Li H, Liu D, Han X, Wingert MJ, Lee LJ, Koelling KW. A review of CO_2 applications in the processing of polymers. Ind Eng Chem Res. 2003;42:6431–56.

Tservistas M, Levy MS, Lo-Yim JYA, O'Kennedy RD, York P, Humphrey GO, et al. The formation of plasmid DNA loaded pharmaceutical powders using SCF technology. Biotechnol Bioeng. 2001;72:12–8.

Turk M, Hils P, Helfgen B, Schaber K, Martin HJ, Wahl MA. Micronization of pharmaceutical substances by the rapid expansion of supercritical solutions (RESS): a promising method to improve bioavailability of poorly soluble pharmaceutical agents. J Supercrit Fluids. 2002;22:75–84.

Varshosaz J, Hassanzadeh F, Mahmoudzadeh M, Sadeghi A. Preparation of cefuroxime axetil nanoparticles by rapid expansion of supercritical fluid technology. Powder Technol. 2009;189:97–102.

Velaga SP, Ghaderi R, Carlfors J. Preparation and characterisation of hydrocortisone particles using a supercritical fluids extraction process. Int J Pharm. 2002;231:155–66.

Vemavarapu C, Mollan MJ, Lodaya M, Needham TE. Design and process aspects of laboratory scale SCF particle formation systems. Int J Pharm. 2005;292:1–16.

Wang TC, Chang PC. Measurement and correlation for the solid solubility of antioxidants sodium L-ascorbate and sodium erythorbate monohydrate in supercritical carbon dioxide. J Chem Eng Data. 2015;60:790–4.

Warwick B, Dehghani F, Foster NR, Biffin JR, Regtop HL. Micronization of copper indomethacin using gas anti-solvent processes. Ind Eng Chem Res. 2002;41:1993–2004.

Wu K, Li J. Precipitation of a biodegradable polymer using compressed carbon dioxide as anti-solvent. J Supercrit Fluids. 2008;46:211–6.

Xiao K, Wang W, Hu D, Hao Z, Qu Y, Liu Y. Preparation of cefquinome nanoparticles by using the supercritical anti-solvent process. J Nanomater. 2015;2015:Article ID 767945.

Yamini Y, Bahramifar N. Solubility of polycyclic aromatic hydrocarbons in supercritical carbon dioxide. J Chem Eng Data. 2000;45:53–6.

Yang H, Zhong C. Modeling of the solubility of aromatic compounds in supercritical carbon dioxide–co solvent systems using SAFT equation of state. J Supercrit Fluids. 2005;33:99–106.

Yasuji T, Takeuchi H, Kawashima Y. Particle design of poorly water-soluble drug substances using supercritical fluid technologies. Adv Drug Deliv Rev. 2008;60:388–98.

Yeo SD, Lee JC. Crystallization of sulfamethizole using the supercritical and liquid anti-solvent processes. J Supercrit Fluids. 2004;30:315–23.

Yeo SD, Lim GB, Debendetti PG, Bernstein H. Formation of microparticulate protein powder using a supercritical fluid anti-solvent. Biotechnol Bioeng. 1993;41:341–6.

Young TJ, Johnston KP, Mishima K, Tanaka H. Encapsulation of lysozyme in a biodegradable polymer by precipitation with a vapor-overliquid anti-solvent. J Pharm Sci. 1999;88:640–50.

Young TJ, Johnston KP, Pace GW, Mishra AK. Phospholipid-stabilized nanoparticles of cyclosporine a by rapid expansion from supercritical to aqueous solution. AAPS PharmSciTech. 2003;5:1–16.

7

Salting Out and Ionic Gelation Manufacturing Techniques for Nanoparticles

Srinivas Reddy Jitta and Lalit Kumar

Abstract

Nanotechnology is currently most explored filed by the researchers especially in novel drug development. Polymeric nanoparticles are the nanomedicine developed by employing nanotechnology in the field of pharmaceutical drug development. Polymeric nanoparticles have many advantages such as less toxicity, targeted drug delivery in several types of diseases include cancer, diabetes, gastrointestinal diseases, pulmonary diseases, and others. The current chapter mainly focused on the various polymers that are used to prepare the nanoparticles. The methodology of different techniques available for the preparation of various kinds of synthetic and natural polymers was discussed focusing mainly on salting-out and ionic gelation crosslinking methods. Further, the latest technologies introduced by the researchers in the recent past for the preparation of polymeric nanoparticles to overcome the limitations of traditional methods are being discussed briefly in the current chapter.

Keywords

Salting out · Ionic gelation · Nanoparticles · Manufacture techniques, etc

1 Introduction

Drug discovery and development is a long journey and involves huge investment. The approximate total cost of developing a new drug in US pharmaceutical industries in the early twenty-first century was estimated at about over a billion dollars. The process of drug development is not only expensive but also a time-consuming procedure as the entire process may take up to 14 years. This creates a tremendous pressure on the industry to reduce the cost and development time and to increase the efficiency. Multiple factors influence the drug development procedure at various stages of the entire process starting from the discovery of a bioactive compound by a chemist to deliver a pharmaceutical agent to the systemic circulation typically by a pharmaceutical dosage form. Physicochemical and biological barriers are the two major issues faced by the researchers during formulation development. Poor water solubility, larger molecular weight, and complications in drug release kinetics are the common physicochemical issues, whereas the drug distribution into various organs after absorption is the biological barrier. Permeability and metabolic

S. R. Jitta · L. Kumar (✉)
Department of Pharmaceutics, Manipal College of Pharmaceutical Sciences, Manipal Academy of Higher Education, Manipal, Udupi, Karnataka, India
e-mail: lalit.kumar@manipal.edu

J. K. Patel, Y. V. Pathak (eds.), *Emerging Technologies for Nanoparticle Manufacturing*,
https://doi.org/10.1007/978-3-030-50703-9_7

stability of the drug molecule plays a key role in developing a suitable formulation (Han and Wang 2016; Lim and Hamid 2018).

2 Nanotechnology in Drug Delivery Systems

Nanotechnology is one of the utmost interesting research areas especially in pharmaceutical drug development, and it is a promising approach to address the problems associated with drug delivery. By applying nanotechnology, it is possible to fabricate new drug delivery systems that can transport the bio-active moiety to the desired cell, organ, or site of action. The term "nanoparticles" was first used in 1976, and nanoparticle technology gained attention in the late 1990s. During the initial days of nanomedicine development, researchers mainly focused on developing nanomedicine mainly concentrating on tumors as the area of interest. Currently, the technology is being explored to develop drugs for various kinds of diseases. The current development in the field of nanotechnology offers plenty of opportunities to get control over the problems associated with conventional dosage forms by the fabrication of nanoparticles that can encapsulate and release drug molecules in a controlled release manner. Nanoparticles are considered as a good candidate for delivery of contraceptives, vaccines, and targeted antibodies. Nanoparticles reduce unwanted side effects by limiting drug release only at specific targets. In the treatment of cancers, the capability of nanoparticles to modify the drug release makes them the ideal choice. In the case of therapeutic areas of ocular diseases, drug treatment requires frequent dosing which is one of the major disadvantages in terms of treatment by conventional dosage forms. Nanoformulations of drugs prepared using biodegradable polymers for these can serve as a suitable drug delivery system for solving problems such as frequent dosing, protection from enzymes, or proteins in the circulation which affect the half-life of the drug. Nanoparticles are usually having a size of 1 nm to 1 μm. Particle size affects the efficiency of drug delivery to a specific target site. Understanding the combinatorial effects of morphological features like size, shape, surface chemistry, and others is very important to design nanoparticles as suitable drug carriers as nanoparticles show phenomena such as quantum size effect. For example, nanoparticles with small size usually enter into tissue extravasations and excreted by renal clearance, whereas nanoparticles with large size are engulfed by the macrophages from systemic circulation reticuloendothelial system (RES)(Galindo-Rodríguez et al. 2005a, b; Wu et al. 2009; Harilall et al. 2013; Krishnamoorthy and Mahalingam 2015; Kadian 2018; Lim and Hamid 2018; Tsai et al. 2018; Jain et al. 2019).

Employing nanotechnology in the field of medicine acquired a rapid growth in the therapeutic areas of several diseases. The anticancer agents prepared by nanotechnology have received approval from the FDA (Food and Drug Administration) because of their better efficiency and minimal toxic effects in comparison to the naked drug. Even though nanomedicine is gaining a lot of attention from the researchers, still there is a large distance between the laboratory bench products and its commercialization. Most of the methods employed in the nanoparticle preparation are still not perfect, and there is a need for improvement and optimization. The scale-up of production methods and characterization of nanoformulations in a highly precise way are laborious, expensive, and time consuming. The variation across the batches is an additional challenge which can hamper the sufficient supply of the nanoformulations to the market needs (Farjadian et al. 2018).

The term nanoparticle is a common name shared by nano-capsule and nano-sphere and is typically defined as the solid and submicron-sized vehicle which may or may not be biodegradable in nature. The intracellular uptake of nanoformulations is greatly affected by its particle size. Apart from the size nature of nanoparticle, surface charge also influences the uptake of the formulation by gut epithelia. Polymeric nanoparticles prepared using lipophilic polymers are known to have more uptake in comparison to the nanoformulations prepared with hydrophilic polymers. In general, hydrophobic polymer-based nanoparticles with

positively charged or uncharged surfaces provide more affinity to follicle-associated epithelia and absorptive enterocytes, whereas nanoparticles with negative charge show less affinity. In contrast to this, nanoparticles prepared with the hydrophilic polymers with a negative charge on the surface may have a strong bio-adhesive nature, because of which absorption takes place by both absorptive enterocytes and M cells in the intestine. Nanoparticles with a combination of both negative and positive surface charge entrapped in a higher hydrophilic matrix are likely to improve the intestinal absorption. Further, surface modification of the nanoparticles also influences drug delivery to the targeted site significantly. The nanoparticles without any surface modification are prone to rapid opsonization by macrophages. The reticuloendothelial system in the spleen and liver is mainly involved in this mechanism and is a major problem for the active targeting of drugs. The RES can recognize the endogenous molecules in systemic circulation and clears by opsonization (Reis et al. 2006).

One of the important goals in the area of drug discovery and development is the synthesis or discovery of new chemical entities with minimal toxic effects and maximum therapeutic benefits. Nanoparticles offer several advantages in this context of drug targeting to the desired tissues and reducing the nonspecific toxicities. Employing biocompatible and biodegradable polymers in the preparation of nanocarrier-based formulations led to the wider application of nanoparticles in drug delivery systems development. The main problem associated with the production of nanoparticles is the synthesis by conventional methods, and on the other side, the chemical synthesis is relatively expensive. Moreover, potential toxic reagents are required for chemical synthesis, requirements for safe disposal which are of environmental concern. Furthermore, the scale-up of nanoparticle synthesis from laboratory to market place is involved with a high level of risk because of the fragility, reactivity, and instability of nanoscale materials. Moreover, the production of nanomaterials is more complicated to engineer in comparison with bulk, so the process involved is more complex and expensive. Reaching the target site efficiently, controlled release of the drug from polymer within time scale, and controlled degradation of the polymer are the other major problems associated with the nanoparticles in the drug delivery system. As per Lipinski's rule of five, drug-like molecules have a moderately lipophilic character and tend to be water insoluble. Hence, poor solubility of the drugs is considered as one of the important problems faced by conventional formulations. When nanoparticles are prepared, the surface area increases, and therefore the rate of dissolution of the drug also increases leading to the improvement in drug bioavailability (Farjadian et al. 2018).

3 Polymeric Nanoparticles

These are the nanoformulations typically of solid particles or dispersions where the drug is encapsulated or conjugated into the polymer matrix. Polymeric nanoparticles are typically having a size of 10 nm to 1 μm range. The development of drug delivery systems of polymer-based nanoparticles is the current research area of interest, and many researchers are working in this field. Polymeric nanoparticles are generally prepared from polymers which are biodegradable and biocompatible in nature, and these systems are being used to improve and alter the pharmacodynamic and pharmacokinetic properties of drugs belonging to various classes. Polymeric nanoparticles have become one of the extensively studied areas in the field of pharmacy and medicine as these are biocompatible with cells and tissues, and also their submicron size and the ability of sustained and controlled release made polymeric nanoparticles as promising drug carrier systems. Polymeric nanoparticles are promising vehicles for delivering drugs, proteins, and nucleic acids such as DNA to the target cell, organ, or site of action. The submicron size of the polymeric nanoparticles helps in effective permeation through the cellular membrane and also avoids the clearance by the RES in the bloodstream. There are several synthetic and natural polymers available, and a few are listed in Tables 7.1 and 7.2.

Nanospheres and nanocapsules are the two subtypes of polymeric nanoparticles that are differed by the concept of how they are entrapped in the matrix of the polymer. The drug is entrapped uniformly and physically in nanocapsules, whereas in nanospheres drug is enclosed in a polymeric membrane. There are several advantages with the polymeric nanoparticles in various fields especially pharmaceutical and medicine. By encapsulating volatile pharmaceutical agents in polymeric nanoparticles, their stability can be improved easily at very low cost in huge quantities by various kinds of methods available. In terms of effectiveness and efficiency, polymeric nanoparticles offer a substantial enhancement over conventional formulations. It is possible to improve the drug concentration releasing at the targeted cell, organ, or site of action by fabricating the polymeric nanoparticles. These are one of the ideal drug carrier systems in the treatment of cancers, delivery of contraceptives, vaccines, and antibiotics for the target site, and it is possible because of the flexibility to alter the drug release kinetics of polymer-based nanoformulations by choosing the choice of suitable polymer (Nagavarma et al. 2012).

4 Drug Releasing Mechanism of Nanoparticles

Once the pharmaceutical agent encapsulated in the polymeric nanoparticle reaches the target site, the drug is released from the carrier by various physicochemical mechanisms such as diffusion caused by the hydration of nanoparticle. Alternatively, the drug is released from the carrier by enzymatic reaction where the polymer undergoes cleavage or degradation or rupture because of the enzymes triggering the drug release from the polymer. A detachment of the drug from the polymer matrix followed by the subsequent release is the other possible mechanism (Nagavarma et al. 2012; Karuppusamy and Venkatesan 2017).

Table 7.1 Commonly used polymers for the preparation of nanoparticles

Polymer type	Name of polymer	Abbreviation or commercial name
Synthetic polymers	Polyglycolides	PGA
	Polylactides	PLA
	Poly(lactide co-glycolides)	PLGA
	Polyorthoesters	POE
	Polycaprolactone	PCL
	Polycyanoacrylates	PCA
	Poly(isobutylcyanoacrylate)	PICBA
	Poly(isohexylcyanoacrylate)	PIHCA
	Poly(n-butylcyanoacrylate)	PBCA
	Poly malic acid	PMA
	Poly glutamic acid	PGA
	Poly(methyl methacrylate)	PMMA
	Poly(N-vinyl pyrrolidone)	PVP
	Poly(acrylic acid)	PAA
	Poly(vinyl alcohol)	PVA
	Poly anhydrides	
	Polyacrylamide	PAM
	Poly(ethylene glycol)	PEG
	Poly(methacrylic acid)	PMA
Natural polymers	Chitosan	
	Alginate	
	Gelatin	
	Albumin	

Table 7.2 Polymeric nanoparticles for drug delivery (Nagavarma et al. 2012; Vauthier and Bouchemal 2009; Kumari et al. 2010)

Polymer type	Name of polymer	Abbreviation or commercial name	Applications	Method of preparation
Natural polymers	Chitosan		Cyclosporin A, ammonium Glycyrrhizinate, BSA	Ionic gelation crosslinking
	Gelatin		Paclitaxel, Didanosine, insulin, chloroquine phosphate	Solvent evaporation, double solvent, ionic gelation crosslinking
Synthetic polymers	Polylactides	PLA	Haloperidol, zidovudine, progesterone	Solvent evaporation, solvent evaporation double emulsion
	Poly(lactide co-glycolides)	PLGA	Taxol, paclitaxel, estradiol, docetaxel, dexamethasone	Solvent evaporation, interfacial deposition, nanoprecipitation, emulsion diffusion
	Polycaprolactone	PCL	Tamoxifen, Clonazepam, insulin, docetaxel	Solvent displacement, solvent evaporation, nanoprecipitation

5 Development of Polymeric Nanoparticles

The formulation approach of polymer-based nanoparticle development for bioactive molecules is mainly based on two categories. The first one is physicochemical interactions such as solvent evaporation and phase separations. The second category is based on chemical reactions, such as the polycondensation of synthetic monomers and polymerization. Physicochemical interactions are to be considered during the development of nanoparticles from water-insoluble hydrophilic polymers such as polylactic acids (PLA), polyacrylates, polymethacrylates, and celluloses. The nature of the polymer is one of the important factors to be considered notably while preparing the nanoparticles especially for the oral administration. The particle size of the prepared nanoparticle shows a predominant effect on the uptake of the formulation by the intestinal tract. Controlling the particle size completely is generally difficult as it depends on the physicochemical properties such as thermal property and hardness and also on the preparation method (du Toit et al. 2008).

Researchers developed several in the recent past for polymer-based nanoformulations development. The selection criteria for the development of polymeric nanoparticles are divided into two categories based on the criteria of whether the nanoparticles are being prepared by polymerization or from preformed polymers (Reis et al. 2006).

5.1 Polymerization

Preparations of polymer-based nanoparticles by polymerization of monomers are usually done by two methods, namely, emulsion polymerization and interfacial polymerization. The first method is further divided considering the type of solvent used as the continuous phase whether it is an organic solvent or aqueous solution. Emulsion polymerization is the fastest and simple method that can be readily scalable also (Reis et al. 2006; du Toit et al. 2008; Haque et al. 2018).

5.1.1 Emulsion-Polymerization Technique

The emulsion technique with organic solvent as a continuous phase involves the use of organic solvents for dissolving polymer, drug, and surfactants to prevent the aggregation of polymers. This is one of the initial techniques developed for nanoparticle development, but the usage of toxic solvents, monomers, initiators, and surfactants in the methodology is the major disadvantage associated with the technique. Nanoparticles of poly(butylcyanoacrylate), poly(ethylcyanoacrylate) (PECA), and poly(methylmethacrylate) (PMMA) are some of the polymeric nanoparticles by this technique (Reis et al. 2006; Haque et al. 2018).

The emulsion technique with the aqueous continuous phase does not require any organic solvent with toxic nature, emulsifier, or surfactant during the preparation of nanoparticles. The initiation of the polymerization process occurs by various mechanisms. The initiation of polymerization occurs with the collision of monomer and initiator molecules that include ions or free radicals. High energy radiation such as ultraviolet and γ-radiation are the alternative methods for the initiation of the polymerization. Nanoparticles of PMMA for vaccines are produced by this technique by using radical initiation of the polymerization reaction. Even though the PMMA nanoparticles preparation by this technique is simple with high entrapment efficiency, the PMMA nanoparticles are associated with disadvantages such as the requirement of physical or chemical initiation and also the nanospheres of PMMA are not biodegradable. The polymerization mechanism by an anionic process is used in the preparation of PACA nanoparticles which can avoid employing high energy radiation. Drugs that are hydrophilic and having sparingly water solubility can be loaded into polymeric nanoparticles prepared with PACA (Reis et al. 2006; Haque et al. 2018).

5.1.2 Interfacial Polymerization Technique

The preparation technique starts with solubilizing monomers and drugs in oil and organic solvent mixture and subsequent addition to the aqueous solution. The polymerization process is initiated by the ions present in the aqueous or continuous phase consisting of surfactants that results in the colloidal suspension. Further, the evaporation under vacuum makes the suspension concentrated. The main advantages associated with this method are high entrapment efficiencies and the polymer formed is in situ which follows the boundary of the inner phase of the emulsion. Nanoparticles preparation using polymerization process results in the polymer of slowly biodegradable or nonbiodegradable in nature. Along with the polymer, other residual molecules of monomers, oligomers, surfactants, etc. are also produced in the polymerization medium which is slightly toxic in nature. There is no need for the purification process to be followed in this method. Though potentially toxic compounds are not used in this method, there is a need for washing of solvents, and replacement by water is required which is a difficult and time-consuming procedure (Reis et al. 2006).

5.2 Development of Polymeric Nanoparticles From Preformed Polymers

Nanoparticles prepared from preformed polymers avoid all the limitations of the polymerization process to produce the nanoparticles. The technique involves the use of preformed polymers instead of monomers in polymeric nanoparticle preparation. Several techniques are existing for the preparation of polymer-based nanoformulations of natural and synthetic polymers by using preformed polymers (Reis et al. 2006).

5.2.1 Emulsification and Solvent Evaporation Method

The method includes two major phases, emulsification of polymer dissolved in the organic solvent followed by evaporation to remove the organic solvent which induces the precipitation of polymer to result in nanoparticle formation. The organic phase in which polymer along with drug is solubilized is added dropwise to the continuous phase in the presence of a dispersing agent and homogenization. In the later part of the method, the solvent is removed by subjecting to high temperatures under reduced pressure. The viscosity of aqueous and organic solvents, amount of dispersing agent, and stirring rate are the few parameters by which the particle size can be controlled during the process of nanoparticle development. Oil in water emulsion is of more interest over the other types of emulsions because water is being used as the non-solvent during the preparation, and it also avoids the recycling of organic solvents, facilitating the washing step, which is one of the main advantages of the method. The technique is more appropriate for the preparation of only liposoluble drugs, and for

the homogenization, there is a need for high energy for scale-up of the method, which are the few limitations associated with this technique (Reis et al. 2006; Pal and Saha 2017). The schematic representation of the method is given in Fig. 7.1.

5.2.2 Solvent Displacement Technique

This technique is also called a nanoprecipitation method. The main steps of the method include preformed polymer precipitation from the external organic phase followed by diffusion of the organic solvent into the external phase facilitated by a stabilizer, usually a surfactant. The drug and polymer are dissolved in an organic solvent which is water miscible and having intermediate polarity, constitutes the internal phase. The organic phase is injected into an aqueous phase containing a stabilizer under continuous stirring. The diffusion of the organic solvent into the aqueous phase facilitates the deposition of polymer on the interphase between the external and internal phases leading to the formation of colloidal suspension. As the organic solvent used is miscible with water, it helps in facilitating the colloidal suspension formation during the process of emulsification. The limitation of the method is that only water-miscible solvents, in which the diffusion rate is sufficient to produce spontaneous emulsification, can be used. Additionally, the method is applicable for the preparation of lipophilic drugs because of the organic solvent miscibility with the continuous phase (Reis et al. 2006; Nagavarma et al. 2012; Krishnamoorthy and Mahalingam 2015). The schematic representation of the method is given in Fig. 7.2.

5.2.3 Interfacial Deposition Technique

This technique is mainly used for the preparation, and basically, it is an emulsification and solidification process. The dispersed phase consists of an organic solvent with minor quantities of oil, and the oil is usually miscible with the organic phase but immiscible with a mixture of polymer and organic solvent. The organic phase which consists of polymer and oil is slowly injected into an aqueous continuous phase leading to the deposition of the polymer nanoparticles. The deposition occurs at the interphase between the aqueous phase and finely dispersed oil droplets forming nanocapsules (Reis et al. 2006).

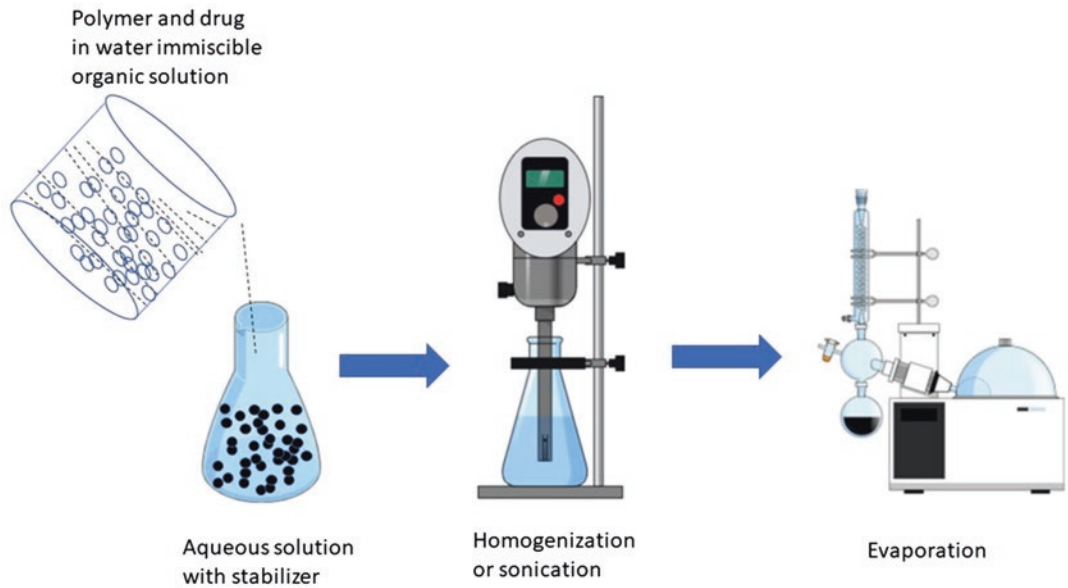

Fig. 7.1 Schematic representation of the emulsification and solvent evaporation method

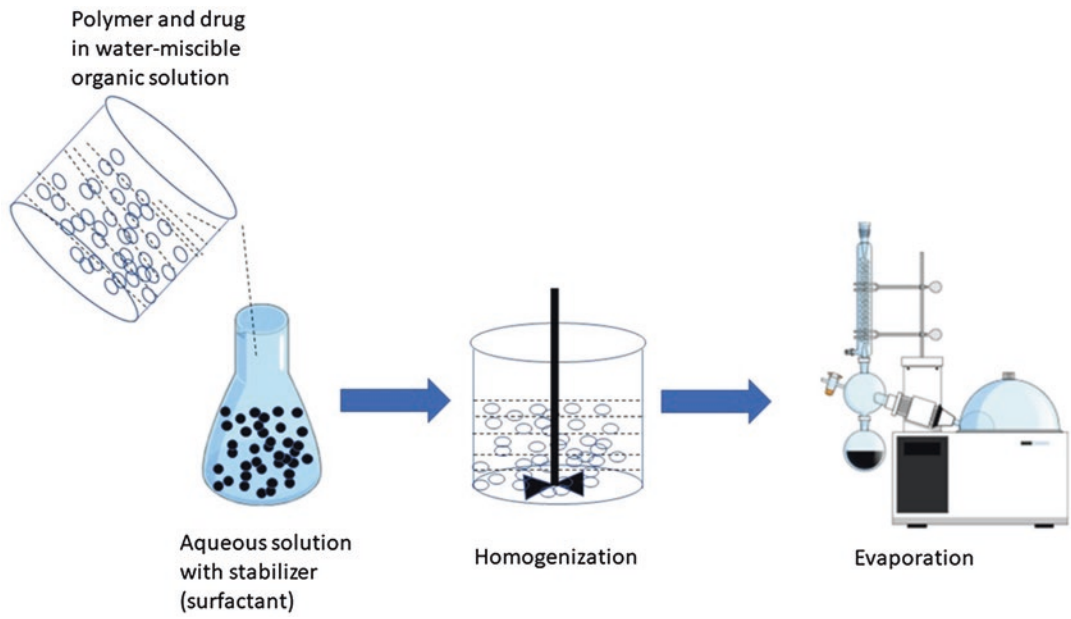

Fig. 7.2 Schematic representation of the solvent displacement method

5.2.4 Emulsification and Solvent Diffusion

This technique is the modified version of the emulsification and solvent evaporation method. The method involves two major steps; in the first step, the encapsulating polymer is dissolved in an organic solvent which is partially water miscible and further saturated with the water for the thermodynamic equilibrium of two liquids. The next step involves the solvent diffusion of the solvent of the organic phase by diluting with water in excess quantities resulting in the precipitation of the polymer to produce nanoparticles. Further, the preparation is subjected to evaporation to remove the solvent. The same method was adopted to develop the salting-out technique for the preparation of nanoparticles. The main advantages of the method include high encapsulation efficiencies, high reproducibility between the batches, and ease of scale-up, and there is no requirement of homogenization during the process. Elimination of large volumes of water and leakage of the drug from the polymer into the continuous phase in the case of water-soluble drugs during the emulsification leading to the lower encapsulation efficiencies are the major limitations associated with the technique (Reis et al. 2006; Nagavarma et al. 2012).

5.2.5 Salting-Out Method

Before 1990 pseudo-latexes, water-insoluble polymeric dispersions in the liquid phase were used to prepare by a method which involves water-immiscible organic solvent. The main principle of the method is the conversion of water-insoluble polymer into an aqueous dispersion. In this process, the first step is to dissolve polymer into an organic solvent which is miscible with water followed by its emulsification into the continuous phase with surfactants of ionic or nonionic in nature. The further emulsion is subjected to homogenization and evaporation to eliminate the solvent. The limitations of the method are: only water-immiscible organic solvents which have to be used for polymer dissolution, the shelf life of the preparation over the period of time, and formation of irreversible hydrolysis or flocculation. High concentration of surfactants used in the preparation which is not suitable for pharmaceutical dosage forms is another drawback of the technique (Bindschaedler et al. 1990).

Bindschaedler et al. patented a procedure called "salting-out" in 1990 for the preparation of a water-insoluble polymer powder which can be re-dispersed easily in the liquid phase. Microparticles of water-insoluble polymer powders in the liquid dispersion state can be prepared by this method by avoiding all the limitations associated with the previous method. An organic solvent that is miscible with water also can be used and is the main advantage of this procedure (Bindschaedler et al. 1990).

The salting-out technique starts with the preparation of oil in water emulsion. The oil phase consists of a water-insoluble polymer, and an active ingredient dissolved in a water-miscible organic solvent. The aqueous phase is a solution or a gel containing a high concentration of salting-out agent and colloidal stabilizer generally a surfactant of ionic or nonionic in nature. The next step is emulsifying the organic phase into the continuous phase usually by mechanical stirring. During this process of mixing, the high concentration of the salt obstructs the solvent diffusion. Once the emulsion is prepared by mechanical mixing of two phases, it is diluted with sufficient water to decrease the concentration of the salting-out agent. It allows diffusion of the organic solvent rapidly into the aqueous phase leading to the formation of the suspension of nanoparticles. The solvent is removed from the suspension by distillation under reduced pressure. Further, the salting-out agent and stabilizer are removed by repeated washings after the ultracentrifugation, and a cross-flow filtration is also effective (Mendoza-Muñoz et al. 2012; Krishnamoorthy and Mahalingam 2015; Karuppusamy and Venkatesan 2017). The schematic representation of the method is given in Fig. 7.3.

Effect of Various Parameters on Salting-Out Technique

The solvents in which polymers dissolved, even though they are miscible with pure water in all proportions when mixed with aqueous solutions of highly concentrated salt or substances and not subject to electrolytic dissociation may lead to the formation of binary phase liquid system. The selection of the combination of polymer and solvent is very crucial as all the combinations leading to precipitation of the polymer in solid form may not be suitable. The common solvents used in this technique are methanol, ethanol, acetone, and acetonitrile. Different polymers are being used by the researchers for the development of polymeric nanoparticles by the salting-out technique. The type and concentration of polymer have a predominant effect on the morphological characteristics of the developed formulation. The most commonly used polymers are poly(lactic acid) (PLA), poly(methacrylates), poly(lactic-co-glycolic acid) (PLGA), cellulose acetate phthalate (CAP), poly(glycolic acid), and poly(caprolactone) (PCL).

The selection of a salting-out agent is a very crucial step in the polymeric nanoparticle development by this method because it has a major role in building the encapsulation efficiency of the formulation. Mineral salts such as aluminum, magnesium, and sodium chlorides, non-electrolytes like sucrose, or a metal sulfate, sulfite, carbonate, nitrate, or phosphate are some of the commonly preferred salting-out agents. Colloidal stabilizers induce the polymer chain conformation in the external phase by anchoring at the interface to form a thick film. It reduces the interfacial tension leading to decreasing the size of the particle. Substances with surfactant properties and the ability to increase the viscosity can be used as colloidal stabilizers**.** For example, poloxamer 127, poloxamer 188, polysorbate 80, and poly(vinyl alcohol) (PVAL) are some of the colloidal stabilizers being used. Various experimental parameters such as stirring rate during the mechanical mixing, a ratio of internal to external phase, the concentration of the polymer, salting-out agent, and colloidal stabilizer can be varied as per the requirement. The selection criteria depend on the type of formulation and the desired output parameters. The concentration of the colloidal stabilizer used for the preparation of nanoparticles and the residual amount after washing steps show an effect on the mean particle size. Konan-Kouakou et al. stated that during the development of nanoparticle development, reducing the concentration of PVAL in the internal phase results

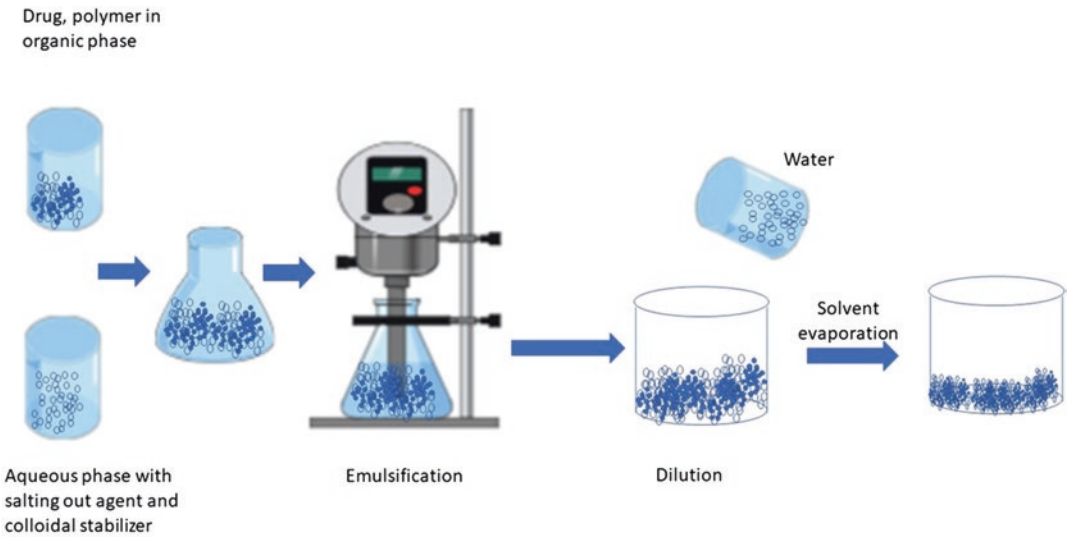

Fig. 7.3 Schematic representation of the salting-out method

in the formation of larger particles. However, the nanoparticle-specific surface area increases linearly with an increase in the residual polymer after the washing steps of the nanoparticles (Bindschaedler et al. 1990; Konan-Kouakou et al. 2005; Mendoza-Muñoz et al. 2012; Bhokare et al. 2015).

Advantages of the Salting-Out Method

- Elevated amounts of polymers can be incorporated in contrast to other methods of preparation where stable dispersions with high polymeric content are difficult to achieve.
- When lipophilic drugs are used, a higher amount of drug loading is possible with improved entrapment efficiency.
- Highly stable polymeric dispersions with high concentrations can be prepared.
- As the salting-out procedure does not require employing temperature, it is helpful in the preparation of heat-sensitive substances.
- Size of the nanoparticle can be controlled.
- It is feasible to scale up the method for the commercial scale.

Disadvantages of the Salting-Out Method

- The method is exclusive for preparation of lipophilic compound-loaded nanoparticles.
- The method is not recommended for hydrophilic compounds as they diffuse into the non-solvent during the process resulting in lower encapsulation (Mendoza-Muñoz et al. 2012; Bhokare et al. 2015).

Scale-Up of the Salting-Out Method

Scale-up is the large-scale manufacturing of a product that comprises the integration of the procedures along with the technology transfer from the small scale. The scale-up procedure is very critical as many times the parameters that are not significant on the lab-scale may become crucial and may lead to the failure of the procedure. Nanoparticle is one of the most promising colloidal drug carrier systems, but lack of information on scale-up technology is hindering the entry into the market. Galindo-Rodríguez et al. scaled up the salting-out method for the development of ibuprofen-loaded nanoparticles. It was a successful attempt to achieve scale-up of 20-fold increase of the lab-scale batches. It is required to maintain the geometric similarities as much as possible to reproduce the quality of the nanoparticles produced by the lab-scale production. The pattern of lab-scale and pilot-scale with respect to the size and distribution was similar which represents the success of the scale-up of the method. The quality of the nanoparticles produced not only depends on the type of materials used but also significantly is affected by the various process parameters applied during the process (Galindo-Rodríguez et al. 2005a, b).

Effect of Process Parameters on the Quality of the Nanoformulation During the Scale-Up of Method

The major issue in the scaling up of the method is mimicking the hydrodynamic conditions of the lab-scale to the large-scale production. For nanoformulations, size is the parameter, especially in the targeted drug delivery approach. The submicron-sized nanoparticles generally have more intracellular uptake than the larger nanoparticles. Small-sized nanoparticles can easily internalize the tumor cells and allow the drug release rapidly into the interior of the cells which leads to the increase in the concentration of the drug at the target site. Particle size of the nano formulation has a huge impact on the drug release profile. As size of the nanoparticles decreases, total fraction of the formulation that is exposed to the medium increases resulting in higher drug release. The particle size of the nanoformulations is predominantly influenced by the characteristics of the precursor emulsion. Processing parameters and physicochemical properties of the organic and aqueous phase show an impact on the diameter of the final droplet of the formulation. The average diameter of nanoparticle decreases predominantly when the stirring rate is increased in lab-scale as well as in pilot-scale production. The homogeneity in the size of the nanoparticles can be achieved at higher stirring rates. The process of coalescence and breakup is simultaneous and their relative kinetics regulate the final size of the droplets. When stirring speed is increased, the breakage forces also increase resulting in finer emulsion droplets formation, thus forming nanoparticles with smaller particle sizes. The homogeneity in the size of the nanoparticles can be achieved at higher stirring rates, and the lower stirring rate results in heterogeneous distribution with larger particles. Lower stirring rates not only results in heterogeneous distribution with larger particles but also affects the reproducibility leading to batch-to-batch variations. In these situations, the lower energy given by the stirrer and the higher viscosity of the dispersion medium because of the colloidal stabilizer and salting-out agent lead to a decline in the efficiency of the breakup process and increase in the coalescence of the droplet, finally leading to the formation of larger particles. Van de Ven et al. analyzed the effect of the organic phase composition on the mean size of the particles. There is an increase in the proportion of DCM in the organic phase where acetone and DMSO are the co-solvents, and the particle size of the PLGA nanoparticles increases gradually. As the water miscibility of the organic phase increases, the average size of the nanoparticles may be lowered significantly. This is because of the lower interface between the organic and continuous phase leading to the droplets with smaller size (Galindo-Rodríguez et al. 2005a, b; Konan-Kouakou et al. 2005; Van de Ven et al. 2012).

The Theoretical Model for the Preparation of Nanoparticles by the Salting-Out Method

Galindo-Rodríguez et al. reported a typical theoretical model of liquid-liquid dispersion systems. This theory was derived from the field of chemical engineering where the theory was originally developed for modeling of emulsion in the micrometric size range. The relationship between the stable drop size and the various parameters is

$$d_{\max} \propto N^{\frac{-6}{5}} \times D^{\frac{-4}{5}} \times \sigma^{\frac{3}{5}} \times \rho_c^{\frac{-3}{5}}$$

where $d_{\max}$ is the maximum stable drop size in meters, D is the diameter stirrer in meters, N is the stirring rate per second, σ is the interfacial tension in Newton meter, and ρ_c is the density of continuous phase in kg/m^3.

The mean diameter of surface-volume value can be used instead of the size of the maximum stable droplet as it is not possible to measure $d_{\max}$. In the same way, the mean diameter can also be substituted if the surface-volume diameter is not available (Galindo-Rodríguez et al. 2005a, b).

Relation of the Rate of Stirring to the Nanoparticle Size

The relation of the mean size of a droplet with the stirring rate can be expressed as follows:

$$d_{\text{mean drop}} = K_1 \left(\frac{\rho_c}{\sigma} \right)^{-0.6} \times D^{-0.8} \times N^{-1.2}$$

where K_1 is the constant.

Further, the emulsions prepared in the same scale D, ρ_c, and σ will be constant, and the logarithmic form of the equation is as follows:

$$\log d_{\text{mean drop}} = \log K_2 - 1.2 \log N$$

where K_2 is a constant.

Since the nanoemulsions are formed during the preparation of nanoparticle, it is not feasible to measure the distribution of the size of the droplets. Assuming each droplet of the emulsion resulting in the formation of a nanoparticle and both are non-porous, the equation can be presented as follows (Galindo-Rodríguez et al. 2005a, b).

$$d_{\text{mean nanoparticle}} \propto d_{\text{mean drop}} \propto N^{-1.2}$$

Model for Drug Transport From the Salted-Out Scaffold

Understanding the principle mechanism by which drugs are released is very significant, and even though the expected efficacy of the developed formulation depends on the physicochemical characteristics of the polymer, the mathematical modeling also plays an important role in this aspect. The two main mechanisms involved during the transportation of drugs are either through fluid-filled pore along with swelling or by polymer erosion. Stress gradient, concentration gradient, and osmotic forces are the typical phenomena that drive the transportation of bioactive molecules from the system. Generation of aqueous pores and subsequent erosion of polymer by which diffusion of drug molecules takes pace causing the drug release is the mechanism generally associated with PLGA-based drug carrier systems. The alternative possibility is by leaching of the drug near to the matrix surface. Partial covalent bonding due to the crosslinking of the polymer in the salting-out method enhances the viscosity of the resulting structure of the system. Ionic strength and the concentration of the electrolytes has a significant effect on the polymer configuration and stability. It is also evident from many studies that the electrolytes may cause retardation of the polymer unraveling and further reduction in the rate of erosion of the polymer. Even though the density of crosslinks is maintained constant with time, the distribution of crosslinks varies according to the time because of the Brownian motion. The rate of erosion of each polymer network may be different than the adjacent network as it depends on the polymer junction fragility.

Mathematical models are outstanding tools for predicting the phenomena that control the drug release rate kinetics of complex polymeric drug carrier systems. Considering the physicochemical diversity of polymers, many researchers developed numerous mathematical models for the release kinetics of drug carrier systems. The kinetic mechanisms involved in the drug release, such as relaxation, erosion, swelling, and diffusion of polymer, can be determined by a suitable mathematical model. These models help to assess the parameters such as interaction parameters, transport phenomena, and kinetic events which control the drug transport from carrier systems. Synchronized operation of all the processes offers a balance between phenomena such as swelling, relaxation, erosion, and diffusion of polymer and drug release that would result in active ideal drug carrier systems. Sibambo et al. reported the optimization of drug-loaded salted-out polymeric scaffold developed by the salting-out method and its evaluation of drug release by applying a kinetic model to interpret the interaction of parameters, events of kinetics, and phenomena involved in drug transport (Sibambo et al. 2009).

Salting-Out Method and Transition of Polymer Properties

Crosslinking and salting-out agents have main implications on the physicochemical and physicomechanical characteristics of polymers that influence the kinetics of the drug release and other mechanisms such as erosion, diffusion, and relaxation. Understanding and elucidation of the mechanism behind this phenomenon are very important to correlate the relationship between the physicochemical and physicomechanical characteristics of polymer and release kinetics of the drug delivery systems. The fluctuation in free energy to the salting-out agent and complex ionic

interactions can be used to modify the 3D network of the polymer by salting out, which alters the morphology, glass-transition temperatures, resilience, and bond vibrations. Altering the configuration and the environment of the matrix by electrolytic inclusions controls the physical rigidity and swelling kinetics. Salting out decreases the hydrogen bonding of the polymeric chain with water molecules leading to the stabilization of water structures of aqueous polymeric solutions. The chemical bonding between the salts and monomers renders the polymeric chains stiff, which further transforms the polymer properties resulting in the dimensionally stable polymers which offer greater integrity in structure making them appropriate for the continued release of drugs. Though the degree of crosslinking controls the polymeric strength, the chemical composition independently controls the degradation rate. Change in the physiochemical properties significantly alters the drug release kinetics. During the drug release from monolithic matrices, the swelling and true dissolution which are the two distinct processes of the polymers could be observed. Swelling systems swell immediately when it comes into contact with dissolution media, and thus hydration rate of the system controls the drug release rate. To avoid the burst release in the initial phase, the polymer used in the preparation of nanoparticles must form a shielding layer of gel before dissolution (Sibambo et al. 2009).

Applications of the Salting-Out Method

Biodegradable nanoparticles are being prepared by the researchers to enhance the therapeutic values of several hydrophilic or hydrophobic drugs by enhancing the solubility, bioavailability, and circulation time. Moreover, these biodegradable nanoparticles reduce the cost of the treatment and also the risk associated with toxicity. Encapsulation of drugs into the biodegradable nanoparticles increases drug specificity, efficacy, tolerability, and therapeutic index of the corresponding drugs. The several advantages associated with nanomedicine include the protection of the drug against premature degradation, enhancement in the absorption of the drug into selected tissues, and interaction with the biological environment thus improving the intracellular penetration. Moreover, the drug-loaded nanoformulations are considered to be more effective than the traditional formulations in terms of targeted drug delivery, controlled release, and therapeutic efficacy. Researchers successfully developed nanomedicines for several drugs related to various dreadful diseases like malaria, cancer, diabetes, HIV-AIDS, tuberculosis, and prion disease. For any kind, polymeric nanodrug delivery system selection of the polymer is a very critical step, and selection criteria generally depend on the characteristics of the polymer-like maximum encapsulation, bioavailability, and retention time. Even though the selection of a type of nanoformulation for a particular drug is a trial-and-error method without any specific rule of thumb, in general, polymeric nanoparticles are preferred than the others. The applications of the salting-out method are given in Table 7.3 (Kumari et al. 2010).

Preparation of PLGA- and PLA-Based Nanoformulations

PLGA (poly-d,l-lactide-co-glycolide) and poly(D, L-lactic acid) (PLA) are the most widely used polymers in the development of nanoparticles in the field of drug delivery system. Hydrolysis of PLGA in body results in the formation of monomers called glycolic acid and lactic acid. Since these monomers are biodegradable in nature, hence PLGA associated toxicity chances are minimal. Poly(D,L-lactic acid) (PLA) is a biocompatible and biodegradable polyester that forms lactic acid monomeric units in the body. Researchers have been using PLA and PLGA for the development of peptide- and protein-based nanoformulations, nano-vaccines, nano-antigen, gene delivery systems with nanoformulations, etc. A variety of micro and nanoparticles can be prepared using different molecular weights of PLA and PLGA polymer with a very low cost and high reproducibility. Most of the nanoparticles prepared by using PLA and PLGA polymers were mainly focused on the development of drug carrier systems for targeting tumors. Apart from the nanoformulation preparations, PLGA has

Table 7.3 Applications of ionic gelation crosslinking method

Type of formulation	Drug name	Organic solvent used	Polymer	Colloidal stabilizer	Salting-out agent	Particle size achieved	References
Nanoparticles	Verteporfin	Tetrahydrofuran	PLGA	PVA	$MgCl_2$ $6H_2O$	167 nm	Konan-Kouakou et al. (2005)
Antibody labeled nanoparticles			PLA		$MgCl_2$ $6H_2O$	170 nm	Cirstoiu-Hapca et al. (2007)
Nanosystem	Isoniazid	Acetone	MAEA	Na CMC	$ZnSO4.7H_2O$	77–414 nm	du Toit et al. (2008)
PLGA scaffolds		Acetone	PLGA	Na_2HPO_4, KH_2PO_4	NaCl, $CaCl_2$, $AlCl_3$	30–100 nm	Sibambo et al. (2008)
Nanoparticles	Plasmid DNA	DCM and acetone	PLGA	PVA	$MgCl_2$ $6H_2O$	240 nm	Fay et al. (2010)
Nanoparticles	Saponin β-aescin	DCM and DMSO	PLGA	PVA	$MgCl_2$ $6H_2O$	272–526 nm	Van de Ven et al. (2012)
HSA nanoparticles	Cabazitaxel	Ethyl alcohol	HSA		Disodium hydrogen phosphate	110–140 nm	Qu et al. (2016)

been successfully used by the scientists in the preparation of surgical sutures, tissue repairing scaffold, and bone plate screws also. The superior hydrophilicity and strong physical strength of PLGA make it a very good controllable drug delivery system for medical applications. Various methods are available for the preparation of polymer-based nanoparticles such as salting out, emulsification-diffusion, solvent emulsion-evaporation, and interfacial deposition. Salting out is a very good substitute method for the most commonly used techniques based on emulsions (Kumari et al. 2010; Lee et al. 2016; Tsai et al. 2018).

The preparation of polymer-based nanoparticles by salting-out method involves two major steps. In first step, polymer (PLGA or PLGA-PEG) and drug are dissolved in an organic solvent such as acetone. The second step involves the subsequent emulsification of the polymer into an aqueous gel containing the salting-out agent using a colloidal stabilizer such as polyvinyl pyrrolidone. The resulting o/w emulsion is diluted with an aqueous solution or water to enhance the diffusion of the organic solvent into the aqueous phase which induces the formation of nanoparticles (Muthu 2009).

Preparation of Polymeric Nanoparticles for Gene Therapy by the Salting-Out Method

Gene therapy for many diseases has shown great potential. Successful gene delivery to the nucleus or cytoplasm and subsequent replacement or regulation of the defective genes result in the effective gene therapy. While delivering a gene to the targeted site of action, several barriers such as cell membrane or endosomal membrane may reduce its efficiency. There is a need for an efficient carrier for delivering a gene to a particular site of action. The cost of the preparation of nanoparticle for gene therapy is one of the reasons behind the hindered applications of gene therapy. The salting-out method is one of the solutions for the preparation of an efficient and cost-effective method for the development of nanoparticles in targeted gene therapy. Song et al. explored the salting-out method for the development of nanoparticles for breast cancer cells. An attempt was made to prepare silk-PEI nanoparticles and magnetic-silk/PEI core-shell nanoparticles for targeted delivery of c-myc antisense oligodeoxynucleotides into MDA-MB-231 breast cancer cells (Song et al. 2019).

Nucleic acids as the therapeutic application for many diseases has been studied extensively in the recent past. The effective delivery of the therapeutic DNA to the targeted site is the current

major limitation in the field of drug delivery. François Fay et al. hypothesized that a combination of emulsion evaporation and salting-out methodology would prepare plasmid DNA-loaded nanoparticles with a minimal application of the sonication. As an encapsulation of plasmid DNA into the polymer is one of the limiting factors in the preparation of circular double-stranded DNA-loaded nanoparticles, sonication of the formulation plays a critical role in the drug loading capacities. Subjecting nanoparticles to sonication for longer times during the preparation steps can cause shear stress leading to the degradation of the DNA and ultimately lower entrapment of the active moiety. A higher level of entrapment of the DNA into the nanoparticles is very important as the dissociation of the surface-adsorbed DNA from the nanoparticles increases rapidly in the acidified environment. Increased entrapment not only avoids nanoparticles from the surface-adsorbed drug leakage but also helps in increased stability and half-life. The cellular internalization efficiencies are significantly influenced by the diameter of the nanoparticles as the particles with different size is taken up at different rates and mechanisms. In general, longer sonication times are required to prepare nanoparticles by most of the methods to get smaller diameters. It was demonstrated that just with 15 s of continuous sonication results in the formation of nanoparticle having a mean diameter nearly 200 nm by using the combined method of emulsion evaporation and salting-out technique (Fay et al. 2010).

Interactions Between Crosslinking Ions and Polymeric Chains

The preparation of nanoparticles using different salts results in producing the nanoparticles with different physicochemical, physicomechanical, and morphological structures. The shape and stereo orientation also depend on the type of salt used along with the polymer in the preparation. Further, the rate of polymer-salt interaction decides the ability of the system to imbibe the water molecule into the matrix, whereas coordination number, atomic size, and reactivity of ions, polymeric substrate, and lattice arrangement nature are the other significant factors to be noted during the process and the following crosslinking.

The salt-polymer ionic interactions depend on ionization energies of crosslinking ions, the thermodynamic stability of water, salts at the polymeric strands of lactide-glycolide, and hydration enthalpy in solution. The intra-ionic and inter-ionic forces and hydrogen bonding in the polymer which is packed with water molecule decide the size of pores and nature of the prepared nanoparticles. Polymeric structures adopt a fixed three-dimensional conformation into chains of crosslinked lattice-glucolide facilitated by the introduction of ions of salting-out agents. Further, the voids formed because of the interconnection of fibers accommodates the water molecules according to the void size due to interactions between polymer chains. The strength and kind of salting-out agents show a significant impact on the transformation of native polymer into a strong structure by the quick process of salting-out and successive crosslinking to attain elasticity. Sibambo et al. reported that PLGA polymeric scaffolds is prepared by a salting-out method using NaCl and $AlCl_3$ as crosslinking agents. The scaffolds prepared with sodium chloride were superior to that of calcium chloride. The physicochemical properties of the salting agent used during the process create an environment that attenuates the viscoelastic nature of the scaffolds. The viscoelastic nature causes densification of the polymeric scaffolds resulting in the scaffold that resists distorting under the extreme stress conditions. The molecular structure of the salt and the chemical backbone of the polymer influences the polymer-salt interactions which control the degree and extent of the bond vibrations at fingerprint regions of the system. As a result, spatial configurations from these interactions lead to the scaffold formation with different morphologies, physicomechanical, and physicochemical properties (Sibambo et al. 2008).

Combination of the Salting-Out Method with Other Methods

Emulsion Solvent Evaporation-Salting-Out Technique

Van de Ven et al. prepared saponin β-aescin-loaded PLGA nanoparticles by employing a combination of emulsion solvent evaporation and the salting-out technique. The first method is suitable for hydrophilic drugs, whereas the latter one is suitable for exclusively lipophilic drugs. Preparation of nanoparticles loaded with water-soluble and amphiphilic drugs is challenging as they end up in low entrapment efficiencies because of the surface-active properties, which leads to settling of the molecules in the emulsion interface. Preparation of nanoparticles proceeds with dissolving polymer and drug in the ratio of 5:1 in an organic solvent. The organic phase consists of various percentages of DCM, DMSO, acetone, and methanol. The organic phase is added to the aqueous phase consisting of a colloidal stabilizer and as the salting-out agent. The prepared emulsion was diluted with a PVA solution for inducing the diffusion of the water-miscible organic solvent leading to the formation of the nanoparticles. A rapid particle formation approach was followed where the partial precipitation of PLGA into nanoparticle formation completed within 30 min. The rapid precipitation approach helps in avoiding the drug leakage of the drug into the continuous phase from the polymer by reducing the solidification time of the emulsion droplet. The preparation was agitated at room temperature to evaporate the DCM used in the organic phase. The obtained nanoparticles were purified by cross-flow filtration to remove unentrapped β-aescin, excess salting-out agent and colloidal stabilizer. The addition of DCM to the organic phase consisting of PLGA and β-aescin helped in reducing the polydispersity index of the formulation. A higher proportion of DMSO increases the size, and this is because the viscosity of the DMSO is more in comparison with acetone and DCM (Van de Ven et al. 2012).

Fay et al. reported the preparation of nanoparticles for the intracellular delivery of plasmid DNA. The researchers combined emulsion evaporation and salting-out agent techniques for the preparation of nanoparticles that entrapped plasmid DNA in PLGA by using DCM and acetone as the dispersed phase. The ice-cold DNA plasmid and the polymer are dissolved in the ice-cold organic solvent and mixed with the aqueous phase consisting of PVA as the colloidal stabilizer and $MgCl_26H_2O$ as the salting-out agent. The addition of the PVA solution initiates the diffusion of the organic solvent and subsequent stirring leads to the formation of nanoparticles (Fay et al. 2010). Donnelly et al. developed Nile red-loaded PLGA nanoparticles by emulsion and salting-out method of preparation using a combination of acetone and DCM as the organic solvent. The Nile red and polymer in an organic solvent are added to an ice-cold solution having PVA as the stabilizer and $MgC_{l2}{\cdot}6H_2O$ as the salting-out agent and subsequent sonication in an ice bath followed by the addition of diluted colloidal stabilizer solution. Further, the stirring of samples to remove the solvent results in the formation of nanoparticles with uniformity in size (Donnelly et al. 2010).

Emulsion-Based and Aqueous-Based Salting-Out Method

In one of the studies, du Toit et al. developed isoniazid nanoparticles, a nano-enabled drug delivery system for controlled drug release at a specific site (pulmonary) with aqueous-based and emulsion-based salting-out approach. Methacrylic acid-ethyl acrylate copolymer (MAEA) has been used as a polymer and zinc sulfate as the salting-out agent in both the methods. For the emulsion-based salting-out approach, drug and polymer are dissolved in an organic solvent such as acetone. Sodium carboxymethylcellulose, a viscosity-enhancing agent, is included to improve the drug release. In aqueous-based salting-out approach, MAEA is redispersed to a latex comprising an aqueous dispersion of MAEA. The solution can be neutralized by adding sodium hydroxide. The procedure follows the pumping of the drug-loaded latex through an atomizer where compressed air is injected to disperse the latex solution to a container consisting of salting-out agents which induce the formation

of aerosolized droplets of drug-loaded nanoparticles. Further, the incubation of this solution allows the formation of discrete and compact nanoparticles. Even though the physicochemical characteristics of nanoparticles prepared by both the methods are the same, the average size of the nanoparticles prepared by emulsion-based approach was lesser than the other method. The polymer concentration has a predominant effect on the particle size of the nanoparticles. A reduction in the concentration of polymer reduces the particle size of the nanoparticles. The nanoparticles prepared by both the methods are showing a slight difference in the drug release profile in vitro, where the initial burst release is slightly more in the nanoparticles of aqueous-based salting-out approach. The formation of crystals and the reaction of salting-out agents with the architecture of the nanoparticles will have an impact on the drug-release profile of the formulation. Also, the polymer-to-drug ratio shows a considerable effect on the yield of the nanoparticles (du Toit et al. 2008).

Water-soluble drugs are prepared by the aqueous-based salting-out method; the drug incorporation efficiencies decrease because of the rapid partitioning of hydrophilic drugs into the aqueous phase leading to lower entrapment of the drug. Apart from the drug nature, the surface area of the nanoparticles also contributes to the loss of the drug during the preparation. The drug release from the nanoparticles is also affected by processing temperature. When higher temperatures are applied during the fabrication of nanoparticles, slower drug release is observed. During the preparation of nanoparticles, the higher temperatures promote the rapid elimination of the solvent leading to the formation of compact polymeric matrices that efficiently entrap the drug within interconnected structures resulting in the controlled release of the drug. The acidic condition of the salting-out agent shows a negative effect on the drug release. The incorporation of the drug into the nanoparticles reduces because of the rapid coalescence of the polymer in the acidic solution resulting in a higher degree of surface deposition of the drug (du Toit et al. 2008).

5.2.6 Supercritical Fluid Technology

A vast number of methods are being developed by the researchers for the development of nanoparticles, but many of them are not environmentally friendly because of the various reasons such as using organic solvents during the process**.** The need for the development of environment-friendly methods motivated researchers towards employing supercritical fluids technology in the production of nanoparticles. Supercritical or compressed fluid-based methods are interesting tools for the preparation of nanoparticles and microparticulate systems. The procedure includes the solubilization of active ingredient and polymer in a supercritical fluid and its subsequent spraying through a nozzle. During the process of spraying, the supercritical fluid is eliminated resulting in the precipitation of the nanoparticles. As the precipitated nanoparticles are free from the solvent producing a high-quality product, the technique is considered as very clean and very much suitable for biopharmaceutical products. Though this technique has several advantages, there are a few disadvantages, such as the process requires high-pressure equipment for producing elevated pressure during the process and compressed supercritical fluids require elaborate recycling measures to lower the energy costs. Moreover, it needs high initial capital investment for the equipment setup, and also it is tough to solubilize polar compounds in supercritical fluids such as CO_2. However, employing cosolvents or surfactants helps to solubilize the polar compounds. Production of polymeric nanoparticles by supercritical fluid technology has been divided into two types, the rapid expansion of supercritical solution and rapid expansion of supercritical solution into a liquid solvent (Reis et al. 2006; Nagavarma et al. 2012; Krishnamoorthy and Mahalingam 2015).

5.2.7 Rapid Expansion of Supercritical Solution (RESS)

The main principle involved in the method is subjecting the polymeric solution to the rapid expansion through a nozzle into the ambient air. The rapid reduction in the pressure along with the higher degree of supersaturation results in nucle-

ation leading to the formation of finely dispersed nanoparticles. The instrumentation setup comprises three main components, a stainless steel mixing chamber with a high-pressure pump, a pre-expansion tube, and a syringe pump. A polymer solution is prepared in a supercritical fluid such as CO_2 at ambient temperature which is driven into the pre-expansion unit where pre-expansion takes place by applying temperature. Followed by this, the solution is released into the atmosphere through the nozzle for the expansion. The particle size and morphology of the nanoparticles are greatly affected by the concentration and degree of saturation of the polymer. As this method is not dealing with any solvents, it is environmentally friendly, and there is no requirement of washing cycles to be performed for the purification of the product, in fact the outcome product will be in its high purity form. The main drawback of the method is the size of the nanoparticles produced that are of microscale rather than nanoscale (Nagavarma et al. 2012).

5.2.8 Rapid Expansion of Supercritical Solution into a Liquid Solvent

This is the slightly modified method of the RESS technique. The method was developed to overcome the major limitations of the RESS method which is the size of the produced nanoparticles. Unlike in the RESS technique, this method involves the expansion of polymeric solution into a solvent unlike the previous method where it is into an ambient atmosphere, and this method is termed as RESOLV. The introduction of the solvent in this method reduces the particle growth during the expansion phase which results in the nanosized particles (Nagavarma et al. 2012).

5.2.9 Electrospraying Technology

Several methods are being used by the researchers for the preparation of nanoparticles, such as spray-drying, microwave heating, microemulsion, and hot-melt extrusion, but these methods are associated with some disadvantages, such as the application of heat during the preparation. Conventional methods such as the wet encapsulation method, which involves multiple steps during the process, compromise the stability and leaching of the drug. Therefore, a technology involving without any application of heat during the process, involving in a lesser number of steps, is found to be in a boom in the field of formulation development. One such approach of nanoparticle development is using electrospraying technology. Electrospraying is being used widely for the encapsulation of not only drug molecules but also various bioactive molecules include quercetin, vitamin E, epigallocatechin, curcumin, and others. The method involves the hydrodynamic atomization of drug solution with or without having polymer in it. The solution is pumped with a metallic needle with the help of a syringe pump at a particular flow rate in the presence of a high voltage electric charge. Because of the electric interactions due to the application of high voltage, the solution gets charged and atomization takes place. The droplets formed are distorted into a Taylor cone, and the solution breaks into a spray of fine droplets. The droplets with a larger surface area are formed because of the atomization of solution, which helps in the evaporation of the solvent, which results in the formation of solid nanoparticles. As this method is rapid and does not involve in the application of any heat during the process, this method is helpful in the development of nanoparticles of thermolabile compounds, and also the procedure involves only one step in the stability and leaching of the molecules during the process which can be avoided. Even though this technique is advantageous in many aspects, low productivity or yield is one of the major obstacles in the commercialization of the technique. Inclusion of multi-nozzle spraying, pressure-assisted spraying, and the rotating spinneret are the few approaches being made by researchers recently to overcome some of the limitations associated with the technology (Rahmani et al. 2015; Yaghoobi et al. 2017; Darade et al. 2018; Giménez et al. 2019; Jayan et al. 2019; Tapia-Hernández et al. 2019).

5.2.10 Ionic Gelation Method

The development of hydrophilic nanoparticles as the drug carriers has involved with a lot of chal-

lenges. The major drawback in the preparation of these nanoparticles is the requirement of organic solvent along with homogenization or sonication. Calvo et al. had reported a method called ionic gelation, a technique used for the preparation of biodegradable nanoparticles and microparticles made of hydrophilic polymers exclusively. The method was developed with the intention of creating a new type of hydrophilic nanoparticles of proteins. Ionic gelation is one of the simplest ways to develop nanoscale delivery systems. It offers a simple and mild preparation method in the aqueous solution. The method is based on the electrostatic interaction between the cations of the polymer with the negatively charged group of polyanionic crosslinking agents, and the process requires the involvement of acidic and alkaline environment. The method starts with the preparation of cationic polymer in the acidified aqueous solution in the presence or absence of a stabilizer, followed by the addition of polyanionic crosslinking agents in the alkaline phase into the acidified aqueous cationic polymer solution. Ionic gelation occurs between a polyanionic crosslinking agent and cationic polymer solution by electrostatic forces and precipitates to form nanoparticles. The ionic gelation method is simple and it does not lead to any structural modifications of the drug. The method is used in the preparation of several kinds of nanoformulations such as chitosan and alginate-based nanoparticles including nanogels, hydrogels, and film-based nanoformulations (Calvo et al. 1997; Sailaja et al. 2011; Wang et al. 2018; Taghizadeh et al. 2019). The schematic representation of the method is given in Fig. 7.4. The applications of ionic gelation crosslinking gelation method are given in Table 7.4.

Chitosan-Based Nanoformulations

Chitosan is a biocompatible, biodegradable, mucoadhesive, and nontoxic polymer consisting of β-1 → 4 linked 2-amino-2-deoxy-glucopyranose and residues of 2-acetamido-2-deoxy-β-D-glucopyranose. The cationic polysaccharide chitosan is used as a polymer based on its ability to undergo liquid-gel transition due to the ionic interaction with a polyanion. Mucoadhesive nature, biocompatibility, and nontoxicity are some of the important properties of chitosan, which render it an interesting biomaterial. Chitosan promotes cross-linkage with a variety of crosslinking agents forming a network to entrap the molecules of interest. The unique structural characteristics of chitosan made researchers use it most frequently for the development of nanoparticles. The nanoformulations prepared with chitosan polymer shows advantages of slow or controlled release, which improve the stability, efficacy, and solubility and decrease the toxicity (Calvo et al. 1997; Kunjachan et al. 2014; Mohammed et al. 2017; Kucukoglu et al. 2019; Naskar et al. 2019; Taghizadeh et al. 2019).

Chitosan-based carrier system for nucleic acids like dsDNA, siDNA, plasmid DNA, peptides, proteins, and oligonucleotides has gained attention from the researchers in recent years. Dhandapani et al. developed dsRNA-loaded chitosan nanoparticles by ionic crosslinking gelation method using TPP as the crosslinking agent. Mean particle size of less than 200 nm was achieved with a good homogeneity of formulation with a PDI value near to 0.2. The surface charge of the prepared nanoparticles was reported as approximately more than +30 indicates the stability of the formulation (Dhandapani et al. 2019).

Characterization of Chitosan

Molecular Weight Determination

In general, chitosan molecular weight is determined by using viscosity data, and hence the molecular weight determined by this method is called viscosity average molecular weight. The method starts with the preparation of different concentrations of chitosan in acidic solution, normally 1% HCl. The viscosity of the prepared solutions is measured by using the viscometer. Then the molecular weight can be calculated using the Mark-Houwink equation given below:

$$[\eta] = KM^{\alpha}$$

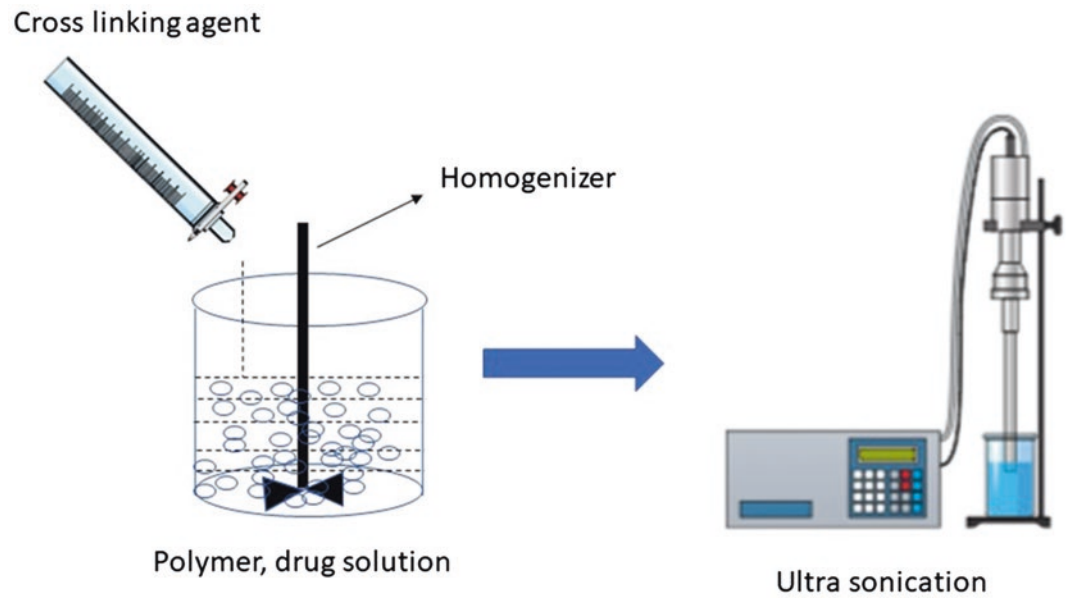

Fig. 7.4 Schematic representation of the ionic crosslinking gelation method

where K and α are constants, M is molecular weight, and $[\eta]$ represents the intrinsic viscosity.

The intrinsic viscosity is defined as the limiting value of the reduced viscosity or inherent viscosity at infinite dilution of the polymer and the equations are given below:

$$\eta_{\text{reduced}} = \left[\frac{(\eta - \eta_0)/\eta_0}{c}\right]$$

$$\eta_{\text{inherent}} = \left[\frac{\ln(\eta/\eta_0)}{c.}\right]$$

where η is the measured viscosity value of chitosan solution, η_o is the measured viscosity value of the solvent, and c is the chitosan solution concentration (Taghizadeh et al. 2019).

Calculation of the Degree of Deacetylation

Chitosan is a linear polysaccharide consisting of N-acetylglucosamine and D-glucosamine units, and it is obtained from the partial deacetylation of chitin. The degree of diacylation is one of the key parameters for the characterization of chitosan, and it is the N-acetylglucosamine units mole fraction in the chain. Determination of degree of diacylation based on the FTIR spectrum is one of the common methods and is estimated from the given equation below:

$$DD = 100 - \frac{\left[\left(\frac{A_{1655}}{A_{3450}}\right)\times 100\right]}{1.33}$$

(A1655, A3450: absorbances at respective wavenumbers, which corresponds to carbonyl and hydroxyl groups, respectively) (Taghizadeh et al. 2019).

Chitosan nanoparticles attracted attention by the researchers in the recent past for the development of nanoparticles as the drug carrier systems as these can avoid the degradation of drugs and improved loading and drug release in a controlled and sustained way. Chitosan nanoparticles are one of the promising drug carriers in the treatment of many disease areas like oncology. Achieving small-sized chitosan nanoparticles is one of the major challenges faced during the development of nanoparticles as the size of the nanoparticle has a predominant effect on their use as vehicles for drug transportation. A wide range of preparation methods is available such as microemulsion, coacervation, reverse micellar technique, and others which require the usage of organic sol-

Table 7.4 Applications of ionic gelation crosslinking method

Type of formulation	Drug name	Polymer	Molecular weight of the polymer	Degree of deacetylation	Crosslinking agent	Particle size achieved	Encapsulation efficiency (approx.)	References
Nanoparticles	Methotrexate	Chitosan	40 k Da	85%	TPP	187.9 nm	53%	Wu et al. (2009)
Nanoparticles	Doxorubicin	Chitosan			CaCl2	320–490.4 nm	56.9–84%	Khalid et al. (2018)
Nanoparticles	Sorbic acid	Chitosan		95%	TPP	327.6 nm		Wang et al. (2018)
Nanoparticles	Insulin	Chitosan	Low	90%	TPP	325.07 nm	73%	Al-nemrawi et al. (2019)
Nanoparticles	Diclofenac	Chitosan	Low and high		TPP	295.33 nm	29%	Alqahtani et al. (2019)
Colon targeted beads	Pterostilbene	Pectin			Zinc acetate	0.96 μm	64%	Ansari et al. (2019)
Nanoparticles	Alpha arbutin	Chitosan	Low	95%	TPP	147–274 nm	71%	Ayumi et al. (2019)
Nanoparticles	Beta arbutin	Chitosan	Low	95%	TPP	211.1–284 nm	77%	Ayumi et al. (2019)
Nanogel	Glibenclamide and quercetin	Chitosan	Low and medium	75 to 85%	TPP	370.4 nm	94%	Chellappan et al. (2019)
Hydrogels		Chitosan	Low	85%	$NaHCO_3$, genipin			Ghavimi et al. (2019)
Nanoparticles	Amoxicillin	Chitosan	Medium		TPP	<100 nm	95%	Hadizadeh and Toraji (2019)
Nanogel	Chlorogenic acid	Chitosan			Calcium phosphate nanoparticles	439 nm	70%	Palaniraj et al. (2019)
Nanoparticles		Chitosan	Different molecular weights	91.02%	TPP	173 nm		Pan et al. (2019)
Nanoparticles	Rotigotine	Chitosan			TPP	75.37 nm	96%	Tzeyung et al. (2019)
Nanoparticles		Chitosan		92.16%	TPP	315.5 nm		Villegas-Peralta et al. (2019)

vents and harmful crosslinking agents that could be toxic. In contrast to this ionic gelation is the method that is based on the electrostatic interaction between cations of chitosan and anions of crosslinking agents that require mild circumstances for drug transportation (Kamat et al. 2015).

Chitosan-Based Nanoparticles and Ionic Gelation Method

Nanoparticles can be prepared by a variety of methods such as ionic gelation, de-solvation method, spray-drying, covalent crosslinking, etc. Nanoparticles prepared by methods like de-solvation and spray-drying result in larger particle sizes, while the crosslinking method can produce particles with lower size. Chitosan nanoparticles developed by conventional methods usually have disadvantages like poor stability and a wide range of size distribution which limits the application in certain cases. Ionic gelation method is attractive for the production of nanoparticles because it is nontoxic, convenient, and controllable without using any organic solvent (Pan et al. 2019).

Typically, the ionic gelation method for the preparation of chitosan nanoparticle involves the addition of a crosslinking agent to the polymer solution as dropwise by slow and unregulated stirring. The method is ecofriendly and safer and results in the formation of nanoparticles with a variable size range of 250–400 nm and charge of +25 to +54 mV. The heterogenicity in the prepared sample shows the effect on physicochemical parameters such as loading efficiency and controlled release of the drug and charge. Variation in properties such as molecular weight of chitosan, the concentration of polymer, and type of crosslinking agent shows a significant impact on the yielding of homogeneous particles. Ultrasonication and radiation amplitude application approach can be employed during the procedure for decreasing the size and polydispersity of the sample (Kamat et al. 2015). Chitosan acts as the chelating agent and inhibits the toxin production by selectively binding trace transition metals. Low molecular weight chitosan enters the cell nucleus and inhibits protein synthesis by interfering with mRNA synthesis. High molecular weight chitosan has the ability to interact with the cell membrane to alter the permeability (Kamat et al. 2015; Pan et al. 2019).

The variation in the concentration of the crosslinking agent, TPP solution, has a predominant impact on the nanoparticle mean diameter. In one of the studies, Villegas-Peralta et al. described the chitosan nanoparticle preparation by two different ionic gelation methods with changing in the type of crosslinking agent, TPP concentration, and maintaining parameters like duration of stirring, concentration, and degree of deacetylation constant. The nanoparticles prepared with lower crosslinking agent concentration result in higher mean size than the one with higher concentration (Villegas-Peralta et al. 2019). Hadizadeh and Toraji reported the preparation of amoxicillin-loaded chitosan nanoparticles. The appropriate size of nanoparticles is very important for controlled release and also the therapeutic efficacy. Nanoparticles loaded with anti-microbial drugs with a submicron size are effective against the cultures of methicillin-susceptible and methicillin-resistant *Staphylococcus aureus*. The chitosan nanoparticles and beads loaded with betamethasone and tetracycline which are developed by the ionic crosslinking method are capable of releasing the drug at a controlled rate (Hadizadeh and Toraji 2019; Taghizadeh et al. 2019).

5.2.11 Microreactor Application in the Preparation of Chitosan Nanoparticles by Ionic Gelation Method

Chitosan nanoparticles prepared by the conventional mixing methods in the crosslinking technique lacks homogeneity and also affect physicochemical parameters of preparation which limit their application. A thorough theoretical analysis of currently available conventional procedures and models of active microreactor were simulated by researchers to design and fabricate

microreactor. A significant difference was observed by the researchers in terms of the size of nanoparticles and the charge of the nanoparticles when prepared in conventional methods and using microreactors. The nanoparticles prepared by microreactor resulted in producing highly monodispersed nanoparticles with adjustable characteristics including entrapment efficiency, drug release, and others. Many other approaches are being investigated by the researchers to find their impact on reducing the size and improving other parameters in the recent past. One of them is microfluidic mixing, a methodology involving the three-dimensional fluid fabrication in a monolith layer which was developed by the researchers recently. This technique offers the regulation over the interaction between reactants and their movement in the reactor in a specified quantity to produce monodispersed particles. Mathematical modeling and geometric designing in fabricating the device helps in achieving the optimal operational parameters. Fine-tuning of parameters such as flow rate of polymer and a crosslinking agent and the collection of the product at outlet makes the difference in yielding a product with desired output parameters. Passive route of preparation of nanoparticles by microfluidics, a general approach followed by researchers, results in a characteristic low Reynolds number because of the scaling effect that is confined to the fluid dynamics to a laminar regime. Slow rate and lower efficiency are the major drawbacks in passive mixing, and hence, active micromixers which disturb the laminar flow shows great potential in the preparation of nanoparticles by ionic gelation method. Active mixing facilitates the mixing by chaotic advection and diffusion and also increases the area of interphase existing between two liquids by complex flow patterns. Active micromixers offer more control and faster mixing in small volumes. The fabrication process of microreactors and fine-tuning of process parameters for controlled synthesis are the two major hurdles associated with this technique. Many attempts were made by researchers for the fabrication of microreactors such as crossflow microfluidic chip-based microreactors for the preparation of monodispersed nanoparticles of chitosan (Kamat et al. 2015).

5.2.12 Theoretical Analysis of Nanoparticle Preparation by Ionic Gelation Method in a Microreactor

Fabrication of microreactor requires a good understanding of the dynamics of conventional and micromixing for the synthesis of chitosan nanoparticles by the ionic gelation method. In the conventional method, mixing does not happen at the center of the mixing reactor. In the microreactor model, basically two inlets are available, one for flow of polymer and the other for crosslinking agent leading to a circular chamber consisting of a magnetic actuator. The chamber consists of a single outlet for the flow of products formed in the chamber. The stirring of the magnetic actuator induces the convergence of fluids that enter into the chamber. The process of diffusion where two different fluids are mixed is one of the dominant mechanisms at the microscale. The microreactor model assumes that the continuity and Navier–Stokes direct the incompressible flow, laminar flow, and steady state and diffusion for species transport by convection. The effectiveness of mixing by the microreactor is calculated by the given formula.

$$M = \sqrt{\frac{\frac{1}{N}\sum_{i=1}^{N}\left(\bar{C} - C_i / \bar{C}\right)^2}{\bar{C}_0\left(1-\bar{C}_0\right)^2}}$$

where C is the concentration, N is the reaction number, and 0 and I are the initial and final concentrations, respectively.

In comparison to conventional methods, microreactors achieve better mixing because of large force with more velocity generated during the process. Though mixing efficiency drops drastically during the initial phase of mixing for both the methods, the efficiency increases in microreactor once it attains saturation.

A clear difference exists between the microreactor and conventional methods in terms of mixing. In the case of conventional method, one reactant is added to the other in a dropwise manner because of which equilibrium reaches faster resulting in a drop in Reynolds number and diffusion leading to laminar flow-like condition. In

microreactor setup, fresh volumes of two liquids enter the chamber because of the continuous flow of reactants and flow out through the outlets at the same time, leading to higher mixing efficiency. During the initial time period of stirring, mixing efficiency increases more significantly and saturates exponentially as the time increases. Kamat et al., in one of the studies, prepared chitosan nanoparticles by ionic gelation technique by using conventional mixing and microreactor mixing methods to understand the advantages of the microreactor mixing method. Researchers carried out simulation studies and observed a better mixing in microreactor in comparison to conventional methods. The nanoparticles prepared by microreactor mixing resulted in significantly lower particle size in comparison with the conventional mixing (Kamat et al. 2015).

5.2.13 Hydrogels of Drug-Loaded Chitosan-Based Nanoparticle

A profound amount of research work was carried out by many researchers on chitosan hydrogels as biodegradable, bioactive, and injectables for bone regenerating applications. In one of the studies, the method of chitosan-based hydrogel injectables with nanocrystals as reinforcing reagent preparation was reported. Genipin and carbonate act as covalent and ionic bond crosslinking agents. The preparations show the controlled release of the active agent calcium phosphate ion. The nanoparticles are prepared by using biopolymers with properties of controlled and sustained release, and the ability to protect drugs against degradation has attracted researchers towards developing a high-performance drug delivery system in the recent past. The preparation of hydrogels by incorporating biopolymeric nanoparticles is helpful in altering the release profile and improving protection from degradation. Many researchers developed nanoparticles (hydrogels) and reported that the preparation of hydrogel systems extends the drug release profile. Chitosan is one of the most extensively used biopolymers for the preparation of nanoparticles because of unique characteristics possessed by chitosan such as biodegradability and biocompatibility and is nontoxic when administered in all the routes of administration. Antimicrobial and therapeutic effects are additional advantages associated with this polymer. Once the nanoparticles are prepared, the next step is the incorporation of chitosan nanoparticles into the polymer. There are various methods of preparations available, and one of the methods reported by Hosseini et al. is the irradiation of PVA solution by an electron beam. Researchers used a 10% PVA solution for the preparation of hydrogels. The required quantity of drug-loaded chitosan-based nanoparticles is dissolved in the PVA solution at room temperature. Then the solution is poured into the mold of poly(ethylene terephthalate) to form a sheet. The prepared sheets are covered with polyethylene film and sealed in polyethylene bags. These bags by irradiating with a high energy electron beam results in the formation of hydrogels (Ghavimi et al. 2019; Hosseini et al. 2019).

5.2.14 Preparation of Alginate-Based Nanoparticles by Ionic Gelation Method

Alginate is a natural polysaccharide usually obtained from the bacterial cell wall, algae, and seaward. The alginate is comprised of monomers of β-D-mannuronic acid and α-L-guluronic acid connected by glycosidic bonding. Alginate is highly biodegradable and biocompatible particularly suitable for biomedical use. Hydrogels prepared from alginate by ionic gelation crosslinking methods have been successfully used for the drug delivery systems development, wound dressing, and tissue regeneration. The stability and mechanical characteristics of alginate have a very important role in all these applications as they affect the applicability and performance of the preparation (Harilall et al. 2013; Dodero et al. 2019; Kadokawa 2019).

Alginate Hydrogels

Ionic gelation is one of the most common techniques used for the alginate hydrogels preparation by using agar molds as a source of bivalent ions. The polymer is diluted with crosslinking agent solutions such as $CaCl_2$, $BaCl_2$, or $SrCl_2$ to approximately1% weight, and the temperature is applied to dissolve the polymer. Agar molds are prepared by keeping the solution in petri dishes at refrigerated conditions for approximately 12 h.

On these molds cylindrical wells are made with the help of metallic cutter and filled with sodium alginate solution. The system is allowed to crosslinking reaction to occur at refrigerated conditions within 2–4 h. The crosslinking time varies according to the requirement of the degree of the crosslinking and the mechanical properties (Dodero et al. 2019).

Factors Influencing the Crosslinking Degree of Alginate-Based Hydrogels

Alginate concentration, crosslinking time, chemical nature, and concentration of the divalent ions are some of the factors that can influence the degree of crosslinking of hydrogels of alginate. Dodero et al. assessed the effect of the most common variables for understanding their influence on the degree of crosslinking in the preparation of alginate-based nanogels by using a method adapted based on the molecular theory of rubber elasticity. A mathematical model helps in predicting the performance in terms of mechanical properties and effective crosslinking degree of nanogels. The validated theoretical model by means of statistical technique and applying RSM is required for better visualization of both the mutual interaction and influence of the selected independent variables on the behavior of the prepared hydrogels (Dodero et al. 2019).

Evaluation of Hydrogels

(a) *Association Efficiency Percentage*

Spectroscopic methods like UV spectra can be used for the evaluation of hydrogels. The spectroscopic method can be used for the confirmation of chitosan nanoparticle formation, the drug association efficiency, and the drug release kinetics from the samples. Centrifugation of the samples separates the nanoparticles in the form of a pellet. Recording the absorbance of the supernatant after centrifugation gives the free drug of the formulation. The percentage of association efficiency can be calculated as follows:

$$\text{Percent association efficiency} = \frac{\left(\text{Total amount of drug} - \text{Free drug}\right)}{\text{Total amount of drug}}$$

The drug release rate of hydrogels can be evaluated by UV spectrophotometry method. The samples are kept in a water bath shaker in distilled water. The UV absorbance calculated for the samples collected at regular time intervals with help of calibration curve gives the mount of drug release (Hosseini et al. 2019).

(b) *Morphology of Hydrogels*

Recording of micrographs of hydrogels with the help of scanning electron microscopy helps in the evaluation of the morphology of hydrogels. The micrographs can be interpreted by various software for image processing and the number (average size) of the samples can be calculated from the following equation:

$$D_n = \frac{\sum D_i . n_i}{\sum n_i}$$

where D_n is the number average size and n_i is the number of particle size with D_i.

The average size along with the percentage yield of nanoparticles formation gives information about the performance of the crosslinking gelation method followed by the preparation of nanoparticles under the optimized conditions (Hosseini et al. 2019).

(c) *FTIR Analysis*

FTIR measurements of particles reveal the interactions between the components of the nanoparticles. It is a well-known interaction between the cations of polymer, and crosslinking agent anions is the basis for the formation of nanoparticles by the ionic crosslinking gelation method. FTIR analysis of the samples helps in depicting the crosslinking mechanism that happened during the preparation. Chitosan shows different peaks representing the different functional groups. A peak that appears in the region

of 3200–3500 cm^{-1} is corresponding to vibrations from primary and secondary amide groups because of N-H stretching and also O-H stretching vibrations. The peaks because of the vibrations of carboxy group stretching and amine group stretching can be seen near 1640 cm^{-1} and 1570 cm^{-1} and vibrations of the C-N stretching show at 1047 cm^{-1}. The crosslinking of chitosan ammonium groups and polyphosphoric groups of TPP can be confirmed by the presence of peaks near 1152 cm^{-1}, 1652 cm^{-1} and the bands at 1570 cm^{-1}, 1640 cm^{-1}(Hosseini et al. 2019; Taghizadeh et al. 2019).

(d) *Drug Release Profile*

The drug adsorbed on the surface causes the abrupt release during the initial time phase, continuing to more than an hour. Then the rate of release becomes slow, and it may appear that during this phase, the swelling of nanoparticles is very slow that the diffusion is difficult. After a relatively larger time where the degree of swelling develops appropriately, the drug releases increase in a linear manner (Hosseini et al. 2019).

(e) *Swelling Behavior of Hydrogels*

There are three major phenomena that take place during the swelling of the hydrogels: (1) diffusion of water molecules into the hydrogels, (2) relaxation of polymer chain, and (3) polymer network expansion into the bulk of the medium. Chitosan nanoparticles have lower hydrophilicity at a pH of 7 and room temperature, which are swelling measurement conditions. The ability of hydrogel swelling declines as the chitosan nanoparticles in PVA hydrogel acts as a barrier against the diffusion of water molecules into the hydrogel network. Moreover, chitosan nanoparticles can lower the swelling capacity of hydrogels because of the possible hydrogen bonding between the chitosan and PVA chains (Hosseini et al. 2019).

The behavior of hydrogel swelling is generally evaluated in deionized water and physiological solution. Because of the loss of free polymer and divalent ions, a decline in the initial swelling degree is observed. Hydrogels prepared by alginate in a saline environment show different behavior than the deionized water environment depending on the conditions used for crosslinking. The water uptake also depends on the concentration of the crosslinking agents used during the preparation. Lower water uptake is observed in samples with a high density of crosslinking agents because of the higher number of constrains between polymer chains. On the other side, the samples with a low density of crosslinking agents show a significant increase in the initial swelling. The procedure of evaluation of swelling of hydrogel starts with the immersion of the hydrogels in the selected medium and checking the weights at regular time intervals until it reaches the equilibrium. Once the equilibrium is reached, the hydrogels are dried in an oven for 24 h under the vacuum at 110 °C. The swelling degree (ϕ) of the samples is determined from the following equation:

$$\Phi = \frac{\left(W_{\text{wet}} - W_{\text{dry}}\right)}{W_{\text{dry}}}$$

where W_{wet} is the weight of the swelled hydrogels and W_{dry} is the weight of the dried hydrogels.

Analyzing the swelling data by Peppa's model explains the kinetic mechanism of hydrogels swelling, and the model is based on the following equation:

$$\frac{M_t}{M_\infty} = kt^n$$

(M_t/M_∞, fractional of hydrogel swelling of the at time t; k, characteristic constant of the hydrogel; n, diffusion exponent)

The coefficient of diffusion of water molecules in the hydrogel system can be determined from the below equation:

$$\frac{M_t}{M_\infty} = 4\left(\frac{Dt}{\pi l^2}\right)^{0.5}$$

where D is the diffusion coefficient (Dodero et al. 2019; Hosseini et al. 2019).

(f) *Crosslinking Degree of Hydrogels*

The degree of crosslinking can be evaluated by subjecting the samples to compression. A rotational rheometer is used to apply compression over the sample. As the sample reaches the

state of equilibrium of swelling, the compressive module can be determined from the slope of the plot of stress vs strain linear region according to the following equation.

$$G = \frac{\sigma}{\gamma}$$

where G is the compression module, σ is the stress, and γ is the strain.

In terms of force (F) and contact area (A) of the sample with the geometry, upper plate stress (σ) is defined as follows:

$$\sigma = \frac{F}{A}$$

Stress (γ) is defined in terms of compressed ratio as follows:

$$\gamma = -\left(\lambda - \lambda^{-2}\right)$$

(λ: compress ratio between the initial and final height of the sample)

With the help of Flory-Rehner theory, the effective crosslinking density of the hydrogels is determined from the following equation:

$$\nu_e = \frac{\left(A \times G\right)}{\left\{R \times T\left(\frac{\phi_{2,r}}{\phi_{2,s}}\right)^{\frac{2}{3}}\right\}\phi_{2,s}}$$

(A, functionality parameter of the crosslinking points; R, universal gas constant; T, absolute temperature; $\phi_{2,r}$, $\phi_{2,s}$, volume fraction of polymer of dried hydrogels and swelled hydrogels) (Dodero et al. 2019)

(g) *Assessment of the Degree of Crosslinking of Hydrogels by Response Surface Methodology (RSM)*

To investigate the influence on the degree of crosslinking of hydrogels, with the help of linear (b_1, b_2, b_3) and interaction terms (b_{12}, b_{13}, b_{23}, b_{123}), models can be developed based on the RSM with a 2^k factorial design. The equation is as follows:

$$y = b_0 + b_1x_1 + b_2x_2 + b_3x_3 + b_{12}x_1x_2 + b_{13}x_1x_3 + b_{23}x_2x_3 + b_{123}x_1x_2x_3 \ldots$$

where y is the system response for the degree of crosslinking, b_0 is the intercept, and x_1, x_2, x_3 are independent variables such as time, the strength of the polymer, and crosslinking agent.

The hydrogels show differences in mechanical behavior when swelling is done in different media. Samples of hydrogel subjected to immersion in deionized water show a higher swelling than the samples in saline media. Apart from this, the samples show differences based on the type of bivalent ion present in the crosslinking agent. For instance, Dodero et al. observed that hydrogels crosslinked with barium ions show a higher compressive modulus than crosslinked counterparts of Ca^{2+} and Sr^{2+}. The probable reason is because of the affinity of Ba^{2+}towards alginate in comparison with Ca^{2+} and Sr^{2+}(Dodero et al. 2019).

Preparation of Sodium Alginate Nanoparticles by Ionic Gelation Method

Sodium alginate is a sodium salt of alginic acid obtained from marine brown algae and is one of the most widely used natural polymer, biocompatible, biodegradable, and mucoadhesive nature and is the advantageous properties of sodium alginate. This polymer consists of two uronic acids, α-L-guluronic, and β-D-mannuronic acids. Guluronic acids exchange Na + ion and react with Ca^{2+} and α-L-guluronic acid groups thus connecting each other by divalent cations. Alginate can transform from sol to gel and vice versa in the presence of ions such as Ca^{2+}, Mg^{2+}, Ba^{2+}, and Sr^{2+}. The transformation is a temperature-dependent manner and is one of its important characteristics. This property of alginate has been helping researchers to prepare hydrogels for a variety of purposes (Khalid et al. 2018; Dodero et al. 2019).

The dimerization of chains of alginate helps in the joining of other chains, leading to the development of a network of gel. Ionotropic gelation property and crosslinked structure of sodium alginate obtained the attention of researchers to use sodium alginate widely in the preparation of nanoparticle by ion gelation method. Khalid et al. developed doxorubicin-loaded sodium alginate nanoparticle by ionic gelation technique and

achieved an average size of less than 0.500 μm using sodium alginate and calcium chloride as polymer and a crosslinking agent (Khalid et al. 2018).

Preparation Sodium Pectin-Based Nanoparticles by Ionic Gelation Method

Pectin is a linear heteropolysaccharide with a long chain of D-galacturonic acid residues with rhamnose forming a part of the polymer backbone and arabinose and galactose forming a side chain. The plant cell wall is the source of pectin, and it is a promising approach in the development of colon targeted drugs. Pectin is classified into low methoxy, high methoxy, amidated, and non-amidated pectin considering amidation and esterification of carboxyl groups. De-esterification of high methoxy pectin results in the formation of amidated low methoxy pectin. Pectin is also used in the treatment and prevention of colorectal cancer. As the solubility of pectin is more in the aqueous phase, preparing an oral formulation to target the colon region by using pectin is a big challenge. This made researchers develop to strategies towards an approach reducing the aqueous solubility of pectin but at the same time making it easily degrade in the colon region. Ansari et al. reported the preparation matrix beads of pterostilbene with the ion gelation method. Zinc acetate is preferred over calcium in the preparation of nanobeads because of the stronger crosslinking capacity of zinc in comparison with calcium. Moreover, zinc pectinate is considered as more suitable for the colon targeting than calcium acetate. Further, the coating of beads with a pH-dependent polymer such as Eudragit S-100 helps in the dissolution of polymer in colon pH conditions (Ansari et al. 2019).

Ionic Gelation Method for the Preparation of Nanogels

Nanogels are the small swollen crosslinked hydrophilic polymer structures that are spherical in shape. These are the nanoparticulate systems having very good applications in the pharmaceutical drug delivery systems development. Nanogels offer sustained, controlled release and targeted drug delivery through the conjugation with other molecules or by changing its chemical structure. Bioactive molecules like drugs, peptides, antigens, carbohydrates, oligonucleotides, proteins, genes, and other inorganic compounds include silver and magnetic nanoparticles. It is possible to avoid the clearance by RES to extend the drug release and circulation time by using nanogels as carrier systems (Chellappan et al. 2019).

Palaniraj et al. reported the preparation of calcium phosphate chitosan porous nanogel-loaded chlorogenic acid biofilm having degradative properties. Ionic gelation method was used to prepare the nanogel by crosslinking the chitosan with calcium phosphate nanoparticles. The researchers reported that, as the formulation was prepared with the chitosan and calcium phosphate, the negative charge and positive charge present on the phosphate ion and chitosan, respectively, help in neutralizing the bacterial growth (Palaniraj et al. 2019).

Ionic Gelation Method for the Development of Nanoparticles Loaded Films

Formulations developed for administration through the buccal cavity offer drug delivery with advantages of bypassing the first-pass metabolism of the drug, high drug stability, rapid absorption, and self-administration of the drug. In one of the studies, Al-nemrawi et al. prepared chitosan nanoparticles loaded with insulin with the ionic gelation method. Buccal films are prepared by the solvent casting method and nanoparticles are introduced into films by dispersion. According to literature, films consisting of nanoparticles have greater mucoadhesive characteristics than blank films. The in vitro drug release studies for the buccal films conducted by the researchers revealed that the slow release is because of both nanoparticles and films. The films retard the drug release more than the nanoparticles which are dispersed in the film. Dispersing the nanoparticles into the films adds an extra advantage of creating one extra barrier for the drug release. The stability studies conducted for the drug loaded into the nanoparticle buccal films show that the drug is stable and is very critical in the

case of drugs like insulin (Al-nemrawi et al. 2019).

5.3 Effect of Process Parameters on the Quality of Nanoformulations

5.3.1 Polymer

The optimization of polymer concentration is very important as it is very crucial in deciding the quality of the formulation in various properties such as the size of the particle, entrapment and loading capacity, drug release profile, and others (Hadizadeh and Toraji 2019). Chitosan nanoparticles are known to show more stability, high antibacterial activity, and low toxicity. Intracellular leakage of chitosan by which positively charged chitosan binds with the negatively charged bacterial surface such as lipopolysaccharides can be explained as the mechanism behind the antibacterial effect of chitosan. The preparation of nanoparticles of antimicrobial drugs with chitosan adds an extra advantage in showing more therapeutic efficacy. Binding of the chitosan to the bacterial membrane permeability causes the leakage of intracellular contents and leads to cell death (Alqahtani et al. 2019).

Alqahtani et al. prepared various diclofenac-loaded chitosan nanoparticles by using the ionic gelation method where chitosan with different molecular weights was used for the preparation of nanoparticles to evaluate the effect of the molecular weight on the antimicrobial activity of the prepared formulations. Researchers reported that the mean particle size of the nanoparticles increases with the increase in the molecular weight of the chitosan without much effect on the distribution. An increase in the molecular weight of the chitosan slightly increases the entrapment efficiency of the nanoparticles, but the difference may be very small and without any statistical significance. The release studies conducted by the researchers show that the release profile is biphasic for the formulations, initial burst release, and slow release in the second phase which is common in most of the nanoformulations. But the researchers identified that an increase in the molecular weight of the chitosan is resulting in a decrease in the release of the drug from the formulation. The nanoformulations prepared by low molecular and high molecular weight chitosan as polymer were showing a high antimicrobial potential than the drug without any polymer (Alqahtani et al. 2019).

5.3.2 Crosslinking Agent

The most commonly used crosslinking agents are sodium tripolyphosphate (TPP), sodium caprylate, geneipin, stearic acid, etc. Sodium citrate, a citrate salt with chelating behavior, exhibits a good potential for use as a crosslinking agent which makes it possible to bind to many ions. Khalid et al. prepared a series of ratios of crosslinking agent to the polymer and by keeping the polymer concentration kept constant and varying the crosslinking agent concentration to identify the suitable ratio of polymer and a crosslinking agent. Deciding an appropriate ration of polymer and crosslinking agent helps in the development of nanoparticles with low mean particle size, particle homogeneity, and maximum particle concentration. The researchers reported that an increase in the concentration of crosslinking agents reduces the mean particle size. In another study, Hadizadeh and Toraji reported that the crosslinking agent is influencing the particle size. The increment in TPP concentration along with chitosan results in nanoparticles with smaller size. Ansari et al. studied the effect of zinc acetate concentration on the entrapment efficiency and in vitro drug release profile. Researchers observed that the higher concentration of crosslinking agent leads to an increase in entrapment efficiency. The increased concentration of crosslinking agents results in a higher degree of crosslinking of polymeric mesh which helps in the formation of a strongly bound matrix to avoid the leakage of drugs from the nanoparticles. Crosslinking agent concentration has a significant effect on the drug release profile in in vitro. The increased concentration of the crosslinking agent results in lowering the release of drugs from nanoparticle, and the reason behind it is that the increased concentration of crosslinking agents leads to higher gel strength and retards the

release of the drug. Chellappan et al. reported the effect of the solvent used for the preparation of crosslinking agents on the quality of the drug-loaded nanogel developed by the ionic crosslinking gelation technique. TPP reagent prepared in PBS pH 7.4 shows better results than the TPP prepared in ultrapure water. The lower concentration of TPP solution results in the smaller particle size, and hence lower concentration of TPP prepared in pH 7.4 is preferred for the preparation of nanogels. Various ratios of crosslinking agents to the polymer results in the formation of nanoparticle with a wide range of particle size. Using a 5:1 ratio of polymer to a crosslinking agent is generally followed to get an optimal size of the nanoparticles (Khalid et al. 2018; Ansari et al. 2019; Chellappan et al. 2019; Hadizadeh and Toraji 2019; Taghizadeh et al. 2019).

5.3.3 Polymer and Drug Ratio

The drug concentration influences major parameters of the nanoparticles such as size, entrapment efficiency, and loading capacity. Hadizadeh and Toraji reported that when the amount of drug increased, the mean particle size increases slightly, and it also improves the entrapment efficiency. In contrast to this, Ansari et al. reported that there is no substantial relation between the drug-polymer ratio to drug release profile and entrapment efficiency. In some other study, Tzeyung et al. assessed the impact of the drug concentration on the size of particles. The mean diameter of particle inclines with the rise in drug concentration. As the drug concentration increases, the ratio of drug to the polymer-crosslinking agent complex changes results in the decrease in the interaction between them. On the other hand, the higher amount of drugs also leads to a decrease in the homogeneity of the formulation. The decrease in the entrapment efficiency was also observed in the same study when the concentration of the drug was increased. When the drug concentration increases, a greater number of drug molecules adsorbed on to the surface of the polymer increase, and these molecules will be separated during the centrifugation step for the separation of nanoparticles. This results in the lower entrapment values of the drug into the nanoparticles (Ansari et al. 2019; Ayumi et al. 2019; Hadizadeh and Toraji 2019; Tzeyung et al. 2019).

5.3.4 Sonication

The application of energy in the form of sonication helps in breaking the glycosidic linkage in the chitosan resulting in the formation of small size droplets. A significant difference in the size of nanoparticles because of sonication was reported by researchers in a few studies (Hadizadeh and Toraji 2019).

5.4 Effect of Morphological and Physicochemical Properties on the Quality of Nanoformulation

The morphological features of polymeric nanoparticles like the size of the particle, surface charge, surface modification, and lipophilicity are the factors that decide the capability of the prepared formulation. Among all these, size and homogeneity in the distribution of particles play a very crucial role in determining the property of their interaction with the cellular membrane which helps permeation through them. It is also to be noted that the requirement of size varies from targeting one tissue or site to the other. The performance of nanoparticles not only depends on the morphology of the polymer used but also on the surface chemistry and molecular weight. The charge on the surface of the nanoparticles is one of the important factors to be considered and plays a significant role in nanoparticle uptake by cells. The charge on the surface of the particles decides whether the particles interact adhere to the counter charged cell membrane or cluster in blood flow. The nanoparticles with a positive charge on their surface enable enhancing its interaction with cells in increasing the rate of cellular internalization. Massive removal of nanoparticles by the macronuclear phagocytic system can be avoided by surface modification. For targeted drug delivery, where the perseverance of nanoformulation in the systemic circulation is needed, surface modification of

nanoparticles can form a network of chains at the surface that helps in repelling the proteins in the plasma and thus enhances the time of circulation in the body and persistence in blood. The molecular weight of the polymer can alter the release mechanism of the formulation. The release rate of the drug from nanoparticles declines with an increase in the polymer molecular weight in in vitro models (Kumari et al. 2010).

5.4.1 Particle Size

The size of the nanoparticle is considered as one of the critical parameters for deciding the quality of the formulation. The small size of the nanoparticles helps in passing through the biological membranes like the blood-brain barrier and enhances drug delivery. The small size of nanoparticles will have unique surface properties when compared to the bulk materials. The surface area increases with a decrease in the size of the nanoparticle, which helps in the solubility of the drug in an aqueous medium and enhances bioavailability. Especially in the treatment of tumors, nanoparticles having small size is advantageous as these formulations will have lower clearance by the RES and also permits the nanoparticles to target the tumor. As the smaller particles have a higher scope of interaction with the cellular membrane owning to their endocytosis, the improved efficiency is possible with the nanoparticles with a small size (Taghizadeh et al. 2019).

The polycation and polyanion concentration have a great impact on the particle size. As the concentration of polymer increases, the average size of the particles increases because of the higher the viscosity of the system (Hadizadeh and Toraji 2019). Chitosan exists as a polycation when dissolved in in acidic solution and when a crosslinking agent is mixed such as TPP which is polyanionic and negatively charged. The interaction takes place between hydroxyl, phosphoric ions of TPP with the positively charged amine groups present on the polymer through electrostatic and hydrogen bonding leading to nanoparticle formation. The nanoparticle formation depends on the availability of free amino groups, which improves the strength of electrostatic interaction between the drug and nanoparticles, which further helps in reducing the particle size. And hence the increase in the concentration of the drug leads to higher particle size (Ayumi et al. 2019).

Hadizadeh and Toraji reported a decrease in the mean diameter of the particles when the concentration of chitosan raised from 0.1% to 0.5%. Nanoparticle size controls the perfusion of the drug through various tissues. For the enhanced time of retention of the drug in tissues, it is required to prepare the nanoparticles with the smaller size as the nanoparticles with larger sizes are easily removed by the macrophages. Apart from therapeutic efficacy, the mean diameter of the particle can also influence the loading and rate of release (Hadizadeh and Toraji 2019). In contrast to this, Tzeyung et al. observed the impact of an increment in chitosan concentration on the size of particles, PDI, and surface charge. The increment is the concentration of polymer causing the rise in the average size of the particle. A higher concentration of polymer results in the increase in the number of chains of chitosan per volume resulting in the larger particle size, and it also causes a decrease in the density of crosslinking between chitosan and crosslinking agent which leads to aggregation resulting in the development of particles with higher diameter. The smaller PDI values show that the prepared nanoparticles by these ionic gelation methods represent the homogeneity of the formulation. In another study, Ayumi et al. observed the same kind of pattern where lower drug concentration results in the nanoparticles with lower size (Ayumi et al. 2019; Tzeyung et al. 2019).

5.4.2 Drug Loading and Entrapment Efficiency

The polymer concentration used in the preparation of formulations shows a predominant effect on drug loading and entrapment efficiency. Increasing the polymer content in the preparation of formulation improves the encapsulation and loading. Drug loading of more than 90% was achieved by the researchers in amoxicillin-loaded chitosan nanoparticles with just 0.1% of chitosan concentration, and it also showed continuous and

controlled release profile. In another study, researchers reported drug loading of more than 84% in sodium alginate nanoparticles loaded with doxorubicin (Khalid et al. 2018; Hadizadeh and Toraji 2019). Dhandapani et al. in one of their studies reported the impact of polymer (chitosan) on the drug loading capacity of dsRNA. The higher concentrations of chitosan results in lower entrapment of dsRNA. In one of the studies, Tzeyung et al. developed the rotigotine nanoparticles with chitosan and TTP by ionic gelation technique. The researchers reported the impact of chitosan concentration on the encapsulation efficiency of the nanoparticles made of chitosan. The increment in the strength of the chitosan leads to a decrease in encapsulation efficiency (Dhandapani et al. 2019; Tzeyung et al. 2019). Ayumi et al., in a study, prepared chitosan nanoparticle of α- and β-arbutin by a mechanism of crosslinking between chitosan and a crosslinking agent. In this study, researchers reported that the high encapsulation was achieved as the heteroatoms of arbutin tend to bond with the protonated chains of chitosan (Ayumi et al. 2019).

5.4.3 Drug Release Kinetics

Nanoparticles show burst release initially because of the weakly bound free drug on nanoparticle surface. As the polymer strength rises, the drug release rate decreases from the formulation. The increased concentration of polymer elevates the buildup through crosslinking between the polymer and crosslinking agent. Further, it causes the retarded release of the entrapped drug from the formulation. Hadizadeh and Toraji observed a rapid release of more than 65% of the drug from the chitosan nanoparticles loaded with amoxicillin within 8 h and later slow release. In another study, Ansari et al. observed a decrease in the rate of release from the beads prepared with a higher concentration of pectin in comparison with the lower concentration, and it is because of the increase in the length of the path that the drug molecules have to transverse (Khalid et al. 2018; Ansari et al. 2019; Hadizadeh and Toraji 2019).

Tzeyung et al. reported the drug release kinetics of the rotigotine chitosan particles developed by the crosslinking technique. The drug release is faster during the first 3 h because of the superficially adsorbed drug on the nanoparticle surface. The remaining drug is released slowly and completes in 24 h. The higher entrapment that resulted from the amplified interaction of the drug with the polymer causes the slow release of the drug from the chitosan nanoparticles (Tzeyung et al. 2019). The release profile of nanogels developed by the ionic crosslinking gelation technique is almost similar to the release profile of other nano-preparations. Chellappan et al. studied the drug release profile of nanogels in comparison with control formulations. A higher percentage of cumulative drug release is observed in the nanogels even after the rapid release in the first 3 h (Chellappan et al. 2019).

5.4.4 Degree of Swelling

As the polymer concentration is raised, the swelling of the polymer is increased. The higher the concentration of polymer, the more the amount of water that imbibes the matrix and shows high swelling. Taghizadeh et al. reported the effect of pH on chitosan beads swelling at two different conditions, pH 4.8 and pH 7.4. It was found that the chitosan beads prepared by the ion gelation method are sensitive to the change in pH with respect to swelling tendency. The swelling tendency is increased when pH was changed for 7.4–4.8. The polar groups present in the chitosan decide the swelling of beads, and it increases with the strengthening of bonding among polar groups. When the media is alkaline, deactivation of amino groups occurs causing the unavailability of lone pairs of electrons of nitrogen atoms leading to the repulsion with OH groups available in the aqueous medium. This causes the inhibition of water molecule and amino group interaction leading to declining in water uptake ultimately the lesser swelling of the beads (Ansari et al. 2019; Taghizadeh et al. 2019).

5.4.5 Zeta Potential

Zeta potential of the nanoparticle suspension is one of the main parameters to be considered for formulation stability, and basically it is a difference in electrical potential between the electroneutral region of the surface layer of the particle

and surrounding dispersion media. Suspension becomes less stable when absolute zeta potential becomes 0 mV. As the zeta potential decreases, flocculation occurs in the suspension because of the attraction of the particles. Flocculated suspensions have a typical zeta potential of – 20 to +20 mV which is a sign of low stability. The stability of the suspension increases with an increase in the zeta potential. A nanoparticle suspension with a high electric surface charge will have repulsive more force between the particles, which prevents the aggregation and results with high zeta potential (Ayumi et al. 2019).

5.4.6 Cellular Uptake of Nanoparticles

The intracellular uptake of nanoparticles is a very important aspect in terms of therapeutic efficacy. The nanoparticle average diameter, shape, and surface potential affects intracellular uptake greatly. There are two main phases in the process of cellular uptake of the nanoparticles, binding of the nanoparticle on the cell membrane and internalization phase. The first phase is most affected by the zeta potential or the surface charge of the nanosuspension, and by varying this factor binding of the nanoparticle to the tissues, directing to the cellular compartments can be controlled. Cellular surfaces consist majorly the negatively charged molecules which take a significant part in the penetration of the particles in topical applications. Nanoparticles with high surface charge show high cellular uptake as the electrostatic force of attractions between the cationic particles and anionic membrane help in strong binding with the cell membrane which facilitates the increase in uptake. After absorption of the nanoparticles onto the cell membrane, the cellular uptake of the nanoparticles is facilitated by various possible mechanisms like pinocytosis, phagocytosis, receptor mediated or nonspecific, or endocytosis (Ayumi et al. 2019).

Even though the exact mechanism behind the antimicrobial nature of chitosan is not clear, one of the assumptions is that the nanoformulations prepared using chitosan will have the cationic charge on the nanoparticle surface because of the ammonia, which helps in interaction with tissues and cell membranes with a negative charge. The smaller size and charge of nanoparticles influence the skin permeability of the nanoparticle and are advantageous especially in the case of nanoformulations intended for the topical application. Chitosan-based nanoformulations are known to have enhanced permeation and delivery of a wide range of drugs. When nanoparticles are prepared with chitosan as a polymer in the case of antimicrobial, the nanoformulations show lower MIC values because of the synergistic activity. The antimicrobial nature of chitosan is more at the acidic environment and also the molecular weight of chitosan is influencing the MIC values (Ayumi et al. 2019; Pan et al. 2019).

5.5 Modified Traditional Methods for the Development of Nanoparticles

Though several methods are available for the development of nanoparticles, continuous efforts are put by researchers to improve the quality of nanoparticles in terms of morphological and therapeutic efficiency and to reduce the toxic effects of the formulations being prepared by the currently available methods. New methods are introduced based on the possible slight modifications of the existing methods. The following are the few techniques developed by the researchers in the recent past for the development of nanoparticles.

5.5.1 Dialysis

Dialysis is a simple and effective method for the preparation of polymeric nanoparticles with small size and narrow distribution. Though the mechanism of dialysis is not fully understood at present, basically the process involves the displacement of the internal phase usually an organic solvent into the aqueous phase across the dialysis membrane leaving the encapsulated drug in a polymer. The method starts with the solubilizing polymer and drug in a suitable organic solvent which is miscible with the water or non-solvent. This solution is placed inside a dialysis tube with appropriate molecular cutoff dialysis membrane

and is placed in an external phase. The polymer aggregates continuously as it loses solubility during the displacement of external phase into non-solvent resulting in nanoparticle formation (Nagavarma et al. 2012; Krishnamoorthy and Mahalingam 2015).

5.5.2 Membrane Evaporation and Emulsion Technique

The technique involves the use of a membrane that separates the organic and aqueous phases during the process. The organic phase consisting of polymer and drug is passed through the membrane into the aqueous phase to form the droplets followed by the detachment from the membrane by the movement of an aqueous medium. The nature of the membrane is whether it is hydrophilic or lipophilic as a function of the external phase (organic or aqueous solution). This results in the formation of nanoparticles with a uniform distribution, and the larger droplet size is the disadvantage in comparison with the conventional emulsion and evaporation technique. There are many parameters that should be considered such as the pore size, pressure applied, and others. The size and distribution of the pores on the membrane decide the nanoparticles produced by the method. The membrane with a pore size less than 200 nm is advisable to expect the nanoparticles with lower size. Applying the pressure across the membrane higher than the critical pressure and keeping the angle of contact as less as possible help in the production of nanoparticles with desired qualities. The membranes such as PTFE (poly(tetrafluoroethylene)) and SPG (Shirasu Porous Glass) are the most commonly used for this technique (Astete and Sabliov 2006).

5.5.3 Premix Membrane Emulsification

Wei et al. reported the preparation of nanoparticles by employing a novel method of preparation that includes a combination of emulsion and premix emulsification procedures. The preparation method includes two major steps, preparation of emulsion by low-speed homogenization process and passing through the membranes such as SPG or PTEE. The low-speed homogenization results in the production of coarse emulsion which is passed through the membrane with high pressure. Further, the emulsion is subjected to evaporation to remove the solvent leading to nanoparticle production. Similar to the previous method, the pore size and its distribution on the membrane and the pressure applied during the extrusion through the membrane decide the quality of the nanoparticles produced (Wei et al. 2008).

5.5.4 Spray-Dry Method

The method is more suitable for the preparation of nanoparticles for hydrophilic drugs. The process involves the preparation of water in oil emulsion, where the oil phase is consisting of a mixture of organic solvents in which polymer is dissolved along with the surfactant of lipophilic in nature. The aqueous phase is prepared by dissolving the hydrophilic drug of interest. The emulsion is prepared by adding the oil phase into the aqueous phase, and the prepared emulsion is sprayed into a hot air chamber by a nozzle. The fine spray because of the nozzle and the evaporation of the solvent because of the hot air facilitate the formation of nanoparticles (Astete and Sabliov 2006).

5.5.5 Spray Solvent Displacement Combined with Dialysis

This method was developed by the researchers by modifying the solvent displacement technique. The process includes the injection of the organic phase into the aqueous phase through a nozzle in the form of a spray. After this, the solvent is removed by the dialysis. The drug is added after the dialysis is processed by adsorption onto the surface of the nanosphere. The addition of stabilizer and further freeze-drying helps in stabilizing the prepared nanoformulation.

6 Conclusion

Several types of nanoformulations are being prepared by the researchers to address the various limitations associated with the conventional dosage forms available at present. Polymeric nanoparticles are one of the most promising

alternative drug delivery systems to conventional formulations. Different kinds of techniques are available for the preparation of different types of synthetic and natural polymers-based nanoparticles for drugs belonging to the various classes of drugs. Each and every method has its typical advantages and at the same time limitations. Methods such as emulsion polymerization and interfacial polymerization technique are used for the preparation of nanoparticles by polymerization of the polymers. Even though these methods are simple and fast, washing steps and only lipophilic drugs can be used are the few limitations associated. The other approach of polymeric nanoparticle preparation is from the preformed polymers. Emulsification and solvent evaporation, solvent displacement, interfacial deposition technique, and emulsification and solvent diffusion technique are some of the preparation methods available for this approach. Most of these methods involve the usage of water-immiscible organic solvent for the solubilization of drug and polymer, and because of this in most cases, only lipophilic drugs are suitable to prepare the nanoparticles. Salting out is one of the methods of nanoparticles where the technique involves the separation of water-miscible organic solvent from the emulsion. The introduction of this method into the nanoparticle preparation addressed most of the limitations associated with the other methods. Combining the salting-out method with the other techniques such as emulsion and aqueous methods adds some additional advantages in some specific characteristics of the nanoparticles that are required.

Ionic gelation is one of the techniques used for the preparation of nanoparticles especially for the compounds which are hydrophilic in nature. As the method is based on the electrostatic interaction of ions and there is no requirement of organic solvent, it is very simple and does not cause any structural changes to the drugs. Chitosan, alginate, and gelatin are some of the natural polymers which are used very frequently to prepare micro and nanoparticles by ionic gelation method. Supercritical fluid technology, dialysis, and membrane evaporation technique are some of the recently developed methods for the preparation of nanoparticles. Combining the recently developed techniques with the available traditional methods helps in developing a novel technology that can address the typical limitations associated with the traditional methods. Continuous in-depth research is required in this filed to make the procedures simple, fast, economical, and eco-friendly.

References

Al-nemrawi NK, Alsharif SS, Alzoubi KH, Alkhatib RQ. Preparation and characterization of insulin chitosan-nanoparticles loaded in buccal films. Pharm Dev Technol. 2019;24(8):967–74.

Alqahtani FY, Aleanizy FS, Tahir EE, Alquadeib BT, Alsarra IA, Alanazi JS, Abdelhady HG. Preparation, characterization, and antibacterial activity of diclofenac-loaded chitosan nanoparticles. Saudi Pharm J. 2019;27(1):82–7.

Ansari M, Sadarani B, Majumdar A. Colon targeted beads loaded with pterostilbene: formulation, optimization, characterization and in vivo evaluation. Saudi Pharm J. 2019;27(1):71–81.

Astete CE, Sabliov CM. Synthesis and characterization of PLGA nanoparticles. J Biomater Dent. 2006;17(3):247–89.

Ayumi NS, Sahudin S, Hussain Z, Hussain M, Samah NHA. Polymeric nanoparticles for topical delivery of alpha and beta arbutin: preparation and characterization. Drug Deliv Transl Res. 2019;9(2):482–96.

Bhokare S, Marathe R, Gaikwad M, Salunke P. Biodegradable polymer based nanoparticles: a novel approach. Int J Pharm Sci Rev Res. 2015;35(1):43–52.

Bindschaedler C, Gurny R, Doelker E. Process for preparing a powder of water-insoluble polymer which can be redispersed in a liquid phase, the resulting powder and utilization thereof. United States Patent. 1990; 4,968,350.

Calvo P, Remuñán-López C, Vila-Jato JL, Alonso MJ. Novel hydrophilic chitosan-polyethylene oxide nanoparticles as protein carriers. J Appl Polym Sci. 1997;63(1):125–32.

Chellappan DK, Yee NJ, Kaur Ambar Jeet Singh BJ, Panneerselvam J, Madheswaran T, Chellian J, Satija S, Mehta M, Gulati M, Gupta G, Dua K. Formulation and characterization of glibenclamide and quercetin-loaded chitosan nanogels targeting skin permeation. Ther Deliv. 2019;10(5):281–93.

Cirstoiu-Hapca A, Bossy-Nobs L, Buchegger F, Gurny R, Delie F. Differential tumor cell targeting of anti-HER2 (Herceptin®) and anti-CD20 (Mabthera®) coupled nanoparticles. Int J Pharm. 2007;331(2):190–6.

Darade A, Pathak S, Sharma S, Patravale V. Atovaquone oral bioavailability enhancement using electrospraying technology. Eur J Pharm Sci. 2018;111:195–204.

Dhandapani RK, Gurusamy D, Howell JL, Palli SR. Development of CS-TPP-dsRNA nanoparticles to enhance RNAi efficiency in the yellow fever mosquito, Aedes aegypti. Sci Rep. 2019;9(1):8775.

Dodero A, Pianella L, Vicini S, Alloisio M, Ottonelli M, Castellano M. Alginate-based hydrogels prepared via ionic gelation: an experimental design approach to predict the crosslinking degree. Eur Polym J. 2019;118:586–94.

Donnelly RF, Morrow DI, Fay F, Scott CJ, Abdelghany S, Singh RRT, Garland MJ, Woolfson AD. Microneedle-mediated intradermal nanoparticle delivery: potential for enhanced local administration of hydrophobic preformed photosensitisers. Photodiagn Photodyn Ther. 2010;7:222–31.

du Toit LC, Pillay V, Choonara YE, Iyuke SE. Formulation and evaluation of a salted-out isoniazid-loaded nanosystem. AAPS PharmSciTech. 2008;9(1):174–81.

Farjadian F, Ghasemi A, Gohari O, Roointan A, Karimi M, Hamblin MR. Nanopharmaceuticals and nanomedicines currently on the market: challenges and opportunities. Nanomedicine. 2018;14(1):93–126.

Fay F, Quinn DJ, Gilmore BF, McCarron PA, Scott CJ. Gene delivery using dimethyldidodecylammonium bromide-coated PLGA nanoparticles. Biomaterials. 2010;31:4214–22.

Galindo-Rodríguez S, Allémann E, Doelker E, Fessi H. Versatility of three techniques for preparing ibuprofen-loaded methacrylic acid copolymer nanoparticles of controlled sizes. J Drug Deliv Sci Tec. 2005a;15(5):347–54.

Galindo-Rodríguez SA, Puel F, Briançon S, Allémann E, Doelker E, Fessi H. Comparative scale-up of three methods for producing ibuprofen-loaded nanoparticles. Eur J Pharm Sci. 2005b;25(4–5):357–67.

Ghavimi SAA, Lungren ES, Stromsdorfer JL, Darkow BT, Nguyen JA, Sun Y, Pfieffer FM, Goldstein CL, Wan C, Ulery BD. Effect of dibasic calcium phosphate incorporation on cellulose nanocrystal/chitosan hydrogel properties for the treatment of vertebral compression fractures. AAPS J. 2019;21:41.

Giménez VMM, Díaz-Rodríguez P, Sanz RL, Vivero-Lopez M, Concheiro A, Diez E, Prado N, Kassuha DE, Alvarez-Lorenzo C, Manucha W. Anandamide-nanoformulation obtained by electrospraying for cardiovascular therapy. Int J Pharm. 2019;566:1–10.

Hadizadeh M, Toraji A. Amoxicillin-loaded polymeric nanoparticles of less than 100 nm: design, preparation and antimicrobial activity against methicillin-resistant staphylococcus aureus. Iran J Sci Technol A. 2019;43(2):379–86.

Han C, Wang B. Factors that impact the developability of drug candidates. In: Drug delivery: principles and applications. Hoboken: Wiley; 2016. p. 1–18.

Haque S, Boyd BJ, McIntosh MP, Pouton CW, Kaminskas LM, Whittaker M. Suggested procedures for the reproducible synthesis of poly (d, l-lactide-co-glycolide) nanoparticles using the emulsification solvent diffusion platform. Curr Nanosci. 2018;14(5):448–53.

Harilall S-L, Choonara YE, Modi G, Tomar LK, Tyagi C, Kumar P, du Toit LC, Iyuke SE, Danckwerts MP, Pillay V. Design and pharmaceutical evaluation of a nano-enabled crosslinked multipolymeric scaffold for prolonged intracranial release of zidovudine. J Pharm Pharm Sci. 2013;16(3):470–85.

Hosseini F, Entezam M, Jafari SH, Khonakdar H-A, Abdouss M. On physical and antibacterial properties and drug release behavior of poly(vinyl alcohol) hydrogels: effect of drug loaded chitosan nanoparticles. Polym-Plast Technol. 2019;58(7):32–741.

Jain S, Cherukupalli SK, Mahmood A, Gorantla S, Rapalli VK, Kumar S, Dubey GS. Emerging nanoparticulate systems: preparation techniques and stimuli responsive release characteristics. J Appl Pharm Sci. 2019;9(08):130–43.

Jayan H, Leena MM, Sundari SS, Moses J, Anandharamakrishnan C. Improvement of bioavailability for resveratrol through encapsulation in zein using electrospraying technique. J Funct Foods. 2019;57:417–24.

Kadian R. Nanoparticles: a promising drug delivery approach. Asian J Pharm Clin Res. 2018;11(1):30–5.

Kadokawa J-i. Dissolution, derivatization, and functionalization of chitin in ionic liquid. Int J Biol Macromol. 2019;123:732–7.

Kamat V, Marathe I, Ghormade V, Bodas D, Paknikar K. Synthesis of monodisperse chitosan nanoparticles and in situ drug loading using active microreactor. ACS Appl Mater Interfaces. 2015;7(41):22839–47.

Karuppusamy C, Venkatesan P. Role of nanoparticles in drug delivery system: a comprehensive review. Int J Pharm Sci Res. 2017;9(3):318.

Khalid A, Bashir S, Sohail M, Amirzada MI. Characterization of doxorubicin nanoparticles prepared by ionic gelation. Trop J Pharm Res. 2018;17(12):2329–34.

Konan-Kouakou YN, Boch R, Gurny R, Allémann E. *In vitro* and *in vivo* activities of verteporfin-loaded nanoparticles. J Control Release. 2005;103:83–91.

Krishnamoorthy K, Mahalingam M. Selection of a suitable method for the preparation of polymeric nanoparticles: multi-criteria decision making approach. Adv Pharm Bull. 2015;5(1):57.

Kucukoglu V, Uzuner H, Kenar H, Karadenizli A. In vitro antibacterial activity of ciprofloxacin loaded chitosan microparticles and their effects on human lung epithelial cells. Int J Pharm. 2019;569:118578.

Kumari A, Yadav SK, Yadav SC. Biodegradable polymeric nanoparticles based drug delivery systems. Colloids Surf B Biointerfaces. 2010;75(1):1–18.

Kunjachan S, Jose S, Lammers T. Understanding the mechanism of ionic gelation for synthesis of chitosan nanoparticles using qualitative techniques. Asian J Pharm Sci. 2014;4(2):148–53.

Lee BK, Yun Y, Park K. PLA micro-and nano-particles. Adv Drug Deliv Rev. 2016;107:176–91.

Lim K, Hamid ZA. Polymer nanoparticle carriers in drug delivery systems: research trend. In: Applications of

nanocomposite materials in drug delivery. San Diego: Elsevier Science & Technology; 2018. p. 217–37.

Mendoza-Muñoz N, Quintanar-Guerrero D, Allémann E. The impact of the salting-out technique on the preparation of colloidal particulate systems for pharmaceutical applications. Recent Pat Drug Deliv Formul. 2012;6(3):236–49.

Mohammed MA, Syeda J, Wasan KM, Wasan EK. An overview of chitosan nanoparticles and its application in non-parenteral drug delivery. Pharmaceutics. 2017;9(4):53.

Muthu M. Nanoparticles based on PLGA and its co-polymer: an overview. Asian J Pharm Sci. 2009;3(4):266–73.

Nagavarma BVN, Yadav HK, Ayaz A, Vasudha L, Shivakumar H. Different techniques for preparation of polymeric nanoparticles-a review. Asian J Pharm Clin Res. 2012;5(3):16–23.

Naskar S, Koutsu K, Sharma S. Chitosan-based nanoparticles as drug delivery systems: a review on two decades of research. J Drug Target. 2019;27(4):379–93.

Pal S, Saha C. Solvent effect in the synthesis of hydrophobic drug-loaded polymer nanoparticles. IET Nanobiotechnol. 2017;11(4):443–7.

Palaniraj S, Murugesan R, Narayan S. Chlorogenic acid-loaded calcium phosphate chitosan nanogel as biofilm degradative materials. Int J Biochem Cell Biol. 2019;114:105566.

Pan C, Qian J, Fan J, Guo H, Gou L, Yang H, Liang C. Preparation nanoparticle by ionic cross-linked emulsified chitosan and its antibacterial activity. Colloid Surf A Physicochem Eng Asp. 2019;568:362–70.

Qu N, Lee RJ, Sun Y, Cai G, Wang J, Wang M, Lu J, Meng Q, Teng L, Wang D, Teng L. Cabazitaxel-loaded human serum albumin nanoparticles as a therapeutic agent against prostate cancer. Int J Nanomedicine. 2016;11:3451–9.

Rahmani S, Villa CH, Dishman AF, Grabowski ME, Pan DC, Durmaz H, Misra AC, Colón-Meléndez L, Solomon MJ, Muzykantov VR. Long-circulating Janus nanoparticles made by electrohydrodynamic co-jetting for systemic drug delivery applications. J Drug Target. 2015;23(7–8):750–8.

Reis CP, Neufeld RJ, Ribeiro AJ, Veiga F. Nanoencapsulation I. Methods for preparation of drug-loaded polymeric nanoparticles. Nanomed-Nanotechnol. 2006;2:8–21.

Sailaja AK, Amareshwar P, Chakravarty P. Different techniques used for the preparation of nanoparticles using natural polymers and their application. Int J Pharm Pharm Sci. 2011;3(2):45–50.

Sibambo SR, Pillay V, Choonara YE, Penny C. A novel salted-out and subsequently crosslinked poly (lactic-co-glycolic acid) polymeric scaffold applied to monolithic drug delivery. J Bioact Compat Polym. 2008;23(2):132–53.

Sibambo SR, Pillay V, Choonara YE, Du Toit LC, Khan RA, Penny C. Kinetic and structural modeling mechanisms of melatonin transport from an electrolytically regulated salted-out PLGA scaffold. J Bioact Compat Polym. 2009;24:266–96.

Song W, Gregory DA, Al-janabi H, Muthana M, Cai Z, Zhao X. Magnetic-silk/polyethyleneimine core-shell nanoparticles for targeted gene delivery into human breast cancer cells. Int J Pharm. 2019;555:322–36.

Taghizadeh MT, Ashassi-Sorkhabi H, Afkari R, Kazempour A. Cross-linked chitosan in nano and bead scales as drug carriers for betamethasone and tetracycline. Int J Biol Macromol. 2019;131:581–8.

Tapia-Hernández JA, Del-Toro-Sánchez CL, Cinco-Moroyoqui FJ, Ruiz-Cruz S, Juárez J, Castro-Enríquez DD, Barreras-Urbina CG, López-Ahumada GA, Rodríguez-Félix F. Gallic acid-loaded zein nanoparticles by electrospraying process. J Food Sci. 2019;84(4):818–31.

Tsai C-H, Wang P-Y, Lin I, Huang H, Liu G-S, Tseng C-L. Ocular drug delivery: role of degradable polymeric nanocarriers for ophthalmic application. Int J Mol Sci. 2018;19(9):2830.

Tzeyung AS, Md S, Bhattamisra SK, Madheswaran T, Alhakamy NA, Aldawsari HM, Radhakrishnan AK. Fabrication, optimization, and evaluation of rotigotine-loaded chitosan nanoparticles for nose-to-brain delivery. Pharmaceutics. 2019;11:26.

Van de Ven H, Vermeersch M, Vandenbroucke R, Matheeussen A, Apers S, Weyenberg W, De Smedt S, Cos P, Maes L, Ludwig A. Intracellular drug delivery in Leishmania-infected macrophages: evaluation of saponin-loaded PLGA nanoparticles. J Drug Target. 2012;20(2):142–54.

Vauthier C, Bouchemal K. Methods for the preparation and manufacture of polymeric nanoparticles. Pharm Res. 2009;26(5):1025–58.

Villegas-Peralta Y, Correa-Murrieta MA, Meza-Escalante ER, Flores-Aquino E, Álvarez-Sánchez J, Sánchez-Duarte RG. Effect of the preparation method in the size of chitosan nanoparticles for the removal of allura red dye. Polym Bull. 2019;76:4415–30.

Wang Q, Wang J, Ding W, Zhang D, Reed K, Zhang B. Alternatives to carcinogenic preservatives in Chinese sausage-Sorbic acid-loaded chitosan/tripolyphosphate nanoparticles. Int J Biol Macromol. 2018;120:28–33.

Wei Q, Wei W, Lai B, Wang L-Y, Wang Y-X, Su Z-G, Ma G-H. Uniform-sized PLA nanoparticles: preparation by premix membrane emulsification. Int J Pharm. 2008;359(1–2):294–7.

Wu P, He X, Wang K, Tan W, He C, Zheng M. A novel methotrexate delivery system based on chitosan-methotrexate covalently conjugated nanoparticles. J Biomed Nanotechnol. 2009;5(5):557–64.

Yaghoobi N, Majidi RF, ali Faramarzi M, Baharifar H, Amani A. Preparation, optimization and activity evaluation of PLGA/streptokinase nanoparticles using electrospray. Adv Pharm Bull. 2017;7(1):131.

8 Nanogel Synthesis by Irradiation of Aqueous Polymer Solutions

S. Duygu Sütekin, Olgun Güven, and Nurettin Şahiner

Abstract

Nanogels/microgels are intramolecularly crosslinked particles with submicron diameters that can swell in a suitable solvent due to their three-dimensional network structure. Nanogels provide beneficial features such as flexibility, biocompatibility, high stability and swelling, fixed shape, large surface/volume ratio, fast stimuli-responsive behavior, etc. Therefore, there is growing interest to further elaborate nanogel formulations in preclinical applications as therapeutics, diagnostics, or nanosensors. However, conventional nanogel synthesis methods may end up with nanogels containing toxic residuals, e.g., initiator, crosslinking agent, and fragments which possess a major disadvantage in biomedical applications requiring tedious purification steps. This chapter reviews the synthesis of nanogels by irradiation of dilute aqueous polymer solutions to induce intramolecular crosslinking by gamma rays or accelerated electrons. This simple, ecofriendly, and cost-effective manufacturing method eliminates the purification step and provides the possibility to produce clean nanogels with desired sizes at room temperature. In the formation of nanogels, the degree of crosslinking can be controlled by polymer solution properties as well as operational parameters such as dose rate of radiation source and total absorbed dose. The method can be applied to many water-soluble polymers, copolymers, or interpolymer complexes for the development of nanogels with desired sizes and properties.

Keywords

Nanogels · Crosslinking · Ionizing radiation · Gamma · E-beam

Abbreviations

ATRP	atom transfer radical polymerization
CinAlg	cinnamoyl alginate
CinPlu	cinnamoyl pluronic F127

S. D. Sütekin · O. Güven (✉)
Department of Chemistry, Hacettepe University, Ankara, Turkey
e-mail: guven@hacettepe.edu.tr

N. Şahiner (✉)
Faculty of Science & Arts, Department of Chemistry, ÇanakkaleOnsekiz Mart University, Çanakkale, Turkey

Department of Chemical and Biomolecular Engineering and Department of Ophthalmology, Morsani College of Medicine, University of South Florida, Tampa, FL, USA

J. K. Patel, Y. V. Pathak (eds.), *Emerging Technologies for Nanoparticle Manufacturing*,
https://doi.org/10.1007/978-3-030-50703-9_8

CMA	4-Methyl-[7- (methacryloyl)oxy] ethyl]oxy]coumarin (coumarin methacrylate)
DMA	N,N-di-methylacrylamide
IUPAC	international union of pure and applied chemistry
NMP	nitroxide-mediated polymerization
RAFT	reversible addition–fragmentation transfer
DMIA	Dimethyl maleinimido acrylamide
HEMA	hydroxyethyl methacrylate
Dex	dextran
NiPAAm	N-isopropylacrylamide
AMPS	acrylamido-2-methylpropane sulfonic acid
AAm	acrylamide
PVME	poly(vinyl methyl ether)
DMAEMA	2-(dimethylamino) ethyl methacrylate
IA	itaconic acid
CEA	2-cinnamoyloxyethyl acrylate
eU	electron energy
PRF	pulse repetitive frequency
PRR	pulse repetition rate
τ	pulse duration
DPP	dose per pulse
I	beam current
Q	volumetric flow rate
R_g	radius of gyration
IPN	interpenetrating network
IPC	interpenetrating complex
INH	isoniazid
CMS	carboxymethyl starch
VPTT	volume phase transition temperature
SLS	sodium lauryl sulfate
APMAM	3-aminopropyl) methacrylamide hydrochloride
mAb	monoclonal antibody
HA-MA	methacrylated hyaluronic acid
AMF	alternating magnetic field
LET	linear energy transfer

1 Introduction

Nanotechnology has emerged as a new era of multidisciplinary science for the design of materials on atomic or molecular scales to be used in nanomedicine, biosensors, microfluidics, diagnostics, targeted drug delivery, etc. Advances in this field introduced many nanomaterials such as liposomes, micelles, biodegradable nanoparticles, and nano/microgels. Over time, an extensive literature has developed on these nanomaterials especially in nanomedicine in order to overcome the problems deriving from the use of large-sized materials such as poor stability, poor bioavailability, and poor solubility. It was reported that more than 40% of market approved drugs and nearly 90% of newly discovered drugs have poor water solubility (Loftsson and Brewster 2010). Nanogels are able to solubilize hydrophobic drugs or therapeutic agents and alter the biodistribution of drugs by some beneficial factors such as stability, ease of functionalization/modification, etc.

Nanogels were obtained from their macroscopic analogues, i.e., hydrogels, composing of three-dimensional network through physical and chemical crosslinking. Macroscopic gels are a specific class of polymers that can swell to a large extent in a solvent by maintaining their network structure in the swollen state with the presence of permanent crosslinks. The term "macroscopic (polymeric) gel" is a general definition that covers other situations where the solvents may vary, e.g., water and body fluids. On the other hand, the term "hydrogel" is proposed where the solvent filling the pores of the network structure is water. Wichterle and Lim introduced the first synthetic hydrogel structure consisting of poly(2-hydroxyethymethacrylate). After their first report on clinical application as soft contact lenses (Wichterle and Lím 1960), there has been an exponential increase in the scientific reports on hydrogels mostly covering applications in adsorption (Kılıç et al. 2005; Pekel et al. 2001; Şahiner et al. 2000; Shafiq et al. 2019), catalysis (Şahiner 2013; Şahiner et al. 2011; Şahiner and Özay 2011), tissue engineering (García et al. 2019; Hou et al. 2019; Liang et al. 2019; Liu et al. 2020; Tibbitt

and Anseth 2009), molecular recognition (Chen et al. 2014; Tomatsu et al. 2006; Yao et al. 2019), and controlled release (Wei et al. 2019; Yuan et al. 2019; Yue et al. 2019) and drug delivery applications (Ekici et al. 2011; Shi et al. 2019; Sılan et al. 2012; Solomevich et al. 2019; Wu et al. 2019) due to their swelling ability and biocompatibility with living tissue.

Nanogels (nanohydrogels) can be defined as nanoscale dispersions of polymer chains (hydrogels) crosslinked in a physical or a chemical way, possessing diameters up to 100 nm (IUPAC). However, submicron gel particles with diameters up to 1 μm have also been classified as nanogels in the early literature. Compared to macroscopic gels, they have much lower viscosity, very high surface area, rapid thermal response, and rapid solution response (i.e., pH sensitivity). Nanogels are commonly synthesized from hydrophilic polymers having functional groups as –COOH, $–NH_2$, $–SO_3H$, $–CONH_2$, etc. They can be comprised of synthetic (co)polymers such as PEG (Nordström et al. 2019), PVP (Sütekin and Güven 2019), PAA (Zhao et al. 2019), PNiPAAm (Chen et al. 2019), or natural polymers including chitosan (Ashrafi et al. 2019), poly(lactic acid) (Can et al. 2019), pullulan (Richa and Roy Choudhury 2020), and hyaluronic acid (Richa and Roy Choudhury 2020), which have commonly been reported in the literature as the raw material of nanogels.

Nano/microgels have been first described in the work of Staudinger in 1935 as a by-product in the form of divinyl benzene microgels (Staudinger and Husemann 1935). However, the term "microgel" was first introduced by Baker in 1949 who worked on emulsions of styrene-butadiene rubbers (SBR) and recognized that these crosslinked structures were intramolecularly crosslinked macromolecules which constituted a new form of polymer molecule. His findings showed that microgels behaved like Einstein spheres, and unlike dissolved linear polymer coils, they show very low solution viscosities (Baker 1949). Since then, an extensive literature has developed on nanogels/nanohydrogels/microgels (Fig. 8.1). The terms "nanogel" and "microgel" are still not fully distinguishable in the literature, and the use of the term "microgel" for submicron structures is still common. However, the term "nanogel" will be used throughout this chapter to cover internally crosslinked macromolecules with diameters in submicron range.

2 Nanosized Particles in Medicine

Nanomedicine integrates nanotechnology with medicine, leading to a groundbreaking advance in the diagnosis and treatment steps with the invent of several systems such as polymer-drug conjugates (Ekladious et al. 2019; Zhou et al. 2019), liposomes (Xia et al. 2019; Zahednezhad et al. 2019), micelles (Cabral et al. 2018; Hanafy et al. 2018; Tambe et al. 2019), nanospheres (Jiang et al. 2019; Lu et al. 2010; Tan et al. 2007), nanocapsules (Yang et al. 2014; Zeng et al. 2018; Zheng et al. 2016), dendrimers (Fan et al. 2019; Jayakumar et al. 2018; Li et al. 2018), and nanogels (Oh et al. 2008). Figure 8.2 shows some of these different architectures schematically. The requirements in the use of these structures as drug delivery systems include small size, biocompatibility, biodegradability, high loading capacity, and prolonged circulation (Brigger et al. 2002; Truong et al. 2015).

There are two methods used for specific targeting using nanosized polymer-drug conjugates. The first one is known as passive targeting where nanoparticle (NP) accumulation through target is made mainly by its size. The second route is to provide site-specific targeting by inducing stimuli-responsive properties (e.g., temperature, pH), ligand-receptor binding, etc. Further details on stimuli-responsive (smart) nanogels will be given in detail.

When nanoparticles are used as drug delivery vehicles for passive tumor targeting, they can easily penetrate and accumulate into tumor tissue due to the enhanced permeability and retention (EPR) effect (Abdalla et al. 2018; Iyer et al. 2006). Figure 8.3 illustrates this effect that, when NPs are administered intravenously, they are unable to penetrate through tight endothelial cells of normal tissue vasculatures, whereas they can

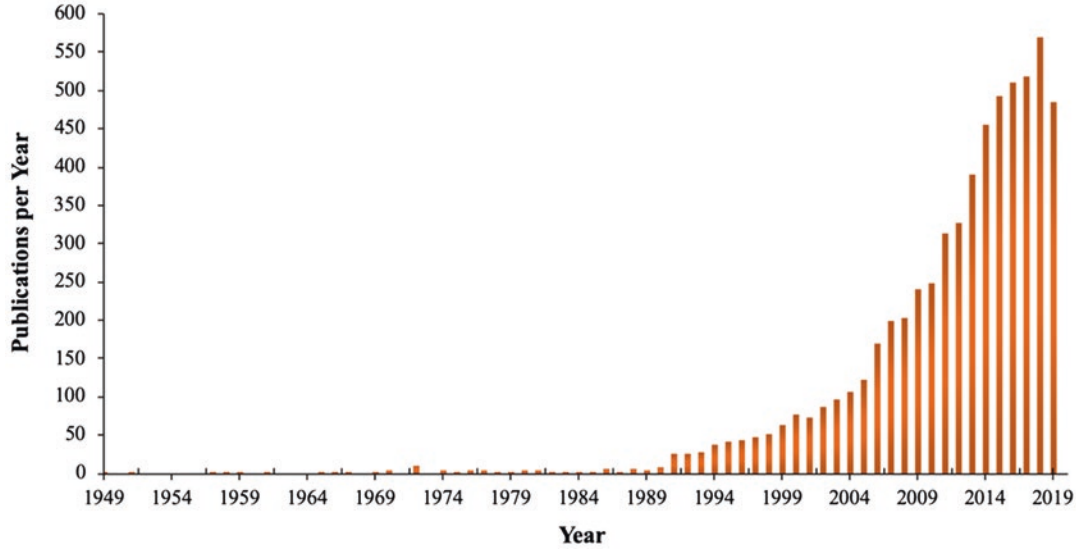

Fig. 8.1 Evolution of the number of publications on nanogels/nanohydrogels/microgels since 1949. (Data taken from web of science citation reports)

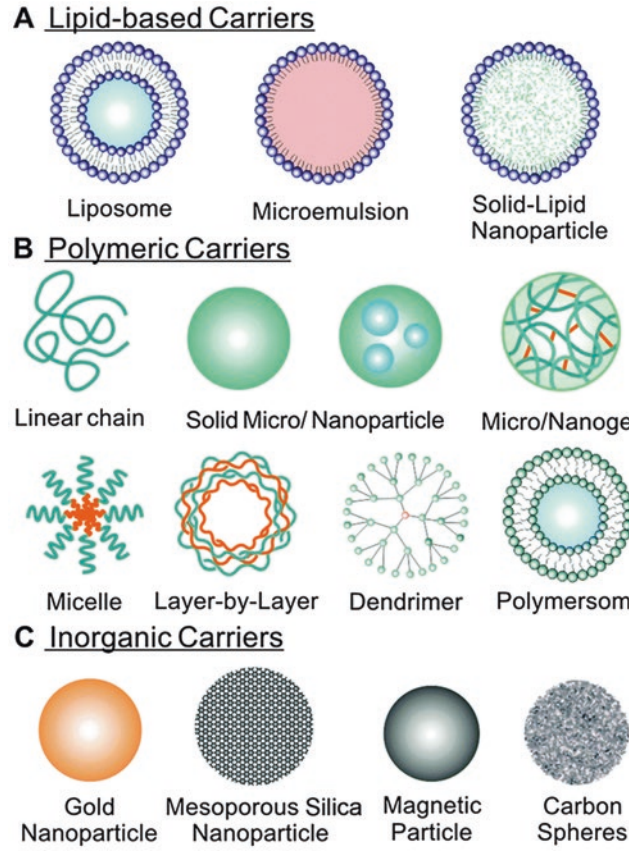

Fig. 8.2 Schematic illustration of various types of micro/nanodrug delivery systems. (Reproduced with permission (Mo et al. 2014), Copyright 2014 The Royal Society of Chemistry)

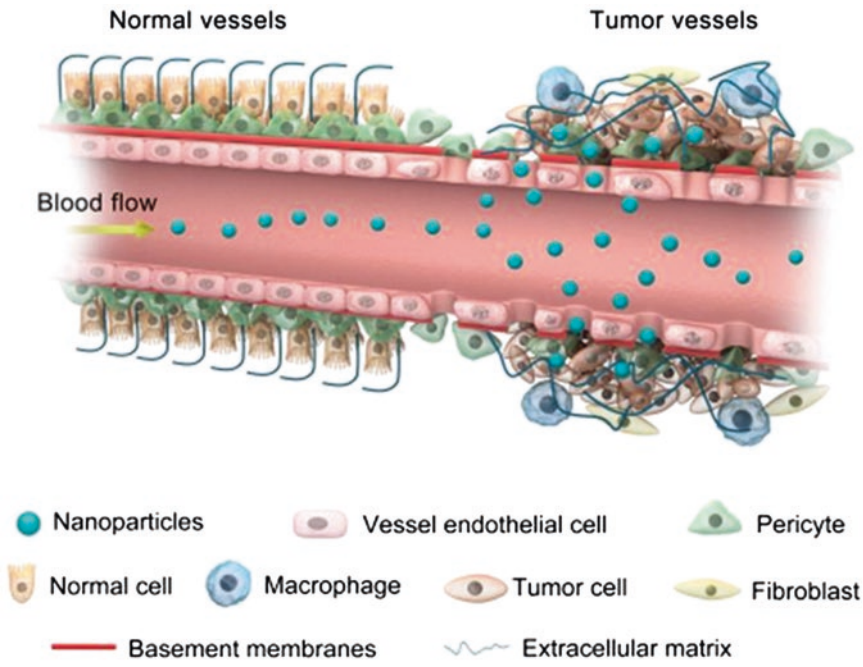

Fig. 8.3 Accumulation of nanoparticles in tumor tissues via the EPR effect. (Reproduced with permission (Abdalla et al. 2018), Creative Commons 2018)

selectively accumulate in metastasized tumor tissue due to its abnormal leaky vasculature structure.

Nanoparticle properties such as size, architecture, and surface characteristics strongly affect the circulation time in blood and the bioavailability of particles in the body by evading RES (Desai et al. 1997; Tong and Cheng 2007). Figure 8.4 emphasizes this event where particles with very small diameters ($d < 5$ nm) can be easily removed from the body by filtration through kidneys. On the other hand, particles having diameters more than 150 nm are entrapped within liver and spleen and will be unable to reach the targeted area. Therefore, NPs with an optimal size between 20 and 150 nm will be eliminated by the mononuclear phagocyte (MPS) system and accumulate in tumor tissues. It should also be noted that particle size plays an important role in the responsiveness to external stimuli since the response rate towards change of stimuli is inversely proportional to the square of the size of the gel (Tanaka and Fillmore, 1979). Moreover, drug loading can also be facilitated by controlling nanoparticle size. For instance, PNiPAAm nanogels with mean diameters from 65 to 450 nm were synthesized and mixed with solid drug nanoparticles of a HIV drug lopinavir to demonstrate how size modifies the drug release behavior. It is evidenced that larger nanogels showed faster release profiles (Town et al. 2019). Longer circulation times can also be reached by controlling surface charge of nanogels to be neutral or slightly negative (Blanco et al. 2015). Figure 8.4 illustrates biodistribution of drugs with different sizes, architectures, and surface properties among lungs, liver, spleen, and kidneys. Therefore, it is of high importance to control the dimensions of nanogels and to gain information about the parameters affecting their size and size distribution.

3 Nanogels: Highlights and Applications

Unlike other polymeric nanoparticles, such as nanospheres, the three-dimensional network of nanogels allows entrapment of biomolecules into

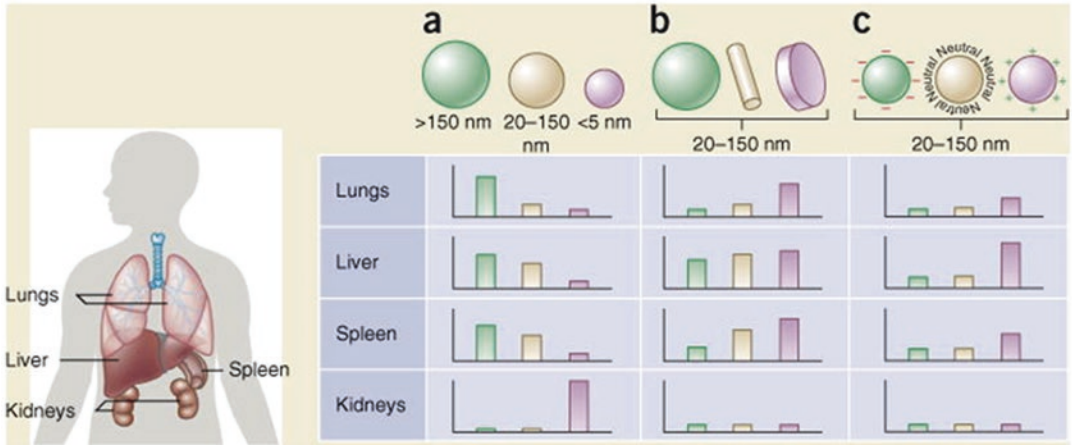

Fig. 8.4 Nanoparticle size, shape, and surface charge dictate biodistribution among different organs including lungs, liver, spleen, and kidneys. (Reproduced with permission (Blanco et al. 2015), Copyright 2015Springer Nature)

their nanospace. Moreover, this network structure promotes increased stability with respect to micelles. Other promising features of nanogels include high water uptake, biocompatibility, flexibility, and fixed shape. Their large surface/volume ratio enables more conjugation with drugs through the presence of functional groups. Nanogel formulations can be classified due to their architecture. Different types of nanogels such as core-shell, layer by layer, and hollow nanogels were presented in the literature for a variety of drug delivery applications (Fig. 8.5).

Spontaneous drug loading can be facilitated by simply mixing aqueous dispersions of nanogels with suitable drug. Thus, sizable and high amount of drug loading (up to 50% of weight) can be achieved. Therefore, many problems arising from drug resistance can be altered, thanks to increased local drug concentration at a targeted site. Nanogel-drug formulations show low buoyant density which enhances their dispersion stability. These properties eliminate the necessity of using organic solvents, additives, or mechanical energy during drug loading. Nanogel-drug formulations can be lyophilized and stored at room temperature, presenting practical advantage for therapeutic applications (Vinogradov et al. 2002, 2005, 2006).

Release of the drug from nanogels can be triggered by near-infrared light (NIR), alternating magnetic field (AMF), ultrasound, etc. (Liu et al. 2015). Moreover, biodegradable nanogels can be used as drug delivery systems that are able to release the drug with the help of degradable bonds, i.e., ester, amide, and anhydride, which are either present in polymer chains or crosslinkers (Elkassih et al. 2019; Zhu et al. 2018). On the other hand, specific examples demand nondegradable nanogels. Lajud et al. performed in vitro studies using fluorescent-labeled liposomal nanogels and chitosan-based hydrogels as a drug delivery system and demonstrated that this hybrid structure can be present under physiological conditions without degradation for at least 2 weeks and can safely transport therapeutic agents from the middle ear to the inner ear (Lajud et al. 2015).

One of the main factors directly affecting the success of nanogel applications is the control of their swelling ability that mostly depend on their chemical structure and degree of crosslinking. However, for smart or responsive nanogels, the swelling degree can be governed by solution pH, ionic strength, and temperature promoting structural changes (Cao et al. 2016; Hajebi et al. 2019). Nanogels obtained from poly(N-isopropyl acrylamide (PNiPAAm) and poly(vinyl methyl ether) (PVME) are some examples to smart nanogels (Kabanov and Vinogradov 2009; Luckanagul et al. 2018). However, current interest is to prepare nanogels with multi-responsive properties that show structural or morphological changes to several factors. For instance, Peng

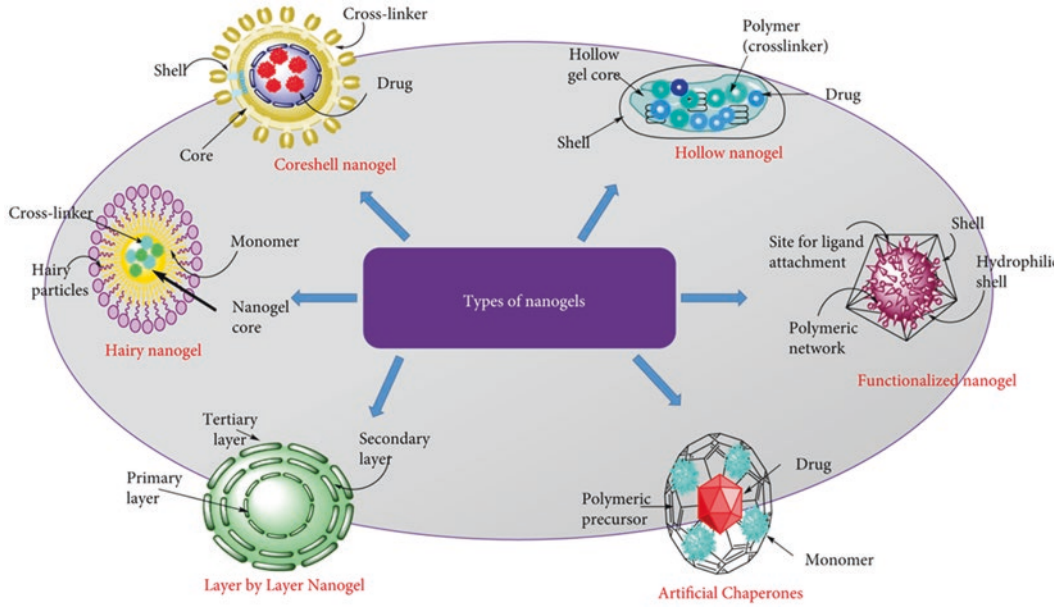

Fig. 8.5 Different types of nanogel formulations. (Reproduced with permission (Sabir et al. 2019), Creative Commons 2019)

et al. synthesized P(N-isopropylacrylamide-co-vinylphenylboronic acid) nanogels for naked eye monitoring of glucose in urine fluid noninvasively. Multi-responsive nanogels were synthesized via emulsion polymerization technique, and they possessed sensitivity to pH, temperature, and glucose concentration. Their self-assembly resulted in observable color changes to glucose concentration as low as 1 mM (Peng et al. 2019).

Nanogels can also serve as matrices for metallic nanoparticles. Liu et al. synthesized reversibly crosslinked nanogels consisting of poly (vinyl alcohol-b-N-vinylcaprolactam) (P(VA-b-VCL)) coating Fe_2O_3 nanoparticles. These nanogels possessed superparamagnetic property; hence, drug release could be performed under AMF. Multiple response mechanisms were carried out with their sensitivity to glucose, pH, and temperature (Liu et al. 2014).

Nanogels can be used as chemical or biological sensors by internalization of a sensing probe. Wu et al. presented a multifunctional core-shell hybrid nanogel for combining optical sensing and cellular imaging of cancer cell and targeting a model anticancer drug temozolomide (TMZ) and photothermal treatment of tumor cells. These properties were provided with the help of Ag-Au bimetallic nanoparticle as core, thermoresponsive crosslinked PEG as shell and incorporated hyaluronic acid (HA) chains onto the surface of nanogels (Fig. 8.6a). The therapeutic efficacy of these multifunctional nanogels was higher than both of chemotherapy and photothermal therapy (Fig. 8.6b) indicating a synergistic multi-stimuli-responsive behavior for the treatment of mouse melanoma B16F10 cells with the TMZ-loaded hybrid nanogels (Wu et al. 2010).

Li et al. proposed a nanogel sensor to function as an ionizing radiation dosimeter in radiotherapy up to 20 kGy based on polyacrylamide nanogel covalently bonded with coumarin-3-carboxylic acid, an IR-sensitive fluorescent probe, and 5(6)-carboxytetramethylrhodamine, an IR reference probe. Figure 8.7 shows the colorimetric fluorescence measurements of PAAm-based nanogels possessing good linearity between 0 and 20 kGy (Li et al. 2019).

Nanogels not only provide internal space for therapeutics but also control their efficacy by their chemical structure. For instance, Weldrick

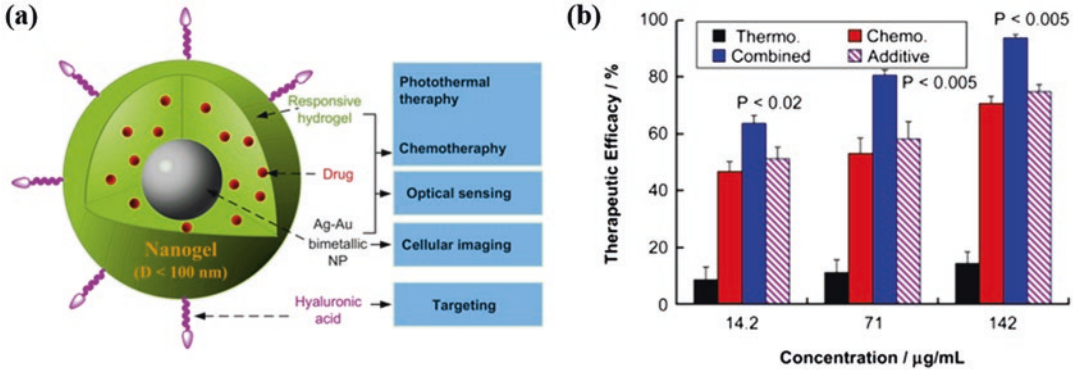

Fig. 8.6 (**a**) Schematic illustration of Ag-Au@PEG-HA hybrid nanogels and (**b**) therapeutic efficacies of photothermal, chemo, and combined treatments with hybrid nanogels. (Reproduced with permission (Wu et al. 2010), Copyright 2010 Elsevier)

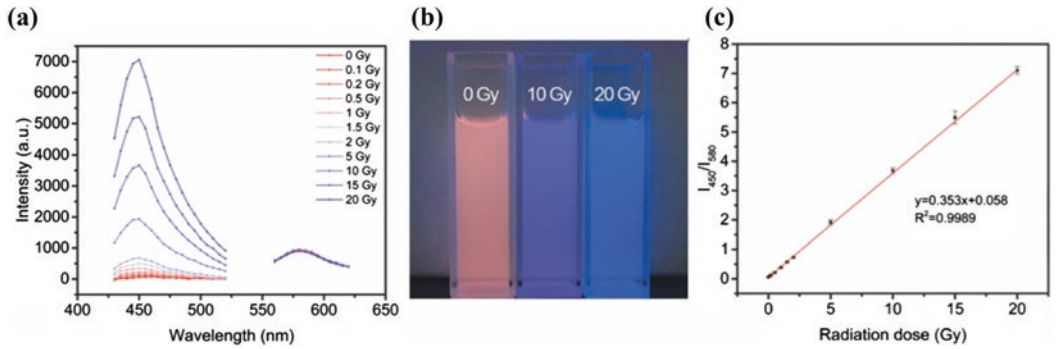

Fig. 8.7 (**a**) Fluorescence emission spectra. (**b**) The photographs of the X-ray-irradiated PAATC nanogel sensors under UV excitation at 365 nm. (**c**) Fluorescence ratio (I450/I580) of the PAATC nanogels after exposure to X-rays in the range of 0–20 Gy. (Reproduced with permission (Li et al. 2019), Copyright 2019 The Royal Society of Chemistry)

et al. developed antibiotic-loaded PAA nanogels coated with cationic poly(ethylene imine) to overcome antibacterial resistance. They observed enhanced antibiotic effect on several bacteria due to the electrostatic attraction between negatively charged bacterial cell wall and positively charged nanogel system (Weldrick et al. 2019).

Several studies on nanogels show that nanogels show low cytotoxicity. For instance, curcumin-loaded nanogels based on gelatin and poly(acrylamidoglycolic)acid showed a profound increase in anticancer activity compared to free curcumin. Synthesized nanogels showed high biocompatibility with cell viability higher than 97% (Madhusudana Rao et al. 2015). Yu et al. performed loading of doxorubicin to hyaluronic acid nanogels containing SiO_2/Fe_3O_4 nanoparticles. They observed a significant decrease in cytotoxicity toward HeLa cells compared to that of free doxorubicin suggesting better cell targeting and cellular uptake of nanogels into target cancer cells (Yu et al. 2016).

Detailed information on the biomedical applications of nanogels can be found in present reviews (Dalwadi and Patel 2015; Liu and An 2014; Neamtu et al. 2017; Niharika et al. 2018; Soni et al. 2016; Tahara and Akiyoshi 2015; Zhang et al. 2016).

Apart from the above-mentioned applications, other important fields include their use as coatings

(Holtz and Asher 1997), super absorbents (Bueno et al. 2009), nanodevices (Van der Linden et al. 2002), nanoreactors (Li et al. 2009) and nanocrystals (Bagde et al. 2019).

4 Synthesis Methods of Nanogels

Several synthetic approaches were proposed to obtain submicron gels. The most explored synthesis methods for the preparation of nanogels are (i) polymerization of monomer or monomer mixtures and (ii) crosslinking of polymers. Other less explored techniques for nanogel synthesis such as photolithography and micromolding are taken out of the scope of this text. Regardless of the synthesis technique, the most important parameters are size, architecture, and colloidal stability, which directly affect the usability of nanogels for a variety of applications.

4.1 Crosslinking/Polymerization of Monomer or Monomer Mixtures

Direct polymerization of vinylic monomers with di- or multifunctional comonomers ends up with crosslinking polymerization. Here the comonomers such as di(meth)acrylates are used as crosslinkers. Crosslinking polymerization techniques are studied intensely over the years to obtain macroscopic networks. Polymerization starts from a monomer or a monomer mixture where the ongoing process is generally free radical polymerization. For the propagation step, reactive sites of the propagating chain may react either with a monomer, with a group that is still reactive on its own chain or with a reactive pendant group on another chain. The latter case will cause branching in polymeric chains, and after a certain point, gelation begins and eventually a three-dimensional network structure will develop (intermolecular crosslinking). This leads the system to a macroscopic gel ("wall to wall" gel) where its dimensions are defined in the limits of the reaction vessel. The other possibility, reaction of the propagating chain with a reactive group on its own chain, can be classified as intramolecular crosslinking. The linear chain will become a coil, and in an ideal case, where only this process occurs, the final product will be a solution containing separate permanent coils with a compact shape fixed with high number of crosslinks. Depending on the synthesis parameters, sizes of these coils may vary, and they can be identified as microgels or nanogels. In practice, separating these two processes and obtaining only one type of product is a challenge due to the fact that most of the time these two processes occur concomitantly.

Direct polymerization of monomers can be applied using conventional free radical polymerization, anionic polymerization, and controlled/living radical polymerization techniques in dilute homogeneous media. In addition, emulsion-based crosslinking polymerization is widely preferred for the synthesis of nanogels under heterogeneous polymerization conditions.

Conventional free-radical crosslinking is the most common route for the synthesis of nanogels because of its simplicity and applicability to different monomers and media. However, there are some drawbacks for this method. Since there is a competition between inter- and intramolecular crosslinking during the propagation step, the synthesis parameters should be carefully controlled especially for free radical crosslinking. One way to favor microgelation over macrogelation is to perform polymerization in highly diluted medium due to the fact that when working in low concentrations the propagating chains are separated from each other and the probability of a crosslink between a reactive group on a propagating chain with a group on another chain is reduced, but in this case recovery of the products can be very low presenting a major disadvantage for large-scale industrial processes. Alternatively, polymerization can be stopped at low conversion to favor microgelation over macrogelation, but this time additional purification of unreacted monomers should be performed.

Direct polymerization of monomers can also be applied under heterogeneous reaction conditions. These include emulsion, inverse emulsion,

precipitation, and dispersion polymerization techniques. In general, emulsion polymerization sorts the microgelation problem out since crosslinking reactions are completed in single micelles that are separated by surfactant layers. Furthermore, since there are so many parameters (i.e., monomers, comonomers, initiators, surfactants, etc.), it is possible to optimize the polymerization process and have a control over particle size, polydispersity, and architecture (Chai et al. 2010; Peng et al. 2010; Zillessen and Bartsch 2010) of nano- or microgels proper for desired applications.

In conventional emulsion polymerization processes, the system is composed of a relatively hydrophobic monomer, initiator, and an oil-in-water (O/W) emulsifier (surfactant) dispersed in aqueous medium by mechanical stirring. Alternatively, the synthesis of hydrophilic nanogels from water-soluble monomers should be performed in a continuous organic phase (W/O) in which case the process is referred to as inverse emulsion polymerization. In general mechanism of emulsion polymerization, initiation takes place in the continuous phase, and monomer droplets (diameter $\approx 10^4$ nm) are emulsified with the aid of a surfactant. Subsequently these monomer droplets lead the system to form monomer micelles that can either be inactive and active during propagation step of FRP. After the consumption of monomers inside the micelle, metastable (kinetically stable) colloidal polymer dispersions (latexes) within the size range of 1–20 μm are produced via FRP in active micelle droplets (Fig. 8.8a). The use of di/multifunctional monomers further promote crosslinking inside the micelles and micro/nanogels are thus formed. The main drawback of classical emulsion polymerization process is that the size of the resultant polymeric particle does not correspond to the initial size of monomer dispersions. Moreover, polymerization can also be performed in monomer droplets and the dispersity of microgels is widened. This phenomenon can be avoided by increasing the amount of surfactant like in the cases of mini- or microemulsion. In miniemulsion process, kinetically stable droplets are formed under high shear by either ultrasonication, high-pressure homogenizer, or high-speed mechanical mixing around the critical micelle concentration (CMC). Thus, kinetically stable gels having diameters between 50 and 500 nm can be synthesized with good control of particle size distribution (Daniloska et al. 2014; Koul et al. 2011; Peres et al. 2018; Šálek et al. 2018). Thermodynamically stable emulsions with very narrow dispersities can be obtained by microemulsion polymerization process by using larger amounts of surfactant (at about 20%) (Fig. 8.8b). This high amount of surfactant induces the system being transparent, single phase with micelles less than 100 nm in diameter. These micelles have an extremely large oil-water interfacial area (~10^5 m^2 dm^{-3} in diameter). The main advantage of this system is the elimination of polymerization in monomer droplets. Hence, by using this technique, nearly monodisperse nano- or microgels can be synthesized which cannot be achieved with other emulsion polymerization techniques (Şahiner 2007, 2018; Şahiner et al. 2007; Şengel and Şahiner 2016). However, the presence of surfactant in higher amounts can be a serious problem since a complete removal of the surfactant should be made mainly due to toxicity concerns. Surfactant-free emulsion process can be a solution for this problem where stabilization was achieved either by ionic groups incorporated into unsaturated oligomers by initiator salts or by oligomers bearing ionic groups at chain ends (Ji et al. 2018; Şahiner and Şengel 2017).

Another common method for the synthesis of nanogels is precipitation polymerization where the initial system is composed of a homogeneous mixture of monomer and initiator in a particular solvent, but the formed polymer is insoluble in the reaction medium. The technique presents an advantage of obtaining nanogels free of any surfactant or stabilizer. This technique is mostly preferred for the development of thermoresponsive nanogels where precipitation can be triggered by changing temperature. Here, the polymer-solvent interactions are weakened by increasing temperature above the lower critical solution temperature (LCST) of the polymer, leading to a phase transition. PNiPAAm is among the most investigated

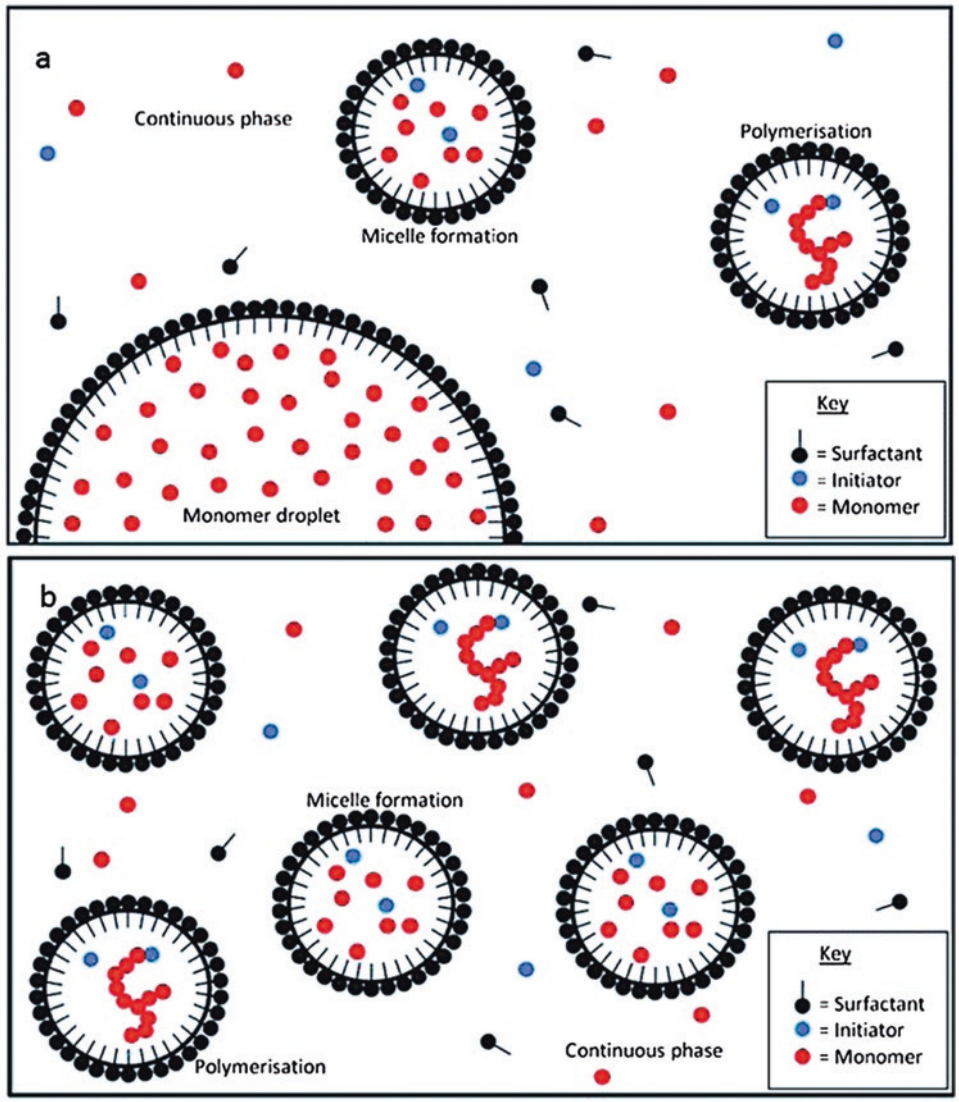

Fig. 8.8 The mechanisms of (**a**) emulsion polymerization and (**b**) microemulsion polymerization (Bonham et al. 2014). (Published by The Royal Society of Chemistry)

stimuli-responsive nanogels showing a LCST (Sahle et al. 2017; Zhou et al. 2015). Other examples include poly(vinylcaprolactam) (Wang et al. 2015) and poly(acrylamide-co-methacrylic acid) (Cenci et al. 2018).

Dispersion polymerization is identical to precipitation polymerization in nature, but the system contains colloidal stabilizers in addition to other compounds for the synthesis of stable nanogels. Thermoresponsive micro- or nanogels with narrow particle size distribution were obtained using this technique (Li et al. 2004, 2016; Şengel and Şahiner 2019).

In the synthesis of nanogels from monomers, UV irradiation is widely used to initiate the polymerization in the presence of photoinitiators and crosslinking with the help of crosslinking agents. Table 8.1 summarizes synthesis parameters, size of the nanogels, and highlights of the studies using UV irradiation method for the production of nanogels.

Table 8.1 Synthesis parameters, size of nanogels and highlights of the studies covering nanogel synthesis by UV-irradiation

Polymer	Synthesis parameters, size, and highlights	References
PNiPAAm-co-P(DMIAAm)	λ = 250–500 nm, t = 0–60 sfv	Vo et al. (2002)
	d = 62 nm	
	Size and swellability of the nanogels controlled by UV irradiation time, concentration of DMIAAm, and surfactant	
PEG-b-P(DMAEMA/CEA)	λ = 350 nm, t = 0–300 min	Yusa et al. (2009)
	d = 28 nm	
	RAFT-mediated copolymerization, micelle formation at pH > 7, UV-induced crosslinking of micelles to yield NGs	
P(NiPAAm-co-CMA)-b-P(DMA-co-CMA)	λ = 320 nm, t = 0–55 min	He et al. (2011)
	d = 47–58 nm	
	Both core- and shell-crosslinked nanogels exhibiting thermal- and photo-responsive properties	
PAAm-DNA	λ = 350 nm, t = 19 min	Kang et al. (2011)
	d = 315 nm	
	Photothermal release of doxorubicin from Au–Ag nanorods (Au–Ag NRs) coated with DNA crosslinked PAAm nanogels	
HA-MA	λ = 365 nm, t = 1–2 h	Messager et al. (2013)
	d = 144–804 nm	
	W/O nanoemulsion nanoreactors crosslinked by UV, effect of degree of methacrylation and no. of incident photons on sizes of NGs, loading of insulin and its pH dependent release	
CinAlg-CinPlu	λ = 365 nm, 400 W, t = 10, 20, 40, 60 min	Wang and Kim (2015)
	T = 10 °C, 20 °C, 30 °C, 40 °C	
	d = 94–213 nm	
	Thermoresponsive structure, heat-induced condensation of Pluronic F127 chains	
HA	λ = 365 nm, t = 1 min	Yu et al. (2016)
	d = 262 nm	
	SiO_2/Fe_3O_4 internalization of NG with endosome membrane components from source cancer cells and loading of doxorubicin	
P(Dex-HEMA)-co-PNiPAAm	λ = 320–400 nm, t = 30 min	Jafari and Kaffashi (2016)
	d = 350 nm	
	Dissolution at low temperature, phase transition, and degradation of the synthesized nanogels	
Polypeptide	λ = 365 nm, t = 20, 40, and 60 s	Jin et al. (2017)
	d = 234 nm	
	Polypeptide−gold nanoparticles hybrid nanogels	

The techniques mentioned up to this point only cover conventional free radical polymerization (FRP). The most important limitation of FRP techniques is that control over molecular weight, dispersity, composition, chain architecture, and functionality is difficult. These limitations strongly affect the structure-property relationship of nanogels for various applications. Recently, controlled radical polymerization (CRP) techniques have emerged to provide a better structural control and functionality. CRP has the advantages of FRP, i.e., the reaction conditions are relatively easy and can be applied to a wide range of monomers. In FRP techniques, the polymerization mechanism consists of a slow initiation with fast propagation and termination, leading to dead-end chains and broad molecular weight distribution. However, in CRP, fast initiation of radicals provides the formation of a large number of growing chains, whereas the terminated chains make up a small proportion of all chains (~1–10%). The remaining

chains are passive (dormant-stationary) chains and are open to reactivity, functionalization, and chain growth. As a result, polymer chains grow at a nearly constant rate, and the chain sizes of the resulting polymer molecules are very close to each other. In this way, polymers with low dispersity (Đ) can be obtained. Block copolymer synthesis is also possible by adding a different monomer to growing chain. Controlled radical polymerization methods include nitroxide-mediated polymerization (NMP), atom transfer radical polymerization (ATRP), and reversible addition-fragmentation chain transfer (RAFT) polymerization. Among these CRP techniques, ATRP (Amamoto et al. 2007; Jin et al. 2010; Jung et al. 2007) and RAFT (An et al. 2007; An et al. 2011a, b; He et al. 2011; Picos-Corrales et al. 2012; Yusa et al. 2009) polymerizations are mostly preferred for the production of functional nanogels with various architectures. However, ATRP has restrictions for acid-functional monomers (e.g., methacrylic acid) or initiators, and the resulting products are contaminated with metal ions; hence further purification should be assessed. RAFT polymerization, on the other hand, can be applied to many monomers, including functional monomers, for different reaction conditions and polymerization techniques such as emulsion and dispersion polymerization (Fu et al. 2017; Ma et al. 2015). More information on this topic can be found in the reviews on the use of controlled polymerization for the synthesis of nanogels (Charleux et al. 2010; Sanson and Rieger 2010).

4.2 Crosslinking of Preformed Polymers

Different from the previous techniques, this method starts from a polymer instead of a monomer or a monomer mixture; thus, it is alternatively called as "monomer-free technique." Here, properties of the product can be easily controlled by choosing the right polymer for synthesis of the desired product (proper grade, molecular weight, etc.). On the other hand, for some polymers whose monomers that don't exist, synthesis step will be impractical or even impossible from monomer-initiated nanogel synthesis. Using polymers as starting materials will also unravel this situation.

Crosslinking can be induced either chemically (covalent bonds) or by physical self-assembly of polymeric chains (non-covalent bonds). Nanogel synthesis by the physical self-assembly of a polymer includes secondary forces such as ionic, electrostatic, van der Waals interactions, or hydrogen bonding or by chain entanglements. Thus, reversible/irreversible destruction can be applied to these physical (pseudo) gels by changing temperature, pH, solvent, etc. Panja et al. synthesized polypeptide nanogels by the self-assembly of mannose-conjugated antimicrobial polypeptide and poly(arginine-r-valine) with Zn^{2+} ions where metal ions act as a coordination center and guanidine (from the arginine moiety) as a ligand (Panja et al. 2019). Zhang et al. prepared chitin nanogels by simply dissolving chitin in NaOH/urea solution by high-speed mechanical stirring. This physical process resulted in spherical nanogels having sizes around 25 nm (Zhang et al. 2019).

Chemical crosslinking method can be applied where the substrate is a preformed linear or branched polymer that contains reactive pendant groups which can undergo crosslinking reaction by an initiator, or a suitable crosslinking agent should be used to react with bifunctional polymers that will result in intramolecular combination. Different crosslinking methods were presented in the literature based on disulfide (Chen et al. 2019; Elkassih et al. 2019), amine (Su et al. 2018), and imine (Madhusudana Rao et al. 2015; Sarika and James 2015) bonds or click chemistry induced crosslinking. Comprehensive reviews on the synthesis of nanogels using these methods were presented in the literature (Khoee and Asadi 2016; Zhang et al. 2015).

5 Radiation-Induced Synthesis of Nanogels

Various radiation sources such as gamma, ultraviolet (UV), e-beam, ion beam, and X-ray have been explored by scientists for (co)polymerization (Sütekin et al. 2018; Sütekin and Güven 2018), surface modification (grafting) (Barsbay et al. 2007; Barsbay and Güven 2009), and crosslinking (Kadlubowski 2014; Şahiner et al. 1998). A significant progress in this field was achieved by using electromagnetic waves with high energy (very short wavelength) sufficient to ionize molecules and lead to chemical changes in the structure by chain scission or crosslinking, referred to as ionizing radiation (Fig. 8.9). Particularly ionizing electromagnetic waves such as gamma and e-beam are mostly used for the synthesis of nanogels to promote intramolecular crosslinking of preformed polymers. However, UV irradiation is also a very common method to prepare nanogels. It should be noted that UV is referred to be non-ionizing for wavelengths higher than 190 nm, and the studies dealing with nanogel synthesis mostly covers UV irradiation around 350 nm (see Table 8.1).

Source-based parameters such as dose rate (i.e., kGy/h for Co-60 gamma sources, current for linear accelerators) and other operational parameters such as absorbed dose and temperature in the radiation cell strongly affect the properties of the resultant materials. Radiation (absorbed) dose is defined as the energy deposited as a result of ionizations and excitations per unit mass of material and has the unit of gray (Gy), where 1 Gy equals to 1 J/kg.

In this technique the initiation step is induced by the absorption of ionizing radiation in the form of gamma rays that are emitted from the nucleus of some unstable (radioactive) atoms like cobalt-60 or cesium-137 or fast electrons that are produced by electron accelerators. The theory behind this method will be discussed in a separate section, but it should first be pointed out that the only difference from the other methods is the initiation step. One can work in bulk, emulsion, or solution; however, the method mentioned here is composed of irradiation of a polymer solution where the effect of ionizing radiation on a polymer chain is mainly "indirect." That means, radiation energy is exclusively absorbed by solvent molecules, and as a result generated reactive species start the initiation. However, to gain control over the process, the theoretical knowledge on radiation chemical aspects should be elaborated. Since most of the syntheses are carried out in aqueous systems, it is crucial to understand the general concepts of water radiolysis and subsequent effects of reactive species on polymeric solutes.

5.1 Radiation Chemistry of Aqueous Systems

An important and distinguishing feature of ionizing radiation is that its absorption is in a nonselective way so that molecules are ionized

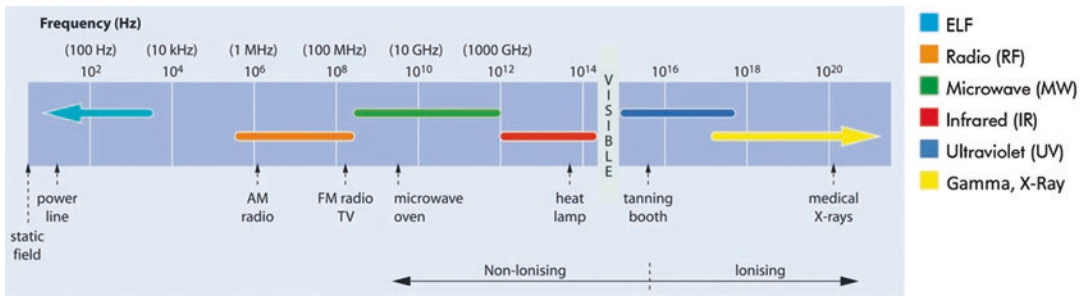

Fig. 8.9 Electromagnetic spectrum. Reproduced from the European Commission, Research Directorate-General, European Communities (2005). Health and Electromagnetic Fields: EU-funded research into the impact of electromagnetic fields and mobile telephones on health, Copyright 2005 European Communities

according to their relative abundance in the medium. Therefore, for dilute solutions, the knowledge of the radiation chemistry of the solvent is the centerpiece. Primary reactive species are predominantly formed in the solvent and then induce secondary chemical effects in minor solutes. This phenomenon is called as "indirect effect." On the other hand, direct effects are dominant in cases where the reactive radicals cannot move freely (i.e., at solute concentrations above 0.1 M for small solutes or in bulk material) (Spinks and Woods 1964).

The action of ionizing radiation on water has been the subject of intensive experimental and theoretical studies. The interest in radiolysis of water arises from its relative simplicity and its biological and ecological importance. The wide variety of aqueous systems is of special interest in radiobiology and nuclear reactor technology.

Historically, the processes taking place when water is subjected to high-energy radiation began to interest scientists only a few years after the first successful separations of weighable amounts of radium salts. Thus, it was found by Curie and Debierne as early as 1901 that solutions of radium salts continually involve hydrogen and oxygen gases (Curie and Debierne 1901). Additionally, formation of H and OH radicals by irradiation of water was first noted by Debierne in 1914 (Debierne 1914). However, systemic studies in radiation chemistry have only been possible with the safe use of gamma-emitting radioisotopes and electron accelerators.

^{60}Co sources and electron beam accelerators are frequently used as radiation sources due to their relatively low cost, availability, and convenience. Gamma photons from ^{60}Co and high-energy electrons from electron beam accelerators produce secondary electrons when they interact with matter. The average linear energy transfer (LET) of ^{60}Co gamma photons or high-energy electrons is approximately 0.2 eV nm^{-1} in aqueous media (Kochanny et al. 1963).

The work of Fricke and coworkers, carried out in the twenties and thirties, described the ferrous sulfate method of dosimetry of ionizing radiations which then formulated the concept of "indirect effect" of radiation on the dissolved substance (Hart 1959) and established the influence of oxygen on the course of radiolysis of aqueous solutions. In 1960s, free radicals mainly H$^{\bullet}$, solvated electron, and $^{\bullet}$OH are considered as the most important intermediates in radiation induced reactions of water and aqueous solutions.

$$H_2O \rightarrow H^{\bullet} + {}^{\bullet}OH \tag{8.1}$$

These radicals are produced as follows. The high-energy photon passing through the water brings about the ionization of the molecules located close to its path, or track:

$$H_2O \rightarrow H_2O^{+} + e^{-} \tag{8.2}$$

The secondary electrons formed have sufficient energy to ionize more molecules of water nearby. The clusters of ions thus produced are called "spurs" (Vereshchinskii and Pikaev 1964).

After these initial approaches, there have been a big progress in radiation chemistry of water and consequently, in the identification of radiolysis products, reaction mechanisms and kinetics of reactions. The current state of knowledge can be summarized by the following reactions:

$$M \rightsquigarrow M^{\bullet+} + e^{-} \tag{8.3}$$

$$H_2O \rightarrow H_2O^{\bullet+} + e^{-} \text{ and } H_2O^{*} \tag{8.4}$$

$$H_2O^{\bullet+} \rightarrow H_2O \rightarrow {}^{\bullet}OH + H_3O^{+} \tag{8.5}$$

$$H_2O^{*} \rightarrow H^{\bullet} + {}^{\bullet}OH, H_2 + O^{\bullet} \tag{8.6}$$

$$e^{-} + nH_2O \rightarrow e^{-}_{aq} \tag{8.7}$$

Reaction 8.4 represents ionization and electronic excitation of water molecules that occur on the timescale of an electronic transition. The electronically excited states H_2O^* are known to dissociate in the vapor phase in reaction 8.6, and the secondary electron which is released in reaction 8.3 is known to be surrounded with polar water molecules and become hydrated e_{aq}^{-}.

As a consequence, final products from the radiolysis of water for low LET radiation such as ^{60}Co γ-rays and fast electrons from an accelerator can be represented as given below:

Table 8.2 Radiation chemical yields (G values) for the radiolysis products of water for low LET radiation (Buxton 2008)

	G-values (μmol J^{-1})
e_{aq}^-	0.28
$^{\bullet}OH$	0.28
H_3O^+	0.28
$H^{\bullet}$	0.062
H_2	0.047
H_2O_2	0.073

$$H_2O \rightsquigarrow e_{aq}^-, H^{\bullet}, {}^{\bullet}OH, H_2, H_2O_2, H_3O^+ \quad (8.8)$$

As shown in Table 8.2, each species generated by irradiation of water has the same or quite different chemical yields.

Here the radiation chemical yields are expressed in μmol J^{-1}. Additionally, it can also be quoted as molecules/100 eV. The conversion factor is:

1 molecule/100 eV = 1.036×10^{-7} mol J^{-1} (or 0.1036 μmol J^{-1}).

$$H_2O \rightsquigarrow 0.44\ e_{aq}^-, 0.028\ H^{\bullet}, 0.056\ {}^{\bullet}OH, 0.11\ H_2, 0.11\ H_2O_2, 0.044\ H_3O^+ \quad (8.9)$$

The principal primary radicals are the hydrated electron (e_{aq}^-), which is the most powerful reducing agent in aqueous systems (standard reduction potential $E^0 = -2.78$ V), and the hydroxyl radical ($^{\bullet}OH$), which is the most powerful oxidizing agent in aqueous systems ($E^0(^{\bullet}OH/OH^-) = 1.90$ V in neutral solution and $E^0(H^+, {}^{\bullet}OH/H_2O) = 2.72$ V in acidic solution) (Buxton 2008). The hydrogen atom ($^{\bullet}H$) is not an important species in neutral or alkaline solution, but it becomes the major reductant ($E^0(H^+/H^{\bullet}) = -2.31$ V) in acidic solution (pH < 3) through reaction of hydrated electron with proton (Spinks and Woods 1964).

$$e_{aq}^- + H^+ \rightarrow H^{\bullet} \quad (8.10)$$

In water radiolysis, approximately equal yields of reducing ($e_{aq}^- + H^{\bullet}$) and oxidizing ($^{\bullet}OH$) species are produced, but generally it is desirable to have either totally reducing or totally oxidizing conditions depending on the ultimate effect to be produced. Choosing the appropriate conditions for generating the species of interest starting with these free radicals is of paramount importance. This can mainly be done by using solutes which alter the proportions of radicalic species.

In order to convert hydrated electrons into oxidizing species, a very practical and frequently used method is to saturate aqueous solution with N_2O ([N_2O] ~ 25 mmol dm^{-3}) (Janata and Schuler 1982):

$$e_{aq}^- + N_2O \rightarrow N_2 + O^{\bullet -} \quad (8.11)$$

$$O^{\bullet -} + H_2O \rightleftharpoons {}^{\bullet}OH + OH^- \quad (8.12)$$

Since $k = 8.7 \times 10^9$ dm^3 mol^{-1} s^{-1} for reaction 8.11, followed by reaction 8.12, the contribution of H to any reactions with N_2O may be less important than $^{\bullet}OH$ reactions ($k = 2.1 \times 10^{-6}$ dm^3 mol^{-1} s^{-1}) (Wardman 1978).

Chemical effects due to hydroxyl radicals (oxidizing conditions) may be further enhanced by the addition of hydrogen peroxide, which acts as a scavenger for hydrogen atoms (and solvated electrons) and at the same time produces more hydroxyl radicals (Hart 1951).

$$H^{\bullet} + H_2O_2 \rightarrow {}^{\bullet}OH + H_2O \quad (8.13)$$

Nanogel formation by irradiation with ionizing radiation mainly depends on $^{\bullet}OH$ and hydrogen atoms produced from water radiolysis which further abstract hydrogen from polymer chains. These carbon-centered polymer radicals can face with competitive reactions such as recombination, disproportionation, hydrogen transfer, or scission (Fig. 8.10). Among these, the most important type is radical recombination, which directly affects the crosslinking hence gelation process.

Nanogels can mainly be synthesized in totally oxidizing conditions, i.e., $^{\bullet}OH$ should be the major species in the reaction with polymer. Therefore, the reducing effect of e_{aq}^- can easily be eliminated by saturating the solution with nitrous oxide according to reactions 8.11 and 8.12. Oxygen is a very efficient radical scavenger

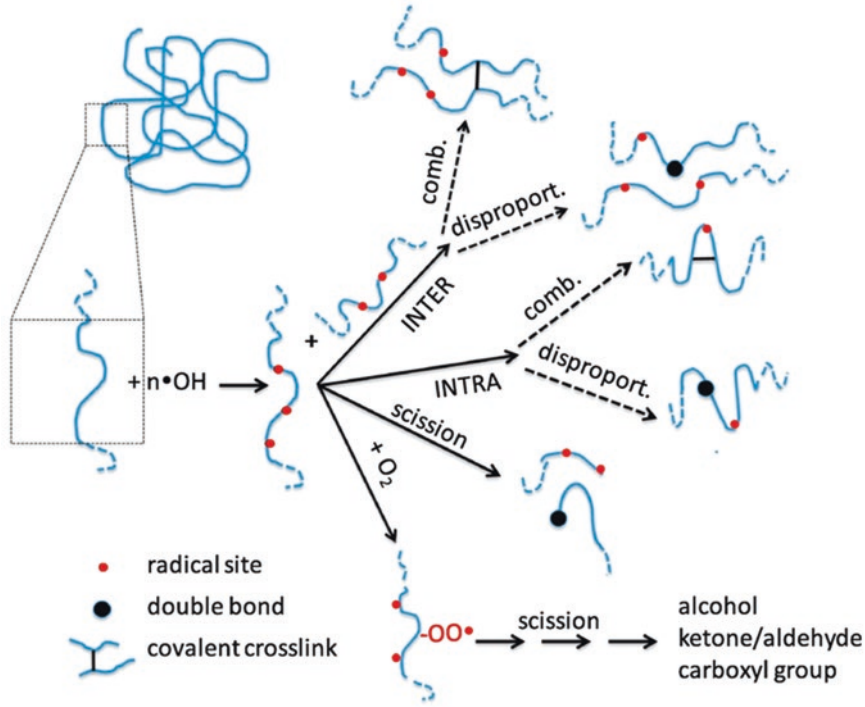

Fig. 8.10 Schematic representation of competitive reactions of polymer radicals in aqueous systems. (Reproduced with permission (Ditta et al. 2019), Copyright 2019 Elsevier)

since reaction of generated macroradicals with dissolved oxygen forms less active peroxyl radical, which would reduce the crosslinking process. Irradiations should also be performed in deoxygenated aqueous solutions to eliminate chain scissions (Ulanski et al. 1996).

The competition between inter- and intramolecular crosslinking in the radiolysis of aqueous polymeric systems was aforementioned. Figure 8.11 represents these routes during crosslinking reactions. As early as in 1959, Dieu and Decreux studied crosslinking of poly(vinyl alcohol) solutions by gamma radiation and found out that intramolecular crosslinking appears to dominate at very low concentrations, whereas at higher concentrations intermolecular crosslinking leads the system to gelation (Dieu and Desreux 1959; Tomoda and Tsuda 1961).

The first report on radiation formation of polymeric nanogels was presented by Ulanski, Janik, and Rosiak in 1998 in which the principles and benefits of nanogel synthesis using ionizing radiation have been revealed. They synthesized nanogels by pulse radiolysis (e-beam) with poly (vinyl alcohol) (PVA), a water-soluble, biocompatible, and crosslinkable polymer in a closed-loop system (Fig. 8.12). They followed molecular weight and intrinsic viscosity[η] changes with increasing total absorbed dose. Intrinsic viscosity was observed to decrease with absorbed dose, despite the increase in molecular weight, contrary to the well-known Mark-Houwink equation, which suggests that the viscosity of a linear polymer chain increases with an increase in its molecular weight. This phenomenon indicated the intramolecular crosslinking leading to shrinkage in polymer coils (Ulański et al. 1998). The study brought an important insight to the literature since they highlighted the requirements to avoid macrogelation and induce intramolecular crosslinking. They concluded that macrogelation can be avoided by working with very low concentrations, i.e., concentrations below threshold concentration for molecular overlap ($c < c^*$) and generating high number of radicals on a single chain, which can be maintained by using

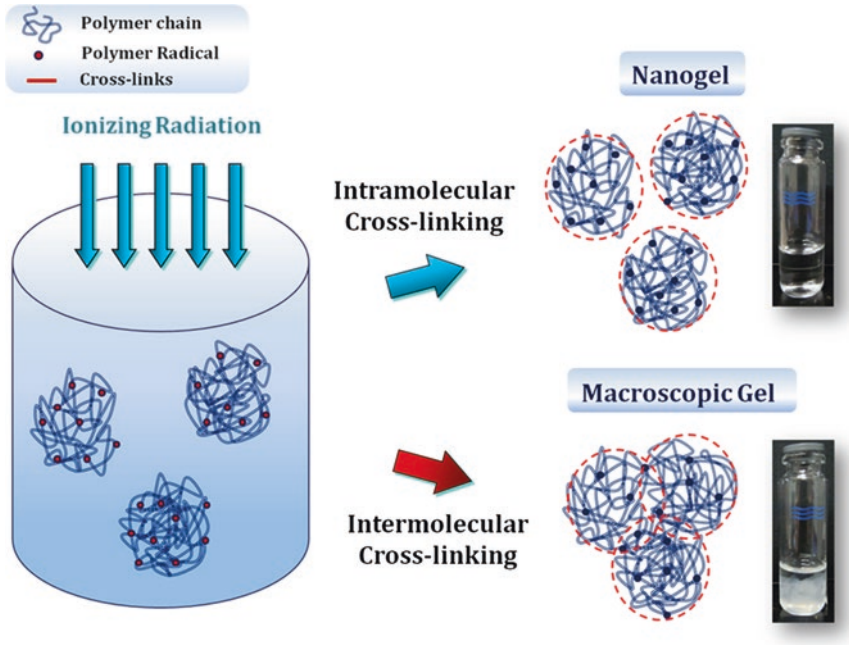

Fig. 8.11 Reaction path for the radiation-induced synthesis of nanogels from polymer solutions, where the system can end up with either a nanogel (via intramolecular crosslinking) or a macroscopic gel (via intermolecular crosslinking)

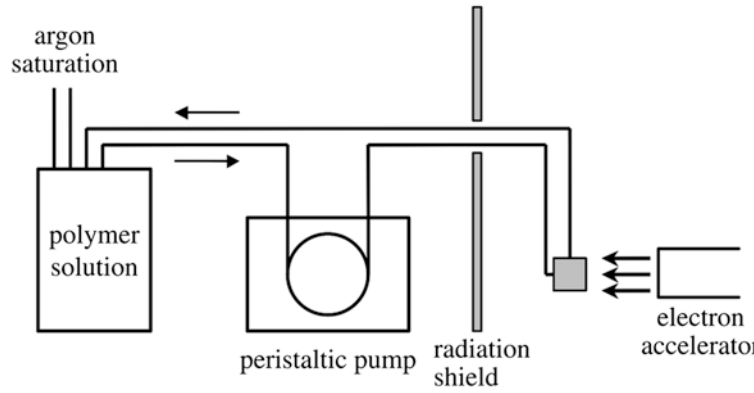

Fig. 8.12 Schematic illustration of the experimental setup (closed-loop system). (Reproduced with permission (Schmidt et al. 2005), Copyright 2005 Elsevier)

high-dose-rate fast electrons that are generated from a linear accelerator or, in general, working with high dose rates.

After the foundation of these requirements, there has been a growing interest in synthesizing nanogels using radiation-induced crosslinking. Valuable reviews have been reported in this field (Dispenza et al. 2016; Ulanski and Rosiak 2004).

The aforementioned inspiring results on nanogel synthesis by pulsed electron-beam further lead the researchers to apply this method to another water-soluble polymer, PVP (Ulanski and Rosiak 1999), and an anionic polyelectrolyte polymer, PAA (Kadlubowski et al. 2003; Ulański et al. 2002). In these studies, evidence of intramolecular crosslinking was supported by limiting viscosity number (intrinsic viscosity), $[\eta]$, and molecular weight and radius of gyration (R_g) measurements as a function of total absorbed dose. In addition, the size of nanogels was observed to be dose dependent. Ulanski et al. further performed Monte Carlo simulations to

explain the kinetics and radical recombination, i.e., inter- or intramolecular crosslinking, upon pulse radiolysis and compared the results with the pulse radiolysis experiment on PEO, and a good agreement was acquired between the two.

J.C. An has proposed a different procedure for the synthesis of PVP nanogels called "template-assisted" ionizing radiation with steady state ^{60}Co gamma-ray irradiation. Preparation of PVP nanogels with diameters ranging from 90 to 190 nm was accomplished by irradiating PVP solutions in nanoporous membrane (Fig. 8.13) where pores of these nanocapillaries control the sizes of nanogels (An 2009).

The use of ionizing radiation in nanogel synthesis can be regarded as the most versatile method compared to other common methods since it allows easy control of properties of end product. Moreover, additional controlling factors such as total absorbed dose and dose rate bring important changes in sizes of nanogels, hence their effectiveness in different application areas. As discussed before, nanogels can alternatively be prepared by using steady-state gamma irradiation with ^{60}Co gamma sources. This technique does not differ from e-beam irradiation in the sense of initiation, reaction mechanism, or application procedure, but controlling factors are limited to total absorbed dose and dose rate. However, pulsed e-beam facilities allow changes in instrumental parameters such as pulse repetition rate (PRR), pulse duration (τ), e-beam current (I), and dose per pulse (DPP) which provide additional control on the course of radical generation and crosslinking reactions and ultimately on the sizes of nanogels. Different operational parameters were summarized in Table 8.3 for the

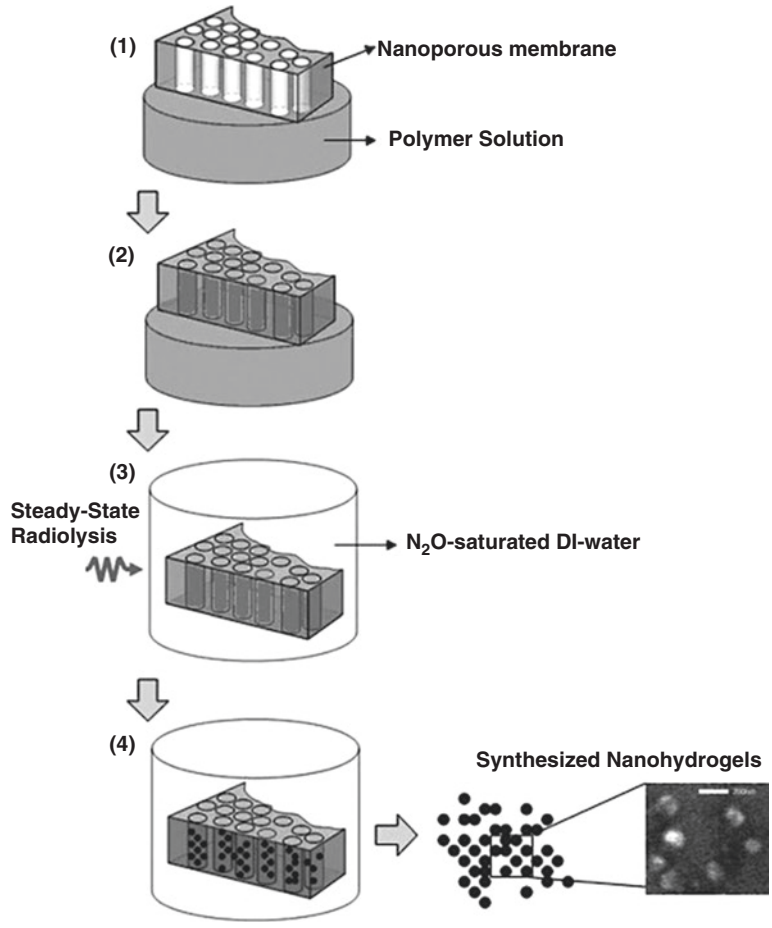

Fig. 8.13 Schematic procedure of the template-assisted γ-ray irradiation. (Reproduced with permission (An 2009), Copyright 2009 The Korean Society of Industrial and Engineering Chemistry, Published by Elsevier B.V)

Table 8.3 Synthesis parameters, size, and highlights of the studies on nanogel synthesis by irradiation of aqueous solutions

Polymer	Synthesis parameters, size, and highlights	References
PVA	*Pulsed electron-beam irradiation*	Ulański et al. (1998)
	eU = 6 MeV, Q = 1 cm^3 s^{-1}, PRF = 1 Hz, DPP = 1.1 kGy,	
	Dose = 1.1 kGy.	
	Radiation-induced synthesis of NGs for the first time, evidence of intramolecular crosslinking by [η] and MW measurements as a function of total absorbed dose	
PVP	*Pulsed electron-beam irradiation*	Ulanski and Rosiak (1999)
	eU = 6 MeV, Q = 2 cm^3 s^{-1}, PRF = 0.5 Hz	
	Dose = 0.32 kGy	
	d = 20–80 nm	
	Evidence of intramolecular crosslinking by R_g and MW measurements as a function of total absorbed dose	
PAA	*Pulsed electron-beam irradiation*	Ulański et al. (2002)
	eU = 6 MeV, τ = 2 μs, PRF = 0.5 Hz, DPP = 1.15 kGy, pH = 2	
	Dose = 1.15–9.2 kGy	
	Evidence of intramolecular crosslinking by [η] and MW measurements as a function of total absorbed dose applied to a polyelectrolyte polymer	
PAA	*Pulsed electron-beam irradiation*	Kadlubowski et al. (2003)
	eU = 6 MeV, Q = 2 cm^3 s^{-1}, τ = 2 μs, PRF = 0.5 Hz, DPP = 1.15 kGy, pH = 2	
	d = 50–95 nm	
	Effect of polymer concentration, total absorbed dose, elaboration of degradation resistance of NGs compared to linear chains	
Gelatin	*Gamma irradiation*	Furusawa et al. (2004)
	DR = 10 kGy/h	
	Dose = 10, 20 kGy	
	d < 20 nm	
	Highly and randomly packed gelatin NGs with conformational stability to temperature changes	
PVP-PAA	*Pulsed electron-beam irradiation*	Henke et al. (2005)
	eU = 6 MeV, τ = 2 μs, PRF = 5 Hz	
	Dose = 0.5–4 kGy	
	d = 17–55 nm	
	Evidence of intramolecular crosslinking in multicomponent H-bonding complexes	
PVME	*Pulsed electron-beam irradiation*	Schmidt et al. (2005)
	eU = 6 MeV, Q = 1 cm^3 s^{-1}, τ = 3 μs, PRF = 0.5 Hz, DPP = 0.96 kGy	
	Dose = 15 kGy	
	d = 10–30 nm	
	Temperature-sensitive NGs, freely draining globular structures	
PEO	*Pulsed electron-beam irradiation*	Ulański et al. (2006)
	eU = 6 MeV, τ = 0.5 μs, DPP = 1–4 kGy	
	Dose = 3.3 kGy	
	Monte Carlo simulations of intrachain crosslinking, good agreement with pulse radiolysis of PEO	

(continued)

Table 8.3 (continued)

Polymer	Synthesis parameters, size, and highlights	References
PVP	*Gamma irradiation*	An (2009)
	DR = 3.5 kGhy/h	
	Dose: 10 kGy	
	d = 90–190 nm	
	Radiation-induced XL in nanoporous membrane, diameter of nanocapillary pore affects the sizes of NGs	
PVP	*Pulsed electron-beam irradiation*	An et al. (2011a, b)
	eU = 7 MeV, I = 200 mA, τ = 3 μs, PRF = 20–300 Hz, DPP = 30–35 Gy at T = 20–77 °C	
	d ~ 20–50 nm	
	Effect of irradiation temperature and PRF on MW and sizes of NGs, evaluation of inter- and intramolecular crosslinking by no. of C-centered free radicals	
CMS	*Pulsed electron-beam irradiation*	Binh et al. (2012)
	eU = 5 MeV, τ = 20 μs, P_E = 150 kW at 5 °C	
	Dose: 6–25 kGy	
	d ~ 25 nm	
	Effects of absorbed dose on MW, [η], and sizes of NGs, enhanced growth of *Lactobacillus* bacteria in the presence of NGs compared to pure polymer	
PEGDA	*Pulsed electron-beam irradiation*	Hamzah et al. (2012)
	eU = 3 MeV	
	Dose = 1–30 kGy	
	d = 95–460 nm	
	Irradiation of inverse micelles with the size ranging from 2 to 8 nm	
PVP	*Pulsed electron-beam irradiation at 0–4 °C*	Dispenza et al. (2012a)
	10 MeV	
	eU = 10 MeV, I = 0.08 μA, τ = 10–12 μs, PRR = 37.5 Hz	
	Dose: 40 kGy	
	d = 26–120 nm	
	Effect of polymer concentration, network spatial organization explained by ^{13}C NMR spin-lattice relaxation spectroscopy and rheology	
PVP-g-APMAM	*Electron-beam irradiation at 5–10 °C*	Dispenza et al. (2012b)
	Facility 1	
	eU = 10 MeV, I = 0.40 μA, τ = 10–12 μs, PRR = 75 Hz, DPP ~ 1.8 Gy, DR: 500 kGy/h	
	Facility 2	
	eU = 10 MeV, I = 0.45 μA, τ = 4.5 μs, PRR = 300 Hz, DPP ~ 13 Gy	
	Dose = 40–80 kGy	
	d = 38–100 nm	
	Crosslinked PVP grafted with APMAM, biocompatible NGs, BSA conjugation, enhanced cellular accumulation of NGs through endocytic pathway, absence of cytotoxicity	
PVP	I. *Gamma irradiation*	Kadlubowski et al. (2012)
	2.0 kGy/h	
	Dose = 0.3–0.7 kGy	
	II. *Pulsed electron-beam irradiation*	
	eU = 6 MeV, τ = 2 μs, Q = 1 cm^3 s^{-1}, PRF = 0.5 Hz, DPP = 0.95 kGy	
	Dose: 0.95–5.7 kGy	
	d = 38–100 nm	
	Two-step irradiation: low-dose-rate irradiation in semi-concentrated polymer solution followed by pulse irradiation of its diluted solution	

(continued)

Table 8.3 (continued)

Polymer	Synthesis parameters, size, and highlights	References
BSA	*Gamma irradiation at 5–10 °C*	Soto Espinoza et al. (2012)
	DR < 1 kGy/h	
	Dose = 0–20 kGy	
	d = 20–40 nm	
	Conservation of 3D structure of protein molecules after irradiation, effect of a co-solvent on NG size	
Bi_2O_3-PVA	*Gamma irradiation*	Zhu et al. (2012)
	DR = 3.72 kGy/h	
	Dose = 265 kGy	
	d~163 nm	
	QDs immobilized into PVA NG, reversible temperature-induced phase transition, entry into B16F10 cells for imaging, temperature-regulated delivery of anticancer drug TMZ	
PVP	*Pulsed electron-beam irradiation at 0–4 °C*	Sabatino et al. (2013)
	eU = 10 MeV, τ = 10–12 μs, PRF = 37.5 Hz, DPP = 0.74 Gy	
	Dose: 40 kGy	
	d = 26–120 nm	
	Concentration effect on network size, intrinsic fluorescence of PVP nanogels	
PAA & Ag/PAA	*Electron-beam irradiation*	Choi et al. (2013)
	eU = 10 MeV, I = 1 mA	
	Dose: 10–150 kGy	
	d ~ 100–500 nm	
	Effect of absorbed dose on zeta potential and sizes of NGs, dose-dependent antibacterial effect against *E. coli* and *S. aureus*, good in vivo wound healing effect	
PVP/PAA	*Gamma irradiation*	Abd El-Rehim et al. (2013a)
	DR = 3.85 kGh/h, T = 10, 35 °C	
	Dose: 10–40 kGy	
	d ~ 60–600 nm	
	Effect of feed (PVP/PAA) composition and concentration, PVP molecular weight, absorbed dose, temperature, and atmosphere on sizes of NGs	
PVP/PAA	*Gamma irradiation*	Abd El-Rehim et al. (2013b)
	DR = 3.85 kGh/h, T = 10, 35 °C	
	Dose: 10–40 kGy	
	d ~ 60–600 nm	
	Encapsulation of pilocarpine, effect of feed composition, and absorbed dose on loading efficiency of pilocarpine into NGs, evaluation ocular applicability, in vitro release study in simulated tear fluid	
PVP-g-AA	*Pulsed electron-beam irradiation*	Grimaldi et al. (2014)
	eU = 10 MeV, I = 0.45 mA, τ = 4.5 μs, PRF = 400 Hz, DPP = 13 Gy	
	Dose: 40 kGy	
	d = 14–40 nm	
	Effect of feed composition on size, surface charge, MW and chemical structure of NGs	
PDMAEMA	*Gamma irradiation*	Meléndez-Ortiz et al. (2014)
	DR: 8 kGy/h	
	Dose: 10–100 kGy	
	d = 26–550 nm	
	Temperature and pH responsive nanogels of PDMAEMA with different sizes at varying amount of crosslinker (EGDMA) and dose	

(continued)

Table 8.3 (continued)

Polymer	Synthesis parameters, size, and highlights	References
PVME	*Pulsed electron-beam irradiation*	Chaykar et al. (2016)
	eU = 1.0 MeV, c < c* and T < LCST	
	Dose: 20, 40 kGy	
	d ~ 70 nm	
	Effect of silica NPs and absorbed dose on VPTT and aggregation behavior of pure and hybrid NGs, investigation of rheological behavior	
PVP-co-APMAM	*Pulsed electron-beam irradiation*	Adamo et al. (2017)
	eU = 10 MeV, 300 Hz	
	Dose: 80 kGy	
	d ~ 200 nm	
	Immune-functionalized NGs by conjugation of mAb, enhanced intracellular localization of conjugated NGs compared to bare NG, target-specific wound healing of conjugated NGs on ECV304 cells	
PVP-PIA	DR = 0.0366 kGy/h	Omar et al. (2017)
	Dose = 30, 40, 50 kGy	
	d = 288–681 nm	
	Encapsulation of INH, higher antimicrobial activity against intracellular mycobacteria tuberculosis than free drug	
CS-g-NVCL	DR = 5.7 kGy/h	Cruz et al. (2017)
	Dose= 1–20 kGy	
	d = 50 to 500 nm	
	Gamma radiation-induced grafting of NVCL onto CS NGs, pH, and thermoresponsive NGs, sustained release of 5-FU	
P(AMPS-co-AAm)	*Gamma irradiation*	Awadallah-F et al. (2018)
	DR = 1.9 kGy/h	
	Dose: 30 kGy	
	d ~ 10–70 nm	
	Effect of SLS concentration and absorbed dose on the pore characteristics and sizes of NGs, in vitro release of 5-fluorouracil (5-FU) at simulated gastric and intestinal fluid	
PAA-PVP IPN	*Gamma irradiation*	Ghaffarlou et al. (2018)
	DR = 0.022 kGy/h	
	Dose = 5,10,15 kGy	
	d = 30–250 nm	
	Effect of pH, MW, and concentration of both polymers on the sizes of precursor IPCs and nanogels derived from	
PAA	*Pulsed electron-beam irradiation*	Matusiak et al. (2018)
	eU = 6 MeV, τ = 2 μs, PRF = 0.5 Hz, DPP = 0.9 kGy	
	d = 56–90 nm	
	Gamma irradiation	
	DR = 0.55 kGy/h	
	d = 100–470 nm	
	Gamma radiolysis resulted in microgels; e-beam radiolysis resulted in nanogels	
PVP-PAA IPN	*Gamma irradiation*	Rattanawongwiboon et al. (2018)
	DR: 0.022 kGy/h	
	Dose: 2 kGy	
	d ~ 200–800 nm	
	Non-aggregating IPCs by control of pH and solvent composition, pH-responsive nanogels from precursor IPCs	

(continued)

Table 8.3 (continued)

Polymer	Synthesis parameters, size, and highlights	References
PVP	I. *Gamma irradiation*	Sütekin and Güven (2019)
	Facility (1) DR = 10 kGy/h	
	Facility (2) DR = 0.8 kGy/h	
	II. *Electron-beam irradiation*	
	Facility (1) eU = 1.3 MeV, DR = 15 kGy/min	
	Facility (2) eU = 7 MeV, DPP = 1 kGy	
	Dose: 5, 10, 15 kGy	
	d = 30–250 nm	
	Comparative study of gamma and e-beam, effect of total absorbed dose, dose rate, polymer concentration, molecular weight on PVP nanogel size, stability up to 2 years.	

eU electron energy, *PRF* pulse repetitive frequency, *PRR* pulse repetition rate, τ pulse duration, *DPP* dose per pulse, *I* beam current, *Q* volumetric flow rate

synthesis of nanogels with gamma and e-beam radiation.

Kadlubowski et al. performed a different approach to obtain PVP nanogels by a two-step synthesis. At first step, gamma irradiation with a low dose rate was applied to PVP solutions having concentration above overlap concentration ($c > c^*$). This step resulted in intermolecular crosslinking evidenced by an increase in molecular weight and coil size. When the desired MW is attained, gamma-irradiated solution is diluted ($c < c^*$) and further subjected to e-beam irradiation as the second stage of irradiation. Thus nanogels with controlled MW and size can be obtained by controlling parameters, i.e., total absorbed dose and concentration in both stages (Kadlubowski et al. 2012).

A comparative study of gamma and e-beam irradiation for the synthesis of PVP nanogels was presented recently. The study includes nanogel synthesis performed by using four different ionizing radiation sources, two of which were gamma and two were e-beam with different dose rates. In addition, the effect of precursor PVP molecular weight and concentration were studied. Table 8.4 summarizes the experimental details about radiation-induced crosslinking of PVP. A clear size and polydispersity reduction was observed for e-beam irradiated samples as a result of high number of radicals generated in a very short irradiation time on separate polymer coils which react with each other intramolecularly, whereas gamma irradiated samples resulted in larger nanogels due to longer irradiation times that allow enough time for diffusion of coils which combine intermolecularly. In addition, molecular weight and concentration of precursor polymer strongly affect the size of obtained nanogels. PVP nanogels with sizes from 30 to 250 nm were obtained reproducibly by controlling polymer and radiation source-based parameters. SEM images also showed that these nanogels were spherical in shape and homogeneous in size distribution (Fig. 8.14). The PVP nanogels were observed to be stable for 2 years at 4 °C evidenced by DLS measurements providing long-term storage of nanogels that is highly important for biomedical applications (Sütekin and Güven 2019). This long-term study was also evidenced for PNiPAAm nanogels synthesized by gamma irradiation (Sütekin et al. 2020).

An et al. investigated the effect of total absorbed dose, pulse repetition rate (PRR), and temperature on molecular weight and sizes of NGs by varying pulse repetition rates from 20 to 300 Hz and temperatures from 20 to 77 °C (Fig. 8.15). A clear decrease in sizes of PVP NGs was accomplished at elevated temperatures as a result of collapsed conformation of PVP chains due to dehydration (An et al. 2011a, b). Several studies including the effect of total absorbed dose on NG size were also performed for different types of polymers such as CMS (Binh et al. 2012), BSA (Soto Espinoza et al. 2012), Ag/PAA (Choi et al. 2013), PVP/PAA (Abd El-Rehim et al. 2013a; Ghaffarlou et al. 2018), PAA/PEO

Table 8.4 Peak mean diameters and PDI values for nanogels synthesized from aqueous PVP solutions having different molecular weights and concentrations by gamma and e-beam irradiation to 10 kGy dose

Unirradiated				Gamma – 10 kGy			e-Beam – 10 kGy		
M_w	Conc. (mg/mL)	d (nm)	PDI		d (nm)	PDI		d (nm)	PDI
1.3×10^6	1	58.9 ± 0.8	0.25	NG1[a]	77.2 ± 0.3	0.18	NG7[c]	48.0 ± 0.4	0.17
1.3×10^6	1	58.9 ± 0.8	0.25	NG2[b]	52.8 ± 0.9	0.27	NG8[d]	35.0 ± 0.3	0.28
3.6×10^5	1	60.8 ± 0.9	0.26	NG3[b]	41.1 ± 0.4	0.25	NG9[d]	32.2 ± 0.5	0.26
1.3×10^6	1.5	60.7 ± 0.7	0.25	NG4[b]	114.5 ± 1.1	0.27	NG10[d]	55.8 ± 0.6	0.30
3.6×10^5	1.5	64.3 ± 0.5	0.26	NG5[b]	59.8 ± 1.6	0.25	NG11[d]	41.3 ± 0.4	0.24
1.3×10^6	2	63.3 ± 0.4	0.26	NG6[a]	247.9 ± 5.7	0.38	NG12[c]	85.9 ± 1.5	0.21

Reproduced with permission (Sütekin and Güven 2019), Copyright 2019 Elsevier
[a]Dose rate = 0.8 kGy/h. [b]Dose rate = 10 kGy/h. [c]Dose rate = 15 kGy/min. [d]Dose rate = 1 kGy/pass

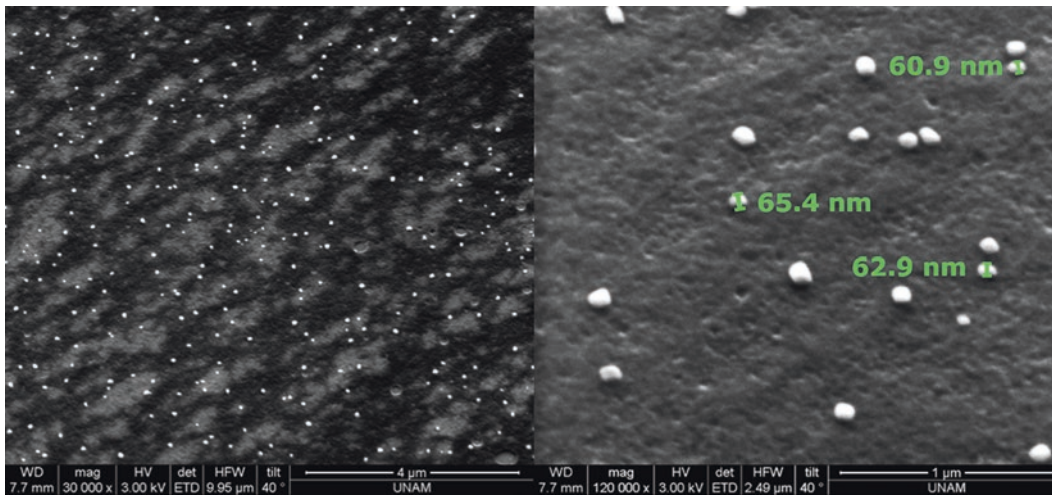

Fig. 8.14 The scanning electron micrographs of PVP nanogels synthesized by radiation induced crosslinking. (Reproduced with permission (Sütekin and Güven 2019), Copyright 2019 Elsevier)

(Rattanawongwiboon et al. 2018), PDMAEMA (Meléndez-Ortiz et al. 2014), and P(AMPS-co-AAm) (Awadallah-F et al. 2018), and pronounced changes in NG sizes were accomplished (see Table 8.3).

Choosing interpenetrating polymer complexes (IPC) as starting materials to obtain nanogel interpenetrating networks (IPN) can be a facile route to obtain nanogels with multifunctional properties. In this way, different properties of polymer pairs can be introduced to a single nanogel system at a single irradiation step, avoiding exhausting synthesis of copolymers by conventional or controlled FRP. Ghaffarlou et al. studied the complexation between PVP and PAA by controlling pH, molecular weight, and concentration of precursor IPCs to obtain pH-responsive IPN nanogels. Table 8.5 shows mean diameters, zeta potentials, and polydispersities of PAA/PVP IPCs and corresponding IPN nanogels. Size reduction due to intramolecular crosslinking was observed for IPN nanogels. PAA/PVP nanogels with homogeneous distribution (low dispersity) were synthesized at low doses (5 and 10 kGy) in a size range of 30 to 250 nm (Ghaffarlou et al. 2018). Similar technique was further applied to obtain pH-responsive PAA/PEO nanogels (Fig. 8.16) (Rattanawongwiboon et al. 2018). In further studies multifunctional nanogels were prepared from PAA/PVIm, PAA/PPVP, and PAA/PAlAm IPCs, and loading and release of BSA and curcumin are being evaluated (Ghaffarlou 2020).

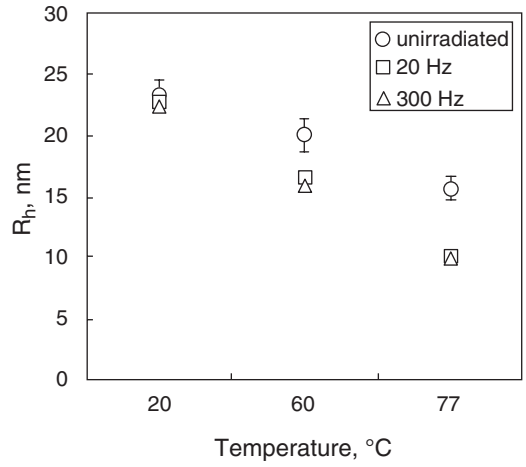

Fig. 8.15 Change in radius of the synthesized PVP nanogels irradiated at different temperatures and pulse repetition rates. (Reprinted with permission (An et al. 2011a, b), Copyright 2011 Elsevier)

Intramolecular crosslinking of polymer chains provides significant changes in the physical properties of the resultant nanogels. Schmidt et al. performed pulsed e-beam irradiation on a temperature-sensitive polymer, PVME below overlap concentration ($c < c^*$) at temperatures below LCST of PVME. An important VPTT decrease was obtained after the formation of radiation-induced crosslinks in polymer chains, from 36 °C to 29 °C (Schmidt et al. 2005). Chaykar et al. also observed significant changes in VPTT of PVME nanogels when the total absorbed dose was changed from 20 kGy to 40 kGy where the VPTTs of nanogels were determined for the first time by rheology (Chaykar et al. 2016). Kadlubowski et al. proved that internally crosslinked PAA NGs showed high resistance to degradation unlike linear PAA linear chains which is important for future applications of nanogels. Furusawa et al. synthesized gelatin nanogel by gamma-initiated crosslinking. They performed circular dichroism (CD) measurements to observe the conformational changes in gelatin NGs and found out that helical structure of gelatin was replaced by random conformation which bring high temperature stability to NGs (Furusawa et al. 2004). Differently, Soto Espinoza et al. observed that gamma irradiation of BSA molecules maintained their three-dimensional structure after internally crosslinked by gamma irradiation (Soto Espinoza et al. 2012).

Nanogels obtained by irradiation of aqueous polymer solutions find attractive applications mainly in biomedical field. Rashed et al. loaded dopamine onto PVP/PAA nanogel obtained by gamma irradiation from a previous study (Abd El-Rehim et al. 2013a). They later investigated in vitro release of dopamine from NGs and found out that the formulation administered dopamine to the brain very rapidly compared to the free drug which can be explained by the size effect, i.e., "Trojan horse effect" (Rashed et al. 2015). Picone et al. conjugated insulin molecule to a nanogel system consisting of a carboxyl-functionalized PVP, a biocompatible polymer, produced by e-beam irradiation (Grimaldi et al. 2014) for the transportation of insulin to the brain by crossing blood-brain barrier. Insulin-conjugated nanogels gave promising results after testing on a cellular Alzheimer's disease system (Picone et al. 2016). The intranasal delivery of this insulin-conjugated nanogel was tested in a following work. High biocompatibility with lack of immunological response was obtained for conjugated nanogels presenting more efficient insulin delivery to the tested brain regions than that of free insulin (Picone et al. 2018). In another study, AntimiR-31 was conjugated to PVP nanogels containing carboxyl groups with a stable amide bond with high conjugation yields. Penetration of NG-AntimiR-31 to cell membrane in the metastatic SW620 colon cancer cells was accomplished (Dispenza et al. 2017).

Irradiation not only provides on-demand generation of nanogels but also controls their effectiveness in their biomedical applications. For example, Choi et al. attained silver-containing PVP nanogels by e-beam irradiation and found out that antibacterial activity against *E. coli* and *S. aureus* is highly dependent to the total absorbed dose which affects nanogel size (Choi et al. 2013). In another work, pilocarpine was encapsulated into PVP/PAA nanogels, and the ocular applicability of this system was evaluated by an in vitro study in simulated tear fluid. They observed that loading efficiency of pilocarpine into nanogels was also dose dependent (Abd El-Rehim et al. 2013b).

Table 8.5 Peak mean diameters, zeta potential, pH, and PDI values for PAA/PVP IPCs and IPC nanogels that are synthesized from aqueous IPC solutions (c = 0.5, 1.0, 1.5 and 2 mg/mL) [a] by gamma irradiation

	Unirradiated				5 kGy-Irradiated				10 kGy-Irradiated			
	pH	Z-Pot. (mV)	d (nm)	PDI	pH	Z-Pot. (mV)	d (nm)	PDI	pH	Z-Pot. (mV)	d (nm)	PDI
IPC1 – 0.5	3.61	–15.4	41	0.212	3.61	–15.4	35	0.125	3.61	–15.4	30	0.121
IPC1 – 1.0	3.45	–17	46	0.201	3.45	–17	38	0.145	3.45	–17	36	0.131
IPC1 – 1.5	3.35	–21.7	58	0.225	3.35	–21.7	51	0.140	3.35	–21.7	49	0.112
IPC1 – 2.0	3.29	–27.4	72	0.234	3.29	–27.4	58	0.143	3.29	–27.4	54	0.101
IPC2 – 0.5	3.77	–16.5	45	0.189	3.77	–16.5	40	0.141	3.77	–16.5	37	0.119
IPC2 – 1.0	3.66	–19.1	51	0.181	3.66	–19.1	45	0.131	3.66	–19.1	39	0.125
IPC2 – 1.5	3.39	–23.2	62	0.211	3.39	–23.2	55	0.193	3.39	–23.2	43	0.105
IPC2 – 2.0	3.27	–29.4	80	0.159	3.27	–29.4	60	0.107	3.27	–29.4	56	0.088
IPC3 – 0.5	3.88	–12.3	249	0.234	3.88	–12.3	122	0.139	3.88	–12.3	108	0.131
IPC3 – 1.0	3.65	–17.3	265	0.263	3.65	–17.3	133	0.155	3.65	–17.3	111	0.127
IPC3 – 1.5	3.44	–22.1	283	0.232	3.44	–22.1	241	0.175	3.44	–22.1	196	0.133
IPC3 – 2.0	3.32	–28.4	307	0.245	3.32	–28.4	249	0.163	3.32	–28.4	225	0.149

Reproduced with permission (Ghaffarlou et al. 2018), Copyright 2018 Elsevier

[a]The abbreviations IPC1, IPC2, and IPC3 denote the combinations of PAA 250,000 g/mol with PVP 360,000 g/mol and PVP 1,300,000 g/mol and PAA 8000 g/mol and PVP 10,000 g/mol, respectively, and the following numbers indicate the corresponding concentrations in mg/mL

6 Conclusions and Future Prospects

Nanogels are nanoscaled analogues of hydrogels and are serious competitors of other nanoparticles in biomedical applications, i.e., nanospheres and liposomes with superior features such as flexibility, large surface area for bioconjugation, high swelling capacity, and high loading (encapsulation) capacity. Stimuli-responsive property can be introduced via the functional groups either present in nanogel main structure or in the outer layer of coated nanogels. Nanogels can also serve as matrices for metallic nanoparticles, photosensitizers, and target-specific ligands especially for combined cancer therapies by different remote triggers. Cytotoxicity studies presented evidence that nanogels are nontoxic to various types of cells.

Although there are various conventional techniques used in the synthesis of nanogels, irradiation of dilute aqueous polymer solutions is gaining popularity in the synthesis of size controlled multifunctional nanogels. This chapter is a humble attempt to review the main characteristics of nanogels, their applications, synthesis parameters, and radiation-induced synthesis of nanogels in particular.

A detailed information about the radiolysis of water and its products was given to reveal the reaction mechanism and controlling factors of radiation-induced crosslinking. A high number of studies are dedicated to the synthesis of nanogels by emulsion polymerizations. These techniques generally require additional purification step of monomers, surfactants, initiators, organic solvents, and/or accelerators. Nanogel synthesis by irradiation of dilute polymer solutions present

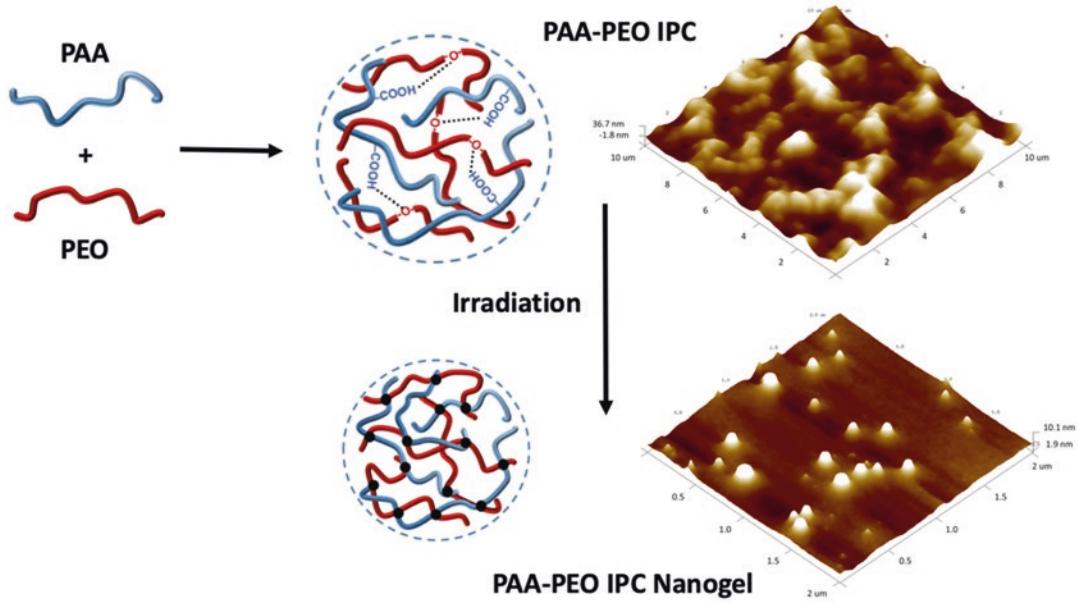

Fig. 8.16 Formation of poly(acrylic acid)-poly(ethylene oxide) (PAA-PEO) nanogels from IPCs by radiation-induced crosslinking. (Reproduced with permission (Rattanawongwiboon et al. 2018), Copyright 2018 Springer-Verlag GmbH Germany, part of Springer Nature)

important advantages since it is a monomer-free method with no requirement of using any additives to initiate or accelerate the crosslinking reactions which is also a room temperature process. In the synthesis of nanogels by irradiation, the most important step is to avoid intermolecular crosslinking of chains to prevent formation of macrogels and obtain submicron gels. The requirements for this strategy have already been proposed by several studies by lowering polymer concentration and the number of radicals on each chain, i.e., dose rates. There are also other operational parameters such as total absorbed dose and temperature which strongly affect the sizes of resultant nanogels. Irradiation by pulsed e-beam provides additional tunable parameters such as beam current, pulse duration, and/or frequency. These operational parameters for the synthesis of several types of nanogels and their corresponding sizes were presented in detail in this chapter. While the radiolysis of many well-known water-soluble polymers is well accomplished, much remains to be explored in working with more complex polymers having double hydrophilic, amphiphilic structures enlarging the applicability of these structures in diverse areas. Moreover, radiolytically stable reagents can be incorporated into the nanogel structure by simultaneous crosslinking and nanoparticle synthesis to obtain novel multifunctional structures to be used in diagnosis and treatment steps. At this stage, upscaling of laboratory applications to pilot and large volume production should be considered.

References

Abd El-Rehim HA, Hegazy ESA, Hamed AA, Swilem AE. Controlling the size and swellability of stimuli-responsive polyvinylpyrrolidone-poly(acrylic acid) nanogels synthesized by gamma radiation-induced template polymerization. Eur Polym J. 2013a;49:601–12. https://doi.org/10.1016/j.eurpolymj.2012.12.002.

Abd El-Rehim HA, Swilem AE, Klingner A, Hegazy ESA, Hamed AA. Developing the potential ophthalmic applications of pilocarpine entrapped into polyvinylpyrrolidone-poly(acrylic acid) nanogel dispersions prepared by γ radiation. Biomacromolecules. 2013b;14:688–98. https://doi.org/10.1021/bm301742m.

Abdalla AME, Xiao L, Ullah MW, Yu M, Ouyang C, Yang G. Current challenges of cancer anti-angiogenic therapy and the promise of nanotherapeutics. Theranostics. 2018;8:533–49. https://doi.org/10.7150/thno.21674.

Adamo G, Grimaldi N, Sabatino MA, Walo M, Dispenza C, Ghersi G. E-beam crosslinked nanogels conjugated with monoclonal antibodies in targeting strategies. Biol Chem. 2017;398:277–87. https://doi.org/10.1515/hsz-2016-0255.

Amamoto Y, Higaki Y, Matsuda Y, Otsuka H, Takahara A. Programmed thermodynamic formation and structure analysis of star-like nanogels with core crosslinked by thermally exchangeable dynamic covalent bonds. J Am Chem Soc. 2007;129:13298–304. https://doi.org/10.1021/ja075447n.

An JC. Synthesis of poly(vinyl pyrrolidone) nanohydrogels by the template-assisted ionizing radiation. J Ind Eng Chem. 2009;15:148–52. https://doi.org/10.1016/j.jiec.2008.09.006.

An Z, Shi Q, Tang W, Tsung CK, Hawker CJ, Stucky GD. Facile RAFT precipitation polymerization for the microwave-assisted synthesis of well-defined, double hydrophilic block copolymers and nanostructured hydrogels. J Am Chem Soc. 2007;129:14493–9. https://doi.org/10.1021/ja0756974.

An Z, Qiu Q, Liu G. Synthesis of architecturally well-defined nanogels via RAFT polymerization for potential bioapplications. Chem Commun. 2011a;47:12424–40. https://doi.org/10.1039/c1cc13955j.

An JC, Weaver A, Kim B, Barkatt A, Poster D, Vreeland WN, Silverman J, Al-Sheikhly M. Radiation-induced synthesis of poly(vinylpyrrolidone) nanogel. Polymer (Guildf). 2011b;52:5746–55. https://doi.org/10.1016/j.polymer.2011.09.056.

Ashrafi B, Rashidipour M, Marzban A, Soroush S, Azadpour M, Delfani S, Ramak P. Mentha piperita essential oils loaded in a chitosan nanogel with inhibitory effect on biofilm formation against S. mutans on the dental surface. Carbohydr Polym. 2019;212:142–9. https://doi.org/10.1016/j.carbpol.2019.02.018.

Awadallah-F A, Abd El-Wahab SY, Al-Shafey HI. Impact of surfactant on the pore and particle sizes of copolymer (2-acrylamido-2-methylpropane sulfonic acid/acrylamide) nanohydrogels for controlled release of 5-fluorouracil. Polym Eng Sci. 2018;58:94–102. https://doi.org/10.1002/pen.24535.

Bagde A, Patel K, Mondal A, Kutlehria S, Chowdhury N, Gebeyehu A, Patel N, Kumar N, Singh M. Combination of UVB absorbing titanium dioxide and quercetin nanogel for skin cancer chemoprevention. AAPS PharmSciTech. 2019;20:240. https://doi.org/10.1208/s12249-019-1424-x.

Baker WO. Microgel, a new macromolecule. Ind Eng Chem. 1949;41:511–20. https://doi.org/10.5254/1.3543023.

Barsbay M, Güven O. A short review of radiation-induced raft-mediated graft copolymerization: a powerful combination for modifying the surface properties of polymers in a controlled manner. Radiat Phys Chem. 2009;78:1054–9. https://doi.org/10.1016/j.radphyschem.2009.06.022.

Barsbay M, Güven O, Stenzel MH, Davis TP, Barner-Kowollik C, Barner L. Verification of controlled grafting of styrene from cellulose via radiation-induced RAFT polymerization. Macromolecules. 2007;40:7140–7. https://doi.org/10.1021/ma070825u.

Binh D, Hong PTT, Duy NN, Duoc NT, Dieu NN. A study on size effect of carboxymethyl starch nanogel crosslinked by electron beam radiation. Radiat Phys Chem. 2012;81:906–12. https://doi.org/10.1016/j.radphyschem.2011.12.016.

Blanco E, Shen H, Ferrari M. Principles of nanoparticle design for overcoming biological barriers to drug delivery. Nat Biotechnol. 2015;33:941–51. https://doi.org/10.1038/nbt.3330.

Bonham JA, Faers MA, Van Duijneveldt JS. Non-aqueous microgel particles: synthesis, properties and applications. Soft Matter. 2014;10:9384–98. https://doi.org/10.1039/c4sm01834f.

Brigger I, Dubernet C, Couvreur P. Nanoparticles in cancer therapy and diagnosis: polymer conjugates for cancer therapy. Adv Drug Deliv Rev. 2002;54:631–51. https://doi.org/10.1016/S0169-409X(02)00044-3.

Bueno VB, Cuccovia IM, Chaimovich H, Catalani LH. PVP superabsorbent nanogels. Colloid Polym Sci. 2009;287:705–13. https://doi.org/10.1007/s00396-009-2017-0.

Buxton GV. An overview of the radiation chemistry of liquids. In: Spotheim-Maurizot M, Mostafavi M, Douki T, Belloni J, editors. Radiation chemistry from basics to applications in material and life sciences. France: EDP Sciences; 2008.

Cabral H, Miyata K, Osada K, Kataoka K. Block copolymer micelles in nanomedicine applications. Chem Rev. 2018;118:6844–92. https://doi.org/10.1021/acs.chemrev.8b00199.

Can M, Ayyala RS, Şahiner N. Crosslinked poly(lactose) microgels and nanogels for biomedical applications. J Colloid Interface Sci. 2019;553:805–12. https://doi.org/10.1016/j.jcis.2019.06.078.

Cao Z, Zhou X, Wang G. Selective release of hydrophobic and hydrophilic cargos from multi-stimuli-responsive nanogels. ACS Appl Mater Interfaces. 2016;8:28888–96. https://doi.org/10.1021/acsami.6b10360.

Cenci L, Tatti R, Tognato R, Ambrosi E, Piotto C, Bossi AM. Synthesis and characterization of peptide-imprinted nanogels of controllable size and affinity. Eur Polym J. 2018;109:453–9. https://doi.org/10.1016/j.eurpolymj.2018.08.031.

Chai S, Zhang J, Yang T, Yuan J, Cheng S. Thermoresponsive microgel decorated with silica nanoparticles in shell: biomimetic synthesis and drug release application. Colloids Surfaces A Physicochem Eng Asp. 2010;356:32–9. https://doi.org/10.1016/j.colsurfa.2009.12.026.

Charleux B, D'Agosto F, Delaittre G. Preparation of hybrid latex particles and core-shell particles through the use of controlled radical polymerization techniques in aqueous media. Adv Polym Sci. 2010;233:125–83. https://doi.org/10.1007/12-2010-64.

Chaykar AS, Goharpey F, Yeganeh JK. Volume phase transition of electron beam cross-linked thermo-responsive PVME nanogels in the presence and absence of nanoparticles: with a view toward rheology and interactions. RSC Adv. 2016;6:9693–708. https://doi.org/10.1039/c5ra21021f.

Chen H, Ma X, Wu S, Tian H. A rapidly self-healing supramolecular polymer hydrogel with photostimulated room-temperature phosphorescence responsiveness. Angew Chemie Int Ed. 2014;53:14149–52. https://doi.org/10.1002/anie.201407402.

Chen J, Wu M, Veroniaina H, Mukhopadhyay S, Li J, Wu Z, Wu Z, Qi X. Poly(N-isopropylacrylamide) derived nanogels demonstrated thermosensitive self-assembly and GSH-triggered drug release for efficient tumor therapy. Polym Chem. 2019;10:4031–41. https://doi.org/10.1039/c9py00537d.

Choi JB, Park JS, Khil MS, Gwon HJ, Lim YM, Jeong SI, Shin YM, Nho YC. Characterization and antimicrobial property of poly(acrylic acid) nanogel containing silver particle prepared by electron beam. Int J Mol Sci. 2013;14:11011–23. https://doi.org/10.3390/ijms140611011.

Cruz A, García-Uriostegui L, Ortega A, Isoshima T, Burillo G. Radiation grafting of N-vinylcaprolactam onto nano and macrogels of chitosan: synthesis and characterization. Carbohydr Polym. 2017;155:303–12. https://doi.org/10.1016/j.carbpol.2016.08.083.

Curie P, Debierne A. Induced radioactivity excited by radium salts. C R Hebd Seances Acad Sci. 1901;133:931–4.

Dalwadi C, Patel G. Application of nanohydrogels in drug delivery systems: recent patents review. Recent Pat Nanotechnol. 2015;9:17–25. https://doi.org/10.2174/1872210509666150101151521.

Daniloska V, Carretero P, Tomovska R, Paulis M, Asua JM. High-performance adhesives resulting from spontaneous formation of nanogels within miniemulsion particles. ACS Appl Mater Interfaces. 2014;6:3559–67. https://doi.org/10.1021/am405752k.

Debierne MA. Recherches sur les gaz produits par les substances radioactives. Décomposition de l'eau Ann Phys (Paris). 1914;9:97–127. https://doi.org/10.1051/anphys/191409020097.

Desai MP, Labhasetwar V, Walter E, Levy RJ, Amidon GL. The mechanism of uptake of biodegradable microparticles in Caco-2 cells is size dependent. Pharm Res. 1997;14:1568–73. https://doi.org/10.1023/A:1012126301290.

Dieu H, Desreux V. Cross-linking of polyvinyl alcohol by gamma radiation. Int J Appl Radiat Isot. 1959;7:71–2. https://doi.org/10.1016/0020-708x(59)90334-5.

Dispenza C, Grimaldi N, Sabatino MA, Todaro S, Bulone D, Giacomazza D, Przybytniak G, Alessi S, Spadaro G. Studies of network organization and dynamics of e-beam crosslinked PVPs: from macro to nano. Radiat Phys Chem. 2012a;81:1349–53. https://doi.org/10.1016/j.radphyschem.2011.11.057.

Dispenza C, Sabatino MA, Grimaldi N, Bulone D, Bondì ML, Casaletto MP, Rigogliuso S, Adamo G, Ghersi G. Minimalism in radiation synthesis of biomedical functional nanogels. Biomacromolecules. 2012b;13:1805–17. https://doi.org/10.1021/bm3003144.

Dispenza C, Spadaro G, Jonsson M. Radiation engineering of multifunctional nanogels. Top Curr Chem. 2016;374 https://doi.org/10.1007/s41061-016-0071-x.

Dispenza C, Sabatino MA, Ajovalasit A, Ditta LA, Ragusa M, Purrello M, Costa V, Conigliaro A, Alessandro R. Nanogel-antimiR-31 conjugates affect colon cancer cells behaviour. RSC Adv. 2017;7:52039–47. https://doi.org/10.1039/c7ra09797b.

Ditta LA, Dahlgren B, Sabatino MA, Dispenza C, Jonsson M. The role of molecular oxygen in the formation of radiation-engineered multifunctional nanogels. Eur Polym J. 2019;114:164–75. https://doi.org/10.1016/j.eurpolymj.2019.02.020.

Ekici S, Ilgın P, Bütün S, Şahiner N. Hyaluronic acid hydrogel particles with tunable charges as potential drug delivery devices. Carbohydr Polym. 2011;84:1306–13. https://doi.org/10.1016/j.carbpol.2011.01.028.

Ekladious I, Colson YL, Grinstaff MW. Polymer–drug conjugate therapeutics: advances, insights and prospects. Nat Rev Drug Discov. 2019; https://doi.org/10.1038/s41573-018-0005-0.

Elkassih SA, Kos P, Xiong H, Siegwart DJ. Degradable redox-responsive disulfide-based nanogel drug carriers: via dithiol oxidation polymerization. Biomater Sci. 2019;7:607–17. https://doi.org/10.1039/c8bm01120f.

Fan Y, Zhang J, Shi M, Li D, Lu C, Cao X, Peng C, Mignani S, Majoral JP, Shi X. Poly(amidoamine) dendrimer-coordinated copper(II) complexes as a theranostic nanoplatform for the radiotherapy-enhanced magnetic resonance imaging and chemotherapy of tumors and tumor metastasis. Nano Lett. 2019;19:1216–26. https://doi.org/10.1021/acs.nanolett.8b04757.

Fu W, Luo C, Morin EA, He W, Li Z, Zhao B. UCST-type thermosensitive hairy nanogels synthesized by RAFT polymerization-induced self-assembly. ACS Macro Lett. 2017;6:127–33. https://doi.org/10.1021/acsmacrolett.6b00888.

Furusawa K, Terao K, Nagasawa N, Yoshii F, Kubota K, Dobashi T. Nanometer-sized gelatin particles prepared by means of gamma-ray irradiation. Colloid Polym Sci. 2004;283:229–33. https://doi.org/10.1007/s00396-004-1211-3.

García JR, Quirós M, Han WM, O'Leary MN, Cox GN, Nusrat A, García AJ. IFN-γ-tethered hydrogels enhance mesenchymal stem cell-based immunomodulation and promote tissue repair. Biomaterials. 2019;220:119403. https://doi.org/10.1016/j.biomaterials.2019.119403.

Ghaffarlou M. Preparation of nanogels by radiation-induced cross-linking of interpolymer complexes in aqueous medium, their characterization and pharmaceutical use. Unpublished doctoral dissertation. Hacettepe University, Ankara, Turkey. 2020.

Ghaffarlou M, Sütekin SD, Güven O. Preparation of nanogels by radiation-induced cross-linking of interpolymer complexes of poly (acrylic acid) with poly (vinyl pyrrolidone) in aqueous medium. Radiat Phys Chem. 2018;142:130–6. https://doi.org/10.1016/j.radphyschem.2017.04.019.

Grimaldi N, Sabatino MA, Przybytniak G, Kaluska I, Bondì ML, Bulone D, Alessi S, Spadaro G, Dispenza C. High-energy radiation processing, a smart approach to obtain PVP-graft-AA nanogels. Radiat Phys Chem. 2014;94:76–9. https://doi.org/10.1016/j.radphyschem.2013.04.012.

Hajebi S, Rabiee N, Bagherzadeh M, Ahmadi S, Rabiee M, Roghani-Mamaqani H, Tahriri M, Tayebi L, Hamblin MR. Stimulus-responsive polymeric nanogels as smart drug delivery systems. Acta Biomater. 2019;92:1–18. https://doi.org/10.1016/j.actbio.2019.05.018.

Hamzah Y, Yunus WMZW, Isa NM, Tajau R, Hashim K, Dahlan KZ. Synthesis of polyethylene glycol diacrylate nanogel using irradiation of inverse micelles technique. E-Polymers. 2012;12 https://doi.org/10.1515/epoly.2012.12.1.533.

Hanafy NAN, El-Kemary M, Leporatti S. Micelles structure development as a strategy to improve smart cancer therapy. Cancers (Basel). 2018;10:238. https://doi.org/10.3390/cancers10070238.

Hart EJ. Mechanism of the γ-ray induced oxidation of formic acid in aqueous solution. J Am Chem Soc. 1951;73:68–73. https://doi.org/10.1021/ja01145a026.

Hart EJ. Development of the radiation chemistry of aqueous solutions. J Chem Educ. 1959;36:266–72. https://doi.org/10.1021/ed036p266.

He J, Yan B, Tremblay L, Zhao Y. Both core- and shell-cross-linked nanogels: photoinduced size change, intraparticle LCST, and interparticle UCST thermal behaviors. Langmuir. 2011;27:436–44. https://doi.org/10.1021/la1040322.

Henke A, Kadlubowski S, Ulanski P, Rosiak JM, Arndt KF. Radiation-induced cross-linking of polyvinylpyrrolidone-poly(acrylic acid) complexes. Nucl Instrum Methods Phys Res Sect B. 2005;236:391–8. https://doi.org/10.1016/j.nimb.2005.04.003.

Holtz JH, Asher SA. Polymerized colloidal crystal hydrogel films as intelligent chemical sensing materials. Nature. 1997;389:829–32. https://doi.org/10.1038/39834.

Hou S, Niu X, Li L, Zhou J, Qian Z, Yao D, Yang F, Ma PX, Fan Y. Simultaneous nano- and microscale structural control of injectable hydrogels via the assembly of nanofibrous protein microparticles for tissue regeneration. Biomaterials. 2019;223:119458. https://doi.org/10.1016/j.biomaterials.2019.119458.

Iyer AK, Khaled G, Fang J, Maeda H. Exploiting the enhanced permeability and retention effect for tumor targeting. Drug Discov Today. 2006;11:812–8. https://doi.org/10.1016/j.drudis.2006.07.005.

Jafari M, Kaffashi B. Synthesis and characterization of a novel solvent-free dextran-HEMA-PNIPAM thermosensitive nanogel. J Macromol Sci Part A Pure Appl Chem. 2016;53:68–74. https://doi.org/10.1080/10601325.2016.1120173.

Janata E, Schuler RH. Rate constant for scavenging eaq- in N2O-saturated solutions. J Phys Chem. 1982;86:2078–84. https://doi.org/10.1021/j100208a035.

Jayakumar K, Camarada MB, Dharuman V, Rajesh R, Venkatesan R, Ju H, Maniraj M, Rai A, Barman SR, Wen Y. Layer-by-layer-assembled AuNPs-decorated first-generation poly(amidoamine) Dendrimer with reduced graphene oxide core as highly sensitive biosensing platform with controllable 3D nanoarchitecture for rapid voltammetric analysis of ultra-trace DNA hybridiza. ACS Appl Mater Interfaces. 2018;10:21541–55. https://doi.org/10.1021/acsami.8b03236.

Ji YL, An QF, Weng XD, Hung WS, Lee KR, Gao CJ. Microstructure and performance of zwitterionic polymeric nanoparticle/polyamide thin-film nanocomposite membranes for salts/organics separation. J Memb Sci. 2018;548:559–71. https://doi.org/10.1016/j.memsci.2017.11.057.

Jiang Y, Tang Y, Miao P. Polydopamine nanosphere@silver nanoclusters for fluorescence detection of multiplex tumor markers. Nanoscale. 2019;11:8119–23. https://doi.org/10.1039/c9nr01307e.

Jin Q, Liu X, Liu G, Ji J. Fabrication of core or shell reversibly photo cross-linked micelles and nanogels from double responsive water-soluble block copolymers. Polymer (Guildf). 2010;51:1311–9. https://doi.org/10.1016/j.polymer.2010.01.026.

Jin RM, Yao MH, Yang J, Zhao DH, Di Zhao Y, Liu B. One-step in situ synthesis of polypeptide-gold nanoparticles hybrid nanogels and their application in targeted photoacoustic imaging. ACS Sustain Chem Eng. 2017;5:9841–7. https://doi.org/10.1021/acssuschemeng.7b01784.

Jung KO, Siegwart DJ, Lee HI, Sherwood G, Peteanu L, Hollinger JO, Kataoka K, Matyjaszewski K. Biodegradable nanogels prepared by atom transfer radical polymerization as potential drug delivery carriers: synthesis, biodegradation, in vitro release, and bioconjugation. J Am Chem Soc. 2007;129:5939–45. https://doi.org/10.1021/ja069150l.

Kabanov AV, Vinogradov SV. Nanogels as pharmaceutical carriers: finite networks of infinite capabilities. Angew Chemie Int Ed. 2009;48:5418–29. https://doi.org/10.1002/anie.200900441.

Kadlubowski S. Radiation-induced synthesis of nanogels based on poly(N-vinyl-2-pyrrolidone) – a review. Radiat Phys Chem. 2014;102:29–39. https://doi.org/10.1016/j.radphyschem.2014.04.016.

Kadlubowski S, Grobelny J, Olejniczak W, Cichomski M, Ulanski P. Pulses of fast electrons as a tool to synthesize poly(acrylic acid) nanogels. Intramolecular cross-linking of linear polymer chains in additive-free

aqueous solution. Macromolecules. 2003;36:2484–92. https://doi.org/10.1021/ma021628s.

Kadlubowski S, Ulanski P, Rosiak JM. Synthesis of tailored nanogels by means of two-stage irradiation. Polymer (Guildf). 2012;53:1985–91. https://doi.org/10.1016/j.polymer.2012.03.018.

Kang H, Trondoli AC, Zhu G, Chen Y, Chang YJ, Liu H, Huang YF, Zhang X, Tan W. Near-infrared light-responsive core-shell nanogels for targeted drug delivery. ACS Nano. 2011;5:5094–9. https://doi.org/10.1021/nn201171r.

Khoee S, Asadi H. Nanogels: chemical approaches to preparation. In: Encyclopedia of biomedical polymers and polymeric biomaterials: Taylor & Francis; 2016. p. 5266–93. https://doi.org/10.1081/e-ebpp-120050693.

Kılıç AG, Malcı S, Çelikbıçak Ö, Şahiner N, Salih B. Gold recovery onto poly(acrylamide-allylthiourea) hydrogels synthesized by treating with gamma radiation. Anal Chim Acta. 2005;547:18–25. https://doi.org/10.1016/j.aca.2005.03.042.

Kochanny GL, Timnick A, Hochanadel CJ, Goodman CD. Radiation chemistry studies of water as related to the initial linear energy transfer of 11-Mev to 23-Mev protons. Radiat Res. 1963;19:462. https://doi.org/10.2307/3571467.

Koul V, Mohamed R, Kuckling D, Adler HJP, Choudhary V. Interpenetrating polymer network (IPN) nanogels based on gelatin and poly(acrylic acid) by inverse miniemulsion technique: synthesis and characterization. Colloids Surfaces B Biointerfaces. 2011;83:204–13. https://doi.org/10.1016/j.colsurfb.2010.11.007.

Lajud SA, Nagda DA, Qiao P, Tanaka N, Civantos A, Gu R, Cheng Z, Tsourkas A, O'Malley BW Jr, Li D. A novel chitosan-hydrogel-based nanoparticle delivery system for local inner ear application. Otol Neurotol. 2015;36:341–7.

Li X, Zuo J, Guo Y, Yuan X. Preparation and characterization of narrowly distributed nanogels with temperature-responsive core and pH-responsive shell. Macromolecules. 2004;37:10042–6. https://doi.org/10.1021/ma048658a.

Li YY, Yang J, Wu WB, Zhang XZ, Zhuo RX. Degradable nanogels as a nanoreactor for growing silica colloids. Langmuir. 2009;25:1923–6. https://doi.org/10.1021/la803902r.

Li Y, Ye Z, Shen L, Xu Y, Zhu A, Wu P, An Z. Formation of multidomain hydrogels via thermally induced assembly of PISA-generated triblock terpolymer nanogels. Macromolecules. 2016;49:3038–48. https://doi.org/10.1021/acs.macromol.5b02538.

Li Y, Zhang X, Zhang Z, Wu H, Xu X, Gu Z. Tumor-adapting and tumor-remodeling AuNR@dendrimer-assembly nanohybrids overcome impermeable multidrug-resistant cancer. Mater Horiz. 2018;5:1047–57. https://doi.org/10.1039/c8mh00694f.

Li W, Nie J, Hu R, Zhao R, Zhu W, Chen X, Li D, Wang L, Hu L. A nanogel sensor for colorimetric fluorescence measurement of ionizing radiation doses. Chem Commun. 2019;55:9614–7. https://doi.org/10.1039/c9cc03680f.

Liang Y, Zhao X, Hu T, Han Y, Guo B. Mussel-inspired, antibacterial, conductive, antioxidant, injectable composite hydrogel wound dressing to promote the regeneration of infected skin. J Colloid Interface Sci. 2019;556:514–28. https://doi.org/10.1016/j.jcis.2019.08.083.

Liu G, An Z. Frontiers in the design and synthesis of advanced nanogels for nanomedicine. Polym Chem. 2014;5:1559–65. https://doi.org/10.1039/c3py01502e.

Liu J, Detrembleur C, Debuigne A, De Pauw-Gillet MC, Mornet S, Vander Elst L, Laurent S, Duguet E, Jérôme C. Glucose-, pH- and thermo-responsive nanogels crosslinked by functional superparamagnetic maghemite nanoparticles as innovative drug delivery systems. J Mater Chem B. 2014;2:1009–23. https://doi.org/10.1039/c3tb21272f.

Liu J, Detrembleur C, Mornet S, Jérôme C, Duguet E. Design of hybrid nanovehicles for remotely triggered drug release: an overview. J Mater Chem B. 2015;3:6117–47.

Liu J, Yang B, Li M, Li J, Wan Y. Enhanced dual network hydrogels consisting of thiolated chitosan and silk fibroin for cartilage tissue engineering. Carbohydr Polym. 2020;227:115335. https://doi.org/10.1016/j.carbpol.2019.115335.

Loftsson T, Brewster ME. Pharmaceutical applications of cyclodextrins: basic science and product development. J Pharm Pharmacol. 2010;62:1607–21. https://doi.org/10.1111/j.2042-7158.2010.01030.x.

Lu W, Zhang G, Zhang R, Flores LG, Huang Q, Gelovani JG, Li C. Tumor site-specific silencing of NF-κB p65 by targeted hollow gold nanosphere-mediated photothermal transfection. Cancer Res. 2010;70:3177–88. https://doi.org/10.1158/0008-5472.CAN-09-3379.

Luckanagul JA, Pitakchatwong C, Ratnatilaka Na Bhuket P, Muangnoi C, Rojsitthisak P, Chirachanchai S, Wang Q, Rojsitthisak P. Chitosan-based polymer hybrids for thermo-responsive nanogel delivery of curcumin. Carbohydr Polym. 2018;181:1119–27. https://doi.org/10.1016/j.carbpol.2017.11.027.

Ma K, Xu Y, An Z. Templateless synthesis of polyacrylamide-based nanogels via RAFT dispersion polymerization. Macromol Rapid Commun. 2015;36:566–70. https://doi.org/10.1002/marc.201400730.

Madhusudana Rao K, Krishna Rao KSV, Ramanjaneyulu G, Ha CS. Curcumin encapsulated pH sensitive gelatin based interpenetrating polymeric network nanogels for anti cancer drug delivery. Int J Pharm. 2015;478:788–95. https://doi.org/10.1016/j.ijpharm.2014.12.001.

Matusiak M, Kadlubowski S, Ulanski P. Radiation-induced synthesis of poly(acrylic acid) nanogels. Radiat Phys Chem. 2018;142:125–9. https://doi.org/10.1016/j.radphyschem.2017.01.037.

Meléndez-Ortiz HI, Peralta RD, Bucio E, Zerrweck-Maldonado L. Preparation of stimuli-responsive nanogels of poly [2-(dimethylamino) ethyl methacrylate] by heterophase and microemulsion polymerization using

gamma radiation. Polym Eng Sci. 2014;54:1625–31. https://doi.org/10.1002/pen.23703.

Messager L, Portecop N, Hachet E, Lapeyre V, Pignot-Paintrand I, Catargi B, Auzély-Velty R, Ravaine V. Photochemical crosslinking of hyaluronic acid confined in nanoemulsions: towards nanogels with a controlled structure. J Mater Chem B. 2013;1:3369–79. https://doi.org/10.1039/c3tb20300j.

Mo R, Jiang T, Di J, Tai W, Gu Z. Emerging micro- and nanotechnology based synthetic approaches for insulin delivery. Chem Soc Rev. 2014;43:3595–629. https://doi.org/10.1039/c3cs60436e.

Neamtu I, Rusu AG, Diaconu A, Nita LE, Chiriac AP. Basic concepts and recent advances in nanogels as carriers for medical applications. Drug Deliv. 2017;24:539–57. https://doi.org/10.1080/10717544.2016.1276232.

Niharika MG, Krishnamoorthy K, Akkala M. Overview on floating drug delivery system. Int J Appl Pharm. 2018;10:65–71. https://doi.org/10.22159/ijap.2018v10i6.28274.

Nordström R, Andrén OCJ, Singh S, Malkoch M, Davoudi M, Schmidtchen A, Malmsten M. Degradable dendritic nanogels as carriers for antimicrobial peptides. J Colloid Interface Sci. 2019;554:592–602. https://doi.org/10.1016/j.jcis.2019.07.028.

Oh JK, Drumright R, Siegwart DJ, Matyjaszewski K. The development of microgels/nanogels for drug delivery applications. Prog Polym Sci. 2008;33:448–77. https://doi.org/10.1016/j.progpolymsci.2008.01.002.

Omar SM, Maziad NA, El-Tantawy NM. Design of isoniazid smart nanogel by gamma radiation-induced template polymerization for biomedical application. Pharm Res. 2017;34:1872–85. https://doi.org/10.1007/s11095-017-2196-1.

Panja S, Bharti R, Dey G, Lynd NA, Chattopadhyay S. Coordination-assisted self-assembled polypeptide nanogels to selectively combat bacterial infection. ACS Appl Mater Interfaces. 2019;11:33599–611. https://doi.org/10.1021/acsami.9b10153.

Pekel N, Şahiner N, Güven O. Use of amidoximated acrylonitrile/N-vinyl 2-pyrrolidone interpenetrating polymer networks for uranyl ion adsorption from aqueous systems. J Appl Polym Sci. 2001;81:2324–9. https://doi.org/10.1002/app.1673.

Peng H, Stolwijk JA, Sun L, Wegener J, Wolfbeis OS. A nanogel for ratiometric fluorescent sensing of intracellular pH values. Angew Chem. 2010;122:4342–5.

Peng M, Yuan S, Shi X, Lu X. Preparation of multiresponsive nanogel and its application in noninvasive glucose naked eye detection. J Appl Polym Sci. 2019;136 https://doi.org/10.1002/app.47933.

Peres LB, dos Anjos RS, Tappertzhofen LC, Feuser PE, de Araújo PHH, Landfester K, Sayer C, Muñoz-Espí R. pH-responsive physically and chemically cross-linked glutamic-acid-based hydrogels and nanogels. Eur Polym J. 2018;101:341–9. https://doi.org/10.1016/j.eurpolymj.2018.02.039.

Picone P, Ditta LA, Sabatino MA, Militello V, San Biagio PL, Di Giacinto ML, Cristaldi L, Nuzzo D, Dispenza C, Giacomazza D, Di Carlo M. Ionizing radiation-engineered nanogels as insulin nanocarriers for the development of a new strategy for the treatment of Alzheimer's disease. Biomaterials. 2016;80:179–94. https://doi.org/10.1016/j.biomaterials.2015.11.057.

Picone P, Sabatino MA, Ditta LA, Amato A, San Biagio PL, Mulè F, Giacomazza D, Dispenza C, Di Carlo M. Nose-to-brain delivery of insulin enhanced by a nanogel carrier. J Control Release. 2018;270:23–36. https://doi.org/10.1016/j.jconrel.2017.11.040.

Picos-Corrales LA, Licea-Claveríe A, Arndt KF. Core-shell nanogels by RAFT crosslinking polymerization: synthesis and characterization. J Polym Sci Part A Polym Chem. 2012;50:4277–87. https://doi.org/10.1002/pola.26235.

Rashed ER, Abd El-Rehim HA, El-Ghazaly MA. Potential efficacy of dopamine loaded-PVP/PAA nanogel in experimental models of parkinsonism: possible disease modifying activity. J Biomed Mater Res Part A. 2015;103:1713–20. https://doi.org/10.1002/jbm.a.35312.

Rattanawongwiboon T, Ghaffarlou M, Sütekin SD, Pasanphan W, Güven O. Preparation of multifunctional poly(acrylic acid)-poly(ethylene oxide) nanogels from their interpolymer complexes by radiation-induced intramolecular crosslinking. Colloid Polym Sci. 2018;296:1599–608. https://doi.org/10.1007/s00396-018-4368-x.

Richa R, Roy Choudhury A. Synthesis of a novel gellan-pullulan nanogel and its application in adsorption of cationic dye from aqueous medium. Carbohydr Polym. 2020;227:115291. https://doi.org/10.1016/j.carbpol.2019.115291.

Sabatino MA, Bulone D, Veres M, Spinella A, Spadaro G, Dispenza C. Structure of e-beam sculptured poly(N-vinylpyrrolidone) networks across different length-scales, from macro to nano. Polymer (Guildf). 2013;54:54–64. https://doi.org/10.1016/j.polymer.2012.11.031.

Sabir F, Asad MI, Qindeel M, Afzal I, Dar MJ, Shah KU, Zeb A, Khan GM, Ahmed N, Din F. Polymeric nanogels as versatile nanoplatforms for biomedical applications. J Nanomater. 2019;2019:1–16. https://doi.org/10.1155/2019/1526186.

Şahiner N. Hydrogel nanonetworks with functional core-shell structure. Eur Polym J. 2007;43:1709–17. https://doi.org/10.1016/j.eurpolymj.2007.01.046.

Şahiner N. Soft and flexible hydrogel templates of different sizes and various functionalities for metal nanoparticle preparation and their use in catalysis. Prog Polym Sci. 2013; https://doi.org/10.1016/j.progpolymsci.2013.06.004.

Şahiner N. One step preparation of polymeric maltitol particles, from a sugar molecule, maltitol for biomedical applications. Mater Sci Eng C. 2018;89:205–12. https://doi.org/10.1016/j.msec.2018.04.017.

Şahiner N, Özay O. Highly charged p(4-vinylpyridine-co-vinylimidazole) particles for versatile applications: biomedical, catalysis and environmental. React Funct

Polym. 2011;71:607–15. https://doi.org/10.1016/j.reactfunctpolym.2011.03.003.

Şahiner N, Şengel SB. Surfactant free synthesis and characterization of poly(vinyl carbazole) microgel and its chemical modifications. Colloids Surfaces A Physicochem Eng Asp. 2017;514:243–50. https://doi.org/10.1016/j.colsurfa.2016.11.068.

Şahiner N, Saraydın D, Karadağ E, Güven O. Swelling and dye adsorption properties of radiation induced N-vinyl-2-pyrrolidone/acrylonitrile hydrogels. Polym Bull. 1998;41:371–8. https://doi.org/10.1007/s002890050376.

Şahiner N, Pekel N, Akkaş P, Güven O. Amidoximation and characterization of new complexing hydrogels prepared from N-vinyl 2-pyrrolidone/acrylonitrile systems. J Macromol Sci Pure Appl Chem. 2000;37(A):1159–72. https://doi.org/10.1081/MA-100101146.

Şahiner N, Alb AM, Graves R, Mandal T, McPherson GL, Reed WF, John VT. Core-shell nanohydrogel structures as tunable delivery systems. Polymer (Guildf). 2007;48:704–11. https://doi.org/10.1016/j.polymer.2006.12.014.

Şahiner N, Özay O, İnger E, Aktaş N. Controllable hydrogen generation by use smart hydrogel reactor containing Ru nano catalyst and magnetic iron nanoparticles. J Power Sources. 2011;196:10105–11. https://doi.org/10.1016/j.jpowsour.2011.08.068.

Sahle FF, Giulbudagian M, Bergueiro J, Lademann J, Calderón M. Dendritic polyglycerol and N -isopropylacrylamide based thermoresponsive nanogels as smart carriers for controlled delivery of drugs through the hair follicle. Nanoscale. 2017;9:172–82. https://doi.org/10.1039/c6nr06435c.

Šálek P, Dvořáková J, Černoch P, Pavlova E, Proks V. Poly(amino acid)-based nanogel by horseradish peroxidase catalyzed crosslinking in an inverse miniemulsion. Colloid Polym Sci. 2018;296:995–1003. https://doi.org/10.1007/s00396-018-4318-7.

Sanson N, Rieger J. Synthesis of nanogels/microgels by conventional and controlled radical crosslinking copolymerization. Polym Chem. 2010;1:965–77. https://doi.org/10.1039/c0py00010h.

Sarika PR, James NR. Preparation and characterisation of gelatin-gum arabic aldehyde nanogels via inverse miniemulsion technique. Int J Biol Macromol. 2015;76:181–7. https://doi.org/10.1016/j.ijbiomac.2015.02.038.

Schmidt T, Janik I, Kadłubowski S, Ulański P, Rosiak JM, Reichelt R, Arndt KF. Pulsed electron beam irradiation of dilute aqueous poly(vinyl methyl ether) solutions. Polymer (Guildf). 2005;46:9908–18. https://doi.org/10.1016/j.polymer.2005.07.077.

Şengel SB, Şahiner N. Poly(vinyl phosphonic acid) nanogels with tailored properties and their use for biomedical and environmental applications. Eur Polym J. 2016;75:264–75. https://doi.org/10.1016/j.eurpolymj.2016.01.007.

Şengel SB, Şahiner N. Synthesis and characterization of poly(N-(2-mercaptoethyl) acrylamide) microgel for biomedical applications. Polym Adv Technol. 2019;30:2109–21. https://doi.org/10.1002/pat.4644.

Shafiq Z, Ajmal M, Kiran S, Zulfiqar S, Yasmeen G, Iqbal M, Farooqi ZH, Ahmad Z, Şahiner N, Mahmood K, Ahmad HB, Al-Harrasi A. Facile synthesis of hydrogel-nickel nanoparticle composites and their applications in adsorption and catalysis. Pure Appl Chem. 2019;91:1567–82. https://doi.org/10.1515/pac-2018-1201.

Shi H, Wang Y, Bao Z, Lin D, Liu H, Yu A, Lei L, Li X, Xu X. Thermosensitive glycol chitosan-based hydrogel as a topical ocular drug delivery system for enhanced ocular bioavailability. Int J Pharm. 2019;570:118688. https://doi.org/10.1016/j.ijpharm.2019.118688.

Sılan C, Akçalı A, Otkun MT, Özbey N, Bütün S, Özay Ö, Şahiner N. Novel hydrogel particles and their IPN films as drug delivery systems with antibacterial properties. Colloids Surfaces B Biointerfaces. 2012;89:248–53. https://doi.org/10.1016/j.colsurfb.2011.09.024.

Solomevich SO, Bychkovsky PM, Yurkshtovich TL, Golub NV, Mirchuk PY, Revtovich MY, Shmak AI. Biodegradable pH-sensitive prospidine-loaded dextran phosphate based hydrogels for local tumor therapy. Carbohydr Polym. 2019;226:115308. https://doi.org/10.1016/j.carbpol.2019.115308.

Soni KS, Desale SS, Bronich TK. Nanogels: An overview of properties, biomedical applications and obstacles to clinical translation. J Control Release. 2016;240:109–26. https://doi.org/10.1016/j.jconrel.2015.11.009.

Soto Espinoza SL, Sánchez ML, Risso V, Smolko EE, Grasselli M. Radiation synthesis of seroalbumin nanoparticles. Radiat Phys Chem. 2012;81:1417–21. https://doi.org/10.1016/j.radphyschem.2011.11.040.

Spinks JWT, Woods RJ. An introduction to radiation chemistry. New York: Wiley; 1964. https://doi.org/10.1126/science.146.3645.760.

Staudinger H, Husemann E. Über hochpolymere Verbindungen, 116. Mitteil.: Über das begrenzt quellbare Poly-styrol. Berichte der Dtsch. Chem Gesellschaft A B Ser. 1935;68:1618–34. https://doi.org/10.1002/cber.19350680841.

Su S, Wang YY, Du FS, Lu H, Li ZC. Dynamic covalent bond-assisted programmed and traceless protein release: high loading nanogel for systemic and cytosolic delivery. Adv Funct Mater. 2018;28:1805287. https://doi.org/10.1002/adfm.201805287.

Sütekin SD, Güven O. Radiation-induced controlled polymerization of acrylic acid by RAFT and RAFT-MADIX methods in protic solvents. Radiat Phys Chem. 2018;142:82–7. https://doi.org/10.1016/j.radphyschem.2017.01.046.

Sütekin SD, Güven O. Application of radiation for the synthesis of poly(n-vinyl pyrrolidone) nanogels with controlled sizes from aqueous solutions. Appl Radiat Isot. 2019;145:161–9. https://doi.org/10.1016/j.apradiso.2018.12.028.

Sütekin SD, Atıcı AB, Güven O, Hoffman AS. Controlling of free radical copolymerization of styrene and maleic anhydride via RAFT process for the preparation of acetaminophen drug conjugates. Radiat Phys

Chem. 2018;148:5–12. https://doi.org/10.1016/j.radphyschem.2018.02.012.
Sütekin, S.D., Kıraç, F., Güven, O., 2020. Facile synthesis of poly(n-vinyl pyrrolidone) and poly(n- isopropylacrylamide) nanogels with controlled sizes. (in publication).
Tahara Y, Akiyoshi K. Current advances in self-assembled nanogel delivery systems for immunotherapy. Adv Drug Deliv Rev. 2015;95:65–76. https://doi.org/10.1016/j.addr.2015.10.004.
Tambe P, Kumar P, Paknikar KM, Gajbhiye V. Smart triblock dendritic unimolecular micelles as pioneering nanomaterials: advancement pertaining to architecture and biomedical applications. J Control Release. 2019;299:64–89. https://doi.org/10.1016/j.jconrel.2019.02.026.
Tan E, Erwin B, Dames S, Voelkerding K, Niemz A. Isothermal DNA amplification with gold nanosphere-based visual colorimetric readout for herpes simplex virus detection. Clin Chem. 2007;53:2017–20. https://doi.org/10.1373/clinchem.2007.091116.
Tanaka T, Fillmore DJ. Kinetics of swelling of gels. J Chem Phys. 1979;70:1214–8. https://doi.org/10.1063/1.437602.
Tibbitt MW, Anseth KS. Hydrogels as extracellular matrix mimics for 3D cell culture. Biotechnol Bioeng. 2009;103:655–63. https://doi.org/10.1002/bit.22361.
Tomatsu I, Hashidzume A, Harada A. Redox-responsive hydrogel system using the molecular recognition of β-cyclodextrin. Macromol Rapid Commun. 2006;27:238–41. https://doi.org/10.1002/marc.200500793.
Tomoda Y, Tsuda M. Some aspects of the crosslinking and degradation of gelatin molecules in aqueous solution irradiated by 60Co γ-rays. J Polym Sci. 1961;54:321–8. https://doi.org/10.1002/pol.1961.1205416005.
Tong R, Cheng J. Anticancer polymeric nanomedicines. Polym Rev. 2007;47:345–81. https://doi.org/10.1080/15583720701455079.
Town AR, Taylor J, Dawson K, Niezabitowska E, Elbaz NM, Corker A, Garcia-Tuñón E, McDonald TO. Tuning HIV drug release from a nanogel-based in situ forming implant by changing nanogel size. J Mater Chem B. 2019;7:373–83. https://doi.org/10.1039/C8TB01597J.
Truong NP, Whittaker MR, Mak CW, Davis TP. The importance of nanoparticle shape in cancer drug delivery. Expert Opin Drug Deliv. 2015;12:129–42. https://doi.org/10.1517/17425247.2014.950564.
Ulanski P, Rosiak JM. Use of radiation technique in the synthesis of polymeric nanogels. Nucl Instrum Methods Phys Res Sect B. 1999;151:356–60. https://doi.org/10.1016/S0168-583X(99)00085-3.
Ulanski P, Rosiak JM. Polymeric nano/microgels. In: Nalwa HS, editor. Encyclopedia of nanoscience and nanotechnology: American Scientific Publishers; 2004. p. 845–71.
Ulanski P, Bothe E, Hildenbrand K, Rosiak JM, Von Sonntag C. Hydroxyl-radical-induced reactions of poly(acrylic acid); a pulse radiolysis, EPR and product study. Part II. Oxygenated aqueous solutions. J Chem Soc Perkin Trans. 1996;2(1):23–8. https://doi.org/10.1039/p29960000023.
Ulański P, Janik I, Rosiak JM. Radiation formation of polymeric nanogels. Radiat Phys Chem. 1998;52:289–94. https://doi.org/10.1016/S0969-806X(98)00155-8.
Ulański P, Kadlubowski S, Rosiak JM. Synthesis of poly(acrylic acid) nanogels by preparative pulse radiolysis. Radiat Phys Chem. 2002;63:533–7. https://doi.org/10.1016/S0969-806X(01)00549-7.
Ulański P, Kadłubowski S, Jeszka JK. Nanogel formation by intrachain radiation-induced cross-linking. Simulation and experiment. Mater Sci Pol. 2006;24:467–76.
Van der Linden H, Herber S, Olthuis W, Bergveld P. Development of stimulus-sensitive hydrogels suitable for actuators and sensors in microanalytical devices. Sens Mater. 2002;14:129–39.
Vereshchinskii IV, Pikaev AK. Introduction to radiation chemistry. New York: Davey; 1964.
Vinogradov SV, Bronich TK, Kabanov AV. Nanosized cationic hydrogels for drug delivery: preparation, properties and interactions with cells. Adv Drug Deliv Rev. 2002;54:135–47. https://doi.org/10.1016/S0169-409X(01)00245-9.
Vinogradov SV, Zeman AD, Batrakova EV, Kabanov AV. Polyplex nanogel formulations for drug delivery of cytotoxic nucleoside analogs. J Control Release. 2005;107:143–57. https://doi.org/10.1016/j.jconrel.2005.06.002.
Vinogradov SV, Kohli E, Zeman AD. Comparison of nanogel drug carriers and their formulations with nucleoside 5′-triphosphates. Pharm Res. 2006;23:920–30. https://doi.org/10.1007/s11095-006-9788-5.
Vo CD, Kuckling D, Adler HJP, Schönhoff M. Preparation of thermosensitive nanogels by photo-cross-linking. Colloid Polym Sci. 2002;280:400–9. https://doi.org/10.1007/s003960100559.
Wang MH, Kim JC. Nanogels composed of Cinnamoyl alginate and Cinnamoyl Pluronic F127. J Dispers Sci Technol. 2015;36:377–83. https://doi.org/10.1080/01932691.2014.913491.
Wang Y, Zheng J, Tian Y, Yang W. Acid degradable poly(vinylcaprolactam)-based nanogels with ketal linkages for drug delivery. J Mater Chem B. 2015;3:5824–32. https://doi.org/10.1039/c5tb00703h.
Wardman P. Application of pulse radiolysis methods to study the reactions and structure of biomolecules. Rep Prog Phys. 1978;41:259–302. https://doi.org/10.1088/0034-4885/41/2/002.
Wei W, Meng C, Wang Y, Huang Y, Du W, Li H, Liu Y, Song H, Tang F. The interaction between self – assembling peptides and emodin and the controlled release of emodin from in-situ hydrogel. Artif Cells Nanomed Biotechnol. 2019;47:3961–75. https://doi.org/10.1080/21691401.2019.1673768.
Weldrick PJ, Iveson S, Hardman MJ, Paunov VN. Breathing new life into old antibiotics: overcoming antibacterial resistance by antibiotic-loaded nanogel carriers with cationic surface functionality. Nanoscale. 2019;11:10472–85. https://doi.org/10.1039/c8nr10022e.

Wichterle O, Lím D. Hydrophilic gels for biological use. Nature. 1960;185:117–8. https://doi.org/10.1038/185117a0.

Wu W, Shen J, Banerjee P, Zhou S. Core-shell hybrid nanogels for integration of optical temperature-sensing, targeted tumor cell imaging, and combined chemo-photothermal treatment. Biomaterials. 2010;31:7555–66. https://doi.org/10.1016/j.biomaterials.2010.06.030.

Wu C, Jiang P, Li W, Guo H, Wang J, Chen J, Prausnitz MR, Wang ZL. Self-powered iontophoretic transdermal drug delivery system driven and regulated by biomechanical motions. Adv Funct Mater. 2019;1907378 https://doi.org/10.1002/adfm.201907378.

Xia Y, Xu C, Zhang X, Ning P, Wang Z, Tian J, Chen X. Liposome-based probes for molecular imaging: from basic research to the bedside. Nanoscale. 2019;11:5822–38. https://doi.org/10.1039/C9NR00207C.

Yang YS, Carney RP, Stellacci F, Irvine DJ. Enhancing radiotherapy by lipid nanocapsule-mediated delivery of amphiphilic gold nanoparticles to intracellular membranes. ACS Nano. 2014;8:8992–9002. https://doi.org/10.1021/nn502146r.

Yao H, Wang J, Fan YQ, Zhou Q, Guan XW, Kan XT, Zhang YM, Lin Q, Wei TB. Supramolecular hydrogel-based AIEgen: construction and dual-channel recognition of negative charged dyes. Dyes Pigments. 2019;167:16–21. https://doi.org/10.1016/j.dyepig.2019.04.011.

Yu J, Zhang Y, Sun W, Wang C, Ranson D, Ye Y, Weng Y, Gu Z. Internalized compartments encapsulated nanogels for targeted drug delivery. Nanoscale. 2016;8:9178–84. https://doi.org/10.1039/c5nr08895j.

Yuan Z, Tsou YH, Zhang XQ, Huang S, Yang Y, Gao M, Ho W, Zhao Q, Ye X, Xu X. Injectable citrate-based hydrogel as an angiogenic biomaterial improves cardiac repair after myocardial infarction. ACS Appl Mater Interfaces. 2019;11:38429–39. https://doi.org/10.1021/acsami.9b12043.

Yue L, Wang S, Wulf V, Willner I. Stiffness-switchable DNA-based constitutional dynamic network hydrogels for self-healing and matrix-guided controlled chemical processes. Nat Commun. 2019;10:4774. https://doi.org/10.1038/s41467-019-12697-2.

Yusa SI, Sugahara M, Endo T, Morishima Y. Preparation and characterization of a pH-responsive nanogel based on a photo-cross-linked micelle formed from block copolymers with controlled structure. Langmuir. 2009;25:5258–65. https://doi.org/10.1021/la803878s.

Zahednezhad F, Saadat M, Valizadeh H, Zakeri-Milani P, Baradaran B. Liposome and immune system interplay: challenges and potentials. J Control Release. 2019;305:194–209. https://doi.org/10.1016/j.jconrel.2019.05.030.

Zeng X, Luo M, Liu G, Wang X, Tao W, Lin Y, Ji X, Nie L, Mei L. Polydopamine-modified black phosphorous nanocapsule with enhanced stability and photothermal performance for tumor multimodal treatments. Adv Sci. 2018;5 https://doi.org/10.1002/advs.201800510.

Zhang X, Malhotra S, Molina M, Haag R. Micro- and nanogels with labile crosslinks-from synthesis to biomedical applications. Chem Soc Rev. 2015;44:1948–73. https://doi.org/10.1039/c4cs00341a.

Zhang H, Zhai Y, Wang J, Zhai G. New progress and prospects: the application of nanogel in drug delivery. Mater Sci Eng C. 2016;60:560–8. https://doi.org/10.1016/j.msec.2015.11.041.

Zhang J, Wu P, Zhao Y, Xue S, Zhu X, Tong J, Zheng S, Chen Y, Shi X, Deng H. A simple mechanical agitation method to fabricate chitin nanogels directly from chitin solution and subsequent surface modification. J Mater Chem B. 2019;7:2226–32. https://doi.org/10.1039/c8tb03158d.

Zhao J, Shu D, Ma Z. Target-inspired Zn 2+ −dependent DNAzyme for ultrasensitive impedimetric aptasensor based on polyacrylic acid nanogel as amplifier. Biosens Bioelectron. 2019;127:161–6. https://doi.org/10.1016/j.bios.2018.12.030.

Zheng YN, Liang WB, Xiong CY, Yuan YL, Chai YQ, Yuan R. Self-enhanced ultrasensitive photoelectrochemical biosensor based on nanocapsule packaging both donor-acceptor-type photoactive material and its sensitizer. Anal Chem. 2016;88:8698–705. https://doi.org/10.1021/acs.analchem.6b01984.

Zhou A, Luo H, Wang Q, Chen L, Zhang TC, Tao T. Magnetic thermoresponsive ionic nanogels as novel draw agents in forward osmosis. RSC Adv. 2015;5:15359–65. https://doi.org/10.1039/c4ra12102c.

Zhou Q, Shao S, Wang J, Xu C, Xiang J, Piao Y, Zhou Z, Yu Q, Tang J, Liu X, Gan Z, Mo R, Gu Z, Shen Y. Enzyme-activatable polymer–drug conjugate augments tumour penetration and treatment efficacy. Nat Nanotechnol. 2019;14:799–809. https://doi.org/10.1038/s41565-019-0485-z.

Zhu H, Li Y, Qiu R, Shi L, Wu W, Zhou S. Responsive fluorescent Bi 2 O 3 @PVA hybrid nanogels for temperature-sensing, dual-modal imaging, and drug delivery. Biomaterials. 2012;33:3058–69. https://doi.org/10.1016/j.biomaterials.2012.01.003.

Zhu Q, Chen X, Xu X, Zhang Y, Zhang C, Mo R. Tumor-specific self-degradable nanogels as potential carriers for systemic delivery of anticancer proteins. Adv Funct Mater. 2018;28:1707371. https://doi.org/10.1002/adfm.201707371.

Zillessen A, Bartsch E. Synthesis of photo-cross-linkable microgel colloids for cluster formation studies. Langmuir. 2010;26:89–96. https://doi.org/10.1021/la9021454.

9 Cellulose Acetate-Based Nanofibers: Synthesis, Manufacturing, and Applications

Ashish Gupta and S. R. Dhakate

Abstract

In the world where plastic has now become a curse to the environment more than a benefit to society due to its non-degradable nature, biodegradable polymers are the only hope. Cellulose, chitosan, and lignin are some of the naturally abundant polymers that need the attention of researchers. The main drawback in biopolymers is the limited spinnability to form fibers to use them in various applications. However, cellulose can be converted to cellulose acetate (CA) by simple acetylation, which in turn becomes spinnable. Electrospinning is nowadays the most prominent technique that has been used for fabricating nanofibers from biopolymers including CA. The CA in form of nanofibers exhibits its importance in a vast field of applications such as drug delivery, antibacterial, sensor, wound dressing, and mechanical transducer due to its biocompatible nature, high porosity, ease of functionality, and high surface to volume ratio. Here, this chapter reports the most recent trends in synthesis and manufacturing of CA-based nanofibers, its composites, and their novel applications.

Keywords

Cellulose acetate · Biopolymer · Electrospinning · Nanofibers · Applications

1 Introduction

Cellulose is a biopolymer that can be obtained from wood and any plant-based material. It is very abundant in nature and thus cost effective. The global market for cellulose acetate (CA) is been reported to reach 750,000 metric tons by 2024 (http://www.strategyr.com/Cellulose_Acetate_Market_Report.asp). Since a long time, cellulose (Rayon) has been used in the manufacturing of fibers via a solution process (wet spinning) technique, followed by conversion to carbon fibers; however due to lower mechanical properties as compared to Poly acrylonitrile (PAN)-based carbon fibers, its use is limited in the development of structural composites. On the other hand, it can be easily functionalized physically and chemically with suitable additives and converted to useful derivatives. Various derivatives of cellulose have been explored till now. Cellulose triacetate is acetate ester of cellulose synthesized primarily in year 1865 by reaction of cellulose with acetic acid (Ibeh 2011). When this solution is poured in water, white flakes called triacetate are precipitated. However, this invention did not directly lead to progress in acetate

A. Gupta · S. R. Dhakate (✉)
CSIR-National Physical Laboratory,
New Delhi, India
e-mail: dhakate@nplindia.org

J. K. Patel, Y. V. Pathak (eds.), *Emerging Technologies for Nanoparticle Manufacturing*,
https://doi.org/10.1007/978-3-030-50703-9_9

fiber spinning until the method of converting triacetate into secondary acetate (diacetate) was discovered by George Miles in 1904 (Hearle and Woodings 2001). This invention solved the problem of directly dissolving triacetate for fiber spinning. CA polymer has advantage over cellulose that it can be electrospun by dissolving in easy solvents and can be reconverted to cellulose fibers by simple deacetylation reaction (Son et al. 2004; Ahmed et al. 2017).

A number of publications have been authored till now on the topic of electrospinning of CA nanofibers starting from 1934 with the first article by Formhals using acetone as a solvent (Anton 1934). However, after long time, Liu and Hsieh (2002) drew nanofibers from CA and since then CA has become more popular among researchers. Web of science shows that since 2002, more than 650 research papers have been published worldwide related to the synthesis and applications of CA nanofibers with 89 in 2018 and 85 in 2019. This shows that researchers are turning toward the use of biopolymers instead of synthetic polymers.

This chapter introduced most recent trends exploring the advancement in synthesis, manufacturing, and applications of CA-based nanofibers. Before delving into CA nanofibers, it would be fruitful to discuss the structure and derivatives of CA followed by electrospinning as a prime method for the synthesis of nanofibers.

2 Derivatives of CA Polymer

CA is being synthesized and manufactured under various brands such as Cellulose triacetate (Arnel® (Celanese, America)), Tricel (British Celanese), Trilan, primary acetate, JPS (Courtaulds), Courpleta (Courtaulds), fibra de triacetate (Esp.), Cellulose Diacetate, etc.

The first commercial production of acetate filament was undertaken by the British Cellulose Co. Ltd. at Spondon, England, in 1921. In 1922, they also launched acetate fiber production in the United States. Cellulose triacetate with chemical equation is $(C_6H_7O_2\ (OOCCH_3)_3)_n$ and was first produced commercially in the United States (1954) by Celanese Corporation. Eastman Kodak was a manufacturer of CTA until March 15, 2007. In 2010, Eastman Chemical announced almost 70% increase in cellulose triacetate output at its Kingsport (TN) manufacturing site to achieve the increasing demand for the chemical's use as an intermediate in the production of polarized films for liquid crystal displays (LCDs). Ethyl cellulose is another derivative of CA (Wang et al. 2013), which is being used for nanofiber synthesis nowadays due to its similar structure to CA. The difference in structure is due to the presence of some ethoxy groups ($–O–CH_2–CH_3$) in place of hydroxyl (–OH) groups (McKeen 2012). However, as compared to other derivatives, CA is more prevalent in nanofiber industry because of the ease in the fiber formation due to large number of solvents available and simple deacetylation processes for cellulosic conversion. In the following section, discussion about the synthesis and manufacturing of CA-based nanofibers is carried out.

3 Synthesis and Manufacturing of CA-Based Nanofibers

Although CA is a thermoplastic material, it cannot be melt spun to nanofibers because of the high melt viscosity due to intramolecular and intermolecular hydrogen bonds. CA butyrate (CAB) a derivative of CA and is a strong shear thinning pseudoplastic fluid, tried for melt-spinning (Wang et al. 2018; Hooshmand et al. 2014). The declined molecular weight of CAB revealed the occurrence of thermal degradation during melt spinning. The melt viscosity of CAB is found to be relatively sensitive to temperature change and it is difficult to achieve particular viscosity until the temperature reaches 230 °C. The diameter of fibers produced from melt spinning of CAB polymer is nearly 100–200 μm. The surface of fibers drawn at 145 °C was as smooth as that of the as-spun fibers, yet fibers drawn to a ratio of 1.5 at 155 °C showed a relatively rough and bumpy surface (Wang et al. 2018). This reveals that the

viscous flow of CAB occurs at a temperature higher than its melting point (150 °C) during drawing process. Therefore, the actual experiment results suggest that the suitable drawing temperature should be between 135 and 150 °C for as-spun fiber with SDR 31. Also, to overcome the brittleness of CAB melt spun fibers, Hooshmand et al. (2014) prepare a composite film of CAB with a plasticizer triethyl citrate (TEC) and cellulose nanocrystal (CNC) gel and extrude them from 0.4 mm spinneret at 160 °C in inert atmosphere. The as-spun fibers were further subjected to a solid state drawing process with a ratio of 1.5 between two rollers. The two rollers have a temperature of 105 and 90 °C, respectively. Scanning Electron Microscope (SEM) analysis (Fig. 9.1) shows that both as-spun (CAB–TEC_{AS}, CAB–TEC–$2CNC_{AS}$, and CAB–TEC–$10CNC_{AS}$) and solid state drawn fibers (CAB–TEC_{DR}, CAB–TEC–$2CNC_{DR}$, and CAB–TEC–$10CNC_{DR}$) have uniform morphology and are free from any defect of crack.

Manufacturing of microfibers from CA is also carried out industrially by wet spinning (Ferguson and Ibrahim 1969), However, electrospinning is recently the prime method of fabricating CA and its derivatives into nanofibers. Electrospinning is a non-mechanical, inexpensive, and fascinating nanofiber technology (Dhakate et al. 2011; Gupta et al. 2017, 2019). It is being used for synthesis and fabrication of useful fibers from synthetic as well as natural polymer.

3.1 Electrospinning Process and Mechanism

Electrospinning was first discussed in a patent by Cooley and co-workers in 1902 as an apparatus to synthesize polymeric fibers with the application of voltage to a polymer solution. The basics for their research comes from the earlier studies on the effect of electrostatic force on water droplet in the seventeenth century and excitation of dielectric liquids under that field in the eighteenth century. But the fundamental idea was studied in a series of patents by Anton Formhals from 1934 to 1944.

Electrospinning instrument consists of major parts, that is, electric voltage, fiber collector, and a syringe pump (Fig. 9.2). It also consists of two electrode systems, where one electrode is connected to the collector and other is connected to a polymer solution

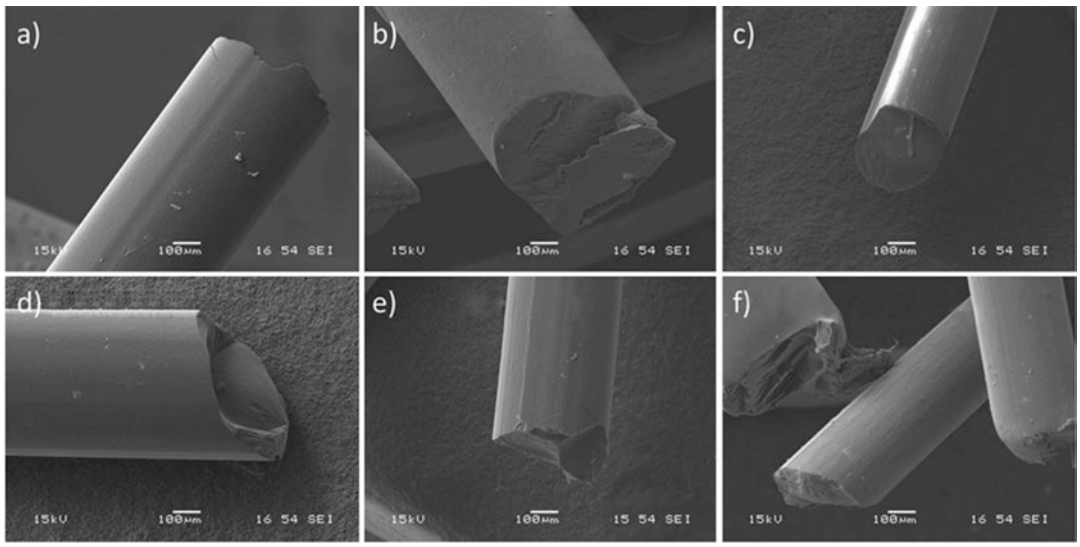

Fig. 9.1 SEM image of the both as-spun and drawn fibers. (**a**) CAB–TEC_{AS}, (**b**) CAB–TEC–$2CNC_{AS}$, (**c**) CAB–TEC–$10CNC_{AS}$, (**d**) CAB–TEC_{DR}, (**e**) CAB–TEC–$2CNC_{DR}$, and (**f**) CAB–TEC–$10CNC_{DR}$ (Hooshmand et al. 2014)

through a metallic needle. The electric voltage is applied on the tip of the syringe needle, which causes adherence of same charges in polymer chains, which results in charge repulsion in one way and dominates surface tension in the other way, forcing splaying or spraying processes (Doshi and Reneker 1995).

The solvent gets evaporated in between and fibers get collected on collector (stationary or moving). The polymer drop from syringe to collector undergoes three main stages which are jet initiation, jet thinning, and jet solidification (Dhakate et al. 2011; Garg and Bowlin 2011).

The nanofiber diameter and length both can be controlled by varying various electrospinning and solution parameters as illustrated in Fig. 9.2. Solution parameters include concentration, viscosity, surface tension, volatilability of solvent conductivity, molecular weight of polymers, etc. Electrospinning or instrument variables consist of tip to collector distance, electric voltage strength, flow rate of solution, type, and speed of fiber collector (Long et al. 2019). Environment factors like temperature and humidity (Cheng et al. 2017) also affect the synthesis and morphology of nanofibers. The most important factor in the nanofiber formation is the solubility of the polymer in the solvent for homogeneous solution preparation.

3.2 Solvent Selection

The focus point in this section is synthesis and manufacturing of CA nanofibers by selecting the appropriate solvent system and optimization of instrumental as well as solution parameters. A number of single as well a combination of solvents have been tried for preparing solution for electrospinning. Single solvents include acetone, chloroform, N,N-dimethylformamide (DMF), dichloromethane (DCM), formic acid, methanol, and pyridine. Dimethylacetamide-Acetone, water-acetone, chloroform–methanol, DCM–methanol, acetic acid-water, and THF-DMSO are among the mixed solvent systems.

The use and selection of solvent remain a hit and trial method and so involves the use of a number of single as well as binary solvents. Based on the Hansen solubility parameters ($D(s-p)<12.40$), CA is soluble in acetic acid (2.68), acetone (5.39), DMAc (5.88), chloroform (8.87), and methanol (12.35). Similarly, CA is soluble in solvents when the Hildebrand solubility (δ) lies between 9.5 and 12.5 $(cal/cm^3)^{1/2}$. So, according to Ghorani et al. acetone and DMAc with Hildebrand solubility parameters of 9.77 and 11.1 $(cal/cm^3)^{1/2}$, respectively, are suitable solvents for CA (Ghorani et al. 2013).

In another work, electrospun CA fibers using pure acetone as a solvent produced both

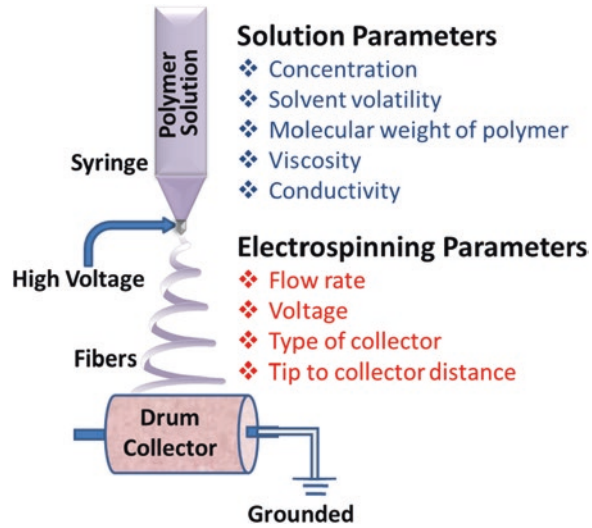

Fig. 9.2 Electrospinning setup and effective variables

cylindrical-and ribbon-shaped fibers of a diameter of 1 μm, whereas CA in 2:1 acetone/DMAc yielded smooth bead-free cylindrical fibers of diameter in the range of 250–350 nm and CA in 3:1 acetic acid/water formed fibers with beads (Majumder et al. 2019).

3.2.1 Acetone-Based Solvent Systems

The CA polymer dissolves in acetone more rapidly as compared to any other solvents but is it is reported that in case of pure acetone due to rapid evaporation the needle gets blocked easily and is required to be cleaned every moment. Hence, another solvent mixed with acetone is preferred to get continuous nanofibers.

(a) Using Water Acetone System

Son et al. (2004) reported acetone: water as a solvent for electrospinning of CA nanofibers. The CA concentration ranged from 9 to 21 wt%, and the water content varied from 5 to 20 wt %. The distance between the needle tip and the ground electrode ranged from 6 to 12 cm. Positive voltage applied to polymer solutions ranged from 8 to 12 kV. Figure 9.3 shows effect of water concentration on CA-based nanofibers. Water delayed the evaporation time of acetone in the system and formed ribbon-like nanofibers with increase in water content. Also, the diameter of nanofibers increased rapidly at water concentration up to 20 wt% (Fig. 9.3d), while on 5 wt% (Fig. 9.3a) water the needle blocked frequently. Hence, it can be assumed that water concentration of 10–15 wt% is suitable to get continuous CA nanofibers.

(b) Acetone-DMF System

Similarly, N,N dimethylformamide (DMF) is also used along with acetone to increase the evaporation time. The 13% of CA solution is prepared in acetone DMF system in volume ratio of 2:1. The solution is stirred for several hours till a homogeneous solution is obtained. In this study, DMF is used to slow down the solvent evaporation during fiber formation (Fathona and Yabuki 2013, 2014). Also, an electric spark (recognized at 4.1 kV) is used in between syringe needle and fiber collector to cut nanofibers of desired length. This shows that it is also possible to get short fibers using the electrospinning technique (Fig. 9.4). Figure 9.4a shows the SEM image of the short fiber with irregular diameter ranging from 500 to 1000 nm, and its magnified image showing a ribbon-like structure in the center (1000 nm). The electric field generated by the electric spark blocked the continuous fiber flow, so that it compressed the mass in the centers of the short fibers. However, at one end the diameter of fiber get reduced to 200–140 nm which is considered due to stretching and cut by periodic voltage and spark energy. While continuous CA nanofibers show smooth morphology and average diameter up to 400 nm.

(c) Using Acetone-DMAc Solvents

It is reported that the acetone-DMAc mix solvent system is the best known solvent for producing continuous nanofibers from CA. Liu and Hsieh (2002) explored a number of solvents for electrospinning of CA, including acetone, DMAc, and acetic acid in mixtures. It is seen that few fibers were obtained from electrospinning CA in pure acetone or acetic acid, while no fibers were observed from electrospinning CA from pure DMAc. They found that electrospinning from acetic acid-DMAc mixtures resulted in fine beaded fibers, while fiber formation from acetone-DMAc was stable and uniform. Fiber morphology varied with both the concentration of CA in the spinning dope and with the ratio of acetone to DMAc in the solvent. It was found that the average diameters of the CA nanofibers can be controlled by changing the composition of the mixed solvent. In another study, 20% CA (M. Wt. 100,000 g/mol) was utilized for electrospinning (Deng et al. 2013). The spinning conditions are a voltage of 16 kV, a flow rate of 0.02 mL/min, and a needle tip-to-collector distance of 16 cm. Mats consist of smooth and uniform nanofibers of average diameter 450 nm, and pore size 710 ± 515 nm are obtained. It is also reported that CA nanofibers using acetone-DMAc can be obtained at a broad range of parameters, that is, 10–25% (by weight), a voltage range of 10–25 kV, and tip-to-collector distances of 10–25 cm.

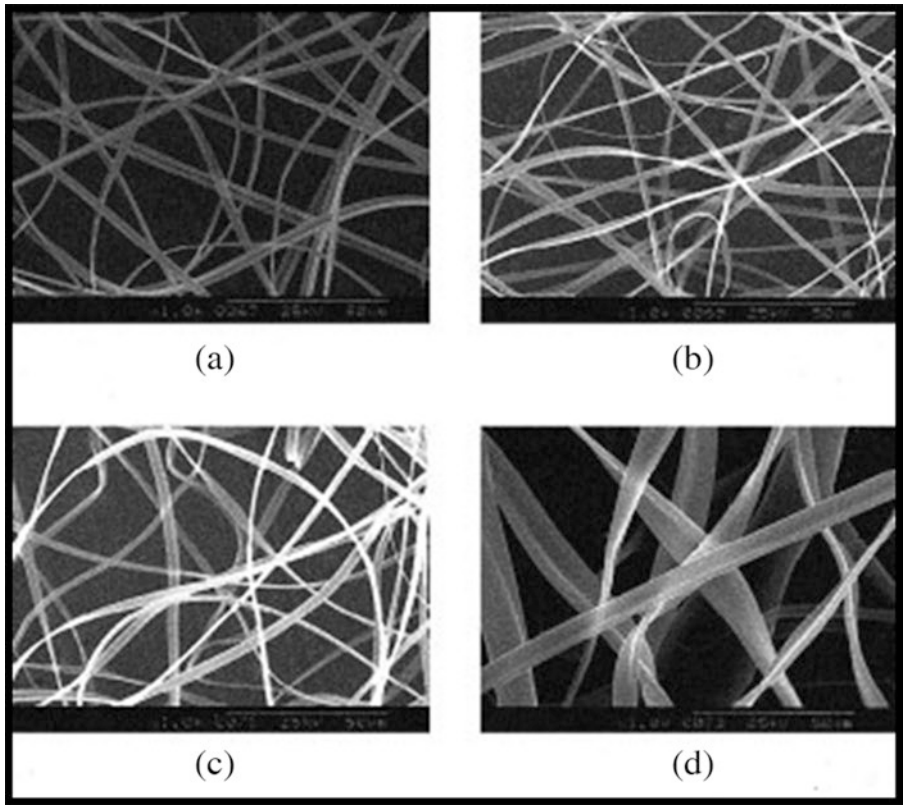

Fig. 9.3 SEM images of electrospun CA fibers from CA/acetone/water solutions (17 wt % CA) at various water concentrations: (**a**) 5 wt %, (**b**) 10 wt %, (**c**) 15 wt %, and (**d**) 20 wt % (Son et al. 2004)

In a study by Kalwar et al., CA nanofibers have been fabricated from different concentrations (13%, 19%, and 25%) of CA by dissolving in the mixture solution of DMAc and acetone (2:1.5 v/v) (Kalwar et al. 2018) followed by electrospinning. It is reported that 13% and 19% concentration of CA results into beaded nanofibers while 25% concentration results into good fibers but with high diameter. In another case, Gaminian et al., a 17 wt% sample of CA is dissolved in a mixture of acetone/DMAc in the volume ratio of 2:1 and stirred for 5 h to achieve the homogeneous solution that is finally considered as a precursor solution for electrospinning. The CA solutions are electrospun at a positive voltage of 20 kV, a needle tip-to-collector distance of 15 cm, and a solution flow rate of 3.0 mL/h. Electrospinning was performed at 20 ± 2 ° C and relative humidity 45–60% (Gaminian and Montazer 2017). CA powder is dissolved in a mixed solvent of 2:1 v/v acetone/DMAc to prepare the base CA solution at a fixed concentration of 15% w/v. Gallic acid (GA)-loaded CA solutions were prepared by dissolving GA powder in the amounts of 10, 20, 30, and 40 wt% based on the weight of CA powder. The electrospun fibers were collected for 12 h on a rotating drum set at 15 cm from the tip of the needle. The electric fields were applied as 15, 18, and 21 kV controlling feed rate at 1 ml/h (Wutticharoenmongkol et al. 2019).

3.2.2 Other Solvent Systems

Acetic acid water has also been used as a solvent system for the synthesis of CA nanofibers. Han et al. used acetic acid with water (Han et al. 2008) and found for the first time that CA nanofibers could be continuously electrospun using a mixed solvent of acetic acid/water. However, CA can be dissolved at acetic acid contents higher than 70 wt%. They studied the effect of solvent com-

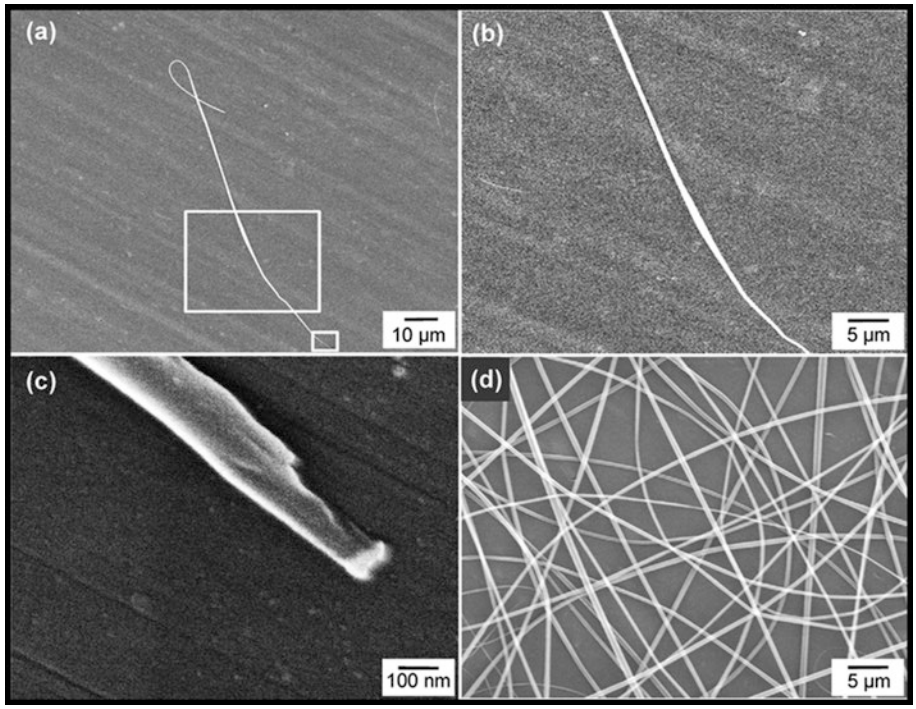

Fig. 9.4 SEM images of (**a**) a short fiber, (**b**) the center of a short fiber, (**c**) the edge of a short fiber, and (**d**) a continuous electrospun fiber without an electric spark (Fathona and Yabuki 2013)

position on the diameter of nanofibers and demonstrated that with increase in acetic acid content from 75 to 95 the nanofiber diameter increases exponentially. Figure 9.5 shows effect of acetic acid content on diameter of nanofibers. The smallest diameter (160 nm) of nanofibers were obtained at acetic acid content 70% (Fig. 9.5a), which increases as 180 nm, 300 nm, 400 nm, 600 nm, and 1300 nm, respectively, for 75 (Fig. 9.5b), 80 (Fig. 9.5c), 85 (Fig. 9.5d), 90 (Fig. 9.5e), and 95% (Fig. 9.5f) content of acetic acid. Recently, Jauhari et al. (2019) fabricated polyvinylpyrrolidione/CA (7,3) blend by dissolving in acetic acid water (ratio 8:2). A series of polymer concentrations are prepared as 5%, 10%, and 15% (w/v) and labeled as FC1, FC2, and FC3. In FC1, beaded fibrous morphology is observed, while in FC2 and FC3 fibers without beads are electrospun. The reason for uniform and nonbeaded fibers at higher concentration is the presence of more polymer chains at specific time in a single droplet. In the context of green energy, Hansen's theory of solubility (Yu et al. 2011) can be applied to select non-toxic binary systems for manufacturing electrospun CA nanofibers by optimization of processing parameters. High packing density is obtained with binary low-volatile alcohols/methyl-ethyl ketone (MEK) solvent mixtures, a decrease in tip to collector distance, and an increase in feed rate (Haas et al. 2010). DCM-methanol mixed solvent in 5:1 v/v ratio were also used for fabricating CA-based nanofibers. The fiber diameters ranged from 300 nm to 2.8 μm (Iliou et al. 2019).

After manufacturing CA nanofibers, it has been applied in various applications such as carbon nanofiber formation (CNF), water purification, and where free hydroxyl groups are required, in which it is converted into pure cellulose by means of deacetylation. Such cellulose is named as deacetylated cellulose (DCA) or regenerated CA (RCA) in literature.

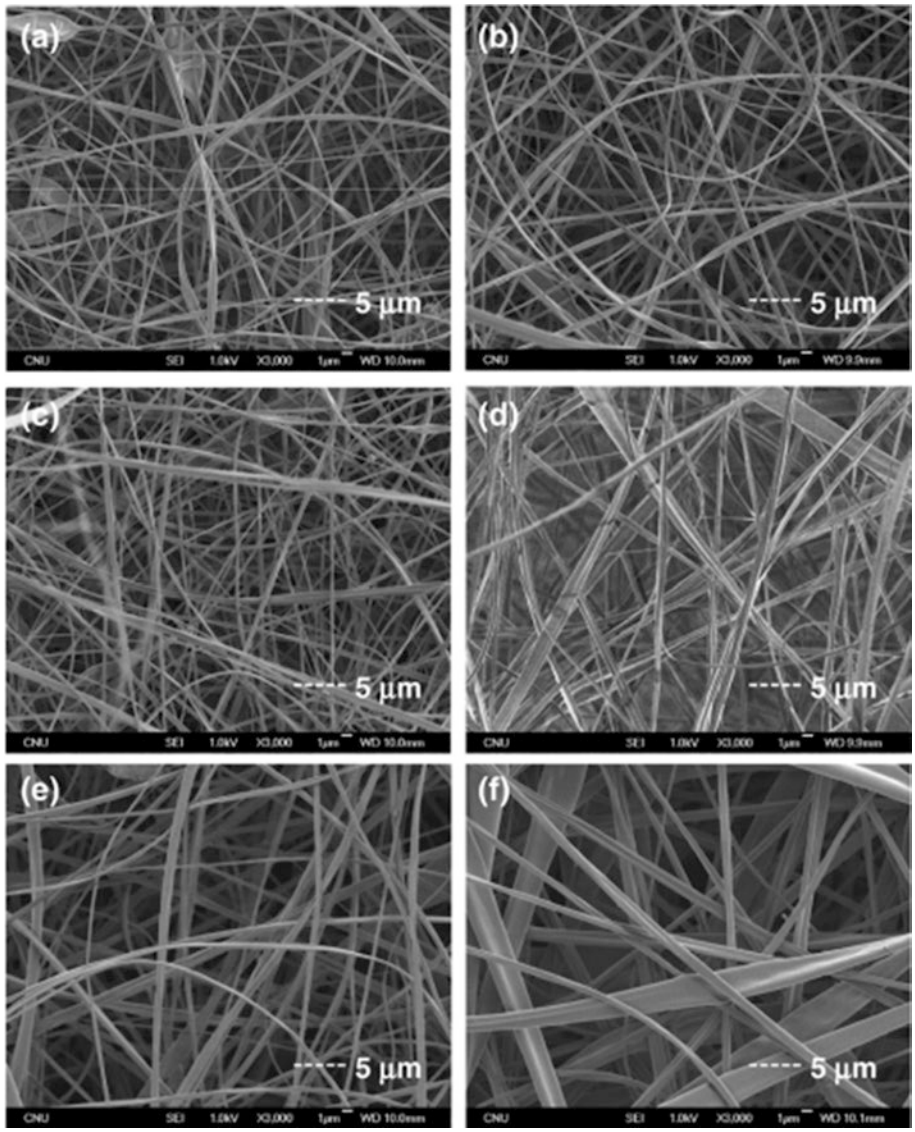

Fig. 9.5 SEM micrographs of the CA nanofibers electrospun from 17 wt% CA solutions in various mixed solvents of acetic acid/water: (**a**) 70/30, (**b**) 75/25, (**c**) 80/20, (**d**) 85/15, (**e**) 90/10, and (**f**) 95/5 (Han et al. 2008)

3.3 Deacetylation Study

As discussed in an earlier section, pure cellulose nanofibers by electrospinning are difficult to produce. However, CA as such or in the form of nanofibers can be subjected to an easy deacetylation process and converted to cellulose nanofibers for its applications wherever required. Generally, the deacetylation process required the use of some hydrolyzing agent such as NaOH, KOH in specific concentration. Liu et al. were first to do deacetylation of cellulose nanofibers (Liu and Hsieh 2002). In this they have dipped CA fibers in 0.2 N NaOH solution in 1:1 w/w EtOH/water for 72 h for stirring. Kalwar et al. (2018) utilized NaOH (0.02 M) ethanol solution, and CA nanofibers are left in the solution for 12 h. After 12 h, fibers are taken out and washed three times with deionized water for the removal of NaOH residues and then dried at 60 °C for

30 min in an incubator and stored for further use. They found that 12 h time is sufficient for deacetylation. Khatri et al. (2012) and Callegari et al. (2011) utilized 0.05 M NaOH solution for 30 h at room temperature for complete deacetylation. A 17% (wt%) of CA solution is prepared in DMF and acetone (DMF: Acetone = 1:2) for the fabrication of CA nanofibers. The solution is continuously stirred for 24 h before electrospinning (Wahab et al. 2019). Figure 9.6 shows SEM images of DMF and acetone solvent-based CA nanofibers before and after deacetylation. The average diameter of the nanofibers reduces from 291 to 289 nm after deacetylation and size distribution regularized.

The distillation process can be characterized using the FTIR technique (Fig. 9.7). The neat CA nanofibers and those treated up to 30 min with NaOH show peaks for C–O at 1745, C–CH_3 at 1375, and C–O–C at 1235 cm^{-1} showing 30 min are not sufficient for deacetylation. The deacetylation can be observed by subsequent decrease and complete removal of acetate group at 1745 cm^{-1}(C=O), 1375 cm^{-1} (C−CH_3), and 1235 cm^{-1} (C–O–C), while increase in peak near 3500 cm^{-1} (O–H) in case of 60 min treatment with NaOH. However, while using NaOH with ethanol water mixture 30 mi are sufficient for ultrasonicated assisted deacetylation. However, to get complete cellulose structure containing –OH group, a 60 min deacetylation is required. It can be seen that there is no adverse effect of ultrasonic cavitation and ethanol formulation on the chemical structure of cellulose. This shows that ethanol-assisted ultrasonic deacetylation by NaOH is far superior and fast as compared to the conventional NaOH approach that takes more than 30 h.

In another method, acetylation is carried out by using 25 mL of an acetone–water mixture (v/v 1/1) at room temperature for 24 h followed by the addition of 12.5 mL of 0.5 N KOH in ethanol. Afterward, excess of alkali (KOH) is removed by titrating with 0.1 N HCl with phenolphthalein as indicator. The nanofibers swell in acetone-water mixture (24 h) and hence OH^- from KOH gets diffused into nanofibers resulting in complete deacetylation. It is suggested that 30 min time is sufficient for complete deacetylation and to get cellulosic structure (Son et al. 2004).

Kim and Lee (2016) reported a novel process of fluorination for deacetylation of CA. Initially, fibers are kept in vacuum and degassed at 60 °C for 1 h followed by mixture of fluorine and nitrogen (F2:N2¼2:8, 4:6, and 6:4) for 10 min and found F_2:N_2 4:6 as optimum. In the first step, the fluorine radical attacks the acetyl group on the CA nanofiber, creating a delocalized negative charge between the oxygen atoms (Fig. 9.8).

The first step is slow and reversible, whereas the other two steps are fast and irreversible. In the final step, the CA nanofiber attains a similar chemical structure to that of cellulose through removal of the acetyl groups (Kang et al. 2008). The introduction of four additional CF bonds is considered from random attack by fluorine radicals at the other carbon positions in the CA nanofiber (Lee 2007). Therefore, the retained C-F4CAF fibrous pattern resulted from the removal of acetyl groups in the CA nanofiber by fluorination.

The ultrasonic-assisted deacetylation was studied at different pH levels, that is, 11, 12, 13, and 14, using NaOH solutions as well as NaOH/EtOH (4:1) solutions. Each nanofiber sample is kept in NaOH and NaOH/EtOH solvents for different time periods (30, 60, and 90 min) in order to investigate the effect of time on the process. The samples are treated at 320 W power output using fixed frequency of 37 kHz. The energy input to the treating bath is 0.97 W/cm^2 and the liquor ratio (solution to nanofiber mass) used was 50:1. For comparison, conventional deacetylation was also carried out using NaOH (0.05 M) at room temperature for 30 h. All the nanofiber samples are thoroughly rinsed off in distilled water until their pH reached neutral (Ahmed et al. 2017).

Further, the degree of deacetylation (DD%) of CA nanofibers can be calculated using the following equation:

$$DD\% = DS_{acetyl} \times 100 / 2.45$$

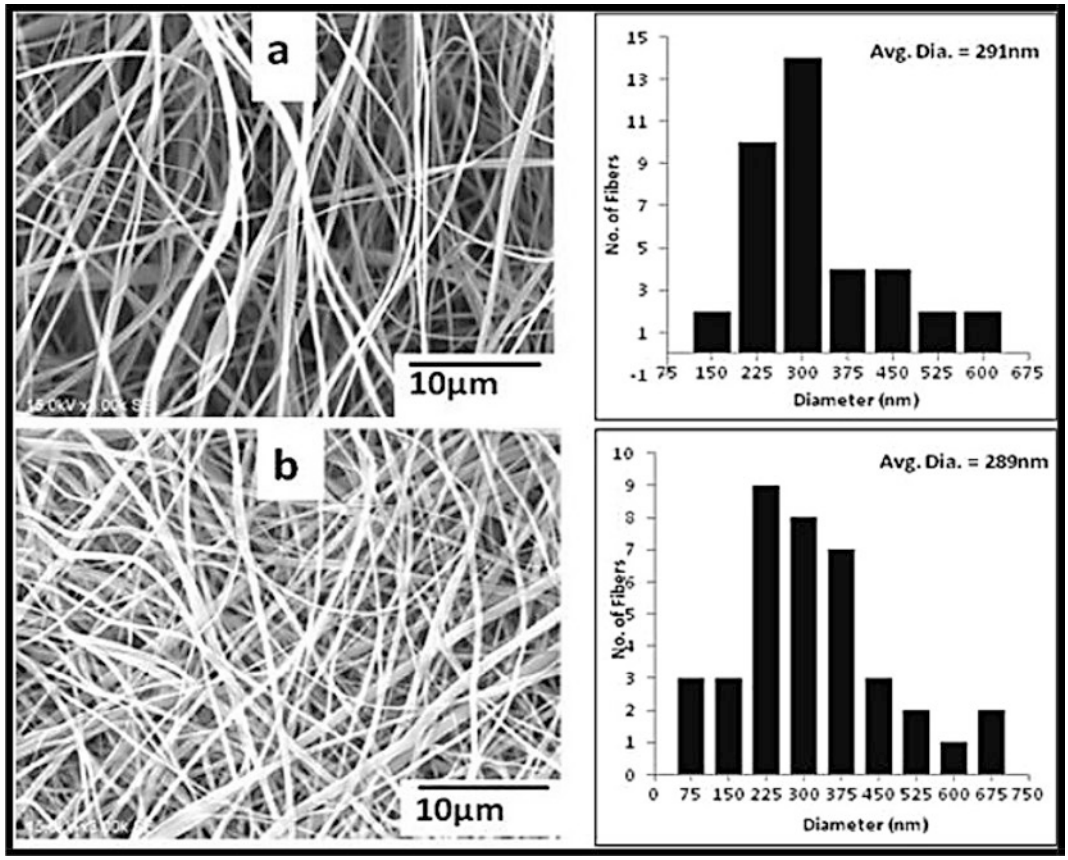

Fig. 9.6 SEM images of CA nanofibers (**a**) before and (**b**) after deacetylation (Wahab et al. 2019)

In order to calculate DD%, an accurately weighed CA nanofiber mat is added to 10 mL of 0.05 M NaOH solution in 1:1 w/w water/EtOH for 24 h under constant stirring. The excess alkali has been titrated with 0.005 M HCl using phenolphthalein as an indicator. The percentage of acetyl in CA was calculated as described by Liu and Heigh (2002):

$$\text{Acetyl}(\%) = \left(V_b \times C_b - V_a \times C_a\right) \times 4.3 / W$$

where W is the sample weight, V_b and C_b are the volume and concentration of base solution, and V_a and C_a are the volume and concentration of acid solution, respectively.

4 Application of CA Nanofibers

CA is a well-known biopolymer which possesses very good hydrophilicity, biocompatibility, and biodegradability (Kai et al. 2014). The hydroxyl groups on the CE govern many of its characteristic properties such as absorbency, chemical reactivity, surface functionality, and its mechanical strength (Jatoi and Khatri 2015). Since a long time, CA fibers are being used as a coating component in photography and eyeglass frame material, cigarette butts. However, as electrospun nanofibers, due to its unique morphology, high surface area, mat-like structure, and ease of functionalization with various additives, its applications are extended to broad areas.

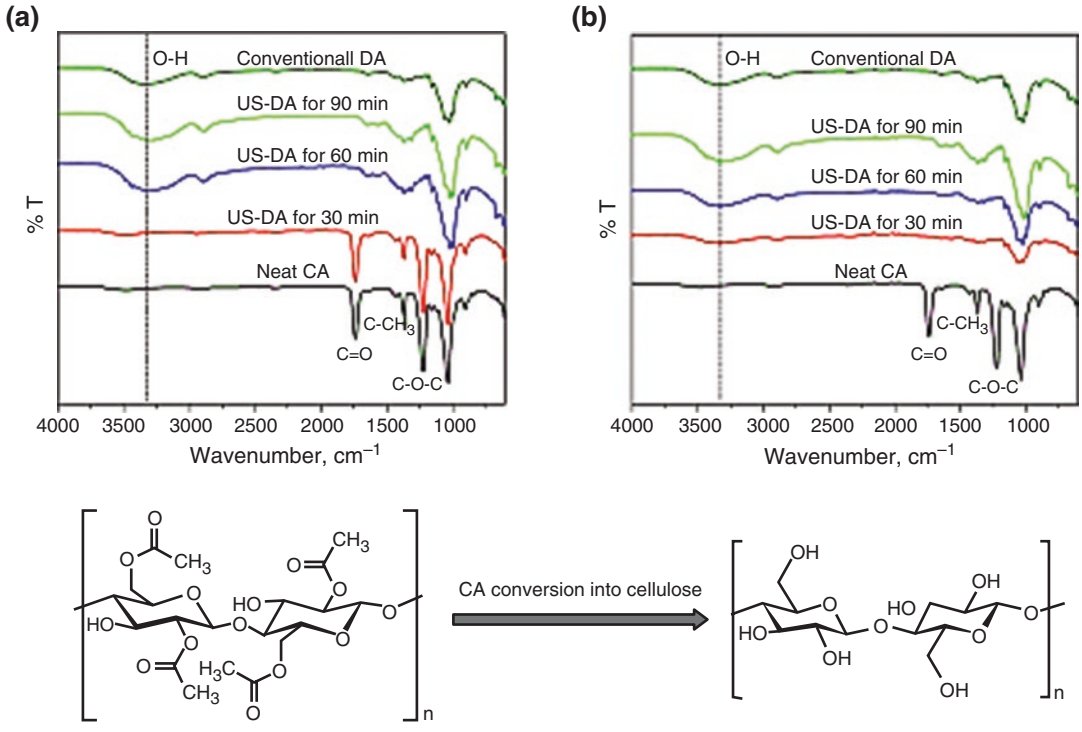

Fig. 9.7 FT-IR spectra of nanofibers deacetylated with (**a**) NaOH and (**b**) NaOH/EtOH (pH 13) (Ahmed et al. 2017)

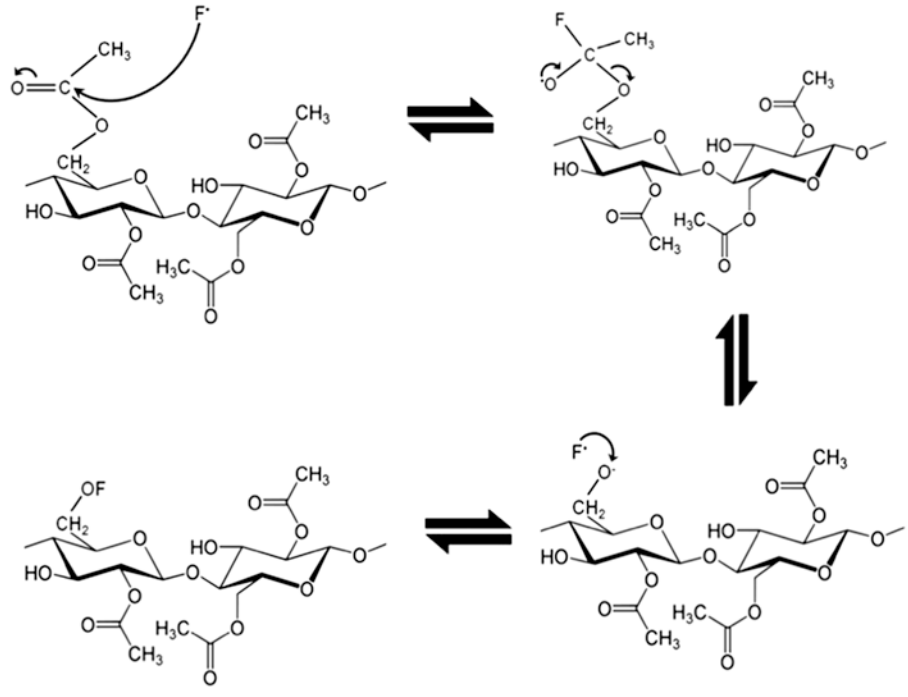

Fig. 9.8 Proposed mechanism of deacetylation of CA by fluorination (Kim and Lee 2016)

These properties of CA and its structure, morphology, and ease of adding useful additives lead to its use in number of applications such as catalysis, sensors biomedical applications (antimicrobial, drug delivery, tissue engineering, enzyme immobilization), water purification, and energy storage (Fig. 9.9).

4.1 Antibacterial Application

Owing to the presence of hydroxyl groups, the CA fibers can possibly be uniformly functionalized with silver ions without using stabilizing agents and demonstrated improved antimicrobial properties (Wahab et al. 2019; Jatoi et al. 2019; Xu et al. 2018; Jang et al. 2014a, b, c). Silver (Ag) is the most used antibacterial agent due to its low or negligible toxicity to human cells as compared to bacteria. Ag acts by denaturing the cell protein by attaching to the thiol group of cysteine, hindering the enzymatic activity of cell and inhibition of DNA replicating capacity in bacterial cell (Choi et al. 2008; Kim et al. 2008).

Kalwar et al. [24] demonstrated incorporation of Ag nanoparticles (AgNPs) in CA nanofibers. CA nanofibers are regenerated using alkali hydrolysis, which reduces the fiber diameter and increases surface roughness. Both the properties are helpful in Ag nanoparticle binding to CA surface. Afterward, a regenerated CA (R-CA) nanofiber patch is immersed in $AgNO_3$ solution followed by immersion in sodium borohydride, where silver nitrate reduced ($AgNO_3$) to AgNPs by sodium borohydride ($NaBH_4$) and attached to the hydroxyl group of R-CA. Figure 9.10a–c shows the Transmission Electron Microscope (TEM) images of immobilized AgNPs on deacetylated NFs at different concentrations: 0.1%, 0.5%, and 1%, respectively, before contact with bacteria. An increase in the number of AgNPs of different sizes attached to R-CA nanofibers can be seen clearly in the TEM image (Fig. 9.10) with increase in concentration. The average size of NPs measured is 43.33 ± 5 nm. The nanofibers were subjected to liquid broth medium having *E. coli* BH5 α and gram positive *S. aureus* for 18 h and the zone of inhibition is measured with a ruler. Figure 9.10d–f shows that AgNPs released from the surface of nanofibers and decreased in size after contact of bacteria, which is due to the release of Ag ions reacting with bacteria.

Figure 9.11 shows the digital photos of the result of zone of inhibition test carried out on *S.*

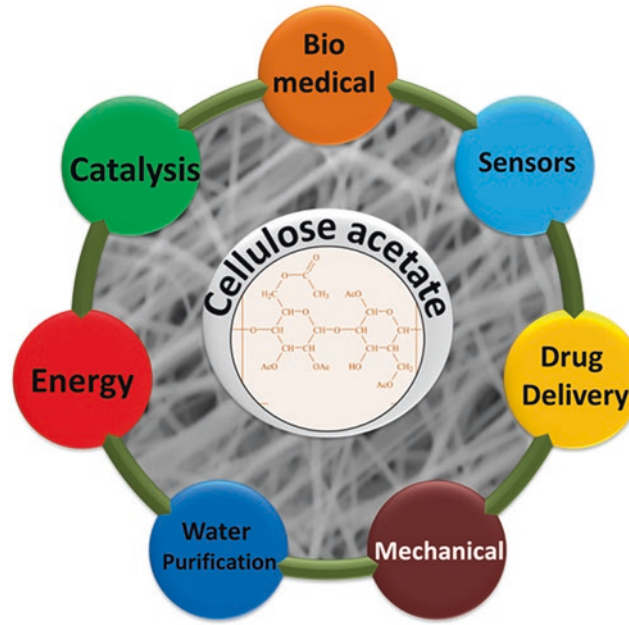

Fig. 9.9 Applications of CA-based nanofibers

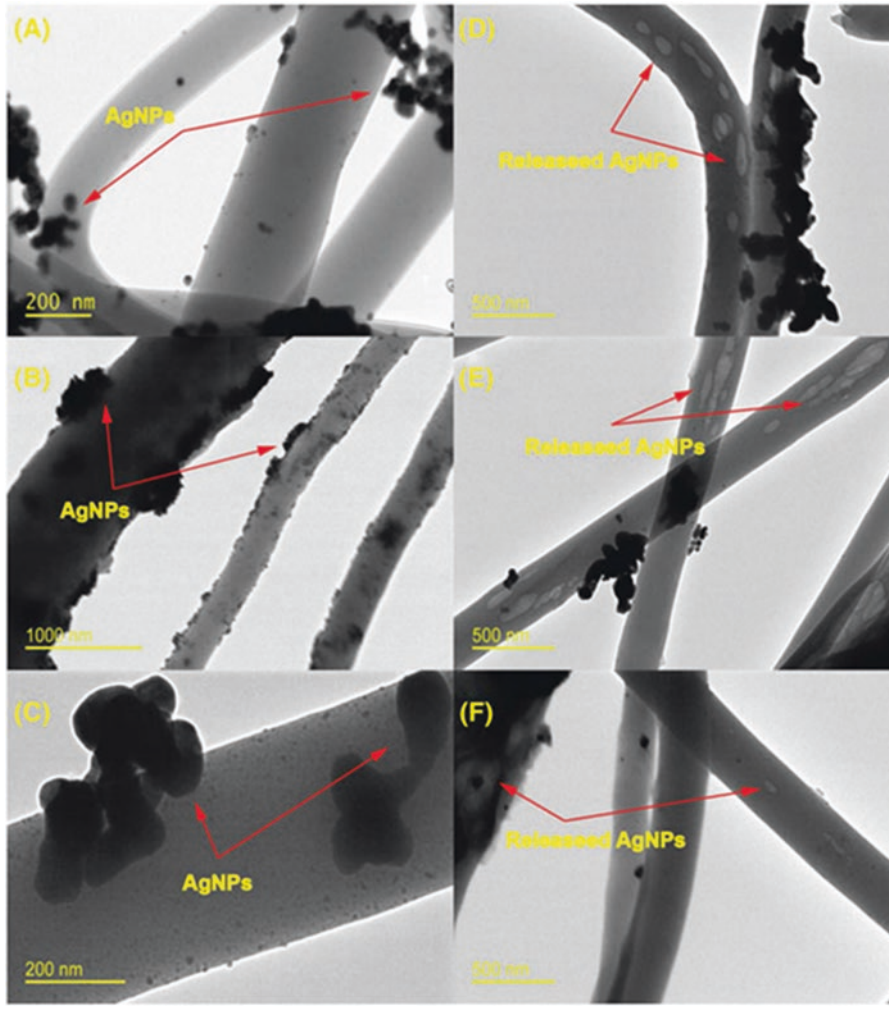

Fig. 9.10 TEM images of immobilized AgNPs on deacetylated NFs at different concentrations: 0.1%, 0.5%, and 1%. (**a**–**b**) before contact of bacteria and (**d**–**f**) after contact of bacteria (Kalwar et al. 2018)

aureus and *E. coli*. Comparing both zones of inhibition, it is reported that Ag has a greater destruction effect on gram negative bacteria than gram positive bacteria. The zone of inhibition found 12, 13.5, and 16 mm for *E. coli* as compared to 11, 12.2, and 14.4 mm for *S. aureus*. The results indicate that these nanofibers can be used as an antibacterial agent, and concentration of AgNPs has an effect on inhibition activity. AgNPs release ions which can onrush on the liposome membrane and, finally, cause death of the species. It is quite possible that these fibers can also be used for anti-fungal application along with antibacterial. However effect against fungus (*Aspergillus niger*) is found lower as observed from the decreasing zone of inhibition 10.5, 11.1, and 12.4 mm as compared to that for bacteria.

AgNPs size (Wahab et al. 2019) and phase (Jang et al. 2014a, b, c) also affect the antimicrobial activity. Wahab et al. (2019) recently generated different sized spherical AgNPs on cellulose nanofiber membranes prepared from deacetylation of CA nanofibers. The cellulose nanofiber membrane (CE) coated with $AgNO_3$ and reduction to Ag particles is carried out by heat treatment and DMF. For thermal reduction, the CEAg samples are heat treated at 160 °C in a simple laboratory drying oven for 1 h, 1.5 h, and

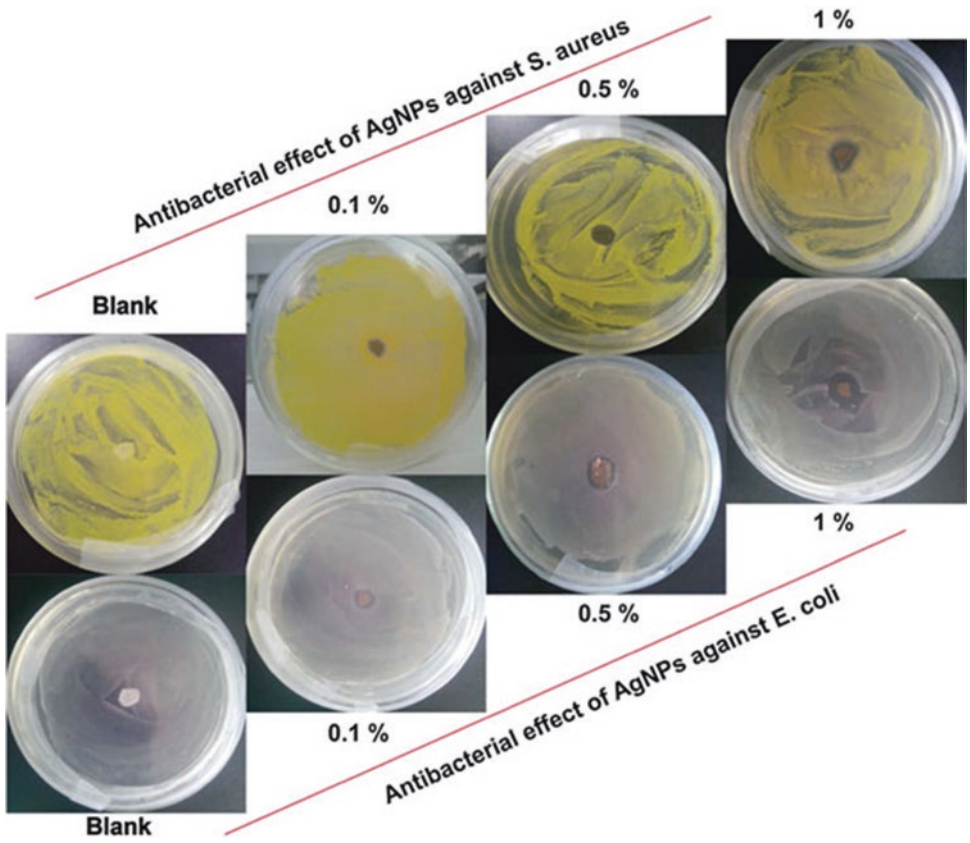

Fig. 9.11 Antibacterial activities against *E. coli* and *S. aureus* with different concentrations: 0.1%, 0.5%, and 1% of AgNPs (Kalwar et al. 2018)

Table 9.1 Antibacterial activity of the CEAgNP nanofibers (area of inhibition zone in mm^2) (Wahab et al. 2019)

Sample	Area of inhibition zone (mm^2)	
	S. aureus	*E. coli*
Contro (CE)	81.87	81.87
CEAgNP1	270.345	223.76
CEAgNP2	316.884	234.227
CEAgNP3	347.1305	269.9637
CEAgNP4	269.6893	186.0683
CEAgNP5	279.5643	202.1973
CEAgNP6	293.3707	268.014

2 h to prepare CEAgNP1, CEAgNP2, and CEAgNP3 nanocomposites. The intermittent soaking of silver-coated CE nanofibers in DMF was performed after every 15 min and the samples are treated for 45 min (CEAgNP4), 1 h (CEAgNP5), and 1.5 h (CEAgNP6). The size of AgNPs in CEAgNP1 and CEAgNP3 centered around 2.5 nm and 4.5 nm, respectively; however, the same in CEAgNP4 and CEAgNP 6 are centered around 4.5 nm and 8.5 nm, respectively.

Antimicrobial activity is tested on *S. aureus and E. coli* bacterial strains. Zone of inhibition is calculated by measuring area around the nanofiber mat as given in Table 9.1. It shows that the zone of inhibition increases with an increase in reduction time for the formation of Ag nanoparticles. Also, the heat treatment method has shown better results as compared to the DMF-based reduction technique. Similarly, Gaminian et al. also prepared Ag-CA composite nanofibers by using dopamine and ultraviolet irradiation as a reducing agent of silver ions. The average size of the synthesized Ag particles is 18 nm having silver contents of 20.3% (wt%) (Gaminian and Montazer 2017).

Another metal oxide with Ag in CA nanofibers can provide better and prolonged antibacte-

rial activity. The TiO_2/AgNP nanocomposite particles (Jatoi et al. 2019) have been synthesized using dopamine hydrochloride (Dopa) to form a polydopamine coating (pDopa) on the TiO_2 nanoparticles followed by treatment with $AgNO_3$ solution to form metallic AgNPs decorated on the TiO_2 nanoparticle surface. Then, these NPs are incorporated in 17 wt% CA by direct electrospinning. With 5% and 10% of NP loading, they achieved nearly 100% cell death with slow release of Ag from the CA polymer matrix. Such formulations also avoid the fast release of Ag, which control both side effects named as argyria and argyrosis (Panyala et al. 2008). However, use of photocatalytic agents such as ZnO and TiO_2 need UV activation before use.

4.2 Drug Delivery

Cellulose and its derivatives are being used in pharmaceutical industry from a long time as excipients due to their non-harmful and biodegradable nature. However, CA in the form of nanofibers is being utilized as a substrate or encapsulation agent for modern drug formulations. The most common route of drug administration is the oral route which has many drawbacks such as systemic adsorption, hepatic metabolism, and need of frequent dosing.

Electrospun nanofibers are being extensively used for delivery of non-steroidal anti-inflammatory drugs (NSAIDs) such as ketoprofen (Yu et al. 2012), naproxen (Li et al. 2014a, b), sulindac (Chung and Kwak 2019), rosmarinic acid (Vatankhah 2018), Acetaminophen (Wang et al. 2015a), Ibuprofen (Celik and Oksuz 2015), etc., for providing local pain reliving effect and bypassing systemic circulation. These drug-loaded nanofibers can be used for transdermal application of mucoadhesive drug delivery.

Recently, it has been highlighted that electrospun polymer nanofibers exhibit an unusual size-dependent behavior, which is a noticeable increase in their mechanical strength with decreasing diameter. Lim et al. (2008) revealed that polymer nanofibers with a smaller diameter have a higher degree of molecular orientation and crystallinity. However, the molecular motion of chains is significantly suppressed when the diameter of Nylon-6 nanofibers decreased, implying that chains confined in a thin polymer nanofiber tend to form a rigid structure. In addition, the release of Rhodamine B molecules from Nylon 6 nanofibers is severely retarded when the diameter of the nanofibers decreased. Chung and Kwak (2019) studied the effect of nanoscale confinement with relation to molecular motion and drug delivery. They prepared nanofibers with different diameters of 260, 350, 530, 620, and 850 nm. It was observed that energy of activation for the main chain motion (E_a, main) increased from 8.64 to11.09 eV with decreasing diameter of CA nanofibers (CN) from 850 to 530 nm. The increase in E_a main implies that the molecular mobility for the reptation-like displacement of main chains decreases with a decrease in the diameter of CNs from 850 to 530 nm. Furthermore, the E_a for the side chain motion (E_a, side) increased from 3.83 to 7.16 eV with decreasing diameter of CNs from 850 to 350 nm, suggesting that the motion of the side chains is suppressed with decreasing diameter. Figure 9.12 shows the effect of diameter on the drug diffusion coefficient (D) value for sulindac loaded CN. The D values for CN-850 and CN-620 are 80.0 and 85.3 $nm^2\ min^{-1}$, respectively. The similar D values indicated that the rate of drug release in CA matrix is similar. However, with decreasing diameter from 620 to 260, the D noticeably decreases. The D values for CN-530, CN-350, and CN-260 are 47.5, 20.4, and 10.3 $nm^2\ min^{-1}$, respectively. These results suggested that the drug tended to be slowly diffused with decreasing diameter of CNs from 620 to 260 nm.

Tungprapa et al. (2007) demonstrated the incorporation of NSAIDS in CA nanofibers by loading four model drugs (sulindac, ibuprofen, naproxen, and indomethacin) using single nozzle electrospinning with a drug loading efficiency of 84–93%. The observations indicate that the obtained fibers have a smooth surface showing all drug encapsulated inside. The drug release from CA-based nanofibers is much faster than cast film-based formulation.

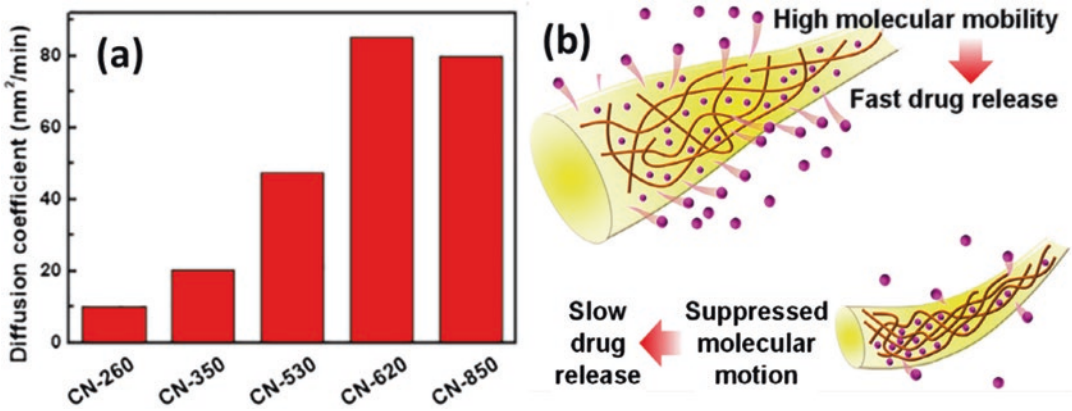

Fig. 9.12 (**a**) Diffusion coefficient (**b**) the proposed effect of confinement on molecular mobility and drug release properties of CA/sulindac nanofibers (Chung and Kwak 2019)

Tri axial electrospinning (Yu et al. 2015; Liu et al. 2019; Yang et al. 2017, 2019) is an engineered technique used to form multicomponent and layered nanofiber membranes. Yang et al. (2019) used triaxial electrospinning to draw CA nanofibers with gliadin and ibuprofen powder in HFIP-TFA (8:2) solvent system. The middle solution is prepared by dissolving a certain amount of CA powder into the mixture of acetone and acetic acid (2:1 v/v). The outer solution was a plain solvent of acetone and acetic acid (2:1 v/v). It reveals that the presence of a CA coating eliminated the initial burst release of ibuprofen seen from a monolithic drug-protein composite, and allowed us to precisely manipulate the drug release (for a 90%) over a time period from 23.5 to 43.9 h in a tunable manner. The constant rate of drug release offered by such systems allows for a constant, therapeutically active, concentration of active pharmaceutical ingredients (API) to be maintained over a prolonged period of time, with no over- or under-dosing.

Cancer is also one of the major problems that attracted the attention of researchers in the past few years. However, only a few studies are available in literature for formulation of anticancer drug using CA-based nanofibers (Absar et al. 2015a, b; Han et al. 2017). Cisplatin is the most researched anticancer drug. Absar et al. reported two approaches; one is single-nozzle electrospinning of CA solution in N-methylmorpholine N-oxide ($NMMO.H_2O$), combined with a solution of cis-diammineplatinum (II) dichloride (cisplatin) dissolved in DMF, another is coaxial electrospinning using sheath solutions of (i) CA and (ii) PEO. A solution of cisplatin in DMF is used as the core solution. The drug-loaded cellulose nanofibers shows particles attached on the surface. These particles are composed of both the polymer and the drug. The CA-cisplatin fibers exhibited drug encapsulation within various diverse morphological conformations: hierarchical structures such as straw-sheaf-shaped particles, dendritic branched nanofibers, and swollen fibers with large beads (Absar et al. 2015a).

The acquired immunodeficiency syndrome (AIDS) caused by human immunodeficiency virus (HIV) infection became a serious health, social, and economic problem all over the world. Fighting HIV has proven to be extremely difficult as it is characterized by a very high genetic variability, resulting in the lack of any currently available vaccine. CA phthalate (CAP) fibers are incorporated with antiviral drugs to prevent man-to-woman HIV transmission. The prevention is made possible as the electrospun CAP fibers are not soluble in healthy vaginal fluid, which has a pH of below 4.5, but are soluble in small amounts of human semen having pH between 7.4 and 8.4. CAP fibers are nontoxic to vaginal epithelial cells at concentration below 2 mg/ml and did not impede the proliferation of the vaginal microbial

flora. Moreover, CAP fibers without anti-HIV drugs also inhibited the HIV infection of CD^{4+} TZMbl cells in vitro. However, further in vivo studies are needed to explore the potential of CAP fibers in preventing HIV transmission during sexual intercourse (Huang et al. 2012).

The most used area of nanofiber-based drug delivery is related to wound dressing. Synthetic as well as natural antibiotics, antifungal, anti-inflammatory drugs have been successfully loaded in CA nanofibers (Wutticharoenmongkol et al. 2019; Samadian et al. 2018; Pilehvar-Soltanahmadi et al. 2018; Kurecic et al. 2018; Hajialyani et al. 2018). Electrospun CA fibers are widely used as carrier of drugs because of their good tissue compatibility and ease of fabrication. Gallic acid is a natural compound obtained from fruits, tea leaves, nuts, and vegetables and known for its efficacy as antioxidant, anti-inflammatory, antifungal, anti-carcinogenic, and antibacterial activities (Wutticharoenmongkol et al. 2019; Karimi-Khouzani et al. 2017).

Wutticharoenmongkol et al. (Wutticharoenmongkol et al. 2019) synthesized CA-based nanofibers with Gallic acid incorporation and tested for antibacterial and antioxidant properties. Antioxidant activity is of concern for investigating the potential for use of fiber mats as carrier for topical and transdermal delivery of GA. The antioxidant activity of the as-released GA was investigated by the 1,1-diphenyl-2-picrylhydrazyl (DPPH) assay (Ghitescu et al. 2015). The antioxidant activity of GA is measured from its release in the acetate buffer and the normal saline. In Fig. 9.13, antioxidant activity comparison between CA-GA electrospun fibers (EF with 20% and 40% GA) and cast film (CF with 20% and 40% GA) shows that as-loaded GA in CF20GA and CF40GA possesses 84.2 ± 0.7% and 84.9 ± 1.4%, while EF20GA and EF40GA shows 83.5 ± 0.5% and 85.1 ± 1.9% activity, respectively.

Kurecic et al. also prepared a multifunctional bio-based system demonstrating its utility in pH detection with controlled release of benjocaine drug and pH-detecting dye bromocresol green (BCG) in situ. CA nanofibers obtained from 17 wt% concentration using electrospinning (Fig. 9.14a) are smooth having a diameter of ~ 600 nm as shown in Fig. 9.14b, while a lower concentration does not form fibers. Figure 9.14c shows a pH-dependent controlled release study where maximum release of benjocaine is observed at pH-9. The accompanying color change of the nanofibrous mats, provided through the encapsulated BCG (from yellow to blue), is noticeable (Fig. 9.14d) within a few seconds after the pH changes from acidic to alkaline (Kurecic et al. 2018).

4.3 Biomedical Applications

A biocompatible and degradable material is always required for tissue engineering applications that lacks cytotoxicity and provides a required environment for promoting cell integration, differentiation, and proliferation. Also, it could be replaced by the regenerated tissue biomaterial. This can be obtained by preparing a three-dimensional biocompatible scaffold compatible with bioactive molecules. The CA with high abundancy provides all these properties and advantages (Konwarh et al. 2013). Electrospinning is a common method to prepare nanofiber scaffolds for tissue engineering. However, the application of electrospun CA nanofibers for tissue engineering is not quite well elaborated in literature databases. So, in this section the following work will describe the application of CA-based nanofibers for tissue engineering.

Along with antimicrobial agents or alone, incorporation of bioactive agents in wound dressing could help the healing process. Reports have shown the remarkable role of calcium in the hemostasis of skin, keratinocyte differentiation, and proliferation (Kawai et al. 2011; Magee et al. 1987). Hydroxyapatite (HAp) is a calcium-based bioceramic and used in tissue engineering applications as well as wound dressing materials. CA-based nanofibers can be used to grow hydroxyapatite, because of the biomimic action of the membrane. A membrane of Poly vinylpyrrolidone (PVP)/CA-based core shell fibers were fabricated by Hou et al. (2018) using electrospinning. Prior to the biomimetic mineralization, the

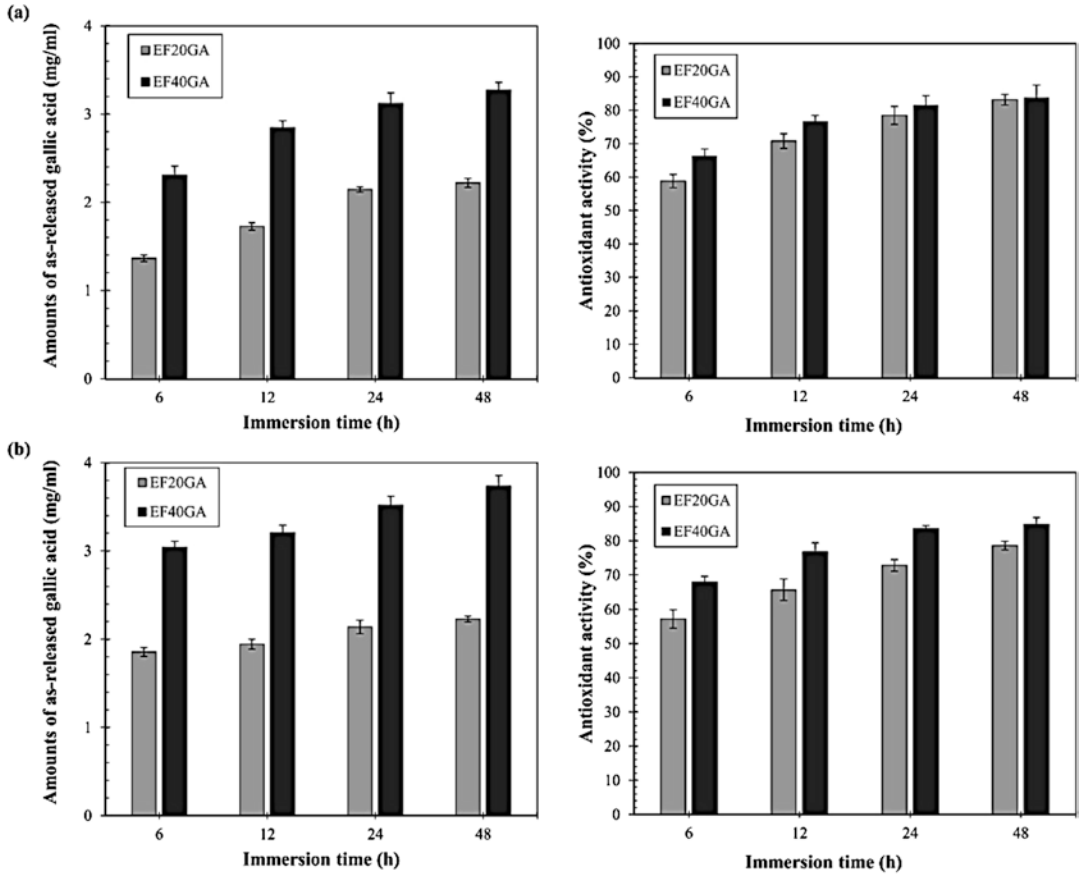

Fig. 9.13 Amounts of as-released GA (left) and antioxidant activity of as-released GA (right) determined by DPPH assay from GA-loaded CA fiber mats at different immersion time points in (**a**) acetate buffer solution at 32 °C and (**b**) normal saline at 37 °C (Wutticharoenmongkol et al. 2019)

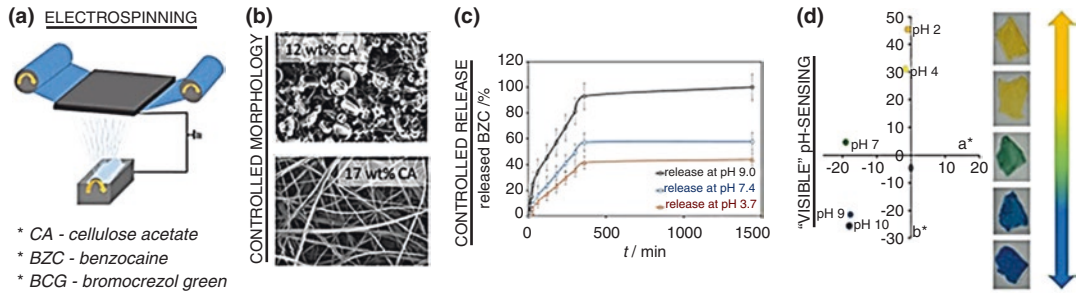

Fig. 9.14 Multifunctional CA-benjocaine bromocresol nanofibers (**a**) method, (**b**) SEM image, (**c**) drug release study, and (**d**) pH sensitivity study (Kurecic et al. 2018)

fibrous membranes are immersed in deionized water and subsequently in ethanol solution. The obtained cellulose scaffold with mineralized HAp to imitate the component of native bone is produced by the simulated body fluid (SBF) immersion method (Jin et al. 2014; Kokubo and Takadama 2006). The nature of the mineral phase on fibers is studied by EDS. The spectra revealed

that the main elements constituting the incubated mineral are carbon, oxygen, calcium, and phosphorus. Calcium and phosphorus could have originated only from the mineral phase, suggesting that the mineral deposited on the surface of the cellulose fibers might have been similar to HAp, which has the molecular formula $Ca10(PO_4)_6(OH)_2$. Furthermore, the calcium to phosphorus (Ca/P) ratio was 1.47, which is close to the theoretical value of 1.67 in HAp.

Samadian et al. (2018) synthesized CA/gelatin/nanohydroxyapatite (CA/Gel/nHAp) nanocomposite fibers containing 12.5, 25, and 50 mg nHAp by electrospinning. It is reported that the interactions between the hydroxyapatite and the polymer particles actually generate as well defects in the internal structure of the membrane (Pandele et al. 2017).

The results showed that the concentration of nHAp has a direct correlation with porosity, water contact angle, water uptake, water vapor transmission rate, and proliferation with L929 cell line. With increase in nHA, contact angle decreases as 61.25 ± 0.75, 58.5 ± 1.5, 57.25 ± 0.75, and 56.5 ± 0.5 for 12.5, 25, and 50 mg of nHA, respectively. Similarly, mechanical strength also decreases but to a lower extent due to increase in porosity. In vitro study carried out for 48 and 72 h shows that cell proliferation on 25 mg nHAp membrane is significantly higher than the other groups 72 h after cell seeding ($p < 0.05$). In vivo study is carried out on six groups of Wistar Rat via a full thickness excision wound. The wound area is measured after 7 days and 14 days. The highest wound closure percent is observed in the CA/Gel þ25 mg nHAp group among all the studied groups with the average wound closure of 66.26 þ 1.91% and 93.56 þ 1.6% on days 7 and 14 post-wounding, respectively.

Chakraborty et al. carried out fabrication of nanofibrous regenerated cellulose scaffolds (RCS) by de-acetylation of electrospun CA scaffolds having CA amount as 9%(B1), 11%(B2), 13%(B3), and 15% (w/v) (B4) prepared in 90:10 (v/v) acetone-water solvent system. After deacetylation, the RCS samples which showed optimum results from the conducted characterization tests are subjected to further in vitro tests for testing the cell adhesion, cell proliferation, and cell viability using MC3T3-E1 osteoblast cell line to determine the viability of the scaffolds as a potential bone-tissue engineering surface (Chakraborty et al. 2019).

Figure 9.15 shows the morphology and adhesion of cells on the RCS scaffolds at intervals of 1, 3, and 5 days. The diameter of nanofibers is in the range 300–500 nm. From Fig. 9.15, rounded cell shapes and their respective adhesion on the B.1 and B.2 scaffold surfaces is observed. This indicates better cell to cell interaction rather than cell to matrix interaction (Liang and Boppart 2009). Additionally, extensive spreading and proliferation of the cells on the surface of the B.3 scaffold after 3 days' and 5 days' time is a sign of better cell to matrix interaction as well as positive cell to cell interactions.

MTT (3-(4, 5-Dimethylthiazol-2-yl)-2,5-Diphenyltetrazolium Bromide) cell assay is used to determine viability of the cells on the surface of the electrospun RCS (Van Meerloo et al. 2011). Cell viability is measured after 4 h using a microplate reader (Multiscan GO, Thermo Scientific) absorbance at 570 nm and at a reference wavelength of 670 nm. Figure 9.16 shows % cell viability of MC3T3-E1 osteoblast cell line w.r.t. control sample. The results show that viability of all RCS samples with respect to control (100%) is greater after 1 and 3 days and lesser than the control in samples B.1 and B.2 after 5 days. But % cell viability is greater than the control in B.3 sample after 5 days. The important thing here is that B.3 RCS sample shows better cell viability than both of B.1 and B.2 RCS scaffolds and also the control after 5 days of cell culture. On the fifth day, cell viabilities of all the mats are decreasing as compared to the results obtained after 3 days, which may be due to the overgrowth of cells on the mats.

Enzyme immobilization is also of great importance and required biocompatible polymers having numerus functional groups for immobilization.

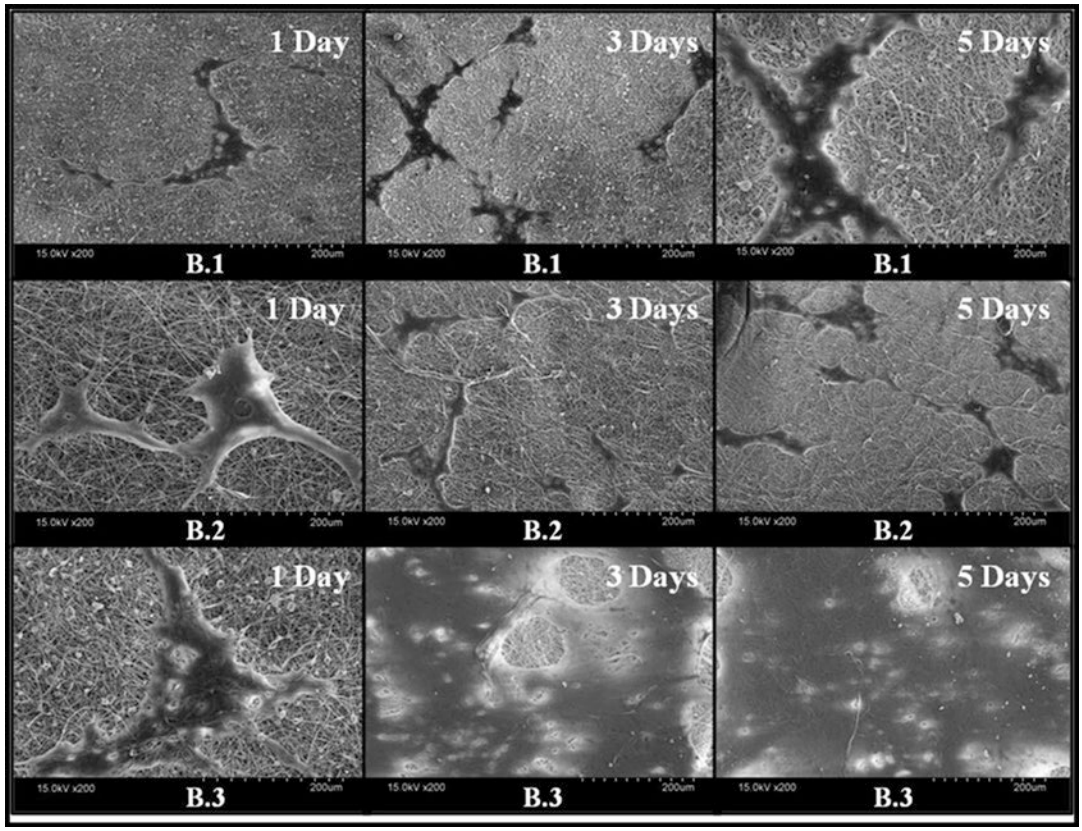

Fig. 9.15 Cells adherence on the surface of B.1, B.2, and B.3 RCS sample scaffolds for different time intervals (Chakraborty et al. 2019)

Such practice enhances the reuse of enzyme in catalyzing various reactions (Huang et al. 2011, 2017; Hu et al. 2019; Demirkan et al. 2018; Chen et al. 2011a). *Candida rugosa lipase* is immobilized on electrospun CA nanofibers by hydrolysis followed by oxidation by $NaIO_4$ (Huang et al. 2011). This generates the aldehyde groups on fiber surfaces which acted as a suitable platform for *Candida rugosa lipase* immobilization. A significant increase in thermostability as well as durability is reported as a result of immobilization. Chen et al. have reported covalent immobilization of *Candida rugosa lipase* using glutaraldehyde as the coupling agent over surface of regenerated electrospun CA. They reported a high activity (9.83×104 U/m^2) for the hydrolysis of olive oil as reaction model. The system consists of pentaethylenehexamine (PEHA) as a spacer. In another work, Demirkan et al. carried out immobilization of protease enzyme over chitosan-blended CA nanofiber mats. Glutaraldehyde (GA) rapidly reacts with the amino groups of the CHI and GA and can also covalently bond to protease enzyme. GA activation effectively increases the cycle number and about 20% of enzyme activity still retained after seven cycles at CA/chitosan samples. This percentage is higher at pure CA nanofiber than CA/chitosan nanofibers and measured around 33.5%. These immobilized enzymes can be used in textile as well as detergent industries (Demirkan et al. 2018).

4.4 Energy Applications

Storage of the existing energies and utilizing the renewable energies has become more and more

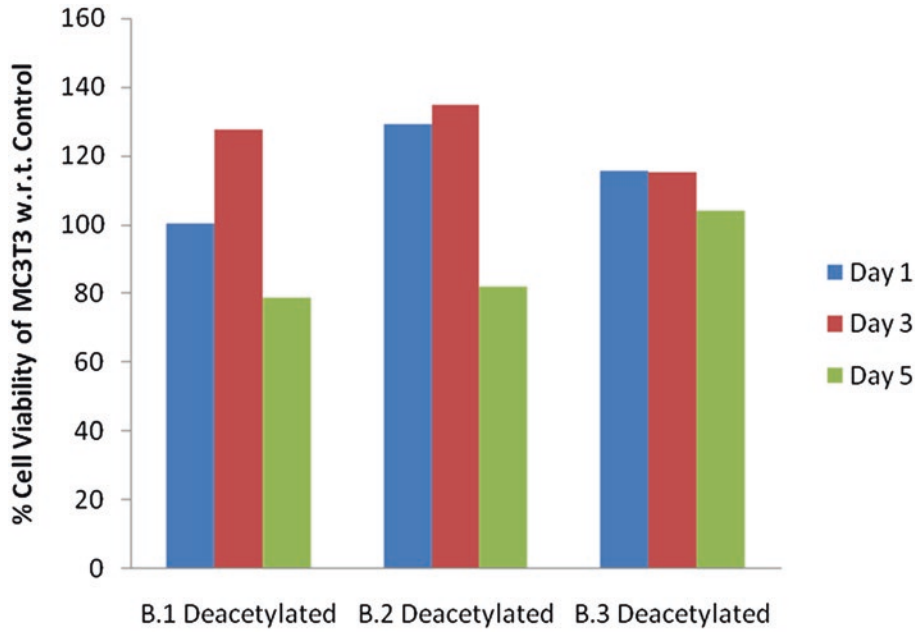

Fig. 9.16 MTT assay for percentage cell viability of MC3T3-E1 cells seeded on the electrospun RCS scaffolds B.1, B.2, and B.3 after 1, 3, and 5 days (Chakraborty et al. 2019)

important due to increase in the demand for energy. The CA-based nanofibers with functional additives and activation have been tested for their application in different kinds of energy storage, that is, thermal energy storage with phase change materials (PCM), supercapacitors, batteries, and dye-sensitized solar cells.

Thermal energy is one of the important energies that can be saved in the forms of sensible, latent, and chemical reaction heat. Phase change materials can store and retrieve the thermal energy in the form of latent heat during any phase transition. So, phase change materials can be combined with polymers such as CA to make phase change fibers (PCF) having advantages as ultrafine size, huge surface-to-volume ratio, and excellent thermal performances (Chen et al. 2013; Rezaei et al. 2014, 2016; Zdraveva et al. 2015; Cai et al. 2013, 2015a, 2017a). In the electrospun CA-based PCFs, CA fiber acts as the matrix and the solid-liquid PCMs act as the phase change ingredient, which could be served as form stable PCMs.

Chen et al. (2011b) fabricated fibers from 15 wt% CA solutions in acetone/DMAc using a core sheath spinneret. They PEG/CA phase change fibers fabricated with PEG content of 37.0 wt% (labeled as PCF-1) and 43.2 wt% (labeled as PCF-2). The sample is subjected to several hundred heating-cooling cycles followed by analyzing morphology and thermal properties. Figure 9.17a, b shows SEM images of PEG/CA fibers with different PEG content. The cylindrical fibers obtained have a smooth surface and diameter 1126 nm which increases to 1552 nm with increasing PEG content. The increase in diameter is similar to PEG/CA fibers reported by conventional electrospinning with a single spinneret (Chen et al. 2011b, 2013). Figure 9.17c shows the morphology of PCF-2 fibers after thermal cycles, which indicates that the coaxial electrospun phase change fibers are typical stable phase change materials. These fibers are washed with deionized water for 24 h to remove PEG content. TEM analysis in Fig. 9.17d shows the core sheath structure can be obtained and PEG is encapsulated completely in a continuous and uniform manner by CA sheath in each fiber during the coaxial electrospinning process.

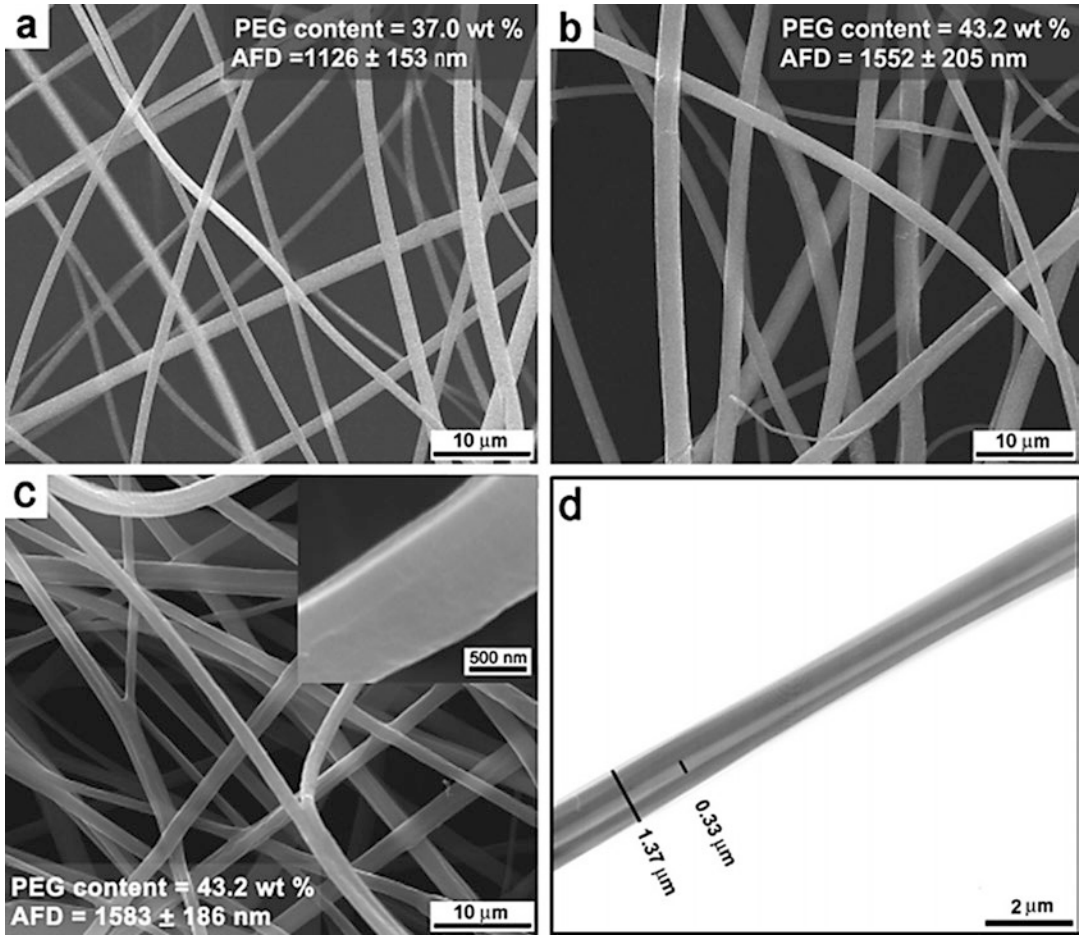

Fig. 9.17 SEM images of (**a**) PCF-1; (**b**) PCF-2; (**c**) PCF-2 after thermal treatment (the inset shows higher magnification image); and (**d**) TEM image of PCF-2 after washing (Chen et al. 2013)

The ultimate strength and ultimate strain of both the composite fibers are lower than those of CA fibers, and decrease with the increase of PEG content. Such reduction in ultimate strength of PEG/CA composite fibers attributed to the introduction of PEG, which weakens the continuous phase structure of CA. Therefore, the addition of PEG is an unfavorable effect to the tensile properties of the composite fibers. However, with the increase of PEG content, the enthalpies of the composite fibers increase and the phase transition temperatures (the onset temperature) have no obvious variation. Pure CA nanofibers do not have any phase change in that temperature range, hence the total latent heats of the fibers are primarily contributed by the phase change in PEG. Hence, PEG content in the composite fibers is the dominating factor of the latent heats of the fibers. The theoretical values of enthalpy of melting and crystallization of the composite fibers are about 65.6 J/g (62.1 J/g) and 76.6 J/g (72.5 J/g), respectively, for PCF-1 and PCF-2. Similarly, Rezaei et al. (2014, 2016) also fabricated PEG/CA nanofibers (PCNs) and demonstrated that a higher diameter of PCNs can present more favorable thermal behavior for advanced applications of thermal energy storage and thermal regulating material fields. As another PCM, a ternary eutectic mixture of capric–myristic–stearic acid (CMS) is incorporated in a binary polymer PVP/CA (Cai et al. 2017a). PVP removal from the CA/PVP nanofibers creates nanoporous features on

the surface of resultant CA nanofiber which increases CMS incorporation capability of the nanofibrous mat. Thermal storage/retrieval capability of the CMS/CA nanofiber based form-stable PCM is evaluated by monitoring temperature change by placing composite nanofibers first at 50°C and then transfering them to ice/water bath i.e. in a 4° C environment. It took only 7 min for the control sample to cool from 50 °C down to 12 °C. Compared to the control sample, the same temperature change from 50 °C to 12 °C took almost five times longer for the form-stable PCM. This shows that porosity is also an important concern for thermal energy storage.

Electrospun carbon nanofibers and their composites have gained much attention over years due to their free-standing and conducting nature; these properties can reduce the cost occurring due to the use of current collector and binder in energy devices. CA has also been used in literature as a precursor to carbon and it can be electrospun easily. Producing carbon fibers from thermoplastic CA fibers is challenging as it loses the morphology during the carbonization. However, the regenerated cellulose fibers can be carbonized to yield carbon fibers. Kakunuri et al. (2017) fabricated carbon nanofibers by heating RCA nanofibers at 240 °C in air prior to carbonization at 900 °C in an inert atmosphere. Electrochemical performance of CA-derived electrospun carbon fibers is studied at 37.2 mA/g. However, after the initial 10 cycles, coulombic efficiency was retained above 90%. Specific reversible capacity is also found stable at 290mAh/g after 100 cycles (Kakunuri et al. 2017). The CA-based nanofibers were also used as the separator in lithium-ion batteries (Weng et al. 2015; Sheng et al. 2017; Zhang et al. 2019a; Bhute and Kondawar 2019). Bhute et al. prepared a polymer electrolyte membrane based on CA/$AgTiO_2$ nanofibers for application as electrode separator (Bhute and Kondawar 2019). At first, silver-doped TiO_2 nanoparticles are prepared by hydrothermal method. These particles are dispersed in PVDF-CA solution prepared in DMF-acetone solvent mixture. Similarly, PVDF-CA nanofibers are also prepared for comparison. PVDF-CA nanofibers show 290% of electrolyte (1 M LiPF6 in EC: DEC (1:1, v/v)) uptake while hybrid nanofibers show 330% after 60 min. The high uptake in both the nanofibers can be attributed to high porosity due to interlaying fiber structure and good hydrophilicity of CA. Such higher uptake provides more ions in the same volume which leads to high ionic conductivity.

Further, the prepared nanofiber membrane is sandwiched between lithium metal as anode and lithium-ion phosphate (LiFePO4) as a cathode (blended with PVDF binder and carbon black). This cell delivered an initial discharge capacity of 170 mAh/g at 0.1C and 100% coulombic efficiency even after 50 cycles.

The CA-based nanofiber membrane can also be used as a supercapacitor that requires good surface area, pore structure, and functional groups. To achieve porous carbon fibers, polymer blending and activation methods have been widely used. Cai et al. prepared carbon nanofibers from RCA (CA nanofibers deacetylated with 0.1 N NaOH/ethanol) nanofibers. Initially RCA nanofibers are immersed in PPy-HCl solution and $FeCl_3$ solution is added dropwise. After washing with water/ethanol mixture and drying, the fibers are subjected to carbonization followed by activation by CO_2 forming N-CNF. For comparison, CA NFs without PPy are also subjected to the same procedure to get CNFs. The electrochemical performance was tested in three electrode systems using KOH as electrolyte. CNFs showed a small rectangle CV curve as compared to N-CNF suggesting higher capacitance of N-CNF. Also, no internal resistance (IR) drop was observed in N-CNF. The N-CNF electrode has a specific capacitance of ~236 F/g at 0.2 A/g, which is substantially higher than the CNF electrode (~105 F/g). The specific capacitance of the N-CNF electrode maintained as high as ~171 F/g at 10 A/g, with ~84.1% retention at 1 A/g (~203.4 F/g). N-CNF electrode also exhibited an excellent cycling stability with less than 2% capacitance loss after 10,000 cycles of charge/discharge at a high current density of 20 A/g indicating a good capacitance retention capability and non-kinetic limited performance (Cai et al. 2015b). In another study, Fan et al.

(2019) used $ZnCl_2$ for activation by dipping RCA nanofibers in $ZnCl_2$ solutions (2%, 5%, 10%, and 20% wt %). These pretreated nanofibers are then subjected to stabilization at temperature 220 °C and carbonization at 700 °C and named it as CACNF-$ZnCl_2$-X, where X denotes the $ZnCl_2$ concentration. It is reported that addition of $ZnCl_2$ not only activates the fibers but also helps in forming nanofibers stable at carbonization temperature. At current density of 0.1 A/g, the specific capacitance was calculated to be 133 F/g, 134 F/g, 170 F/g, and 202 F/g for CACNF-$ZnCl_2$-2%, CACNF-$ZnCl_2$-5%, CACNF$ZnCl_2$-10%, and CACNF-$ZnCl_2$-20%, respectively. It is revealed that the specific capacitance becomes stable for all samples when the current density is higher than 2 A/g. The CACNF$ZnCl_2$-20% electrode shows maximum discharge times, either at high current densities or at low current densities, indicating the best electrochemical performance. One of the reasons for the best performance is highest surface area (1188 m^2/g) among other samples. Also, only slight IR drop is observed at high current loading, indicating the high-rate capability and little internal resistance (Fan et al. 2019). Cai et al. (2015b), further, prepared N-CNF/$Ni(OH)_2$ nanofibers by using $Ni(OH)_2$ doping, and an asymmetric capacitor is designed with N-CNF as the other electrode. The capacitor device operated at the window of 1.6 V and the scan rate of 1 mV s^{-1} has a high specific capacitance of ~172 F g^{-1}, which is approximately 1.4, 1.6, and 1.8 times higher than that at a voltage window of 1.4, 1.2, and 1.0 V (same scan rate), respectively, from N-CNF-based symmetric supercapacitors. The maximum energy density for asymmetric supercapacitor operating at 1.6 V voltage windows was ~ 51 Wh/kg at a power density of ~0.9 kW/kg.

In another report by Cai et al. (2016) interbonded CA-based carbon nanofibers have been engineered and demonstrated high specific capacitance (~241.4 F/g at the current density of 1.0 A/g), excellent cycling stability (99.9% capacitance retention after 10,000 cycles), and larger power capability (~84.1 kW/kg).

4.5 Sensor

The use of CA-based NFs (nanofibers) has also been extended to reach bio-sensing and different types of electrical devices such as optical sensor (Yang et al. 2009), colorimetric sensor (Hu et al. 2017), ethanol (Mulijani et al. 2018), strain sensor (Fu et al. 2019), and fish spoilage indicator (Aghaei et al. 2018). In brewery, it takes a long time to check alcohol concentration in product liquors, by using distillation method and gas chromatography or liquid chromatography.

Mulijani et al. (2018) prepared an optical sensor–based device for ethanol sensor. This sensor has been fabricated by binding Nile Red to a CA nanofiber membrane that has previously been subjected to an exhaustive base hydrolysis. Nile red is almost non-fluorescent in water and other polar solvents but undergoes fluorescence enhancement and large absorption and emission blue shifts in nonpolar environments (excitation/emission maxima ~552/636 nm in methanol). The hydroxyl group of cellulose plays a vital role in immobilizing the Nile red dye via ternary amine group.

The performance of optical sensor is evaluated for ethanol, methanol, and propanol to measure the polarity and selectivity of optic sensor toward the alcohol derivatives. Fluorescence intensity of optic sensor membrane for methanol 5%, ethanol 5%, and propanol 5% is 15,113.56, 16,573.75, and 18,495.97, respectively. The difference in the intensity is due to difference in structure and polarity of these derivatives.

Similarly, alizarin-loaded CA nanofibers have been demonstrated as fish spoilage sensor. In this study by Agheai et al. (2018), fish fillets have been cut into 100 g slices under sterile conditions placed in sterile jars. Nanosensors are placed in the head space of the jars, which are then kept under refrigeration temperature at 4 °C. The sensor works on detection of total volatile basic nitrogen (TVB-N) and total viable count (TVC). When fibers are exposed to these, the color of the fibers changes to dark brick from pale yellow as the content of TVB-N increases.

Flexible and wearable electronic textiles as sensor can meet the technological demands of

modern society. Fu et al. (2019) reported the application of Reduced Graphene Oxide (RGO)/CA electronic textiles as a strain sensor. In the process, well-aligned electrospun CA nanofibers with belt-like morphology deposited with GO aqueous colloid. Due to the enhanced capillary force of the well-aligned CA nanofibers, GO solution is effectively drawn downward. After being hot pressed, the GO sheets are thermally reduced into RGO environmentally, which highly improves the conductivity as a result.

To investigate viability of RGO/CA composite mat as a strain sensor, the current change in the RGO/CA membrane with a certain voltage at 3 V during the movement is recorded. It is found that as the finger bends downward, the detected current rises and stabilizes at a certain value. Such an improved sensitivity is likely because the conductive RGO sheets can be stretched well after being bent. To evaluate the sensitivity of the RGO/CA membrane, they clenched the finger to a large degree and then unclenched slightly and detected a clear linear change in current. On the other hand, the RGO/CA membrane can also be utilized to monitor the pressure. The resistance decreases when an increased pressure is applied on the RGO/CA membrane, as the deposited RGO sheets may be stretched and then better combined with the CA substrate.

4.6 Mechanical Properties

Electrospun nanofiber membranes have been criticized due to their low mechanical strength. So, mechanical properties of electrospun nanofibers and their composites are of great concern for their various applications such as filtration, osmosis, and desalination where high flux is required (Bui and McCutcheon 2013). Although there are many research papers that deal with mechanical properties of different composite nanofibers, here discussion on the recent research work, specifically on mechanical properties, will be carried out. In composite materials, the use of a filler compound increases the strength of the polymer; similarly some nanofillers such as carbon nanotubes (CNTs) and graphene oxide have been used to increase the strength of CA nanofibers. Salama et al. (2018a) reported the effect of CNTs as filler on the mechanical properties of CA-based nanofibers. For the preparation of CA/CNT composite nanofibers, the dispersion of CNT in the mixture of the polymer and solvents is obtained by stirring for 30 min at 30 °C, and then, the mixture prepared by sonication for 40 min at 60 °C, and this process is repeated for the five samples with different CNT contents (0.05, 0.1, 0.5, 1, and 1.5 wt%). The diameter of pure CA nanofibers is in the range of 515 ± 45 nm. With increase in amount of CNTs from 0.05 to 1.5 wt% the fiber diameter decreases from 415 nm to 305 nm, respectively; this is due to increase in solution conductivity and more stretching and whipping motion exerted on nanofibers.

Figure 9.18 shows the stress–strain curve and Young's modulus pure and composite fibers. It shows that both strain and stress rate increases with the increase in content of CNTs up to 0.5 wt%, however later it decreases with further increase in CNT content, that is, 1 and 1.5 wt%. Young's modulus also follows the same trend for increase in CNT content. Young's modulus increases from 200 to 1100 MPa for 0.5 wt% CNT-loaded CA nanofibers, and afterward it decreases to 840 and 760 MPa for 1 wt% and 1.5 wt % samples. This shows that the amount of CNTs well dispersible in CA matrix is 0.5 wt%. Graphene oxide (GO) (Aboamera et al. 2018, 2019) is also a good nanofiller for attaining good mechanical applications due to more functional groups and 2D structure as compared to CNTs. Similar to the above case, different concentrations of GO, that is, 0.05, 0.5, 1, and 1.5 wt. were added to CA nanofibers during electrospinning. Here too, similar to CNTs in the previous case, the diameter of nanofibers decreases with an increase in GO content. The composite nanofibers having GO content 1.5 wt% shows high tensile strength (97.5 MPa), which improved to about 73% compared to 49 MPa for the pure CA nanofibers. Also, Young's modulus increases 75% for 1.5 wt% GO containing nanofibers.

In a study by Gopiraman et al. (2013) CA/graphene and CA/graphene functionalized with –COOH group were synthesized. Young's modulus

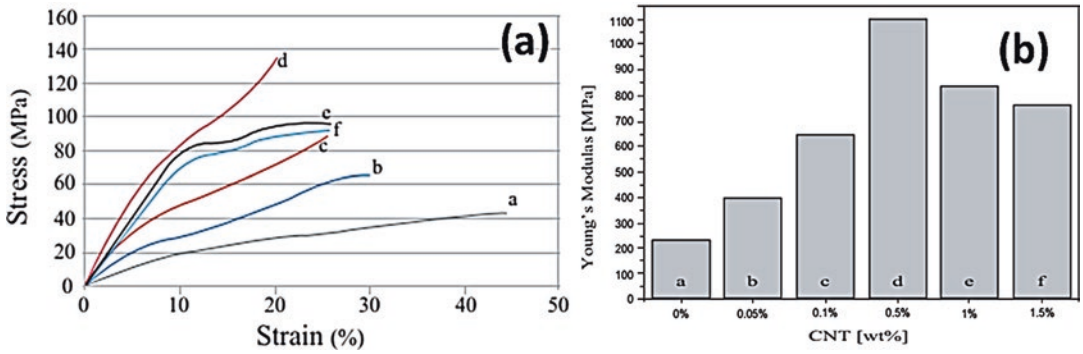

Fig. 9.18 Stress–strain curve and Young's modulus of (**a**) pure CA, (**b**) CA/CNT 0.05 wt%, (**c**) CA/CNT 0.1 wt%, (**d**) CA/CNT 0.5 wt%, (**e**) CA/CNT 1 wt%, and (**f**) CA/CNT 1.5 wt% (Salama et al. 2018a)

of CA/graphene hybrid nanofiber mat with 4 wt% graphene was found to be 739.8 MPa, which was about three times higher than that of pure CA nanofiber mat. The CA/graphene-COOH hybrid nanofiber mat with 4.0 wt% graphene-COOH showed the highest Young's modulus, which was approximately 3.7 times higher than that of pure CA nanofiber mat (~245.5 MPa), suggesting that mechanical properties of such hybrid nanofibers were increased with increasing amounts of graphene-COOH nano-additives. A similar tendency was also observed for CA/graphene hybrid nanofibers. However, at 5 wt% graphene or graphene-COOH contents, Young's modulus of the hybrid CA nanofibers started to decrease, which is again due to agglomeration of graphene in the nanofibers (Gopiraman et al. 2013). To enhance the mechanical properties of RCA nanofibers, the annealing and the saponification of electrospun cellulose-acetate nanofibers (CA-NF) have been investigated (Inukai et al. 2018; Ali et al. 2019a). It was found that by increasing the annealing time of CA-NF at 50 °C from 0 to 12 h, the crystallinity of RC-NF increased from 37% to 41%, which became constant after 12 h. Also, the Young's modulus of RC-NF was found to increase from 11.2 to 28.0 GPa by increasing the annealing time from 0 to 12 h, which also became constant after 12 h. However, on increasing annealing temperature to 75 and 100 °C, Young's modulus increases up to 4 h and 0.5 h, respectively, and afterward becomes constant. This is due to increase in crystallinity with increase in annealing temperature which in turn decreases the annealing time.

Ag nanoparticles into the structure of cellulose nanofibers can improve the tensile strength by interaction with hydroxyl groups of cellulose nanofibers regenerated in the alkali condition from CA (Gaminian and Montazer 2017). Polydopamine coating on RCA nanofibers generates a highly stable polymer layer that enhances tensile strain of the modified RCA nanofibers from 10.88 to 13.40% and stress from 1.49 to 1.85 MPa. It was reported that UV irradiation increases polydopamine formation rate and reduction of Ag ions to Ag nanoparticles in a short time and then enhances the tensile strength. So with 120 min UV irradiation, tensile strength increases from 13.40 to 18.06 which further increases to 21.27 and 21.38% on addition of 0.1 and 0.2 wt% $AgNO_3$. Increasing AgNO3 to 0.2 wt% causes more Ag nanoparticles that provides more interfacial interactions and higher tensile strength. However, further increase in $AgNO_3$ concentration shows no effect on tensile strength. UV irradiation increases polydopamine formation rate and reduction of Ag ions to Ag nanoparticles in a short time and then enhances the tensile strength (Gaminian and Montazer 2017).

4.7 Water Purification

CA-based nanofibers have a list of most suitable properties such as hydrophilicity, free-OH group for functionalization, biocompatible nature, and good mechanical strength. All these make it a

good candidate for application in water purification from pollutants such as harmful dyes (Aboamera et al. 2018; Chen et al. 2014; Gaminian and Montazer 2018; Keskin et al. 2015; Mokhena et al. 2015; Olaru et al. 2014, 2019; Wang et al. 2015b; Xiao et al. 2018; Zhou et al. 2016), heavy metals, arsenic, fluoride, copper, chromium, and organic impurities.

Dye removal from water can be done by either photo-catalytic degradation or by adsorption mechanism. Wang et al. (2015b) synthesized CA/TiO_2-based nanofiber composite for the removal of methyl blue as a model dye. The TiO_2 in different concentrations (1%, 3%, 5 wt%) is incorporated in 14.5 wt% of CA by electrospinning. The 3 cm × 3 cm patches from each fiber sheet are placed in different 10 ppm dye solution. It is observed that with 0, 1, 3, 5 wt% TiO_2 contents, the concentration of MB reduced by about 5%, 20%, 65%, and 90%, respectively, after 4 h of mercury lamp exposure. Also, the recycling capability of CA/TiO_2 composite ultrafine fibers is investigated, which shows that the MB removal rate of CA/TiO_2 composite nanofibers with 1, 3, and 5 wt% TiO_2 NPs is decreased after 5 cycles by 5%. Therefore, as-spun CA/TiO_2 composite nanofibers were confirmed to be effective for cycling use in dyeing water treatment. Instead of incorporating TiO_2 particles in nanofibers, Salama et al. (2018b) attached amine-functionalized TiO_2 nanoparticles on as prepared CA-CNT electrospun nanofibers. For chemical bonding or crosslinking between CA-CNT nanofibers and TiO_2-NH_2, the CA-CNT fibers are first treated with glutaraldehyde followed by immersion in TiO_2-NH_2 nanoparticles. Photocatalytic degradation of MB and indigo carmine dyes is studied under UV light (UV lamp (315–400 nm) of 40 watts). Different MB and IC concentrations are used (10, 30, 50 mg/L) and at different pH starting from 2 to 8. It is found that during the first 90 min of effective irradiation, the degradation rate is high, reaching 80% for IC and 52% for MB. However, dye degradation rate decreases after reaching 95% degradation (after 120 min for IC and 210 min for MB). In a novel approach by Rohani et al. (2017), CA/heteropolyacid (HPA) is produced as green and recyclable nanophotocatalyst fibers with 0, 1, 2, 3, and 4 wt% HPA contents, concentration of MO reduced by about 15%, 53%, 93.1%, and 97.8%, respectively, after 25 min. Similarly, Abomera et al. fabricated CA/GO composite nanofibers via electrospinning technique, followed by crosslinking TiO_2-NH_2 nanoparticles (Aboamera et al. 2018) for IC and MB dye removal. They also crosslinked the adsorption-based materials that have also been explored within CA-based nanofibers for physisorption or chemisorption of dye molecules (Gaminian and Montazer 2018; Olaru et al. 2019). Gaminian and Montazer (2018) propose the use of CA/carbon black (CB) nanofibers for MB dye adsorption from aqueous solution. CB not only helps in dye adsorption but also increases thermal stability and electrical conductivity of fibers which further helps in getting low-diameter fibers via electrospinning. The percentage removal of MB after 300 min with CA/CB-based CNFs is 95.46%, which is higher than that of CA-based CNFs (75%). The maximum adsorption capacity of CNFs/CB for MB is 84.6 mg/g. The results reveal that Freundlich isotherm shows the good agreement with the experimental data with correlation coefficient of 0.98 in comparison to the low correlation coefficient of Langmuir isotherm (0.79) due to the presence of heterogeneous surface of CA/CB-based CNFs. In another study, the CA/polyaniline/β-cyclodextrin (PANI/β-CD) composite fibers were fabricated using electrospinning (Ali et al. 2019b). These composite fibers, however, show a lower adsorption capacity of 48 mg/g for MB as compared to the above case. It is observed that there are hydrogen bonds between the H-atom of OH group of β-CD and N-atom of MB. Also, there is π-π stacking between the aromatic rings of PANI and MB. The adsorption studies of CA-PANI/β-CD nanosorbent shows that 100%, 97.11%, 95.03%, and 93.45% of MB dye is removed from the seawater, industrial wastewater, municipal wastewater, and tap water, respectively (Ali et al. 2019b).

Heavy metals (Pb (Hamad et al. 2019; Senthamizhan et al. 2016), As (Kumar et al. 2019; Rani Agrawal et al. 2019), Fe (Hamad et al. 2019), Cr (Cai et al. 2017b), Cu (Senthamizhan et al. 2015; Zhang et al. 2019b;

Zhou et al. 2011), and Hg (Bansal et al. 2018; Zou et al. 2017)) are also one of the most common water pollutants and their contamination level in water differs from place to place. A green approach for the removal of Pb (II) and Fe(III) is adapted by Hamad et al. (2019). Electrospinning of CA nanofibers in the acetone-DMF solvent system is carried out followed by impregnation with HAp nanoparticles (3 wt%). Adsorption of Pb (II) and Fe (III) at pH 6.0 suggested that the positively charged species could bind through electrostatic attraction to negatively charged functional groups on the surface of the adsorbent, because more functional groups carrying negative charges would be exposed at this pH. The maximum rapid adsorption is acquired in 35 and 40 min for Pb (II) and Fe (III) ions up to 99.7% and 95.46%, respectively. The adsorption occurred by binding between pollutants and CA-HAp nanofibers, surface complexation, ion exchange, and hydrogen bonding sites on CA/HAp nanofibers. The binding capacity of these fibers is observed more toward Pb(II) followed by Fe(III). Arsenic is another heavy metal (metalloid) attaining attention of researchers worldwide (Sharma et al. 2014; Agrawal et al. 2018). CA/chitosan-based nanofibers have been manufactured using the electrospinning method followed by treatment with sodium bicarbonate (Na_2CO_3) for the removal of As (V), Pb (II), and Cu (II) ions from water. The adsorption capacity of As(V), Pb(II), and Cu(II) ions increases with contact time and reach to the maximum adsorption capacity 26.1, 39.5, and 80.7 mg/g, respectively. From the isotherm model, the maximum adsorption capacity is calculated as 39.4, 57.4, and 112.6 mg/g for As(V), Pb(II), and Cu(II), respectively.

4.8 Miscellaneous Application

Besides the above applications, CA-based nanofibers have also been applied to other areas such as flame retardant (Jiang et al. 2019), pest repellant (Iliou et al. 2019), dyeing processes (Babar et al. 2018; Khatri et al. 2013a, b, 2014, 2016, 2017), odor adsorbent (Ghorani et al. 2019), ion exchangers (Zhang et al. 2018), and as UV protective textile (Nasouri 2019). Cellulose is a textile material used in cloths and CA can be converted to cellulose easily by deacetylation and can be used in dying purpose. Babar et al. (2018) have reported a colorful, breathable dual-layer CA (CA)/dyed CA (DCA) nanofiber membrane with exceptional directional moisture transport performance. The DCA layer offers good wettability, hydrophilic nature, dye fixation, high color yield, and colorfast performance against washing. The inner layer is made up of pure CA nanofibers. These dual-layer nanofiber membranes offered a high color yield of 16.33 with ~82% dye fixation and reasonably high water vapor transport rate (12.11 kg/d/m^{-2}), suggesting to be a potential substrate for fast sweat release applications. The overall moisture management capacity is excellent as 0.89.

Citronella oil–loaded CA nanofibers are synthesized via electrospinning and used as mosquito repellent systems against Asian tiger mosquito *Aedes albopictu.* A single layer and triple layer nanofiber mat was prepared using CA and PVP by incorporating citronella oil in DCM methanol mixture. These fibers have shown high repellent activity for at least 4 weeks. Specifically, after one-week exposure, the repellency of the samples increases from 44% to 77%, with the single-layer CA and PVP systems providing the highest protection from mosquitoes. Triple-layer systems show an increase in their repellency, while in the case of the single-layer CA and PVP mats the repellency marginally decreased in 4 weeks. This is due to the sustained diffusion of citronella oil through three layers as compared to fast diffusion from a single layer (Iliou et al. 2019).

CA materials have low fire retardancy due to easy flammability with identical limiting oxygen index, that is, 18, which limits its application in fire-critical areas. Recently, Jiang et al. prepared Mg-doped CA nanofibers that have shown promising results as fire-retardants. CA nanofibers were doped with flower-shaped hydromagnesite (MgO-P) and magnesium oxide (MgO) materials (prepared by precipitation method). All three fibers are subjected to alcohol burner and infrared

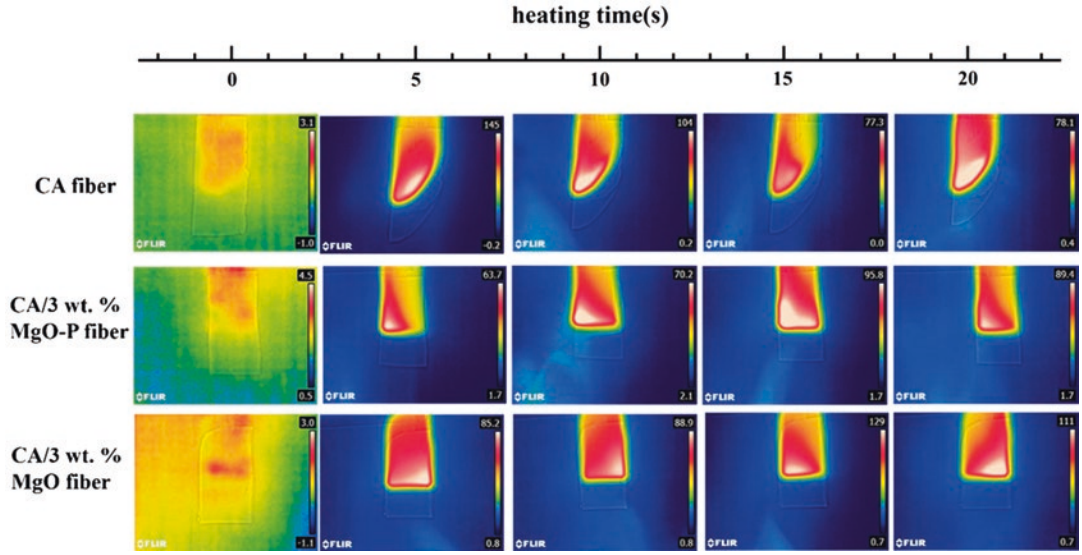

Fig. 9.19 Infrared thermography images of electrospun CA, CA/3 wt% MgO-P, and CA/3 wt% MgO nanofibers after being heated for different time durations (Jiang et al. 2019)

thermography (IT) is carried out. Figure 9.19 shows the IT image of CA as such, CA/3 wt% MgO-P and CA/3 wt% MgO nanofibers. The CA mat shrank after being heated only for 5 s, while both the CA/3 wt% MgO-P and CA/3 wt% MgO show excellent dimension stability even after being heated for 20 s. In case of CA, the temperature dropped down from 145 to 104 °C after 5 s of heating due to the shrinkage. MgO-P shows the lowest temperature below 95.8 °C during the whole heating procedure, also the yellow area in CA/3 wt% MgO-P and CA/3 wt% MgO nanofibers is bigger, which implies that it bears lower heat conductive velocity and is the best flame retardant among the three nanofibers (Jiang et al. 2019).

5 Conclusion

CA is easily spinnable by electrospinning technique using a number of single and mixed solvents. Melt spinning of pure CA is not possible, and for derivatives it gives micrometer diameter fibers. CA nanofibers itself can be used as drug carriers for cancer, AIDS, local analgesic, and wound dressing applications. The biocompatible nature of CA nanofibers makes it suitable for its application in biomedical tissue and bone engineering as well as water purification. It is also possible to improve mechanical properties of CA nanofiber mats for its application to withstand high flux. RCA nanofibers have hydroxyl functional groups that have been proven useful in binding with functional materials for sensor, adsorption, energy, and dying applications. However, CA-based nanofibers are needed to be explored more for food technology and mechanical applications.

References

Aboamera NM, Mohamed A, Salama A, Osman TA, Khattab A. An effective removal of organic dyes using surface functionalized cellulose acetate/graphene oxide composite nanofibers. Cellulose. 2018;25(7):4155–66.

Aboamera NM, Mohamed A, Salama A, Osman TA, Khattab A. Characterization and mechanical properties of electrospun cellulose acetate/graphene oxide composite nanofibers. Mech Adv Mater Struct. 2019;26(9):765–9.

Absar S, Khan M, Edwards K, Neumann J. Investigation of synthesis and processing of cellulose, cellulose acetate and poly(ethylene oxide) nanofibers incorporat-

ing anti-cancer/tumor drug cis-diammineplatinum (II) dichloride using electrospinning techniques. J Polym Eng. 2015a;35(9):867–78.

Absar S, Khan M, Edwards K, Calamas D, ASME. Electrospinning of cisplatin-loaded cellulose nanofibers for cancer drug delivery. New York: American Society of Mechanical Engineers; 2015b.

Aghaei Z, Emadzadeh B, Ghorani B, Kadkhodaee R. Cellulose acetate nanofibres containing alizarin as a halochromic sensor for the qualitative assessment of rainbow trout fish spoilage. Food Bioprocess Technol. 2018;11(5):1087–95.

Agrawal PR, Singh N, Kumari S, Dhakate SR. Multiwall carbon nanotube embedded phenolic resin-based carbon foam for the removal of As (V) from contaminated water. Mater Res Express. 2018;5(3):035601.

Ahmed F, Arbab AA, Jatoi AW, Khatri M, Memon N, Khatri Z, et al. Ultrasonic-assisted deacetylation of cellulose acetate nanofibers: a rapid method to produce cellulose nanofibers. Ultrason Sonochem. 2017;36:319–25.

Ali MM, Pakkang N, Taira S, Koda K, Itoyama K, Uraki Y. Direct electrospinning of cellulose acetate onto polyurethane sheet and effect of its saponification on mechanical properties. J Wood Chem Technol. 2019a;39(4):282–95.

Ali ASM, El-Aassar MR, Hashem FS, Moussa NA. Surface modified of cellulose acetate electrospun nanofibers by polyaniline/β-cyclodextrin composite for removal of cationic dye from aqueous medium. Fiber Polym. 2019b;20(10):2057–69.

Anton F. Process and apparatus for preparing artificial threads. Google Patents 1934.

Babar AA, Miao DY, Ali N, Zhao J, Wang XF, Yu JY, et al. Breathable and colorful cellulose acetate-based nanofibrous membranes for directional moisture transport. ACS Appl Mater Interfaces. 2018;10(26):22866–75.

Bansal M, Ram B, Chauhan GS, Kaushik A. L-cysteine functionalized bagasse cellulose nanofibers for mercury (II) ions adsorption. Int J Biol Macromol. 2018;112:728–36.

Bhute MV, Kondawar SB. Electrospun poly(vinylidene fluoride)/cellulose acetate/AgTiO2 nanofibers polymer electrolyte membrane for lithium ion battery. Solid State Ionics. 2019;333:38–44.

Bui NN, McCutcheon JR. Hydrophilic nanofibers as new supports for thin film composite membranes for engineered osmosis. Environ Sci Technol. 2013;47(3):1761–9.

Cai YB, Gao CT, Zhang T, Zhang Z, Wei QF, Du JM, et al. Influences of expanded graphite on structural morphology and thermal performance of composite phase change materials consisting of fatty acid eutectics and electrospun PA6 nanofibrous mats. Renew Energy. 2013;57:163–70.

Cai YB, Liu MM, Song XF, Zhang J, Wei QF, Zhang LF. A form-stable phase change material made with a cellulose acetate nanofibrous mat from bicomponent electrospinning and incorporated capric-myristic-stearic acid ternary eutectic mixture for thermal energy storage/retrieval. RSC Adv. 2015a;5(102):84245–51.

Cai J, Niu HT, Li ZY, Du Y, Cizek P, Xie ZL, et al. High-performance Supercapacitor electrode materials from cellulose-derived carbon nanofibers. ACS Appl Mater Interfaces. 2015b;7(27):14946–53.

Cai J, Niu HT, Wang HX, Shao H, Fang J, He JR, et al. High-performance supercapacitor electrode from cellulose-derived, inter-bonded carbon nanofibers. J Power Sources. 2016;324:302–8.

Cai YB, Song XF, Liu MM, Li F, Xie MS, Cai DL, et al. Flexible cellulose acetate nano-felts absorbed with capric-myristic-stearic acid ternary eutectic mixture as form-stable phase-change materials for thermal energy storage/retrieval. J Therm Anal Calorim. 2017a;128(2):661–73.

Cai J, Lei M, Zhang Q, He JR, Chen T, Liu S, et al. Electrospun composite nanofiber mats of cellulose@organically modified montmorillonite for heavy metal ion removal: design, characterization, evaluation of absorption performance. Compos A Appl Sci Manuf. 2017b;92:10–6.

Callegari G, Tyomkin I, Kornev KG, Neimark AV, Hsieh YL. Absorption and transport properties of ultra-fine cellulose webs. J Colloid Interface Sci. 2011;353(1):290–3.

Celik G, Oksuz AU. Controlled release of ibuprofen from electrospun biocompatible nanofibers with in situ QCM measurements. J Macromol Sci A Pure Appl Chem. 2015;52(1):76–83.

Chakraborty PK, Adhikari J, Saha P. Facile fabrication of electrospun regenerated cellulose nanofiber scaffold for potential bone-tissue engineering application. Int J Biol Macromol. 2019;122:644–52.

Chen PC, Huang XJ, Huang F, Ou Y, Chen MR, Xu ZK. Immobilization of lipase onto cellulose ultrafine fiber membrane for oil hydrolysis in high performance bioreactor. Cellulose. 2011a;18(6):1563–71.

Chen CZ, Wang LG, Huang Y. Electrospun phase change fibers based on polyethylene glycol/cellulose acetate blends. Appl Energy. 2011b;88(9):3133–9.

Chen CZ, Zhao YY, Liu WM. Electrospun polyethylene glycol/cellulose acetate phase change fibers with core-sheath structure for thermal energy storage. Renew Energy. 2013;60:222–5.

Chen SL, Huang XJ, Xu ZK. Decoration of phthalocyanine on multiwalled carbon nanotubes/cellulose nanofibers nanocomposite for decoloration of dye wastewater. Compos Sci Technol. 2014;101:11–6.

Cheng M, Qin ZY, Hu S, Yu HY, Zhu MF. Use of electrospinning to directly fabricate three-dimensional nanofiber stacks of cellulose acetate under high relative humidity condition. Cellulose. 2017;24(1):219–29.

Choi O, Deng KK, Kim N-J, Ross L, Surampalli RY, Hu Z. The inhibitory effects of silver nanoparticles, silver ions, and silver chloride colloids on microbial growth. Water Res. 2008;42(12):3066–74.

Chung J, Kwak SY. Effect of nanoscale confinement on molecular mobility and drug release properties of cel-

lulose acetate/sulindac nanofibers. J Appl Polym Sci. 2019;136(33):47863.
Demirkan E, Avci T, Aykut Y. Protease immobilization on cellulose monoacetate/chitosan-blended nanofibers. J Ind Text. 2018;47(8):2092–111.
Deng L, Young RJ, Kinloch IA, Zhu Y, Eichhorn SJ. Carbon nanofibres produced from electrospun cellulose nanofibres. Carbon. 2013;58:66–75.
Dhakate SR, Gupta A, Chaudhari A, Tawale J, Mathur RB. Morphology and thermal properties of PAN copolymer based electrospun nanofibers. Synth Met. 2011;161(5):411–9.
Doshi J, Reneker DH. Electrospinning process and applications of electrospun fibers. J Electrost. 1995;35(2):151–60.
Fan QC, Ma C, Wu LQ, Wei CB, Wang HH, Song Y, et al. Preparation of cellulose acetate derived carbon nanofibers by ZnCl2 activation as a supercapacitor electrode. RSC Adv. 2019;9(12):6419–28.
Fathona IW, Yabuki A. One-step fabrication of short electrospun fibers using an electric spark. J Mater Process Technol. 2013;213(11):1894–9.
Fathona IW, Yabuki A. A simple one-step fabrication of short polymer nanofibers via electrospinning. J Mater Sci. 2014;49(9):3519–28.
Ferguson J, Ibrahim KM. The wet spinning of secondary cellulose acetate: solution rheology and filament spinnability. Polymer. 1969;10:135–45.
Fu WL, Dai YQ, Meng XY, Xu WL, Zhou J, Liu ZG, et al. Electronic textiles based on aligned electrospun belt-like cellulose acetate nanofibers and graphene sheets: portable, scalable and eco-friendly strain sensor. Nanotechnology. 2019;30(4):045602.
Gaminian H, Montazer M. Decorating silver nanoparticles on electrospun cellulose nanofibers through a facile method by dopamine and ultraviolet irradiation. Cellulose. 2017;24(8):3179–90.
Gaminian H, Montazer M. Carbon black enhanced conductivity, carbon yield and dye adsorption of sustainable cellulose derived carbon nanofibers. Cellulose. 2018;25(9):5227–40.
Garg K, Bowlin GL. Electrospinning jets and nanofibrous structures. Biomicrofluidics. 2011;5(1):013403.
Ghitescu R-E, Popa A-M, Popa VI, Rossi RM, Fortunato G. Encapsulation of polyphenols into pHEMA e-spun fibers and determination of their antioxidant activities. Int J Pharm. 2015;494(1):278–87.
Ghorani B, Russell SJ, Goswami P. Controlled morphology and mechanical characterisation of electrospun cellulose acetate fibre webs, Int J Polym Sci. 2013;2013. https://doi.org/10.1155/2013/256161.
Ghorani B, Kadkhodaee R, Rajabzadeh G, Tucker N. Assembly of odour adsorbent nanofilters by incorporating cyclodextrin molecules into electrospun cellulose acetate webs. React Funct Polym. 2019;134:121–32.
Gopiraman M, Fujimori K, Zeeshan K, Kim BS, Kim IS. Structural and mechanical properties of cellulose acetate/graphene hybrid nanofibers: spectroscopic investigations. Express Polym Lett. 2013;7(6):554–63.
Gupta A, Dhakate SR, Pal P, Dey A, Iyer PK, Singh DK. Effect of graphitization temperature on structure and electrical conductivity of poly-acrylonitrile based carbon fibers. Diam Relat Mater. 2017;78:31–8.
Gupta A, Gurunathan P, Ramesha K, Singh M, Dhakate SR. Effect of heat treatment temperature on energy storage performance of PAN co-MMA based carbon nanofibers as freestanding lithium ion batteries anode. Energy Storage. 2019;1(6):e89.
Haas D, Heinrich S, Greil P. Solvent control of cellulose acetate nanofibre felt structure produced by electrospinning. J Mater Sci. 2010;45(5):1299–306.
Hajialyani M, Tewari D, Sobarzo-Sanchez E, Nabavi SM, Farzaei MH, Abdollahi M. Natural product-based nanomedicines for wound healing purposes: therapeutic targets and drug delivery systems. Int J Nanomedicine. 2018;13:5023–43.
Hamad AA, Hassouna MS, Shalaby TI, Elkady MF, Abd Elkawi MA, Hamad HA. Electrospun cellulose acetate nanofiber incorporated with hydroxyapatite for removal of heavy metals. Int J Biol Macromol. 2019;151:1299–313.
Han SO, Youk JH, Min KD, Kang YO, Park WH. Electrospinning of cellulose acetate nanofibers using a mixed solvent of acetic acid/water: effects of solvent composition on the fiber diameter. Mater Lett. 2008;62(4–5):759–62.
Han D, Sherman S, Filocamo S, Steckl AJ. Long-term antimicrobial effect of nisin released from electrospun triaxial fiber membranes. Acta Biomater. 2017;53:242–9.
Hearle JW, Woodings C. Fibers related to cellulose, regenerated cellulose fibers. Sawston/Cambridge, UK: Woodhead Publishing; 2001. p. 156–73.
Hooshmand S, Aitomäki Y, Skrifvars M, Mathew AP, Oksman K. All-cellulose nanocomposite fibers produced by melt spinning cellulose acetate butyrate and cellulose nanocrystals. Cellulose. 2014;21(4):2665–78.
Hou JZ, Wang YH, Xue HL, Dou YL. Biomimetic growth of hydroxyapatite on electrospun CA/PVP Core-Shell nanofiber membranes. Polymers. 2018;10(9):1032.
Hu L, Yan XW, Li Q, Zhang XJ, Shan D. Br-PADAP embedded in cellulose acetate electrospun nanofibers: colorimetric sensor strips for visual uranyl recognition. J Hazard Mater. 2017;329:205–10.
Hu MX, Li JN, Guo Q, Zhu YQ, Niu HM. Probiotics biofilm-integrated electrospun nanofiber membranes: a new starter culture for fermented milk production. J Agric Food Chem. 2019;67(11):3198–208.
Huang X-J, Chen P-C, Huang F, Ou Y, Chen M-R, Xu Z-K. Immobilization of Candida rugosa lipase on electrospun cellulose nanofiber membrane. J Mol Catal B Enzym. 2011;70(3–4):95–100.
Huang C, Soenen SJ, van Gulck E, Vanham G, Rejman J, Van Calenbergh S, et al. Electrospun cellulose acetate phthalate fibers for semen induced anti-HIV vaginal drug delivery. Biomaterials. 2012;33(3):962–9.
Huang WJ, Zhan YF, Shi XW, Chen JJ, Deng HB, Du YM. Controllable immobilization of naringinase on

electrospun cellulose acetate nanofibers and their application to juice debittering. Int J Biol Macromol. 2017;98:630–6.

Ibeh CC. Thermoplastic materials: properties, manufacturing methods, and applications. Boca Raton: CRC Press; 2011.

Iliou K, Kikionis S, Petrakis PV, Ioannou E, Roussis V. Citronella oil-loaded electrospun micro/nanofibrous matrices as sustained repellency systems for the Asian tiger mosquito Aedes albopictus. Pest Manag Sci. 2019;75(8):2142–7.

Inukai S, Kurokawa N, Hotta A. Annealing and saponification of electrospun cellulose-acetate nanofibers used as reinforcement materials for composites. Compos A Appl Sci Manuf. 2018;113:158–65.

Jang KH, Kang YO, Lee TS, Park WH. Photocatalytic activities of cellulose-based nanofibers with different silver phases: silver ions and nanoparticles. Carbohydr Polym. 2014a;102:956–61.

Jang KH, Kang YO, Park WH. Functional cellulose-based nanofibers with catalytic activity: effect of Ag content and Ag phase. Int J Biol Macromol. 2014b;67:394–400.

Jang KH, Yu YJ, Lee YH, Kang YO, Park WH. Antimicrobial activity of cellulose-based nanofibers with different Ag phases. Mater Lett. 2014c;116:146–9.

Jatoi AW, Khatri Z. Influence of amino-functional macro and micro silicone softeners on the properties of cotton fabric. Mehran Univ Res J Eng Technol. 2015;34(1):70–4.

Jatoi AW, Kim IS, Ni QQ. Cellulose acetate nanofibers embedded with AgNPs anchored TiO2 nanoparticles for long term excellent antibacterial applications. Carbohydr Polym. 2019;207:640–9.

Jauhari J, Wiranata S, Rahma A, Nawawi Z, Sriyanti I. Polyvinylpyrrolidone/cellulose acetate nanofibers synthesized using electrospinning method and their characteristics. Mater Res Express. 2019;6(6):064002.

Jiang L, Li K, Yang HY, Liu X, Xu WL, Deng B. Significantly improved flame-retardancy of cellulose acetate nanofiber by Mg-based nano flaky petal. Cellulose. 2019;26(9):5211–26.

Jin L, Feng Z-Q, Wang T, Ren Z, Ma S, Wu J, et al. A novel fluffy hydroxylapatite fiber scaffold with deep interconnected pores designed for three-dimensional cell culture. J Mater Chem B. 2014;2(1):129–36.

Kai D, Liow SS, Loh XJ. Biodegradable polymers for electrospinning: towards biomedical applications. Mater Sci Eng C. 2014;45:659–70.

Kakunuri M, Araga R, Khandelwal M, Sharma CS. Cellulose acetate derived free-standing electrospun carbon nanofibrous mat as anode material for rechargeable lithium-ion battery. ECS Trans. 2017;80(10):419–24.

Kalwar K, Hu L, Li DL, Shan D. AgNPs incorporated on deacetylated electrospun cellulose nanofibers and their effect on the antimicrobial activity. Polym Adv Technol. 2018;29(1):394–400.

Kang K, Cho K, Lim H, Kim J. Investigation of surface morphology of cellulose acetate micromould after deacetylation. J Phys D Appl Phys. 2008;41(19):195403.

Karimi-Khouzani O, Heidarian E, Amini SA. Anti-inflammatory and ameliorative effects of gallic acid on fluoxetine-induced oxidative stress and liver damage in rats. Pharmacol Rep. 2017;69(4):830–5.

Kawai K, Larson BJ, Ishise H, Carre AL, Nishimoto S, Longaker M, et al. Calcium-based nanoparticles accelerate skin wound healing. PLoS One. 2011;6(11):e27106.

Keskin NOS, Celebioglu A, Sarioglu OF, Ozkan AD, Uyar T, Tekinay T. Removal of a reactive dye and hexavalent chromium by a reusable bacteria attached electrospun nanofibrous web. RSC Adv. 2015;5(106):86867–74.

Khatri Z, Wei K, Kim BS, Kim IS. Effect of deacetylation on wicking behavior of co-electrospun cellulose acetate/polyvinyl alcohol nanofibers blend. Carbohydr Polym. 2012;87(3):2183–8.

Khatri Z, Khatri A, Saleem U, Mayakrishnan G, Kim BS, Wei K, et al. Pad dyeing of cellulose acetate nanofibres with disperse dyes. Color Technol. 2013a;129(2):159–63.

Khatri Z, Mayakrishnan G, Hirata Y, Wei K, Kim IS. Cationic-cellulose nanofibers: preparation and dyeability with anionic reactive dyes for apparel application. Carbohydr Polym. 2013b;91(1):434–43.

Khatri Z, Ahmed F, Jhatial AK, Abro MI, Mayakrishnan G, Kim IS. Cold pad-batch dyeing of cellulose nanofibers with reactive dyes. Cellulose. 2014;21(4):3089–95.

Khatri M, Ahmed F, Jatoi AW, Mahar RB, Khatri Z, Kim IS. Ultrasonic dyeing of cellulose nanofibers. Ultrason Sonochem. 2016;31:350–4.

Khatri M, Ahmed F, Shaikh I, Phan DN, Khan Q, Khatri Z, et al. Dyeing and characterization of regenerated cellulose nanofibers with vat dyes. Carbohydr Polym. 2017;174:443–9.

Kim MI, Lee YS. Deacetylation of cellulose acetate nanofibers by fluorination for carbon nanofibers. Mater Lett. 2016;181:236–9.

Kim JY, Lee C, Cho M, Yoon J. Enhanced inactivation of E. coli and MS-2 phage by silver ions combined with UV-A and visible light irradiation. Water Res. 2008;42(1):356–62.

Kokubo T, Takadama H. How useful is SBF in predicting in vivo bone bioactivity? Biomaterials. 2006;27(15):2907–15.

Konwarh R, Karak N, Misra M. Electrospun cellulose acetate nanofibers: the present status and gamut of biotechnological applications. Biotechnol Adv. 2013;31(4):421–37.

Kumar M, Rao TS, Isloor AM, Ibrahim GS, Ismail N, Ismail AF, et al. Use of cellulose acetate/polyphenylsulfone derivatives to fabricate ultrafiltration hollow fiber membranes for the removal of arsenic from drinking water. Int J Biol Macromol. 2019;129:715–27.

Kurecic M, Maver T, Virant N, Ojstrsek A, Gradisnik L, Hribernik S, et al. A multifunctional electrospun and dual nano-carrier biobased system for simultaneous

detection of pH in the wound bed and controlled release of benzocaine. Cellulose. 2018;25(12):7277–97.
Lee Y-S. Syntheses and properties of fluorinated carbon materials. J Fluor Chem. 2007;128(4):392–403.
Li Z, Kang HL, Che N, Liu ZJ, Li PP, Li WW, et al. Controlled release of liposome-encapsulated naproxen from core-sheath electrospun nanofibers. Carbohydr Polym. 2014a;111:18–24.
Li Z, Kang HL, Che N, Liu ZJ, Li PP, Li WW, et al. Effects of electrode reversal on the distribution of naproxen in the electrospun cellulose acetate nanofibers. J Nanomater. 2014b;2014:1–8.
Liang X, Boppart SA. Biomechanical properties of in vivo human skin from dynamic optical coherence elastography. IEEE Trans Biomed Eng. 2009;57(4):953–9.
Lim C, Tan E, Ng S. Effects of crystalline morphology on the tensile properties of electrospun polymer nanofibers. Appl Phys Lett. 2008;92(14):141908.
Liu HQ, Hsieh YL. Ultrafine fibrous cellulose membranes from electrospinning of cellulose acetate. J Polym Sci B Polym Phys. 2002;40(18):2119–29.
Liu XK, Yang YY, Yu DG, Zhu MJ, Zhao M, Williams GR. Tunable zero-order drug delivery systems created by modified triaxial electrospinning. Chem Eng J. 2019;356:886–94.
Long Y-Z, Yan X, Wang X-X, Zhang J, Yu M. Electrospinning: the setup and procedure. In: Electrospinning: nanofabrication and applications. Amsterdam: Elsevier; 2019. p. 21–52.
Magee AI, Lytton NA, Watt FM. Calcium-induced changes in cytoskeleton and motility of cultured human keratinocytes. Exp Cell Res. 1987;172(1):43–53.
Majumder S, Matin MA, Sharif A, Arafat MT. Understanding solubility, spinnability and electrospinning behaviour of cellulose acetate using different solvent systems. Bull Mater Sci. 2019;42(4):171.
McKeen L. 12-renewable resource and biodegradable polymers. In: The effect of sterilization on plastics and elastomers. Amsterdam: Elsevier; 2012. p. 305–17.
Mokhena TC, Jacobs V, Luyt AS. A review on electrospun bio-based polymers for water treatment. Express Polym Lett. 2015;9(10):839–80.
Mulijani S, Iswantini D, Wicaksono R, Notriawan D. Optical sensor based chemical modification as a porous cellulose acetate film and its application for ethanol sensor. In: IOP conference series: materials science and engineering. London: IOP Publishing; 2018 p. 012014.
Nasouri K. Fabrication of lightweight and flexible cellulose acetate composite nanofibers for high-performance ultra violet protective materials. Polym Compos. 2019;40(8):3325–32.
Olaru N, Calin G, Olaru L. Zinc oxide nanocrystals grown on cellulose acetate butyrate nanofiber mats and their potential photocatalytic activity for dye degradation. Ind Eng Chem Res. 2014;53(46):17968–75.
Olaru N, Anghel N, Pascariu P, Ailiesei G. Synthesis and testing of cellulose acetate nicotinate as adsorbent for rhodamine B dye. J Appl Polym Sci. 2019;136(29):47772.
Pandele AM, Comanici FE, Carp CA, Miculescu F, Voicu SI, Thakur VK, et al. Synthesis and characterization of cellulose acetate-hydroxyapatite micro and nano composites membranes for water purification and biomedical applications. Vacuum. 2017;146:599–605.
Panyala NR, Peña-Méndez EM, Havel J. Silver or silver nanoparticles: a hazardous threat to the environment and human health? J Appl Biomed. 2008;6(3):117–29.
Pilehvar-Soltanahmadi Y, Dadashpour M, Mohajeri A, Fattahi A, Sheervalilou R, Zarghami N. An overview on application of natural substances incorporated with electrospun nanofibrous scaffolds to development of innovative wound dressings. Mini-Rev Med Chem. 2018;18(5):414–27.
Rani Agrawal P, Singh N, Kumari S, Dhakate SR. The removal of pentavalent arsenic by graphite intercalation compound functionalized carbon foam from contaminated water. J Hazard Mater. 2019;377:274–83.
Rezaei B, Askari M, Shoushtari AM, Malek RAM. The effect of diameter on the thermal properties of the modeled shape-stabilized phase change nanofibers (PCNs). J Therm Anal Calorim. 2014;118(3):1619–29.
Rezaei B, Ghani M, Askari M, Shoushtari AM, Malek RMA. Fabrication of thermal intelligent core/shell nanofibers by the solution coaxial electrospinning process, Adv Polym Technol. 2016;35(1). https://doi.org/10.1002/adv.21534.
Rohani M, Bamoharram FF, Khosravi M, Baharara J, Heravi MM. Preparation and characterisation of preyssler heteropolyacid-cellulose acetate hybrid nanofibers: a new, green and recyclable nanocatalyst for photodegradation of methyl orange as the model dye. J Exp Nanosci. 2017;12(1):1–13.
Salama A, Mohamed A, Aboamera NM, Osman T, Khattab A. Characterization and mechanical properties of cellulose acetate/carbon nanotube composite nanofibers. Adv Polym Technol. 2018a;37(7):2446–51.
Salama A, Mohamed A, Aboamera NM, Osman TA, Khattab A. Photocatalytic degradation of organic dyes using composite nanofibers under UV irradiation. Appl Nanosci. 2018b;8(1–2):155–61.
Samadian H, Salehi M, Farzamfar S, Vaez A, Ehterami A, Sahrapeyma H, et al. In vitro and in vivo evaluation of electrospun cellulose acetate/gelatin/hydroxyapatite nanocomposite mats for wound dressing applications. Artif Cell Nanomed Biotechnol. 2018;46:S964–S74.
Senthamizhan A, Celebioglu A, Balusamy B, Uyar T. Immobilization of gold nanoclusters inside porous electrospun fibers for selective detection of Cu(II): a strategic approach to shielding pristine performance. Sci Rep. 2015;5:15608.
Senthamizhan A, Balusamy B, Celebioglu A, Uyar T. "Nanotraps" in porous electrospun fibers for effective removal of lead(II) in water. J Mater Chem A. 2016;4(7):2484–93.
Sharma R, Singh N, Gupta A, Tiwari S, Tiwari SK, Dhakate SR. Electrospun chitosan–polyvinyl alcohol composite nanofibers loaded with cerium for efficient removal of arsenic from contaminated water. J Mater Chem A. 2014;2(39):16669–77.

Sheng J, Tong S, He Z, Yang R. Recent developments of cellulose materials for lithium-ion battery separators. Cellulose. 2017;24(10):4103–22.

Son WK, Youk JH, Lee TS, Park WH. Electrospinning of ultrafine cellulose acetate fibers: studies of a new solvent system and deacetylation of ultrafine cellulose acetate fibers. J Polym Sci B Polym Phys. 2004;42(1):5–11.

Tungprapa S, Jangchud I, Supaphol P. Release characteristics of four model drugs from drug-loaded electrospun cellulose acetate fiber mats. Polymer. 2007;48(17):5030–41.

Van Meerloo J, Kaspers GJ, Cloos J. Cell sensitivity assays: the MTT assay. In: Cancer cell culture. Totowa: Springer; 2011. p. 237–45.

Vatankhah E. Rosmarinic acid-loaded electrospun nanofibers: in vitro release kinetic study and bioactivity assessment. Eng Life Sci. 2018;18(10):732–42.

Wahab JA, Kim IS, Ni QQ. A comparative study on synthesis of AgNPs on cellulose nanofibers by thermal treatment and DMF for antibacterial activities. Mater Sci Eng C Mater Biol Appl. 2019;98:1179–95.

Wang X, He GQ, Liu HY, Zheng GF, Sun DH. Fabrication and morphological control of electrospun ethyl cellulose nanofibers. New York: IEEE; 2013.

Wang X, Li XY, Li Y, Zou H, Yu DG, Cai JS. Electrospun acetaminophen-loaded cellulose acetate nanofibers fabricated using an epoxy-coated spinneret. E-Polymers. 2015a;15(5):311–5.

Wang SD, Ma Q, Liu H, Wang K, Ling LZ, Zhang KQ. Robust electrospinning cellulose acetate@TiO2 ultrafine fibers for dyeing water treatment by photocatalytic reactions. RSC Adv. 2015b;5(51):40521–30.

Wang X, Wang Y, Xia Y, Huang S, Wang Y, Qiu Y. Preparation, structure, and properties of melt spun cellulose acetate butyrate fibers. Text Res J. 2018;88(13):1491–504.

Weng B, Xu F, Alcoutlabi M, Mao Y, Lozano K. Fibrous cellulose membrane mass produced via forcespinning® for lithium-ion battery separators. Cellulose. 2015;22(2):1311–20.

Wutticharoenmongkol P, Hannirojram P, Nuthong P. Gallic acid-loaded electrospun cellulose acetate nanofibers as potential wound dressing materials. Polym Adv Technol. 2019;30(4):1135–47.

Xiao JL, Lv WY, Song YH, Zheng Q. Graphene/nanofiber aerogels: performance regulation towards multiple applications in dye adsorption and oil/water separation. Chem Eng J. 2018;338:202–10.

Xu YJ, Li SS, Yue XP, Lu WL. Review of silver nanoparticles (AgNPs)-cellulose antibacterial composites. BioResources. 2018;13(1):2150–70.

Yang YF, Fan X, Long YY, Su K, Zou DC, Li N, et al. A simple fabrication of electrospun nanofiber sensing materials based on fluorophore-doped polymer. J Mater Chem. 2009;19(39):7290–5.

Yang GZ, Li JJ, Yu DG, He MF, Yang JH, Williams GR. Nanosized sustained-release drug depots fabricated using modified tri-axial electrospinning. Acta Biomater. 2017;53:233–41.

Yang YY, Li WB, Yu DG, Wang GH, Williams GR, Zhang Z. Tunable drug release from nanofibers coated with blank cellulose acetate layers fabricated using tri-axial electrospinning. Carbohydr Polym. 2019;203:228–37.

Yu H, Hu J, Chang J. Selective separation of wood components based on Hansen's theory of solubility. Ind Eng Chem Res. 2011;50(12):7513–9.

Yu DG, Yu JH, Chen L, Williams GR, Wang X. Modified coaxial electrospinning for the preparation of high-quality ketoprofen-loaded cellulose acetate nanofibers. Carbohydr Polym. 2012;90(2):1016–23.

Yu DG, Li XY, Wang X, Yang JH, Bligh SWA, Williams GR. Nanofibers fabricated using triaxial electrospinning as zero order drug delivery systems. ACS Appl Mater Interfaces. 2015;7(33):18891–7.

Zdraveva E, Fang J, Mijovic B, Lin T. Electrospun poly(vinyl alcohol)/phase change material Fibers: morphology, heat properties, and stability. Ind Eng Chem Res. 2015;54(35):8706–12.

Zhang SL, Tanioka A, Matsumoto H. Nanofibers as novel platform for high-functional ion exchangers. J Chem Technol Biotechnol. 2018;93(10):2791–803.

Zhang T-W, Tian T, Shen B, Song Y-H, Yao H-B. Recent advances on biopolymer fiber based membranes for lithium-ion battery separators. Compos Commun. 2019a;14:7–14.

Zhang K, Li ZJ, Deng NP, Ju JG, Li YF, Cheng BW, et al. Tree-like cellulose nanofiber membranes modified by citric acid for heavy metal ion (Cu2+) removal. Cellulose. 2019b;26(2):945–58.

Zhou WT, He JX, Cui SZ, Gao WD. Preparation of electrospun silk fibroin/cellulose acetate blend nanofibers and their applications to heavy metal ions adsorption. Fiber Polym. 2011;12(4):431–7.

Zhou ZD, Peng XW, Zhong LX, Wu L, Cao XF, Sun RC. Electrospun cellulose acetate supported Ag@AgCl composites with facet-dependent photocatalytic properties on degradation of organic dyes under visible-light irradiation. Carbohydr Polym. 2016;136:322–8.

Zou H, Lv PF, Wang X, Wu D, Yu DG. Electrospun poly(2-aminothiazole)/cellulose acetate fiber membrane for removing Hg(II) from water, J Appl Polym Sci. 2017;134(21). https://doi.org/10.1002/app.44879.

Production of Nanofibers, Environmental Challenges and Solutions

10

Rachna Rana and Swati Gupta

Abstract

Nanofibers are gaining popularity due to their unique characteristics of mechanical strength and large surface area owing to their nanosize. These properties make them preferable over macromaterials. History, methodology, applications and environmental challenges are discussed in this chapter. Advancement in technology is opening up new ways for preparation of nanofibers. However, electrospinning remains the most suited methodology. Suitability of nanofibers in clinical use makes them a potential tool in biomedical purposes for drug delivery, tissue engineering and biological dressing. High filtration efficiency and porosity in structure of nanofibers match the requirements of use in protective clothing in warfare, firefighting, etc. Nanofibers have paved a way in novel applications in energy generation, healthcare sector and environmental treatment. Degree of variability in applications for nanofibers enriches it with wide scope of research and development. This chapter aims to present detailed study of applications of nanofibers in various fields along with considering their hazardous toxicity to the environment. A brief explanation on patent aspect of nanofiber is also described for a practical clarity on the topic. This chapter also provides future perspective and expectations for the benefit of the reader. The future challenges of nanofibers give the direction to scope of research and improvement in the existing knowledge.

Keywords

Nanofibers · Tissue engineering · Electrospinning · Drug delivery · Energy Storage

1 Introduction

Nanotechnology is the branch of science that deals with the physical and chemical properties and unique characteristics of matter of nanoscale range. It is the science that deals with the study of functionalities of matter in the size range of 0.1–100 nm. The particles in nanoscale range possess electrical, magnetic, mechanical, thermal and biological properties because of their minute size due to which they are gaining popularity. These properties are unique which makes them varied from macromaterials. The various nanomaterials utilized in pharmaceutical and other industries are nanotubes, nanofibers, nanorods, nanowires, nanocrystals, two-dimensional nanosheets, etc. This chapter deals with properties, history, manu-

R. Rana · S. Gupta (✉)
Amity Institute of Pharmacy, Amity University, Noida, Uttar Pradesh, India

J. K. Patel, Y. V. Pathak (eds.), *Emerging Technologies for Nanoparticle Manufacturing*,
https://doi.org/10.1007/978-3-030-50703-9_10

facturing, applications and environmental challenges of nanofibers. Nanofiber is a combination of two words, namely, 'nano' and 'fiber', which translates into slender, elongated fibers or thread-like structures with diameter in nanoscale range (~50–300 nm) (Almetwally et al. 2017). Nanofibers are gaining popularity as carriers for delivery of biological substances due to their suitability in clinical use in humans. A number of reviews have been published on the interaction patterns of nanofibers with cells and its applications in clinical use. The small diameter of nanofibers mimics the size scale of extracellular matrix (ECM) fibers, which supports its use for biomedical purposes. High surface area-to-volume ratio and porosity in structure make nanofibers a better candidate for drug loading and many other advanced applications as compared to macro- or microscale carrier systems. This property also imparts better adhesion to cell receptors after the administration by providing a strong cell matrix interaction. Nanofibers show higher rates of protein adsorption as compared to macromaterials which aids in better attachment to biological surfaces. Protein adsorption of nanofibers can be supported by an example of poly(L-lactic acid) (PLLA) fibers of nanoscale range (50–500 nm) attributing to four times higher rates of adsorption of proteins as compared to porous PLLA of macroscale range. A number of reviews have been published based on nanofibers signifying their popularity and applicability. The mechanical properties of nanofibers including the parameters such as tensile modulus, tensile strength and shear modulus have been shown to increase with decrease in diameter. Such behaviour can be due to the increased macromolecular chain alignment within the nanofibers of higher degree of crystallinity. These mechanical properties help in altering cell behaviour and resisting the forces from the cell cytoskeleton by providing required tension and strength (Dahlin et al. 2011). Various materials such as natural polymers, synthetic polymers, semiconducting nanomaterials, etc. have been utilized to prepare nanofibers. Continuous efforts are being made for the synthesis, characterization of nanofibers and exploration of new applications such as energy generation, environmental treatment and healthcare advancements (Lim 2017). It is interesting to know that nanofibers can be utilized in gene delivery, drug delivery, tissue engineering, energy transfer systems, batteries, fuel cells, capacitors, biotechnology, security and defence (Almetwally et al. 2017). Attempts have been made to adopt polymeric nanofibers in tissue engineering for the regeneration of various tissues (Dahlin et al. 2011). It is also observed by several researchers that nanofibers can enhance cellular activity as compared to the flat surfaces or microfibers of the same material as a result of large surface-to-volume ratio. Thus, nanofibers can be utilized for the cell proliferation, excretion and differentiation in cell culture (Moutsatsou et al. 2017). Nanofibers are gifted for forming porous meshlike structures. These porous structures of nanofibers can be modified into different pore sizes and shapes as per the requirement. On the other hand, conventional porous structures are rigid, although, if required, the porous structure of nanofibers can be linked together to impart rigidity. Chemical functionalities and surface properties can be tailored by changing the synthesis environment, conditions and reactants. Out of many methods of synthesis of nanofibers, electrospinning is the most frequently employed method due to its easy process and high production rate. Electrospinning is a profoundly productive method for the synthesis of porous nanofibers (Ramakrishna et al. 2006). Nanofibers prepared by electrospinning technique have been proven to be useful for filtration, protective clothing, healthcare, nanocatalysis and tissue scaffolds (Shooto et al. 2016). Electrospun nanofibers can be classified on the basis of their application as follows: bone engineering, cartilage engineering, tissue engineering, vascular tissue engineering, drug delivery, wound dressing and heart tissue engineering (Kanani and Bahrami 2010). Electrospinning is the most versatile, profoundly employed method of production of nanofibers in industry and academia to produce varied fibrous assemblies at low cost (Moutsatsou et al. 2017). Amongst all the available methods of nanofiber fabrication, electrospinning is the most effective method (Radacsi et al. 2018). In certain cases, it

is feasible to use nanofiber composites rather than monophasic nanofibers. Nanofiber composites are composed of two or more phases of nanofibers combined together. This modification helps in altering the physical, chemical and biological properties presented by monophasic nanofibers. Thus, desired alterations are also possible with nanofibers. Nanofiber composites include two phases, namely, continuous or primary phase and discontinuous phase or secondary phase. The secondary phase is embedded in the primary phase. In such association, the properties of each phase of nanofiber synergize the effect of the other. Considerable efforts are needed for producing or inventing such possible and efficient combinations to optimize the activity. This chapter aims to cover a detailed information about nanofibers and their composites along with environmental challenges which hinder their encouragement for biomedical purposes (Ramalingam and Ramakrishna 2017).

2 History

Discoveries for development of nanofibers hold the history of about four centuries. William Gilbert during the late 1600s started working in the direction of developing electrospinning technology. He observed that a charged amber piece was capable of pulling its positions to take up the shape of a cone when transferred close to a water droplet on a dry surface. This was named as Taylor cone. Later in 1749, a scientist named Nollet presented the disintegration of a water jet on being charged. In 1902, a US patent was granted to J. F. Cooley under the title 'Apparatus for electrically dispersing fibers' for recognizing this process as 'electrospinning'. Zeleny, a scientist, took forward the studies about it in 1914. In 1952, Vonnegut and Neubauer developed fine streams (0.1 mm diameter) using highly electrified droplets. In 1962, a patent was granted to Simons for an apparatus designed to produce non-wovens using electrospinning technique. After the popularity of ultra-fine fibers in nanoscale range, electrospinning started gaining importance. In 1981, Larrondo and Manley experimented the electrospinning technique by using melting polymer process. By the twentieth century, this phenomenon gained popularity by its name 'electrospinning'. Continuous exploration has been carried out for the development of nanofibers and other materials using electrospinning technique since then. Ramakrishna et al. published a book on nanofibers and electrospinning technique in 2005. Nowadays many more techniques such as freeze drying, phase separation, CO2 laser supersonic drawing, etc. have been developed and are being utilized for the synthesis of nanofibers and other nanomaterials. Research is continuously being carried out to extend its applications in different fields apart from pharmaceutics as well. Many companies use electrospinning technique for air filtration, fuel battery systems, etc. More and more articles and research papers are published every year (Barhoum et al. 2017) (Moutsatsou et al. 2017) (Karakaş 2015). Table 10.1 summarizes the history of nanofibers.

3 Method of Preparation

There are diverse approaches used for the manufacturing of nanofibers. Depending on the feasibility any of the techniques can be utilized for the fabrication of fibers at nanoscale range. Techniques for nanofiber production are described in Fig. 10.1.

(i) *Phase separation*
In this technique, polymer is blended with solvent and gelated. The solvent is then extracted leaving behind residue. It is then subjected to freezing and freeze drying for phase separation which happens as a result of physical inconsistency.

(ii) *Bicomponent extrusion*
Bicomponent extrusion technique is used to extrude two fibers from one spinneret. Different types of bicomponent fibers can be islands in the sea, segmented pie, sheath core, side by side and eccentric as shown in Fig. 10.2. In islands-in-the-sea fibers, one polymer is suspended into the matrix of the other polymer melt before extrusion. The

Table 10.1 History of nanofibers

Scientist	Year	Description
William Gilbert	Late 1600s	Described Taylor cone phenomenon
Nollet	1749	Disintegration of water jet on being charged
J. F. Cooley	1902	US patent for recognizing electrospinning
Zeleny	1914	Further studies on electrospinning
Vonnegut and Neubauer	1952	Development of fine streams using highly electrified droplets
Simons	1962	Patent on non-woven-producing apparatus
Larrondo and Manley	1981	Electrospinning experimentation using melting polymer process

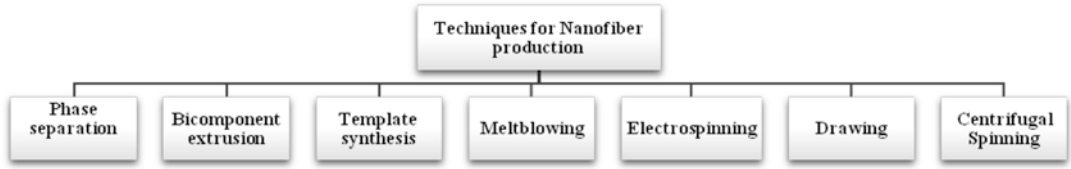

Fig. 10.1 Various techniques for nanofiber production

suspended island polymer may have uniform or non-uniform diameters. Polymers are mixed in the predetermined ratio as drops of one polymer into the melt of another to fabricate fibers. After extrusion, fibers are subjected to fast cooling to ensure solidification of polymer mixture. For separation of the polymers, heat, chemical or mechanical techniques can be carried out. For fabricating segmented pie and side-by-side type of bicomponent fibers, polymers are fed into the feed where they are separated by septum or edges to come out from the same spinneret together in side-by-side alignment. Sheath core and eccentric bicomponent fibers can be fabricated by pipe in pipe method where each pipe holds a different polymer for the envelope type of arrangement.

(iii) *Drawing*

This method is used for viscoelastic material which can withstand the stress even after high degree of deformation during pulling. The material should be cohesive enough to handle pulling stress and deform as required too. This method is based on dry spinning technique at molecular level. This technique is generally employed at laboratory level only, thus having limited industrial application. The manufacturing unit for drawing technique involves a SiO2 surface, a micropipette and a micromanipulator. A micropipette is plunged into the polymer droplet near the contact line through a micromanipulator. It is then removed at a speed of 1 × 10–4 ms-1 to form a nanofiber. The pulled fiber is removed from the micropipette end, and the process is continued with every drop. With increased evaporation, the viscosity of the material also increases.

(iv) *Centrifugal spinning*

Centrifugal spinning has been recently popularized for the construction of nanofibers to address the shortcomings of electrospinning. Centrifugal spinning is 500 times faster in terms of production as compared to electrospinning. Electrospinning is only applicable for materials with dielectric properties, whereas centrifugal spinning does not have dielectric restrictions. Electrospinning technique is also expensive, slow, and requires electric fields and spinning, which is not suitable for every material. These drawbacks can be overcome using centrifugal spinning technique which requires centrifugal force for spinning rather than high-voltage electric fields. Centrifugal spinning is used for the fabrication of carbon, metal nanofibers, etc. Centrifugal spinning technique was used by Hooper in 1924

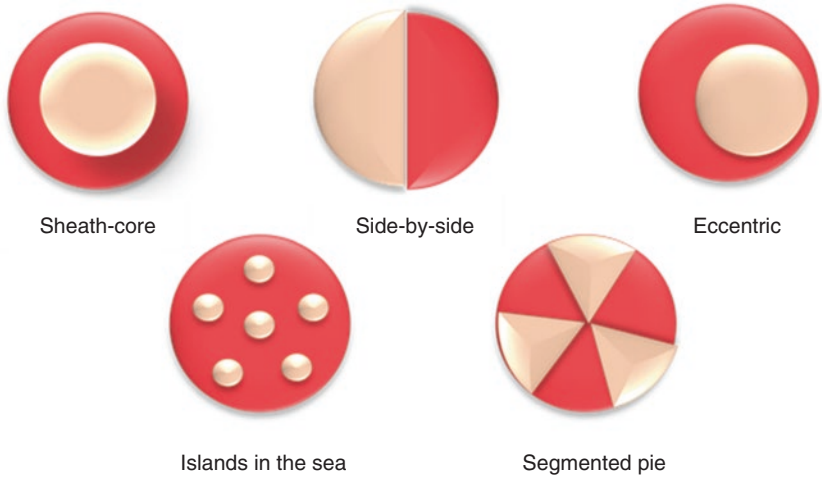

Fig. 10.2 Different types of bicomponentfibers

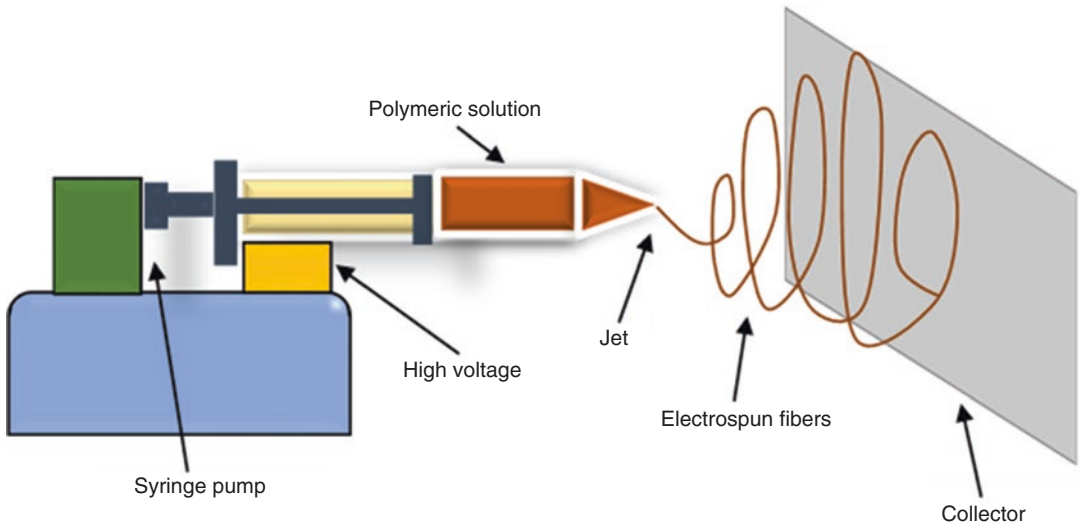

Fig. 10.3 Set-up for electrospinning

to develop artificial silk threads from viscose. The development of fibers by centrifugal spinning technique relies upon two forces, namely, centrifugal force and Laplace force. For the fabrication of nanofibers using centrifugal spinning, polymer solution stream is forced through the orifice to form a jet as a result of centrifugal and hydrostatic pressure. These forces overcome the flow-resistant capillary forces, and the polymer solution starts to flow through the nozzle as a jet. Further, force is increased to extend the jet and increase surface area. The polymer jet so produced stretches towards the collector wall. As the jet reaches the collector wall, its diameter is significantly reduced. Finally, the solvent is evaporated to form the fibers by shrinkage. The diameter or the thickness of the fibers depends on the solidification of the fibers. Highly volatile solvent is easily evaporated leading to fast solidification, and thus thick fibers are formed. On the other hand, less volatile solvent produces very thin fibers as it gets

enough time for jet extension. The spinning process apart from volatility also depends on orifice radius, solution surface tension, temperature, distance between nozzle and collector wall, spinneret angular velocity and polymer viscosity (Almetwally et al. 2017).

4 Rising Applications of Nanofibers

Nanofibers possess unique characteristics due to their large surface area-to-volume ratio. These characteristics make nanofibers the attractive candidate for various applications in energy storage, healthcare, environmental remedy, biomedical engineering, water treatment, electronic devices, etc. Fig. 10.4 depicts various applications of nanofibers.

4.1 Tissue Engineering

Tissue engineering aims at repairing, replacing, maintaining or improving the function of specific organs or tissues. The main obstacle in tissue engineering is to compose and fabricate scaffolds that are biomimetic to the naturally available extracellular matrix of cells and tissues. In vitro and in vivo studies show that electrospun nanofibrous scaffolds are a revolution for enhancing cell attachment, proliferation, differentiation and penetration (Karakaş 2015).

4.1.1 Bone Tissue Engineering

Natural bone is composed of organic and inorganic components (hydroxyapatite crystals mainly). Ninety per cent of the organic bone matrix is composed of collagen. Collagen present in the bones exists mainly in the collagen type I fibril form. Fibers present in bones have diameter of about 50 nm. In bone tissue engineering, poly-

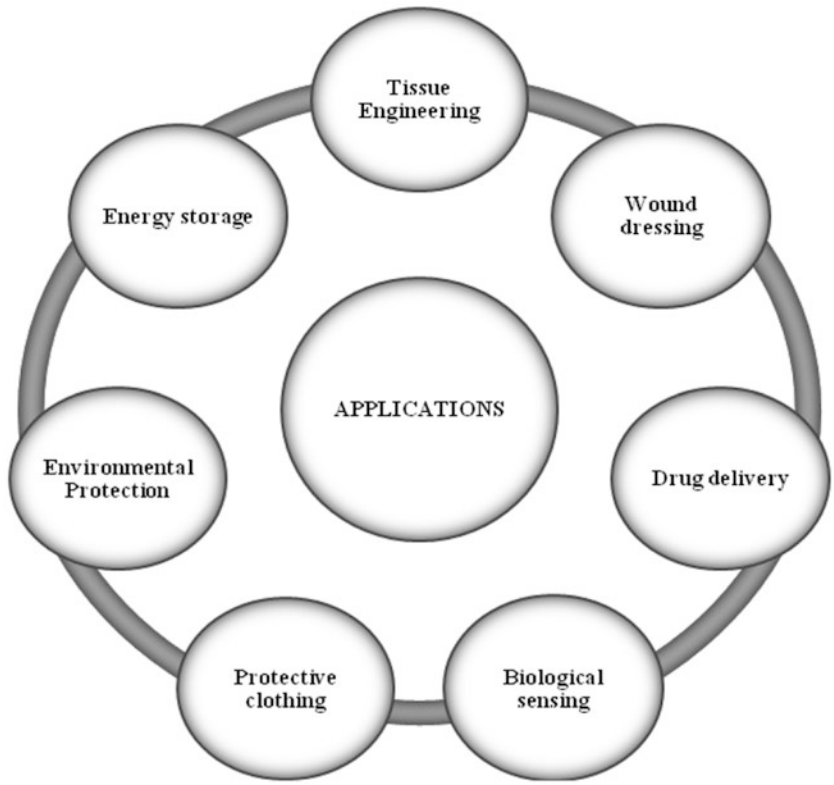

Fig. 10.4 Various applications of nanofibers

meric nanofibers can be fabricated in a similar size range to mimic the behaviour of bone extracellular matrix (Dahlin et al. 2011). In bone tissue engineering, the scaffolds are designed by taking the reference from physical characteristics of bone tissues, for instance, hardness, mechanical strength, 3D structure and porosity (Vasita and Katti 2006). Electrospinning is a suitable method to produce ultra-fine fibers to mimic bone extracellular matrix (Karakaş 2015). Several experiments have been practiced to demonstrate the revolution of polymeric nanofibers in bone tissue engineering in in vitro and in vivo conditions (Dahlin et al. 2011). Electrospun nanofibers made from polymers such as chitosan, collagen, poly(e-caprolactone) (PCL) and gelatin have been proved to be superior than other extensively examined polymers for bone tissue engineering (Barhoum et al.). Yoshimoto et al., in an in vitro study, fabricated microporous PCL scaffolds by electrospinning with fibers in size range 20 nm to 5 mm. Scanning electron microscope (SEM), immunohistochemical and histological studies, demonstrated prevalence in mineralization and differentiation of mesenchymal stem cells of rat derived from the bone marrow. PCL scaffolds of fiber diameter of about 370 nm have also been shown to be effective in contributing to higher levels of alkaline phosphatase activity, osteocalcin, osteopontin, adherence and generation of mesenchymal stem cells. In an in vivo study, PCL scaffolds were implanted for a time period of 4 weeks in rat omenta. It was observed that cells were capable of differentiating and infiltrating the scaffolds along with promotion in collagen type I production and mineralization. This suggests that PCL scaffolds are the promising candidate for bone tissue engineering (Kanani and Bahrami 2010). In many studies, scaffolds have been formed in combination of both micro- and nanofibers. The microfibers provide large pore size, whereas nanofibers aid in cell adhesion and contact. In a study, PCL nanofibers were fabricated with fibers of diameter 600 nm by electrospinning. The nanofibers so produced were seeded with mesenchymal stem cell culture in osteogenic media. It was observed that cell infiltration into the scaffolds was limited and cell spreading was enhanced improving the cell proliferation and differentiation although cell attachment did not improve. Composite fibers have also been proved to show osteoinductive effects. In a study, composite nanofibers were developed using BMP-2, PEO, silk and hydroxyapatite nanoparticles, and it was observed that bone formation and osteogenic differentiation were greatly enhanced (Dahlin et al. 2011). In a study, Kim et al. demonstrated the silk fibroin designed by electrospinning technique as a device for use in bone engineering and periodontal regenerative treatment. Results demonstrated that levels of osteocalcin and cell number increased significantly aiding cell proliferation and differentiation. In vivo study showed complete healing of bone defect with new bone. Thus, it was concluded by the authors that silk fibroin membrane can be utilized as a significant tool in bone regeneration (Kanani and Bahrami 2010).

4.1.2 Tendon and Ligament Tissue Engineering

Tendons and ligaments are the tough bands composed of connective tissue that is responsible for body movement, bending and stability. Any injury to the tendon or ligament may lead to an irreversible damage of the surrounding tissues which do not heal naturally. Conventional treatments for such injuries are not completely effective for repair. In such cases, nanofibers can be used for tissue and ligament tissue engineering as proved by recent advances (Vasita and Katti 2006). The mechanical loading observed in tendons and ligaments is unidirectional that leads to anisotropic mechanical properties. Therefore, mesenchymal stem cells or fibroblasts are cultured on aligned fibers to fabricate a similar anisotropic framework. The aligned fibers mimic the anisotropic tissues and, therefore, are a promising tool for tendon and ligament tissue engineering. The braided fabrics commonly used as scaffold show low cell seeding, cell infiltration, mass transfer and mechanical strength. However, knitted microfibers can overcome these challenges except cell seeding which is still complicated. A combination of knitted microfiber and nanofiber can be utilized to impart desired

mechanical strength provided by microfiber and adequate surface area for cell attachment by nanofiber structures. In a study, poly(lactic-co-glycolic acid) (PLGA) nanofibers were spun over the PLGA microfiber scaffold that showed better cell seeding, proliferation and function (Dahlin et al. 2011). In a study, Lee and co-workers seeded the polyurethane nanofibers on human ligament fibroblasts (HLFs) to study the effect of alignment and mechanical stimuli direction on the formation of human ligament fibroblast extracellular matrix. The authors used a rotating target to fabricate aligned electrospun fibers. It was observed that HLFs possessed spindle shape and were aligned in the direction of nanofibers. The production of collagen also enhanced when compared to randomly aligned nanofibers. The authors also observed that HLFs were extra sensitive to longitudinal mechanical strain. This study justified the use of aligned nanofibers for the treatment of ligament injury (Vasita and Katti 2006).

4.1.3 Cartilage Tissue Engineering

Cartilage lines the surface of the joints to serve lubrication and protection to the bones. The cartilage tissues are mainly composed of collagen, chondrocytes, water and proteoglycans. The tensile strength is provided to the cartilage by the mesh structure of the fibrils composed of collagen. The mesh structure helps in trapping the molecules in the structure. The chondrocytes are deeply embedded in the extracellular matrix and therefore are restricted for availability in repairing the injury. Also, chondrocytes are avascular tissues due to which their self-regeneration is limited. Nanofibers have been thus frequently investigated for its fibrous structure for cartilage tissue engineering. The main challenge is to maintain the chondrocytic phenotype. When chondrocytes are cultured in vitro, they dedifferentiate into collagen type II and proteoglycans. Therefore, different approaches have been utilized to promote redifferentiation of chondrocytes and prevent dedifferentiation. In a study, PCL nanofibrous scaffolds were constructed and explored for its ability to promote chondrocyte expansion. It was observed that chondrocytes significantly proliferated and expanded in tissue culture. The influence of fiber diameter on chondrocyte morphology was also explored. It was concluded that nanofibrous scaffolds supported cell proliferation and maintained rounded morphology, whereas cells grown on microfibers were spread well. In a study carried out on swine model, mesenchymal stem cells of humans were implanted on nanofibrous PCL scaffolds which led to the creation of hyaline-like cartilage having smooth surface. Nanofibrous scaffolds can be easily fixed on the tissues by sutures and do not need periosteal covering. Thus, morbidity correlated with the surgeries can be reduced (Dahlin et al. 2011). In a study carried out by Kisiday and co-workers, cartilage repair was examined by fabricating self-assembling peptide hydrogel scaffold using the KDK-12 peptide in a sequence AcN-KLDLKLDLKLDLCNH2 where K stands for lysine, D for aspartic acid and L for leucine and seeding it with bovine chondrocytes. Then self-assembly into the hydrogel was allowed. It was observed from the study that the chondrocytes produced cartilage-like extracellular matrix which was rich in type II collagen and proteoglycan. Continuous deposition of glycosaminoglycan-rich matrix by the chondrocytes was also observed increasing the mechanical properties to the ECM. Thus, it can be concluded that self-assembling peptide hydrogel scaffold can be utilized in cartilage tissue engineering as a suitable candidate (Vasita and Katti 2006).

4.1.4 Neural Tissue Engineering

A number of neural disorders may occur due to degeneration of neurons or damage of glial cells. Neural injuries may lead to permanent loss of function in the central nervous system. Neural tissue engineering can play a significant role in repair of such neural injuries supported by normal or genetically engineered cells or ECM substitutes along with nanofibrous scaffold systems for drug delivery (Vasita and Katti 2006). Significant efforts have been made to utilize nanofibers for the repair of peripheral or central neurons. The structure of nanofibers mimics the structure of fibrous components of the neural extracellular matrix. In addition to this, nanofi-

bers also can direct the sprouting of axon and deliver the neurotrophic factors to the target site of the injury. In many cases, nanofibers have also been reported to affect cell generation, differentiation and growth patterns of neural stem cells. The arrangement of the nanofibers can affect the elongation of neural stem cell and outgrowth of neurite in the direction of the nanofibers aligned. Effective neural guidance conduits are embedded into the tissue to support axonal sprouting and diffusion of neurotrophic factors and prohibit the fibrous tissue growth into the defect (Dahlin et al. 2011). In a separate work, nanofibrous scaffolds of collagen were produced to promote the presynaptic maturation of neural stem cell (NSC)-derived neurons towards the generation of neural network (Lim 2017). Yang and co-workers investigated the role of electrospun nanofibrous scaffold made from poly(L-lactic acid) (PLLA) for neural tissue engineering by determining its influence on neural stem cells (NSCs). They observed that nanofibers in the size range of 150–350 nm that were randomly oriented favoured the cell adhesion and differentiation of NSC due to the large surface area and roughness of the nanofibrous scaffolds. In another study, Yang and co-workers demonstrated the role of aligned nanofibers in tissue engineering. They collected the aligned nanofibers from the edge of a rotating disc and designed a 3D scaffold of desired thickness. The oriented nanofibers in the scaffold were then investigated for its influence on NSCs. The results indicated elongation of NSCs and neurite outgrowth along the direction of the fiber orientation. Also, the NSCs showed increase in rate of differentiation as compared to microfibers. The diameter of the fibers also affects the neural stem cell behaviour. It was reported that with decrease in diameter of the nanofibers, the rate of proliferation and differentiation got increased. Thus, it can be concluded from the study that PLLA scaffolds possess a potential for its use as a tool for neural tissue engineering (Yang et al. 2005). In another study carried out by Semino and co-workers, self-assembling peptide scaffolds were fabricated to investigate 3D culture and cell entrapment. For this study, neural progenitor cells and hippocampal slice were removed from the dentate gyrus region and cultured on self-assembled nanofibrous scaffold. It was observed that neurons and glial cells got migrated and entrapped into the peptide scaffold to a depth of about 400–500 μm from the edge of the tissue slice after 1 week of culturing. The cells entrapped into the peptide scaffold were collected from the migration zone and utilized for initiating new cultures. During the experiment it was observed that the neural cell mitotic activity maintained for 3 days following migration since the nanofibrous scaffold mimics the ECM of the neural cells. The study supports the development of technology for in vitro isolation of neural progenitor cell and enrichment for neural tissue engineering (Vasita and Katti 2006) (Dahlin et al. 2011).

4.1.5 Cardiovascular Tissue Engineering

Extracellular matrix in cardiac tissues causes cardiomyocytes to produce cell bundles like fibers. The fibrous bundles in cardiac tissues undergo elongation and alignment to couple with adjacent fibrils. Thus, any polymeric structure which assists the cardiomyocyte alignment can be used in cardiovascular tissue engineering for its biomimetic role. From studies it has been demonstrated that electrospun fibers of poly(L-lactide-co-ε-caprolactone) P(LLA-CL) having average diameter near to 550 nm supported the adhesion and generation of human coronary artery, endothelial cells and smooth muscle cells. The alignment of P(LLA-CL) further increase the smooth muscle cell adhesion and proliferation. The role of density of nanofibers on its biomimetic effect was also observed and noted that best outcome is achieved in a density range of 30–50 nanofibers/mm. Further approaches have been focused on changing the surface characteristics of nanofibers to enhance the biomimetic effect in cardiac tissue engineering. Separately in another study, hydrophobin coating was used for the immobilization of anti-CD31 onto the surface of nanofibers of PCL. It was reported that binding of endothelial cells of human umbilical vein was drastically enhanced. To mimic basal lamina, in a study, gelatin was grafted covalently onto the surface-modified PCL constructs developed by electros-

pinning. It was observed that gelatin grafting enhanced endothelial cell spreading and overall growth of cells. The cells cultured on aligned fibers showed alignment in the direction of the fibers. In another study, collagen was directly introduced into the electrospinning process to fabricate collagen-blended P(LLA-CL) fibers and was observed to enhance endothelial cell spreading, adhesion and viability. Efforts have been done to investigate use of self-assembling peptides as a tool for cardiovascular tissue engineering which were reported to be able to self-assemble to form a nanofiber network in vivo when injected into the myocardium (Dahlin et al. 2011). Zong and co-workers fabricated poly(lactide)- and poly(glycolide)-based (PLGA) scaffolds that were non-woven and biodegradable. The scaffolds were used to study the structural and functional effects of fine-textured matrices with submicron features on cardiac myocyte growth. In vitro studies demonstrated a dose-response effect of the poly(glycolide) concentration on the rate of degradation. The non-woven matrix had a nanofibrous structure which supported the isotropic or anisotropic growth of the cardiomyocytes. It was concluded from the study that by adjusting the geometry and chemistry of micro- or nano-textured surfaces, it is possible to alter the structure and function of engineered cardiac tissues (Kanani and Bahrami 2010).

4.1.6 Skin Tissue Engineering

Skin tissue engineering is gaining attention for the healing of skin wounds. Wounds on skin under normal circumstances heal by the development of epithelialized scar tissues. Normal regeneration of cells is impaired if large epidermal areas are required to be replaced, although dermis layer has more scope for regeneration. The scar tissue so formed lacks strength, elasticity and flexibility when compared to normal dermis layer. Therefore, scar tissues are cosmetically undesirable. In a study, Min and co-workers fabricated electrospun non-woven silk fibroin nanofibers followed by coating with type I collagen to explore its use as a tool in skin tissue engineering. The authors observed that the porosity and large surface area-to-volume ratio of the produced nanofibers resulted in adhesion of keratinocytes/fibroblast and cell spreading. The study suggested that silk fibroin nanofibers possess great potential in skin tissue engineering (Vasita and Katti 2006). Electrospun nanofibers can also be used for producing skincare masks for skin healing, therapeutic effect and cleansing (Karakaş 2015). The nanofiber masks can also be impregnated with skin-revitalizing factors for skin renewal (Ramakrishna et al. 2006).

4.1.7 Blood Vessel (Vascular Tissue Engineering)

Vascular structures comprise of three layers, namely, tunica intima, tunica media and tunica adventitia. The innermost tunica intima layer is composed of non-thrombogenic endothelial cells in monolayer. Tunica media layer is composed of concentrically arranged smooth muscle cells. Tunica adventitia which is the external layer is composed of collagenous ECM and fibroblasts. ECM is the main part of the vascular system and comprises of collagen (type I and III), elastin, proteoglycans and glycoproteins. Collagen provides tensile rigidity against rupture, elastin provides elasticity, and proteoglycans provide compressibility to the blood vessel. The first case reported in vascular tissue engineering was in 1986 by Weinberg and Bell who developed artificial artery based on collagen scaffold. Nanofibers are utilized in vascular tissue engineering due to their biomimetic behaviour with ECM of blood vessels. In a study, Mo and co-workers developed poly(L-lactide-co-ε-caprolactone) [P(LLA-CL)] nanofibers by electrospinning and culturing on vascular system. It was observed that both smooth muscle cells and endothelial cells showed adhesion and proliferation on scaffold. Thus, it was concluded that the developed nanostructures can be used as a tool in vascular tissue engineering. Matthews et al. disclosed from their study that electrospun nanofibers of collagen encourage cell growth and seepage of cells into the developed matrix. Luong-Van et al. produced PCL nanofibers using electrospinning technique and embedded it with heparin. They observed that there was sustained release of heparin from the nanofibers for over 14 days. The developed nanofibers were

biocompatible, and it was concluded that electrospun PCL fibers are a potential tool for distribution of heparin to the site of vascular grafts. In another study, collagen, elastin and PLGA blend were used to fabricate nanofibers using electrospinning which showed that composition of tissue and mechanical characteristics were similar to blood vessels. Inoguchi et al. fabricated tubular scaffold made up of elastomeric poly(L-lactide-co-ε-caprolactone) fabrics using electrospinning technique at varied wall thickness to design a 'mechanoactive' artificial vascular graft of small diameter. The authors concluded that as the electrospinning time is increased, the thickness of the wall of the fabricated tube also increased. The fabricated scaffold was exposed to static- and dynamic-type flow conditions to evaluate the dependence of mechanical responses on thickness of the wall. Static condition demonstrated that decrease in wall thickness leads to more compliant tube. Dynamic flow condition produced by custom-designed arterial circulatory system showed increase in strain (relative increment in diameter per pulse) with decline in wall thickness similar to the native artery. Thus, it was demonstrated that tubular scaffold with mechanoactive property can be developed from an elastomeric PLCL and ELSP technique. Mo et al. developed collagen-chitosan and P(LLA-CL) nanofibers using electrospinning. They concluded from their study that by varying the collagen content in the collagen-chitosan complex nanofibers, the mechanical properties change. It was observed that smooth muscle cells grew rapidly on collagen nanofibers compared to P(LLA-CL). In a study, Zhang et al. fabricated the scaffolds of silk fibroin to induce vascular cell growth and cultured on human aortic endothelial cell (HAEC) and human coronary artery smooth muscle cell (HCASMC). The random non-woven silk nanofibrous scaffolds were observed within 5 days following seeding for the alignment pattern and elongation of HCASMCs. In the study, HCASMCs were also evaluated for the formation of extracellular cell matrix and transcription levels. The authors concluded from the study that the developed scaffolds enhanced the growth and expansion of HAECs and HCASMCs. Tillman et al. prepared polycaprolactone (PCL) collagen scaffolds by electrospinning and evaluated on the basis of in vivo stability studies in rabbit aorta-iliac bypass model. It was observed that under physiologic conditions, electrospun scaffolds supported adhesion and proliferation of vascular cells. When exposed to blood, endothelialized grafts resisted adherence of platelets. The developed scaffolds retained the structural integrity for a period of about 1 month of implantation in vivo. It was supported through this study that nanofibrous scaffolds prepared by electrospinning when combined with vascular cells may be considered as an alternative to prosthetic vascular grafts in vascular tissue engineering (Kanani and Bahrami 2010) (Vasita and Katti 2006).

4.2 Wound Dressing

In order to heal wounds, dressing plays a vital role in protection, removal of exudates, prevention of microorganisms and improved appearances. It was observed that a blister healed faster when left unbroken. This led to the interest in designing wound dressing materials. Wound dressing aids in conglutination of wounds since wound beds have moist nutritious territory which provides favourable conditions for microbial growth (Kanani and Bahrami 2010). Since electrospun nanofiber scaffolds are identical to the structure of an extracellular matrix, it can be used in wound dressing. Nanofiber scaffolds are better than traditional dressings in terms of cell attachment, proliferation and formation of new skin without scar tissue. Moreover, antimicrobial agents, vitamins, growth factors and drugs can be loaded in nanofiber scaffolds. The electrospun nanofibers have large surface area and porosity which can rapidly attract fibroblasts to the dermis and then release extracellular matrix components such as cytokines helpful for repairing damaged tissues. The traditional dressing has pore size insufficient to protect wounds from bacterial invasion through aerosol particle-capturing mechanism. Nanofibers also induce haemostatis, facilitate cell respiration and absorb wound exudates. Nanofibers are flexible which facilitate 3D

dressing. It does not require frequent changing as it operates in moist environment and thus reduces pain (Barhoum et al.). Nanofibers of biodegradable polymers can also be directly sprayed on the open wound to heal faster than traditional cotton gauze (Karakaş 2015). Latest advances in nanotechnology have enabled the use of nanofibers in wound healing overcoming the shortcomings of traditional dressings. In a study, Powell et al. developed nanofibrous scaffolds of collagen from bovine source using freeze-drying and electrospinning technique. Results showed that there was no considerable difference between electrospun collagen skin substitutes (ECSS) and freeze-drying collagen skin substitutes (FCSS) in terms of surface hydration, cellular organization and cell proliferation. The rates of grafting in athymic mice were observed to be 87.5% in FCSS and 100% in ECSS. At week 8, bovine collagen remained in the wound in FCSS, whereas bovine collagen did not persist in ECSS group. The authors concluded from the study that electrospun scaffolds can be better than freeze-dried scaffolds for skin substitutes. Rho et al. fabricated collagen type I nanofibrous matrix with average diameter of460nm and cross-linked it by vapours of glutaraldehyde. The porosity observed in collagen matrix elucidated decline to 71% from 89% during the process. Three groups, namely, uncoated collagen nanofibers, collagen nanofibers treated with collagen type I and laminin-treated collagen nanofibers, were examined for their effects on cytocompatibility, cell behaviour, open-wound healing and cell-collagen nanofiber interaction. Results showed low cell adhesion observed on uncoated collagen nanofibers as compared to collagen nanofibrous matrices treated with type I collagen or laminin; therefore it was concluded that electrospun scaffolds treated with collagen or laminin displayed enhanced results. In another study, Muzzarelli et al. evaluated the effects of chitosan and chitin on repairing the different wounds. Noh et al. developed chitin nanofibrous matrices and tested them for biodegradability and cell behaviour. The developed chitin nanofibers were compared with commercially available chitin microfibers (Beschitin W®; Chi-M), and it was observed that during 15 days of degradation in vitro, the rate of degradation was higher in Chi-N compared to Chi-M. During in vivo studies, Chi-N was grafted into rat subcutaneous tissue, and within 28 days, degradation was observed, but inflammation did not appear on nanofiber surfaces or in surrounding tissues. Results showed that relatively high cell attachment and spreading of cells occurred on Chi-N compared to Chi-M. On treating Chi-N with type I collagen, cellular response significantly increased. From the study, it was concluded that chitin nanofibers have adequate characterizations required for wound healing and chitosan, which is the derivative of chitin, is more suited for healing of wounds due to its high solubility in inorganic solvents and few organic solvents. Gholipour and co-workers developed a nanofibrous web of chitosan-polyvinyl alcohol (PVA) blend solutions in different ratios that is characterized by SEM, FTIR and DSC. They found that 25/75Cs/PVA is the best ratio. In vitro studies showed that the developed web possessed excellent antimicrobial activity against Gram-negative bacteria (*Pseudomonas aeruginosa*) and thus can be used for the purpose of dressing of wounds. In another study, Rujitanaroj et al. developed ultra-fine gelatin fiber mats with antimicrobial effect for burn wounds by using gelatin solution 22%w/v in 70 vol% acetic acid containing 2.5 wt% AgNO3. Silver nanoparticles containing gelatin solution were fabricated, and the average diameter of the developed silver nanoparticles ranged from 11 to 20 nm. Electrospinning of both the base and silver nanoparticles containing gelatin solution resulted in smooth fibers of average diameter of w230 and w280nm, respectively. The silver-containing gelatin fiber mats were further characterized for release of silver nanoparticles and antibacterial activity in burn wounds. Results concluded that the antibacterial activity was greatest against *Pseudomonas aeruginosa*, followed by *Staphylococcus aureus*, *Escherichia coli* and methicillin-resistant *S. aureus*. Authors suggested the use of silver nanoparticle-loaded gelatin fiber mats in dressings in burn wounds (Kanani and Bahrami 2010). Khil et al. developed electrospun polyurethane nanofibrous membrane for the purpose of wound

dressing which displayed controlled evaporative loss, optimum oxygen permeability and porosity suitable for fluid drainage. From the histological examination, it was observed that epithelialization rate was improved and secretion in the dermis was well controlled by electrospun membrane cover. Authors suggested that nanofibrous polyurethane membrane is significantly useful in wound dressing and drug can also be loaded in it to further enhance the effect (Vasita and Katti 2006). In a similar study, Verreck and co-workers electrospun polyurethane nanofibrous mat and loaded it with itraconazole and ketanserin to study the drug release for wound healing. An amorphous nanodispersion of both drugs was prepared separately with polyurethane. It was observed that at low drug loading, itraconazole release was a linear function of the square root of time suggesting Fickian kinetics with no initial drug burst, whereas ketanserin demonstrated biphasic release pattern. It was concluded that polyurethane nanofibrous mats can be used for controlled drug delivery-based wound dressing. Thakur et al. developed a poly(L-lactic acid) (PLLA)-based dual drug release electrospun scaffold containing lidocaine and mupirocin using dual spinneret electrospinning apparatus. Drug release patterns observed showed that lidocaine hydrochloride displayed an initial burst with 80% release within an hour followed by a plateau, whereas mupirocin exhibited sustained release after a 5% release in first hour. Based on the release profiles, it was concluded that dual spinneret technique is better than single spinneret technique for wound healing since the presence of two drugs in same polymer matrix alters the release kinetics of at least one drug (Kanani and Bahrami 2010). In a study, chitosan/polyethylene oxide (PEG)/green tea extract nanofibers were fabricated with controllable diameter by electrospinning technique. The developed nanofibers possessed antibacterial activity against both Gram-positive and Gram-negative bacteria and showed improved rate of healing of wounds. In another study, authors fabricated electrospun nanofibers for wound dressing based on two natural biopolymers, i.e. chitosan and sericin. The developed non-woven composite nanofibers were found to be non-toxic and biocompatible. The nanofibers demonstrated antibacterial activity against both Gram-negative and Gram-positive bacteria due to synergistic biological effects of two natural polymers (Lim 2017). Chitosan nanofibers can also be loaded with curcumin for wound healing. PCL-poly(ethylene glycol) nanofibers were loaded with 0.5% weight of curcumin. The developed nanofibers showed excellent wound healing properties (Mohammadi et al. 2018).

4.3 Drug Delivery

Nanofibers offer a promising advantage of its use as carriers for delivery of drugs and therapeutic agents as they exhibit large surface area and microporous structure which is suitable for encapsulation and direct incorporation of therapeutic agents (Lim 2017). Nowadays, many types of drugs such as antibiotics, proteins, DNA, RNA and anticancer agents can be embodied into electrospun nanofibers. Nanofiber material can be employed to control the drug release also via diffusion or diffusion and scaffold degradation. Different types of drug loading techniques such as coating, encapsulation and embedding can be utilized to give control over drug release kinetics. Nanofibers can provide controlled drug release which is more favourable these days over conventional dosage forms due to reduced toxicity, improved therapeutic effect and predesigned drug release. Nanofibrous carriers can offer site-specific drug delivery to the target tissue and also provide the advantage of encapsulation of more than one drug directly into the fibers. A number of researches have been put forward to examine the role of nanofibers produced by electrospinning technique in drug delivery and modification of release kinetics. In a study, Kenway and co-workers fabricated nanofibers of three types: polycaprolactone (PCL) as biodegradable polymer, polyurethane (PU) as a nonbiodegradable polymer and blend of both polymers. They embedded ketoprofen drug in all polymer solutions and examined the release kinetics. UV spectroscopy showed simi-

lar drug release profiles in all three types of nanofibers, although, mechanical properties were reported to be improved in blend of PCL and PU. Kenway et al. fabricated nanofibrous mats composed of PLA, poly(ethylene-co-vinyl acetate) (PEVA) and a blend of two polymers in 50:50 ratio by electrospinning technique. The developed nanofibrous mats were loaded with tetracycline hydrochloride, and drug release was examined. Drug release profiles obtained demonstrated that PEVA showed faster release compared to PLA or polymer blend. The drug release profiles were also compared with corresponding cast films which showed that electrospun mats tended to have greater release due to their large surface area. Zong et al. fabricated bioabsorbable amorphous poly(D, L-lactic acid) (PDLA) and semi-crystalline poly(L-lactic acid) (PLLA) nanofiber non-woven membranes loaded with Mefoxin. The fabricated non-woven membrane exhibited uniform structures with average diameter of 160 nm. UV spectroscopy showed that over 90% typical loading efficiency of Mefoxin is exhibited in PDLA. It was concluded that the drug functionality was not affected by the gentle electrospinning process making electrospun nanofibers safe for the delivery of therapeutic agents. Yang et al. developed gelatin/PVA bicomponent nanofibers by electrospinning process and examined the drug release of raspberry ketone (RK). Burst release of the drug was observed in the first hour, which further reached a plateau after 2 hours. The authors concluded that addition of PVA enhanced the tensile strength and elongation at break of the membrane and drug release could be modified by altering the cross-linking time by glutaraldehyde vapour, ratio of GEL and PVA in matrix. In another study, Maretschek et al. designed nanofibers by electrospinning process of emulsions comprising of an organic poly(L-lactide) solution and aqueous protein solution. Cytochrome C was encapsulated in the nanofibers and protein release was investigated. The protein release was found to be dependent on the surface tension of the release medium. It was explained that the morphology of the resulting nanofibers is affected by the addition of different amounts of hydrophilic polymer to the aqueous phase (Kanani and Bahrami 2010). In a study, nanofiber-based platform was developed for the delivery of peptides across the blood-brain barrier to stimulate the pharmacological response. The nanofibers were prepared through self-assembly of amphiphilic peptide. The active peptide epitope surrounded the nanofiber core. It was observed that peptide degradation was prevented by the nanofibrous configuration and the amphiphilic nature of the peptide facilitated the transport of peptide across the blood-brain barrier. In another study, gelatin nanofiber-based platform was used for the localized transient delivery of miRNA-based therapeutic agent (miR-29a inhibitor) for the synthesis of extracellular matrix and cell deposition. The release of the therapeutic agent observed was continuous for 72 h with enhanced synthesis of osteonectin from pre-osteoblastic cells grown on nanofibers. A transdermal patch based on biodegradable PVA-sodium alginate composite nanofiber was also successfully developed in a study for the delivery of antibiotic ciprofloxacin. In another study, coaxial electrospinning technique was utilized for fabricating biocompatible core-shell nanofibers using two water-soluble polymers: PVA and chitosan. The anticancer drug doxorubicin (DOX) was embedded into the developed nanofiber core for the treatment of ovarian cancer. Results concluded that DOX could be delivered to the target site and the release profile could be adjusted by altering the PVA-chitosan ratio in the nanofiber core. The developed nanofiber core significantly diminished the attachment and proliferation of the cancer cells supporting its use in ovarian cancer chemotherapy (Lim 2017). Verreck and co-workers developed polyurethane nanofibrous scaffolds incorporated with water-insoluble drugs: itraconazole and ketanserin. From the study it was observed that amorphous nanodispersion of the drugs on scaffolds was formed due to the fast solvent evaporation. This elucidated that the release of water-insoluble drugs from water-insoluble polymers is possible (Vasita and Katti 2006). Nanofibers have the application in gene encoding. DNA can be covalently attached to

carbon nanofiber array and inserted into the cells where DNA is expressed without affecting the cell viability (Ramakrishna et al. 2006). Luu et al. developed PLGA- and PLA-PEG-based nanofibrous scaffold for the delivery of DNA plasmid. The formulated scaffold showed controlled release of DNA at the target site causing cell transfection and bioactivity. The transfection activity was found to be greater compared to addition of naked DNA into the culture medium. The study suggested that nanofibrous scaffold are well suited for the delivery of intact DNA and release can be modified by altering the properties of nanofibers. In a study, Jia et al. formulated polystyrene nanofibers by electrospinning and loaded it with alpha-chymotrypsin. The author observed the biotransformation efficiency of the nanofibers. Results elucidated that nanofibrous enzyme system had improved hydrolytic activity compared to immobilized enzyme. Nanofibrous system showed three times more nonaqueous activity compared to immobilized enzyme in organic solvents. The overall stability of the enzyme also improved due to less structural denaturation. Thus, it was suggested that nanofibers can be utilized as catalytic systems in biotransformation. Similarly, Zeng and coworkers designed PVA nanofibers for delivery of proteins. The nanofibers were incorporated with bovine serum albumin or luciferase proteins and coated with poly(p-xylylene) (PPX). Both coated and uncoated nanofibrous scaffolds were compared for release profile and bioactivity of proteins. It was observed that PPX-coated nanofibers showed decelerated release as compared to uncoated PVA nanofibers suggesting the employment of nanofibrous scaffolds for controlled release of protein or enzymes (Vasita and Katti 2006). For cosmetic purpose, nanofibers can also be utilized in developing masks impregnated with skin-revitalizing factors that help skin renewal for the maintenance of healthy skin (Ramakrishna et al. 2006). All the studies conclude the potential of nanofibrous scaffold systems for drug delivery; therefore, efforts should be made in more advancement of nanofiber technology in this direction.

4.4 Protective Clothing

Nanofibers can be used in protective clothing due to their characteristic properties such as large surface area, high porosity, high filtration efficiency, etc.; high porous structure of electrospun nanofibers provides breathable nature to the structure along with small pore size which can help in filtration of harmful chemicals in aerosol forms. Thus, nanofibers laid down in a layered form can form efficient protective clothing for use (Karakaş 2015). Military, firefighter, etc. require protective clothing for protection against mustard gas, bacterial spores, cyanides, viruses, etc. The currently available protective suits are based on full barrier protection which is very heavy in weight and cause moisture retention. Nanofibers on the other hand are very light weighed and are sensitive to the presence of chemical or biological toxins. The warfare agents can be chemically modified by attachment of oximes, chloramines or cyclodextrins to improve the efficiency for protection. Chemical modification of functionalized fibers with paraoxon and dimethyl methylphosphonate showed decontamination. Metal nanoparticles have also been proved to be good decomposing agents for warfare agents. Nanofibers could also provide better tear strength for battlefield dresses (Ramakrishna et al. 2006).

4.5 Environmental Protection

Environmental protection is important for ensuring the safe future. New solutions have been continuously explored for water treatment, air purification, waste treatment, etc. (Fig. 10.5). Nanofiber technology can be employed for such purposes as they mainly involve the usage of membranes. Nanofibers when used in filtration membranes provide higher efficiency compared to conventional fibers. Large surface area and porous structure of nanofibers ensure better adsorption of contaminants. Companies like DuPont, AMSOIL and Donaldson have developed nanofibers for filtration purpose (Karakaş 2015). In biotechnology, biomacromolecules, ligands or cells can be impregnated into nanofi-

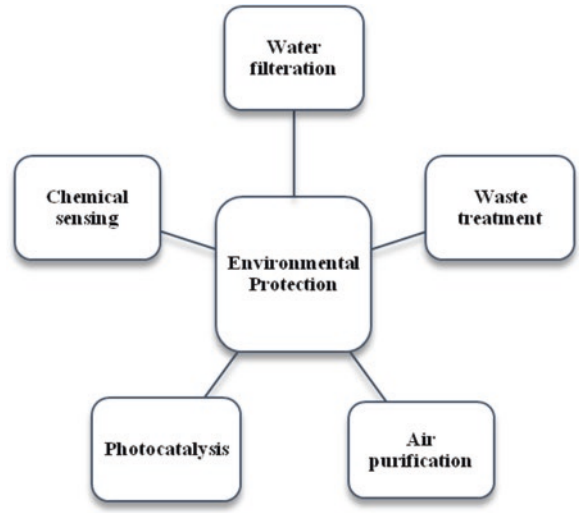

Fig. 10.5 Applications of nanofibers in environmental protection

ber membranes for water or protein purification, enzymatic catalysis or biosensing. Ligands should be bonded covalently to prevent the leaching of ligands during filtration. Studies suggest that nanofibers in the diameter range of 1 μm to 5 μm show high efficiency in filtration of airborne particles. Moreover, the membrane could be cleaned for the recovery after usage for filtration. Nanofiber membranes based on cellulose were functionalized with Cibacron blue for purifying albumin protein. Ceramic nanomaterials like iron oxides and hydrated alumina/alumina hydroxide could be functionalized in polymer nanofibers for designing affinity membranes for water purification (Ramakrishna et al. 2006). Nanofibrous membranes can be designed to specifically adsorb metal ions that have high toxicity and accumulative nature in living organisms. This makes them more suitable for drinking water treatment than conventional membrane. Many manufacturing industries release fine particles into the atmosphere leading to air pollution. This is the cause for many respiratory and cardiovascular diseases. Although, electrospun nanofibers are extremely long fibers making them difficult to enter the body through inhalation. Polyacrylonitrile (PAN) composite membrane has been developed for filtration purpose. The developed nanofiber filters possess high filtration rate and pressure drop. The filtration efficiency can also be enhanced by mixing nanofibers into fibrous filter media. Many authors have evaluated the application of nanofibers in the adsorption of volatile organic compounds from the air (Barhoum et al.). Poly(methyl methacrylate) (PMMA) nanofiber membrane has been introduced with β-cyclodextrin which is a cyclic oligosaccharide having affinity towards hydrophobic organic molecules. The developed membrane could be used for removal of organic waste from water that inhibits the life to sustain in it (Ramakrishna et al. 2006). Research has been made recently to explore the role of nanofibers in oil/water separation also. In a study, Li et al. developed pH-sensitive nanofiber membrane using PMMA-b-P4VP and underwater oleophilic/hydrophilic PMMA. The developed membrane allowed passage of oil selectively, whereas water remained at the initial state. On treating the membrane with acidic water before separation, the process of separation reversed allowing water to pass through it and oil remaining at initial state. Authors concluded that both separation processes were highly efficient and the developed membrane showed numerous cycles of switchable wettability. Nanofibers can also be incorporated with TiO2, silver or quaternary ammonium salt containing cationic polymers to exhibit antimicrobial activity. In a study, polyvinyl alcohol nanofibers were electrospun by using benzyltriethylammonium chloride as the antimicrobial agent. The developed nanofiber membrane

showed efficient removal of *E. coli* and *S. aureus* under dynamic flow conditions (Barhoum et al.). The cellulose nanofibers were formulated and coated with MnO2 for the purpose of methylene blue removal. The developed hybrid nanofibers showed excellent adsorption efficiency and oxidation in methylene blue decolourization. In another study, aerogel based on quaternary NH3-functionalized cellulose nanofibers was prepared and evaluated for heavy metal adsorbent activity. Study showed that the nanofiber-based aerogel efficiently removed the metallic ion Cr (VI) during water treatment (Lim 2017). In another study, polyvinyl alcohol nanofibers and polyvinyl alcohol benzene tetracarboxylate nanofibers were fabricated and incorporated with strontium, lanthanum and antimony. The developed nanofibers were evaluated for lead adsorption activity in water systems. Results elucidated that the so-formed nanofibers showed monolayer sorption of lead in a rapid and spontaneous manner (Shooto et al. 2016). Fe nanoparticle-loaded polyaniline (PANI) composite nanofibers rapidly removed organic and inorganic contaminants from water such as arsenic, chromium and Congo red dye. Polybenzimidazole (PBI) nanofibers can be used for the removal of oxidized organosulphur compounds due to the selectivity of PBI nanofibers towards sulphone-containing compounds. The composite polymeric nanofibers have also been synthesized composed of poly(ethylene terephthalate) (PET) and PVA polymer-based hydrophobic/hydrophilic interpenetrating network composite nanofiber (HH-IPN-CNF) by electrospinning technique for the purpose of support layer in forward osmosis membrane. The resultant support layer significantly improved the forward osmosis membrane flux. Apart from this, photocatalysis gained interest after Fujishima and Honda presented a report on photoelectron chemical splitting of water. Nanofibers have been investigated for their use in hydrogen generation and degradation of toxic chemicals and pollutants that are hazardous to the environment. Titanium dioxide has been considered as an efficient photocatalyst due to its low toxicity, high photochemical stability and photocatalytic activity. Various nanofibers based on TiO2 have been designed in the past few years. In a study, silver nanoparticle-based TiO2 nanofibers were formulated for the purpose of photocatalytic degradation of rhodamine B and phenol. Similarly, SnO2/TiO2 nanofibers were formulated for degradation of rhodamine B under UV-visible light. In another study, TiO2/SiO2 nanofibers were formulated and coated with PANI for the photocatalytic degradation under visible light of methyl orange (Lim 2017). Singh et al. developed highly mesoporous zinc oxide nanofibers which showed enhanced interaction with polycyclic hydrocarbons (aromatic) such as anthracene and naphthalene and thus had higher UV light photodegradation rate. Bedfort and co-workers developed photocatalytic textile fibers with self-cleaning property by using cellulose acetate nanofiber as core and TiO2 as shell fiber. The developed nanofibers were able to degrade the dyes like key acid blue and sulphorhodamine at moderate exposure to light. Peining et al. developed TiO2 nanofibers and incorporated graphene in it. The photocatalytic activity of the developed nanofibers was compared with TiO2 nanofibers and mechanically mixed graphene and TiO2 nanofibers. It was observed that graphene-loaded nanofibers showed better photodegradation of methyl orange. Li et al. doped nitrogen into TiO2 nanofibers and evaluated the photodegradation of rhodamine B dye that was found to be 12 times more than the pure TiO2 nanofibers (Sundaramurthy et al. 2014). Nanofibers can also be employed in chemical gas sensing for the detection of quality of air and presence of toxic gases. Semiconductor oxide like MoO3, TiO2 or SnO2 can be functionalized in nanofibers as they show electrical resistance. This resistance is sensitive to chemical gases such as ammonia or nitroxide and, thus, can be useful in toxic gas sensing. Nanofibers are highly sensitive and stable for chemical gas detection as a result of their extremely porous structure and high surface area that improve the mass transport and diffusion of gases (Ramakrishna et al. 2006). Nanofibers can be altered for improving the efficiency of gas sensing by improving the surface area or incorporation of metal ions. Nanofibers based on p-type Cr2O3 and Co3O4 oxide semiconductor were

developed for the sensing of ethanol. Porous hollow SnO2 nanofibers were designed for fast sensing of ethanol. Similarly, GaN nanofibers were formulated for the sensing of ethanol with high sensitivity and fast response time. Au-doped SnO2 nanofibers were developed through sol-gel-based electrospinning for sensing CO. Polymeric chitosan/PANI nanofibers were developed for the sensing of chemicals like alcohols and amines (Lim 2017).

4.6 Biological Sensing

Due to the presence of immobilization sites in nanofibers, they can be used for biosensing of biomolecules. Large surface area of nanofibers provides higher efficiency in detecting the active species. Nanofibers also possess electrocatalytic properties which further assists in biosensing (Lim 2017). Nanofiber-based biosensors provide high sensitivity and specificity. In a study, polypyrrole nanofibers were impregnated with avidin protein for biosensing the biotin-labelled biomolecules like DNA. Poly(acrylic acid)-poly(pyrene methanol) was employed for biosensing the organic and inorganic impurities. The detection of metal ion impurities on nanofiber surface was marked by quenching of fluorescence (Ramakrishna et al. 2006). TiO2 nanofiber mat was used as biosensing platform for the detection of esterified cholesterol. Cholesterol esterase and cholesterol oxidase were immobilized covalently to the TiO2 nanofiber mat-based biosensor. The results demonstrated higher efficiency of biosensing the cholesterol due to the high sensitivity of nanofibers and enhanced charge transfer. In another study, polycarbonate-polycaprolactone nanofiber core-shell was developed for designing oxygen sensor. The sensor was embedded with oxygen-sensitive luminescence probe. The resulting sensor was used for the investigation of tumour hypoxia. The authors concluded that the biosensor was efficient in locating the hypoxic areas present around aggregates of glioblastoma cell (Lim 2017). Cu2O nanoparticle-doped hollow carbon nanofibers were fabricated for their use in biological sensing of glucose. The developed electrochemical biosensor showed promising results of detection limit down to 0.48 mM for glucose (Li et al. 2018).

4.7 Energy Storage

In order to meet the current concern about fossil fuel depletion and nature deterioration, researches have been carried out to invent new strategies for energy Conversion and development of storage devices. The highly porous structure and large surface area of nanofibers have developed interest for their use in energy production applications. Nanofibers can be utilized in designing energy storage devices, fuel cells, solar cells and hydrogen production (Fig. 10.6). Graphite nanofibers can be used for hydrogen storage as the small pores allow aggregation of hydrogen molecules between graphite layers leading to improved storage capacity. Nanofibers can also be used in fabrication of free-standing electrodes as they result in better storage of energy compared to conventional electrodes which contain inert materials, carbon black and binder. In a study, Iqbal and co-workers developed composite membranes with Fe3O4-doped carbon nanofibers uniformly anchored with MnO2 particles. The developed membranes were used as flexible electrodes in high-performance supercapacitor. The resulting electrodes showed improved efficiency of harvesting solar energy (Barhoum

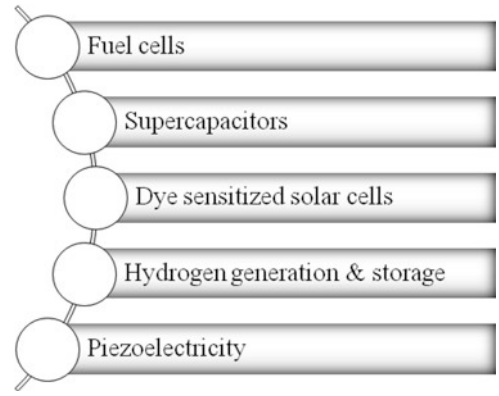

Fig. 10.6 Applications of nanofibers in energy storage and protection

et al.). In another study, cellulose nanofibers were integrated with carbon nanotubes to fabricate the non-woven highly porous macrofiber mat for supercapacitor. The fabricated supercapacitor showed excellent stability and electrochemical properties. The macrofiber mat was investigated for damage reliability, and it was observed that even after various degrees of damage, the mats were damage reliable (Lim 2017). In a study, carbon nanofibers were functionalized with deposition of silver, platinum and palladium to fabricate electrodes in order to increase the electrical conductivity in supercapacitors. It was reported that the cyclic voltammetry performance significantly increased. Improved rate capability and excellent life cycle were reported (Li et al. 2019). Electrospun nanofibers can be used as an alternative to Pt catalyst in fuel cells (Karakaş 2015). A microbial fuel cell anode was developed from nanocomposite based on nanofiber for the generation of bioenergy utilizing microbial catalyst. In another study, Liu et al. produced carbon fuel cell anode based on hollow nanofibers of Ce0.6Mn0.3Fe0.1O2. As the contact area is increased between fuels and anode by using nanofibers, the catalytic activity gets increased for oxidation of carbon monoxide (Barhoum et al.). Ji et al. developed a porous PAN/SiO2 nanofiber composite to be employed as anode material in lithium ion battery without the addition of non-active carbon black or binder. The resulting anode had magnified area compared to conventional battery. Similarly, Qie et al. used polypyrrole to synthesize porous nanofiber composite for lithium ion batteries. Zheng et al. prepared polystyrene CNF composite utilizing aluminium oxide templates. The authors achieved 730 mAh/g reversible capacity after 150 cycles. It was concluded that the developed structure overcame the problem of random diffusion of polysulphides. Lithium ions' fast transport was reported (Feng et al. 2014). Kim et al. and Choi et al. used poly(vinylidene fluoride) (PVDF) to fabricate nanofiber membrane for lithium battery. The nanofiber membrane displayed high uptake of lithium electrolyte. Therefore, more quantity of electrolyte can be held in thinner batteries. Moreover, energy density/weight also increases compared to conventional batteries (Ramakrishna et al. 2006). Nanofibrous structures can also be made from different piezoelectric materials for mechanical energy harvesting as they have higher capability of energy scavenging (Karakaş 2015). Piezoelectric devices use mechanical forces by scavenging to generate power and convert it into electrical energy. In a study, it was reported that PVDF nanofiber webs were developed and integrated into energy-harvesting device utilizing mechanical to electrical conversions. The developed needleless electrospun nanofiber webs showed excellent energy conversion compared to nanofibers produced by needle-based electrospinning. In another study, PVDF-TrFE nanofibers were fabricated which showed excellent piezoelectric property (Lim 2017). Nanofibers have been produced for dye-sensitized solar cells as the photoelectrode material as they exhibit excellent charge transport properties. Barakat and co-workers fabricated Pd-Co-doped carbon nanofibers as an electrode material in dye-sensitized solar cells. The resulting solar cell showed improved iodine reduction on the surface of electrode and overall good performance. He and co-workers fabricated two types of TiO2 nanotubes for dye-sensitized solar cell photoanode. The resulting electrode showed high short-circuit current density and good device efficiency (Sundaramurthy et al. 2014). In a study, TiO2 nanofibers were fabricated and blended with ZnO nanoparticles to develop photoanode films for dye-sensitized solar cells. The resulting composite photoanode films demonstrated improved light scattering and diminished recombination of electron. This resulted in improved efficiency in energy conversion. Similarly, CNT/TiO2 composite nanofibers were developed as the anode material in dye-sensitized solar cell. The composite nanofibers resulted in enhanced power conversion. In solar energy-harvesting techniques, solution-based organic photovoltaics have also been recognized. In a separate study, bilayer of alkoxy naphthalene-based polymer nanofiber/fullerene was constructed as the organic photovoltaic resulting in excellent photocurrent density (Lim 2017). Hydrogen is also being used in sustainable energy generation due

to its zero emission of CO2 and high energy. Recently, investigations are done to evaluate the use of nanostructured hydrogen storage material for energy storage. Nanofibers can decrease the diffusion path for hydrogen and reduce the reactive interface thickness. Carbon-coated Li3N nanofibers were produced for hydrogen storage which showed improved diffusion of hydrogen for reaction due to the presence of micro-, meso- and macropores on the porous carbon walls of nanofibers. In 1972, Honda and Fujishima demonstrated a method utilizing TiO2 as the electrode for the production of hydrogen by photocatalytic water splitting. Continuous efforts have been made since then to investigate the fabrication of nanostructured electrodes for hydrogen generation (Sundaramurthy et al. 2014). Nanofibers can be employed for hydrogen generation to further improve the energy conversion efficiency. Core-shell TiO2/CdSe nanofiber film was produced for the purpose of hydrogen generation photoelectrochemically. The so formed nanofiber film provided more active sites for oxidation and thus improved the efficiency of separation of photo-generated charges. Similarly, SrTiO3 nanofibers produced by electrospinning displayed improved photocatalytic hydrogen generation under UV light (Lim 2017).

5 Toxicity

Nanofibers continue to be used in numerous fields from tissue engineering to energy production. The biomimetic property of nanofibers makes them ideal for tissue engineering. Their ultra-fine structure and mechanical strength open up the channels for application in batteries, water purification systems, supercapacitors, etc. Nanofibers make their way into textile industry to produce protective clothing and warfare. Despite all these benefits, nanofibers are still lesser evaluated for their toxicity in clinical use. Data for clinical use of nanofibers is limited to ensure the safety. Nanofibers are morphologically similar to pathogenic fibers, e.g. asbestos. The potential risk of nanofiber usage in clinical set-up may cause potential health problems. The structural-activity relationship of nanofibers elucidate the promotion of fiber-type pathogenicity. Titanium dioxide nanofibers are one of the most commonly employed nanofibers. On in vivo application, TiO2 nanofibers show inflammation and certain degree of cytotoxicity. TiO2 nanofibers are mostly used in solar cells, catalysts, etc. In a study, TiO2 nanofiber cytotoxicity was evaluated, and it was observed that TiO2 nanofibers showed increased cytotoxicity, epithelial barrier perturbation and haemolysis. The effect of TiO2 nanofiber was found to be worrying for its use in tissue engineering (Allegri et al. 2016). It is important to carefully address the possible toxicity related to nanofibers, while the investigations are carried out on their roles in different purposes.

6 Patents

Considering the applications of nanofibers, various attempts have been taken to investigate and make new inventions for purposes in tissue engineering, filtration, biosensing, fabric development, etc. Some of the recent patent applications are described in the Table 10.2.

On the basis of PATENTSCOPE database of the international Patent Cooperation Treaty (PCT) applications, the number of patent applications related to nanofibers has been observed to rapidly increase in the past few years. The pattern of growth can be attributed to the safe use of nanofiber in various fields contributing to revolutionized interest of the researchers. The number of patent applications from year 1997 to 2019 has been demonstrated in Fig. 10.7.

7 Future Perspective and Expectations

In this chapter varied applications of nanofibers due to their exceptional physical, chemical and biological properties were discussed in detail. This chapter highlights the basic introduction, method of production, applications, toxicity and patents on nanofibers. For the production of nanofibers, electrospinning is the most widely

Table 10.2 Recent patent applications based on nanofiber

Patent publication no.	Inventors	Title	Description
US20190352819	Marcio D. Lima et al.	Nanofiber fabric	Fabric composed of nanofibers with adhesives in limited area is disclosed. The developed fabric preserves the important characteristics of nanofibers (Lima et al., 2019).
US20190352822	Marcio D. Lima et al.	Tear-resistant nanofiber sheet	The present invention discusses about the placement of nanofiber yarns in contact with nanofiber sheets to provide extra mechanical strength to the resulting nanofiber sheet. Infiltrating material can also be added into the interstitial spaces to further form a continuous network (Lima et al., 2019).
US20190348680	Hiroki Yamashita et al.	Positive-electrode active material for secondary cell and method for manufacturing same	Manufacturing method for positive electrode active material based on cellulose nanofiber is disclosed. Such electrode exhibits improved charge/discharge properties in lithium or sodium ion secondary cell (Yamashita et al. 2019).
WO2019217767	Martin et al.	Nanofiber-hydrogel composites for enhanced soft tissue replacement and regeneration	Method for preparing gel disposed with nanofibers for developing a composite material for the purpose of soft tissue engineering is discussed (Martin et al. 2019).
US20190327966	Wael Mamdouh et al.	Polyvinyl alcohol-chitosan composite-soluble electrospun nanofibers for disinfectant antibacterial and anti-corrosion applications	Composite nanofiber can be fabricated using the composition disclosed in the patent. Composition comprises of natural chitosan, polyvinyl alcohol, ascorbic acid and citric acid to provide antibacterial, disinfectant or anti-corrosion properties (Ahmed et al. 2019).
US20190323979	David J. Cammenga et al.	Nanofiber smoke detection calibration	Patent discloses a detector including nanofiber chemical sensor for the sensing of airborne material indicated by changes in electrical characteristics (Cammenga et al. 2019).
EP3554572	Byron Mary M et al.	Infection-fighting drug-eluting device	The patent discloses an implantable medical device for eluting drug. The medical device is composed of polymer substrate, nanofibers and antimicrobial drug for fighting against infection (Byron et al. 2019).
US20190314152	Magdi Yacoub et al.	Expandable aortic or pulmonary root	Method of preparation of synthetic root and a support layer based on nanofiber is disclosed. This invention can be beneficial in tissue engineering of aortic or pulmonary root (Yacoub and Heart Biotech Nano Ltd 2019).
WO2019199630	Costella et al.	Nanofiber-reinforced hydrogel medical dressings	In the present invention, medical dressings are designed from electrospun nanofiber non-woven mats embedded in chitosan hydrogel matrix. The developed dressings are transparent, flexible and mechanically stronger. The dressings discussed are claimed to be more suited for ocular wounds (Costella et al. 2019).
US20190309197	Jae-Uk Chu et al.	Thermal adhesive containing tetrapod zinc oxide and alumina nanofiber	Present invention discusses epoxy resin, zinc oxide and alumina nanofiber-based thermal adhesive. This adhesive can exhibit significantly high heat conductivity. The resin may include a catalyst and curing agent (Chu et al. 2019).

(continued)

Table 10.2 (continued)

Patent publication no.	Inventors	Title	Description
US20190310223	Tamara Floyd Smith et al.	Carbon nanofiber sensor for non-enzymatic glucose detection and methods of glucose detection using such carbon nanofiber sensor	Method for development of glucose detection sensor based on nanofiber without the usage of enzymes is discussed. The present invention also discloses the method of detection of glucose by the discussed nanofiber sensor (Smith et al. 2019).
US20190305290	Arvinder Singh et al.	Free-standing, binder-free metal monoxide/suboxide nanofiber as cathodes or anodes for batteries	The invention discusses method for producing nanofiber mat-based anodes, cathodes and batteries (Singh and Kalra 2019).
US20190299133	Jens Neumann et al.	Filter medium, method for producing same and use of the filter medium in a filter element	The present invention discloses method of production of filter medium comprising of substrate layer, nanofiber layer and an adhesive layer (Neumann et al. 2019).
US20190291057	Ui Young Jeong et al.	Filter assembly, method for manufacturing same and filter module comprising same	The disclosed filter assembly comprising of nanofiber layer, hydrophilic coating and support layer is proposed to exhibit good chemical resistance and water permeability (Jeong et al. 2019).
CN209188190	Zhang Kaiqiang et al.	Intelligent oil-water separator	Nanofiber-based oil-water separator is designed. The separator can intelligently separate oil and water based on centrifugal force as oil is lighter than water (Zhang et al. 2019).

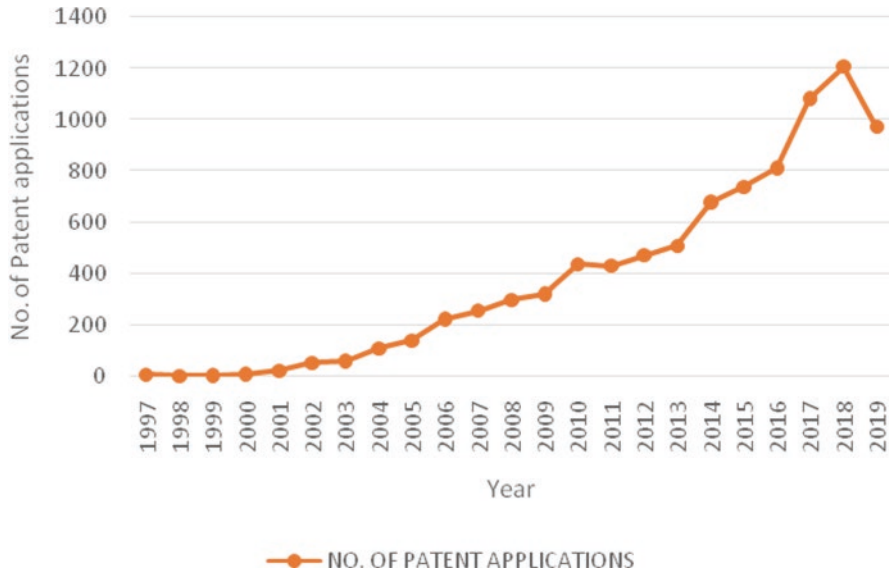

Fig. 10.7 Number of patent application from 1997 to 2019 as per PATENTSCOPE database

employed technique (Almetwally et al. 2017). The flexibility in modifying surface functionalities of nanofibers attract interest of both industrialists and academicians for diverse applications in tissue engineering, energy generation, drug delivery, biosensing, ultrafiltration, textile, etc. It also attracts the researchers to meet the recent challenges of nanofibers in toxicity and commercial production of high-quality, rigorous clinical studies (Barhoum

et al.). In tissue engineering, the main challenge is to improve the clinical application. Sufficient studies of nanofibers to support the efficacy and eliminate the toxicity in clinical set-up are necessary (Lim 2017). The methods of production other than electrospinning such as self-assembly and phase separation are not suitable for large-scale production. Thus, advancement in different production methods on commercial scale is required. The application of mathematical models for characterization and behaviour studies of nanofibers can improve the current trend of nanofiber handling. The drug delivery by nanofibers can be further improved to predict and control the release profiles of therapeutic agents (Dahlin et al. 2011). The urgent need of water treatment and environmental protection can be met by the use of nanofibers. In future, researches can be made for incorporating other nanostructures into the structure of nanofibers to impart additional roles in ultrafiltration and sensing (Lim 2017). In future development of nanofibers for humidity or temperature sensing is expected. The present materials should be improved in performance by altering structural orientations without compromising with the mechanical properties (Feng et al. 2014). Fiber formation by electrospinning is now based not only on natural or synthetic polymers but also on metals, ceramics and organic/inorganic composite system (Karakaş 2015). In recent years, there is a demand of wearable, lightweight electronics. Nanofibers have been employed in energy storage devices and generation but now additional efforts are required to meet the recent demands. This will need more robust methods of nanofiber production that can produce nanofibers with tolerance to mechanical deformations. It is important to bridge the gap between academia and industry. Most of the researches are confined to academia. It is important to translate the recent advancements to the industry as well so that nanofibers can be utilized in improving our day-to-day life (Lim 2017).

References

Ahmed WMSS, Kegere J, American University in Cairo (2019) Polyvinyl alcohol/chitosan composite soluble electrospun nanofibers for disinfectant antibacterial and anti-corrosion applications. U.S. Patent Application 16/349,393.

Allegri M, Bianchi MG, Chiu M, Varet J, Costa AL, Ortelli S, Blosi M, Bussolati O, Poland CA, Bergamaschi E. Shape-related toxicity of titanium dioxide nanofibres. PLoS One. 2016;11(3):e0151365.

Almetwally AA, El-Sakhawy M, Elshakankery MH, Kasem MH. Technology of nano-fibers: production techniques and properties-critical review. J Text Assoc. 2017;78:5–14.

Barhoum, A., Rasouli, R., Zadeh, M.Y. and Bechelany, M., 2017. Nanofibers technology: history and developments.

Byron MM, Wulfman DR, Fruci A, Mcgraw A, Frankson D, Sherwood GJ, Delaney JT, Aremu AO, Cardiac Pacemakers Inc. Infection fighting drug eluting device: E.P. Patent Application 17830060; 2019.

Cammenga DJ, Geerlings KL, Nemes JC, Tonar WL, Christian DE, Tuttle DD, Niu X, Gentex Corp. Nanofiber smoke detection calibration: U.S. Patent Application 16/387,593; 2019.

Chu JU, Chang-Kook JANG, Song SJ, Seung-Won SONG, Youngyiel Precision Co Ltd. Thermal adhesive containing tetrapod zinc oxide and alumina nanofiber: U.S. Patent Application 16/373,280; 2019.

Costella LA, Tison CK, Patterson M, Broderick K, Woodard L, Gasbarre M, Luna Innovations Incorporated. Nanofiber-reinforced hydrogel medical dressings: U.S. Patent Application 2019/026,254; 2019.

Dahlin RL, Kasper FK, Mikos AG. Polymeric nanofibers in tissue engineering. Tissue Eng Part B Rev. 2011;17(5):349–64.

Feng L, Xie N, Zhong J. Carbon nanofibers and their composites: a review of synthesizing, properties and applications. Materials. 2014;7(5):3919–45.

Jeong UY, Seo IY, Amogreentech Co Ltd. Filter assembly, method for manufacturing same, and filter module comprising same: U.S. Patent Application 16/305,954; 2019.

Kanani AG, Bahrami SH. Review on electrospun nanofibers scaffold and biomedical applications. Trends Biomater Artif Organs. 2010;24(2):93–115.

Karakaş H. Electrospinning of nanofibers and there applications: Istanbul Technical University, Textile Technologies and Design Faculty; 2015.

Li Y, Cai R, Lü R, Gao L, Qin S. Template synthesis of the Cu2O nanoparticle-doped hollow carbon nanofibres and their application as non-enzymatic glucose biosensors. R Soc Open Sci. 2018;5(12):181474.

Li Z, Qi S, Liang Y, Zhang Z, Li X, Dong H. Plasma surface functionalization of carbon nanofibres with silver, palladium and platinum nanoparticles for cost-effective and high-performance supercapacitors. Micromachines. 2019;10(1):2.

Lim CT. Nanofiber technology: current status and emerging developments. Prog Polym Sci. 2017;70:1–17.

Lima MD, Lintec of America Inc. Nanofiber fabric: U.S. Patent Application 16/364,933; 2019a.

Lima MD, Lintec of America Inc. Tear resistant nanofiber sheet: U.S. Patent Application 16/364,955; 2019b.

Martin R, Reddy S, Colbert K, Mao H, Johns Hopkins University. Nanofiber-hydrogel composites for enhanced soft tissue replacement and regeneration: U.S. Patent Application 2019/031,638; 2019.

Mohammadi MA, Rostami M, Beikzadeh S, Raeisi M, Tabibiazar M, Yousefi M. Electrospun nanofibers as advanced antibacterial platforms: a review of recent studies. Int J Pharm Sci Res. 2018;10(2):463–73.

Moutsatsou P, Coopman K, Georgiadou S. Biocompatibility assessment of conducting PANI/Chitosan nanofibers for wound healing applications. Polymers. 2017;9(12):687.

Neumann J, Brosi H, Mann+ Hummel GmbH. Filter medium, method for producing same, and use of the filter medium in a filter element: U.S. Patent Application 16/442,480; 2019.

Radacsi N, Campos FD, Chisholm CR, Giapis KP. Spontaneous formation of nanoparticles on electrospun nanofibres. Nat Commun. 2018;9(1):4740.

Ramakrishna S, Fujihara K, Teo WE, Yong T, Ma Z, Ramaseshan R. Electrospun nanofibers: solving global issues. Mater Today. 2006;9(3):40–50.

Ramalingam M, Ramakrishna S. Nanofiber composites for biomedical applications: Woodhead Publishing; 2017.

Shooto ND, Dikio CW, Wankasi D, Sikhwivhilu LM, Mtunzi FM, Dikio ED. Novel PVA/MOF nanofibres: fabrication, evaluation and adsorption of lead ions from aqueous solution. Nanoscale Res Lett. 2016;11(1):414.

Singh A, Kalra V. Free-standing, binder-free metal monoxide/suboxide nanofiber as cathodes or anodes for batteries: U.S. Patent Application 16/372,067; 2019.

Smith TF, Tigner J, Koehne J, Tuskegee University. Carbon nanofiber sensor for non-enzymatic glucose detection and methods of glucose detection using such carbon nanofiber sensor: U.S. Patent Application 16/364,694; 2019.

Sundaramurthy J, Li N, Kumar PS, Ramakrishna S. Perspective of electrospun nanofibers in energy and environment. Biofuel Res J. 2014;1(2):44–54.

Vasita R, Katti DS. Nanofibers and their applications in tissue engineering. Int J Nanomed. 2006;1(1):15.

Yacoub M, Heart Biotech Nano Ltd. Expandable aortic or pulmonary root: U.S. Patent Application 16/383,366; 2019.

Yamashita H, Hatsumori T, Ogami T, Taiheiyo Cement Corp. Positive-electrode active material for secondary cell, and method for manufacturing same: U.S. Patent Application 16/515,489; 2019.

Yang F, Murugan R, Wang S, Ramakrishna S. Electrospinning of nano/micro scale poly (L-lactic acid) aligned fibers and their potential in neural tissue engineering. Biomaterials. 2005;26(15):2603–10.

Zhang K, Liu Z, Chen P, Jia J, Henan Shuozhijia Environmental Protection Technology Co Ltd. Intelligent oil-water separator.C.N: Patent Application 201821462245.6; 2019.

Part III

Lipid Nanoparticles

High-Pressure Homogenization Techniques for Nanoparticles

11

Preksha Vinchhi, Jayvadan K. Patel, and Mayur M. Patel

Abstract

High-pressure homogenization (HPH) has been employed for unit operations like comminution, mixing, and stabilization of pharmaceutical solids and nanoparticles. With advancing nanotechnology, the HPH technique has undergone discernible evolution and has broadened the scope of its pharmaceutical applications by facilitating particle engineering. An in-depth understanding of fluid dynamics has helped the researchers devise innovative designs for high-pressure homogenizers with higher processing capacity and efficiency. The present chapter provides useful insights on the fundamentals involved in the process of HPH of colloidal dispersions, basic instrumentation of homogenizers, and theories on forces involved in homogenization. HPH has the distinct advantage of being one of the most versatile and scalable processing methods for the preparation of different vesicular and non-vesicular lipid-based nanosystems such as nanoemulsions, solid lipid nanoparticles (SLNs), nanostructured lipid carriers (NLCs), nanocrystals, as well as polymeric nanoparticles. The chapter has summarized the effect of various processing and product variables on characteristics of the aforementioned nanoparticle formulations. The chapter provides a comprehensive overview of the processing attributes of HPH that may facilitate the development of nanoparticles to attain desirable pharmaceutical attributes.

Keywords

Nanoparticles · Particle engineering · Homogenization pressure · Homogenization cycles · Fragmentation and disruption

1 Introduction

The concept of homogeneity and heterogeneity is derived on the basis of uniformity in a substance or a system, wherein the homogeneity signifies uniformity in a character or composition, while heterogeneity designates nonuniformity. The applicability of these notions is possible at a diverse level of intricacy from atoms or molecules to galaxies. The term "homogenization" denotes "to render uniformity throughout in terms of structure, composition, and character." Homogenizing is an umbrella word depicting multiple unit operations like mixing, blending,

P. Vinchhi · M. M. Patel (✉)
Department of Pharmaceutics, Institute of Pharmacy, Nirma University, Ahmedabad, Gujarat, India

J. K. Patel
Nootan Pharmacy College, Sankalchand Patel University, Visnagar, Gujarat, India

J. K. Patel, Y. V. Pathak (eds.), *Emerging Technologies for Nanoparticle Manufacturing*,
https://doi.org/10.1007/978-3-030-50703-9_11

dispersing, disrupting, emulsifying, stirring, etc. (Dhankhar 2014). In 1899, Auguste Gaulin discovered and patented the process of homogenization of milk and pioneered the pressure homogenization method (Gaulin 1904). Gaulin's equipment was portrayed in 1900 at Paris world's fair having a three-piston thruster and filtration tubes working at pressures up to 30 MPa. Conventional homogenizers or standard homogenizers protracted about 50 MPa pressure range since then. Nowadays to enhance the proficiency and outcome of the process, high-pressure homogenizers operating at pressure as high as 100–500 MPa are developed.

HPH technique is exceedingly utilized in the sector of food and beverage preparation, pharmaceutical, chemical, cosmetics, and personal care industries. The major utilization of the HPH technique in the pharmaceutical arena is for numerous purposes like particle size reduction, preparation of highly stable emulsions or suspensions, mixing, increasing product stability and consistency, micronization, nanonization, etc. The process often ensues smaller and monodisperse particles that provide stability to the dispersions and increases its shelf-life. The HPH technique ensures drastic size reduction owing to the action of very high sheer, acceleration, pressure, turbulence, and impact forces on the subjected particles. The technique comes under top-down approach in which the particles subjected for size reduction are dispersed in nonsolvent media and passed through HPH. With the advent of nano-formulations in the pharmaceutical sector, the employment of the HPH technique for producing nanoparticles has increased. Nowadays, nanoparticle research has become a great interest to the scientific community because of well-known benefits in drug delivery approaches like controlled and targeted drug release, increased drug bioavailability, increased drug effectiveness, and stability. HPH technique allows the formulation of uniform and consistent nano-sized particles more efficiently owing to the combined effect of high pressure and mechanical forces (Yadav and Kale 2019). A detailed understanding of the effect of HPH processing parameters on nanoparticles size, stability, polydispersity index (PDI), and the surface charge will provide a benefit in formulating nanoparticles with desired characteristics. The chapter mainly focuses on the fundamentals of homogenization technique including its instrumentation, working principle, theories of homogenization, its application in various lipid-based nanoparticles, nanocrystals and polymeric nanoparticles, process analytical technique for HPH, scale-up aspect, and future perspectives.

2 Fundamentals of High-Pressure Homogenization

HPH is a process in which the fluid, i.e., the product to be homogenized (premix), is subjected under high pressure through homogenizing nozzle comprising a very narrow gap. The premix fed in the high-pressure homogenizer can be a suspension, emulsion or dispersion subjected for size reduction, droplet breakup, and homogenization. HPH technique provides enormous energy for breaking down particles efficiently to nanoscale. The commonly used units for pressure indication include bar, psi, and MPa. The instruments, operating pressure ranges from 50 to 500 MPa in which the instrument working at 200 MPa or above that, are termed as ultrahigh-pressure homogenizer (UHPH) (Dumay et al. 2013). Preliminarily, the premix under high pressure passes through a narrow gap or the homogenization valve from the inlet chamber to the outlet chamber of the homogenizer. A schematic representation of the HPH process is given in Fig. 11.1. According to Bernoulli's principle, the increase in velocity proportionally decreases the pressure; thus in the gap, the pressure decreases tremendously due to very high velocity. Moreover, the pressure applied through the pump should be such that the Laplace pressure imparting resistance against droplet deformation or breakup can be surmounted. The Laplace pressure increases to a certain level with the decrease in droplet diameter; thus the smaller the particle size, the higher is the pressure required for its breakup (Digby 2002; Yong et al. 2017).

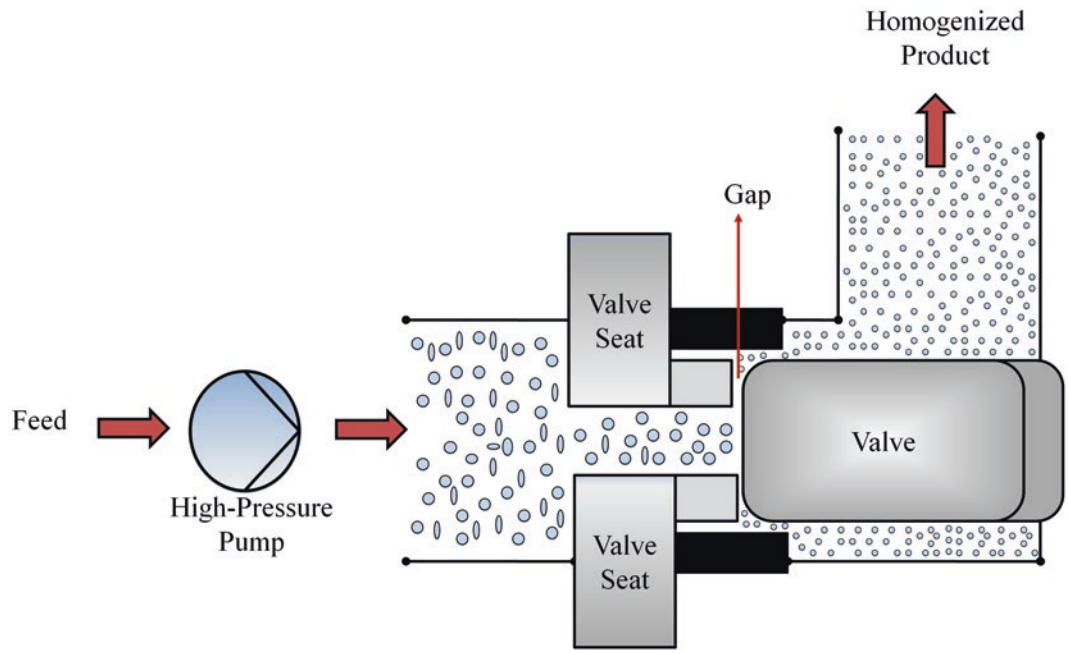

Fig. 11.1 Schematic representation of HPH technique

3 Instrumentation of High-Pressure Homogenizer

The high-pressure homogenizer instrument encompasses two main components responsible for homogenization and size reduction: (a) high-pressure pump and (b) homogenizing valve. The equipment used for pharmaceutical and food industries is usually fabricated using stainless steel of high-quality grade. The use of corrosion-resistant and wear-resistant material is a major concern for complying with the safety guidelines by the regulatory agencies. The modern homogenizing valves are usually constructed using tungsten carbide, nierite, and zirconium oxide for the purpose of inculcating corrosion-resistant characteristics and producing mechanically efficient valves that can withstand intense hydrodynamic forces. Modified equipments with soundproof or anti-vibration casing and facilities like steam in place (SIP) and clean in place (CIP) are also provided in certain new models (Yadav and Kale 2019).

There are basically two main categories of high-pressure homogenizers bifurcated on the basis of the geometry of the disruption unit and the flow pattern of the fluid: (1) piston gap homogenizer and (2) jet stream homogenizer. A piston gap homogenizer cannot achieve very high pressure ranges as that of Microfluidizer (jet stream homogenizer). The difference between both the assemblies is the valve design that is discussed further in Sects. 3.2.1 and 3.2.2. The main components of the homogenizer assembly affecting the homogenization process are high-pressure pump, valve assembly, impact ring, and O ring. The valve assembly can be considered as the heart of the instrument as the homogenization is completely dependent on the valve geometry and type of valve assembly. The integral parts of high-pressure homogenizer are discussed further in detail.

3.1 High-Pressure Pump

The integral part of high-pressure homogenizer equipment is high-pressure pumps that regulate the pressure under which the premix will be forced through the narrow gap. The largest part of

the homogenizer equipment in consideration of volume and weight includes the pumps and the motors for pressurizing the flow. Generally, laboratory-scale HPH encompasses 1 piston high-pressure pump, while production-scale or pilot-scale HPH has 3–5 piston high-pressure pump (Håkansson 2018b). The pump is usually pneumatically or electrically actuated and is made up of highly resistant materials. The diameter of the piston affects the attainable pressure and the capacity of the instrument. Piston with smaller diameter results in a high-pressure but moderate-capacity machine, while piston with large diameter confers moderate-pressure but a high-capacity machine. A piston pump often generates a pulsating flow that results in flow variations that causes acceleration and deceleration of the liquid in the downstream and upstream pipes of the equipment. These flow variations lead to vibrations and create possibilities of pipe breakage as well. The major effect due to pressure fluctuation occurs when there is a sudden pressure drop in the valve inlet. When the inlet temperature drops below the products boiling point, cavitation bubbles are generated that implodes on the valve. Dampers are often used to surmount the intense wear on valve walls owing to the cavitation effect. Heat exchangers are sometimes added to control the temperature increase that occurs due to increased pressure.

3.2 Homogenization Valve

The homogenization valve design and geometry play an indispensable role in the size reduction and droplet disruption of the premix. Among various parts of the homogenizer, the valve assembly is the most crucial component affecting the homogenization. The standard valve assembly generally comprises a valve rod and valve seat that forms a narrow gap in between. The fluid flow undergoes an intense increase in velocity and decrease in pressure while passing through the valve gap that leads to disruption of particles. After passing through the gap generally, the flow impinges on the impact ring and in turn gets deflected by a particular angle from where the homogenized product exits (Martínez-Monteagudo et al. 2017). On the basis of the number of valves used, high-pressure homogenizer can be categorized as one-stage homogenizer (single-valve assembly) and two-stage homogenizer (two-valve assembly). One-stage homogenizer is sufficient for most of the products, although, in cases where maximum size reduction with narrow particle size distribution is essential, a two-stage homogenizer is required. Usually, the products that require highly efficient homogenization, viz., high-fat content products, are subjected to the two-stage homogenizer. The second stage, where pressure equivalent to 10% of total pressure is applied, reduces the clumping and controls back pressure. Depending on the application, several types of homogenization valves are available commercially. Numerous patents have been granted to date for a variety of homogenization valves with different design and geometry. There are three main types of homogenization valves based on the design, flow, operating pressure, and scalability. The three main types are (1) radial diffuser valve, (2) counter jet valve, (3) and axial flow through orifice valve as represented in Fig. 11.2.

3.2.1 Radial Diffuser Valve

The radial diffuser valve is the most common type of homogenizing dispersion unit that consists of a mobile valve seat and an axial valve face. The mobile valve seat enables variation of homogenization pressure through adjusting upstream flow and the slit width. The flow enters through a nozzle and further gets deflected consecutively at a 90° into two coaxial annular chambers. The maximum pressure level up to 150 MPa can be obtained by this valve assembly. Gandini and Grandi studied the effect on homogenization efficiency by increasing the number of homogenization valves and reported that there was no significant improvement in homogenization efficiency (Gandini and Grandi 2006). The pressure variations while passing through a flat radial diffuser valve were studied by Phipps. While entering into the inlet, due to the intense increase in velocity, the pressure suddenly drops. Furthermore, the formation of vapor bubbles

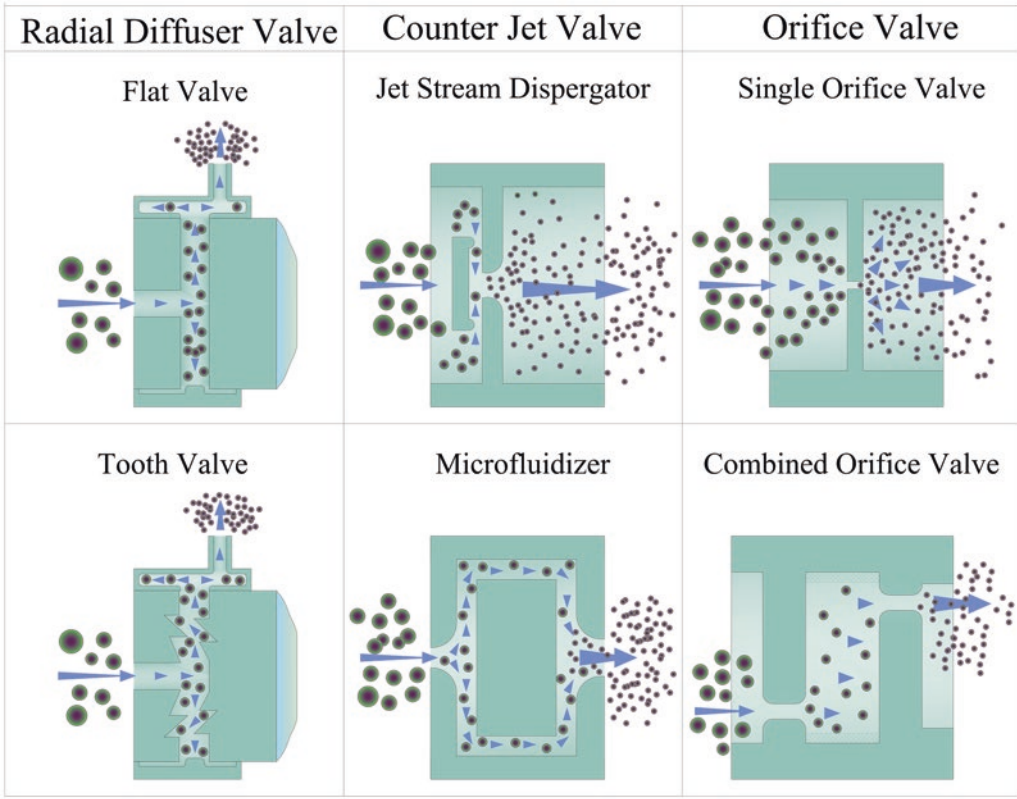

Fig. 11.2 Schematic representation of different valve designs for high-pressure homogenizer

converts the flow into two-phase flow, i.e., vapor/liquid flow. Thereafter due to compression shock, the vapor bubbles collapse due to a rise in pressure again. Based on the pressure variation study, Phipps explained that the disruption of droplet mainly occurs in the inlet of the homogenization slit (Phipps 1974). However, the exact phenomena described by various researchers remain contradictory as the accessibility to the very small dimensions and extreme conditions during homogenization is difficult. Also, many variables influence the homogenization process; thus complete theory is not established.

3.2.2 Counter Jet Valve

The counter jet dispergators involve impingement of jet streams from opposite directions leading to particle size reduction and homogenization. Alike radial diffusers, counter jet valves do not have movable parts and thus allow higher pressure range up to 300 MPa. Bayer AG patented a jet dispergator consisting of two orifices (axially opposing) and sharp edge inlets. On the basis of experimental results, the length/diameter optimal ratio reported is between 1.5 and 2 range and the optimal diameter of the bore is 0.3 mm to 1 mm. For attaining mean droplet diameter x by jet dispergator, Klinksiek and Koglin gave the following equation:

$$X = \frac{C \cdot d_B^{0.165} \cdot \gamma^{0.365} \cdot \eta_d^{0.495}}{\Delta p_H^{0.6} \cdot \eta_k^{0.025} \cdot \rho_d^{0.235}}$$

where C = constant dependent on product; Δp_H = inclined differential pressure; ɣ = interfacial tension; ρ_d = dynamic viscosity of disperse phase; η_d = dynamic viscosity of disperse phase; and η_k = dynamic viscosity of continuous phase. Stang studied the impact of collision of jet emulsion on mean droplet diameter. He concluded that there is no significant influence of collision because as per the experiment the laminar extension flow at the bore of the orifice leads to droplet

disruption. The experiment with setup of one orifice and two or four orifices resulted in the smallest mean droplet diameter with one orifice setup. The number of orifices does not impact on homogenization quality, but for scale-up, higher number of orifice is beneficial (Schultz et al. 2004).

Another widely used homogenization dispergator based on the collision of jet streams is Microfluidizer®. In Microfluidizer® the premix gets divided into two microchannels that are directed toward each other, and they collide in the interaction chamber. The fluid velocity gets increased around tenfold in the microchannels, and then under pressure, the opposite streams impinge. The outlet is ninefold bigger than the diameter of the microchannel; thus the pressure gets discharged in the outlet chamber. Similar to the case of jet dispergators, Stang does not consider collision as the only mechanism for reduction of size. As per experiments, he considered a combination of turbulent flow in the interaction chamber as well as the laminar extensional flow in the inlet as the mechanism of size reduction. The Microfluidizer showed an enhanced reduction in mean droplet diameter compared to radial diffusers, which was studied by Robin et al. Since the original design development, numerous modifications are reported in the jet dispergator valve assembly. To increase the volume stream, Y-chamber valve or jet to jet valve was developed as multi-slotted Y channels can also be incorporated for increasing the volume capacity. Z-chamber design or jet to wall valve assembly was developed to produce effective microemulsion and reduce the rise in temperature. It has been reported on the basis of experiments that the Y-chamber valve assembly gives more uniform droplet size distribution compared to the Z-chamber valve assembly. The counter jet valves commercially available are capable of handling large volume scale up to 1000 L h^{-1}, and 200 MPa pressure is the key advantage of counter jet valves. Contrarily when pressure level more than 200 MPa is desired, there is a need for extremely high flow rates, as the design of the valve is such that the flow rate controls the homogenization pressure. Thus, a great amount of energy input is required, which is the disadvantage of counter jet dispergators (Schultz et al. 2004).

3.2.3 Axial Flow Through Orifice Valve

Axial flow through orifice valve (also known as nozzle aggregate) has an orifice with sharp edge inlet and outlet through which the pressurized fluid enters axially. Like counter jet dispergators, nozzle aggregates also do not contain any movable parts and thus provide the advantage of working at very high-pressure ranges. Experiment using a high-speed video system has been done to study the mechanism of droplet disruption. The study showed that the droplet breaks up after passing through the nozzle bore when the laminar flow changes to turbulent flow in the core part of the open jet. F Hoffmann-La Roche AG patented a novel type of combined orifice valve for stronger breakdown and improved droplet stabilization. The valve design has an arrangement of three consecutive orifices, wherein the second orifice has a larger diameter than the first and third orifices. High turbulence is created in the second chamber having a larger diameter. Compared to simple orifice valves, combined orifice valves have the capability of producing smaller mean droplet diameters. The turbulence chamber in the combined orifice valve is responsible for achieving a smaller mean droplet diameter. The residence time in combined orifice valves is higher, so even the surfactants with low-medium adsorption velocities can successfully give highly stable products and smaller-sized products.

3.3 Impact Rings and "O" Rings

The high-velocity liquid passing out from the valve gap strikes firstly with the impact ring. The impact ring prevents the damaging of the chamber due to an annular high-pressure fan. The impact ring is also known as the breaker ring as the fluid after leaving the gap firstly strikes perpendicularly to the impact ring (Kelly and Muske 2004). Most of the poppet-type valves have a breaker ring in the valve assembly. In the valve

packing, an O ring is fitted to prevent the leakage and seal the interface. It is made up of an elastomer loop usually by ethylene propylene diene monomer. However, the O ring might sometimes get contaminated with the crevices or clefts and, in turn, lead to leakage. To avoid the chances of contamination, Avestin introduced oped emulsifiers where no O ring is required.

4 Theories of Homogenization

4.1 Shear

High shear is produced owing to the disruption of fluid motion while passing through the minute gap of the homogenization valve. The change in fluid motion, in turn, leads to enhanced shear effect within the fluid system as well as among the valve seat and the fluid system (Martínez-Monteagudo et al. 2017). High shear is produced mainly in the inlet chamber and boundary layers of the gap in the valve. In the case of solid particle, the velocity gradient will impart a force on the particle and cause rotation, while in the case of liquid droplet, the elongation and deformation of drop occur. The term "shear" specifically indicates the elongation of dispersed-phase droplets followed by droplet breakup due to the high-velocity gradient surrounding the droplet. The fluid acceleration in the inlet chamber gives rise to elongational stress G on the droplet. Deformation of drop from spherical to ellipsoidal shape increases with an increase in elongational stress. However, the interfacial tension counteracts the deformation due to shear stress. The deformation extent is usually expressed in terms of capillary number. The droplet breakup is expected when sufficiently large deformation takes place, i.e., capillary number exceeds the critical limit.

$$Ca = \frac{G\mu cD}{2\gamma}$$

Hydrodynamic modeling and experiments have represented that the maximum shear rate G depends on the gap height and velocity of fluid passing from the gap.

$$G \propto \frac{Ug}{h}$$

The shear rate G can be used in order to determine the fragmentation stress on the droplet by the following equation:

$$\sigma frag = \mu cG$$

Contrarily, this fragmentation stress is experienced by the droplets for a very short duration of time, i.e., before entering the gap. Thus, deformation timescale can be expressed as:

$$\tau def = \frac{\mu D}{\sigma frag}$$

Walstra argued that as the fragmentation stress experienced by droplet will be for a very short duration, only low-viscosity drops will get fragmented due to laminar shear. It was concluded that the laminar shear in the inlet chamber will be unable to fragment the highly viscous drops. In the high-pressure homogenizer, the second region exhibiting high laminar shear is laminar boundary layers of the gap. Maximum droplets pass through the center of the gap as per the flow profile; thus the boundary layer extending in the center of the gap has a significant impact on fragmentation. The boundary layer thickness δ and gap distance correlation, x, as per flat plate approximation, can be stated as:

$$\delta(x) = 5\frac{x\sqrt{vc}}{\sqrt{Ugx}}$$

The boundary layer merges only if the gap length is long enough to give $\delta(x = lg) = h/2$. Herein, the difference in laboratory HPH and production-scale HPH can be noticed as the boundary layer had an impact on small-scale homogenizers but not on production-scale homogenizers.

4.2 Turbulence

The passage of fluid gets abruptly reduced to about 100–1000-fold, which generates a high degree of the velocity gradient. The turbulence

created by the highly irregular motion is considered as the chief phenomena responsible for efficient mixing, homogenization, and emulsification. The turbulent flow causes different mixing zones in which fluid particles undergo complicated and unpredictable paths leading to enhanced mass transfer, heat, and momentum (Martínez-Monteagudo et al. 2017). Turbulent eddies (coherent structures formed at different length scales) and heat are generated due to the dissipative nature of turbulence that sequentially offers adequate energy for the disruption of particles. Kolmogorov theoretically described the interaction of turbulent eddies with the drops that lead to the fragmentation of drops. Furthermore, the Kolmogorov-Hinze model described two mechanisms: (1) turbulent inertial fragmentation and (2) turbulent viscous fragmentation. According to turbulent inertial fragmentation, the fragmentation occurs by small eddies, while in the case of turbulent viscous fragmentation, disruption occurs by large whirlpools (Steiner et al. 2006). Furthermore, the theory of maximum size (dmax) that a droplet withstands was established by linking Kolmogorov's theory with the Laplace pressure, which was mathematically expressed as:

$$\mathrm{dmax} \approx \varepsilon^{-0.4} \times \gamma^{0.6} \times \rho^{-0.2}$$

where ε expresses the average amount of energy dissipated per time, γ is the interfacial tension, and ρ indicated the density (Hinze 1955).

The Reynolds number is very high at the exit of the gap, which indicates the formation of a turbulent jet.

$$\mathrm{Re} = \frac{Q}{\pi rev}$$

According to Kelemen et al., at Re > 14,000, kinetic energy gets converted to turbulence, and a turbulent jet is formed (Kelemen et al. 2014). The fragmentation rate in turbulent flow can be estimated by the turbulent kinetic energy dissipation rate by using the following equation:

$$\eta = \left(\frac{V_C^3}{\varepsilon} \right)^{1/4}$$

where ε = rate of dissipation of turbulent kinetic energy and Vc = kinematic viscosity of continuous phase. Breakup visualization studies have reported that the size reduction occurs in the downstream near the outlet chamber (Innings and Trägårdh 2005). This can be attributed to the turbulent energy force. The large turbulent eddies get further broken up to smaller size until they can be damped out of the viscous fluid. The eddies having a similar size as that of the droplet are able to break them more efficiently. The visualization experiments have represented that the droplet breakup occurs at the position where the turbulent flow has transformed its energy to suitable length scales (Håkansson et al. 2013).

4.3 Cavitation

Another mechanism involved in droplet breakup is cavitation that occurs as a result of the large pressure drop encountered by the liquid while passing through the valve. The fluid velocity in the gap increases by several folds owing to the narrow gap size. Thus, considering the energy conservation, the high-velocity region will be having high dynamic pressure but a very low static pressure. Formation of cavities within the fluid and its subsequent collapse occur when the static pressure falls below the vapor pressure. The bubbles/cavities collapse and generate shock waves that cause particle size reduction in the fluid. Cavitation can be quantified by Thoma number (Th)/cavitation number (Nc).

$$Nc = \frac{P\infty - P_v(T)}{0.5\ \rho_c V_\infty^2}$$

where $P\infty$ = upstream static pressure; $P_v(T)$ = vapor pressure at temperature of fluid; ρ_c = velocity of continuous phase; V_∞^2 = characteristic fluid velocity; and Nc = cavitation number.

Several experiments performed by researchers have demonstrated cavitation phenomena ensuing in HPH. On the basis of cavitating flow properties including the light scattering of

vapor bubbles, ultrasonic emissions, wear, and free radical formation, cavitation phenomena have been studied. In the HPH valve, the cavitation occurs at the beginning and inside the gap due to high local velocity and has been confirmed by several gap visualization experiments. With an increase in homogenization pressure, the cavitation increases, and contrarily, employing the second homogenization stage, the cavitation bubbles decrease. Cavitation being the mechanism for droplet breakup is beneficial in HPH, but on the counterpart, it also leads to wear in the HPH valve when it occurs in close proximity to the walls. This, in turn, causes a decrease in HPH valve efficiency for suitable size reduction and homogenization (Innings et al. 2011).

5 Process Analytical Techniques for High-Pressure Homogenization

The efficiency or the outcome of high-pressure homogenizer can be known by studying the particle size or particle size distribution of the obtained product. However, the influence of pressure, geometry of the device, or formulation on the homogenization efficiency in detail cannot be known with particle size analysis. The final product analysis gives the combined effect of superimposed mechanisms, but the effect of each intermediate step cannot be justified. Understanding the influence of all intermediate steps allows a deeper understanding of the selection of proper design and processing parameters for formulating products with desired properties. For understanding the droplet/particle deformation or disruption, inline measurement is necessary. However, inline measurement is often challenging due to high velocity, complex flow patterns, and high-pressure ranges contributing to the HPH process. Recently, several optical measurement methods have been established to understand the inline parameters influencing homogenization efficiency. An overview of different optical measurement methods is given in Table 11.1 (Bisten and Schuchmann 2016).

6 Applications of High-Pressure Homogenization in Nanoparticles Development

In the pharmaceutical industries, the HPH technique can be employed for the preparation of stable emulsions, suspensions, colloidal dispersions, as well as various types of nanoparticles. The high pressure and intense energy produced during HPH allow efficient particle size reduction and also yield uniform monodisperse particles and highly stable product. Apparently, the known advantages of nano-sizing in the pharmaceutical field have increased research and development in the field of nanoparticles for drug delivery (Möschwitzer 2010). However, most of the techniques have a major issue of scalability due to complex processing and product parameters affecting nanoparticle formation. Applying quality by design approach can be beneficial to understand various interdependent parameters involved. HPH is a technique that can be used also at a larger scale, so it provides an advantage over other competing techniques of nanoparticle production. The issues of traditional size reduction techniques like polymorph transformation, metal contamination, and high amorphization do not prevail in the HPH technique. The technique is also suitable for both aqueous and nonaqueous systems. The factors affecting the HPH process for nanoparticle preparations should be considered during nanoparticle preparation. Basically, the processing variable and product variable affect homogenization efficiency. The process variables are homogenization pressure, the number of homogenization cycles, valve and impingement design, flow rate, and temperature. In the case of nanoparticles, the product variables like initial size range, the viscosity of the medium, sample concentration, and sample volume play an indispensable role affecting homogenization efficiency (Yadav and Kale 2019). Different nanoparticles require different processing conditions according to the product characteristics that need to be optimized while performing HPH for producing nano-formulations. The application of the HPH technique for different types of nanoparticles has been discussed further.

Table 11.1 Optical measurement techniques for process analysis of HPH (Bisten and Schuchmann 2016)

Optical measurement method	Description
High-speed image processing (HSIP)	The HSIP method is based on capturing images of inline events within a very short time duration. A high-speed camera with a light source and good resolution is connected to a computer for visualization. In the breakup of droplet visualization, capture in minimum time with minimum motion blur is necessary. Droplet deformation or breakup can be investigated by this method, but on the contrary, velocity profiles or local stresses cannot be calculated and are the limitations of the HSIP method
Particle image velocimetry (PIV)	The PIV method allows visualization of disruption as well as the measurement of local velocity fields. It involves the addition of tracer particles that follow the flow pattern. Pulsed laser light is used to illuminate the tracer particles. High-speed and high-resolution camera captures double images (two images at a particular time difference) of the tracer particles that are at a 90° to the light beam. From the displacement between double images, the velocity field is calculated. The cross-correlation or autocorrelation method is usually applied for further processing
Microparticle image velocimetry (μPIV)	The macroscopic PIV technique is modified to a microscale to characterize flow patterns in microfluidic devices. There is a difference in illumination in PIV and μPIV methods. In μPIV technique whole volume is illuminated. The laser light gets absorbed by fluorescent particles, and thereafter they emit light at a different wavelength. The further process includes the same steps as in the PIV technique. However, the visualization of small droplets is difficult, and temporal and spatial resolution limitations are the drawbacks of this method
Shadow graphic imaging	The method is employed for visualization of cavitation pattern. There is a light source in line with the camera. The cavitation forms gas bubbles that in turn block the light and reflect it back forming a shadow. The camera records the shadow and describes the flow pattern. Thus, the area where the cavitation occurs can be established by visualization of the shadow. However, the gas bubble collapse cannot be determined by this method
Sono-chemiluminescence (SCL)	Luminol is added to the fluid that emits light on the collapse of cavitation bubbles. This is due to the formation of free OH radicals that oxidizes luminol and forms an intermediate product. The intermediate product on decomposition emits light that is detected by a camera or a sensor. The method provides an advantage to measure the intensity of gas bubble collapse. However, velocity measurement is not possible by this method

6.1 High-Pressure Homogenization for Lipid-Based Nanoparticles

6.1.1 Solid Lipid Nanoparticles (SLNs) and Nanostructured Lipid Carriers (NLCs)

SLNs and NLCs are a new generation of colloidal carriers that are derivative of o/w emulsion in which oil drops are replaced by solid lipids. Owing to their distinct advantages like controlled and targeted drug release, biocompatible and biodegradable nature of most of the lipids, increased drug stability, and easy scalability, SLNs and NLCs are attracting major attention in the pharmaceutical industry. SLNs are considered as first-generation lipid nanoparticles wherein drug-entrapped solid lipid nanospheres are dispersed in the surfactant-stabilized aqueous phase. NLCs were developed to overcome the drawbacks of SLNs like low drug loading and stability issues. NLCs comprise of liquid lipids along with solid lipids in the lipid core that enhances the drug loading capacity (Rawal and Patel 2018,

2019). In 1992, Siekmann and Wetesen and Muller et al. in 1993 introduced the HPH technique for formulating SLNs and NLCs. Furthermore, the HPH technique for lipid colloidal carriers was patented by Muller and Lucks in 1996 (Muller et al. 2011). Among various methods proposed for the preparation of SLNs and NLCs, HPH is most widely used. Researchers have developed numerous therapeutically effective SLNs and NLCs employing HPH technique (Sinhmar et al. 2018a, b; Mathur et al. 2019; Khatri et al. 2019; Chokshi et al. 2019). A summary of various experiments done for the preparation of SLNs and NLCs employing the HPH technique is given in Table 11.2.

For the preparation of SLNs and NLCs, there are two types of HPH techniques based on the process temperature: (1) hot homogenization and (2) cold homogenization. In both the techniques, initially, the drug is dissolved in lipid at 5–10 °C above the melting point of lipid.

1. Hot homogenization

In hot homogenization, the complete process is carried out at a temperature higher than the lipid's melting point; thus it can be considered as the homogenization of an emulsion. Primarily, using a high-shear device, a pre-emulsion of drug-entrapped lipid melt and aqueous surfactant phase is prepared. The lipid melt and aqueous phase subjected to emulsify are kept at the same temperature (5–10 °C above the melting point of lipid). Immediately after the pre-emulsion is formed, it is subjected to high-pressure homogenizer for further size reduction. The high temperature allows higher size reduction due to lower inner-phase viscosity. Contrarily, chances of drug degradation are higher at high temperatures. Also, the higher pressure leads to increased sample temperature (almost 10 °C at 500 bar). Homogenization requires at least 5 cycles at 500–1000 bar for sufficient size reduction that apparently increases sample temperature as well. After cooling of the product, the primary homogenized product, i.e., nanoemulsion, converts to colloidal dispersion (Mehnert and Mäder 2012; Ganesan and Narayanasamy 2017). Figure 11.3. represents the hot homogenization process for the preparation of SLNs/NLCs.

2. Cold homogenization

To overcome the drawbacks of hot homogenization such as drug degradation at high temperature and chances of drug expulsion in the aqueous phase during homogenization, cold homogenization technique has been established. In cold homogenization, the lipid remains in solid state; thus it can be correlated with high-pressure milling of suspension. The first step of solubilizing drugs in lipid melt remains the same as in hot homogenization, although, further steps are carried out at a lower temperature range. After the dissolution of the drug in lipid melt, it is rapidly cooled by liquid nitrogen or dry ice. Immediate cooling at very low temperatures leads to uniform distribution of the drug in the lipid phase. The drug-lipid solid mixture is further milled to form microparticles by mortar milling or ball milling. At lower temperatures the fragility of lipids increases so particle comminution occurs efficiently. The milled drug-loaded lipid microparticles are added to the cold aqueous surfactant solution and subjected to HPH. The cold homogenization avoids the higher temperature exposure but does not completely surmount it due to the dissolution of the drug in lipid melt in the preliminary step. Higher particle size and broader size distribution of nanocarriers are observed in cold homogenized samples compared to hot homogenization samples (Naseri et al. 2015). Figure 11.4 represents the cold homogenization process for the preparation of SLNs/NLCs.

6.1.2 Nanoemulsion

HPH technology has two main advantages that have made it very attractive for the formulation of nanoemulsion: (1) the intense energy and hydrodynamic stresses are beneficial for achieving small droplet sizes; (2) it is well-tested technology for large-scale continuous production. The formulation parameters like disperse-phase volume, emulsifiers, and surfactants and process parameters like homogenization pressure, number of cycles, and temperature have a major effect on nanoemulsion quality. The disperse-phase volume affects the process of fragmentation of droplets. The dispersed-phase droplets in the

Table 11.2 Summary of research findings related to SLNs and NLCs formulated by employing HPH technique

Type of nanocarrier	Drug/active moiety	Lipids used	Surfactant/ co-surfactant	HPH used	Homogenization pressure (bar)	Homogenization cycles	Particle size (nm)	PDI	References
1. Solid lipid nanoparticles (SLNs)	Rifampicin	Compritol 888 ATO	Polysorbate 80	Panda Plus 2000, GEA (Niro Soavi, Germany)	1000	12	456 ± 11	0.205 ± 0.03	Chokshi et al. (2018)
	Citral	Glyceryl monostearate (GMS)	Tween 80 and Span 80 (1:1)	AH100D, ATS Engineering Inc., Vancouver, Canada	500	2	194 ± 2.19	0.358 ± 0.04	Tian et al. (2018)
	Progesterone	Tristearin	Poloxamer 188	Panda Plus 2000/ GEA (Niro Soavi, Parma, Italy)	1000	1–3	181 ± 14	0.031	Esposito et al. (2017)
	Astaxanthin	Stearic acid	Tween 20	AH-basic, Shanghai, China	300	15	167 ± 18.1	0.19 ± 0.042	Li et al. (2016)
	Dibucaine	Myristyl myristate	Poloxamer 188	Panda homogenizer (Niro Soavi, Parma, Italy)	600	3	234.33 ± 42.87	0.32 ± 0.01	Barbosa et al. (2018)
	Dibucaine	Cetyl palmitate	Poloxamer 188	Panda homogenizer (Niro Soavi, Parma, Italy)	600	3	239.37 ± 18.31	0.18 ± 0.03	
	Voriconazole	Witepsol® W35	Polysorbate 80	Avestin Emulsiflex B15 instrument (Avestin Europe GmbH, Germany)	600	5	182 ± 4.1	0.269 ± 0.01	Füredi et al. (2017)
	Artemether	Glyceryl monostearate: Compritol (50:50)	Poloxamer 188	Panda Plus 2000 (Niro Soavi, Germany)	1000	10	419 ± 09 nm	0.235 ± 0.02	Khatri et al. (2018)

2. Nanostructured lipid carrier (NLCs)	Quercetin	Glyceryl monostearate (GMS), linseed oil	Polyglycerol-6 monostearate, Tween 80, 1,1-propylene glycol	FB-110, LiTu Mechanical Equipment Engineering Co., Ltd., Shanghai, China	800	6	95.6 ± 0.3	0.253 ± 0.010	Huang et al. (2017)
	Ondansetron hydrochloride	Tristearin, Phosal 53MCT	Tween 80	Emulsiflex C3, Avestin, ON, Canada	500	6	266 ± 10	0.280 ± 0.007	Duong et al. (2019)
	Minoxidil	Stearic acid, oleic acid	Tween 80, Span 80	M-110P Microfluidics, Newton, USA	1380	2	281.4 ± 7.4	0.207 ± 0.009	Wang et al. (2017b)
	Ibuprofen	Witepsol E85, Miglyol 812	Lutrol F68	Emulsiflex C3 high-pressure homogenizer (Avestin Europe GmbH, Mannheim, Germany)	600	5	107.47 ± 14.4	0.18 ± 0.3	Sütő et al. (2016)
	5-Fluorouracil	Precirol® ATO 5, Labrasol®	Poloxamer 188, Solutol® HS15	Emulsiflex C3; Avestin, Ottawa, ON, Canada	1500	5	208.32 ± 8.21	0.352 ± 0.060	Rajinikanth and Chellian (2016)
	Budesonide	Compritol 888 ATO, Labrafac WL 1349	Span® 80	Panda Plus, GEA Niro Soavi, Italy	700	5	284.0 ± 4.53	0.155 ± 0.06	Sinhmar et al. (2018a)
	Domperidone	Palmitic acid, oleic acid	Tween 80	Panda 2 K, NS1001L Spezial, GEA Niro Soavi, Lübeck, Germany	500	5	283.97 ± 2.25	0.176 ± 0.015	Tetyczka et al. (2017)
	Voriconazole	Compritol 888 ATO, Miglyol 812N	Tween 80, Solutol HS 15	Nano DeBEE; BEE International, Easton, MA, USA	1380	3	45.62 ± 0.53	0.18 ± 0.01	Tian et al. (2017)
	Citral	Hydrogenated palm oil (HPO), lipoid S-100 and olive oil	Tween 80	High-pressure homogenizer (Avestin, Ottawa, ON, Canada)	1000	15	54.12 ± 0.30	0.224 ± 0.005	Nordin et al. (2018)

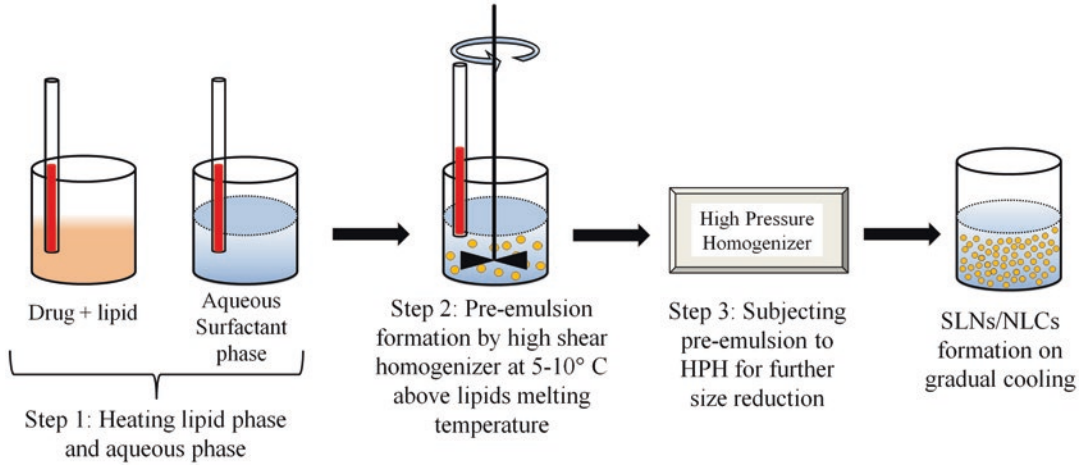

Fig. 11.3 Hot high-pressure homogenization process

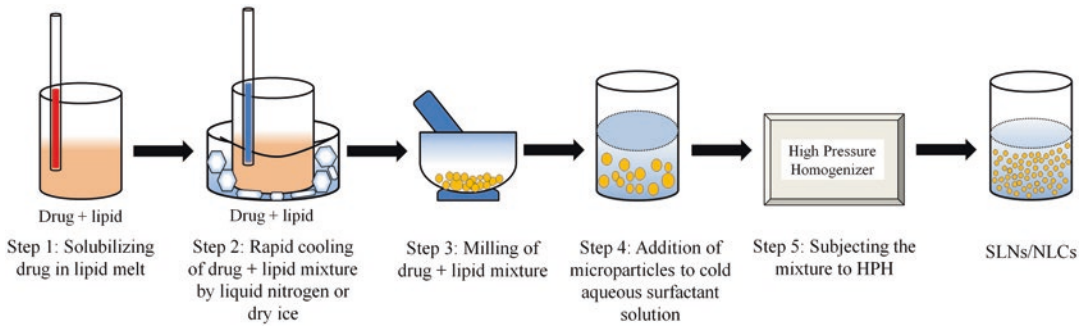

Fig. 11.4 Cold high-pressure homogenization process

flow lead to an increase in viscosity as well as viscous stresses. With increased viscosity, the drop formation and its fragmentation become complicated. However, the effect of higher viscosity of dispersed phase is less in orifice-type valves and jet dispergators (Håkansson 2018a). Stang reported laminar extension flow in jet dispergators and orifice valves leading to droplet disruption in spite of higher viscosity. There is also an effect of the disperse phase on the turbulent energy that on the basis of droplet size can lead to either attenuation or enhancement of turbulent stresses. Thus, the disperse-phase volume can significantly affect the homogenization mechanism (Stang et al. 2001). Surfactants and emulsifiers have the same role in nanoemulsion formulation by HPH as in the case of any emulsification process. They reduce the interfacial tension and thereby increase the fragmentation rate and decrease the chances of recoalescence. However, under HPH the emulsifier has a very short time to stabilize the new fragments as high-intensity passage time is very short. It takes only 10 μs for the emulsion to pass through the valve gap; thus the stabilization may be problematic in such a short duration. Also, the intense high pressure might cause changes or break covalent bonds and, in turn, may decrease the emulsifying efficiency of emulsifiers. Apart from the product parameters, process parameter like temperature also affects the emulsion quality. Experimental studies have investigated that the product temperature increases with homogenization pressure (19–23 °C temperature increase per 100 MPa

increase in pressure) (Mao et al. 2010; Benzaria et al. 2014).

Almost all the experiments done for preparing nanoemulsion by HPH have concluded that nanoemulsion prepared by HPH is more stable on storage and has desired characteristics and droplet size less than 500 nm. As per the trials, not all nanoemulsion requires the same homogenization pressure to attain a particular droplet size, viz., studies of nanoemulsion having the same droplet size (200 nm) have required different pressure (50 MPa to 200 MPa). Thus, no specific homogenization pressure can be concluded for nanoemulsion formation because the droplet size depends on several other factors as well. Another process parameter is HPH passages/HPH cycles. There is a requirement of at least 2–3 passages for nanoemulsion preparation. For laboratory scale, recirculation is possible, but in the case of industrial continuous processing, 2–3 homogenizers need to be connected in a series that in turn increases the production cost. After processing the nanoemulsion at a certain pressure and after many numbers of passages, a phenomenon of droplet size increase termed as "recoalescence" occurs. Various experimental studies have been done to justify the mechanism of recoalescence. Lee et al. in his experimental study observed that after five passages recoalescence occurred. He attributed the reason that due to temperature increase coalescence rate increased. However, an increase in temperature leads to a decrease in fluid viscosity, and thus his reason for a coalescence rate increase is not justifiable (Lee et al. 2014). Ali et al. suggested two mechanisms for recoalescence based on his experiment, viz., denaturation of emulsifier due to higher passages through the HPH valve and another aspect very less adsorption time (Ali et al. 2016). Various studies have reported such findings representing the denaturation of emulsifiers while passing through HPH. Floury et al. reported that during HPH methylcellulose underwent degradation (Floury et al. 2002). Conformational changes and degradation in barley wax even at low homogenization pressure 5–20 MPa were also reported (Floury et al. 2002). However, several studies have also shown no conformational changes or damage in emulsifiers in overprocessed nanoemulsion. Thus, to what extent the emulsifier deformation affects recoalescence still needs to be evaluated further. Several studies have reported various factors affecting the HPH process for nanoemulsion formulation. Mistry et al. studied the effect of stabilizers and HPH on chemical and physical properties of curcumin-containing chitosan/glycerol monooleate nanoemulsion. Polyvinyl alcohol and poloxamer 407 were the two stabilizers used for oil in water chitosan/GMO nanoemulsion stabilization. The results represented that three homogenization cycles reduced 50–65% droplet size; further increasing cycles did not significantly reduce the size (Mistry and Mohapatra 2012). Sharma et al. studied the effect of HPH on rutin- (active moiety) and TPGS (emulsifier)-loaded nanoemulsion. Comparison of the nanoemulsion characteristics like droplet size, zeta potential, and in vitro drug release was done for rutin-loaded nanoemulsion prepared by HPH method and spontaneous emulsion method. Compared to nanoemulsion prepared by spontaneous emulsification method, the nanoemulsion prepared by HPH represented increased in vitro release and smaller droplet size. The nanoemulsion by HPH also showed increased permeability in ex vivo studies compared to rutin suspension. The homogenization pressure of 200 MPa and 4 homogenization cycles was found to be optimum (Sharma et al. 2015). Another novel approach of using ultrasound along with HPH to reduce the energy requirement of individual processes was done by Calligaris et al. Tween 80 and Span 80 (1:1) blend and 15% (w/w) oil in water mixture were homogenized at 20–100 MPa prior to or after 20–60 s of ultra-sonification. While comparing nanoemulsion with individual method, nanoemulsion prepared by the combination was found to be more stable with a lower mean size (Calligaris et al. 2016).

6.1.3 Liposomes

Liposomes are lipid-based artificial nanovesicles of spherical geometry comprising of a phospholipid bilayer. The key advantage of liposomes is that they can entrap hydrophobic material within

the phospholipid bilayer and hydrophilic material in the internal aqueous core. The conventional methods for the preparation of liposomes are film hydration method, reverse-phase evaporation, freeze thawing, extrusion, ethanol injection method, etc. These traditional methods have a requirement of organic solvents and very complicated processing steps. HPH technique allows easy scale-up as well as does not require the use of toxic solvents. Wang et al. developed phytosterol- and phytosterol ester-encapsulated soy phospholipid liposomes employing HPH. The phospholipid and phytosterol dispersion in 3,4-morpholinopropanesulfonic acid (MOPS) buffer was initially pre-homogenized in an Ultra-Turrax homogenizer at 22,000 rpm for 5 min. Furthermore, the pre-emulsion was subjected to high-pressure homogenizer (Microfluidizer) at 690 bar pressure, 80 °C. The liposomes formulated by Microfluidizer were highly stable, and TEM images showed that most of the structures are unilamellar and some appeared multivesicular. The study provided an outlook for pharmaceutical and nutraceutical companies toward using Microfluidizer for the preparation of liposomes to deliver bioactive agents (Wang et al. 2017a). Another approach that encompasses the use of HPH in liposome manufacturing is preparing liposomes by conventional approaches and further reducing their size in a high-pressure homogenizer. The size distribution of the liposomes depends on processing parameters like the number of homogenizing cycles and homogenization pressure. Apart from that, the sample related factors like composition of the bulk medium, phospholipid concentration and composition, liposome lamellarity, and initial size distribution of the liposomes. Barnadas et al. studied the effect of homogenization process parameters like the effect of recirculation mode and non-recirculation mode of the Microfluidizer. Along with process parameters, the effect of sample parameters like phospholipid and ethanol concentration was also studied. In a non-recirculation mode, the study depicted a continuous effect of pressure on the liposome size (increase in pressure led to a decrease in liposome diameter). In the case of homogenization cycles, there was no significant effect on the mean diameter after seven cycles. While in a recirculation mode, at the homogenization outset, there is an increase in size distribution width initially because small quantities of suspension in the reservoir get mixed with the processed sample. But when liposomes attain a certain small size, the width of size distribution decreases. The study for determining the effect of ethanol concentration and phospholipid concentration represented that under fixed conditions the liposome diameter decreased and size distribution became narrower with increased concentration of ethanol (Barnadas-Rodríguez and Sabés 2001).

Kyun et al. studied the effect of HPH on the physicochemical properties of cationic polymer-coated liposomes. Non-coated liposomes, chitosan-coated liposomes, and Eudragit-coated liposomes were formulated employing the HPH method. There was an effect on homogenization pressure, the ratio of core material to lecithin, and the number of homogenization cycles on mean size, PDI, encapsulation efficiency, and surface charge of the non-coated liposomes. The experimental results depicted that three homogenizing cycles and 1000 bar pressure gave the optimal results. There was a decrease in particle size and PDI with increase in pressure and number of cycles. However, with an increase in homogenization pressure, the encapsulation efficiency decreased. At 500 bar, the encapsulation efficiency was highest, but the particle size and PDI were higher. Thus, 1000 bar was selected for preparation of liposomes with desired characteristics (Kyun et al. 2014).

6.2 High-Pressure Homogenization for Nanocrystals

Nanocrystals are basically drug particles of submicron sizes that have a semicrystalline state with a high surface area. HPH is one of the most important techniques for the production of nanocrystals. When nanocrystals are dispersed and stabilized in a dispersion medium, nanosuspension is formed (Keck and Müller 2006). Various

processes based on the HPH technique have been patented by several industries. DissoCube® technology was the first HPH-based technology that was granted a patent for pure aqueous homogenization of particles. Another HPH-based technology named as Nanopure® was patented by PharmaSol GmbH, Berlin, for non-aqueous media milling of drug particles to form nanosuspension. Herein, isotonic hydrophilic solvents such as aqueous solution of polyethylene glycol (PEG) or glycerol are used for the production of parenteral nanosuspensions. Yet another HPH-based method, used for the production of nanosuspensions, was patented under the name NANOEDGE® by Baxter pharmaceuticals to overcome the problem of uncontrolled crystal growth, associated with the traditional precipitation method by combining this bottom-up approach with the top-down process of HPH.

6.2.1 DissoCube®

This technology was based upon the fact that large cavitation forces are generated upon subjecting the drug dispersion in an aqueous medium to piston gap homogenization. Based on Bernoulli's principle, in a closed system, the flow volume of liquid is constant per section. Hence, upon passing an aqueous drug dispersion through a narrow orifice diameter, enormous dynamic pressure is generated with a simultaneous decrease in static pressure. Reduction in static pressure results in reduced vapor pressure, due to which, the liquid starts to boil and form gas bubbles that get imploded on leaving the homogenization gap. The resultant cavitational forces are believed to contribute to the size reduction of drug dispersion to nano-size and form nanocrystal/nanosuspension. The process of nanocrystal formation depends on the powder density of the homogenizer, temperature, and number of homogenization cycles. In addition to this, initial particle size should be <1 mm, and the pre-homogenized drug powder should be monodisperse to prevent physical destabilization.

6.2.2 Nanopure®

This specialized HPH technique also referred to as "deep-freeze homogenization" is used for the development of specialized nanocrystals/nanosuspensions in which the drug particles are dispersed in non-aqueous hydrophilic media such as PEG 400, PEG 600, or water-glycerol mixtures. Some examples of such pharmaceutical nanocrystals are nanosuspensions to be filled in capsules or hydrolytically unstable drug nanosuspensions that can be diluted prior to their administration with aqueous vehicle to have dry products with low moisture content. In contrast to cavitation being the driving force for size reduction of nanoparticles in the DissoCube® technology, the driving force for size reduction using the Nanopure® technology involves size reduction at zero or subzero temperatures (−20 °C). This technology provides a subtle method for the size reduction of thermolabile drugs and the drugs that have the aforementioned prerequisites. This method has also been employed to homogenize drug powder in melted solid/semi-solid PEG like PEG 1000 or PEG 6000 and to obtain nanocrystals that can be filled in hard gelatin capsule directly or after grinding the solidified PEG nanosuspension.

6.2.3 NANOEDGE®

As described earlier, this technique involves size reduction using HPH after the precipitation step of the bottom-up approach. The main advantage of this process is that it yields nanoparticles in a state wherein a balance of particle energy is achieved to attain good particle stability of the nanocrystals. Moreover, irrespective of the initial state of the material (amorphous, semicrystalline, or crystalline), the precipitated particles undergo "annealing" step when processed using this patented HPH technology and are transformed to a crystalline state. However, this technique has a prerequisite of having a predefined solvent and an anti-solvent for the chosen drug to facilitate drug precipitation. Despite these advantages, the method has drawbacks of using solvents that need to be removed from the product for regulatory approval and being more expensive. Some examples of nanocrystals/nanosuspensions produced using HPH have been described here in detail.

Solid concentration/solid content of nanosuspension is one of the major parameters affecting particle size reduction using HPH. Typically, the process of HPH is more efficient at solid concentrations<10%. The research work of Krause and Muller demonstrates the production of nanosuspensions at typically high solid contents (20 and 30%) with the use of different amounts of surfactants. The factors that led to an efficient nanonization of powders with high solid content were observed to be pre-milling, homogenizer design, and product viscosity. The pre-milling step typically involves operating HPH at 100 bar for 2 cycles, followed by 2 cycles at 500 bar and 2 cycles at 1000 bar. However, this step may be obviated if the initial powder size is to a fine degree. It was observed that there was a significant increase in the viscosity of suspension with an increase in the solid content to >40% and yield of paste. Processing such high-viscosity materials can be difficult with the lab-scale high-pressure homogenizers and demands large-scale piston gap homogenizers to be employed. It can be summarized from the undertaken research work that in order to achieve particle sizes similar to that for the low solid concentration suspensions (<10%), homogenization cycles can be increased (to achieve high total disintegration energy), and a homogenizer design that facilitates active transport of suspension should be used (Krause and Muller 2001).

In a research work of Karadag et al., quercetin nanocrystals were prepared using HPH technology to enhance its water solubility and bioavailability. The optimized quercetin nanocrystals were formed by dispersing (0.5%w/w) quercetin in aqueous solution of Tween 80 at 70 °C for 20 min. This coarse dispersion was subjected to further size reduction using the high-shear homogenizer (Ultra-Turrax T-25 basic, IKA Works Inc., Wilmington, NC, USA) at 24,000 rpm for 5 min. The dispersion thus obtained was subjected to filtration through Whatman cellulose filters (grade 3, 6 μm mesh). Further size reduction was carried out using a high-pressure homogenizer (Emulsiflex C3, 90 Avestin Inc., Ottowa, Canada) at 50 to 200 MPa and 40 cycles. It was observed that on increasing the homogenization pressure, there was a decrease in the particle size. Almost 50% size reduction was observed after two cycles. However, the rate of size reduction was reduced on the further increase and was found to get stagnant after 10 cycles. The particle size and PDI of nanocrystals thus obtained were observed to be ~430 nm and 0.2, respectively. Also, fluctuations in PDI have been observed in between the homogenization cycles, indicating the formation of reversible aggregates that get comminuted during subsequent cycles. The predominating size reduction force involved in the processing of the quercetin nanocrystals was observed to be cavitation (Karadag et al. 2014).

In a similar study performed by Sun et al., itraconazole (ITZ) nanosuspension was prepared using HPH and evaluated for the effect of stabilizer on particle size, zeta potential, and surface morphology. For the preparation of ITZ nanosuspension, the researchers subjected the coarse ITZ powder to homogenization in aqueous stabilizer solution using Ultra-Turrax T-25 (Jahnke & Kunkel, Staufen, Germany) at 8000 rpm for 1 min. The dispersion thus prepared was subjected to HPH using AH100D (ATS Engineering Inc., Shanghai, China). The dispersion was processed for two homogenization cycles at 150, 500, and 1000 bar and repeated at 1350 bar for several cycles to obtain the desired particle size. The ITZ nanosuspension was evaluated for deducing the effect of multiple stabilizer system (Lutrol F127 and sodium lauryl sulfate (SLS)) on particle size using central composite design. There was no alteration in the crystalline form of ITZ after being processed by HPH. However, the in vitro dissolution rate was observed to be directly proportional to the size of the ITZ nanocrystals. The in vivo pharmacokinetics in rats showed a significant enhancement of drug concentration-time curve and maximal plasma concentration (AUC) with the ITZ nanosuspensions ($n = 3$) (Sun et al. 2011).

In the past decade, several research works have been performed for facilitating the formation of solid dispersions of nanocrystals. In a research work performed by Ye et al., nanosuspension of Efavirenz (EFZ) were prepared by

HPH and converted to a solid dispersion by combining it with the hot-melt extrusion process. The EFZ nanodispersion was stabilized using Kollidon® 30 and sodium lauryl sulfate (SLS), followed by its blending in the extruder barrel with Soluplus®. Particle size reduction was significant with an increase in the homogenization cycles till an optimum, after which there was no further size reduction. The particle size of ~320 nm was achieved on subjecting 2% drug suspension to homogenization for 20 homogenization cycles at 1500 bar. While HPH was performed efficiently at % drug loading of 2% and 4%, the % drug loading of 8% was observed to block the HPH. There was a significant increase in the dissolution rate of EFZ with the nanocrystals, due to increased wetting ability and surface area (Ye et al. 2016).

6.3 High-Pressure Homogenization for Polymeric Nanoparticles

Polymeric nanoparticles are generally of two types, nanospheres and nanocapsules, wherein the active moiety is encapsulated within the polymeric material. Emulsification solvent evaporation, salting out method, precipitation method, supercritical fluid technology, and ionic gelation method are the general methods used for the preparation of polymeric nanoparticles. The HPH method is usually employed for further size reduction and producing uniform monodisperse particles. Various experimental studies done by researchers have proved the efficiency of the HPH technique to produce smaller and uniform particle sizes. Also, the redispersibility and stability of the nanoparticles are found to be increased by employing HPH for its production. Lamprecht et al. developed PLG/PCL 50:50 polymeric nanoparticles by double emulsion pressure homogenization technique and checked the influence of process parameters on the preparation of nanoparticles. The homogenization time, amount of polymer, and surfactant amount were influencing the particle size and particle size distribution. The experimental results depicted that the homogenization time up to 3 min was effective for maximum size reduction and size distribution. After 3 min, the particle size and polydispersity index increased which might be due to decreased stability of double emulsion leading to uncontrolled coalescence (Lamprecht et al. 2000). Another study includes the preparation of 5-fluorouracil-loaded PLGA nanoparticles by a high-pressure homogenization-emulsification method. The nanoparticle preparation owes a benefit of increasing bioavailability of 5-FU. As 5-FU is a hydrophilic drug, the w/o/w emulsion method is most appropriate. However, to achieve proper size reduction and monodisperse particles, HPH can be beneficial. Optimum cycles and homogenization pressure were found to be 3 cycles at 800 bar pressure as per the experimental trials. The particle size range obtained was 75 nm to 102 nm and the mean diameter was 85 nm. The polydispersity index was 0.10 to 0.18, which indicates that the HPH was effective enough to get uniform small-sized particles (Li et al. 2008). Aimin Shi et al. formulated starch nanoparticles by combined mini-emulsion cross-linking and HPH technique. The influence of processing parameters on stability and particle size was studied. The coarse emulsion when subjected to high-pressure homogenizer at 10 MPa to 60 MPa and 1–5 passes produced small-sized and uniform particles (Shi et al. 2011). Dong et al. prepared paclitaxel-incorporated PLGA nanoparticles employing the HPH technique. The author described three advantages of using HPH for particle size reduction, viz., excellent redispersibility of nanoparticles, uniform particle production, and easy scalability. The experiments for adjusting the homogenization pressure and cycles revealed that there was no significant influence of very high pressure on particle size. The pressure range of 86 MPa to 155 MPa gave a particle size range of 200–300 nm. A homogenization pressure of 86 MPa and 1 cycle also gave a sufficient nano-size. Also, the entrapment efficiency decreased with an increase in pressure and cycles; thus lower pressure and one cycle can be considered optimum for this formulation (Dong and Feng 2007).

7 Scale-Up and Industrialization Perspective

The key advantage of employing HPH techniques for nanoparticle preparation is that the high-pressure homogenizers of different sizes and capacities are available. Talking about other techniques of nanoparticle preparation, a major problem remains the scalability issue. Contrarily, HPH provides easy scale-up as various models, viz., benchtop models/laboratory-scale models with 10 L/h capacity, pilot-scale models with 100 L/h capacity, as well as large production scale 100,000 L/h, are available. Currently, high-pressure homogenizers are widely used in food and beverage preparation, cosmetics, nutraceuticals, as well as pharmaceuticals for industrial manufacturing of stable emulsions, suspensions, and colloidal dispersions. Thus, the fact that already the mature technique is well established at industrial scale manufacturing makes it more convenient for the manufacturing of nanoparticles. However, there are certain factors like change in geometry of valve, change in flow rate, gap height, as well as different fluid volume which have an effect on the homogenization results at laboratory scale and industrial scale. The optimization of the flow rate, homogenization pressure, and number of homogenizing cycles for nanoparticle production should be done for obtaining nanoparticles with desirable properties at an industrial scale as well. As a concluding remark, it can be said that compared to other competing manufacturing techniques of nanoparticles, HPH has an advantage as large-scale production is possible. Conversely, theoretical analysis of pressure loses, cavitation number, and Reynolds number suggests differences in the capacity of homogenization by different scale homogenizers. However, more experimental insights are necessary for studying the factors involved in different scale production in terms of homogenization efficiency as well as stability of homogenized products obtained.

8 Concluding Remark and Future Prospects

High-pressure homogenization is a versatile technique providing numerous advantages for the manufacturing of nanoparticles with desirable characteristics and stability. The technique utilizes mechanical action as well as pressure that provides a benefit to achieve nano-sized particles having uniform structures and lower PDI. The type of high-pressure homogenizer, valve design, geometry, type of pressure pump, and processing parameters have a prodigious influence on the final homogenized product. A deeper understanding of the forces acting on the size reduction, viz., shear, turbulence, and cavitation, will provide an outlook to achieve the desired product quality. Several factors affecting the therapeutic outcome of the nano-products like improved targetability, bioavailability, stability, etc. get influenced by the processing parameters of the HPH technique. The modifications and improvements were done in the HPH technology and allow flexibility and improved functionality in obtaining the nanoparticles with the desired pharmaceutical application. Newer valve designs and improved instrumentation enable the homogenizer to achieve higher durability and withstand higher pressure levels. At both industrial as well as research levels, the technique has a bright future and a broader impact on formulating highly stable nano-formulations with desired characteristics because of the key advantage of scalability.

Acknowledgment and Fundings The authors are grateful to Nirma University, Ahmedabad, India, for providing financial assistance in the form of Major Research Project (NU/Ph.D./Major Res Pro/IP/16-17/669). The authors are also thankful to the Department of Science and Technology (DST), Fund for Improvement of S&T Infrastructure (FIST) (Grant No.: SR/FST/LSI-607/2014), government of India, for providing the necessary funding to establish an equipment facility. Ms. Preksha Vinchhi is also grateful to Nirma University for providing the Junior Research Fellowship.

References

Ali A, et al. β-Lactoglobulin stabilized nanoemulsions – formulation and process factors affecting droplet size and nanoemulsion stability. Int J Pharm. 2016;500(1–2):291–304. https://doi.org/10.1016/j.ijpharm.2016.01.035.

Barbosa RDM, et al. Solid lipid nanoparticles for dibucaine sustained release. Pharmaceutics. 2018;10(4):1–17. https://doi.org/10.3390/pharmaceutics10040231.

Barnadas-Rodríguez R, Sabés M. Factors involved in the production of liposomes with a high-pressure homogenizer. Int J Pharm. 2001;213(1–2):175–86. https://doi.org/10.1016/S0378-5173(00)00661-X.

Benzaria A, et al. UHPH-processed O/W submicron emulsions stabilised with a lipid-based surfactant: physicochemical characteristics and behaviour on in vitro TC7-cell monolayers and ex vivo pig's ear skin. Colloids Surf B: Biointerfaces. 2014;116:237–46. https://doi.org/10.1016/j.colsurfb.2013.12.050.

Bisten A, Schuchmann HP. Optical measuring methods for the investigation of high-pressure homogenisation. PRO. 2016;4(4):6–9. https://doi.org/10.3390/pr4040041.

Calligaris S, et al. Nanoemulsion preparation by combining high pressure homogenization and high power ultrasound at low energy densities. Food Res Int. 2016;83:25–30. https://doi.org/10.1016/j.foodres.2016.01.033.

Chokshi NV, Khatri HN, Patel MM. Formulation, optimization, and characterization of rifampicin-loaded solid lipid nanoparticles for the treatment of tuberculosis. Drug Dev Ind Pharm. 2018;44(12):1975–89. https://doi.org/10.1080/03639045.2018.1506472.

Chokshi NV, Khatri HN, Patel MM. Fabrication and optimization of isoniazid loaded lipid nanoparticulate systems for the treatment of tuberculosis. Adv Sci Eng Med. 2019;11(8):741–57.

Dhankhar P. Homogenization fundamentals. IOSR J Eng. 2014;4(5):01–8. https://doi.org/10.9790/3021-04540108.

Digby S. High pressure homogenisation. Process Eng. 2002;83(5):33.

Dong Y, Feng S. Poly (d,l-lactide-co-glycolide) (PLGA) nanoparticles prepared by high pressure homogenization for paclitaxel chemotherapy. Int J Pharm. 2007;342:208–14. https://doi.org/10.1016/j.ijpharm.2007.04.031.

Dumay E, et al. Technological aspects and potential applications of (ultra) high-pressure homogenisation. Trends Food Sci Technol. 2013;31(1):13–26. https://doi.org/10.1016/j.tifs.2012.03.005.kele20.

Duong VA, et al. Nanostructured lipid carriers containing ondansetron hydrochloride by cold high-pressure homogenization method: Preparation, characterization, and pharmacokinetic evaluation. J Drug Deliv Sci Technol. 2019;53(July):101185. Elsevier. https://doi.org/10.1016/j.jddst.2019.101185.

Esposito E, et al. Progesterone lipid nanoparticles: scaling up and in vivo human study. Eur J Pharm Biopharm. 2017;119:437–46. https://doi.org/10.1016/j.ejpb.2017.07.015.

Floury J, et al. Degradation of methylcellulose during ultra-high pressure homogenisation. Food Hydrocoll. 2002;16(1):47–53. https://doi.org/10.1016/S0268-005X(01)00039-X.

Füredi P, et al. Development and characterization of the voriconazole loaded lipid-based nanoparticles. J Pharm Biomed Anal. 2017;132:184–9. https://doi.org/10.1016/j.jpba.2016.09.047.

Gandini and Grandi. Homogeniser for the continuous treatment of fluids at very high pressure. Patent no. US 7,661,873 B2. 2006.

Ganesan P, Narayanasamy D. Lipid nanoparticles: different preparation techniques, characterization, hurdles, and strategies for the production of solid lipid nanoparticles and nanostructured lipid carriers for oral drug delivery. Sustain Chem Pharm. 2017;6:37–56. https://doi.org/10.1016/j.scp.2017.07.002.

Gaulin A. A. gaulin. system for intimately mixing milk. (756). Patent no. 756953. 1904.

Håkansson A. Fabrication of nanoemulsions by high-pressure valve homogenization. In: Jafari S, McClements D, editors. Nanoemulsions: formulation, applications, and characterization; 2018a. p. 175–206. https://doi.org/10.1016/B978-0-12-811838-2.00007-2.

Håkansson A. Flow pulsation plays an important role for high-pressure homogenization in laboratory-scale. Chem Eng Res Des. 2018b;138:472–81. https://doi.org/10.1016/j.cherd.2018.09.015.

Håkansson A, et al. Velocity measurements of turbulent two-phase flow in a high-pressure homogenizer model. Chem Eng Commun. 2013;200(1):93–114. https://doi.org/10.1080/00986445.2012.691921.

Hinze JO. Fundamentals of the hydrodynamic mechanism of splitting in dispersion processes. AICHE J. 1955;1(3):289–95. https://doi.org/10.1002/aic.690010303.

Huang J, et al. Nanostructured lipid carrier (NLC) as a strategy for encapsulation of quercetin and linseed oil: preparation and in vitro characterization studies. J Food Eng. 2017;215:1–12. https://doi.org/10.1016/j.jfoodeng.2017.07.002.

Innings F, Trägårdh C. Visualization of the drop deformation and break-up process in a high pressure homogenizer. Chem Eng Technol. 2005;28(8):882–91. https://doi.org/10.1002/ceat.200500080.

Innings F, et al. Understanding and analysis of wear in homogenizers for processing liquid food. Wear. 2011;271(9–10):2588–98. https://doi.org/10.1016/j.wear.2011.01.084.

Karadag A, Ozcelik B, Huang Q. Quercetin nanosuspensions produced by high-pressure homogenization.

J Agric Food Chem. 2014;62:1852–9. https://doi.org/10.1021/jf404065p.

Keck CM, Müller RH. Drug nanocrystals of poorly soluble drugs produced by high pressure homogenisation. Eur J Pharm Biopharm. 2006;62(1):3–16. https://doi.org/10.1016/j.ejpb.2005.05.009.

Kelemen K, Schuch AC, Schuchmann HP. Influence of flow conditions in high-pressure orifices on droplet disruption of oil-in-water emulsions. Chem Eng Technol. 2014;37(7):1227–34. https://doi.org/10.1002/ceat.201400037.

Kelly WJ, Muske ÆKR. Optimal operation of high-pressure homogenization for intracellular product recovery. Bioprocess Biosyst Eng. 2004;27:25–37. https://doi.org/10.1007/s00449-004-0378-9.

Khatri H, Chokshi N, Rawal S, Patel MM. Fabrication, characterization and optimization of artemether loaded PEGylated solid lipid nanoparticles for the treatment of lung cancer. Mater Res Express. 2018;6(4):045014. https://doi.org/10.1088/2053-1591/aaf8a3.

Khatri H, Chokshi N, Rawal S, Patel B, Patel MM. Formulation and optimization of paclitaxel loaded lipid nanoparticles and their in vitro cytotoxicity studies using H1299 lung cancer cell lines. Adv Sci Eng Med. 2019;11(12):1202–17.

Krause KP, Müller RH. Production and characterisation of highly concentrated nanosuspensions by high pressure homogenisation. Int J Pharm. 2001;214(1–2):21–4. https://doi.org/10.1016/S0378-5173(00)00626-8.

Kyun S, et al. Colloids and surfaces a: physicochemical and engineering aspects factors influencing the physicochemical characteristics of cationic polymer-coated liposomes prepared by high-pressure homogenization. Colloids Surf A Physicochem Eng Asp. 2014;454:8–15. https://doi.org/10.1016/j.colsurfa.2014.03.095.

Lamprecht A, Ubrich N, Pe MH. Influences of process parameters on nanoparticle preparation performed by a double emulsion pressure homogenization technique. Int J Pharma. 2000;196:177–82.

Lee L, et al. Production of water-in-oil nanoemulsions using high pressure homogenisation: a study on droplet break-up. J Food Eng. 2014;131:33–7. https://doi.org/10.1016/j.jfoodeng.2014.01.024.

Li X, et al. PLGA nanoparticles for the oral delivery of 5-fluorouracil using high pressure homogenization-emulsification as the preparation method and in vitro/in vivo studies. Drug Dev Ind Pharm. 2008;34(1):107–15. https://doi.org/10.1080/03639040701484593.

Li M, et al. Preparation and stability of astaxanthin solid lipid nanoparticles based on stearic acid. Eur J Lipid Sci Technol. 2016;118(4):592–602. https://doi.org/10.1002/ejlt.201400650.

Mao L, et al. Effects of homogenization models and emulsifiers on the physicochemical properties of β-carotene nanoemulsions. J Dispers Sci Technol. 2010;31(7):986–93. https://doi.org/10.1080/01932690903224482.

Martínez-Monteagudo SI, Yan B, Balasubramaniam VM. Engineering process characterization of high-pressure homogenization – from laboratory to industrial scale. Food Eng Rev. 2017;9(3):143–69. https://doi.org/10.1007/s12393-016-9151-5.

Mathur P, et al. Fabrication, optimization, and in vitro evaluation of docetaxel-loaded nanostructured lipid carriers for improved anticancer activity. J Liposome Res. 2019:1–15. https://doi.org/10.1080/08982104.2019.1614055.

Mehnert W, Mäder K. Solid lipid nanoparticles: production, characterization and applications. Adv Drug Deliv Rev. 2012:83–101. https://doi.org/10.1016/j.addr.2012.09.021.

Mistry PH, Mohapatra SK. Effect of high-pressure homogenization and stabilizers on the physicochemical properties of curcumin-loaded glycerol monooleate/chitosan nanostructures. Nanomedicine. 2012;7(120):1863–76.

Möschwitzer J. Nanotechnology: pharmaceutical development process. Am Pharma Rev. 2010:54–9.

Muller H, Shegokar R, Keck M. 20 years of lipid nanoparticles (SLN & NLC): present state of development and industrial applications. Curr Drug Discov Technol. 2011;8(3):207–27. https://doi.org/10.2174/157016311796799062.

Naseri N, Valizadeh H, Zakeri-Milani P. Solid lipid nanoparticles and nanostructured lipid carriers: structure preparation and application. Adv Pharma Bull. 2015;5(3):305–13. https://doi.org/10.15171/apb.2015.043.

Nordin N, et al. Characterization and toxicity of citral incorporated with nanostructured lipid carrier. PeerJ. 2018;2018(1):1–19. https://doi.org/10.7717/peerj.3916.

Phipps LW. Some operating characteristics of a simple homogenizing poppet valve; pressure profiles and separation: zone of fat globule dispersion. J Dairy Res. 1974;41(3):339–47. https://doi.org/10.1017/S0022029900019786.

Rajinikanth PS, Chellian J. Development and evaluation of nanostructured lipid carrier-based hydrogel for topical delivery of 5-fluorouracil. Int J Nanomedicine. 2016;11:5067–77. https://doi.org/10.2147/IJN.S117511.

Rawal SU, Patel MM. Lipid nanoparticulate systems-modern versatile drug carriers. In: Grumezescu A, editor. lipid nanocarriers for drug targeting: Elsevier; 2018. p. 49–138. https://doi.org/10.1016/b978-0-12-813687-4.00002-5.

Rawal S, Patel MM. Threatening cancer with nanoparticle aided combination oncotherapy. J Control Release. 2019;301(March):76–109. Elsevier. https://doi.org/10.1016/j.jconrel.2019.03.015.

Schultz S, et al. High-pressure homogenization as a process for emulsion formation. Chem Eng Technol. 2004;27(4):361–8. https://doi.org/10.1002/ceat.200406111.

Sharma S, et al. Effect of high-pressure homogenization on formulation of TPGS loaded nanoemulsion of rutin – pharmacodynamic and antioxidant studies.

Drug Deliv. 2015;22(4):541–51. https://doi.org/10.3109/10717544.2014.893382.

Shi AM, et al. Preparation of starch-based nanoparticles through high-pressure homogenization and miniemulsion cross-linking: influence of various process parameters on particle size and stability. Carbohydr Polym. 2011;83(4):1604–10. https://doi.org/10.1016/j.carbpol.2010.10.011.

Sinhmar, et al. Process, optimization, and characterization of budesonide-loaded nanostructured lipid carriers for the treatment of inflammatory bowel disease. Drug Dev Ind Pharm. 2018a;44(7):1078–89. https://doi.org/10.1080/03639045.2018.1434194.

Sinhmar, et al. Surface engineered lipid nanoparticle-mediated site-specific drug delivery system for the treatment of inflammatory bowel disease. Artif Cells Nanomed Biotechnol. 2018b;46(sup 2):565–78. https://doi.org/10.1080/21691401.2018.1463232.

Stang M, Schuchmann H, Schubert H. Emulsification in high-pressure homogenizers. Eng Life Sci. 2001;1(4):151. https://doi.org/10.1002/1618-2863(200110)1:4<151::AID-ELSC151>3.0.CO;2-D.

Steiner H, et al. Numerical simulation and experimental study of emulsification in a narrow-gap homogenizer. Chem Eng Sci. 2006;61(17):5841–55. https://doi.org/10.1016/j.ces.2006.04.016.

Sun W, Mao S, Shi Y, Li LC, Fang L. Nanonization of itraconazole by high pressure homogenization: stabilizer optimization and effect of particle size on oral absorption. J Pharm Sci. 2011;100(8):3365–73.

Sütő B, et al. Development of ibuprofen-loaded nanostructured lipid carrier-based gels: characterization and investigation of in vitro and in vivo penetration through the skin. Int J Nanomedicine. 2016;11:1201–12. https://doi.org/10.2147/IJN.S99198.

Tetyczka C, et al. Development of nanostructured lipid carriers for intraoral delivery of domperidone. Int J Pharm. 2017;526(1–2):188–98. https://doi.org/10.1016/j.ijpharm.2017.04.076.

Tian B, et al. Enhanced antifungal activity of voriconazole-loaded nanostructured lipid carriers against Candida albicans with a dimorphic switching model. Int J Nanomedicine. 2017;12:7131–41. https://doi.org/10.2147/IJN.S145695.

Tian H, et al. Preparation and characterization of citral-loaded solid lipid nanoparticles. Food Chem. 2018;248:78–85. https://doi.org/10.1016/j.foodchem.2017.11.091.

Wang FC, Acevedo N, Marangoni AG. Encapsulation of phytosterols and phytosterol esters in liposomes made with soy phospholipids by high pressure homogenization. Food Funct. 2017a;8(11):3964–9. https://doi.org/10.1039/C7FO00905D.

Wang W, et al. Preparation and characterization of minoxidil loaded nanostructured lipid carriers. AAPS PharmSciTech. 2017b;18(2):509–16. https://doi.org/10.1208/s12249-016-0519-x.

Yadav KS, Kale K. High pressure homogenizer in pharmaceuticals: understanding its critical processing parameters and applications. J Pharm Innov. 2019; https://doi.org/10.1007/s12247-019-09413-4.

Ye X, et al. Conjugation of hot-melt extrusion with high-pressure homogenization: a novel method of continuously preparing nanocrystal solid dispersions. AAPS PharmSciTech. 2016;17(1):78–88. https://doi.org/10.1208/s12249-015-0389-7.

Yong AP, Islam MA, Hasan N. A review: effect of pressure on homogenization. Nat Sci. 2017;35(1):1–22.

12

Solvent Emulsification Evaporation and Solvent Emulsification Diffusion Techniques for Nanoparticles

Sunita A. Chaudhary, Dasharath M. Patel, Jayvadan K. Patel, and Deepa H. Patel

Abstract

Nowadays, there has been an increased demand of nanoparticulate-based drug delivery as nanoparticles (NPs) generally give more advantages over the conventional drug carriers for targeting in various parameters like more drug encapsulation, more stability and site specificity, sustained release profile and the ability to deliver both lyophilic and lyophobic types of drug particles using different modes of administration. Nanocarriers have been expansively studied as particulate drug delivery in the field of pharmaceuticals, due to their controlled and sustained release properties, small size and biocompatibility with body tissues. Manufacturing technique used to prepare nanoparticles plays a vital role in achieving their desired properties for a particular application. Several methods to formulate nanoparticles have been developed during the last many decades, and these are classified based on whether the particle formation undergoes a polymerization reaction or a nanoparticle forms directly from a preformed polymer or ionic gelation method. The choice of method for the preparation of nanoparticle is highly dependent on the physicochemical properties of both the polymer and the drug compound. Polymeric nanoparticles are generally manufactured by polymerization of monomers using anionic polymer or by preparing homogeneous dispersion of the dissolved polymers which gives nanoparticles using various methods such as solvent evaporation, emulsification solvent diffusion, salting out, emulsification diffusion and supercritical fluid (SCF) technology. This chapter emphasizes on how emulsification followed by solvent evaporation and solvent diffusion permits an emulsion of a polymer solution to customize as nanoparticles. The chapter also provides concise information on recent trends of research in specified domain.

Keywords

Nanoparticles · Emulsification solvent evaporation · Emulsification solvent diffusion

S. A, Chaudhary (✉)
Arihant School of Pharmacy & Bio Research Institute, Gandhinagar, Gujarat, India

D. M. Patel
Graduate School of Pharmacy, Gujarat Technological University, Ahmedabad, Gujarat, India

J. K. Patel
Nootan Pharmacy College, Sankalchand Patel University, Visnagar, Gujarat, India

D. H. Patel
Parul Institute of Pharmacy and Research, Faculty of Pharmacy, Parul University, Vadodara, India

J. K. Patel, Y. V. Pathak (eds.), *Emerging Technologies for Nanoparticle Manufacturing*,
https://doi.org/10.1007/978-3-030-50703-9_12

1 Introduction

Current advances in drug development research arise from the multidisciplinary research by association of scientists from various fields such as chemistry, biology, pharmacology, medicine and engineering. Similar to such research for new active substances, controlled drug delivery technology represents one of the front-line areas of science, which also involves multidisciplinary scientific approach (Patil 2016). In particular, the involvement of nanoscience and physical chemistry of colloids seems very decisive, but the concepts proposed in nanotechnology have been executed to the profound limitation of the pharmaceutical applications. Much focus has been given to novel modes of drug administration because the most commonly used pills, tablets and parenteral solution were inadequate for many active pharmaceutical ingredients. The technological advances in nanotechnology make it more technical and accurate with a touch of interdisciplinary effect (Ahmad et al. 2012). Polymeric nanoparticles are defined as submicron (1–1000 nm) colloidal particles comprising active pharmaceutical ingredients encapsulated within or adsorbed to macromolecular polymer system (Chang 1992). The drug is dissolved, entrapped, encapsulated or attached to a nanoparticle matrix. Nanoparticles, nanospheres or nanocapsules can be obtained depending upon the use of manufacturing technique. Nanoparticles are carriers in which the drug is enclosed by a suitable polymeric membrane, whereas nanospheres are matrix carrier in which the drug is distributed homogenously as matrix (Catarina et al. 2006). Many types of drug delivery systems, namely, emulsions, gels, aqueous suspensions of microgel particles, liposomes and solid lipid particles, have been widely investigated. Polymeric colloidal carriers made of biocompatible polymers offer many technical advantages in terms of stability, processability and versatility for various applications (Domenico et al. 2019). These kind of delivery systems present numerous benefits to the physician and the patient compared to conventional dosage forms, which mainly include reduced toxicity, enhanced stability of the active substance, more encapsulation of drug and slow delivery rates that allow spacing out the doses or reducing concentration of active substance in the formulation; these advantages result in improved efficacy with decreased side effects, patient compliance and convenience (Brannon-Peppas and Blanchette 2004). These are the reasons why polymeric particulate carriers are most widely used in drug delivery technology. Passive and active drug targeting can be achieved by controlling particle magnitude including size and surface properties. Nanoparticles offer some specific advantages to increase the stability of active pharmaceutical ingredient (API) and retain useful modified release characteristics. The benefits of nanoparticles as a nanocarrier include (Mohanraj and Chen 2006) enhanced therapeutic value and reduced toxic effects; controlled or sustained release of drug; high drug loading; achievement of site-specific targeting by developing magnetic nanoparticle; suitable for various routes including ocular, oral, nasal and parenteral; and because of larger surface area, rapid dissolution of drug in body fluids, such as the human body with rapid absorption and more bioavailability.

2 Commonly Used Polymers for Nanoparticles

The general polymers used to manufacture nanoparticles should be biodegradable, biocompatible and non-toxic and should not give any type of antigenic effect (Yu et al. 2016).

2.1 Natural Polymers

The mostly natural-occurring polymers are used to prepare nanoparticles like albumin, chitosan, gelatin and sodium alginate.

2.2 Synthetic Polymers

Polyvinyl alcohol (PVA), polylactides, poly(lactic-co-glycolic acid) (PLGA), polygly-

colides, polyacrylic acid, polyacrylamide, polyglutamic acid, polymalic acid, polymethyl methacrylate, polyethylene glycol and polymethacrylic acid are some the commonly used synthetic polymers.

3 Mechanisms of Drug Release from Nanoparticles

The overall performance of nanoparticle is governed by capacity of a nanoparticle to release encapsulated drug. The polymeric nanoparticles release the drug when it reaches the targeted site by following the three mechanisms: (1) diffusion of drug molecule due to the swelling of the polymer nanoparticles by hydration, (2) rupture of the polymer at site of action by an enzymatic action resulting in releasing the drug from the encapsulated inner core and (3) desorption of surface adhered drug at the targeted site from the hydrated and swelled nanoparticles (Gi-Ho et al. 2017). Various nanoparticle properties like particle size, charge on the surface and its shape handle critical roles in generating actual functional drug delivery system by various mechanisms.

3.1 Effect of Particle Size

Size of nanoparticle play vital role in cell interaction, degradation and elimination of nanoparticle. The main focus of controlling particle size is avoidance of reticuloendothelial system (RES) uptake for degradation. By avoiding RES circulation time, the bioavailability of nanoparticles can be increased (Couvreur et al. 1995). Desai et al. (1996) studied that nanoparticle uptake of an in situ rat intestinal loop model demonstrated 15- to 250-fold increase in cellular uptake of small size nanoparticle when compared with larger microparticles.

3.2 Effect of Particle Charge

Stability of nanoparticle can be influenced by presence of charge on the surface of nanocarriers. A highly charged system offers more gradation of repulsion force between similar particles. This generated repulsive force leads to stabilization of nanoparticles and prevents aggregation (Nagavarma et al. 2012). Nanoparticles formulated with more evidential surface charges have shown to be more stabilize nanoparticle and prevent its further aggregation.

3.3 Effect of Particle Shape

Particle shape has been identified as a new physical parameter which has exerted tremendous impact on cellular uptake and biodistribution. A recent study has identified that there is a lower uptake of nanoparticle by macrophages due to its oblate shape which favours more circulation in the blood. Afterwards, this enhances the residence of nanoparticles in the blood and increases their probabilities of attaining their target site. Besides macrophages, the nanoparticle shape also favours endocytosis by normal and cancer cells (Sahay et al. 2010).

4 Methods for Preparation of Nanoparticles

Nanocarriers can be produced from various materials like natural polymer including polysaccharides and proteins, as well as by using synthetic polymers. The choice of polymeric materials depends on critical factors like (a) size of nanoparticles, (b) drug properties like solubility and stability in water, (c) surface characteristics such as surface charge and penetrability, (d) ability of biodegradation with good biocompatibility and less toxicity and (e) expected drug release pattern (Pathak and Thassu 2009). Nanoparticles can be obtained either by polymerization reactions or by dispersion of preformed polymers, either natural or synthetic. From literature, it was found that emulsion polymerization is the most frequently used polymerization method to produce nanoparticles but is less used for the purpose of encapsulation and drug delivery. Studies have been carried out on polyalkyl cyanoacrylate

nanoparticles which are prepared by emulsion polymerization processes. Other techniques like nano-encapsulation techniques using preformed polymers are preferable due to the toxic effects of residual substance present after a polymerization reaction and also adverse reaction with drug (Tiwari et al. 2012). The knowledge of proper selection of the nanoparticle manufacturing methods is a key issue for the research scientist who is involved with drug delivery research and development. Some preparation methods have been specifically developed for the manufacturing of nanoparticles from natural macromolecules or preformed synthetic polymers due to their easy implementation and lower toxicity potential. Most novel and widely used methods to prepare polymeric nanoparticles are solvent emulsification diffusion process and solvent emulsification evaporation method.

4.1 Emulsification Solvent Diffusion Process

4.1.1 Introduction

This is the most widely used method for preparation of nanoparticles. In this technique, all the ingredients that are required in the final dispersed phase are solubilized in an organic solvent. The organic solvent is chosen such that it is partially soluble in water and the aqueous system is consequently saturated with the organic phase so as to keep the thermodynamic partition equilibrium of the dispersed and dispersing phases (Allemann et al. 1993). The selected polymer and the drug are dissolved in a water-immiscible organic phase and further saturated with water to ensure the thermodynamic equilibrium of both solvent systems. Successively, saturated solvent phase containing polymer-water is emulsified in an aqueous solution containing stabilizer such as polyvinyl alcohol in water which leads to solvent diffusion to the external phase and the formation of nanoparticles in solvent phase (Petros and DeSimone 2010), as shown in Fig. 12.1. Once there is a formation of emulsion, then emulsified droplets are diluted in water which leads to an interaction between emulsion droplets and dilution phase, which further leads to the precipitation of polymer due to poor solvency of polymer. In this method two possible mechanisms observed in the formation of nanoparticle are mechanism due to mechanical means and the particle formation from droplet of emulsion (Zaida Urbán et al. 2010).

4.1.2 Mechanism

Emulsion of droplet size 2–5 μm was obtained by emulsification of oil and water using mechanical shear. Successively, the slow diffusional motion of water-immiscible solvents into the aqueous phase takes place, and precipitation of polymer starts until it reaches limiting concentration for polymer; phase separation occurs from the interface. Thus, each emulsion droplet forms individual polymer nanoparticle when the solvent is extracted (Feng et al. 2010). In general, good emulsion homogenization such as in ultrasonication produces droplets with a diameter < 0.5 μm, and thus, a similar size is yielded for nanoparticles (Brannon-Peppas and Blanchette 2004).

Mechanical Mechanism

Quintanar-Guerrero et al. (2005) had proposed the mechanical approach to prepare the nanoparticle using emulsification solvent diffusion method and using principle of polymer precipitation and interfacial phenomenon. In this method, strong interfacial tension difference cannot be determined by variation of interfacial concentration due to partial water miscibility of solvent and saturation level by water to maintain equilibrium during emulsification stage. Higher concentration of stabilizing agent in this method will drastically reduce the interfacial tension which reduces the globule size up to significant level. It is also mentioned that interface between hydrophilic and lipophilic phase is exposed to high mechanical force in the process of emulsification. Shear force leads to increase in energy in molecules, and the presence of surfactant plays important role in controlling the size of nanoparticle. After complete diffusion of solvent, submicron particle will be formed if stabilizing agent is present at liquid interface (Murthy 2007).

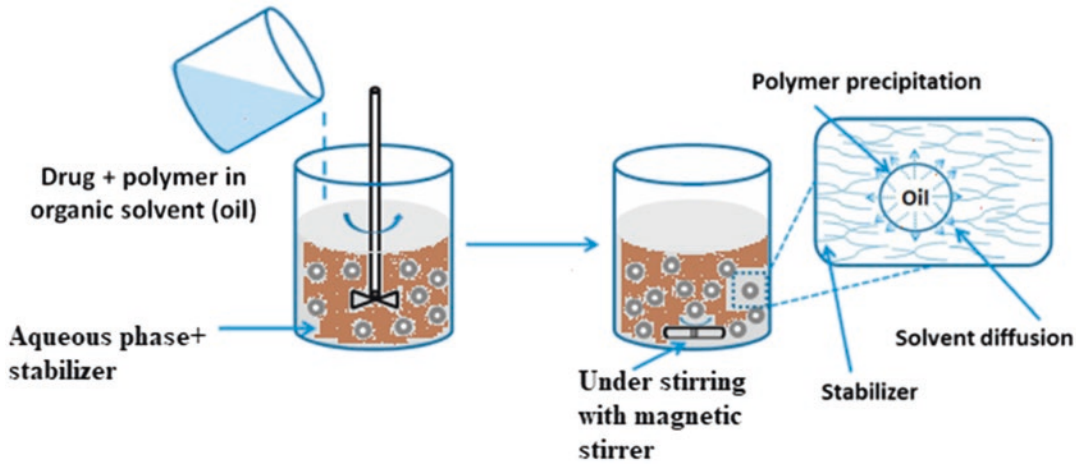

Fig. 12.1 Nanoparticle by emulsification solvent diffusion method

Formation of Particle from Emulsion Droplet

Galindo-Rodriguez et al. (2004) supported the mechanism of particle formation by this approach. It was suggested that particle size is always less than emulsion droplet. The droplet formation in organic phase was given by binary break-up mechanism in which the droplet is continuously broken down in two possible fragments until hydrodynamic condition is achieved. Also droplet formation was governed by capillary disruption in which droplet is strained to produce elongated filaments which further convert to fragment depending upon capillary number. To obtain controlled particle size, many processing parameters need to be controlled like temperature, stirring speed, stirring time, organic to aqueous phase ratio and also order of phase mixing. Aubrey et al. (2017) studied the effect of order of mixing of different phase on particle size. When organic phase was added drop wise to the aqueous phase decrease the particle size.

4.1.3 Effect of Various Factors on Controlling Size of Particles

Nature of Polymer

Nature and type of polymer highly stimulates the size and stability of nanoparticle prepared by emulsification solvent diffusion method. Zeta potential of particle is always negative if it is prepared by non-ionic stabilizing agent due to availability of carboxylic acid group in the surface of particle (Zhang et al. 2008). When the concentration of polymer is high, different behaviours are observed due to difference in molecular size and molecular arrangement. If polymer concentration is too high, then it leads to increase in particle size of particle; it may be due to the increase in viscosity which leads to Ostwald's ripening.

Effect of Stabilizing Agent

Stabilizing agent plays a key role in controlling physical stability dispersion containing submicron-level particles. Concentration and nature of stabilizing agent affect the size and stability of the particle. Stabilizing agent plays a key role as surfactant in the formation of emulsion droplet and shape formation governed by the presence of stabilizer. Stabilizing agent lowers interfacial tension between aqueous and organic phase by adsorption on the interface of solvent phase formed during emulsification step which leads to the decrease in particle size. The remaining quantity is used for preventing aggregation during dilution phase by steric, electrostatic and electro-steric effect (Xu et al. 2013).

Effect of Solvent

Solvent influences particle size and zeta potential of submicron particles. Murakami et al. (2000) suggested that particle size and yield of particles are highly influenced by affinity of polymer towards solvent. Solubility parameter and interaction parameter are used for studying the behaviour of the particle system. Lower solvent-water interaction parameter means higher solvent-water affinity for solvent diffusion. However, more polymer-solvent interaction parameter facilitates solvent diffusion. Thus, major affinity of polymer and solvent as well as solvent-water leads to larger particle size. Higher affinity of polymer solvent causes difficulty in solvent diffusion which causes insufficient solvent migration towards the external phase. Thus, particle size seems to be larger. Many physicochemical properties of solvent like surface tension, viscosity, density and water solubility affect particle size. Lower values of all these properties lower the particle size. Precipitation of particle is due to different molecular arrangement of polymeric chain obtained, depending upon solvent used. Typical organic solvents that are partially soluble in water are those of medium polarity like ethyl acetate, methyl ethyl ketone, benzyl alcohol and propylene carbonate (McNamara and Tofail 2017). Many researchers have developed nanoparticle using this emulsification solvent diffusion as shown in Table 12.1.

4.1.4 Advantages and Disadvantages

This technique gives many advantages like more encapsulation capacity compared to other method of manufacturing with no requirement for homogenization. It also gives higher batch-to-batch reproducibility with ease of scale-up, simplicity and narrow size distribution. This process allows a precise control of particle size that is difficult with other usual method of preparation of nanoparticles like nano-precipitation. Major limitation of using this technique is leakage of water-soluble drug into the external phase during emulsification which may reduce encapsulation efficiency (Kudr et al. 2017).

4.2 Emulsification Solvent Evaporation Method

4.2.1 Introduction

From the different processes for manufacturing nanoparticle, the emulsification solvent evaporation method is well recognized. It is a method with huge popularity because of its easiness, and it mainly allows effective encapsulation of various compounds which are lipophilic in nature. Emulsification solvent evaporation involves two steps. The first one consists of the dissolution of the polymer and the drug in a volatile organic solvent. In the past, dichloromethane and chloroform were frequently used, but these have now been replaced by ethyl acetate to minimize residual solvent toxicity concerns. Initially there is an aqueous phase used for emulsification of the polymer. During the second step, polymer solvent is evaporated, which leads to polymer precipitation on a central core to give nanoparticles as shown in Fig. 12.2. The nanoparticles are collected by ultracentrifugation and washed with distilled water to remove stabilizer residue or any free drug and lyophilized for storage (Liu et al. 2008). Recently modification takes place in this method which is known as high-pressure emulsification, followed by solvent evaporation method. This method involves first preparation of emulsion followed by homogenization using high pressure, and further it is subjected to stirring to evaporate organic solvent. Various parameters like type and amount of dispersing agent, stirring rate, temperature and viscosity of both organic and aqueous phases highly influence the size of particle. Conversely this method can be applied to lipophilic drugs, and restrictions are enforced by the scale-up issue.

4.2.2 Mechanism of Formation of Nanoparticles

Mechanism of nanoparticle formation depends on type of polymer used for preparation. Coalescence of single or multiple droplets is observed in emulsion during preparation of nanoparticle. Then it is followed by stabilization using surfactant during solvent evaporation (Moinard-Chécot et al. 2008). When ethyl cellu-

Table 12.1 Drug, polymer, stabilizer and solvent used for emulsification solvent diffusion process

Sr. no.	Name of drug	Polymer	Stabilizer	Solvent	Size	References
1	Meso-tetra(hydroxyphenyl) porphyrin	PLGA (p-THPP	PVA	Dichloromethane	200 nm	Konan et al. (2003)
2	Doxorubicin	PLGA	PVA	Ethyl acetate, methanol	180 nm	Pieper et al. (2017)
3	Cyclosporine (cy-A-)	Glyceryl behenate (Compritol® ATO 888)	Lauroyl macrogolglycerides (Gelucire® 44/14)	Ethyl acetate	280 nm	Zaida Urbán (2010)
4	Lecithin and taurodeoxycholic acid sodium salt	Glyceryl monostearate	–	Benzyl alcohol	250 nm	Trotta et al. (2003)
5	Blank	PLA	PVA	Polycarbonate	212	Quintanar-Guerrero et al. (1997)
6	Omapatrilat	PLA	Poloxomer 188	Ethyl acetate	170 nm	Tamayo-Esquivel et al. (2006)
7	Docetaxel	Lecithin	PEG 2000	Chloroform	230 nm	Nijaporn et al. (2009)
8	Curcumin	PLGA	PVA	Ethylene (ETH), acetone (ACE)	180 nm	Cen et al. (2014)
9	Clobetasol propionate	Monostearin	Poloxamer 188	N hexane	250 nm	Yuan et al. (2008)
10	Rifampicin	Polycaprolactone	Pluronic F68	Ethyl acetate	100 nm	Mi-Yeon et al. (2009)
11	Blank	Poly(ε-caprolactone)	Polyvinyl alcohol	Ethyl acetate	260 nm	Asim et al. (2012)
12	Oestrogen	Poly(D,L-lactide-co-glycolide) (PLGA)	Didodecyldimethylammonium bromide (DMAB)	Propylene carbonate (PC)	100 nm	Hye-Young et al. (2001)
13	*Cymbopogon citratus*	PLGA	PVA	DCM	280 nm	Kessiane et al. (2019)
14	Insulin	HPMC	PVA	Acetone	183 nm	Fang et al. (2019)
15	Sertaconazole	Stearic acid	Labrafac	Ethanol: acetone	272 nm	Naser et al. (2019)
16	Tretinoin	Glyceryl monostearate, Compritol 888 ATO®, Dynasan 116® and Cutina CBS®	Epikuron 200®, Tween 20 and Tween 80	Benzyl alcohol	230 nm	Weissig and Elbayoumi (2019)

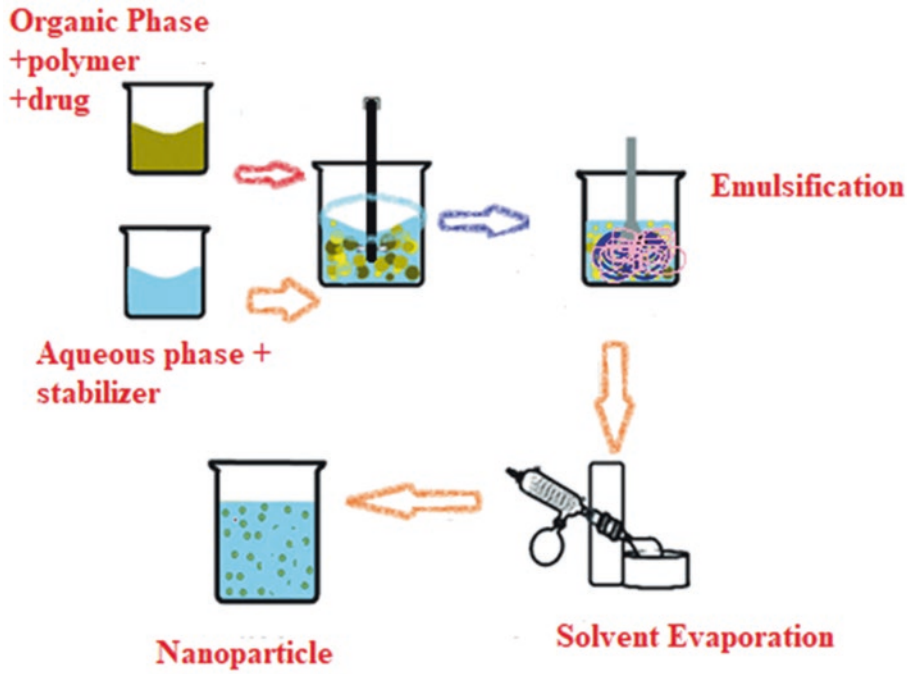

Fig. 12.2 Nanoparticle by emulsification solvent evaporation method

lose (EC) was used, emulsion droplet starts to coalescence before obtaining stable nanoparticle which is free from any traces of solvent during evaporation, and nanoparticles were generated from several droplets. In contrast, when polylactic acid (PLA) was employed, limited or no coalescence occurred; therefore, a nanoparticle was formed from a single droplet. Differences were attributed to the surface activity properties of the polymers; EC is surface active, whereas PLA has no interfacial adsorption. The major disadvantage of emulsification solvent evaporation is its poor efficiency in the incorporation of hydrophilic drugs such as peptides, proteins and genetic material (Vanderhoff et al. 1979). Many researchers have developed nanoparticle using emulsification solvent evaporation as shown in Table 12.2.

4.2.3 Factors Influencing Nanoencapsulation Process

Various factors affect final nanoparticles obtained including (a) solubility of the drug, (b) type and concentration of polymer, (c) the ratio of drug/polymer, (d) the organic solvent utilized, (e) concentration and nature of stabilizer utilized, (f) stirring speed and temperature of the emulsification process and (g) the volume and viscosities of the dispersed and continuous phases (Paliwal et al. 2014). Manipulation of these variables has been shown possible to optimize nanoparticle size and maximize efficiency of encapsulation as shown in Fig. 12.3.

Type of Polymer

Copolymers of lactic and glycolic acids (PLGA) are the most frequently used polymer to prepare nanocarrier systems due to their safety profile and Food and Drug Administration (FDA) approvals in humans. Non-biodegradability and biocompatibility property make successful use of drug carriers, like ethyl cellulose (EC) and polymethyl methacrylate. The selection of polymer used depends on the anticipated drug release pattern, which is mostly controlled by physical and chemical properties of polymer system (Khinast et al. 2013). If a single polymer system is unable to provide satisfactory drug release, then copolymer is manufactured from two individually different polymers. The characteristics of the

Table 12.2 Drug, polymer, stabilizer and solvent used for emulsification solvent evaporation process

Sr. no.	Drug	Polymer	Stabilizer	Solvent	Particle size	References
1	Paclitaxel	PLGA and vitamin E TPGS	PVA, Poloxomer 188	Dichloromethane	230 nm	Navneet et al. (2016)
2	Ketoprofen	Eudragit E100 Eudragit RS 100	PVA	Acetone	120 nm	Le Thi (2012)
3	Aceclofenac	Ethyl cellulose	PVA	Dichloromethane	10 um	Gupta et al. (2013)
4	Rifampicin	PLGA	PVA	Dichloromethane	360 nm	Tripathi et al. (2010)
5	Haemagglutinin (HA)	PLGA	PVA	Dichloromethane	216 nm	Lemoine and Preat (1998)
6	Zidovudine	PLA	PVA	Methylene chloride	320 nm	Mainardes et al. (2010)
7	Progesterone	Poly(hydroxybutyrate-co-hydroxyvalerate), poly(ε-caprolactone) poly(L-lactic acid)	PEG	Chloroform	140 nm	Fernanda et al. (2015)
8	Ketoprofen	Eudragit E100	Sodium dodecyl sulphate	Chloroform	150 nm	Le Thi (2009)
9	Levofloxacin	Poly(lactic-co-glycolic acid) (PLGA) and chitosan (CS)	PVA	Dichloromethane	430 nm	Manuel et al. (2019)
10	Praziquantel	Poly(D,L-lactide-co-glycolide) (PLGA)	PVA	Methylene chloride		Rubiana et al. (2006)
11	Dexamethasone	PLGA	PVA	Acetone		Seda et al. (2019)

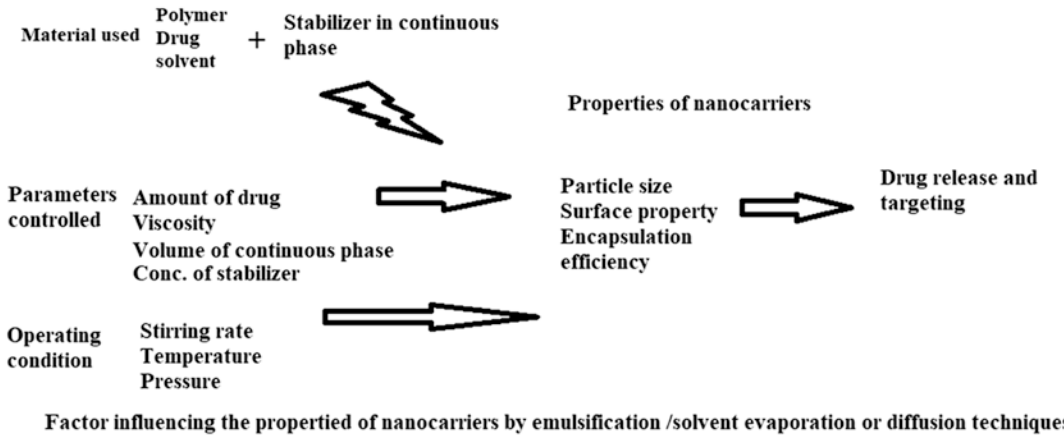

Fig. 12.3 Factors affecting nanoparticle properties using emulsification solvent evaporation

copolymer are enhanced because it consists of two segments on the chain like PLGA.

The Organic Solvent

Emulsification solvent evaporation has some specific selection criteria for solvent like ability to dissolve the chosen polymer and having poor solubility in the external phase; solvent with high volatility, low toxicity and a low boiling point is expected. Methylene chloride is the most effective solvent for the preparation of nanoparticle because of its rapid evaporation which may be due to low boiling point and also high level of immiscibility with water. More solvent evapora-

tion rate of methylene chloride may be due to high vapour pressure compared to other solvents. Chloroform was frequently used earlier but it is progressively substituted by methylene chloride due to its toxicity and relatively low vapour pressure. The commonly used solvents in this method are dichloromethane (DCM) and ethyl acetate. Other more toxic solvents used are chloroform and acetonitrile. When single organic solvent is not able to solubilize the drug, a mixture of solvent is required; the most commonly used solvent mixture is DCM-ethanol (Sovan et al. 2011).

Concentration and Type of Stabilizer

The surfactant is normally engaged in the distribution of aqueous phase in to its immiscible phase and for the maintenance of equilibrium condition in emulsion. It diminishes the surface tension of external phase, prevents the amalgamation and accumulation of drops and stabilizes the emulsion. A selection of proper surfactant is able to give nanoparticle of a regular size and a controlled particle size distribution, with a more expectable and stable drug release. Depending upon nature of the hydrophilic part of surfactant molecule, they are classified as non-ionic, anionic, cationic and amphoteric. For the mostly prepared emulsion using methylene chloride/water, typical non-ionic stabilizers like partially hydrolysed PVA, methylcellulose, tweens and spans as well as anionic surfactant like sodium dodecyl sulphate were used (Rao and Geckeler 2011). Commonly used stabilizers include polyvinyl alcohol (PVA), poloxamer 127, poloxamer 188 and polysorbate 80 among others.

Stirring Speed and Temperature of the Emulsification Process

Speed of stirring will control the particle size and its uniformity. The solvent evaporation rate can be enhanced either by increasing the temperature of the continuous phase or by reducing the use of vacuum to reduce pressure in the reactor.

The Volume and Viscosities of the Dispersed and Continuous Phases

Viscosity of dispersed phase was proportionally related to the polymer concentration and the molecular weight. Increasing viscosity also improves entrapment efficiency and size also. Polymers used in this method are PLGA, polyglycolic acid (PGA), PLA, ethyl cellulose (EC), cellulose acetate phthalate (CAP), polycaprolactone (PCL), poly(hydroxybutyrate) (PHB) and poly(β-hydroxybutyrate) (PBHB) (Mody et al. 2010).

5 Advanced Emulsification Techniques

5.1 Membrane Emulsification

In high-pressure homogenization and ultrasonication, there is a stability issue of potential candidate due to high-energy input which leads to the progress of membrane emulsification solvent evaporation method. This method combined emulsification by low-energy conventional process and premix membrane emulsification has been proposed. The coarse emulsion obtained by low-speed stator homogenization is extruded through membrane under excess pressure to form uniform-sized nanoparticles. In premix membrane emulsification process for nanoparticle preparation, the size of the coarse emulsions was reduced to nanoscale due to high transmembrane pressure which leads to droplet disruption. The most commonly used membranes for oil-in-water emulsions are hydrophilic Shirasu porous glass (SPG) membranes and for water-in-oil emulsions polytetrafluoroethylene (PTFE) membranes. The solvent present in the nanoemulsion is removed either by prolonged stirring or evaporating under vacuum conditions. The solvent commonly used is ethyl acetate due to its relatively high boiling point. SPG membrane pore size is critical to the manufacturing of uniformly sized nanoparticles. Droplet size can be controlled by the membrane type, the crossflow velocity and the transmembrane pressure; with increased transmembrane pressure, small-sized particles with narrow-sized distribution were obtained. Advantages of this modification cover narrow-sized distribution of nanoparticle and high productivity, simplicity and suitability for synthetic and natural polymers (Liu et al. 2010). Biodegradable materials such as

poly(lactic-co-glycolic acid) (PLGA), polycaprolactone (PCL), sodium alginate, chitosan, polylactide (PLA), Eudragit, etc. are employed.

Qiang Weim et al. (2008) had developed nanoparticles by a simplistic method combining premix membrane emulsification followed by solvent removal for the first time. Initially there is a preparation of coarse emulsions, additional premix membrane emulsification with very high pressure was employed to achieve uniform-sized nanodroplets, and nanoparticles were formed by further solidification. Polylactide was designated as a model polymer. Type of organic solvent, the volume ratio of oil phase and external water phase, pore size of the microporous membrane and transmembrane pressure played key roles for the size of nanoparticle. The novel method also has the advantages of high productivity, simplicity and easy scale-up.

5.2 High-Pressure Emulsification

The nanometric size of the emulsion droplet is controlled by applying high-shear forces usually by high-speed stirring or ultrasonication. Another way to obtain very-small-sized oily globules is by means of a high-pressure homogenizer. In general, the high-pressure emulsification and solvent evaporation method consist of forming a coarse emulsion with the polymer and the drug in an organic solvent and an aqueous solution with a stabilizer agent; this emulsion is transferred into a high-pressure homogenizer, and the emulsification is performed at high pressure by recycling the emulsion by several cycles (Jaiswal et al. 2004). High-pressure emulsification has been employed to prepare pharmaceutical nanoemulsions.

Lamprecht et al. (1999) investigated nanoparticles as effective drug carriers for biological proteins. The bovine serum albumin is a hydrophilic protein which is incorporated within NP. The double emulsification has been chosen due to high solubility of the protein in water using a Microfluidizer as homogenization device with PLGA and PCL polymer and has been used for the preparation of the nanoparticles. The bovine serum albumin encapsulation was high up to 80%, and drug release pattern was categorized by a significant initial rapid release for both PLGA and PCL nanoparticle. An increased release rate was attained at the last dissolution study for PLGA nanoparticle up to 92% compared with PCL nanoparticle up to 72%.

5.3 Microchannel Emulsification

Microchannel technology was proposed to prepare tiny microchannels embedded in silicon plate. Emulsified droplets are formed by pushing the dispersed phase through the microchannels. Microchannel emulsification decreases interfacial tension, which is the driving force for formation of droplets (Kawakatsu et al. 1997).

Sugiura et al. (2004) developed aqueous multiple emulsion by double emulsification using microchannel emulsification in second step. They used a high-speed homogenizer for the initial phase of emulsification step due to low output rate of microchannel emulsification.

6 Conclusion

The major aim of this chapter is to highlight the different manufacturing techniques accessible for manufacturing of nanoparticles. It was perceived that among the various possible available methods, nanoparticle requires a suitable selection of technique. Depending on the physical and chemical properties of a drug, it is promising to select the most suitable method for manufacturing and a suitable polymer to produce nanoparticles with preferred particle size with good drug loading efficiency. Methods used to prepare nanoparticle like emulsification solvent diffusion and solvent evaporation are simple, and they rely on the use of pharmaceutically acceptable solvents, biocompatible polymers and surfactants. The versatility of both these methods is demonstrated by the use of modified polymers to enable the production of modified nanoparticle with control particle size and targetability. Reports on the scale-up and production of large batches of nanoparticles in a reproducible way using emulsification solvent diffusion and evaporation are expected to increase.

References

Ahmad MU, Ali SM, Ahmad I. Applications of nanotechnology in pharmaceutical development. In: Lipids in nanotechnology; Academic Press and AOCS Press, USA, 2012. p. 171–90.

Allemann E, Gurny R, Doekler E. Drug-loaded nanoparticles preparation methods and drug targeting issues. Eur J Pharm Biopharm. 1993;39:173–91.

Asim U, Shahid N, Naveed R. Selection of a suitable method for the synthesis of copper nanoparticles. Nano. 2012;7(5):18.

Aubrey E, et al. Enhanced cellular uptake of size-separated lipophilic silicon nanoparticles. Sci Rep. 2017;7:Article number: 43731.

Brannon-Peppas L, Blanchette JO. Nanoparticle and targeted systems for cancer therapy. Adv Drug Deliv Rev. 2004;56(11):1649–59.

Catarina PR, Ronald JN, Antonio JR. Nano capsulation 1. Method of preparation of drug – loaded polymeric nanoparticles. Nano Technol Biol Med. 2006;2:8–21.

Cen C, et al. A modified spontaneous emulsification solvent diffusion method for the preparation of curcumin-loaded PLGA nanoparticles with enhanced in vitro anti-tumor activity. Front Mater Sci. 2014;8(4):332–42.

Chang TMS, Microcapsules and nanoparticles in medicine and pharmacy, edited by M. Donbrow, CRC Press, London; 1992. p. 323.

Couvreur P, Dubernet C, Puisieux F. Controlled drug delivery with nano particles: current possibilities and future trends. Eur J Pharm Biopharm. 1995;41:2–13.

Desai MP, Labhasetwar V, Amidon GL, et al. Gastrointestinal uptake of biodegradable microparticles: effect of particle size. Pharm Res. 1996;13(12):1838–45.

Domenico L, Mikhail AK, Maria TC. Smart nanoparticles for drug delivery application: development of versatile nanocarrier platforms in biotechnology and nanomedicine. J Nanomater. 2019; Article ID 3702518, 26 pages

Fang Y, et al. Gastrointestinal responsive polymeric nanoparticle for oral delivery of nanoparticle, characterization and in vivo evaluation. J Pharm Sci. 2019;108:2994–3002.

Feng X, Lv F, Liu L, et al. Conjugated polymer nanoparticles for drug delivery and imaging. Appl Mater Interfaces. 2010;2(8):2429–35.

Fernanda VL, et al. Characterization of progesterone loaded biodegradable blend polymeric nanoparticles. Ciência Rural. 2015;45(11):2082–8.

Galindo-Rodriguez S, Allémann E, Fessi H, Doelker E. Physicochemical parameters associated with nanoparticle formation in the salting-out, emulsification-diffusion, and nanoprecipitation methods. Pharm Res. 2004;21:1428–39.

Gi-Ho S, Beom JL, Cheong WC. Mechanisms of drug release from advanced drug formulations such as polymeric-based drug-delivery systems and lipid nanoparticles. J Pharm Investig. 2017;47:287–96.

Gupta J, Mohan G, Prabakaran L, Gupta R. Emulsion solvent diffusion evaporation technique: formulation design optimization and investigation of aceclofenac loaded ethyl cellulose microspheres. Int J Drug Dev Res. 2013 October–December;5(4):336–49.

Hye-Young K, Jun-Young L, Sung-Wook C, Yangsoo J, Jung-Hyun K. Preparation of PLGA nanoparticles containing estrogen by emulsification–diffusion method. Colloids Surf A Physicochem Eng Asp. 2001;182:123–30.

Jaiswal J, Gupta SK, Kreuter J. Preparation of biodegradable cyclosporine nanoparticles by high-pressure emulsification-solvent evaporation process. J Control Release. 2004;96:169–78.

Kawakatsu T, Kikuchi Y, Nakajima M. Regular-sized cell creation in microchannel emulsification by visual microprocessing method. J Am Oil Chem Soc. 1997;74:317–21.

Kessiane BA, et al. PLGA nanoparticles optimized by Box-Behnken for efficient encapsulation of therapeutic Cymbopogon citratus essential oil. Colloids Surf B: Biointerfaces. 2019;18:935–42.

Khinast J, Baumgartner R, Roblegg E. Nano-extrusion: a one-step process for manufacturing of solid nanoparticle formulations directly from the liquid phase. AAPS Pharm Sci Tech. 2013;14(2):601–4.

Konan YN, Berton M, Gurny R, Allémann E. Enhanced photodynamic activity of meso-tetra(4-hydroxyphenyl)porphyrin by incorporation into sub-200 nm nanoparticles. Eur J Pharm Sci. 2003;18(3–4):241–9.

Kudr J, Haddad Y, Richtera L, Heger Z, Cernak M, Adam V, et al. Magnetic nanoparticles: from design and synthesis to real world applications. Nano. 2017;7(9):243.

Lamprecht A, Ubrich N, Pérez MH, Lehr C-M, Hoffman M, Maincent P. Biodegradable monodispersed nanoparticles prepared by pressure homogenization-emulsification. Int J Pharm. 1999;184(1):97–105.

Le Thi MH. Preparation of drug nanoparticles by emulsion evaporation method. APCTP–ASEAN workshop on advanced materials science and nanotechnology. J Phys Conf Ser. 2009;187:012047.

Le Thi MH. Preparation and characterisation of nanoparticles containing ketoprofen and acrylic polymers prepared by emulsion solvent evaporation method. J Exp Nanosci. 2012;7(2):189–97.

Lemoine D, Preat V. Polymeric nanoparticles as delivery system for influenza virus glycoproteins. J Control Release. 1998;54:15–27.

Liu Z, Jiao Y, Wang Y, Zhou C, Zhang Z. Polysaccharides-based nanoparticles as drug delivery systems. Adv Drug Deliv Rev. 2008;60(15):1650–62.

Liu W, Yang X, Ho WWS. Preparation of uniform-sized multiple emulsions and micro/nano particulates for drug delivery by membrane emulsification. J Pharm Sci. 2010;100:75–93.

Mainardes RM, et al. Intranasal delivery of zidovudine by PLA and PLA-PEG blend nanoparticles. Int J Pharm. 2010;395:266–71.

Manuel LL, et al. Optimized preparation of levofloxacin loaded polymeric nanoparticles. Pharmaceutics. 2019;11:1–13.

McNamara K, Tofail SAM. Nanoparticles in biomedical applications. Adv in Phys X. 2017;2(1):54–88.

Mi-Yeon L, et al. Development of a novel nanocapsule formulation by emulsion-diffusion combined with high hydrostatic pressure. J Microencapsul. 2009;26(2):122–9.

Mody VV, Siwale R, Singh A, et al. Introduction to metallic nanoparticles. J Pharm Bioallied Sci. 2010;2(4):282–9.

Mohanraj VJ, Chen Y. Nanoparticles – a review. Trop J Pharm Res. 2006;5(1):561–73.

Moinard-Chécot D, Chevalier Y, Briançon S, Beney L, Fessi H. Mechanism of nanocapsules formation by the emulsion–diffusion process. J Colloid Interface Sci. 2008;317:458–68.

Murakami H, et al. Further application of a modified spontaneous emulsification solvent diffusion method to various types of PLGA and PLA polymers for preparation of nanoparticles. Powder Technol. 2000;107(1-2):137–43.

Murthy SK. Nanoparticles in modern medicine: state of the art and future challenges. Int J Nanomedicine. 2007;2(2):129–41.

Nagavarma BVN, Hemant KS, Yadav A, Vasudh LS, Shivakumar HG. Different techniques for preparation of polymeric nanoparticles – a review. Asian J Pharm Clin Res. 2012;5(3):16 23.

Naser T, et al. Thermosensitive hydrogel containing sertaconazole loaded nanostructured lipid carriers for potential treatment of fungal keratitis. Pharm Dev Technol. 2019;24(7):891–901.

Navneet S, Parshotam M, Senshang L. Effect of process and formulation variables on the preparation of parenteral paclitaxel-loaded biodegradable polymeric nanoparticles: a co-surfactant study. Asian J Pharm Sci. 2016;11:404–16.

Nijaporn Y, Brian RS, Zhengrong C. Nanoparticles engineered from lecithin-in-water emulsions as a potential delivery system for docetaxel. Int J Pharm. 2009 September 8;379(1):174–80.

Paliwal R, Babu RJ, Palakurthi S. Nanomedicine scale-up technologies: feasibilities and challenges. AAPS Pharm Sci Tech. 2014;15(6):1527–34.

Pathak Y, Thassu D. Drug delivery, nanoparticles, formulation and characterization. In: Pathak Y, Thassu D, Swarbrick J, editors. Drugs and the pharmaceutical sciences. New York: Informa Healthcare; 2009. p. 394.

Patil J. Multidisciplinary research opportunities: need of the hour. J Pharmacovigil. 2016;4:147.

Petros RA, DeSimone JM. Strategies in the design of nanoparticles for therapeutic applications. Nat Rev Drug Discov. 2010;9(8):615.

Pieper S, et al. Doxorubicin loaded PLGA nanoparticle – a systemic evaluation for preparation technique and evaluation. Mater Today Proc. 2017;4:S188–92.

Quing W, et al. Uniform size PLA nanoparticle: preparation by premix membrane emulsification. Int J Pharm. 2008;359:294–7.

Quintanar-Guerrero D, Allemann E, Doelker E, Fessi H. A mechanistic study of the formation of polymer nanoparticle by the emulsification-diffusion technique. Colloid Polym Sci. 1997;275:640–7.

Quintanar-Guerrero D, Tamayo-Esquivel D, Ganem-Quintanar A, Allémann E, Doelker E. Adaptation and optimization of the emulsification – diffusion technique to prepare lipidic nanospheres. Eur J Pharm Sci. 2005;26(2):211–8.

Rao JP, Geckeler KE. Polymer nanoparticles: preparation techniques and size-control parameters. Prog Polym Sci. 2011;36:887–913.

Rubiana MM, et al. Thermoanalytical study of praziquantel-loaded PLGA nanoparticles. Braz J Pharm Sci. 2006;42(4):523–30.

Sahay G, Alakhova DY, Kabanov AV. Endocytosis of nanomedicines. J Control Release. 2010;145(3):182–95.

Seda R, et al. Dexamethasone-loaded PLGA-nanoparticles for potential local treatment of oral precancerous lesions. Pharm Dev Technol. 2019;25(2):149–58.

Sovan LP, Utpal J, Manna PK, Mohanta GP, Nanoparticle MR. An overview of preparation and characterization. J Appl Pharm Sci. 2011;1(6):228–34.

Sugiura S, et al. Preparation characteristics of water-in-oil-in-water multiple emulsions using microchannel emulsification. J Colloid Interface Sci. 2004;270(1):221–8.

Tamayo-Esquivel D, Ganem-Quintanar A, Martinez AL, Navarrete Rodriguez M, Rodriguez-Romo S, Quintanar-Guerrero D. Evaluation of the enhanced oral effect of omapatrilat-monolein nanoparticles prepared by the emulsification-diffusion method. J Nanosci Nanotechnol. 2006;6(9–10):3134–8.

Tiwari G, Tiwari R, Sriwastawa B, et al. Drug delivery systems: an updated review. Int J Pharm Investig. 2012;2(1):2–11.

Tripathi A, et al. PLGA nanoparticles of anti tubercular drug: drug loading and release studies of a water in-soluble drug. Int J Pharm Tech Res. 2010;2(3):2116–23.

Trotta M, Debernardi F, Caputo O. Preparation of solid lipid nanoparticles by a solvent emulsification-diffusion technique. Int J Pharm. 2003;257(1-2):153–60.

Vanderhoff JW, El Aasser MS, Ugelstad J. Polymer emulsification process. US4177177. 1979.

Weissig V, Elbayoumi T, editors. Pharmaceutical nanotechnology: basic protocols, Methods in molecular biology, vol. 2000. New York: Springer; 2019.

Xu W, Ling P, Zhang T. Polymeric micelles, a promising drug delivery system to enhance bioavailability of poorly water-soluble drugs. J Drug Deliv. 2013;2013. Article ID 340315, 15 pages https://doi.org/10.1155/2013/340315.

Yu X, Trase I, Ren M, Duval K, Guo X, Chen Z. Design of nanoparticle-based carriers for targeted drug delivery. J Nanomater. 2016; Article ID 1087250, 15

Yuan H, et al. Solid lipid nanoparticle prepared by solvent diffusion method in a non reactor system. Colloids Surf B: Biointerfaces. 2008;61:132–7.

Zaida Urbán M. Preparation and characterization of solid lipid nanoparticles containing cyclosporine by the emulsification-diffusion method. Int J Nanomedicine. 2010;5:611–20.

Zaida Urbán M, Adriana G, et al. Preparation and characterization of solid lipid nanoparticles containing cyclosporine by the emulsification-diffusion method. Int J Nanomedicine. 2010;5:611–20.

Zhang L, Gu F, Chan J, Wang A, Langer R, Farokhzad O. Nanoparticles in medicine: therapeutic applications and developments. Clin Pharmacol Ther. 2008;83(5):761–9.

13 Ultrasound-Activated Nanoparticles

Gayatri Gopal Shetgaonkar and Lalit Kumar

1 Introduction

Mechanical sound wave which has periodic vibrations and frequencies of more than 20 KHz, which in turn is more than upper human audible range frequency, is known as ultrasound (US) wave (Abu Zidan et al. 2011). It is produced through a transducer that utilizes piezoelectric component or an electromagnetic inductor which has the capability of converting electrical signal into mechanical vibrations and vice versa (Hangiandreou 2003).

Devices producing ultrasound wave consist of parts like a transducer, transmitter pulse generator, compensating amplifier, focusing control unit, digital processor, and display system (Carovac et al. 2011). It generates action through thermal and nonthermal impacts. Thermal impact relates to temperature increases because of the absorption of ultrasonic wave that leads to tissues' mechanical compression and decompression (Dalecki 2004). Owing to the friction, energy produced is lost and converted to heat. Nonthermal effect of ultrasound leads to complex procedures like stable and inertial cavitation, radiation forces, and microstreaming (Hizadifar et al. 2017). This leads to rise in temperature and mechanical stresses such as microjets and microstreams specifically. The gas pocket in fluid oscillates around an equilibrium radius during non-inertial cavitation and can thus continue to remain for a number of cycles of acoustic compression and decompression. This leads to streams of fluid and mixing of medium due to mechanical stress. Figure 13.1a depicts these processes involved. Inertial cavitation is a method of fast development and brutal collapse of gas bubbles trapped in a liquid during ultrasound exposure (Deng et al. 1996). High temperature and pressure are generated during such collapse, releasing elevated power. Inertial cavitation can cause heat dissociation of water and therefore reactive oxygen species (ROS) generation (Rosenthal et al. 2004).

Ultrasound is used for therapy and diagnosis of the diseases in medical field (Miller et al. 2012). Biological effect generated through ultrasound is dependent on intensity and ultrasound wave frequency. When compared with other external stimulus method, it has shown safety, good penetration capacity, and low operation and instrument cost in therapy (Klibanov and Hossack 2015).

Ultrasound stimulus is also used for treatment of soft tissue injury, wound healing, edema resolution, and tissue scar softening. Ultrasound-mediated bone growth stimulation has been approved by US FDA as class III device. It was also studied that ultrasound-based lipolysis and

G. G. Shetgaonkar · L. Kumar (✉)
Department of Pharmaceutics, Manipal College of Pharmaceutical Sciences, Manipal Academy of Higher Education, Manipal, Udupi, Karnataka, India
e-mail: lalit.kumar@manipal.edu

J. K. Patel, Y. V. Pathak (eds.), *Emerging Technologies for Nanoparticle Manufacturing*,
https://doi.org/10.1007/978-3-030-50703-9_13

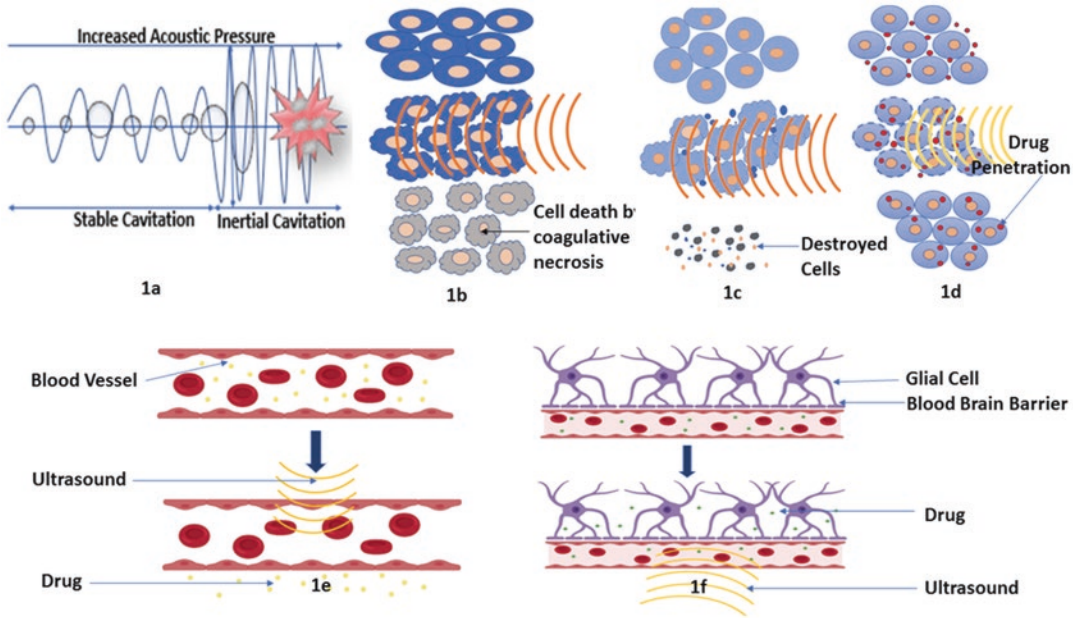

Fig. 13.1 (**a**) Compression and decompression cycle of microbubble under ultrasound influence. (**b–f**) Ultrasound use in thermal ablation, mechanical destruction, sonoporation, enhancement of vascular permeability, and blood-brain barrier opening, respectively

liposuction techniques are used for cosmetic surgery (Bellini et al. 2017).

2 High-Intensity Focused Ultrasound

High-intensity focused ultrasound (HIFU) or focused ultrasound surgery (FUS) is a tissue removal method which uses the frequencies in the range of range 0.8–3.5 MHz used as an alternative to surgical removal of tumors (Haar and Coussios 2007; Orsi et al. 2010) and for Alzheimer's disease treatment (Nicodemus et al. 2019), uterine fibroids (Mahmoud et al. 2014), and kidney stones. Further this pulse is of high amplitude compared to ultrasound wave used for standard diagnostic purpose and has short duty cycle. The wave thus selectively damages focused region because of constructive-type interference produced by ultrasound wave at desired focus, in millimeter resolution.

Conventionally, it leads to generation of temperature increase (>50 °C) in targeted tissue leading to denaturation of protein, shrinkage of cell, destruction of membrane, and coagulation necrosis as it uses more acoustic doses with long as well as highly repetitive pulse (Yildirim et al. 2017). Even though HIFU is used for killing of breast, prostrate, kidney, liver, bone, and pancreas tumors (Hsiao et al. 2016), the curative results of present HIFU is not satisfactory because of difficulties to produce the necessary high-acoustic doses particularly for intense and highly vascularized cell growths (Yildirim et al. 2017). As a result, reoccurrence is mostly seen for tumors because of incomplete removal of tissues (Maestroni et al. 2018). It was also studied that a strong-intensity HIFU can damage healthy cells and tissues leading to off-targeted effect like skin burns and nerve damage (Yildirim et al. 2017). Figure 13.1b–f explains the use of ultrasound in thermal ablation, mechanical destruction, sonoporation, enhancement of vascular permeability, and blood-brain barrier opening (www.fusfoundation.org).

Further the destruction volume generated after HIFU treatment is large in the shape of cigar with

dimensions of 1–3 mm × 8–15 mm and thus nonspecifically destroys tissue. Thus, this method cannot be used for treatment of small nodules and micrometastases. Further destruction of blood vessels of tumors avoids removal of residual cells by additional treatment like chemotherapy or immunotherapy (Yildirim et al. 2017).

Focused ultrasound with high intensity is applied at desired local area leading to invasive ablations of tissue. It produces effect leading to irreversible and complete cell destruction in the targeted region through coagulative necrosis, reducing the potential for heat to harm the nonirradiated region of the tissue. Nonthermal shock like acoustic cavitation, microstreaming, and radiation forces generates shear stress leading to destruction of membrane and cell death as shown in Fig. 13.2a.

It is also applied for molecules like antineoplastic drugs, antibodies, gene, and others (Han et al. 2017). Table 13.1 illustrates types of nonthermal processes and respective ultrasound frequencies. Biological systems have shown very elevated sensitivity to signs and drugs in spatiotemporal conditions. Drug delivery systems based on polymer show a steady release rate. They have also been researched for accomplishing sustained and targeted release of bioactive molecules.

Study is being carried out wherein release of drug from ionically interconnected hydrogels using a quasi-digital ultrasound is done wherein it can be either enhanced or turned off on demand using ultrasound. It was found that the materials are not permanently damaged by ultrasound, but in deficiency of ultrasound stimulus, these hydrogels can self-repair the cross-structure further preventing the drug release. In vitro trials showed that a temporarily brief, high-dose drug exposure burst can be used to enhance mitoxantrone toxic effect to breast cancer cells. Further researchers also produced a system of hydrogels containing mitoxantrones for xenograft tumor treatment. The application of this principle regularly

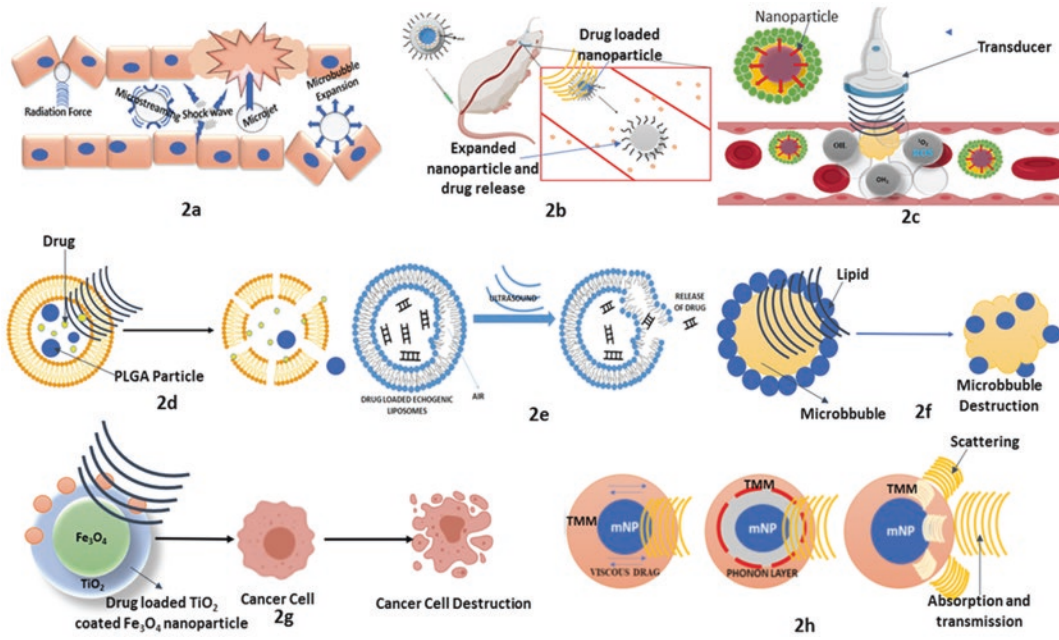

Fig. 13.2 (**a**) Ultrasound-mediated nonthermal method of cellular destruction. (**b**, **c**) Process of drug release from nanoparticle (NP) triggered by ultrasound. (**d**) Process of drug release and PLGA particle entrapped in liposome activated by ultrasound. (**e**) Ultrasound-mediated release of drug from echogenic liposome. (**f**) Ultrasound-activated drug release from microbubble liposome complex

Table 13.1 Types of sonosensitizers and their therapeutic effects

Category of sonosensitizer	Sonosensitizer	Particle size	Ultrasound irradiation	Therapeutic effect
Lipid-coated microbubble	Biotinylated decafluorobutane microbubble with biotinylated liposomes	100 nm	1 MHz	Ultrasound-activated release of thrombin from the pendant leads to acceleration of blood clotting
Polymeric nanoparticle (NP)	PEGylated PLGA nanoparticle loaded with microRNAs	115.3 ± 18 nm	4 MHz	1.9–3.7-fold increase enhanced delivery compared to nano-control nanoparticle
Titanium dioxide (semiconductor)	Au-TiO2 nanocomposite	200 nm	–	Enhanced ROS generation leading to complete suppression of the tumors
Metallic nanoparticle	Fe_3O_4 nanoparticles	11 ± 3 nm	1 MHz	Significant decrease in viability of the MCF-7 cells
Porous nanoparticles	Silicon nanoparticle	100 nm	1–3 MHz	Suppression of cancer cell proliferation

decreased the tumor growth over the use of sustained release of drug individually. It was discovered that daily drug release stimulated by ultrasound considerably reduces tumor development with regard to release of continuous drug alone. It was also concluded that this technology is useful for a wide variety of polymers and bioactives. Thus, it is a helpful instrument to study how the factor delivery timing controls the fate of cell in vivo (Huebsch et al. 2014).

Further, to reduce the side effects associated with chemotherapeutic drugs, it is necessary to entrap the drug molecule in a carrier with organic or inorganic chemical nature in nano- or microforms resulting in the production of reduced leaking in the circulation. The carrier should cause immediate drug release once in the tumor and is considered as one of the important aspects in delivery of the drug sector to prevent or limit exposure to healthy tissue. Thus, this leads to challenges in developing a delivery system with two of these opposing characteristics.

Further, it becomes difficult to develop a triggering strategy that can change the delivery system circulating from stable form to unstable form, which causes drug release. Distinctive mechanical actuator is being accomplished by exploiting the changes in size which happen when microbubble (1–10 μM) interacts with ultrasound, enabling fast release of drugs and facilitating delivery to neighboring cells (Ibsen et al. 2013). Hence, ultrasound can be focused a few cubic millimeters, allowing for the precise control tissue location where microbubble is destabilized yet capable of delivering the encapsulated drug. In addition to this, the use of ultrasound as trigger for delivery of drug using microbubble provides a path of visualizing the microbubble loaded with ultrasound through low-pressure ultrasound.

Initially, hematoporphyrin was used for cancer cell sonodynamic therapy (SDT), which is used as photosensitizer; however, the clinical use of photodynamic therapy is limited for cancerous cell surface due to the incapability of photo energy to penetrate deeply in the tissues (Kuroki et al. 2007).

3 Ultrasound-Driven Nanoparticle-Assisted Stimulation

Sonodynamic therapy is a developmental approach involving a mixture of low-intensity ultrasound and high-tech nontoxic chemical agent known as sonosensitizers (Wan et al. 2016). Mostly, molecules such as porphyrins and xanthene dyes were used in photodynamic therapy as sonosensitizer, because they were originally used as photosensitizers. However, when activated by ultrasound, it produces ROS-mediated cytotoxic impact.

The majority of these sonosensitizers are extremely hydrophobic, which readily aggregates in a physiological environment that reduces its efficacy and thus affects pharmacokinetic behavior (Varges et al., 2004). These molecules are also poisonous in nature and demonstrate low tissue selectivity. This limits sonosensitizer's clinical implementation. The implementation of different kinds of strong and soft particles of micron and nano-size in conjunction with SDT demonstrates excellent capability to solve these critical problems (Serpe et al. 2012). Figure 13.2b and c depicts the process of ultrasound-assisted nanoparticle delivery and activation of it.

The existence of nanoparticles shows an enhancement in biocompatibility, bodily distribution, and selectivity toward diseased tissue. The presence of nanoparticles in liquid also paves a way as site of nucleation for cavitation bubbles, reducing limits for cavitation and hence improving effectiveness of sonodynamic therapy (SDT). The type of nanoparticles used for sonodynamic therapy is reported in Table 13.2.

3.1 Detailed Mechanism of NP-Assisted SDT

The process of nanoparticle-assisted sonodynamic therapy involves two steps. First is communication between ultrasonic waves and nanoparticles. Here the nanoparticle acts as initiators of sonodynamic process. Next is development of therapeutic effect.

Table 13.2 Nonthermal process of cellular destruction and respective ultrasound frequency (Rychak et al. 2005); (Manasseh et al. 2010); (Ohl et al. 2015); (Ce Guo et al. 2018)

Processes	Ultrasound frequency
Radiation force	2.0 MHz
Microstreaming	2.4 kHz
Shock wave	15 kHz
Microjets	3.24 MHz
Microbubble expansion	10 MHz

3.2 Interaction of Nanoparticle and Ultrasound

The use of ultrasound with intensity in range of 0.5–4 W/cm^2 is incapable of generating heat as well as mechanical disruption in healthy cells resulting in enhanced safety. Thus, high energy is desired, but it causes cytotoxic effect like temperature increase or initiation of inertial cavitation generation.

It is possible to use high-energy shock wave to minimize the impact of temperature while improving cavitation. Further, studies are also reported on use of single acoustic pulse with a broad frequency range (20 MHz) and elevated pressure amplitude (up to 20 MPa) that leads to disturbance of an in vitro neuroblastoma (Serpe et al. 2012).

Inertial cavitation involves brutal crash of the bubble on exposure under ultrasound. It was studied that as ultrasound moves through a liquid/tissue, a bubble of gas which is present in the liquid undergoes oscillation under applied acoustic field. The succeeding paragraph explains the interaction of ultrasound and nanoparticles.

3.3 Development of Therapeutic Effect

3.3.1 Chemical Effect of Ultrasound-Assisted Activation of Nanoparticle

Increase in acoustic pressure makes the oscillation volatile, and thus the bubble breaks down producing incredibly high temperature and stress in the middle of the collapse bubble (Morch et al. 2015). This is used to produce ROS by hemolytic breaking of water molecule or to generate chemical changes in or within imploding bubble. The intensity of ultrasound capable of generating cavitation of inertial type is known as cavitation limit and is affected by features of irradiating medium like temperature, viscosity, and presence of impurities. The presence of nanoparticle in aqueous solution is shown to reduce limit of cavitation. Nanoparticles present on the surface and

in the cavities have capability to stabilize the nanobubbles.

In the context of SDT, nanoparticles can generate inertial cavitation in or near the desired targeted cells when activated with short strength ultrasound and lead to cytotoxic impacts. It is therefore a fundamental mechanism behind sonodynamic therapy. The studies thus seek to increase the efficacy of SDT aided by the nanoparticles which focus mainly on enhancing nanoparticles capacity to cause inertial cavitation.

Thus, studies aimed at enhancing the efficacy of nanoparticle-assisted sonodynamic therapy which should therefore concentrate mainly on enhancing nanoparticles' capacity to cause inertial cavitation. After defining the function of acoustic cavitation as the initial mechanism behind nanoparticle-assisted sonodynamic therapy, another mechanism producing final therapeutic effect is as follows.

Imploding bubble in the presence of water and oxygen is considered as nano-sonochemical reactor to produce ROS. These unstable molecules generate elevated toxic effect if they are produced inside the cells like oxidative stress, DNA damage, apoptosis, and lipid peroxidation of cell membrane.

The presence of ROS scavenger like histidine, mannitol, and superoxide dismutase protects desired cells from sonodynamic therapeutic effect that confirms ROS in the impact of sonodynamic therapy. In addition to the chemical mechanism, impact resulting from the implosion of the cavitation bubble, cytotoxic effect plays a significant part. This impact reveals acoustic streaming, fluid microjets, and wave of shock. Thus, ROS produced for the duration of the cavitation bubble collapse can be considered as one of the probable mechanism prominent to SDT therapeutic effect (Canavese et al. 2018).

3.3.2 Mechanical Effect of Ultrasound-Assisted Activation of Nanoparticle

Apart from generation of chemical effect, effects generated by implosion of cavitating bubble, a mechanical effect plays a role in causing cytotoxic effect. The effects produced are acoustic streaming, shock wave, and liquid microjets. These are generated by cavitating bubble crash and thus can harm membranes of cells as well as intracellular elements mechanically. In addition, if bubble present intracellulary is more than the quantity of cell during the expansion stage, destruction of the cell caused by means of the mechanical forces is observed. The increased cell death caused by ultrasound was primarily because of mechanical stress like physical disruption in cell membranes.

Further since cavitation generated is to be considered as source for concentration of the externally applied energy of ultrasound, it is mandatory that part of this energy could be transformed to the nanoparticles. The effect produced on cavitation is sonoluminescence. It is the light emission from the cavitating bubble and can be regarded during bubble collapse owing to relaxation of excited chemical species. It was also hypothesized that emission of light from cavitating bubble could be absorbed by sonosensitizers, and thus similar to photodynamic therapy mechanism, excited sonosensitizers generate an electron hole pair that further leads to production of ROS in aqueous milieu (Canavese et al. 2018).

3.3.3 Metal Oxide Nanoparticles and TiO_2 Activation

As metal oxide nanoparticles like TiO_2 NPs can act as photosensitizers for photodynamic therapy, the use of these nanoparticles can enhance the SDT efficacy by using sonoluminescence as a mechanism for production of ROS showing toxicity toward cells (Bogdan et al. 2017).

Using this hypothesis, to improve their quantum yield, functionalization of TiO_2 nanoparticles with gold nanoparticles (Au TiO_2) was carried out. This fictionalization improved the time of recombination by entrapping excited electron while increasing the absorption spectrum through plasmon resonance on the surface. TiO_2 NPs generated more ROS than bare TiO_2 NPs resulting in in vivo tumor growth being completely suppressed.

In addition to this size of sonosensitizers, morphology and surface chemistry also increase

the capability of TiO_2 to generate acoustic cavitation by entrapping large gas nanobubbles on its surface. It results in enhanced cavitation activity, increased generation of ROS, and therefore toxic effect (Canavese et al. 2018).

The writer suggested that the cytotoxic effect of sonodynamic therapy is triggered inside or near the collapsing bubbles by the chemical activation of the sonosensitizers. The temperature generated by inertial containment of gas in the collapse of the bubble either can trigger pyrolysis of sonosensitizers instantly or can lead to response with ROS produced by cavitation eventually forming free radicals based on the cytotoxic sensitizer.

It is assumed that cavitation generated high temperature and ROS chemically activate the nanoparticles. Hence, the bubble collapse is expected to be present near their original location, i.e., the NP surface. It is thus the case with drug delivery system based on ROS or nanoparticles reacting with oxidative stress.

Acoustic cavitation is also produced through NP mechanical stimulation like mesoporous surface formation, structural changes, and development of extremely reactive surface of new metal oxide. Thus, delivery of nanoparticles aided by ultrasound can be regarded as a mixture of distinct processes.

Nanoparticles can be categorized as nanosensitizers carrying sonosensitizers based on the functions of nanoparticles in sonodynamic therapy. Ultrasound-assisted nanoparticles include mediated liposomes, lipid monolayer-coated microbubble, polymeric nanoparticles, metallic nanoparticles, porous silica nanoparticles, and semiconductive nanoparticles (Canavese et al. 2018).

Liposome Type

Liposome-based drug delivery system is developed by lipid bilayer arrays created by self-assembly that separates hydrophilic and hydrophobic areas; hence it can carry vast arrays of materials like sonosensitizers, therapeutic agents, genes, protein peptides, and contrast agents. It is thus used for imaging and diagnosis under irradiation of ultrasound. Intravenously administered conventional forms of chemotherapeutic agents were assigned not precisely in the body (Wu et al. 2014; Zhao et al. 2018). Both tumorous and tissues of normal types are affected, thereby limiting the dose inside the tumor and causing suboptimal therapy because of surplus toxicity. Drug delivery to targeted system assures to increase drug therapy window by enhancing targeted tissue delivery and also ratio of targeted and nontargeted tissue.

The goal of targeted drug delivery is to reduce uptake of nondiscriminate toxic agents and enhance accumulation of drug at desired site. These drug molecules are directly attached to targeting agents or complexed with vehicle having targeting moieties to target drug to specific systems in tissues within body. The main technology behind nanomedicine and nanostructure-mediated targeted drug delivery is capable of improving bioavailability of drug, enhancement in timely drug release, as well as enhanced drug targeting (Patra et al. 2018).

Glioblastoma, glial cell neoplasm belonging to grade IV tumor as per World Health Organization (WHO), is the most aggressive type of cancer. Only 30–35% subset of patients has shown benefits from temozolomide chemotherapy in which tumors show methylation of the O6 promoter area methylguanine DNA methyltransferase (MGMT) gene. To increase the benefits of this therapy to more number of patients, magnetic resonance imaging-guided microbubble-based low-intensity focused ultrasound (LIFU) is applied in the blood-brain barrier opening transiently and producing a liposome-charged small molecule MGMT inactivator in mice having temozolomide-resistant gliomas as these therapeutic molecules are hard to be used. It was seen that O6-(4-bromothenyl)-guanine (O6BTG) a derivative of liposome has the capacity to effectively target MGMT, thus increasing sensitivity of in vitro cells of gliomas obtained from murine and human to drug temozolomide.

Also image-guided LIFU is used to mediate the deliverance of stable liposomal MGT inactivator present in tumor causing potent in vivo depletion of MGMT. Further combination along with temozolomide chemotherapy, treatment car-

ried out using new liposomal MGMT inactivator facilitation by LIFU-based blood-brain barrier opening decreases tumor production and thus considerably extends glioma-bearing mice survival (Papachristodoulou et al. 2019).

In another study, in order to improve tumor destruction which may lead to reduction in associated side effects, a new ultrasound-based liposomal system for targeting drugs to tumor was developed. Ultrasound-responsive agents were used in the studies of PLGA nanoparticles instead of standard microbubble. The new ultrasonic liposomes that encapsulate nanoparticles of PLGA type have the capability for use as new antitumor system in drug delivery. Figure 13.2d depicts the process of release of drug and PLGA nanoparticles entrapped in liposome under impact of ultrasound.

Ultrasound-based drug delivery was created using thermosensitive polymer (TSP) (NIPMAM-co-NIPAM)-altered liposomes that sensitized the liposomes to elevated temperatures. Furthermore, ultrasound irradiation (USI) augmented the use of releases of drug from TSP liposomes by cancer cells.

The mechanism for releasing liposomes from ultrasound-mediated drug release has been explored. The findings showed that the carriers unique release mechanism caused variations in ultrasound drug release kinetics acquired for distinct liposomal compositions. The developed liposomes have been evaluated for morphology, mean size, and distribution in size before and after a specified exposure of ultrasound. Cryo-transmission electron microscopy, dynamic light dispersion, and asymmetric field flow fractionation along with multiangle light dispersion showed an important shift in the mean particle size, size distribution, and morphology of the ultrasound using DOPE-dependent liposomes, directing toward irreversible vesicle disturbance and simultaneous drug release. By comparing after ultrasound implementation, the hydrogenated soy phosphatidylcholine (HSPC)-developed liposomes remain unchanged, suggesting porous mechanism for release.

By enhancing efficacy and decreasing systemic toxicity, targeted drug delivery using ultrasound-generated hyperthermia may lead to enhancing the therapeutic index of chemotherapeutic drugs. Specifically, a dual compartment container, transparent in nature for acoustic pressure, is used wherein thermosensitive liposomes are suspended in cell culture medium and are placed in glycerol, a medium that absorbs temperature. In case of glycerol, ultrasound produces hyperthermia that heats the conductive thermosensitive liposomes and produces encapsulated drug release. Acoustic conditions are theoretically obtained and thus experimentally validated for required hypothermia. Doxorubicin (DOX) was released from thermosensitive liposomes by 80%.

This research explored cancer cell destruction using ultrasound and liposomes that are free of drugs that contained perfluoropentane (ePFC5) emulsion and were commodified using avidin as ligand and Japanese hemagglutinating virus envelop in order to enhance liposome combination with cells. Such type of liposomes is referred as avidin/HVJ liposomes laden with ePFC5. Ultrasound irradiation activates ePFC5-loaded liposomes.

Drug delivery based on image-sensitive liposomes (iTSLs) and high-intensity focused ultrasound has been studied as novel and noninvasive way to targeted anticancer drug therapy. FUS-generated hyperthermia is used to release drug from these systems as external trigger mechanism. Subablative hyperthermia has been used to modify the penetration of tumor blood vessels and thus improve the absorption of nanoparticles. Here the preparation and use of thermosensitive liposomes labeled as magnetic resonance imaging (MRI) and near-infrared fluorescence (NIRF) for imaging and monitoring biodistribution and drug release in a murine cancer model was researched. iTSLs have been prepared to encapsulate topotecan, a chemotherapeutic agent that can be tracked by a rise in its inherent drug fluorescence when released into tumors. FUS was introduced with feedback via subcutaneous thermocouples for maintenance and monitoring of hypothermic temperature. Immediately after liposome administration, iTSL growth in tumors was noted using imaging techniques of NIRF

types. Mild hyperthermia induced by FUS (3 min at 42 °C, 30 min after IV administration) significantly enhanced uptake of iTSLs. Co-localized increase in topotecan fluorescence emissions was also noted instantly after FUS was applied, showing fast release of drugs. A second mild hyperthermia treatment implemented 1 h after the first seemed to amplify the phenomenon of enhanced accumulation of iTSLs and simultaneous topotecan release. Due to FUS medicines, MRI in vitro also verified improved iTSL uptake. Next image findings show the impact of hyperthermia on carrier and drug uptake. Combination of real-time imaging with FUS used for hyperthermia can be used as instrument for tumor-dependent drug delivery (Centelles et al. 2018).

The potential effect of penetrating phospholipid membrane shown by ultrasound has increased the capacity to use ultrasound as a way of increasing the delivery of anticancer drugs through liposomes to tumor. In the study carried out, new ultrasound-sensitive or sonosensitive doxorubicin-trapped liposomes are recorded as the major lipid-based element based on 1,2 distearoyl-sn-glycero-3-phosphatidylethanolamine (DSPE). A range of bilayer composition of lipids were studied using experimental design in relation to US-activated in vitro release of drug and also serum stability of drug retention. A powerful association among DSPE content and sonosensitivity was stated by multivariate data analysis, both alone and in interplay with cholesterol. After 6 min of US exposure, the most model formulation showed about 70% release of doxorubicin. Compared to conventional PEGylated liposomal doxorubicin, this showed sevenfold increase in rate of release. The important increase in liposomal sonosensitivity demonstrates the potential of liposomal lipid structure in engineering for US drug delivery (Evien et al. 2010).

In the research study, it was proven that the potential of targeted and ultrasonic-based delivery of drug systems that utilizes liposomes that are modified using poly(NIPMAM-co-NIPAM) as polymer (TSP) to sensitize these liposomes to enhanced temperatures. These TSP-modified liposomes (TSP liposomes) released encapsulated calcein for 30s at 0.5 W/cm^2 under 1 MHz ultrasound irradiation and for 5 min at 42 °C under incubation (Ninomiya et al. 2014).

One of the most prevalent and deadly microvascular complications shown in diabetes is diabetic nephropathy (DN). The objective associated with this research is to study whether coenzyme Q10 (CoQ10) an antioxidant coupled using ultrasound-targeted microbubble destruction (UTMD) can reverse early stages of diabetic nephropathy progression. CoQ10 shows excellent capacity for early DN treatment. But due to its low aqueous solubility and nonspecific distribution, the clinical use of CoQ10 was restricted. Liposomes thus loaded using CoQ10 is thus ready and can be coupled for early DN theranostics with ultrasound microbubble (Yue et al. 2017).

Novel polyethylene glycol modified liposomes entrapping gas responsive to ultrasound and reporting the mixture of US and bubble liposomes (BLs) useful for direct transmission of siRNA to cytoplasm. After intravenous administration, the delivery of siRNA is impacted by nuclease degradation. In this research cationic lipid was used, 1, 2-dioleoyl-3-trimethylammonium-propane (DOTAP) for developing innovative siRNA-loaded BLs (si-BLs). These siRNAs could be loaded to DOTAP-containing BLs and serum-stable siRNA-loaded BLs. A particular impact of gene silencing was also accomplished through si-BL transfection. The mixture of si-BLs and US exposure can therefore be used to deliver siRNA to a particular tissue through systemic injection (Endo-Takahashi et al. 2012).

Echogenic-type liposomes (ELIP) has shown capacity as carrier for targeting oligonucleotides (ODN), beyond diagnostic agent, specifically if agent release is triggered and uptake of it is enhanced using ultrasound at targeted site. This study aims to co-encapsulate air and NF-κB decoy ODN within ELIP to allow ultrasound for releasing encapsulated ODN from ELIP and quantify definitely the ELIP release from encapsulated ODN using ultrasound application. The process is depicted in Fig 13.2e. These results indicate prospective applications for atheroscle-

rosis gene therapy and thus other illnesses (Buchanan et al. 2010).

Lipid-Coated Microbubble Type

Ultrasound-mediated drug delivery is used as targeting mechanism that will enhance the action of drug at specific sites. The objective of the study is the use of focused ultrasound field on the bubble that carries a drug that in the targeted regions destroys and thus releases the drug. These drugs are attached to the microbubble shell such as plasmid DNA attached to the surface of microbubble using electrostatic interaction or trapped in a shell of microbubble like in the case of paclitaxel, a hydrophobic drug. The first strategy is restricted if lipid monolayer is used to develop the shell of microbubble and thus is used to enhance drug payload inside the bubble (Klibanov et al. 2010). Figure 13.2f shows the release of drug from liposome microbubble pendant complexes activated by ultrasound.

Liposome conjugates and microbubble filled with gas can be used as pendant-like structure wherein liposomes coat the microbubble surface to be used as drug delivery carriers. Ultrasound-based release of dyes entrapped inside the liposomes for microbubble insonation present in the vicinity of giant liposome is observed. Thus, it is seen that liposomes that are attached to microbubble surface get ruptured when ultrasound-based treatment is used. The use of liposome and microbubble composite for delivery of drug in comparison to simple microbubble preparations broadens the range of substance to be used like proteins (e.g., enzymes or antibodies) or other types of hydrophilic drugs that are not otherwise seen in association with the shell of microbubble in stable order (Klibanov et al. 2010).

Studies discussed explain the use of the ultrasound-based release of the drug present inside the liposome microbubble makeup.

A study based on the preparation of an ultrasound-based drug delivery system utilizing the context of liposome-coated pendant-type complex of microbubble was developed. A streptavidin linker was used to coat biotinylated decafluorobutane microbubble with biotinylated liposomes. Liposomes with calcein and thrombin were prepared. By using 100 nm liposomes, more than 1 um^3 payload volume per microbubble liposome was used based on the original calcein concentration. Insonation of in vitro microbubble liposome pendant led in the full destruction of microbubbles (MBs) and the release of a substantial proportion of material that was trapped. Ultrasound treatment with 1 MHz led to around 30% release of trapped calcein that was calculated with utilization of the fluorescence quenching test. A chromogenic substrate research estimated the release of thrombin from liposome complexed with microbubble (11% of trapped material) because of ultrasound therapy. Ultrasound-activated discharge of thrombin from developed pendant leads to quickening of blood clotting process (Klibanov et al. 2010).

Lipid monolayer-coated microbubble is utilized for latest ultrasound molecular imaging technique to determine vascular areas that show certain surface proteins. The microbubbles are functionalized using targeting ligand that has the capacity to bind to required microbubble holding cells as remaining unbound microbubbles are removed from circulation. The extremely reflective microbubbles left behind can be detected by subsequent ultrasound scanning. The method based on ultrasound scanning and detection leads to microbubble destruction, generating the fragments of monolayer lipid (Ibsen et al. 2014). A majority of fragments observed were big enough to show resistance to endocytosis processed by the receptor. The fragments were not seen for 96 min of incorporation into cell lipid membrane. It was also not seen breaking into smaller parts or changing shape but was seen undergoing translation and rotation through the cell surface. These big fragments remain on the surface of the target cells for a time period and also impacts on blood flow through microcapillaries (Ibsen et al. 2014).

Parkinson's disease (PD), a type of neurodegenerative diseases, is characterized in substantia through loss of neurons releasing dopamine. Neurotropic factor like GDNF derived from glial cells has shown neuroprotective impact on PD rats. It was found that ultrasound-activated lipid-modified GDNF type of microsphere that produces GDNF after low-frequency ultrasound

stimulation in a continuous way can decrease neonatal rats' hypoxic-based ischemic injury. In the research, it was explored whether lipid-coated GDNF microsphere in rat model of PD has the potential to produce neuroprotective impact in PD rats (Wang et al. 2014).

Next the research aims in determining the efficacy of lipid-entrapped microbubble and effect of ultrasound in recanalization of graft thrombi in arteriovenous passage and the impact of attenuation of tissue on the rate achievement. In four canines a total of 55 thrombotic occlusions have been developed. Two distinct US intensities of 1 MHz were randomly handled with thrombosed grafts, small (0.4–0.6 W/cm^2) and high (10 W/cm^2). Microbubble intragraft was contrasted using saline intragraft and the same dose of microbubble-provided IV. In the presence and lack of a tissue mimicking phantom, IV microbubble was also provided. High-intensity US (10 W/cm^2) with microbubble intragraft generated considerably greater patentability and flow rating than US saline. The US had greater achievement rates in recanalizing thrombosed grafts with IV microbubbles than the US alone had at all intensities. Attenuation leads to both low and high intensities and effective recanalization happened. The US and microbubble are capable of recanalizing thrombosis of the acute arteriovenous graft. In the presence of tissue attenuation, higher intensities may be required (Xie et al. 2005). In case of ultrasound-mediated delivery of combination therapy for an ovarian xenograft model, multifunctional oxygen and paclitaxel charged microbubble were developed. Compared to other therapeutic alternatives, a superior therapeutic result was accomplished by intravenous administration of oxygen- and paclitaxel-loaded microbubbles (OPLMBs) accompanied by ultrasound mediation. Immunohistochemical analyses of the dissected tumor tissue verified enhanced apoptosis of the tumor and decreased after therapy expression of VEGF. Western blot techniques verified the reduction in HIF-1α and P-gp expressions. Experiment indicates that OPLMB ultrasound mediation can be used as a potential drug delivery approach for therapy utilizing drug combination in ovarian cancer (Liu et al. 2015).

The objective of the research was to improve the persistence of in vitro microbubble circulation for medical imaging apps and targeted delivery of drugs. The approach involves investigating the effect of in-plane rigidity of the monolayer of lipid to decrease microbubble destruction rate by keeping the size, concentration, and architecture of microbubble surface constant. Here estimating the impact on the cohesive surface energy of the acyl chain length of the main diacyl phosphatidylcholine (PC) lipid and interlipid distance, based on these results, it was hypothesized that the stability of microbubbles and the persistence of the in vivo ultrasound contrast would increase monotonically as the length of the acyl chain increased. Thus, in the study, the stability of microbubble *in vitro* with and without ultrasound exposure was carried out.

The study shows a sharp increase in stability between DPPC and DSPC that relates to wrinkling shift, showing the initiation of important resistance to shear on surface and permeation of gas. In vitro- and in vivo-based stability comparison of microbubble covered using pure DPPC with lung surfactants extracted results in further proof that shows the impact of wrinkling shift. Stability of microbubble against ultrasound-free dilution and persistence of in vitro ultrasound comparison show a monotonic rise from DSPC to DBPC with acyl chain length. Stability drop was also observed precipitously from DBPC to DLiPC for all types of measurements to further enhance the length of the lipid acyl chain. This result indicates that hydrophobic mismatch present between primary PC lipid and DSPE-PEG 5000 lipopolymer-based emulsifier causes a less stable surface microstructure. Further these findings help in the hypothesis related to the role of in-plane rigidity to enhance microbubble circulation lifetime (Garg et al. 2013)

Polymeric Nanoparticles

Attachment of sensitizer drugs or lipidic surface contrast agents can result in particle instability. It was suggested to solve this issue with polymeric

microbubbles. It also demonstrates in vitro and in vivo selective toxicity.

In this research a study on intended and validated platform for delivery of PEGylated poly(lactic-co-glycolic acid) (PLGA) nanoparticles (FDA-approved product) loaded with microRNAs to profound tissue in pig model was carried out. These small RNAs reprogram tumor cells and sensitize them for chemotherapy. Anticancer miRNA has to be encapsulated into the nanocarrier to overcome their brief half-life and intravascular circulation and generate controlled and sustained release of the same into tumor cells. Ultrasound focused on a targeted region along with gas-filled microbubble offers a noninvasive way to enhance tumor vascular permeability and boost drug-charged particle delivery effectiveness. In this research, a single handheld curvilinear ultrasound array with clinical-grade contrast agent SonoVue was used for image-guided treatment. In this initially validation of phantom platform was carried out to optimize the acoustic-based amount of microbubble cavitation like peak negative pressure, pulse length, and pulse repetition frequency. Next it was tested in vitro by supplying pig liver and kidney with PLGA nanoparticles co-loaded with antisense miRNA-21 and antisense miRNA 10b. Increased miRNA deliverance was seen (1.9–3.7-fold increase) as compared to untreated control regions due to ultrasound treatment. Further, extremely fluorescent semiconducting polymer nanoparticles in order to evaluate the extravasation of nanoparticles. Nanoparticle in the extravascular compartment was suggested by fluorescent microscopy. Hematoxylin and eosin staining of treated tissue did not show any harm to the tissue. The findings described in this manuscript indicate that the suggested platform may be used. Nanoparticle in the extravascular compartment was suggested by fluorescent microscopy. Hematoxylin and eosin staining of treated tissue did not show any harm to the tissue. The findings described in this manuscript indicate that the suggested platform can be used to enhance the miRNA delivery from nanoparticles loaded in big animal models securely and noninvasively to target areas in profound organs (Ianni et al. 2019).

Next a study is carried out in ultrasound-reactive nanoparticle aggregates (NPAs) which shows disintegration in slow release nanoscale, drug delivery devices that are used at specific locations through local application of low-energy US. The properties of these mechanically activated NPA made up of polymeric nanoparticles have been adjusted by adjusting the molecular weight of polymer, nanoparticle precursor size, and percentage of excipients used to hold the NPA together, thus reducing stability issues as shown in the case of microbubble-based drug carrier (Papa et al. 2017). This idea was applied further to practice by manufacturing NPAs consisting of doxorubicin (DOX)-charged nanoparticles and testing their capacity to cure tumors through ultrasound activation. Trials on mouse showed considerably higher effectiveness for targeting tumor with ultrasound-activated NPAs as compared with PLGA nanoparticle controls (with or without ultrasound application) or intact NPAs. Further DOX-loaded nanoparticles were injected and exposed locally to US energy; this enhanced method to concentrate nanoparticles at tumor site causes a significantly greater amount of reduction in volume of tumor as compared to using tumors which have been treated with 20 times higher free drug dose (Papa et al. 2017).

Multifunctional ultrasound contrast agents (UCAs) combining ultrasonic diagnosis with tumor treatment have gained enormous attention due to their excellent biocompatibility and elevated capacity to penetrate biologically. Nevertheless, in future studies, nanoscale UCAs with appropriate size and excellent therapeutic effect continue to be created. Here hybrid cerasomes loaded with indocyanine green and L-menthol (ICG-MCNs) were manufactured as a multifunctional theranostic nanoplatform with elevated structural stability and aqueous photostability. Mutual support with ICGs' photothermal effect, heating-caused L-menthol triphase transition could generate ongoing gas microbubbles for improved ultrasound imaging. Therefore, the resulting ICG-MCNs are expected to be a compe-

tent candidate for US phototherapy and imaging (Yang et al. 2019).

The production of pathological stimulus-dependent nanoplatform with theranostic functions has become increasingly interesting. Thus, it found ketalized maltodextrin (KMD) nanoparticle that is capable of simultaneously delivering therapeutic and imaging features to acidic circumstances like in the case of inflammation. KMD was produced by combining acid-cleavable hydrophobic moiety with maltodextrin through carbonate bond as platform for theranostic nanoparticles. To produce carbon dioxide bubbles, KMD nanoparticle could undergo acid-triggered hydrolytic degradation, amplifying the ultrasound signal. Silymarin as a model drug was used to evaluate the potential of KMD nanoparticles as a drug carrier. KMD nanoparticles showed substantially increased ultrasound contrast at acidic pH and release acid-triggered drug payloads. The translational potential of silymarin-loaded KMD (S-KMD) nanoparticle as ultrasound contrast agents and therapeutic agents has been carefully assessed using acetaminophen (APAP)-induced acute liver failure models of cell culture and mouse models. S-KMD nanoparticles showed considerably increased ultrasound contrast in the APAP-intoxicated liver and substantially suppressed hepatic damage by inhibiting pro-inflammatory cytokine expression. These findings show that KMD nanoparticles have extraordinary potential for multiple-type inflammation as theranostics agents (Go et al. 2018).

A Trojan horse approach for cancer treatment using nonviral nano-vector-transfected tumor tropical mesenchymal stem cells is presented here. In this study mesoporous silica nanoparticle responsive to ultrasound was covered using polycation (i.e., with two different molecular weight plasmids). After treatment using silica nanoparticles, the appearance of green fluorescent protein was studied in mesenchymal stem cells obtained from decidua. The most active form of nanoparticle was further used to induce expression of the two suicide gene: cytosine deaminase and uracil phosphoribosyltransferase that causes cell transformation into poisonous drug (5-fluorouridine monophoshate) and nontoxic prodrug (5-flurocytosine). In the cancer cell line (NMU cells) that transfected vehicle cells, decidua obtained mesenchymal-based stem cells, and the effects for manufacturing of toxicity-based final product was also studied (Paris et al. 2019).

Recently, there has been excellent interest in cell-mediated cancer therapy. Tumor-entrapping cells exert anticancer impacts via inherent capabilities, through therapeutic gene transfection or acting as vehicles for therapeutic nanoparticles. Ultrasonic mesoporous silica nanoparticle (capable of carrying anticancer drug) is developed to behave as nonviral transfection agent for human mesenchymal stem cells. The successful transfection is used for the treatment of tumor tropical human mesenchymal stem cells. The transfection of vehicle cell is analyzed using different expression plasmids. The carrier cell is capable of converting toxic prodrug into an extremely toxic molecule on transfection using two suicide genes which in an in vitro coculture model can also kill adjacent cancer cells. This research opens the door to a host of approaches whereby human mesenchymal stem cells can transport both genes and drug-loaded nanoparticles to tumor tissues.

Mesoporous silica nanoparticles have been identified as appropriate carrier for drug delivery, but after systemic administration, enhanced delivery of drug to target tissue becomes a challenge. For cavitation activity to be identified in actual time, two distinct ultrasound frequencies 0.5 or 1.6 MHz with pressure in range of 0.5–4 MHz are used. The recognized ideal ultrasound-mediated conditions were used to generate dye-loaded nanoparticles as a model for drug-loaded nanocarriers, with fluorescence microscopy analyzing the amount of extravasation. Further these nanoparticles are co-injected with submicrometric polymer cavitation nuclei as a mode of promoting cavitation activity and also decreasing acoustic pressure required in situ to achieve extravasation. Comparison of cavitation energy and penetration with mesoporous silica nanocarriers and thus submicrometric cavitation nuclei can help to increase nanocarrier extravasation, thus enabling subsequent release of sustained release drugs from the particles trapped in tumor tissue (Paris et al. 2018).

Effectively eradicating *C. albicans* is hard with traditional antifungal agents, primarily due to low *C. albicans* permeability. The cell wall of *albicans* produces a powerful resistance to drugs. The aim of the study involves exploring synergistic fungicidal impact as well as fundamental mechanisms associated with low-frequency as well as low-intensity ultrasound that is coupled along amphotericin B-loaded nanoparticle (AmB-NPs) therapy along with *C. albicans*. AmB-NPs were developed using double emulsion technique of poly(lactic-co-glycolic acid). *C. albicans* was handled for 15 min with AmB-NPs combined with 0.30 W/cm^2 ultrasound irradiation of 42 kHz. The finding shows that the application of ultrasound improved the antibacterial efficacy of AmB-NPs ($P < 0.01$) and the antifungal efficacy improved considerably as amount of drug-charged nanoparticles under ultrasonic irradiation increased. After combined therapy of AmB-NPs and ultrasound, albicans experienced the most serious harm and loss of ordinary microbial morphology as disclosed by electron microscope. Further studies were carried out on the secured application of low-frequency ultrasound using exposed skin and debated the possible mechanism of ultrasound-enhanced fungicidal activity. Observations show that the mechanism can be associated with the impact of ultrasonic cavitation and an increase in species of intracellular reactive oxygen (Yang et al. 2018).

Various studies have shown that entrapment of the drug in nanoparticle improves the efficacy and thus reduces toxic effect produced as compared with standard chemotherapy. However, due to multiple biological obstacles and irregular tumor perfusion, nanoparticle delivery is inadequate as well as heterogeneous. Here a study on distinctive multifunctional drug delivery scheme composed of stabilized microbubble by polymeric nanoparticles (NPMBs), allowing the delivery of ultrasound-mediated drugs, is carried out. The objective involves examination process of ultrasound-based delivery of drug and to study whether there was therapeutic benefit from enhanced tumor uptake. It was described by cellular absorption and toxicity, circulation, and biodistribution. Tumors were studied using ultrasound of different pressure and length of pulse after intravenous injection of NPMBs in mice, and further distribution of the nanoparticle was pictured in tumor segment. No impacts of low pressure were noted, while full destruction of bubble at greater pressures enhanced tumor uptake 2.3 times without harm to the tissue. In a successful proof of concept research, in which all tumors showed regression into complete remission, an improved therapeutic effect was demonstrated (Snipstad et al. 2017).

Due to the potential toxicity of standard agents, the design of secure and effective diagnostic/therapeutic agents for treating cancer in hospitals continues to be difficult. While the annual incidence of neuroblastomas is not so high, the diseases happen primarily in kids, a population susceptible to toxic contrast agents and therapeutics. A study showed that cancer-targeting, gas-generating polymeric nanoparticles are helpful as an ultrasound (US) imaging and neuroblastoma treatment instrument. In this study poly(D, L-lactide-co-glycolide) to encapsulate calcium carbonate and develop gas-generating polymer nanoparticles (GNPs) was used. Under acidic circumstances, these nanoparticles release carbon dioxide bubble and improve signals of ultrasound.

Once GNPs were altered with the rabies virus glycoprotein (RVG) peptide, a targeting moiety for neuroblastoma RVG-GNPs accumulates at the site of tumor and significantly enhances US signal in a mouse model bearing a tumor. Further intravenous administration of RVG-GNPs decreases development of the tumor in the mouse model without using standard therapeutic agents. This approach for development of theranostic agents with disease targeting capacity can provide a helpful strategy for cancer identification and cancer treatment, enabling a secure and effective clinical application with fewer side effects than standard agents (Lee et al. 2016).

Ultrasound-induced microbubble cavitation may result in increased permeability across natural tumor obstacles like walls of blood vessel or cell membrane, resulting in enhanced therapeutic delivery to targeted tissues. Further enhanced delivery of smaller (<1 nm) molecule is shown at

acoustic pressure less than 1 MPa both in vitro and in vivo; the effectiveness of delivery of bigger (>100 nm) therapeutic carrier to cancer continues to be uncertain and thus needs greater stress for adequate delivery of molecule. Enhancement in the delivery of the bigger drug carrier such as FDA-approved PEGylated poly(lactic-co-glycolic acid) nanoparticles (PLGA-PEG-NP) has important clinical importance because it has been shown that these nanoparticles protect encapsulated drugs from blood circulation degradation and enable the slow and prolonged release of encapsulated drugs at the target place. Different acoustic parameters were explored in this research to promote the effective delivery of two nanocarriers, a fluorescent semiconducting polymer model drug nanoparticle as well as PLGA-PEG-NP into human colon xenografts in mice. First the amount of cavitation generated by different acoustic parameters (pressure, duration of pulse, and frequency of pulse repetition) and concentration of microbubble in a phantom-imitating tissue was studied. Next in vivo experiments were conducted to determine nanocarrier penetration depth using different acoustic pressures ranging from 1.7 to 6.9 MPa.

PLGA-PEG-NP was entrapped in a therapeutic microRNA, miR-122, and thus the quantity of miR-122 delivered was evaluated by RT-PCR quantitatively. Findings indicate the greatest impact of acoustic pressure on cavitation. A rise in stress from 0.8 to 6.9 MPa in phantom studies led in an almost 50-fold enhancement in cavitation. In vivo, as the pressure amplified from 1.7 to 6.9 MPa, the quantity of nanoparticles placed in cancer xenograft increased from 4- to 14-fold, and thus median penetration deepness of extravasated nanoparticles enlarged from 1.3-fold to 3-fold as compared with control conditions deprived of ultrasound, as observed from 3D-type confocal microscopy. By providing miR-122-charged PLGA-PEG-NP using ideal acoustic configurations with minimal tissue harm, miR-122 delivery to ultrasound and microbubble tumors is 7.9-fold greater as compared with ultrasound-free therapy. The research thus shows that microbubble cavitation generated by ultrasound has been a helpful instrument for delivering in vivo cancer with therapeutic effect miR-charged nanocarriers (Wang et al. 2015).

Extracellular matrix which is packed densely and in rigid form in tumor cells can inhibit drug carriers' deeper penetration and thus reduces their therapeutic effectiveness. Here, the ECM remodeling approach is suggested by pulsed high-intensity focused ultrasound (pulsed HIFU) technology for enhancing tumor targeting of nanoparticles. It was reported that intravenously injected Cy5.5-labeled glycol chitosan nanoparticle (Cy5.5-CNP) tumor-targeting effectiveness and tissue penetration are highly reserved in tumor tissue consisting of elevated levels of collagen and hyaluronic content in ECM-rich A549 tumor consisting mice compared to ECM-poor SCC7.

When collagenase or hyaluronidase was treated with intra-tumoral injection, the quantity of collagen and hyaluronic content reduced in ECM containing A549 tumor tissues, and thus more Cy5.5 NPs penetrated in the tumor tissue which is confirmed by noninvasive optical imaging.

Further, ECM-rich A549 tumor tissue is treated with low power of pulsed HIFU (20 W/cm^2) wherein acute tissue damage is not seen so as to break down the firm ECM structure. As projected, the tumor tissue of A549 showed remodeling of the ECM framework following noninvasive exposure to pulsed HIFU, resulting in amplified blood flow, lowered collagen content, as well as reduced CNP penetration. In case of pulsed HIFU-treated A549 tissue tumor, targeting efficiency of tumor was 2.5 times more than that of untreated tissue of tumor. These findings suggest that pulse HIFU ECM remodeling and collagen structure disturbance are promising ways of enhancing nanoparticles' profound tissue penetration and tumor targeting in ECM-rich tumor tissue (Lee et al. 2017).

Therapy based on central nervous system (CNS) illness like brain tumors, Alzheimer's, Parkinson's, and stroke is hampered by the blood-brain barrier (BBB). In order to generate desired effect in the brain, therapeutics can bypass the BBB and also penetrate the brain parenchyma.

Here study on distinctive mixture of noninvasive strategy to BBB permeabilization with therapeutically appropriate platform of nanoparticle and polymer was carried out which quickly penetrates brain microenvironment. With intravenous microbubbles (MBs), MR-guided focused ultrasound (FUS) can interrupt the BBB locally and reversibly by submillimeter spatial precision. Dense poly(ethylene-co-glycol) (PEG)-covered, brain-penetrating nanoparticles (BPNs) in ordinary rat brain tissue are long-acting and tenfold slower than water diffusion. Following intravenous model administration and decomposable BPNs in case of ordinary healthy rats, it showed secured pressure-based deliverance of 60 nm BPNs to the brain parenchyma for the areas in which FUS and MB disrupt the BBB. Delivery of BPNs using MR-directed FUS has the ability for enhancing treatment efficacy of many illnesses of CNS, while reducing systemic side effects by delivering long-term well-dispersed drug delivery to selected brain areas (Nancea et al. 2017).

Chemotherapeutic drugs administered by systemic way are ineffective due to bad therapeutic index for invasive brain tumor therapy. Extracellular matrix which is dense and raised interstitial pressure generate a blood tumor barrier in glial cell cancer despite of existence of heterogeneously leaky microvessels that prevent drug delivery and distribution. Further the intact blood-brain barrier protects invasive cancer cells beyond the tumors' MRI-enhancing edge. The research was conducted to study whether brain-penetrating nanoparticles (BPNs) with thick polyethylene glycol surface coatings and loaded with cisplatin could be supplied with MR image-guided focused ultrasound (MRgFUS) across tumor and obstacles of blood brain barrier and whether this therapy can control glioma development and hence invasiveness. Further in tumor models, BPN delivery across the intact BBB was also significantly improved just beyond the tumor limit. It was shown that a CDDP-loaded BPN (CDDP-BPN) formulation, consisting of a mixture of polyaspartic acid (PAA) and strongly PEGylated polyaspartic acid (PAA -PEG), was extremely stable, provided release of drug was extended and was efficient against in vitro F98 cells. These CDDP-BPNs were supplied to orthotropic F98 glioma using MRgFUS from systemic circulation, resulting significantly in reduction of tumor invasiveness, and development also enhanced survival of the animal. Thus, it was concluded that the therapy can provide strong fresh strategy to the treatment of invasive gliomas, especially to prevent and control recurrence (Timbie et al. 2017).

Metallic Nanoparticles

Antibacterial activity of silver nanoparticles has been studied and used. In this study the impact of applying therapeutic ultrasound in the presence of silver nanoparticles of less than 100 nm on human ovarian carcinoma cells A2780 was studied. MTT assay and lifetime microscopy examined the viability of cell. The presence of nanoparticles in cells was studied using electron transmission microscopy. Experiments showed a considerable reduction in cell-based viability, which has been affected by collective effect of ultrasound and silver nanoparticles. The experiments demonstrate an important impact of applying these two variables successively. After incubation the presence of nanoparticles within the cells was shown. These findings indicate the use of ultrasound as a factor which in the presence of silver nanoparticles has impact on cell viability (Bernard et al. 2014).

Nanoprobes, small particles that circulate in the vascular system and have the ability to reach tumor tissue by means of endothelial gap, produce a fresh method for precise tumor surveillance and, molecular-level image-based antitumor therapy. The study involves a polymeric multifunctional nanoparticle probe loaded using gold nanorods (Au-NRs) and liquid perfluorocarbon (perfluorinated hexane/PFH) and conjugated using monoclonal antibody (MAGE-1 antibody) to melanoma-linked antigen genes (MAGE) targeting melanomas and was prepared by double emulsion and carbodiimide methods as targeted photoacoustic/ultrasound dual-mode imaging contrast agents (MAGE-Au-PFH-NPs). In vitro targeted delivery to cells showed large amount of MAGE-Au-PFH-NPs in targeted group around B16 melanoma cells. In the case of targeted

group, the photoacoustic signal was increased significantly and the in vivo period was longer than that in the untargeted group. Further in the case of photoacoustic instruments in vitro, the photoacoustic signal produced using nanoprobes was enhanced using Au-NR concentration. After laser irradiation carried at 808 nm, the improved signal was identified using ultrasound. Biocompatibility and cytotoxicity tests showed enhanced biological security for MAGE-Au-PFH-NPs. The MAGE-Au-PFH-NPs have been used as dual-mode photoacoustic/ultrasound contrast agent that is used as a base for tumor targeting, tracking, and therapy (Li et al. 2018).

Glioblastoma (GBM), a glial cell tumor, is the most prevalent as well as the most aggressive type of brain tumor with elevated morbidity and mortality rates. A strategy is urgently required to boost the effectiveness of accessible drugs and improve the delivery of chemotherapy over the blood-brain barrier (BBB). Along with MR-based focused ultrasound (MRgFUS), researchers explored the ability of cisplatin-conjugated gold nanoparticle (GNP-UP-Cis) to intensify GBM therapy. Viability assays have shown that GNP-UP-Cis significantly inhibits GBM cell growth relative to free cisplatin and demonstrates marked synergy with radiation therapy. In addition, increased DNA damage was noted in GNP-UP-Cis-treated cells along with increased platinum levels as a result of γH2AX phosphorylation. In vitro, the development of GBM tumors was significantly decreased by GNP-UP-Cis, and MRgFUS resulted in enhanced BBB permeability and distribution of GNP drugs to the brain tissue. Our studies indicate that GNP-Cis conjugates and MRgFUS can be used to deliver targeted chemotherapy to brain tumors in a focused manner (Coluccia et al. 2018).

Titanium Dioxide Nanoparticle (Semiconductor) Type

Like in the case of most of the nanoparticles, titanium dioxide is used as photocatalyst that generates reactive oxygen species (ROS) through the effect of ultrasound irradiation (Farner et al. 2019). This causes cancer cell death as well as harmful chemical degradation and microorganism inactivation (Blake et al. 1999). Further nanoparticles of TiO_2 can also be used as photocatalyst for cancer cell injury. Further nanoparticle surface was modified to target ROS impact on desired cells, and thus antibody immobilized TiO_2 NPs can be applied to cause photolytic degradation of cancer cells (Ninomiya et al. 2012).

Further it was studied that TiO_2 can be used as sonocatalyst; specifically these particles can improve production of hydroxyl ion radical by destruction of ultrasound even in the absence of light deprived of UV irradiation. This sonocatalytic results generated by TiO_2 nanoparticles can be used for studying destruction of definite types of chemicals and hence microorganism inactivation.

Further it was found that TiO_2 can be used as sonocatalyst; specifically TiO_2 nanoparticles can generate hydroxyl radical using ultrasound irradiation even in the absence of light without UV light irradiation. These sonocatalytic results generated by TiO_2 nanoparticles can be used for studying chemical degradation and thus microorganism inactivation.

Further utilizing the sonocatalytic effect generated due to TiO_2 NPs on injury to cancer cells, TiO_2 NPs modified with targeting proteins are integrated with cancer cells and stimulated sonocatalytically to generate OH radicals that causes injury to the cell membrane.

Thus the cell-destroying factors of TiO_2/US treatment are considered to be roughly divided into the following:

1. Chemical factors like ROS resulted from TiO_2 activation under ultrasound irradiation causing oxidation of the cell membrane
2. Physical factors such as shear stress derived from the collapse of cavitation bubbles which causes cell membrane disruption

With regard to the chemical factor for TiO_2/US therapy when TiO_2 NPs are integrated into the cells, the ROS can affect the cells more efficiently because when produced on the TiO_2 surface, ROS has very short half-lives. Thus modification of the TiO_2 NPs with biomolecule specifically binding to target cells is an intelligent SDT approach. In general, therefore TiO_2 NPs showing nonspecific incorporation cannot be used as practical

SDT sonosensitizers as this will also respond to ultrasound stimulation to ordinary cells close to tumors.

Thus, in general, TiO_2 NPs which exhibit non-specific incorporation cannot be used as a practical sonosensitizer for SDT since it would also accumulate to normal cells in the vicinity of the tumors that would react to ultrasound stimulus.

The following are the studies carried out using TiO_2 nanoparticle as sonosensitizers.

Although sonodynamic therapy is used as alternative potential to conventional form of photodynamic therapy, sonosensitizers of low quantum yield such as TiO_2 nanoparticles produce a major problem. In this strategy, hydrophilized Au-TiO_2 nanocomposites (HAu-TiO_2 NCs) have been used as sonosensitizers for enhanced SDT. Physicochemical properties of HAu-TiO_2 NCs have been carefully researched and contrasted without gold deposition with their counterparts. A large quantity of reactive oxygen species was produced after exposing HAu-TiO_2 NCs to ultrasound, causing the destruction of tumor growth on systemic administration. Overall it was determined that gold composite with TiO_2 NPs increases the ROS generation concentration considerably, utilizing its potential as SDT agent for cancer therapy (Deepagan et al. 2016).

A new therapeutic approach for malignant gliomas is anticipated to be sonodynamic therapy. Ultrasound can activate, a photosensitizer, a titanium dioxide nanoparticle. In this research, a comparison was created in vitro between photodynamic and sonodynamic damage on U251 human glioblastoma cell lines using water-dispersed TiO_2 nanoparticles. Through the adsorption of chemically altered polyethylene glycol on the TiO_2 surface, water-dispersed TiO2 nanoparticles were built. U251 monolayer cells were incubated for 3 h in cultural medium including 100 μg/mL of TiO2/PEG and subsequently irradiated by ultraviolet light (5.0 mW/cm^2) or 1.0 MHz ultrasound (1.0 W/cm^2) to assess cytotoxicity. MTT assay estimates cell survival 24 h after irradiation. The photodynamic cytotoxic effect upon 20 min of ultrasound light exposure was not seen in the presence of TiO_2/PEG, whereas the sonodynamic cytotoxicity effect was nearly proportional to the sonication time. Furthermore, radical scavenger nearly inhibited the photodynamic cytotoxicity of TiO_2/PEG, while suppression of the sonodynamic cytotoxic impact was not important. Results of multiple fluorescent stains showed that cells treated with ultrasound lost their viability instantly after irradiation and particularly damaged cell membrane compared to cells treated with ultraviolet. These results demonstrated a prospective implementation of TiO_2/PEG as new treatment method for malignant gliomas for sonodynamic therapy and found that the TiO_2/PEG-mediated mechanism for sonodynamic cytotoxicity differ from photodynamic cytotoxic therapy (Yamaguchi et al. 2011).

Sonodynamic therapy (SDT) is a fresh method of activating definite sensitizers of chemical for cancer therapy using ultrasound (US). Here in the research, in vitro and in vivo irradiation explored the influence of US-coupled nanoparticle of titanium dioxide on melanoma cell. In the presence and or absence of TiO_2, cells of melanomas (C32) are destroyed with US. Immediately after US irradiation, cell viability was measured (1 MHz, 0.5 and 1.0 W/cm^2 for 10 s). Measuring tumor volume regression explored the impact of the mixture of TiO_2 and US exposure (1 MHz, 1.0 W/cm^2, 2-min duration) on subcutaneously implanted strong C32 tumors in mice. The cell viability in the presence of TiO_2 was considerably reduced only after US irradiation. Result from the in vivo irradiation showed important inhibition of tumor development in TiO_2 and US-treated groups. It is the first post to show the cell-killing impact of TiO_2 nanoparticles under US in vitro and in vivo irradiation (Harada et al. 2011).

A study was carried out on sonodynamic therapy for cancer cells using the delivery of nanoparticles of TiO_2 modified with protein precisely identifying target cells and thus following its generation of TiO_2NP hydroxyl radical triggered by internal ultrasound irradiation called as TiO_2/US therapy. This research first examined HepG2 cell uptake conducted with pre-S1/S2 (protein recognizing hepatocyte, model) modified by TiO_2 NPs for 24 h. It went 6 h for the cells to take up

enough of the TiO_2 NPs. Next the impact of TiO_2/US therapy on the development of HepG2 cells was investigated for 96 h after the 1 MHz ultrasound (0.1 W/cm^2, 30 s) was irradiated to the cells that integrated the TiO_2 NPs. After therapy with TiO_2/US, apoptosis was noted at 6 h. Although no cell injury was noted until 24 h after therapy, at 96 h, the feasible concentration of cells had worsened to 46% of the control. Finally, a mouse xenograft model was treated with the TiO_2/US treatment. The pre-S1/S2 immobilized TiO_2 (0.1 mg was injected) straight into tumors accompanied by an ultrasound irradiation of 1 MHz for 60 s at 1.0 W/cm^2. Tumor development could be hindered up to 28 days, which is associated to regulation circumstances as a consequence of therapy repeated five times within 13 days (Ninomiya et al. 2012).

The noninvasive photodynamic therapy was restricted to the treatment of superficial tumors, mainly due to bad light penetration of the tissue as the source of the energy. Here study on a long-circulating titanium dioxide nanoparticle ($HTiO_2$ NP) which is activated by using ultrasound to produce reactive oxygen species (ROS). $HTiO_2$ NPs efficiently blocked the progress of superficial tumors following ultrasound-mediated treatments when systematically administered to mice. In multiple fold tumor tissue, we evaluated the concentration of pro-inflammatory cytokines, and intense vascular harm was noted. Further ultrasound treatment using $HTiO_2$ NPs too repressed at least 15-fold development of deeply located liver tumors compared to non-ultrasound treatment animals. This research offers the first demonstration that $HTiO_2$ NPs can be used as sensitizers for in vitro sonodynamic therapy (You et al. 2016).

In another study in order to enhance targeting of the drug and combination therapy, titanium dioxide entrapped Fe_3O_4 nanoparticle wherein TiO_2 acts as the sonosensitizer. In this combination strategy, doxorubicin has been incorporated. In the incubation of these nanoparticles with cancer cells, ROS is produced efficiently on irradiation using ultrasound. This combination therapy thus produces stronger synergistic effect causing stronger cytotoxicity and hence more therapeutic effect. Thus, it also proved to be highly effective in enhancing therapy and thus reduced side effects.

Fe_3O_4 Nanoparticles

From the different types of nanoparticles, magnetic nanoparticles (MNPs) like Fe_3O_4 (magnetite) and Fe_2O_3 (maghemite) have shown to attract a lot of attention, specifically those that show superparamagnetic properties (SPIONs), which are desired nanoparticles for biomedical uses. For instance, it is used for biological purposes like cell isolation, drug delivery, MRI-based diagnosis, cellular imaging, and hyperthermia. The toxic effect of MNPs in biological environment is based on a number of factors related to properties of NP like size, concentration, surface properties, and structure properties. As per cellular study, the main toxicity caused by MNPs is stress generated by oxidation which is primarily generated by incomplete reduction of oxygen and thus affects cell metabolism and enhances apoptosis. MNPs can thus be used in therapy of cancer for cancer cell destruction (Arora et al., 2012). Figure 13.2g shows the release of doxorubicin from TiO_2-coated Fe_3O_4 nanoparticle (Shen et al. 2015).

The cavitation generated by ultrasound produces the ROS in cells, and thus by accumulating enough of ROS in cells, a cascade of events is produced inside the cells that causes apoptosis. ROS generated in the cavitation produces harmful effects on DNA of cells and also disrupts normal functions of mitochondria.

The cavitation generates hydroxyl radicals through Fenton's reaction. The results of these reactions are two different oxygen radical species with water as a byproduct. The reaction sequence is given below:

$$Fe^{2+} + H_2O_2 + H+ \rightarrow Fe^{3+} + HO\bullet + H_2O$$

$$Fe^{3+} + H_2O_2 \rightarrow Fe^{2+} + HOO\bullet + H$$

The reduction of free iron, the Fenton reaction, is incomplete, whereas the use of ultrasound wave can produce superoxide radical that improves iron release from ferritin, providing a pool of active Fe^{2+} to catalyze the Fenton reac-

tion. It is shown that there is a large amount of increase in ROS production that shows an increase in Fe ions leading to more cellular toxic effect.

The following is the research carried out using a combination of effect of nanoparticles of Fe_3O_4 and ultrasound waves of therapeutic importance in the viability of cancer cells. In the study, a sonosensitizer therapeutic ultrasonic wave with 1 MHz frequency and various levels of Fe_3O_4 nanoparticles were explored to understand the combined impact on MCF-7 cell line. In short cells were split into distinct groups: control cells that came into contact with nanoparticles and cells affected by mixture of nanoparticles and ultrasound wave on exposure to cells and ultrasound wave. Finally, to detect cytotoxicity impacts, a cell viability assay was used. Experimental findings showed an important reduction in cell viability affected by combined ultrasound field action and Fe_3O_4 nanoparticles as associated to the distinct exposure of Fe_3O_4 nanoparticles or ultrasonic field. Ultrasound waves and Fe ions may have a synergistic impact due to manufacturing of lethal free radicals (Fard et al. 2015).

Silicon Nanoparticles

Porous silicon biocompatible and biodegradable NPs are very promising, which are verified for multiple medical apps by their preclinical studies. Porous silicon nanoparticles (PSi NPs) have been explored extensively as drug delivery nanocontainers, fluorescent labels, and reactive oxygen photosensitizers. PSi NPs have been extensively explored as drug delivery nanocontainers, fluorescent labels, and photosensitizers of reactive oxygen. To explain the possible mechanism of therapeutic effect of USI in the presence of PSi NPs and to ensure their potential for the SDT, two main hypotheses should be considered. The first one assumes the local heating of nanoparticles in ultrasonic field, i.e., local hyperthermia. The second is based on the assumption that PSi NPs initiate acoustic cavitation, which causes intense mechanical movement and cell destruction. In case of PSi NPs, one should take into account gas bubbles related both to the residual dissolved air inside the pores and gaseous products of silicon dissolution, i.e., hydrogen.

The following data explain the studies carried out using porous silicon nanoparticles and ultrasound.

A significant reduction in the cavitation limit was noted for ultrasound irradiation (USI) with therapeutic frequency (0.88 MHz) and intensity (about 1 W/cm^2) in aqueous suspension of porous silicon nanoparticles (PSi NPs) with dimension of about 100 nm compared to pure water. This impact is described by PSi NP porous morphology, which encourages cavitation bubble nucleation. In vitro studies disclosed a suppression of cancer cell proliferation with the introduced PSi NPs following USI exposure linked to improved cavitation procedures, resulting in cell destruction. The results obtained shows that PSi NPs in mild cancer therapy are prospective for application as sonosensitizers. Biodegradable polymer (dextran) was used to cover luminescent porous silicon nanoparticle with mean size of about 100 nm and was investigated as potential sensitizer for ultrasound-assisted therapy. The effective absorption of nanoparticles by cancer cells in vitro was disclosed by luminescent confocal microscopy. The nanoparticles were found to be almost nontoxic to 0.1 mg/mL and 30 mg/kg as confirmed by experiments in vitro and in vivo, respectively. Following a combination of nanoparticles and therapeutic ultrasound irradiation with frequencies of 1–3 MHz and intensities of 1–2 W/cm^2, a powerful suppression of cancer cell proliferation was noted (Osminkina et al. 2015).

Sonodynamic therapy is a noninvasive method of the development of cancer treatment based on acoustic cavitation selectively activating a sonosensitizer agent. The activated sonosensitizer agent could produce species of reactive oxygen leading to death of cancer cells. Next researchers explored the potential of core shell polymethyl methacrylate nanoparticles (NPs) loaded with meso-tetrakis (4-sulfonatophenyl) porphyrin (TPPS) as an innovative sensitizing scheme, i.e., TPPS-NPs. Once charged to NPs, the sonosensitizing properties of TPPS were significantly enhanced, thus enhancing the efficacy

of the sonodynamic therapy in an in vitro neuroblastoma model (Canaparo et al. 2013).

Dendrimer Type

Peptide dendrimers are radially branched macromolecules comprising a central and/or peripheral peptide chain branching with the properties of being an effective carrier for drugs and biomolecules. With respect to other polymers used, dendrimers offer advantages with respect to size, polydispersity, encapsulation, and scaffolding properties. Several studies have been carried out on dendrimer-based treatment utilizing intravenous, intraperitoneal, transmucosal, oral, transdermal, and ocular route. Considering this, a study has been designed to determine individual and combined effect of peptide dendrimers and low-frequency ultrasound on transdermal delivery of ketoprofen. Studies showed that the synthesized peptide dendrimer increases transdermal permeation of ketoprofen and showed enhanced enhancement ratio of 3.25 as compared to passive diffusion of drug alone in vitro. Further combination of peptide dendrimer treatment and ultrasound application worked in synergy showing enhancement ratio up to 1369.15. In vivo studies demonstrated that dendrimer- and ultrasound-assisted permeation of drug achieved much higher plasma concentration of drug compared to passive diffusion. The excised mouse skin after in vivo permeation study with dendrimers and ultrasound did not show major toxic reactions. This study thus proves that arginine-terminated peptide dendrimer combined with sonophoresis enhances transdermal permeation of ketoprofen (Manikkath et al. 2017).

Similar line studies were carried out to investigate the combined effect of dendrimers and low-frequency ultrasound on the transdermal delivery of ketoprofen. Both PAMAM dendrimers and sonophoresis used individually increased the transdermal permeation of drug, but combination of these two techniques showed enhancement in permeation of the drug wherein pretreatment mode of dendrimer application showed higher drug permeation (Manikkath et al. 2017). These studies thus show enhancement in skin delivery of biomolecules.

3.4 Correlation Between Acoustic Cavitation Noise and Yield Enhancement of Sonochemical Reaction by Alumina Particle Addition

Chemical response leading to generation of hydroxyl radical oxidants, ozone, and hydroxyl peroxide from the hot place generated by violent collapse of cavitation bubble produced in a fluid irradiated using severe ultrasound is known as sonochemical response. It was identified that the broadband component present in the frequency spectrum of acoustic noise is known as white noise, and it has the intensity corresponding to the quantity of cavitation bubbles which has shown activity in chemical, physical, and biological processes. The noise is obtained through nonlinear-type pulsations of bubble such as shock wave generation from bubble and acoustic emission produced through chaotically oscillating bubble. It was observed that addition of particle has the ability to further increase yield for sonochemical reaction.

The process is seen due to the presence of particle in the medium that offers nucleation site for cavitation bubble due to its surface roughness that leads to reduction in limit of cavitation when ultrasound causes irradiation of liquid. This addition of particle is anticipated to produce rise in amount of bubbles; however whether the rise in amount of bubbles due to addition of particle is liable for increasing the output of sonochemical response has not been proven till now.

Furthermore in one study, the effect of particles addition on the sonochemical response as a guide for oxidation reaction that utilizes ultrasound irradiation either in the presence or lack of alumina-dependent particles by measuring the associated frequency spectrum of applied intensity of sound and also absorption for release of iodide from an aqueous solution of KI was determined. Also, in addition to it, the time associated with temperature in degassed or in the air-saturated liquid which is irradiated using ultrasound is determined either in the presence or in the absence of alumina-based particles and is studied. Further a rise in the output associated

with sonochemical response by addition of particles that utilizes suitable quantity as well as size was also observed.

During such particle addition, the acoustic noise associated which along with rise in liquid temperature associated with cavitation bubble increases. This helps further to enhance sonochemical response (Tuziuti et al. 2005).

3.5 Ultrasound-Propelled Nanocups for Drug Delivery

As discussed, earlier cavitation is a dynamic behavior shown by bubble in response to positive and negative pressure stages, shown in response to an ultrasound wave resulting in growing and contraction of the bubble. This uncontrolled growth under specific conditions reduces the stress in the cavity until gas fluid is not able to help the inertia of surrounding liquid, and hence the cavity generated collapses violently. Thus in order to enhance the penetration as well as extravasation of free drugs in various application, microstreaming connected with such cavitation activity has been shown.

All the trials that aims at mechanically enhancing delivery of drugs to tumors have used shell microbubble that has been approved for use as an ultrasound-based contrast agent for diagnostic purpose in clinical application (Sun et al. 2005). However, the relatively big microbubbles are disrupted using ultrasound exposure at the wave amplitude needed to enhance delivery of drug and thus preventing its ability to increase drug penetration.

However, cavitation activity is also shown to be maintained for 30s or less even in the presence of these types of developments. It is thus not consistent with need to enhance drug delivery and penetration into tumors, specifically for tens of minutes to circulate. Further in order to maintain cavitation-mediated drug transport, numerous injections of microbubbles are required. Yet it is possible in the small animal models the requirement for repeated injections or continuous infusions that will cross the maximum allowable human dose (0.06 mL/kg) for these agents. To tackle this type of restriction, a new solid-gas nanoparticle which is capable of maintaining cavitation at ultrasonic pressure amplitude generated using standard diagnostic transducer and therapeutic ultrasound devices for several minutes was developed. Thus, a biocompatible nanoparticle having the shape of a cup, also known as nanocups, has been intended in order to trap surface nanobubbles that detach and collapse after being exposed to ultrasound.

On contact to ultrasound, the nanobubble which has been stabilized nucleates a cavitation which allows surrounding fluid to be actively micropumped and any agents present in it. Measurement was further carried out using in vitro and in vivo method to determine the cavitation activity and thus related cavitation enhanced transport of drug. In the presence of nanocups and ultrasound, the model demonstrates considerably increased extravasation of model drug. The nanocup itself also penetrates well beyond the vessel wall, sometimes far beyond the molecular drug (Kwan et al. 2015).

3.6 Cytotoxicity of Sonodynamic Therapy

SDT's cytotoxicity is a difficult subject and it is not easy to understand the toxicity processes. However, it is mainly affected by the nature and characteristics of ultrasound, and nanoparticles are thus affected by environmental conditions. Like different sonosensitizers that have shown different behaviors in the same experiment conditions, even their category is the same as in the case of NPs of metal oxide type. Also, various ultrasound parameters like frequency and intensity can produce different types of results in the presence of sonosensitizers of the same type. Further all the ultrasound or sound-based therapy have proved the toxicity produced.

These types of toxicity mechanisms are dependent on the nature and features associated with US and NPs as well as affected by environmental circumstances. Further different sonosensitizers show different types of behavior under the same type of experimental conditions, even if

it has the tendency to belong to the same type of category as that of metal oxide NPs. Further in case of same type of sonosensitizer, different types of ultrasound parameters like frequency and intensity lead to generation of different types of responses. Usually all the SDT trials proved treatment-associated toxicity showing cell-associated viability.

First oxidative stress plays an important role in SDT-generated cytotoxicity. ROS is produced above cell-tolerated boundaries, resulting in the production of oxidative stress and oxidative lesions in cell structures. Next the type of cell destruction caused ranges from one context to another, and hence either apoptosis or necrosis is shown. The nature of the ROS depends on the type of methods used to detect them.

First oxidative stress seems to play a key role in SDT-induced cytotoxicity. ROS is generated above the cell-tolerated boundaries, resulting in oxidative stress and oxidative lesions in cellular structures. The sort of cell death caused varies from one context to another, and either apoptosis or necrosis is reported. Next the type of ROS involved depends on the method utilized to detect it (e.g., electron paramagnetic resonance (EPR) spectroscopy, flow cytometry, spectrofluorometry), molecule used to identify them (e.g., specific fluorescent and chemiluminescent sensors, electron spin resonance (ESR) spin traps, or ROS scavengers), and type of experimental conditions used (temperature, duration of testing). However even though ROS is difficult to identify, a range of observed ROS-based biological impact confirms the existence. These impacts involve apoptosis induction, lipid-based peroxidation and mitochondrial capacity loss, damage to DNA, and activation produced by different ROS-based signaling pathways. This singlet oxygen radical is among all the recognized ROS engaged in SDT phase.

Sonoluminiscent hotspot generated on the surface of the sonosensitizer through ultrasound is responsible for the generation of oxidizing compound. The singlet oxygen generated is responsible for cell destruction impact like membrane and cytoskeletal harm, DNA destruction, and mitochondrial potential loss. The effect is associated with highly reactive compound mostly with generation of ROS and is often shown in combination with other effects called as sonochemical ones.

This type of effect is produced via the action of ultrasound on aqueous medium (implosion of bubble and release of energy) or from the structure of cell and NPs direct interaction. During the process of sonodynamic therapy, safety associated with each of the element has been considered; neither stimulus nor the sonosensitizer is poisonous; however cytotoxicity is generated when it has been mixed with each other.

The oxidizing compound is generated through the action of sonoluminiscent hotspot present on the sonosensitizer that is generated through ultrasonic energy. Further presence of singlet oxygen has been connected with diverse cell viability impacts like membrane and cytoskeletal harm, fragmentation of DNA and loss of mitochondrial capacity in the membrane, damage to DNA, and various ROS signaling pathway activation. Singlet oxygen radical is among all the recognized ROS engaged in SDT phase.

Further the sonochemical effects associated with these highly reactive compounds and more in general with ROS generation have been detected along with other types of effect knows as sonomechanical effects. Such type arises either from action of ultrasound on aqueous medium (implosion of bubble and release of energy) or by direct impact of NPs on cell structures. The result generated is mechanical damage and thus consequent production of cell death using mechanical pathway.

Thus, the basic goal associated with nanoparticle-based SDT is destruction of cells that depend on combined therapy based on ultrasound and nanoparticles (Canavese et al. 2018).

3.7 Ultrasound-Related Toxicity

High-intensity focused ultrasound has tendency to cause highly damaging effect on viability of the cells and hence ablation of tumor. However, in the case of SDT, cytotoxicity associated with low-intensity ultrasound (US) (below 5 W/cm^2)

should be considered. Intensity of the ultrasound wave is an important parameter to be taken into account during cytotoxicity, and the difference associated along with it generates various toxic impacts in the biological system, even in the range of small intensities. The cytotoxicity can be tuned by merely changing the intensities associated with the ultrasound. It was also found that the ratio of cell apoptosis to necrosis has been determined by intensities of US stimulus used.

US-based cavitation is dependent on the creation of the small gas bubbles in tissue due to US vibration, and hence harm produced for biological structures is because of inertial cavitation, whereby bubble destruction produces an aggressive mechanism leading to cell structure destruction. Instead different damage mechanisms are connected with acoustic streaming. This is a fluid motion owing to the wave of ultrasound that is produced through ultrasound energy shift to the fluid. This may lead to motion generation through propagation of the ultrasound beam (bulk streaming) or the stream eddies around a vibrating bubble (microstreaming). The method is less aggressive than the cavitation itself. In addition, other than structural impacts, it is shown that low-intensity US cavitation produces change in the associated cellular toxicity like synthesis of protein and manufacturing of cytokine. This functional effect produced can be justified by utilizing mechanoreceptor activation which is capable of identifying mechanical stimulation produced by ultrasound. This type of the activation can be interpreted as a type of cellular reaction to regeneration that is created using cell to combat the treatment-directed damage. Thus, it can be concluded that cytotoxicity produced by ultrasound is linked not to mechanical damage but also to chemical species, i.e., ROS. Due to this sonosensitizers have been used in order to enhance the output generated by ultrasound treatment even though the cell damage can be produced by synergistic effect of two or only one (Canavese et al. 2018).

Several metal oxide NPs on both prokaryotic and eukaryotic cells have been shown to show inherent cytotoxicity. The cytotoxic impact mechanisms are complicated and are hard to generalize. In reality they are dependent on the concentration and physicochemical features of the particular metal oxides, which in the biological competition also influence their conduct. However out of all the literature-suggested cytotoxicity mechanisms, three of them deserve consideration when applying SDT: ROS generation, cell membrane destruction, and metal ion release. In the case of ROS generation, certain studies show the ability of metal oxide-based nanoparticles even in the absence of any motive to generate ROS. This is shown in the case of components or compound having semiconductor properties. Electrons can readily move with the adsorbed species to the particle surface, leaving highly reactive holes in the conductive band which is further dependent on the flaws of NP crystal structure. In addition to this, ROS can be obtained from indirect process that involves interaction between NPs and electron transport chain present in the mitochondrial cell apparatus. Cell membrane destruction through mechanical process is the second mechanism involved. Finally, because of the dissolution of the metal oxide-based NPs in aqueous media, release of metal ion is considered as a major toxicity cause associated with NPs. These metal-based toxicities have been poorly studied and are specific for each metal. Like in the case of ZnO NPs, dissolution into Zn^{+2} leads to mitochondrial apoptosis and toxicity of protein disorders owing to the activation of particular cellular reactions (Canavese et al. 2018).

4 Nanoparticle-Assisted Ultrasound in Cancer Therapy Clinical Application

Microbubbles coupled with ultrasound lead to the creation of pores in the cell membrane; they also open the endothelial junctions, thus enhancing vessel permeability and improving extravasation of co-administered drugs. Phospholipidic microbubble in association with ultrasound has been used to enhance the response of cancer patients. However, the disadvantage associated with microbubble is larger size, and to overcome

this size limit, nanoscale ultrasound contrast agents like nanobubbles, echogenic liposomes, micelles, and nanodroplets have been proposed which are able to extravasate from the blood vessels to the tissues and transport the drug deeper into malignant cells leading to new theranostic capabilities.

There are still few obstacles to translate the ultrasound-mediated drug delivery from nanostructures to clinical setting. For example, the comprehension of the cytotoxic mechanisms taking place in vivo has to be clarified. Similarly, the biological effect has to be monitored, and it is also important to understand the biodistribution and pharmacokinetics of NPs coupled with ultrasound when delivered in vivo.

Sonodynamic therapy has exhibited profound physical and chemical changes on cellular structure. It has also shown notable efficiency against a variety of neoplastic cell lines. It has also shown efficacy both in vitro and in vivo against multiple adherent neoplastic cell lines with particular promise against leukemia cells.

Sonoflora, a sonosensitizer, is able to generate singlet oxygen on interaction with proper ultrasound wave and induces cellular necrosis. It has been studied for advanced breast carcinoma. Similarly, another group studied SDT with two new chlorophyll-derived sonosensitizing agents and proved by in vitro studies on human breast and lung cancer cell lines that SDT is strongly synergistic with chemotherapy. Other clinical case studies were conducted in patients with locally advanced and inoperable pancreatic cancers. They were treated using a customized configuration of commercial clinical ultrasound scanners in the presence of MBs. The combination of ultrasound, microbubble, and chemotherapy in these clinical settings increased the number of treatment cycles prolonging the quality of life in patients with pancreatic adenocarcinomas compared to chemotherapy treatment. Thus, nanoparticles are successfully assisting ultrasound applications in particular sonodynamic competing with other more traditional techniques for cancer diagnosis and treatment.

The role of nanoparticle sonosensitizer should be further investigated and understood especially for those particles having a multifunctional and synergistic effect with ultrasound action. Together with the NP properties, ultrasound irradiation can be optimized to improve the generation of cavitating bubbles and consequently the therapeutic outcome of NP-assisted STD (Xiaohuai et al. 2008; Lentacker et al. 2009; Kaneko and Willmann 2012; Kotopuslis et al. 2013; Dimcevski et al. 2016; Guvener et al. 2017; Canavese et al. 2018).

5 Use of Ultrasound-Assisted Nanoparticle in Removal of Pollutants from Environment

Apart from using this strategy for therapeutic and diagnostic purpose, it can also have an important role to play in the removal of toxic agents from the environment.

Dye pollutants have a complex molecular, toxic, nondegradable, and stable structure that cause harmful effects when entering the environment. Eosin B is a chemical dye used in textiles and hygienic industries and has a highly toxic impact because of its aromatic properties. Different methods have been used for its elimination like biological, coagulation, and adsorption method. However, the use of other methods like sonocatalysis and photocatalysis has been suggested as the abovementioned methods are difficult to implement. Further, the use of ultrasound in the removal of the natural contaminants has been preferred due to the low cost, high efficiency, and energy saving.

The mechanism involves cavitation that produces increased temperature and pressure. This process involves creation, gradual growth, and ultimately eruption of a series of bubbles by application of ultrasound to the solution causing shock wave. During this process the generated hotspot is capable of converting water molecule into highly reactive species like hydroxyl free radicals, hydrogen, and hydrogen peroxide leading to destruction of these harmful contaminants.

These hydroxyl radicals are generally strong oxidizing agents that have the tendency to attack and destroy all organic-based pollutant to small molecule and thus convert them to H_2O and CO_2. The presence of solid particles increases the mass transfer coefficient of contaminants between catalyst surface and liquid. Various catalysts studied are TiO_2, $KNbO_3$, CdSe, Bi_2O_3, CdS, and ZnO. Of this ZnO has been widely used in the process of sonocatalysis in order to remove organic pollutants due to its specific properties, low cost and nontoxicity (Mahadavi and Siamak 2019).

Next a similar line study has been carried on ibuprofen. It is an analgesic and anti-inflammatory drug which is used commonly and is considered as pollutant in the marine setting. Hence study is carried out in order to determine the efficiency of ultrasonic process in the presence of titanium dioxide nanoparticle catalyst as well as hydrogen peroxide for degradation of ibuprofen from the aqueous solutions. The results indicate that the ultrasonic wave which is combined along with titanium dioxide nanoparticle has shown highest efficiency for ibuprofen degradation from the aqueous solutions. Further parameters like hydrogen peroxide concentration, pH, frequency, total organic carbon, and sonication time were effective in degrading ibuprofen efficiency (Ahmadpoura et al. 2019).

6 Equipment Used in Ultrasound-Assisted Drug Delivery System

Ultrasound is used in the therapeutic process as image-guided delivery of drugs and genes to different tissues. Ultrasound-mediated therapeutic delivery has acquired an attention as it delivers the drugs to target areas like tumor, thereby reducing systemic dose and toxicity. Due to wide availability of ultrasound, portability, inexpensive properties, as well as ability to focus on the targeted region without any invasion with precision, ultrasound-based drug delivery can be considered as an effective way for treatment of cancer that is not accessible to ultrasound.

By sonoporation process, ultrasound and microbubble-based cavitation produces temporary or permanent blood vessel wall pores and thus significantly improves therapeutic delivery in the extravascular region of interest. US MB-based drug delivery is triggered by both stable and inertial cavitation of microbubbles. When microbubbles oscillate stably without collapsing in the acoustic field, stable cavitation is seen, while when microbubble grows and collapses violently, it is known as inertial cavitation. As stated before both processes lead to exertion of mechanical forces on adjacent tissue, while microbubble collapse leads to production of secondary mechanical effects like shockwaves and liquid jetting which enhance sonoporation effects. Based on the type and concentration of microbubble and carrier for drug, the combination of certain ultrasound parameters like frequency, intensity, mechanical index, and ultrasound exposure duration can affect the drug delivery efficacy mediated by ultrasound. Hence it is important to understand the basics of ultrasound equipment. Figure 13.3a shows the components of the equipment.

The process consists of handheld probe (transducer) which is placed and moved over the patient directly. A water-containing gel is packed for coupling of ultrasounds between patients and transducer. A piezoelectric component present in the transducer generates a sound wave. The frequency of the sound ranges from 2 to 18 MHz. Further the sound is generated by the shape of the transducer or from the complex set of control pulses from the ultrasound scanner machine. It results in the production of the arc-shaped waves of ultrasound from the transducer face. These waves travel through the body and then focused at the desired depth. New technology-based transducers use phase array techniques that cause the machine to change its focus depth and hence direction.

All the piezoelectric transducers are ceramic types. To produce 2D image, the ultrasound-based image is swept. Also, transducer has been swept mechanically by moving or rotating 1D phase array transducers in order to seep the beam electronically. Data generated can be processed

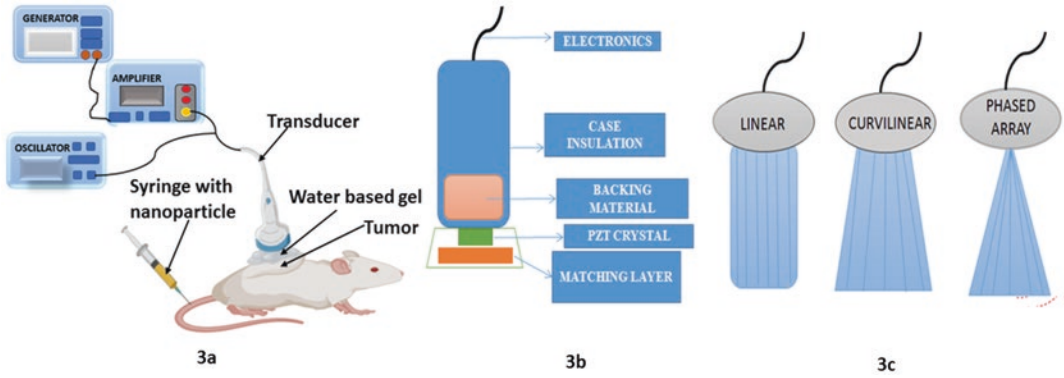

Fig. 13.3 (**a**) Basic components of ultrasound equipment. (**b**, **c**) Components of transducer and types of transducer

and has been used to produce an image which shows 2D presentation of the slice in the body. 3D image is produced by utilizing a series of adjacent 2D images. Majorly a specialized probe which scans mechanically a conventional 2D image transducer has been used. Further since the mechanical-based scanning is slow, it becomes problematic to generate 3D image of the tissue moving. Recently 2D-based array transducer that moves/sweeps the beam in the 3D wave has been developed. Figure 13.3b and c depicts the basic components of transducer and type of transducers.

Different types of modes used for ultrasound-based medical imaging include the following:

A-type mode – simple type of ultrasound. Here a single transducer is involved in scanning lines through the body, and the echoes have been plotted on screen as the function of the depth. Also, when ultrasound has been used for therapeutic uses and focuses on specific type of tumor or the calculus, it is also called as A mode that results in specific focus by the destructive wave energy.

B-type mode – transducers based on linear-type array have been used that scan a plane via a body that is observed as 2D-type image.

M-type mode – represents the motion. In this mode, sequence of B-type mode scans, whose images follow each other in sequence on scanning. Thus directs the doctors to observe and measure motion range, as the organ boundaries that produce reflections related to the probe.

Parts of ultrasound device include a transducer, transmitter pulse generator, compensating amplifier, control unit for focusing, a digital processor, and display system. Inverter is a part that converts electrical type of signals into the mechanical form and vice versa. When it is activated, these types of inverter are leaned on the body; it generates an ultrasonic beam. These waves are then focused using beam, ultrasonic mirrors, and by electronic means.

Medical ultrasound transducer, an echoscopic probe, is a device which is placed on a patient's body and consists of one or more ultrasound-based transducers, i.e., linear probe, sectoral probe, probe in which the ring changer focusing is performed, rocking mirror test, and convex probe.

Linear type of probe has been used at all the locations in which an access window present in the body is large. This inverter poses the ability to convert electrical type signals into mechanical one and vice versa.

6.1 Parameters of Ultrasound Affecting Drug Delivery

6.1.1 Frequency of Ultrasound

On the basis of tissues and the organism model, the frequency of ultrasound used for delivery of drug varies from kHz to MHz. In the case of therapeutic applications, frequency used is lower than for diagnostic uses. Optimum effect of therapy is obtained due to deeper penetration of ultra-

sound in the tissue at lower frequency. Further ultrasound frequency used is based on the kind of microbubble used as use of this ultrasound frequency near or same as that of resonant frequency of microbubble produces stable microbubble cavitation.

6.1.2 Intensity

Intensities which have been used for delivery of the drug range from 0.3 to 3 W/cm^2. Further FDA has approved the intensities that cause less than 1 °C rise in temperature. But high intensities of ultrasound have been used when pulse cycles/ultrasound frequency and/or pulse repetition frequency (pulses/sec) is reduced, resulting in low duty cycles (pulse length × pulse repetition frequency) and, thus, decreased temporal average intensity (duty cycle ultrasound intensity).

6.1.3 Mechanical Index

Mechanical index of ultrasound is the peak negative pressure (in MPa) divided by the square root of center frequency (in MHz). Mechanical index of ultrasound and intensity is proportional to acoustic pressure applied, and hence it is used as an alternative parameter. MI has also shown direct proportionality relation with cavitation activity. To prevent uncoated effect due to temperature, MI ranges from 0.2 to 1.9 hence reducing direct damage to tissue.

6.1.4 Treatment Duration

Duration of ultrasound used for treatment is dependent on the time utilized by ultrasound to produce stable or the inertial-type cavitation and thus sonoporation, thereby preventing thermal effects which are not necessary. Further the type and location of the tissue treated determines the duration for which ultrasound is used in drug delivery. High pressure that causes immediate type of inertial cavitation, continuous or multiple microbubble injections, and extended treatment time leads to enhancement in efficacy of drug delivery. But high pressure leads to unnecessary damage to tissue. At low pressure the time required for stable oscillations of microbubble and also required for obtaining optimum delivery of drug because of increased time of treatment at reduced pressure produces heating effects. As a result of which, duration of treatment as therapeutic protocol part is optimized for treatment indications (Chowdhary et al. 2017).

7 Effect of Microbubble Dynamics on Therapy

In ultrasound stimuli-based microbubble-mediated drug delivery, dynamics of microbubble with the immediate setting plays a significant part. Cavitation behavior is significantly altered under distinct settings, which in turn has a drastic effect on drug delivery results. It is not possible to apply single microbubble dynamics that only communicate with the surrounding setting to various microbubbles that communicate with microenvironment as well as with one another. In the event of numerous microbubble ranges between two microbubbles, the impact of microbubble and border on cavitation is shown. Adjacent boundaries and microbubble reduce cavitation by limiting microbubble development. In the process of numerous microbubble ranges between two microbubbles, microbubble and border exhibit cavitation impact. Microbubble cavitation (stable or inertial) has been shown to exert forces on deformable tissue limits in reaction to ultrasound exposure, which will in turn influence microbubble behavior. Next when microbubble has been injected in the blood vessels, it leads to communication between each other, and thus the associated sonoporation, cavitation, and drug delivery process are also affected by these types of interactions.

It was also found in the studies that reduction in the inter-microbubble distance can lead to increase of its lifetime which is not having any direct proportionality impact on the improvement in delivery of the drugs. Next, two or more of the microbubble can also join together to form a single microbubble through the impact of high-pressure ultrasound during the sonoporation process. Even though cavitation of fused microbubble can produce larger mechanical forces causing bigger pore size, it can also lead to tissue damage. It was also studied that less concentra-

tion of microbubble causes less uniform treatment, whereas the higher concentration of it leads to irreversible tissue damage (Chowdhary et al. 2017).

8 Conclusion

The use of smart and stimuli-responsive drug delivery is a rapidly growing area of biomaterial research. On the basis of this, ultrasound can be considered as one of the important role player for diagnostic and therapeutic purpose. Further use of various types of nanomaterial having either soft or hard nanomaterial has been studied for enhancing its efficacy which is attained using focused targeting of the ultrasound on the desired site for therapy. Besides this the concept of US-driven nanoparticle can be used to eliminate toxins from the setting as well as reduction of oil viscosity. The impact generated is either chemical based producing reactive oxygen species or physical leading to generation of shock, microstreaming, and radiation forces. As described in the literature, detailed mechanisms for the toxic effects are yet to be studied for further implementation of this therapy in the clinical use. In order to understand added applications, interdisciplinary scientific research has to be carried out in the future settings.

References

Abu Zidan FM, Henry AF, Corr P. Clinical ultrasound physics. J Emerg Trauma Shock. 2011;4(4):501–3.

Ahmadpoura N, Sayadia MH, Verma A, Mansouri B. Ultrasonic degradation of ibuprofen from the aqueous solution in the presence of titanium dioxide nanoparticles/hydrogen peroxide. Desalin Water Treat. 2019;145:291–9.

Bellini E, Grieco MP, Raposio E. A journey through liposuction and liposculture: Review. Ann Med Surg (Lond). 2017;24:53–60.

Bernard V, Mornstein V, Jaros J, Sedlackova M, Skorpikova J. Combined effect of silver nanoparticles and therapeutically ultrasound on ovarian carcinoma cells A2780. J Appl Biomed. 2014;12:1–9.

Blake DM, Maness P, Huang Z, Wolfrum EJ, Huang J. Application of the photocatalytic chemistry of titanium dioxide to disinfection and the killing of cancer cells. Separat Purific Method. 1999;28(1):1–50.

Bogdan J, Pławińska-Czarnak J, Zarzyńska J. Nanoparticles of titanium and zinc oxides as novel agents in tumor treatment: a review. Nanoscale Res Lett. 2017;12:225.

Buchanan KD, Huang SL, Kim H, McPherson D, Mac Donald R. Encapsulation of NF-kappa B decoy oligonucleotides within echogenic liposomes and ultrasound-triggered release. J Control Release. 2010;141(2):193–8.

Canaparo R, Varchi G, Ballestri M, Foglietta F, Sotgiu G, Guerrini A, Francovich A, Civera P, Frairia R, Serpe L. Polymeric nanoparticles enhance the sonodynamic activity of meso-tetrakis (4-sulfonatophenyl) porphyrin in an in vitro neuroblastoma model. Int J Nanomedicine. 2013;8:4247–63.

Canavese G, Ancona A, Racca L, Canta M, Dumontel B, Barbaresco F, Limongi T, Cauda V. Nanoparticle-assisted ultrasound: a special focus on sonodynamic therapy against cancer. Chem Eng J. 2018;340:155–72.

Carovac A, Smajlovic F, Junuzovic D. Application of ultrasound in medicine. Acta Inform Med. 2011;19(3):168–71.

Ce Guo. The relationship between the collapsing cavitation bubble and its microjets near a rigid wall under an ultrasound field. Chapter 5. 2018;73–89.

Centelles MN, Wright M, So PW, Amrahli M, Xu XY, Stebbing J, Miller AD, Gedroyc W, Thanou M. Image-guided thermosensitive liposomes for focused ultrasound drug delivery: using NIRF-labelled lipids and topotecan to visualise the effects of hyperthermia in tumours. J Control Release. 2018;280:87–98.

Chowdhary SM, Lee T, Willmann JK. Ultrasound guided drug delivery in cancer. Ultrasonography. 2017;36(3):171–84.

Coluccia D, Figueiredo CA, Wu MY, Riemenschneider AN, Diaz R, Luck A, Smith C, Das S, Ackerley C, O'Reilly M, Hynynen K, Rutka JT. Enhancing glioblastoma treatment using cisplatin gold nanoparticle conjugates and targeted delivery with magnetic resonance guided focused ultrasound. Nanomedicine. 2018;14(4):1137–48.

Dalecki D. Mechanical bioeffects of ultrasound. Annu Rev Biomed Eng. 2004;6:229–48.

Deepagan VG, You DG, Wooram U, Ko H, Kwon S, Choi KY, Ra YG, Lee JY, Lee DS, Kim K, Ick C K, Par JH. Long circulating Au-TiO2 Nanocomposite as a Sonosensitizer for ROS-Mediated Eradication of Cancer. Nano Lett. 2016;16:6257–64.

Deng CX, Xu Q, Apfel RE, Holland CK. Inertial cavitation produced by pulsed ultrasound in controlled host media. J Acoust Soc Am. 1996:1199–208.

Dimcevski G, Kotopoulis S, Bjanes T, Hoem D, Schjott J, Gjertsen BT, et al. A human cliica trial using ultrasound and microbubble to enhance gemticabine treatment of inoperable pancreatic cancer. J Control Release. 2016;243:172–81.

Endo-Takahashi Y, Negishi Y, Kato Y, Suzuki R, Maruyama K, Aramaki Y. Efficient siRNA delivery

using novel siRNA-loaded bubble liposomes and ultrasound. Int J Pharm. 2012;422(1–2):504–9.

Evien TJ, Nilssen EA, Rognvaldsson S, Brandl M, Fossheim SL. Distearoylphosphotidylethalonamine based liposomes for ultrasound mediated drug delivery. Eur J Pharm Biopharm. 2010;75(3):327–33.

Fard AE, Zarepour A, Zarrabi A, Shanei A, Salehi H. Synergistic effect of the combination of triethyleneglycol modified Fe_3O_4 nanoparticles and ultrasound wave on MCF-7 cells. Journal of Magnetism and Magnetic Materials.2015; 394, 44–49.

Farner JM, Cheong RS, Mahe E, Anand H, Tufenkji N. Comparing TiO_2 nanoparticle formulations: stability and photo reactivity are key factors in acute toxicity to daphnia magna. Environ Sci Nano. 2019;6(8):2532–43.

Garg S, Thomas AA, Borden MA. The effect of lipid monolayer in-plane rigidity on in vivo microbubble circulation persistence. Biomaterials. 2013;34(28):6862–70.

Go Y, Lee H, Jeong L, Sun S, Hong E, Jung E, Ko C, Noh J, Park S, Lee, Chulgyu S, Dongwon L. Acid-triggered echogenic nanoparticles for contrast-enhanced ultrasound imaging and therapy of acute liver failure. Biomaterials. 2018;186:22–30.

Guvener N, Appold L, Lorenzi F d, Golombek SK, Rizzo LY, Lammers T, Kiessling F. Recent advances in ultrasound-based diagnosis and therapy with micro and nanometer sized formulations. Methods. 2017;130:4–13.

Haar GT, Coussios C. High intensity focused ultrasound: physical principles and devices. Int J Hyperthermia. 2007; 23(2):89–104.

Han H, Lee H, Kim K, Ki H. Effect of high intensity focused ultrasound (HIFU) in conjunction with a nanomedicines-microbubble complex for enhanced drug delivery. J Control Release. 2017;266:75–86.

Hangiandreou NJ. AAPM/RSNA physics tutorial for residents. Topics in US: B-mode US: Basic concepts and new technology. Radiographics. 2003;23:1019–33.

Harada Y, Ogawa K, Irie Y, Endo H, Feril LB Jr, Uemura T, Tachibana K. Ultrasound activation of TiO_2 in melanoma tumors. J Control Release. 2011;149(2):190–5.

Hizadifar Z, Babyn P, Chapman D. Mechanical and biological effect of ultrasound: a review of present knowledge. Ultrasound Med Biol. 2017;43:1085–104.

Hsiao Y, Kuo S, Tsai HD, et al. Clinical application of high-intensity focused ultrasound in cancer therapy. J Cancer. 2016;7(3):225–31.

Hubesh N, Kearney J, Zhao X, Kim J, Cezar CA, Suo Z, Mooney DJ. Ultrasound-triggered disruption and self-healing of reversibly cross-linked hydrogels for drug delivery and enhanced chemotherapy. Proc Natl AcadSci USA. 2014;111(27):9762–7.

Ianni TD, Bose RJC, Sukumar UK, Bachawall S, Wang H, Telichko A, Herickhoff CD, Robinson E, Baker S, Vilches Moure Jose G, Felt SA, Gambhir SS, Paulmurugan R, Dahl J. Ultrasound- and microbubble-mediated targeted delivery of therapeutic microRNA-loaded nanocarriers to deep liver and kidney tissues in pigs, license to bioRxiv under CC-BY-NC-ND 4.0 International License, Referred on 16 09 2019.

Ibsen S, Schutt CE, Esener S. Microbubble-mediated ultrasound therapy: a review of its potential in cancer treatment. Drug Des Devel Ther. 2013;7:375–88.

Ibsen S, Guixin S, Carolyn S, Linda S, Kyle DS, Michael B, Viviana S, Dmitri S, Michael B, Sadik E. The behavior of lipid debris left on cell surfaces from microbubble based ultrasound molecular imaging. Ultrasonics. 2014;54(8):2090–8.

Kaneko OF, Willmann JK. Ultrasound for molecular imaging and therapy in cancer. Quant Imaging Med Surg. 2012;2:87–97.

Klibanov AL, Hossack J. Ultrasound in radiology: from anatomic, functional, molecular imaging to drug delivery and image-guided therapy. Investig Radiol. 2015;50(9):657–70.

Klibanov AL, Shevchenko TI, Raju BI, Seip R, Chin CT. Ultrasound-triggered release of materials entrapped in microbubble-liposome constructs: a tool for targeted drug delivery. J Control Release. 2010;148(1):13–7.

Kotopuslis S, Dimcevski G, Gilja OH, Hoem D, Postema M. Treatment of human pancreatic cancer using combined ultrasound, microbubble, and gemcitabine: a clinical case study. Med Phys. 2013;40:072902.

Kuroki M, Hachimine K, Abe H, Shibaguchi H, Kuroki M, Maekawa S, Yanagisawa J, Kinugasa T, Tanaka T, Yamashita Y. Sonodynamic therapy of cancer using novel sonosensitizers. Anticancer Res. 2007;27(6A):3673–7.

Kwan JJ, Myers R, Coviello CM, Graham SM, Shah AR, Stride E, Carlisle RC, Coussios CC. Ultrasound-propelled nanocups for drug delivery. Small. 2015;11(39):5305–14.

Lee J, Min HS, You DG, Kim K, Kwon IC, Rhim T, Lee KY. Theranostic gas-generating nanoparticles for targeted ultrasound imaging and treatment of neuroblastoma. J Control Release. 2016;223:197–206.

Lee S, Han H, Koo H, Na JH, Yoon HY, Lee KE, Lee H, Kim H, Kwon IC, Kim K. Extracellular matrix remodeling in vivo for enhancing tumor targeting efficiency of nanoparticle drug carriers using the pulsed high intensity focused ultrasound. J Control Release. 2017;263:68–78.

Lentacker I, De Smedth SC, Sanders NN. Drug loaded microbubble design for ultrasound triggered delivery. Soft Matter. 2009;5:2161–70.

Li X, Wang D, Ran H, Hao L, Cao Y, Ao M, Zhang N, Song J, Zhang L, Yi H, Wang Z, Li P. A preliminary study of photoacoustic/ultrasound dual mode imaging in melanoma using MAGE targeted gold nanoparticles. Biochem Biophys Res Commun. 2018;502(2):255–61.

Liu L, Chang S, Sun J, Zhu S, Yin M, Zhu Y, Wang Z, Xu RX. Ultrasound-mediated destruction of paclitaxel and oxygen loaded lipid microbubbles for combination therapy in ovarian cancer xenografts. Cancer Letters. 2015; 361(1):147–154.

Maestroni U, Morandin F, Ferretti S, Dinale F, Ziglioli F. Recurrence of prostate cancer after HIFU. Proposal of a novel predictive index. Acta Biomed. 2018;89(2):220–6.

Mahadavi RS, Siamak AT. Enhancement of ultrasound assisted degradation of Eosin B in the presence of nanoparticles of ZnO as sonocatalyst. Ultrason Sonochem. 2019;51:230–40.

Mahmoud MZ, Alkhorayef M, Alzimami KS, Aljuhani MS, Abdelmoneim S. High-Intensity Focused Ultrasound (HIFU) in uterine fibroid treatment: review study. Pol J Radiol. 2014;79:384–90.

Manikkath J, Hegde A, Kalthur G, Parekh H, Mutalik S. Influence of peptide dendrimers and sonophoresis on the transdermal delivery of ketoprofen. Int J Pharm. 2017;521:110–9.

Miller D, Smith N, Bailey M, Czarnota G, Kullervo H, Makin I. American institute of ultrasound in medicine bioeffects committee. Overview of therapeutic. Ultrasound Applications and Safety Considerations. J Ultrasound Med. 2012;31(4):623–34.

Morch KA. Cavitation inception from bubble nuclei. Interface Focus. 2015;5(5):20150006.

Nancea E, Timbiec K, Millerd GW, Songc J, Louttitc C, Klibanov AL, Shihb T, Swaminathanb G, Tamargoa RJ, Woodworth GF, Hanes J, Price RJ. J Control Release. 2017; 1–12.

Nicodemus NE, Becerra S, Kuhn TP, Packham HR, Duncan J, Mahdavi K, Iovine J, Kesari S, Pereles S, Whitney M, Mamoun M, Franc D, Bystritsky A, Jordan S. Focused transcranial ultrasound for treatment of neurodegenerative dementia. Alzheimer's Dement (NY). 2019;5:374–81.

Ninomiya K, Ogino C, Oshima S, Sonoke S, Kuroda S, Shimizu N. Targeted sonodynamic therapy using protein-modified TiO_2 nanoparticles. Ultrason Sonochem. 2012;19:607–14.

Ninomiya K, Kawabata S, Tashita H, Shimizu N. Ultrasound-mediated drug delivery using liposomes modified with a thermosensitive polymer. Ultrasonics Sonochemistry. 2014; 21(1):310–316.

Ohl S-W, Klaseboer E, Khoo BC. Bubbles with shock waves and ultrasound: a review. Interface Focus. 2015;5:20150019.

Orsi F, Arnone P, Chen W, Zhang L. High intensity focused ultrasound ablation: a new therapeutic option for solid tumors. J Cancer Res Ther. 2010;6(4):414–20.

Osminkina LA, Nikolaev AL, Sviridov AP, Andronova NV, Tamarov KP, Gongalsky MB, Kudryavtsev AA, Treshalina HM, Yu T. Porous silicon nanoparticles as efficient sensitizers for sonodynamic therapy of cancer. Microporous Mesoporous Material. 2015;210:169–75.

Papa AL, Korin N, Kanapathipillai M, Mammoto A, Mammoto T, Jiang A, Mannix R, Uzun O, Johnson C, Bhatta D, Cuneo G, Ingber DE. Ultrasound sensitive nanoparticle aggregates for targeted drug delivery. Biomaterials. 2017;139:187–94.

Papachristodoulou A, Signorell RD, Werner B, Brambilla D, Luciani P, Cavusoglu M, Grandjean J, Silginer M, Rudin M, Martin E, Weller M, Roth P, Leroux JC. Chemotherapy sensitization of glioblastoma by focused ultrasound-mediated delivery of therapeutic liposomes. J Control Release. 2019;295:130–9.

Paris JL, de la Torre P, Cabañas MV, Manzano M, Flores AI, Vallet-Regí M. Suicide-gene transfection of tumor-tropic placental stem cells employing ultrasound-responsive nanoparticles. ActaBiomater. 2019;83:372–8.

Paris JL, Mannaris C, Cabañas MV, Carlisle R, Manzano M, Vallet-Regí M, Coussios CC. Ultrasound-mediated cavitation-enhanced extravasation of mesoporous silica nanoparticles for controlled-release drug delivery. Chemical Engineering Journal. 2018; 340: 2–8.

Patra JK, Das G, Fraceto LF, Campos EVRC, Rodriguez-Torres MP, Acosta-Torres LS, Diaz-Torres LA, Grillo R, Swamy MK, Shivesh S, Habtemariam S, Han-Seung S. Nano based drug delivery systems: recent developments and future prospects. J Nanobiotechnology. 2018;16:71.

Rosenthal I, Sostaric JZ, Riesz P. Sonodynamic therapy – a review of the synergistic effects of drugs and ultrasound. Ultrason Sonochem. 2004;11:349–63.

Rychak JJ, Klibanov AL, Hossack JA. Acoustic radiation force enhances targeted delivery of ultrasound contrast microbubbles: *In vitro* verification. IEEE Trans Ultrason Ferroelectr Freq Control. 2005;52(3):421–33.

Serpe L, Foglietta F, Canaparo R. Nanosonotechnology: the next challenge in cancer sonodynamic therapy. Nanotechnol Rev. 2012;1:173–82.

Shen S, Wu L, Xie M, Shen H, Qi X, Yan Y, Ge Y, Jin Y. Core shell structured Fe_3O_4 @TiO_2 – doxorubicin nanoparticles for targeted chemo – sonodynamic therapy of cancer. Int J Pharm. 2015;486:380–8.

Snipstad S, Berg S, Morch Y, Bjorkoy A, Sulheim E, Hansen R, Grimstad I, Vanwamel A, Torp AMS, Davis CDL. Ultrasound improves the delivery and therapeutic effect of nanoparticle-stabilized microbubbles in breast cancer xenografts. Ultrasound Med Biol. 2017;43(11):2651–69.

Sun Y, Kruse DE, Dayton PA, Ferrara KW. High-frequency dynamics of ultrasound contrast agents. IEEE Trans Ultrason Ferroelectr Freq Control. 2005;52(11):1981–91.

Tuziuti T, Yasui K, Sivakumar M, Iida Y, Miyoshi N. Correlation between acoustic cavitation noise and yield enhancement of sonochemical reaction by particle addition. J PhysChem A. 2005;109(21):4869–72.

Timbie KF, Afzal U, Date A, Zhang C, Song J, Wilson Miller G, Suk JS, Hanes J, Price RJ. MR image-guided delivery of cisplatin-loaded brain-penetrating nanoparticles to invasive glioma with focused ultrasound. J Control Release. 2017;263:120–131.

Varges A, Pegaz B, Debefve E, Konan-Kouakou Y, Lange N, Ballini J. P., Bergh H. van den, Gurny R, Delie F. Improved photodynamic activity of porphyrin loaded into nanoparticles: an in vivo evaluation using chick embryos. Int J Pharm. 2004;286:131–145.

Wahajuddin, Arora S. Superparamagnetic iron oxide nanoparticles: magnetic nanoplatforms as drug carriers. Int J Nanomedicine. 2012;7:3445–71.

Wan GY, Liu Y, Chen BW, Liu YY, Wang YS, Zhang N. Recent advances of sonodynamic therapy in cancer treatment. Cancer Biol Med. 2016;13(3):325–38.

Wang X, Cui G, Yang X, Zhang Z, Shi H, Zu J, Hua F, Shen X. Intracerebral administration of ultrasound-induced dissolution of lipid-coated GDNF microbubbles provides neuroprotection in a rat model of Parkinson's disease. Brain Res Bull. 2014;103:60–5.

Wang TY, Choe JW, Pu K, Devulapally R, Bachawal S, Machtaler S, Choudhary SM, Luong R, Tian L, Khuri Yakub B, Rao J, Paulmurugan R, Willmann JK. Ultrasound guided delivery of micro RNA loaded nanoparticles into cancer. J Control Release. 2015;203:99–108.

Wu Q, Yang Z, Nie Y, Shi Y, Fan D. Multi-drug resistance in cancer chemotherapeutics: mechanisms and lab approaches. Cancer Lett. 2014;347:159–66.

www.fusfoundation.org.

Xiaohuai W, Lewis TJ, Mitchell D. The tumoricidal effect of sonodynamic therapy (SDT) on S-180 sarcoma in mice. Integr Cancer Ther. 2008;7:96–102.

Xie F, Tsutsui JM, Lof J, Unger EC, Johanning J, Culp WC, Matsunaga T, Porter TR. Effectiveness of lipid microbubble and ultrasound in declotting thrombosis. Ultrasound Med Biol. 2005;31(7):979–85.

Yamaguchi S, Kobayashi H, Narita T, Kanehira K, Sonezaki S, Kudo N, Kubota Y, Terasaka S, Houkin K. Sonodynamic therapy using water-dispersed TiO_2-polyethylene glycol compound on glioma cells: comparison of cytotoxic mechanism with photodynamic therapy. Ultrason Sonochem. 2011;18(5):1197–204.

Yang M, Xie S, Adhikari VP, Dong Y, Du Y, Li D. The synergistic fungicidal effect of low-frequency and low-intensity ultrasound with Amphotericin B-loaded nanoparticles on C. albicans *in vitro*. Int J Pharm. 2018;542(1–2):232–41.

Yang X, Wang C, Ding M, Zhang C, Wang W, Cao Z. Indocynanine green (ICG) – Menthol loaded cerasomal nanoparticles for ultrasound imaging and photothermal therapy against tumor. Mater Lett. 2019;255:126534.

Yildirim A, Chattaraj R, Blum NT, Shi D, Kumar K, Goodwin AP. Phospholipid capped mesoporous nanoparticles for targeted high intensity focused ultrasound ablation. Adv Healthc Mater. 2017;6(18)

You DG, Deepgan VG, Um W, Jeon S, Sejin S, Chang H, Yoon H, Cho YW, Maggie S, Lee S, Pomper MG, Kwon IC, Kim K, Park JH. ROS-generating TiO_2 nanoparticles for non-invasive sonodynamic therapy of cancer. Sci Rep. 2016;6:1–12.

Yue T, Xu HL, Chen PP, Zheng L, Huang Q, Sheng WS, Zhuang YD, Jiao LZ, Chi TT, Zhu Ge DL, Liu JJ, Zhao YZ, Lan L. Combination of coenzyme Q10-loaded liposomes with ultrasound targeted microbubbles destruction (UTMD) for early theranostics of diabetic nephropathy. Int J Pharm. 2017;528(1–2):664–74.

Zhao C, Cheng R, Yang Zhe Y, Tian ZM. Nanotechnology for cancer therapy based on chemotherapy. Molecules. 2018;23(4):826.

Multiple Emulsions: Emphasizing on Industrial Applications

14

Pratishtha, Manish Kumar Gupta, and Swati Gupta

Abstract

Multiple emulsions generally consist of three phases. They can be O/W/O and W/O/W types of multiple emulsions. Multiple emulsions are prepared by incorporating preformulated macroemulsion (i.e., either O/W or W/O emulsions) into the respective aqueous or oil phase as required with the help of sufficient and appropriate emulsifier. For example, O/W and W/O emulsions are incorporated in oil phase and aqueous phase, respectively. Multiple emulsions are preferred over macroemulsions due to the sustained release mechanism of multiple emulsions that helps in the prolongation of drug release or slow release of drug which further delays/prolongs the drug stay in the body for therapeutic action. Demands for multiple emulsions are increasing as they can also be used as red blood cell substitute, oxygen substitute, bioavailability enhancer, etc. Multiple emulsions are eligible to target bioactivity, and they can also be used in drug overdose treatment. Multiple emulsions have a tendency to enhance the drug absorption in the gastrointestinal tract (GIT) when administered orally. They act as local immunosuppressant as they can reduce the immune system's activity. Targeted delivery of peptides and proteins can be achieved by using multiple emulsions because they can easily encapsulate peptide or proteins within the innermost layer. Multiple emulsions play a vital role in cosmetics as well as in health-care products; there are various cosmeceutical products available in the market such as moisturizer, sunscreen lotion, cleanser, antiperspirant, shaving cream, etc. for their moisturizing capability, protective nature, cleansing ability, sun protection, etc.

Keywords

Emulsions · Targeting · Evaluation · Industrial applications

1 Introduction

Emulsions are biphasic liquid dosage forms intended for oral or topical route of administration for attaining desired therapeutic effect of the drug dispersed in the formulation. The two phases of emulsions are, namely, continuous phase and dispersed phase. Emulsions are mainly of two types, i.e., oil in water emulsions (O/W) and water in oil emulsions (W/O). Basic differences

Pratishtha · S. Gupta (✉)
Amity Institute of Pharmacy, Amity University Uttar Pradesh, Noida, India

M. K. Gupta
SGT College of Pharmacy, SGT University, Gurugram, India

J. K. Patel, Y. V. Pathak (eds.), *Emerging Technologies for Nanoparticle Manufacturing*,
https://doi.org/10.1007/978-3-030-50703-9_14

Table 14.1 Difference between O/W and W/O emulsion

Oil in water emulsions (O/W)	Water in oil emulsions (W/O)
Water is in continuous phase, whereas oil is in dispersed phase.	Oil is in continuous phase, whereas water is in dispersed phase.
They are easy to wash due to their nonsticky or nongreasy nature.	They are sticky or greasy due to the presence of oil in continuous phase and therefore may not be easy to wash with only water and thus require soap to wash it.
It is preferred for oral use as it can mask the bitter taste of oil and thus is acceptable by patients.	Presence of oil in continuous phase gives the bitter taste therefore oral administration is avoided.
Topical application of O/W emulsion is preferred as it is easy to wash.	Topical application provides moisture to the surface.
Example: Milk, vanishing cream, etc.	Example: Cold cream

between O/W and W/O emulsions are described in Table 14.1. But emulsions can further be classified as double or multiple emulsions (O/W/O or W/O/W emulsions), microemulsion, nanoemulsion, etc.

Oil in water emulsions consist of oil in dispersed phase, whereas water in continuous phase or in other words oil part is dispersed in water, i.e., present as continuous phase. However, in water in oil-type emulsions, water is dispersed phase and oil is continuous phase. There are chances for both phases to have difficulty in incorporation due to their different nature; therefore to overcome this problem, some chemicals or substances having properties such as to be miscible with both the oil phase and water phase need to be incorporated. These substances are capable to mix easily or with the help of heat with both phases and thus allow incorporation of both oil and water phases. These substances acquiring such potency to hold together both unlikely natured or differently natured liquids to form an emulsion are called as emulsifiers. Examples of emulsifier are beeswax, soft paraffin, tragacanth, gum acacia, guar gum, etc. Various factors have been observed obstructing either the formation of emulsion or the type of emulsion such as emulsifiers, phase volume, ratio of each phase, etc. There are few tests available to detect the type of emulsion such as dye test, conductivity test, fluorescence test, etc. which are described briefly in Table 14.2.

2 Multiple Emulsions

Unlike macroemulsions, i.e., simple oil in water (O/W) emulsion and water in oil (W/O) emulsion, multiple emulsions have three phases. Formulating multiple emulsions helps in controlled or sustained release of drug. Multiple emulsions can be defined as a complex of both oil in water (O/W) and water in oil (W/O) type of emulsions. Multiple emulsions can be O/W/O and W/O/W type, which is briefly discussed in Table 14.3. In case of water in oil in water (W/O/W) type of multiple emulsions, first, water in oil (W/O) type of emulsion is prepared using suitable emulsifier (hydrophobic or lipophilic emulsifiers are preferred to disperse aqueous phase into oil, i.e., continuous phase), and then prepared W/O emulsions are incorporated in aqueous or water phase with the help of hydrophilic emulsifiers (stabilize the formulation), resulting in W/O/W emulsions which are best suited in delayed release of the drug molecule. Whereas in case of oil in water in oil (O/W/O)-type emulsions, O/W emulsions are prepared using hydrophilic emulsifiers and then are mixed in further oily phase (continuous phase). The use of hydrophilic and lipophilic surfactants enhances the stability of multiple emulsions. Multiple emulsions have vesicular structure dispersed as globules separated by layers of oil/aqueous phase accordingly (Nafisi and Maibach 2017). In multiple emulsion systems, the solute has to transverse from inner miscible phase to outer miscible phase by the middle immiscible organic phase; it is also known as liquid membrane system (Kumar et al. 2012). Generally, multiple emulsions are used in cosmetics, food, and pharmaceuticals. They give a smooth touch after topical application due to their fine texture.

Table 14.2 Test for detection of emulsion type

S. no.	Name of test	Procedure	O/W	W/O
1.	Dye test	Add few drops of dye (water-soluble dye or oil-soluble dye) in the prepared emulsion. Coloration of emulsion is observed either as whole or in droplets. Example of water-soluble dye – brilliant blue and methylene blue. Example of oil-soluble dye – scarlet red.	Water-soluble dye when mixed with O/W emulsion colors the whole emulsion because water is in continuous phase, whereas oil-soluble dye only colors the oil droplets dispersed throughout the emulsion.	Oil-soluble dye when mixed with W/O emulsion colors the emulsion fully, but in case of water-soluble dye, they color the emulsion partially or the droplets of water present in the emulsion.
2.	Dilution test	In this test, water is added in the emulsion and allowed to mix using the appropriate method of mixing. Stability of emulsion is observed after keeping it for a few minutes.	O/W emulsion will remain stable even after adding water in emulsion as majority of emulsion consists of water (continuous phase), and thus water is readily miscible with O/W emulsion resulting in stable emulsion.	After addition of water in W/O emulsion, it becomes unstable due to the presence of excessive amount of water, and this can also lead to phase inversion.
3.	Electrical conductivity test	A setup is arranged containing electrodes, a beaker, a light bulb, wire, and emulsion to be tested. Emulsion is poured into the beaker, and electrodes are placed in the beaker vertically, and bulb is connected to the electrodes with the help of wire. Observe the glowing or flickering of the bulb.	In case of O/W emulsions, bulb glows continuously because water is a good conductor of electricity and in this case, water is in continuous phase.	Bulb either flickers a bit or does not glow because water is in disperse phase and only present in the form of globules in W/O emulsions.
4.	Fluorescence test	Fluorescence test is susceptible for fluorescent oils only which under ultraviolet light shows the fluorescence. Emulsion is subjected to observation under microscope in the presence of UV light, and the pattern of fluorescence is observed.	Fluorescence is observed in W/O emulsion as small droplets due to the presence of oil in dispersed phase.	Majority of emulsion is observed to be fluorescent because oil is present as continuous phase.

Source: Jaiswal et al. (2015) and Ferreira et al. (2010)

In pharmaceutics and cosmetics, multiple emulsions are mainly used for their protective nature as they prevent the degradation of active ingredients present in cosmetics or pharmaceutical products (medicated multiple emulsions for topical and oral use) and also allow controlled release of drug due to globular or vesicular dispersion within multiple layers of oil and aqueous phase. In the case of cosmetics, nonionic surfactants are preferred. Multiple emulsions with milk immunoglobulin can protect drug or active ingredient from alkali, acid, and protease enzyme. Multiple emulsions can behave as internal reservoir for drug or active compounds by entrapping them within the inner layer forming a vesicular structure surrounded by other oil and aqueous phase accordingly (Nafisi and Maibach 2017). Examples of products/formulations in which multiple emulsions are used for their protective, nutritive, and moisturizing effects are sunscreens, antiperspirants, shaving creams, hand creams, makeup cleansers, etc.

Table 14.3 Difference between O/W/O and W/O/W multiple emulsions

Water in oil in water (W/O/W) emulsion	Oil in water in oil (O/W/O) emulsion	References
W/O/W emulsions consist of water droplets dispersed in oil phase forming water in oil emulsion and then incorporating this W/O emulsion in an aqueous phase resulting in W/O/W emulsion. It could be either a two-component or three-component formulation (e.g., $W_1/O/W_1$ or $W_1/O/W_2$ emulsion) (Fig. 14.1).	O/W/O emulsions consist of water droplets dispersed in oil phase forming oil in water emulsion and then incorporating this O/W emulsion in an oil phase resulting in O/W/O emulsion. In this, one type of oil or two different oils can be used to prepare O/W/O emulsion (Fig. 14.1).	Nafisi and Maibach (2017)

2.1 Evaluation of Multiple Emulsions

2.1.1 Microscopic Evaluation

The microscopic evaluation of multiple emulsions is used for the determination of consistency, color, and homogeneity.

2.1.2 Macroscopic Evaluation

Multiple emulsions are evaluated using a macroscope to detect the globule size and size distribution in emulsion.

2.1.3 Zeta Potential Test

Zeta potential test is done for the detection of electrokinetic potential of colloidal dispersion. It can be determined using the Smoluchowski equation:

$$\tau = \frac{4\pi n\mu}{\varepsilon E} \times 10^3$$

where

τ = zeta potential

n = dispersion medium's viscosity

μ = velocity of migration

ε = dielectric constant

E = potential gradient

2.1.4 Entrapment Efficiency Test

Entrapment efficiency test is one of most important evaluation parameters. It is used to determine the amount or concentration of drug entrapped within the globules of multiple emulsion. It can be determined using the following equation:

$$\%\text{Entrapment efficiency} = \frac{\text{Total drug incorporated} - \text{Free drug}}{\text{Total drug}} \times 100$$

2.1.5 Viscosity

Viscosity test is used to determine the thickness of the emulsion due to the internal friction of particles. Viscosity of emulsion can be determined using Brookfield viscometer.

2.1.6 Drug Release Rate Test

Drug release test helps to check the release rate of drug from multiple emulsions and to find out the order of drug release (first- and zero-order drug release).

2.1.7 pH Test

pH test is used to detect the pH of the emulsion. It can be determined using pH meter (manual or digital pH meter).

2.2 Theory of Emulsification

2.2.1 Monomolecular Adsorption Theory

In monomolecular adsorption theory, surfactants get adsorbed at the oil and water interface forming monomolecular film and reducing surface tension. A combination of hydrophilic and hydrophobic emulsifiers is being used in aqueous and oil phase, respectively, for complex film formation at interface.

2.2.2 Oriented Wedge Theory

In oriented wedge theory of emulsion, emulsifying agent forms a curved monomolecular layer surrounding the internal-phase droplet of emulsion. Molecules of emulsifier orient at inter phase and form a hydrated complex. For example, emulsifying agent gets mixed with more prefera-

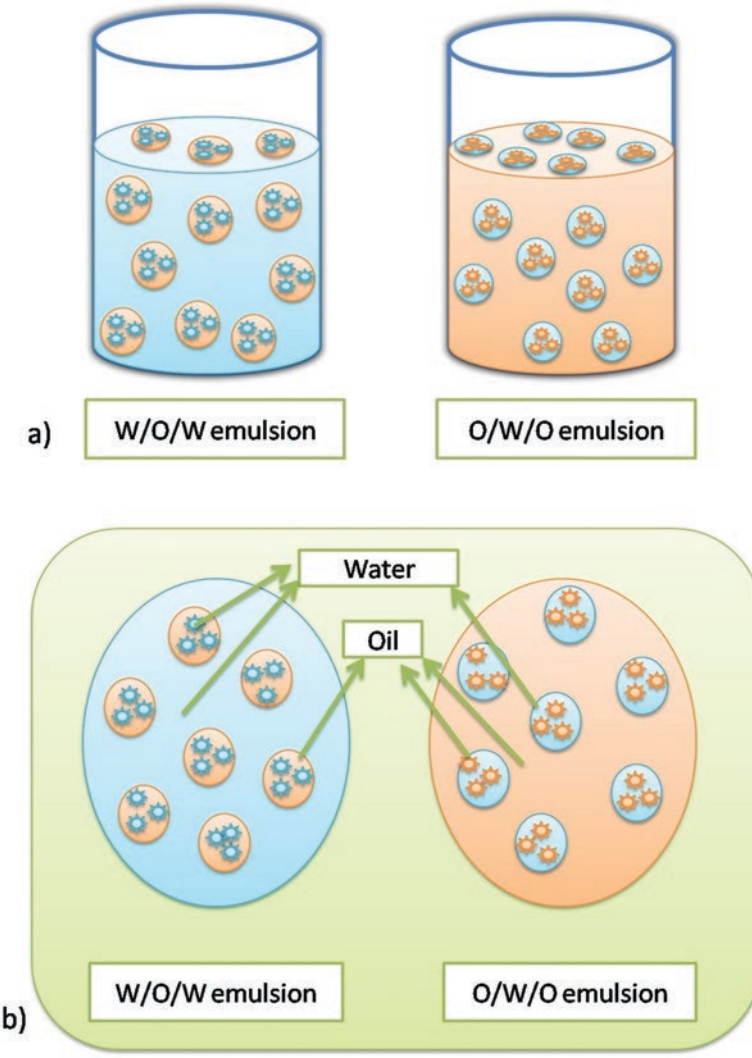

Fig. 14.1 Type of multiple emulsions: (**a**) two beakers containing W/O/W and O/W/O emulsions showing globular dispersion of W/O and O/W emulsions, respectively, whereas (**b**) describes the presence of oil and water in W/O/W and O/W/O multiple emulsions

ble liquid among two immiscible liquid, i.e., aqueous and oil.

2.2.3 Oriented Adsorption Theory

In oriented adsorption theory of emulsions, the emulsifier gets adsorb at the interface of emulsion resulting in the formation of a mechanical film. This theory also offers the stable emulsion, or in other words, emulsion stabilizes after oriented adsorption of emulsifiers at interface of liquid. But, the drawback of this theory is that it is unable to explain the type of emulsion formed.

2.2.4 Plastic or Interfacial Film Theory

In plastic or interfacial film theory, the emulsifying agent remains between oil and water interfacial surface, surrounding the inner droplet of internal phase as a thin layer of film adsorbed on the surface of drops. The degree of stability of emulsion specify the formation of type of emulsion depending upon the emulsifiers used, for example, oil-soluble emulsifiers promote and encourage the W/O type of emulsions, whereas water-soluble emulsifiers encourage the formation of O/W-type emulsions.

2.2.5 Surface Tension Theory

In the case of surface tension theory of emulsions, the emulsifying agent reduces the interfacial tension between the two immiscible liquids. Apparently, the surfactant reduces the size of larger globules into small globules, whereas it also avoids the formation of large globules by coalescing of small ones.

2.2.6 Interfacial Tension Theory

Interfacial tensions take place in between the boundaries of two immiscible liquids due to the presence of interfacial forces and cause the liquids to resist breakage and become spherical resulting in reduction of surface tension. Interfacial tension theory of emulsification states that the increase in interfacial tension makes emulsification difficult, whereas decrease in interfacial tension enables easy emulsification.

2.2.7 Viscosity Theory

Viscosity theory of emulsion simply states that increase in viscosity results in more stable emulsion whereas low viscosity causes formation of unstable emulsion. This theory perfectly describes the emulsions containing gums as emulsifying agents, but it fails to explain the higher-stability emulsions with low viscosity, such as milk.

2.3 Drug Release Mechanism in Multiple Emulsion

Multiple emulsions consist of different layers of oil and water. Generally, the innermost layer of multiple emulsions consists (or encapsulates) maximum amount of therapeutic agent or drug which releases with different pattern or mechanism based on the nature of drug and the environment. These mechanisms of drug release can be classified as follows.

2.3.1 Diffusion Mechanism

Diffusion mechanism of drug release is most common. In a stable multiple emulsion, the diffusion of unionized hydrophobic drugs takes place via oil phase which is considered as semipermeable liquid membrane (Fig. 14.2). This semipermeable layer allows the slow diffusion of drug and its release into the body system for intended therapeutic effect.

2.3.2 Thinning of Oil Membrane

This mechanism of drug transport or drug release takes place through the thin membrane of oil phase. The membrane thinning of oil phase takes place due to the difference in osmotic pressure between the outer and inner aqueous phases. Increase in osmotic pressure will decrease the thickness of oil layer which provides easier passage for the drug and water molecules to pass through (Fig. 14.3).

2.3.3 Rupture of Oil Phase

The name or title of the drug release mechanism itself states that release of drug in multiple emulsions takes place when the oil layer present in between gets ruptured. This phenomenon of rupturing the oil layer which is responsible to separate inner and outer aqueous phases will lead to uniting or mixing of both aqueous phases and eventually release the drug for its pharmacological action (Fig. 14.4).

2.3.4 Carrier-Mediated Transport or Facilitated Diffusion

In carrier-mediated drug release or transport, a carrier molecule is responsible for delivering an ionic and hydrophilic drug molecule to the external aqueous phase from the inner aqueous phase. This facilitation allows easy and effective drug transport. The compatibility of drug and carrier molecules allows the drug molecule to bind to the carrier molecule which helps it to cross the nonionic lipophilic oil layer of multiple emulsion. This facilitated diffusion or carrier-mediated drug transport can also be called as “pumping system” as the carrier molecule behaves as a pump by pumping out the drug molecules from the inner aqueous phase to the external aqueous phase (Fig. 14.5).

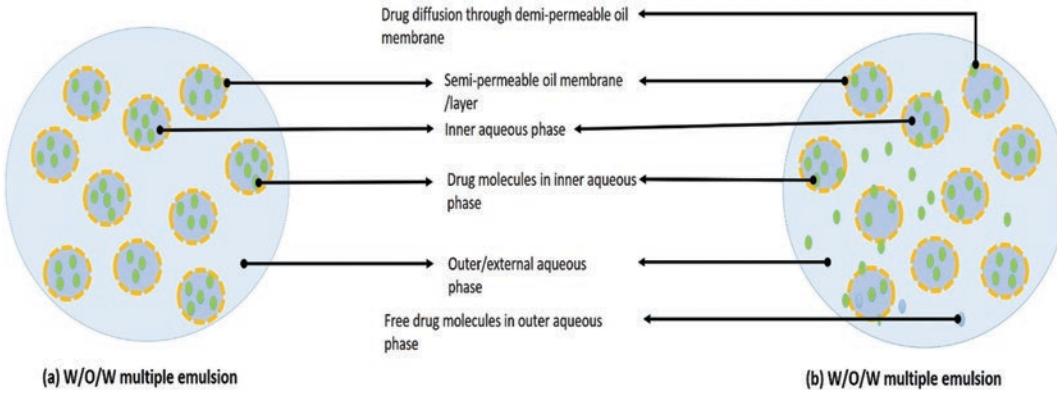

Fig. 14.2 W/O/W multiple emulsion showing (**a**) an outer aqueous phase carrying semipermeable oil layer encapsulating drug molecules. (**b**) Semipermeable oil layer providing easy passage for diffusion of drug molecules from inner to external/outer external phase

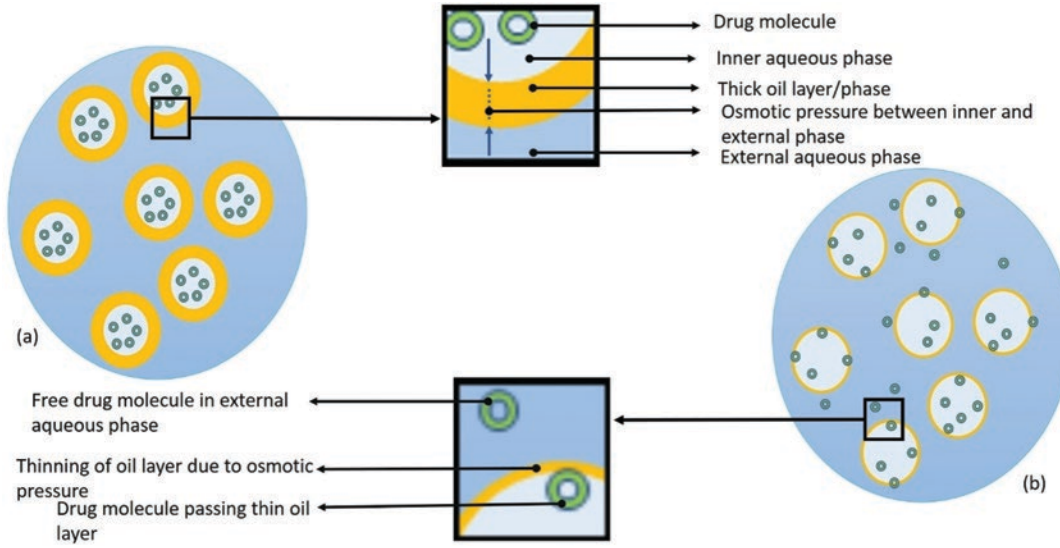

Fig. 14.3 (**a**) W/O/W multiple emulsion having thick oil layer and osmotic pressure from both inner and outer phases on oil layer. (**b**) Thinning of oil layer due to osmotic pressure allowing drug molecules to pass through oil layer to outer aqueous phase to give required therapeutic effect/action

2.3.5 Swelling or Breakdown Process

The swelling or breakdown process of drug release in multiple emulsions takes place only when the presence of concentration gradient is observed in between outer and inner aqueous phases. The presence of concentration gradients swells out the drug molecules present in the innermost aqueous phase, i.e., surrounded by an oil layer separating it from outer aqueous phase. Due to the swelling of drug molecules, the surface area of drug molecules increases, which need to expand their area, and thus it breaks the oil layer and releases the drug (Fig. 14.6).

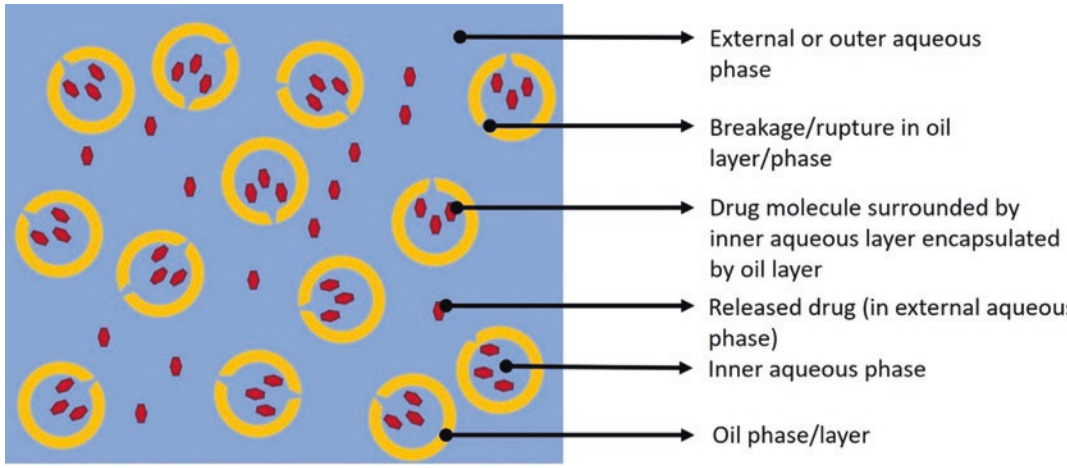

Fig. 14.4 W/O/W multiple emulsions having rupture in oil layer allowing the drug molecules to release in external aqueous phase providing pharmacological action

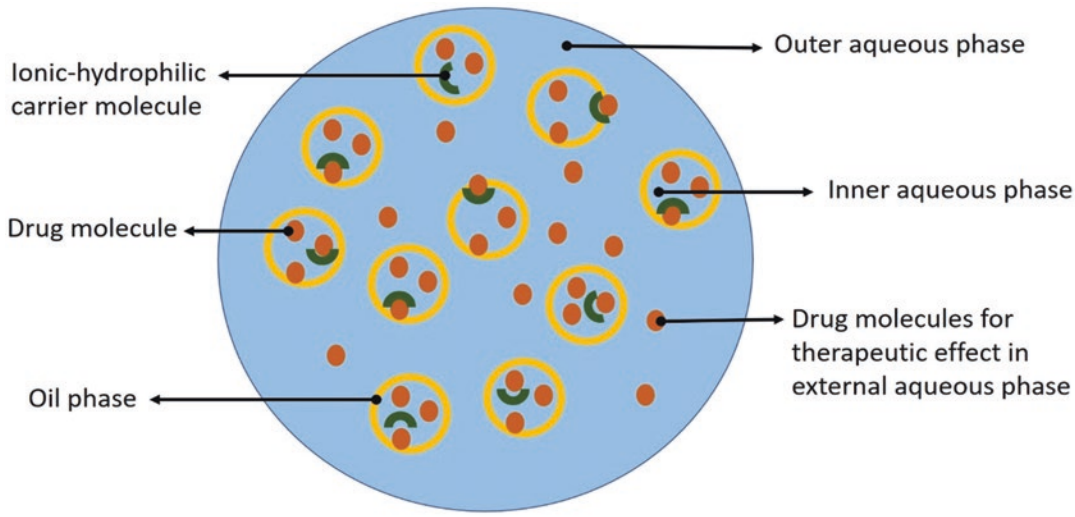

Fig. 14.5 Drug release takes place with the help of ionic-hydrophilic carrier molecule, which pumps out the drug molecules in external aqueous phase, which will further release for therapeutic effect

3 Industrial Applications of Multiple Emulsions

3.1 Controlled and Sustained Release

Controlled drug delivery enables the prolonged drug release with a specified release rate (Yun et al. 2015), whereas sustained release of drug is also meant for prolonged drug release but without any specific drug release rate (Lowinger et al. 2018). Sustained and controlled release of drug can be achieved with the help of reservoir or vesicular type of formulations that can encapsulate drug within layer(s) such as multiple emulsion, liposomes, etc. Multiple emulsions are more potent for both controlled and sustained drug release due to the presence of several layers which surround the drug to be released for its therapeutic action. In both systems, probably the dispersed drug remains within the innermost layer/globules of multiple emulsions and hence

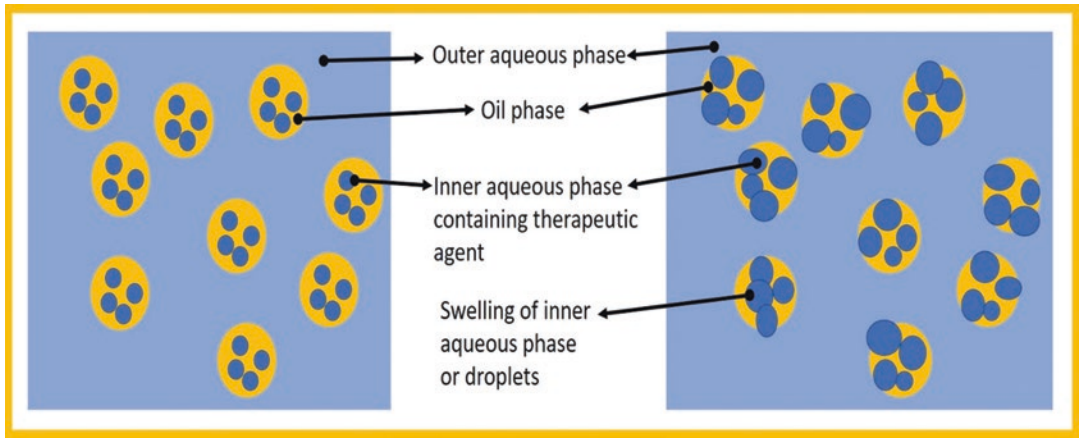

Fig. 14.6 Inner aqueous phase containing therapeutic agent swells after administration, and this process releases the drug for pharmacological action

prevents the deterioration of drug before reaching the targeted site for release. Moreover, parenteral administration of W/O/W emulsions is preferred due to their low viscosity and good stability (Mishra et al. 2011; Oh et al. 1998).

3.2 Inverse Targeting

The reticuloendothelial system (RES) is responsible for small particle clearance from the circulation even after intravenous administration (Talegaonkar and Vyas 2005). But RES clearance of colloidal carrier may act as a disadvantage. Excessive uptake and repeat dosing of colloidal carrier may result in the impairment of host defense system and may lead to blockage of the RES (Allen et al. 1984). Inverse targeting is a method or process of avoiding RES uptake of colloidal carriers (Lazo and Hacker 1985). For avoiding colloidal carrier uptake by the RES, few strategies have been opted previously such as by injecting blank colloidal carriers (Illum et al. 1986) or dextran sulfate macromolecules (Patel et al. 1983) in large amount before injecting therapeutic formulation to suppress RES function. Other methods or strategies for inverse targeting are modification of size, hydrophilicity, rigidity, surface charge, and composition of colloidal carriers. But in the case of multiple emulsions, change in size, rigidity, and surface charge is not easy, although, coating hydrophilic substances over hydrophobic particles has shown reduced RES uptake. Talegaonkar and Vyas had used gelatinization method of inner aqueous phase to prepare poloxamer 403 containing diclofenac sphere in oil in water (S/O/W)-type multiple emulsions (Talegaonkar and Vyas 2005). Poloxamer 403 were tested for inverse targeting and found to be effective in reducing RES uptake of drugs most probably in the liver, non-RES tissues (such as lungs and inflammatory tissues), and brain (Vladisavljević and Williams 2005).

3.3 Vaccine Adjuvant

Vaccine is a substance prepared from causative agent of disease to build immunity against that disease and it also helps in the stimulation of antibodies (Di Pasquale et al. 2015), whereas an adjuvant is an agent that enhances the activity or effect of agents or substances used alongside (Coffman et al. 2010). Adjuvant is used along with vaccines to enhance their pharmacological and immunological activity for more antibody production in the body resulting in long-lasting immunity. Herbert was first to come up with the idea of using multiple emulsions (i.e., W/O/W emulsion) as an adjuvant for antigen (Herbert 1965). R. Verma and Jaiswal studied *Pasteurella multocida* infection which is caused due to cat or dog bite, and therefore they indulge their knowledge in developing multiple emulsion vaccine.

Both cell-mediated and humoral responses were observed in multiple emulsion vaccine against *Pasteurella multocida* infection. However, hemorrhagic septicemia can also be controlled effectively with this multiple emulsion vaccine prepared by Verma and Jaiswal (Verma and Jaiswal 1997). W/O/W multiple emulsion containing influenza virus surface antigen hemagglutinin was prepared, and Wistar albino rat was used for in vitro as well as in vivo characterization resulting in an effective vaccine against influenza virus with adjuvant properties (Fox et al. 2011; Leclercq et al. 2011).

3.4 Oxygen Substitute

Oxygen plays a major role in the human body. Normally, oxygen level in blood fluctuates approximately between 75 mm Hg and 100 mm Hg, but when it falls below 60 mm Hg, it is considered as low blood oxygen level. In such emergency conditions to maintain oxygen level in the body, multiple emulsions are used to encapsulate oxygen. Zheng S. et al. developed hemoglobin in oil in water (Hb/O/W)-type multiple emulsion encapsulating concentrated solution of hemoglobin (Hb) which serves as oxygen substitute in the human body. Hb/O/W is also used as blood or red blood cell substitute (Zheng et al. 1993).

3.5 Red Blood Cell Substitute

Red blood cells (RBCs) are present in blood fluid and are discoid in shape. Although RBCs are responsible for carrying oxygen to the lungs as well as to other body parts, they also participate in coagulation and inflammatory processes (Pretorius 2013). As discussed above in multiple emulsion used as oxygen substitute, it also acts as RBC substitute. The Hb/O/W multiple emulsion prepared by Zheng et al. during their study consisted of concentrated solution of hemoglobin encapsulated within the oil phase (Zheng et al. 1993), which was further dispersed in an isotonic saline solution (Borwanker et al. 1988). This multiple emulsion acts as artificial RBC as it carries oxygen, whereas the oil phase encapsulating hemoglobin acts as a membrane for gaseous (oxygen and carbon dioxide) exchange (Borwanker et al. 1988). The small droplet size of pharmacologically compatible oil encapsulating hemoglobin within allows it to flow easily through blood vessels enabling its availability to other body parts.

3.6 Bioavailability Enhancer

Bioavailability is defined as the rate of drug absorption and its availability at the targeted site or where the drug has to show its intended action (Chow 2014), whereas, bioavailability enhancers are the substances that have the capability to increase or enhance bioavailability (Kesarwani and Gupta 2013). Multiple emulsions are preferred for oral administration due to their property to enhance bioavailability. They are preferred for protection of drugs that are lipophilic in nature or poorly water-soluble drugs which may undergo first pass metabolism and may degrade.

3.7 Enzyme Immobilization

Enzyme immobilization is a process responsible for restricting free movement of enzymes; therefore, it enables the prolonged availability of enzymes to substrate (Datta et al. 2013). Various techniques such as encapsulation, entrapment, adsorption, cross-linking, and covalent binding have been used for immobilization of enzymes (Tamer et al. 2016). Multiple emulsions carry enzymatic conversions of substances that are insoluble in water or that are highly lipophilic substrates, for example, steroids. The microdroplets also known as "water pool" contain the enzymes, whereas the substrate solution remains within organic solvent. For example, for urease, immobilization hydrocarbon-based liquid surfactant membranes have been used (May and Li 1974).

3.8 Drug Overdose Treatment

Drug overdose can either be accidental or can be intentional which cause severe, mild, or major effects and can also lead to death. The overdosage of drugs can be controlled in early stages by neutralizing and eliminating (if possible) the effect of excessive amount of drug from the body. Chiang et al. in 1978 used barbiturates for treatment of drug overdose (Chiang et al. 1978). Utilization of difference in pH can be used by this system to treat drug overdose. The innermost layer of multiple emulsion consists of basic buffer that acts as inner aqueous phase, and after oral administration, the acidic pH of the stomach surrounding the multiple emulsion acts as an outer or external aqueous phase.

3.9 Targeting of Bioactives

Bioactives are the substances that are capable to influence physiological activity as well as cellular activity of human or animal body after administration (Santos et al. 2019). Bioactive compounds have the ability to influence intake of energy; also it can reduce pro-inflammatory state as well as oxidative stress and metabolic disorders (Siriwardhana et al. 2013). Targeting of bioactives is an important application by which the pharmacologically active agents can be targeted to the specific site. This application mostly benefits chemotherapy in cancer patients where cytotoxic therapeutic agents or drugs cause serious damage to non-cancer cells and tissues. Multiple emulsions act as lymphotropic carriers and help in targeting bioactives. Intramuscular or intraperitoneal administration of multiple emulsions leads the droplets of emulsions to reach regional lymph nodes as well as lymphatic system. Therefore, bioactive agent-loaded multiple emulsions can achieve various levels by specific targeting. Takahashi et al. 1973 studied delivery of labeled 5-flurouracil to regional lymph nodes following intratesticular administration. The formulation showed that within 15 min the emulsion droplets reached regional lymph nodes within and remained there for more than 7 days (Takahashi et al. 1973). W/O/W emulsion system also gave highest levels within the regional lymph nodes than other systems such as aqueous solution, water in oil (W/O) emulsions, and oil in water (O/W) emulsions.

3.10 Delivery of Proteins and Peptides

Proteins are macromolecules that are derived from amino acid; therefore amino acids are also known as building blocks of proteins. Generally proteins consist of 20 different amino acids which can be achieved after complete hydrolysis of proteins (Blanco and Blanco 2017). Small chains of amino acids are called peptides, which can be obtained after partial hydrolysis of protein polypeptide chains (González de Llano and Polo Sánchez 2003). Multiple emulsions are unique as they have the tendency to separate all three phases from each other. This phenomenon is especially important for bioactive molecules that cannot appropriately stay stabilized in solid state. The aqueous-phase separation enables highly specialized environments, conducive to protein activity. The conventional systems have a major drawback, that is, physical instability, which further restricts their wider applications. Attempts to improve physical stability of aqueous dispersions via interfacial complexation and use of microemulsions could improve short-term stability. Toorisaka et al. 2003 developed insulin solid in oil in water (S/O/W) emulsion for oral administration. Ultrasonication method was used to disperse insulin coated with surfactant in oil, which was homogenized to mix with outer water phase, and finally, the S/O/W emulsion thus obtained was adjusted to a constant particle size by passage via the Shirasu porous glass (SPG) membrane. Oral administration of S/O/W emulsion in rats showed hypoglycemic activity for a long period (Toorisaka et al. 2003).

3.11 Local Immunosuppression

The efficacy to suppress or reduce the activity of the immune system locally is termed as local immunosuppression (Streilein and Taylor 2001). An attempt to deliver immunosuppressive agents to specific targeted organs or tissues provided the information that multiple emulsions have the potential to enhance immunosuppressive efficacy and avoid complication of systemic immunosuppression. Therefore, to deliver immunosuppressants, W/O/W multiple emulsion has been developed. It has been suggested that tacrolimus W/O/W emulsion possesses pharmacokinetic benefits of local immunosuppression. The significant decrease in tacrolimus levels in the brain and kidney was observed as well as increase in tacrolimus levels in the liver and spleen.

3.12 Absorption Enhancement via GIT

The gastrointestinal tract (GIT) sometimes restricts the absorption of drugs due to the presence of enzymes. Omotosho, 1990, had developed a W/O/W multiple emulsion of griseofulvin. It was observed that griseofulvin multiple emulsion had increased oral absorption than in simple oil in water (O/W) emulsion as well as conventional tablets of griseofulvin. Administration of griseofulvin in W/O/W emulsion may lead to enhancement of therapeutic efficacy of the drug (Omotosho et al. 1990). To improve the mucosal absorption of poorly absorbed drugs, Kajita, 2000, prepared and evaluated multiple emulsion loaded with vancomycin hydrochloride incorporated with unsaturated fatty acids. The emulsion incorporating C18 unsaturated fatty acids or docosahexaenoic acid enhanced the drug absorption after rectal and colonic dosing and proved useful carriers as they improve the absorption of poorly absorbable drugs via the intestinal tract (Kajita et al. 2000). A similar system was investigated for increase in rectal bioavailability for insulin.

3.13 Taste Masking

Conventional formulations had a drawback of unwanted taste that is unacceptable by patients. Therefore, multiple emulsions had been coined for taste masking. Thus, chloroquine, an antimalarial agent, was encapsulated within multiple emulsions for treatment of malaria and had been found capable to mask the bitter taste efficiently (Vaziri and Warburton 1994). Multiple emulsions are also reported to mask the taste of chlorpromazine, i.e., an antipsychotic drug (Lokhande 2019).

3.14 Cosmetics and Health Care

Generally, both simple emulsions such as oil in water and water in oil emulsions have been used for cosmetics and toiletries. Emulsions are usually used for their moisturizing, protective, and nutritive properties when they are applied as moisturizers, sunscreen, hand cream, antiperspirant, cleanser for makeup, shaving creams, etc. It has been reported that $O_1/W/O_2$ multiple emulsions have better sun protection ability than simple emulsions. Laugel et al. 2000 reported incorporation of silicones within O/W/O multiple emulsions loaded with dimethicones, as an efficient means of modulating penetration and distribution of drugs in the skin. O/W/O multiple emulsions carrying silicones have two major advantages: (1) silicones with lowest molecular weight decrease oily touch due to large range of viscosity; (2) after topical application of silicone O/W/O multiple emulsions, silicones influence skin distribution activities (Laugel et al. 2000).

4 Miscellaneous

W. J. Herbert in 1965 had developed a multiple emulsion using mineral oil as oil phase. Herbert incorporated antigen within multiple emulsion resulting in an antigen adjuvant promoting the production of antibody as well as prolonging their responses. In comparison to normal water in oil emulsions, this mineral oil antigen adjuvant multiple emulsion had low viscosity which

enables the easy injection of multiple emulsion even with fine needles. Another benefit of this formulation was the use of less amount of oil to contain the antigen within. This emulsion was stable (Herbert 1965).

Elson et al. in 1970 had formulated vinblastine sulfate water in oil in water (W/O/W) multiple emulsion for sustained release of vinblastine sulfate. Generally, increase in bone marrow cells is observed after administering the dose remains for a little while only, whereas, when a single aqueous injection of vinblastine sulfate multiple emulsion is administered, the bone marrow cells increase gradually in metaphase even after 4 h. Result had proven the continuous increase in bone marrow cells arrested in metaphase even after 48 h of single-dose administration. It offers the benefit of low or less dose(s) and better patient compliance.

Takahashi et al. had been working on anticancer agents, and they observed that lymphatic capillaries have the ability to absorb lipids; therefore, they deliver the large amount of water-soluble anticancer drugs using fat emulsion to the regional lymph nodes. To serve this purpose, they developed W/O/W multiple emulsion with increased concentration of 3H-5-fluorouracil (i.e., anticancer agent) which was delivered using intratesticular injection. 5-Fluorouracil showed promising results, and it also had better radioactivity than in conventional emulsions (Takahashi et al. 1973).

In 1974, Christine J. Benoy et al. had developed a water in oil in water-type multiple emulsion using a combination of methotrexate and cytosine arabinoside which is used in the treatment of leukemia (both lymphocytic leukemia and granulocytic leukemia). Parenteral administration of methotrexate W/O/W emulsion resulted in the enhancement of the therapeutic effect in rat Walker tumor as well as in mouse R1 lymphoma. Sustained pharmacological action was observed after administering the multiple emulsion parenterally due to slow drug release. It also shows prolonged therapeutic effect. Single dose of W/O/W emulsion containing cytosine arabinoside gives similar effect as five daily doses of aqueous solution of cytosine arabinoside against lymphoma. Therefore, reduced dose is an advantage of this formulation (Benoy et al. 1974).

May and Li in 1974 had formulated multiple emulsion for enzyme immobilization. Development of various diseases takes place due to urease activity of microbial sources, whereas urease is generally found in various bacteria, fungi, algae, soil, plants, etc. Urease, which is present in plants, is detected for their inhibitory activities and therefore is used as vaccine against microbial infections. Urease acts as a virulence factor; it is accountable for pathogenesis in humans and has various clinical applications (May and Li 1974).

In 1989, Omotosho et al. had developed methotrexate multiple emulsion. Although methotrexate is an antineoplastic drug, Omotosho et al. used it for its effectiveness in cancer chemotherapy. This multiple emulsion tends to have sustained delivery, therefore giving prolonged therapeutic effect. After parenteral administration of multiple emulsion, enhanced therapeutic actions were observed against rat Walker tumor and mouse lymphoma (Omotosho et al. 1989).

References

Allen TM, Murray L, MacKeigan S, Shah M. Chronic liposome administration in mice: effects on reticuloendothelial function and tissue distribution. J Pharmacol Exp Ther. 1984;229:267–75.

Benoy CJ, Schneider R, Elson LA, Jones M. Enhancement of the cancer chemotherapeutic effect of the cell cycle phase specific agents methotrexate and cytosine arabinoside when given as a water-oil-water emulsion. Eu J Cancer (1965). 1974;10:27–33. https://doi.org/10.1016/0014-2964(74)90034-6.

Blanco A, Blanco G. Chapter 3 – Proteins. In: Blanco A, Blanco G, editors. Medical biochemistry. London/San Diego: Academic Press; 2017. p. 21–71. https://doi.org/10.1016/B978-0-12-803550-4.00003-3.

Borwanker CM, Pfeiffer SB, Zheng S, Beissinger RL, Wasan DT, Sehgal LR, Rosen AL. Formulation and characterization of a multiple emulsion for use as a red blood cell substitute. Biotechnol Prog. 1988;4:210–7. https://doi.org/10.1002/btpr.5420040404.

Chiang C-W, Fuller GC, Frankenfeld JW, Rhodes CT. Potential of liquid membranes for drug overdose treatment: in vitro studies. J Pharm Sci. 1978;67:63–6. https://doi.org/10.1002/jps.2600670117.

Chow SC. Bioavailability and bioequivalence in drug development. Wiley Interdiscip Rev Comput Stat. 2014;6:304–12. https://doi.org/10.1002/wics.1310.

Coffman RL, Sher A, Seder RA. Vaccine adjuvants: putting innate immunity to work. Immunity. 2010;33:492–503. https://doi.org/10.1016/j.immuni.2010.10.002.

Datta S, Christena LR, Rajaram YRS. Enzyme immobilization: an overview on techniques and support materials. 3 Biotech. 2013;3:1–9. https://doi.org/10.1007/s13205-012-0071-7.

Di Pasquale A, Preiss S, Tavares Da Silva F, Garçon N. Vaccine adjuvants: from 1920 to 2015 and beyond. Vaccines (Basel). 2015;3:320–43. https://doi.org/10.3390/vaccines3020320.

Ferreira MRA, Santiago RR, de Souza TP, Egito EST, Oliveira EE, Soares LAL. Development and evaluation of emulsions from Carapa guianensis (Andiroba) oil. AAPS PharmSciTech. 2010;11:1383–90. https://doi.org/10.1208/s12249-010-9491-z.

Fox CB, Baldwin SL, Duthie MS, Reed SG, Vedvick TS. Immunomodulatory and physical effects of oil composition in vaccine adjuvant emulsions. Vaccine. 2011;29:9563–72. https://doi.org/10.1016/j.vaccine.2011.08.089.

González de Llano D, Polo Sánchez C. PEPTIDES. In: Caballero B, editor. Encyclopedia of food sciences and nutrition. 2nd ed. Oxford: Academic Press; 2003. p. 4468–73. https://doi.org/10.1016/B0-12-227055-X/00906-8.

Herbert WJ. Multiple emulsions. A new form of mineral-oil antigen adjuvant. Lancet. 1965;286:771. https://doi.org/10.1016/s0140-6736(65)90816-0.

Illum L, Thomas NW, Davis SS. Effect of a selected suppression of the reticuloendothelial system on the distribution of model carrier particles. J Pharm Sci. 1986;75:16–22. https://doi.org/10.1002/jps.2600750105.

Jaiswal M, Dudhe R, Sharma PK. Nanoemulsion: an advanced mode of drug delivery system. 3 Biotech. 2015;5:123–7. https://doi.org/10.1007/s13205-014-0214-0.

Kajita M, Morishita M, Takayama K, Chiba Y, Tokiwa S, Nagai T. Enhanced enteral bioavailability of vancomycin using water-in-oil-in-water multiple emulsion incorporating highly purified unsaturated fatty acid. J Pharm Sci. 2000;89:1243–52. https://doi.org/10.1002/1520-6017(200010)89:10<1243::AID-JPS2>3.0.CO;2-C

Kesarwani K, Gupta R. Bioavailability enhancers of herbal origin: an overview. Asian Pac J Trop Biomed. 2013;3:253–66. https://doi.org/10.1016/S2221-1691(13)60060-X.

Kumar R, Kumar MS, Mahadevan N. Multiple emulsions: a review. Int J Recent Adv Pharm Res. 2012;2:9–19. https://doi.org/10.17010//2012/v5i2/60128.

Laugel C, Rafidison P, Potard G, Aguadisch L, Baillet A. Modulated release of triterpenic compounds from a O/W/O multiple emulsion formulated with dimethicones: infrared spectrophotometric and differential calorimetric approaches. J Control Release. 2000;63:7–17. https://doi.org/10.1016/s0168-3659(99)00169-8.

Lazo J, Hacker M. Organ-directed toxicology of antitumor agents. Symposium summary. Fed Proc. 1985;44:2335–8.

Leclercq SY, dos Santos RMM, Macedo LB, Campos PC, Ferreira TC, de Almeida JG, Seniuk JGT, Serakides R, Silva-Cunha A, Fialho SL. Evaluation of water-in-oil-in-water multiple emulsion and microemulsion as potential adjuvants for immunization with rabies antigen. Eur J Pharm Sci. 2011;43:378–85. https://doi.org/10.1016/j.ejps.2011.05.008.

Lokhande SS. Recent trends in multiple emulsion – a comprehensive review. Asian J Res Pharma Sci. 2019;9:201–8. https://doi.org/10.5958/2231-5659.2019.00032.8.

Lowinger MB, Barrett SE, Zhang F, Williams RO. Sustained release drug delivery applications of polyurethanes. Pharmaceutics. 2018;10:55. https://doi.org/10.3390/pharmaceutics10020055.

May SW, Li NN. Encapsulation of enzymes in liquid membrane emulsions. In: Pye EK, Wingard LB, editors. Enzyme engineering, vol. 2. Boston: Springer US; 1974. p. 77–82. https://doi.org/10.1007/978-1-4615-8897-9_11.

Mishra B, Sahoo BL, Mishra M, Shukla D, Kumar V. Design of a controlled release liquid formulation of lamotrigine. Daru. 2011;19:126–37.

Nafisi S, Maibach HI. Chapter 22 – nanotechnology in cosmetics. In: Sakamoto K, Lochhead RY, Maibach HI, Yamashita Y, editors. Cosmetic science and technology. Amsterdam: Elsevier; 2017. p. 337–69. https://doi.org/10.1016/B978-0-12-802005-0.00022-7.

Oh I, Kang YG, Lee YB, Shin SC, Kim CK. Prolonged release of tegafur from S/O/W multiple emulsion. Drug Dev Ind Pharm. 1998;24:889–94. https://doi.org/10.3109/03639049809097268.

Omotosho JA, Whateley TL, Florence AT. Methotrexate transport from the internal phase of multiple w/o/w emulsions. J Microencapsul. 1989;6:183–92. https://doi.org/10.3109/02652048909098019.

Omotosho JA, Florence AT, Whateley TL. Absorption and lymphatic uptake of 5-fluorouracil in the rat following oral administration of w/o/w multiple emulsions. Int J Pharm. 1990;61:51–6. https://doi.org/10.1016/0378-5173(90)90043-4.

Patel KR, Li MP, Baldeschwieler JD. Suppression of liver uptake of liposomes by dextran sulfate 500. Proc Natl Acad Sci U S A. 1983;80:6518–22. https://doi.org/10.1073/pnas.80.21.6518.

Pretorius E. The adaptability of red blood cells. Cardiovasc Diabetol. 2013;12:63. https://doi.org/10.1186/1475-2840-12-63.

Santos DI, Saraiva JMA, Vicente AA, Moldão-Martins M. 2-Methods for determining bioavailability and bioaccessibility of bioactive compounds and nutrients. In: Barba FJ, Saraiva JMA, Cravotto G, Lorenzo JM, editors. Innovative thermal and non-thermal processing, Bioaccessibility and Bioavailability of Nutrients and Bioactive Compounds. Sawston: Woodhead

Publishing; 2019. p. 23–54. https://doi.org/10.1016/B978-0-12-814174-8.00002-0.

Siriwardhana N, Kalupahana NS, Cekanova M, LeMieux M, Greer B, Moustaid-Moussa N. Modulation of adipose tissue inflammation by bioactive food compounds. J Nutr Biochem. 2013;24:613–23. https://doi.org/10.1016/j.jnutbio.2012.12.013.

Streilein JW, Taylor AW. Local immunosuppression: the eye. In: Thomson AW, editor. Therapeutic immunosuppression, immunology and medicine series. Dordrecht: Springer; 2001. p. 275–321. https://doi.org/10.1007/978-94-010-0765-8_11.

Takahashi T, Mizuno M, Fujita Y, Ueda S, Nishioka B, Majima S. Increased concentration of anticancer agents in regional lymph nodes by fat emulsions, with special reference to chemotherapy of metastasis. GANN Japan J Cancer Res. 1973;64:345–350_1. https://doi.org/10.20772/cancersci1959.64.4_345.

Talegaonkar S, Vyas SP. Inverse targeting of diclofenac sodium to reticuloendothelial system-rich organs by sphere-in-oil-in-water (s/o/w) multiple emulsion containing poloxamer 403. J Drug Target. 2005;13:173–8. https://doi.org/10.1080/10611860500065104.

Tamer T, Omer A, Hassan M. Methods of enzyme immobilization. Int J Curr Pharma Rev Res. 2016;7:385–92.

Toorisaka E, Ono H, Arimori K, Kamiya N, Goto M. Hypoglycemic effect of surfactant-coated insulin solubilized in a novel solid-in-oil-in-water (S/O/W) emulsion. Int J Pharm. 2003;252:271–4. https://doi.org/10.1016/s0378-5173(02)00674-9.

Vaziri A, Warburton B. Slow release of chloroquine phosphate from multiple taste-masked W/O/W multiple emulsions. J Microencapsul. 1994;11:641–8. https://doi.org/10.3109/02652049409051114.

Verma R, Jaiswal TN. Protection, humoral and cell-mediated immune responses in calves immunized with multiple emulsion haemorrhagic septicaemia vaccine. Vaccine. 1997;15:1254–60. https://doi.org/10.1016/s0264-410x(97)00025-x.

Vladisavljević GT, Williams RA. Recent developments in manufacturing emulsions and particulate products using membranes. Adv Colloid Interface Sci. 2005;113:1–20. https://doi.org/10.1016/j.cis.2004.10.002.

Yun YH, Lee BK, Park K. Controlled drug delivery: historical perspective for the next generation. J Control Release. 2015;219:2–7. https://doi.org/10.1016/j.jconrel.2015.10.005.

Zheng S, Zheng Y, Beissinger RL, Wasan DT, McCormick DL. Hemoglobin multiple emulsion as an oxygen delivery system. Biochim Biophys Acta. 1993;1158:65–74. https://doi.org/10.1016/0304-4165(93)90098-s.

15 Membrane Techniques for the Preparation of Nanomaterials

Komal Parmar, Jayvadan K. Patel, and Deepak Bhatia

Abstract

Nanomaterials are always in demand owing to its wide variety of applications in various fields of science. Various methods are available for the synthesis of nanomaterials, but membrane techniques proved to be efficient in the preparation of nanoparticles. The present chapter reviews the membrane techniques reported in the fabrication of various types of nanomaterials such as nanowires, nanorods, nanospheres, and others.

Keywords

Membrane · Techniques · Nanomaterials · Template

K. Parmar (✉)
ROFEL, Shri G.M. Bilakhia College of Pharmacy, Vapi, Gujarat, India

J. K. Patel
Nootan Pharmacy College, Sankalchand Patel University, Visnagar, Gujarat, India

D. Bhatia
Shenandoah University – ICPH Fairfax, Bernard J. Dunn School of Pharmacy, Fairfax, VA, USA

1 Introduction

Nowadays terms like "nanoscience" and "nanotechnology" are not only limited to the research field but also used in day to day life. The applied science involves the technology at nanoscale, which is about 1–100 nanometers. Nanomaterials are used in wide array of science including electronics (Kamyshny and Magdassi 2019), optics (Shen et al. 2000), composite materials (Sahay et al. 2014), energy storage (Liu et al. 2017), electrochemistry (Li et al. 2009), food science (Singh et al. 2017), and health science (Chen et al. 2013). Nanomaterials are nanotech product designed to be very small with unique physical and chemical characteristics that prevails at nanoscale. The physical and chemical properties at nanoscale are largely varied than their large-scale version, which can prove to be beneficial. For instance, nanoscale particles are reported to cross the complex blood-brain barrier, which can further host for targeted health benefits (Saraiva et al. 2016; Thomsen et al. 2015). Thus, since the discovery of nanomaterials, a deep interest has been developed for these nano-objects, and extensive research has been done. These nano-objects with their large surface area show trenchant thermal, mechanical, optical, electronic, and chemical properties as compared to its bulk counterpart. This unique characteristic is developed due to the quantum size of the material (Roduner 2006). The nanomaterials can be clas-

J. K. Patel, Y. V. Pathak (eds.), *Emerging Technologies for Nanoparticle Manufacturing*,
https://doi.org/10.1007/978-3-030-50703-9_15

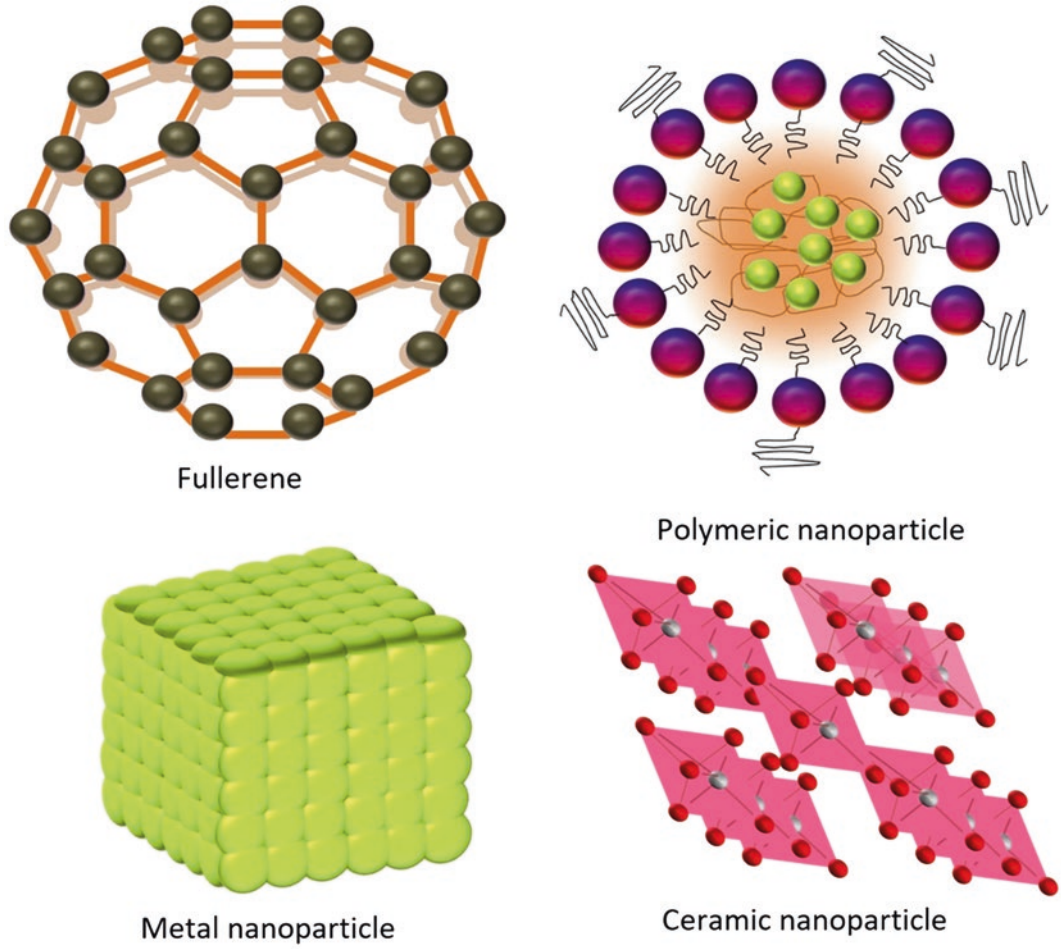

Fig. 15.1 Various types of nanomaterials

sified into various groups, namely, fullerenes, metal nanoparticles, ceramic nanoparticles, and polymeric nanoparticles (Fig. 15.1).

Significant development has been made in the improvement of methods for the synthesis of nanomaterials. Methods are classified into physical, chemical, biological, and hybrid approaches. Physical approaches can be further classified into mechanical methods, such as high-energy ball milling (Yadav et al. 2012) and melt blending (Bikiaris et al. 2006), and vapor methods, such as physical vapor deposition (Horprathum et al. 2014), laser ablation (Kim et al. 2017), sputter deposition (Galdino et al. 2017), and electric arc (El-Khatib et al. 2018). Chemical approaches can be classified into five major classes, viz., (i) colloidal methods (Kang et al. 2007), (ii) sol-gel processes (Mackenzie and Bescher 2007), (iii) water-in-oil microemulsion methods (Malik et al. 2012), (iv) hydrothermal synthesis (Darr et al. 2017), and (v) polyol method (Fievet et al. 2018). Biological methods involve the use of DNA (Seeman 2010), microorganisms (Sharma et al. 2015), and enzymes (Kolhatkar et al. 2015). Hybrid methods include electrochemical method (Singaravelan and Alwar 2015), chemical vapor deposition (Manawi et al. 2018), and microwave-assisted reverse microemulsion method (Lu et al. 2016).

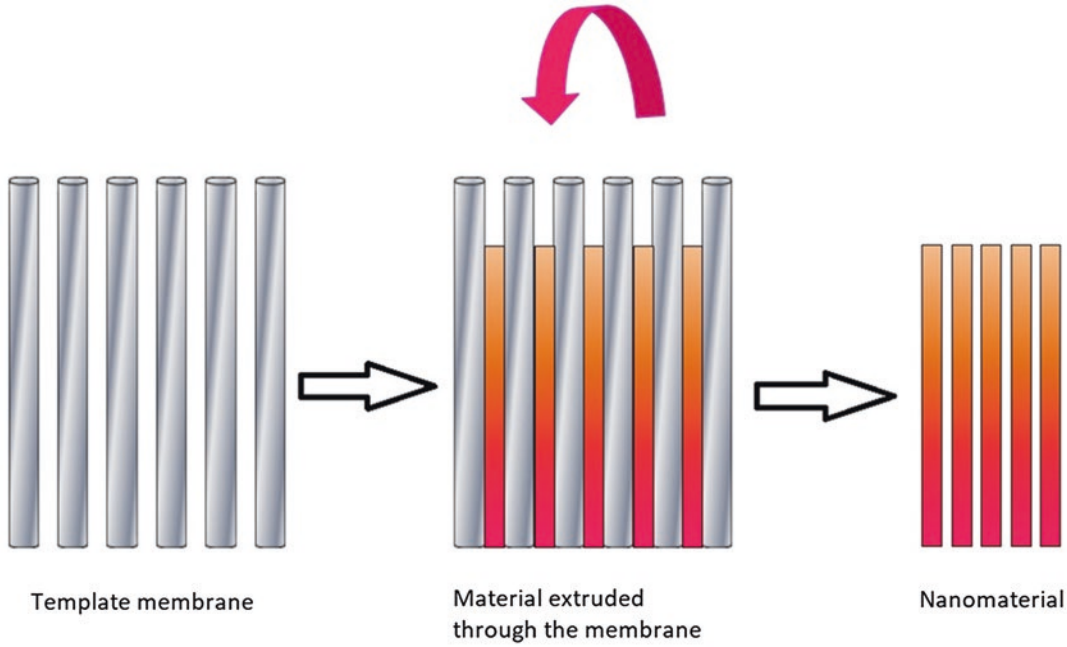

Fig. 15.2 Schematic representation of extrusion of nanomaterial through template membrane

2 Membrane Approach

Membrane-based approach for the synthesis of nanomaterials is known since the 1990s. The general approach for nanomaterial preparation is "template method" because the pores of the nanoporous membranes are utilized as template in the fabrication of nanomaterials. Figure 15.2 demonstrates the mechanism of process of forming nanomaterials when entered into a membrane. Membranes contain cylindrical pores of definite length and width. Material is extruded through the membrane under pressure resulting into formation of nanomaterials. Template method is utilized to fabricate nanotubes and nanowires. Another method in membrane technique uses membrane contactor to prepare nanomaterials. Figure 15.3 exhibits the working principle of the method in which one phase is introduced in the membrane through the pores and another phase flows tangentially to the membrane surface. Nanomaterials are produced when both phases come into contact with each other. Polymeric nanoparticles, solid lipid nanoparticles, and nanocrystals can be prepared using this technique.

3 Template Method

Over the past few decades, template method has proved to be the most successful method for the fabrication of nanomaterials. The method generally involves formation of desired materials in the nano-range of the pores of the membrane. Depending on the physical characteristics of the nanopore membrane, size, shape, and structure of the fabricated nanomaterial can be managed. Morphology of the nanomaterials can be changed during the process by controlling the nucleation and growth of nuclei. Three basic steps involved in the template method of fabrication of nanomaterials are (i) preparation of template; (ii) application of some synthetic approach like sol-gel, precipitation, etc.; and (iii) template removal. Templates are classified into two groups soft and hard templates based on the structure of the template material.

Removal of template is the last step in the process of nanomaterial fabrication. Method selection is made such that the physical and chemical properties of the nanomaterials remain unaf-

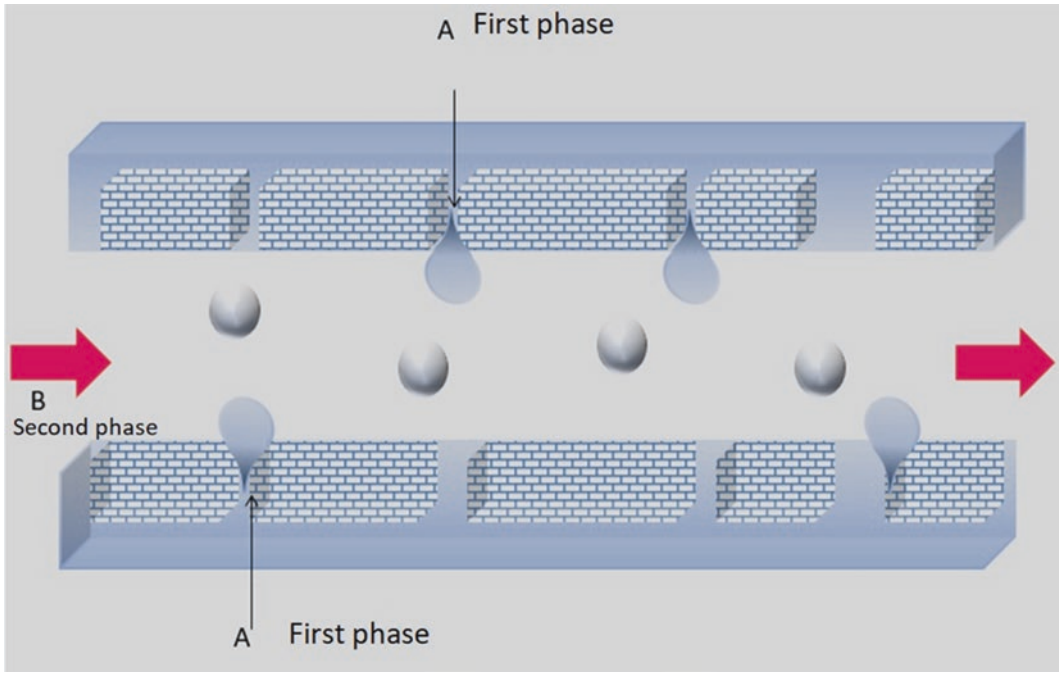

Fig. 15.3 Working principle of the template method

fected. Removal methods are classified as physical (e.g., dissolution) and chemical (e.g., calcination and etching).

4 Hard Template

The name itself suggests the property of hard template, which is made up of rigid and stable material like polymers, silica, and carbon. Hard template is also known as exotemplate method and determines the size and morphology of the mesoporous structure. The process is analogous to casting method in metallurgy, where the template acts as casting molds. Thus, it is referred as nanocasting, where the casting process is at nano-level. Various types of hard templates are available, such as mesoporous silica, porous anodic aluminum oxide (AAO), and carbon.

Mesoporous silica is explored as hard template due to its well organized structure and pores, high surface area, high thermal stability, low toxicity, and high compatibility with wide variety of materials (Deng et al. 2017). Upon removal of the template mold, the metal precursors will take the shape of the mesoporous silica hard template. Mesoporous silica such as SBA-15 is commonly used for the fabrication of mesoporous nanostructures. For example, silica templates with cylindrical channels will yield nanowires (Lu and Schuth 2005), template with spherical pores will give nanospheres (Lu and Schuth 2006), and template with bicontinuous pores will produce bicontinuous mesostructures (Yang and Zhao 2005). SBA-15 has distinct characteristics such as uniform hexagonal pores with narrow pore size distribution ranging between 5 nm and 15 nm, wall thickness of about 3.1 to 6.4 nm, and internal surface area of about 400–900 m^2/g (Thielemann et al. 2011). Takai and co-workers synthesized nanowires of noble metals (Pt, Ag, and Au) by using SBA-15 powder as template through vapor-infiltration process employing dimethylamine borane as reducing agent (Takai et al. 2010). Seo and co-workers reported synthesis of carbon nanomaterials using mesoporous silica as template. SBA-15, SBA-16, and KIT-6 mesoporous silica templates were employed for the synthesis. Further the templates were impregnated with mineral acids such as

Table 15.1 Various mesoporous silica used as hard template

Mesoporous silica type	Material synthesized	Precursor	References
SBA-15	CdS nanowire	Cadmium xanthate	Yuan et al. (2009)
SBA-15	Mesoporous carbon	Polyacrylonitrile	Kruk et al. (2005)
SBA-15 and B56-E-20	Mesoporous PAF-45HX	Biphenyl	Li et al. (2018)
SBA-15 and KIT-6	Co_3O_4 nanostructures	Cobalt oxide	Rumplecker et al. (2007)
KIT-6	Mesoporous carbon	Sucrose	Dai et al. (2010)
MCM-48	Osmium and platinum 3D nanonetworks	Organometallic	Lee et al. (2006)
MCF	Mesostructured graphitic carbon nitride materials	Carbon tetrachloride and ethylenediamine	Xu et al. (2013)
HMS aluminosilicate	Mesoporous carbon	Phenol and formaldehyde	Lee et al. (2000)
MSUF	Mesocellular carbon foam	Sulfur	Jeong et al. (2017)
SBA-15	Mesoporous NiO	Nickel	Wahab and Darain (2014)
SBA-15 and KIT-6	Mesoporous and nanowire SnO_2 anode	SnO_2	Kim and Cho (2008)
SBA-15	Mesoporous $NiCo_2O_4$ nanowires	$Ni(NO_3)_2{\cdot}6H_2O$ and $Co(NO_3)_2{\cdot}6H_2O$	Wang et al. (2018a, b)
SBA-15	Mesoporous $CoFe_2O_4$ and $CoLa_{0.12}Fe_{1.88}O_4$	$Co(NO_3)_3{\cdot}6H_2O$ and $Fe(NO_3)_3{\cdot}9H_2O$	Shang et al. (2018)
KIT-6	Mesoporous Fe-In_2O_3	Indium and ferric nitrate salts	Zhao et al. (2014)
KIT-6	Mesoporous structures of In_2O_3-decorated NiO	Nickel nitrate	Dong and Liu (2018)
MCM-48	Mesoporous CeO_2	Cerium nitrate	Ji et al. (2008)
KIT-6	Mesoporous Fe_3O_4/CeO_2	CeO_2 and $Fe(NO_3)_3{\cdot}9H_2O$	Li et al. (2017)
KIT-6	Mesoporous WO_3	Phosphotungstic acid hydrate	Villa et al. (2015)
KIT-6	Mesoporous Fe_2O_3–TiO_2	$Ti(OCH_2CH_3)_4$	Park et al. (2017)
KIT-6	Mesoporous Fe_3O_4	$Fe(NO_3)_3.9H_2O$	Zhu et al. (2017)
SBA-15	Mesoporous MnO_2	$Mn(NO_3)_2.6H_2O$	Zhi et al. (2014)
KIT-6	Mesoporous MnO2	$Mn(NO_3)_2.4H_2O$	Bai et al. (2016)
SBA-15	Mesoporous transition metal sulfide@N-doped carbon composites	MClx (metal chlorides) and methionine	Zhu et al. (2019)
SBA-15	SnO_2 nanowires	$SnCl_2 \cdot 2H_2O$	Zhang et al. (2011)

phosphoric acid and sulfuric acid which formed as ester with the surface silanol and thereby prevented external carbon deposition (Seo et al. 2015a, b). Different mesoporous silica exploited for the synthesis of various nanomaterials are demonstrated in Table 15.1.

Porous anodic aluminum oxide (AAO) is widely exploited in the preparation of nanomaterials because of its flexibility and quantum-level pore size. Generally, the template is prepared from alumina sheet using electrochemical methods. Porous alumina is a self-organized structure resembling to honeycomb formed by high-density arrangement of ordered and parallel pores with diameter of 100–500 nm, pore density ranging from 10^7 to 10^{11} pore/cm^2, and diameter of 1–300 μm (Chen et al. 2012, Ide et al. 2017). Porous anodic alumina is reported in the preparation of a wide variety of nanomaterials, viz., nanowires, nanotubes, and nanodots. In one study, researchers had synthesized biological active surface-modified nanowires of anticancer drug (paclitaxel) by solvent annealing method using AAO templates. The surface was modified using n-octadecyltrichlorosilane, which thereby prevented agglomeration of nanowires (Abumaree et al. 2011). Copper nanowires were synthesized using a galvanic displacement pro-

cess in combination with AAO templates. AAO template was prepared by anodizing alumina with oxalic acid. Nanowires were fabricated to use as an electrode for electrochemical denitrification (Ganapathi et al. 2019). Gold nanodot arrays were fabricated using AAO template with controlled size between 20 and 80 nm using nanoimprint method (Kwon et al. 2011). In another study, Mn-doped K0.5Na0.5NbO3 nanodots were synthesized on an Nb-doped $SrTiO_3$substrate by means of AAO template. Resulting nanodots had a diameter of 50 nm and thickness of 34 nm (Ahn and Son 2016). Carbon nanotubes are reported to be fabricated by AAO template method using impregnation method (Peng Xiang et al. 2012), microwave plasma chemical vapor deposition method (Zuidema et al. 2013), and catalytic chemical vapor deposition method (Hekmat et al. 2017) and employing microwave radiation (Dadras and Faraji 2018).

Carbon is one of the abundant elements found in nature. It can be present in different structures with various physical and chemical properties. Carbon is being exploited as template for synthesis of a wide variety of nanomaterials due to its thermal and chemical stability (Zhu et al. 2012). It has uniform pore distribution and has diameter less than 50 nm and high specific area (Zhang et al. 2016). Hollow metal oxide fibers (TiO_2 and Fe_2O_3) have been synthesized using activated carbon fibers as the templates employing impregnation and heat treatment (Yuan et al. 2006). In another study, metal oxide nanowall structures of α-Fe_2O_3 were fabricated using carbon nanowalls as template by plasma-enhanced chemical vapor deposition technique (Akikubo et al. 2019). Metal oxide hollow spheres of Cr_2O_3, α-Fe_2O_3, Co_3O_4, NiO, and ZnO have been fabricated employing glucose derived-carbonaceous spheres as sacrificial templates. Respective metal oxides were used as precursors (Abdelaal and Harbrecht 2014). Researchers demonstrated the use of carbon nanofibers as template in the fabrication of porous metal oxide nanowires of Fe_2O_3, Co_3O_4, NiO, and CuO. These nanowires were further studied for their photocatalytic performance in which porous Fe_2O_3 showed the best results (Fan et al. 2015).

5 Soft Template

Soft templates are not fixed, rigid structures but are formed during the process of fabrication of nanoparticles. Because of some intermolecular or intramolecular force of interaction, the aggregate is formed with specific structure. The inorganic materials deposit on the surface or interface of these templates by means of some methods, namely, electrochemical deposition, chemical deposition, and/or other deposition techniques. This process of deposition leads to the formation of particles of definite shape and size. Soft templates show wide variety of application in the fabrication of nanomaterials due its versatile characteristics, easy method of preparation, nontoxicity, and repeatability. It is also known as endotemplate method in which structure-directing agents like surfactants arrange to self-assemblies (micelles) leading to mesopores (2–30 nm). The assemblies are governed by weak forces like non-covalent bonds, van der Waals force, and electrostatic attraction (Zhang et al. 2019).

Mainly soft templates include cationic, anionic, nonionic, and mixed surfactant systems to synthesize self-assembled porous structures. Mixed anionic surfactants such as sodium dodecyl benzene sulfonate and sodium dodecyl sulfate were used as template in the synthesis of mesoporous silica nanoparticles. The co-structure-directing agent employed was 3-aminopropyltrimethoxysilane (Gai et al. 2016). In another study, mesoporous hollow silica nanoparticles were synthesized using dual soft template system. Cationic surfactant cetyltrimethylammonium bromide along with triblock copolymer poly(styrene-b-2-vinyl pyridine-b-ethylene oxide) with a center void of about 17 nm was used to fabricate the nanoparticles. The ion interaction between cationic surfactant and silica leads to formation of mesostructures (Li et al. 2015). Shen and co-workers fabricated three-dimensional dendritic biodegradable mesoporous silica nanospheres using cationic cetyltrimethylammonium chloride as soft template and triethanolamine as catalyst (Shen et al. 2014).

Polymers possessing properties like large molecular weight, stability, and diverse molecu-

lar structure are used as soft template for the synthesis of nanomaterials. Block copolymers are generally utilized for the synthesis of nanomaterials by soft template method. Linear arrangement of blocks of monomers leads to more than one characteristic and thereby becomes helpful in the nanomaterial's fabrication. Choma and co-workers synthesized mesoporous carbon containing silver nanoparticles using soft template method. Triblock copolymer $EO_{101}PO_{56}EO_{101}$ was used as soft template, while resorcinol and formaldehyde were employed as carbon precursors (Choma et al. 2011). Nanostructured titania materials were fabricated using randomly methylated beta-cyclodextrin and block copolymer P123 as soft template. Controlled amount of cyclodextrin promoted sphericity of particles (Lannoy et al. 2014).

Many researchers employed a combination of hard and soft template techniques to exploit each templating characteristics in the preparation of nanomaterials. A combination of hard and soft template methods were employed in the preparation of silica hollow microcoils with nanostructred walls. Acid group (-COOH)-functionalized carbon microcoils were used as hard template, whereas hexadecyltrimethylammonium bromide (a surfactant) or perylenebis(dicarboximide) (amphiphilic dye aggregates) was used as soft templates (Rodriguez-Abreu et al. 2011). In another research, Zhang and co-workers fabricated hollow mesoporous silica nanoparticles via a facile soft-hard template route. Carbon nanosphere was used as hard template, and cetyltrimethylammonium bromide was utilized as soft template (Zhang et al. 2015).

Thermal stability is a concern with hydrocarbon-based polymer templates undergoing thermal treatment. However, carbonization of polymer templates helps to improve thermal stability but is limited to a certain extent. Also carbonized polymer template can undergo oxidation resulting into breakdown of the porous structure. Another method is to couple inorganic elements with polymer templates where inorganic nanoparticles serve as hard template and polymers as soft template. Thus, advantages of both hard and soft template methods can be achieved, and this combination is known as colloidal template method. Kang and co-workers demonstrated colloidal template method for the synthesis of $C@MoS_2$ nanoadsorbents. Colloidal microporous organic network nanotemplates were prepared through the networking of organic building blocks in the presence of poly(vinylpyrrolidone). MoS_2precursors were incorporated into the nanotemplates, and heat treatment led to surface-engineered core-shell nanoadsorbents. $C@MoS_2$ nanoparticles with a diameter of 80 nm, a negative zeta potential (−39.5 mV), a high surface area (508 $m^2 g^{-1}$), and excellent adsorption performance toward cationic dyes were successfully prepared using colloidal template method (Kang et al. 2019).

6 Membrane Contactor

In membrane contactor technique, one phase is introduced into another phase through the membrane pores. The other phase is flowing perpendicular to the membrane surface. Pore droplets are formed at the pore outlets and are solidified in the second phase flowing tangentially to the membrane surface (Fig. 15.4). The process has similarity to membrane emulsification technique (Fig. 15.5) in which oil in water, water in oil, or multiemulsions are prepared. In some process mixing and reaction such as polymerization, precipitation occurs between two phases inside the membrane unit. Polymeric hollow fibers and tubelike inorganic membranes are generally employed in the fabrication of nanomaterials using membrane contactor technique. For instance, nanoparticles of $BaSO_4$ were fabricated employing hollow fiber ultrafiltration membrane using membrane contactor technique (Jia and Liu 2002). In another work, nanoparticles with average size of 360 nm were prepared using ceramic membranes with an active ZrO_2 layer on an Al_2O_3-TiO_2 support (Charcosset and Fessi 2006). Various nanoparticles prepared using membrane contactor technique include polymeric nanoparticles, solid lipid nanoparticles, and inorganic nanoparticles (Table 15.2).

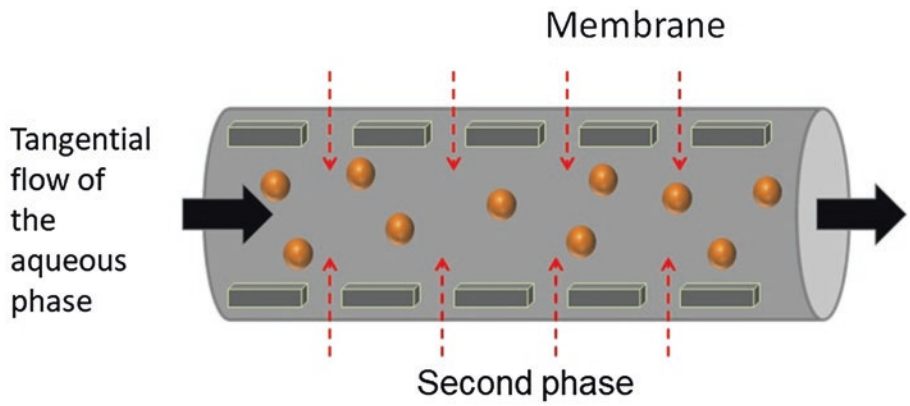

Fig. 15.4 Schematic representation of membrane contactor technique

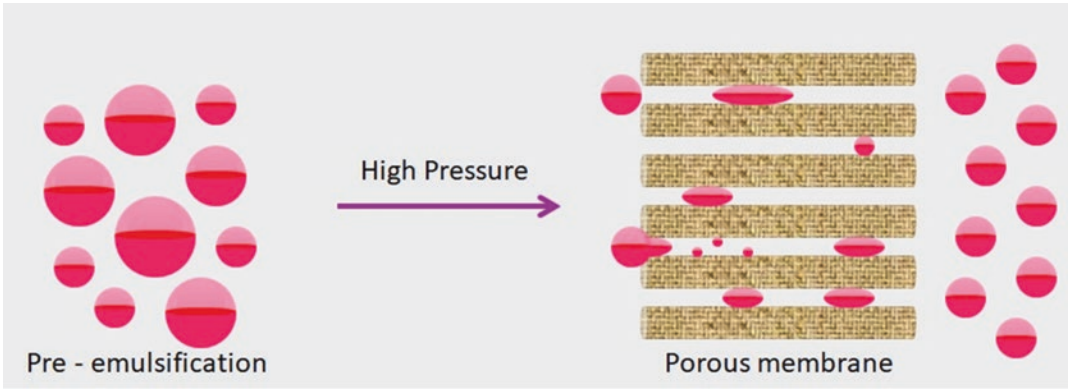

Fig. 15.5 Schematic representation of membrane emulsification method for the preparation of nanomaterials

7 Miscellaneous Methods

Membrane techniques are investigated extensively using various novel materials as membrane for synthesis of nanoparticles. For instance, Wang and co-workers used eggshell as membrane template in fabrication of MnO_2 nanoparticles from potassium permanganate by in situ redox reaction (Wang et al. 2018a, b). In another work, tin oxide nanoparticles were synthesized from tin chloride dihydrate using eggshell as biotemplate (Selvakumari et al. 2018). Nanoparticle size ranged from 13 to 40 nm. Gold nanorods were synthesized by electrochemical template synthesis using track-etched polycarbonate membrane. Chloroauric acid ($HauCl_4$) was employed as precursor in the preparation of gold nanorods and mercury as cathode for the electrochemical deposition process (Sharma et al. 2012). In another such work, AgCl microstructures and Pt nanowires were fabricated using etched ion track polycarbonate as membrane template employing simple ion exchange mechanism (Kumar and Chakarvarti 2012, Naderi et al. 2012). Shirasu porous glass (SPG) membranes are utilized by various researchers in the preparation of nanoparticles. Itraconazole nanoparticles were fabricated using SPG membrane using antisolvent precipitation method (Seo et al. 2015a, b). In another such work, polymeric nanoparticles (around 300 nm in size) of docetaxel were prepared by SPG membrane emulsification method using poly(lactide)-D-α-tocopheryl polyethylene glycol 1000 succinate polymer (Yu et al. 2013).

Membrane techniques for fabrication of nanomaterials were introduced since the 1980s, and

Table 15.2 Examples of nanoparticles prepared using membrane contactor technique

Product	Membrane type	References
$CaCO_3$ nanoparticles	Polypropylene hollow fiber	Jia et al. (2013)
$CaCO_3$, $SrCO_3$, $Al(OH)_3$, and Al nanoparticles	Polypropylene hollow fiber	Jia et al. (2009)
Albumin nanoparticles	Porous glass	Yedomon et al. (2013)
Solid lipid nanoparticles	Ceramic membranes with an active ZrO_2 layer on an Al_2O_3-TiO_2 support	El-Harati et al. (2006)
Polycaprolactone 10,000 nanoparticles	Ceramic membranes with an active ZrO_2 layer on an Al_2O_3-TiO_2 support	Charcosset and Fessi (2005)
Solid lipid nanoparticles	Ceramic membranes with an active ZrO_2 layer on an Al_2O_3-TiO_2 support	Charcosset et al. (2005)
$CaCO_3$ nanoparticles	Polypropylene hollow fiber	Jia et al. (2010)
Gold nanoparticles, polycaprolactone nanoparticles, biodegradable micelles from poly(ε-caprolactone)/ poly(ethylene glycol) diblock copolymers and liposomes	Nickel microengineered membrane	Vladisavljevic (2019)
$BaSO_4$ nanoparticles	Hollow fiber membrane	Jia and Liu (2002)
CeO_2Nanoparticles	Stainless steel microfiltration membrane	Yao et al. (2017)
ZnO nanoparticles	Stainless steel microfiltration membrane	Wang et al. (2010)
Silica nanoparticles	Stainless steel microfiltration membrane	Zhang et al. (2014)
Indium tin oxide nanoparticles	Stainless steel microfiltration membrane	Wang et al. (2016)
ZnO nanoparticles	Stainless steel microfiltration membrane	Huang et al. (2013)
Pseudoboehmite nanoparticles	Stainless steel microfiltration membrane	Wang et al. (2011)

till today various new membranes are investigated and reported for the same. Membrane template methods are widely used among the other methods available for the synthesis of nanoparticles. However, new polymers and materials are exploited for the efficient preparation of nanoparticles.

References

Abdelaal HM, Harbrecht B. Template-assisted synthesis of metal oxide hollow spheres utilizing glucose derived-carbonaceous spheres as sacrificial templates. J Adv Chem Eng. 2014;5(1):116. https://doi.org/10.4172/2090-4568.1000116.

Abumaree MH, Zhu L, Bardeen CJ, Al-Suwaidan SD, Al-Kaysi RO. Fabrication of biologically active surface-modified taxol nanowires using anodic aluminum oxide templates. RSC Adv. 2011;1(5):884–92.

Ahn Y, Son JY. Fabrication and ferroelectric characterization of Mn-doped K0.5Na0.5NbO3 nanodots using an anodic aluminum oxide template. Mater Lett. 2016;185:119–22.

Akikubo K, Kawaguchi N, Tachibana M. Synthesis of metal oxide nanowall structures using a carbon nanowall template. Jpn J Appl Phys. 2019;58(9):090912. https://doi.org/10.7567/1347-4065/ab37fe.

Bai B, Qiao Q, Li J, Hao J. Synthesis of three-dimensional ordered mesoporous MnO_2 and its catalytic performance in formaldehyde oxidation. Chin J Catal. 2016;37:27–31.

Bikiaris DM, Papageorgiou GZ, Pavlidou E, Vouroutzis N, Palatzoglou P, Karayannidis GP. Preparation by melt mixing and characterization of isotactic polypropylene/SiO_2 nanocomposites containing untreated and surface-treated nanoparticles. J Appl Polym Sci. 2006;100(4):2684–96.

Charcosset C, Fessi H. Preparation of nanoparticles with a membrane contactor. J Membr Sci. 2005;266:115–20.

Charcosset C, Fessi H. A membrane contactor for the preparation of nanoparticles. Desalination. 2006;200:568–9.

Charcosset C, El-Harati A, Fessi H. Preparation of solid lipid nanoparticles using a membrane contactor. J Control Release. 2005;108:112–20.

Chen CC, Fang D, Luo ZP. Fabrication and characterization of highly-ordered valve-metal oxide nanotubes and their derivative nanostructures. Rev Nanosci Nanotechnol. 2012;1:229–56.

Chen S, Zhang Q, Hou Y, Zhang J, Liang XJ. Nanomaterials in medicine and pharmaceuticals: nanoscale materials developed with less toxicity and more efficacy. Eur J Nanomed. 2013;5(2):61–79.

Choma J, Jedynak K, Gorka J, Jaroniec M. Soft-templating synthesis and adsorption properties of mesoporous carbons with embedded silver nanoparticles. Adsorption. 2011;17(3):461–6.

Dadras S, Faraji M. Improved carbon nanotube growth inside an anodic aluminum oxide template using microwave radiation. J Phys Chem Solids. 2018;116:203–8.

Dai W, Zheng M, Zhao Y, Liao S, Ji G, Cao J. Template synthesis of three-dimensional cubic ordered mesoporous carbon with tunable pore sizes. Nanoscale Res Lett. 2010;5:103–7.

Darr JA, Zhang J, Makwana NM, Weng X. Continuous hydrothermal synthesis of inorganic nanoparticles: applications and future directions. Chem Rev. 2017;117(17):11125–238.

Deng X, Chen K, Tuysuz H. Protocol for the nanocasting method: preparation of ordered mesoporous metal oxides. Chem Mater. 2017;29(1):40–52.

Dong Z, Liu S. In_2O_3-decorated ordered mesoporous NiO for enhanced NO_2 sensing at room temperature. J Mater Sci Mater Electron. 2018;29(4):2645–53.

El-Harati AA, Charcosset C, Fessi H. Influence of the formulation for solid lipid nanoparticles prepared with a membrane contactor. Pharm Dev Technol. 2006;11:153–7.

El-Khatib AM, Badawi MS, Ghatass ZF, Mohamed MM, Elkhatib M. Synthesize of silver nanoparticles by arc discharge method using two different rotational electrode shapes. J Clust Sci. 2018;29(6):1169–75.

Fan W, Li M, Xu J, Bai H, Zhang R, Chen C. Synthesis and photocatalytic property of porous metal oxides nanowires based on carbon nanofiber template. Funct Mater Lett. 2015;8(2):1550018. https://doi.org/10.1142/S1793604715500186.

Fievet F, Ammar-Merah S, Brayner R, Chau F, Giraud M, Mammeri F, Peron J, Piguemal JY, Sicard L, Viau G. The polyol process: a unique method for easy access to metal nanoparticles with tailored sizes, shapes and compositions. Chem Soc Rev. 2018;47(14):5187–233.

Gai F, Zhou T, Chu G, Li Y, Liu Y, Huo Q, Akhtar F. Mixed anionic surfactant-templated mesoporous silica nanoparticles for fluorescence detection of Fe^{3+}. Dalton Trans. 2016;45:508–14.

Galdino NM, Brehm GS, Bussamara R, Goncalves WDG, Abarca G, Scholten JD. Sputtering deposition of gold nanoparticles onto graphene oxide functionalized with ionic liquids: biosensor materials for cholesterol detection. J Mater Chem B. 2017;5(48):9482–6.

Ganapathi A, Swaminathan P, Neelakantan L. Anodic aluminum oxide template assisted synthesis of copper nanowires using a galvanic displacement process for electrochemical denitrification. ACS Appl Nano Mater. 2019;2(9):5981–8. https://doi.org/10.1021/acsanm.9b01409.

Hekmat F, Sohrabi B, Rahmanifar MS. Effect of template on the structure of carbon nanotubes grown by catalytic chemical vapor deposition method. Mod Chem Appl. 2017;5(1):207. https://doi.org/10.4172/2329-6798.1000207.

Horprathum M, Eiamchai P, Kaewkhao J, Chananonnawathorn C, Patthanasettakul V, Limwichean S, Nuntawong N, Chindaudom P. Fabrication of nanostructure by physical vapor deposition with glancing angle deposition technique and its applications. AIP Conf Proc. 2014;1617:7. https://doi.org/10.1063/1.4897091.

Huang C, Wang Y, Luo G. Preparation of highly dispersed and small-sized ZnO nanoparticles in a membrane dispersion microreactor and their photocatalytic degradation. Ind Eng Chem Res. 2013;52:5683–90.

Ide S, Capraz OO, Shrotriya P, Hebert KR. Oxide microstructural changes accompanying pore formation during anodic oxidation of aluminum. Electrochim Acta. 2017;232:303–9.

Jeong TG, Chun J, Cho BW, Lee J, Kim YT. Enhanced performance of sulfur-infiltrated bimodal mesoporous carbon foam by chemical solution deposition as cathode materials for lithium sulfur batteries. Sci Rep. 2017;7:Article ID: 42238.

Ji P, Zhang J, Chen F, Anpo M. Ordered mesoporous CeO_2 synthesized by nanocasting from cubic Ia3d mesoporous MCM-48 silica: formation, characterization and photocatalytic activity. J Phys Chem C. 2008;112:17809–13.

Jia Z, Liu Z. Synthesis of nanosized BaSO4 particles with a membrane reactor: effects of operating parameters. J Membr Sci. 2002;209:153–61.

Jia Z, Chang Q, Qin J, Hong X. Preparation of nanoparticles with a gas–liquid membrane contactor. J Membr Sci. 2009;342:1–5.

Jia Z, Chang Q, Qin J, Sun H. Preparation of nanoparticles with a continuous gas–liquid membrane contactor: absorption process. J Membr Sci. 2010;352:50–4.

Jia Z, Chang Q, Qin J, Mamat A. Preparation of calcium carbonate nanoparticles with a continuous gas-liquid membrane contactor: particles morphology and membrane fouling. Chin J Chem Eng. 2013;21(2):121–6.

Kamyshny A, Magdassi S. Conductive nanomaterials for 2D and 3D printed flexible electronics. Chem Soc Rev. 2019;48(6):1712–40.

Kang L, Wang Z, Cao Z, Ma Y, Fu H, Yao J. Colloid chemical reaction route to the preparation of nearly monodispersed perylene nanoparticles: size-tunable synthesis and three-dimensional self-organization. J Am Chem Soc. 2007;129(23):7305–12.

Kang SY, Kang CW, Kim DW, Myung Y, Choi J, Lee SM, Kim HJ, Ko YJ, Son SU. Colloidal template synthe-

sis of nanomaterials by using Microporous organic nanoparticles: the case of C@MoS2 nanoadsorbents. Chem Asian J. 2019; https://doi.org/10.1002/asia.201900885.

Kim H, Cho J. Hard templating synthesis of mesoporous and nanowire SnO_2 lithium battery anode materials. J Mater Chem. 2008;18:771–5.

Kim M, Osone S, Kim T, Higashi H, Seto T. Synthesis of nanoparticles by laser ablation: a review. KONA Powder Part J. 2017;34:80–90.

Kolhatkar AG, Dannongoda C, Kourentzi K, Jamison AC, Nekrashevich I, Kar A, Cacao E, Strych U, Rusakova I, Martirosyan KS, Litvinov D, Lee TR, Willson RC. Enzymatic synthesis of magnetic nanoparticles. Int J Mol Sci. 2015;16(4):7535–50.

Kruk M, Dufour B, Celer EB, Kowalewski T, Jaroniec M, Matyjaszewski K. Synthesis of mesoporous carbons using ordered and disordered mesoporous silica templates and polyacrylonitrile as carbon precursor. J Phys Chem B. 2005;109(19):9216–25.

Kumar S, Chakarvarti SK. Chemical synthesis of AgCl microstructures using etched ion track polycarbonate membranes. Synth Reactivity Inorg Metal Org Nano-Metal Chem. 2012;42:1242–5.

Kwon N, Kim N, Yeon J, Yeom G, Chung I. Fabrication of ordered Au nanodot arrays utilizing anodic aluminum oxide templates formed on Si substrate. J Vac Sci Technol B. 2011;29:031805. https://doi.org/10.1116/1.3592431.

Lannoy A, Bleta R, Machut C, Monflier E, Ponchel A. Block copolymer–cyclodextrin supramolecular assemblies as soft templates for the synthesis of titania materials with controlled crystallinity, porosity and photocatalytic activity. RSC Adv. 2014;4:40061. https://doi.org/10.1039/c4ra05994h.

Lee J, Yoon S, Oh SM, Shin CH, Hyeon T. Development of a new mesoporous carbon using an HMS aluminosilicate template. Adv Mater. 2000;12(5):359–62.

Lee CH, Lee K, Chang S, Park JT, Kim B. Highly efficient MCM-48-based template synthesis of osmium and platinum 3-D nano networks. Bull Kor Chem Soc. 2006;27(1):130–2.

Li H, Liu S, Dai Z, Bao J, Yang X. Applications of nanomaterials in electrochemical enzyme biosensors. Sensors. 2009;9(11):8547–61.

Li Y, Bastakoti BP, Imura M, Tang J, Aldalbahi A, Torad NL, Yamauchi Y. Dual soft-template system based on colloidal chemistry for the synthesis of hollow mesoporous silica nanoparticles. Chemistry. 2015;21(17):6375–80.

Li K, Zhao Y, Song C, Guo X. Magnetic ordered mesoporous Fe_3O_4/CeO_2 composites with synergy of adsorption and Fenton catalysis. Appl Surf Sci. 2017;425:526–34.

Li J, Ren H, Zou X, Cai K, Zhao N, Zhu G. Hard-template synthesis of micro-mesoporous organic frameworks with controlled hierarchicity. Chem Commun. 2018;54(60):8335–8.

Liu Y, Zhou G, Liu K, Cui Y. Design of complex nanomaterials for energy storage: past success and future opportunity. Acc Chem Res. 2017;50(12):2895–905.

Lu AH, Schuth F. Nanocasting pathways to create ordered mesoporous solids. C R Chim. 2005;8:609–20.

Lu AH, Schuth F. Nanocasting: a versatile strategy for creating nanostructured porous materials. Adv Mater. 2006;18:1793–805.

Lu CY, Puig T, Obradors X, Ricart S, Ros J. Ultra-fast microwave-assisted reverse microemulsion synthesis of $Fe_3O_4@SiO_2$ core–shell nanoparticles as a highly recyclable silver nanoparticle catalytic platform in the reduction of 4-nitroaniline. RCS Adv. 2016;6(91):88762–9.

Mackenzie JD, Bescher EP. Chemical routes in the synthesis of nanomaterials using the sol–gel process. Acc Chem Res. 2007;40(9):810–8.

Malik MA, Wani MY, Hashim MA. Microemulsion method: a novel route to synthesize organic and inorganic nanomaterials: 1st nano update. Arab J Chem. 2012;5(4):397–417.

Manawi YM, Ihsanullah SA, Al-Ansari T, Atieh MA. A review of carbon nanomaterials' synthesis via the chemical vapor deposition (CVD) method. Materials (Basel). 2018;11(5):822. https://doi.org/10.3390/ma11050822.

Naderi N, Hashim MR, Rouhi J. Synthesis and characterization of Pt nanowires electrodeposited into the cylindrical pores of polycarbonate membranes. Int J Electrochem Sci. 2012;7:8481–6.

Peng Xiang H, Chang L, Chao S, Hui MC. Carbon nanotubes prepared by anodic aluminum oxide template method. Chin Sci Bull. 2012;57(2–3):187–204.

Rodriguez-Abreu C, Vilanova N, Solans C, Ujihara M, Imae T, Lopez-Quintela A, Motojima S. A combination of hard and soft templating for the fabrication of silica hollow microcoils with nanostructured walls. Nanoscale Res Lett. 2011;6(1):330. https://doi.org/10.1186/1556-276X-6-330.

Roduner E. Size matters: why nanomaterials are different. Chem Soc Rev. 2006;35:583–92.

Rumplecker A, Kleitz F, Salabas EL, Schuth F. Hard templating pathways for the synthesis of nanostructured porous Co_3O_4. Chem Mater. 2007;19:485–96.

Sahay R, Reddy VJ, Ramakrishna S. Synthesis and applications of multifunctional composite nanomaterials. Int J Mech Mater Eng. 2014;9:25. https://doi.org/10.1186/s40712-014-0025-4.

Saraiva C, Praça C, Ferreira R, Santos T, Ferreira L, Bernardino L. Nanoparticle-mediated brain drug delivery: overcoming blood-brain barrier to treat neurodegenerative diseases. J Control Release. 2016;235:34–47.

Seeman NC. Nanomaterials based on DNA. Annu Rev Biochem. 2010;79:65–87.

Selvakumari JC, Nishanthi ST, Dhanalakshmi J, Ahila M, Padiyan DP. Bio-active synthesis of tin oxide nanoparticles using eggshell membrane for energy storage application. Appl Surf Sci. 2018;441:530–7.

Seo JW, Kim KJ, Kim SH, Hwang KM, Seok SH, Park ES. Effect of process parameters on formation and aggregation of nanoparticles prepared with a Shirasu porous glass membrane. Chem Pharm Bull. 2015a;63(10):792–8.

Seo Y, Kim K, Jung Y, Ryoo R. Synthesis of mesoporous carbons using silica templates impregnated with mineral acids. Microporous Mesoporous Mater. 2015b;207:156–62.

Shang T, Lu Q, Chao L, Qin Y, Yun Y, Yun G. Effects of ordered mesoporous structure and La-doping on the microwave absorbing properties of $CoFe_2O_4$. Appl Surf Sci. 2018;434:234–42.

Sharma MK, Ambolikar AS, Aggarwal SK. Electrochemical synthesis of gold nanorods in track-etched polycarbonate membrane using removable mercury cathode. In: Diallo MS, Fromer NA, Jhon MS, editors. Nanotechnology for sustainable development. Cham: Springer; 2012. p. 349–58.

Sharma D, Kanchi S, Bisetty K. Biogenic synthesis of nanoparticles: a review. Arab J Chem. 2015; https://doi.org/10.1016/j.arabjc.2015.11.002.

Shen Y, Friend CS, Jiang Y, Swiatkiewicz J, Prasad PN. Nanophotonics: interactions, materials, and applications. J Phys Chem B. 2000;104(47) https://doi.org/10.1021/jp0031395.

Shen D, Yang J, Li X, Zhou L, Zhang R, Li W, Chen L, Wang R, Zhang F, Zhao D. Biphase stratification approach to three-dimensional dendritic biodegradable mesoporous silica nanospheres. Nano Lett. 2014;14(2):923–32.

Singaravelan R, Alwar SBS. Electrochemical synthesis, characterisation and phytogenic properties of silver nanoparticles. Appl Nanosci. 2015;5(8):983–91.

Singh T, Shukla S, Kumar P, Wahla V, Bajpai VK, Rather IA. Application of nanotechnology in food science: perception and overview. Front Microbiol. 2017;8:1501.

Takai A, Doi Y, Yamauchi Y, Kuroda K. Soft-chemical approach of noble metal nanowires templated from mesoporous silica (SBA-15) through vapor infiltration of a reducing agent. J Phys Chem C. 2010;114(17):7586–93.

Thielemann JP, Girgsdies F, Schlogl R, Hess C. Pore structure and surface area of silica SBA-15: influence of washing and scale-up. Beilstein J Nanotechnol. 2011;2:110–8.

Thomsen LB, Thomsen MS, Moos T. Targeted drug delivery to the brain using magnetic nanoparticles. Ther Deliv. 2015;6(10):1145–55.

Villa K, Murcia-Lopez S, Andreu T, Morante JR. Mesoporous WO_3 photocatalyst for the partial oxidation of methane to methanol using electron scavengers. Appl Catal B Environ. 2015;163:150–5.

Vladisavljevic GT. Production of nanoparticles using membrane contactors and microfluidic devices. https://repository.lboro.ac.uk/account/articles/9246356. Accessed on 4th Oct 2019.

Wahab MA, Darain F. Nano-hard template synthesis of pure mesoporous NiO and its application for streptavidin protein immobilization. Nanotechnology. 2014;25(16):165701. https://doi.org/10.1088/0957-4484/25/16/165701.

Wang Y, Zhang C, Bi S, Luo G. Preparation of ZnO nanoparticles using the direct precipitation method in a membrane dispersion micro-structured reactor. Powder Technol. 2010;202:130–6.

Wang Y, Xu D, Sun H, Luo G. Preparation of pseudo-boehmite with a large pore volume and a large pore size by using a membrane-dispersion microstructured reactor through the reaction of CO_2 and a $NaAlO_2$ solution. Ind Eng Chem Res. 2011;50:3889–94.

Wang J, Zhang F, Wang Y, Luo G, Cai W. A size-controllable preparation method for indium tin oxide particles using a membrane dispersion micromixer. Chem Eng J. 2016;293:1–8.

Wang Q, Jin K, Lv Z, Yang D, Xu J, Hong B, Wang X. Synthesis and pseudo capacitive performance of ordered mesoporous $NiCo_2O_4$ nanowires. Int J Electrochem Sci. 2018a;13:11675–83.

Wang Q, Ma C, Tang J, Zhang C, Ma L. Eggshell membrane-templated MnO_2 nanoparticles: facile synthesis and tetracycline hydrochloride decontamination. Nanoscale Res Lett. 2018b;13:255. https://doi.org/10.1186/s11671-018-2679-y.

Xu J, Shen K, Xue B, Li YX, Cao Y. Synthesis of three-dimensional mesostructured graphitic carbon nitride materials and their application as heterogeneous catalysts for knoevenagel condensation reactions. Catal Lett. 2013;143(6):600–9.

Yadav TP, Yadav RM, Singh DP. Mechanical milling: a top down approach for the synthesis of nanomaterials and nanocomposites. Nanosci Nanotechnol. 2012;2(3):22–48.

Yang H, Zhao D. Synthesis of replica mesostructures by the nanocasting strategy. J Mater Chem A. 2005;15:1217–31.

Yao H, Wang Y, Luo G. A size-controllable precipitation method to prepare CeO_2 nanoparticles in a membrane dispersion microreactor. Ind Eng Chem Res. 2017;56:4993–9.

Yedomon B, Fessi H, Charcosset C. Preparation of Bovine Serum Albumin (BSA) nanoparticles by desolvation using a membrane contactor: a new tool for large scale production. Eur J Pharm Biopharm. 2013;85:398–405.

Yu Y, Tan S, Zhao S, Zhuang X, Song Q, Wang Y, Zhou Q, Zhang Z. Antitumor activity of docetaxel-loaded polymeric nanoparticles fabricated by Shirasu porous glass membrane-emulsification technique. Int J Nanomedicine. 2013;8:2641–52.

Yuan R, Fu X, Wang X, Liu P, Wu L, Xu Y, Wang X, Wang Z. Template synthesis of hollow metal oxide fibers with hierarchical architecture. Chem Mater. 2006;18(19):4700–5.

Yuan N, Cheng G, An Y, Du Z, Wu S. Ordered mesostructured CdS nanowire arrays with rectifying properties. Nanoscale Res Lett. 2009;4:414–9.

Zhang H, Tan Z, Xu P, Oh K, Wu R, Shi W, Jiao Z. Preparation of SnO_2 nanowires by solvent-free method using mesoporous silica template and their gas sensitive properties. J Nanosci Nanotechnol. 2011;11:11114–8.

Zhang T, Wang Y, Luo G, Bai S. Preparation of highly dispersed precipitated nanosilica in a membrane dispersion microreactor. Chem Eng J. 2014;258:327–33.

Zhang H, Xu H, Wu M, Zhong Y, Wang D, Zheng J. A soft–hard template approach towards hollow mesoporous silica nanoparticles with rough surfaces for controlled drug delivery and protein adsorption. J Mater Chem B. 2015;3(31):6480–9.

Zhang L, Zhang T, Gao R, Tang D, Tang J, Zhan Z. Preparation and characterization of mesoporous carbon materials of chinese medicine residue with high specific surface areas. Chem Eng Trans. 2016;55:79–84.

Zhang L, Jin L, Liu B, He J. Templated growth of crystalline mesoporous materials: from soft/hard templates to colloidal templates. Front Chem. 2019; https://doi.org/10.3389/fchem.2019.00022.

Zhao J, Yang T, Liu Y, Wang Z, Li X, Sun Y, Du Y, Li Y, Lu G. Enhancement of NO_2 gas sensing response based on ordered mesoporous Fe-doped In_2O_3. Sensors Actuators B. 2014;191:806–12.

Zhi B, Ding H, Wang D, Cao Y, Zhang Y, Wang X, Liu Y, Huo Q. Ordered mesoporous MnO_2 as a synergetic adsorbent for effective arsenic (iii) removal. J Mater Chem A. 2014;2(7):2374–82.

Zhu K, Sun J, Zhang H, Liu J, Wang Y. Carbon as a hard template for nano material catalysts. J Nat Gas Chem. 2012;21:215–32.

Zhu S, Dong B, Yu Y, Bu L, Deng J, Zhou S. Heterogeneous catalysis of ozone using ordered mesoporous Fe_3O_4 for degradation of atrazine. Chem Eng J. 2017;328:527–35.

Zhu J, Chen Z, Jia L, Lu Y, Wei X, Wang X, Wu WD, Han N, Li Y, Wu Z. Solvent-free nanocasting toward universal synthesis of ordered mesoporous transition metal sulfide@N-doped carbon composites for electrochemical applications. Nano Res. 2019;12(9):2250–8.

Zuidema J, Ruan X, Fisher TS. Optical properties of ordered carbon nanotube arrays grown in porous anodic alumina templates. Opt Express. 2013;21(19):22053–62.

16 Self-Assembling Lipid Nanoparticles/Nanosystems (SLNN) Using Hydrophilic Solvents: Overview and Industrial Uses

Jeffrey S. Reynolds, Nicole McCardy, Julian Bejarano, and Deborah Duffey

Abstract

Self-assembling lipid nanoparticle systems come in a variety of structural arrangements, sizes, morphologies, and compositions. Lipid nanoparticles have become a significant option to increase the stability and control the release of many active compounds of interest for pharmaceutical and food and beverage industries allowing the development of safer and more effective formula or products. A comprehensive summary of self-assembling nanoparticle systems is beneficial for the nanoparticle field, both academic and professional toward aiding awareness of the subject and its benefits. An overview of self-assembling lipid nanoparticle systems is presented with emphasis on nanostructures, properties, production methods, and key characteristics of importance for industrial applications. Special emphasis is placed on lamellar phase dispersions, termed liposomes, relevant properties, long history of use, and their key role as vehicle of a variety of therapeutic agents. Additional details of each characteristic of self-assembling lipid nanoparticle systems are presented along with information regarding benefits of particular self-assembling lipid nanoparticle systems. Examples of the self-assembling lipid nanoparticle systems within various industrial sectors including pharmaceutical, cosmetic, nutraceutical, and food and beverage are described, as well as the relevance of self-assembling lipid nanoparticle systems within the particular industrial segment. Additionally, details of value and/or benefit to the specific industrial segment are presented.

Keywords

Self-assembling · Lipid nanoparticles · Nanovesicles · Pharmaceutical · Delivery systems · Food · Beverage · Cosmetic · Industrial · Application

1 Overview and Types of Self-Assembling Nanolipid Particles and Systems (SLNN)

Self-assembly is a spontaneous feature observed in a variety of biological materials. It is defined as the regular assembly of very small molecular entities to become larger supramolecular structures as a result of various noncovalent interactions, including hydrogen bonding, coordination, van der Waals forces, and electrostatic and hydrophobic interactions, among others. These supra-

J. S. Reynolds ✉) · N. McCardy · J. Bejarano
D. Duffey
Dermazone Solutions Inc., St. Petersburg, FL, USA
e-mail: jReynolds@dermazone.com

J. K. Patel, Y. V. Pathak (eds.), *Emerging Technologies for Nanoparticle Manufacturing*,
https://doi.org/10.1007/978-3-030-50703-9_16

molecular assemblies have additional and unique functions/properties, which would not be possible in the isolated single structure alone.

Lipids are an example of the biological compounds with self-assembling capacities. Lipids are generally amphiphilic in nature (*amphi* meaning two and *philic* meaning liking or loving). The lipid molecule has two parts: a hydrophilic head group, which has affinity for water and the alkyl chain(s), and a hydrophobic tail group, which has low to no affinity to water. This special amphiphilic behavior governs the self-assembling process of lipids when mixed with an aqueous medium. Self-assembled structures of lipids are commonly seen in many biological structures, such as the cell plasma membrane and the densely folded membranes in the mitochondria (Shanmugam and Banerjee 2011).

Self-assembling lipid nanoparticles or nanostructured lipid particles (SLNNs) have gained substantial interest for nanomedicine applications such as diagnostic and drug delivery due to their simple formulation process, notable biocompatibility, and biodegradability. The high interest in these self-assembled lipid nanosystems as delivery vehicles for therapeutic agents also is based on their hydrophilic and hydrophobic domains, which permit the incorporation of compounds with a variety of physicochemical properties. Additionally, their complex internal lipid nanoarchitecture permits the sustained release of the entrapped therapeutic agents.

During the self-assembling process, lipids will form various liquid crystalline phases. This process is termed polymorphism. The polymorphism can be influenced by small changes in molecular or ambient properties leading to morphology and phase changes (Barauskas et al. 2005). For example, amphiphilic lipids spontaneously self-assemble and form thermodynamically stable phases on exposure to an excess of water. A pioneering study to understand better lyotropic liquid crystalline phases (formed by dissolving an amphiphilic mesogen in a suitable solvent) is shown in the work conducted by Luzzati and Husson (1962), which employed x-ray scattering techniques to demonstrate clearly that lipids can self-assemble into different phase structures. In particular, some of the commonly encountered mesophases are (1) the bilayer lamellar phases (L_α); (2) the 2D inverse hexagonal structure (H_{II}); (3) the 3D ordered micellar cubic (I_{II} or Fd3m) and bicontinuous cubic (V_{II}) phases; and (5) the disordered phases of reverse isotropic micelles (L_{II}) and swollen sponges (L_{III}) (Luzzati and Husson 1962; Tan et al. 2018).

The type of lipid structure formed is governed by the molecular packing of the lipid molecules, which is represented by their critical packing parameter (CPP) defined as (Tan et al. 2018)

$$\mathrm{CPP} = \frac{V_s}{a_0 l}$$

where V_s is the hydrophobic or hydrocarbon chain volume, a_0 is the effective head group area, and l is the critical length of the lipid tail or hydrophobic chain. The CPP can be influenced by elemental factors including the concentration and spontaneous curvature of the lipid molecules as well as environmental parameters including temperature, water content, ionic strength, and pH. When the CPP value is <0.5, space is dominated by the large hydrophilic head groups, and the lipids adopt a conical structure as the head groups occupy a greater surface and generally favor the formation of positively curved micelles (e.g., spherical micelles, worm-like or cylindrical micelles, ribbons, tubules, cubic or non-inverted hexagonal [H_I] phase) (Fig. 16.1). If CPP is between 0.5 and 1, the curvature of the self-assembled lipids is close to zero leading to positively curved L_α phases (bilayer vesicles). Whereas when CPP is >1, it refers to large hydrophobic tail groups, where the lipid adopts a wedge shape as hydrocarbon tail chains are larger than that of the head group, leading to the formation of highly negatively curved inverted phases such as inverted micelles and inverted-cubic (V_{II}) or inverted-hexagonal (H_{II}) phases (Shanmugam and Banerjee 2011; Tan et al. 2018).

Figure 16.2 shows the different self-assembled lipid nanostructures formed with varying CPP.

The different self-assembled lipid arrangements might be formed through different lipid

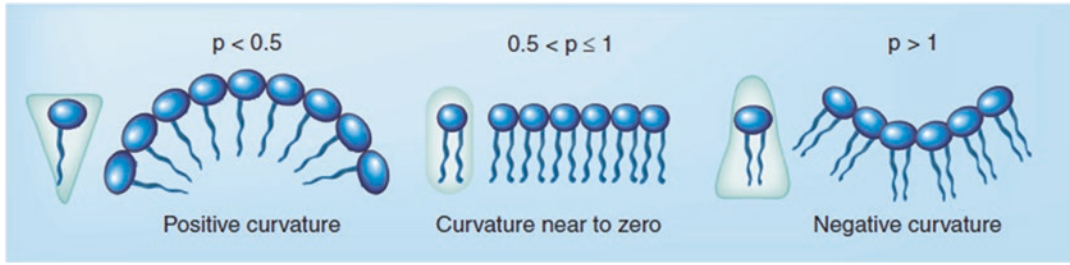

Fig. 16.1 Packaging parameters of liquid crystalline phases and their shape and curvature. (Reprinted with permission from Shanmugam and Banerjee 2011)

transitions such as (1) transition between ordered lamellar phases (e.g., crystal to gel, gel to gel, crystal to crystal), (2) transition because of chain melting (lipids form a lamellar gel phase at low temperature, which switches to a fluid phase at high temperature), and (3) transition within the single phase (the transition occurs between the same fluid phase lamellar to hexagonal or cubic or vice versa) (Shanmugam and Banerjee 2011). The stable intermediates of the lamellar structures are known as mesophasic supramolecular structures or non-lamellar structures. Examples of these mesophases are cubosomes, hexosomes, and supramolecular structures (tubules, ribbons, lipoplexes, and cochleates, among others) (Shanmugam and Banerjee 2011). Cubosomes and hexosomes are dispersed particles of the highly ordered, non-lamellar structures of V_{II} and H_{II} phases, respectively. With the aid of steric stabilizers, these bulk mesophases can be dispersed to form stable nanoparticles that contain the internal cubic or hexagonal phase. Furthermore, their internal nanostructure can be tuned by additives that enable control of the drug diffusion rate, size selectivity, and stimuli responsiveness of the nanosystems.

The simplest and most studied of the self-assembled lipid nanostructures are the lamellar phase dispersions, termed liposomes, discovered by Bangham and coworkers in the 1960s (Bangham and Horne 1964). Liposomes are vesicles of a range of shapes self-assembled by amphiphilic lipid molecules in a hydrophilic solution. For example, if the vesicle is formed by a single lipid bilayer, this is called a unilamellar vesicle (ULV). Similarly, if the vesicle is formed by multiple lipid bilayers, it would be called a multilamellar vesicle (MLV). Sometimes, a large vesicle engulfs similar or different sized smaller vesicles, which is called an oligo-vesicular vesicle (OVV). Based on their particle size, unilamellar vesicles are broadly categorized into small (SUV, 20–100 nm), large (LUV, 100–1000 nm), and giant (GUV, >1 μm) unilamellar vesicles (Kulkarni 2016). Figure 16.3 shows this categorization of the vesicles.

For drug delivery application, hydrophilic therapeutic agents can be entrapped into the aqueous liposome core, while hydrophobic therapeutic agents can be incorporated into the liposomal membranes or lipid bilayers (Shanmugam and Banerjee 2011).

There are a number of different vesicles that can be used for drug delivery. Among the most studied, we can find conventional liposomes, transfersomes, niosomes, and ethosomes. Lyphazome®, a novel and proprietary liposomal encapsulation system, will also be discussed.

Conventional liposomes are composed of phospholipids, which in water form lipid bilayer spheres enclosing aqueous cores. Phospholipids are amphiphilic, and this characteristic is responsible for the formation of vesicles in aqueous solutions caused by hydrogen bonding, van der Waals forces, and other electrostatic interactions. This vesicle structure means that liposomes can encapsulate hydrophilic molecules inside their core or lipophilic molecules into their lipid bilayer (Shukla et al. 2017).

Transfersomes are vesicular systems with highly stress-adaptive and stress-responsive properties. The main components of a transfer-

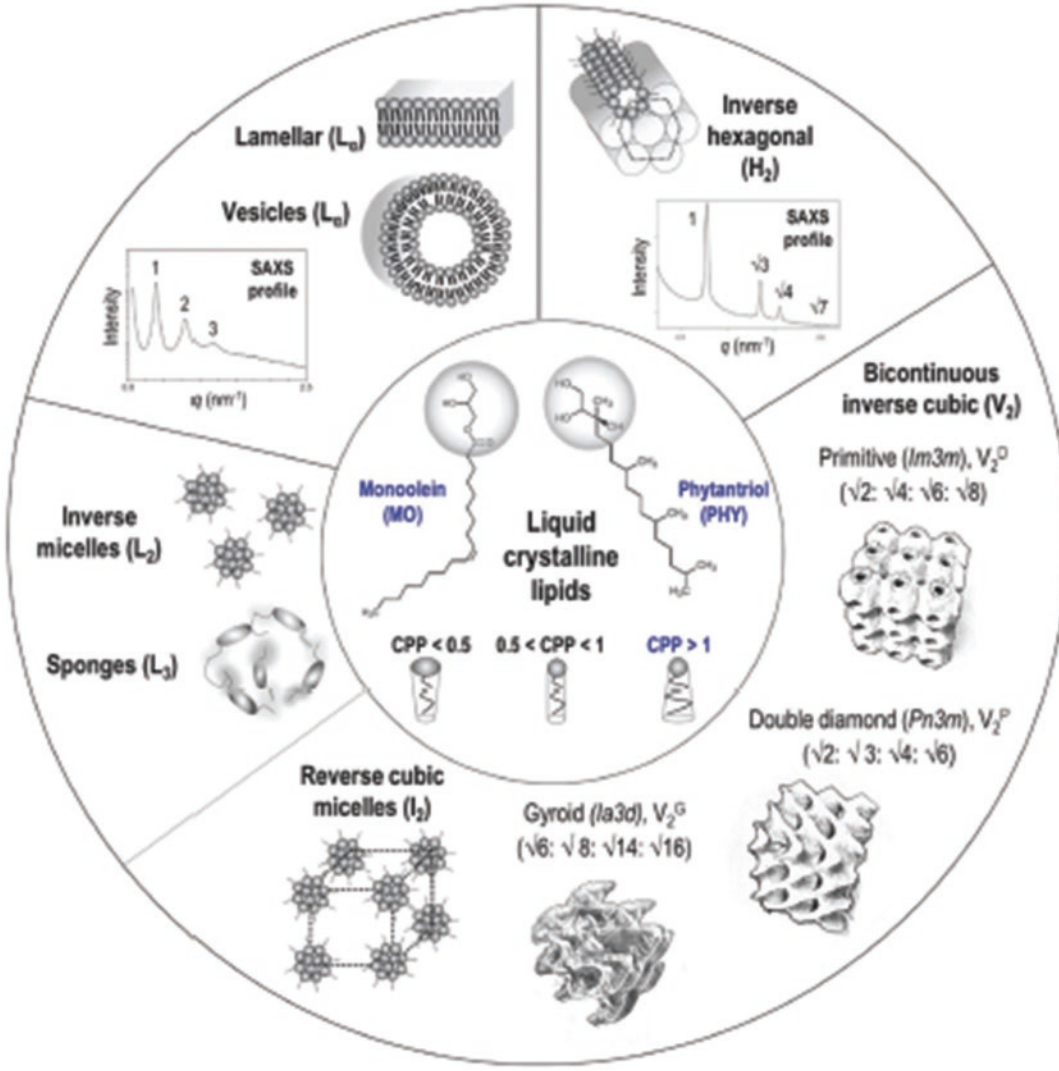

Fig. 16.2 Self-assembled lipid nanostructures with varying CPP. Characteristic diffraction spacing ratios by small-angle x-ray scattering (SAXS) are shown. (Reprinted with permission from Tan et al. 2018)

some are phospholipids like soy phosphatidylcholine which is the vesicle forming agent, surfactants (e.g., sodium cholate or sorbitan esters and polysorbates), and solvents (e.g., ethanol and methanol, among others). Surfactants act as an edge activator that destabilizes the lipid bilayers and increases the deformability of the vesicle. Formulations may also contain some ethanol (less than about 10%) and a lipid concentration (typically less than about 10% in the final aqueous lipid suspension). Transfersomes have the ability to deform and pass through narrow pores (from five to ten times less than their own diameter) without measurable loss. This function gives better penetration keeping an intact vesicular structure. They generally have high entrapment efficiency like the case of lipophilic drug (~90%). Transfersomes also serve as a carrier for both low and high molecular weight drugs (Pawar et al. 2016).

Niosomes are one of the promising drug carriers that have a lipid bilayer structure and are formed by self-association. The self-assembly of nonionic surfactants in aqueous media results in a

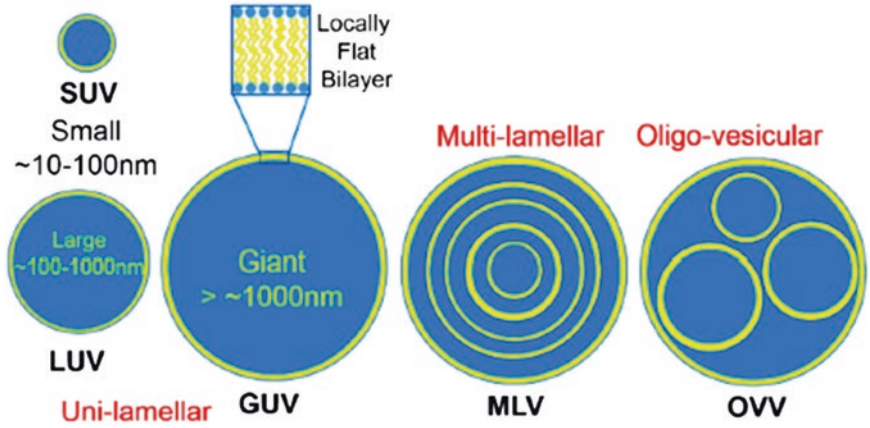

Fig. 16.3 Schematic diagram of vesicles according to their size and lamellarity. (Reprinted with permission from Kulkarni 2016)

closed bilayer structure. A high interfacial tension between water and the hydrophobic tails of the amphiphile causes them to associate. The steric and hydrophilic repulsion between the head groups of nonionic surfactants ensure that hydrophilic termini point outward in contact with water. The assembly into closed bilayers usually requires some input of mechanical or heat energy. Niosomes are biodegradable, biocompatible, and non-immunogenic. They have long shelf life, exhibit high stability, and enable the delivery of drugs at target site in a controlled and/or sustained manner. Various types of nonionic surfactants have been reported to form niosomes and enable the entrapment of a large number of drugs with a wide range of solubility (Seleci et al. 2016).

Ethosomes are phospholipid-based elastic nanovesicles containing a high content of ethanol (20–45%) and water. Ethanol is known as an efficient permeation enhancer and has been added in vesicular systems to prepare elastic nanovesicles. It can interact with the polar head group region of the lipid molecules, which causes a reduction of the melting point of the stratum corneum lipids on skin. This reduction in melt point increases lipid fluidity and cell membrane permeability. The high flexibility of vesicular membranes from the added ethanol permits the elastic vesicles to squeeze through the pores, which are much smaller than the ethosome diameters. Ethosomes are platforms for the delivery of large and diverse groups of drugs (e.g., peptides, protein molecules) (Verma and Pathak 2010).

Lyphazomes® are lipid nanoparticles that are formed from a precursor solution that have lipid nanostructures with average mean diameters from 1 to 20 nm. The precursor solution is a proprietary blend of ethanol, lecithin (with a >50% of phosphatidylcholine), and water. Lyphazomes® can be loaded with a variety of passenger molecules, and assemblies of these particles into a hydrophilic solvent result in a vehicle population of a desired size. Single application or multifunction assemblies can be formed and range in size from about 30 to about 200 nm (https://patents.justia.com/patent/8597678).

2 Production Methods

In general, the production of lipid nanoparticles can be performed by both "top-down" and "bottom-up" techniques. The top-down approach applies precise tools that allow an accurate reduction of the size and structure of the material, whereas the bottom-up approaches are based mostly in physicochemical processes that involve the use of materials derived from either self-assembly or self-organization molecular processes (Roos and Livney 2017). The main disadvantage of the top-down approach is the

requirement of high-energy sources for the formation of lipid nanostructures. In addition, during the breakdown process, there is possibility of compromising the stability of the encapsulated molecule (Shanmugam and Banerjee 2011). Bottom-up is more common in self-assembling nanoencapsulation, as it is generally simpler and requires less energy to form colloidally stable nano-sized particles via spontaneous self-assembly of molecules (Roos and Livney 2017). Figure 16.4 shows a schematic diagram of these two approaches to produce lipid nanostructures including some of the most used production methods for each approach.

Nanoemulsions can be produced by either a top-down or a bottom-up approach. Top-down emulsification techniques use high-energy techniques to exert high shear on oil-water-surfactant mixtures or primary emulsions, e.g., using various homogenizers for disrupting oil-water interfaces in order to produce droplet breakdown and size reduction to the desired nanoscale. Otherwise, bottom-up nanoemulsification techniques do not require special equipment and rely on the properties of the surfactant, oil, and water system, utilizing low-energy processes such as simple mixing methods or by changing system conditions such as temperature or pH to induce spontaneous formation of nanodroplets by surfactant self-assembly (Roos and Livney 2017).

For example, cubosome synthesis using a bottom-up technique starts with a molecular solution, rather than a bulk material, allowing cubosomes to form and crystallize from precursors at molecular scale. The main advantage of the bottom-up approach is that it can be easily adopted for production at a large scale (Shanmugam and Banerjee 2011).

There are a variety of conventional techniques that can be used to produce lamellar lipid nanostructures like liposomal formulations. All methods for producing liposomes require lipids to be combined by some means with an aqueous phase producing the self-assembling of lipids leading to the formation of vesicles. Usually, top-down techniques (e.g., extrusion, sonication, high-shear homogenization) are used after the self-assembling process to allow the homogenization

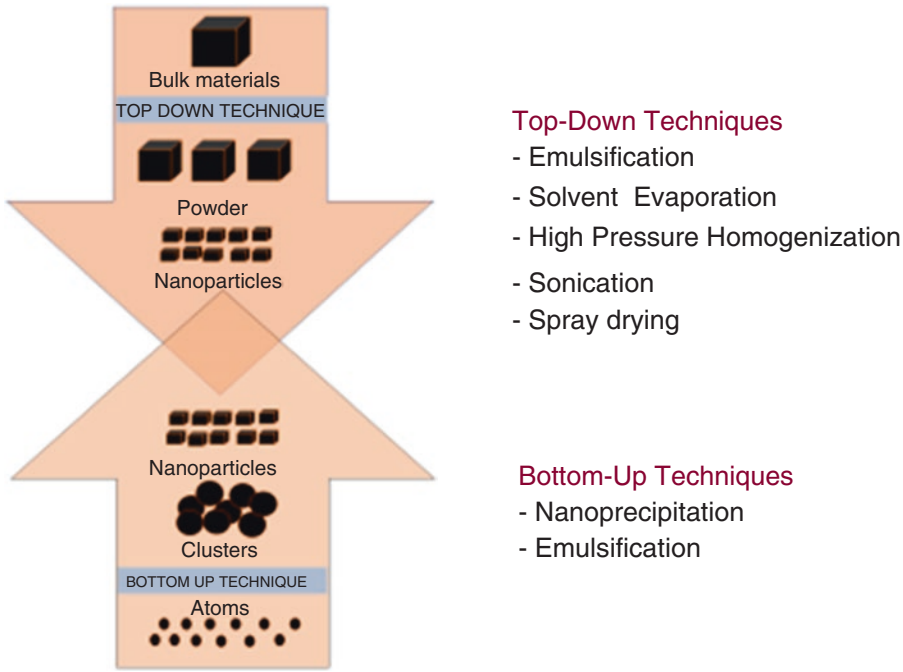

Fig. 16.4 Scheme of top-down and bottom-up techniques used for lipid nanoparticle production. (Adapted with permission from Rai et al. 2019)

and reduction of the particle size. Typical methods for liposome production are:

Bangham method (thin lipid film and hydration): It involves the dissolution of lipids into an organic phase and subsequent removal of the organic solvent by evaporation (time-consuming stage) to form a lipid film. The final step is the dispersion or hydration of the lipid film with aqueous media. Active agents can be added to either the organic or aqueous phase. Liposomes with several microns in size and consequently MLV are produced, limiting their extended industrial use due to low entrapment efficiency especially for water-soluble active agents, difficulty in removing the organic solvent, and small-scale production. Subsequent techniques for size reduction are recommended (Maherani et al. 2011). For example, an additional step of *extrusion* can be used to produce ULV by forcing the aqueous suspension of MLV through polycarbonate filters with defined pore size. The particle size distribution of ULV is a function of the number of passes through the extruder membrane. This approach enables production of very consistent particle sizes.

Detergent depletion method: It is based on the formation of detergent-lipid micelles, followed by the removal of the detergent to form liposomes (time-consuming stage). It is a mild process useful for a wide variety of vesicle types and highly homogeneous liposomes. The disadvantages of this method are: final concentration of liposomes in the solution and entrapment of hydrophobic compounds are low as well as the detergent remains in the formulation (Maherani et al. 2011).

Injection methods: The ethanol and ether injection methods involve the dissolution of the lipids into ether or ethanol, followed by the injection of the lipid solution into an aqueous medium, thus forming liposomes. The extraction of solvents is required but is easier for the ether injection method. LUVs are formed as the injection speed increases. The ether injection method produces a more concentrated liposomal product with higher entrapment efficiencies compared to ethanol injection. On the other hand, the ethanol injection method is rapid, simple, and reproducible for production of a ready-to-use liposome solution. The inkjet method is a variation of the ethanol injection with excellent control on particle size and high potential for scaling up (Maherani et al. 2011).

Reverse phase evaporation method: The reverse phase evaporation method is based on the creation of reversed micelles in the aqueous phase with a central core surrounded by lipids and dispersed in an organic solvent. Reversed micelles are produced by dissolving the lipids in an organic solvent, adding a small volume of aqueous phase, and sonicating the solution to produce inverted micelles. The organic solvent is removed using a rotary evaporator resulting in a viscous gel. When sufficient solvent has been removed, the gel collapses, and an aqueous suspension of vesicles is formed (Yu et al. 2018).

High-pressure homogenization (HPH) method: High shear stress produces high pressures (100–2000 bar), resulting in disruption of particles into the nanometer range. This method is divided into hot homogenization and cold homogenization. The former gives lower particle size because of the decreased viscosity of the phase at a higher temperature but may result in an increased degradation rate of the active material in the liposome core. The latter was developed to overcome the limitations of the hot homogenization, incurred by high temperatures, and involves the solubilization or dispersion of the active material at about 5–10 °C above the phase transition temperature of the liposome (Yu et al. 2018). This technique is especially useful to produce very small liposomes suitable for intravenous applications.

Besides those described above, there are other techniques that have been used for the production of liposomes, such as microfluidic channel method, heating method, dense gas techniques, supercritical fluid methods, and solvent dilution.

3 Relevant Characteristics of Self-Assembling Lipid Nanoparticles/Nanosystems for Industrial Applications

3.1 Manufacturing and Scale-Up

Some SLNNs are very easy to manufacture. For example, most of the bottom-up preparation techniques involve only minimal mixing conditions. Depending on the SLNN system, high shear homogenization or ultrasonication can be required. For Lyphazomes®, the mixing style does not appear to be a critical process parameter for their formation in that any type of stirring can be used, such as a magnetic spin bar, propeller mixing, and hand mixing by spatula or even transfer pipette (https://patents.justia.com/patent/8597678). Process conditions beyond mixing style may be critical, e.g., mixing speed, mixing duration, mixing temperature, and possibly shear rate. Mixing vessel style is another area that may not be noncritical to the success of the system. Unlike other nanoparticle systems which require specialized equipment, SLNN may not require unique equipment, regardless of batch scale. Size is only a factor when considering suitable capacity for the mixing type. As one increases the size of the batch, the size of the mixer is easily increased, e.g., a larger diameter propeller or spin bar.

3.2 Size Control and Customization

Particle size distribution is often the nemesis of most nanoencapsulation systems. SLNNs are capable of producing tightly distributed particle size ranges as defined by very low polydispersity indices, <0.3%. The range for SLNN can be as low as 30 nm and as high as 1000 nm. Furthermore, the preparation technique and composition optimization can allow for customization of particle size and range, as well as the possibility of containing multiple particle distributions within a single system (https://patents.justia.com/patent/8597678).

3.3 Safety

The safety of any system is of paramount importance. The complete system should not contain any toxic compounds and should potentiate the toxicity of any other compound or that of the overall system. Some commercially available nanoparticle systems may contain compounds that pose a safety concern, such as gold nanoparticles (Alkilany and Murphy 2010). Although this concern does not remove these systems from consideration, it is an aspect that requires careful evaluation of the benefit versus the potential for complications from their toxicity. Many SLNN systems contain ingredients considered to be GRAS (generally recognized as safe) for both topical and internal dosage routes. The qualitative composition of these systems uses water, natural lipids, and a hydrophilic solvent (taken from such compounds as ethyl alcohol, glycerin, polyethylene glycol 400, and other similar solvents) (Kullenberg et al. 2012). For example, lecithin is used as lipid source in the Lyphazome® system and has been reviewed and considered safe by the US Food and Drug Administration at levels up to 325 mg per dose for oral dosage forms and up to 1.4% (w/w) for topical dosage forms (FDA Inactive Ingredients Database 2020).

3.4 Multiple Passenger Loading

SLNN technology can encapsulate a variety of compounds, both hydrophilic and lipophilic. That is, SLNNs are capable of encapsulating a hydrophilic compound and a lipophilic compound into a common encapsulation matrix. Furthermore, SLNNs can handle multiple compounds within a given encapsulation matrix. This aspect makes for some interesting possibilities in drug delivery.

3.5 Bioavailability Enhancement

All drug delivery systems seek to improve the bioavailability of the drug substance, whether through enhanced release from vehicle, enhanced

solubility in biological fluids, and/or improved permeability through biological membranes (Beg et al. 2011; Savjan et al. 2012). SLNNs have been demonstrated to provide drug delivery benefits via various routes. Refer to Sect. 4 for additional details of enhancements observed. One example of SLNNs is comprised of an external phospholipid bilayer which mimics the cell walls in the body which facilitates transport across the membrane (Alberts et al. 2002). The ability of SLNN to encapsulate poorly soluble compounds within its lipid bilayer or internal phase and sub-micron-to-nanometer size enables increased solubility in most aqueous systems without compromising particle suspension (Cooper 2000). This combination of all three bioavailability enhancement techniques (small particle size, enhanced solubility of passenger molecule, and enhanced permeability from the phospholipid bilayer) makes SLNN a good candidate for a drug delivery system across a wide variety of pharmaceutical compounds.

3.6 High Loading Efficiency

The encapsulation efficiency of SLNNs depends on the lipophilicity of the molecule. Lipophilic compounds are favored passenger molecules because of their affinity with the lipids used in creating SLNNs. Those compounds which are highly lipophilic will exhibit higher loading efficiencies in SLNNs, ranging upwards of 100% loading. On the other hand, hydrophilic substances will still load into SLNN, but at a lower efficiency compared to lipophilic compounds. The hydrophilic loading is more challenging to predict and mostly depends on the nature of the hydrophilic compound, concentration, and type of preparation process and can be variable depending on the specific compound and any adjunct compounds added to the system. Loading efficiency also will depend on the ratio of passenger molecule to phospholipid. That is, increased loading efficiency can be realized by increasing the amount of phospholipid relative to the amount of the passenger molecule. There is an optimal balance though between cost of additional phospholipid and any increased loading efficiency (Zucker et al. 2009).

3.7 Flavor Modulation

Deepak et al. (Deepak et al. 2012) identified that pharmaceutically active compounds may result in poor patient compliance because of poor taste characteristics, mostly resulting from bitterness. Patient compliance with dosing instructions is a critical component contributing to the success of any given treatment regimen. Deepak et al. (2012) speculated that improving the taste profile of a pharmaceutically active ingredient could help toward ensuring patient compliance and thus increase overall success of the corresponding treatment regimen. Given that liposomes have been recognized as a means of rendering certain components of taste (sweet, sour, salty, and bitter) undetectable (or at least less detectable) to the human tongue (Rowat et al. 2019), SLNNs in general are expected to provide a similar benefit. In many cases, a complete coverage and elimination of the off-taste is not achieved, but a sufficient reduction in perception of off-taste is achieved such that conventional means of taste masking can overcome the residual off-taste (Gala and Chauhan 2014). In either case, the unpleasant sensor experience is mitigated making for a more tolerable treatment option and thus better compliance and success in treatment.

3.8 Optical Clarity

Oftentimes, the formulator considering the use of a nanoparticle delivery system may desire the finished product to be as clear as possible, approaching the quality of filtered water. This task can be reached via the use of nanoparticle technologies, specifically those systems that can produce particles below 100 nm (Shafiqa et al. 2018). In SLNN® systems such as Lyphazomes, size can be dialed down into the range of less than 30 nm for apparent optical clarity. Particles up to about 100 nm retain a reasonable degree of clarity, whereas particles above 100 nm will begin to

exhibit some translucency, depending on total concentration of the SLNN® particles. This aspect becomes most valuable in the beverage industry for infusing water with various lipophilic compounds while retaining the typical clarity of purified water (Jeevanandam et al. 2018).

3.9 Shelf and Product Stability

Yadav et al. (2011) suggested that traditional liposome-like systems were inherently unstable, making them unsuitable for drug delivery systems. However, they acknowledged that certain adjunctive compounds (e.g., pegylation, stealth) could be added to the system to improve the stability of the vesicles. Modified SLNNs are resistant to degradation and alteration resulting from the typical conditions required to assess forced degradation. These include photolysis, hydrolysis, and oxidation (Blessy et al. 2014). Thermal exposure may have an effect on the particle depending on the type and composition. SLNN can provide enhanced stability of otherwise labile passenger molecules. This was seen in the example of CBD encapsulated Lyphazomes®, which were added to water, with a final CBD concentration of 92.6 mg/g. CBD levels were seen to be stable after 3 months at room temperature (25 °C) and 40 °C. Table 16.1 provides details of the particle size and cannabidiol assay results.

It is believed that the encapsulation of the passenger molecule in an inert environment such as the phospholipid bilayer when properly encapsulated can protect the passenger molecule from degradation by environmental insults, such as oxygen and moisture. Although not entirely impermeable, the lipid bilayer prevents typical environmental factors from affecting the content of the liposome. Thermal exposure is an external force that has been shown to have an influence on SLNN® stability. Particle size will change to some extent dependent on the duration and severity of thermal exposure (Kono 2001).

Table 16.1 CBD water stability results

Time point	Temperature	Particle size (nm)	CBD assay (mg/g)
T0	25 °C	195.5	92.4
1 month	25 °C	198.7	91.5
2 months	25 °C	203.5	92.0
3 months	25 °C	187.6	91.3
1 month	40 °C	196.1	90.9
3 months	40 °C	196.8	90.1

3.10 Other Considerations

It should be recognized that although SLNNs present many characteristics beneficial for use in industrial applications, there are some challenges one must consider when using SLNN. For example, the choice of solvent to use must consider the eventual manufacturing site and dosage delivery route. Ethanol is often used in the formation of certain SLNN (Verma and Pathak 2010). Ethanol is flammable and specialized equipment is required by law to prevent fires and explosions when working with large quantities of ethanol (or other flammable liquids). Another solvent often used in certain SLNNs is propylene glycol. Propylene glycol can be used in some oral dosage forms but must be limited (FDA Inactive Ingredients Database 2020). Secondly, SLNNs may not be suitable for every type of desired passenger molecule. Those compounds which are not soluble (or cannot be dissolved) in solvents appropriate for use with SLNNs cannot be successfully encapsulated using SLNNs. For example, active compounds containing fibers, insoluble particulates, or crystal residues would not be suitable to be encapsulated into SLNNs. These, along with other potential disadvantages, must be considered and investigated before determining the possible industrial uses.

4 Industrial Applications

4.1 Pharmaceutical

SLNNs have significant promise for the improvement of drug delivery systems, as they can act as vehicles for hydrophilic and hydrophobic drugs for the treatment of cancer, fungal and bacterial

infections, vaccines, etc. (Alavi et al. 2017). SLNNs like liposomes have shown potential in stabilizing therapeutic compounds, improving the distribution of compounds to the desired site, reducing challenges with cellular and tissue uptake, promoting biocompatibility, and increasing the ability to carry large drug payloads. Since SLNNs are able to entrap both lipophilic and hydrophilic compounds, a wide range of drugs can be encapsulated and optimized, depending on the physicochemical and biophysical properties of the drug (Sercombe et al. 2015).

There are many examples of SLNNs currently being used in drug delivery or undergoing research. For example, niosome vesicles have been shown in vivo to provide sustained release of peptides and proteins through oral administration (Gharbavi et al. 2018). Another example is seen in the cancer treatment medication Doxil, which is an IV chemotherapy medication that utilizes liposomes to reduce the destruction of the drug by the body's immune system, to reduce toxicity of the active ingredient (doxorubicin) to the body, and to enable the medication to remain in the body for an increased period of time (Waterhouse et al. 2001). When compared to the free-form version of the drug (doxorubicin), Doxil provided a greater lifetime cumulative dose of doxorubicin to be administered and allowed for a safer administration at higher doses.

The Lyphazome® Technology is also currently being evaluated in OTC and Rx formulations. For instance, a 2% miconazole formula utilizing Lyphazomes® was evaluated over the course of 4 months on four patients with noticeable toenail fungal conditions. Significant improvement of condition was shown with the use of the product over the treatment period, indicating the potential benefits of Lyphazomes® in such a system.

4.2 Cosmetic

SLNNs have been utilized in cosmetics since the mid-1980s, where they first appeared in a Christian Dior antiaging cream (Ashtiani et al. 2016). Since then, many cosmetic companies have used lipid nanosystems to boost the effects of their products. In particular, liposomes can act as carrier vehicles for botanical agents to encourage their penetration into the skin barrier, which can lead to an enhanced cosmetic benefit. Unloaded liposomes have demonstrated efficacy in enhancing skin benefits, as they interact with skin lipids, proteins, and carbohydrates to encourage skin homeostasis and support the defensive properties of the stratum corneum. The addition of SLNNs to a cosmetic product can improve the overall efficiency of the product, increase stability, provide targeted skin delivery, and increase the economic value of the product.

As mentioned, there are many examples of the SLNN technology currently being utilized or undergoing investigation in cosmetics. For example, ethosomes containing niacinamide were evaluated in vitro using Franz diffusion cells with porcine skin and compared with a non-ethosome niacinamide acting as the control (Wu et al. 2015). It was seen that with the ethosome encapsulated niacinamide, significantly higher skin permeability was observed.

Another example of the use of a particular SLNN, Lyphazome®, was its use in a topical moisturizing lotion. This was a third-party sponsored program performed as part of a thesis supporting a master's degree in pharmacy (Foti 1998). The study compared three moisturizers: an OTC lotion containing water and glycerin (OTC lotion), a lotion containing Lyphazomes® (Lyphazome® lotion), and a lotion containing alpha-hydroxy acids (AHA lotion). Hairless mice were used in this study, and the transepidermal water loss (TEWL) was evaluated. TEWL is a function of the skin lipid barrier, temperature, and external environment (Friberg et al. 1990; Grice and Bettley 1967) and is used to characterize skin barrier function, where low TEWL values are associated with healthy, hydrated skin and high TEWL values are associated with impaired, dry skin. The moisturizers were applied daily to the specimen over a 16-day period. During that time, all lotions showed an increase in water activity for up to 45 min following each application of the product. However, once application of product was discontinued, the Lyphazome® lotion showed a sustained elevation

of skin hydration for an additional 96 h. This demonstrated that the Lyphazome® lotion was more effective at maintaining higher levels of skin hydration than either the OTC or AHA lotion.

4.3 Beverage and Food

The use of nanotechnology is a continuing area of interest for the food and beverage, agricultural, and nutraceutical industries, where it is being used to improve processing and production (Berger 2019). The use of SLNNs in food and beverages has many potential benefits including better encapsulation and more efficient release of active ingredients. Incorporation of nano-molecular agents such as nanoemulsions, liposomes, micelles, and Lyphazomes® into food and beverage systems has resulted in improved properties, including protecting the actives, controlled/enhanced delivery, increased product stability, and masking unpleasant taste (Berger 2019).

According to the 2006 European Nanotechnology Gateway forum, a food is characterized as a "nanofood" when nanotechnology is used during the cultivation, production, processing, or packaging of the food (Tiju and Morrison 2006). For example, in agriculture, nano-capsules have been utilized to enhance the delivery of pesticides, fertilizers, and other relevant materials to agricultural crops. Another example is seen with transfersomes, where they were shown to effectively encapsulate taxifolin (a flavanonol with antioxidant properties, used in nutraceuticals and supplements) with encapsulation efficiencies of 72–75% (Hasibi et al. 2019). Taxifolin, which typically has low bioavailability, was seen to have over 90% release in gastrointestinal conditions when encapsulated with transfersomes. Another example is seen in Frozun® Spirits, an alcoholic frozen dessert product, where Lyphazomes® are employed to help stabilize the freezing of alcohol at levels greater than 6% alcohol by volume for their ice creams and gelatos (Frozun Spirits Infused Desserts and Cocktails 2018). Enhanced delivery of key actives is also a common use of nanotechnology in beverages. To demonstrate this property, a pharmacokinetic study was done on an "energy boost" liquid formula that utilized caffeine as the active ingredient at 1.2% (12 mg/g). The study employed a single dose of 72 mg of caffeine, and a total of four subjects participated. Three formulas were prepared for the study, two using Lyphazome®-encapsulated caffeine at different particle sizes (200 and 50 nm) and one using non-encapsulated caffeine. Blood was collected at pre-dose, 0.25, 0.5, 0.75, 1, 1.5, 2, 4, 6, and 12 hours on the day of treatment. Samples were tested for caffeine concentration. Figure 16.5 provides graphic representation of the caffeine level in the blood samples taken.

The Lyphazome® enhanced drink with particle sizes of 200 nm displayed a slightly more rapid uptake of caffeine with longer retention than the free-form caffeine version. The Lyphazome® enhanced drink with particle sizes of 50 nm showed a slightly slower uptake of caffeine than the drink with particle sizes of 200 nm, although this may be a function of a higher baseline caffeine level. Results suggest that the particle sizes may affect the delivery of an active to the body. From these examples, it is clear that SLNNs can have a beneficial place in the food and beverage industry. Further research is ongoing to discover additional benefits.

4.4 Cannabis

The cannabis plant has been used medicinally for centuries with its therapeutic potential still being investigated. Within the last 20 years, cannabis has entered a modern age of research, as it is being considered for a variety of industries, such as pharmaceutical, cosmetic, food, and beverage. The cannabis plant consists of over 100 phytocannabinoids, which are lipophilic compounds that interact primarily with receptors of the endocannabinoid system. The endocannabinoid receptors participate in many biological processes, such as pain, memory, mood, appetite, stress, sleep, metabolism, immune function, and reproductive function (Laurentiis et al. 2014). The most well-known phytocannabinoids are tetrahy-

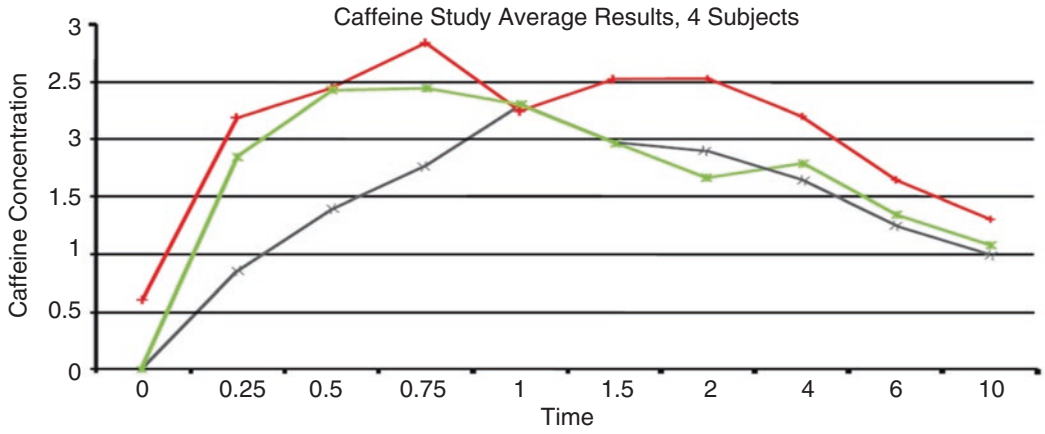

Fig. 16.5 Pharmacokinetic study of encapsulated vs free-form caffeine at 1.2% in an oral drink formulation

drocannabinol (THC) and cannabidiol (CBD), but others are gaining recognition as well, such as cannabigerol (CBG), cannabinol (CBN), and cannabichromene (CBC) (Elsohly et al. 2017).

Efficient and safe delivery of the various cannabinoids to the body has become a popular topic. Historically, smoking or vaping cannabis has been the optimum route of delivery but has potential dangers associated with lung exposure and damage. Therefore, additional routes of administration are being considered. In general, cannabinoids have been found to have very low oral and skin bioavailability and medium sublingual bioavailability (Elsohly et al. 2017; Huestis 2007). A potential improvement of cannabinoid bioavailability is using nanoencapsulation. Using nanoencapsulation technologies to entrap cannabinoids can improve the solubility of the hydrophobic compounds and increase their stability against light and temperature (Puglia and Santonocito 2019).

Nanotechnology in the field of cannabis is a moderately new area of research where extensive work is currently being done to understand the possible advantages. One way nanotechnology is being utilized in this industry is through nanoemulsions, where the droplet size is reduced to sizes between 20 and 600 nm for a number of purposes, such as an increase in solubility and bioavailability (Sajal et al. 2008). Another way it is used is in liposomal encapsulation of the cannabinoid. To demonstrate the use of SLNN technology to encapsulate a cannabinoid, two versions of a 2% (w/w) CBD lotion were prepared: one with Lyphazome®-encapsulated CBD and the other with non-encapsulated CBD. Particle sizes of the Lyphazome®-encapsulated CBD were measured and tested in triplicate. Table 16.2 and Fig. 16.6 show the particle size distribution test results.

Table 16.2 Lyphazome®-encapsulated CBD dynamic light scattering results

Sample name	Diameter (nm)	Polydispersity index (PDI)
Encapsulated CBD	207	0.248
	211	0.375
	194	0.259

The CBD encapsulated with Lyphazomes® showed an average particle size of 204 nm. The polydispersity index (PDI) is a measure of the heterogeneity of the particle sizes with an average of 0.294. A PDI of less than 0.3 indicates a mono-disperse system. Therefore, the values show a mono-disperse array of CBD encapsulated particles.

An ex vivo penetration study was conducted using confocal Raman microscopy to detect the CBD through the layers of cadaver skin samples. The cadaver skin samples were treated topically with the 2% CBD lotion with Lyphazomes® or the 2% CBD lotion without Lyphazomes® and placed in a Franz Cell for 3 hours and 20 hours at 34 °C. After treatment, the skin was assembled

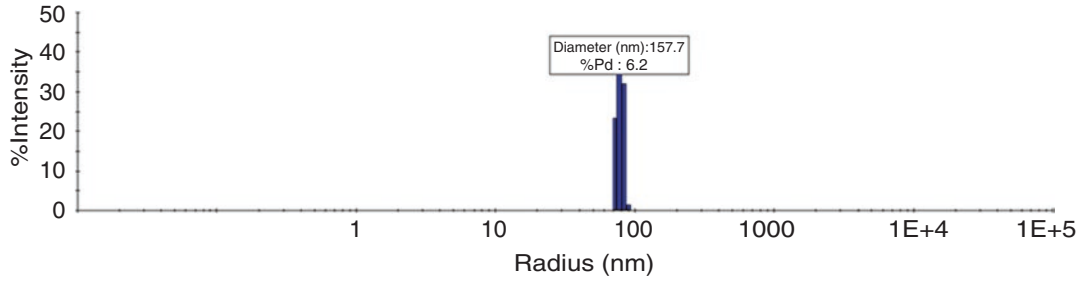

Fig. 16.6 Particle size distribution of the Lyphazome®-encapsulated CBD system

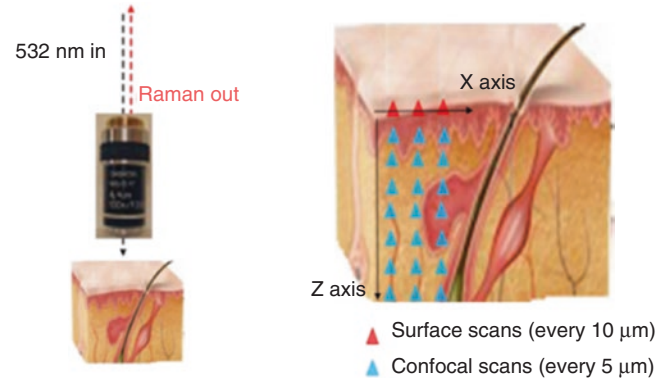

Fig. 16.7 Raman spectroscopy setup

into a proprietary brass cell and kept hydrated during scanning by confocal Raman spectroscopy (WITec system). Typical confocal Raman image size (xz) was 40 × 30 µm (first sets) or 30 × 40 µm (second sets) at 2 µm spatial resolution. The spectroscopic parameters used were spectral range, 172–180 cm^{-1}; laser excitation, 532 nm; laser power, 20 mW; and laser exposure, 20 s. The deposition and penetration of CBD into the skin sample were evaluated by comparing the Raman spectra of the skin treated with the lotion samples and the untreated skin sample. Figure 16.7 shows the Raman measurement system.

The skin treated topically with the Lyphazomes® CBD lotion exhibited a deeper penetration of CBD after 3-hour treatment. CBD can be detected inside the epidermis up to ~15 µm, whereas for the skin treated with the CBD lotion without Lyphazomes®, the active barely penetrated into the skin. After a 20-hour skin exposure to the Lyphazome® CBD lotion, the active penetrated deeper inside the epidermis up to ~25 µm. For the skin exposed to the 2% CBD lotion without Lyphazomes®, the CBD remained at the surface. The results achieved indicate that topical formulations containing Lyphazome®-encapsulated CBD penetrate deeper faster and to greater extent and therefore are expected to have improved benefits. Figure 16.8 shows the Raman Microscopy test results.

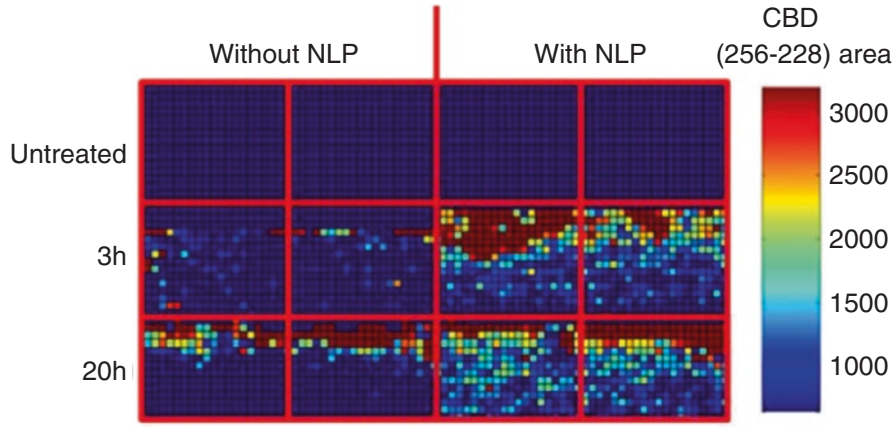

Fig. 16.8 Raman images of the skin cross-section showing the 245 cm^{-1} peak area (CBD concentration) for each skin sample at 3 h and 20 h

References

Alavi M, et al. Application of various types of liposomes in drug delivery systems. Adv Pharm Bull. 2017;7(1):3–9. https://doi.org/10.15171/apb.2017.002.

Alberts B, Johnson A, Lewis J, et al. Molecular biology of the cell. 4th ed. New York: Garland Science; 2002. The lipid bilayer. Available from: https://www.ncbi.nlm.nih.gov/books/NBK26871/

Alkilany AM, Murphy CJ. Toxicity and cellular uptake of gold nanoparticles: what we have learned so far? J Nanoparticle Res. 2010;12(7):2313–2333. Retrieved on 17 February 2020 from https://www.ncbi.nlm.nih.gov/pmc/articles/PMC2988217/

Ashtiani H, Reza A, et al. Liposomes in cosmetics. J Skin Stem Cell. 2016;3(3) https://doi.org/10.5812/jssc.65815.

Bangham AD, Horne RW. Negative staining of phospholipids and their structural modification by surface-active agents as observed in the electron microscope. J Mol Biol. 1964;8:660–8.

Barauskas J, Johnsson M, Tiberg F. Self-assembled lipid superstructures: beyond vesicles and liposomes. Nano Lett. 2005;5(8):1615–9.

Beg S, Swain S, Rizwan M, Irfanuddin M, Malini DS. Bioavailability enhancement strategies: basics, formulation approaches and regulatory considerations. Curr Drug Delivery. 2011;8 6:691–702. https://doi.org/10.2174/156720111797635504. Retrieved on 13 February 2020 from https://sci-hub.tw/10.2174/156720111797635504

Berger M. Nanotechnology in food, Nanowerk, 24 Apr. 2019; (2019). www.nanowerk.com/nanotechnology-in-food.php

Cooper GM. The cell: a molecular approach. 2nd ed. Sunderland: Sinauer Associates; 2000. Cell membranes. Available from: https://www.ncbi.nlm.nih.gov/books/NBK9928/

Deepak S, Singh M, Kumar D, Singh G, Rarthore MS. Taste masking technologies: a novel approach for the improvement of organoleptic property of pharmaceutically active substance. Int Res J Pharm. 2012;3(4):108–116. Retrieved on 13 February 2020 from https://www.researchgate.net/publication/236152461_Taste_Masking_Technologies_A_Novel_Approach_for_the_improvement_of_Organoleptic_Property_of_Pharmaceutically_Active_Substance

Elsohly MA, et al. Phytochemistry of Cannabis sativa L. Prog Chem Org Nat Prod. 2017;103:1–36. https://doi.org/10.1007/978-3-319-45541-9_1.

FDA Inactive Ingredients Database. 2020. Retrieved on 11 February 2020 from https://www.accessdata.fda.gov/scripts/cder/iig/index.cfm?event=BasicSearch.page

Foti D. Investigation of the effects of moisturizers on the biomechanical skin properties of hydration and elasticity for the hairless mouse. Master's thesis – University of South Florida; 1998.

Friberg SE, et al. Water permeation of reaggregated stratum corneum with model lipids. J Investig Dermatol. 1990;94(3):377–80. https://doi.org/10.1111/1523-1747.ep12874497.

Frozun Spirits Infused Desserts & Cocktails. Frozun Spirits Infusion; 2018. 28 Dec. 2018, www.frozun.com/

Gala U, Chauhan H. Taste masking techniques in the pharmaceutical industry. Am Pharm Rev. 2014. Retrieved on 13 February 2020 from https://www.americanpharmaceuticalreview.com/Featured-Articles/163483-Taste-Masking-Techniques-in-the-Pharmaceutical-Industry/

Gharbavi M, et al. Niosome: a promising nanocarrier for natural drug delivery through blood-brain barrier. Adv Pharmacol Sci. 2018:1–15. https://doi.org/10.1155/2018/6847971.

Grice K, Bettley FR. The effect of skin temperature and vascular change on the rate of transepidermal

water loss. Br J Dermatol, U.S. National Library of Medicine, Nov. 1967; 1967. www.ncbi.nlm.nih.gov/pubmed/6072763

Hasibi F, et al. Formulation and characterization of taxifolin-loaded lipid nanovesicles (liposomes, niosomes, and transfersomes) for beverage fortification. Eur J Lipid Sci Technol. 2019;122(2):1900105. https://doi.org/10.1002/ejlt.201900105.

Huestis MA. Human cannabinoid pharmacokinetics. Chem Biodivers Wiley Online Library;(2007. onlinelibrary.wiley.com/doi/https://doi.org/10.1002/cbdv.200790152/references

Jeevanandam J, Barhoum A, ChanYS, Dufresne A, Danquah MK. Review on nanoparticles and nanostructured materials: history, sources, toxicity and regulations. Beilstein J Nanotechnol. 2018;9:1050–1074. Retrieved on 13 February 2020 from https://www.ncbi.nlm.nih.gov/pmc/articles/PMC5905289/

Kono K. Thermosensitive polymer-modified liposomes. Adv Drug Deliv Rev. 2001;53(3):307–319. https://doi.org/10.1016/S0169-409X(01)00204-6. Retrieved on 13 February 2020 from https://www.sciencedirect.com/science/article/abs/pii/S0169409X01002046

Kulkarni CV. Lipid self-assemblies and nanostructured emulsions for cosmetic formulations. Cosmetics. 2016;3:37. https://doi.org/10.3390/cosmetics3040037.

Kullenberg D, Taylor LA, Schneider M, Massing U. Health effects of dietary phospholipids. Lipids Health Dis. 2012;11(3):1–34. Retrieved on 11 February 2020 from https://www.ncbi.nlm.nih.gov/pmc/articles/PMC3316137/

Laurentiis A, et al. Role of the endocannabinoid system in the neuroendocrine responses to inflammation. Curr Pharm Des. 2014;20(29):4697–706. https://doi.org/10.2174/13816128206614013021295 7.

Luzzati V, Husson F. The structure of the liquid-crystalline phases of lipid-water systems. J Cell Biol. 1962;12:207–19.

Maherani B, Arab-Tehrany E, Mozafari MR, Gaiani C, Linder M. Liposomes: a review of manufacturing techniques and targeting strategies. Curr Nanosci. 2011;7:436–52.

Pawar AY, Jadhav KR, Chaudhari LH. Transfersome: a novel technique which improves transdermal permeability. Asian J Pharm. 2016;10(4):S425.

Puglia C, Santonocito D. Cosmeceuticals: nanotechnology-based strategies for the delivery of phytocompounds. Curr Pharm Des. 2019;25(21):2314–22. https://doi.org/10.2174/1381612825666190709211101.

Rai R, Alwani S, Badea I. Polymeric nanoparticles in gene therapy: new avenues of design and optimization for delivery applications. Polymers. 2019;11:745. https://doi.org/10.3390/polym11040745.

Roos YH, Livney YD. Chapter 5: Nanoencapsulation technologies. In: Engineering foods for bioactives stability and delivery. New York: Springer; 2017. p. 143–69.

Rowat P, et al. Nanoemulsion: the hottest new trend in the Cannabis beverages industry; 2019. Greencamp, greencamp.com/nanoemulsion-the-hottest-new-trend-in-the-cannabis-beverages-industry/

Sajal JK, Uday SR, Surrendra V. Taste masking in pharmaceuticals: an update. J Pharm Res. 2008;1(2):126–30. Retrieved 20 February 2020 from https://www.researchgate.net/publication/38109421_Taste_masking_in_pharmaceuticals_An_update

Savjan KT, Gajjar AK, Savjani JK. Drug solubility: importance and enhancement techniques. Int Scholar Res Notices Pharma. 2012;2012:1–10. https://doi.org/10.5402/2012/195727. Retrieved on 13 February 2020 from https://www.hindawi.com/journals/isrn/2012/195727/

Seleci DA, Seleci M, Walter J-G, Stahl F, Scheper T. Niosomes as nanoparticular drug carriers: fundamentals and recent applications. J Nanomater. 2016;2016:Article ID 7372306, 13 pages.

Sercombe L, et al. Advances and challenges of liposome assisted drug delivery. Front Pharmacol. 2015;6:286. https://doi.org/10.3389/fphar.2015.00286.

Shafiqa AR, Aziz AA, Mehrdel B. Nanoparticle optical properties: size dependence of a single gold spherical nanoparticle. J Phys Conf Ser. 2018;1083:1–6. https://doi.org/10.1088/1742-6596/1083/1/012040. Retrieved on 13 February 2020 from https://iopscience.iop.org/article/10.1088/1742-6596/1083/1/012040/pdf

Shanmugam T, Banerjee R. Nanostructured self assembled lipid materials for drug delivery and tissue engineering. Ther Deliv. 2011;2(11):1485–516.

Shukla S, Haldorai Y, Hwang SK, Bajpai VK, Huh YS, Han Y-K. Current demands for food-approved liposome nanoparticles in food and safety sector. Front Microbiol. 2017;8:Article 239805. https://doi.org/10.3389/fmicb.2017.02398.

Tan A, Hong L, Du JD, Boyd BJ. Self-assembled nanostructured lipid systems: is there a link between structure and cytotoxicity? Adv Sci. 2018;6(3):1801223.

Tiju J, Morrison M. Nanotechnology applications in food and agriculture. Institute of Nanotechnology; 2006. p. 2–14.

US Patent 8,597,678. Nanolipidic particles. Issued 22 December 2006. Retrieved on 17 February 2020 from https://patents.justia.com/patent/8597678

Verma, Pathak K. Therapeutic and cosmeceutical potential of ethosomes: an overview. J Adv Pharm Technol Res. 2010;1(3):274–82.

Waterhouse DN, et al. A comparison of liposomal formulations of doxorubicin with drug administered in free form. Drug Saf. 2001;24(12):903–20. https://doi.org/10.2165/00002018-200124120-00004.

Wu W, et al. Oral delivery of liposomes. Ther Deliv. 2015;6(11):1239–41. https://doi.org/10.4155/tde.15.69.

Yadav AV, Murthy MS, Shete AS, Sakhare S. Stability aspects of liposomes. Indian J Pharm Educ Res. 2011;45(4):402–413. Retrieved on 13 February

2020 from http://www.ijper.org/sites/default/files/IJPER_45_4_13.pdf

Yu H, Park J-Y, Kwon C W, Hong S-C, Park K-M, Chang P-S. An overview of nanotechnology in food science: preparative methods, practical applications, and safety. J Chem. 2018; 2018:Article ID 5427978, 10 pages https://doi.org/10.1155/2018/5427978.

Zucker D, Marcus D, Barenholz Y, Goldblum A. Liposome drugs' loading efficiency: a working model based on loading conditions and drug's physicochemical properties. J Control Release. 2009;139(1):73–80. https://doi.org/10.1016/j.jconrel.2009.05.036. Retrieved on 13 February 2020 from sci-hub.tw/10.1016/j.jconrel.2009.05.036

Nanoemulsions: An Emerging Technology in Drug Delivery

17

Sharmeen Rafique, Nandita G. Das, and Sudip K. Das

Abstract

Nanoemulsions are a class of two-phase liquid systems with an internal phase droplet size of less than 200 nm. Although two-phase emulsion systems have been known for decades, the concept of nanoemulsions is fairly recent. Nanoemulsion stability is far more reliable than traditional two-phase "macro"-emulsion systems, which has led to nanoemulsions becoming an attractive option for the delivery of diverse categories of lipophilic small molecule drugs and bioactive agents. This chapter presents an overview of the theories underlying the formulation of emulsions for maximum stability and potential for scale-up. Both low and high energy dispersive techniques have been discussed with suggestions of suitable equipment. Various techniques for formulation have been discussed with specific attention to the nature of the drug and suitability of the excipients. Correlations have been established between stability of nanoemulsions and the nature and concentration of the surfactant, cosurfactant, oil phase, and temperature. A brief section has been devoted to the in vitro characterization of nanoemulsions with reference to instrumentation and techniques used in the pharmaceutical industry. The last part of the chapter is devoted to the application of nanoemulsions in anticancer drug delivery, with examples on how these novel delivery systems can enhance the efficacy of anticancer drugs while significantly reducing the toxic effects of the chemotherapeutic agents.

Keywords

Nanoemulsion · Surfactants · Formulation factors · Low energy manufacture · High energy manufacture · In vitro evaluation · Anticancer drug delivery

1 Introduction

An emulsion is defined as a two-phase system of two or more immiscible liquids that are thermodynamically and/or mechanically stabilized by an emulsifier. Nanoemulsions could be used for delivery of both hydrophobic and hydrophilic drugs, and the internal droplet size range is limited to 20–200 nm (Solans and Solé 2012). The term "nanoemulsion" was introduced by

S. Rafique
Department of Pharmaceutical Sciences, Butler University, Indianapolis, IN, USA

Leminos Laboratories, Mumbai, India

N. G. Das · S. K. Das (✉)
Department of Pharmaceutical Sciences, Butler University, Indianapolis, IN, USA
e-mail: sdas@butler.edu

J. K. Patel, Y. V. Pathak (eds.), *Emerging Technologies for Nanoparticle Manufacturing*,
https://doi.org/10.1007/978-3-030-50703-9_17

Nakajima in 1993 (Nakajima et al. 1993). Nanoemulsions follow the same theories as the conventional emulsions and are often referred to as "submicron emulsions" or "micellar phases" (Russel et al. 1991). Similar to emulsions, nanoemulsions are composed of at least three components, i.e., oil phase, water phase, and surfactant and/or cosurfactant. Nanoemulsions in which the water phase forms the continuous phase are called O/W emulsions, while emulsions in which the oil phase forms the continuous phase and water is the dispersed phase are called W/O emulsions. Most of the nanoemulsions reported in literature for therapeutic drug delivery are based on O/W systems. In recent years, double emulsions or multiple emulsions have been developed in which one type of emulsion is dispersed into another continuous phase such as O/W/O and W/O/W. In general, nanoemulsions are relatively stable (devoid of creaming or cracking) compared to the conventional emulsions and can be formulated using either high shear (mechanical) or by using surfactants (thermodynamic, low shear) or both, in combination.

Recently, there has been extensive research related to injectable emulsions. Intralipid® was the very first intravenous emulsion in the market. It is basically an O/W emulsion containing 10% or 20% or 30% soybean oil which is stabilized using 1.2% of egg phospholipids and 2.25% glycerol, which also acts as an osmotic agent. These formulations allow the infusion of large amounts of energy in relatively less volume of fluid via the peripheral veins. Propofol is a widely used intravenous anesthetic, which is formulated and marketed as a submicron emulsion.

The biological fate of intravenously administered nanoemulsions is dependent on their uptake by target and non-target tissues and the catabolic pathways of the emulsions (Nishikawa et al. 1998). Following IV administration, the oil droplets in the O/W nanoemulsion get captured by the macrophages in reticuloendothelial system (RES) (Becher 1983). It is possible to develop O/W nanoemulsions which can escape the RES and hence have longer circulation time in the blood. This can be achieved by coating with a hydrophilic polymer, namely, poloxamer 338. Pegylated polyethylene (PEG-PE), which is a PEG derivative, also decreases RES uptake in emulsions (Benita 1998a). The emulsion droplets may also bind to apolipoproteins, due to which they can undergo rapid elimination (lipolysis) which is similar to the degradation pathways of lipoproteins. It was observed that an emulsion containing egg yolk phosphatidylcholine (EYPC) was eliminated rapidly as compared to distearoyl phosphatidylcholine (DSPC) emulsions (Clark and Derksen 1987). Another example is an emulsion containing 1-palmitoyl-2-oleoylphosphatidylcholine (POPC), which shows three times higher attainment of apolipoprotein Cs as compared to the one emulsified with dipalmitoylphosphatidylcholine (DPPC) (Redgrave et al. 1992). Hence, it is essential for the emulsions to remain free of apolipoprotein in order to escape their metabolic pathways. Table 17.1 shows the differences between conventional emulsions or microemulsion and nanoemulsions in terms of the physicochemical and thermodynamic principles.

2 Theories of Nanoemulsion Formation

The concepts and theories of nanoemulsion formation are very similar to that of two-phase conventional emulsions because the general physicochemical properties do not change much except for the size. Figure 17.1 depicts a diagram of W/O or O/W nanoemulsion and orientation of the surfactant at the interface (Singh et al. 2017). Interfacial tension is the basic property of an interface and arises due to the attractive forces between the molecules of two different fluids. The imbalanced forces at the interface cause the two immiscible liquids to separate. The interface which occurs between two liquids gets deformed into a liquid film which gets converted into large droplets that further break down into small droplets. This breakdown of droplets is opposed by Laplace pressure (Garti and Aserin 1996). Hence, surfactants act as stabilizers by reducing this gra-

Table 17.1 Comparison of conventional emulsions and nanoemulsions

Characteristics	Conventional emulsions/ microemulsion	Nanoemulsions
Dispersed droplet size	A few μm to a few mm	10–100 nm
Appearance	Milky	Translucent to transparent
Nature of the emulsion	O/W or W/O	O/W or W/O
Stability	Thermodynamically unstable	Thermodynamically semi-stable
Time-dependent kinetics	Rate of increase in droplet size is fast	Rate of increase in droplet size is slow
Mode of separation of phases (flocculation)	Dependent on the order of mixing of ingredients	Independent of the order of mixing of ingredients
Concentration of surfactant	1–20% (Bagwe et al. 2001)	> 10%, up to 50%, without any shear stress 2.5% with high shear stress (Pinnamaneni et al. 2003)
Cosurfactant used	No (Bagwe et al. 2001)	Yes
Energy	Require energy to formulate	Can be formulated without any external energy and high concentration of surfactants

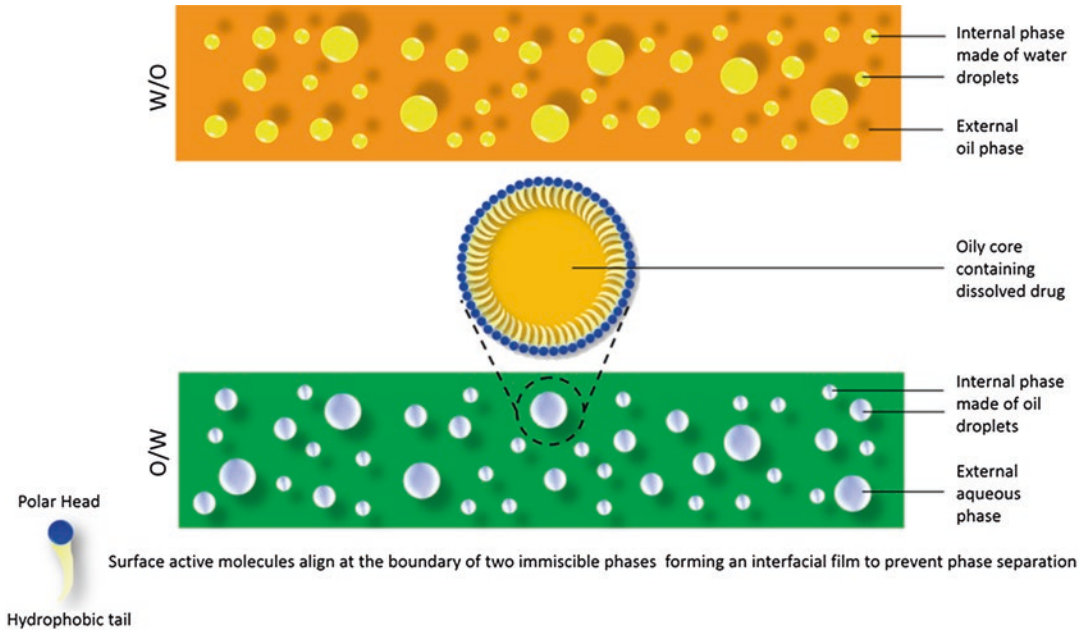

Fig. 17.1 Schematic diagram of W/O and O/W nanoemulsions with presence of surfactant at the interface. (Reproduced with permission)

dient pressure. They adsorb on the surface of the droplets altering their properties and hence reducing the interfacial tension and the Laplace pressure. The surfactants also form a film or the continuous phase between the droplets. Hence, the successful formation of an emulsion depends on maintaining the emulsion in a stable state by opposing the interfacial tension.

3 Formulation of Nanoemulsions

There are various techniques used for the formation of emulsions. In condensation method, the vapor of the dispersed phase is injected below the surface of the other liquid. These vapors become supersaturated and undergo condensation to form very small particles (Chidambaran and Burgess 2005). Dispersion method involves the applica-

tion of force to disrupt the film at the interface and form very small droplets. In the past, grinding mills were used to reduce the particle size with the help of a dispersion medium. These grinding mills offered several drawbacks such as increased risk of contamination, long periods of time required in attaining the desired particle size, and difficulty in cleaning. Also, it is difficult to scale up the process since the variables involved such as mill size, media volume, and processing time do not have any linear relationship.

Nanoemulsions consist of three main components: oil phase, water phase, and surfactant and/or cosurfactant. Surfactants are amphiphilic molecules containing both polar and nonpolar regions. They contain both a hydrophilic and a lipophilic portion, and they are categorized on this basis as to their hydrophile-lipophile balance (HLB) value. HLB concept was introduced by Griffin in the 1940s (Griffin 1954). The HLB range is usually between 1 and 20 (Salager 2000). The high HLB numbers are designated to surfactants with high lipophilic characteristics. In addition to surfactants, HLB values are also assigned to oils. For the successful formation of an emulsion, the HLB of the surfactant chosen should be similar to the HLB of the oil. Surfactants prevent flocculation and coalescence by contributing to the repulsive and London dispersion forces. It is not an easy task to select a surfactant for a particular formulation. Surfactants with low HLB values produce W/O emulsions and vice versa. According to Bancroft's rule, the continuous phase will be the one in which the surfactant will be soluble. Davies demonstrated that the greater the energy barrier to coalescence, the higher will be its HLB value (Garti and Aserin 1996). They reduce the gradient pressure by adsorbing on the O/W interface and also altering their properties. Surfactants place themselves at the interface, where the hydrophilic head remains in solution (water) and the hydrophobic head parks itself near the oil phase. The hydrophobic head is usually a charged or neutral polymeric chain, and the tail is a single or double hydrocarbon chain with or without aromatic groups. Depending on whether the surfactants contain a positive or negative charge, they are termed cationic and anionic, respectively. The most widely used surfactant in the industry is nonionic in nature. These differ from the ionic surfactants by the absence of a charge. Nonionic surfactants are known to be less irritant than the cationic or anionic surfactants and are also compatible with other surfactants. Another advantage of nonionic surfactants is that they are capable of forming nanoemulsions even without a cosurfactant (Bagwe et al. 2001). Above a certain surfactant concentration, i.e., the critical micelle concentration (CMC), colloidal aggregates (micelles) are formed. The hydrophobic core of the micelle can accommodate organic substances within itself. This increase in solubility of a substance due to the formation of micelles is called "solubilization." This solubilized substance may partition itself between the continuous phase, the interior of the micelle, and the interfacial surface. Therefore, the interface may consist of not only the surfactant by itself but also other substances on the interface, called cosurfactants. It is well-known that the inner core of the micelle solubilizes the nonpolar molecules. However, solubilization is higher in nanoemulsions as compared to micelles (Benita 1998b). One molecule of surfactant is capable of dissolving10–30 molecules of oil in O/W emulsions and 10–300 water molecules in case of W/O emulsions (Garti and Aserin 1996).

3.1 Formulation of Nanoemulsion by Low-Energy Method

Although the most common method for formulation of nanoemulsions involves the use of high shear stress, in combination with some surface-active agents, low-energy process is gaining popularity because of the better intestinal permeability of poorly soluble drugs(Buyukozturk et al. 2010) by delivering a concentrated emulsion in a compact capsule. Self-emulsifying drug delivery systems are isotropic mixes of oils, surfactants, and solvents which form emulsions on mixing with water (Gursoy and Benita 2004). These mainly differ from regular emulsions containing large amounts of surfactants and requir-

ing little to no energy during the emulsion formation process. Therefore, it is possible to deliver the mixture of anhydrous drug in a mixture of oil and surfactant which forms a spontaneous emulsion when it comes in contact with the aqueous medium in gastrointestinal tract (GI) (Rani et al. 2019). It is important that the drug dissolves in the aqueous environment of the gastrointestinal tract and at the same time it should be sufficiently lipophilic so that it can partition across the lipid membrane bilayer. The oils present in the emulsions have been advantageously used as vehicles for lipophilic drugs. Oils also cause an increase in the amount of lipophilic drug transported by the lymphatic system which further increases the bioavailability via the GI tract (Gershanik and Benita 2000). Improved drug absorption by self-nano/micro-emulsifying drug delivery systems has been reported in a number of studies. Cyclosporin oral bioavailability was reported to be increased severalfold with low inter- and intra-subject variability when given in submicron emulsion vs conventional emulsion formulation (Kovarik et al. 1994). When ontazolast was administered as self-micro emulsifying formulation, it showed improved oral bioavailability compared to a suspension administration (Hauss et al. 1998). A novel formulation of self-micro emulsifying formulation with hydroxypropyl methylcellulose (HPMC) was developed that showed fivefold greater AUC values of paclitaxel (Gao et al. 2003).

3.2 Formulation of Nanoemulsion by High Energy Methods

High energy emulsification methods involve high-shear and/or high-pressure homogenization and ultrasonication. The main goal is to reduce the droplet size of the internal phase by collision, compression, or cavitation. The major issue in the processing of nanoemulsion using the high shear process is generation of heat, resulting in high temperature of the mixture. A number of drugs, including macromolecules, would be unstable at high shear and high temperature. Two different types of equipment can be used for the preparation of nanoemulsions using high energy methods.

3.2.1 High Shear Rotor-Stator Mixers

Rotor-stator mixers consist of a fast-spinning inner rotor with a stationary outer sheath (stator) to homogenize samples through mechanical tearing, shear fluid forces, and/or cavitation (the rapid formation and collapse of bubbles). Often, the outer sheath is perforated such as in Silverson L5MA (Silverson Machines, MA) that works in a few stages that draws the mixture of the liquid into the rotor/stator assembly, produces shearing action between the rotor blade and the inner walls of the stator, and forces the mixture out through the perforated stator toward the side of the vessels while the new mixture is pulled into the head. The advantages of these types of mixers are (1) efficient and precise shear action, (2) robust equipment, and (3) possibility of extrapolating the formulation variables to a pilot batch. On the other hand, due to the inherent high shear stress, the temperature of the formulation increases unless the sample is chilled externally. Also, it could be a challenge to process very small sample volume.

3.2.2 High Pressure Microfluidizer

This method involves impingement of mixture of oil and water phase from two microchannels that collide with each other at a chamber at a very high pressure (about 30,000 psi). The liquid-liquid interaction occurs vigorously in the narrow microchannels (Chidambaran and Burgess 2005). The heterogeneous mixture of phases is passed through the interaction chamber repeatedly to produce the desired dispersed droplet size. The droplet size decreases as the pressure of homogenization is increased or by increasing the number of passages. The major advantage of this process is the production of droplet size less than 100 nm with a narrow distribution of size range (Maali and Mosavian 2013). One such instrument, LM10 Microfluidizer (Microfluidics, MA), has been referred in many publications (Pinnamaneni et al. 2003). Microfluidization offers several advantages over homogenization such as reduced particle size, low cost, increased

output, use of broad range of pressure up to 40,000 psi, reduced contamination, easy to clean, and easy to scale up.

4 Factors Affecting Formulation of Nanoemulsions

4.1 Surfactant

The choice of surfactant for the particular oil being used is a major influence in emulsion formulation. There are three crucial factors (Bagwe et al. 2001) for the successful production of nanoemulsion:

(i) The interfacial tension at the O/W interface should be very low.
(ii) The concentration of the surfactant should be 10–40% in order to cover the new surface formed by the oil dispersed in water within the nanoemulsion.
(iii) The interfacial film should possess low surface viscosity and low fluidity so that the spontaneous formation of nanoemulsions can occur. Also, the surfactant should have sufficient lipophilicity to provide the correct curve at the interface of the nanoemulsion (Ghosh and Murthy 2006).

4.2 Cosurfactant

Another major factor influencing the stability of nanoemulsions is the achievement of very low interfacial tension. Since nanoemulsions form a very large surface area due to the high number of droplets at the oil-water interface, their stability can be accomplished only if the positive interfacial energy is compensated by the negative free energy of mixing. Cosurfactants help in reducing the interfacial tension to this low level (Ghosh and Murthy 2006). A study carried out to determine the effect of cosurfactant Pluronic L61 on the cytotoxicity of doxorubicin showed a 290- and 700-fold increase in the sensitivity of CHRC5 and MCF-7/ADR cell lines, respectively (Venne et al. 1996). Another study tested the effects of Pluronic L61 and Pluronic F127 on the anticancer activity of doxorubicin (SP1049C). This study demonstrated that SP1049C has higher activity than doxorubicin due to increased drug uptake and inhibition of the drug efflux proteins (Alakhov et al. 1999). They also fluidize the interfacial film by placing themselves between the surfactant molecules. It has been proposed that if the surfactant is soluble in the oil phase, it will rapidly go in the oil phase and will not be available in the water phase. Cosurfactants of short alcohol chain lengths will readily diffuse in and be available at the oil-water interface. The length of the alcohol cosurfactant is also a factor influencing the curvature. It has been reported that long-chain alcohols swell the oil group region more than the short-chain alcohols (Ghosh and Murthy 2006). However, alcohols are not being used in the industry anymore due to toxicity issues. They have been replaced by PEG derivatives, poloxamers, polyethylene glycol, polyol esters, and various other surfactants.

4.3 Oil Phase

The nature of the oil component has an influence on the droplet curvature by penetrating and causing the tail group region of the surfactant to swell. The short-chain oils are known to penetrate better than the long-chain oils. They cause an increase in the swelling which increases the negative curvature and further reduces the HLB. Triglycerides like Labrafac™, Labrafil™, and Lauroglycol™ (Gattefosse, NJ) are some of the oils being used. The particle size of the medium-chain triglyceride emulsions was found to be less than those of Intralipid®. In addition, oxidative stability of the oil should be considered in formulation of nanoemulsion.

4.4 Surfactant-Cosurfactant Ratio

The difference in packing of the surfactant and cosurfactant at the oil-water interface is a major influence on the properties of microemulsions. Haskell et al. compared the particle size from

samples of Intralipid® with medium-chain triglyceride containing O/W emulsions. They used increasing concentrations (0%, 1.25%, 2.5%, 5%) of cosurfactant in the medium-chain triglyceride emulsions. The particle size of the emulsions was found to be inversely proportional to the concentrations of the cosurfactant (Haskell et al. 1998). A study showed how the microemulsion area changed on altering the ratios of Tween 20 and Cremophor EL as surfactants (Li et al. 2005).

4.5 Temperature

Temperature is another important factor affecting the characteristics of nanoemulsions. Nonionic surfactants increase the sensitivity of the nanoemulsions to temperature. O/W emulsions could invert to W/O emulsions at high temperatures, but at intermediate temperatures, the O/W emulsions form bi-continuous nanoemulsions. Phase inversion is referred to as a sudden event in which the internal phase of the emulsion forms the external phase, i.e., O/W emulsion inverts into W/O emulsion. This occurs when the emulsifier does not have the appropriate HLB which causes it to migrate from the interface to the continuous phase. Hence, phase inversion temperature is the temperature at which a surfactant switches its affinity from aqueous phase to oil phase, causing a change in the emulsion type (Salager 2000). Shinoda et al. have shown that W/O emulsions containing nonionic surfactants become less soluble in water as the temperature increases and they leave the interface which causes the emulsions to invert (Garti and Aserin 1996).

5 In Vitro Characterization of Nanoemulsions

5.1 Particle Size

This is an extremely important parameter for evaluation of nanoemulsion stability. Gao et al. studied the effect of each component of the emulsion on its particle size. They concluded that a mix of 10:5:4 ratio of Cremophor EL™, Transcutol™, and Captex 355™ was ideal to obtain a stable microemulsion with a small droplet size (Gao et al. 1998). A narrow particle size distribution is an indicator of a stable emulsion. Generally, a size range of 20–200 nm is ideal, and particle sizes greater than 1 μm can be of concern clinically. If the size exceeds 5 μm, the formulation is considered clinically undesirable since it carries the risk of causing pulmonary embolism. USP <729> test requires two analytical techniques: dynamic light scattering (DLS), or laser diffraction, to measure the mean and standard deviation of the distribution and light obscuration to measure the large tails >5 μm. The particle size distribution of emulsion formulations can be determined by various methods such as photon correlation spectroscopy (PCS/DLS), quasi-elastic light scattering, and intensity fluctuation spectroscopy. The PCS method provides intensity average equivalent diameter which is then converted to volume average diameter.

Transmission electron microscopy and freeze-fracture electron microscopy (FFEM) are used to study the microstructure of the nanoemulsions. In this technique, the nanoemulsion is frozen rapidly to avoid crystallization or phase separation (Bolzinger-Thevenin et al. 1999). This is achieved by plunging the sample in liquid cryogen by spray freezing.

Conductivity and viscosity measurements: Conductivity measurements indicate the nature of the emulsions, i.e., W/O or O/W type, and it also proves the presence of phase inversion phenomenon (Mehta and Bala 1999). Various sophisticated techniques such as small-angle X-ray scattering (SAXS), small-angle neutron scattering (SANS), and dynamic light scattering (DLS) are used to characterize the emulsion structure. In addition, the desired viscosity could maintain the emulsion at the right level of flocculated state.

Nuclear magnetic resonance (NMR) techniques are useful in instituting the phase diagrams. In this technique, a two- or three-phase character can also be detected with a single-phase domain (Shinoda et al. 1991).

Surface charge (zeta potential): A stable dispersion of the droplets of the internal phase requires separation of the droplets to prevent

aggregation. Substantial positive or negative surface charge assures uniform dispersion of the internal phase of the nanoemulsion. The process of Ostwald ripening can also be due to low zeta potential of the nanoemulsion, which could lead to destabilization (Solans and Solé 2012). The surfactant type and medium pH could affect the zeta potential of nanoemulsions.

5.2 Physical Stability Studies for Nanoemulsions

Creaming, flocculation, and coalescence are events that lead to emulsion instability. The movement of droplets and their interference could cause them to deform in the disperse system. Viscosity of the external phase has been found to be directly proportional to the shelf life of the emulsions. Flocculation usually precedes creaming. It involves reversible aggregation of the internal phase into three-dimensional structures. Coalescence occurs due to the aggregation of the smaller droplets to form large drops. Unlike flocculation, in coalescence, the interfacial film is integral. Accelerated tests are commonly used to predict the long-term stability of the emulsion formulation. The shelf life of the emulsions is evaluated at relatively high humidity and elevated temperatures. The Arrhenius equation on particle size growth is used to determine the shelf life of the emulsions. The emulsions are stable at higher temperatures as compared to the ones stored at low temperatures. This is because freezing causes the formation of ice crystals which increases the pressure and hence destroys the shape of the emulsion (Rieger 1986). Steam sterilization, excessive shaking, and freeze-thaw cycles could also destabilize an emulsion. Post formulation, the emulsion is subjected to different stress conditions during transportation and aging. These tests involve the assessment of the pH, zeta potential, particle size, and drug content before and after the tests. These help find out the degradation products which can be expected on long storage conditions. Also, physical changes such as increased particle size, change in pH, and creaming can be tracked. Shelf life tests also include sterility tests and pyrogen testing.

5.3 Drug Release Studies

Drug release is indirectly dependent on the stability of the emulsion. The drug will be instantly released in the continuous phase during coalescence of the internal phase, and the oil droplets will be broken down to be released in the medium (Rosoff 1996). Reverse micelles are involved in transport of both ionized and unionized substances (Magdassi et al. 1984). In case of facilitated diffusion, the carrier molecule interacts with the drug in the membrane and makes it lipophilic (Barker and Hadgraft 1981). Wetting is an essential phenomenon for increased bioavailability. If the emulsion displays hydrophobic qualities, the entrapped air remains on the surface causing the emulsion to become unstable and display poor dissolution characteristics. Hence, poor wetting causes entrapped air which decreases the effective surface area for dissolution, thereby decreasing bioavailability. It is known that the smaller the particle size, the larger will be the surface area. The rate of dissolution will increase as the surface area increases. Viscosity is also a factor affecting the release of drug from the formulation.

A recent review by D'Souza discussed in vitro drug research setups for nano-delivery systems (D'Souza 2014). The dialysis method is most common for assessing the in vitro release of drugs from nanoemulsion. The nanoemulsions are introduced into a dialysis bag (suitable molecular weight cutoff for release of the entrapped drug) containing release media (inner media/compartment) that is placed in a larger vessel containing release media (outer media/compartment) and agitated to disturb the saturated boundary layer adjacent to the outer layer of the dialysis bag.

6 Nanoemulsions in Anticancer Drug Delivery

Recently, nanoemulsions have received considerable attention for the treatment of cancer. Most of the anticancer drugs are hydrophobic in nature, which poses major delivery issues. Emulsions form an attractive dosage form for the delivery of these hydrophobic drugs as the oil phase can solubilize and improve the bioavailability and therefore the therapeutic efficacy of the drug (Bagwe et al. 2001). Nanoemulsions can be formulated using biodegradable and biocompatible materials (Benita 1998b). They have a small droplet size, are easy to manufacture, and have a relatively long shelf life. As nanoemulsions use limited amount of surfactants compared to microemulsions or "solubilized" formulations (e.g., Taxol®, where the highly hydrophobic drug paclitaxel is solubilized with Cremophor® EL and pure ethanol), they can reduce the overall volume of the delivery vehicle introduced into the body of the patient, causing a reduction in toxic effects. Among the components of a nanoemulsion, the surfactants can increase the permeability of the cell membrane, hence enhancing drug absorption. Many diblock copolymer-type surfactants such as Pluronic P85 have in themselves been proven to possess anticancer activity (Evers et al. 2000). A study carried out to determine the chemo-sensitizing effects of Pluronic P85 in the MRP overexpressing cell line MDCKII showed that P85 effectively sensitized these cells to the effects of antineoplastic agents (Batrakova et al. 2003).

A unique advantage of emulsions is potentially the use of a physiological abnormality of cancer tissues in enhancing drug delivery to solid tumors, namely, angiogenesis that refers to the growth of new blood vessels in the body. Tumors stimulate this growth of new blood vessels in order to bring about a constant supply of blood for food and oxygen. It is a natural body process and gets activated by angiogenesis-stimulating growth factors. However, the vessels in cancer tissue differ from the normal blood vessels by having extensive extravasation, caused by vascular mediators such as bradykinin, nitric oxide, and cytokines such as VPF/VEGF. Also, the cancer tissue differs from the normal tissues by having a defective vascular design and having impaired lymphatic clearance from the interstitial tissues. Due to enhanced extravasation and impaired clearance, the lipid droplets of an O/W emulsion could potentially stay in the interstitial cavity for prolonged periods. This phenomenon is called enhanced permeability and retention (EPR) (Maeda et al. 2000). Cytotoxic drugs with large molecular size and long half-lives show enhanced EPR effect. The $t_{1/2}$ of neocarzinostatin in mice was found to be 1.8 min, whereas the $t_{1/2}$ of poly(styrene-co-maleic acid) half-n-butyl ester copolymer was 19 min, i.e., almost a tenfold increase (Fang et al. 2004). Another characteristic required for an increase in EPR is that the nanoemulsions should be either neutral or anionic (Maeda 1991). If the delivery system is cationic, it will be adsorbed on the negative surface of the cell and hence will have a short life span in the body. SMANCS is a prototype macromolecular anticancer agent mainly used with Lipiodol® (Maeda and Matsumura 1989). Lipiodol is basically an iodinated ethyl ester of poppy seed oil and is administered from the hepatic artery and the bronchial artery. SMANCS (styrene maleic acid neocarzinostatin) remains in the tumor at high concentrations for a long time due to the EPR effect. Hence, tumor vasculature can prove to be an exceptional target for delivery of large size anticancer agents or nanometer size lipid droplets.

An evaluation of microemulsions containing methotrexate on MCF-7 breast cancer cell line showed that the microemulsion exerted greater cytotoxic effect as compared to the solution form (Karasulu et al. 2007). The Caco-2 cell line was used to study the cytotoxic action of the formulation. It was also reported that methotrexate exerts more action on the tumor cells by inducing apoptosis. Another study indicated that arsenic trioxide containing microemulsions showed greater cytotoxic activity on the MDAH2774 ovarian cancer cell line as compared to the solutions (Terek et al. 2006) Goldstein carried out a study to determine the efficacy of paclitaxel palmitate loaded anti-HER2 immunoemulsions in prostate

cancer model overexpressing the HER2 receptor (Goldstein et al. 2007). The anti-HER2 immunoemulsion is basically a delivery system consisting of a cationic emulsion which has a covalent sharing with a monoclonal antibody, Herceptin. The immunoemulsion was found to have greater effects as compared to the cationic emulsion.

A study was carried out in which all-trans retinoic acid (ATRA) was added in an emulsion. ATRA has anticancer properties in some cancer cell lines. Studies show that ATRA was distributed evenly in the body system and demonstrated increased accumulation in the liver as compared to the solution form of ATRA. Liver has been known to be a target organ of tumor metastases which plays an important role in determining the survival time of the patient. In order to evaluate the capability of the ATRA incorporated emulsions over hepatic metastases, the number of metastatic colonies on the liver was measured. The survival time of the mice was also observed. The number of metastatic colonies in mice treated with ATRA in 5% HCO-60 micelles was found to be significantly lower compared to the control (Chansri et al. 2006). Also, the survival time of mice treated with ATRA emulsion was higher than that of mice treated with ATRA solution form.

Prete et al. carried out a study involving a cholesterol-rich nanoemulsion (LDE) containing etoposide oleate. The B16 tumor-bearing mice model was used to carry out the study. The LDE-etoposide oleate formulation was compared with the commercial etoposide, and it was found that the LDE-etoposide oleate showed greater plasma half-life and AUC as compared to the commercial formulation. At a dose of 17 μmol kg^{-1}, the LDE-etoposide oleate showed higher cell kill compared to the commercial formulation. The survival curves of the tumor-bearing mice treated with LDE-etoposide oleate at higher dose showed 67% survival rate as opposed to treatments of smaller doses which showed 50% survival rate. The commercial product showed only a 22% survival rate (Prete et al. 2006). A study involving a cholesterol-rich nanoemulsion containing paclitaxel was done to determine the tumor uptake. These LDE-containing nanoemulsions were found to have a greater half-life and AUC than the paclitaxel-Cremophor formulation (Dias et al. 2007). Also, the uptake of the LDE concentrates in the tumor tissues was found to be higher than in the normal tissues.

Karasulu et al. prepared an arsenic trioxide containing microemulsion and observed the anticancer effects of this formulation on MCF-7 breast cancer cell line. Increased antitumor activity was seen in the cells at 5×10^{-6}MAs_2O_3 concentration. At concentration of 1.6×10^{-9} M, almost 80% cell kill was observed. This low concentration showed a 1000 times higher cytotoxic action as compared to the regular As_2O_3 solution (Yeşim Karasulu et al. 2004). Another study compared the antitumor activity of LDE-paclitaxel with the commercial product in the NCI-H292 cancer cell line. The antitumor effect of the two formulations was not found to be statistically different. LDE by itself did not exert any effect on cell survival but Cremophor EL caused a reduction in cell survival. Higher antitumor effect of commercial paclitaxel was attributed to the supplementary growth inhibitory activity of Cremophor EL. Acute toxicity studies were also carried out in rats, and LDE demonstrated reduced drug toxicity. The LD50 for LDE-paclitaxel and the commercial paclitaxel was reported to be 324 mg/kg and 31.8 mg/kg, respectively (Rodrigues et al. 2002). The antitumor agent carmustine was incorporated in cholesterol-rich emulsion, and its cytotoxicity was studied ex vivo. The biodistribution was also studied in mice. It was found that LDE-carmustine was taken up by the tumor cells at higher levels compared to the normal cells (Maranhao et al. 2002). A clinical study was carried out in 42 patients to establish the toxicity outline for the formulation. The patients exposed to LDE-carmustine showed reduced side effects. Studies were carried out using a mouse model to determine if a subcutaneous injection of nanoemulsion is effective against tumor growth in neuroblastoma. It was found that the suspension formulation was ineffective in reducing neuroblastoma tumor growth while the nanoemulsions caused a 65% reduction in the growth of tumor cells (Kuo et al. 2007).

7 Conclusion

Nanomedicine has progressed as a novel area of drug delivery for targeting the drug to a particular tissue and/or to increase the bioavailability and reduce the toxicity of a drug. Nanoemulsion is a part of the colloidal delivery systems that presents a unique opportunity for the delivery of a drug for targeting as well as solubilization of hydrophobic drugs. Most of the nanoemulsions use generally recognized as safe (GRAS) excipients that are biodegradable and biocompatible. There are fewer challenges in formulation and pilot scale study of nanoemulsions compared to solid biodegradable nanoparticles. One of the most important production criteria for nanoemulsion that can be controlled reproducibly is the narrow size distribution of the nanoemulsion droplets. In recent years, we have observed a large number of reports in the area of nanoemulsions for anticancer drugs.

Conflict Statement None.

References

Alakhov V, Klinski E, Li S, Pietrzynski G, Venne A, Batrakova E, Bronitch T, Kabanov A. Block copolymer-based formulation of doxorubicin. From cell screen to clinical trials. Colloids Surf B: Biointerfaces. 1999;16(1–4):113–34.

Bagwe RP, Palla JKB, Patanjali PK. Improved drug delivery using. Crit Rev Ther Drug Carrier Syst. 2001;18(1):77–140.

Barker N, Hadgraft J. Facilitated percutaneous absorption: a model system. Int J Pharm. 1981;8(3):193–202.

Batrakova EV, Li S, Alakhov VY, Elmquist WF, Miller DW, Kabanov AV. Sensitization of cells overexpressing multidrug-resistant proteins by pluronic P85. Pharm Res. 2003;20(10):1581–90.

Becher P, editor. Encyclopedia of emulsion technology – Volume 1. Basic theory. New York: Marcel Dekker, Inc.; 1983. p. 725.

Benita S. Biofate of fat emulsions. In: Benita S, editor. Submicron emulsions in drug targeting and delivery. 1st ed. Singapore: Harwood Academic Publisher; 1998a. p. 99–118.

Benita S. Introduction and overview. In: Benita S, editor. Submicron emulsions in drug targeting and delivery. 1st ed. Singapore: Harwood Academic Publisher; 1998b. p. 1–3.

Bolzinger-Thevenin MA, Grossiord JL, Poelman MC. Characterization of a sucrose ester microemulsion by freeze fracture electron micrograph and small angle neutron scattering experiments. Langmuir. 1999;15(7):2307–15.

Buyukozturk F, Benneyan JC, Carrier RL. Impact of emulsion-based drug delivery systems on intestinal permeability and drug release kinetics. J Control Release. 2010;142(1):22–30.

Chansri N, Kawakami S, Yamashita F, Hashida M. Inhibition of liver metastasis by all-trans retinoic acid incorporated into O/W emulsions in mice. Int J Pharm. 2006;321(1–2):42–9.

Chidambaran N, Burgess D. Emulsions: design and manufacture. In: Burgess DJ, editor. Injectable dispersed systems. Boca Raton: Taylor & Francis; 2005. p. 213–41.

Clark SB, Derksen A. Phosphatidylcholine composition of emulsions influences triacylglycerol lipolysis and clearance from plasma. Biochim Biophys Acta. 1987;920(1):37–46.

D'Souza S. A review of in vitro drug release test methods for nano-sized dosage forms. Adv Pharm. 2014;2014:304757.

Dias ML, Carvalho JP, Rodrigues DG, Graziani SR, Maranhao RC. Pharmacokinetics and tumor uptake of a derivatized form of paclitaxel associated to a cholesterol-rich nanoemulsion (LDE) in patients with gynecologic cancers. Cancer Chemother Pharmacol. 2007;59(1):105–11.

Evers R, Kool M, Smith AJ, Van Deemter L, De Haas M, Borst P. Inhibitory effect of the reversal agents V-104, GF120918 and Pluronic L61 on MDR1 Pgp-, MRP1-and MRP2-mediated transport. Br J Cancer. 2000;83(3):366–74.

Fang J, Sawa T, Maeda H. Factors and mechanism of "EPR" effect and the enhanced antitumor effects of macromolecular drugs including SMANCS. In: Polymer drugs in the clinical stage. Boston: Springer; 2004. p. 29–49.

Gao ZG, Choi HG, Shin HJ, Park KM, Lim SJ, Hwang KJ, Kim CK. Physicochemical characterization and evaluation of a microemulsion system for oral delivery of cyclosporin A. Int J Pharm. 1998;161(1):75–86.

Gao P, Rush BD, Pfund WP, Huang T, Bauer JM, Morozowich W, Kuo MS, Hageman MJ. Development of a supersaturable SEDDS (S-SEDDS) formulation of paclitaxel with improved oral bioavailability. J Pharm Sci. 2003;92(12):2386–98.

Garti A, and Aserin A. Pharmaceutical emulsions, double emulsions, and microemulsions. In: Benita S, ed. Microencapsulation. New York: Marcel Dekker, Inc.; 1996. p. 411–534.

Gershanik T, Benita S. Self-dispersing lipid formulations for improving oral absorption of lipophilic drugs. Eur J Pharm Biopharm. 2000;50(1):179–88.

Ghosh PK, Murthy RSR. Microemulsions: a potential drug delivery system. Curr Drug Deliv. 2006;3(2):167–80.

Goldstein D, Gofrit O, Nyska A, Benita S. Anti-HER2 cationic immunoemulsion as a potential targeted drug delivery system for the treatment of prostate cancer. Cancer Res. 2007;67(1):269–75.

Griffin WC. Calculation of HLB values of non-ionic surfactants. J Soc Cosmet Chem. 1954;5:249–56.

Gursoy RN, Benita S. Self-emulsifying drug delivery systems (SEDDS) for improved oral delivery of lipophilic drugs. Biomed Pharmacother. 2004;58(3): 173–82.

Haskell RJ, Shifflett JR, Elzinga PA. Particle-sizing technologies for submicron emulsions. In: Submicron emulsions in drug targeting and delivery, vol. 9. Amsterdam: Harwood Academic Publishers; 1998. p. 21–98.

Hauss DJ, Fogal SE, Ficorilli JV, Price CA, Roy T, Jayaraj AA, Keirns JJ. Lipid-based delivery systems for improving the bioavailability and lymphatic transport of a poorly water-soluble LTB4 inhibitor. J Pharm Sci. 1998;87(2):164–9.

Karasulu HY, Karabulut B, Göker E, Güneri T, Gabor F. Controlled release of methotrexate from w/o microemulsion and its in vitro antitumor activity. Drug Deliv. 2007;14(4):225–33.

Kovarik JM, Mueller EA, Kutz K, Van Bree JB, Tetzloff W. Reduced inter-and intraindividual variability in cyclosporine pharmacokinetics from a microemulsion formulation. J Pharm Sci. 1994;83(3):444–6.

Kuo F, Kotyla T, Wilson T, Kifle L, Panagiotou T, Gruverman I, Tagne JB, Shea T, Nicolosi R. A nanoemulsion of an anti-oxidant synergy formulation reduces tumor growth rate in neuroblastoma-bearing nude mice. J Exp Ther Oncol. 2007;6(2):129–35.

Li P, Ghosh A, Wagner RF, Krill S, Joshi YM, Serajuddin AT. Effect of combined use of nonionic surfactant on formation of oil-in-water microemulsions. Int J Pharm. 2005;288(1):27–34.

Maali A, Mosavian MH. Preparation and application of nanoemulsions in the last decade (2000–2010). J Dispers Sci Technol. 2013;34(1):92–105.

Maeda H. SMANCS and polymer-conjugated macromolecular drugs: advantages in cancer chemotherapy. Adv Drug Deliv Rev. 1991;6(2):181–202.

Maeda HAYM, Matsumura Y. Tumoritropic and lymphotropic principles of macromolecular drugs. Crit Rev Ther Drug Carrier Syst. 1989;6(3):193–210.

Maeda H, Wu J, Sawa T, Matsumura Y, Hori K. Tumor vascular permeability and the EPR effect in macromolecular therapeutics: a review. J Control Release. 2000;65(1–2):271–84.

Magdassi S, Frenkel M, Garti N. On the factors affecting the yield of preparation and stability of multiple emulsions. J Dispers Sci Andtechnol. 1984;5(1):49–59.

Maranhao RC, Graziani SR, Yamaguchi N, Melo RF, Latrilha MC, Rodrigues DG, Couto RD, Schreier S, Buzaid AC. Association of carmustine with a lipid emulsion: in vitro, in vivo and preliminary studies in cancer patients. Cancer Chemother Pharmacol. 2002;49(6):487–98.

Mehta SK, Bala K. Phase behavior, structural effects, and volumetric and transport properties in nonaqueous microemulsions. Phys Rev E. 1999;59(4):4317.

Nakajima H, Tomomasa S, Okabe M. Proceedings of first world emulsion conference, vol. 1. Paris: EDS; 1993. p. 1–11.

Nishikawa M, Takakura Y, Hashida M. Biofate of fat emulsions. In: Submicron emulsions in drug targeting and delivery, vol. 9. Amsterdam: Harwood Academic Publisher; 1998. p. 99–118.

Pinnamaneni S, Das NG, Das SK. Comparison of oil-in-water emulsions manufactured by microfluidization and homogenization. Die Pharmazie. 2003;58(8):554–8.

Prete ACL, Maria DA, Rodrigues DBG, Valduga CJ, Ibañez OC, Maranhão RC. Evaluation in melanoma-bearing mice of an etoposide derivative associated to a cholesterol-rich nanoemulsion. J Pharm Pharmacol. 2006;58(6):801–8.

Rani S, Rana R, Saraogi GK, Kumar V, Gupta U. Self-emulsifying oral lipid drug delivery systems: advances and challenges. AAPS PharmSciTech. 2019;20(3):129.

Redgrave TG, Rakic V, Mortimer BC, Mamo JC. Effects of sphingomyelin and phosphatidylcholine acyl chains on the clearance of triacylglycerol-rich lipoproteins from plasma. Studies with lipid emulsions in rats. Biochim Biophys Acta. 1992;1126(1):65–72.

Rieger MM. Emulsions. In: Lachman L, Lieberman H, Kanig J, editors. The theory and practice of industrial pharmacy. 3rd ed. Philadelphia: Lea & Febiger; 1986. p. 502–32.

Rodrigues DG, Covolan CC, Coradi ST, Barboza R, Maranhão RC. Use of a cholesterol-rich emulsion that binds to low-density lipoprotein receptors as a vehicle for paclitaxel. J Pharm Pharmacol. 2002;54(6): 765–72.

Rosoff M. Specialized pharmaceutical emulsions. In: Lieberman HA, Rieger MM, Banker GS, editors. Pharmaceutical dosage forms: disperse systems. 2nd ed. New York: Marcel Dekker, Inc.; 1996. p. 1–35.

Russel WB, Russel WB, Saville DA, Schowalter WR. Colloidal dispersions. New York: Cambridge University Press; 1991.

Salager JL. Formulation concepts for the emulsion maker. In: Nielloud F, Mart-Mestres G, editors. Pharmaceutical emulsions and suspensions. New York: Marcel Dekker, Inc.; 2000. p. 19–68.

Shinoda K, Araki M, Sadaghiani A, Khan A, Lindman B. Lecithin-based microemulsions: phase behavior and microstructure. J Phys Chem. 1991;95(2): 989–93.

Singh Y, Meher JG, Raval K, Khan FA, Chaurasia M, Jain NK, Chourasia MK. Nanoemulsion: concepts, development and applications in drug delivery. J Control Release. 2017;252:28–49.

Solans C, Solé I. Nano-emulsions: formation by low-energy methods. Curr Opin Colloid Interface Sci. 2012;17(5):246–54.

Terek MC, Karabulut B, Selvi N, Akman L, Karasulu Y, Ozguney I, Sanli AU, Uslu R, Ozsaran A. Arsenic trioxide–loaded, microemulsion-enhanced cytotoxicity on MDAH 2774 ovarian carcinoma cell line. Int J Gynecol Cancer. 2006;16(2):532–7.

Venne A, Li S, Mandeville R, Kabanov A, Alakhov V. Hypersensitizing effect of pluronic L61 on cytotoxic activity, transport, and subcellular distribution of doxorubicin in multiple drug-resistant cells. Cancer Res. 1996;56(16):3626–9.

Yeşim Karasulu H, Karabulut B, Kantarci G, Özgüney I, Sezgin C, Sanli UA, Göker E. Preparation of arsenic trioxide-loaded microemulsion and its enhanced cytotoxicity on MCF-7 breast carcinoma cell line. Drug Deliv. 2004;11(6):345–50.

Part IV

Metallic Nanoparticles

18

Manufacturing Techniques for Carbon Nanotubes, Gold Nanoparticles, and Silver Nanoparticles

Tejal Mehta, Renuka Mishra, Chintan Pansara, Chetan Dhal, Namdev Dhas, Kartik Hariharan, and Jayvadan K. Patel

Abstract

Extensive research has been focused around organic and inorganic nanoparticles (NP) due to their unique and abundant benefits such as superior drug loading, biocompatibility, and role in drug delivery, biosensing, and theranostic. Among the organic NPs, carbon nanotubes (CNT), graphene NP, and fullerenes are widely explored, while gold and silver are extensively used for inorganic NP in biomedicine. The fabrication of CNT and its types like single-walled CNT (SWCNT) and double-walled CNT using conventional methods like arc discharge method, laser ablation, and chemical vapor deposition has been considered in detail. The traditional method of preparation of gold NPs (GNPs) is chemical reduction method which uses toxic chemicals or yields by-products which may compromise its inert characteristic. Thus, the current trend has been shifted toward the synthesis of GNPs using green method. In the last few decades, incredible innovations have come up regarding the applications and methods of fabrication of silver nanoparticles (AgNPs). Similar to methods used for the fabrication of GNPs, AgNPs are also manufactured by various chemical methods such as reduction, light-mediated ion implant. The additional method which has been extensively explored is green synthesis of AgNPs using plants, bacteria, and fungi. This chapter provides an insight into the commonly used techniques as well as recently explored techniques in preparation of carbon nanotubes, gold NPs (GNP), and AgNPs.

Keywords

Manufacturing · Carbon nanotubes · Single-walled carbon nanotubes (SWCNT) · Gold nanoparticles · Silver nanoparticles · Green synthesis · Chemical synthesis

1 Introduction

Carbon nanotubes (CNTs) are relatively new nanomaterials known to the public for nearly 20 years; however, their history is somewhat longer. CNTs were first discovered and identified by Radushkevich and Lukyanovich in 1952 (Radushkevich and Lukyanovich 1952) and then

T. Mehta (✉) · R. Mishra · C. Pansara · C. Dhal
N. Dhas · K. Hariharan
Department of Pharmaceutics, Institute of Pharmacy, Nirma University, Ahmedabad, Gujarat, India
e-mail: tejal.shah@nirmauni.ac.in

J. K. Patel
Nootan Pharmacy College, Sankalchand Patel University, Visnagar, Gujarat, India

J. K. Patel, Y. V. Pathak (eds.), *Emerging Technologies for Nanoparticle Manufacturing*,
https://doi.org/10.1007/978-3-030-50703-9_18

observed by Oberlin et al. (1976) in 1976 as single (or double)-walled CNTs. In later history, the discovery of CNTs is credited to Iijima as the first scientist to depict preparation method of multi-walled CNTs (MWCNTs) after a random event during 1991 test of new arc evaporation technique for C60 carbon molecules (Iijima 1991). CNTs have attracted many researchers owing to their unique properties such as excellent electrical, mechanical, and thermal properties and larger surface area and a wide range of applications (Baughman et al. 2002). Nevertheless, in order to scale up at industrial level for increasing quantity and improving quality of the manufactured CNTs, it is necessary to develop new techniques for synthesis or improvement in the existing techniques. Generally, CNTs are divided into two types: single-walled CNTs (SWCNTs) and MWCNTs. SWCNTs are made up of a single sheet of graphene that is wrapped around itself forming a cylindrical tube. This is difficult to obtain, however they are unique because of higher stability and better mechanical properties. The SWCNTs possess a diameter in the range of 0.4–3 nm, and the length can be more than 10 mm, which can act as a good template for study in one-dimensional mesoscopic physics system (Dekker 1999). The MWCNTs are formed by two or more layers of concentric atoms, i.e., they are formed by two or more SWCNTs.

Gold nanoparticles in recent years have garnered significant interest due to their inherent optical and electrical properties when scaled down to nano-size which finally results in varied and diverse applications in biomedical field. These noble metals being inert in nature are devoid of significant toxicity in appropriate concentrations. Manufacturing techniques established previously were chemical reduction based which evolved through the years to explore different aspects like physical ablation techniques, sonochemical-based techniques, etc. The toxicity when preparing gold nanoparticles by chemical reduction often has increased due to the use of different chemicals and surfactants, and this has necessitated toward the use of green method–based synthesis of gold nanoparticles in recent years. The literature discussed here gives a brief overview of different techniques explored over the years for preparation of gold nanoparticles.

There is recent focus on understanding the relationship between the physicochemical properties of nanomaterials and their potential risk to the human health and the surrounding environment day by day. Due to the growing popularity of silver nanoparticles (AgNPs) in consumer commodities, an effort has been placed to verify the safety of AgNPs along with the need to understand the mechanism of action for its antimicrobial effects. Due to unique properties of nanoparticles such as smaller particle size in nanoscale and higher surface area, which can significantly change physical, chemical, and biological properties, their significance has increased tremendously leading to numerous applications. One such application of surface-modified silver is in the field of antimicrobial effectiveness (Rai and Duran 2011). The beneficial effect of colloidal silver has been known for many years, but thorough studies on its outcome on the environment have recently begun. Preliminary studies have proved that AgNPs influence microbes and microbial cells principally due to the release of low concentration of silver ion from the nanoparticles.

In order to satisfy the requirements of AgNPs, a variety of approaches have been employed for the synthesis of nanoparticles. Generally, traditional physical and chemical methods are very costly and harmful. Interestingly, biologically prepared AgNPs from biological sources including bacteria, fungi, yeast, algae, or plants show superior yield, solubility, and good stability. Among numerous synthetic methods used for manufacturing AgNPs, biological methods seem to be less complicated, quick, nontoxic, and green approaches that can produce specific size and morphology under optimized conditions for research. A green chemistry approach promises the synthesis of AgNPs. Over the years, green nanotechnological advancements through biological resources have emerged significantly for synthesis and fabrication of metal nanoparticles (Gahlawat and Choudhury 2019). The methods of synthesis of AgNPs can be broadly divided into wet chemistry, ion implants, and biological sources.

2 Manufacturing Techniques for Carbon Nanotubes

2.1 Fabrication Methods for CNTs

Several methods have been evolved for the fabrication of CNTs, viz., chemical vapor deposition (CVD), laser ablation, arc discharge, electrolysis, and sonochemical/hydrothermal method. Each method has its own advantages and limitations. Fabrication methods for development of CNTs involve different mechanisms with varying levels of purity. The ultimate aim is to develop CNTs with greater purity and improve synthesis processes, which results in reduction of fabrication cost.

2.1.1 Arc Discharge Method

Lijima et al. utilized the arc method in the discovery of CNTs. This method involves the electric discharge of two electrodes (cathode and anode) of graphite inside a steel chamber, containing inert gas at high pressure (Sales 2003). In addition to this, in this method, helium/argon/methane gases are utilized, and the pressure is nearly 50–500 torr with temperature greater than 1700 °C with the catalyst Co and Fe in carbon, which has been confirmed first in SWCNT synthesis. This method causes the CNT expansion with fewer structural defects in comparison with other methods (Al Hasan 2019). The CNT-based quality produced by electric arc method is based on the quality and quantity of the catalyst, the pressure, the geometry of the system, inert gas nature, temperature, and electric current of the cathode and anode distancing during the process (Droppa Junior 2004; Teixeira 2010). The anode is composed of graphite and metals, such as Co, Ni, Pd, Pt, Ag, and Fe, and mixtures of Ni, Fe, and Co with other elements like Fe-NO, Ni-Cu, Co-Ni, Ni-Ti, Co-Cu, etc. The metal catalyst plays an important role in the process yield (Prasek et al. 2011). Iijima et al. fabricated SWCNTs with diameter of 1 nm (Iijima and Ichihashi 1993); however, Bethune et al. developed SWCNTs with a diameter of 1.2 nm by using co-evaporation of Co and carbon in an arc generator, and walls were made of single thick atomic layer (Bethune et al. 1993). Additionally, Ajayan et al. also used co-catalyst for synthesis of SWCNTs with a diameter of 1–2 nm utilizing arc discharge in helium atmosphere. Ni is one of the most utilized catalysts in the synthesis of SWCNTs (Ajayan et al. 1993). Furthermore, Saito et al. fabricated single-layer CNTs involving platinum-group metals (Pd, Ir, Ru, Pt, Os, and Rh) using the arc discharge method. The results indicated that Pt, Pd, and Rh demonstrated catalytic activity for growing SWCNTs; however, other metals were not able to show the catalytic activity. The results demonstrated that the diameter size of core Rh-based CNTs was found to be 20–30 nm. However, the diameter size of core Pd-based SWCNTs was found to be 50–200 nm (Saito et al. 1996). Furthermore, Zhao et al. investigated the effect of catalysts in the fabrication of SWCNTs using modified arc discharge method. In this technique, helium buffer gas with a pressure of 500 torr, an arc current of 100 A, and a temperature of 600 °C was kept constant. Nevertheless, the chemical composition of catalysts such as Co-Ni, Ni-In, FeS-Ni-Mg + zeolite, FeS-Ni-Mg, La-Mg, Nb, La-Ni-Mg, Co-Mg, Ni-Y_2O_3, Ga-Mg, Co-Y_2O_3, and Mo-Co-Mg was varied in the experiment. All the aforementioned catalysts with a content of 3 wt% of mixture of powder graphite and catalyst were considered. The results indicated that the SWCNTs were produced at large scale using Co-Ni and Fe-Ni-Mg as the catalysts. However, instead of SWCNTs, the amorphous carbon on the soot was produced using Co-Mg, Ga-Mg, and La-Mg as catalysts. The rest of the catalysts were able to produce a very small amount of SWCNTs. From the results, it can be concluded that S and Fe or few transition metals can effectively initiate the growth of SWCNTs. However, bimetal powders of catalysts including Mg cannot activate the carbon clusters to form regular CNTs. In conclusion, it can be said that FeS and Ni or few transition metals as a catalyst can increase the production of SWCNTs. Therefore, suitable catalyst or a combination of catalysts plays a significant role in the production of SWCNTs (Zhao et al. 2019).

Compared to SWCNTs and MWCNTs, the fabrication methods for double-walled carbon nanotube (DWCNT) deposition are more complicated. However, a number of successful investigations have been carried out to produce DWCNTs using arc discharge method. For instance, Hutchinson et al. (2001) fabricated DWCNTs by arc discharge method using an atmosphere of hydrogen and argon mixture. Additionally, graphite rod was used as an anode with a diameter of 8.2 mm filled with catalysts. The mixture of Co, S, Ni, and Fe was utilized as a catalyst. With advancement, Sugai et al. (2003) developed DWCNTs with high quality by high-temperature pulsed arc discharge method using Y/Ni alloy catalysts. Furthermore, Huang et al. (2003) developed DWCNTs with high resistance to high-temperature (about 720 °C) oxidation in air without additional annealing even after acid treatment. This can be explained by in situ defect-healing effect of the bowl-like cathode and the absence of reactive gases during arc discharge.

The arc discharge method of MWCNTs is simple in case when all the growth conditions are ensured. With the approach of two electrodes, there is increase in the temperature, which is around 3000 °C to 4000 °C, following which there is a deposition of carbon in the form of black soot on the walls of the chamber and the negative electrodes, thus forming the MWCNTs. Moreover there is formation of some amount of amorphous carbon, fullerenes, and graphite sheets (Droppa Junior 2004; Teixeira 2010). The graphite usually water-cooled electrodes with diameters between 6 mm and 12 mm in a chamber filled with helium at subatmospheric pressure (Prasek et al. 2011). Additionally, direct current arc discharge technique is one of the most efficient techniques to fabricate carbon-based nanoplatforms. Owing to its efficiency in fabrication and great commercial value, there was breakthrough in synthesis of C60 by direct current arc discharge method using helium atmosphere. This method can fabricate carbon-based nanoplatforms like SWCNTs, MWCNTs, spherical carbon NPs, carbon nanohorns, and graphene. In this method, the aforementioned nanoplatforms are collected from different positions. For example, MWCNTs and graphene-based NPs are collected from anode deposit (Liang et al. 2014); however, SWCNTs are collected from cathode deposits (Liang et al. 2012). Additionally, Li et al. investigated that flow rate of H2 buffer gas enhances or accelerates the growth process of graphene owing to which carbon-based nanomaterials deposit fast onto the chamber. The rapid flow of gas plays a significant role in separation and exfoliation of few-layer graphene to single-layer graphene (Li et al. 2014). Furthermore, Li et al. investigated that under N2 atmosphere, the dimensions of carbon nanomaterials and the diameter and length of CNTs gradually decrease (Li et al. 2017). For instance, Zhang et al. investigated the controllable synthesis of carbon nanomaterials using direct current arc discharge method. The transmission electron microscopy (TEM) results indicated that spherical carbon NPs were obtained with size range of 30–80 nm under argon and nitrogen atmosphere as buffer gas. However, few graphene sheets were obtained when exposed to hydrogen atmosphere with a size ranging from 200 nm to 400 nm. The results indicated that atmosphere plays a significant role in controlling the morphology of carbon nanomaterials using direct current arc discharge technique. Furthermore, the researcher investigated the effect of gas pressure; the results indicated that spherical carbon nanomaterials produced were amorphous and aggregated under the argon atmosphere at 40 kPa and 50 kPa pressure due to low temperature gradient. However, when the argon pressure was increased to 70 kPa, the structure of carbon nanomaterials was clearly seen. In this case, long residence time of primary particles was responsible for aggregation. Increase in gas pressure leads to increase in temperature gradient, thereby facilitating carbon clusters to be deposited into the inner side of chamber by intense quenching (Zhang et al. 2019). However, many studies have utilized methane or hydrogen atmosphere in arc discharge method. Additionally, Wang et al. investigated the effect of various atmospheres on the morphology of CNTs. The researchers utilized direct current arc discharge of graphite electrodes in methane and helium. By evaporation under high arc current and high-pres-

sure methane gas, thick NTs embellished with many carbon NPs were obtained. However, utilizing anode with a diameter of 6 mm, an arc current of 20 A, and a methane gas pressure of around 50 torr can lead to the formation of long and thin MWCNTs (Wang et al. 1996).

Generally, the production of CNTs is the presence of impurities that affects the final properties of CNTs as material that could be used in some special applications. Hence, there are different studies carried out by the researchers dealing with this problem. The purification of CNTs can be carried out using various methods such as oxidation, filtration, annealing, ultrasonication, and thermal and acidic treatment (Prasek et al. 2011).

2.1.2 Laser Ablation or Laser Vaporization Technique

The CNT synthesis using laser ablation was first reported by Gao et al. in 1995. This technique for the fabrication of CNTs is similar to arc discharge technique. Both techniques have a similar principle, i.e., both methods utilize the condensation of carbon atoms generated from the vaporization of graphite targets (Rakhi 2019). However, this method includes the use of light source, which is absent in arc discharge process. According to the literature, laser ablation method can produce SWCNTs with greater than 90% of purity. This method includes various factors and rate-limiting steps, viz., type of gas, temperature, target material, light sources, and pressure which regulates the production of CNTs. Both carbon atom and graphite rod can act as carbon feedstock for nanotube growth when suspended in surrounding atmosphere in reaction chamber. The growth of CNTs in the reaction zone can be tuned by supply of carbon feedstock to ensure pure and defect-free CNT formation (Scott et al. 2001). Additionally, in this method, during the synthesis of CNTs, there is formation of fullerenes as an intermediate which further degrades into lower fragments by laser effects, and this disintegrated fragments of carbon act as feedstock for further growth of CNTs (Das et al. 2016). As SWCNTs have to be collected from water-cooled chamber of laser ablation process, SWCNT formation occurs near/at graphite target in the proximity of laser attack surface. Greater target ablation can be achieved by laser irradiation by maintaining the appropriate temperature in reaction chamber (Das et al. 2016). The hot plasma plume is generated owing to high-temperature ablation of target material which supports proper and fast growth of SWCNTs in gas phase (Journet et al. 1997; Su and Zhang 2015). In this method, the graphite target is placed in a quartz tube surrounded by a furnace at around 1200 °C. The carbon soot produced by the vaporization of graphite electrode by continuous or pulse laser is transferred to a water-cooled Cu collector with the help of a constant flow of inert gas (helium and argon) (Scott et al. 2001; Dillon et al. 2000; Braidy et al. 2002; Guo et al. 1995). Furthermore, the growth of CNTs can be explained by "scooter" mechanism (Thess et al. 1996). According to this mechanism, on the open edge of nanotubes, a single transition metal atom (Co, Fe, or Ni) gets chemisorbed. This metal atom circulates around the open end of the tube and absorbs small carbon molecules leading to the formation of graphite-like sheet. The metal atom must be highly effective in catalyzing the nanotube growth, and it must have a sufficient high electronegativity so as to prevent the formation of fullerenes. The growth of CNTs continues until many catalyst atoms aggregate on the end of the nanotube. These formed large catalyst clusters will either become over-coated with sufficient carbon to terminate the catalytic activity or get detached from the tip. The CNT tip will thus be terminated either with a fullerene-like cap or with a catalyst particle (Rakhi 2019).

2.1.3 Chemical Vapor Deposition (CVD)

The synthesis of CNTs can also be fabricated by another method, i.e., CVD. CVD is the most intensively studied technique for the large production of various types of CNTs (Kumar et al. 2017; Ferreira et al. 2016). In this technique, the growth of the CNTs can be promoted by pyrolysis of hydrocarbons or heating the gaseous hydrocarbon sources, viz., methane, acetylene, ethylene, ethanol, and CO, to 600 °C to 1000 °C with transition metal catalysts such as Co, Fe, and Ni (Kohl 2001; Yaceman et al. 1993). CNTs

can be fabricated with controlled growth of nanotubes, good alignment, and production at larger scale using this method (Ren et al. 1999). Additionally, control over shell number and diameter can also be achieved (Hou et al. 2008). Several steps are involved in CVD. Firstly, substrates are coated with the help of catalyst metal particles. Secondly, the substrate is placed in the furnace where the catalyst metal particles are subjected to reduction treatment upon heating under NH3 or H2. Then, the hydrogen gas or CO is let into a furnace. Hydrocarbon molecules are prone to catalytic decomposition which led to deposition of carbon on the catalyst particles at temperature ranging from 500 °C to 1200 °C (Rakhi 2019). The synthesis of SWCNTs requires higher temperature, i.e., 600 °C to 1150 °C, in the presence of mixture of inert gases such as argon and H2, and the synthesis of MWCNTs requires lower temperature, i.e., 500 °C to 800 °C, in the presence of inert gas atmosphere (Kiselev et al. 2006). In this regard, the temperature required for the fabrication of CNTs using CVD is lower as compared to arc discharge method. The structure of MWCNTs obtained by arc discharge technique is significantly different from the structure generated from CVD. As compared to arc discharge, the CVD produces less crystalline MWCNTs and exhibits more defects in MWCNTs (Rakhi 2019). Depending on the catalyst, spiral growth of MWCNTs can occur in CVD. CVD can produce the MWCNTs with greater diameter with a particle size of 100 nm. This method involves the growth of nanotubes perpendicular to the substrate; thus, the length of MWCNTs can be determined easily (Grobert et al. 1999). There are several substrates utilized in this method such as stainless steel, Si, Ni, Cu, SiO2, glass or Ti/Cu/Si, tungsten foil, and graphite. Many studies also utilized mesoporous silica; it may show a templating role in guiding the initial growth of CNTs (Afolabi et al. 2011; Dumpala et al. 2011). CVD method is broadly classified into thermal enhanced CVD and plasma enhanced (catalytic) CVD, and is considered as the standard technique which is more feasible and economical for large-scale production of CNTs. There are several other methods used for the fabrication of CNTs, such as microwave plasma CVD, oxygen-assisted CVD, radiofrequency CVD, and hot-filament CVD. In this technique, catalysts are responsible for decomposition of carbon source either via heat (thermal CVD) or plasma irradiation (plasma CVD) and its new nucleation to obtain CNTs (Prasek et al. 2011).

3 Manufacturing Techniques for Gold Nanoparticles

3.1 Chemical Reduction Technique

Turkevich method was one of the most widely accepted techniques that laid the foundation for further development in synthesis of gold nanoparticles. It is based on chemical reduction technique using sodium citrate under boiling conditions. Under boiling conditions, the sodium citrate was converted to dicarboxy acetone that played multiple roles as reducing agent, seeding agent, and stabilizing agent. The precursor chloroauric acid was boiled initially, and then the reducing agent was added to it. Briefly, in experimental setup, 95 ml of chloroauric acid solution (containing 5 mg of Au) was heated to the boiling point, and 5 ml of 1% sodium citrate solution was added to the boiling solution with good stirring. After about a minute, a very faint grayish pink or grayish blue tone appeared, and in a period of 5 min, it darkened to deep wine and red color (Turkevich et al. 1953).

Frens in 1973, during his study on different size-dependent phenomena like Brownian motion, light scattering, and sedimentation of particles, focused on synthesis of different sizes of gold nanoparticles by varying the concentration of citrate to reduce gold by using the traditional Turkevich method. As the ratio of reactants was changed, a change in nucleation and growth rate was expected. In the procedure described by Frens, 50 ml of 0.01% $HAuCl_4$ was heated to the boiling point, and 0.5 ml of 1% trisodium citrate was added. Initially, the solution turned bluish indicating nucleation, and then it turned wine red after 1 min. The formation of gold nanoparticles

completed after a period of 5 min. Neither prolonged heating after that period or increasing citrate concentration after that resulted in any change or formation of nanoparticles in suspension. The change in sizes was analyzed after adding different volumes of trisodium citrate after boiling (Frens 1973).

Sivaraman et al. modified the Turkevich process by reversing the order of addition of sodium citrate. The molar ratio (MR) was such that sodium citrate was at least five times more than $HAuCl_4$. Keeping the overall reaction volume to 25 ml, sodium citrate of 5.2 mM of 24.75 ml was prepared and kept for boiling. To this 0.25 ml, 25.4 mM $HAuCl_4$ was added to get an overall concentration of 0.254 mM. This resulted in formation of monodisperse 10 nm gold colloids at less than 2 min as compared to standard addition where it took up to 10mins. It is essential that MR is at least 5, or else reversing the addition does not have any significant affect (Sivaraman et al. 2011).

3.2 Two-Phase System-Based Reduction

Brust and Schiffrin used a two-phase system to synthesize thiol decorated gold nanoparticles. Phase transfer from aqueous to organic phase was employed to get monodisperse gold nanoparticles. Initially, aqueous tetrachloroaurate solution was prepared and mixed with organic phase toluene containing tetraoctylammonium bromide (TOAB), which acted as a phase transfer agent. This was mixed thoroughly till tetrachloroaurate was transferred to organic phase to which dodecanethiol was added. To this, aqueous organic phase containing sodium borohydride was added that acted as a reducing agent. The organic phase was subsequently evaporated and recrystallized with ethanol (Brust et al. 1994).

3.2.1 Electrospray-Assisted Chemical Reduction

The effects of method of addition of precursor to the reducing agent solution were studied by Soliwoda wherein gold(III) chloride hydrate was reduced with the help of octadecyl amino methanol (ODAM). ODAM here played the role of both reducing agent and stabilizer. The precursor solution of gold(III) chloride hydrate was prepared in isopropanol, and this was added to reductive solution consisting of ODAM in cyclohexane and formaldehyde prepared separately. The addition of precursor solution to reductive solution was done either by electrospray method in which the precursor solution was sprayed as fine mist, or by capillary technique in which the precursor solution was added to reductive solution as a continuous flow. The gold nanoparticles produced by capillary method showed a polydisperse sample, and that produced by electrospray technique had a monodisperse and much smaller particle size (Soliwoda et al. 2015).

3.3 Surfactant-Aided Preparation of Gold Nanoparticles

Gold nanoparticles can be prepared using surfactant to get nanorods using electrochemical technique or seed-mediated technique. Electrochemical technique yields higher amount of gold nanorods as compared to seed-mediated growth method.

3.3.1 Seed-Mediated Growth Method

Seed-mediated growth method employs formation of seed solution initially, which is subsequently added to growth solution to allow the nanoparticles of required dimensions to grow. Nikoobakht et al. prepared seed solution of CTAB and $HAuCl_4$ in reducing agent solution $NaBH_4$ at room temperature. After this, $HAuCl_4$ was added in the growth solution consisting of CTAB and $AgNO_3$ and mixed. To this solution, a mild reducing agent (ascorbic acid) was added and mixed till color changed from dark yellow to colorless. To this solution, finally, the seed solution was added, which resulted in preparation of nanorods after 20mins of mixing at room temperature. The nanorods formed had an aspect ratio of length to width of 4.7 and had plasmon bands less than 850 nm.

In the same study, another approach to prepare nanorods of plasmon width more than 850 nm was utilized. A mixture of surfactants consisting of benzyldimethylhexadecylammonium chloride (BDAC) and CTAB was used to which $AgNO_3$ was added. Following this, $HAuCl_4$ was added and mixed gently, and to this solution, the mild reducing agent ascorbic acid was added. To this solution, the seed solution was added that resulted in completion of growth of nanorods after 1 h. The preparation by this method resulted in obtaining nanorods having plasmon width more than 850 nm and lesser nanospheres in the solution (Nikoobakht and El-Sayed 2003).

3.3.2 Electrochemical Method of Preparation

Electrochemical method of preparation employs the use of cathode and anode plates in an electrolyte solution. Yu et al. utilized gold plates as anode and platinum plates as cathode in an electrolyte surfactant solution hexadecyltrimethylammonium bromide (CTAB), which was cationic in nature. CTAB played the role of cationic electrolyte solution, rod-shaped inducing agent, and stabilizer of formed nanoparticles. A current of 3A for a time of 30 min was employed to produce electrolysis that resulted in conversion of bulk gold from anode to gold nanoparticles in the interface of cathode and electrolyte solution. The synthesis was carried out under ultrasonication at 38 °C. Acetone was added as cylinder-shape inducing agent in the micellar structure of CTAB that resulted in formation of Au nanorods (Yu et al. 1997).

3.4 Sonochemical-Assisted Reduction of Gold Nanoparticles

Sonochemical technique is based on the use of ultrasound to create microbubbles and cavitation in them due to high temperature leading to generation of radicals. In water, it leads to formation of H^+ and OH^- ions. The radicals reduce the Au^{3+} to Au^0 to form the gold nanoparticles. Okitsu et al. found that the use of organic solvents in such conditions accelerated the formation of gold nanoparticles. The formation of gold nanoparticle was achieved by reducing $NaAuCl_4$ in the presence of 2-propanol. The ultrasonic bath was maintained at constant temperature at 200 kHz and 200 W. 2-Propanol is converted to reducing radical generated by pyrolysis in the presence of ultrasonic conditions (Okitsu et al. 2001).

$$\left(CH_3\right)_2 CHOH + {}^{\bullet}OH + {}^{\bullet}H \rightarrow \left(CH_3\right)_2 COH \rightarrow \text{Pyrolysis radicals}$$

These pyrolysis radicals reduce the Au^{3+}:
gold(III) + reducing radical → gold(II)
gold(II) + reducing radical → gold(I)
gold(I) + reducing radical → gold(0)

3.4.1 Sonochemical-Assisted Chemical Reduction Using Ionic Liquid

Jin et al. used sonochemistry-based acoustic cavitation phenomenon to produce gold nanoparticles with the aid of H_2O_2 as a reducing agent in the presence of ionic liquid that acted as a gold capturing agent. Ionic liquids which have the ability to become miscible with organic as well as aqueous solution due to their dual characteristic to change their cationic and anionic character acted as green solvent. The thiol-linked ionic liquids could produce gold nanoparticles in the size range of 2–5 nm. Briefly, thiol-functionalized ionic liquid [1-(2′, 3′-dimercaptoacetoxypropyl)-3-methylimidazolium, 3″-mercapto-1″-propanesulfonic acid (TFIL)] was treated with aqueous solution of $HAuCl_4$ (0.25 mM, 5 ml) at different concentrations corresponding to the Au/S molar ratio of 2:1, 1:1, 1:2, 1:4, and 1:8, respectively. After stirring for 5 min, reducing agent H_2O_2 was added to the ionic liquid solution containing precursor $HAuCl_4$ acid. Subsequently, the solution was placed in ultrasonic bath with circulating water at 25 °C. Sonochemical treatment of 40 KHz and 80 W was provided that resulted in the change of color of solution from light yellow to red. The prepared AuNP stayed stable for several weeks without precipitation. Characterization using TEM analysis revealed the least particle size was obtained in an Au/S

ratio of 1:2 wherein the size of particles was around 3 nm (Jin et al. 2007).

3.5 Green Method–Based Reduction

Metal ions of iron, silver, gold, etc., have been reduced using extracts of plants like *Jasminum sambac*, *Rosa rugosa*, *Magnolia kobus* and *Diospyros kaki*, *Ocimum sanctum*, *Aerva lanata*, *Coriandrum sativum*, *Phyllanthus*, and henna. The secondary metabolites present in these plants serve as both reducing agent and stabilizing agent after the AuNP is formed. In a particular study by Yulizaret al., the *Polyscias scutellaria* leaves acted to reduce precursor gold solution. Initially, the *Polyscias scutellaria* leaves were extracted in a mixture of organic and aqueous solvents. Different fractions of extract were then used to reduce $HAuCl_4$ solution in the presence of UV radiation (Yulizar et al. 2017).

Dzimitrowicz et al. utilized plants of *Lamiaceae* family, *Mentha piperita*, *Salvia officinalis*, and *Melissa officinalis*, which are members of the *Nepetoideae* subfamily, to prepare extracts in the synthesis of gold nanoparticles. Components like hydroxyl group of phenolic compounds, secondary amines, and nitriles of the extract play the role of a reducing agent in reducing Au^{+3} to Au^0. The leaves of the plants were extracted in double distilled water, and then the precursor solution $HAuCl_4$ was treated with it. Further reduction in size of AuNP was anticipated by the use of direct current atmospheric pressure glow micro-discharge (dc-APGD). Discharge system was constructed of argon nozzle microjet which acted as anode and a flowing liquid as cathode which was the AuNP solution treated with plant extract. But the use of dc-APGD resulted in rise in particle size.

Apart from this, research on the use of several other plants and their extracts in production of gold nanoparticles has been carried out (Table 18.1), with a perspective of obtaining a safe and biocompatible final product.

3.6 Physical Techniques to Prepare Gold Nanoparticles

Physical techniques are majorly top-down techniques that synthesize nanoparticles from larger sized bulk gold. Laser ablation is the most frequently employed technique to get AuNP from bulk gold. Unlike wet chemistry, initially, prepared gold nanoparticles were without surfactant, which led to highly polydisperse and aggregated nanoparticles. Mafune et al. synthesized sodium dodecyl sulfate stabilized laser-irradiated gold nanoparticles. Laser ablation at 1064 nm was employed in a surfactant SDS solution containing gold plate of 99.9% purity. The laser fluence used was of the power of 800 mJ/pulse/cm^2 that led to the formation of gold nanoparticles of 8.0 nm. This was further subjected to laser-induced fragmentation in which a laser irradiation of 532 nm was employed. The photons of this laser interacted with the electrons of the nanoparticles which led to heating of the nanoparticle to its boiling point. This leads to formation of fragments that allow the growth of nanoparticles (Mafuné et al. 2002).

Gold nanoparticles have also been prepared by similar laser ablation technique in pure water. Gold plates were exposed to laser wavelengths of 532 nm with different optical energy of 10–250 J/cm^2 and 5–40 J/$cm^2$and then further exposed to laser of 532 nm and 266 nm. The laser implication on gold plate resulted in ablation-induced plume formation of gold atoms and clusters over the surface of the plate. These atoms and clusters tend to form embryonic nanoparticles and subsequently grow into nanoparticles. Gold nanoparticles having size less than 15 nm could be achieved by this process in pure water without the use of surfactants (Tarasenko et al. 2006).

Table 18.1 Gold nanoparticles synthesized by green method

Sr. no	Source	Description	Size of AuNP	Shape of AuNP	References
1	*Plumeria alba* flower extract (PAFE)	Aqueous extract of 1% PAFE and 5% PAFE was utilized in which the amine groups of the phytoconstituents acted as reducing agents.	Size with 1% PAFE = 28 ± 5.6 and size with 5% PAFE = 15.6 ± 3.4 nm	Spherical	Mata et al. (2016)
2	Fructus Amomi (cardamom)	Aqueous extract of Fructus Amomi and its constituents like phenols, tannins, and terpenoids were responsible for reduction and capping of gold nanoparticles.	269.9 nm	Spherical	Soshnikova et al. (2018)
3	Thermophilic filamentous fungi	The cell-free protein extracts, mycelia of the fungi were used for reduction of gold.	1–80 nm	Spherical and hexagonal	Molnár et al. (2018)
4	*Staphylococcus warneri*	The intracellular protein extract of *Staphylococcus warneri* was utilized to reduce the precursor gold solution.	81 nm	Spherical	Nag et al. (2018)
5	Marine red algae	Carrageenan oligosaccharide (CAO) from red algae acted as reducing agent and stabilizing agent on formed AuNP.	35 ± 8 nm	Ellipsoidal shape	Chen et al. (2018)
6	Hyperbranched polymers	Hyperbranched polyethylenimine-terminal isobutyramide (HPEI-IBAm) acted as a template and its amine group as reducing agent. Overall HPEI-IBAm also acted as a stabilizing agent for gold nanoparticles.	–	Spheroid shape	Liu et al. (2018)
7	Marine red seaweed *Gracilaria verrucosa*	Aqueous extract of *G. verrucosa* which contained various protein, phenolic, and aromatic constituents was responsible for reducing and stabilizing AuNP.	73.12 nm	60% spherical shapes and 20% triangular shapes were obtained	Chellapandian et al. (2019)
8	Vitamin B8 (inositol)	Inositol which is a strong reducing agent oxidizes itself to produce inosose form to reduce gold nanoparticles.	1.95 nm	Spherical	Halawa et al. (2018)
9	Mannan polysaccharide	Mannan polysaccharide acted as reducing, capping, as well as stabilizing agent for prepared AuNP.	9.18 ± 0.71 nm	Spherical	Uthaman et al. (2018)
10	*Ziziphus zizyphus*	Aqueous leaf extract of *Ziziphus zizyphus* and its phytoconstituents acted as reducing agent to form gold nanoparticles.	51.8 ± 0.8 nm	Majorly spherical shapes. Triangular and hexagonal platelet shaped also observed	Aljabali et al. (2018)

(continued)

Table 18.1 (continued)

Sr. no	Source	Description	Size of AuNP	Shape of AuNP	References
11	*Artemisia dracunculus* (tarragon)	The aqueous leaf extracts of *Artemisia dracunculus* which contained phenolic and flavonoid compounds were responsible for reducing the precursor gold solution.	Different shapes had different sizes and range was 30–100 nm	Spherical, hexagonal, triangular, nanobox shaped	Wacławek et al. (2018)
12	*Annona squamosa* L (AS)	The peel of fruit extracts of *Annona squamosa* L (AS) containing hydroxyl and carbonyl functional groups in its constituents acted as reducing as well as stabilizing agent for formation of gold nanoparticles in the presence of microwave irradiation.	5–10 nm	Spherical	Gangapuram et al. (2018)
13	*Eucalyptus globulus and Rosmarinus officinalis*	Aqueous extracts and natural essential oils of both *Eucalyptus globulus and Rosmarinus officinalis*	i. *E. globulus* – aqueous extract, 12.8 nm Natural oil, 42 nm ii. *R. officinalis* Aqueous extract, 8.66 nm Natural essential oil, 60.7 nm	i. Majorly spherical shaped for aqueous extracts ii. Essential oil extract showed majorly spherical but also triangular, rods, etc.	Dzimitrowicz et al. (2019)
14	*Chaenomeles sinensis*	Aqueous fruit extracts of *Chaenomeles sinensis* containing flavonoids and triterpenes were responsible for reducing gold solution and capping of AuNPs.	Core size 40 nm	Spherical, icosahedral	Oh et al. (2018)
15	*Platycodon grandiflorum*	The triterpenoid platycodon saponins from Platycodi Radix through aqueous extract were obtained and used in reducing precursor gold solution.	14.94 ± 2.14 nm	Spherical	Choi et al. (2018)

4 Manufacturing Techniques for Silver Nanoparticles

4.1 Wet Chemistry

4.1.1 Monosaccharide Reduction

There are many methods of AgNP manufacturing; one of those methods is monosaccharide reduction method. In this method, glucose, fructose, maltose, and maltodextrins are used as reducing agents, but sucrose is not used as a reducing agent. It is generally a simple technique which involves the single-step process to reduce silver ion to AgNPs (Iravani et al. 2014). The use of reducing sugar along with alkali and $AgNO_3$ also yields AgNPs at high pH levels. The free aldehyde and ketone in reducing sugar facilitate monosaccharides to get oxidized into gluconate (El-Rafie et al. 2014).

Reducing agents must have a free ketone group which enables them to go through tautomerization (Darroudi et al. 2011). Whereas, if the aldehydes are present in the reducing agents, they will be trapped in cyclic form and do not qualify as reducing agents. For example, glucose has an aldehyde functional group that is able to reduce

silver cations to silver atoms and is then oxidized to gluconic acid. The oxidation reaction for the sugars occurs in aqueous solutions. The capping agent is also not present when heated.

4.1.2 Citrate Reduction

AgNPs are prepared by sodium citrate reduction of $AgNO_3$. One of the most common methods of manufacturing AgNPs is citrate reduction. M. C. Lea, in 1889, for the first time successfully developed a citrate-stabilized silver colloid (Graf et al. 2003). Using trisodium citrate, reduction of silver nitrate or silver perchlorate to colloidal silver can be done. The synthesis is normally done at higher temperature (~100 °C) to increase the monodispersity of the particle considering the size and shape of the particles (Wojtysiak and Kudelski 2012). The citrate ion acts as a reducing agent as well as a capping agent, making it a valuable agent in the production of AgNPs owing to its very brief reaction period (Nowack et al. 2011). However, the silver particles have wide size distribution with different geometrical shapes. To obtain uniform size and shape particles, addition of stronger reducing agents to the reaction is often used (Wojtysiak and Kudelski 2012; Jin and Dong 2003).

4.1.3 Reduction by Sodium Borohydride

The following reaction takes place in the synthesis of AgNPs using $NaBH_4$ as a reducing agent:

$$Ag^{+} + BH_4^{-} + 3H_2O \rightarrow Ag0 + B(OH)_3 + 3.5H_2$$

Metal atom forms the nanoparticle nuclei, and this reduction mechanism is similar to that of the reduction using citrate. The advantage of using sodium borohydride over citrate is that it provides improved monodispersity of the nanoparticles. The rationale behind the improved monodispersity is the strong behavior of $NaBH_4$ than citrate as a reducing agent (Bahrig et al. 2014). The effect of reducing agent strength can be observed by studying a LaMer diagram which illustrates the nucleation and growth of nanoparticles. The development of nucleation and growth through the LaMer mechanism is split into three steps:

(I) Rapid growth in the concentration of free monomer in the solution.
(II) The monomer undergoes burst nucleation which drastically decreases the concentration of free monomers in solution. The rate of this nucleation is described as "effectively infinite," and after this point, there is almost no nucleation occurring due to the low concentration of monomers after this point.
(III) Following nucleation, growth occurs under the control of the diffusion of the monomers through the solution (Thanh et al. 2014).

When weak reducing agent like citrate is used, there is simultaneous new nuclei formation and growth of earlier nuclei (Liu et al. 2009; Bastús et al. 2011). This is the main reason behind the decreased monodispersity of nuclei with citrates. A strong reducing agent like $NaBH_4$ provides nuclei formation in shorter duration of time and a good yield potential of monodispersed AgNPs (Song et al. 2009). Particles produced by using reducing agents must have surface stabilization in order to avoid unwanted particle cluster or bonding with each other, growth, or coarsening (Jana et al. 2001; Mallick et al. 2001). Since the nanoparticles have greater surface area to volume ratio, they may allow rapid agglomeration, and this can be prevented by diminishing the surface energy (Bahrig et al. 2014). This decrease in surface energy can be responded by adding an agent which will be adsorb to the surface of the nanoparticles and decreases the activity of the particle surface, thus inhibiting particle agglomeration according to the DLVO theory (Jana et al. 2001; Kim et al. 2005). Chemicals which adsorb to the nanoparticle surface are referred as ligands. For example, $NaBH_4$ in large quantities, polyvinylpyrrolidone (PVP) (Pierrat et al. 2007), SDS (Song et al. 2009; Pierrat et al. 2007), and dodecane thiol. There are number of general methods to eliminate nanoparticles from solution; this can be done by evaporating the solvent or by adding a chemical entity in the solution that decreases the

solubility of the nanoparticles. These methods lead to precipitation of the nanoparticles.

4.1.4 Polyol Process

This method of manufacturing is important where the size and the shape of the nanoparticles are the most important aspects and a narrow size distribution is desired. Generally, this synthesis begins with the heating of a polyol such as ethylene glycol, 1,5-pentanediol, or 1,2-propylene glycol, Ag^+ source, and a capping agent. The Ag^+ source is reduced by the polyol to form a colloidal nanoparticle (Wiley et al. 2004). This method is extremely susceptible to reaction parameters like change in temperature, chemical nature, and concentration of reactants (Leonard et al. 2005). Therefore, the size and shape of the nanoparticles can be controlled, and varied shapes of particles like quasi-spheres, pyramids, spheres, and wires can be produced by changing these variables (Leonard et al. 2005; Coskun et al. 2011; Smetana et al. 2005).

4.1.5 Seed-Mediated Process

This is a synthetic method which produces the small, stable nuclei in a separate chemical environment to a desired size and shape. It consists of two steps, namely, nucleation and growth. This synthetic process of manufacturing is more popular in controlling the morphology of nanoparticles; this can be easily achieved by varying the following factors in the process like ligand, nucleation reaction time, and concentration of reducing agent (Wu et al. 2016). The nucleation step of seed growth comprises the reduction of metal ions to metal atoms. Period of nucleation needs to be kept short in order to control the size distribution of the seeds and to get monodispersity of particles. This can be studied using the LaMer model (Thanh et al. 2014; LaMer and Dinegar 1950). Smaller nanoparticles referred to as seeds are typically stabilized by the ligands, which are usually small organic molecules attached to the surface of the nanoparticles that prevent the seed growth. Ligands prevent particle agglomeration by increasing the energy barrier of coagulation. Ligand binding attraction and selectivity can be utilized to monitor geometry and growth of nanoparticles. The balance among attractive and repulsive forces in colloidal solutions is demonstrated by the DLVO theory (Kim et al. 2005). The ligand to be used in seed synthesis should have medium to low binding affinity to allow for exchange during the growth phase. Nano-seeds can be produced by positioning the seeds in a growth solution comprising a low concentration of a metal source and ligands. The ligands will readily exchange with active seed ligands and a low concentration of weak reducing agent. Growth is the outcome of the competition among surface energy and bulk energy. The balance between the energy of growth and dissolution is the rationale for uniform growth only on active seeds (Navrotsky 2004). Growth occurs by the accumulation of metal atoms from the growth solution to the seeds and ligand exchange between the growth ligands and the seed ligands (Liu et al. 2009). Ultimately, to control the size and geometry of the nanoparticles, parameters to be controlled include the concentration of metal precursor and ligand and reaction conditions. Anisotropic particles, i.e., nonspherical particles, can be the result of dissimilar growth in the particles (Bastús et al. 2011).

4.1.6 Light-Mediated Process

Generation of AgNPs from Ag^+ is mainly dependent upon the redox potential of the reducing agents (Wu et al. 2008). Agents with greater negative redox potential than Ag^+ will rapidly produce AgNPs by reducing the Ag^+. It is proven that light has enormous capability to obtain, energize, and bring electrons from water to reduce various ions. This ability of light can be exploited to reduce Ag^+. This light-mediated method supports the reduction of Ag^+ to Ag^0 and also helps prompt oxidation of Ag^0 to Ag_2O by release of oxygen through photolysis of water to produce biphasic AgNPs (Manikprabhu et al. 2016).

4.1.7 Silver Mirror Reaction

This manufacturing technique involves conversion of $AgNO_3$ to $Ag(NH_3)OH$ which is further reduced to colloidal silver in the presence of sugar containing aldehyde group (Qu and Dai 2005). The size and geometry of the produced

nanoparticles is a challenge to control, and frequently, the particles have wide distribution range. However, this manufacturing method is frequently used for thin coatings of silver nanoparticles onto surfaces (Li et al. 2012).

4.1.8 Ion Implant

This method is widely used to create AgNPs implanted in different surfaces like glass, polyurethane, silicone, polyethene, and poly(methyl methacrylate). Particles are implanted onto the surface using high accelerating voltage with constant current density of ion beam which produces the monodisperse AgNPs. An additional increase in the ion beam dosage can reduce the nanoparticle size and density onto the target material, whereas an ion beam working at a high accelerating voltage with a slowly rising current density is found to yield an increase in the nanoparticle size (Popok et al. 2005). There are a few proposed mechanisms that can result in the lower nanoparticle size. These are destruction of AgNPs on collision to the material, splitting of the sample surface, particle fusion upon heating, and dissociation. It involves processes of diffusion and clustering which can be divided into separate subprocesses like implantation, diffusion, and growth. High temperature in implantation process will increase the impurity (Stepanov 2010). Implant temperature and ion beam current density are critical in order to achieve a monodisperse nanoparticle size. After implantation on the surface, the beam currents can be increased as the with increase in surface conductivity. This is followed by diffusion of nanoparticles in the material surface. This diffused particle now acts as a seed for the growth of the uniform monodispersed nanoparticles.

4.2 Biological Route

The major requirement for the production of silver nanoparticle through the biological source is resistance of the organism to silver ions (Rai and Duran 2011; Gahlawat and Choudhury 2019). The usual fabrication method of nanoparticles involves either "top-down" or "bottom-up strategy" (Ahmed et al. 2016a). Biological method for synthesizing nanoparticles has become a promising substitute for established techniques (Singh et al. 2016). The microbial route provides an inexpensive and reliable way for producing nanoparticles with various sizes, shapes, compositions, and physicochemical compositions (Pattanayak et al. 2013). Biosynthesizing of nanoparticles does not require capping or stabilizing agent as the biomolecules perform the function themselves (Sintubin et al. 2012; Mukherjee et al. 2012; Zsembik 2005).

4.2.1 Synthesis of AgNPs Through Bacteria and Fungi

Microbial synthesis of AgNPs can occur intracellularly or extracellularly (Roy et al. 2019). Intracellular production of AgNPs occurs after the accumulation of silver inside the cell. Accumulation of silver leads to nucleation of AgNPs inside the live microbial cells. The cells are harvested for an optimum time before they are given special treatment to release synthesized nanoparticles (Roy et al. 2019). The extracellular secretion plays an important role in the synthesis of AgNPs. Although the exact mechanism is unknown, proposed mechanism involves reduction of the Ag^+ ions in the presence of several biomolecules such as enzymes, proteins, amino acids, polysaccharides, and vitamins. The most accepted mechanism is based on the presence of enzyme nitrate reductase (Jin and Dong 2003; Kumar et al. 2007; Pandian et al. 2010; Kalimuthu et al. 2008; Rai et al. 2008). Nitrate reductase, an enzyme of the nitrogen cycle, is responsible for the conversion of nitrate (NO_3^-) to nitrite (NO_2^-) (Durán et al. 2005). During this conversion, the generated electron gets transferred to free silver ion (Ag^+) reducing it to (Ag^0) (Iijima and Ichihashi 1993; Hutchison et al. 2001; Roy et al. 2019). The use of specific enzyme α-NADPH (nicotinamide adenine dinucleotide phosphate)-dependent nitrate reductase as a homogenous catalase in the synthesis of nanoparticles plays an important role by down-streaming the process (Zomorodian et al. 2016; Baymiller et al. 2017). The most preferred method for the biosynthesis is extracellular route as it does not require

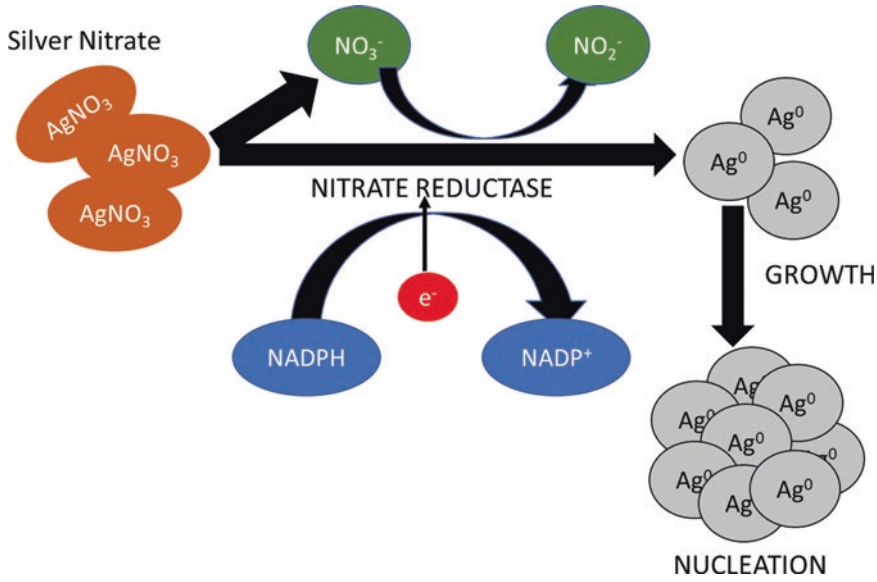

Fig. 18.1 Mechanism of nitrate reductase

extraction of prepared AgNPs from the cells (Guilger-Casagrande and de Lima 2019). Once the method for manufacturing gets established, high yield can be obtained by performing optimization of temperature, pH, biological load, etc. Figure 18.1 depicts the nitrate reductase mechanism helpful in the synthesis of AgNPs.

Bacteria

For the production of AgNPs from bacterial colonies, an Erlenmeyer flask containing Luria Bertani medium (LB) or Luria-Bertani medium plus nitrate (LBN) or Luria-Bertani medium plus lactose (LBE) or nutrient broth or Mueller-Hinton broth is used for sufficient time at 37 °C at 100 rpm. The obtained bacterial suspension is centrifuged between 5000 and 15,000 rpm for 10 min to obtain cell-free supernatant. Different concentration of silver nitrate solution with a maximum concentration of 1 mM is added to the supernatant solution in a different Erlenmeyer flask, and cell-free suspension is added to the flask. These flasks and their positive, negative controls are subjected to incubation at 37 °C at 100 rpm for sufficient time. Light or dark conditions are maintained depending upon the type of bacteria. Production of AgNPs can be confirmed with visual color change from light brown to dark brown and through ultraviolet-visible spectroscopic method of analysis (Zomorodian et al. 2016; Baymiller et al. 2017; Guilger-Casagrande and de Lima 2019; Deljou and Goudarzi 2016; Eswari et al. 2018; Hamouda et al. 2019; Kumar et al. 2016; Sani et al. 2017; Das et al. 2014; Siddiqi et al. 2018; Abostate and Partila 2015; Baltazar-Encarnación et al. 2019; Khaleghi et al. 2017). AgNPs of varying shapes were developed by researchers working on different bacterial colonies. Most of the findings report that the AgNPs were spherical having a particle size between 1 and 50 nm (Gahlawat and Choudhury 2019). Some researchers reported that triangular and hexagonal AgNPs could also be obtained using *Pseudomonas stutzeri*, a special type of bacteria found in the silver mines (Klaus et al. 1999). The bacterial colonies which were explored for the synthesis of AgNPs include *Pseudomonas aeruginosa*, *Brevibacterium casei*, *Bacillus cereus*, *Gluconacetobacter xylinus*, *Streptomyces coelicolor*, *Bacillus subtilis*, *Salmonella typhimurium*, *Bacillus atrophaeus*, *Lactobacillus rhamnosus*, *Gordonia amicalis*, *Actinobateria* sp., *Sinomonas mesophila*, *Nocardiopsis flavescens*, *Streptomyces griseo-*

planus, *Phanerochaete chrysosporium*, *Weissella oryzae*, *Serratia nematodiphila*, *Ochrobactrum* sp., *Shewanella loihica*, *Escherichia coli*, *Klebsiella pneumoniae*, and *Deinococcus radiodurans* (Gahlawat and Choudhury 2019; Zsembik 2005; Singh 2019).

Fungi

Fungi are an attractive and efficient source for the synthesis of AgNPs. They have a higher resistance to metals, and their extracellular protein and enzyme secretion is comparatively higher than bacterial colonies (Balaji et al. 2009; Netala et al. 2016; Du et al. 2015). Fungi produce a larger volume of biomass which is easy to filter and possess resistance to agitation and pressure in comparison to bacterial biomass (Gade et al. 2008; Velusamy et al. 2016). Fungi can be cultivated at large scale and lead to production of nanoparticles with controlled size and morphology (Velusamy et al. 2016; Ahluwalia et al. 2014; Satish et al. 2015). Similar to the process discussed for intracellular synthesis using bacterial colonies, metal precursor is added to the mycelial culture. Consequently, the internalization of precursor promotes formation of AgNPs. Nanoparticles are extracted by using chemical treatment, centrifugation, and filtration (Molnár et al. 2018; Castro-Longoria et al. 2011; Rajput et al. 2016).

Briefly, extracellular synthesis of AgNPs from fungi involves the growth of mycelium in Erlenmeyer flask over suitable media such as Vogel's Minimal Medium, Malt Extract Broth, Potato Dextrose Broth, seed medium, malt extract glucose yeast peptone media. The media are supplemented with glucose and peptone to enhance mycelium production. Fungi are allowed to grow for 48–96 h at 32 °C, and later growth media are separated by centrifugation at 5000 x g (rcf) to 10,000 x g for 10 min. The biomass is filtered through Whatman filter paper no. 1 or 3, resuspended in distilled water for 24–48 h, and filtered again. To the filtrate, silver nitrate at a maximum concentration of 1 mM is added and allowed to convert into AgNPs. The conversion is checked visually or by UV-Vis spectroscopic analysis between 400 and 450 nm (Gade et al. 2008; Castro-Longoria et al. 2011; Singhal et al. 2011; Sintubin et al. 2009; Gudikandula et al. 2017; Vahabi et al. 2011; Gudikandula and Charya Maringanti 2016; Ottoni et al. 2017; Elamawi et al. 2018; Shaligram et al. 2009; Rose et al. 2019).

AgNPs synthesized from fungi have spherical, quasispheroidal, hexagonal, pseudospherical, cubical, cuboctahedral, icosahedral, rod-shaped, irregular, roughly spherical, oval, and ellipsoidal shapes. The typical particle size of nanoparticles can be as low as 5 nm and goes up to 200 nm (Rai and Duran 2011; Gahlawat and Choudhury 2019; Roy et al. 2019; Singh 2019; Ovais et al. 2018). The size of nanoparticles depends upon the species, temperature, pH, dispersion medium, and presence or absence of a capping agent (Khandel and Shahi 2018; Lee and Jun 2019). The fungal species explored till date for the synthesis are *Penicillium* sp., *Curvularia lunata*, *Raphanus sativus*, *Pleurotus ostreatus*, *Cryptococcus laurentii*, *Candida* sp., *Rhodotorula* sp., *Saccharomyces cerevisiae*, *Trichoderma harzianum*, *Aspergillus foetidus*, *Cladosporium* sp., and *Rhizopus stolonifer* (Rai and Duran 2011; Gahlawat and Choudhury 2019; Roy et al. 2019; Singh 2019; Ovais et al. 2018).

The production yield can be optimized by the culture conditions such as rate of agitation, time, temperature, pH, the quantity of biomass, and the concentration of silver nitrate (Zielonka and Klimek-Ochab 2017). Temperature plays a vital role in affecting the biomass and rate of conversion of Ag^+ to Ag^0. Certain microbes showed linear relation between temperature and amount of biomass. The time required for synthesis considerably decreases, and rate considerably increases with increase in temperature, indicating faster and scalable process (Elamawi et al. 2018; Almasaudi 2018; Birla et al. 2013). During the synthesis, adjustment of pH helps in modifying various characters of nanoparticles (Nayak et al. 2011). Higher pH allows higher stabilization of metal ion, resulting in increase in production at alkaline pH (Sintubin et al. 2009). Ideal concentration of silver nitrate as a precursor in extracellular scheme is 1 mM (Saxena et al. 2016). Some researchers have confirmed that smaller nanopar-

ticles are synthesized with lower levels of metal precursor; however, contrasting results were obtained with some species (Phanjom and Ahmed 2017). The amount of biomass may or may not affect the synthesis and characters of AgNPs. Some cases reported that lower biomass content yielded higher number of nanoparticles, while other reports showed the opposite (Elamawi et al. 2018; Birla et al. 2013; Balakumaran et al. 2015). Therefore, it is important to optimize the amount of biomass responsible for desired physicochemical characteristics of the AgNPs.

4.2.2 Biological Synthesis of AgNPs: Through Plants

Synthesis of AgNPs through plant source is eco-friendly, nonpathogenic, rapid, and economical. Plants have several primary and secondary metabolites such as proteins, amino acids, enzymes, carbohydrates, polysaccharides, alkaloids, tannins, phenolics, saponins, terpenoids, and vitamins (Kulkarni and Muddapur 2014; Sun et al. 2014). These agents act as reducing agents and stabilizers during the synthesis of AgNPs.

For the synthesis of AgNPs, the plant part is collected and washed multiple times such as twice or thrice with water which removes epiphyte, necrotic plants, and debris. The clean plant parts are dried in sunshade for sufficient time, specifically 10–15 days. The dried crushed plant parts with increased surface area are boiled with water to liberate plant components. The resulting solution is filtered to collect infusion media. The infusion media are then mixed with different concentrations of silver nitrate with a maximum level up to 1 mM. The conversion of Ag^+ ions to Ag^0 is monitored visually with time and quantified through UV-visible spectroscopic analysis between 400 and 450 nm (Hebbalalu et al. 2013; Eisa et al. 2019; Dhand et al. 2016; de Barros et al. 2018; Chung et al. 2016; Allafchian et al. 2016; Christopher et al. 2015; Ahmed et al. 2016b).

AgNPs have been prepared using various plant parts such as leaves, seeds, peel, fruit, rhizomes, whole plant, and inflorescence. Although most of the researchers obtained spherical AgNPs using plant extract, other shapes of the AgNPs obtained were quasispheroidal, flower-shaped, triangular, pentagonal, hexagonal, circular, and quasilinear. The size of the AgNPs obtained was as low as 0.5 nm and as high as 350 nm. Some researchers have reported the biological activity of AgNPs from plant origin having a particle size below 50 nm (Sintubin et al. 2012; Allafchian et al. 2016). Some of the plants from which nanoparticles have been prepared are *Acorus calamus*, *Boerhaavia diffusa*, tea extract, *Tribulus terrestris*, *Cocos nucifera*, *Abutilon indicum*, *Cymbopogon citratus*, *Acalypha indica*, *Centella asiatica*, *Argyreia nervosa*, *Brassica rapa*, *Vitex negundo*, *Melia dubia*, *Thevetia peruviana*, *Pogostemon benghalensis*, *Trachyspermum ammi*, *Swietenia mahagoni*, *Moringa oleifera*, *Acalypha indica*, *Allium sativum*, aloe vera, *Eucalyptus* hybrid, *Datura metel*, *Carica papaya*, and *Nelumbo nucifera (*Allafchian et al. 2016*).*

4.3 Product and Functionalization

Production of AgNPs can be synthetically modified to yield nonspherical and functionalized AgNPs with materials such as silica. Functionalization benefit in producing surface-modified AgNPs includes different types of coatings, sizes, and shapes.

4.3.1 Anisotropic Structure

Anisotropic AgNPs can be prepared because silver exhibits localized surface plasmon resonance (LSPR) because of its smaller size.

Most of the methods used for the synthesis of AgNPs involve seed mediation approach, i.e., synthesizing smaller nanoparticle, usually between 3 and 5 nm. These AgNPs can be grown into larger nanoparticles having a triangular shape. Synthesis of these AgNPs involves physical admixture of $AgNO_3$ and sodium citrate in aqueous media followed by rapid addition of $NaBH_4$. This initiates the production of AgNPs. An additional amount of $AgNO_3$ is added to the seed solution at low temperature yielding generation of triangular AgNPs with modulation of excess $AgNO_3$ with ascorbic acid (Dong et al. 2010). Photo mediation can also transform existing AgNPs into a triangular shape

by exposing the reaction mixture to high-intensity light (Xue et al. 2008).

This seed mediation process can be modified by altering the reducing as well as capping agent. Cube-shaped and rod-shaped AgNPs can be produced by using reducing agent such as ethylene glycol and PVP as capping agent (Chang et al. 2011; Zeng et al. 2010). Ageing $AgNO_3$ solution before being used benefits in the production of wire-shaped AgNPs (Chang et al. 2011).

4.3.2 Coating with Silica

AgNPs can be coated with silica by adsorbing PVP over the surface of AgNPs by mixing them with an aqueous solution of PVP. Separation of PVP-coated AgNPs can be mediated through centrifugation process. The coated AgNPs are stirred in a solution containing ethanol, ammonia, and tris(hydroxymethyl)methyl]-2-aminoethanesulfonic acid (TES) to promote formation of surrounding layer of ether-linked silicon dioxide. Modifications in the amount of TES can produce shells of varying thickness (Graf et al. 2003).

5 Concluding Remarks and Future Perspectives

Tremendous research is ongoing on CNTs, AuNPs, and AgNPs for the treatment of various diseases. However, the challenges like reproducibility, scalability, cost-effectiveness, etc., need to be strengthened for commercialization of these products in the market. AuNPs have been prepared by different methods, and the most facile method to prepare is by chemical reduction technique. Chemical reduction technique faces issues like reproducibility and concentration-dependent toxicity which needs to be monitored. Physical methods like laser ablation and sonochemical-assisted reduction give narrow particle size range as well but are expensive. Green method-based reduction has been amply explored as it does not use chemicals that can pose a risk of toxicity. Recent years have witnessed the use of AuNPs in imaging along with therapy which necessitates that the prepared AuNPs are pure, stable, and nontoxic. Over the years, AgNPs have been synthesized from $AgNO_3$ using physical, chemical, and biological methods. These techniques involve the conversion of $AgNO_3$ to elemental state followed by growth of nanoparticles. Physical and chemical methods of AgNP synthesis are costly and involve usage of hazardous chemicals. In turn, biological method is helpful in synthesizing AgNPs, is cost-effective, stable, quick, and nontoxic, and produces higher yield. Biological methods can be modified to generate AgNPs having size between 0.5 nm and 500 nm and various shapes. However, there could be concerns about industrial scalability with these methods to provide uniform size and shape of nanoparticles. We expect that with the newer technology, polymers, and targeting, it is expected that more products will be available in the market by 2025.

Acknowledgment The authors would like to acknowledge Institute of Pharmacy, Nirma University, Ahmedabad, for providing PhD research facilities to Mr. Chetan Dhal, Mr. Chintan Pansara, Mr. Kartik Hariharan, and Mr. Namdev Dhas. The authors also acknowledge the Council for Scientific and Industrial Research for providing Senior Research Fellowship to Mr. Chetan Dhal (09/1048(008)/2018 EMR-I) and Mr. Namdev Dhas (09/1048(007)/2018 EMR-I). The authors also acknowledge Nirma University for providing Junior Research Fellowship to Mr. Chintan Pansara and Mr. Kartik Hariharan.

Conflict of Interests The authors have no conflict of interest.

References

Abostate M, Partila A. Microbial production of silver nanoparticles by Pseudomonas aeruginosa cell free extract. J Ecol Health Environ. 2015;3:91–8.

Afolabi A, Abdulkareem A, Mhlanga S, Iyuke S. Synthesis and purification of bimetallic catalysed carbon nanotubes in a horizontal CVD reactor. J Exp Nanosci. 2011;6(3):248–62.

Ahluwalia V, Kumar J, Sisodia R, Shakil NA, Walia S. Green synthesis of silver nanoparticles by Trichoderma harzianum and their bio-efficacy evaluation against Staphylococcus aureus and Klebsiella pneumonia. Ind Crop Prod. 2014;55:202–6.

Ahmed S, Ahmad M, Swami BL, Ikram S. A review on plants extract mediated synthesis of silver

nanoparticles for antimicrobial applications: a green expertise. J Adv Res. 2016a;7(1):17–28.
Ahmed S, Saifullah AM, Swami BL, Ikram S. Green synthesis of silver nanoparticles using Azadirachta indica aqueous leaf extract. J Radiat Res Appl Sci. 2016b;9(1):1–7.
Ajayan P, Lambert J, Bernier P, Barbedette L, Colliex C, Planeix J. Growth morphologies during cobalt-catalyzed single-shell carbon nanotube synthesis. Chem Phys Lett. 1993;215(5):509–17.
Al Hasan NHJ. Methods on preparation of single walled carbon nanotubes. Int Invent Sci J. 2019;3(03):513–9.
Aljabali AA, Akkam Y, Al Zoubi MS, Al-Batayneh KM, Al-Trad B, Abo Alrob O, et al. Synthesis of gold nanoparticles using leaf extract of Ziziphus zizyphus and their antimicrobial activity. Nano. 2018;8(3):174.
Allafchian A, Mirahmadi-Zare S, Jalali S, Hashemi S, Vahabi M. Green synthesis of silver nanoparticles using phlomis leaf extract and investigation of their antibacterial activity. J Nanostruct Chem. 2016;6(2):129–35.
Almasaudi SB. Acinetobacter spp. as nosocomial pathogens: epidemiology and resistance features. Saudi J Biol Sci. 2018;25(3):586–96.
Bahrig L, Hickey SG, Eychmüller A. Mesocrystalline materials and the involvement of oriented attachment–a review. CrystEngComm. 2014;16(40):9408–24.
Balaji D, Basavaraja S, Deshpande R, Mahesh DB, Prabhakar B, Venkataraman A. Extracellular biosynthesis of functionalized silver nanoparticles by strains of Cladosporium cladosporioides fungus. Colloids Surf B Biointerfaces. 2009;68(1):88–92.
Balakumaran M, Ramachandran R, Kalaichelvan P. Exploitation of endophytic fungus, Guignardia mangiferae for extracellular synthesis of silver nanoparticles and their in vitro biological activities. Microbiol Res. 2015;178:9–17.
Baltazar-Encarnación E, Escárcega-González CE, Vasto-Anzaldo XG, Cantú-Cárdenas ME, Morones-Ramírez JR. Silver nanoparticles synthesized through green methods using Escherichia coli top 10 (Ec-Ts) growth culture medium exhibit antimicrobial properties against nongrowing bacterial strains. J Nanomater. 2019;2019
Bastús NG, Comenge J, Puntes V. Kinetically controlled seeded growth synthesis of citrate-stabilized gold nanoparticles of up to 200 nm: size focusing versus Ostwald ripening. Langmuir. 2011;27(17):11098–105.
Baughman RH, Zakhidov AA, De Heer WA. Carbon nanotubes – the route toward applications. Science. 2002;297(5582):787–92.
Baymiller M, Gobble A, Huang F. Rapid one-step synthesis of gold nanoparticles using the ubiquitous coenzyme NADH. Matters. 2017;3(7):e201705000007.
Bethune D, Kiang CH, De Vries M, Gorman G, Savoy R, Vazquez J, et al. Cobalt-catalysed growth of carbon nanotubes with single-atomic-layer walls. Nature. 1993;363(6430):605–7.
Birla SS, Gaikwad SC, Gade AK, Rai MK. Rapid synthesis of silver nanoparticles from Fusarium oxysporum by optimizing physicocultural conditions. Sci World J. 2013;2013:1–12.
Braidy N, El Khakani M, Botton G. Single-wall carbon nanotubes synthesis by means of UV laser vaporization. Chem Phys Lett. 2002;354(1–2):88–92.
Brust M, Walker M, Bethell D, Schiffrin DJ, Whyman R. Synthesis of thiol-derivatised gold nanoparticles in a two-phase liquid–liquid system. J Chem Soc Chem Commun. 1994;(7):801–2.
Castro-Longoria E, Vilchis-Nestor AR, Avalos-Borja M. Biosynthesis of silver, gold and bimetallic nanoparticles using the filamentous fungus Neurospora crassa. Colloids Surf B Biointerfaces. 2011;83(1):42–8.
Chang S, Chen K, Hua Q, Ma Y, Huang W. Evidence for the growth mechanisms of silver nanocubes and nanowires. J Phys Chem C. 2011;115(16):7979–86.
Chellapandian C, Ramkumar B, Puja P, Shanmuganathan R, Pugazhendhi A, Kumar P. Gold nanoparticles using red seaweed Gracilaria verrucosa: green synthesis, characterization and biocompatibility studies. Process Biochem. 2019;80:58–63.
Chen X, Zhao X, Gao Y, Yin J, Bai M, Wang F. Green synthesis of gold nanoparticles using carrageenan oligosaccharide and their in vitro antitumor activity. Mar Drugs. 2018;16(8):277.
Choi Y, Kang S, Cha S-H, Kim H-S, Song K, Lee YJ, et al. Platycodon saponins from Platycodi Radix (Platycodon grandiflorum) for the green synthesis of gold and silver nanoparticles. Nanoscale Res Lett. 2018;13(1):1–10.
Christopher JG, Saswati B, Ezilrani P. Optimization of parameters for biosynthesis of silver nanoparticles using leaf extract of Aegle marmelos. Braz Arch Biol Technol. 2015;58(5):702–10.
Chung I-M, Park I, Seung-Hyun K, Thiruvengadam M, Rajakumar G. Plant-mediated synthesis of silver nanoparticles: their characteristic properties and therapeutic applications. Nanoscale Res Lett. 2016;11(1):40.
Coskun S, Aksoy B, Unalan HE. Polyol synthesis of silver nanowires: an extensive parametric study. Cryst Growth Des. 2011;11(11):4963–9.
Darroudi M, Ahmad MB, Abdullah AH, Ibrahim NA. Green synthesis and characterization of gelatin-based and sugar-reduced silver nanoparticles. Int J Nanomedicine. 2011;6:569.
Das VL, Thomas R, Varghese RT, Soniya E, Mathew J, Radhakrishnan E. Extracellular synthesis of silver nanoparticles by the Bacillus strain CS 11 isolated from industrialized area. 3 Biotech. 2014;4(2):121–6.
Das R, Shahnavaz Z, Ali ME, Islam MM, Hamid SBA. Can we optimize arc discharge and laser ablation for well-controlled carbon nanotube synthesis? Nanoscale Res Lett. 2016;11(1):510.
de Barros CHN, Cruz GCF, Mayrink W, Tasic L. Bio-based synthesis of silver nanoparticles from orange waste: effects of distinct biomolecule coatings on size, morphology, and antimicrobial activity. Nanotechnol Sci Appl. 2018;11:1.

Dekker C. Carbon nanotubes as molecular quantum wires. Phys Today. 1999;52:22–30.
Deljou A, Goudarzi S. Green extracellular synthesis of the silver nanoparticles using thermophilic Bacillus sp. AZ1 and its antimicrobial activity against several human pathogenetic bacteria. Iran J Biotechnol. 2016;14(2):25.
Dhand V, Soumya L, Bharadwaj S, Chakra S, Bhatt D, Sreedhar B. Green synthesis of silver nanoparticles using Coffea arabica seed extract and its antibacterial activity. Mater Sci Eng C. 2016;58:36–43.
Dillon A, Parilla P, Alleman J, Perkins J, Heben M. Controlling single-wall nanotube diameters with variation in laser pulse power. Chem Phys Lett. 2000;316(1–2):13–8.
Dong X, Ji X, Jing J, Li M, Li J, Yang W. Synthesis of triangular silver nanoprisms by stepwise reduction of sodium borohydride and trisodium citrate. J Phys Chem C. 2010;114(5):2070–4.
Droppa Junior R. Síntese e caracterização de nanotubos e fulerenos nitrogenados gerados por arco elétrico. 2004.
Du L, Xu Q, Huang M, Xian L, Feng J-X. Synthesis of small silver nanoparticles under light radiation by fungus Penicillium oxalicum and its application for the catalytic reduction of methylene blue. Mater Chem Phys. 2015;160:40–7.
Dumpala S, Jasinski JB, Sumanasekera GU, Sunkara MK. Large area synthesis of conical carbon nanotube arrays on graphite and tungsten foil substrates. Carbon. 2011;49(8):2725–34.
Durán N, Marcato PD, Alves OL, De Souza GI, Esposito E. Mechanistic aspects of biosynthesis of silver nanoparticles by several Fusarium oxysporum strains. J Nanobiotechnol. 2005;3(1):8.
Dzimitrowicz A, Berent S, Motyka A, Jamroz P, Kurcbach K, Sledz W, et al. Comparison of the characteristics of gold nanoparticles synthesized using aqueous plant extracts and natural plant essential oils of Eucalyptus globulus and Rosmarinus officinalis. Arab J Chem. 2019;12(8):4795–805.
Eisa WH, Zayed MF, Anis B, Abbas LM, Ali SS, Mostafa AM. Clean production of powdery silver nanoparticles using Zingiber officinale: the structural and catalytic properties. J Clean Prod. 2019;241:118398.
Elamawi RM, Al-Harbi RE, Hendi AA. Biosynthesis and characterization of silver nanoparticles using Trichoderma longibrachiatum and their effect on phytopathogenic fungi. Egypt J Biol Pest Control. 2018;28(1):28.
El-Rafie M, Ahmed HB, Zahran M. Facile precursor for synthesis of silver nanoparticles using alkali treated maize starch. Int Sch Res Notices. 2014;2014:702396.
Eswari JS, Dhagat S, Mishra P. Biosurfactant assisted silver nanoparticle synthesis: a critical analysis of its drug design aspects. Adv Nat Sci Nanosci Nanotechnol. 2018;9(4):045007.
Ferreira FV, Cividanes LDS, Brito FS, BRCd M, Franceschi W, Simonetti EAN, et al. Functionalizing graphene and carbon nanotubes: a review. Cham: Springer; 2016.
Frens G. Controlled nucleation for the regulation of the particle size in monodisperse gold suspensions. Nat Phys Sci. 1973;241(105):20–2.
Gade A, Bonde P, Ingle A, Marcato P, Duran N, Rai M. Exploitation of Aspergillus niger for synthesis of silver nanoparticles. J Biobaased Mater Bioenergy. 2008;2(3):243–7.
Gahlawat G, Choudhury AR. A review on the biosynthesis of metal and metal salt nanoparticles by microbes. RSC Adv. 2019;9(23):12944–67.
Gangapuram BR, Bandi R, Alle M, Dadigala R, Kotu GM, Guttena V. Microwave assisted rapid green synthesis of gold nanoparticles using Annona squamosa L peel extract for the efficient catalytic reduction of organic pollutants. J Mol Struct. 2018;1167:305–15.
Graf C, Vossen DL, Imhof A, van Blaaderen A. A general method to coat colloidal particles with silica. Langmuir. 2003;19(17):6693–700.
Grobert N, Hsu W, Zhu Y, Hare J, Kroto H, Walton D, et al. Enhanced magnetic coercivities in Fe nanowires. Appl Phys Lett. 1999;75(21):3363–5.
Gudikandula K, Charya Maringanti S. Synthesis of silver nanoparticles by chemical and biological methods and their antimicrobial properties. J Exp Nanosci. 2016;11(9):714–21.
Gudikandula K, Vadapally P, Charya MS. Biogenic synthesis of silver nanoparticles from white rot fungi: their characterization and antibacterial studies. OpenNano. 2017;2:64–78.
Guilger-Casagrande M, de Lima R. Synthesis of silver nanoparticles mediated by Fungi: a review. Front Bioeng Biotechnol. 2019;7:287.
Guo T, Nikolaev P, Thess A, Colbert DT, Smalley RE. Catalytic growth of single-walled nanotubes by laser vaporization. Chem Phys Lett. 1995;243(1–2):49–54.
Halawa MI, Wu F, Nsabimana A, Lou B, Xu G. Inositol directed facile “green” synthesis of fluorescent gold nanoclusters as selective and sensitive detecting probes of ferric ions. Sensors Actuators B Chem. 2018;257:980–7.
Hamouda RA, Hussein MH, Abo-elmagd RA, Bawazir SS. Synthesis and biological characterization of silver nanoparticles derived from the cyanobacterium Oscillatoria limnetica. Sci Rep. 2019;9(1):1–17.
Hebbalalu D, Lalley J, Nadagouda MN, Varma RS. Greener techniques for the synthesis of silver nanoparticles using plant extracts, enzymes, bacteria, biodegradable polymers, and microwaves. ACS Sustain Chem Eng. 2013;1(7):703–12.
Hou P-X, Liu C, Cheng H-M. Purification of carbon nanotubes. Carbon. 2008;46(15):2003–25.
Huang H, Kajiura H, Tsutsui S, Murakami Y, Ata M. High-quality double-walled carbon nanotube super bundles grown in a hydrogen-free atmosphere. J Phys Chem B. 2003;107(34):8794–8.
Hutchison J, Kiselev N, Krinichnaya E, Krestinin A, Loutfy R, Morawsky A, et al. Double-walled carbon

nanotubes fabricated by a hydrogen arc discharge method. Carbon. 2001;39(5):761–70.
Iijima S. Helical microtubules of graphitic carbon. Nature. 1991;354(6348):56–8.
Iijima S, Ichihashi T. Single-shell carbon nanotubes of 1-nm diameter. Nature. 1993;363(6430):603–5.
Iravani S, Korbekandi H, Mirmohammadi SV, Zolfaghari B. Synthesis of silver nanoparticles: chemical, physical and biological methods. Res Pharm Sci. 2014;9(6):385.
Jana NR, Gearheart L, Murphy CJ. Seeding growth for size control of 5–40 nm diameter gold nanoparticles. Langmuir. 2001;17(22):6782–6.
Jin Y, Dong S. One-pot synthesis and characterization of novel silver– gold bimetallic nanostructures with hollow interiors and bearing Nanospikes. J Phys Chem B. 2003;107(47):12902–5.
Jin Y, Wang P, Yin D, Liu J, Qin L, Yu N, et al. Gold nanoparticles prepared by sonochemical method in thiol-functionalized ionic liquid. Colloids Surf A Physicochem Eng Asp. 2007;302(1–3):366–70.
Journet C, Maser W, Bernier P, Loiseau A, de La Chapelle ML, Lefrant S, et al. Large-scale production of single-walled carbon nanotubes by the electric-arc technique. Nature. 1997;388(6644):756–8.
Kalimuthu K, Babu RS, Venkataraman D, Bilal M, Gurunathan S. Biosynthesis of silver nanocrystals by Bacillus licheniformis. Colloids Surf B Biointerfaces. 2008;65(1):150–3.
Khaleghi M, Madani M, Parsia P. Biosynthesis characteristic of silver nanoparticles produced by mine soil Bacteria isolation, Kerman, Iran. Int J Nanosci Nanotechnol. 2017;13(4):307–13.
Khandel P, Shahi SK. Mycogenic nanoparticles and their bio-prospective applications: current status and future challenges. J Nanostruct Chem. 2018;8(4):369–91.
Kim T, Lee K, M-s G, Joo S-W. Control of gold nanoparticle aggregates by manipulation of interparticle interaction. Langmuir. 2005;21(21):9524–8.
Kiselev N, Krestinin A, Raevskii A, Zhigalina O, Zvereva G, Kislov M, et al. Extreme-length carbon nanofilaments with single-walled nanotube cores grown by pyrolysis of methane or acetylene. Carbon. 2006;44(11):2289–300.
Klaus T, Joerger R, Olsson E, Granqvist C-G. Silver-based crystalline nanoparticles, microbially fabricated. Proc Natl Acad Sci. 1999;96(24):13611–4.
Kohl D. Function and applications of gas sensors. J Phys D Appl Phys. 2001;34(19):R125.
Kulkarni N, Muddapur U. Biosynthesis of metal nanoparticles: a review. J Nanotechnol. 2014;2014:1–8.
Kumar SA, Abyaneh MK, Gosavi S, Kulkarni SK, Pasricha R, Ahmad A, et al. Nitrate reductase-mediated synthesis of silver nanoparticles from $AgNO_3$. Biotechnol Lett. 2007;29(3):439–45.
Kumar A, Kumar B, Ghosh A, Tiwari M, Reyaz M. Microbial production of silver nanoparticles (Agnps) by Some bacterial isolates. Int J Biotechnol Biochem. 2016;12(2):95–110.
Kumar S, Rani R, Dilbaghi N, Tankeshwar K, Kim K-H. Carbon nanotubes: a novel material for multifaceted applications in human healthcare. Chem Soc Rev. 2017;46(1):158–96.
LaMer VK, Dinegar RH. Theory, production and mechanism of formation of monodispersed hydrosols. J Am Chem Soc. 1950;72(11):4847–54.
Lee SH, Jun B-H. Silver nanoparticles: synthesis and application for nanomedicine. Int J Mol Sci. 2019;20(4):865.
Leonard BM, Bhuvanesh NS, Schaak RE. Low-temperature polyol synthesis of AuCuSn2 and AuNiSn2: using solution chemistry to access ternary intermetallic compounds as nanocrystals. J Am Chem Soc. 2005;127(20):7326–7.
Li X, Shen J, Du A, Zhang Z, Gao G, Yang H, et al. Facile synthesis of silver nanoparticles with high concentration via a CTAB-induced silver mirror reaction. Colloids Surf A Physicochem Eng Asp. 2012;400:73–9.
Li B, Song X, Zhang P. Raman-assessed structural evolution of as-deposited few-layer graphene by He/H_2 arc discharge during rapid-cooling thinning treatment. Carbon. 2014;66:426–35.
Li B, Nan Y, Zhang P, Song X. Reducing dimensions of nanocarbons in electric arc plasma via rapid flow treatment. Diam Relat Mater. 2017;73:148–53.
Liang F, Shimizu T, Tanaka M, Choi S, Watanabe T. Selective preparation of polyhedral graphite particles and multi-wall carbon nanotubes by a transferred arc under atmospheric pressure. Diam Relat Mater. 2012;30:70–6.
Liang F, Tanaka M, Choi S, Watanabe T. Measurement of anode surface temperature in carbon nanomaterial production by arc discharge method. Mater Res Bull. 2014;60:158–65.
Liu J, He F, Gunn TM, Zhao D, Roberts CB. Precise seed-mediated growth and size-controlled synthesis of palladium nanoparticles using a green chemistry approach. Langmuir. 2009;25(12):7116–28.
Liu X, Zhu C, Xu L, Dai Y, Liu Y, Liu Y. Green and facile synthesis of highly stable gold nanoparticles via hyperbranched polymer in-situ reduction and their application in Ag+ detection and separation. Polymers. 2018;10(1):42.
Mafuné F, Kohno J-y, Takeda Y, Kondow T. Full physical preparation of size-selected gold nanoparticles in solution: laser ablation and laser-induced size control. J Phys Chem B. 2002;106(31):7575–7.
Mallick K, Wang Z, Pal T. Seed-mediated successive growth of gold particles accomplished by UV irradiation: a photochemical approach for size-controlled synthesis. J Photochem Photobiol A Chem. 2001;140(1):75–80.
Manikprabhu D, Cheng J, Chen W, Sunkara AK, Mane SB, Kumar R, et al. Sunlight mediated synthesis of silver nanoparticles by a novel actinobacterium (Sinomonas mesophila MPKL 26) and its antimicrobial activity against multi drug resistant Staphylococcus aureus. J Photochem Photobiol B Biol. 2016;158:202–5.

Mata R, Bhaskaran A, Sadras SR. Green-synthesized gold nanoparticles from Plumeria alba flower extract to augment catalytic degradation of organic dyes and inhibit bacterial growth. Particuology. 2016;24:78–86.

Molnár Z, Bódai V, Szakacs G, Erdélyi B, Fogarassy Z, Sáfrán G, et al. Green synthesis of gold nanoparticles by thermophilic filamentous fungi. Sci Rep. 2018;8(1):1–12.

Mukherjee S, Sushma V, Patra S, Barui AK, Bhadra MP, Sreedhar B, et al. Green chemistry approach for the synthesis and stabilization of biocompatible gold nanoparticles and their potential applications in cancer therapy. Nanotechnology. 2012;23(45):455103.

Nag S, Pramanik A, Chattopadhyay D, Bhattacharyya M. Green-fabrication of gold nanomaterials using Staphylococcus warneri from Sundarbans estuary: an effective recyclable nanocatalyst for degrading nitro aromatic pollutants. Environ Sci Pollut Res. 2018;25(3):2331–49.

Navrotsky A. Energetic clues to pathways to biomineralization: precursors, clusters, and nanoparticles. Proc Natl Acad Sci. 2004;101(33):12096–101.

Nayak RR, Pradhan N, Behera D, Pradhan KM, Mishra S, Sukla LB, et al. Green synthesis of silver nanoparticle by Penicillium purpurogenum NPMF: the process and optimization. J Nanopart Res. 2011;13(8):3129–37.

Netala VR, Bethu MS, Pushpalatha B, Baki VB, Aishwarya S, Rao JV, et al. Biogenesis of silver nanoparticles using endophytic fungus Pestalotiopsis microspora and evaluation of their antioxidant and anticancer activities. Int J Nanomedicine. 2016;11:5683.

Nikoobakht B, El-Sayed MA. Preparation and growth mechanism of gold nanorods (NRs) using seed-mediated growth method. Chem Mater. 2003;15(10):1957–62.

Nowack B, Krug HF, Height M. 120 years of nanosilver history: implications for policy makers. Environ Sci Technol. 2011;45:1177–83.

Oberlin A, Endo M, Koyama T. Filamentous growth of carbon through benzene decomposition. J Cryst Growth. 1976;32(3):335–49.

Oh KH, Soshnikova V, Markus J, Kim YJ, Lee SC, Singh P, et al. Biosynthesized gold and silver nanoparticles by aqueous fruit extract of Chaenomeles sinensis and screening of their biomedical activities. Artif Cells Nanomed Biotechnol. 2018;46(3):599–606.

Okitsu K, Yue A, Tanabe S, Matsumoto H, Yobiko Y. Formation of colloidal gold nanoparticles in an ultrasonic field: control of rate of gold (III) reduction and size of formed gold particles. Langmuir. 2001;17(25):7717–20.

Ottoni CA, Simões MF, Fernandes S, Dos Santos JG, Da Silva ES, de Souza RFB, et al. Screening of filamentous fungi for antimicrobial silver nanoparticles synthesis. AMB Express. 2017;7(1):1–10.

Ovais M, Khalil AT, Ayaz M, Ahmad I, Nethi SK, Mukherjee S. Biosynthesis of metal nanoparticles via microbial enzymes: a mechanistic approach. Int J Mol Sci. 2018;19(12):4100.

Pandian SRK, Deepak V, Kalishwaralal K, Viswanathan P, Gurunathan S. Mechanism of bactericidal activity of Silver Nitrate-a concentration dependent bi-functional molecule. Braz J Microbiol. 2010;41(3):805–9.

Pattanayak M, Mohapatra D, Nayak P. Green synthesis and characterization of zero valent iron nanoparticles from the leaf extract of Syzygium aromaticum (clove). Middle-East J Sci Res. 2013;18(5):623–6.

Phanjom P, Ahmed G. Effect of different physicochemical conditions on the synthesis of silver nanoparticles using fungal cell filtrate of Aspergillus oryzae (MTCC No. 1846) and their antibacterial effect. Adv Nat Sci Nanosci Nanotechnol. 2017;8(4):045016.

Pierrat S, Zins I, Breivogel A, Sönnichsen C. Self-assembly of small gold colloids with functionalized gold nanorods. Nano Lett. 2007;7(2):259–63.

Popok V, Stepanov A, Odzhaev V. Synthesis of silver nanoparticles by the ion implantation method and investigation of their optical properties. J Appl Spectrosc. 2005;72(2):229–34.

Prasek J, Drbohlavova J, Chomoucka J, Hubalek J, Jasek O, Adam V, et al. Methods for carbon nanotubes synthesis. J Mater Chem. 2011;21(40):15872–84.

Qu L, Dai L. Novel silver nanostructures from silver mirror reaction on reactive substrates. J Phys Chem B. 2005;109(29):13985–90.

Radushkevich L, Lukyanovich V. About the structure of carbon formed by thermal decomposition of carbon monoxide on iron substrate. J Phys Chem (Moscow). 1952;26:88–95.

Rai M, Duran N. Metal nanoparticles in microbiology. Berlin/Heidelberg: Springer Science & Business Media; 2011.

Rai M, Yadav A, Gade A. CRC 675—current trends in phytosynthesis of metal nanoparticles. Crit Rev Biotechnol. 2008;28(4):277–84.

Rajput S, Werezuk R, Lange RM, McDermott MT. Fungal isolate optimized for biogenesis of silver nanoparticles with enhanced colloidal stability. Langmuir. 2016;32(34):8688–97.

Rakhi R. Preparation and properties of manipulated carbon nanotube composites and applications. In: Nanocarbon and its composites: Elsevier; 2019. p. 489–520.

Ren Z, Huang Z, Wang D, Wen J, Xu J, Wang J, et al. Growth of a single freestanding multiwall carbon nanotube on each nanonickel dot. Appl Phys Lett. 1999;75(8):1086–8.

Rose GK, Soni R, Rishi P, Soni SK. Optimization of the biological synthesis of silver nanoparticles using Penicillium oxalicum GRS-1 and their antimicrobial effects against common food-borne pathogens. Green Process Synth. 2019;8(1):144–56.

Roy A, Bulut O, Some S, Mandal AK, Yilmaz MD. Green synthesis of silver nanoparticles: biomolecule-nanoparticle organizations targeting antimicrobial activity. RSC Adv. 2019;9(5):2673–702.

Saito Y, Nishikubo K, Kawabata K, Matsumoto T. Carbon nanocapsules and single-layered nanotubes produced with platinum-group metals (Ru, Rh, Pd, Os, Ir, Pt) by arc discharge. J Appl Phys. 1996;80(5):3062–7.

Sales R. Materiais Compósitos Reforçados com Nanotubos de Carbono 2013.

Sani N, Aminu B, Mukhtar M. Eco-friendly synthesis of silver nanoparticles using Lactobacillus delbrueckii subsp. bulgaricus isolated from kindrimo (locally fermented milk) in Kano State, Nigeria. Bayero J Pure Appl Sci. 2017;10(1):481–8.

Satish S, Baker S, Rakshith D, Satish S. Mycosynthesis of silver nanoparticles bearing antibacterial activity Azmath Pasha. Saudi Pharm J. 2015;24(2):140–6.

Saxena J, Sharma PK, Sharma MM, Singh A. Process optimization for green synthesis of silver nanoparticles by Sclerotinia sclerotiorum MTCC 8785 and evaluation of its antibacterial properties. Springerplus. 2016;5(1):1–10.

Scott CD, Arepalli S, Nikolaev P, Smalley RE. Growth mechanisms for single-wall carbon nanotubes in a laser-ablation process. Appl Phys A Mater Sci Process. 2001;72(5):573–80.

Shaligram NS, Bule M, Bhambure R, Singhal RS, Singh SK, Szakacs G, et al. Biosynthesis of silver nanoparticles using aqueous extract from the compactin producing fungal strain. Process Biochem. 2009;44(8):939–43.

Siddiqi KS, Husen A, Rao RA. A review on biosynthesis of silver nanoparticles and their biocidal properties. J Nanobiotechnol. 2018;16(1):14.

Singh I. Biosynthesis of silver nanoparticle from fungi, algae and bacteria. Eur J Biol Res. 2019;9(1):45–56.

Singh P, Kim Y-J, Zhang D, Yang D-C. Biological synthesis of nanoparticles from plants and microorganisms. Trends Biotechnol. 2016;34(7):588–99.

Singhal G, Bhavesh R, Kasariya K, Sharma AR, Singh RP. Biosynthesis of silver nanoparticles using Ocimum sanctum (Tulsi) leaf extract and screening its antimicrobial activity. J Nanopart Res. 2011;13(7):2981–8.

Sintubin L, De Windt W, Dick J, Mast J, Van Der Ha D, Verstraete W, et al. Lactic acid bacteria as reducing and capping agent for the fast and efficient production of silver nanoparticles. Appl Microbiol Biotechnol. 2009;84(4):741–9.

Sintubin L, Verstraete W, Boon N. Biologically produced nanosilver: current state and future perspectives. Biotechnol Bioeng. 2012;109(10):2422–36.

Sivaraman SK, Kumar S, Santhanam V. Monodisperse sub-10 nm gold nanoparticles by reversing the order of addition in Turkevich method–the role of chloroauric acid. J Colloid Interface Sci. 2011;361(2):543–7.

Smetana AB, Klabunde KJ, Sorensen CM. Synthesis of spherical silver nanoparticles by digestive ripening, stabilization with various agents, and their 3-D and 2-D superlattice formation. J Colloid Interface Sci. 2005;284(2):521–6.

Soliwoda K, Rosowski M, Tomaszewska E, Tkacz-Szczesna B, Celichowski G, Psarski M, et al. Synthesis of monodisperse gold nanoparticles via electrospray-assisted chemical reduction method in cyclohexane. Colloids Surf A Physicochem Eng Asp. 2015;482:148–53.

Song KC, Lee SM, Park TS, Lee BS. Preparation of colloidal silver nanoparticles by chemical reduction method. Korean J Chem Eng. 2009;26(1):153–5.

Soshnikova V, Kim YJ, Singh P, Huo Y, Markus J, Ahn S, et al. Cardamom fruits as a green resource for facile synthesis of gold and silver nanoparticles and their biological applications. Artif Cells Nanomed Biotechnol. 2018;46(1):108–17.

Stepanov A. Synthesis of silver nanoparticles in dielectric matrix by ion implantation: a review. Rev Adv Mater Sci. 2010;26:1/2):1–29.

Su Y, Zhang Y. Carbon nanomaterials synthesized by arc discharge hot plasma. Carbon. 2015;83:90–9.

Sugai T, Yoshida H, Shimada T, Okazaki T, Shinohara H, Bandow S. New synthesis of high-quality double-walled carbon nanotubes by high-temperature pulsed arc discharge. Nano Lett. 2003;3(6):769–73.

Sun Q, Cai X, Li J, Zheng M, Chen Z, Yu C-P. Green synthesis of silver nanoparticles using tea leaf extract and evaluation of their stability and antibacterial activity. Colloids Surf A Physicochem Eng Asp. 2014;444:226–31.

Tarasenko N, Butsen A, Nevar E, Savastenko N. Synthesis of nanosized particles during laser ablation of gold in water. Appl Surf Sci. 2006;252(13):4439–44.

Teixeira A. Síntese de Nanotubos de Carbono por CVD utilizando catalisadores à base de Ferro e Molibdênio suportados em matrizes cerâmicas. Belo Horizonte:[sn]. 2010.

Thanh NT, Maclean N, Mahiddine S. Mechanisms of nucleation and growth of nanoparticles in solution. Chem Rev. 2014;114(15):7610–30.

Thess A, Lee R, Nikolaev P, Dai H, Petit P, Robert J, et al. Crystalline ropes of metallic carbon nanotubes. Science. 1996;273(5274):483–7.

Turkevich J, Stevenson PC, Hillier J. The formation of colloidal gold. J Phys Chem. 1953;57(7):670–3.

Uthaman S, Kim HS, Revuri V, Min J-J, Lee Y-K, Huh KM, et al. Green synthesis of bioactive polysaccharide-capped gold nanoparticles for lymph node CT imaging. Carbohydr Polym. 2018;181:27–33.

Vahabi K, Mansoori GA, Karimi S. Biosynthesis of silver nanoparticles by fungus Trichoderma reesei (a route for large-scale production of AgNPs). Insciences J. 2011;1(1):65–79.

Velusamy P, Kumar GV, Jeyanthi V, Das J, Pachaiappan R. Bio-inspired green nanoparticles: synthesis, mechanism, and antibacterial application. Toxicol Res. 2016;32(2):95–102.

Wacławek S, Gončuková Z, Adach K, Fijałkowski M, Černík M. Green synthesis of gold nanoparticles using Artemisia dracunculus extract: control of the shape and size by varying synthesis conditions. Environ Sci Pollut Res. 2018;25(24):24210–9.

Wang M, Zhao X, Ohkohchi M, Ando Y. Carbon nanotubes grown on the surface of cathode deposit by arc discharge. Fuller Sci Technol. 1996;4(5):1027–39.

Wiley B, Herricks T, Sun Y, Xia Y. Polyol synthesis of silver nanoparticles: use of chloride and oxygen to pro-

mote the formation of single-crystal, truncated cubes and tetrahedrons. Nano Lett. 2004;4(9):1733–9.

Wojtysiak S, Kudelski A. Influence of oxygen on the process of formation of silver nanoparticles during citrate/borohydride synthesis of silver sols. Colloids Surf A Physicochem Eng Asp. 2012;410:45–51.

Wu X, Redmond PL, Liu H, Chen Y, Steigerwald M, Brus L. Photovoltage mechanism for room light conversion of citrate stabilized silver nanocrystal seeds to large nanoprisms. J Am Chem Soc. 2008;130(29):9500–6.

Wu S, Han C, Iocozzia J, Lu M, Ge R, Xu R, et al. Germanium-based nanomaterials for rechargeable batteries. Angew Chem Int Ed. 2016;55(28):7898–922.

Xue C, Métraux GS, Millstone JE, Mirkin CA. Mechanistic study of photomediated triangular silver nanoprism growth. J Am Chem Soc. 2008;130(26):8337–44.

Yaceman M, Yoshida M, Rendson J, Santiestaban G. Catalytic growth of carbon microtubules with fullerene structure. Appl Phys Lett. 1993;62:202–4.

Yu Y-Y, Chang S-S, Lee C-L, Wang CC. Gold nanorods: electrochemical synthesis and optical properties. J Phys Chem B. 1997;101(34):6661–4.

Yulizar Y, Utari T, Ariyanta HA, Maulina D. Green method for synthesis of gold nanoparticles using polyscias scutellaria leaf extract under uv light and their catalytic activity to reduce methylene blue. J Nanomater. 2017;2017

Zeng J, Zheng Y, Rycenga M, Tao J, Li Z-Y, Zhang Q, et al. Controlling the shapes of silver nanocrystals with different capping agents. J Am Chem Soc. 2010;132(25):8552–3.

Zhang D, Ye K, Yao Y, Liang F, Qu T, Ma W, et al. Controllable synthesis of carbon nanomaterials by direct current arc discharge from the inner wall of the chamber. Carbon. 2019;142:278–84.

Zhao X, Zhao T, Peng X, Hu J, Yang W. Catalyst effect on the preparation of single-walled carbon nanotubes by a modified arc discharge. Fullerenes Nanotubes Carbon Nanostruct. 2019;27(1):52–7.

Zielonka A, Klimek-Ochab M. Fungal synthesis of size-defined nanoparticles. Adv Nat Sci Nanosci Nanotechnol. 2017;8(4):043001.

Zomorodian K, Pourshahid S, Sadatsharifi A, Mehryar P, Pakshir K, Rahimi MJ, et al. Biosynthesis and characterization of silver nanoparticles by Aspergillus species. Biomed Res Int. 2016;2016:1–6.

Zsembik BA. Health issues in Latino families and households. In: Handbook of families & health: interdisciplinary perspectives. Thousand Oaks: Sage Publications; 2005. p. 40–61.

19 Radio Frequency Plasma-Based Synthesis of Metallic Nanoparticles for Biomedical Application

Vignesh Nagarajan, Sanjay Sudan, and Kuldeep Sharma

Abstract

This chapter involves the plasma synthesis of nanoparticulate powders. Using induction-coupled plasma (ICP) is the new way of producing high purity nanopowders on an industrial scale. All this is made possible by TEKNA, the leading producer of nanomaterial synthesizing machines. The concept of plasma synthesis is used quite comprehensively; it encompasses all the processes by which charged particles are kept. Therefore, the topic of this project ranges from high temperature processes and microwave processes to the laser and flame synthesis of nanopowders. For each of the processes discussed in this chapter, the product characteristics are explained. Not only being a means of producing high purity powders, IPS is known for having a clean heat source that lacks induced contaminants assuring high-grade products. This complex technology is based on utilizing high voltage being passed through a coil with a conductor placed in between the coil to produce a large amount of heat at the conductor owing to the effect of electromagnetic induction. With flowing gas being used as the conductor, it will reach high temperature extremes because of ionization of the gas into a plasma. The most common gases used in this system include argon, hydrogen, and oxygen as carriers. The IPS machine uses micron-sized powders as the feed, which is then carried through the system by a carrier gas, commonly argon. These are then ionized together or vaporized to a plasma state, the fourth state of matter at extreme temperatures producing ionized metal, which are then subjected to a quenching gas, ensuring homogenous nucleation. The size of the nanoparticles, ranging from 20 to 100 nm based on several parameters, is to be closely calculated and followed to ensure the desired nanoparticle size outcome. These include: temperature; feed dispersion; gas composition; quenching gas; feed rate; carrier gas; carrier gas temperature; torch temperature; raw material. The particle morphology and distribution of nanopowders were significantly influenced by the powder feed rate, the induction of plasma power, and the volume of the sheath gas. The average particle size monotonously increased with the increase in powder feed rate. The nanopowder distribution became more and more concentrated as the induction plasma power increased. The average size of nanopowder decreased obviously with the increase in H_2 proportion.

V. Nagarajan (✉) · S. Sudan · K. Sharma
Saveer Matrix Nano Private Ltd, Noida, UP, India
e-mail: Vignesh@matrixnano.onmicrosoft.com

J. K. Patel, Y. V. Pathak (eds.), *Emerging Technologies for Nanoparticle Manufacturing*,
https://doi.org/10.1007/978-3-030-50703-9_19

Keywords

Induction-coupled plasma · Nanopowder · Quenching · Nanocrystals · Silver

1 Introduction

In the past couple of years, bringing the era of micromaterial to the verge of ending, nanomaterials have been replacing them because of their unique characteristic properties, in contrast to micromaterials, which replaced mesh material within a decade. The extremely small size of 10^9 nm, giving them a higher surface to volume ratio, enables these nanomaterials to exhibit great physical and chemical properties that play an important role in various industries involving material science being an atom to all disciplines of science (Akyildiz and Ozturk 2010). Nanomaterials play a crucial role in biomedicine, with a wide range of applications such as drug delivery, cancer therapy or bioimaging. An industrial concern for large-scale manufacturing and consistency is the replacement of the conventional chemical process involving reducing toxicity and oxidants that are not only used for synthesis but also stabilization. This makes industrial nanomaterials manufacturing expensive in comparison with micromaterials manufacturing and not a feasible process owing to its long duration and lack of consistency. The unique approach from the top-down and bottom-up, or rather a combination of the two, is basically the use of gas phase synthesis or plasma. In terms of reality in the industrial manufacturing of materials, plasma technology is the most prominent method for nanomaterials manufacturing (Aminorroaya et al. 2011). Plasma is considered the fourth state of matter. Plasma processes are one of a kind gas phase processes with a package of essential advantages. The most significant aspect is its high efficiency with regard to energy consumption and in the case of proper selection of operating conditions such as temperature, feed dispersion, gas composition, quenching gas, feed rate, carrier gas, feed rate, carrier gas temperature, torch temperature, raw material, and extremely narrow particle size distributions. Narrow particle size distributions are obtained because particle formation in plasma synthesis is, in contrast to conventional gas phase synthesis, not necessarily a random process; instead, it may be controlled by particle charging. Thus, there are many different demands with regard to product quality and quantity (Atias Adrian et al. 2011; Bystrzejewski et al. 2005).

1.1 Coupling Mechanism

The fundamental events regulating the operation of plasmas coupled inductively (Fig. 19.1) are essentially like those of metal induction heating, known since the beginning of the century and having found numerous large-scale industrial applications over the last 40 years. However, with induction plasmas, the fact that the "load" is the conductive plasma gas with a substantially lower electrical conductivity than most metals has a direct influence on the optimal combination of frequency, size, and power needed to maintain a stable discharge. The comparatively easy channel system created by Freeman and Chase in 1968, based on a near comparison with metal induction heating, best demonstrates the coupling system. Energy equilibrium, the general effectiveness of power, is an instant problem in the layout of any plasma-producing machine. This is described as the proportion of the electricity accessible to the engine as enthalpy in the plasma fluid at the torch entrance (Bystrzejewski et al. 2005). Unlike the DC torches, which can be constructed with a total power effectiveness of 60–80%, the effectiveness of inductively connected plasma torches typically ranges from 40 to 60%. The main losses are the radio frequency (RF) transmitter, the connection between the magnet and the load, and the power transferred to the plasma containment pipe. A loss breakdown in a typical RF plasma induction scheme is shown in Fig. 19.7. It should be noted that the losses of the oscillator tube are almost constant and equal to 20% of the platform power, whereas the losses of

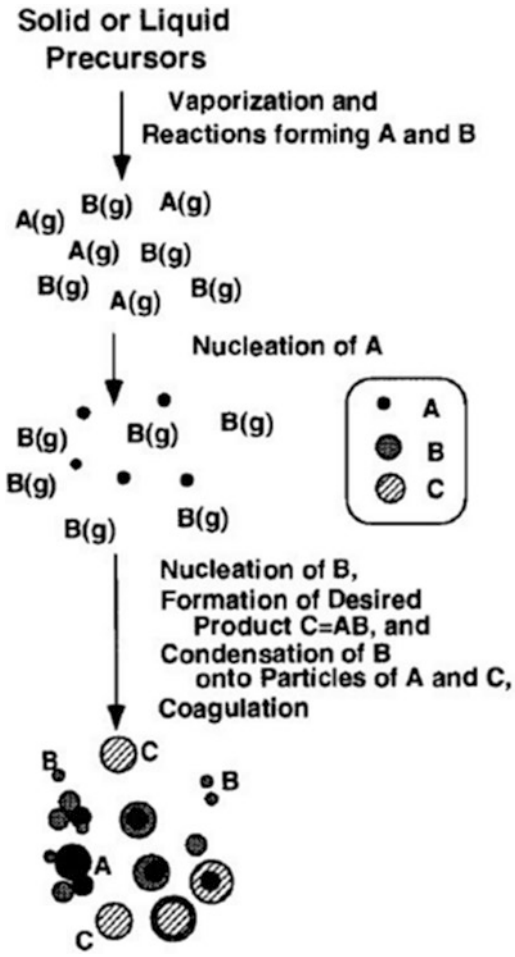

Fig. 19.1 Particle formation in a two-component system

transmission and coil were only 9% in this case. The loss of the lamp shaft, on the other hand, decreases significantly with the rise in the proportion of (rn/rc) owing to the enhanced electromagnetic bonding, whereas the loss of conduction, wind, and radiation pressure on the walls of the cell containment pipe rises as the proportion of the water to the cell radius rises, owing to the closeness of the water to the cabinet roof (Jeon et al. 2011; Yan et al. 2013). However, it should be observed that the interpretation of the above power effectiveness measurements should be strongly linked to the use of the plasma torch for induction. For example, if the torch were to be used as a gas heater with the materials to be injected into the tail flame at the torch exit, then an energy efficiency of about 50% would be realistic. The scenario is entirely distinct if the material to be handled is axially inserted into the coil region's release core. This is merely because, in this situation, in the general power equilibrium, the lamp wall losses should not be taken into consideration (de Jongh et al. 2007).

1.2 Electric and Magnetic Fields

Magnetic field intensity probe measurements were performed using water cooled miniature probes (Gresback et al. 2011). Noncooled probes were also used under temporary circumstances (Gupta et al. 2009). Typical electrical field strength radial models are shown in the existence and lack of release at the midsection of the induction coil (Gresback et al. 2011). The range of the oscillator was 2 to 6 MHz and it was forecast that the wasted energy was 25 kW (Lee et al. 2010). As predicted, owing to the contact between the applied magnetic force and the induction forces in the discharge, the existence of the discharge results in a significant reduction of the electric field strength in the middle of the coil. The axial measurements of electromagnetic field strength along the centerline of the torch afterward reveal an analogous impact (Gupta et al. 2009). In this situation, a torch worked with a 9-MHz oscillator frequency and an energy rate of 27 kW. This corresponds to the situation without the flame, whereas curves 2 and 3 relate to air and argon release. It is obvious that the predictions that could be made using such a model may be very useful when it comes to the optimization of the injection condition of a given powder or an aerosol with the objectives of obtaining either a physical and/or a chemical change in the powder or simply evaporating them completely, as is the case in spectrochemical analysis (Lei et al. 2009) (Fig. 19.2).

2 Related Work

Bernardi and Liang (1999) investigated the effects of coil and torch geometry with a 3D numerical model for an argon atmospheric pressure RFICP torch. In this study, conventional helicoidal, double-stage, planar coil geometries,

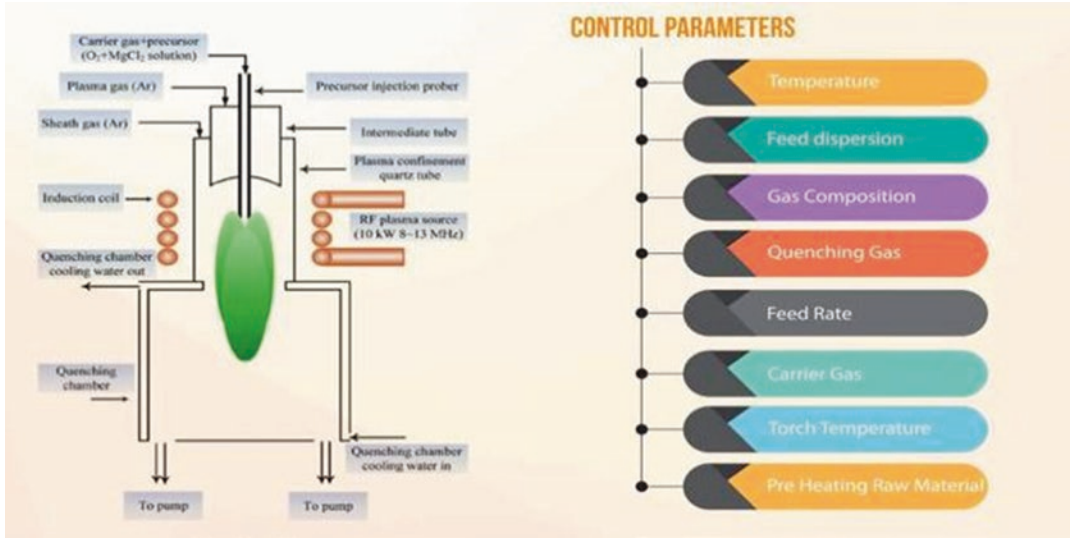

Fig. 19.2 Principle behind the induction-coupled plasma system

and an elliptical cross section torch were compared (Fig. 19.3).

With the conventional coil, a displacement of plasma toward the confinement tube (toward the front and rear ends of the coil) is reported because the induction coils was asymmetric. In the case of double-stage geometry, the plasma volume extends axially and RF power is dissipated on the upper part of the torch. In the planar torch, axial symmetry of the power and temperature distribution is observed, whereas elliptical coils appear asymmetric along the minor axis (Mandal and Gregory 2010). Conventional helicoidal turns are usually used in powder synthesis applications with several coil turns depending on the plasma operating power and powder production capacity. As the change of induction coils for an existing induction-coupled plasma (ICP) system is not usually practical, it can be considered a constant parameter in most cases, after a choice of the proper plasma system was made (Oelerich 2001). As can be seen in Eq. (2.5), skin depth increases with decreasing working coil frequency. Colombo et al. (2010) compared the particle trajectories under two different coil frequencies (3 MHz and 13.56 MHz) for a RFICP torch with a non-axisymmetric reaction chamber, and it was shown that for the 3-MHz frequency, larger particles follow a straight line, but smaller particles deviate from the axial direction. The frequency is changed during the tuning of an RF generator, but usually altered within the allowable limits; thus, it may not be changed freely when studying with a specific RFICP torch (Reilly Jr and Wiswall Jr 1968). During the nitridation of $MoSi_2$ in an electric plasma plant, Soucy (2001) examined the impact of current parameters. The plasma scheme being studied was RF with a 50-kW energy. Plasma plate strength, tank temperature, sheath gas structure, and quench fluid stream rate were the method parameters researched. The results obtained through a plasma flow enthalpy probe without the injection of $MoSi_2$ powders showed that at a chamber pressure of 0.4 bar, the maximum temperatures were 7400 K and 6500 K respectively for a plate power of 40 and 25 kW. The plasma quantity was also greater at elevated energy: 85 m/s at 40 kW. As for the stress impact, they discovered that in the event of 0.8 bar, the cloud temperature was about 1000 K greater than the stress of 0.4 bar (25 kW panel energy). The highest speed was 0.8 bar at 47 m/s. This should be contrasted with a speed of 0.4 bar of 72 m/s. Nishiyama (1996) and Reinmann and Akram (1997) outlined the control features of the air temperature and speed domains of argon plasma by RF induction in comparable research. The gas temperature increased slightly in all regions of the

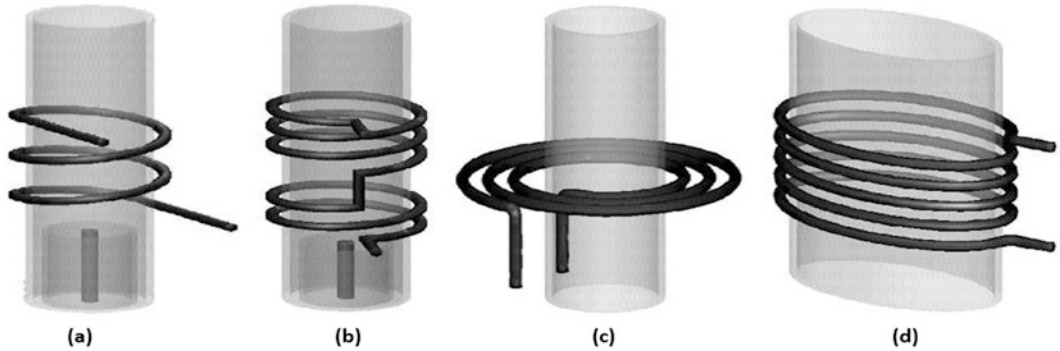

Fig. 19.3 Types of induction coupling coils. (**a**) Conventional helicoidal coil with 2.5 turns, (**b**) double-stage coil, (**c**) planar coil, (**d**) elliptical coil

plasma when the power was increased, the axial velocity increased in the central region, and the maximum point of velocity shifted toward the center axis. Punjabi (2012) and Schwyn (1988) reported similar results; Ar, N_2 and air were used as plasma fuel and increased plasma key temperature and extended plasma quantity were observed. Pristavita (2011) researched the manufacturing of coal nanoparticles and examined the stress impact in RF plasma. In this work, methane gas was added to the plasma (argon) gas by 0.6 {7 vol percent. The plasma lamp was connected to a conical tank with a span of 50 cm and an extension angle of 14 cm. Figure 19.3 was taken from their job, showing simulation outcomes at distinct stress concentrations for temperature and speed allocation. As seen in this pure gas (means with out any mixure) gas velocities reduced with growing stress (0.2, 0.55, and 1 bar) at 10 kW of energy, and plasma temperatures stayed nearly constant. The impact of atmospheric heat and stress on fullerene chemistry was explored in the literature by Wang (2003) and Pfeiffer (2014). The plasma induction lamp used had a 1.67 MHz oscillator with a peak output of 200 kW, pressure varied from about 0.2 to 0.67 bar under blended air Ar and He/Ar. C-Si blended precursors were supplied at a speed of 5 g/min to the plasma and the platform energy was maintained at 30 kW. Adding helium gas and low-pressure operation was discovered to be useful for fullerene synthesis. Based on calculations in this research, the highest rotational speeds at 0.2, 0.5, and 0.67 bar pressure were 160, 90, 75 m/s respectively. Three distinct combinations of fuel have been screened in this research: pure Ar, 70% He/30% Ar combination, and plain He. It was noted that in all gas combinations the highest temperature values were almost equivalent by the structure of the fluid; pure He had the largest reduction with a value of 7300 K. For 70% He/30% Ar and plain Ar , the respective numbers were 5200 K and 1700 K (Burak Aktekin 2013; Vons et al. 2010, 2011). Temperature reduced close to the quench area in the event of radial quenching, and mass proportion focused on the longitudinal direction. For the no quench situation, the largest particles (around 90 nm) were recorded. Owing to recirculation and reduced temperatures there, particles close to the walls and reactor entrance were larger for all three instances. As a second parameter, the feeding rate was changed, and it was seen that the nil particle size increased for all quenching positions with the increasing number of precursors fed to the plasma. Shigeta and Watanabe (2008) and Mangolini (2005) also explored the anti-cooling situation using a plasma energy of 3 kW. The counter stream cooling was discovered to trigger a dramatic reduction in plasma tail temperature arising in the creation of nanoparticles being promoted. Although nanoparticles for cooling without counterflow position were formed near the reactor walls, in the downstream region (below the plasma reball) counterflow was produced in addition to the region near the reactor wall for counterflow cooling. Furthermore, the development

processes of metals including B, Cr, Fe, Mo, Pt, and Si were also researched in this process and forecast the dominant method of nucleation (Ding et al. 2006; Gresback et al. 2011) (Fig. 19.4).

Kobayashi et al. (2008) further indicated in their research, that nearly all precursors evaporated when the ice level was 0.33 g/min. This was unlike a feed speed of 1.7 and 3.5 g/min, where non-evaporated particles were present. The quantity of completely evaporated dust improved with the growing dust transport speed, but the evaporation proportion reduced. Increasing the feeding frequency thus led to larger particles (condensed from the gas stage). (Figs. 19.5 and 19.6).

When the stress was raised to a greater value, the particle residence time improved (Jiayin et al. 2010). It was also seen that the degree of supersaturation was increased with the growing quantity of copper vapor, leading to larger particles flowing to increased heterogeneous nucleation. The stream speed of oxygen introduced to the sheath material was altered as a third method parameter and it was revealed that the addition of oxygen improved the evaporation proportion and chip size flowing to elevated water heat conductivity (Li et al. 2007). Research by Shin et al. (2006) has experimentally proven the impacts of precursor feed level and core fluid stream rate using appropriate plasma diagnostic methods such as the enthalpy test method, optical emission detection, and laser light extinction measurements. A RF ICP lamp (2035 kW, 13.56 MHz) running at 0.4 bar stress (ArH_2) was supplied with alumina powders with a mean diameter of 4.7 m. The transport frequency of the precursor and the stream frequency of the main argon gas altered from 1.44.7 g/min to 627 standard liter per minute (SLPM). Decreasing carrier gas flow led in increased enthalpy and an increased plasma key temperature gradient. The quantity of flame processed precursors and the quantity of fresh batch of powders gathered were also greater when the carrier oxygen flow was low. Results of optical emission spectroscopy found that Al emission intensity declined with the elevated feeding prices of precursors, suggesting a trend from a precursor-deficient system to a power-deficient system with higher feeding prices (Al emission intensity was thought to be a measure of precursor vaporization) (Jurbergs et al. 2006). Guo et al. (1997) researched RF plasma (3-MHz frequency, energy up to 52.2 kW) synthesis of ultrafine SiC powder. The effect on the products of plasma plate strength, injection probe location, and gas structure was explored. Powders were produced through the response of Argon and oxygen. By using argon as a carrier gas, oxygen was introduced axially to the coil core. Methane and the carrier gas were combined. In short, by altering system parameters, it is feasible to regulate plasma properties, corresponding to item features. The plasma form and heat distribution are primarily determined by the coil and flashlight geometry. Coil frequency impacts the plasma's surface thickness and generally operates at reduced frequencies with elevated energy devices. These parameters are not merely controllable for a specified plasma scheme; therefore, on the grounds of the overall demands for the planned study region, these must be considered before the establishment phase of a scheme. The plate strength with torch pressure are two significant parameters that can be readily regulated. The result of greater working energy is greater plasma size and higher temperature. Another impact is seen on the gas speed, where higher energy levels cause a greater speed of axial gas (Hirasawa et al. 2006). Although energy affects the gas speed, it is working stress that has the greatest effect. Increasing stress reduces the speed considerably, whereas the plasma temperature may increase slightly. The moment of particle stay depends exclusively on the speed of the plasma fluid as it determines the moment of particle exposure to the atmosphere. Lower flame stress could therefore be said to result in a short residence time and relatively less effective precursor evaporation. Because of their distinct heat and electrical characteristics, the structure of the fluids supplied into the lamp is another significant parameter. Compared with He, N_2, O_2, and water, the volume of the elevated heat area in the atmosphere was revealed to be greater for Ar petrol, adding gasses with greater heat conductivity (such as He and H_2) to Ar plasma fuel for more effective plasma precursor heat therapy (Gupta et al. 2009). It has been noted that adding He to Ar increases the plasma tail temperature gra-

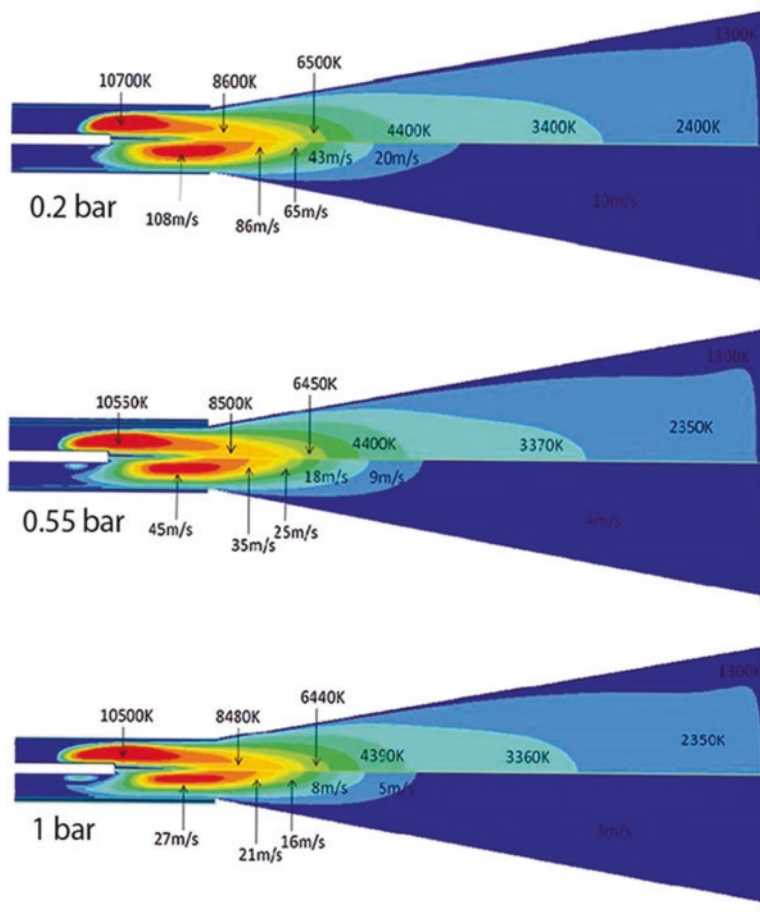

Fig. 19.4 Temperature (upper half) and velocity (lower half) distribution at different pressures. (Pristavita et al. 2011)

dient. The feeding place of a secondary gas is also essential, for example, because of its elevated heat conductivity. In addition, He as a carrier gas has been observed to raise the plasma's internal temperature. In comparison, flowing to its reduced electrical conductivity (skin impact), an addition to sheath fuel was reported to reduce the size of the area of elevated temperature of the plasma. As anticipated, the suppression of the gas stream speed considerably affects the particle size of the products. Quenching avoids further particle development and new solids are gathered from the scheme with growing stream speeds. Despite the location of the quenching gas injection, counter flow quenching results in an abrupt drop in plasma Cap-temperature. The frequency and location of precursor feeding mainly impact the percentage of evaporation (Dal Negro et al. 2001). Higher feeding speed improves the quantity of vaporized solids, but it also leads to greater non-evaporated precursor proportion and greater particle size.

2.1 Tekna's Induction of Plasma-Based Nano Spheroidizer PL35Kw to Produce Powders

Metal and metal oxide nanopowder manufacturing using plasma technology requires remote, interruption-free powder feeding to have a spherical shape, ensuring the highest packing density achievable, a specific particle size distribution, a high flow ability, as well as an internal particle structure that is free of pores. Despite the various advantages that commercially available powders can offer in terms of affordability and/or ease of availability, they rarely meet all the requirements listed above (Fig. 19.7).

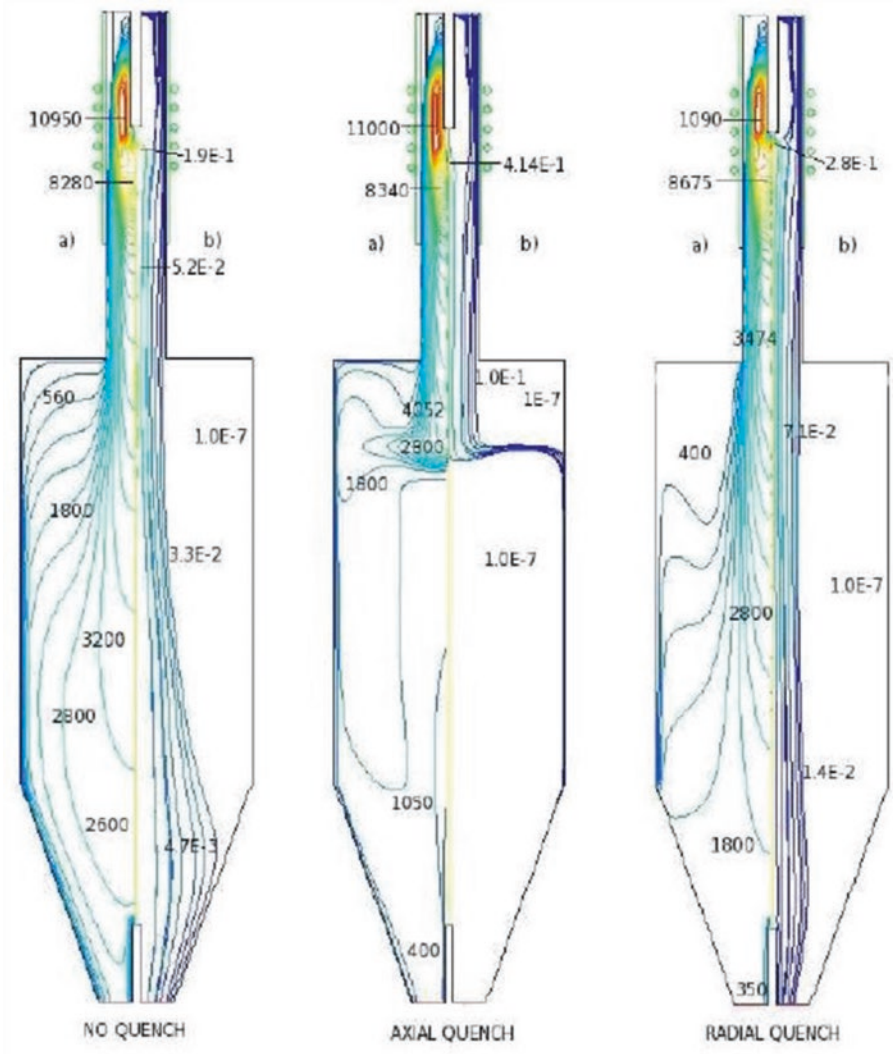

Fig. 19.5 Temperature contour lines and mass fraction path lines for three different quenching positions. (Mendoza Gonzales et al. 2006)

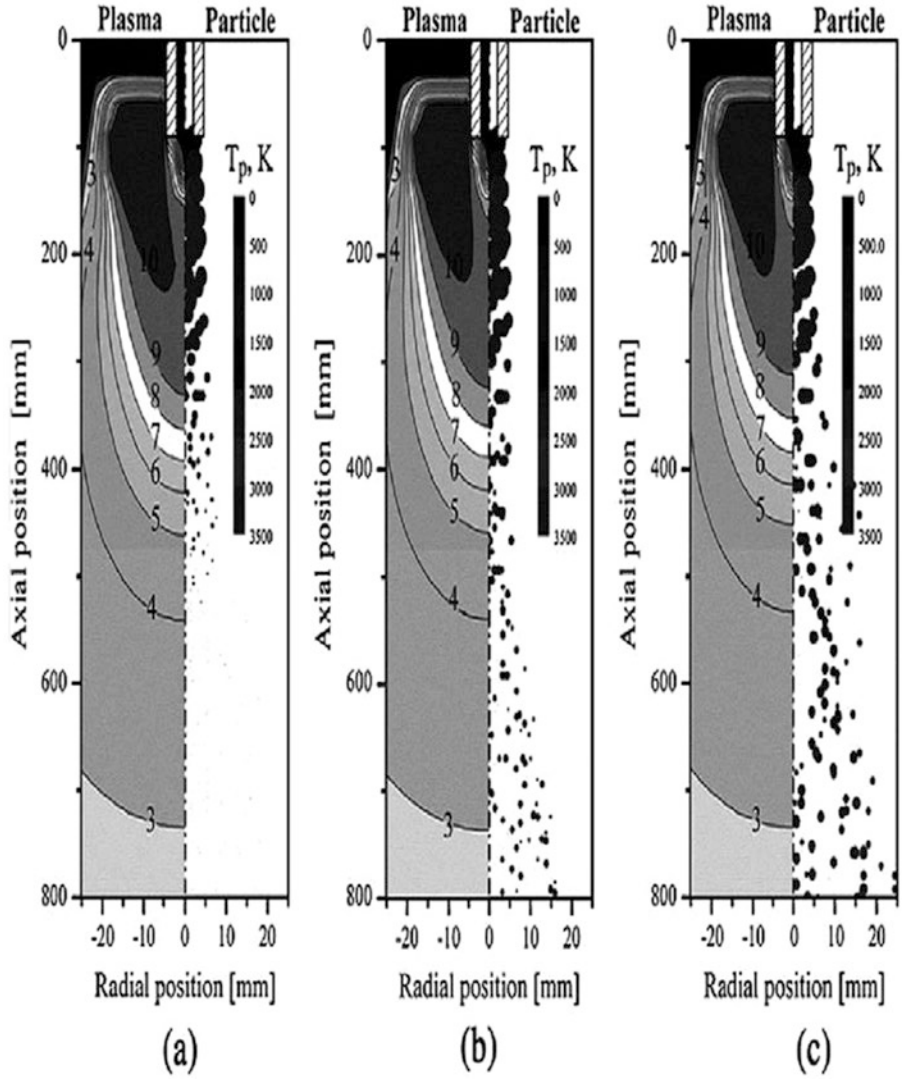

Fig. 19.6 Numerical analysis of the thermal plasma revealing the temperature distribution and particle trajectory with the change in particle size as well. (**a**) 0.33 g/min, (**b**) 1.7 g/min, (**c**) 3.5 g/min (Kobayashi et al. 2008) and 0.67 bar in order to see the impact of stress, and the working speed was held steady at 1.7 g/min

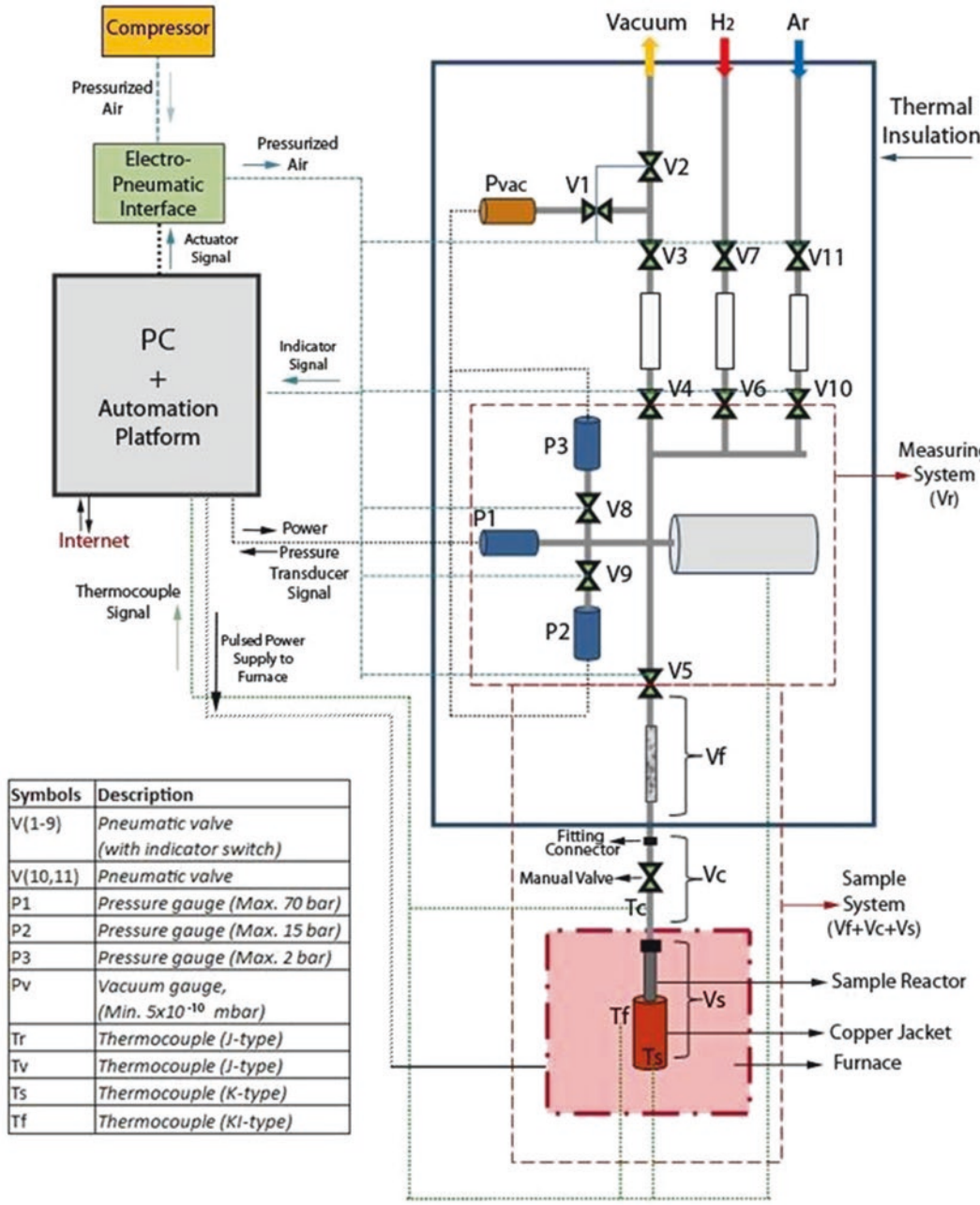

Symbols	Description
V(1-9)	*Pneumatic valve (with indicator switch)*
V(10,11)	*Pneumatic valve*
P1	*Pressure gauge (Max. 70 bar)*
P2	*Pressure gauge (Max. 15 bar)*
P3	*Pressure gauge (Max. 2 bar)*
Pv	*Vacuum gauge, (Min. $5x10^{-10}$ mbar)*
Tr	*Thermocouple (J-type)*
Tv	*Thermocouple (J-type)*
Ts	*Thermocouple (K-type)*
Tf	*Thermocouple (KI-type)*

Fig. 19.7 Schematic representation of the induction plasma system

2.2 Experimental Design and Operating Parameters

2.2.1 Induction Plasma Torch

Main Components

- *Induction coil*: to create magnetic and electrical fields.
- *Quartz tube*: to separate central and sheath gases.
- *Ceramic tube*: to confine plasma.

Gas Distribution

- *Carrier*: conveys the precursor (powder); Ar, usually preferred between 5 to 8 SLPM for 30 kW.
- *Central*: plasma-forming gas by ionization; Ar, maximum to be 20 SLPM for 30 kW.
- *Sheath*: stabilizes plasma and protects the ceramic tube; Ar + Auxillary (usually between 0 to 10 SLPM) (Fig. 19.8).

2.2.2 Containment Effect

To determine the effect of plasma containment, under the same operating conditions, computations were made for a confined and free plasma discharge. In the case of free plasma discharge, the plasma-containing tube extends only 15 nm beyond the end of the induction coil, while having the same diameter as that used for the confined plasma calculations. At this stage, in an atmospheric environment, the plasma appeared as a free jet that was supposed to be the same as the air fuel (argon). In the case of both confined and free plasma, the dimensions of the induction coil and the gas distributor were the same. Typical streamlines, temperature, and swirl contours were acquired for a vertically upward centered plasma under circumstances of free flow and with an average flow inlet velocity of 13.3 m/s. It is noted that, under the same operational conditions, the stream held in the induction region is analogous to that acquired for the restricted plasma. Beyond the holding area, the heated plasma gas flows vertically upward, leading to a significant quantity of ambient gas. The mass flow speed of the trained gas, as stated by the stream function values, may be greater than that of the plasma gas.

2.2.3 Effect of the Central Carrier Gas

Also researched is the influence of core injection on the areas of stream and temperature for a limited plasma (Pfeiffer et al. 2014). In this scenario the torch design was comparable with that shown on Fig. 19.6. Computations were performed with the momentum and energy equations written for both argon and nitrogen plasma gas in terms of their primitive variables. Indicates the calculated isotherms and streamlines for a 3-MHz oscillator frequency argon plasma, a 3-kW energy rate, and distinct main injection flow speeds (Q1 = 100 l/min). It should be noted that the corresponding plasma gas flow rate, Q, is maintained constant whereas the sheath gas flow rate, Q, is adjusted so that the total flow rate, Q is constant. As the core injection stream increases, the entry area near the centerline cools down, pushing the elevated heat area (T > 9600 K) nearer to the cell containment pipe wall. With the increase of Q1 over the investigated range, the temperature and flow yield at the torch exit do not change significantly.

2.2.4 Effect of the Total Gas Flow Rate

Computations were performed to determine the influence on the fluid and temperature ranges in the torch of improving the actual gas flow level, Q0. In this case, Q1 will be kept zero while Q2 and Q3 will be increased proportionally to give

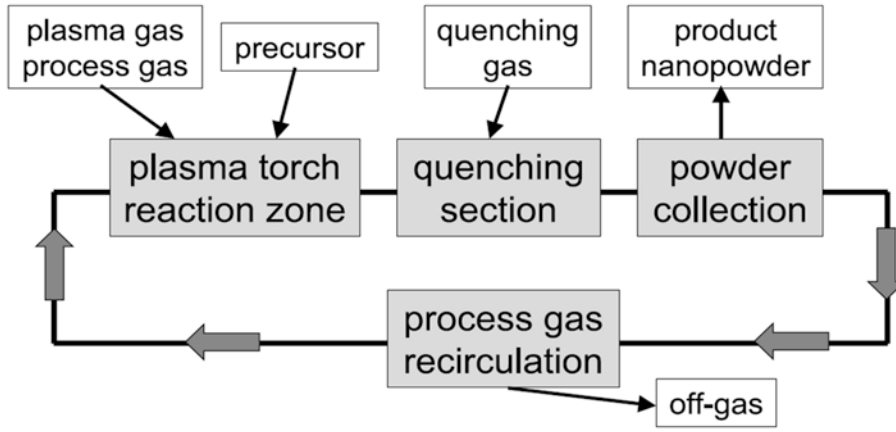

Fig. 19.8 Process flow diagram of a production plant using induction-coupled plasma

Q0 values ranging from 20 to 50 (sec/min). Under atmospheric stress, the plasma gas is regarded as argon and the overall power rate is 5 kW. The results demonstrate that by accelerating the sheath gas stream speed, the areas near the plasma housing pipe wall are significantly cooled. As the test is performed for a steady complete dissipated energy in the plasma, a corresponding temperature rise is noted in the initial conducting area. For a continuous flow velocity of 20 (1/mm) (Fig. 19.4), the local heat flow through the wall reaches its largest value near the downstream end of the circuit. This appears to overlap with the stagnation point where the secondary recirculation area of the wall starts. As the fluid stress rises, there is a drastic reduction in the heat flux to the wall in the coil region. However, the maximum heat flux point systematically moves downstream of the induction coil. As an example, the trajectories of fine silver particles with a diameter of 10,200 pm injected into the discharge region of a confined argon induction plasma are given in Fig. 19.29 Cheng et al. (2010). A summary of the pertinent physical properties of pure silver used in these calculations is given in Table 19.3. In this case, the plasma confinement tube had an internal diameter of 28 mm. The central powder carrier gas, and intermediate and sheath gas flow rates were set to 0.4, 2.0, and 16.0 1/mm respectively. The oscillator frequency was 3 MHz and the net power dissipated in the discharge was 3.77 kW. In the representation of the trajectories given in Fig. 19.4, the size of the circles used to indicate the position of the particles is also an indication, although not to scale, of their diameter. Moreover, an open circle indicates a solid particle whereas a dark circle represents a liquid droplet.

2.2.5 Optimal Parameters of Silver Nano Spheroids

Analyzing the impact of each single plasma parameter on nano spheroids, we can conclude an optimized parameter setting on the basis of a comprehensive discussion on multiple factors. The key plasma parameters of silver nano spheroids by induction plasma are shown in Table 19.4. It is known that the application of silver nano spheroids is restricted by two critical factors. One is the production rate, and the other is the precursor conversion rate. The Brunauer -Emmett -Teller (BET) test results of silver nano spheroids after optimizing parameters are shown in Table 19.5. The average particle size of silver nano spheroids is less than 55 nm, and the mass production rate of nanopowder has attained a hectogram level per hour. The high production rate of 327 g/h reveals the high efficiency of silver nano spheroid production, and in the 81.8% conversion rate lies a solid foundation for the massive application of silver nano spheroids (Table 19.1).

Table 19.1 Optimal parameters for the production of silver

Parameters	Value
Sheath gas Ar:H2 (SLPM of Ar)	75
Quench gas (SLPM of Ar)	480
Central gas (SLPM of Ar)	18
Plate power (kW)	19
Plate voltage	3.58
Feed rate (g/min)	5
Reactor pressure (psi)	11.4

psi pounds per square inch, *SLPM* standard liter per minute

2.2.6 Powder Feed Rate

- Definition
  - Powder feed in the system per unit of time (g/min; kg/h).
  - Change by varying stroke on powder feeder Vibrator PFV or motor speed on Powder feed Disperser (PFD) powder Feed reciprocator (PRF).
  - Optimization = stable feed rate.

During the plasma method, the powder feed speed plays a significant part in silver oxide nano spheroids. Three powder feed rates, 100, 400, and 800 g/h, are accepted. Figure 19.9 demonstrates the silver nano spheroid transmission electron micrographs at various dust feed rates. The particle size allocation of nanoparticles at the vapor feed speed of 100 g/h is apparently relatively small. Most of the particle sizes range from 150 to 200 nm. The allocation of particle size is widening as the speed of the powder feed rises. When the dust transport frequency is 800 g/h, the allocation of dust is seriously irregular. Many tiny nanoparticles adhered to the surface of the large particles; when the dust transport frequency is 800 g/h, the allocation of dust is seriously irregular. Some large solids measure up to the micrometer scale. BET assessment results are consistent with silver nano spheroid transmission electron micrographs. The median particle size of silver nano spheroids is 171 nm at a powder feed rate of 100 g/h, whereas the median particle size rises to 304 nm at a dust feed rate of 800 g/h. Monotonically, the median particle size rises as the speed of the dust feed rises. As the dust supply frequency rises from 100 to 800 g/h, there is a sharp increase in the amount of coarse powders traveling through the plasma area, which raises the power requirement for nano spheroidization. The plasma energy is corrected, however, which is too restricted to allow full vaporization of coarse powders at a 800 g/h powder feed rate. The nano spheroidization effectiveness of silver is due to the low thermal intake of vapor at an elevated powder feed frequency (Fig. 19.9 and Table 19.2).

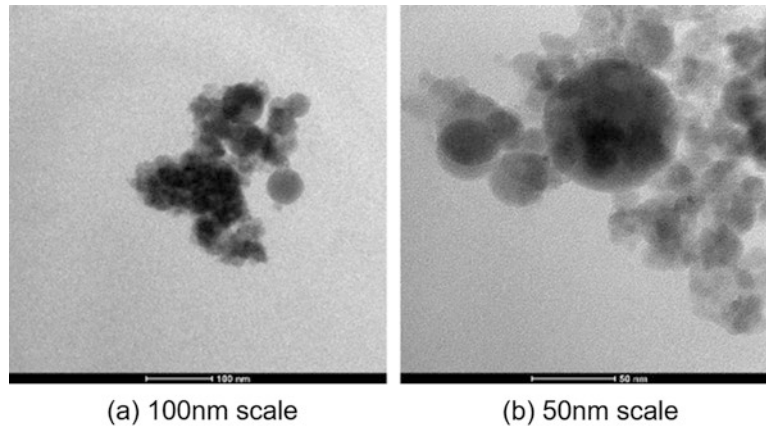

Fig. 19.9 Particle formation in a two-component system. (**a**) 100-nm scale. (**b**) 50-nm scale

Table 19.2 Brunauer–Emmett–Teller (BET) test values for different plasma power (conducted at IPR Gujarat)

Induction plasma power (kW)	The BET value (m^2/g)	Particle size (nm)
15 kW	26.878	58 nm
22 kW	19.654	46 nm
30 kW	12.548	32 nm

Impact of Raising the Feed Rate

- Poor energy distribution.
- Nano: increases powder diameter.
- Sphero: decreases percentage spheroidization.
- Less energy per particle.
- Risk of clogging into the probe or tube.

Impact of Lowering the Feed Rate

- Lower production rates.
- Higher production costs.
- Nano: less production.
- Sphero: lower yield owing to evaporation.

2.2.7 Plasma Particle Interaction Effects

Although the assumption of a dilute system has generally been accepted for the calculation of individual particle trajectories and temperature histories under plasma conditions, the interpretation of the results obtained is greatly hindered by the simple fact that any application of plasma technology for the inflight processing of powders will have to be carried out under sufficiently high loading conditions in order to make efficient use of the thermal energy available in the plasma. With the local cooling of the plasma owing to the presence of the particles, model predictions using the low loading assumption can be substantially incorrect. In an attempt to take into account the plasma particle interaction effects, Boulos and his collaborators (Baldwin et al. 2002) developed a mathematical model, which, through the iterative procedure illustrated in Brunauer–Emmett–Teller (BET) continuously updates the computed plasma temperature, velocity, and concentration yields. The interaction between the stochastic single-particle trajectory calculations and those of the continuum low, temperature and concentration yields is incorporated through the use of appropriate source/sink terms in the respective continuity, momentum, energy, and mass transfer equations. These are estimated using the so-called particle source in the cell model (PSI-cell) Si et al. (2003).

2.2.8 Dispersion of Biomedical Silver and Metal Oxide Nanopowders (as per GMP)

The following method is written for the preparation of dispersion of silver nano spheroids (AgNps) in deionized (DI) water (50 mg/l concentration).

Materials

1. One large glass beaker (1 l)
2. Volumetric
3. (Glass) flask (1 l).
4. DI water (resistivity of 18 Ω).
5. Ultrasonic probe 3 (Cole-Parmer R 130 Watt Ultrasonic Processors (50/60 Hz, VAC 220); product number EW0471451); the titanium probe measures 6 mm (1/4″) and is tuned to resonate at 20 kHz, 50 kHz).
6. Mini lab jack.
7. Stainless steel spatula.
8. Disposable pipette (preferably standard glass Pasteur pipette, 150 mm long).
9. Vial 2 containing nano spheroids (AgNps; 50 mg).
10. Vial 3 (precleaned, with no specific dimensions) to contain a suitable volume of DI water with between 20 to 1%.

Method Step 1: to create a thick paste, add a few drops of DI water (with 20 to 1 %) taken from vial 3 using a glass pipette to the nanoparticles powder in vial 2. Do this using a precleaned spatula while mixing and apply enough energy to remove visible aggregates in the paste. The purpose of this wetting step is to adequately replace the solid–air interface with a solid–

liquid interface, as recommended by guidelines in BS ISO 14887 (2000) ('Sample preparation dispersing procedures for liquid powders').

Step 2: add the rest of the DI water from vial 3 into vial 2 (containing the paste of nanoparticles powder) and gently mix using a clean spatula.

Step 3: place vial 2 on to a lab jack and insert the ultrasonic probe tip halfway down the small vial. Deagglomerate using an ultrasonic probe for 20 s (at 90% amplitude; this should give a temperature rise of 5 °C in the dispersion). The operator should determine the acceptable temperature rise during sonication in the given time period. If a longer sonication time is required, then the operator must provide better control of the temperature inside the vial. One option is to immerse vial 2 in an ice bath during sonication. Ensure that the tip is not touching the sides of the glass vial. In addition, do not place your hands near the deagglomerating unit while it is operating.

Step 4: once completed, transfer the nanoparticle suspension to the desired total volume (to make the "stock) and mix gently with a glass rod. Flush the small vial with further DI Water (or liquid media) and add this to the rest of the suspension. This "washing" step is important to ensure that all of the nanoparticles are transferred from the small vial to the larger beaker, so that the dosage measurement (by mass) can be interpreted accurately. Gently stir with a glass rod. For greater accuracy, make up the desired volume using the appropriate volumetric flask/pipette.

Step 5: the dispersion is now ready for analysis. For the nanoparticle analysis, this will involve the sample splitting of the "stock". From guidelines found in ISO 14488: 2007 (Particulate materials sampling and sample splitting for the determination of particulate properties), sample splitting using a pipette is recommended as this method (relative to sample splitting using multiple capillary tubes) is simple to do and less prone to contamination. Prior to taking an aliquot out of the stock, agitate the stock dispersion.

3 Results and Discussion

3.1 Characterization of Biomedical Silver Nanoparticles

3.1.1 UV-Vis Spectrum

The Uv-Vis spectrum analysis was primarily performed to confirm the formation of silver nanoparticles based on the expectance and presence of the standard absorbance peak within a range of 400–420 nm, which was exhibited by our materials, both on the day of synthesis and 20 days post-synthesis (Fig. 19.10).

3.1.2 Dynamic Light Scattering

Dynamic light scattering (DLS) was performed for the silver nanomaterial as a primary confirmation of the size of the nanomaterial synthesized by using a Malvern Zetasizer NZ, the powder was dispersed in DI water by probe sonication based on our regular quality control protocols, and the tests were performed at room temperature to avoid varying hydrodynamic motions. The sample was tested during three time phases: one on the same day of synthesis, which gave us a hydrodynamic size of silver nanopowder and gave us a zeta average of 48 nm, giving a 100% intensity peak at 31.78 nm with an acceptable standard deviation of 3. 77 nm. The sample was rechecked 20 days later to confirm the shelf life of the material after storing it in a dark foiled bottle in a vacuum. The sample gave peaks within the same range below 40 nm with a standard deviation of 6.77 nm and a maximum intensity peak at 37.28 nm with an intensity of 86% (Figs. 19.11 and 19.12).

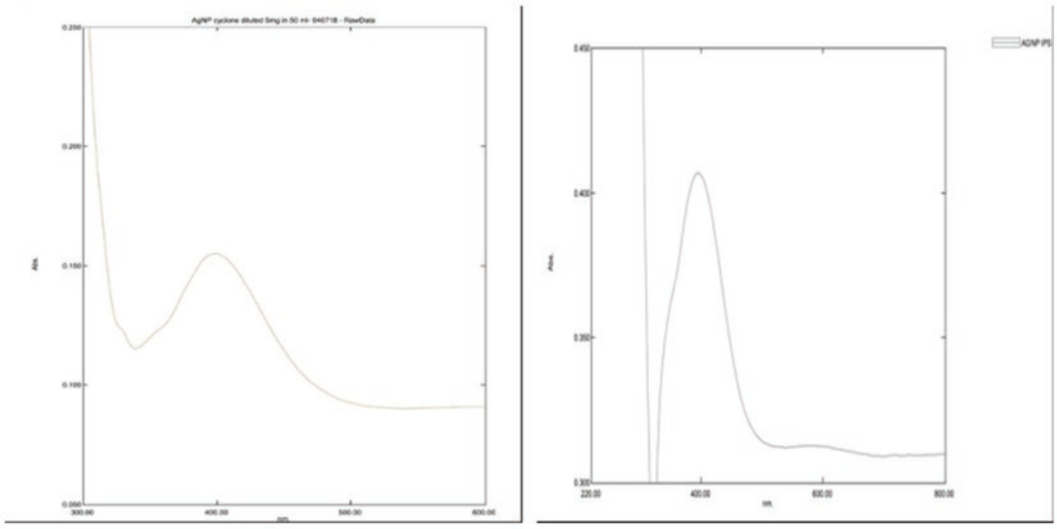

Fig. 19.10 UV-Vis spectrum of Silver Nano Particles (AgNps) (**a**) Cyclone canister. (**b**) Mid-canister

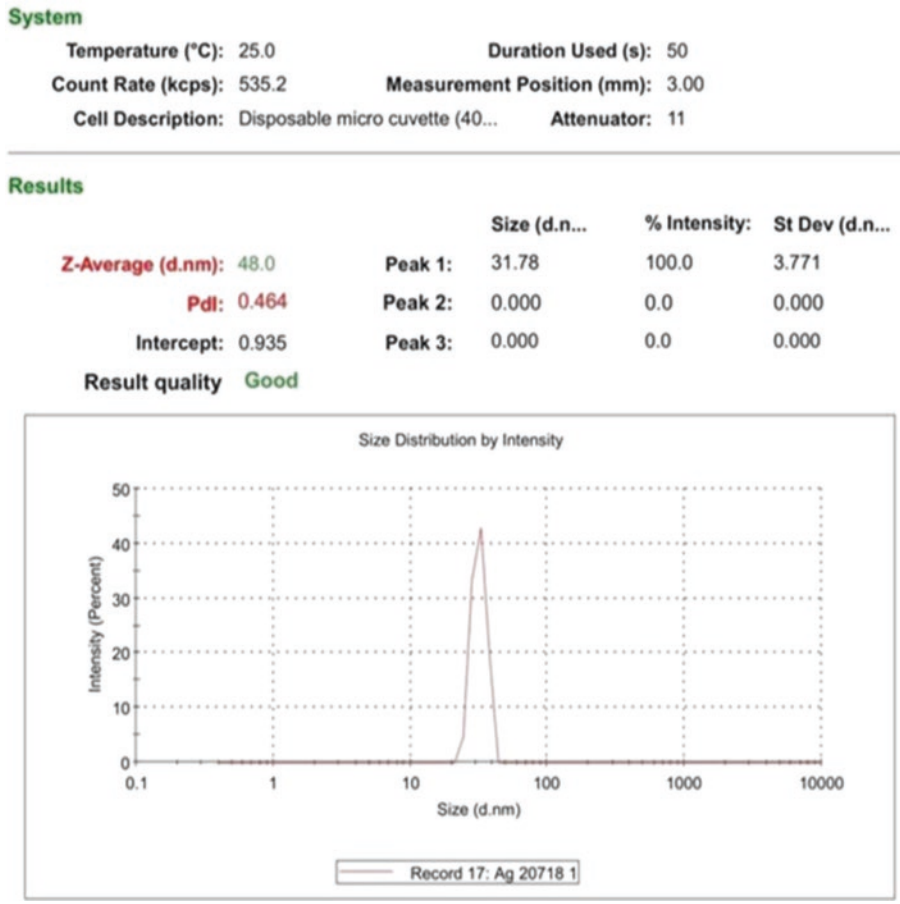

Fig. 19.11 Dynamic light scattering of Silver Nano Particles (AgNps) after synthesis

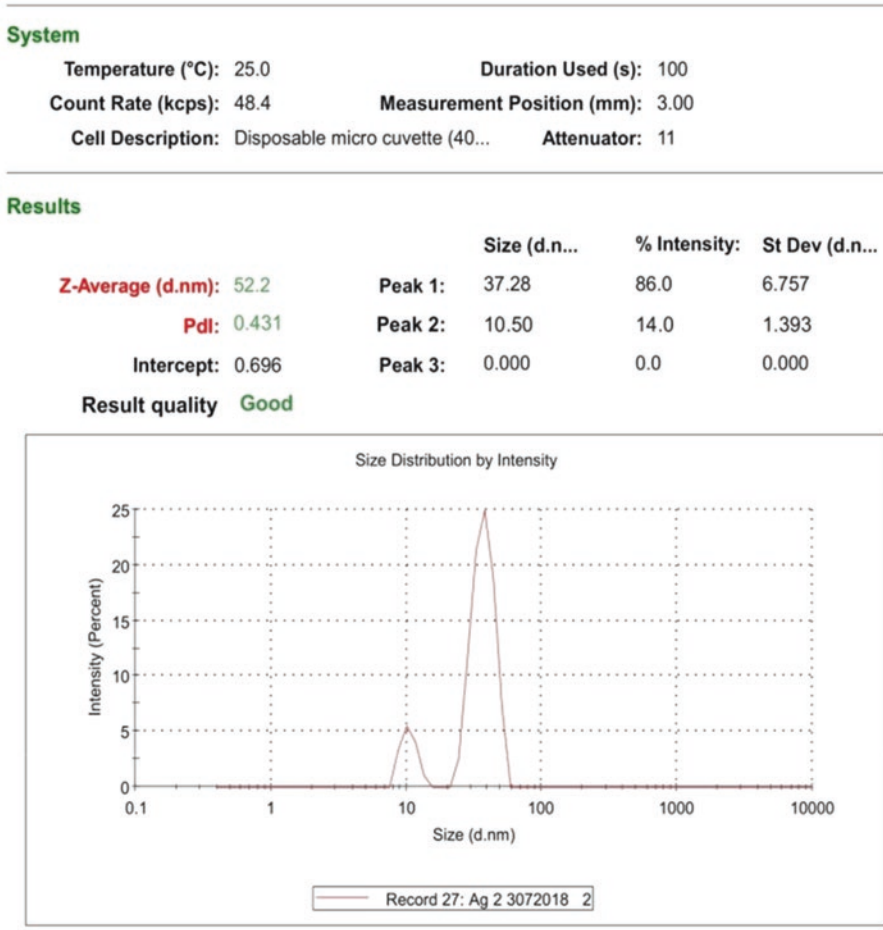

Fig. 19.12 Dynamic light scattering of Silver Nano Particles (AgNps) after 20 days after synthesis to check agglomeration

3.1.3 Zeta Potential

The zeta potential of the above silver nanopowder was performed in ethanol as a dispersant, by sonicating for 30 min in ethanol and the dilution and filtration was carried out as per company quality control protocol. The zeta values ranged between 15 and 17 mV, which falls within the desired range of standards between -30 and +30 mV, showing greater stability and good activity (Fig. 19.13).

3.1.4 X-Ray Diffraction Report (Figs. 19.14, 19.15, and 19.16)

3.1.5 Characterization of Biomedical Metal Oxide Nanoparticles (Figs. 19.17 and 19.18)

3.1.6 Antimicrobial Study for Silver for Wound Healing Gels/ Pharma Grade Disinfectants

Minimal inhibitory concentration (MIC) determination: IPS Silver Nano Particles (AgNps) were exploited to determine their MIC against *Enterobacter aerogenes* (Gram-negative) and *Bacillus subtilis* (Gram-positive). Inoculum was maintained to 0.5 McFarland dilution for performing the MIC test according to Clinical Laboratory Standard Institute (CLSI) guidelines. Amoxicillin and streptomycin were positive controls for comparative analysis. Antimicrobial activity of IPS AgNP was validated using various bacterial and fungal cultures (Figs. 19.2, 19.3;

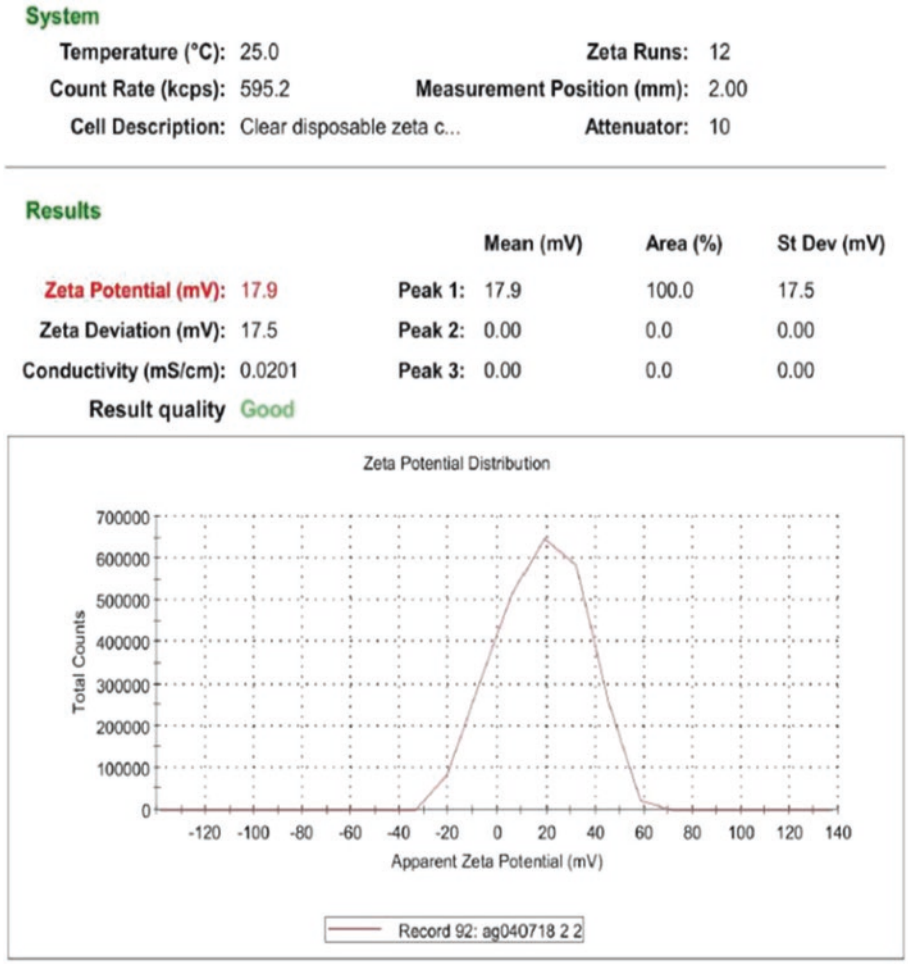

Fig. 19.13 Zeta potential of Silver Nano Particles (AgNps) after synthesis to check stability and surface charge

Phase classification

Name	Silver
Mineral Name	Silver
Formula	Ag
I/Icor	19.120001
Sample Name	9013045
Quality	C (calculated)

References

Publication	
Bibliography	Suh I.-K., Ohta H., Waseda Y., "High-temperature thermal expansion of six metallic elements measured by dilatation method and X-ray diffraction Locality: synthetic Sample: at T = 293 K", Journal of Materials Science **23**, 757-760 (1988)
Origin of data	
Source of entry	COD (Crystallography Open Database)
Link to orig. entry	9013045

Crystal structure

Crystallographic data	
Space group	F m -3 m (225)
Crystal system	Cubic
Cell parameters	a= 4.0860 Å
Cell meas. conditions	T= 293.0 K

Crystal structure

Crystallographic data	
Space group	F m -3 m (225)
Crystal system	Cubic
Cell parameters	a= 4.0860 Å
Cell meas. conditions	T= 293.0 K

Atom coordinates

Element	Oxid.	x	y	z	Bi	Focc.
Ag		0.000	0.000	0.000	1.000000	1.000000

Diffraction data

Diffraction lines

d [Å]	Int.	h	k	l	Mult.
2.3591	1000.0	1	1	1	8
2.0430	467.8	2	0	0	6
1.4446	256.1	2	0	2	12
1.2320	271.7	3	1	1	24
1.1795	76.9	2	2	2	8
1.0215	37.0	4	0	0	6
0.9374	129.9	3	1	3	24
0.9137	128.9	4	0	2	24
0.8341	152.0	4	2	2	24
0.7864	360.0	3	3	3	8

Experimental

Physical Properties	
Calc. density	10.50300 g/cm³

Fig. 19.14 Phase analysis of nanosilver

Name	Silver
Mineral Name	Silver
Formula	Ag
I/Icor	19.139999
Sample Name	9013047
Quality	C (calculated)
Publication	
Bibliography	Suh I.-K., Ohta H., Waseda Y., "High-temperature thermal expansion of six metallic elements measured by dilatation method and X-ray diffraction Locality: synthetic
Origin of data	
Source of	COD (Crystallography Open Database)
Link to orig. entry	9013047
Crystal structure	
Crystallographic data	
Space group	F m -3 m (225)
Crystal system	Cubic
Cell parameters	a= 4.1170 Å
Cell meas.	T= 671.0 K

Atom coordinates

Element	Oxid.	x	y	z	Bi	Focc
Ag		0.000	0.000	0.000	1.000000	1.000000

Diffraction data

Diffraction lines

d [Å]	Int.	h	k	l
2.3770	1000.0	1	1	1	8
2.0585	468.7	2	0	0	6
1.4556	257.8	2	0	2	12
1.2413	273.2	3	1	1	24
1.1885	77.2	2	2	2	8
1.0293	36.7	4	0	0	6
0.9445	127.5	3	1	3	24
0.9206	125.9	4	0	2	24
0.8404	144.0	4	2	2	24
0.7923	304.2	3	3	3	8

Experimental	
Physical Properties	
Calc. density	10.26600 g/cm³

Fig. 19.15 Phase analysis of nanosilver

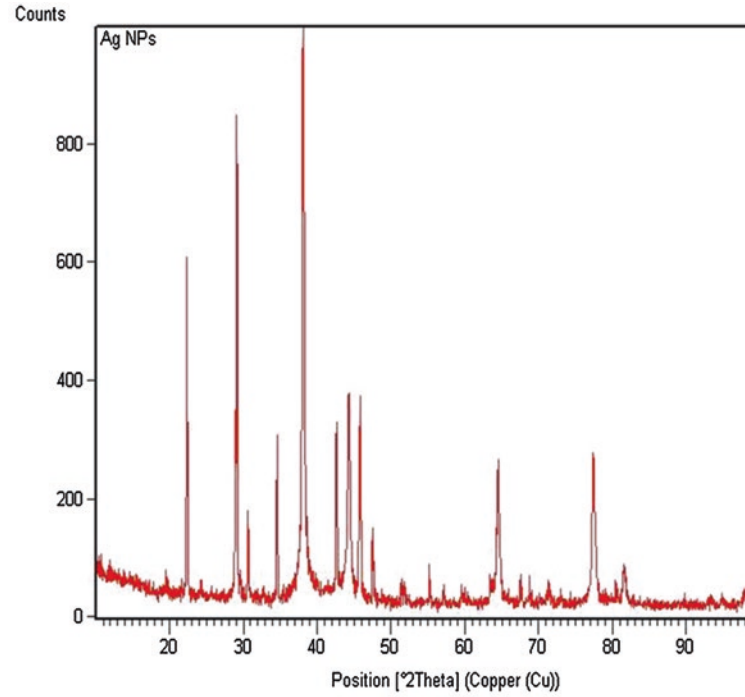

Fig. 19.16 X-ray diffraction pattern of silver nano spheroids

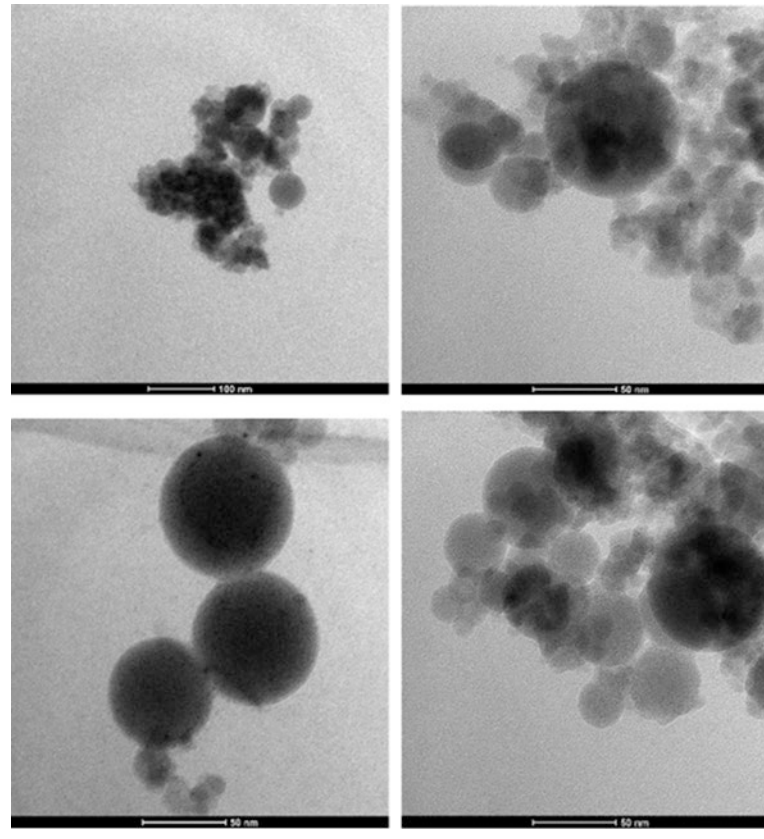

Fig. 19.17 Transmission electron microscopy images of titanium dioxide

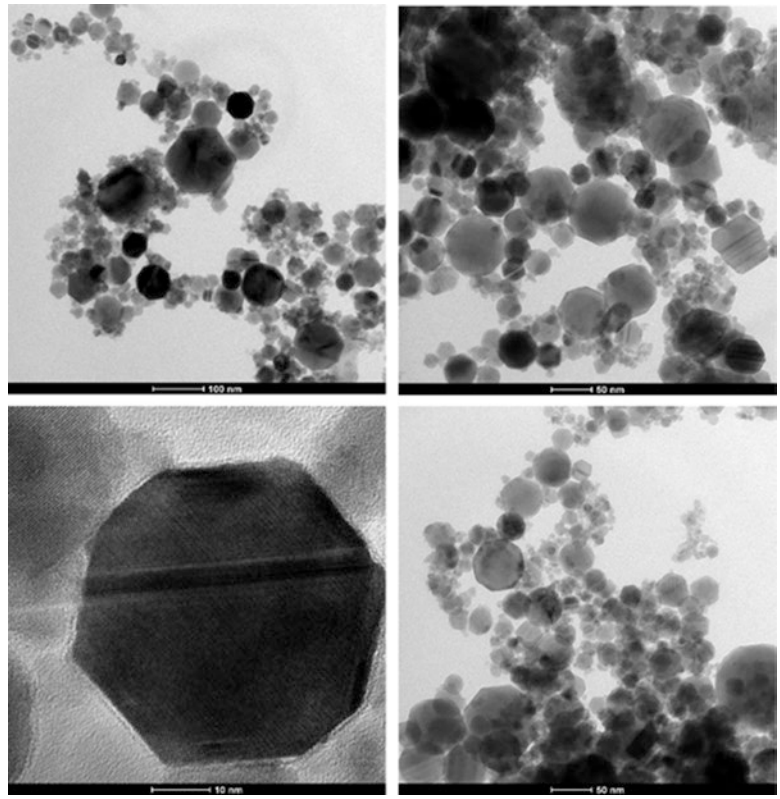

Fig. 19.18 Transmission electron microscopy images of silver-coated graphene

Tables 19.2, 19.3). MIC was found to be 12.5 g/ml for both bacterial and fungal inhibition, which is almost close to the commercial antimicrobial agents (Figs. 19.19 and 19.20, Table 19.3).

As is evident from Table 19.4, IPS AgNP is active against both bacteria, whereas amoxicillin is more active against *Bacillus subtilis* and streptomycin is more active against *Enterobacter aerogenes*. These results are undergoing further validation (Tables 19.5, 19.6, and 19.7).

Zone inhibition test: IPS AgNP were exploited to determine their zone of inhibition against *Enterobacter aerogenes* (Gram-negative) and *Bacillus subtilis* (Gram-positive). To study the zone of inhibition, the gel diffusion method was employed. Initially, bacterial suspension was made to get dilution of 0.5 on the McFarland scale (1 * 108 CFU/ml) and spread onto agar plates according to CLSI guidelines. Amoxicillin and streptomycin were positive controls for comparative analysis. As is evident from Table 19.8, IPS AgNP has exhibited a zone of inhibition almost like streptomycin and amoxicillin (Table 19.9; Fig. 19.21).

Table 19.3 Sample identification

Sample name	Size (in nm)	Zeta potential (mV)	Uv_{max} (nm)
IPS AgNP	58	15.6	408

4 Conclusion

Silver nanoparticles are being used in numerous technologies and incorporated into a wide array of consumer products that take advantage of their desirable optical, conductive, and antibacterial properties.

1. Diagnostic applications: silver nanoparticles are used in biosensors and numerous assays where the silver nanoparticle materials can be used as biological tags for quantitative detection.
2. Antibacterial applications: silver nanoparticles are incorporated in apparel, footwear, paints, wound dressings, appliances, cosmetics, and plastics.

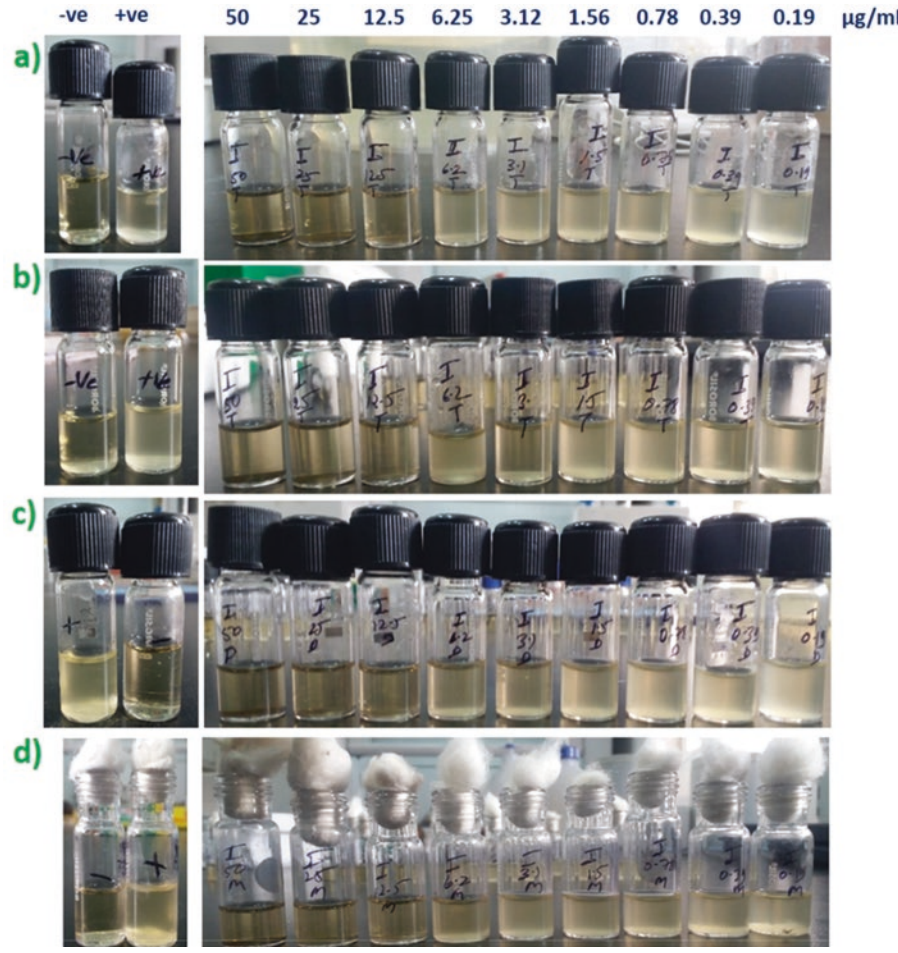

Fig. 19.19 Photographic representation of antibacterial activity of IPS AgNP against (**a**) *E. coli*, (**b**) *Staphylococcus aureus*, (**c**) *Pseudomonas aeruginosa*, and (**d**) *Bacillus subtilis* using the broth dilution method. For Minimal inhibitory concentration data please refer to the Results and Discussion section

Table 19.4 Minimal inhibitory concentration (MIC) of IPS Silver Nanoparticles (AgNPs) in comparison with amoxicillin and streptomycin

	Enterobacter aerogenes	Bacillus subtilis
Sample name	(MIC in g)	(MIC in g)
IPS AgNP	137.5	93.7
Amoxicillin	>500	23.4
Streptomycin	93.7	>500

Table 19.5 Minimum inhibitory concentration (MIC) of IPS Silver Nanoparticles (AgNPs) in comparison with bulk Ag powder, enrofloxacin, and ampicillin

	E. coli	S. aureus
Sample name	(MIC in g/ml)	(MIC in g/ml)
IPS AgNP	12.50	12.50
Bulk Ag powder	>50	>50
Enrofloxacin	1,710.45	2,271.70
Ampicillin	2,341.20	3,382.30

Table 19.6 Minimum inhibitory concentration (MIC) of IPS Silver Nanoparticles (AgNPs) in comparison with bulk Ag powder, enrofloxacin, and ampicillin

Sample name	*P. aeruginosa* (MIC in g/ml)	*Bacillus subtilis* (MIC in g/ml)
IPS AgNP	12.50	12.50
Bulk Ag powder	>50	>50
Enrofloxacin	13.15	11.56
Ampicillin	22.70	41.16

Table 19.7 Minimum inhibitory concentration (MIC) of IPS Silver Nanoparticles (AgNPs) in comparison with bulk Ag powder, thiabendazole, and clioquinol

Sample name	*Aspergillus niger* (g/ml)	*Penicillium oxalicum* (g/ml)
IPS AgNP	12.50	12.50
Bulk Ag powder	>50	>50
Thiabendazole	12.50	0.390
Clioquinol	18.219	1.560

3. Conductive applications: silver nanoparticles are used in conductive inks and integrated into composites to enhance thermal and electrical conductivity.
4. Optical applications: silver nanoparticles are used to efficiently harvest light and for enhanced optical spectroscopies, including metal-enhanced fluorescence and surface-enhanced Raman scattering (Fig. 19.22).

5 Objective: To Test the Efficiency of the Matrix Nano Water Disinfectant

Result: pH of the sample water {7.7 (Table 19.10).

The sample was incubated for 10–15 min and plated on a Luria Bertani agar plate to check for CFU. 200 ul of the samples A, B, C, and D were added to 2 ml of the Luria Bertani broth for a turbidity check.

Table 19.8 Zone of inhibition test for IPS Silver Nanoparticles (AgNPs) in comparison with streptomycin and amoxicillin

Name and concentration of compound (g)	Zone of inhibition (mm) *Enterobacter aerogenes*	Zone of inhibition (mm) *Bacillus subtilis*
IPS Silver Nanoparticles (AgNPs)		
20	13.60	15.01
50	13.60	15.30
100	13.80	17.60
200	14.80	16.31
Streptomycin		
20	19.61	
50	21.61	
100	23.60	
200	26.60	
Amoxicillin		
20	19.61	13.60
50	21.61	13.81
100	23.60	15.02
200	26.60	18.00

Table 19.9 Zone of inhibition test for IPS Silver Nanoparticles (AgNPs) against *E. coli*

Concentration in (μg/g)	Zone of inhibition in mm
10	12, 12, 12, 11
25	11, 14, 14, 16
50	15, 15, 17, 17
100	15, 15, 16, 17

Observation: the sample water is contaminated and treatment results in 100% clearance of the bacterial contaminant.

Procedure

1. The matrix nano disinfectant was tested in 15 batches at different concentrations.
2. The samples were taken from three different locations, and the experiment was carried out for 3 months by the Pradeep research group at IIT MADRAS (Table 19.11).

Result: at a concentration of 5 ppm, the bactericidal effect of the disinfectant is observed.

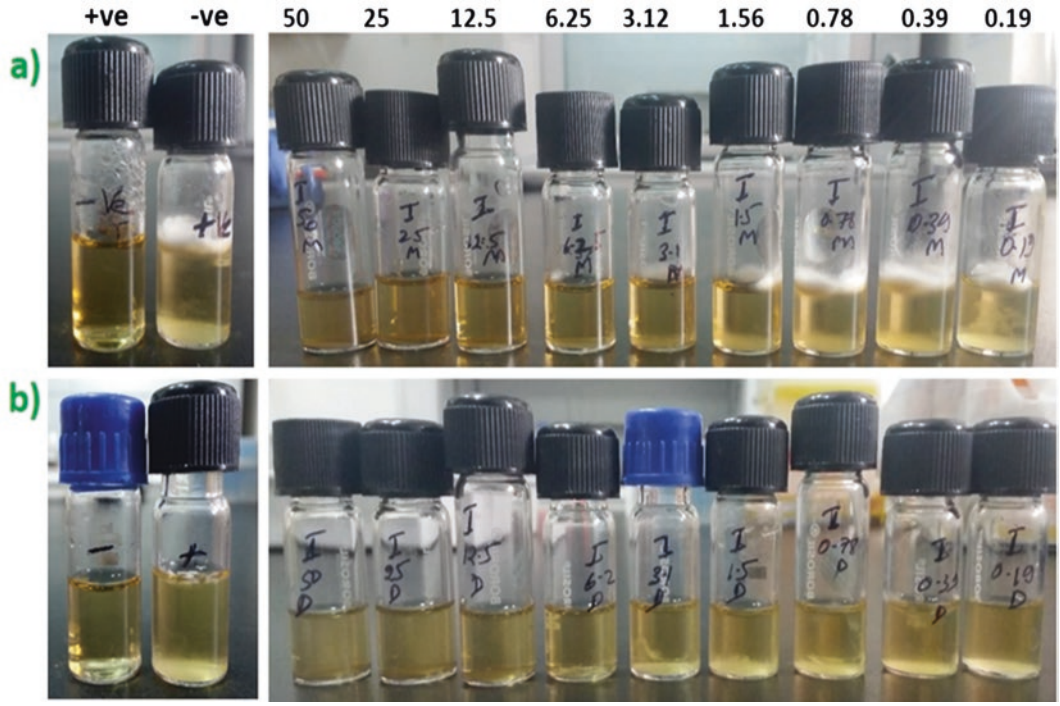

Fig. 19.20 Photographic representation of antifungal activity of IPS Silver Nanoparticles (AgNPs) against (**a**) *Aspergillus niger* and (**b**) *Penicillium oxalicum* using the broth dilution method

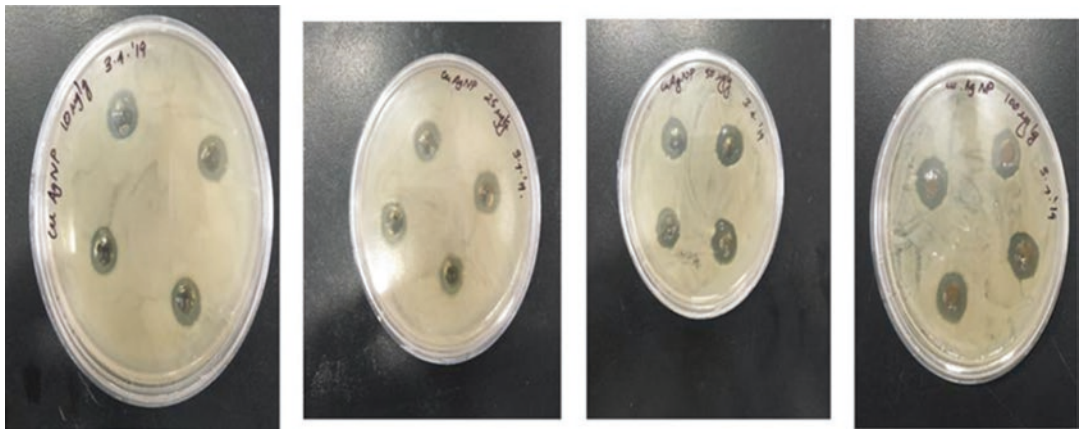

Fig. 19.21 Zone of inhibition test

Acknowledgement I would like to heartily thank Dr. Y. Srinivas Rao, chief scientist of the Nanotechnology Innovation Centre, who helped me with the antimicrobial study of plasma-synthesized nano silver. I would also like to thank my machine operator, Vivek Sharma, for being there with me through various trials and experiments. This was all possible because of the blessing of my Mom and Dad, who constantly supported me to be a nanotechnologist. In addition, I would also want to acknowledge my friend, Miss Risha Jain, who constantly kept me motivated during my experiments and trials.

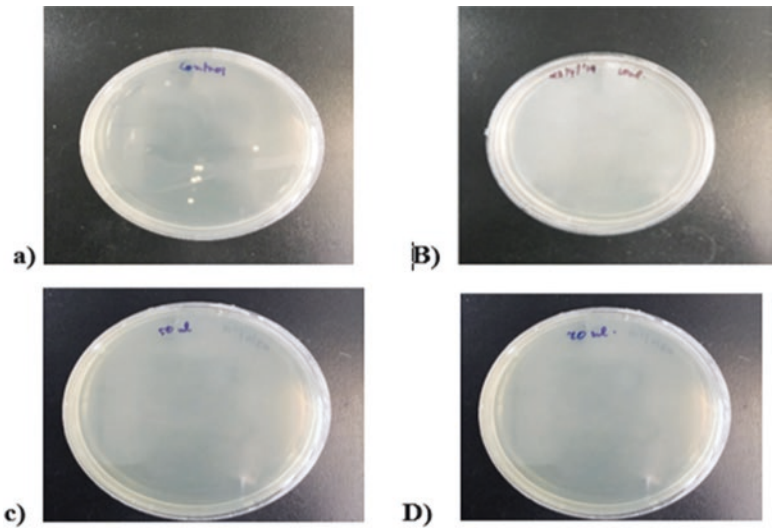

Fig. 19.22 (**a**) Control sample plated in Luria Bertani agar, (**b**) sample A plated, (**c**) sample B plated, (**d**) sample C plated

Table 19.10 Effect of disinfectant in water

	Control	Sample A	Sample B	Sample C
Disinfectant (in liters)		10	70	50
Water sample (in milliliters)	10	10	10	10

Table 19.11 Comparison of the antibacterial effect of sample 1 (matrix nano) and sample (colloid silver)

	Bacteria count in control (CFU/ml)	Bacteria count in sample 1	Bacteria control in sample 2
Time (h)	Concentration of silver = 0 ppm	Concentration of silver = 5 ppm	Concentration of silver = 5 ppm
0	1*10^6	1*10^6	1*10^6
1	1*10^6	1*10^4	1*10^5
1.5	1*10^6	3*10^2	1*10^5
24	1*10^6	1*10^2	4*10^2

References

Akyildiz H, Ozturk T. Hydrogen sorption in crystalline and amorphous Mg–Cu thin films. J Alloys Compd. 2010;492(12):745–50.

Aminorroaya S, Ranjbar A, Cho YH, Liu HK, Dahle AK. Hydrogen storage properties of mg10 wt.% Ni alloy co-catalysed with niobium and multiwalled carbon nanotubes. Int J Hydrog Energy. 2011;36(1):571–9.

Anastasopol A, er TVP, Middelkoop J, La font U, Perez RJC, Ott AS, Mulder FM, Eijt SWH. Reduced enthalpy of metal hydride formation for Mg–Ti nanocomposites produced by spark discharge generation. J Am Chem Soc. 2013;135(21):7891–900.

Atias-Adrian IC, Deorsola FA, Ortigoza-Villalba GA, De Benedetti B, Baricco M. Development of nanostructured Mg_2Ni alloys for hydrogen storage applications. Int J Hydrog Energy. 2011;36(13):7897–901.

Baldwin RK, Pettigrew KA, Garno JC, Power PP, Liu G, Kauzlarich SM. Room temperature solution synthesis of alkyl capped tetrahedral shaped silicon nanocrystals. J Am Chem Soc. 2002;124(7):1150–1.

Burak Aktekin. Induction plasma synthesis of Mg-Ni nanoparticles. PhD thesis, Middle East Technical University; 2013.

Bystrzejewski M, Huczko A, Lange H. Arc plasma route to carbon encapsulated magnetic nanoparticles for biomedical applications. Sensors Actuators B Chem. 2005;109(1):81–5.

Cheng KY, Anthony R, Kortshagen UR, Holmes RJ. Hybrid silicon nanocrystal organic light emitting devices for infrared electroluminescence. Nano Lett. 2010;10(4):1154–7.

Dal Negro L, Pavesi L, Pucker G, Franzo G, Priolo F. Optical gain in silicon nanocrystals. Opt Mater. 2001;17(12):41–4.

de Jongh PE, Wagemans RWP, Eggenhuisen TM, Dauvillier BS, Radstake PB, Meeldijk JD, Geus JW, de Jong KP. The preparation of carbon supported magnesium nanoparticles using melt in infiltration. Chem Mater. 2007;19(24):6052–7.

Ding Y, Dong Y, Bapat A, Nowak JD, Barry Carter C, Kortshagen UR, Campbell SA. Single nanoparticle semiconductor devices. IEEE Trans on Electron Devices. 2006;53(10):2525–31.

Gresback R, Nozaki T, Okazaki K. Synthesis and oxidation of luminescent silicon nanocrystals from silicon tetrachloride by very high frequency nonthermal plasma. Nanotechnology. 2011;22(30):305605.

Gupta A, Swihart MT, Wiggers H. Luminescent colloidal dispersion of silicon quantum dots from microwave plasma synthesis: exploring the photoluminescence behavior across the visible spectrum. Adv Funct Mater. 2009;19(5):696–703.

Hirasawa M, Orii T, Seto T. Size-dependent crystallization of Si nanoparticles. Appl Phys Lett. 2006;88(9):093119.

Jeon K-J, Moon HR, Ruminski AM, Jiang B, Kisielowski C, Bardhan R, Urban JJ. Air stable magnesium nanocomposites provide rapid and high capacity hydrogen storage without using heavy metal catalysts. Nat Mater. 2011;10(4):286.

Jiayin G, Xiaobao F, Dolbec R, Siwen X, Jurewicz J, Boulos M. Development of nano powder synthesis using induction plasma. Plasma Sci Technol. 2010;12(2):188.

Jurbergs D, Rogojina E, Mangolini L, Kortshagen U. Silicon nanocrystals with ensemble quantum yields exceeding 60%. Appl Phys Lett. 2006;88(23):233116.

Lee JG, Li P, Choi CJ, Dong XL. Synthesis of Mn–Al alloy nanoparticles by plasma arc discharge. Thin Solid Films. 2010;519(1):81–5.

Lee JK, Yoon WY, Kim BK. Electrochemical behavior of Si nanoparticle anode coated with diamond like carbon for lithium ion battery. J Electrochem Soc. 2012;159(11):A1844–8.

Lei JP, Huang H, Dong XL, Sun JP, Lu B, Lei MK, Wang Q, Dong C, Cao GZ. Formation and hydrogen storage properties of in situ prepared Mg–Cu alloy nanoparticles by arc discharge. Int J Hydrog Energy. 2009;34(19):8127–34.

Li JG, Ikeda M, Ye R, Moriyoshi Y, Ishigaki T. Control of particle size and phase formation of TiO_2 nanoparticles synthesized in RF induction plasma. J Phys D Appl Phys. 2007;40(8):2348.

Liang G, Huot J, Boily S, Van Neste A, Schulz R. Hydrogen storage properties of the mechanically milled MgH_2–V nanocomposite. J Alloys Compd. 1999;291(12):295–9.

Mandal TK, Gregory DH. Hydrogen: a future energy vector for sustainable development. Proc Inst Mech Eng C J Mech Eng Sci. 2010;224(3):539–58.

Mangolini L. Synthesis, properties, and applications of silicon nanocrystals. J Vac Sci Technol B Microelectron Nanometer Struct. 2013;31(2):020801.

Mangolini L, Thimsen E, Kortshagen U. High yield plasma synthesis of luminescent silicon nanocrystals. Nano Lett. 2005;5(4):655–9.

Oelerich W, Klassen T, Bormann R. Metal oxides as catalysts for improved hydrogen sorption in nanocrystalline mg-based materials. J Alloys Compd. 2001;315(12):237–42.

Ostraat ML, De Blauwe JW, Green ML, Bell LD, Brongersma ML, Casperson J, Flagan RC, Atwater HA. Synthesis and characterization of aerosol silicon nanocrystal non-volatile fatigated memory devices. Appl Phys Lett. 2001;79(3):433–5.

Petermann N, Stein N, Schierning G, Theissmann R, Stoib B, Brandt MS, Hecht C, Schulz C, Wiggers H. Plasma synthesis of nanostructures for improved thermoelectric properties. J Phys D Appl Phys. 2011;44(17):174034.

Pfeiffer TV, Feng J, Schmidt Ott A. New developments in spark production of nanoparticles. Adv Powder Technol. 2014;25(1):56–70.

Reilly JJ Jr, Wiswall RH Jr. Reaction of hydrogen with alloys of magnesium and nickel and the formation of Mg2NiH4. Inorg Chem. 1968;7(11):2254–6.

Reinmann R, Akram M. Temporal investigation of a fast spark discharge in chemically inert gases. J Phys D Appl Phys. 1997;30(7):1125.

Schwyn S, Garwin E, SchmidtOtt A. Aerosol generation by spark discharge. J Aerosol Sci. 1988;19(5):639–42.

Si PZ, Zhang ZD, Geng DY, You CY, Zhao XG, Zhang WS. Synthesis and characteristics of carbon coated iron and nickel nanocapsules produced by arc discharge in ethanol vapor. Carbon. 2003;41(2):247–51.

Vons VA, Leegwater H, Legerstee WJ, Eijt SWH, Schmidt Ott A. Hydrogen storage properties of spark generated palladium nanoparticles. Int J Hydrog Energy. 2010;35(11):5479–89.

Vons VA, Anastasopol A, Legerstee WJ, Mulder FM, Eijt SWH, Schmidt Ott A. Low temperature hydrogen desorption and the structural properties of spark discharge generated mg nanoparticles. Acta Mater. 2011;59(8):3070–80.

Vyas D, Jain P, Agarwal G, Jain A, Jain IP. Hydrogen storage properties of Mg_2Ni affected by Cr catalyst. Int J Hydrog Energy. 2012;37(21):16013–7.

Yan Y, Au YS, Rentsch D, Remhof A, de Jongh PE, Zuttel A. Reversible hydrogen storage in $Mg(Bh_4)_2$/carbon nanocomposites. J Mater Chem A. 2013;1(37):11177–83.

Zaluska A, Zaluski L, Strom Olsen JO. Synergy of hydrogen sorption in ball milled hydrides of Mg and Mg_2Ni. J Alloys Compd. 1999;289(12):197–206.

Zhang X, Yang R, Yang J, Zhao W, Zheng J, Tian W h, Li X g. Synthesis of magnesium nanoparticles with superior hydrogen storage properties by acetylene plasma metal reaction. Int J Hydrog Energy. 2011;36(8):4967–75.

Techniques for Accurate Sizing of Nanoparticles

20

Hemant K. S. Yadav, Afrasim Moin,
Roua Abdulazem Okla, and Raghad Issa Odeh

Abstract

Nanotechnology is having vast applications. Nanoparticles have shown promising results in drug delivery. There are various techniques to prepare nanoparticles. After the preparation, the measurement of size of nanoparticle is very important. The chapter focusses on different techniques which are used for accurate measuring of various nanoparticles along with nanoparticles properties like surface charge and particle size. The chapter describes various techniques like transmission electron microscopy, dynamic light scattering, atomic force microscopy, tunable resistive pulse sensing, etc. along with the principles involved, advantages, and limitations. It also briefly describes about the challenges in nanoparticles characterization.

Keywords

Nanoparticles · Particle size · Techniques · Challenges

H. K. S. Yadav (✉) · R. A. Okla · R. I. Odeh
RAK College of Pharmaceutical Sciences, RAK Medical and Health University,
Ras Al Khaimah, UAE
e-mail: hemant@rakmhsu.ac.ae

A. Moin
Department of Pharmaceutics, University of Hail,
Hail, Saudi Arabia

1 Introduction

Bio-nanotechnology has been introduced recently in medical fields. The major part of this science is nanoparticles. Nanoparticles are defined as the particles whose size ranges in the nano-scale. These nanoparticles are used as vehicles for nanomedicines. Besides this application, they have other applications, as they act as markers in immunohistochemistry and detectors for biosensors. In addition, nanoparticles are preferred over conventional dosage forms due to their efficiency, since they are less toxic, exhibit fewer side effects, provide controlled release of the drug, and have the ability to deliver the drug directly to its target. Recent applications are majorly in the field of biomedical and pharmaceutical sciences, in which nanoparticles are used as drug delivery systems, diagnostic tools, and transdermal patches. The use of nanoparticles as drug delivery system has been considered economic and more beneficial to health because fewer materials are used in the composition of the drug product, leading to increased efficiency and more stable drug product; therefore, characterization of nanoparticles before they are formulated is very important. Characterization includes studying their particle size, surface charge, shape, degree of aggregation, and size distribution (Carvalho et al. 2018).

J. K. Patel, Y. V. Pathak (eds.), *Emerging Technologies for Nanoparticle Manufacturing*,
https://doi.org/10.1007/978-3-030-50703-9_20

2 Importance of Nanoparticle Properties

2.1 Surface Charge

Surface charge is an important parameter to be studied for a nanoparticle. The nanoparticle can be either positively charged, negatively charged, or neutral. The least efficiency exists when the nanoparticle is neutral. In addition, neutral nanoparticles aggregate, leading to precipitation. When nanoparticles enter the body, they interact with the biological fluids by binding to proteins which will change their surface charge; then they will be delivered to their target sites. Since the cell membrane is negatively charged, positively charged nanoparticles are preferred over neutral and negatively charged nanoparticles. So, positively charged nanoparticles bind to the cell membrane strongly due to the electrostatic forces. Therefore, undesired consequences can be prevented such as platelet aggregation and hemolysis (Carvalho et al. 2018).

2.2 Particle Size

Nanoparticles' size range is between 10 and 1000 nm. If they fall in a smaller size range (i.e., less than 10 nm) or a larger range (i.e., more than 1000 nm), then they will not achieve their desired therapeutic action, and they might show undesired side effects. Therefore, nanoparticles with a normal size range can permeate through cell membranes and cannot be detected by the reticuloendothelial system. Detection of nanoparticles by the reticuloendothelial system results in harder nanoparticle targeting. On the other hand, if they are smaller than 10 nm, their pharmacokinetics will change, in which faster clearance will occur as a result of a faster distribution of the nanoparticles. Nevertheless, nanoparticles that are larger than 1000 nm can precipitate at the site of injection, leading to the accumulation of nanoparticles. Another possible consequence of larger nanoparticle is entrapment of those nanoparticles by the liver, spleen, and lungs. So, while designing the nanoparticles, their sizes are considered as the most important feature to be studied. Their sizes must be adjusted to deliver the loaded amount of the drug with the desired distribution (Carvalho et al. 2018).

The particle size of the nanoparticles can act as a barrier, which makes the characterization process incomplete due to analysis difficulty. Therefore, for a successful characterization process, a comprehensive approach about the techniques used is required. So, a combination of different techniques may be used. Furthermore, limitations and strengths of the characterization techniques used must be known to have a background about the strategy which will be followed for the nanoparticle characterization, in which the analyzer will know whether only one or more than one technique will be used to provide the optimum results.

The most common techniques that are used to determine the nanoparticle size are transmission electron microscopy (TEM) and dynamic light scattering (DLS). Other techniques include atomic force microscopy (AFM), nanoparticle tracking analysis (NTA), single particle inductively coupled plasma mass spectrometry (SP-ICP-MS), tunable resistive pulse sensing (TRPS), and differential centrifugal sedimentation (DCS) (Bell et al. 2012).

3 Method and Techniques Available to Determine Nanoparticle Size

3.1 Transmission Electron Microscopy (TEM) Technique

3.1.1 Overview About the Technique

Transmission electron microscopy (TEM) is one of the techniques used to characterize the synthesized nanoparticles. To visualize the samples of nanoparticles under the electron microscope, there are two different ways; depending on their chemical composition, if the nanoparticles contain heavy atoms such as gold, silver, and iron, they are easily observed under the electron microscope without staining due to their high electron density. Another form of nanoparticles

requires staining due to their low electron density. Furthermore, osmium tetroxide can increase the electron density in case of lipid-based nanoparticles to visualize them.

3.1.2 Functions of TEM

For any active material to be effective after its administration, an interaction between the active material and the biological membrane will occur. Studying their properties through TEM requires adequate knowledge about their ability to cross the plasma membrane and their degradation. The contact of nanoparticles with the plasma membrane can be with a single nanoparticle or with a cluster of nanoparticles. After they become in contact with the plasma membrane, they enter the cell through endocytosis. So, TEM technique can be used to provide more details about this interaction between the nanoparticles and the plasma membrane. Another role for TEM technique is the identification of any structural modification of the nanoparticle including break in the membrane, enlargement in the mitochondria due to a swelling, or any change in the mitochondria (Malatesta 2016).

3.1.3 Samples in TEM

The characteristics of the ideal sample which must be used in the TEM are with large number of individual particles and free from any aggregation of nanoparticles. The number of the nanoparticles which is detected by TEM is affected by the concentration of the nanoparticles in the sample solution. However, the use of a diluted sample solution is not preferred in case of TEM because longer capture time is required than in concentrated sample solutions in order to obtain the desired number of nanoparticles.

3.2 Standardization and Reporting in TEM

The instrument used in TEM technique is calibrated, and the operator must run a standard test regularly in order to provide accurate results and adequate instrument performance, which match the manufacturer specifications resulting in validation of the instrument. When the nanoparticles which are measured by this technique are measured by another technique, as DLS, the results will not match with each other. This is because of differences in mean weight obtained from each technique. When reporting the results after the measurement by TEM, several values and parameters must be included in the final report. The most important one is the mean particle size. Other parameters can be included in this report, as any parameter that has been measured, such as frame size and pixel dimensions (Bonevich and Haller 2010).

3.3 Advantages and Limitations of TEM

All techniques used for any application have advantages and limitations; hence, other techniques will be discovered and developed later. TEM is considered as a powerful technique. Consequently, it can be used in different fields of studies, including scientific, educational, and industrial studies. When applying this technique in any study, it provides information about the structure of the material, surface features, shape, and size. In addition, if proper training is given to the operator, it will be easy to perform. The limitations included that the equipment used is large and expensive. Furthermore, the sample preparation is considered as a difficult and laborious process. Finally, when reporting the results, the images obtained are black and white (https://www.microscopemaster.com/transmission-electron-microscope.html).

3.4 Dynamic Light Scattering

3.4.1 Overview About the Technique

The dispersion of nanoparticles in a liquid is not completely homogeneous because of the Brownian movement of the particles, so at a given time, some areas will contain more particles than the others. This feature can be used to measure the particle size by light scattering means, i.e., the nanoparticles tend to scatter the light when it is

exposed to a beam of incident light; because of the Doppler effect, a spectral broadening will be achieved (Langevin et al. 2018).

The equation (D/λ^2) is used to calculate the coefficient of particle diffusion (D) and λ which is the wavelength of light (Kerker 1969). For example, the NPs (nanoparticles) have a radius of 20 nm in water and a λ of 600 nm; the broadening will have a frequency of 1000 Hz; this frequency will be compared to the frequency of the normal light (1014–1015 Hz); as the broadening is very small, monochromatic laser sources must be used. Through determining the intensity of the scattering or the broadening lines, alternatively, D can be calculated. From D, the particle size can be obtained. This method is called dynamic light scattering (DLS) (Berne and Pecora 2000).

This method can be used for different types of dispersions with small changes in the calculation; it can be used for monodisperse spherical particles (Nel et al. 2009; Anguissola et al. 2014; Zhang et al. 2012; Wang et al. 2013), polydisperse spherical particles (Guarnieri et al. 2014; Sabella et al. 2014), and anisotropic spherical particles (De Matteis et al. 2015; DeLoid et al. 2017).

DLS, often referred to as photon correlation spectroscopy, is one of the very commonly utilized techniques to determine the size of nanoparticles. The use of DLS technique for determining the nanoparticle size has numerous advantages and has been broadly used to determine their hydrodynamic size. The measurement process can be done quickly, and it does not require much time; it is not destructive for the sample; it is an automated process; hence, it does not require intensive labor (Lim et al. 2013).

4 Recommendations to Reduce Errors During the Use of DLS for Sizing

For consistent size determination through utilizing DLS, here are some recommendations, and these are valid to any DLS instrument.

1. Different instruments have different modes of analysis (cumulant, CONTIN). So, it is better to cross-check your results obtained using different methods with each other. One of the most seen cases is that sometimes the different method will give different results; in this case, it is recommended to choose the values listed by the cumulant method which are less sensitive to noise.
2. The use of low g2 value and a large range of correlation times can cause more errors during the measurement and analysis, so these parameters must be controlled so as to minimize the effect of noise during the cumulant analysis and in order to limit the possible influence of the noise on data processing.
3. A very critical parameter that must be considered during DLS is that the measurement will not be considered reliable if it is under the minimum detected intensity. If this problem happened with the use of DLS instruments, it can be fixed by removing attenuators. If this cannot be done, the time of acquisition can be increased, so just do the measuring for a longer time. If even this does not give better outcomes, you can increase the concentration of the particles in the sample.
4. In some cases of instrument errors when the instrument is not giving accurate corresponding noise level, the change of optical filters or the size of the detection pinhole can be considered to alter the intensity.
5. The sonication step is very important to break down and prevent the agglomeration. So, in order to ensure the reliability and repeatability of the procedure, calibration of the sonication energy must be done every time (Langevin et al. 2018).

5 Atomic Force Microscopy (AFM)

Atomic force microscopy (AFM) is a microscopy technique which is specialized in measuring certain parameters like height and friction. Therefore, it can be used to measure the particle size of the nanoparticles through measuring their heights. In other words, if the particles to be analyzed through this type of microscope are spherical

particles as nanoparticles, then the height measurement is considered as their diameter; to measure the particle size. When preparing the nanoparticle samples, the sample must be dispersed on a flat surface in order to proceed for the measurement through AFM. Nevertheless, the nanoparticles present in the sample must be characterized with a surface roughness that is less than the surface roughness of the normal nanoparticles.

At the end, when the results are obtained in the form of images, the images will be in the form of three-dimensional surface profile, unlike other microscopic techniques, as electron microscope. Electron microscopic technique provides two-dimensional image at the end of the measurement process. Inspection is required for the microscope to validate the process. Inspection is performed by optical microscope inspection. This inspection provides extra magnification of the sample to be tested by using light microscope. Inspection must be performed before conducting AFM measurement (Grobelny et al. 2009).

6 Nanoparticle Tracking Analysis (NTA)

6.1 Principle of NTA

Nanoparticle tracking analysis is a sizing technique of nanoparticles. It was established in 2006. The principle of NTA is based on the ability of particles to be analyzed to scatter the light as well as on their Brownian movement in a liquid dispersion. In the liquid sample, the particles will be exposed to a laser light, and this light as it passes through the medium will be scattered by the action of particles present. Then this light is tracked using a camera to which a software based on the principles of Stokes–Einstein equation will be implanted to determine the size of each particle individually. Hence, the NTA can provide good information about the particle concentration and not just about the size (Jean-Marie et al. 2018).

NTA depends on the refractive index of the nanoparticle, i.e., the speed at which the light travels through a medium. It combines the use of laser light scattering microscopy technique and charge-coupled device camera. This combination enhances the visualization of the nanoparticles in a solution. After the visualization, the software will recognize the nanoparticles according to their Brownian movement and diffusion speed. This technique is able to measure the protein particle size, ranging from 50–100 to 600–1000 nm. It can measure the size of other particles, ranging from 30 to 1000 nm (Filipe et al. 2010).

Nanoparticle tracking analysis measures the nanoparticle size depending on the refractive index of the nanoparticles. Therefore, the sample will be irradiated by a laser beam, in which the light will scatter as a result of the particles' Brownian movement. The charge-coupled device camera records the particles. The size of the recorded individual particles will be determined based on modified Stokes–Einstein equation (Coriolis Pharma).

6.2 Importance of Nanoparticle Tracking Analysis

Several protein formulations can be spoiled, or their quality can be affected due to the presence of the protein aggregations. Their effect can result in poor product quality and unwanted immunogenicity. Therefore, several techniques are available for thorough protein aggregate characterization, such as NTA (nanoparticle tracking analysis). But still these techniques are not measuring the protein aggregate properties due to the heterogenicity of the protein aggregates.

As any technique, this technique has limitations and advantages. The first advantage is that it is applicable to different types of samples: monodisperse and polydisperse. It is more efficient when applied to monodisperse systems, whereas more development is required when a polydisperse system is involved in the study. It can easily detect the contaminants present in the sample, such as dust, microorganisms, and any aggregate. Besides the protein aggregation characterization, it has the ability to monitor heat-induced aggregations resulting in background formation about

the aggregation kinetics. The sample concentration is limited to 10^7–10^9 mg/ml. It is less reproducible than other techniques. During characterization, only expert operators can perform this technique, and several parameters must be adjusted. After each measurement, the chamber where the sample is kept must be cleaned. For each measurement, it can take up to 1 h (Filipe et al. 2010).

6.3 Single Particle Inductively Coupled Plasma Mass Spectrometry (SP-ICP-MS)

One of the most useful techniques available for sizing nanoparticles is the single particle inductively coupled plasma mass spectrometry (SP-ICP-MS); it is an innovative analytical method which could overcome many of the challenges in the sizing process especially for the environmental samples (Laborda et al. 2014).

This technique is mainly used for liquid samples, so the samples to be analyzed are introduced into the instrument as polydisperse droplets in the form of an aerosol through a nebulization system; when the droplets are inside the plasma, evaporation of the sample occurs, and the particles will be volatilized, atomized, and after that ionized. The next step is the extraction of the ions by the use of mass spectroscopy; the particles will get separated according to their mass/charge ratio and are detected. While measuring the particle size, two samples can be considered:

1. In case if the particles are soluble in the solution and they are homogeneously distributed in the aerosol droplets, as the solution containing the particles goes inside the plasma, the rate of elements entering and travelling through the plasma toward the detector in the form of ions is assumed to be constant; eventually, the readings will give a steady signal.
2. On the other hand, if the sample used is in a suspension form, after nebulization, the particles will not be distributed homogeneously; hence, the element will be in isolated particles and cannot be detected properly, so in this case, the dilution of the sample may help to detect the ions generated from each individual particle (Laborda et al. 2016).

Then, as the signal of each passed particle is recorded or in case of packs of ions, the reading will be recorded as pulses according to the acquisition frequency used. The analysis can be either done by means of fast data acquisition (<104 Hz, i.e., using reading times >100 μs) or under lower frequencies (i.e., at reading times in the millisecond range) (Laborda et al. 2016).

During the SP-ICP-MS, the signals are recorded as events; each consists of single readings or pulses above a steady baseline (that is because of the background at the mass recorded or may be due to the presence of dissolved forms of the element measured), and according to the ions detected from each particle measured, the intensity of the event will differ. Then, a graph is plotted for event intensity against event intensity frequency to obtain histograms (Laborda et al. 2014). From these data according to Degueldre and Favarger, theoretical basis can be applied to measure the particle size (Degueldre and Favarger 2003).

The SP-ICP-MS instrument involves programmed software which is designed on the basis of different protocols to process the data collected after running the sample in the instrument (Tuoriniemi et al. 2012; Liu et al. 2014; Laborda et al. 2013; Cornelis and Hassellöv et al. 2014).

After collecting the data, some calculations are required to calculate the particle size and concentration; they are available on https://www.wur.nl/en/Research-Results/Research-Institutes/food-safety-research/show-rikilt/Single-Particle-Calculation-tool.htm.

SP-ICP-MS has the advantage of an element specific atomic spectrometry technique compared to ICP-MS, which uses a particle counting technique, since measurements are done on the basis of particle-by-particle principles. By using SP-ICP-MS, the following measurements can be obtained:

1. The presence of a particular element as particulate or dissolved (qualitative analysis).
2. Information about the mass characteristics of the particles detected that can be transformed into data of particle size on the condition that

the data about the composition, shape, and density of the element is known or assumed.
3. The particle number concentration and mass concentration can be obtained (quantitative analysis) (Laborda et al. 2016).

7 Tunable Resistive Pulse Sensing (TRPS)

Tunable resistive pulse sensing (TRPS) is a subtype of resistive pulse sensing (RPS) analytical techniques that utilizes the principle of particle by particle for the detection and analysis of colloidal systems containing particles of 40 nm to hundreds of micrometer diameter. In TRPS, a suspension of the colloidal particles and a conductive solution are passed through a membrane. TRPS technology has been commonly used in the biology field as it allows high-throughput analysis of particles and biomolecules (Coulter 1953).

The name of this technique refers to the adjustability of the pore size of the membrane used as the pore substrate is an elastomer; hence, the membrane can be stretched on an mm length, so eventually technical alteration of the pore size on a nanoscale level can be achieved. This unique feature of TRPS provides significant advantages compared to static ones. These advantages include real-time adjustments to suit the analyte used; if blockage happens during data capturing, the membrane can be stretched for recovery; also manual optimization of the stretch, voltage, and pressure to the analyte used and hence the signal-to-noise ratio of the resistive pulse signals can be done which will enhance the sensitivity of the instrument (Sowerby et al. 2007).

TRPS is mainly used to measure the size of particles that are assumed to be spherical, so the analysis will be very sensitive and will have high-resolution results (Sikora et al. 2016; Vogel et al. 2016; Vogel et al. 2011; Weatherall et al. 2016; Willmott et al. 2018; De Vrij et al. 2013; Maas et al. 2014; Roberts et al. 2010, 2012). TRPS can be utilized for nonspherical analytes such as viruses (Allen et al. 2014), bacteria (Heider and Metzner 2014), and self-assembled aggregates (McDaniel et al. 2014).

In case of a simple spherical particle, the principle of TRPS is applied, as the relationship between the particle volume and magnitude of the resistive pulse ΔR produced by a TRPS instrument is linear, so the diameter of the sphere with equivalent volume impermeable to ions can be determined with high accuracy using Eq. 20.1 (Deblois et al. 1977).

$$\Delta R / R = d^3 / D^2 L \tag{20.1}$$

where:
R is the pore resistance.
D is the pore diameter.
d is the particle diameter.
L is the effective pore length (that is the geometric length + 0.8 D) (Deblois et al. 1977).

Also, in more complicated cases, TRPS can be used with different equation to understand the measurement process (Kozak et al. 2011).

8 Differential Centrifugal Sedimentation

Differential centrifugal sedimentation (DCS), also known as centrifugal photo-sedimentation, is a novel, innovative, and simple particle size characterization technique, which has become "reborn" in recent years. Earlier boundaries and problems with the technique of sedimentation have been fixed by utilizing new developments in technology, and some technical changes in the instrumentation and the disk design. DCS is nowadays a powerful device to determine size distribution of the nanoparticle which is around 2 nm (Minelli et al. 2018).

DCS can give high-resolution size distributions of nanoparticles. DCS deals with the time the nanoparticles take to settle or deposit in a fluid when exposed to a centrifugal energy. This time that NPs require for sedimentation depends on two factors which are the density and particle size of the NPs. In order to determine the particle size of nanoparticles, an analytical centrifugation approach based on measurements of line-start

centrifugal sedimentation and flotation is used (Mahl et al. 2011).

The main principle behind the DCS is the separation of nanoparticles according to their sizes by means of centrifugal sedimentation process which is done by a CPS Disc Centrifuge (CPS Instruments, Inc.) in a rotating disk containing a solvent density gradient. The particles are moving toward the outer edge of the disk in a rate that is totally dependent on their sizes; as the particles are moving, they pass through a light source and are continuously detected, and this data is converted to size distribution.

The sedimentation velocity of a particle is directly proportional to the second power of its diameter, and transportation time is calibrated. The calibration should be done using standard particle that has a uniform and identified size such as polystyrene beads. The total size distribution is calculated by sampling >1 × 109 particles, and that is many orders of magnitude bigger than other size-determining methods which only sample hundreds to thousands of samples (https://nano.imra.com/size-measurement-by-disc-centrifugation/).

9 Zeta Sizer Equipment

One of the equipment that are used for nanoparticle size measurement is zeta sizer (nano zeta sizer). It is a high-performance two-angle particle and molecular size analyzer. Besides molecular size analysis, it is able to analyze the molecular weights of the molecules and nanoparticles using static light scattering. The sizes that can be detected by zeta sizer range from 0.3 nm to 10 μm, whereas the molecular weight down to 980 daltons can be detected. In addition, it provides the ability to investigate the zeta potential of the molecules and nanoparticles involved in the study by using electrophoretic light scattering. Furthermore, viscosity and viscoelasticity of the particles involved in the study can be measured due to the microrheology option. Mobility of the proteins can also be measured due to the presence of the protein measurement option, and 0.1 mg/ml concentration of protein solution can be detected. This device is also able to detect the fluorescent samples like anthracene because a filter option is present. To minimize errors, automation of measurements is done by using auto-titrator option.

Different zeta sizers are different from each other in one system component, which is the optic. Two types are present in the zeta sizers: 90 degree scattering optics and NIBS (non-invasive backscatter) optics. The performance of zeta sizers with NIBS optics is better than the performance of the zeta sizers with 90 degree scattering optics. This is because NIBS optics have the ability to detect the aggregates and measure the particle size in different concentrations, in which the sample can be diluted or concentrated, i.e., sample concentration ranges from 0.1 ppm to 40% w/v (Malvern Panalytical).

Zeta sizer device is composed of a small chamber for placing the sample cuvette. This chamber has a cover, to be closed after placing the sample. Cuvettes that are used are of two shapes, depending on the property to be measured. For determining the zeta potential, a cuvette of 0.75 ml volume is used. The cuvette is closed; the cover has two holes, through which the sample will be injected using a syringe. Cuvette cover has two gold-plated electrodes which is used to attach an electric source, resulting in voltage application. When voltage is applied, particles will move inside the cuvette. Particle movement will be used then to determine the surface charge and zeta potential. Cuvettes used for particle size measurement have three different volumes: 40 μL, 100 μL, and 1.5 ml (Malvern).

The parameters to be measured using this device are determined by the combination of three different sizing techniques: dynamic light scattering, laser Doppler micro-electrophoresis, and static light scattering. Each technique is designed to measure a specific parameter; dynamic light scattering is used to measure the particle and molecular size, laser Doppler micro-electrophoresis is used to measure the zeta potential, and static light scattering is used to measure the molecular weight of proteins and polymers.

Dynamic light scattering technique depends on the Brownian movement of the particles in the sample loaded. Brownian movement is defined as the random movement of particles in a liquid due to the bombardment by the molecules that surround them. Particles of different sizes will diffuse at different speeds; that is, small particles will diffuse more quickly than larger particles. So, the time required for small particles to diffuse is shorter than diffusion time for large particles. When relating these two variables to each other, the size can be determined (Malvern Panalytical).

10 Nanoparticle Characterization Challenges

Nanoparticles are known to be sensitive in nature. So, their characterization process must be performed carefully. As a result of nanoparticle sensitivity, their properties can change following any change in their surrounding media. Some of the changes that can occur include particle aggregation, size changes, and reaction with environment leading to oxidation or absorption of contaminants. The challenge in nanoparticle characterization is relating the dependence of their manufacturing properties to their stability, storage conditions, and health benefits.

Different techniques are employed in the particle size measurement of nanoparticles in order to avoid any inaccurate result. Nevertheless, the application of a single technique can lead to inadequate measurement due to the limitations of some techniques. DLS is the most commonly used technique, although it has some limitations which make the measurement process complicated sometimes. Specificity of DLS is less when the sample is polydisperse or it is a heterogeneous sample. In addition, DLS is not applicable to nonspherical nanoparticles. Another technique used is electron microscopy; it affects the stability of the synthesized nanoparticles by affecting their properties through staining in order to be observed under the microscope (https://www.azom.com/article.aspx?ArticleID=13104).

11 Conclusion

The field of nanotechnology characterization is very important; as it includes research areas on nanotoxicology which helps in the identification of the potential harm of nanoparticles. Most of the toxic effects in case of nanoparticles result from inaccurate sizes during the production of nanoparticle. Therefore, different techniques and instruments are employed to get the accurate particle size measurement of the synthesized nanoparticles. The purpose of employing different techniques is to get the optimum accuracy. Sometimes, a combination of different techniques can also be used.

References

Allen CS, Loo JFC, Yu S, Kong SK, Chan T-F. Monitoring bacterial growth using tunable resistive pulse sensing with a pore-based technique. Appl Microbiol Biotechnol. 2014;98:855–62.

Anguissola S, et al. High content analysis provides mechanistic insights on the pathways of toxicity induced by amine-modified polystyrene nanoparticles. PLoS One. 2014;9(9):e108025.

Bell NC, Minelli C, Tompkins J, Stevens MM, Shard AG. Emerging techniques for submicrometer particle sizing applied to stober silica. Langmuir. 2012;28:10860–72. https://doi.org/10.1021/la301351k.

Berne BJ, Pecora R. Dynamic light scattering: with applications to chemistry, biology, and physics. Mineola: Dover Publications; 2000.

Bonevich JE, Haller WK. Measuring the size of nanoparticle using transmission Electron microscopy (TEM). Gaithersburg: National Institute of Standards and Technology; 2010.

Carvalho PM, Felicio MR, Santos NC, Goncalves S, Domingues MM. Application of light scattering techniques to nanoparticle characterization and development. Front Chem. 2018;6:237.

Coriolis Pharma. Nanoparticle tracking analysis. https://www.coriolis-pharma.com/nanoparticle-tracking-analysis-nta

Cornelis G, Hassellöv M. A signal deconvolution method to discriminate smaller nanoparticles in single-particle ICP-MS. J Anal At Spectrom. 2014;29:134.

W.H Coulter. Means for counting particles suspended in a fluid. United States Patent Office, Chicago, 20th Oct 1953, pg; 3–9.

De Matteis V, et al. Negligible particle-specific toxicity mechanism of silver nanoparticles: the role

of Ag+ ion release in the cytosol. Nanomedicine. 2015;11(3):731–9.
De Vrij J, Maas SLN, Van Nispen M, Sena-Esteves M, Limpens RWA, Koster AJ, Leenstra S, Lamfers ML, Broekman MLD. Quantification of nanosized extracellular membrane vesicles with scanning ion occlusion sensing. Nanomedicine. 2013;8:1443–58.
Deblois RW, Bean CP, Wesley RKA. Electrokinetic measurements with submicron particles and pores by the resistive pulse technique. J Colloid Interface Sci. 1977;61:323–35.
Degueldre C, Favarger P-Y. Colloid analysis by single particle inductively coupled plasma-mass spectroscopy: a feasibility study. Colloids Surf A Physicochem Eng Asp. 2003;217:137.
DeLoid GM, et al. Preparation, characterization, and in vitro dosimetry of dispersed, engineered nanomaterials. Nat Protoc. 2017;12:355.
Filipe V, Hawe A, Jiskoot W. Critical evaluation of nanoparticle tracking analysis by nano sight for the measurement of nanoparticle and protein aggregates. Pharm Res. 2010 May;27(5):796–810. [Pub Med].
Grobelny J, Del Rio FW, Pradeep N, Kim D-I, Hackley VA, Cook RF. Size measurement of nanoparticles by atomic force microscopy. Gaithersburg: National Institute of Standards and Technology; 2009.
Guarnieri D, et al. Transport across the cell-membrane dictates nanoparticle fate and toxicity: a new paradigm in nanotoxicology. Nanoscale. 2014;6:10264–73.
Heider S, Metzner C. Quantitative real-time single particle analysis of virions. Virology. 2014;462:199–206.
Jean-Marie CG, Chantalat L, Moriscot C, Cambedouzou J, Odorico M, Ravaux J, Podor R, Gerdil A, Habert A, Herlin-Boime N, Chen S-w W, Pellequer J-L. On the operational aspects of measuring nanoparticle sizes. Nanomaterials (Basel). 2018;9(1):18.
Kerker M. The scattering of light and other electromagnetic radiation. London: Academic Press; 1969.
Kozak D, Anderson W, Vogel R, Trau M. Advances in resistive pulse sensors: devices bridging the void between molecular and microscopic detection. Nano Today. 2011;6:531–45.
Laborda F, Jiménez-Lamana J, Bolea E, Castillo JR. Single particle inductively coupled plasma mass spectrometry: A powerful tool for nano-analysis. J Anal At Spectrom. 2013;28:1220.
Laborda F, Bolea E, Jiménez-Lamana J. Single particle inductively coupled plasma mass spectrometry: A powerful tool for nanoanalysis. Anal Chem. 2014;86:3–7.
Laborda F, Bolea E, Jiménez-Lamana J. Single particle inductively coupled plasma mass spectrometry for the analysis of inorganic engineered nanoparticles in environmental samples. Trends Environ Anal Chem. 2016;9:15–23. https://doi.org/10.1016/J.TEAC.2016.02.001.
Langevin D, Raspaud E, Mariot S, Knyazev A, Stocco A, Salonen A, Luch A, Haase A, Trouiller B, Relier C, Lozano O, Thomas S, Salvati A, Dawson K. Towards reproducible measurement of nanoparticle size using dynamic light scattering: Important controls and considerations. NanoImpact. 2018;10:161–7.
Lim J, Yeap SP, Che HX, Low SC. Characterization of magnetic nanoparticle by dynamic light scattering. Nanoscale Res Lett. 2013;8(381):1–14.
Liu J, Murphy KE, MacCuspie RI, Winchester MR. Capabilities of single particle inductively coupled plasma mass spectrometry for the size measurement of nanoparticles: a case study on gold nanoparticles. AnalChem 2014;86:3405.
Maas SLN, De Vrij J, Broekman MLD. Quantification and size-profiling of extracellular vesicles using tunable resistive pulse sensing. J Vis Exp. 2014;19(92):e51623.
Mahl D, Diendorf J, Meyer-Zaika W, Epple M. Possibilities and limitations of different analytical methods for the size determination of a bimodal dispersion of metallic nanoparticles. Colloids Surf A. 2011;377:386–92.
Malatesta M. Transmission electron microscopy for nanomedicine: novel applications for long-established techniques. Eur J Histochem. 2016;60(4):2751.
Malvern. Zeta sizer nano series, user manual.
Malvern Panalytical. Zeta sizer Nano ZS. https://www.malvernpanalytical.com/en/products/product-range/zetasizer-range/zetasizer-nano-range/zetasizer-nano-zs. Copyright 2019 – Malvern Panalytical Ltd is a Spertric company.
McDaniel JR, Weitzhandler I, Prevost S, Vargo KB, Appavou M-S, Hammer DA, Gradzielski M, Chilkoti A. Noncanonical self-assembly of highly asymmetric genetically encoded polypeptide amphiphiles into cylindrical micelles. Nano Lett. 2014;14:6590–8.
Minelli C, Sikora A, Garcia-Diez R, Sparnacci K, Gollwitzer C, Krumrey M, Sharda AG. Measuring the size and density of nanoparticles by centrifugal sedimentation and flotation. Anal Methods. 2018;10:1725.
Nel AE, et al. Understanding biophysicochemical interactions at the nano-bio interface. Nat Mater. 2009;8(7):543–57.
Roberts GS, Kozak D, Anderson W, Broom MF, Vogel R, Trau M. Tunable nano/micropores for particle detection and discrimination: scanning ion occlusion spectroscopy. Small. 2010;6:2653–8.
Roberts GS, Yu S, Zeng Q, Chan LCL, Anderson W, Colby AH, Grinstaff MW, Reid S, Vogel R. Tunable pores for measuring concentrations of synthetic and biological nanoparticle dispersions. Biosens Bioelectron. 2012;31:17–25.
Sabella S, et al. A general mechanism for intracellular toxicity of metal-containing nanoparticles. Nanoscale. 2014;6(12):7052–61.
Sikora A, Shard AG, Minelli C. Size and ζ-potential measurement of silica nanoparticles in serum using tunable resistive pulse sensing. Langmuir. 2016;32:2216–24.
Sowerby SJ, Broom MF, Petersen GB. Dynamically resizable nanometre-scale apertures for molecular sensing. Sens Actuators B: Chem. 2007;123:325–30.
Tuoriniemi J, Cornelis G, Hassellöv M. Size discrimination and detection capabilities of single-particle

ICPMS for environmental analysis of silver nanoparticles. Anal Chem. 2012;84:3965.
Vogel R, Willmott G, Kozak D, Roberts GS, Anderson W, Groenewegen L, Glossop B, Barnett A, Turner A, Trau M. Quantitative sizing of nano/microparticles with a tunable elastomeric pore sensor. Anal Chem. 2011;83:3499–506.
Vogel R, Coumans FAW, Maltesen RG, Boing AN, Bonnington KE, Broekman ML, Broom MF, Buzás EI, Christiansen G, Hajji N. A standardized method to determine the concentration of extracellular vesicles using tunable resistive pulse sensing. J Extracell Vesicles. 2016;5:31242.
Wang F, et al. Time resolved study of cell death mechanisms induced by amine-modified polystyrene nanoparticles. Nanoscale. 2013;5(22):10868–76.
Weatherall E, Hauer P, Vogel R, Willmott GR. Pulse size distributions in tunable resistive pulse sensing. Anal Chem. 2016;88:8648–56.
Willmott GR. Tunable resistive pulse sensing: better size and charge measurements for submicrometer colloids. Anal Chem. 2018;90:2987–95.
Zhang H, et al. Processing pathway dependence of amorphous silica nanoparticle toxicity: colloidal vs pyrolytic. J Am Chem Soc. 2012;134(38):15790–804.

21

Silver Nanoparticle Synthesis from Cyanobacteria: Environmental and Biomedical Applications

Md. Nafe Aziz, Almaz Zaki, Irshad Ahamad, and Tasneem Fatma

Abstract

Silver and silver salts have been utilized from the ancient civilization, but silver nanoparticles have been utilized recently. Physical and chemical methods such as reduction of silver salt solution, thermal decomposition of silver compound, and sonication have been utilized for the synthesis of nanoparticle. These methods are simple and can achieve the complex morphology but limit their application in the area of healthcare because of associated toxicity and biocompatibility problems. In order to overcome this, researchers have proposed biogenic approach as a cleaner, economical, eco-friendly, and sustainable route for nanoparticle synthesis. This process reduces the need of hazardous chemicals and decreases the need of downstream processing, which makes the process more economical and less energy intensive. Silver nanoparticles (AgNPs) can be synthesized by bacteria, cyanobacteria, fungi, and algae. The microbes are having ability to function under variable extremes of temperature, pressure, and pH which makes them more attractive. In particular, silver-based nanomaterials have emerged as a promising potential in biomedical applications and are utilized in cosmetic, biosensor, nanofertilizer, nanopesticides, bioimaging, targeted drug and gene delivery, etc. AgNPs are also used in packaging to prevent damage of food products by pathogens. Due to biocompatibility, biogenic AgNPs are much attractive in the nanomedicine and medical devices.

Keywords

Silver nanoparticles · Cyanobacteria · Biogenic synthesis · Biomedical applications

M. N. Aziz · A. Zaki · I. Ahamad · T. Fatma (✉)
Department of Biosciences, Jamia Millia Islamia (Central University), New Delhi, India

Biosynthesis of nanoparticle is an important area in the field of nanotechnology which has economic and eco-friendly benefits. Biogenic silver nanoparticles can be synthesized by bacteria, cyanobacteria, fungus, algae, and plants. In particular, silver-based nanomaterials have emerged as a promising potential in biomedical applications and are utilized in cosmetic, biosensor, nanofertilizer, nanopesticides, bioimaging, targeted drug, gene delivery, etc. Due to biocompatibility, AgNPs are much attractive in the nanomedicine and medical devices.

J. K. Patel, Y. V. Pathak (eds.), *Emerging Technologies for Nanoparticle Manufacturing*,
https://doi.org/10.1007/978-3-030-50703-9_21

1 Introduction

"Nano" is a Greek word meaning dwarf or extremely small and indicates one in a billionth (10^{-9}). The nanotechnology is the study of synthesizing, manipulating, and designing nanomaterials in the range of 1–100 nm (Nouailhat 2010). The nanomaterial with distinctive physicochemical properties has the potential to develop new systems, structures, and devices. Nanoparticles of any compound show unique and different properties (optical, electronic, thermal, catalytic, and chemical) from their bulk compound due to their high surface area to volume ratio. Nanoparticles are used in many biomedical applications, such as biosensors, diagnostic tools, cancer treatment, targeted drug, and gene delivery (Sadowski 2010). These qualities have attracted researchers to uncover novel techniques (chemical, physical, and biological) to synthesize various kinds of metallic (gold, titanium, copper, cobalt, selenium, iron, zinc, silver, etc.) and nonmetallic (silicon, carbon, phosphorus, etc.) nanoparticles with broad biological and nonbiological applications. Among them, silver nanoparticles are considered as the most applicable and efficacious (Rai et al. 2009) and thus gained the maximum attention. AgNPs exhibited the highest level of commercialization, accounting for 55.4% of the nanomaterial-based consumer products existing in the market (313 out of 565) (Agnihotri et al. 2014). Consequently, nanosilver becomes the nucleus of the nanoindustry. According to the Khanna et al. (2019), nanomaterials (e.g., AgNPs) are classified based on shape and dimension (quantum dots, platelets, and particles), phase composition (crystalline, coated particles and aerogels), and nature of the material (pure and bimetallic, e.g., Ag-Au, Zn-Ag).

Though conventional techniques (physical and chemical methods) take less time to synthesize a large amount of nanoparticles, they require toxic chemicals like reducing and capping/stabilizing agents (sodium citrate, ascorbate, sodium borohydride (NaBH4), elemental hydrogen, polyol process, Tollens reagent, N,N-dimethylformamide) which make them environmentally unfriendly (Iravani et al. 2014; Gurunathan et al. 2015). Therefore, biogenic synthesis of nanoparticles emerged as an alternative. Biological method is convenient, safe, and ecofriendly which does not require high energy and utilizes biological macromolecules (proteins, carbohydrates, lipids, and secondary metabolites) as reducing and stabilizing agents. Various biological resources like bacteria, cyanobacteria, fungi, and plants have been used for silver nanoparticle synthesis. Cyanobacteria have attracted special attention for synthesis of nanomaterials due to high growth rate (faster doubling time), easy scalability, and low cost (Fatma et al. 2007).

So far, a number of cyanobacterial taxa belonging to orders Nostocales (Morsy 2014), Oscillatoriales, and Synchococcales (Lengke et al. 2007; Sudha et al. 2013) have been used for the synthesis of AgNPs. Recently, many researchers have synthesized AgNPs using cyanobacteria. For the first time, *Plectonema boryanum* UTEX 485 based intracellular and extracellular AgNPs were synthesized by Lengke et al. (2007). Tsibakhashvili et al. (2011) carried out extracellular synthesis of AgNPs via *Spirulina platensis*. Screening of cyanobacterial species (*Aphanothece*, *Oscillatoria*, *Microcoleus*, *Aphanocapsa*, *Phormidium*, *Lyngbya*, *Gloeocapsa*, and *Synechococcus*) isolated from mangroves was performed for extracellular AgNP synthesis by Sudha et al. (2013). The water-soluble extracellular polysaccharide of *Nostoc commune* was employed for the fabrication of AgNPs without using surfactant and capping agent (Morsy 2014). In our lab, the cyanobacterial extracts of 30 strains were screened for their ability to synthesize AgNPs (Husain et al. 2015). Mubarak et al. (2011) synthesized AgNPs using *Oscillatoria willei* NTDM01. Microalgae like *Scenedesmus abundance* and *Chlorella pyrenoidosa* were also utilized for AgNP synthesis using cell extract (Aziz et al. 2014, 2015). AgNPs were also synthesized extracellularly from macroalgae such as *Sargassum longifolium* (Kumar et al. 2012), *Gracilaria corticata* (Kumar et al. 2013b), *Ulva lactuca* (Kumar et al. 2013a), *Sargassum muti-*

cum (Azizi et al. 2013), and *Acanthophora spicifera* (Ibraheem et al. 2016).

2 Synthesis of Silver Nanoparticles

Metal nanoparticle synthesis can be done by bottom-up and top-down methods (Husen and Siddiqi 2014). AgNP synthesis is traditionally done through chemical methods using reducing chemicals, electrochemical reaction using high voltage and current, and irradiation-assisted chemical using radiation energy and pyrolysis methods (Zhang et al. 2007). The capping agents [cetyltrimethylammonium bromide (CTAB), polyvinylpyrrolidone (PVP), sodium dodecyl sulfate (SDS), thioglycerol (TG), mercaptoethanol (ME), sodium hexametaphosphate (SHMP)] are used during the chemical synthesis of nanoparticles (Rahdar 2013). Physical methods include arc discharge, physical vapor condensation, energy ball milling method, and direct current magnetron sputtering (Tien et al. 2008; Abou El-Nour et al. 2010; Asanithi et al. 2012) that are nontoxic, as highly reactive chemicals are not used, but they require high energy. Biogenic nanoparticle synthesis is based on the bottom-up approach that involves metal salt and cell extract with reducing and stabilizing agent (Thakkar et al. 2010; Nath and Banerjee 2013). The biogenic AgNPs obtained from bacteria, fungi, yeast, algae, cyanobacteria, and plant extracts have several advantages over the chemical and physical methods. This route is simple, cost-effective, eco-friendly, and biocompatible (Husen and Siddiqi 2014). Biogenic synthesis of AgNPs may be intracellular or extracellular. Extracellular synthesis of nanoparticles is cheap, favors large-scale production, and requires simpler downstream processing. Thus, the extracellular method for the synthesis of nanoparticles is preferred in comparison to the intracellular method.

Cyanobacterial extract consists of carbohydrates, proteins, minerals, and polyunsaturated fatty acids along with antioxidants (polyphenols, tocopherols), carotenoids (carotene, xanthophyll), chlorophylls, and phycobilins (phycocyanin, phycoerythrin) which act as reducing agents (Michalak and Chojnacka 2015). Intracellular synthesis occurs inside the microbial cells. During synthesis of nanoparticles in extracellular medium, the cyanobacterial cell extract is incubated with metal precursor solution ($AgNO_3$). A color change (reddish brown) in the reaction mixture indicates the reduction of $AgNO_3$ to AgNPs. The reducing agents (e.g., NADPH-dependent nitrate reductase) present in the extract react with the Ag^+ ions in the reaction mixture, thus forming thermodynamically stable nanoparticles (Sharma et al. 2015; Fawcett et al. 2017; Aziz et al. 2019).

3 Morphology of AgNPs

Particle size plays an important role in determining the properties of nanoparticles. The shape and size of the biogenic AgNPs vary due to altered reaction conditions and cell constituents. The reported size of the cyanobacterial AgNPs ranges from 5 to 90 nm, e.g., 10 nm by *Plectonema boryanum* (Lengke et al. 2007), 10–15 nm by *Spirulina platensis* (Mahdieh et al. 2012), and 10–25 nm by *Oscillatoria willei* (Mubarak et al. 2011). Generally, AgNPs are spherical in shape, but other shapes like cubic, pentagonal, hexagonal, and octahedral were also reported (Husain et al. 2015). Uniform shape and size can be obtained during biogenic synthesis under identical conditions (Sudha et al. 2013). The type of energy commonly used during the synthesis of the nanoparticles stimulates the change in the shape. The dynamic nature and shape of the synthesized nanoparticles greatly affect their chemical properties (Baer et al. 2013).

4 Characterization of Silver Nanomaterials

Nanoparticles are subjected to various characterization techniques to ascertain their size, shape, distribution, surface morphology, and surface area. Spectroscopic and diffractographic techniques involved in the characterization include UV-visible spectroscopy for optical properties,

dynamic light scattering (DLS) for structural properties (particle size distribution and hydrodynamic diameter), energy dispersive spectroscopy (EDS) for elemental composition, X-ray diffraction (XRD) for crystalline structure, Fourier transform infrared spectroscopy (FTIR) for identifying all biomolecules, and X-ray photoelectron spectroscopy (XPS) for identifying oxidation state and zeta potential for surface charge (Menon et al. 2017; Shah et al. 2015). Scanning electron microscopy (SEM), transmission electron microscopy (TEM), high-resolution transmission electron microscopy (HR-TEM), and atomic force microscopy (AFM) are employed to determine the size and morphological features of NPs (Aziz et al. 2015; Aziz et al. 2016).

5 Biotechnological Significance of Biogenic AgNPs

AgNPs synthesized from cyanobacterial sources are used as conventional medicines and antibacterial (Sharma et al. 2015), anticancer (Govindaraju et al. 2015), and antifungal agents (Azizi et al. 2013). Apart from medicinal applications, the AgNPs have extensive applicability in cosmetics, food packaging, sensing devices, and environmental health (Iravani et al. 2014; Husain et al. 2019).

5.1 Biomedical Application of AgNPs

AgNPs fabricated from various cyanobacterial sources have been utilized in following biological fields.

5.1.1 Antimicrobial Activities of AgNPs

Microbial infections have presented a persistent threat to human health despite the pioneering breakthroughs in antibiotics and antiseptics. Excessive antibiotic use/misuse has resulted in growing resistance to such treatment strategies. Notably, the outbreak of antibiotic resistance has resulted in nosocomial infections, such as urinary tract infections, pneumonia, and bloodstream infections. In the United States alone, roughly 1.7 million estimated nosocomial infections, primarily from bacteria and fungi, are responsible for 99,000 deaths each year (Klevens et al. 2007). In this milieu, metallic silver, especially in the form of nanoparticles and nanostructured substrates, has received considerable attention for antibacterial activity (Husain et al. 2015; Prasad et al. 2016).

The cubic AgNPs of 33–81 nm obtained from ethanolic extract of *Acanthophora spicifera* are effective against *Staphylococcus aureus*, *Bacillus subtilis*, *Salmonella* sp., *Escherichia coli*, and yeast strain *Candida albicans* (Ibraheem et al. 2016). The AgNPs synthesized from cellular metabolites of *Microcoleus* sp. show antibacterial effect against *Escherichia coli*, *Proteus vulgaris*, *Salmonella typhi*, *Vibrio cholerae*, *B. subtilis*, *S. aureus*, *Streptococcus*, and *Corynebacterium* (Sudha et al. 2013). Biosynthesized spherical AgNPs in 18–46 nm range from *Gracilaria corticata* have an effective antifungal activity against *Candida albicans* and *Candida glabrata* (Kumar et al. 2013b). AgNPs synthesized from using the aqueous extract of *Gelidiella acerosa* exhibited antifungal property against *Humicola insolens*, *Fusarium dimerum*, *Mucor indicus*, and *Trichoderma reesei* (Vivek et al. 2011). *Sargassum longifolium*-mediated AgNPs showed antifungal activity against the pathogenic fungi *Aspergillus fumigatus*, *C. albicans*, and *Fusarium* sp. (Kumar et al. 2012).

The smaller nanoparticles showed higher disruption of the cell membrane by adhering to its surface and consequently penetrating the cell and further damaging the DNA. Loo et al. (2018) explained that AgNPs bind to the thiol group of proteins and disrupt the bacterial respiratory chain leading to generation of reactive oxygen species (ROS) causing oxidative stress and cell damage. Nanoparticles have high affinity for phosphorus and nitrogen, thus adversely affecting the DNA replication and cellular metabolism (Kim et al. 2007; Nanda and Saravanan 2009; Lemire et al. 2013). Small (5–20 nm) human

serum albumin stabilized silver nanoparticles exhibited a dose-dependent anti-retrovirus activity and inhibited HIV-1 replication (Sun et al. 2005).

5.1.2 Anticancer Activities of AgNPs

Chemotherapy and radiation therapy commonly used for cancer therapy destroy both normal and cancer cells (Brown 2002). In order to overcome this disadvantage, AgNPs were successfully applied due to high surface area to volume ratio and high binding activity, distinctive catalytic, bactericidal, therapeutic activities, and stability (Yezhelyev et al. 2006). AgNPs exhibit their anticancer activity by inducing ROS generation and apoptosis (Fig. 21.1) (Mishra et al. 2017; Aziz et al. 2019). AgNPs exhibit a strong cationic surface charge due to capping under physiological conditions, whereas cancer cells have higher concentration of anionic phospholipids on their surface (Erdogan et al. 2019). Thus, the interaction of negatively charged cancer cells with positively charged AgNPs by electrostatic interactions and phagocytosis is favored that promotes the cellular uptake and cytotoxicity (Erdogan et al. 2019). Sanpui et al. (2011) demonstrated that the chitosan-mediated AgNPs disrupt the normal cellular function and also affect membrane integrity by inducing apoptotic signaling genes of mammalian cells, leading to death. Asharani et al. (2009) and Franco-Molina et al. (2010) reported that AgNPs inhibit proliferation of human glioblastoma cells and human breast cancer cells.

Algae-derived silver nanoparticles showed good in vitro cytotoxicity in malignant cell line, e.g., human breast (MCF-7) cell line and human colon cancer (HCT-116) cell line (Bhattacharya and Gupta 2005). Macroalgal (*Turbinaria turbinata*) and some microalgal (*Anabaena oryzae*, *Nostoc muscorum*, and *Calothrix marchica*) derived AgNPs showed high cytotoxic effect against *Ehrlich ascites* carcinoma (EAC) (Khalifa et al. 2016).

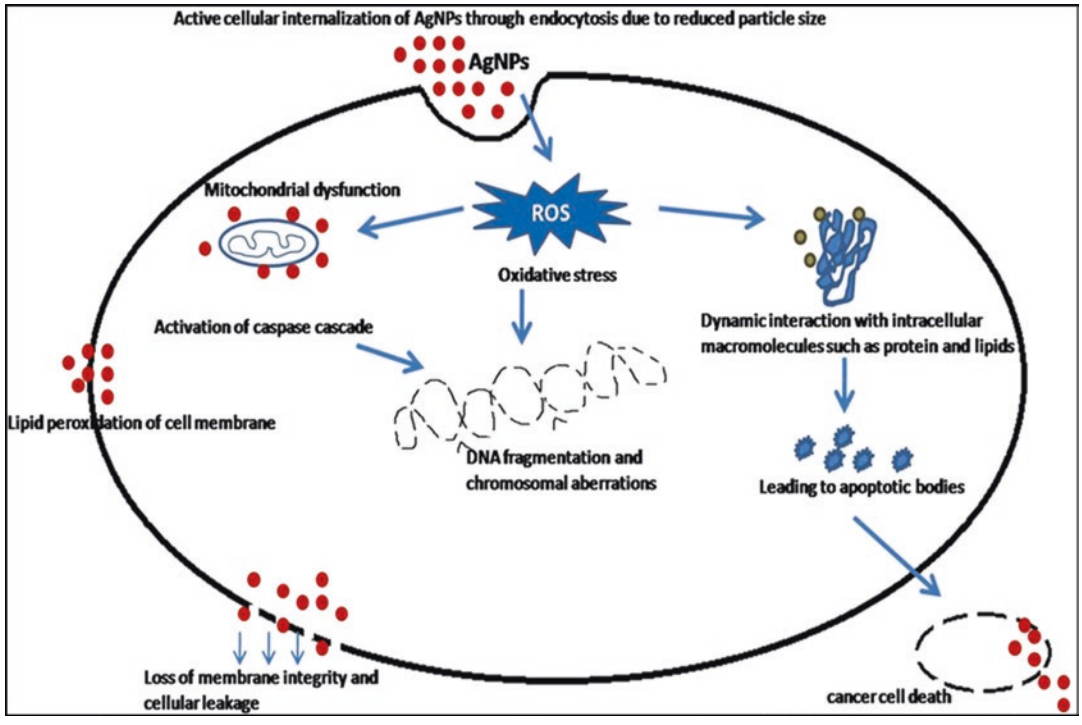

Fig. 21.1 Mechanism behind the cytotoxicity of the AgNPs against cancerous cells (Aziz et al. 2019)

5.1.3 Antifouling Agents

Antifouling agents are substances which are utilized to remove or prevent biofouling phenomenon by organisms on wetted surfaces. Biofouling is associated with medical devices, membranes, paper manufacturing, food processing industries, underwater construction, and desalination plants. In biofouling industry, AgNP is used as coat (Beyth et al. 2008; Roe et al. 2008) or impregnated or embedded (Vijayan et al. 2016) that inhibits the bacterial adhesion and the biofilm formation. AgNPs from *Turbinaria conoides* (spherical in shape, 2–17 nm size) were efficient in controlling biofilm formation by inhibiting the growth of *E. coli*, *Salmonella* spp., *Serratia liquefaciens*, and *Aeromonas hydrophila*; thus, they act as potent antifouling agents (Vijayan et al. 2014). The "coat" made of phytagel and Apcomin zinc chrome paint glazed with AgNPs synthesized from *Turbinaria ornata* restricted the growth of 15 biofilm isolates with maximum inhibition in *E. coli* (71.9%) due to the secretion of extracellular polymeric substances (EPS) (Krishnan et al. 2015).

5.1.4 Food Packaging

Today, there is an increase in the demands for "ready to eat," "ready to cook," and "ready to use" food; this had consequently increased the dependence on food processing. But the main issue during food processing is the protection against foodborne pathogens like *Salmonella* nontyphoidal, *Campylobacter*, *Listeria*, and *Escherichia coli* (Morris 2011). Prevention of foodborne diseases associated with food packaging requires a special food packaging technique that releases active biocide substances in order to improve the quality of the food and delay the food spoilage. Thus, the use of nanomaterials is growing in food packaging (Carbone et al. 2015). Metal nanoparticles with their potent antimicrobial properties are therefore used as "active packaging" (Duncan 2011). Emerging metal nanoparticles with biocidal properties are Cu, Zn, Au, Ti, and Ag (Toker et al. 2013); among them, silver nanoparticles (AgNPs) demonstrated to have the most effective bactericidal properties against a wide range of pathogenic microorganisms, including bacteria, yeasts, fungi, and viruses (Rai et al. 2009; Martinez-Abad et al. 2012). AgNPs can be hosted in different matrices such as polymers and stabilizing agents such as citrates and long-chain alcohols (Toker et al. 2013). AgNPs can be coated, absorbed, or directly incorporated in the synthesis processes of packaging materials (Martinez-Abad et al. 2012). Few examples of AgNPs used commercially in packaging are given in Table 21.1.

5.1.5 Medical Devices

Medical devices like central venous catheters (CVC), wound drains, and catheters for continuous ambulatory peritoneal dialysis (CAPD) may cause microbial infection due to the patient-

Table 21.1 Nanocomposite packaging based on AgNPs/degradable polymeric matrices (Carbone et al. 2016)

Polymer matrix	Tested food	Tested microorganisms	References
LDPE + Ag, ZnONPs	Orange juice	Yeast, molds, total aerobic bacteria	Emamifar et al. (2010)
LDPE + AgNPs	Barberry	Total aerobic bacteria	Motlagh et al. (2012)
PVC + AgNPs	Minced beef	Total mesophilic bacteria, *E. coli*, *S. aureus*	Mahdi et al. (2012)
EVOH + AgNPs	Chicken, pork, cheese, lettuce, apples, peels, eggshells	*Salmonella* spp., *L. monocytogenes*	Martinez-Abad et al. (2012)
Polyethylene + Ag, TiO_2 NPs	Fresh apples, white slice bread, fresh carrots, soft cheese, atmosphere packaging milk powder, fresh orange juice	*Penicillium*, *Lactobacillus*	Metak and Ajaal (2013)
Polyethylene + Ag, TiO_2 NPs	Fresh apples, white slice bread, fresh carrots, soft cheese, atmosphere packaging milk powder, fresh orange juice	*S. aureus*, *coliforms*, *E. coli*, *Listeria*	Metak (2015)

derived glycoprotein coating (conditioning film) which deposits on implant (Baumgartner and Cooper 1996). Several approaches have been applied to prevent building related illness (BRI) through surface coating such as surface modification by gas plasma, and they appear to reduce microbial adhesion in vitro but are ineffective in vivo (Everaert et al. 1998). In an attempt to address these shortcomings, the broad antimicrobial spectrum of AgNPs has been impregnated into medical devices (Furno et al. 2004). AgNP-impregnated central venous catheters (CVC) significantly decreased the rate of catheter-related blood stream infections than in the conventional practice (Samuela and Guggenbichler 2004). Surface modification of implants using AgNPs does not affect their biocompatibility while resulting in an added benefit due to increased antibacterial properties (Cao et al. 2010).

5.1.6 AgNPs in Wound Dressing

The skin is the largest organ in the body of vertebrates, and it is an important natural barrier to protect internal organs from chemical or mechanical damage. To date, substantial efforts have been made to provide effective treatment for burns, abrasions, exposure to chemical/biological agents, and other skin lesions. An ideal wound dressing possesses special properties such as good biocompatibility, sufficient physical protection against bacterial intrusions, high porosity for gas exchange, and promotion of epithelialization (Rujitanaroj et al. 2008; Khil et al. 2003). Special attention has been paid to nanofibrous membranes that are produced by electrospinning. Acticoat is a commercial wound dressing and is made up of two layers of polyamide ester membranes covered with nanocrystalline silver (Unnithan et al. 2012; Valchou et al. 2007). Among the various antimicrobial agents that are available, silver nanoparticles (AgNPs) have been recognized to have a broad spectrum and to be highly effective in treating infectious wounds (Agarwal et al. 2011). They also overcome several problems associated with previously used wound dressings like tissue irritation and insufficiently wide spectrum of antifungal properties.

5.2 Environmental Applications of AgNPs

There is a growing production and application of silver nanoparticles (AgNPs) in various areas including catalysis, consumer products, food technology, textiles/fabrics, as well as medical products and devices. It was reported that about 25% of the >1300 nanomaterial-containing consumer products contain AgNPs.

5.2.1 Textiles

Textiles containing nano-silver make up the majority of commercially available nano-functionalized materials (Blaser et al. 2008; Walser et al. 2011). AgNPs are used in T-shirts, socks, underwear, and sports clothing, but the most important application is in medical field because of the high risks of contamination associated with surgical suits (Benn and Westerhoff 2008; Freeman et al. 2012). There are different ways to produce AgNP functionalized textiles can be produced either by embedding into the fibers or applied to the surface of the fibers. Nanomaterials are expected to either improve the existing properties or bring new functionalities to textiles such as dirt and water repellence, breathability, UV protection, conductive and antistatic properties, wear and wrinkle resistance, and resistance to stains, bacteria, or fungi. NanoHorizons Inc., USA, is a company that enhances their fabrics with silver nanoparticles to reduce odor.

5.2.2 Bioremediation

It has been found that nanomaterials provide a wonderful platform for remediating environmental pollution (chemical and biological). The AgNPs fabricated from *Ulva lactuca* and *Microchaete* degrade azo dyes, methyl orange and methyl red, respectively, photocatalytically under visible light (Kumar et al. 2013a, b; Husain et al. 2019). According to Liu et al. (2007), on visible light irradiation, an electron from AgNPs moves to an excited state, and this leaves behind a hole. Water, which is adsorbed on the surface of AgNPs, reacts with the hole and gets oxidized to give hydroxyl radical. Radicals such as $HO^{\bullet}$ and $^{\bullet}O^{2-}$ degrade methyl orange by interacting with

the aromatic ring of the methyl orange and opening the azo bond and hydroxylated ring to yield CO_2, H_2O, SO_4^{2-}, NO_3^-, and NH_4^+ ions.

In recent years, with the development of nanotechnology, AgNPs have also been successfully applied in household water and wastewater disinfection. AgNPs attached to filter materials have been considered promising for water disinfection due to their high antibacterial activity and cost-effectiveness (Quang et al. 2013).

5.2.3 Nanopesticides

Biogenic metal nanoparticles are less hazardous, are eco-friendly, and are considered as alternatives to chemical pesticides (organochlorine, organophosphorus, carbamate, triazine pesticides, etc.). Nanocapsules with AgNPs are used for the delivery of pesticides because they reduce the frequent application of chemicals. *Moringa oleifera* (drumstick) leaf extract (Mo-LE)-mediated AgNPs showed larvicidal and pupicidal toxicity against *Musca domestica* and insecticidal activity against *Aedes aegypti* and *Culex quinquefasciatus* (Abdel-Gawad 2018; Sujitha et al. 2015; Murugan et al. 2015). *Manilkara zapota* (sapodilla) leaf extract-mediated AgNPs were effective against the adults of *M. domestica* (Kamaraj et al. 2012).

5.2.4 Nanofertilizer

Nanoparticles are recognized as efficient agrochemical agents as they improve the crop productivity and nutrient uptake by plants. Nanoparticles penetrate the cuticle and tissues of the plants easily, thus allowing their effective release to the target area. It has great influence on plant growth and development such as germination, root-shoot ratio, seedling growth, root growth, root elongation, and senescence inhibition (Shah and Belozerova 2009).

Application of AgNPs in the plant is effective due to their small size, easy solubility, and diffusible nature that renders for rapid and complete absorption/uptake by the plant catering the nutritional needs and deficiencies in the crop plant (Raliya and Tarafdar 2013). Nowadays, large amounts of commercial fertilizers are used in the form of urea, nitrate, etc., but they have toxic effects on the plants and the beneficial microflora. It has been reported that silver nanoparticles could be used to enhance seed germination potential in many plants (Duhan et al. 2017).

6 Conclusion

Due to diverse properties, AgNPs are one of the most important and versatile materials with various benefits and applications to humans. The cyanobacterial biomolecules act as both reducing and stabilizing agents during silver nanoparticles synthesis. Day by day, AgNP demands are increasing due to its various applications (bioimaging, drug delivery, biosensors, and gene delivery). Due to biocompatibility, easy accessibility, and low cost, AgNPs have opened their greater use in the biomedical field. In the near future, it may appear as a smart weapon against multidrug-resistant microorganisms. Besides, AgNPs are also serving as herbicides, pesticides, and fertilizers.

References

Abdel-Gawad RM. Insecticidal activity of *Moringa oleifera* synthesized silver and zinc nanoparticles against the house fly, *Musca domestica L.* Autumn. 2018;11(4):19–30.

Abou El-Nour KMM, Eftaiha A, Al-Warthan A, Ammar RAA. Synthesis and applications of silver nanoparticles. Arab J Chem. 2010;3:135–40.

Agarwal A, Guthrie KM, Czuprynski CJ, Schurr MJ, McAnulty JF, Murphy CJ, Abbott NL. Polymeric multilayers that contain silver nanoparticles can be stamped onto biological tissues to provide antibacterial activity. Adv Funct Mater. 2011;21:1863–73.

Agnihotri S, Mukherji S, Mukherji S. Size-controlled silver nanoparticles synthesized over the range 5–100 nm using the same protocol and their antibacterial efficacy. RSC Adv. 2014;4:3974–83. https://doi.org/10.1039/C3RA44507K.

Asanithi P, Chaiyakun S, Limsuwan P. Growth of silver nanoparticles by DC magnetron sputtering. J Nanomater. 2012;2012:8. https://doi.org/10.1155/2012/963609.

Asharani PV, Mun GLK, Hande MP, Valiyaveettil S. Cytotoxicity and genotoxicity of silver nanoparticles in human cells. ACS Nano. 2009;3:279–90. https://doi.org/10.1021/nn800596w.

Aziz N, Fatma T, Varma A, Prasad R. Biogenic synthesis of silver nanoparticles using *Scenedesmus abundans* and evaluation of their antibacterial activity. J Nanoparticle. 2014;2014:1–6. https://doi.org/10.1155/2014/689419.

Aziz N, Faraz M, Pandey R, Shakir M, Fatma T, Varma A, Barman I, Prasad R. Facile algae-derived route to biogenic silver nanoparticles: synthesis, antibacterial and photocatalytic properties. Langmuir. 2015;31:11605–12.

Aziz N, Pandey R, Barman I, Prasad R. Leveraging the attributes of *Mucor hiemalis*-derived silver nanoparticles for a synergistic broad-spectrum antimicrobial platform. Front Microbiol. 2016;7(1984):1–11.

Aziz N, Faraz M, Sherwani MA, Fatma T, Prasad R. Illuminating the anticancerous efficacy of a new fungal chassis for silver nanoparticle synthesis. Front Chem. 2019;7:65.

Azizi S, Namvar F, Mahdavi M, Ahmad M, Mohammad R. Biosynthesis of silver nanoparticles using brown marine macroalga *Sargassum muticum* aqueous extract. Materials. 2013;6:5942–50.

Baer DR, Engelhard MH, Johnson GE. Surface characterization of nanomaterials and nanoparticles: important needs and challenging opportunities. J Vac Sci Technol. 2013;31(5):Article ID 050820.

Baumgartner JN, Cooper SL. Bacterial adhesion on polyurethane surfaces conditioned with thrombus components. ASAIO J. 1996;42:M476–9.

Benn TM, Westerhoff P. Nanoparticle silver released into water from commercially available sock fabrics. Environ Sci Technol. 2008;42(11):4133–9.

Beyth N, Haddad HY, Hadar BL, Farber YI, Domb AJ, Weiss EI. Surface antimicrobial activity and biocompatibility of incorporated polyethylenimine nanoparticles. Biomaterials. 2008;29(31):4157–63.

Bhattacharya D, Gupta RK. Nanotechnology and potential of microorganisms. Crit Rev Biotechnol. 2005;25:199–204.

Blaser SA, Scheringer M, MacLeod M, Hungerbühler K. Estimation of cumulative aquatic exposure and risk due to silver: contribution of nano-functionalized plastics and textiles. Sci Total Environ. 2008;390:396–409.

Brown K. Breast cancer chemoprevention: risk-benefit effects of the antioestrogen tamoxifen. Expert Opin Drug Saf. 2002;1:253–67. https://doi.org/10.1093/mutage/gep022.

Cao H, Liu X, Meng F, Chu PK. Silver nanoparticles-modified films versus biomedical device-associated infections. Wiley Interdiscip Rev Nanomed Nanobiotechnol. 2010;2:670–84.

Carbone M, Sabbatella G, Antonaroli S, Remita H, Orlando V, Biagioni S, Nucara A. Exogenous control over intracellular acidification: enhancement via proton caged compounds coupled to gold nanoparticles. Biochim Biophys Acta Gen Subj. 2015;1850:2304–7.

Carbone M, Donia DT, Sabbatella G, Antiochia R. Silver nanoparticles in polymeric matrices for fresh food packaging. J King Saud Univ Sci. 2016;28(4):273–9. https://doi.org/10.1016/j.jksus.2016.05.004.

Duhan JS, Kumar R, Kumar N. Nanotechnology: The new perspective in precision agriculture. Biotechnol Rep. 2017;2017:11–23.

Duncan TV. Applications of nanotechnology in food packaging and food safety: barrier materials, antimicrobials and sensors. J Colloid Interface Sci. 2011;363(1):1–24. https://doi.org/10.1016/j.jcis.2011.07.017.

Emamifar A, Kadivar M, Shahedi M, Soleimanian-Zad S. Evaluation of nanocomposite packaging containing Ag and ZnO on shelf life of fresh orange juice. Innovative Food Sci Emerg Technol. 2010;11:742–8.

Erdogan O, Abbak M, Demirbolat GM, Birtekocak F, Aksel M. Green synthesis of silver nanoparticles via *Cynara scolymus* leaf extracts: The characterization, anticancer potential with photodynamic therapy in MCF7 cells. PLoS One. 2019;14(6):e0216496. https://doi.org/10.1371/journal.pone.0216496.

Everaert EPJM, Van de Belt-Gritter B, Van der Mei HC, Busscher HJ, Verkerke GJ, Dijk F, Mahieu HF, Reitsma A. In vitro and in vivo microbial adhesion and growth on argon plasma-treated silicone rubber voice prostheses. J Mater Sci Mater Med. 1998;9:147–57.

Fatma T, Khan MA, Choudhary M. Impact of environmental pollution on cyanobacterial proline content. J Appl Phycol. 2007;19:625–9. https://doi.org/10.1007/s10811-007-9195-2.

Fawcett D, Verduin JJ, Shah M, Sharma SB, Poinern GEJ. A review of current research into the biogenic synthesis of metal and metal oxide nanoparticles via marine algae and seagrasses. J Nanosci. 2017;2017:15.

Franco-Molina MA, Mendoza-Gamboa E, Sierra-Rivera CA, Gómez-Flores RA, Zapata-Benavides P, Castillo-Tello P. Antitumor activity of colloidal silver on MCF-7 human breast cancer cells. J Exp Clin Cancer Res. 2010;29:148. https://doi.org/10.1186/1756-9966-29-148.

Freeman AI, Halladay LJ, Cripps P. The effect of silver impregnation of surgical scrub suits on surface bacterial contamination. Vet J. 2012;192(3):489–93.

Furno F, Morley KS, Wong B, Sharp BL, Arnold PL, Howdle SM, Bayston R, Brown PD, Winship PD, Reid HJ. Silver nanoparticles and polymeric medical devices: a new approach to prevention of infection? J Antimicrob Chemother. 2004;54(6):1019–24. https://doi.org/10.1093/jac/dkh478.

Govindaraju K, Krishnamoorthy K, Alsagaby SA, Singaravelu G, Premanathan M. Green synthesis of silver nanoparticles for selective toxicity towards cancer cells. IET Nanobiotechnol. 2015;9:325–30.

Gurunathan S, Park JH, Han JW, Kim JH. Comparative assessment of the apoptotic potential of silver nanoparticles synthesized by *Bacillus tequilensis* and *Calocybe indica* in MDA-MB-231 human breast cancer cells: Targeting p53 for anticancer therapy. Int J Nanomedicine. 2015;10(1):4203–23. https://doi.org/10.2147/IJN.S83953.

Husain S, Sardar M, Fatma T. Screening of cyanobacterial extracts for synthesis of silver nanoparticles. World J Microbiol Biotechnol. 2015;31(8):1279–83. https://doi.org/10.1007/s11274-015-1869-3.

Husain S, Afreen S, Yasin D, Afzal B, Fatma T. Cyanobacteria as a bioreactor for synthesis of silver nanoparticles-an effect of different reaction conditions on the size of nanoparticles and their dye decolorization ability. J Microbiol Methods. 2019;162:77–82.

Husen A, Siddiqi KS. Phytosynthesis of nanoparticles: concept, controversy and application. Nanoscale Res Lett. 2014;9:229.

Ibraheem IBM, Abd-Elaziz BEE, Saad WF, Fathy WA. Green biosynthesis of silver nanoparticles using marine red algae *Acanthophora spicifera* and its antimicrobial activity. J Nanomed Nanotechnol. 2016;7:1–4.

Iravani S, Korbekandi H, Mirmohammadi SV, Zolfaghari B. Synthesis of silver nanoparticles: chemical, physical and biological methods. Res Pharm Sci. 2014;9(6):385–406.

Kamaraj C, Rajakumar G, Rahuman AA, Velayutham K, Bagavan A, Zahir AA, Elango G. Feeding deterrent activity of synthesized silver nanoparticles using *Manilkara zapota* leaf extract against the house fly, *Musca domestica* (Diptera: Muscidae). Parasitol Res. 2012;111(6):2439–48. https://doi.org/10.1007/s00436-011-2689-5.

Khalifa K, Hamouda R, Hanafy D, Hamza A. In vitro antitumor activity of silver nanoparticles biosynthesized by marine algae. Dig J Nanomater Biostruct. 2016;11:213–21.

Khanna P, Kaur A, Goyal D. Algae-based metallic nanoparticles: Synthesis, characterization and applications. J Microbiol Methods. 2019;163:105656.

Khil MS, Cha DI, Kim HY, Kim IS, Bhattarai N. Electrospun nanofibrous polyurethane membrane as wound dressing. J Biomed Mater Res B Appl Biomater. 2003;67B:675–9.

Kim JS, Kuk E, Yu EN, Kim JH, Park SJ, Lee HJ, Kim SH, Park YK, Park YH, Hwang CY. Antimicrobial effects of silver nanoparticles. Nanomedicine. 2007;3:95–101.

Klevens RM, Edwards JR, Richards CL, Horan TC, Gaynes RP, Pollock DA. Estimating health care-associated infections and deaths in U.S. hospitals, 2002. Public Health Rep. 2007;122:160–6.

Krishnan M, Sivanandham V, Hans-Uwe D, Murugaiah SG, Seeni P, Gopalan S, Rathinam AJ. Antifouling assessments on biogenic nanoparticles: a field study from polluted off shore platform. Mar Pollut Bull. 2015;101:816–25.

Kumar P, Selvi SS, Praba AL, Selvaraj M. Antibacterial activity and in-vitro cytotoxicity assay against brine shrimp using silver nanoparticles synthesized from *Sargassum ilicifolium*. Dig J Nanomater Biostruct. 2012;7:1447–55.

Kumar P, Govindaraju M, Senthamilselvi S, Premkumar K. Photocatalytic degradation of methyl orange dye using silver (Ag) nanoparticles synthesized from *Ulva lactuca*. Colloids Surf B: Biointerfaces. 2013a;103:658–61.

Kumar P, Selvi SS, Govindaraju M. Seaweed-mediated biosynthesis of silver nanoparticles using *Gracilaria corticata* for its antifungal activity against Candida spp. Appl Nanosci. 2013b;3:495–500.

Lemire JA, Harrison JJ, Turner RJ. Antimicrobial activity of metals: mechanisms, molecular targets and applications. Nat Rev Microbiol. 2013;11:371–84.

Lengke MF, Fleet ME, Southam G. Biosynthesis of silver nanoparticles by filamentous cyanobacteria from a silver (I) nitrate complex. Langmuir. 2007;23:2694–9.

Liu Z, Sun D, Guo P, Leckie JO. One-Step fabrication and high photo-catalytic activity of porous TiO_2 hollow aggregates by using a low-temperature hydrothermal method without templates. Chem Eur J. 2007;13:1851–5.

Loo YY, Rukayadi Y, Nor-Khaizura MA, Kuan CH, Chieng BW, Nishibuchi M, Radu S. In vitro antimicrobial activity of green synthesized silver nanoparticles against selected gram-negative foodborne pathogens. Front Microbiol. 2018;16(9):1555. https://doi.org/10.3389/fmicb.2018.01555.

Mahdi SS, Vadood R, Nourdahr R. Study on the antimicrobial effect of nanosilver tray packaging of minced beef at refrigerator temperature. Glob Veterinaria. 2012;9:284–9.

Mahdieh M, Zolanvari A, Azimee AS, Mahdieh M. Green biosynthesis of silver nanoparticles by *Spirulina platensis*. Sci Iran. 2012;19(3):926–9. https://doi.org/10.1016/j.scient.2012.01.010.

Martinez-Abad A, Lagaron JM, Ocio MJ. Development and characterization of silver-based antimicrobial ethylene-vinyl alcohol copolymer (EVOH) films for food-packaging applications. J Agric Food Chem. 2012;60:5350–9.

Menon S, Rajeshkumar S, Kumar V. A review on biogenic synthesis of gold nanoparticles, characterization, and its applications. Resour Effic Technol. 2017;3(4):516–27.

Metak AM. Effects of nanocomposites based nano-silver and nano-titanium dioxideon food packaging materials. Int J Appl Sci Technol. 2015;5:26–40.

Metak AM, Ajaal TT. Investigation on polymer based nano-silver as food packaging materials. Int J Biol Food Vet Agric Eng. 2013;7:772–7.

Michalak I, Chojnacka K. Algae as production systems of bioactive compounds. Eng Life Sci. 2015;15:160–76.

Mishra S, Singh B, Naqvi A. Potential of biosynthesized silver nanoparticles using *Stenotrophomonas* sp. BHU-S7 (MTCC 5978) for management of soil-borne and foliar phytopathogens. Sci Rep. 2017;7:45154. https://doi.org/10.1038/srep45154.

Morris JK. How safe is our food? Emerg Infect Dis. 2011;17:126–8.

Morsy SMI. Role of surfactants in nanotechnology and their applications. Int J Curr Microbiol App Sci. 2014;3(5):237–60.

Motlagh NV, Mosavian MTH, Mortazavi SA. Effect of polyethylene packaging modified with silver particles on the microbial, sensory and appearance of dried barberry. Packag Technol Sci. 2012;26:39–49.

Mubarak AD, Sasikala M, Gunasekaran M, Thajuddin N. Biosynthesis and characterization of silver nanopar-

ticles using marine cyanobacterium, *Oscillatoria willei* NTDM 01. Dig J Nanomater Biostruct. 2011;6(2):385–90.

Murugan K, Samidoss CM, Panneerselvam C, Higuchi A, Roni M, Suresh U, Chandramohan B, Subramaniam J, Madhiyazhagan P, Dinesh D, Rajaganesh R. Seaweed-synthesized silver nanoparticles: an eco-friendly tool in the fight against *Plasmodium falciparum* and its vector *Anopheles stephensi*? Parasitol Res. 2015;114:4087–97.

Nanda A, Saravanan M. Biosynthesis of silver nanoparticles from *Staphylococcus aureus* and its antimicrobial activity against MRSA and MRSE. Nanomedicine. 2009;5:452–6.

Nath D, Banerjee P. Green nanotechnology–a new hope for medical biology. Environ Toxicol Pharmacol. 2013;36:997–1104.

Nouailhat A. An introduction to nanoscience and nanotechnology: Wiley; 2010. https://doi.org/10.1002/9780470610954.

Prasad R, Pandey R, Barman I. Engineering tailored nanoparticles with microbes: quo vadis? Wiley Interdiscip Rev Nanomed Nanobiotechnol. 2016;8(2):316–30.

Quang DV, Sarawade PB, Jeon SJ. Effective water disinfection using silver nanoparticle containing silica beads. Appl Surf Sci. 2013;266:280–7.

Rahdar A. Effect of mercaptoethanol and Na_2S dropwise addition rate on zinc sulfide semiconductor nanocrystals: synthesis and characterization. J Nanostruct Chem. 2013;3:61.

Rai M, Yadav A, Gade A. Silver nanoparticles as a new generation of antimicrobials. Biotechnol Adv. 2009;27(1):76–83. https://doi.org/10.1016/j.biotechadv.2008.09.002.

Raliya R, Tarafdar JC. ZnO nanoparticle biosynthesis and its effect on phosphorous-mobilizing enzyme secretion and gum contents in cluster bean (*Cyamopsis tetragonoloba* L.). Agric Res. 2013;2:48–57.

Roe D, Karandikar B, Bonn-Savage N, Gibbins B, Roullet JB. Antimicrobial surface functionalization of plastic catheters by silver nanoparticles. J Antimicrob Chemother. 2008;61(4):869–76.

Rujitanaroj PO, Pimpha N, Supaphol P. Wound-dressing materials with antibacterial activity from electrospun gelatin fiber mats containing silver nanoparticles. Polymer. 2008;49:4723–32.

Sadowski Z. Biosynthesis and application of silver and gold nanoparticles. In: Perez DP, editor. Silver nanoparticles. Rijeka: IntechOpen; 2010. https://doi.org/10.5772/8508.

Samuela U, Guggenbichler JP. Prevention of catheter-related infections: the potential of a new nano-silver impregnated catheter. Int J Antimicrob Agents. 2004;23:75–8.

Sanpui P, Chattopadhyay A, Ghosh SS. Induction of apoptosis in cancer cells at low silver nanoparticle concentrations using chitosan nanocarrier. ACS App Mat Interfaces. 2011;3:218–28. https://doi.org/10.1021/am100840c.

Shah V, Belozerova I. Influence of metal nanoparticles on the soil microbial community and germination of lettuce seeds. Water Air Soil Pollut. 2009;197:143–8.

Shah M, Fawcett D, Sharma S, Tripathy S, Poinern G. Green synthesis of metallic nanoparticles via biological entities. Materials. 2015;8:7278–308.

Sharma A, Sharma S, Sharma K, Chetri SP, Vashishtha A, Singh P, Kumar R, Rathi B, Agrawal V. Algae as crucial organisms in advancing nanotechnology: a systematic review. J Appl Phycol. 2015;28:1759–74.

Sudha SS, Amanickam K, Rengaramanujam J. Microalgae mediated synthesis of silver nanoparticles and their antibacterial activity against pathogenic bacteria. Indian J Exp Biol. 2013;51(5):393–9.

Sujitha V, Murugan K, Paulpandi M, Panneerselvam C, Suresh U, Roni M, Nicoletti M, Higuchi A, Madhiyazhagan P, Subramaniam J, Dinesh D, Vadivalagan C, Chandramohan B, Alarfaj AA, Munusamy MA, Barnard DR, Benelli G. Green-synthesized silver nanoparticles as a novel control tool against dengue virus (DEN-2) and its primary vector *Aedes aegypti*. Parasitol Res. 2015;114(9):3315–25. https://doi.org/10.1007/s00436-015-4556-2.

Sun RWY, Chen R, Chung NPY, Ho CM, Lin CLS, Che CM. Silver nanoparticles fabricated in hepes buffer exhibit cytoprotective activities toward HIV-1 infected cells. Chem Commun. 2005;40:5059–61.

Thakkar KN, Mhatre SS, Parikh RY. Biological synthesis of metallic nanoparticles. Nanomedicine. 2010;6:257–62.

Tien DC, Liao CY, Huang JC, Tseng KH, Lung JK, Tsung TT, Kao WS, Tsai TH, Cheng TW, Yu BS, Lin HM, Stobinski L. Novel technique for preparing a nano-silver water suspension by the arc-discharge method. Advanced Study Center Co. Ltd. Rev Adv Mater Sci. 2008;18:750.

Toker RD, Kayaman-Apohan N, Kahraman MV. UV-curable nano-silver containing polyurethane based organic–inorganic hybrid coatings. Prog Org Coat. 2013;76:1243–50.

Tsibakhashvili NY, Kirkesali EI, Pataraya DT, Gurielidze MA, Kalabegishvili TL, Gvarjaladze DN, Tsertsvadze GI, Frontasyeva MV, Zinicovscaia II, Wakstein MS, Khakhanov SN. Microbial synthesis of silver nanoparticles by *Streptomyces glaucus* and *Spirulina platensis*. Adv Sci Lett. 2011;4:1–10.

Unnithan AR, Barakat NAM, Pichiah PBT, Gnanasekaran G, Nirmala R, Cha YS, Jung CH, El-Newehy M, Kim HY. Wound-dressing materials with antibacterial activity from electrospun polyurethane-dextran nanofiber mats containing ciprofloxacin HCl. Carbohydr Polym. 2012;90:1786–93.

Vijayan SR, Santhiyagu P, Singamuthu M, Kumari Ahila N, Jayaraman R, Ethiraj K. Synthesis and characterization of silver and gold nanoparticles using aqueous extract of seaweed, *Turbinaria conoides*, and their antimicrofouling activity. Sci World J. 2014;2014:938272.

Vijayan SR, Santhiyagu P, Ramasamy R, Arivalagan P, Kumar G, Ethiraj K, Ramaswamy BR. Seaweeds:

a resource for marine bionanotechnology. Enzym Microb Technol. 2016;95:45–57.

Vivek M, Kumar PS, Steffi S, Sudha S. Biogenic silver nanoparticles by *Gelidiella acerosa* extract and their antifungal effects. Avicenna J Med Biotechnol. 2011;3(3):143–8.

Vlachou E, Chipp E, Shale E, Wilson YT, Papini R, Moiemen NS. The safety of nanocrystalline silver dressings on burns: A study of systemic silver absorption. Burns. 2007;33:979–85.

Walser T, Demou E, Lang DJ, Hellweg S. Prospective environmental life cycle assessment of nanosilver t-shirts. Environ Sci Technol. 2011;45:4570–8.

Yezhelyev MV, Gao X, Xing Y, Al-Hajj A, Nie S, O'Regan RM. Emerging use of nanoparticles in diagnosis and treatment of breast cancer. Lancet Oncol. 2006;7:657–67.

Zhang W, Qiao X, Chen J. Synthesis of nanosilver colloidal particles in water/oil microemulsion. Col Surf A Physicochem Eng Asp. 2007;299:22–8.

Selenium Nanoparticles: Green Synthesis and Exploitation

22

Bushra Afzal and Tasneem Fatma

Abstract

Selenium (Se) is a crucial trace element required by all living organisms, and its deficiency as well as excess is known to cause many diseases. Selenium as selenite and selenate is toxic in comparison to selenium nanoparticles (SeNPs), which have no toxicity. SeNPs can be synthesized by physical, chemical, and biological methods. The biosynthesized SeNPs are red-colored, stable structures. Different microorganisms like plants, bacteria, cyanobacteria, fungus, etc., have been used to synthesize SeNPs due to the presence of many reducing biomolecules. Parameters that govern their synthesis are reaction time, temperature, pH, and reactant concentration. Microbial synthesis of SeNPs is a two-step reduction process from SeO_4^{-2} to $SeO_3^{-2}$and then to insoluble elemental selenium (Se^0). These reactions are catalyzed by selenate and selenite reductases. SeNPs act as potent antioxidant, antibacterial, anti-inflammatory, chemopreventive, and chemotherapeutic agents. Conjugation of SeNPs with antibiotics enhances their anticancer efficacy. SeNPs also have applications in nanobiosensors and environmental remediation.

Keywords

Selenium · Selenium nanoparticles · Anticancer · Antimicrobial · Antioxidant

1 Introduction

Selenium is an essential trace mineral which gets incorporated into proteins and plays a role in prevention of cellular damage, regulation of the thyroid gland, and immune system functioning (Zhang et al. 2005). Se acts as a cofactor for thioredoxin reductases and glutathione peroxidases (Wadhwani et al. 2016). In the environment, Se exists in different oxidation states and forms like ionic selenite (Na_2SeO^4), selenite (Na_2SeO^3), solid state Se (0), selenocysteine/selenomethionine (SeMet), etc. Selenium nanoparticles (SeNPs) show low cytotoxicity and some unique properties in comparison to selenium (Se) compounds and thus have many added medicinal applications including cancer therapy (Forootanfar et al. 2014a; Benko et al. 2012).

Conventionally, SeNPs can be synthesized through physical (hydrothermal techniques, UV radiation, and laser ablation) and chemical methods (acid decomposition, precipitation, catalytic reduction using ascorbic acid, sodium dodecyl sulfate, sulfur dioxide, glucose, etc.)

B. Afzal · T. Fatma (✉)
Cyanobacterial Biotechnology Laboratory, Department of Biosciences, Jamia Millia Islamia, New Delhi, India

J. K. Patel, Y. V. Pathak (eds.), *Emerging Technologies for Nanoparticle Manufacturing*,
https://doi.org/10.1007/978-3-030-50703-9_22

(Wadhwani et al. 2016). These methods use harsh chemicals, high temperature, and acidic pH which makes the nanoparticles unsafe and toxic for biomedical use. Therefore, the need for synthesis of SeNPs by biological method became acute. Moreover, biogenic SeNPs are more stable due to coating of biomolecules that reduces nanoparticle aggregation (Nancharaiah and Lens 2015).

Some proteins that are reported to play a significant role in the SeNP synthesis and in their stability are selenium factor A (Sef A) (Butler et al. 2012), metalloid reductases (Rar A) (Lenz et al. 2011), propanol-preferring alcohol dehydrogenase (AdhP) (Dobias et al. 2011), and bovine serum albumin (BSA) (Kaur et al. 2009). Proteins containing aromatic amino acids like tryptophan, phenylalanine, and tyrosine also play a significant role in the synthesis of SeNP (Li et al. 2007). Some biologically active compounds present in plants like phenols, flavonoids, lignin, etc., are found to be responsible for the synthesis of SeNPs (Prasad and Selvaraj 2014; Kokila et al. 2017).

2 Biosynthesis of Selenium Nanoparticles

Considering the biocompatible and eco-friendly nature of nanoparticles, many organisms are used as bioresource as they possess active compounds like proteins, carbohydrates, cardiac glycosides, saponins, flavonoids, phenols, alkaloids, steroids, and amino acids that reduce selenium salts to SeNPs (Li et al. 2007; Prasad and Selvaraj 2014).

2.1 SeNP Synthesis by Bacteria and Actinomycetes

Many bacteria synthesize SeNPs during their detoxification and resistance mechanism (Kessi et al. 1999). Synthesis of SeNPs can be intracellular, extracellular, or membrane bound (Table 22.1). *Salmonella heidelberg* grown in sodium selenite (Na_2SeO_3) form red amorphous, intracellular SeNPs (McCready et al. 1966).

According to the current nomenclature, particles having the size range between 1 and 100 nm are called nanoparticles. But, Se nanomaterials having size range more than 100 nm are also reported in the past. Newly isolated, aerobically growing *Duganella* sp. and *Agrobacterium* sp. from soils of Punjab, India, form spherical SeNPs in the size range 140–200 and 185–190 nm, respectively, from water-soluble selenite (Bajaj et al. 2012). The SeNPs in the size range 28–123 nm have also been synthesized from actinomycetes (*Streptomyces microflavus* strain FSHJ31) that were characterized by UV-Vis spectroscopy, transmission electron microscopy (TEM), energy dispersive X-ray analysis (EDX), and Fourier-transform infrared spectroscopy (FTIR) (Forootanfar et al. 2014b). Bimetallic nanoparticles of Se with semiconducting properties, e.g., ZnSe nanoparticles (Pearce et al. 2008) and CdSe nanoparticles (Ayano et al. 2014) from *Veillonella atypica and Pseudomonas* sp. strain RB, respectively, were also attempted. Their biomedical potential is yet to be explored.

2.2 SeNP Synthesis by Fungi

Fungi are also reported to synthesize SeNPs (Table 22.2). Zare et al. (2013) synthesized spherical SeNPs with an average size of 47 nm from *Aspergillus terreus* extracellularly by the culture supernatant and then characterized by UV-Vis spectroscopy, dynamic light scattering (DLS), and scanning electron microscopy (SEM). Sarkar et al. (2011) used the culture filtrate of *Alternaria alternata* to synthesize red-colored, monodispersive, amorphous, spherical SeNPs having size range between 30 and150 nm. Their FTIR suggested that the protein shell is responsible for the stabilization of SeNPs. Edible *Lentinula edodes* is also found to synthesize intense red-colored, spherical, 18–16-nm-sized SeNPs (Vetchinkina et al. 2013).

Table 22.1 Selenium nanoparticles synthesized by bacteria and actinomycetes

Organism	Size (nm)	Shape	Location	References
Bacteria				
Bacillus cereus	150–200	Spherical	Intracellular	Dhanjal and Cameotra (2010)
Bacillus sp. MSh-1	80–220	Spherical	Intracellular	Shakibaie et al. (2010)
Bacillus selenitireducens	300	Spherical	Extracellular	Oremland et al. (2004)
Bacillus subtilis	50–400	Spherical	Extracellular	Wang et al. (2010)
Duganella sp.	140–200	Spherical	Extracellular	Bajaj et al., (2012)
Escherichia coli K-12	24–122	Spherical	Extracellular	Dobias et al. (2011)
Enterobacter cloacae SLD1a-1	100	Spherical	Near cell surface	Losi and Frankenberger (1997)
Enterobacter cloacae SLD1a-1	–	–	Periplasmic membrane	Watts et al. (2003)
Geobacter sulfurreducens	40–700	Spherical	–	Fellowes et al. (2011)
Klebsiella pneumonia	90–320	Spherical	Intracellular	Kazempour et al. (2013)
Lactobacillus acidophilus	–	Spherical	Intracellular	Domokos-Szabolcsy et al. (2012)
Lactobacillus plantarum	>250	–	Intracellular	Yazdi et al. (2013)
Microbacterium sp. *ARB05*	30–150	Spherical	Extracellular	Prasad et al. (2012)
Moraxella bovis	–	–	Intracellular	Biswas et al. (2011)
Pseudomonas aeruginosa	140	Spherical	Extracellular	Dwivedi et al. (2013)
Pseudomonas alcaliphila	50–500	Spherical	Intracellular	Zhang et al. (2011)
Pseudomonas fluorescens	–	–	Intracellular	Garbisu et al. (1996)
Pseudomonas putida KT2440	–	–	Bound to membrane	Avendaño et al. (2016)
Pseudomonas stutzeri	100–500	Spherical	Extracellular	Lortie et al. (1992)
Rhodospirillum rubrum	–	Spherical	Intracellular	Kessi et al. (1999)
Shewanella sp.	11–20	Spherical	Intracellular	Filipe et al. (2010)
Sulfurospirillum barnesii	300	Spherical	Extracellular	Oremland et al. (2004)
Selenihalanaerobacter shriftii	300	Spherical	Extracellular	Oremland et al. (2004)
Shewanella oneidensis MR 1	100	Spherical	Intracellular	Li et al. (2014)
Stenotrophomonas maltophilia	≤270	Spherical	Near cell wall	Dungan et al. (2003)
Stenotrophomonas maltophilia	–	–	–	Lampis et al. (2014)
Zoogloea ramigera	30–150	Spherical	Extracellular	Srivastava and Mukhopadhyay (2013)
Actinomycetes				
Streptomyces microflavus	28–123	–	–	Forootanfar et al. (2014a, b)
Streptomyces bikiniensis	17	Rods	–	Ahmad et al. (2015)

Table 22.2 SeNPs synthesized by fungi

Fungus	Size (nm)	Shape	Location	Reference
Alternaria alternata	30–150	Spherical	Extracellular	Sarkar et al. (2011)
Aspergillus terreus	47	Spherical	Extracellular	Zare et al. (2013)
Fusarium sp.	–	–	Hyphae and conidia	Gharieb et al. (1995)
Gliocladium roseum	20–80 nm	Spherical	Extracellular	Srivastava and Mukhopadhyay (2013)
Saccharomyces cerevisiae	30–100	–	Extracellular	Hariharan et al. (2012)
Trichoderma reesei	–	Needle-like	Hyphae and conidia	Gharieb et al. (1995)
Rhizobium sp. strain B1	–	–	–	Hunter and Kuykendall (2007)
Lentinula edodes	16–18	Spherical	Mycelia and hyphae	Vetchinkina et al. (2013)

2.3 SeNP Synthesis by Plants

Li et al. (2007) synthesized red, amorphous α-Se/protein composites by using 30 kDa protein from *Capsicum annuum*. This protein not only reduces the SeO_3^{2-} ions to Se^0 but also controls the nucle-

Table 22.3 SeNPs synthesized by angiospermic plants

Plants	Size (nm)	Shape	Location	Reference
Allium sativum	40–100	Spherical	Extracellular	Anu et al. (2017)
Capsicum annuum	200–500	Polygonal	Leaf extract	Li et al. (2007)
Diospyros montana	4 to 16	Spherical	Leaf extract	Kokila et al. (2017)
Pantoea agglomerans	30–300	Spherical	Intracellular	Torres et al. (2012)
Lemon	60–80	–	Leaf extract	Prasad et al. (2013)
Trigonella foenum-graecum	50–150	Spherical	Seed extract	Ramamurthy et al. (2013)
Terminalia arjuna	10–80	Polydispersed	Leaf extract	Prasad and Selvaraj (2014)
Vitis vinifera	3–18	Spherical	Fruit extract	Sharma et al. (2014)
Psidium guajava	8–20	Spherical	Leaf extract	Alam et al. (2019)

ation and growth of Se^0. The size and shell thickness of the α-Se/protein composites increase with increasing leaf extract concentration and decrease at low pH. Sharma et al. (2014) synthesized red, spherical, 3–18 nm sized lignin capped SeNPs using dried *Vitis vinifera* extract. Alam et al. (2018) synthesized small sized (8–20 nm) SeNPs by alcoholic extract of a guava (*Psidium guajava*) leaf. Their FTIR spectroscopy suggested the role of phenolic compounds in SeNP synthesis. These SeNPs showed good antibacterial effect against both gram-positive and gram-negative bacteria. Good anticancer activity was obtained against HepG2 and CHO cell lines. Details of plant-based SeNPs are summarized in Table 22.3.

2.4 Synthesis by Algae and Cyanobacteria

The extracts of algae and cyanobacteria are rich in photosynthetic pigments and secondary metabolites that reduce metals to synthesize metal nanoparticles like AuNPs, AgNPs, and SeNPs (Parial et al. 2012; Aziz et al. 2014; Husain et al. 2015, 2019; Singh et al. 2015; Afzal et al. 2019). Chen et al. (2008) used polysaccharides of *Undaria pinnatifida* (edible seaweed) for synthesis of SeNPs and suggested their chemopreventive role for human cancers, especially melanoma cancer. Though scientific work with special emphasis on SeNP synthesis through cyanobacteria started in current decade, indirect evidences for its synthesis may be traced back from the 1970s as accidental observations. Kumar and Prakash (1971) observed red-colored granules in the liquid medium of selenite-treated *Anacystis nidulans* and *Anabaena variabilis*. Sielicki and Burnham (1973) also noticed the cell associated granules in *Phormidium luridum* var. *olivacea* after exposure to high selenite. According to Pronina et al. (2002), *Spirulina platensis* reduce the Se(IV) to Se(0)/SeNPs within the cell that ooze out to the cell surface. Hnain et al. (2013) optimized and synthesized the SeNPs (220 nm) intracellularly in *Synechococcus leopoliensis*. Yang et al. (2012) used *Spirulina* polysaccharides (SPS) for capping of chemically synthesized SeNPs that showed increased anticancer efficacy. Recently, we have screened 20 cell-free cyanobacterial extracts for the synthesis of SeNPs (Afzal et al. 2019). Table 22.4 shows different algae and cyanobacteria which have been reported for the SeNP synthesis.

3 Mechanism of Biosynthesis of SeNPs

3.1 Intracellular Synthesis of SeNPs

The intracellular mechanism explains the transportation of selenium ions into the microbial cell to form nanoparticles mediated by cellular enzymes. The intracellular mechanism of selenite and selenate reduction has been studied in three organisms, viz., *Enterobacter cloacae SLD1a-1(*Yee et al. 2007), *Escherichia coli* (Kessi and Hanselmann 2004), and *Thauera selenatis* (Butler et al. 2012). Selenite reduction is a two-

Table 22.4 SeNPs synthesized by algae and cyanobacteria

Organism	Size (nm)	Shape	Location	References
Algae				
Undaria pinnatifida	59	Spherical	Extracellular	Chen et al. (2008)
Cyanobacteria				
Arthrospira indica SOSA-4	11.8	Spherical	Extracellular	Afzal et al. (2019)
Arthrospira maxima SAE-4988	16.2	Spherical	Extracellular	
Arthrospira indica SAE-84	60	Spherical	Extracellular	
Calothrix brevissema NCCU-65	25.6	Spherical	Extracellular	
Chroococcus NCCU-207	18.2	Spherical	Extracellular	
Gloeocapsa gelatinosa NCCU-430	13.2	Spherical	Extracellular	
Lyngbya NCCU-102	18.9	Spherical	Extracellular	
Microchaete sp. NCCU-342	15.2	Spherical	Extracellular	
Nostoc muscorum NCCU-442	18.6	Spherical	Extracellular	
Nostoc punctiforme	26	Spherical	Extracellular	
Nostoc sphericum	22.4	Spherical	Extracellular	
Oscillatoria sp. NCCU-369	13.6	Spherical	Extracellular	
Phormidium sp. NCCU-104	14	Spherical	Extracellular	
Plectonema sp. NCCU-204	18.3	Spherical	Extracellular	
Scytonema sp. NCCU-126	24	Spherical	Extracellular	
Spirulina CPCC-695	18.2	Spherical	Extracellular	
Spirulina platensis NCCU-S5	21.4	Spherical	Extracellular	
Synechocystis NCCU-370	18.9	Spherical	Extracellular	
Westiellopsis prolifica NCCU-331	17.5	Spherical	Extracellular	
Synechococcus leopoliensis	220	Spherical	On cell surface	Hnain et al. (2013)
Spirulina platensis	20–50	Spherical	Extracellular	Yang et al. (2012)

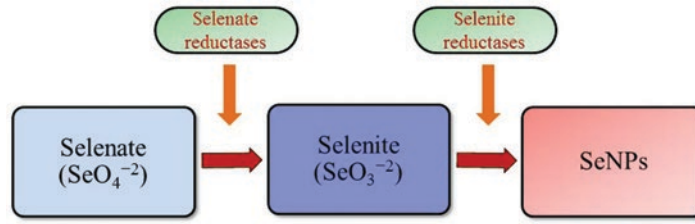

Fig. 22.1 General mechanism of selenate and selenite reduction

step reduction process: (i) selenate reductases convert selenate (SeO_4^{-2}) to selenite (SeO_3^{-2}) and (ii) selenite to insoluble elemental selenium (Se^0)/SeNPs by nonspecific selenite reductases (Fig. 22.1).

Selenate reductase is the crucial enzyme for the selenate reduction which exists in soluble and membranous forms in many bacteria (Butler et al. 2012; Ma et al. 2009; Yee et al. 2007; Watts et al. 2003). A trimeric unit SerABCD operon encodes for selenate reductase in periplasm (Butler et al. 2012) that is active in both aerobic and anaerobic conditions. In *Enterobacter cloacae* SLD1a-1, the expression of selenate reductases is regulated by fumarate-nitrate reduction regulator (FNR), which is an anaerobic regulatory gene (Yee et al. 2007).

Selenite reduction is catalyzed by selenite reductases (Dwivedi et al. 2013; Garbisu et al. 1995). Molybdenum acts as an activator for selenite reductase, but tungsten acts as an inhibitor for the enzyme (Watts et al. 2003). In *Shewanella oneidensis*, anaerobic respiration and reduction of selenite take place simultaneously (Li et al. 2014). According to Butler et al. (2012), glutathione reduces selenite to Se0 (SeNPs) in a stepwise manner. Initially, selenite is converted to selenodiglutathione (GS-Se-SG) by donating electrons. Then, thioredoxin reductase (TR) or glutathione reductase (GR) reduces the selenodi-

glutathione to selenopersulfide of glutathione which dismutates into reduced glutathione and elemental Se/SeNPs. SeNPs formed during exponential growth phase get released into the surrounding medium during stationary phase causing irreversible damage to the cell wall (Kessi and Hanselmann 2004).

3.2 Extracellular Mechanism

In nature, the extracellular synthesis refers to the synthesis of nanoparticles outside the cell and is executed by the compounds that ooze out from the cell such as ions, various proteins/enzymes, pigments, and non-protein entities like RNA, DNA, hormones, antioxidants, and lipids (Mata et al. 2009; Vijayan et al. 2014). But during in vitro biogenic nanoparticle synthesis, either crude cell extracts or their individual components are used as reducing and capping agents (Fig. 22.2). For extract preparation, pretreatments with detergents, blending, crushing in mortar and pestle, and heating or their combinations are used.

Incubation temperature is a very crucial parameter for the synthesis of SeNPs. The optimized temperature for *Enterococcus faecalis* and *Acetobacter* sp. SW30 was 37 °C (Shoeibi and Mashreghi 2017; Wadhwani et al. 2017), while for *Gliocladium roseum*, it was 30 °C (Srivastava and Mukhopadhyay 2015). For cyanobacteria, optimal temperature was 32 °C (Afzal et al. 2019). Time taken for SeNP synthesis also varied. It was 5 min by *Diospyros montana* extract (Kokila et al. 2017). Srivastava and Mukhopadhyay (2015) observed that the synthesis time for SeNPs from *Gliocladium roseum* is only one day. Hnain et al. (2013) found that the intracellular synthesis of SeNPs by *Synechococcus leopoliensis* takes 9 days. In our study, ten cyanobacterial extracts took 2 days, and the rest of the extracts took 3 to 5 days (Afzal et al. 2019). Fast reduction reactions in some organisms may be due to the presence of higher quantity of enzymatic or nonenzymatic reducing substances. After optimizing the reaction conditions, it has been observed by our group that the extract from cyanobacterial *Anabaena variabilis* can synthesize the SeNPs only in 1 day (communicated).

So far, the leaf extracts of ginger (Menon et al. 2019), *Vitis vinifera* (Sharma et al. 2014), *Psidium guajava* (Alam et al. 2019), and *Diospyros montana* (Kokila et al. 2017) are used for SeNP synthesis. Algal and cyanobacterial polysaccharides act as reducing and capping agents for SeNPs (Chen et al. 2008; Yang et al. 2012). Proteins containing aromatic amino acids like tryptophan, phenylalanine, and tyrosine play a much significant role in the synthesis (Li et al. 2007). A protein, selenium factor A (Sef A) with a size of ~94.5 kDa, has been found to play an important role in the export of SeNPs across cytoplasm and stabilizing the nanoparticles (Butler et al. 2012). Metalloid reductase Rar A is a binding protein that provides

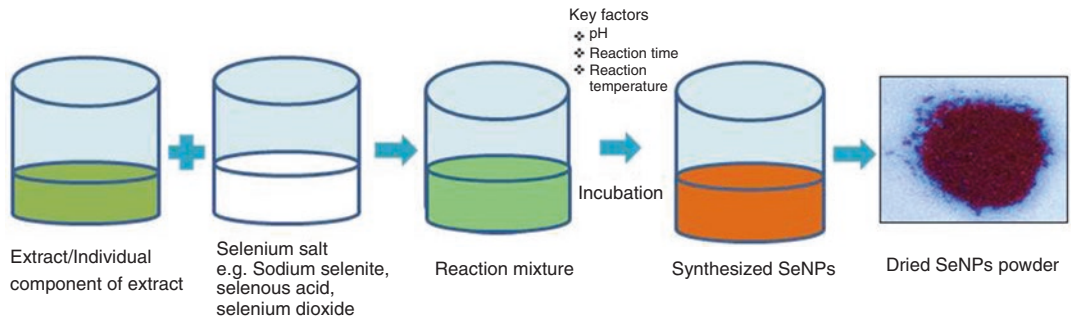

Fig. 22.2 Extracellular synthesis of SeNPs

stability to SeNPs (Lenz et al. 2011). Propanol-preferring alcohol dehydrogenase (AdhP) controls the SeNP size distribution (Dobias et al. 2011), while bovine serum albumin (BSA) influences the shape of SeNPs (Kaur et al. 2009).

4 Applications of Biosynthesized SeNPs

SeNPs have a wide range of applications in therapeutics, medicine, biosensors, and bioremediation (Fig. 22.3).

4.1 Biosynthesized SeNPs in Medicine

SeNPs have variety of applications in medicine like antioxidant, antimicrobial, and anticancer agents.

4.1.1 Antimicrobial Activity

SeNPs exhibit an excellent antimicrobial activity against different bacteria, yeast, and fungi. They show size and concentration-dependent effects against the investigated microorganisms. According to Zonaro et al. (2015), SeNPs synthesized by *Stenotrophomonas maltophilia* SeITE02 possess antimicrobial activity against *Escherichia coli* JM109, *Pseudomonas aeruginosa* PAO1, and *Staphylococcus aureus* ATCC 25923. Se nanocomposites synthesized by *Saccharomyces cerevisiae* have antimicrobial activity against

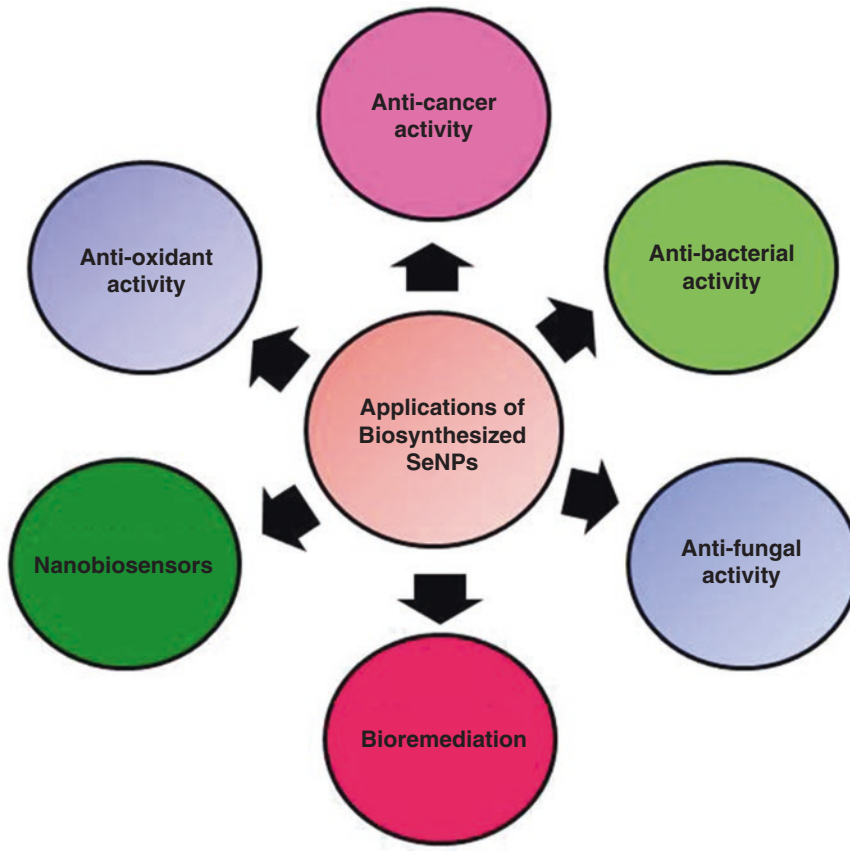

Fig. 22.3 Applications of SeNPs

nosocomial infection causing pathogenic bacteria (Hariharan et al. 2012).

Biogenic SeNPs produced by *Klebsiella pneumoniae* showed antifungal effectiveness against *Aspergillus* and *Malassezia* (Shahverdi et al. 2010). SeNPs synthesized from *Bacillus* sp. MSh-1 kill amastigotes and promastigotes of *Leishmania major* and *Leishmania infantum* (Soflaei et al. 2014; Beheshti et al. 2013) and platyhelminth *Echinococcus granulosus*, which causes cystic hydatid disease in humans (Mahmoudvand et al. 2014). *Anabaena variabilis*-mediated SeNPs also showed antimicrobial activity against *Escherichia coli*, *Streptococcus aureus, Klebsiella pneumonia*, *Bacillus subtilis*, and *Candida* sp. in a dose-dependent manner (communicated).

4.1.2 Antioxidant Activity of Biosynthesized SeNPs

SeNPs showed better scavenging activity than SeO_2 for reactive oxygen species (ROS) such as superoxide anion ($O_2^{\bullet-}$), singlet oxygen ($^1O_2$), 1,1-diphenyl-2-picrylhydrazyl (DPPH), and carbon-centered free radicals (Forootanfar et al. 2014a). According to Torres et al. (2012), smaller sized and L-cystine stabilized SeNPs show higher antioxidant activity. We also found that the smallest cyanobacterial SeNPs showed higher antioxidant activity (Afzal et al. 2019).

4.1.3 Anticancer Activity of Biosynthesized SeNPs

SeNPs show anticancer activity against lung cancer (Ali et al. 2013) and liver and breast cancer (Ahmad et al. 2015). Like antioxidant activity, smaller sized SeNPs show better anticancer activity. Selenium nanorods synthesized by *Streptomyces bikiniensis* strain Ess_amA1 showed anticancer activity against HepG2 and MCF-7 human cancer cells. The mechanisms of SeNP activity include (a) initiation of cellular and mitochondrial apoptosis; (b) prevention of metastasis by inhibiting the expression of matrix metalloproteinases; (c) endogenous copper mobilization; (d) increased oxidative stress, immune surveillance, and carcinogen detoxification; (e) arrest of cell cycle at S phase; and (f) inhibition of angiogenesis and tumor cell invasion. SeNPs synthesized from the leaf extract of *Terminalia arjuna* give protection against cell death and DNA damage (Prasad and Selvaraj 2014). SeNPs from *Lactobacillus brevis* showed activity against metastatic breast cancer along with induction of immune response (Yazdi et al. 2012).

According to Yang et al. (2012), SeNPs synthesized by polysaccharides of *Spirulina* inhibit the tumor growth by triggering apoptosis and assist in targeted nanoparticle delivery in cancerous cells through the specific interactions between the biomolecules like lectins and carbohydrates present on the surface of the cell. They also found that conjugates of SeNPs and doxorubicin help in the uptake of antibiotic in the cell, thereby increasing their cytotoxic effects against cancerous cells.

4.2 SeNPs in Nanobiosensors

Wang et al. (2010) reported that the nanobiosensor modified by *Bacillus subtilis*-derived SeNPs shows better electrocatalytic activity for H_2O_2. Biosensors with larger size range SeNPs (50 to 400 nm) have better detection limit (8×10^{-8} M) in comparison to chemically synthesized SeNPs of smaller size (10 nm) with detection limit (9.2×10^{-7} M). They suggested that SeNP-based biosensors have a wide range of applications related to the detection of H_2O_2 in food, pharmaceutical, clinical, industrial, and environmental analyses.

4.3 SeNPs in Bioremediation

Reduction reactions in which the toxic forms of Se (selenite and selenate) reduce to the nontoxic forms (elemental Se/SeNPs) are the basic mechanism to eliminate Se from the nature (Garbisu et al. 1996). They developed a bacterial treatment system to reduce the selenium contamination from streams using *Pseudomonas fluorescens*

and *Bacillus subtilis*. Similarly, bioremediation of seleniferous compounds was done by *Enterobacter cloacae* SLD1a-1 in the agricultural drainage water (Losi and Frankenberger 1997). Heating is also found to induce the conversion of SeNPs from amorphous Se to crystalline form, which can be easily removed from the settled wastewater (Lenz et al. 2009). Jiang et al. (2012), found that *Shewanella putrefaciens* is able to co-remove mercury and selenium from aqueous medium.

5 Summary and Future Perspective

SeNPs can be synthesized by physical, chemical, and biological methods. The biological SeNPs are stable and eco-friendly due to the presence of biomolecules on their surface. Cellular extracts, bacteria, cyanobacteria, fungus, and plants are capable to synthesize SeNPs. They can be synthesized by intracellular and extracellular modes. Intracellular SeNP synthesis is part of the resistance mechanism used by some organisms to counter toxic effects of high selenium doses present in their surroundings. These SeNPs may ooze out. During extracellular synthesis, crude extracts or purified compounds of organisms are used as a source of reducing and stabilizing agent. Effect of biological source and reaction conditions can be controlled for optimizing yield and size of SeNPs. Smaller biosynthesized SeNPs have large applications than selenium salts. In order to increase the efficacy of SeNPs, experiments are needed to be carried out to study the surface functionalization of SeNPs with drugs.

Acknowledgments B. Afzal is thankful to ICMR (Indian Council of Medical Research), New Delhi, for giving funding as ICMR-SRF.

References

Afzal B, Yasin D, Husain S, Zaki A, Srivastava P, Kumar R, Fatma T. Screening of cyanobacterial strains for the selenium nanoparticles synthesis and their anti-oxidant activity. Biocatal Agric Biotechnol. 2019;21:101307.

Ahmad MS, Yasser MM, Sholkamy EN, Ali AM, Mehanni MM. Anticancer activity of biostabilized selenium nanorods synthesized by *Streptomyces bikiniensis* strain Ess_amA-1. Int J Nanomedicine. 2015;10:3389.

Alam H, Khatoon N, Raza M, Ghosh PC, Sardar M. Synthesis and characterization of nano selenium using plant biomolecules and their potential applications. BioNanoScience. 2019;9(1):96–104.

Ali EN, El-Sonbaty SM, Salem FM. Evaluation of selenium nanoparticles as a potential chemopreventive agent against lung carcinoma. Int J Pharm Biol Sci. 2013;2(4):38–46.

Anu K, Singaravelu G, Murugan K, Benelli G. Green-synthesis of selenium nanoparticles using garlic cloves (*Allium sativum*): biophysical characterization and cytotoxicity on vero cells. J Clust Sci. 2017;28(1):551–63.

Avendaño R, Chaves N, Fuentes P, Sánchez E, Jiménez JI, Chavarría M. Production of selenium nanoparticles in *Pseudomonas putida* KT2440. Sci Rep. 2016;6:37155.

Ayano H, Miyake M, Terasawa K, Kuroda M, Soda S, Sakaguchi T, Ike M. Isolation of a selenite-reducing and cadmium-resistant bacterium *Pseudomonas sp*. strain RB for microbial synthesis of CdSe nanoparticles. J Biosci Bioeng. 2014;117(5):576–81.

Aziz N, Fatma T, Varma A, Prasad R. Biogenic synthesis of silver nanoparticles using *Scenedesmus abundans* and evaluation of their antibacterial activity. J Nanopart. 2014;2014:1–6.

Bajaj M, Schmidt S, Winter J. Formation of Se (0) nanoparticles by *Duganella sp.* and *Agrobacterium sp*. isolated from Se-laden soil of North-East Punjab, India. Microb Cell Factories. 2012;11(1):64.

Beheshti N, Soflaei S, Shakibaie M, Yazdi MH, Ghaffarifar F, Dalimi A, Shahverdi AR. Efficacy of biogenic selenium nanoparticles against *Leishmania major*: in vitro and in vivo studies. J Trace Elem Med Biol. 2013;27(3):203–7.

Benko I, Nagy G, Tanczos B, Ungvari E, Sztrik A, Eszenyi P, Prokisch J, Banfalvi G. Subacute toxicity of nano-selenium compared to other selenium species in mice. Environ Toxicol Chem. 2012;31(12):2812–20.

Biswas KC, Barton LL, Tsui WL, Shuman K, Gillespie J, Eze CS. A novel method for the measurement of elemental selenium produced by bacterial reduction of selenite. J Microbiol Methods. 2011;86(2):140–4.

Butler CS, Debieux CM, Dridge EJ, Splatt P, Wright M. Biomineralization of selenium by the selenate-respiring bacterium *Thauera selenatis*. Biochem Soc Trans. 2012;40(6):1239–43.

Chen T, Wong YS, Zheng W, Bai Y, Huang L. Selenium nanoparticles fabricated in *Undaria pinnatifida* polysaccharide solutions induce mitochondria-mediated apoptosis in A375 human melanoma cells. Colloids Surf B: Biointerfaces. 2008;67(1):26–31.

Dhanjal S, Cameotra SS. Aerobic biogenesis of selenium nanospheres by *Bacillus cereus* isolated from coalmine soil. Microb Cell Factories. 2010;9(1):52.

Dobias J, Suvorova EI, Bernier-Latmani R. Role of proteins in controlling selenium nanoparticle size. Nanotechnology. 2011;22(19):195605.

Domokos-Szabolcsy E, Marton L, Sztrik A, Babka B, Prokisch J, Fari M. Accumulation of red elemental selenium nanoparticles and their biological effects in *Nicotiana tabacum*. Plant Growth Regul. 2012;68(3):525–31.

Dungan RS, Yates SR, Frankenberger WT Jr. Transformations of selenate and selenite by *Stenotrophomonas maltophilia* isolated from a seleniferous agricultural drainage pond sediment. Environ Microbiol. 2003;5(4):287–95.

Dwivedi S, Alkhedhairy AA, Ahamed M, Musarrat J. Biomimetic synthesis of selenium nanospheres by bacterial strain JS-11 and its role as a biosensor for nanotoxicity assessment: a novel Se-bioassay. PLoS One. 2013;8(3):57404.

Fellowes JW, Pattrick RAD, Green DI, Dent A, Lloyd JR, Pearce CI. Use of biogenic and abiotic elemental selenium nanospheres to sequester elemental mercury released from mercury contaminated museum specimens. J Hazard Mater. 2011;189(3):660–9.

Filipe V, Hawe A, Jiskoot W. Critical evaluation of nanoparticle tracking analysis (NTA) by NanoSight for the measurement of nanoparticles and protein aggregates. Pharm Res. 2010;27(5):796–810.

Forootanfar H, Adeli-Sardou M, Nikkhoo M, Mehrabani M, Amir-Heidari B, Shahverdi AR, Shakibaie M. Antioxidant and cytotoxic effect of biologically synthesized selenium nanoparticles in comparison to selenium dioxide. J Trace Elem Med Biol. 2014a;28(1):75–9.

Forootanfar H, Zare B, Fasihi-Bam H, Amirpour-Rostami S, Ameri A, Shakibaie M, Torabi Nami M. Biosynthesis and characterization of selenium nanoparticles produced by terrestrial actinomycete *Streptomyces microflavus strain* FSHJ31. Res Rev J Microbiol Biotechnol. 2014b;3(1):47–53.

Garbisu C, Gonzalez S, Yang WH, Yee BC, Carlson DL, Yee A, Smith NR, Otero R, Buchanan BB, Leighton T. Physiological mechanisms regulating the conversion of selenite to elemental selenium by *Bacillus subtilis*. BioFactors (Oxford, England). 1995;5(1):29–37.

Garbisu C, Ishii T, Leighton T, Buchanan BB. Bacterial reduction of selenite to elemental selenium. Chem Geol. 1996;132(1–4):199–204.

Gharieb MM, Wilkinson SC, Gadd GM. Reduction of selenium oxyanions by unicellular, polymorphic and filamentous fungi: cellular location of reduced selenium and implications for tolerance. J Ind Microbiol. 1995;14(3–4):300–11.

Hariharan H, Al-Dhabi NA, Karuppiah P, Rajaram SK. Microbial synthesis of selenium nanocomposite using *Saccharomyces cerevisiae* and its antimicrobial activity against pathogens causing nosocomial infection. Chalcogenide Lett. 2012;9(12):509–15.

Hnain A, Brooks J, Lefebvre DD. The synthesis of elemental selenium particles by *Synechococcus leopoliensis*. Appl Microbiol Biotechnol. 2013;97(24):10511–9.

Hunter WJ, Kuykendall LD. Reduction of selenite to elemental red selenium by *Rhizobium sp.* strain B1. Curr Microbiol. 2007;55(4):344–9.

Husain S, Sardar M, Fatma T. Screening of cyanobacterial extracts for synthesis of silver nanoparticles. World J Microbiol Biotechnol. 2015;31(8):1279–83.

Husain S, Afreen S, Yasin D, Afzal B, Fatma T. Cyanobacteria as a bioreactor for synthesis of silver nanoparticles-an effect of different reaction conditions on the size of nanoparticles and their dye decolorization ability. J Microbiol Methods. 2019;162:77–82.

Jiang S, Ho CT, Lee JH, Van Duong H, Han S, Hur HG. Mercury capture into biogenic amorphous selenium nanospheres produced by mercury resistant *Shewanella putrefaciens 200*. Chemosphere. 2012;87(6):621–4.

Kaur G, Iqbal M, Bakshi MS. Biomineralization of fine selenium crystalline rods and amorphous spheres. J Phys Chem C. 2009;113(31):13670–6.

Kazempour ZB, Yazdi MH, Rafii F, Shahverdi AR. Sub-inhibitory concentration of biogenic selenium nanoparticles lacks post antifungal effect for *Aspergillus niger* and *Candida albicans* and stimulates the growth of *Aspergillus niger*. Iran J Microbiol. 2013;5(1):81.

Kessi J, Hanselmann KW. Similarities between the abiotic reduction of selenite with glutathione and the dissimilatory reaction mediated by *Rhodospirillum rubrum* and *Escherichia coli*. J Biol Chem. 2004;279(49):50662–9.

Kessi J, Ramuz M, Wehrli E, Spycher M, Bachofen R. Reduction of selenite and detoxification of elemental selenium by the phototrophic bacterium *Rhodospirillum rubrum*. Appl Environ Microbiol. 1999;65(11):4734–40.

Kokila K, Elavarasan N, Sujatha V. *Diospyros montana* leaf extract-mediated synthesis of selenium nanoparticles and their biological applications. New J Chem. 2017;41(15):7481–90.

Kumar HD, Prakash G. Toxicity of selenium to the blue-green algae, *Anacystis nidulans* and *Anabaena variabilis*. Ann Bot. 1971;35(3):697–705.

Lampis S, Zonaro E, Bertolini C, Bernardi P, Butler CS, Vallini G. Delayed formation of zero-valent selenium nanoparticles by *Bacillus mycoides* SeITE01 as a consequence of selenite reduction under aerobic conditions. Microb Cell Factories. 2014;13(1):35.

Lenz M, Van Aelst AC, Smit M, Corvini PFX, Lens PN. Biological production of selenium nanoparticles from waste waters. In: Advanced materials research, vol. 71: Trans Tech Publications; 2009. p. 721–4.

Lenz M, Kolvenbach B, Gygax B, Moes S, Corvini PF. Shedding light on selenium biomineralization: proteins associated with bionanominerals. Appl Environ Microbiol. 2011;77(13):4676–80.

Li S, Shen Y, Xie A, Yu X, Zhang X, Yang L, Li C. Rapid, room-temperature synthesis of amorphous selenium/

protein composites using *Capsicum annuum* L extract. Nanotechnology. 2007;18(40):405101.

Li DB, Cheng YY, Wu C, Li WW, Li N, Yang ZC, Tong ZH, Yu HQ. Selenite reduction by *Shewanella oneidensis* MR-1 is mediated by fumarate reductase in periplasm. Sci Rep. 2014;4:3735.

Lortie L, Gould WD, Rajan S, McCready RGL, Cheng KJ. Reduction of selenate and selenite to elemental selenium by a *Pseudomonas stutzeri* isolate. Appl Environ Microbiol. 1992;58(12):4042–4.

Losi ME, Frankenberger WT. Reduction of selenium oxyanions by *Enterobacter cloacae* SLD1a-1: isolation and growth of the bacterium and its expulsion of selenium particles. Appl Environ Microbiol. 1997;63(8):3079–84.

Ma J, Kobayashi DY, Yee N. Role of menaquinone biosynthesis genes in selenate reduction by *Enterobacter cloacae* SLD1a-1 and *Escherichia coli* K12. Environ Microbiol. 2009;11(1):149–58.

Mahmoudvand H, Harandi MF, Shakibaie M, Aflatoonian MR, ZiaAli N, Makki MS, Jahanbakhsh S. Scolicidal effects of biogenic selenium nanoparticles against protoscolices of hydatid cysts. Int J Surg. 2014;12(5):399–403.

Mata YN, Torres E, Blazquez ML, Ballester A, González FMJA, Munoz JA. Gold (III) biosorption and bioreduction with the brown alga *Fucus vesiculosus*. J Hazard Mater. 2009;166(2–3):612–8.

McCready RGL, Campbell JN, Payne JI. Selenite reduction by *Salmonella heidelberg*. Can J Microbiol. 1966;12(4):703–14.

Menon S, KS SD, Agarwal H, Shanmugam VK. Efficacy of biogenic Selenium nanoparticles from an extract of ginger towards evaluation on anti-microbial and anti-oxidant activities. Colloid Interf Sci Commun. 2019;29:1–8.

Nancharaiah YV, Lens PN. Selenium biomineralization for biotechnological applications. Trends Biotechnol. 2015;33(6):323–30.

Oremland RS, Herbel MJ, Blum JS, Langley S, Beveridge TJ, Ajayan PM, Sutto T, Ellis AV, Curran S. Structural and spectral features of selenium nanospheres produced by Se-respiring bacteria. Appl Environ Microbiol. 2004;70(1):52–60.

Parial D, Patra HK, Dasgupta AK, Pal R. Screening of different algae for green synthesis of gold nanoparticles. Eur J Phycol. 2012;47(1):22–9.

Pearce CI, Coker VS, Charnock JM, Pattrick RA, Mosselmans JFW, Law N, Beveridge TJ, Lloyd JR. Microbial manufacture of chalcogenide-based nanoparticles via the reduction of selenite using *Veillonella atypica*: an in situ EXAFS study. Nanotechnology. 2008;19(15):155603.

Prasad KS, Selvaraj K. Biogenic synthesis of selenium nanoparticles and their effect on As (III)-induced toxicity on human lymphocytes. Biol Trace Elem Res. 2014;157(3):275–83.

Prasad KS, Vyas P, Prajapati V, Patel P, Selvaraj K. Biomimetic synthesis of selenium nanoparticles using cell-free extract of *Microbacterium sp*. ARB05. Micro & Nano Lett. 2012;7(1):1–4.

Prasad KS, Patel H, Patel T, Patel K, Selvaraj K. Biosynthesis of Se nanoparticles and its effect on UV-induced DNA damage. Colloids Surf B: Biointerfaces. 2013;103:261–6.

Pronina NA, Kovshova YI, Popova VV, Lapin AB, Alekseeva SG, Baum RF, Mishina IM, Tsoglin LN. The effect of selenite ions on growth and selenium accumulation in *Spirulina platensis*. Russ J Plant Physiol. 2002;49(2):235–41.

Ramamurthy CH, Sampath KS, Arunkumar P, et al. Green synthesis and characterization of selenium nanoparticles and its augmented cytotoxicity with doxorubicin on cancer cells. Bioprocess Biosyst Eng. 2013;36(8):1131–9.

Sarkar J, Dey P, Saha S, Acharya K. Mycosynthesis of selenium nanoparticles. Micro & Nano Lett. 2011;6(8):599–602.

Shahverdi AR, Fakhimi A, Mosavat G, Jafari-Fesharaki P, Rezaie S, Rezayat SM. Antifungal activity of biogenic selenium nanoparticles. World Appl Sci J. 2010;10(8):918–22.

Shakibaie M, Khorramizadeh MR, Faramarzi MA, Sabzevari O, Shahverdi AR. Biosynthesis and recovery of selenium nanoparticles and the effects on matrix metalloproteinase-2 expression. Biotechnol Appl Biochem. 2010;56(1):7–15.

Sharma G, Sharma A, Bhavesh R, Park J, Ganbold B, Nam JS, Lee SS. Biomolecule-mediated synthesis of selenium nanoparticles using dried *Vitis vinifera* (raisin) extract. Molecules. 2014;19(3):2761–70.

Shoeibi S, Mashreghi M. Biosynthesis of selenium nanoparticles using *Enterococcus faecalis* and evaluation of their antibacterial activities. J Trace Elem Med Biol. 2017;39:135–9.

Sielicki M, Burnham JC. The effect of selenite on the physiological and morphological properties of the blue-green *alga Phormidium luridum var. olivacea 1*. J Phycol. 1973;9(4):509–14.

Singh R, Shedbalkar UU, Wadhwani SA, Chopade BA. Bacteriagenic silver nanoparticles: synthesis, mechanism, and applications. Appl Microbiol Biotechnol. 2015;99(11):4579–93.

Soflaei S, Dalimi A, Abdoli A, Kamali M, Nasiri V, Shakibaie M, Tat M. Anti-leishmanial activities of selenium nanoparticles and selenium dioxide on *Leishmania infantum*. Comp Clin Pathol. 2014;23(1):15–20.

Srivastava N, Mukhopadhyay M. Biosynthesis and structural characterization of selenium nanoparticles mediated by *Zooglea ramigera*. Powder Technol. 2013;244:26–9.

Srivastava N, Mukhopadhyay M. Biosynthesis and structural characterization of selenium nanoparticles using *Gliocladium roseum*. J Clust Sci. 2015;26(5):1473–82.

Torres SK, Campos VL, León CG, Rodríguez-Llamazares SM, Rojas SM, Gonzalez M, Smith C, Mondaca MA. Biosynthesis of selenium nanoparticles by

Pantoea agglomerans and their antioxidant activity. J Nanopart Res. 2012;14(11):1236.

Vetchinkina E, Loshchinina E, Kursky V, Nikitina V. Reduction of organic and inorganic selenium compounds by the edible medicinal basidiomycete *Lentinula edodes* and the accumulation of elemental selenium nanoparticles in its mycelium. J Microbiol. 2013;51(6):829–35.

Vijayan SR, Santhiyagu P, Singamuthu M, Kumari Ahila N, Jayaraman R, Ethiraj K. Synthesis and characterization of silver and gold nanoparticles using aqueous extract of seaweed, *Turbinaria conoides*, and their antimicrofouling activity. Sci World J. 2014;2014.

Wadhwani SA, Shedbalkar UU, Singh R, Chopade BA. Biogenic selenium nanoparticles: current status and future prospects. Appl Microbiol Biotechnol. 2016;100(6):2555–66.

Wadhwani SA, Gorain M, Banerjee P, Shedbalkar UU, Singh R, Kundu GC, Chopade BA. Green synthesis of selenium nanoparticles using *Acinetobacter sp.* SW30: optimization, characterization and its anticancer activity in breast cancer cells. Int J Nanomed. 2017;12:6841.

Wang T, Yang L, Zhang B, Liu J. Extracellular biosynthesis and transformation of selenium nanoparticles and application in H_2O_2 biosensor. Colloids Surf B: Biointerfaces. 2010;80(1):94–102.

Watts CA, Ridley H, Condie KL, Leaver JT, Richardson DJ, Butler CS. Selenate reduction by *Enterobacter cloacae* SLD1a^{-1} is catalysed by a molybdenum-dependent membrane-bound enzyme that is distinct from the membrane-bound nitrate reductase. FEMS Microbiol Lett. 2003;228(2):273–9.

Yang F, Tang Q, Zhong X, Bai Y, Chen T, Zhang Y, Li Y, Zheng W. Surface decoration by *Spirulina* polysaccharide enhances the cellular uptake and anticancer efficacy of selenium nanoparticles. Int J Nanomedicine. 2012;7:835.

Yazdi MH, Mahdavi M, Varastehmoradi B, Faramarzi MA, Shahverdi AR. The immunostimulatory effect of biogenic selenium nanoparticles on the 4T1 breast cancer model: an in vivo study. Biol Trace Elem Res. 2012;149(1):22–8.

Yazdi MH, Mahdavi M, Setayesh N, Esfandyar M, Shahverdi AR. Selenium nanoparticle-enriched *Lactobacillus brevis* causes more efficient immune responses in vivo and reduces the liver metastasis in metastatic form of mouse breast cancer. DARU J Pharm Sci. 2013;21(1):33.

Yee N, Ma J, Dalia A, Boonfueng T, Kobayashi DY. Se (VI) reduction and the precipitation of Se (0) by the facultative bacterium *Enterobacter cloacae* SLD1a^{-1} are regulated by FNR. Appl Environ Microbiol. 2007;73(6):1914–20.

Zare B, Babaie S, Setayesh N, Shahverdi AR. Isolation and characterization of a fungus for extracellular synthesis of small selenium nanoparticles. Nanomed J. 2013;1(1):13–9.

Zhang J, Wang H, Yan X, Zhang L. Comparison of short-term toxicity between Nano-Se and selenite in mice. Life Sci. 2005;76(10):1099–109.

Zhang W, Chen Z, Liu H, Zhang L, Gao P, Li D. Biosynthesis and structural characteristics of selenium nanoparticles by *Pseudomonas alcaliphila*. Colloids Surf B: Biointerfaces. 2011;88(1):196–201.

Zonaro E, Lampis S, Turner RJ, Qazi SJS, Vallini G. Biogenic selenium and tellurium nanoparticles synthesized by environmental microbial isolates efficaciously inhibit bacterial planktonic cultures and biofilms. Front Microbiol. 2015;6:584.

Part V

Quality Control for Nanoparticles

23

Practical Guidelines for the Characterization and Quality Control of Nanoparticles in the Pharmaceutical Industry

Fanny Varenne and Christine Vauthier

Abstract

Nanomaterials (NMs) are used in a wide range of applications bringing completely new properties to a material or considerable improving pristine material property. In the medical domain where they are named nanomedicines, their usefulness was found to resolve drug delivery challenges and to improve performances of imaging-based diagnostic methods. Some carry activity on their own giving birth to new types of medicines. Whatever the application of the nanomaterial is for, a quality assessment is needed to ensure the repeatability and efficiency of industrial processes and in turn activity and safety of the product. This chapter was aimed to discuss the characterization of physicochemical parameters that can be used to define a nanomaterial. It gives basis in metrology and explains how it can be used to develop validated procedures for the characterization of the main physicochemical parameters that define NMs including their transfer to be used in many laboratories. Examples discussed in the chapter include the measurement of the size of NMs, the evaluation of the size distribution and of the zeta potential. The development of validated procedures for the characterization of NMs is in its infant ages facing challenges that are discussed in this chapter.

Keywords

Characterization · Size · Zeta potential · Size distribution · Metrology

Abbreviations

ANOVA	Analysis of variance
AUC	Analytical ultracentrifugation
AFM	Atomic force microscopy
CD	Circular dichroism
CE	Capillary electrophoresis
CLS	Centrifugal liquid sedimentation
CRM	Certified reference material
DCS	Differential centrifugal sedimentation
DLS	Dynamic light scattering
DSC	Differential scanning calorimetry
ELS	Electrophoretic light scattering
EM	Electron microscopy

F. Varenne · C. Vauthier (✉)
University Paris-Saclay, UMR CNRS 8612, Institut Galien Paris-Saclay, Châtenay-Malabry, France
e-mail: christine.vauthier@universite-paris-saclay.fr

J. K. Patel, Y. V. Pathak (eds.), *Emerging Technologies for Nanoparticle Manufacturing*,
https://doi.org/10.1007/978-3-030-50703-9_23

ES-DMA	Electrospray-differential mobility analysis
FFF	Field flow fractionation
GE	Gel electrophoresis
GUM	Guide to the expression of uncertainty in measurement
HDC	Hydrodynamic chromatography
ICH	International Conference on Harmonisation of Technical Requirements for Registration of Pharmaceuticals for Human Use
IR	Infrared spectroscopy
ISO	International Organization for Standardization
ITC	Isothermal titration calorimetry
MS	Mass spectrometry
NIST	National Institute of Standards and Technology
NM(s)	Nanomaterial(s)
NMR	Nuclear magnetic resonance
NP(s)	Nanoparticle(s)
NTA	Nanoparticle tracking analysis
PALS	Phase analysis light scattering
PSD	Particle size distribution
RM	Reference material
SAXS	Small-angle X-ray scattering
SEC	Size exclusion chromatography
SEM	Scanning electron microscopy
SLS	Static light scattering
sp-ICP-MS	Single particle inductively coupled plasma-mass spectrometry
TEM	Transmission electron microscopy
TRPS	Tunable resistive pulse sensing
XPS	X-ray photoelectron spectroscopy
XRD	X-ray diffraction
ZP	Zeta potential

1 Introduction

Over the last decades, nanomaterials (NMs) have become extremely popular thanks to unique properties that can be exploited in different fields such as energy (Ravi and Vadukumpully 2016; Dessie et al. 2019), transportation (Jung et al. 2005; Ali et al. 2018), industry (Khalil et al. 2017; Jørgensen 2009), food (Dubascoux and Wyser 2019), cosmetics (Katz et al. 2015), and medicine (Han et al. 2019; Abd Elkodous et al. 2019). They can occur with different structures and be composed of various matter such as metals, that is, titanium oxide, gold, silver, platinum, and ferric oxides, polymers, lipids, carbons including carbon nanotubes, graphene derivatives, nanodiamonds, and fullerenes.

Many NMs have found interest in medical applications. Pharmaceuticals and medical devices based on the use of these technologies were called nanomedicines. They include various types of nano-objects which vary in their structure and composition. It was a rapidly growing field over the past two decades but several aspects on their definition remain under debate. There is a need to clarify the classification of the different types of nanomedicines occurring with complex structures (Castagnola et al. 2017). Regarding the size, the definition given for a NM proposed by authorities in early 2010 is too narrow to include all types of nanomedicines as it excludes many nanomedicines whose size is larger (200–300 nm) than the upper limit given in the official definition based on at least one dimension lower than 100 nm for 50% of the number size distribution of NMs. Nevertheless, a consensus is established on the need to provide with relevant quality control procedures to assess product quality insuring repeatability and reproducibility of the safety and efficacy on a batch-to-batch basis. This can be achieved performing the characterization of NMs by the use of validated procedures under conditions compatible with quality control (Varenne et al. 2015a, b; Loeschner et al. 2015; Linsinger et al. 2013; Dudkiewicz et al. 2015; Braun et al. 2011a) or methods whose performances have been proven by interlaboratory comparisons (Linsinger et al. 2014; Weigel et al. 2017; Lamberty et al. 2011) thus ensuring reliable results. The reliability of measurements can be ensured by defining a series of handling precautions and quality criteria for good measurements (Varenne et al. 2015a, b, c, d). The selection of

relevant methods to characterize properties of NMs should be performed by comparing available methods to provide reliable measurements (Varenne et al. 2016a; Till et al. 2016; Teulon et al. 2018; Sokolova et al. 2011; Grombe et al. 2014; Cascio et al. 2014; Anderson et al. 2013; Sikora et al. 2015; Borchert et al. 2005; Aichele et al. 2015). It is noteworthy that the characterization of physicochemical parameters of NMs in general remains a difficult task even for parameters including the size of the nano-object and the distribution of size, the surface charge using automatic measurement instruments. Most characterization methods of NMs require a preparation of the sample that will be used to perform measurements with the specifically designed method. This can include a dilution of the sample or the realization of a dry depot on a substrate. Whatever the modalities for the preparation of the sample, efforts are needed to ensure that measurements will be representative of the original dispersions of NMs (Varenne et al. 2015a, b, c, d; Ghomrasni et al. 2020; Wagner et al. 2015; Delvallée et al. 2015). This chapter aims to give some practical guidelines to characterize nanomedicine-based pharmaceuticals in the quality control assessment perspective.

2 Characterization of Materials

The characterization of NMs under conditions compatible with quality control is a societal task. NMs are characterized by two different types of parameters. For instance, the composition, the concentration, the structure, and the surface functionalization of the NMs are general parameters which are not restricted to NMs, although methods for the determination of the concentration are very specific. Specific characteristics of NMs include their size parameters, giving the size, the particle size distribution (PSD), and the agglomeration or aggregation state, their surface properties as surface charge through the evaluation of the zeta potential (ZP), reactive surface, surface area and porosity, and their shape (Hassellöv and Kaegi 2009; Guidance manual for the testing of manufactured nanomaterials 2010). These characteristics should be characterized as suggested by the technical committee of International Organization for Standardization (ISO TC 229 – Nanotechnologies) and the OECD Working Party on Manufactured Nanomaterials. Modifications of size parameters and surface properties of nanomedicines can affect their biological fate hence biological efficacy and safety (Shekunov et al. 2007; Gaumet et al. 2008). Size parameters and surface properties of NMs are among paramount factors to evaluate in order to assess repeatability and reproducibility and efficiency of industrial processes and product quality (Li 2010). Table 23.1 summarizes the different methods that are available to assess specific physicochemical parameters of NMs. It points out direct and indirect methods and those that can be applied in routine analysis. Table 23.2 overviews the general physicochemical parameters that are used to describe the properties of NMs. It highlights the methods that can be applied to assess these general parameters. It is noteworthy that the evaluation of the concentration of NMs can be performed using the methods specific to the NMs. The application of any mentioned method of characterization in quality control analysis needs to be validated according to general procedures used in metrology in order to provide uncertainties associated to the measurement of the physicochemical parameter of NMs using a given method and applying a specific measurement procedure.

3 General Consideration to Achieve Quality Control Analysis and Metrology: Validation and Transfer of Analytical Procedures

The characterization of NMs is necessary to describe the properties of the NMs composing nanomedicines thus achieving safety-efficiency

Table 23.1 Specific physicochemical parameters used to describe properties of NMs (Hassellöv and Kaegi 2009; Linsinger et al. 2012)

Physicochemical parameter	Definition	Method	Measurand
Size, PSD, and agglomeration or aggregation state	***Size***: Physical dimensions of NM evaluated with specific size measurement method with given experimental conditions.	***Batch***	
		Acoustic techniques (Aichele et al. 2015; Dukhin 2020)	Volume-based diameter and PSD
		DLS (Varenne et al. 2015b, 2016a, b; Sokolova et al. 2011; Cascio et al. 2014; Anderson et al. 2013 Ruseva et al. 2018)[b]	Hydrodynamic diameter/Scattering intensity-based PSD
		SLS (Varenne et al. 2016a; Kaasalainen et al. 2017)	Gyration diameter (Rayleigh)/Scattering intensity-based PSD
		SAXS (Borchert et al. 2005; Geertsen et al. 2018; Agbabiaka et al. 2019; Sakurai 2017)	Gyration diameter (Guiner)/Scattering intensity-based PSD
		XRD (Borchert et al. 2005)	Scherrer's diameter/No PSD
	PSD: Proportion of distinct populations with different NM sizes of a given dispersion of NMs.	***Single***	
		– ***Direct method***	
		EM (Varenne et al. 2016a; Sokolova et al. 2011; Anderson et al. 2013; Borchert et al. 2005)	Equivalent spherical diameter or Feret's diameter/Number-based PSD
		AFM (Varenne et al. 2016a; Couteau and Roebben 2011)	Height or diameter from analysis of images in (x-y) dimension/Number-based PSD
	Agglomeration: NMs bounded by weak interaction as Van der Waals force and electrostatic interactions (ISO/TS 27687 2008).	– ***Indirect method***	
		NTA (Varenne et al. 2016a; Sokolova et al. 2011; Anderson et al. 2013)	Hydrodynamic diameter/Number-based PSD
		TRPS (Varenne et al. 2016a; Anderson et al. 2013; Vogel et al. 2016)	Raw diameter/Number-based PSD
		sp-ICP-MS (Geertsen et al. 2018; Montoro Bustos et al. 2018)	Height of intensity of detected pulse/Mass-based PSD
		ES-DMA (Lenggoro et al. 2002; Elzey et al. 2013)	Mobility diameter/Number-based PSD
	Aggregation: NMs bounded by interaction with higher intensity such as covalent binding (ISO/TS 27687 2008).	***Separative***	
		AUC (Mehn et al. 2017; Planken and Cölfen 2010)	Sedimentation diameter/Density-based PSD
		CE (Chang et al. 2008; d'Orlyé et al. 2008a, b)	Apparent mobility (or electrophoretic mobility)/PSD depending on detector used
		DCS (known as CLS) (Cascio et al. 2014; Anderson et al. 2013)	Sedimentation diameter/Extinction intensity-based PSD
		FFF (Varenne et al. 2016a; Cascio et al. 2014; Wagner et al. 2015; Caputo et al. 2019)	Retention time/PSD depending on detector used
		HDC (Williams et al. 2002)	Retention time/PSD depending on detector used
		SEC (Ingebrigtsen and Brandl 2002)	Retention time/PSD depending on detector used

Surface charge	***Evaluation of ZP***: Charged NMs are surrounded by electrical double layer formed with opposite charged ions (Stern layer with strongly bound ions) and diffuse layer with weakly bound ions) in ionic dispersant. Ions from diffuse layer are sharing from ions of bulk dispersant with movement of NM. The potential on shear surface corresponds to ZP (Bhattacharjee 2016).	***Batch***	
		ELS (Varenne et al. 2015a, 2019a) [b]	Electrophoretic mobility
		Acoustic techniques (Dukhin and Parlia 2014; O'Brien et al. 1995)	Electrophoretic mobility
		Indirect single method	
		NTA (Sikora et al. 2015; Wilson and Green 2017)	Electrophoretic mobility
		TRPS (Sikora et al. 2015, 2016; Vogel et al. 2017)	Electrophoretic mobility
		Separative	
		CE (Ramírez-García et al. 2017a; Ohshima 2001; Oukacine et al. 2011)	Electrophoretic mobility
Reactive surface	Surface of NMs available to interact with different mediums such as biological medium, i.e., with biomolecules.	CE (Ramírez-García et al. 2017b; Coty et al. 2018; Oszwałdowski et al. 2010)	Apparent mobility (or electrophoretic mobility) or area
		DLS (Goy-López et al. 2012; Piella et al. 2017)	Hydrodynamic diameter
		ES-DMA (Pease et al. 2007; Tsai et al. 2011)	Mobility diameter
		GE (Coty et al. 2016)[b]	Degree of complement pathway
		ITC (Mandal et al. 2013; Atri et al. 2015; Winzen et al. 2015)[b]	Released or absorbed heat from binding event providing thermodynamic parameters
Surface area and porosity	Developed surface of NMs including surface area of open pores.	Brunauer, Emmett, and Teller method (Zhou et al. 2019)[b]	Adsorption of gas molecules as N_2 on surface of NMs (adsorption isotherm)
Shape[a]	Geometrical description of NMs.	***Direct method***	
		EM	Aspect ratio described with dimensionless terms such as elongation ratio, flatness ratio, sphericity, circularity, and rugosity
		AFM	
		Indirect method	
		AUC (Urban et al. 2016)	Shape factor
		SAXS (Sakurai 2017)	Shape form factor

AFM Atomic force microscopy, *AUC* Analytical ultracentrifugation, *CE* capillary electrophoresis, *CLS* Centrifugal liquid sedimentation, *DCS* Differential centrifugal sedimentation, *DLS* Dynamic light scattering, *ELS* Electrophoretic light scattering, *EM* Electron microscopy, *ES-DMA* Electrospray-differential mobility analysis, *FFF* Field flow fractionation, *GE* Gel electrophoresis, *HDC* Hydrodynamic chromatography, *ITC* Isothermal titration calorimetry, *NM(s)* Nanomaterial(s), *NTA* Nanoparticle tracking analysis, *PSD* Particle size distribution, *SAXS* Small-angle X-ray scattering, *SEC* Size exclusion chromatography, *SLS* Static light scattering, *sp-ICP-MS* Single particle inductively coupled plasma-mass spectrometry, *TRPS* Tunable resistive pulse sensing, *XRD* X-ray diffraction, *ZP* Zeta potential

[a]Evaluation of agglomeration or aggregation state of NMs can be performed with methodologies applied to determine the shape of NMs

[b]Used in routine

Table 23.2 General parameters used to describe properties of NMs

Physicochemical parameter	Definition	Method
Concentration	Number of NMs per volume unit	ES-DMA, NTA, TRPS, sp-ICP-MS
Composition	Chemical and molecular structure of NMs	MS, NMR, sp-ICP-MS
Structure	Structure state	IR, CD, DSC, NMR, SAXS, XRD
Surface functionalization	Chemical and molecular structure at the surface of NMs	IR, XPS

CD circular dichroism, *DSC* Differential scanning calorimetry, *ES-DMA* Electrospray-differential mobility analysis, *IR* Infrared spectroscopy, *MS* Mass spectrometry, *NM(s)* Nanomaterial(s), *NMR* Nuclear magnetic resonance, *NTA* Nanoparticle tracking analysis, *SAXS* Small-angle X-ray scattering, *sp-ICP-MS* Single particle inductively coupled plasma-mass spectrometry, *TRPS* Tunable resistive pulse sensing, *XPS* X-ray photoelectron spectroscopy, *XRD* X-ray diffraction

and batch-to-batch consistency. In practice, very few methods are available to achieve the characterization of nanomedicines on a routine basis considerably limiting the number of parameters that can be included in quality control assessment. It is noteworthy that almost all methods are indirect methods, which means that the parameter measured by the instrument is then used to calculate the property desired to determine. Models developed to convert the measure into the measurand can be quite complexed, restricting the application of the technique to the characterization of a narrow range of NMs. Standardization of size measurement methods is paramount to provide results that are comparable between laboratories. For instance, the widely used method for size determination by dynamic light scattering (DLS) can be applied on spherical NMs with a narrow size distribution. Results are biased while the polydispersity increases, and the method is inappropriate to characterize the size of non-spherical particles. Measurements should be performed under conditions compatible with quality control that requires the use of standardized procedures. The procedures should be validated and uncertainties should be evaluated with a reference NM close to that which will be analyzed. Moreover, instruments must be qualified using appropriate reference NMs including materials from National Institute of Standards and Technology (NIST) when available. In the quality control assessment procedure for the analysis of a NM, the reference NMs should be analyzed before and after the analysis of "unknown" NMs by the same validated measurement procedure.

The evaluation of physicochemical properties of NMs should be performed under conditions which are compatible with quality control to provide reliable characterization. Reliability of results can be appreciated with associated measurement uncertainty determined through the validation of analytical procedures. The validation of analytical procedures consists in providing guarantees with certified reference material (CRM) or reference material (RM) that analytical procedures are sufficiently acceptable, reliable, and adequate for elements of their scope (ICH 1994; ISO 5725-1 1994; Ahuja and Scypinski 2001). Moreover, laboratories should prove that their analysts are able to perform analytical procedures with similar results (Ahuja and Scypinski 2001; Code of Federal Regulations; USP 37, General Information 1224). Hence, there is a need to provide guidelines to ensure quality control and thereby to evaluate the safety and toxicity of NMs. Draft guidance documents are provided for manufactured NMs, indicating various methods that can be applied to evaluate these parameters (Guidance manual for the testing of manufactured nanomaterials 2010; ISO/TS 80004-6 2013). Nevertheless, no indication is given to validate and transfer analytical procedures applied to the characterization of NMs and to provide uncertainty closed to results (Guidance manual for the testing of manufactured nanomaterials 2010).

Although many parameters can be used to define one NM, only a few are really accessible for a routine analysis using marketed instruments or having been the subject of standards from International Organization for Standardization (ISO) description as size (ISO 13318-3 2004; ISO 13318-2 2007; ISO 13318-1 2001; ISO

22412 2017; ISO/TS 21362 2018; ISO 13321 1996; ISO 29301 2017; ISO/DIS 21363; ISO/DIS 19749; ISO 13322-1 2014; ISO/TS 13762 2001; ISO 11039 2012; ISO 27911 2011; ISO 20998-1 2006; ISO 20998-2 2013; ISO 20998-3 2017; ISO/DIS 15900), surface charge (ISO 13099-3 2012; ISO 13099-2 2012; ISO 13099-1 2012), shape (ISO/DIS 21363; ISO/DIS 19749; ISO/TS 10797 2012), surface area (ISO 18852 2012; ISO 18757 2003), and reactive surface (ISO/AWI TS 23459).

3.1 Validation and Transfer of Analytical Procedures

Whatever the type of analysis, it follows a well-established analytical procedure describing in detail all steps needed to carry out a given analysis. All analytical procedures will follow a life cycle which includes a validation stage and a transfer stage as illustrated in Fig. 23.1. The validation is achieved applying strict metrology concepts which aim to prove that the analytical procedure is sufficiently acceptable, reliable, and adequate for the elements of its scope (ICH 1994; ISO 5725-1 1994; Ahuja and Scypinski 2001). The validation is generally achieved using CRM or RM. It consists of performing numerous measurements of these materials following the described procedure. The results are then analyzed with appropriate statistical analytical methods. The guide to the expression of uncertainty in measurement (GUM) outlines statistical

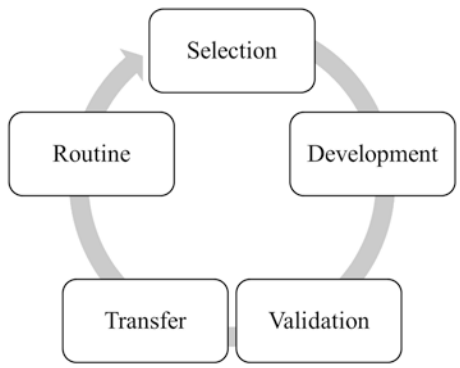

Fig. 23.1 Life cycle of analytical procedure

methodologies to interpret raw data of validation as analysis of variance (ANOVA) (Evaluation of measurement data – guide to the expression of uncertainty in measurement 2008). The different parameters evaluating performances of analytical procedures were summarized in Table 23.3. The validation of analytical procedure permits to assess to the associated expanded uncertainty expressing reliability of results provided with validated analytical procedure (Evaluation of measurement data - guide to the expression of uncertainty in measurement. 2008). CRM is a material that is metrologically characterized with valid procedure for one or more specified properties (ISO Guide 35 2006). Analysis certificate providing value of specified property with corresponding uncertainty and metrological traceability is produced with CRM. RM is a homogeneous and stable material toward one or more specified properties (ISO Guide 35 2006). It is adequate for its used in process of measurement of specified property. When it is possible, it is important to validate the analytical procedure with a material certified for the analytical method that will be used. The number of CRM and RM available to validate methods of characterization of NMs is limited. Size CRM generally consists in monodispersed NMs. Only one consists in bimodal dispersion of silica nanoparticles (NPs) certified at 18.2 and 84 nm with electron microscopy (EM) (ERM-FD102). There is only one available CRM with assigned SI-traceable values of positive electrophoretic mobility (NIST Standard Reference Material® 1980, value: 2.53 ± 0.12 $\mu m.cm.V^{-1}.s^{-1}$). It is noteworthy that there is another CRM with a negative value of ZP (ERM-FD100, value: 43.0 ± 21.8 mV (Braun et al. 2011b)). However, the uncertainty of the certified value of ZP of this standard is about 50% of the certified value. Other CRMs are currently under development (Levin et al. 2018). Polystyrene latex particles–based standard is commercially available but it is not a CRM (DTS1235 from Malvern, value: 42.0 ± 4.2 mV).

Besides having appropriate CRM or RM, validation also needs to investigate adequate parameters. No official specific guidelines were yet established to perform the validation of a

Table 23.3 Overview of parameters used to describe the performance of analytical procedures (ICH 1994; ISO 5725-1 1994; Ahuja and Scypinski 2001)

Parameter	Definition
Specificity	Ability of analytical procedure to perform unambiguously analysis of substance in the presence of impurities, degradation products, or matrix.
Linearity	Ability of analytical procedure to provide results directly proportional to the concentration of substance in samples for a given range of concentrations.
Trueness	Difference between the average value provided by a large series of test results and the accepted value, i.e., conventional true value or accepted reference value highlighted systematic errors (bias).
Precision	Degree of dispersion of a series of test results provided with multiple sampling of same homogeneous sample carried out under stipulated experimental conditions pointed random errors. Three distinguished levels: *Repeatability (or intra-assay precision):* repetition performed with same experimental conditions including method, instrument, laboratory, and analyst over a short period of time, i.e., same day. *Intermediate precision (or within laboratories variations):* repetition carried out by varying factors as day, analyst, or equipment within the same laboratory. *Reproducibility (or inter-laboratories variations):* repetition performed in different laboratories.
Range	Interval whose boundaries are defined by lowest and highest concentrations of substance and for which appropriate level of trueness, precision, and linearity of analytical procedure have been proved.
Detection limit	Lowest quantity of substance that can be detected but not necessarily quantified as exact value.
Quantification limit	Lowest quantity of substance that can be quantified with acceptable trueness and precision.
Robustness	Ability of analytical procedure to remain non-affected by small deliberate variations in experimental conditions.
System suitability testing	Developed tests to control equipment, electronics, stability of sample, or analytical operations.

measurement procedure characterizing NMs. The guidelines Q2(R1) from International Conference on Harmonisation of Technical Requirements for Registration of Pharmaceuticals for Human Use (ICH guidelines Q2(R1)) was established only for the validation of most common types of analytical procedures including identification tests, quantitative tests for impurities' content, limit tests for the control of impurities, and quantitative tests of the active moiety in samples of drug substance or drug product or other selected components in the drug product (ICH 1994). Other types of analytical procedures such as dissolution testing of drug products and the evaluation of particle size of drug substance have not been addressed in this document. This guideline mentioned that the validation of these analytical procedures is equally important to those listed herein and may be considered in subsequent documents. Although this guideline did not provide any specific information on how validation of NM characterization procedures should be carried out, concepts to achieve such validations can be drawn from it. The selection of studied parameters should be adapted on a case-by-case basis.

Other official documents propose some lines to perform validation of measurement procedures applicable to the characterization of NMs. Standards from ISO suggest to study trueness and precision, that is, repeatability and intermediate precision of procedures used to evaluate the ZP of NMs with ELS coupled to phase analysis light scattering (PALS) (ISO 13099-2 2012) and precision, that is, repeatability and reproducibility of procedures applied to evaluate the size of NMs by DLS (ISO 22412 2017). However, no indication about the number of samples needed to study each parameter and statistical methodologies to interpret raw data was given in ISO standards (ISO 22412 2017; ISO 13099-2 2012). The Nanomedicine Characterization Laboratory

(Frederick, MD, USA) proposes standardized procedures to evaluate the size of NMs with DLS (Hackley and Clogston 2007), atomic force microscopy (AFM) (Grobelny et al. 2009), transmission electron microscopy (TEM) (Bonevich and Haller 2010), scanning electron microscopy (SEM) (Vladár and Ming 2011), and electrospray-differential mobility analysis (ES-DMA) (Pease III et al. 2010) or to evaluate ZP (Clogston 2009). It was reported that procedures used for evaluating the size of NMs by DLS (Hackley and Clogston 2007) and procedures applied to size evaluation of NMs with SEM (Vladár and Ming 2011) should be validated. Last decade, Shekunov et al. and Gaumet et al. were the first to carry out reflexion about the reliability of results for NM characterization through size measurement with acceptable trueness (Shekunov et al. 2007; Gaumet et al. 2008).

A measurement procedure validated in one laboratory can be transferred to other laboratories through a transfer approach. The aim is to demonstrate that the procedure validated by the sending laboratory can be applied in the other laboratories, named receiving laboratories, with the same performances. It must prove that receiving laboratories are able to carry out analytical procedure by providing similar results as the sending laboratory (Ahuja and Scypinski 2001; Code of Federal Regulations; USP 37, General Information 1224). Approaches that can be used to achieve the transfer of an analytical procedure are described by the Food and Drug Administration (FDA) (Ahuja and Scypinski 2001) and the USP Pharmacopeia (USP 37, General Information 1224). They are also described in the *Handbook of Modern Pharmaceutical Analysis* (Ahuja and Scypinski 2001). The different approaches that can be included in a transfer of analytical procedure are summarized in Table 23.4. Their selection to achieve the transfer of a given analytical procedure depends on risk assessment, complexity, criticality, and the aim of the analytical procedure. In general, during the analytical stage, each laboratory including the sending laboratory and all receiving laboratories analyze the same batch of samples. Data obtained from the different laboratories are compared and confronted to acceptance criteria that are defined depending on the method. It is noteworthy that no specific information is provided to perform the transfer of physicochemical characterization procedures of NMs. The selection of a suitable approach to transfer such a procedure should be adapted on a case-to-case basis.

Table 23.4 Overview of approaches used for the transfer of analytical procedures (Ahuja and Scypinski 2001; Code of Federal Regulations; USP 37, General Information 1224)

Approach	Definition
Comparative testing	Analysis of defined number of samples from the same batch performed by sending and receiving laboratories.
Interlaboratory covalidation	Participation of receiving laboratories in part of process of validation of the analytical procedure such as precision study, i.e., investigation of reproducibility.
Revalidation	Partial or complete validation of analytical procedure by the receiving laboratories. *Used when variations in analytical procedure are provided or no suitable samples are available.*
Verification	Demonstration of performance of receiving laboratories by comparison between results obtained by the receiving laboratories and certified results provided with certificate of CRM or by the sending laboratory or by checking conformance of results provided by receiving laboratories with respect of performance criteria.
Application	Demonstration of performance of receiving laboratories by application according to control test procedure by checking the conformance of results provided by receiving laboratories with respect to performance criteria defined in test procedure.
Transfer waiver	The receiving laboratories are considered to be able to perform the analytical procedure without investigation of their performance.

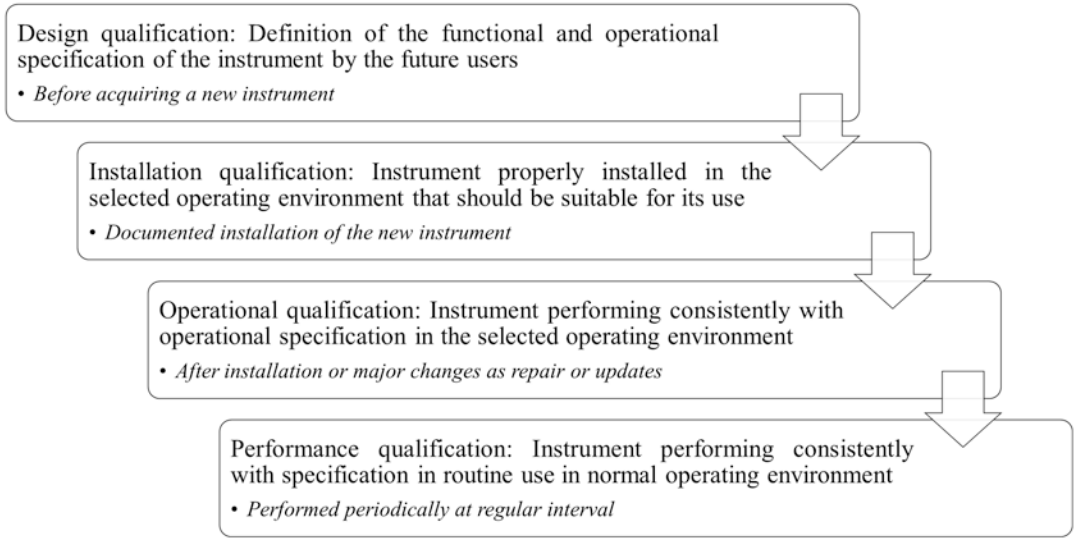

Fig. 23.2 Stages of qualification of an instrument

3.2 Qualification of Instrument

The qualification of an instrument is achieved to provide documented evidence that the instrument performs with specification. According to the ISO standard and the Good Manufacturing Practices, the instruments should be calibrated or checked by appropriate methods with suitable control samples as traceably calibrated materials at defined periods (ISO 9001 2008; Good manufacturing practices). There are different stages of qualification covering the life of an instrument from its design to its utilization in routine (Fig. 23.2).

This aspect was introduced in the ISO standard devoted to the measurement of size of NMs by DLS (ISO 22412 2017). The ISO standard mentions that the qualification of the instrument should be performed after installation (operational qualification) and at regular time intervals (performance qualification) with a dispersion of materials with certified size. CRM with values assigned for DLS using the same algorithm to determine the size of the CRM should be used to carry out the qualification of the instrument. It is mentioned that the chemistry and the morphology of the NMs constituting the CRM should match the test samples as closely as possible. It is noteworthy that, alternatively, certified dispersions of polystyrene latex with narrow size distribution with average particle diameter as evaluated by DLS or EM can be used for the qualification of instrument. The qualification of the instrument can be evaluated either from five repeat measurements of size of CRM by comparing the difference between the measured average and the certified values and the expanded uncertainty closed to the measured average value (Linsinger 2005) or from three repeat measurements of size of CRM carried out before and after the measurement of the size of unknown NMs; the size of the CRM should be within the range of size determined during the validation of the procedure used to evaluate the size of unknown NMs (Varenne et al. 2015b, 2016b). If the qualification fails, it can indicate a mistake in the preparation of the dispersion or the instability of the dispersion or the failure of the instrument.

4 Validation of Procedures Evaluating Physicochemical

Parameters of NMs: Examples

4.1 Size Measurement by Dynamic Light Scattering

DLS is a major technique used to measure the size of NMs. This method is very popular thanks to the existence of easy to use affordable marketed measurement instruments. DLS was also implemented to achieve continuous measurements using a glass capillary mounted in classical laboratory instrument (Ruseva et al. 2018). Results provided with this method are reliable considering NMs of homogenously distributed size have a narrow size distribution (Varenne et al. 2015b, 2016b). However, this technique should be applied with caution when characterizing the size of unknown NMs as bias on measurements can be introduced in the case of non-homogenous in size dispersions or of dispersions showing a wide or complex polydispersity (Varenne et al. 2016a; Sokolova et al. 2011; Cascio et al. 2014; Anderson et al. 2013; Langevin et al. 2018a; Elizalde et al. 2000).

Very few works have reported size results with associated measurement uncertainty ensuring reliable characterization of size of NMs by DLS (Varenne et al. 2015b, 2016b, 2019b; Braun et al. 2011a). The preparation of the sample to perform size measurement by DLS is particularly a critical step (Varenne et al. 2015b, d, 2016b; Braun et al. 2011a; Langevin et al. 2018a, b). The presence of dust may compromise the size measurement of NMs. It is necessary to prepare diluted samples of NMs with freshly filtered dispersants with 0.22 µm filter and flasks with caps should be pre-rinsed with filtered ultrapure water and stored in a dust-free environment. Bias can be introduced with the quality of measurement macrocuvettes. Cuvettes showing defects on the optical faces must be discarded while they can represent 85% of the units in a box depending on suppliers and quality. The measurement cuvettes should be cleaned with filtered ultrapure water and stored in a dust-free environment until use. The measurement cuvettes should be used only once to avoid cross-contamination. The volume of sample introduced in the macrocuvette should be sufficient to permit the passage of the laser into the sample. The larger the volume is, the longer the equilibration time is to let the sample reach the temperature of measurement. Indeed, the temperature of the sample during measurement is paramount to control to provide with reliable size results as the measured parameter is the diffusion coefficient from which the size is calculated using the Stokes and Einstein equation. Artifacts due to degassing of the samples may be created with high difference between the temperature of the sample and the temperature of measurement. The equilibration time should be long enough for the sample to achieve the temperature of measurement. A minimum of 1 min per degree of difference should be considered for a volume sample of approximately 1 mL. Optimal concentration of the dispersions of NMs to carry out size measurement should be optimized for the intensity of the signal to be within the range recommended by the supplier of the instrument used. For this purpose, the curve representing the intensity of the signal as a function of the concentration of NMs should be established and the optimal concentration is selected on the linear part of this curve (Cao 2003).

Some quality criteria should be defined and followed to ensure reliable results (Varenne et al. 2015b, d). For size measurement by DLS, the quality of the correlogram reflecting the probability to find the NMs at the same place after a few times and the count rate curve corresponding to the number of photons collected by the detector associated to each run during measurements can be followed during the size measurement. After measurement, the raw correlogram, the intercept describing the amplitude of the correlogram that is close to the signal-to-noise ratio, the mean count rate, and the cumulant fit error can be inspected. The cumulant fit error is the closeness of agreement between the experimental raw correlogram and the calculated correlogram by means of the cumulant method described in the ISO standard (ISO 22412 2017).

It is noteworthy that an ISO standard dealing with good practice for DLS measurements is under development (ISO/PRF TR 22814).

The selection of the CRM or RM is crucial. NIST Traceable Particle Size Standards consisting in polystyrene latex standard with SI-traceable certified values by TEM can be used to validate the developed procedures. These CRM are spherical NPs known to not swell in aqueous dispersions and appeared quite monodisperse as acknowledged by the low PDI (PDI < 0.05) and available from 50 to 900 nm. These CRMs should be diluted in NaCl 10 mM for suppressing the electrical double layer and ensuring that the measured hydrodynamic diameter was the same as expected by TEM as described in the ISO standard (ISO 13321 1996). Other CRM with traceable mean diameter of 20, 30, and 40 nm by DLS are available.

The developed procedures should be validated by studying robustness, precision, that is, repeatability and intermediate precision, and trueness to evaluate the expanded uncertainties of the procedures. The robustness is investigated by varying experimental parameters that may influence measurements of size of NMs permitting to provide indication on the reliability under normal conditions of use of the proposed procedures. This study is a preliminary step before transferring methods to other laboratories or performing collaborative studies. The repeatability is performed by measuring the size of the CRM carried out successively in the same day and the intermediate precision by measuring the size of the CRM performed in different days. In the experimental nested design proposed by Varenne et al., to investigate the precision of the procedure, three samples of diluted CRM at optimal concentration were analyzed per day (Varenne et al. 2015b). Each sample was analyzed in triplicate, that is, three successive size measurements were performed on each sample. This experimental nested design permits to investigate the influence of the factors days, samples, and replicates that are considered as random (Fig. 23.3). The raw data were interpreted by means of ANOVA permitting to investigate the variability between days, between samples variability analyzed on the same day (within days), and between replicates variability of a sample (within samples). Appropriate statistical models were developed to interpret the raw

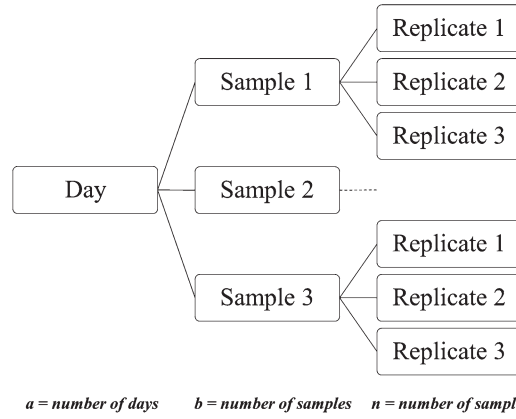

Fig. 23.3 Experimental nested design to investigate the precision of procedure. The factors days, samples, and replicates are studied and the symbols a, b, and n correspond to the number of levels of a nested factor within the factor above ranked

data. According to the ISO standard (ISO 22412 2017), the relative uncertainties of repeatability and reproducibility should be below 2% and 5%, respectively. This ISO standard mentions any information about the evaluation of intermediate precision to evaluate the influence of factors as the instrument and/or the analyst or over a longer period of time (i.e., typically on different days) (ISO 22412 2017). It is suggested to investigate the trueness of the developed procedure. However, no limit was provided for the relative uncertainty of trueness (ISO 22412 2017). According to the literature, the limits of the relative uncertainties of intermediate precision and trueness may be set at 5% and 10% for intermediate precision and trueness, respectively.

Qualified size measurements should be provided to characterize unknown NMs by DLS under quality control conditions. The procedure proposed by Varenne et al. included (1) the control of the absorption spectrum of NMs for ensuring that no absorption band appears at the wavelength of the laser source of the measurement instrument, (2) the evaluation of the optimal concentration of the dispersions of NMs, and (3) the measure of the size of unknown dispersions of NMs at the determined optimal concentration under operational or performance qualification of the instrument (Varenne et al. 2015b, 2016b). It

means that the size of CRM whose size and nature is close to the size of the investigated NMs should be measured before and after the evaluation of the size of investigated NMs permitting to evaluate the size of monodispersed NMs under conditions compatible with quality control assessments.

Validated size measurement procedures using DLS proposed by Varenne et al. were suitable to measure the size of a wide range of NMs including polymer NPs, liposomes, and inorganic NPs as silica NPs (Varenne et al. 2015b, 2016b). However, it was found unsuitable to evaluate the size of NPs having a high density such as anastase TiO_2 and magnetic NPs whose sizes are in the upper limit of the measurement instrument (Varenne et al. 2019b).

4.2 Evaluation of the Particle Size Distribution

Evaluating the PSD of a dispersion of NMs is a difficult issue. Several size measurement methods present major inherent limitations that hamper reliable determination of the PSD of NM dispersions that have a wide or complex PSD. Besides, there is only one multimodal CRM (ERM-FD102) including silica particles of two sizes, 18.2 and 84 nm certified by EM. However, this CRM is not certified to be used for the determination of PSD. Without an appropriate reference dispersion of NMs, the performance of a method applied to measure PSD cannot be evaluated. No official procedure has been proposed to characterize the PSD of NMs. The scientific community recommended to apply two methods at least based on two different physical principles. One of the methods should be based on a direct size measurement method including image analysis of particles obtained from AFM, SEM, or TEM or it should include a separative size stage combined with batch size measurement method as detector (Varenne et al. 2016a; Caputo et al. 2019; Rice et al. 2013).

It is noteworthy that the DLS method needs to be used with caution while applied to characterize size and PSD of unknown NMs although this technique is widely used in routine. The intensity of the scattered light is proportional to the power six of the radius of NMs. Thus, the intensity of the scattered light due to the large NMs can cover the signal produced by the smaller NMs of the dispersion. Important bias was reported with this method when it is applied for the determination of the size and PSD of NMs having a wide or complex size distribution although it is reliable while applied to the characterization of NMs having a narrow size distribution (Varenne et al. 2016a; Marucco et al. 2019).

Direct size measurement methods include EM and AFM (Varenne et al. 2016a; Rice et al. 2013; Song et al. 2009). The size of the NMs is measured directly from images obtained for the NMs. The preparation of samples for observations by EM and AFM consists in the spreading of the NMs on a sample holding (Ghomrasni et al. 2020; Delvallée et al. 2015). This preparation is critical for the quality of the subsequent image analysis process used to determine PSD and may require that a specific procedure may be developed for each NM (Varenne et al. 2020). NMs of the dispersion must be randomly distributed on the surface of the sample holder (carbon grid or mica substrate). It is also preferable that NMs will be well individualized to avoid distortions due to the proximity of neighbor NMs (Fig 23.4a) and to facilitate image processing measurements. It may be difficult to obtain a random deposition of NMs on sample holder from a dispersion of NMs having a high PSD as a segregation according to the NM size may occur as illustrated in the Fig.23.4b. For this reason, it is recommended to evaluate the PSD performing orthogonal measurements with different methods (Varenne et al. 2016a; Sokolova et al. 2011; Cascio et al. 2014; Anderson et al. 2013; Caputo et al. 2019; Ingebrigtsen and Brandl 2002).

To evaluate PSD from direct methods, size measurements must be performed on a sufficiently large number of NMs. The debate around the number of NMs that should be considered remains open. The ISO standard suggests that the size of one thousand individual NMs should be measured that seems not always possible to achieve due to sample preparation constrains

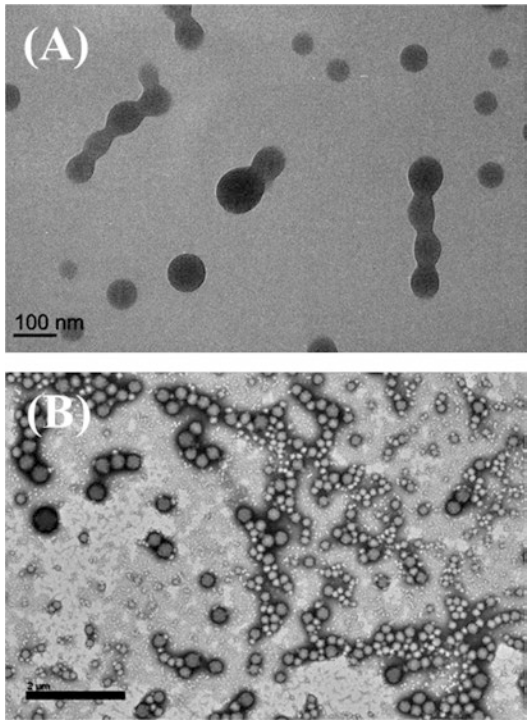

Fig. 23.4 Electron micrograph of unstained poly(isobutyl cyanoacrylate) NPs deposited on a formvar-carbon coated cupper grid for EM. (**a**) Projected image of single particles appeared circular suggesting that the particles were spherical. In contrast, particles included in agglomerates appeared distorted due to the close contact with their neighbors. Scale bar: 100 nm. (**b**) Segregation according to particle size occurred during sample preparation of a highly polydisperse dispersion of the NPs. Scale bare: 2 µm. Evaluation of shape, size, and PSD by EM requires that NPs will be well individualized on the sample holder and randomly distributed over the surface of the sample holder

(ISO 13322-1 2004). A much lower number of NMs was considered in different works. Song *et al.* studied the PSD of a dispersion of synthetic gold NPs consisting in one population of size with a polydisperse distribution and showed that the PSD provided by counting a few hundred NPs was similar to the one produced by the analysis of one thousand NPs (Song et al. 2009). Varenne *et al.* investigated the PSD of a multimodal dispersion of polymer NPs from the "real-life" obtaining similar PSD from three independent evaluations performed by measuring samples including around three hundred NPs (Varenne et al. 2020). A number of at least five hundred NPs was considered in an interlaboratory comparison of the evaluation of the PSD of NPs performed by TEM indicating a good performance of the method considering this number of NPs (Rice et al. 2013). Rice *et al.* have found that the best model to use to interpret raw data evaluating the PSD was the lognormal reference model as it provided with the lower relative standard errors (RSEs) compared with other size distribution reference models tested in their work while determining the PSD of their NM (Rice et al. 2013).

4.3 Evaluation of Zeta Potential Using Electrophoresis Light Scattering

Reliable evaluation of ZP of NMs by electrophoretic light scattering (ELS) also requires the validation of measurement procedures. An ISO standard gives guidelines for good practices in the evaluation of ZP (ISO/TR 19997 2018). Another ISO standard indicates the thresholds for the relative standard uncertainties of repeatability, intermediate precision, and trueness that should be used for the validation of procedures to evaluate ZP (ISO 13099-2 2012).

A similar strategy than that applied to validate the procedure of size measurements may be applied (Varenne et al. 2015a, c, 2019a, b). In short, as for size measurements performed by DLS, the preparation of samples to evaluate ZP by ELS is a key step (Varenne et al. 2015a, c, 2019a, b). The presence of dust in samples can be avoided preparing dilutions with fresh filter dispersants with 0.22 µm filter just before use. All flasks with caps devoted to the preparation of dispersant and samples are needed to be pre-cleaned with filtered ultrapure water and stored in a dust-free environment. Selection of high-quality measurement cell is needed as optical defects including scratches and/or apparent impurities in the polycarbonate faces may interfere with optical measurements. Beside cell cleanliness appearance, electrodes should be homogenous and well attached on both the inside and outside of the cell measurement to insure a homogeneous electric field. The cells including caps should be

rinsed with appropriate filtered solvent and stored in a dust-free environment before using. The cells should be used only once to prevent cross-contamination. The temperature of the sample is a critical parameter. Large differences between the temperature of the sample and the temperature of measurement may generate artefacts during measurements due to the degassing of the samples.

Optimal concentration of the dispersions of NMs to evaluate ZP should be evaluated using methods based on the equilibrium dilution procedure mentioned in the ISO standard (ISO 13099-1 2012). This procedure consists in maintaining the composition and the concentration of dispersant identical between diluted samples.

The quality of data may be appreciated by means of defined quality criteria achieved during measurement and on the raw data (Varenne et al. 2015a, c). For example, the phase plot showing phase difference between the measured frequency and the reference frequency as a function of time and the count rate curve giving the number of photons detected by the photomultiplier associated to each run can be inspected during measurement. The final phase plot, the frequency plot corresponding to the Fourier Transform analysis of the slow field reversal part of the analysis used to evaluate ZP distribution and the mean count rate, can be controlled on the raw data.

Experimental measurement procedures established to evaluate the ZP of an NM must be validated using reference NMs. Only two were developed so far. One CRM is available with assigned SI-traceable values of positive electrophoretic mobility (NIST Standard Reference Material® 1980). It is noteworthy that this CRM tends to adsorb on the intern surface of measurement cells made of polycarbonate (Varenne et al. 2015a). For this reason, measurement cells should be preconditioned with the dilute dispersions of NMs before introducing fresh samples and carrying out the analysis as explained in the notice of use. To validate procedures for NMs with a negative ZP, it necessary to use one negative ZP RM classified as a transfer standard. This type of standard has been referenced to an accepted standard by the scientific community as there is no CRM with acceptable uncertainty of the certified value of ZP (Braun et al. 2011b).

The procedures should be validated by investigating robustness, precision, that is, repeatability and intermediate precision, and trueness to determine the expanded uncertainties of the procedures. The same experimental design than the one presented in Fig. 23.2 may be used to investigate the precision of the developed procedures. The repeatability can be determined with successive evaluation of ZP of the RM on the same day while the intermediate precision can be assessed by carrying out the evaluation of ZP of the RM for various days. The ISO standard gives thresholds for the relative standard uncertainties of repeatability, intermediate precision, and trueness (10%, 15%, and 10%, respectively) (ISO 13099-2 2012).

Qualified evaluation of ZP can be performed following the same procedure than the one described for the measurement of size of NMs. According to the mode used to perform the evaluation of ZP, the proposed procedures by Varenne et al. can be applied to the characterization of NMs including polymer NPs and liposomes, but were not appropriate to evaluate the ZP of dense NPs such as titanium dioxide NPs (Varenne et al. 2015a, 2019a, b). In any case, the evaluation of ZP of an NM is not trivial as many parameters can influence the final results (Skoglund et al. 2017). A series of advices on how to interpret and report measurements of ZP was proposed based on the evaluation of the ZP of metal NPs dispersed in complex media of relevance for studies on nanotoxicology and environmental interactions (Skoglund et al. 2017).

4.4 Transfer

Once validated in one laboratory, it has to be demonstrated that the validated procedure can be applied in other laboratories with the same performances. A transfer of the procedure is needed to prove that the results of measurements are similar in all laboratories. Such transfer was achieved for very few procedures applied to the characterization of NMs (Weigel et al. 2017;

Langevin et al. 2018a, b; Varenne et al. 2017; Franks et al. 2019). For instance, procedures to characterize size and ZP of NMs by DLS and ELS, respectively, were transferred from one sending laboratory to other laboratories (Varenne et al. 2017). Two situations were considered. In the first case, the sending and receiving laboratories were equipped with the same measurement instrument (same wavelength of the laser source). A comparative test performed on the same batch of CRM or RM was proposed to show that performances of the receiving laboratories were similar to those of the sending laboratory taking into account handling precautions, crucial factor highlighted by the validation carried out by the sending laboratory and measurement quality criteria. In the second case, the sending and receiving laboratories were not equipped with the same instrument (different wavelength of the laser source). It was then suggested to perform a partial validation to prove the ability of receiving laboratories to perform the procedures. This partial validation was based on the study of the precision, that is, repeatability and intermediate precision, and the trueness to assess the expanded uncertainties of the procedure. To achieve the transfer of a procedure, it is important that all partners carry on measurements of the same batch of CRM or RM. Results of measurements obtained by the different laboratories are compared using statistical analytical methods. A development of appropriate methods was proposed in the work of Varenne et al. based on the β-expectation tolerance interval method and ANOVA (Varenne et al. 2017).

5 Conclusion

Main issues found for the characterization of NMs were considered in the present chapter. It discussed the validation of analytical procedures based on metrology approaches to be applied to assess the quality analysis of NMs. The reflexion associated basis in metrology and their application to the method of characterization of the main physicochemical parameters that are used to define NMs. This analysis pointed out the urgent need to standardize, validate, and transfer analytical procedures applied to characterize NMs. This is paramount to ensure the reliability of results obtained from the quality assessment of NMs which, in turn, is needed to ensure their safety providing proof of the repeatability and efficiency of industrial processes producing NM-based products. Today, physicochemical characterization of NMs associated with metrology remains a challenge for future development in all application fields. Quality assessment of NMs is still in its infant age. Efforts are on the way to provide with more official guidelines to perform validation and transfer of measurement procedures and develop appropriate RM including CRM. Besides, several validated measurement procedures and results from interlaboratory measurement comparisons were published in the literature that can now serve as basis to go further setting up quality control procedures for NMs.

References

Abd Elkodous M, El-Sayyad GS, Abdelrahman IY, El-Bastawisy HS, Mohamed AE, Mosallam FM, Nasser HA, Gobara M, Baraka A, Elsayed MA, et al. Therapeutic and diagnostic potential of nanomaterials for enhanced biomedical applications. Colloids Surf B Biointerfaces. 2019;180:411–28. https://doi.org/10.1016/j.colsurfb.2019.05.008.

Agbabiaka A, Wiltfong M, Park C. Small angle X-ray scattering technique for the particle size distribution of nonporous nanoparticles. https://new.hindawi.com/journals/jnp/2013/640436/. Accessed 27 Dec 2019. https://doi.org/10.1155/2013/640436.

Ahuja S, Scypinski S. Handbook of modern pharmaceutical analysis: Elsevier; 2001.

Aichele CP, Venkataramani D, Smay JE, McCann MH, Richter S, Khanzadeh-Moradllo M, Aboustait M, Ley MT. A comparison of automated scanning electron microscopy (ASEM) and acoustic attenuation spectroscopy (AAS) instruments for particle sizing. Colloids Surf A Physicochem Eng Aspects. 2015;479:46–51. https://doi.org/10.1016/j.colsurfa.2015.03.052.

Ali MKA, Fuming P, Younus HA, Abdelkareem MAA, Essa FA, Elagouz A, Xianjun H. Fuel economy in gasoline engines using Al_2O_3/TiO_2 nanomaterials as nanolubricant additives. Appl Energy. 2018;211:461–78. https://doi.org/10.1016/j.apenergy.2017.11.013.

Anderson W, Kozak D, Coleman VA, Jämting ÅK, Trau M. A comparative study of submicron particle sizing platforms: accuracy, precision and resolution analysis

of polydisperse particle size distributions. J Colloid Interf Sci. 2013;405:322–30. https://doi.org/10.1016/j.jcis.2013.02.030.

Atri MS, Saboury AA, Ahmad F. Biological applications of isothermal titration calorimetry. Phys Chem Res. 2015;3(4):319–30. https://doi.org/10.22036/pcr.2015.11066.

Bhattacharjee S. DLS and zeta potential – what they are and what they are not? J Control Release. 2016;235:337–51. https://doi.org/10.1016/j.jconrel.2016.06.017.

Bonevich JE; Haller WK. NIST – NCL joint assay protocol, PCC-7, measuring the size of nanoparticles using transmission electron microscopy (TEM). 2010.

Borchert H, Shevchenko EV, Robert A, Mekis I, Kornowski A, Grübel G, Weller H. Determination of nanocrystal sizes: a comparison of TEM, SAXS, and XRD studies of highly monodisperse CoPt3 particles. Langmuir. 2005;21(5):1931–6. https://doi.org/10.1021/la0477183.

Braun A, Couteau O, Franks K, Kestens V, Roebben G, Lamberty A, Linsinger TPJ. Validation of dynamic light scattering and centrifugal liquid sedimentation methods for nanoparticle characterisation. Adv Powder Technol. 2011a;22(6):766–70. https://doi.org/10.1016/j.apt.2010.11.001.

Braun A, Franks K, Kestens V, Roebben G, Lamberty A, Linsinger TPJ. Certification of equivalent spherical diameters of silica nanoparticles in water – certified reference material ERM®-FD100. March 22, 2011b.

Cao A. Light scattering. Recent applications. Anal Lett. 2003;36(15):3185–225. https://doi.org/10.1081/AL-120026567.

Caputo F, Arnould A, Bacia M, Ling WL, Rustique E, Texier I, Mello AP, Couffin A-C. Measuring particle size distribution by asymmetric flow field flow fractionation: a powerful method for the preclinical characterization of lipid-based nanoparticles. Mol Pharm. 2019;16(2):756–67. https://doi.org/10.1021/acs.molpharmaceut.8b01033.

Cascio C, Gilliland D, Rossi F, Calzolai L, Contado C. Critical experimental evaluation of key methods to detect, size and quantify nanoparticulate silver. Anal Chem. 2014;86(24):12143–51. https://doi.org/10.1021/ac503307r.

Castagnola V, Cookman J, de Araújo JM, Polo E, Cai Q, Silveira CP, Krpetić Ž, Yan Y, Boselli L, Dawson KA. Towards a classification strategy for complex nanostructures. Nanoscale Horiz. 2017;2(4):187–98. https://doi.org/10.1039/C6NH00219F.

Chang T-H, Liu F-K, Chang Y-C, Chu T-C. Rapidly characterizing the growth of Au nanoparticles by CE. Chromatographia. 2008;67(9):723–30. https://doi.org/10.1365/s10337-008-0594-6.

Clogston JD. NCL method PCC-2, measuring zeta potential of nanoparticles. 2009.

Code of Federal Regulations, U.S. Food and Administration, 21CFR §211.194.

Coty J-B, Varenne F, Vachon J-J, Vauthier C. Serial multiple crossed immunoelectrophoresis at a microscale: a stamp-sized 2D immunoanalysis of protein C3 activation caused by nanoparticles. Electrophoresis. 2016;37(17–18):2401–9. https://doi.org/10.1002/elps.201500572.

Coty J-B, Varenne F, Benmalek A, Garsaa O, Le Potier I, Taverna M, Smadja C, Vauthier C. Characterization of nanomedicines' surface coverage using molecular probes and capillary electrophoresis. Eur J Pharma Biopharma. 2018;130:48–58. https://doi.org/10.1016/j.ejpb.2018.06.014.

Couteau O, Roebben G. Measurement of the size of spherical nanoparticles by means of atomic force microscopy. Meas Sci Technol. 2011;22(6):065101. https://doi.org/10.1088/0957-0233/22/6/065101.

d'Orlyé F, Varenne A, Gareil P. Size-based characterization of nanometric cationic maghemite particles using capillary zone electrophoresis. Electrophoresis. 2008a;29(18):3768–78. https://doi.org/10.1002/elps.200800123.

d'Orlyé F, Varenne A, Gareil P. Determination of nanoparticle diffusion coefficients by Taylor dispersion analysis using a capillary electrophoresis instrument. J Chromatogr A. 2008b;1204(2):226–32. https://doi.org/10.1016/j.chroma.2008.08.008.

Delvallée A, Feltin N, Ducourtieux S, Trabelsi M, Hochepied JF. Direct comparison of AFM and SEM measurements on the same set of nanoparticles. Meas Sci Technol. 2015;26(8):085601. https://doi.org/10.1088/0957-0233/26/8/085601.

Dessie Y, Tadesse S, Eswaramoorthy R, Abebe B. Recent developments in manganese oxide based nanomaterials with oxygen reduction reaction functionalities for energy conversion and storage applications: a review. J Sci Adv Mater Dev. 2019;4(3):353–69. https://doi.org/10.1016/j.jsamd.2019.07.001.

Dubascoux S, Wyser Y. Nanomaterials in food: an overview; 2019. p. 110–7.

Dudkiewicz A, Boxall ABA, Chaudhry Q, Mølhave K, Tiede K, Hofmann P, Linsinger TPJ. Uncertainties of size measurements in electron microscopy characterization of nanomaterials in foods. Food Chem. 2015;176:472–9. https://doi.org/10.1016/j.foodchem.2014.12.071.

Dukhin AS. Chapter 3.2.4 – Acoustic spectroscopy for particle size measurement of concentrated nanodispersions. In: Hodoroaba V-D, Unger WES, Shard AG, editors. Characterization of nanoparticles, Micro and nano technologies: Elsevier; 2020. p. 197–211. https://doi.org/10.1016/B978-0-12-814182-3.00013-4.

Dukhin AS, Parlia S. Measuring zeta potential of protein nano-particles using electroacoustics. Colloids Surf B Biointerfaces. 2014;121:257–63. https://doi.org/10.1016/j.colsurfb.2014.02.048.

Elizalde O, Leal GP, Leiza JR. Particle size distribution measurements of polymeric dispersions: a comparative study. Particle Particle Syst Charact. 2000;17(5–6):236–43. https://doi.org/10.1002/1521-4117(200012)17:5/6<236::AID-PPSC236>3.0.CO;2-0.

Elzey S, Tsai D-H, Yu LL, Winchester MR, Kelley ME, Hackley VA. Real-time size discrimination and elemental analysis of gold nanoparticles using

ES-DMA coupled to ICP-MS. Anal Bioanal Chem. 2013;405(7):2279–88. https://doi.org/10.1007/s00216-012-6617-z.

Evaluation of measurement data – guide to the expression of uncertainty in measurement. JCGM:2008 GUM 1995 with minor corrections 100AD.

Franks K, Kestens V, Braun A, Roebben G, Linsinger TPJ. Non-equivalence of different evaluation algorithms to derive mean particle size from dynamic light scattering data. J Nanopart Res. 2019;21(9):195. https://doi.org/10.1007/s11051-019-4630-2.

Gaumet M, Vargas A, Gurny R, Delie F. Nanoparticles for drug delivery: the need for precision in reporting particle size parameters. Eur J Pharma Biopharma. 2008;69(1):1–9. https://doi.org/10.1016/j.ejpb.2007.08.001.

Geertsen V, Barruet E, Gobeaux F, Lacour J-L, Taché O. Contribution to accurate spherical gold nanoparticle size determination by single-particle inductively coupled mass spectrometry: a comparison with small-angle X-ray scattering. Anal Chem. 2018;90(16):9742–50. https://doi.org/10.1021/acs.analchem.8b01167.

Ghomrasni NB, Chivas-Joly C, Devoille L, Hochepied J-F, Feltin N. Challenges in sample preparation for measuring nanoparticles size by scanning electron microscopy from suspensions, powder form and complex media. Powder Technol. 2020;359:226–37. https://doi.org/10.1016/j.powtec.2019.10.022.

Good manufacturing practices, qualification and validation.

Goy-López S, Juárez J, Alatorre-Meda M, Casals E, Puntes VF, Taboada P, Mosquera V. Physicochemical characteristics of protein–NP bioconjugates: the role of particle curvature and solution conditions on human serum albumin conformation and fibrillogenesis inhibition. Langmuir. 2012;28(24):9113–26. https://doi.org/10.1021/la300402w.

Grobelny J, DelRio FW, Pradeep N, Kim D-I, Hackley VAH, Cook RF. NIST – NCL Joint assay protocol, PCC-6, size measurement of nanoparticles using atomic force. Microscopy. 2009;

Grombe R, Charoud-Got J, Emteborg H, Linsinger TPJ, Seghers J, Wagner S, von der Kammer F, Hofmann T, Dudkiewicz A, Llinas M, et al. Production of reference materials for the detection and size determination of silica nanoparticles in tomato soup. Anal Bioanal Chem. 2014;406(16):3895–907. https://doi.org/10.1007/s00216-013-7554-1.

Guidance manual for the testing of manufactured nanomaterials: OECD's Sponsorship Programme; First Revision. 2010.

Hackley VA, Clogston JD. NIST-NCL joint assay protocol, PCC-1 Version 1.2, measuring the size of nanoparticles in aqueous media using batch-mode dynamic light scattering. 2007.

Han HJ, Ekweremadu C, Patel N. Advanced drug delivery system with nanomaterials for personalised medicine to treat breast cancer. J Drug Deliv Sci Technol. 2019;52:1051–60. https://doi.org/10.1016/j.jddst.2019.05.024.

Hassellöv M, Kaegi R. Analysis and characterization of manufactured nanoparticles in aquatic environments. 2009; https://doi.org/10.1002/9781444307504.ch6.

ICH harmonized tripartite guideline, validation of analytical procedures: text and methodology Q2(R1). 1994.

Ingebrigtsen L, Brandl M. Determination of the size distribution of liposomes by SEC fractionation, and PCS analysis and enzymatic assay of lipid content. AAPS PharmSciTech. 2002;3(2):9–15. https://doi.org/10.1208/pt030207.

ISO 11039:2012: Surface chemical analysis – scanning-probe microscopy – measurement of drift rate.

ISO 13099-1:2012(E): Colloidal systems – methods for zeta-potential determination – part 1: electroacoustic and electrokinetic phenomena.

ISO 13099-2:2012(E): Colloidal systems – methods for zeta-potential determination – part 2: optical methods.

ISO 13099-3:2012(E): Colloidal systems – methods for zeta-potential determination – part 3: acoustic methods.

ISO 13318-1:2001: Determination of particle size distribution by centrifugal liquid sedimentation methods – part 1: general principles and guidelines.

ISO 13318-2:2007: Determination of particle size distribution by centrifugal liquid sedimentation methods – part 2: photocentrifuge method.

ISO 13318-3:2004: Determination of particle size distribution by centrifugal liquid sedimentation methods – part 3: centrifugal x-ray method.

ISO 13321:1996(E). Particle size analysis – photon correlation spectroscopy.

ISO 13322-1:2004: Particle size analysis – image analysis methods – part 1: static image analysis methods.

ISO 13322-1:2014: Particle size analysis – image analysis methods – part 1: static image analysis methods.

ISO 18757:2003: Fine ceramics (advanced ceramics, advanced technical ceramics) – determination of specific surface area of ceramic powders by gas adsorption using the BET method.

ISO 18852:2012: Rubber compounding ingredients – determination of multipoint nitrogen surface area (NSA) and statistical thickness surface area (STSA).

ISO 20998-1:2006: Measurement and characterization of particles by acoustic methods – part 1: concepts and procedures in ultrasonic attenuation spectroscopy.

ISO 20998-2:2013: Measurement and characterization of particles by acoustic methods – part 2: guidelines for linear theory.

ISO 20998-3:2017: Measurement and characterization of particles by acoustic methods – part 3: guidelines for non-linear theory.

ISO 22412:2017: Particle size analysis – dynamic light scattering (DLS).

ISO 27911:2011: Surface chemical analysis – scanning-probe microscopy – definition and calibration of the lateral resolution of a near-field optical microscope.

ISO 29301:2017 Microbeam analysis – analytical electron microscopy – methods for calibrating image magnification by using reference materials with periodic structures.
ISO 5725-1:1994: Accuracy (trueness and precision) of measurement methods and results – part 1: general principles and definitions.
ISO 9001:2008: Quality management systems – requirements.
ISO Guide 35:2006: Reference materials – general and statistical principles for certification.
ISO/AWI TS 23459: Nanotechnologies – assessment of protein secondary structure following an interaction with nanomaterials using circular dichroism spectroscopy.
ISO/DIS 15900: Determination of particle size distribution – differential electrical mobility analysis for aerosol particles.
ISO/DIS 19749: Nanotechnologies – measurements of particle size and shape distributions by scanning electron microscopy.
ISO/DIS 21363: Nanotechnologies - Measurements of Particle Size and Shape Distributions by Transmission Electron Microscopy.
ISO/PRF TR 22814: Good practice for dynamic light scattering (DLS) measurements.
ISO/TR 19997:2018: Guidelines for good practices in zeta-potential measurement.
ISO/TS 10797:2012 Nanotechnologies – characterization of single-wall carbon nanotubes using transmission electron microscopy.
ISO/TS 13762:2001: Particle size analysis – small angle x-ray scattering method.
ISO/TS 21362:2018: Nanotechnologies – analysis of nano-objects using asymmetrical-flow and centrifugal field-flow fractionation.
ISO/TS 27687:2008: Nanotechnologies – terminology and definitions for nano-objects – nanoparticle, nanofibre and nanoplate.
ISO/TS 80004-6:2013: Nanotechnologies – vocabulary – part 6: nano-object characterization.
Jørgensen B. Gas-phase oxidation of aqueous ethanol by nanoparticle vanadia/anatase catalysts. Top Catal. 2009;52(3):253–7. https://doi.org/10.1007/s11244-008-9161-5.
Jung H, Kittelson DB, Zachariah MR. The influence of a cerium additive on ultrafine diesel particle emissions and kinetics of oxidation. Combust Flame. 2005;142(3):276–88. https://doi.org/10.1016/j.combustflame.2004.11.015.
Kaasalainen M, Aseyev V, von Haartman E, Karaman DŞ, Mäkilä E, Tenhu H, Rosenholm J, Salonen J. Size, stability, and porosity of mesoporous nanoparticles characterized with light scattering. Nanoscale Res Lett. 2017;12(1):74. https://doi.org/10.1186/s11671-017-1853-y.
Katz LM, Dewan K, Bronaugh RL. Nanotechnology in cosmetics. Food Chem Toxicol. 2015;85:127–37. https://doi.org/10.1016/j.fct.2015.06.020.
Khalil M, Jan BM, Tong CW, Berawi MA. Advanced nanomaterials in oil and gas industry: design, application and challenges. Appl Energy. 2017;191:287–310. https://doi.org/10.1016/j.apenergy.2017.01.074.
Lamberty A, Franks K, Braun A, Kestens V, Roebben G, Linsinger TPJ. Interlaboratory comparison for the measurement of particle size and zeta potential of silica nanoparticles in an aqueous suspension. J Nanopart Res. 2011;13(12):7317–29. https://doi.org/10.1007/s11051-011-0624-4.
Langevin D, Raspaud E, Mariot S, Knyazev A, Stocco A, Salonen A, Luch A, Haase A, Trouiller B, Relier C, et al. Towards reproducible measurement of nanoparticle size using dynamic light scattering: important controls and considerations. NanoImpact. 2018a;10:161–7. https://doi.org/10.1016/j.impact.2018.04.002.
Langevin D, Lozano O, Salvati A, Kestens V, Monopoli M, Raspaud E, Mariot S, Salonen A, Thomas S, Driessen M, et al. Inter-laboratory comparison of nanoparticle size measurements using dynamic light scattering and differential centrifugal sedimentation. NanoImpact. 2018b;10:97–107. https://doi.org/10.1016/j.impact.2017.12.004.
Lenggoro IW, Xia B, Okuyama K, de la Mora JF. Sizing of colloidal nanoparticles by electrospray and differential mobility analyzer methods. Langmuir. 2002;18(12):4584–91. https://doi.org/10.1021/la015667t.
Levin AD, Alenichev MK, Masalov VM, Sukhinina NS, Emelchenko GA. Developing of standard reference materials of the electrokinetic (zeta) potential of nanoparticles. Nanotechnol Russia. 2018;13(1):90–5. https://doi.org/10.1134/S1995078018010068.
Li C. Structure controlling and process scale-up in the fabrication of nanomaterials. Front Chem Eng China. 2010;4(1):18–25. https://doi.org/10.1007/s11705-009-0305-3.
Linsinger TPJ ERM application note 1: comparison of a measurement result with the certified value. 2005.
Linsinger TPJ, Roebben G, Gilliland D, Calzolai L, Rossi F, Gibson N, Klein C. Requirements on measurements for the implementation of the European Commission definition of the term "Nanomaterial." JRC Reference Reports 2012.
Linsinger TPJ, Chaudhry Q, Dehalu V, Delahaut P, Dudkiewicz A, Grombe R, von der Kammer F, Larsen EH, Legros S, Loeschner K, et al. Validation of methods for the detection and quantification of engineered nanoparticles in food. Food Chem. 2013;138(2):1959–66. https://doi.org/10.1016/j.foodchem.2012.11.074.
Linsinger TPJ, Peters R, Weigel S. International interlaboratory study for sizing and quantification of ag nanoparticles in food simulants by single-particle ICPMS. Anal Bioanal Chem. 2014;406(16):3835–43. https://doi.org/10.1007/s00216-013-7559-9.
Loeschner K, Navratilova J, Grombe R, Linsinger TPJ, Købler C, Mølhave K, Larsen EH. In-house validation of a method for determination of silver nanoparticles in chicken meat based on asymmetric flow field-flow fractionation and inductively coupled plasma mass

spectrometric detection. Food Chem. 2015;181:78–84. https://doi.org/10.1016/j.foodchem.2015.02.033.

Mandal S, Hossain M, Devi PS, Kumar GS, Chaudhuri K. Interaction of carbon nanoparticles to serum albumin: elucidation of the extent of perturbation of serum albumin conformations and thermodynamical parameters. J Hazard Mater. 2013;248–249:238–45. https://doi.org/10.1016/j.jhazmat.2013.01.009.

Marucco A, Aldieri E, Leinardi R, Bergamaschi E, Riganti C, Fenoglio I. Applicability and limitations in the characterization of poly-dispersed engineered nanomaterials in cell media by dynamic light scattering (DLS). Materials (Basel). 2019;12(23) https://doi.org/10.3390/ma12233833.

Mehn D, Iavicoli P, Cabaleiro N, Borgos SE, Caputo F, Geiss O, Calzolai L, Rossi F, Gilliland D. Analytical ultracentrifugation for analysis of doxorubicin loaded liposomes. Int J Pharm. 2017;523(1):320–6. https://doi.org/10.1016/j.ijpharm.2017.03.046.

Montoro Bustos AR, Purushotham KP, Possolo A, Farkas N, Vladár AE, Murphy KE, Winchester MR. Validation of single particle ICP-MS for routine measurements of nanoparticle size and number size distribution. Anal Chem. 2018;90(24):14376–86. https://doi.org/10.1021/acs.analchem.8b03871.

O'Brien RW, Cannon DW, Rowlands WN. Electroacoustic determination of particle size and zeta potential. J Colloid Interf Sci. 1995;173(2):406–18. https://doi.org/10.1006/jcis.1995.1341.

Ohshima H. Approximate analytic expression for the electrophoretic mobility of a spherical colloidal particle. J Colloid Interf Sci. 2001;239(2):587–90. https://doi.org/10.1006/jcis.2001.7608.

Oszwałdowski S, Zawistowska K, Grigsby LK, Roberts KP. Capillary electrophoretic separation and characterizations of CdSe quantum dots. Cent Eur J Chem. 2010;8(4):806–19. https://doi.org/10.2478/s11532-010-0052-9.

Oukacine F, Morel A, Cottet H. Characterization of carboxylated nanolatexes by capillary electrophoresis. Langmuir. 2011;27(7):4040–7. https://doi.org/10.1021/la1048562.

Pease III LF, Tsai DH, Zangmeister RA, Zachariah MR, Tarlov MJ. NIST – NCL joint assay protocol, PCC-10, analysis of gold nanoparticles by electrospray differential mobility analysis (ES-DMA). 2010.

Pease LF, Tsai D-H, Zangmeister RA, Zachariah MR, Tarlov MJ. Quantifying the surface coverage of conjugate molecules on functionalized nanoparticles. J Phys Chem C. 2007;111(46):17155–7. https://doi.org/10.1021/jp075571t.

Piella J, Bastús NG, Puntes V. Size-dependent protein–nanoparticle interactions in citrate-stabilized gold nanoparticles: the emergence of the protein corona. Bioconjugate Chem. 2017;28(1):88–97. https://doi.org/10.1021/acs.bioconjchem.6b00575.

Planken KL, Cölfen H. Analytical ultracentrifugation of colloids. Nanoscale. 2010;2(10):1849–69. https://doi.org/10.1039/C0NR00215A.

Ramírez-García G, Oluwole DO, Nxele SR, d'Orlyé F, Nyokong T, Bedioui F, Varenne A. Characterization of phthalocyanine functionalized quantum dots by dynamic light scattering, laser Doppler, and capillary electrophoresis. Anal Bioanal Chem. 2017a;409(6):1707–15. https://doi.org/10.1007/s00216-016-0120-x.

Ramírez-García G, d'Orlyé F, Gutiérrez-Granados S, Martínez-Alfaro M, Mignet N, Richard C, Varenne A. Electrokinetic hummel-dreyer characterization of nanoparticle-plasma protein corona: the non-specific interactions between PEG-modified persistent luminescence nanoparticles and albumin. Colloids Surf B Biointerfaces. 2017b;159:437–44. https://doi.org/10.1016/j.colsurfb.2017.08.012.

Ravi S, Vadukumpully S. Sustainable carbon nanomaterials: recent advances and its applications in energy and environmental remediation. J Environ Chem Eng. 2016;4(1):835–56. https://doi.org/10.1016/j.jece.2015.11.026.

Rice SB, Chan C, Brown SC, Eschbach P, Han L, Ensor DS, Stefaniak AB, Bonevich J, Vladár AE, Hight Walker AR, et al. Particle size distributions by transmission electron microscopy: an interlaboratory comparison case study. Metrologia. 2013;50(6):663–78. https://doi.org/10.1088/0026-1394/50/6/663.

Ruseva V, Lyons M, Powell J, Austin J, Malm A, Corbett J. Capillary dynamic light scattering: continuous hydrodynamic particle size from the nano to the micro-scale. Colloids Surf A Physicochem Eng Aspects. 2018;558:504–11. https://doi.org/10.1016/j.colsurfa.2018.09.022.

Sakurai S. SAXS evaluation of size distribution for nanoparticles. X-ray Scatter. 2017; https://doi.org/10.5772/65049.

Shekunov BY, Chattopadhyay P, Tong HHY, Chow AHL. Particle size analysis in pharmaceutics: principles, methods and applications. Pharm Res. 2007;24(2):203–27. https://doi.org/10.1007/s11095-006-9146-7.

Sikora A, Bartczak D, Geißler D, Kestens V, Roebben G, Ramaye Y, Varga Z, Palmai M, Shard AG, Goenaga-Infante H, et al. A systematic comparison of different techniques to determine the zeta potential of silica nanoparticles in biological medium. Anal Methods. 2015;7(23):9835–43. https://doi.org/10.1039/C5AY02014J.

Sikora A, Shard AG, Minelli C. Size and ζ-potential measurement of silica nanoparticles in serum using tunable resistive pulse sensing. Langmuir. 2016;32(9):2216–24. https://doi.org/10.1021/acs.langmuir.5b04160.

Skoglund S, Hedberg J, Yunda E, Godymchuk A, Blomberg E, Odnevall Wallinder I. Difficulties and flaws in performing accurate determinations of zeta potentials of metal nanoparticles in complex solutions—four case studies. PLoS One. 2017;12(7) https://doi.org/10.1371/journal.pone.0181735.

Sokolova V, Ludwig A-K, Hornung S, Rotan O, Horn PA, Epple M, Giebel B. Characterisation of exosomes

derived from human cells by nanoparticle tracking analysis and scanning electron microscopy. Colloids Surf B Biointerfaces. 2011;87(1):146–50. https://doi.org/10.1016/j.colsurfb.2011.05.013.

Song NW, Park KM, Lee I-H, Huh H. Uncertainty estimation of nanoparticle size distribution from a finite number of data obtained by microscopic analysis. Metrologia. 2009;46(5):480–8. https://doi.org/10.1088/0026-1394/46/5/012.

Teulon J-M, Godon C, Chantalat L, Moriscot C, Cambedouzou J, Odorico M, Ravaux J, Podor R, Gerdil A, Habert A, et al. On the operational aspects of measuring nanoparticle sizes. Nanomaterials (Basel). 2018;9(1) https://doi.org/10.3390/nano9010018.

Till U, Gibot L, Mingotaud A-F, Ehrhart J, Wasungu L, Mingotaud C, Souchard J-P, Poinso A, Rols M-P, Violleau F, et al. Drug release by direct jump from poly(ethylene-glycol-b-ε-caprolactone) nano-vector to cell membrane. Molecules. 2016;21(12) https://doi.org/10.3390/molecules21121643.

Tsai D-H, DelRio FW, Keene AM, Tyner KM, MacCuspie RI, Cho TJ, Zachariah MR, Hackley VA. Adsorption and conformation of serum albumin protein on gold nanoparticles investigated using dimensional measurements and in situ spectroscopic methods. Langmuir. 2011;27(6):2464–77. https://doi.org/10.1021/la104124d.

Urban MJ, Holder IT, Schmid M, Fernandez Espin V, Garcia de la Torre J, Hartig JS, Cölfen H. Shape analysis of DNA–Au hybrid particles by analytical ultracentrifugation. ACS Nano. 2016;10(8):7418–27. https://doi.org/10.1021/acsnano.6b01377.

USP 37, General Information 1224: Transfer of Analytical Procedure.

Varenne F, Botton J, Merlet C, Vachon J-J, Geiger S, Infante IC, Chehimi MM, Vauthier C. Standardization and validation of a protocol of zeta potential measurements by electrophoretic light scattering for nanomaterial characterization. Colloids Surf A Physicochem Eng Aspects. 2015a;486:218–31. https://doi.org/10.1016/j.colsurfa.2015.08.044.

Varenne F, Botton J, Merlet C, Beck-Broichsitter M, Legrand F-X, Vauthier C. Standardization and validation of a protocol of size measurements by dynamic light scattering for monodispersed stable nanomaterial characterization. Colloids Surf A Physicochem Eng Aspects. 2015b;486:124–38. https://doi.org/10.1016/j.colsurfa.2015.08.043.

Varenne F, Botton J, Merlet C, Vachon J-J, Geiger S, Infante IC, Chehimi M, Vauthier C. Toward a standardization of physico-chemical protocols for nanomedicine characterization: II. Zeta potential measurements. In 17th International Congress of Metrology; EDP Sciences, 2015c; p 14003. https://doi.org/10.1051/metrology/20150014003.

Varenne F, Botton J, Merlet C, Beck-Broichsitter M, Legrand F-X, Vauthier C. Toward a standardization of physico-chemical protocols for nanomedicine characterization: I. Size measurements. In 17th International Congress of Metrology; EDP Sciences, 2015d; p 14002. https://doi.org/10.1051/metrology/20150014002.

Varenne F, Makky A, Gaucher-Delmas M, Violleau F, Vauthier C. Multimodal dispersion of nanoparticles: a comprehensive evaluation of size distribution with 9 size measurement methods. Pharm Res. 2016a;33(5):1220–34. https://doi.org/10.1007/s11095-016-1867-7.

Varenne F, Botton J, Merlet C, Hillaireau H, Legrand F-X, Barratt G, Vauthier C. Size of monodispersed nanomaterials evaluated by dynamic light scattering: protocol validated for measurements of 60 and 203nm diameter nanomaterials is now extended to 100 and 400nm. Int J Pharma. 2016b;515(1):245–53. https://doi.org/10.1016/j.ijpharm.2016.10.016.

Varenne F, Rustique E, Botton J, Coty J-B, Lanusse G, Ait Lahcen M, Rio L, Zandanel C, Lemarchand C, Germain M, et al. Towards quality assessed characterization of nanomaterial: transfer of validated protocols for size measurement by dynamic light scattering and evaluation of zeta potential by electrophoretic light scattering. Int J Pharma. 2017;528(1):299–311. https://doi.org/10.1016/j.ijpharm.2017.06.006.

Varenne F, Coty J-B, Botton J, Legrand F-X, Hillaireau H, Barratt G, Vauthier C. Evaluation of zeta potential of nanomaterials by electrophoretic light scattering: fast field reversal versus slow field reversal modes. Talanta. 2019a;205:120062. https://doi.org/10.1016/j.talanta.2019.06.062.

Varenne F, Hillaireau H, Bataille J, Smadja C, Barratt G, Vauthier C. Application of validated protocols to characterize size and zeta potential of dispersed materials using light scattering methods. Colloids Surf A Physicochem Eng Aspects. 2019b;560:418–25. https://doi.org/10.1016/j.colsurfa.2018.09.006.

Varenne F, Devoille L, Makky A, Feltin N, Violleau F, Barratt G, Vauthier C. Evaluation of size distribution of a multimodal dispersion of polymer nanoparticles by microscopy after different methods of deposition J Drug Deliv Sci Tec. 2020;60:102047. https://doi.org/10.1016/j.jddst.2020.102047.

Vladár AE, Ming B. NIST – NCL joint assay protocol, PCC-15, measuring the size of colloidal gold nanoparticles using high-resolution scanning electron microscopy. 2011.

Vogel R, Coumans FAW, Maltesen RG, Böing AN, Bonnington KE, Broekman ML, Broom MF, Buzás EI, Christiansen G, Hajji N, et al. A standardized method to determine the concentration of extracellular vesicles using tunable resistive pulse sensing. J Extracell Vesicles. 2016;5:31242. https://doi.org/10.3402/jev.v5.31242.

Vogel R, Pal AK, Jambhrunkar S, Patel P, Thakur SS, Reátegui E, Parekh HS, Saá P, Stassinopoulos A, Broom MF. High-resolution single particle zeta potential characterisation of biological nanoparticles using tunable resistive pulse sensing. Sci Rep. 2017;7(1):1–13. https://doi.org/10.1038/s41598-017-14981-x.

Wagner S, Legros S, Loeschner K, Liu J, Navratilova J, Grombe R, Linsinger TPJ, Larsen EH, von der

Kammer F, Hofmann T. First steps towards a generic sample preparation scheme for inorganic engineered nanoparticles in a complex matrix for detection, characterization, and quantification by asymmetric flow-field flow fractionation coupled to multi-angle light scattering and ICP-MS. J Anal At Spectrom. 2015;30(6):1286–96. https://doi.org/10.1039/C4JA00471J.

Weigel S, Peters R, Loeschner K, Grombe R, Linsinger TPJ. Results of an interlaboratory method performance study for the size determination and quantification of silver nanoparticles in chicken meat by single-particle inductively coupled plasma mass spectrometry (Sp-ICP-MS). Anal Bioanal Chem. 2017;409(20):4839–48. https://doi.org/10.1007/s00216-017-0427-2.

Williams A, Varela E, Meehan E, Tribe K. Characterisation of nanoparticulate systems by hydrodynamic chromatography. Int J Pharma. 2002;242(1):295–9. https://doi.org/10.1016/S0378-5173(02)00191-6.

Wilson DR, Green JJ. Nanoparticle tracking analysis for determination of hydrodynamic diameter, concentration, and zeta-potential of polyplex nanoparticles. In: Petrosko SH, Day ES, editors. Biomedical nanotechnology: methods and protocols, Methods in molecular biology. New York: Springer; 2017. p. 31–46. https://doi.org/10.1007/978-1-4939-6840-4_3.

Winzen S, Schoettler S, Baier G, Rosenauer C, Mailaender V, Landfester K, Mohr K. Complementary analysis of the hard and soft protein corona: sample preparation critically effects corona composition. Nanoscale. 2015;7(7):2992–3001. https://doi.org/10.1039/C4NR05982D.

Zhou M, Wei Z, Qiao H, Zhu L, Yang H, Xia T. Particle size and pore structure characterization of silver nanoparticles prepared by confined Arc plasma. https://new.hindawi.com/journals/jnm/2009/968058/. Accessed 26 Dec 2019. https://doi.org/10.1155/2009/968058.

Part VI

Challenges in Scale-Up Production of Nanoparticles

24

Nanomedicine Scale-Up Technologies: Feasibilities and Challenges

Dasharath M. Patel, Nitesh N. Patel, and Jayvadan K. Patel

Abstract

Size, shape, morphology, size distribution, targetability, and functionality of developed nanoparticles are the key parameters for their effective biomedical applications. Such desired characteristics should be reproducible and scalable. The production of nanoparticles is a challenging task in terms of reproducibility of size and monodispersity. Desired reproducible drug release profile from nanoparticles is required to further establish batch-to-batch uniformity and quality performance by in vitro in vivo correlation performance. The method of nanoparticle production depends on many factors including intention of application, material used for preparation, nature of bioactive to be loaded, etc. The suitable selection of materials and appropriate method of production of nanodevices is required because the in vitro and in vivo performances of the systems depend on the material characteristics as well as the production method. The preparation methods that require the use of organic solvents and the removal of residual solvents from the final product can often be tedious. The regulatory guidelines require the manufacturers to ensure the purity and safety of the final nanoparticle-based formulations. Numerous methods have been developed in order to produce nanoparticles of desired characteristics. Emerging methods such as membrane extrusion, supercritical fluid technology, and microfluidizer technology have scale-up capabilities with few products of these technologies in the market. However, application of these methods for developing targeted and surface functionalized nanoparticles at large scale is still debatable. This chapter summarizes an overview of nanoparticle production methods, scale-up issues highlighting industrial applicability, and challenges associated with their successful application as clinical nanomedicine.

Keywords

Nanoparticles · Scale-up · Challenges · Drug delivery · Drug targeting

D. M. Patel (✉)
Graduate School of Pharmacy, Gujarat Technological University, Ahmedabad, Gujarat, India

N. N. Patel
Formulation Development, Emcure Pharmaceuticals Limited, Adalaj, Gujarat, India

J. K. Patel
Nootan Pharmacy College, Sankalchand Patel University, Visnagar, Gujarat, India

J. K. Patel, Y. V. Pathak (eds.), *Emerging Technologies for Nanoparticle Manufacturing*,
https://doi.org/10.1007/978-3-030-50703-9_24

1 Introduction

Small molecule chemotherapeutics have their own limitations as the efficacy of chemotherapeutics is often weakened by drawbacks such as poor solubility, bioavailability, and in discriminant toxicity. Once injected, small molecule drugs pass through the liver and undergo metabolism by cytochrome P450 and other enzymes (Guengerich 1999). This first-pass metabolism often targets important moieties installed for target specificity and solubility, rendering drugs inactive or with modified profiles of toxicity and bioavailability. They are rapidly excreted from the body, thus requiring large doses that damage the organs of drug clearance. Severe nephrotoxicity by cisplatin (Courjault et al. 1993) and camptothecin-induced toxicity (Scott et al. 1994) are reported. Likewise, other cells in active growth such as bone marrow and digestive tissues are affected, causing most of the side effects associated with chemotherapy. In general, changing salt forms or formulation conditions as well as synthetic modifications to the drug can address these challenges; however, some drugs can acquire additional toxicity or diminished activity (Morgan et al. 2003; Mueller 2009).

Alternatively, delivery platforms such as polymers, liposomes, and nanoparticles are being explored as effective methods to modulate drug activity (Duncan 2003; Torchilin 2005; Peer et al. 2007; Yoo et al. 2011; Fox et al. 2009). Macromolecular carriers transport drugs to the site of action, thereby limiting metabolism and toxicity. Carriers should possess a number of favorable features including water solubility, lack of toxicity and immunogenicity, long circulation times with half-lives ranging from hours to days, the capacity for high drug loading, and ideally the potential to degrade into nontoxic components. Because the pharmacokinetics of the drug are dictated by the carrier, important factors such as drug release rates and blood circulation time can be modulated by changes to the delivery system. Furthermore, there is the potential for significantly higher tumor accumulation as compared to the small molecule drug due to the passive targeting phenomenon known as the enhanced permeation and retention (EPR) effect (Matsumura and Maeda 1986). Macromolecules in the bloodstream can more easily access the interstitial space in tumor tissue and accumulate due to the lack of lymphatic drainage with minimum distribution to normal tissue in contrast to the distribution of small molecules throughout the body that leads to poor tumor targeting and more systemic toxicities.

Huge research literature is published in the last two decades focusing on preparation of nanocarriers for drug delivery and targeting. However, it is more challenging to scale up these laboratory-scale experiments to actual production scale as compared to scale-up of other conventional formulation such as tablets and capsules. This chapter covers various nanocarriers with special emphasis on the challenges involved in scale-up and large-scale production of these carriers.

2 Nanocarriers for Drug Delivery and Targeting

Nanotechnology has tremendously revolutionized the pharmaceutical and biomedical research. Controlled drug or gene delivery, vaccine delivery, and cell-based diagnosis are featured in the applications of nanoparticles (Brannon-Peppas and Blanchette 2004; Langer 1998). Polymer, lipid, polymer-lipid grafts, metallic nanoparticles, carbon nanotubes, etc. have been widely explored in the new generation "nanomedicines." These nanosystems are synthesized in the laboratory using different techniques which vary significantly from case to case. Therefore, it becomes necessary to understand the method of production of these nanosystems and the scale-up issues thereof for the various systems designed to perform specific biomedical applications.Table 24.1 summarizes different nanoformulations which have been reached up to scale-up, production, or commercial scale as drug delivery system.

Table 24.1 Polymer nanoparticles and synthetic polymer particles combined with drugs or biologics

Name	Material description	Nanoparticle advantage	Indication(s)	Approval year
Adagen®/pegademase bovine (Sigma-Tau Pharmaceuticals)	PEGylated adenosine deaminase enzyme	Improved circulation time and decreased immunogenicity	Severe combined immunodeficiency disease (SCID)	1990
Oncaspar®/pegaspargase (Enzon Pharmaceuticals)	Polymer-protein conjugate (PEGylated L-asparaginase)	Improved stability of protein through PEGylation	Acute lymphoblastic leukemia	1994
Copaxone®/Glatopa (Teva)	Random copolymer of L-glutamate, L-alanine, L-lysine, and L-tyrosine	Large amino acid-based polymer with controlled molecular weight and clearance characteristics	Multiple sclerosis (MS)	1996
Renagel®[sevelamer hydrochloride]/ Renagel®[sevelamer carbonate] (Sanofi)	Polyallylamine hydrochloride)	Increased circulation and therapeutic delivery	Chronic kidney disease	2000
PegIntron® (Merck)	PEGylated IFN alpha-2a protein	Improved stability of protein through PEGylation	Hepatitis C	2001
Neulasta®/pegfilgrastim (Amgen)	PEGylated GCSF protein	Improved stability of protein through PEGylation	Chemotherapy-induced neutropenia	2002
Eligard® (Tolmar)	Leuprolide acetate and polymer (PLGH (poly (D,L-lactide-co-glycolide))	Controlled delivery of payload with longer circulation time	Prostate cancer	2002
Pegasys® (Genentech)	PEGylated IFN alpha-2a protein	Improved stability of protein through PEGylation	Hepatitis B; hepatitis C	2002
Somavert®/pegvisomant (Pfizer)	PEGylated HGH receptor antagonist	Improved stability of protein through PEGylation	Acromegaly	2003
Macugen®/pegaptanib (Bausch + Lomb)	PEGylated anti-VEGF aptamer (vascular endothelial growth factor) aptamer	Improved stability of aptamer as a result of PEGylation	Macular degeneration, neovascular age-related	2004
Mircera®/methoxy polyethylene glycol-epoetin beta (Hoffmann-La Roche)	Chemically synthesized ESA (erythropoiesis-stimulating agent)	Improved stability of aptamer as a result of PEGylation	Anemia associated with chronic kidney disease	2007
Cimzia®/certolizumab pegol (UCB)	PEGylated antibody fragment (certolizumab)	Improved circulation time and greater stability in vivo	Crohn's disease, rheumatoid arthritis, psoriatic arthritis, ankylosing spondylitis	2008; 2009; 2013; 2013
Krystexxa®/pegloticase (Horizon)	Polymer-protein conjugate (PEGylated porcine-like uricase)	Improved stability of protein through PEGylation; introduction of unique mammalian protein	Chronic gout	2010
Plegridy® (Biogen)	Polymer-protein conjugate (PEGylated IFN beta-1a)	Improved stability of protein through PEGylation	Multiple sclerosis	2014

(continued)

Table 24.1 (continued)

Name	Material description	Nanoparticle advantage	Indication(s)	Approval year
ADYNOVATE (Baxalta)	Polymer-protein conjugate (PEGylated factor VIII)	Improved stability of protein through PEGylation	Hemophilia	2015
Zilretta	Triamcinolone acetonide with a polylactic-*co*-glycolic acid (PLGA) matrix microspheres	Extended pain relief over 12 weeks	Osteoarthritis of the knee	2017
Rebinyn	Coagulation factor IX (recombinant) glycoPEGylated	Effective control in 95% of bleeding episodes; 98% of bleeds were treated with 1–2 infusions	Control and prevention of bleeding episodes and prevention of bleeding in the perioperative setting for hemophilia B patients	2017
Liposome formulations combined with drugs or biologics				
DaunoXome® (Galen)	Liposomal daunorubicin	Increased delivery to tumor site; lower systemic toxicity arising from side effects	Karposi's sarcoma	1995
Abelcet® (Sigma-Tau)	Liposomal amphotericin B lipid complex	Reduced toxicity	Fungal infections	1995
Doxil®/Caelyx™ (Janssen)	Liposomal doxorubicin	Improved delivery to site of disease; decrease in systemic toxicity of free drug	Karposi's sarcoma; ovarian cancer; multiple myeloma	1995; 2005; 2008
DepoCyt© (Sigma-Tau)	Liposomal cytarabine	Increased delivery to tumor site; lower systemic toxicity arising from side effects	Lymphomatous meningitis	1996
AmBisome® (Gilead Sciences)	Liposomal amphotericin B	Reduced nephrotoxicity	Fungal/protozoal infections	1997
Curosurf®/poractant alfa (Chiesi Farmaceutici	Liposome-proteins SP-B and SP-C	Increased delivery for smaller volume; reduced toxicity	Pulmonary surfactant for respiratory distress syndrome	1999
Visudyne® (Bausch + Lomb)	Liposomal verteporfin	Increased delivery to site of diseased vessels; photosensitive release	Macular degeneration, wet age-related; myopia; ocular histoplasmosis	2000
DepoDur® (Pacira Pharmaceuticals)	Liposomal morphine sulphate	Extended release	Analgesia (postoperative)	2004
Marqibo® (Onco TCS)	Liposomal vincristine	Increased delivery to tumor site; lower systemic toxicity arising from side effects	Acute lymphoblastic leukemia	2012
Onivyde® (Merrimack)	Liposomal irinotecan	Increased delivery to tumor site; lower systemic toxicity arising from side effects	Pancreatic cancer	2015

Vyxeos (Jazz Pharmaceuticals)	Liposomal combination of daunorubicin and cytarabine	Sustained release of the molecules and co-loaded two molecules with synergistic antitumor activity	Acute myeloid leukemia (AML) or AMLA with myelodysplasia-related changes (AML-MRC)	2017
Micellar nanoparticles combined with drugs or biologics				
Estrasorb™ (Novavax)	Micellar estradiol	Controlled delivery of therapeutics	Menopausal therapy	2003
Protein nanoparticles combined with drugs or biologics				
Ontak® (Eisai Inc)	Engineered protein combining IL-2 and diphtheria toxin	Targeted T cell specificity; lysosomal escape	Cutaneous T-cell lymphoma	1999
Abraxane®/ABI-007 (Celgene)	Albumin-bound paclitaxel nanoparticles	Improved solubility; improved delivery to tumor	Breast cancer; NSCLC; pancreatic cancer	2005; 2012; 2013
Nanocrystals				
INFeD® (Sanofi-Aventis)	Iron dextran (low MW)	Allows increased dose	Iron deficiency in chronic kidney disease (CKD)	1957
DexIron®/Dexferrum® (Sanofi-Aventis)	Iron dextran (low MW)	Allows increased dose	Iron deficiency in chronic kidney disease (CKD)	1957
Feridex®/Endorem® (AMAG Pharmaceuticals)	SPION coated with dextran	Superparamagnetic character	Imaging agent	1996 (2008)
Ferrlecit® (Sanofi-Aventis)	Sodium ferric gluconate	Allows increased dose	Iron deficiency in chronic kidney disease (CKD)	1999
Venofer® (Luitpold Pharmaceuticals)	Iron sucrose	Allows increased dose	Iron deficiency in chronic kidney disease (CKD)	2000
Rapamune® (Wyeth Pharmaceuticals)	Sirolimus	Increased bioavailability	Immunosuppressant	2000
Megace ES® (Par Pharmaceuticals)	Megestrol acetate	Reduced dosing	Anti-anorexic	2001
GastroMARK™; umirem® (AMAG Pharmaceuticals)	SPION coated with silicone	Superparamagnetic character	Imaging agent	2001 (2009)
Avinza® (Pfizer)	Morphine sulphate	Increased drug loading and bioavailability; extended release	Psychostimulant	2002 (2015)
Ritalin LA® (Novartis)	Methylphenidate HCl	Increased drug loading and bioavailability	Psychostimulant	2002
Zanaflex® (Acorda)	Tizanidine HCl	Increased drug loading and bioavailability	Muscle relaxant	2002
Vitoss® (Stryker)	Calcium phosphate	Mimics bone structure allowing cell adhesion and growth	Bone substitute	2003

(continued)

Table 24.1 (continued)

Name	Material description	Nanoparticle advantage	Indication(s)	Approval year
Emend® (Merck)	Aprepitant	Surface area allows faster absorption and increases bioavailability	Antiemetic	2003
OsSatura® (IsoTis Orthobiologics)	Hydroxyapatite	Mimics bone structure allowing cell adhesion and growth	Bone substitute	2003
Tricor® (Lupin Atlantis)	Fenofibrate	Increases bioavailability; simplifies administration	Hyperlipidemia	2004
Ostim® (Heraeus Kulzer)	Hydroxyapatite	Mimics bone structure allowing cell adhesion and growth	Bone substitute	2004
Focalin XR® (Novartis)	Dexmethylphenidate HCl	Increased drug loading and bioavailability	Psychostimulant	2005
nanOss® (Rti Surgical)	Hydroxyapatite	Mimics bone structure allowing cell adhesion and growth	Bone substitute	2005
EquivaBone® (Zimmer Biomet)	Hydroxyapatite	Mimics bone structure	Bone substitute	2009
Feraheme™/ferumoxytol (AMAG Pharmaceuticals)	Ferumoxytol SPION with polyglucose sorbitol carboxymethylether	Magnetite suspension allows for prolonged steady release, decreasing number of doses	Iron deficiency anemia in chronic kidney disease (CKD)	2009
Invega® Sustenna® (Janssen Pharmaceuticals)	Paliperidone palmitate	Allows slow release of injectable low solubility drug	Schizophrenia; schizoaffective disorder	2009; 2014
Inorganic and metallic nanoparticles NanoTherm®(MagForce)	Iron oxide	Allows cell uptake and introduces superparamagnetism	Glioblastoma	2010
Ryanodex® (Eagle Pharmaceuticals)	Dantrolene sodium	Faster administration at higher doses	Malignant hypothermia	2014

2.1 Liposomes

They were discovered by Alec Bangham in 1960. Liposomes are used in the pharmaceutical and cosmetics industry for the transportation of diverse molecules and are among the most studied carrier system for drug delivery. Liposomes are an engrained formulation strategy to improve the drug delivery. They are vesicles of spherical form composed of phospholipids and steroids usually in the 50–450 nm size range (Bozzuto and Molinari 2015). They are considered as better drug delivery vehicles because of their analogous nature to the cell membranes. It has also been proved that they make therapeutic compounds stable, improve their biodistribution, can be used with hydrophilic and hydrophobic drugs and are also biocompatible and biodegradable. Liposomes are divided into four types. *Conventional-type liposome* consists of a lipid bilayer which can make either anionic, cationic, or neutral cholesterol and phospholipids, which surrounds an aqueous core material. In this case, both the lipid bilayer and the aqueous space can be filled with hydrophobic or hydrophilic materials, respectively. *PEGylated liposome* contains polyethylene glycol (PEG) incorporated to the surface of liposome to achieve steric equilibrium. *Ligand-targeted liposome* contains ligands like antibodies, carbohydrates, and peptides that are linked to the surface of the liposome or to the end of previously attached PEG chains. *Theranostic liposome* is a blend of the previous three types of liposomes and generally consists of a nanoparticle along with a targeting, imaging, and a therapeutic element (Sercombe et al. 2015).

The typical synthesis procedure for liposomes involves thin layer hydration, mechanical agitation, solvent evaporation, solvent injection and the surfactant solubilization (Kotla et al. 2017). The important aspect of liposomes is that the drugs that are trapped within them are not bioavailable until they are released. Therefore, their accumulation in particular sites is very important to increase drug bioavailability within the therapeutic window at the right rates and times. Drug loading in liposomes is attained by active (drug encapsulated after liposome formation) and passive (drug encapsulated during liposome formation) approaches (Akbarzadeh et al. 2013). Hydrophilic drugs such as ampicillin and, 5-fluoro-deoxyuridine are typically confined in the aqueous core of the liposome, and thus, their encapsulation does not depend on any modification in the drug/lipid ratio. However, the hydrophobic drugs such as amphotericin B and indomethacin were found in the acyl hydrocarbon chain of the liposome, and thus their engulfing is subjected to the characteristics of the acyl chain (Mohan et al. 2014). The well-described passive loading approaches are mechanical dispersion, solvent dispersion, and detergent removal (Akbarzadeh et al. 2013).

There are obstacles with the use of liposomes for drug delivery purposes in the form of the reticuloendothelial system (RES), opsonization and immunogenicity, although there are factors like EPR that can be utilized in order to boost the drug delivery efficiency of the liposomes (Sercombe et al. 2015; Akbarzadeh et al. 2013). Once liposomes get into the body, they run into opsonins, high-density lipoproteins (HDLs), and low-density lipoproteins (LDLs) while circulating in the bloodstream by themselves. Opsonins (e.g., immunoglobulins and fibronectin) assist RES on recognizing and eliminating liposomes. HDLs and LDLs have interactions with liposomes and decrease their stability. Liposomes tend to gather more in the sites like the liver and the spleen, and this is an advantage because then a high concentration of liposomes can help treat pathogenic diseases, although in the case of cancers this can lead to a delay in the removal of lipophilic anticancer drugs. This is the reason why as mentioned at the beginning, different types of liposomes have been developed, in this case PEGylated ones. Dimov et al. (Dimov et al. 2017) reported a continuous procedure of flow system for the synthesis, functionalization, and cleansing of liposomes consisting of vesicles under 300 nm in a lab-on-chip that are useful and potential candidates for cost-intensive drugs or protein encapsulation development. This is very important because costs of production also determine whether or not a specific drug can be commercialized. Liposome-based systems have now

been permitted by the FDA (Sercombe et al. 2015; Akbarzadeh et al. 2013; Zylberberg and Matosevic 2016; Sapsford et al. 2013; Zhang et al. 2008).

2.2 Polymeric Micelles

Polymeric micelles are nanostructures made of amphiphilic block copolymers that gather by itself to form a core-shell structure in the aqueous solution. The hydrophobic core can be loaded with hydrophobic drugs (e.g., camptothecin, docetaxel, paclitaxel); at the same time the hydrophilic shell makes the whole system soluble in water and stabilizes the core. Polymeric micelles are under 100 nm in size and normally have a narrow distribution to avoid fast renal excretion, thus permitting their accumulation in tumor tissues through the EPR effect. In addition, their polymeric shell restrains nonspecific interactions with biological components. These nanostructures have a strong prospective for hydrophobic drug delivery since their interior core structure permits the assimilation of these kinds of drugs resulting in enhancement of stability and bioavailability (Miyata et al. 2011; Xu et al. 2013).

Polymeric micelles are synthesized by two approaches: (1) convenient solvent-based direct dissolution of polymer followed by dialysis process or (2) precipitation of one block by adding a solvent (Xu et al. 2013; Kulthe et al. 2012). The factors like hydrophobic chain size in the amphiphilic molecule, amphiphile concentration, solvent system, and temperature affect the micelle formation (Devarajan and Jain 2015). The micelle assembly creation starts when the critical micelle concentration (CMC) is reached by the amphiphilic molecules (Kulthe et al. 2012). Drugs are loaded within polymeric micelles by three common methodologies such as direct dissolution process, solvent evaporation process, and the dialysis process. As of the direct dissolution process, the copolymer and the drugs combine with each other by themselves in the water medium and form a drug loaded with the micelles. While in the solvent evaporation process, the copolymer and the intended drug are dissolved using a volatile organic solvent, and finally, in case of the dialysis process, both the drug in solution and the copolymer in the organic solvent are combined in the dialysis bag and then dialyzed with the formation of the micelle (Mourya et al. 2011).

The targeting of the drugs using different polymeric micelles as established by various mechanisms of action including the boosted penetrability and the holding effect stimuli, complexing of a definite aiming ligand molecule to the surface of the micelle, or by combination of the monoclonal antibodies to the micelle corona (Wakaskar 2017). Polymeric micelles are reported to be applicable for both the drug delivery in cancer (Kulthe et al. 2012) and for ocular drug delivery in the posterior ocular tissues (Mandal et al. 2017). In the work by Li et al. (Li et al. 2016), dasatinib was encapsulated within nanoparticles prepared from micellation of PEG-b-PC, to treat proliferative vitreoretinopathy (PVR), their size was 55 nm with a narrow distribution, and they turned out to be noncytotoxic to ARPE-19 cells. This micellar formulation ominously repressed the cell proliferation, attachment, and relocation in comparison to the free drugs.

2.3 Dendrimers

Dendrimers are highly bifurcated, monodisperse, well-defined, and three-dimensional structures. They are globular-shaped and their surface is functionalized easily in a controlled way, which makes these structures excellent candidates as drug delivery agents (Kesharwani et al. 2015; Zhu and Shi 2013; Madaan et al. 2014). Dendrimers can be synthesized by means of two approaches: The first one is the different route in which the dendrimer starts formation from its core and then it is extended outward, and the second is the convergent one, which starts from the outside of the dendrimer (Cheng et al. 2008). Dendrimers are grouped into several kinds according to their functionalization moieties: PAMAM, PPI, liquid crystalline, core-shell, chiral, peptide, glycodendrimers, and PAMAMOS, being PAMAM the most studied for oral drug

delivery because it is water soluble and it can pass through the epithelial tissue boosting their transfer via the paracellular pathway (Noriega-Luna et al. 2014). Dendrimers are limited in their clinical applications because of the presence of amine groups. These groups are positively charged or cationic which makes them toxic; hence dendrimers are usually modified in order to reduce this toxicity issue or to eliminate it. Drug loading in dendrimers is performed via the following mechanisms: simple encapsulation, electrostatic interaction, and covalent conjugation (Tripathy and Das 2013).

Drug is basically delivered by the dendrimers following two different paths, a) by the in vivo degradation of drug dendrimer's covalent bonding on the basis of availability of suitable enzymes or favorable environment that could cleave the bonds and b) by discharge of the drug due to changes in the physical environment like pH, temperature, etc. (Tripathy and Das 2013). Dendrimers have been developed for transdermal, oral, ocular, pulmonary, and in targeted drug delivery (Kesharwani et al. 2014).

Jain et al. (Jain et al. 2014) have described the folate attached poly-L-lysine dendrimers (doxorubicin hydrochloride) as a capable cancer prevention drug carrier model for pH-dependent drug discharge, target specificity, and antiangiogenic and anticancer prospective; it was shown that doxorubicin-folate-conjugated poly-L-lysine dendrimers increased the concentration of doxorubicin in the tumor by 121.5-fold after 24 h compared with free doxorubicin. Similarly, Kaur et al. (Kaur et al. 2017) developed folate-conjugated polypropylene imine dendrimers (FA-PPI) as a methotrexate (MTX) nanocarriers, for pH-sensitive drug release, selective targeting to cancer cells, and anticancer treatment. The in vitro studies on them showed sustained release, increased cell uptake, and low cytotoxicity on MCF-7 cell lines (39). Further, it has to be pointed out that the developed formulations, methotrexate (MTX)-loaded and folic acid-conjugated 5.0G PPI (MTX-FA-PPI), were selectively taken up by the tumor cells in comparison with the free drug, methotrexate (MTX).

2.4 Inorganic Nanoparticles

Inorganic nanoparticles include silver, gold, iron oxide, and silica nanoparticle. Studies focused on them are not as many as there are on other nanoparticle types discussed in this section although they show some potential applications. However, only few of the nanoparticles have been accepted for its clinical use, whereas the majority of them are still in the clinical trial stage. Metal nanoparticles, silver and gold, have particular properties like SPR (surface plasmon resonance) that liposomes, dendrimers, and micelles do not possess. They showed several advantages such as good biocompatibility and versatility when it comes to surface functionalization.

Studies on their drug delivery-related activity have not been able to clear out whether the particulate or ionized form is actually related to their toxicity, and even though two mechanisms have been proposed, namely, paracellular transport and transcytosis, there is not enough information about their in vivo transport and uptake mechanism (Choi et al. 2013). Drugs can be conjugated to gold nanoparticle (AuNPs) surfaces via ionic or covalent bonding and physical absorption, and they can deliver them and control their release through biological stimuli or light activation (Kong et al. 2017). Silver nanoparticles exhibited antimicrobial activity, but as for drug delivery, very few studies have been carried out, for example, Prusty and Swain (Prusty and Swain 2018) synthesized an interlinked and spongy polyacrylamide/dextran nano-hydrogel hybrid system with covalently attached silver nanoparticles for the release of ornidazole which turned out to have an in vitro release of 98.5. Similarly in another study, the iron oxide nanoparticles were synthesized using laser pyrolysis method and were covered with violamycine B1 and antracyclinic antibiotics and tested against the MCF-7 cells for its cytotoxicity and the anti-proliferation properties along with its comparison with the commercially available iron oxide nanoparticles (Marcu et al. 2013).

2.5 Nanocrystals

Nanocrystals are pure solid drug particles within 1000 nm range. These are 100% drug without any carrier molecule attached to it and are usually stabilized by using polymeric steric stabilizers or surfactants. A nanocrystal suspension in a marginal liquid medium is normally alleviated by addition of a surfactant agent known as nano-suspension. In this case, the dispersing medium is mostly water or any aqueous or non-aqueous media including liquid polyethylene glycol and oils (Junyaprasert 2015; Du et al. 2015). Nanocrystals possess specific characters that permit them to overcome difficulties like increased saturation solubility, increased dissolution velocity, and increased glueyness to surface/cell membranes. The process by which nanocrystals are synthesized is divided into top-down and bottom-up approaches. The top-down approaches include sono-crystallization, precipitation, high-gravity controlled precipitation technology, multi-inlet vortex mixing techniques, and limited impinging liquid jet precipitation technique (Junyaprasert 2015). However, use of an organic solvent and its removal at the end makes this process quite expensive. The bottom-up approach involves grinding procedures along with homogenization at higher pressure. Among all of the methods, milling, high-pressure homogenization, and precipitation are the most used methods for the production of nanocrystals. The mechanisms by which nanocrystals support the absorption of a drug to the system include enhancement of solubility, suspension rate, and capacity to hold intestinal wall firmly (Junyaprasert 2015). Ni et al. (Ni et al. 2017) embedded cinaciguat nanocrystals in chitosan microparticles for pulmonary drug delivery of the hydrophobic drug. The nanoparticles were contrived for continuous release of the drug taking advantage of the swelling and muco-adhesive potential of the polymer. They found that inhalation efficacy might be conceded under the disease conditions, so more studies are needed to prove that this system has more potential (Ni et al. 2017).

2.6 Metallic Nanoparticles

In recent years, the interest of using metallic nanoparticles has been growing in different medical applications, such as bioimaging, biosensors, target/sustained drug delivery, hyperthermia, and photoablation therapy. In addition, the modification and functionalization of these nanoparticles with specific functional groups allow them to bind to antibodies, drugs, and other ligands, making these systems more promising in biomedical applications. Although the most extensively studied metallic nanoparticles are gold, silver, iron, and copper, a crescent interest has been exploited regarding other kinds of metallic nanoparticles, such as zinc oxide, titanium oxide, platinum, selenium, gadolinium, palladium, and cerium dioxide among others (McNamara and Tofail 2015, 2017; Kudr et al. 2017).

2.7 Protein and Polysaccharide Nanoparticles

Polysaccharides and proteins are collectively called as natural biopolymers and are extracted from biological sources such as plants, animals, microorganisms, and marine sources (Shimpi 2017; Perale and Hilborn 2016). Protein-based nanoparticles are generally decomposable, metabolizable, and easy to functionalize for its attachment to specific drugs and other targeting ligands. They are normally produced by using two different systems, (a) from water-soluble proteins like bovine and human serum albumin and (b) from insoluble ones like zein and gliadin (Lohcharoenkal et al. 2014). The usual methods to synthesize them are coacervation/desolvation, emulsion/solvent extraction, complex coacervation, and electrospraying. The protein-based nanoparticles are chemically altered in order to combine targeting ligands that identify exact cells and tissues to promote and augment their targeting mechanism (Lohcharoenkal et al. 2014). Similarly, the polysaccharides are composed of sugar units (monosaccharides) linked through O-glycosidic bonds. The composition of these monomers as well as their biological source

is able to confer to these polysaccharides a series of specific physical-chemical properties (Perale and Hilborn 2016; Liu et al. 2008; Huang et al. 2018). One of the main drawbacks of the use of polysaccharides in the nanomedicine field is its degradation (oxidation) characteristics at high temperatures (above their melting point) which are often required in industrial processes. Besides, most of the polysaccharides are soluble in water, which limits their application in some fields of nanomedicine, such as tissue engineering (Poole-Warren et al. 2015; Pertici 2017). However, techniques such as cross-linking of the polymer chains have been employed in order to guarantee stability of the polysaccharide chains, guaranteeing them stability in aqueous environments (Poole-Warren et al. 2015; Pertici 2017). The success of these biopolymers in nanomedicine and drug delivery is due to their versatility and specified properties such as since they can originate from soft gels, flexible fibers, and hard shapes, they can be porous or non-porous; they have great similarity with components of the extracellular matrix, which may be able to avoid immunological reactions (Shimpi 2017; Cardoso et al. 2016).

3 Scale-Up and Production of Nanoparticle Formulations

The production of nanoparticles is a challenging task in terms of reproducibility of size and polydispersity (Paliwal et al. 2014). The method of nanoparticle production depends on many factors including intention of synthesis, i.e., application, material used for preparation, nature of bioactive to be loaded, etc. The suitable selection of materials and appropriate method of production of nanodevices are required because the in vitro and in vivo performances of the systems depend on the material characteristics as well as the production method (Paliwal et al. 2014). The preparation methods that require the use of organic solvents and the removal of residual solvents from the final product can often be tedious. The regulatory guidelines require the manufacturers to ensure the purity and safety of the final nanoparticle-based formulations. The present article provides an overview of nanoparticle production methods, scale-up issues highlighting industrial applicability, and challenges associated with their successful application in clinical nanomedicine.

3.1 Unit Operations or Steps Involved in Production of Nanoparticle Formulations

Several unit operations are very commonly used in the production of nanoparticle formulation which involves, but not limited to, (1) homogenization and formation of course emulsion or dispersion, (2) size reduction of formed emulsion or dispersion, (3) solvent evaporation, and (4) purification of formulation.

3.1.1 Homogenization and Formation of Course Emulsion or Dispersion

Formation of homogeneous emulsions or dispersion is critical to the effectiveness of any given product. There is a huge difference between achieving stability or homogeneity in the lab and in an industrial format. Scaling is a significant challenge for many labs and corporations because industrial machines have difficulty achieving the same level of shear and force that a laboratory machine can achieve. This is particularly challenging because scaling requires use of the same method to achieve the same result with very different machinery. Below are a few specific factors that should be considered when creating a stable emulsion in the laboratory and transforming it in production.

There are a number of techniques available to achieve the homogenization starting from simple magnetic stirrer to high-speed stirrer to rotor-stator-based high-speed or high-sheer homogenizers.

The field of homogenizing encompasses a very broad area. The word homogenize means "to make or render homogeneous," while homogeneous means "having the same composition,

structure, or character throughout." Homogenizing is what is called an umbrella word – a word which covers a very large area (Dhankhar 2014). When someone says that they are homogenizing, they may mean that they are actually doing one or more of the following: blending, mixing, disrupting, emulsifying, dispersing, stirring, etc. (Dhankhar 2014). The current processes or methods of homogenizing can be broken down into three major categories: (1) ultrasonic homogenizing, (2) pressure homogenizing, and (3) mechanical homogenizing.

Ultrasonic Homogenizing

One widely used method to disrupt cells is ultrasonic disruption (Dhankhar 2014). These devices work by generating intense sonic pressure waves in a liquid media. The pressure waves cause streaming in the liquid and, under the right conditions, rapid formation of microbubbles which grow and coalesce until they reach their resonant size, vibrate violently, and eventually collapse. This phenomenon is called cavitation. The implosion of the vapor phase bubbles generates a shock wave with sufficient energy to break covalent bonds. Shear from the imploding cavitation bubbles as well as from eddying induced by the vibrating sonic transducer disrupts cells (Dhankhar 2014). There are several external variables which must be optimized to achieve efficient cell disruption. These variables are tip amplitude and intensity, temperature, cell concentration, pressure, vessel capacity, and shape.

Modem ultrasonic processors use piezoelectric generators made of lead zirconate titanate crystals. The vibrations are transmitted down a titanium metal horn or probe tuned to make the processor unit resonate at 15–25 kHz. The rated power of ultrasonic processors varies from 10 to 375 watts (Homogenizers 2019). Low power output does not necessarily mean that the cell disintegrator is less powerful because lower power transducers are generally matched to probes having smaller tips. It is the power density at the tip that counts. Higher output power is required to maintain the desired amplitude and intensity under conditions of increased load such as high viscosity or pressure. The larger the horn, the more power is required to drive it and the larger the volume of sample that can be processed. On the other hand, larger ultrasonic disintegrators generate considerable heat during operation and will necessitate aggressive external cooling of the sample. Typical maximum tip amplitudes are 30–250 urn, and resultant output intensities are in the range of 200–2000 W/sq.cm. The temperature of the sample suspension should be as low as possible. In addition to addressing the usual concerns about temperature liability of proteins, low media temperatures promote high-intensity shock front propagation. So ideally, the temperature of the ultrasonicated fluid should be kept just above its freezing point. The ultrasonic disintegrator generates considerable heat during processing and this complicates matters. Disruption can also be enhanced by increased hydrostatic pressure (typically 15–60 psi) and increased viscosity, providing the ultrasonic processor has sufficient power to overcome the increased load demand, and the associated sample heating problems can be solved. For microorganisms the addition of glass beads in the 0.05 to 0.5 mm size range enhances cell disruption by focusing energy released by the bubble implosions and by physical crushing. Beads are almost essential for disruption of spores and yeast. A good ratio is one volume of beads to two volumes of liquid. Tough tissues such as skin and muscle should be macerated first in a blender or the like and confined to a small vessel during ultrasonic treatment. The tip should not be placed so shallow in the vessel as to allow foaming. Antifoaming agents or other materials which lower surface tension should be avoided. Finally, one must keep in mind that free radicals are formed in ultrasonic processes and that they are capable of reading with biological materials such as proteins, polysaccharides, or nucleic acids. Damage by oxidative free radicals can be minimized by including scavengers like cysteine, dithiothreitol, or other SH compounds in the media or by saturating the sample with a protective atmosphere of helium or hydrogen gas. For practical reasons, the tip diameter of ultrasonic horns cannot exceed about 3 inches. This sets a limit on the scale-up of these devices. While standard-sized ultrasonic

disrupters have been adapted to continuous operation by placing the probe tip in a chamber through which a stream of cells flow, cooling and free radical release present problems (Dhankhar 2014; Homogenizers 2019).

Pressure Homogenizing

High-pressure homogenizers have been used to homogenized two phases for many years. This type of homogenizer works by forcing cell suspensions through a very narrow channel or orifice under pressure. Subsequently and depending on the type of high-pressure homogenizer, they may or may not impinge at high velocity on a hard-impact ring or against another high-velocity stream of one phase coming from the opposite direction (Dhankhar 2014; Homogenizers 2019). Machines which include the impingement design are more effective than those which do not. Disruption of the vesicle occurs by a combination of the large pressure drop, highly focused turbulent eddies, and strong shearing forces (Dhankhar 2014; Homogenizers 2019). The rate of vesicle disruption is proportional to approximately the third power of the turbulent velocity of the product flowing through the homogenizer channel, which in turn is directly proportional to the applied pressure (Dhankhar 2014; Homogenizers 2019). Thus, the higher the pressure, the higher the efficiency of disruption per pass through the machine. The operating parameters which affect the efficiency of high-pressure homogenizers are pressure, temperature, number of passes, valve and impingement design, and flow rate.

High-pressure homogenizers have long been the best available means to mechanically homogenize two phases on a large scale. Animal tissue also can be processed, but the tissue must be pretreated with a blade blender, rotor-stator homogenizer, or paddle blender. The supremacy of high-pressure homogenizers is now being challenged by bead mill homogenizers. Still, in terms of throughput, the largest industrial models of high-pressure homogenizers outperform bead mills. The maximum volume of dispersion per hour that can be treated by the larger commercial machines is 4500 liters for high-pressure homogenizers versus about 1200 liters for bead mills. Even larger capacity high-pressure homogenizers are available, but their efficiency in homogenization has not been documented. This throughput advantage is diminished somewhat by the fact that most high-pressure homogenizers require several passes of the process to achieve high levels of homogenization, whereas bead mills frequently need only one (Dhankhar 2014; Homogenizers 2019).

A familiar commercial high-pressure homogenizer for the laboratory is the French press which uses a motor-driven piston inside a steel cylinder to develop pressures up to 40,000 psi. Pressurized sample suspensions up to 35 mL are bled through a needle valve at a rate of about 1 mL/min. Because the process generates heat, the sample, piston, and cylinder are usually precooled. Generally, the higher the pressure, the fewer the passes. Most high-pressure homogenizers used for homogenization were adapted from commercial equipment designed to produce emulsions and homogenates in the food and pharmaceutical industries. They combine high pressure with an impingement valve. Capacities of continuous homogenizers vary from 55 to 4500 L/hat 10–17% w/v dispersion concentrations. With the larger capacity machines, several passes are needed to achieve high homogenization. Considerable heat can be generated during operation of these homogenizers, and therefore a heat exchanger attached to the outlet port is essential (Dhankhar 2014; Homogenizers 2019).

Mechanical Homogenizers

Mechanical homogenizers can be broken down into two separate categories, a) rotor-stator homogenizers and b) blade-type homogenizers.

Rotor-Stator Homogenizers

Rotor-stator homogenizers (also called colloid mills or Willems homogenizers) generally outperform cutting blade-type blenders and are well suited for emulsion type of product. Homogenization with the rotor-stator homogenizer involves hydraulic and mechanical shear as well as cavitation (Dhankhar 2014; Homogenizers 2019). Some people in the homogenizing field also claim that there is to a lesser extent high-

energy sonic and ultrasonic pressure gradients involved, while some do not believe in the theory that high-energy sonic and ultrasonic pressure gradients are involved with mechanical homogenizers. The only thing that ultrasonic and mechanical (rotor-stator) homogenizing have in common is that both methods generate and use to some degree cavitation. Cavitation is defined as the formation and collapse of low-pressure vapor cavities in a flowing liquid. Cavitation is generated as you move a solid object through a liquid at a high rate of speed. In ultrasonics the object being moved is the probe which is being vibrated at a very high rate of speed generating cavitation. In mechanical homogenizing (rotor-stator), the blade (rotor) is being moved through the liquid at a high rate of speed generating cavitation. The rotor-stator generator-type homogenizer was first developed to make dispersions and emulsions, and most biological tissues are quickly and thoroughly homogenized with this apparatus. There the material is centrifugally thrown outward in a pump-like fashion to exit through the slots or holes. Because the rotor (blade) turns at a very high rpm, the dispersion is rapidly reduced in size by a combination of extreme turbulence, cavitation, and scissor-like mechanical shearing occurring within the narrow gap between the rotor and the stator (Dhankhar 2014; Homogenizers 2019). Since most rotor-stator homogenizers have an open configuration, the product is repeatedly recirculated. The process is fast, and depending on the toughness of the sample, desired results will usually be obtained in 15–120 s. For the recovery of vesicle or emulsion or complexes, shorter times are used and the rotor speed is reduced. The variables to be optimized for maximum efficiency (Dhankhar 2014; Homogenizers 2019) are design and size of rotor-stator (generator), rotor tip speed, initial size of sample, viscosity of medium, time of processing or flow rate, volume of medium and concentration of sample, shape of vessel, and positioning of rotor-stator.

The size of the rotor-stator probe (also called generator) can vary from the diameter of a pencil for 0.01–10 mL sample volumes to much larger units having batch capacities up to 19,000 L or, for online units, capabilities of 68,000 L/h. Rotor speeds vary from 3000 rpm for large units to 8000–60,000 rpm for the smaller units. In principle, the rotor speed of the homogenizer should be doubled for each halving of the rotor diameter. It is not the rpm's of the motor but the tip velocity of the rotor that is the important operating parameter (Dhankhar 2014; Homogenizers 2019). Other factors such as rotor-stator design, which there are many, materials used in construction, and ease of leaning are also important factors to consider in selecting a rotor-stator homogenizer. Laboratory-sized rotor-stator homogenizers process liquid samples in the 0.01 mL to 20 L range. The capacity of the rotor-stator should be matched to the viscosity and volume of the medium and with the type and amount of plant and animal tissue to be processed. The speed and efficiency of homogenization is greatly degraded by using too small a homogenizer, and the volume range over which a given homogenizer rotor-stator size will function efficiently is only about tenfold. Also, most of the laboratory-sized homogenizers function properly only with liquid samples in the low to medium viscosity range (<10,000 cps). This must be balanced against the practical observation that concentrated samples, by colliding more frequently, are broken up more rapidly. Higher viscosity samples can be processed but require specially shaped homogenization vessels or unique rotor-stator configurations. The size of the sample prior to processing with the homogenizer must be small enough to be drawn inside the stator. Therefore, samples often must be pre-chopped, cut, or fragmented. Foaming and aerosols can be a problem with rotor-stator homogenizers. Keeping the tip of the homogenizer well submerged within the media and the use of properly sized vessels help with the first problem. Square-shaped or fluted vessels give better results than round vessels, and it is also beneficial to hold the immersed tip off center (Dhankhar 2014; Homogenizers 2019). Aerosols can be minimized by using covered vessels. There are no aerosols with in-line homogenizers. Even though a number of the laboratory rotor-stator homogenizers use sealed motors, none of them are truly explosion-proof. Due caution

should be followed when using flammable organic solvents by conducting the homogenization in a well-ventilated hood. On the positive side, rotor-stator homogenizers generate minimal heat during operation, and this can be easily dissipated by cooling the homogenization vessel in ice water during processing. The larger rotor-stator homogenizers are either scaled-up versions of the laboratory models or in-line homogenizers. The latter contain teeth on the edge of a horizontally oriented, multibladed, high-speed impeller aligned in close tolerance to matching teeth in a static liner (Dhankhar 2014; Homogenizers 2019).

Blade-Type Homogenizers

Although less efficient than rotor-stator homogenizers, blade homogenizers (also called blenders) have been used for many years to produce homogeneous slurry. The cutting blades on this class of homogenizer are either bottom or top driven and rotate at speeds of 6000 to 50,000 rpm. Blenders are not suitable for disruption of hard material. Sometimes addition of polyethylene imine, metal chelators, or detergents such as Triton X-100 or Tween-80 also helps. Blade homogenizers are available for a range of liquid sample sizes from 0.01 mL to multi-gallons. Some of the higher rpm homogenizers can reduce tissue samples to a consistent particulate size with distributions as small as 4um as determined by flow cytometric analysis (Dhankhar 2014; Homogenizers 2019).

3.1.2 Size Reduction of Formed Emulsion or Dispersion

Several methods are reported in the literature for the size reduction of nanoparticles depending upon the type of material such as polymer, lipid, and metal. All the methods to be discussed in subsequent section can be classified in bottom-up (i.e., starting from a dissolved molecule to a precipitate) and top-down processes (i.e., starting from a macro-size drug powder to be reduced to smaller one). The latter one has been adopted by pharmaceutical industry at large. However, bottom-up approach is less popular at industrial level as this approach needs removal of the traces of the remaining solvent which is a difficult process (Junghanns and Müller 2008).

For bottom-up category, homogenization cum size control is taking place simultaneously. In this techniques, size reduction is generally not required; instead control on formed precipitated is required. Nanocrystallization is frequently used in this category (Paliwal et al. 2014).

Nanocrystallization

Nanocrystallization directly converts poorly water-soluble drugs into nanoparticles with altered physical properties (Junghanns and Müller 2008). Several formulations developed by nanocrystallization method are available in the market including aprepitant, fenofibrate, and sirolimus. The nanoparticle may be crystalline or amorphous depending upon the production technology and processing of the material. It is possible to develop nanocrystals of desired shape and size by controlling the process parameters. The drug nanocrystals are developed by three approaches, i.e., precipitation, homogenization methods (such as microfluidizer technology), and milling (Paliwal et al. 2014).

Nanoprecipitation is a simple technique which is generally adopted for preformed polymers. Briefly, the polymer is dissolved in a water-miscible organic solvent, and the solvent is then diffused in the aqueous medium in the presence of a surfactant, leading to the instantaneous formation of a colloidal suspension (Petros and DeSimone 2010). This is also known as solvent displacement technique. The method is useful for the preparation of nanocapsules, which is a reservoir type of nanosystem. A high drug payload can be achieved using this technique in nanocapsules; however, its usefulness is limited to water-miscible solvents (better for lipophilic drug encapsulation), and it cannot be adopted for water-immiscible solvents (inefficient to encapsulate hydrophilic drugs). The assembly and stability of drug nanoparticles depend on super saturation and precipitation. The controlling factors for nanoprecipitation method are nucleation and growth kinetics, which decide the final particle size and the size distribution (Merisko-Liversidge et al. 2003). Similarly, the phase of

the drug in nanoparticle form (i.e., crystalline or amorphous) has major impact on stability and bioavailability in vivo (Paliwal et al. 2014).

Sometimes alone precipitation is insufficient to control the size of formed precipitates. So along with precipitation, homogenization or milling method is used to control the size of formed nanocrystals (Paliwal et al. 2014).

For top-down approach, formed homogeneous dispersion (micron in size) will be subjected to size reduction by different approaches, which will be discussed in subsequent section.

Microfluidizer Technology

Microfluidizer technology is fairly latest and one of the most emerging technologies adopted for producing nanoparticles (Microfluidizer®, Microfluidics Inc.). A frontal collision occurs between the two fluids under high-pressure conditions (up to 1700 bar) (BRUNO and MCILWRICK 2001). During collision of the fluids, many changes take place simultaneously such as shear forces and cavitation forces (Tunick et al. 2002). To stabilize developed nanoparticles, surfactants are added in the solution. In order to get the desired size of nanoparticles, several cycles (may range from 50 to even 100) are required which is the limitation of this method. Microfluidic-based liposome preparation is recently reported in the literature (Mijajlovic et al. 2013). This technology offers a number of advantages over the more traditional methods of preparation of liposomes such as extrusion and sonication. Microfluidic hydrodynamic focusing has been used to synthesize nanoparticles and vesicles of various lipids (Mijajlovic et al. 2013; Hung and Lee 2007; Park et al. 2010; Napoli et al. 2011).

Milling Method

Milling is a traditional process of nanoformulation production. NanoCrystals® technology employs generally a bead or a pearl mill in order to get drug nanoparticles. One can develop ultrafine suspensions of drugs using a ball mill (Junghanns and Müller 2008). The principle of size reduction is generation of shear forces of impact by the milling media, which leads to nanoparticles (Xing et al. 2013). The factors affecting size and physical stability of nanoparticles include milling media, dispersion medium, and the stabilizer. However, the chances of product contamination with erosion of the milling material and a comparatively long milling time in case of crystalline drugs and scale-up limitation are some of the unfavorable features of this technique (Paliwal et al. 2014).

Extrusion

Extrusion is a simple method of nanoparticle production. Converting hydrophobic drugs directly into nanoparticles is a scalable and less costly method. Manual extrusion using gas-tight syringes and polycarbonate membranes is a common technique. However, it may develop heterogeneity especially when one uses pore sizes less than 100 nm. This happens due to variability of manual pressure applied each time (Aydin et al. 2011). Recently, Guo et al. reported a nanoporous membrane extrusion method for nanoparticle production of hydrophobic drugs (Guo et al. 2013). This method induces precipitation of drug-loaded nanoparticles at the exits of nanopores. Recently, Khinast et al. reported a novel one-step process for converting a liquid stabilized nano-suspension into a solid formulation via hot-melt extrusion combined with an internal devolatilization process (Khinast et al. 2013). In this process, the polymer is fed into the extruder and allowed to melt. Subsequently, a stable nanosuspension is added to this via side-feeding devices. The water is then removed by devolatilization and the polymer solidified at the outlet. Currently commercially available pegylated liposomal formulation doxil involves extrusion as size reduction technique.

Supercritical Fluid Technology

One of the most promising techniques of nanoparticle production is supercritical fluid (SCF) technology. Mild temperature conditions and avoidance of organic solvent in the production of polymeric nanoparticles are clear benefits of this technique over the others (Elizondo et al. 2012). Pressure and temperature are simultaneously higher for an SCF than those at the critical point.

SCF can be used for various purposes in the nanoparticle production as follows: [A] solvent-rapid expansion from supercritical solutions process, [B] swelling and plasticizing agent-gas saturated solution process, [C] an gas-antisolvent or supercritical antisolvent process or aerosol solvent extraction system process and solution-enhanced dispersion by SCF process, and [D] a solvent for polymerization in dispersed media. The formulation scientist gets advantages like particle de-aggregation, improved solubility and dissolution rate, controlled release, and drug absorption enhancement with this method (Sheth et al. 2012; Byrappa et al. 2008; Sun et al. 2005). In order to get desired properties of nanoparticles such as size and size distribution, morphology, inner core structure, and minimal residual solvent concentration, this method is the most suitable. The remarkable feature of SCF technique is that particles with smooth surfaces, small particle size and distribution, and free flowing can be obtained. However, the poor solvent power of CO_2, the cost, and use of large amount of the CO_2 are few limitations as well (Sheth et al. 2012).

High-Pressure Homogenization

High-pressure homogenization can be classified into two parts: hot homogenization and cold homogenization. Hot homogenization is carried out at temperature above the melting point of the lipid and is applied to lipophilic drugs (Corrias and Lai 2011; Vyas et al. 2008; Lamprecht et al. 1999). Drug-loaded lipid (in melted form) and aqueous phase are mixed by a high-shear mixer, keeping both at the same temperature. It is important to note that the final form of the nanoparticle largely depends upon quality of pre-emulsion, which is often a nanoemulsion. The dispersed phase in the nanoemulsion congeals upon cooling down to room temperature forming the lipid nanoparticles. However; this method is not suitable for the thermolabile drugs. Other limitation is that the drug distribution and loss into the aqueous phase take place in the homogenization process. An alternative approach of lipid nanoparticle production is cold homogenization. This is a type of high-pressure milling of suspension in which lipid with the drug is melted and solidified quickly to get lipid microparticles. The developed microparticles are subsequently processed for high-speed stirring in cold aqueous surfactant followed by homogenization below room temperature to convert them into nanoparticles. If we compare both the methods, it can be inferred that hot high-pressure homogenization is suitable for high lipid concentrations and produces very narrow particle size distributions (Hou et al. 2003). However, cold homogenization process yields large particles with broad size distribution. This method also limits thermal exposure to the drug and offers negligible degradation of temperature-sensitive biomolecules including drugs. Factors affecting size distribution of lipid nanoparticles in both hot and cold homogenization include temperature, type of homogenizer, pressure, and homogenization cycles.

Microemulsion

Gasco and coworkers (Gasco 1993) developed lipid nanoparticles using microemulsion technique. Briefly, lipid nanoparticles can be obtained from hot microemulsion consisted of low melting lipids, an emulsifier, co-surfactant, and water. Further, this microemulsion is added into excess cold water under stirring which results in the precipitation of lipid phase forming nanoparticles. Subsequently, the excess water is removed by a suitable method like ultrafiltration or lyophilization. The remarkable feature of this method is that nanoparticles can be produced without energy inputs and hence are suitable for loading thermolabile drugs in lipid nanoparticles. Factors like composition, temperature gradient, and pH of the medium significantly affect the product quality. The limitations are requirement of removal of excess water from lipid nanoparticles and high concentration of surfactant and co-surfactant. The latter one is highly important from regulatory prospects and should be kept in mind when designing this protocol for nanoparticle production.

Ultrasonication

Ultrasonication can be opted for the preparation of lipid nanoparticles from preformed microparticles (Bose and Michniak-Kohn 2013). The size

Table 24.2 Feasibility and challenges of different size reduction techniques

Method	Remarks	Limitations
Nanoprecipitation	Small particle size, low cost	Difficulties in controlling particle growth, applicability to lipophilic drugs only
Supercritical fluid technology (SCF)	Narrow particle size distribution, mild operating temperatures, and absence of residual solvent	Poor solvent power of CO_2, the cost and necessity of voluminous usage of the CO_2
Extrusion	Simple, inexpensive, easy scale-up, solvent free, fast and continuous process, low cost	Application of temperature and downstream processing are necessary
Microfluidizer	Precise control of the size	Relatively more number of cycles are required
High-pressure homogenization	Scale-up feasibility and no use of organic solvent	Larger particles and broader size distribution of lipid nanoparticles in case of cold process, while hot process is not suitable for thermolabile drugs, energy-intensive process
Microemulsion	Scale-up feasibility, low mechanical energy input	High concentration of surfactant and co-surfactant is used, low nanoparticle concentration
Ultrasonication	For preformed microparticles, reduced shear stress	Broader particle size distribution, chances of potential metal contamination by probe particles, physical instability like particle growth upon storage

of nanoparticles can be controlled by varying the frequency and intensity of ultrasonication. Furthermore, a combination of high-speed stirring and ultrasonication at higher temperature can also be explored. However, the broader particle size distribution is a major limitation along with potential metal contamination arising from the sonication probe.

Table 24.2 summarizes the comparative advantages and disadvantages of the different techniques discussed in the above section.

3.1.3 Solvent Evaporation

After synthesis, several types of treatments may be necessary to apply on nanoparticle dispersions including purification, sterilization, and preparation for storage. Purification is often required to remove traces of impurities such as residual organic solvent, excess of surfactants, salts and large polymer aggregates (Vauthier and Bouchemal 2009). Volatile organic solvents can be removed by evaporation under reduced pressure.

Solvent removal or concentration is an essential process for pharmaceutical, chemical, and biotechnology industries, in applications where it is necessary to reduce solvent amount to a certain extent to facilitate formulation or analysis of molecules of interest. The use of drying or concentration techniques in natural products, medicinal or chemical research, and production of flavors or fragrances is quite widespread, yet, preparative purification remains their most common application (Sabine Kleinhans and Schönenberger 2007; Abeysena and Darrington 2013).

Due to a large diversity of sample types and solvents, various commercial systems have been developed over the years to accommodate the wide range of applications – no universal solution being available at the moment (Sabine Kleinhans and Schönenberger 2007; Abeysena and Darrington 2013).

Many drying techniques can typically meet the specificities of a given process; hence, in general, several dryers could do the job. The choice of the most appropriate solution therefore depends on several criteria, the key conditions being that the dryer must be able to handle the amount of samples required by the application, should deal with sample variations and product requirements, and should carry the substance from feed to exit if necessary (Sabine Kleinhans and Schönenberger 2007; Abeysena and Darrington 2013). The use of the latest equipment, together with a good, up-to-date understanding of the process in a theoretical, applicative, and practical level enables method optimization for faster sample drying or concentration.

Following are the commonly used solutions in the pharmaceutical industry for evaporation:

Rotary Evaporator

Rotary evaporators have been designed for quick and gentle evaporation and condensation of solvents. They are usually used for the separation of highly volatile solvents from liquids or solids with a high boiling point. Rotary evaporation can commonly be used for solvent removal from the final stage of a reaction or the separation of mixed solvents, the precipitation of suspensions or solutions, the concentration of liquids, the recrystallization of a sample to remove impurities, the drying of powder or granulates, the synthesis of chemicals, Soxhlet extractions, or solvent recycling, for example.

The rotation of the sample flask increases the surface area of the mixture, thereby improving the heat transfer and making the process faster. This also makes the vaporization easier and avoids local overheating and incrustation. It also reduces retarded boiling and foaming. The vacuum lowers the boiling point, making low-temperature evaporations possible (Sabine Kleinhans and Schönenberger 2007).

Rotary evaporators can range in size from benchtop/lab-scale instruments (200 mL–2 L) up to 20–50 L process scale units. Their main components usually are a vacuum pump to lower the pressure in the system, a heating bath to control the heating of the sample vessel, a condenser and a chiller to condense the evaporated solvent and recover it, a collection vessel to recover the previously evaporated and condensed solvent, a motor to rotate the flask, and another one to lower and lift the vessel into the bath.

To enable a successful evaporation performance, the rule of thumb suggests that there should be a 20 °C temperature difference between the cooling and the boiling temperatures and between the boiling and the bath temperatures. Recommended parameters would be 20/40/60 °C; however this could be modified when the product must not be heated to 40 °C or whenever solvent boils at a temperature lower than 40 °C under atmospheric pressure. The vacuum and cooling conditions are ideal when the condensate covers approximately half to three quarters of the height of the condenser (Sabine Kleinhans and Schönenberger 2007).

Many criteria will then determine the choice of the most appropriate rotary evaporation solution for a process. A wide range of solutions covering essential needs, as well as specific demands, can be found. When many samples need to be concentrated or dried, systems that evaporate in parallel could be more adequate than rotary evaporation. Vortex evaporator systems are essentially similar than rotary evaporator, but they allow the evaporation of several sample in parallel.

Thin Film Evaporators

Agitated thin-film evaporation has been very successful with difficult-to-handle products. Simply stated, the method quickly separates the volatile from the less volatile components using indirect heat transfer and mechanical agitation of the flowing product film under controlled conditions (Hyde and Glover 1997).

The separation is normally made under vacuum conditions to maximize ΔT while maintaining the most favorable product temperature and to maximize volatile stripping and recovery. A variety of thin-film evaporator designs is commercially available today. Thin-film evaporators can be either vertical or horizontal and can have cylindrical or tapered thermal bodies and rotors. The agitated thin-film or "wiped-film" evaporator consists of two major assemblies: a heated body and a rotor. The rotor may be one of several zero-clearance designs (wiping), a rigid fixed-clearance type or, in the case of a tapered rotor, an adjustable-clearance construction may be used (Hyde and Glover 1997). The majority of thin-film evaporators in operation today is the vertical design with a cylindrical fixed-clearance rotor.

Within the vertical design evaporator, the product enters the unit tangentially above the heated zone and is distributed evenly over the inner circumference of the body wall by rotor. Product spirals down the wall, while bow waves developed by the rotor blades generate highly turbulent flow and optimum heat flux. Volatile components evaporate rapidly. Vapors can flow either concurrently or, more commonly, counter-

currently and are ready for condensing or subsequentprocessing as they leave the unit. Nonvolatile components are discharged at the bottom outlet (Hyde and Glover 1997).

Continuous washing by the bow waves minimizes fouling of the thermal wall where the product or residue is most concentrated. The combination of short residence time, narrow residence time distribution, high turbulence, and rapid surface renewal permits the agitated thin-film evaporator to successfully handle heat-sensitive, viscous, and fouling streams. Low product inventory and operation at near-equilibrium conditions in the process zone are important for highly reactive products. Agitated thin-film evaporators have a wide processing flexibility, and a single system can often be designed to process different products under varied operating conditions. Agitated thin-film technology is a good choice for processes or products containing vaporizable or partly vaporizable components that must be removed to improve quality, yield/recovery, operating economy or environmental containment (Hyde and Glover 1997).

Spray Dryer

Spray drying is a widely applied method to convert aqueous or organic solutions, emulsions, dispersions, and suspensions into a dry powder.

Spray drying is accomplished by dissolving, emulsifying, or dispersing the core substance in a solvent or in a solution of carrier material. The material is then atomized and sprayed into the drying chamber where a hot stream of drying gas will help evaporate the solvent to produce dry solid particles that will further be separated from the gas stream and collected (Sabine Kleinhans and Schönenberger 2007; Mishra 2015; Xin and Mujumdar 2009).

The process parameters, the properties of the feed, and the equipment design are variables that can be adjusted to modify the characteristics of the final product.

Spray drying can be considered a high-throughput process since it is drying very quickly compared to other drying techniques. It provides the advantage of weight and volume reduction. The transformation of a liquid product into a dry powder is done in a single step, which makes the method advantageous in terms of costs, scale-up, and process simplification. The powder can be fully engineered and processed into tablets/capsules without milling or other secondary processing; moreover, most temperature-sensitive substances like enzymes, proteins, antibiotics, etc. can be spray dried without major loss of activity (Sabine Kleinhans and Schönenberger 2007; Mishra 2015; Xin and Mujumdar 2009; Sosnik and Seremeta 2015; Spray Drying vs Freeze Drying 2015; Freeze Drying vs Spray Drying 2019).

Due to a loss of product on the wall of the drying chamber and into the exhaust air, yields in laboratory-scale experiments are far from optimal and are reported to be in the range of 20–70% (88–90). At industrial scale however, yields increase with larger scale setups since the lost fraction is a smaller part of the production volume. Insufficient forces of liquid atomization and the ineffectiveness of the cyclone to effectively separate fine particles with a diameter below 2 μm makes the production and the recovery of submicron particles tedious. This phenomenon has to be considered in the development of drug delivery systems such as intravenous administrated pharmaceuticals (Mishra 2015; Xin and Mujumdar 2009; Sosnik and Seremeta 2015). Laboratory-scale spray drying also fails to produce particles with a size range above 50 μm, similar to those produced at large scale. This needs to be taken into account during lab-scale screening since it could lead to some issue later during scale-up when dissolution profile of particles and powders are important parameters.

Freeze-Drying

Freeze-drying or lyophilization is an effective way of drying a material. It is using the physical principle of sublimation, which involves the direct transition between the solid and the gaseous phase, bypassing the liquid phase. The frozen sample is dried under vacuum without being allowed to thaw. This process is suitable for a wide range of applications such as the preservation of delicate material against degradation or

decomposition, the preservation of product characteristics and initial shape, the conservation of products that require fast rehydration, or the conditioning of product for further use.

The crucial parameters in freeze-drying are pressure and temperature. A typical freeze-drying process involves two stages: freezing and primary drying. For some samples a secondary drying might be required in order to remove solvent molecules tightly attached to the sample and reduce moisture.

Each process step has distinctive requirements in terms of pressure and temperature depending on sample characteristics (BUCHI Labortechnik AG 2019).

Size and shape of the ice crystals depend on the cooling speed and define the freeze-drying ability; rapid cooling results in small ice crystals, while slower cooling leads to larger ice crystals. In terms of freeze-drying, small ice crystals are more challenging to remove from the product than large ones. Yet, the freezing temperature of a formulation is defined by its characteristics and composition (BUCHI Labortechnik AG 2019).

Formulations can generally freeze in two different ways; eutectic mixtures contain substances that freeze at lower temperatures than the water surrounding them. When cooling a eutectic mixture, water is the first to separate from the substances and it freezes to ice. The formulation may now appear frozen, but the remaining substances are actually still liquid. They form concentrated areas that freeze eventually at temperatures below the freezing point of water. The temperature where all components of the mixture are properly frozen is called eutectic temperature. This is the critical temperature of the formulation and the maximum temperature the formulation can endure during the freeze-drying process. Applying vacuum to an incompletely frozen eutectic mixture may result in the destruction of the product as unfrozen components expand when placed under vacuum (BUCHI Labortechnik AG 2019).

The other class of mixtures is amorphous and forms into glassy states when frozen. With decreasing temperature, the formulation becomes more and more viscous and eventually freezes to a vitreous solid at the glass transition point. For amorphous products, the critical point in terms of stability is called collapse temperature. The collapse temperature is typically slightly lower than the glass transition point. Amorphous products are generally very challenging to freeze-dry (BUCHI Labortechnik AG 2019).

The first drying phase – the primary drying – removes the bulk of water within the product by sublimation. The temperature of the product is defined by the pressure in the drying chamber and the heat input must be carefully controlled. The ideal product temperature is as high as possible to maximize the vapor pressure difference between the sample and the condenser, though at the same time it must remain below the product's critical temperature to preserve the frozen character. By using heated shelves, the set temperature is slowly approached at a defined heating rate (BUCHI Labortechnik AG 2019).

The vast majority of the water should be removed by the end of the primary drying phase. The residual moisture content of the product may now be 5–10% due to water bound to the matrix. At this stage, ice should not be present anymore. The secondary drying step removes the adsorbed water molecules by desorption. In order to achieve ideal conditions for desorption, the lowest possible pressure as well as a further increase of the shelf temperature is required. Again, product stability must be considered when choosing the shelf temperature. Secondary drying is usually performed for shorter time periods. At the end of secondary drying, the product moisture content should be in the range of 1–5% (BUCHI Labortechnik AG 2019).

Freeze-drying is usually the favorite choice for the preservation of a wide range of pharmaceutical, mainly when stability in the liquid state is not adequate, storage requirements are too rigorous, or when the product is required in solid form. It is well suited for formulations that do not require further processing after drying since they can be filled directly in vials, which can be sealed in the drying after the cycle, in order to avoid potential contaminations. Freeze-drying strengths lie in the low process temperatures, high yields, great product uniformity, and often, high quality in terms of activity, water content, and/or stabil-

ity. The accurate control of the process enables the production of a product of the highest quality since it minimizes risk of intrinsic product properties such as collapse, eutectic melt, or glass transition temperatures being exceeded (Spray Drying vs Freeze Drying 2015; Freeze Drying vs Spray Drying 2019).

Even though freeze-drying shows non-negligible benefits for sensitive products, industries are investigating alternative methods such as spray drying, due to the high cost, long process time, and limited volumes associated with lyophilization at production scale.

3.1.4 Purification of Formulation

After synthesis, several types of treatments may be necessary to apply on nanoparticle dispersions including purification, sterilization, and preparation for storage. Purification is often required to remove traces of impurities such as residual organic solvent, excess of surfactants, salts, and large polymer aggregates (Vauthier and Bouchemal 2009). Volatile organic solvents can be removed by evaporation under reduced pressure.

The composition of colloidal nanomaterials is a key point, since it affects not only its transport, delivery, and biodistribution in vivo, but, most importantly, it can contribute to toxicity-related problems (Dobrovolskaia et al. 2016; Lin et al. 2014; Crist et al. 2012; Sapsford et al. 2011). For this reason, to ensure a safe formulation, free of contaminants, a purification step is strongly recommended, followed by a physicochemical characterization, before starting preclinical and clinical analysis. There are several techniques available to purify the nanomaterial which will be discussed in subsequent section.

Filtration

Filtration is a purification method, specifically used to sterilize nanomaterial colloidal dispersions. This method is advantageous as a sterilization technique for thermolabile compounds (Dobrovolskaia and SE 2013). In addition, it represents a rapid, commercially available, cost-effective, and simple technique. Although it can be performed under atmospheric pressure, usually, it is performed taking advantage of special devices with filters, which are centrifuged, thus increasing the speed and efficiency of the process (Sapsford et al. 2011; Roy et al. 2012). An aspect that could be considered as a drawback is that filtration of large volumes could produce clogging of the filters, reason for which filters are single-use devices (Scopes 1994). Membrane pore size ratings are in the 0.1 μm to 10.0 μm range for particle and microbial removal and below 0.1 μm pore size for virus filtration. The current standard pore size for sterilizing grade filters is 0.1 μm or 0.22 μm depending on the supplier. Specialized "nanofilters" are also marketed for filtration-based removal for certain virus classes. Dead-end filtration is generally unsuccessful because nanoparticles concentrate at the pores resulting in a "filter cake" that blocks the filter. To overcome the disadvantage of dead-end filtration, industry generally uses cross-flow filtration which is to be discussed in the next section.

Cross-Flow Filtration

Cross-flow filtration (CFF) overcomes this problem by providing a flow of particles at a tangent to the pores under high pressure. The pressure allows particles smaller than the pore size to permeate the membrane while the tangential flow prevents the formation of a filter cake.

CFF is a rapid and efficient method for separating and purifying process flow. It can be used to recover and purify solutions from small volumes (10 mL) up to thousands of liters. With TFF the feed flows tangentially over the surface of the membrane, where a portion flows through the membrane as permeate. Key operating variables include transmembrane pressure (TMP), feed cross-flow velocity (ΔP), increased turbulence (enhances mass transfer), process flux, temperature, volume concentration factor, and number of diafiltration wash volumes.

Transmembrane pressure and cross-flow velocity are important variables. The transmembrane pressure drives fluid through the membrane, taking the permeable molecules with it. Cross-flow velocity is the rate that the solution flows through a feed channel and across the membrane. Its force sweeps away any molecules

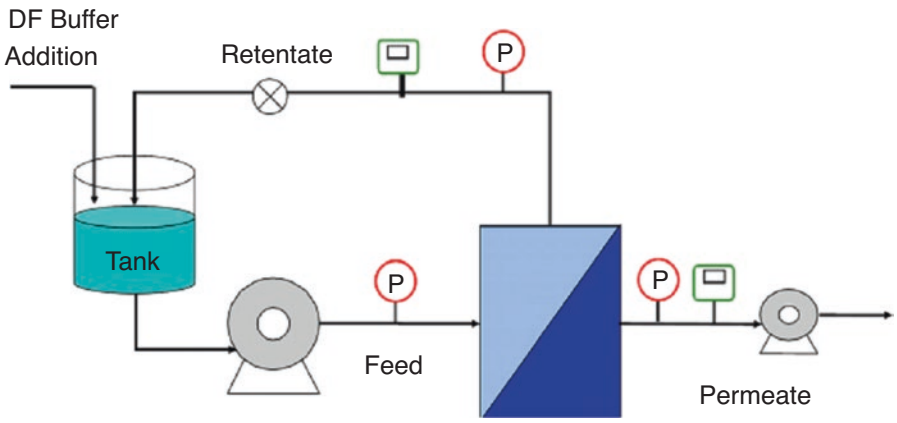

Fig. 24.1 Basic schematic diagram of cross-flow filtration

which might foul the membrane and cause filtrate flow to be restricted (Fig. 24.1).

It is possible to optimize the process relative to time and process volume because both concentration and diafiltration are performed on the same membrane and equipment. By concentrating a sample before diafiltration, a much smaller volume is required for diafiltration. For example, starting with 1 L of product, it takes 1 L(1 DV)of diafiltration buffer to remove 50% of the salt by discontinuous diafiltration. If the product were first concentrated 10× to 100 mL, then it would only require 100 mL of diafiltration buffer to remove 50% of the salt. Note that in both cases the final salt concentration in the sample (concentrate)is the same. However, the concentrated solution will be more viscous. Actual viscosity is dependent on the characteristics of the specific molecules that make up the sample. This viscosity effect becomes very significant as the product concentration increases above a few percent. With increased viscosity, the filtrate flux rate will be lower. Although the process volume is reduced tenfold, the time will not be reduced proportionately.

In diafiltration, the filtrate flux rate remains relatively constant during the process except if the sample viscosity changes due to concentration effects or if changes in the ionic environment change the conformation of a retained molecule and its permeability.

Centrifugation

Centrifugation is another technique useful for the purification of nanomaterials. It consists of the application of a centrifugal force to enhance the precipitation of nanomaterials due to the increased gravitational field (Scopes 1994). Different kinds of centrifugation exist, such as the conventional centrifugation, ultracentrifugation, and gradient centrifugation, whose use depends on the objective of the study and on the nanomaterial type, specifically on their size (Sapsford et al. 2011). Centrifugation is more efficient than filtration. It is a rapid, facile, and economic technique, able to be used for different kinds of nanomedicines. In addition, low amounts of sample are required. However, the centrifugation of large volumes requires special equipment, and in some cases, difficulties on resuspending sediment nanomaterials appear, specifically when working with soft matter, which are not always possible to recover their dispersion liquid state (Sapsford et al. 2011; Scopes 1994). Apart from the use of centrifugation to purify nanomedicines, it has been also used to concentrate nanomedicines, to change their dispersant, and to separate conjugated nanomaterials from those nonconjugated (Sapsford et al. 2011). For example, Fornaguera et al. (Fornaguera et al. 2015) centrifuged PLGA nanoparticles to purify them from the surfactant traces and to concentrate them.

Table 24.3 Feasibility and challenges of different purification techniques

Processing method	Attributes	Benefits	Limitations
Direct flow filtration	Mocroporous, charged filter media, cellulose pads	Simple, reliable, and easily scalable method	Volume and throughput are limited
Tangential flow filtration	Molecular weight cut off of membrane, surface area of membrane	Capable of handling large harvest volumes	Long processing time
Centrifugation	Speed (rotation per minute), centrifugal force, handling volume	Capable of handling very large harvest volumes	Open process, hence contamination and safety issues
Chromatographic purification	Presence of affinity ligands	High throughput, high purity	High initial cost

Chromatographic Purification

Liquid chromatography is a purification method employing a packed resin bed, through which flows a solution containing a mixture of solutes. Specific solutes are differentially bound or slowed as they contact the bed, while others pass through without interacting with the packed resin. The large majority of chromatography steps used in the purification of mAbs and other protein-based biotherapeutics are those in which some constituents bind or interact with a ligand of the stationary phase (packed resin) absolutely while others pass through with no interaction. The bound components are then removed or eluted by the gradual or stepwise change of the composition of the mobile phase (such as through the use of buffers) run through the packed resin bed, such that bound feed constituents are ideally eluted separately from the product of interest. In bind-elute methods, the product is what binds, while in flow-through methods, the product passes through while other unwanted elements of the feed are temporarily bound.

The functional or chromatographically active groups of the stationary phase may be charged (as in ion exchange chromatography), of specific biochemical make-up with affinity for certain feed components (as in affinity chromatography), hydrophobic (hydrophobic interaction chromatography), or some combination of the above (mixed mode).

The chromatographic media (resins) selected for various stages in the downstream process typically have some properties in common like high particle porosity and internal pore surface area for high dynamic binding capacity of either the product of interest or contaminants and impurities and relatively larger resin particle diameter as compared to analytical and other small-scale resins so that resistance to flow is minimized.

Ideally, the chromatographic media should have an average pore size that facilitate relatively less hindered diffusion of target molecules into the back, out of the pores and adsorptive surfaces. This is necessary to maintain a dynamic binding capacity at high levels without any need of decreasing the flow rate during chromatographic purification. Comparative evaluation with respect to method and its attribute is summarized in Table 24.3.

4 Concluding Remarks

The size, shape, morphology, size distribution, targetability, and functionality of developed nanoparticles are the key parameters for their effective biomedical applications. Such desired characteristics should be reproducible and scalable. A desired reproducible drug release profile from nanoparticles is required to further establish batch-to-batch uniformity and quality performance by in vitro in vivo correlation (IVIVC) performance. At present, very little data is avail-

able to establish such critically important parameters of quality control of nanomedicine. Even, till date, no officially established drug release method is available for their evaluation. Mostly, conventional official dissolution methods (established for solid dosage forms) such as paddle or basket method are generally used to perform the same. Dialysis method is also used in various variants (reverse dialysis, rotating dialysis, double dialysis, etc.) to estimate drug release of nanoparticles; however, these methods need validation. Since, nanomedicines are specialized nanounits which have been developed to deliver the bioactive very precisely to their biological targets, an effective way is needed to generate IVIVC for them to ensure their quality production. Despite significant advances in health science and pharmaceutical industry, selection of the method and material is affected by market demands too. One of the important aspects for scale-up production of nanoparticles is the cost of the finished product and also consumable market (Burnett and Tyshenko 2010; Vladisavljević et al. 2013). For more details, readers are suggested to go through an article written by Hock et al. (Hock et al. 2011).

There are several components associated with scale-up of a nanomedicine product from bench to the market. For example, nature of material and its generally regarded as safe (GRAS) status, toxicological features associated with size and shape of nanoparticle (Buzea et al. 2007), in vivo biodegradability of nanocarriers, and balancing of multicomponent system at large scale are a few of them. One has to be careful before selection of materials, solvent, procedure of nanoparticle development, cost, and acceptability of finished product both by clinicians and patients. During scale-up of laboratory method, sometimes the desired features of nanoparticles are lost. For example, in a study of scale-up of nanoparticle prepared using emulsion method, it was observed that increase in impeller speed and agitation time, particle size was decreased although entrapment efficiency was not altered (Colombo et al. 2001). Selection of nanoparticle production method is also important to save time during pilot batch production from scale-up point of view. In a comparative study of ibuprofen-loaded nanoparticles, it was found that nanoprecipitation method took less time (about 2 h) than emulsion-based method (about 3 h) for nanoparticle production (Galindo-Rodríguez et al. 2005). After optimization of therapeutic need, market demand, research and development, production steps, scale-up feasibilities, clinical trials, and regulatory issues, a nanomedicine product reaches to market. Some of the commercially available nanomedicine products for the therapeutic purposes are Doxil® (Bridgewater, USA), DaunoXome (Gilead), Abraxane® (Abraxis Bioscience), AmBisome® (Gilead), Estrasorb (Novavax), Emend (Elan), Megace ES (Elan), TriCor (Elan), and Triglide (SkyePharma). In addition, nanoparticle-based formulations currently available for in vivo imaging include Resovist (Schering), Feridex (Advanced Magnetics), and Gastromark (Advanced Magnetics). The nanomedicine products no doubt are superior in therapeutic performances than conventional drug delivery systems and hence are highly demanded. The overall market for the nanomedicine product in the year 2012 was about 12 billion dollars (Wagner et al. 2006).

Numerous methods have been developed in order to produce nanoparticles of desired characteristics. Emerging methods such as membrane extrusion, supercritical fluid technology, and microfluidizer technology have scale-up capabilities, and few products of these technologies are in the market. However, application of these methods for developing targeted and surface functionalized nanoparticles at large scale is still debatable. On the basis of presently available literature, it seems promising that nanomedicine will translate many products from laboratory to market in the future for various kinds of therapeutics and clinical purposes.

References

Abeysena I, Darrington R. Understanding concentration and evaporation technology: part 1: basic principles of commonly used evaporation techniques. Am Lab Tech notes. 2013;131586.

Akbarzadeh A, Rezaei-Sadabady R, Davaran S, Joo SW, Zarghami N, Hanifehpour Y, et al. Liposome: classification, preparation, and applications. Nanoscale Res Lett. 2013;8(1):102.

Aydin E, Planell JA, Hasirci V. Hydroxyapatite nanorod-reinforced biodegradable poly (L-lactic acid) composites for bone plate applications. J Mater Sci Mater Med. 2011;22(11):2413–27.

Bose S, Michniak-Kohn B. Preparation and characterization of lipid based nanosystems for topical delivery of quercetin. Eur J Pharm Sci. 2013;48(3):442–52.

Bozzuto G, Molinari A. Liposomes as nanomedical devices. Int J Nanomedicine. 2015;10:975.

Brannon-Peppas L, Blanchette JO. Nanoparticle and targeted systems for cancer therapy. Adv Drug Deliv Rev. 2004;56(11):1649–59.

Bruno RP, Mcilwrick R. Microfluidizer® processor technology for high performance particle size reduction, mixing and dispersion. Paperback APV. 2001;42:77–89.

BUCHI Labortechnik AG, Freeze Drying Adviser 2017 [cited 2019 28 Sep 2019]. Available from: https://www.buchi.com/en/node/5661

Burnett K, Tyshenko MG. A comparison of human capital levels and the future prospect of the nanotechnology industry in early sector investors and recent emerging markets. Int J Nanotechnol. 2010;7(2–3):187–208.

Buzea C, Pacheco II, Robbie K. Nanomaterials and nanoparticles: sources and toxicity. Biointerphases. 2007;2(4):MR17–71.

Byrappa K, Ohara S, Adschiri T. Nanoparticles synthesis using supercritical fluid technology–towards biomedical applications. Adv Drug Deliv Rev. 2008;60(3):299–327.

Cardoso M, Costa R, Mano J. Marine origin polysaccharides in drug delivery systems. Mar Drugs. 2016;14(2):34.

Cheng Y, Xu Z, Ma M, Xu T. Dendrimers as drug carriers: applications in different routes of drug administration. J Pharm Sci. 2008;97(1):123–43.

Choi S-J, Lee JK, Jeong J, Choy J-H. Toxicity evaluation of inorganic nanoparticles: considerations and challenges. Mol Cell Toxicol. 2013;9(3):205–10.

Colombo A, Briançon S, Lieto J, Fessi H. Project, design, and use of a pilot plant for nanocapsule production. Drug Dev Ind Pharm. 2001;27(10):1063–72.

Corrias F, Lai F. New methods for lipid nanoparticles preparation. Recent Pat Drug Deliv Formul. 2011;5(3):201–13.

Courjault F, Leroy D, Coquery I, Toutain H. Platinum complex-induced dysfunction of cultured renal proximal tubule cells. Arch Toxicol. 1993;67(5):338–46.

Crist RM, Grossman JH, Patri AK, Stern ST, Dobrovolskaia MA, Adiseshaiah PP, et al. Common pitfalls in nanotechnology: lessons learned from NCI's nanotechnology characterization laboratory. Integr Biol. 2012;5(1):66–73.

Devarajan PV, Jain S. Targeted drug delivery: concepts and design. Cham: Springer; 2015.

Dhankhar P. Homogenization fundamentals. IOSR J Eng. 2014;4(5):01–8.

Dimov N, Kastner E, Hussain M, Perrie Y, Szita N. Formation and purification of tailored liposomes for drug delivery using a module-based micro continuous-flow system. Sci Rep. 2017;7(1):12045.

Dobrovolskaia MA, SE MN. Handbook of immunological properties of engineered nanomaterials. Hackensack: World Scientific; 2013.

Dobrovolskaia MA, Shurin M, Shvedova AA. Current understanding of interactions between nanoparticles and the immune system. Toxicol Appl Pharmacol. 2016;299:78–89.

Du J, Li X, Zhao H, Zhou Y, Wang L, Tian S, et al. Nanosuspensions of poorly water-soluble drugs prepared by bottom-up technologies. Int J Pharm. 2015;495(2):738–49.

Duncan R. The dawning era of polymer therapeutics. Nat Rev Drug Discov. 2003;2(5):347.

Elizondo E, Veciana J, Ventosa N. Nanostructuring molecular materials as particles and vesicles for drug delivery, using compressed and supercritical fluids. Nanomed Nanotechnol Biol Med. 2012;7(9):1391–408.

Fornaguera C, Llinàs M, Solans C, Calderó G. Design and in vitro evaluation of biocompatible dexamethasone-loaded nanoparticle dispersions, obtained from nano-emulsions, for inhalatory therapy. Colloids Surf B: Biointerfaces. 2015;125:58–64.

Fox ME, Szoka FC, Fréchet JM. Soluble polymer carriers for the treatment of cancer: the importance of molecular architecture. Acc Chem Res. 2009;42(8):1141–51.

Freeze Drying vs Spray Drying: is it essentially quality vs cost? 2017 [cited 2019 28 Sep 2019]. Available from: https://biopharma.co.uk/blog/2017/03/15/freeze-drying-vs-spray-drying-is-it-essentially-quality-vs-cost/

Galindo-Rodríguez SA, Puel F, Briançon S, Allémann E, Doelker E, Fessi H. Comparative scale-up of three methods for producing ibuprofen-loaded nanoparticles. Eur J Pharm Sci. 2005;25(4–5):357–67.

Gasco MR. Method for producing solid lipid microspheres having a narrow size distribution: Google Patents; 1993.

Guengerich FP. Cytochrome P-450 3A4: regulation and role in drug metabolism. Annu Rev Pharmacol Toxicol. 1999;39:1–17.

Guo P, Hsu TM, Zhao Y, Martin CR, Zare RN. Preparing amorphous hydrophobic drug nanoparticles by nanoporous membrane extrusion. Nanomed Nanotechnol Biol Med. 2013;8(3):333–41.

Hock SC, Ying YM, Wah CL. A review of the current scientific and regulatory status of nanomedicines and the challenges ahead. PDA J Pharm Sci Technol. 2011;65(2):177–95.

Homogenizers PS. The field of homogenizing 2019. Available from: https://proscientific.com/the-field-of-homogenizing

Hou D, Xie C, Huang K, Zhu C. The production and characteristics of solid lipid nanoparticles (SLNs). Biomaterials. 2003;24(10):1781–5.

Huang J, Deng Y, Ren J, Chen G, Wang G, Wang F, et al. Novel in situ forming hydrogel based on xanthan and chitosan re-gelifying in liquids for local drug delivery. Carbohydr Polym. 2018;186:54–63.

Hung L-H, Lee AP. Microfluidic devices for the synthesis of nanoparticles and biomaterials. J Med Biol Eng. 2007;27(1):1.

Hyde W, Glover W. Evaporation of difficult products-Agitated thin-film evaporation overcomes common problems. Chem Process. 1997;60(2):59.

Jain K, Gupta U, Jain NK. Dendronized nanoconjugates of lysine and folate for treatment of cancer. Eur J Pharm Biopharm. 2014;87(3):500–9.

Junghanns J-UA, Müller RH. Nanocrystal technology, drug delivery and clinical applications. Int J Nanomedicine. 2008;3(3):295.

Junyaprasert VB. Morakul B. Nanocrystals for enhancement of oral bioavailability of poorly water-soluble drugs. Asian J Pharm Sci. 2015;10(1):13–23.

Kaur A, Jain K, Mehra NK, Jain N. Development and characterization of surface engineered PPI dendrimers for targeted drug delivery. Artif Cells Nanomed Biotechnol. 2017;45(3):414–25.

Kesharwani P, Jain K, Jain NK. Dendrimer as nanocarrier for drug delivery. Prog Polym Sci. 2014;39(2):268–307.

Kesharwani P, Xie L, Banerjee S, Mao G, Padhye S, Sarkar FH, et al. Hyaluronic acid-conjugated polyamidoamine dendrimers for targeted delivery of 3, 4-difluorobenzylidene curcumin to CD44 overexpressing pancreatic cancer cells. Colloids Surf B: Biointerfaces. 2015;136:413–23.

Khinast J, Baumgartner R, Roblegg E. Nano-extrusion: a one-step process for manufacturing of solid nanoparticle formulations directly from the liquid phase. AAPS PharmSciTech. 2013;14(2):601–4.

Kong F-Y, Zhang J-W, Li R-F, Wang Z-X, Wang W-J, Wang W. Unique roles of gold nanoparticles in drug delivery, targeting and imaging applications. Molecules. 2017;22(9):1445.

Kotla NG, Chandrasekar B, Rooney P, Sivaraman G, Larrañaga A, Krishna KV, et al. Biomimetic lipid-based nanosystems for enhanced dermal delivery of drugs and bioactive agents. ACS Biomater Sci Eng. 2017;3(7):1262–72.

Kudr J, Haddad Y, Richtera L, Heger Z, Cernak M, Adam V, et al. Magnetic nanoparticles: from design and synthesis to real world applications. Nano. 2017;7(9):243.

Kulthe SS, Choudhari YM, Inamdar NN, Mourya V. Polymeric micelles: authoritative aspects for drug delivery. Des Monomers Polym. 2012;15(5):465–521.

Lamprecht A, Ubrich N, Pérez MH, Lehr C-M, Hoffman M, Maincent P. Biodegradable monodispersed nanoparticles prepared by pressure homogenization-emulsification. Int J Pharm. 1999;184(1):97–105.

Langer R. Drug delivery and targeting. Nature. 1998;392:5–10.

Li Q, Lai KL, Chan PS, Leung SC, Li HY, Fang Y, et al. Micellar delivery of dasatinib for the inhibition of pathologic cellular processes of the retinal pigment epithelium. Colloids Surf B: Biointerfaces. 2016;140:278–86.

Lin P-C, Lin S, Wang PC, Sridhar R. Techniques for physicochemical characterization of nanomaterials. Biotechnol Adv. 2014;32(4):711–26.

Liu Z, Jiao Y, Wang Y, Zhou C, Zhang Z. Polysaccharides-based nanoparticles as drug delivery systems. Adv Drug Deliv Rev. 2008;60(15):1650–62.

Lohcharoenkal W, Wang L, Chen YC, Rojanasakul Y. Protein nanoparticles as drug delivery carriers for cancer therapy. Biomed Res Int 2014;2014.

Madaan K, Kumar S, Poonia N, Lather V, Pandita D. Dendrimers in drug delivery and targeting: drug-dendrimer interactions and toxicity issues. J Pharm Bioallied Sci. 2014;6(3):139.

Mandal A, Bisht R, Rupenthal ID, Mitra AK. Polymeric micelles for ocular drug delivery: from structural frameworks to recent preclinical studies. J Control Release. 2017;248:96–116.

Marcu A, Pop S, Dumitrache F, Mocanu M, Niculite C, Gherghiceanu M, et al. Magnetic iron oxide nanoparticles as drug delivery system in breast cancer. Appl Surf Sci. 2013;281:60–5.

Matsumura Y, Maeda H. A new concept for macromolecular therapeutics in cancer chemotherapy: mechanism of tumoritropic accumulation of proteins and the antitumor agent smancs. Cancer Res. 1986;46(12 Part 1):6387–92.

McNamara K, Tofail SA. Nanosystems: the use of nanoalloys, metallic, bimetallic, and magnetic nanoparticles in biomedical applications. Phys Chem Chem Phys. 2015;17(42):27981–95.

McNamara K, Tofail SAM. Nanoparticles in biomedical applications. Adv Phys X. 2017;2(1):54–88.

Merisko-Liversidge E, Liversidge GG, Cooper ER. Nanosizing: a formulation approach for poorly-water-soluble compounds. Eur J Pharm Sci. 2003;18(2):113–20.

Mijajlovic M, Wright D, Zivkovic V, Bi J, Biggs MJ. Microfluidic hydrodynamic focusing based synthesis of POPC liposomes for model biological systems. Colloids Surf B: Biointerfaces. 2013;104:276–81.

Mishra M. Handbook of encapsulation and controlled release. Boca Raton: CRC Press; 2015.

Miyata K, Christie RJ, Kataoka K. Polymeric micelles for nano-scale drug delivery. React Funct Polym. 2011;71(3):227–34.

Mohan A, Narayanan S, Sethuraman S, Krishnan UM. Novel resveratrol and 5-fluorouracil coencapsulated in PEGylated nanoliposomes improve chemotherapeutic efficacy of combination against head and neck squamous cell carcinoma. Biomed Res Int. 2014;2014:424239.

Morgan MT, Carnahan MA, Immoos CE, Ribeiro AA, Finkelstein S, Lee SJ, et al. Dendritic molecular capsules for hydrophobic compounds. J Am Chem Soc. 2003;125(50):15485–9.

Mourya V, Inamdar N, Nawale R, Kulthe S. Polymeric micelles: general considerations and their applications. Indian J Pharm Educ Res. 2011;45(2):128–38.

Mueller CE. Prodrug approaches for enhancing the bioavailability of drugs with low solubility. Chem Biodivers. 2009;6(11):2071–83.

Napoli M, Atzberger P, Pennathur S. Experimental study of the separation behavior of nanoparticles in micro-and nanochannels. Microfluid Nanofluid. 2011;10(1):69–80.

Ni R, Zhao J, Liu Q, Liang Z, Muenster U, Mao S. Nanocrystals embedded in chitosan-based respirable swellable microparticles as dry powder for sustained pulmonary drug delivery. Eur J Pharm Sci. 2017;99:137–46.

Noriega-Luna B, Godínez LA, Rodríguez FJ, Rodríguez A, Larrea G, Sosa-Ferreyra C, et al. Applications of dendrimers in drug delivery agents, diagnosis, therapy, and detection. J Nanomater. 2014;2014:39.

Paliwal R, Babu RJ, Palakurthi S. Nanomedicine scale-up technologies: feasibilities and challenges. AAPS PharmSciTech. 2014;15(6):1527–34.

Park JI, Saffari A, Kumar S, Günther A, Kumacheva E. Microfluidic synthesis of polymer and inorganic particulate materials. Annu Rev Mater Res. 2010;40:415–43.

Peer D, Karp JM, Hong S, Farokhzad OC, Margalit R, Langer R. Nanocarriers as an emerging platform for cancer therapy. Nat Nanotechnol. 2007;2(12):751.

Perale G, Hilborn J. Bioresorbable polymers for biomedical applications: from fundamentals to translational medicine. Duxford: Woodhead Publishing; 2016.

Pertici G. Introduction to bioresorbable polymers for biomedical applications. Bioresorbable polymers for biomedical applications. Amsterdam: Elsevier; 2017. p. 3–29.

Petros RA, DeSimone JM. Strategies in the design of nanoparticles for therapeutic applications. Nat Rev Drug Discov. 2010;9(8):615.

Poole-Warren L, Martens P, Green R. Biosynthetic polymers for medical applications. San Diego: Elsevier; 2015.

Prusty K, Swain SK. Nano silver decorated polyacrylamide/dextran nanohydrogels hybrid composites for drug delivery applications. Mater Sci Eng C. 2018;85:130–41.

Roy S, Jain V, Bajpai R, Ghosh P, Pente A, Singh B, et al. Formation of carbon nanotube bucky paper and feasibility study for filtration at the nano and molecular scale. J Phys Chem C. 2012;116(35):19025–31.

Sabine Kleinhans CA, Schönenberger G. The LaboratoryAssistant 2007. Available from: https://www.buchi.com/sites/default/files/Buechi_Laborassistent_short_Version_0.pdf

Sapsford KE, Tyner KM, Dair BJ, Deschamps JR, Medintz IL. Analyzing nanomaterial bioconjugates: a review of current and emerging purification and characterization techniques. Anal Chem. 2011;83(12):4453–88.

Sapsford KE, Algar WR, Berti L, Gemmill KB, Casey BJ, Oh E, et al. Functionalizing nanoparticles with biological molecules: developing chemistries that facilitate nanotechnology. Chem Rev. 2013;113(3):1904–2074.

Scopes RK. Making an extract. In: Protein purification. New York: Springer; 1994. p. 22–43.

Scott DO, Bindra DS, Sutton SC, Stella VJ. Urinary and biliary disposition of the lactone and carboxylate forms of 20 (S)-camptothecin in rats. Drug Metab Dispos. 1994;22(3):438–42.

Sercombe L, Veerati T, Moheimani F, Wu SY, Sood AK, Hua S. Advances and challenges of liposome assisted drug delivery. Front Pharmacol. 2015;6:286.

Sheth P, Sandhu H, Singhal D, Malick W, Shah N, Serpil KM. Nanoparticles in the pharmaceutical industry and the use of supercritical fluid technologies for nanoparticle production. Curr Drug Deliv. 2012;9(3):269–84.

Shimpi NG. Biodegradable and biocompatible polymer composites: processing, properties and applications: Woodhead Publishing; 2017.

Sosnik A, Seremeta KP. Advantages and challenges of the spray-drying technology for the production of pure drug particles and drug-loaded polymeric carriers. Adv Colloid Interf Sci. 2015;223:40–54.

Spray Drying vs Freeze Drying. 2015.

Sun YP, Meziani MJ, Pathak P, Qu L. Polymeric nanoparticles from rapid expansion of supercritical fluid solution. Chem Eur J. 2005;11(5):1366–73.

Torchilin VP. Recent advances with liposomes as pharmaceutical carriers. Nat Rev Drug Discov. 2005;4(2):145.

Tripathy S, Das MK. Dendrimers and their applications as novel drug delivery carriers. J Appl Pharm Sci. 2013;3(9):142–9.

Tunick MH, Van Hekken DL, Cooke PH, Malin EL. Transmission electron microscopy of mozzarella cheeses made from microfluidized milk. J Agric Food Chem. 2002;50(1):99–103.

Vauthier C, Bouchemal K. Methods for the preparation and manufacture of polymeric nanoparticles. Pharm Res. 2009;26(5):1025–58.

Vladisavljević GT, Khalid N, Neves MA, Kuroiwa T, Nakajima M, Uemura K, et al. Industrial lab-on-a-chip: design, applications and scale-up for drug discovery and delivery. Adv Drug Deliv Rev. 2013;65(11–12):1626–63.

Vyas S, Rai S, Paliwal R, Gupta PN, Khatri K, Goyal AK, et al. Solid lipid nanoparticles (SLNs) as a rising tool in drug delivery science: one step up in nanotechnology. Curr Nanosci. 2008;4(1):30–44.

Wagner V, Dullaart A, Bock A-K, Zweck A. The emerging nanomedicine landscape. Nat Biotechnol. 2006;24(10):1211.

Wakaskar RR. Polymeric micelles for drug delivery. Int J Drug Dev Res. 2017;9:1–2.

Xin HL, Mujumdar AS. Spray drying and its application in food processing. Innov Food Eng. 2009:303–29.

Xing T, Sunarso J, Yang W, Yin Y, Glushenkov AM, Li LH, et al. Ball milling: a green mechanochemical approach for synthesis of nitrogen doped carbon nanoparticles. Nanoscale. 2013;5(17):7970–6.

Xu W, Ling P, Zhang T. Polymeric micelles, a promising drug delivery system to enhance bioavailability of poorly water-soluble drugs. J Drug Deliv. 2013;2013:340315.

Yoo J-W, Irvine DJ, Discher DE, Mitragotri S. Bio-inspired, bioengineered and biomimetic drug delivery carriers. Nat Rev Drug Discov. 2011;10(7):521.

Zhang L, Gu F, Chan J, Wang A, Langer R, Farokhzad O. Nanoparticles in medicine: therapeutic applications and developments. Clin Pharmacol Ther. 2008;83(5):761–9.

Zhu J, Shi X. Dendrimer-based nanodevices for targeted drug delivery applications. J Mater Chem B. 2013;1(34):4199–211.

Zylberberg C, Matosevic S. Pharmaceutical liposomal drug delivery: a review of new delivery systems and a look at the regulatory landscape. Drug Deliv. 2016;23(9):3319–29.

Patent Survey on Recent Technology for Nanoparticles

25

Manish P. Patel and Jayvadan K. Patel

Abstract

A patent is a form of right granted by the government to an inventor, giving the owner the right to exclude others from making, using, selling, offering to sell, and importing an invention for a limited period of time, in exchange for the public disclosure of the invention. An invention generally has to fulfill three main requirements: it has to be new, not obvious, and have an industrial application. The chapter represents patent distribution according to the different types of nanoparticles used as well as the patent distribution according to the responses to different stimuli; the highest responses tend to fall under the receptor-/aptamer-mediated category. Receptors/aptamers are used as an attractive strategy to enhance the therapeutic index of drugs and to specifically deliver these agents to the defined target cells, thus keeping them away from healthy cells, which are sensitive to the toxic effects of the drugs. The chapter also focuses on patent distribution according to the routes of administration of the drug particle; the most commonly used route is parenteral, owing to the fact that the effects of the medication are much rapid and that it can be administered directly to the site. Also discussed is the patent distribution on the basis of form of delivery. Earlier known as lipid vesicles, the recent most popular form of delivery of the drugs are liposomes, as is evident from the graph. The exceptionally high use of liposomes accounts to the fact that they have high retention rates and excellent targeted sustained release. The patent distribution trends relate the five broad classifications of cancer types. Most widely treated cancer is carcinoma, which contributes the highest ratio of patents as analyzed. Carcinoma class includes the most common type of cancers occurring in humans and can be cured using the technology implying nanoparticles, while sarcoma cancers, related to bone and the connective tissues, is a very complex category and is difficult to treat using any technique

Keywords

Nanocrystals · Drug delivery · Route of administration · Cancer · Computed tomography

M. P. Patel (✉)
L M College of Pharmacy, Ahmedabad, India

J. K. Patel
Nootan Pharmacy College, Sankalchand Patel University, Visnagar, Gujarat, India

J. K. Patel, Y. V. Pathak (eds.), *Emerging Technologies for Nanoparticle Manufacturing*,
https://doi.org/10.1007/978-3-030-50703-9_25

1 Introduction

Nanoscale refers to size dimensions between approximately 1 and 100 nm (or more appropriately 0.2 and 100 nm) because at this scale the properties of materials differ with respect to their physical, chemical, and biological properties from a larger scale. Any form of a material that has one or more dimensions in the nanoscale is known as nanomaterial (Sekhon 2014). Nanoparticles have unique biological properties like small size and large surface area-to-volume ratio which allow them to bind, absorb, and carry compounds such as small-molecule drugs, DNA, RNA, proteins and probe with high efficiency (Compositions and methods for modified dendrimer nanoparticle vaccine delivery. US201562222515P).

2 Nanoparticle Types

- Liposomes are the simplest forms of nanovectors (hollow- or solid-structured nanoparticles which can be filled with various anticancer drugs, targeting moieties and detection agents) which are made up of lipids enclosing water core (Hosen 2015).
- Dendrimers are artificial macromolecules having treelike structures in which atoms are arranged in many branches that radiate from a central core.
- Nanoshells are nanoparticles composed of a gold shell surrounding a semiconductor.
- Nanowires are sensing wires coated with antibodies like molecules to bind to proteins of interest. Silicon nanowires are real-time detectors for molecular binding effects (Singh 2017).
- Fullerenes are nanostructured arrangement of carbon atoms in specific soccer-like architecture. They may also form nanotubes which are cylindrical carbon atom assemblies. Fullerenes have found several specific sensing applications.
- Quantum dots are inorganic fluorescent semiconductor nanoparticles composed of 10–50 atoms with a diameter ranging 2–10 nm (Cai and Chen 2007).
- Gold nanoparticles have been used in vitro based on their ability to scatter visible light (Sokolov et al. 2003).
- Carbon nanotubes are cylinders of several graphite layers with a diameter in nanometers. They may be classified into single-walled carbon nanotubes and multiwalled carbon nanotubes. Due to their unique electronic, thermal, and structural characteristics of carbon nanotubes, they offer a unique approach for drug and gene delivery (Tanaka et al. 2004).
- Nanobiosensors are devices used for detection of an analyte through combination of a sensitive biological component, and transducer along with a detector component is termed as a biosensor (Mody 2011).

3 When Is a Nanotechnology Novel?

As a general rule, size is not a sufficient condition to establish the novelty of an invention. Some nanotechnology inventions, however, involve nanoscale formulations of previously disclosed chemical compounds, structures, and materials. Does this mean that these inventions are not patentable (www.crnano.org/whatis.htm)?

When nanoscale inventions exhibit properties that are, in some measure, unanticipated or different from those found in larger-scale prior art, exceptions have been made. For example, in BASF v Orica Australia, the EPO's Technical Board of Appeals (TBA) held that a prior patent which disclosed polymer nanoparticles larger than 111 nm did not destroy the novelty of a subsequent application by Orica for nanoparticles smaller than 100 nm. Orica's smaller particles exhibited remarkably improved technical properties resulting in a glossier coat compared to the larger particles protected under the prior patent. The difference in properties was held to be sufficient to impart novelty. But does an invention lack novelty if it claims to use particles in a range of sizes that overlap with those disclosed in the prior art? Generally, even the slightest overlap is

sufficient to destroy novelty, but exceptions have been liberally applied to nanoscale inventions. Under the EPO's approach to assessing novelty of these so-called selection inventions, the overlap must be narrow relative to the larger prior art range, sufficiently far removed from the larger range, and indicative of an invention, for example, by exhibiting a new or unexpected effect that occurs only within the selected subrange. The new effect does not, of itself, render the subrange novel; rather, it permits the inference that the subrange has been specifically selected to provide a technical advantage or resolve a technical issue in the prior art and that it is, therefore, novel. Additionally, the EPO assesses the relevance of the subrange to prior art documents by asking whether a person skilled in the art would seriously contemplate applying the technical teachings of the prior art in the range of overlap (www.nanotech-now.com).

The EPO's TBA applied this measure in a recent case involving Smithkline Beecham Biologicals v Wyeth Holdings Corporation (www.nanotech-now.com). The question was whether Smithkline's patent application on a hepatitis B vaccine adjuvant (www.nano.gov/html/facts/whatIsNano.html) lipid measuring 60–120 nm lacked novelty in light of a prior patent on a similar adjuvant with particles measuring 80–500 nm. The TBA found that Smithkline's patent was novel because the overlap was:

- Narrow – only 10% of the larger range in the earlier patent.
- At the extreme lower end of the prior art range.
- Exhibited significantly improved adjuvancy – the smaller particles resulted in an unexpected and favorable shift in immune response.

Moreover, the prior art gave little guidance on how to prepare the smaller particles. A skilled person who followed the vaccine supplier's protocol would have produced particles of between 115 and 951 nm. The technical teachings in the prior art were, therefore, not considered relevant to Smithkline's patent application. Granting patents for inventions falling within such overlapping ranges has become more common in nanotechnology than in any other field. Arguably, this creates a fragmented patent proprietorship landscape with multiple "blocking" patents on the same invention. The existence of "a dense web of overlapping rights" creates uncertainty and inhibits inventors in "designing around" existing patents. Such a dead weight of patents for inventions falling within overlapping ranges already overshadows research on nanotubes, nanowires, nanocrystals, and nanoemulsions and threatens to severely arrest innovation and the further development of the nanotechnology sector (www.nano.gov/html/facts/whatIsNano.html).

4 When Is a Nanotechnology Non-obvious/Inventive?

In addition to proving novelty, a nanotechnology patent application must pass the test of non-obviousness. Generally, an invention is considered obvious if it miniaturizes known elements, performing the same function, and yields no more than might be expected from the diminished size. Technology is considered non-obvious if it produces new and unexpected results or serves previously unrecognized functions that overcome a technical problem relating to the prior art. As practically all nanoscale technologies display these characteristics, only those results which are not likely to emerge from extrapolations by a skilled person working with smaller structures are deemed patentable.

In the Smithkline Beecham Biologicals v Wyeth Holdings Corporation case, the vaccine adjuvant was held to be inventive because of its unexpectedly improved effect and the fact that nothing in the prior art had suggested that a skilled person might consider reducing the particle size to achieve that advantage (www.nanotech-now.com/basics.htm).

Nanotechnology applications can pass the non-obvious test if the invention affords a significant technological advantage over prior art, for example, by enabling a skilled person to practice the previously disclosed invention at the nanoscale for the first time. In BASF v Orica Australia [13], Orica's claimed invention involved manufacturing polymer particles at

100 nms or less by initiating polymerization at temperatures below 40 °C. BASF argued that the invention was obvious because a prior patent had disclosed the same manufacturing process using temperatures below 50 °C to yield particles averaging 111 nms or more. They argued that a skilled person exercising no inventive effort and repeating reactions on a trial-and-error basis for all temperatures between 0 °C and 50 °C would have derived sub-100 nm particles at temperatures below 40 °C. The EPO rejected this argument and reasoned that the prior patent suggested using temperatures not exceeding 50 °C. While this "did not rule out the use of temperatures below 40°C, it was far from suggesting their use." Moreover, the patent was aimed at manufacturing particles larger than 111 nms only. A skilled person following the teachings of the prior patent would not have used temperatures below 40 °C or foreseen that lower temperatures would result in particles smaller than 100 nms. The TBA held that Orica's invention provided, for the first time, a method of creating smaller variants of polymer nanoparticles and was, therefore, inventive (Dang et al. 2010).

Types of Nanomaterials (Fig. 25.1)

5 Current and Future Developments

In search for a more effective solution to address the challenges in cancer therapy for improved therapeutic efficacy and reduced adverse effects, the advent and advancement of nanotechnology has shed promising light on both cancer diagnostics and therapy. The use of nanostructures as delivery vehicles for cytotoxic agents in chemotherapy can improve the overall pharmacokinetics and biodistribution of these drugs while significantly reducing the unwanted side effects. Meanwhile, these nanostructures can also be modified with chemical and/or biochemical moieties, which bind specifically to the targeted tissues for better confinement of the treatment to the diseased tissues (Zhao et al. 2018).

Besides their function for targeted drug delivery, some nanostructures themselves can act as active anticancer therapeutics as a result of their inherent optical and dielectric properties, magnetic susceptibility, and thermal or electrical conductivity. In recognition of the multifaceted advantages of nanostructures, especially their antitumor effectiveness in cancer therapy, extensive efforts have been made to fabricate various nanomaterials. However, the

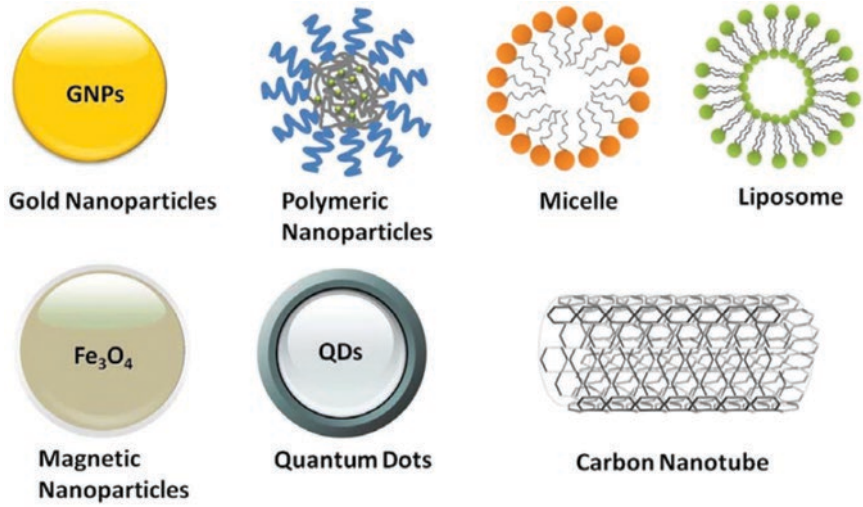

Fig. 25.1 Types of nanomaterials

bulk properties of materials cannot be simply applied to the materials on the nanoscale. In particular, the interaction profile of various nanomaterials with biological system, including their biodistribution and biosafety, needs to be reevaluated prior to their clinical applications. Among them, one crucial concern is the potential toxicity of nanomaterials. The small size of nanoparticles allows them to penetrate into tissue and accumulate inside cells, and the large surface area would lead to more interactions between nanoparticles and cells as well as the intracellular organelles. The cellular response to nanomaterials is often dependent on the concentration of nanomaterials and is related to other physicochemical properties, such as size and geometries, raising the complexity of the studies on the interaction between biological system and nanoparticles. It is believed that insightful understandings of the cellular uptake mechanism and intracellular destination can provide guidance to better design the targeting strategies with optimal compositions. Once these issues are resolved, multifunctional nanostructures will significantly expand our capabilities for innovative oncological interventions with high efficiency and specificity (Zhao et al. 2018).

5.1 Patents in Nanotechnology

A patent is a form of right granted by the government to an inventor, giving the owner the right to exclude others from making, using, selling, offering to sell, and importing an invention for a limited period of time, in exchange for the public disclosure of the invention. An invention generally has to fulfill three main requirements: it has to be new, not obvious, and have an industrial application (Ranjan and Dasgupta 2016) (Fig. 25.2).

- **List of FDA-Approved Nanotechnology-Based Products and Clinical Trials** (Ventola 2017)
  - Adagen®/pegademase bovine (Sigma-Tau Pharmaceuticals), a formulated PEGylated adenosine deaminase enzyme with improved circulation time and decreased immunogenicity for severe combined immunodeficiency disease (SCID) in 1990.
  - Cimzia®/certolizumab pegol (UCB), a formulated PEGylated antibody fragment (certolizumab) with improved circulation time and greater stability in vivo for Crohn's disease, rheumatoid arthritis, psoriatic arthritis, and ankylosing spondylitis in 2008, 2009, 2013, and 2013 successively.
  - Copaxone®/Glatopa (Teva), a formulated random copolymer of l-glutamate, l-lanine, l-lysine, and l-tyrosine large amino-acid-based polymer with controlled molecular weight and clearance characteristics for multiple sclerosis (MS) in 1996.
  - Eligard® (Tolmar), a formulated leuprolide acetate and polymer (PLGH (poly (dl-lactide-co-glycolide)) with controlled delivery of payload with longer circulation time for prostate cancer in 2002.
  - Macugen®/pegaptanib (Bausch + Lomb), a formulated PEGylated anti-VEGF (vascular endothelial growth factor) aptamer with improved stability of aptamer as a result of PEGylation for macular degeneration and neovascular age-related in 2004.
  - Mircera®/methoxy polyethylene glycol-epoetin beta (Hoffmann-La Roche), a formulated chemically synthesized ESA (erythropoiesis-stimulating agent) with improved stability of aptamer as a result of PEGylation for anemia associated with chronic kidney disease in 2007.
  - Neulasta®/pegfilgrastim (Amgen), a formulated PEGylated GCSF protein with improved stability of protein through PEGylation for chemotherapy-induced neutropenia in 2002.
  - Pegasys® (Genentech), a formulated PEGylated IFN alpha-2a protein with improved stability of protein through PEGylation for hepatitis B and hepatitis C in 2002.
  - PegIntron® (Merck), a formulated PEGylated IFN alpha-2a protein with improved stability of protein through PEGylation for hepatitis C in 2001.
  - Renagel®[sevelamer hydrochloride]/Renagel®[sevelamer carbonate] (Sanofi), a

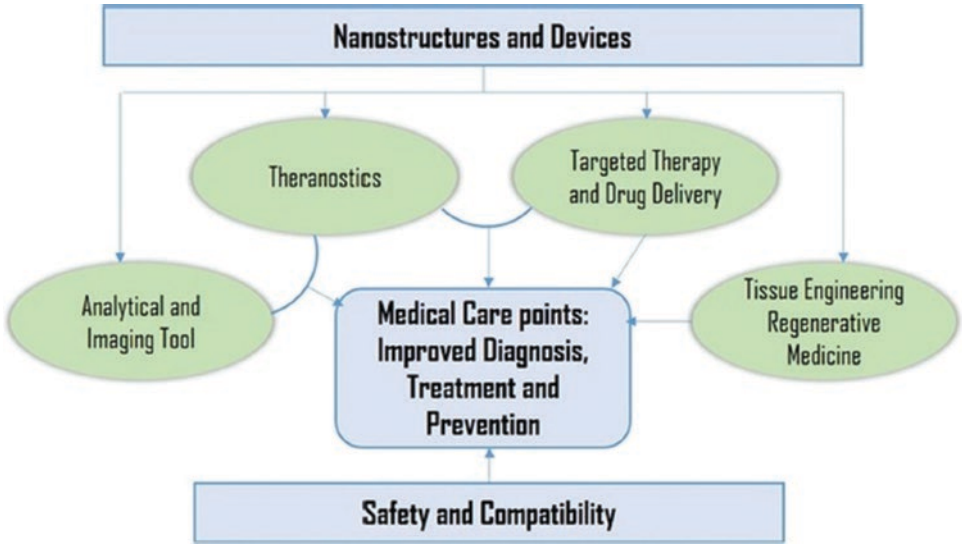

Fig. 25.2 Nanostructures and devices

formulated poly(allylamine hydrochloride) with increased circulation and therapeutic delivery for chronic kidney disease in 2000.
- Somavert®/pegvisomant (Pfizer), a formulated PEGylated HGH receptor antagonist with improved stability of protein through PEGylation acromegaly in 2003.
- Oncaspar®/pegaspargase (Enzon Pharmaceuticals), a formulated polymer-protein conjugate (PEGylated l-asparaginase) with improved stability of protein through PEGylation for acute lymphoblastic leukemia in 1994.
- Krystexxa®/pegloticase (Horizon), a formulated polymer-protein conjugate (PEGylated porcine-like uricase) with improved stability of protein through PEGylation and introduction of unique mammalian protein for chronic gout in 2010.
- Plegridy® (Biogen), a formulated polymer-protein conjugate (PEGylated IFN beta-1a) with improved stability of protein through PEGylation for multiple sclerosis in 2014.
- ADYNOVATE (Baxalta), a formulated polymer-protein conjugate (PEGylated factor VIII) with improved stability of protein through PEGylation for hemophilia in 2015.
- Zilretta, a formulated triamcinolone acetonide with a poly-lactic-*co*-glycolic acid (PLGA) matrix microspheres with extended pain relief over 12 weeks for osteoarthritis (OA) of the knee in 2017.
- Rebinyn, a formulated coagulation factor IX (recombinant) glyco-PEGylated for effective control in 95% of bleeding episodes; 98% of bleeds were treated with one to two infusions for control and prevention of bleeding,episodes and prevention of bleeding in the perioperative setting for hemophilia B patients in 2017.

- **Micellar Nanoparticles Combined with Drugs or Biologics** (Wang et al. 2014)
  - Estrasorb™ (Novavax), a formulated micellar estradiol with controlled delivery of therapeutic for menopausal therapy in 2003.
- **Protein Nanoparticles Combined with Drugs or Biologics** (Miele et al. 2009)
  - Abraxane®/ABI-007 (Celgene), a formulated albumin-bound paclitaxel nanoparticles with improved solubility and improved delivery to tumor for breast cancer,

NSCLC, and pancreatic cancer in 2005, 2012, and 2013 successively.
  - Ontak® (Eisai Inc), a formulated engineered protein combining IL-2 and diphtheria toxin for targeted T-cell specificity and lysosomal escape cutaneous T-cell lymphoma in 1999.
- **Nanocrystals** (Patra et al. 2018)
  - Emend® (Merck), a formulated aprepitant with surface area that allows faster absorption and increases bioavailability for antiemetic in 2003.
  - Tricor® (Lupin Atlantis), a formulated fenofibrate with increased bioavailability that simplifies administration for hyperlipidemia in 2004.
  - Rapamune® (Wyeth Pharmaceuticals), a formulated sirolimus with increased bioavailability for immunosuppressant in 2000.
  - Megace ES® (Par Pharmaceuticals), a formulated megestrol acetate with reduced dosing for anti-anorexic in 2001.
  - Avinza® (Pfizer), a formulated morphine sulphate with increased drug loading and bioavailability; extended release which is psychostimulant in 2002 (2015).
  - Focalin XR® (Novartis), a formulated dexmethylphenidate HCl with increased drug loading and bioavailability for psychostimulant in 2005.
  - Ritalin LA® (Novartis), a formulated methylphenidate HCl with increased drug loading and bioavailability for psychostimulant in 2002.
  - Zanaflex® (Acorda), a formulated tizanidine HCl with increase d drug loading and bioavailability for muscle relaxant in 2002.
  - Vitoss® (Stryker), a formulated calcium phosphate which mimics bone structure allowing cell adhesion and growth as bone substitute in 2003.
  - Ostim® (Heraeus Kulzer), a formulated hydroxyapatite which mimics bone structure allowing cell adhesion and growth as bone substitute in 2004.
  - OsSatura® (IsoTis Orthobiologics), a formulated hydroxyapatite which mimics bone structure allowing cell adhesion and growth as bone substitute in 2003.
  - nanOss® (RTI Surgical), a formulated hydroxyapatite which mimics bone structure allowing cell adhesion and growth as bone substitute in 2005.
  - EquivaBone® (Zimmer Biomet), a formulated hydroxyapatite which mimics bone structure as bone substitute in 2009.
  - Invega® Sustenna® (Janssen Pharmaceuticals), a formulated paliperidone palmitate which allows slow release of injectable with low solubility drug for schizophrenia and schizoaffective disorder in 2009 and 2014.
  - Ryanodex® (Eagle Pharmaceuticals), a formulated dantrolene sodium with faster administration at higher doses for malignant hypothermia in 2014.
  - Inorganic and metallic nanoparticles NanoTherm® (MagForce), a formulated iron oxide which allows cell uptake and introduces super paramagnetism for glioblastoma in 2010.
  - Feraheme™/ferumoxytol (AMAG Pharmaceuticals), a formulated ferumoxytol SPION with polyglucose sorbitol carboxymethyl ether magnetite suspension which allows for prolonged steady release, decreasing number of doses for anemia iron deficiency in chronic kidney disease (CKD) in 2009.
  - Venofer® (Luitpold Pharmaceuticals), a formulated iron sucrose which allows increased dose for iron deficiency in chronic kidney disease (CKD) in 2000.
  - Ferrlecit® (Sanofi-Aventis), a formulated sodium ferric gluconate which allows increased dose for iron deficiency in chronic kidney disease (CKD) in 1999.
  - INFeD® (Sanofi-Aventis), a formulated iron dextran (low MW) which allows increased dose for iron deficiency in chronic kidney disease (CKD) in 1957.
  - DexIron®/Dexferrum® (Sanofi-Aventis), a formulated iron dextran (low MW) which

allows increased dose for iron deficiency in chronic kidney disease (CKD) in 1957.
- Feridex®/Endorem® (AMAG Pharmaceuticals), a formulated SPION coated with dextran with superparamagnetic character as imaging agent in 1996 (2008).
- GastroMARK™; umirem® (AMAG Pharmaceuticals), a formulated SPION coated with silicone superparamagnetic character as imaging agent in 2001 (2009).
- Adagen® (Sigma-Tau Pharmaceuticals), a formulated pegademase bovine with PEGylated adenosine deaminase enzyme for immunodeficiency disease to improve circulation time in body and decrease immunogenicity in 1990.
- Oncaspar® (Enzon Pharmaceuticals), a formulated l-asparaginase with PEGylated l-asparaginase for acute lymphoblastic leukemia improved protein stability due to PEGylation in 1994.
- Copaxone® (Teva), a formulated glatopa l-glutamate, l-alanine, l-lysine, and l-tyrosine random copolymer for multiple sclerosis in regulation of clearance and polymer with controlled molecular weight in 1996.
- Renagel® (Sanofi), a formulated sevelamer hydrochloride or sevelamer carbonate with poly(allylamine hydrochloride) for chronic renal diseases with increased site-specific delivery and increase in circulation time in body in 2000.
- PegIntron® (Merck, a) formulated interferon-alpha (IFN-α2b) with PEGylated IFN-α2b protein for hepatitis C with improved protein stability due to PEGylation in 2001.
- Pegasys® (Genentech), a formulated interferon-alpha (IFN-α2a) with PEGylated IFN-α2a protein for hepatitis B and C with improved protein stability due to PEGylation in 2002.
- Eligard® (Tolmar), a formulated leuprolide acetate with polymer (PLGH (poly(dl-lactide-co-glycolide) for prostate cancer with prolonged drug delivery and circulation time in body in 2002.
- Neulasta® (Amgen), a formulated PEGfilgrastim with PEGylated granulocyte colony-stimulating factor (GCSF) protein for neutropenia induced by chemotherapy for improved protein stability due to PEGylation in 2002.
- Somavert® (Pfizer), a formulated PEGvisomant with PEGylated HGH receptor antagonist for acromegaly with improved protein stability due to PEGylation in 2003.
- Macugen® (Bausch + Lomb), a formulated PEG-aptanib with PEGylated anti-vascular endothelial growth factor aptamer for macular degeneration; neovascular age-related (decreased vision) for improved stability due to PEGylation in 2004.
- Mircera® (Hoffmann-La Roche), a formulated methoxy polyethylene glycol-epoetin beta which is chemically synthesized erythropoiesis-stimulating agent for anemia associated with renal failure due to diseases with improved stability due PEGylation in 2007.
- Cimzia® (UCB) formulated certolizumab pegol with PEGylated antibody fragment (certolizumab) for Crohn's disease, rheumatoid arthritis, psoriatic arthritis, and ankylosing spondylitis to increase stability and circulation time in the body in 2008, 2009, 2013, and 2013 successively.
- Krystexxa® (Horizon), a formulated PEGloticase with PEGylated porcine-like uricase for chronic gout with improved protein stability due to PEGylation in 2010.
- Plegridy® (Biogen), a formulated interferon-beta (IFN-β1a) with PEGylated IFN-β1a protein for multiple sclerosis with improved protein stability due to PEGylation in 2015.
- ADYNOVATE (Baxalta), a formulated factor VIII with PEGylated factor VIII for hemophilia with improved protein stability due to PEGylation in 2015.
- Rapamune® (Wyeth Pharmaceuticals), a formulated sirolimus nanocrystal as immu-

nosuppressant with increased bioavailability in 2000.
- Megace ES® (Par Pharmaceuticals), a formulated megestrol acetate with nanocrystals as anti-anorexic with reduced posology in 2001.
- Avinza® (Pfizer), a formulated morphine sulfate with nanocrystals as mental stimulant with prolonged release and increased bioavailability in 2002/2015.
- Ritalin LA® (Novartis), a formulated methylphenidate HCl with nanocrystals as mental stimulant with increased drug loading and bioavailability in 2002.
- Zanaflex® (Acorda), a formulated tizanidine HCl with nanocrystals as muscle relaxant with increased bioavailability and decreased posology in 2002.
- Emend® (Merck), a formulated aprepitant with nanocrystals as antiemetic drug with increased absorption and bioavailability in 2003.
- Vitoss® (Stryker), a formulated calcium phosphate with nanocrystals as bone substitute which mimics bone structure by cell adhesion and growth in 2003.
- OsSatura® (IsoTis Orthobiologics), a formulated hydroxyapatite with nanocrystals as bone substitute which mimics bone structure by cell adhesion and growth in 2003.
- Ostim® (Heraeus Kulzer), a formulated hydroxyapatite with nanocrystals as bone substitute which mimics bone structure by cell adhesion and growth in 2004.
- Tricor® (Lupin Atlantis), a formulated fenofibrate with nanocrystals for hyperlipidemia with increased bioavailability in 2004.
- Focalin XR® (Novartis), a formulated dexmethylphenidate HCl with nanocrystals as mental stimulant with increased bioavailability in 2005.
- nanOss® (RTI Surgical), a formulated hydroxyapatite with nanocrystals as bone substitute which mimics the bone structure by cell adhesion and growth in 2005.
- EquivaBone® (Zimmer Biomet), a formulated hydroxyapatite with nanocrystals as bone substitute which mimics the bone structure in 2009.
- Invega® Sustenna® (Janssen Pharmaceuticals), a formulated paliperidone palmitate with nanocrystals for schizophrenia and schizoaffective disorder with decreased release of poor water-soluble drugs in 2009/2014.

Nanotechnology is a rapidly expanding field, encompassing the development of man-made materials in the 5–200 nanometer size range. This dimension vastly exceeds that of standard organic molecules, but its lower range approaches that of many proteins and biological macromolecules. In the scientific world, the term “nano” is, however, somewhat ambiguous since it does not designate the same reality for physicists, chemists, and biologists. Conceptually, nanotechnologies in general and nanoparticles in particular have revolutionized the administration of medicines. There is, nevertheless, a wide consensus that nanotechnology represents not simply a miniaturization of larger objects but the preparation of nanomaterials with physical and chemical properties which dramatically differ from those of bulk materials, because they are on a nanometric scale. Nanotechnology involves the engineering of functional systems at the molecular scale. Such systems are characterized by unique physical, optical, and electronic features that are attractive for disciplines ranging from materials science to biomedicine. One of the most active research areas of nanotechnology is nanomedicine, which applies nanotechnology to highly specific medical interventions for the prevention, diagnosis, and treatment of diseases. By virtue of their unique physicochemical properties, nanoparticles have shown promise in delivering a range of molecules to desired sites in the body. To develop safer and more effective therapeutic nanoparti-

cles, researchers have designed novel multifunctional nanoparticle platforms for cell/tissue-specific targeting, sustained or triggered drug delivery, co-delivery of synergistic drug combinations, etc. Advances in biocompatible nanoscale drug carriers such as liposomes and polymeric nanoparticles have enabled more efficient and safer delivery of a myriad of drugs. Advantages in nanoparticle drug delivery, particularly at the systemic level, include longer circulation half-lives, improved pharmacokinetics, and reduced side effects. In cancer treatments, nanoparticles can further rely on the enhanced permeability and retention effect caused by leaky tumor for better drug accumulation at the tumor sites. These benefits have made therapeutic nanoparticles a promising candidate to replace traditional chemotherapy, where intravenous injection of toxic agents poses a serious threat to healthy tissues and results in dose-limiting side effects (Jeevanandam et al. 2018).

The emergence of nanotechnology has made a significant impact on clinical therapeutics in the last two decades. Advances in biocompatible nanoscale drug carriers such as liposomes and polymeric nanoparticles have enabled more efficient and safer delivery of a myriad of drugs. Advantages in nanoparticle drug delivery, particularly at the systemic level, include longer circulation half-lives, improved pharmacokinetics, and reduced side effects. In cancer treatments, nanoparticles can further rely on the enhanced permeability and retention effect caused by leaky tumor vasculatures for better drug accumulation at the tumor sites (Shi et al. 2010).

Nanoparticles have the advantage of targeting cancer by simply being accumulated and entrapped in tumors (passive targeting). The phenomenon is called the enhanced permeation and retention effect, caused by leaky angiogenetic vessels and poor lymphatic drainage, and has been used to explain why macromolecules and nanoparticles are found at higher ratios in tumors compared to normal tissues (Shi et al. 2010).

Figure 25.3 represents the patent distribution according to the different types of nanoparticles used. As evident from the graph, the use of polymeric drug nanoparticles is the highest as it increases the therapeutic performance of poorly soluble drugs in any route of administration. The unique characteristics of noble metal nanoparticles, such as high surface-to-volume ratio, broad optical properties, ease of synthesis, and facile surface chemistry and functionalization, hold pledge in the clinical field for cancer therapeutics, thus, ranking them as second most widely used material form. Moreover, metals like gold and silver can efficiently convert light or radiofrequencies into heat, thus enabling thermal ablation of targeted cancer cells. For example, patent **US20100029544A1** talks about the new heteroalkyl polymer-based nanoparticles used for treating cardiovascular diseases and cancer. The graph also very clearly depicts a significant number of patents involving the use of gold nanoparticles because of their basic tendency to stick to the site of action, i.e., tumor. Patent **US20070031337A1** discloses the use of gold nanoparticles using proton therapy to treat the tumor cells (www.lexxinnova.com n.d.).

Figure 25.4 represents the patent distribution according to the responses to different stimuli. As visible from the graph, the highest responses tend to fall under the receptor/aptamer mediated category. Receptors/aptamers are used as an attractive strategy to enhance the therapeutic index of drugs and to specifically deliver these agents to the defined target cells, thus keeping them away from healthy cells, which are sensitive to the toxic effects of the drugs. Ultrasound field coupled with low pH factors and polymer nanoparticles is widely used as vesicles for treating carcinoma group of cancers. These dually responsive vesicles show no cytotoxicity below 250 μg/ml and can encapsulate anticancer drugs, exhibiting retarded release profile and controllable release rate when subjected to ultrasound radiation or varying pH in tris buffer at 37 °C. However, the evolution of stimulus-responsive vesicles from bench to bedside still seems far away for the limitations of current stimulus forms such as ultrasound, light, photothermal, etc. For example, patent **US20080131366A1** discloses diagnosing and treating a patient with solid tumor (lymphoma) comprising of nanoparticles which respond to the steroid receptor. Likewise in patent **US20120259152A1**, radiation, as a stimulus, is

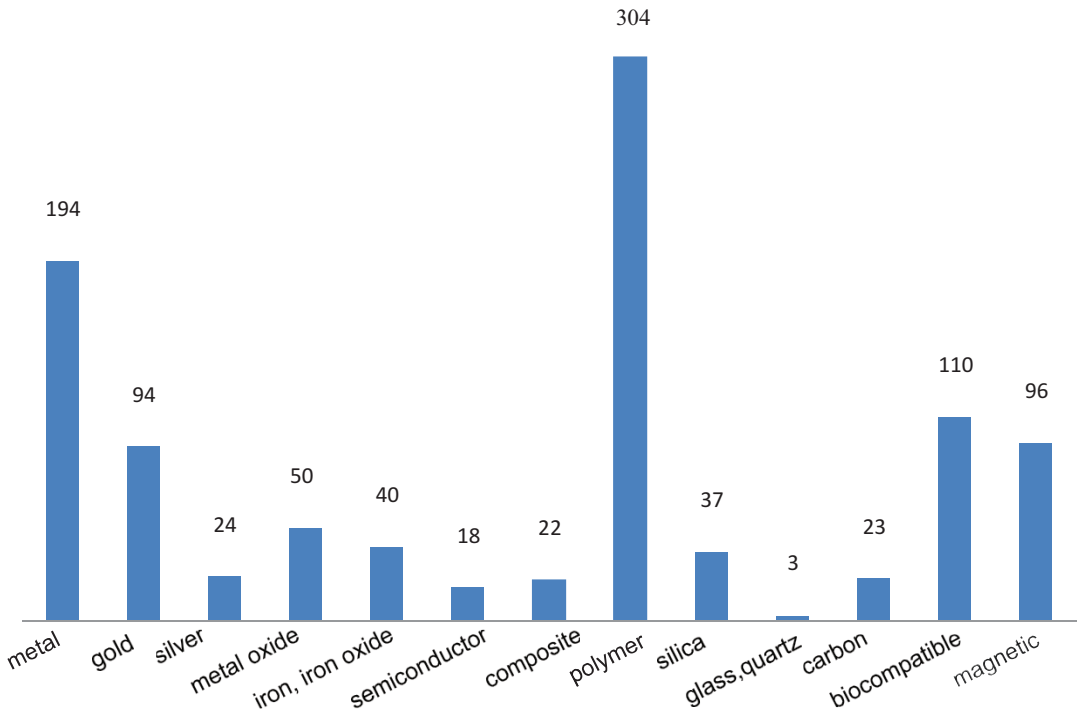

Fig. 25.3 Patent distribution on the basis of nanoparticle types

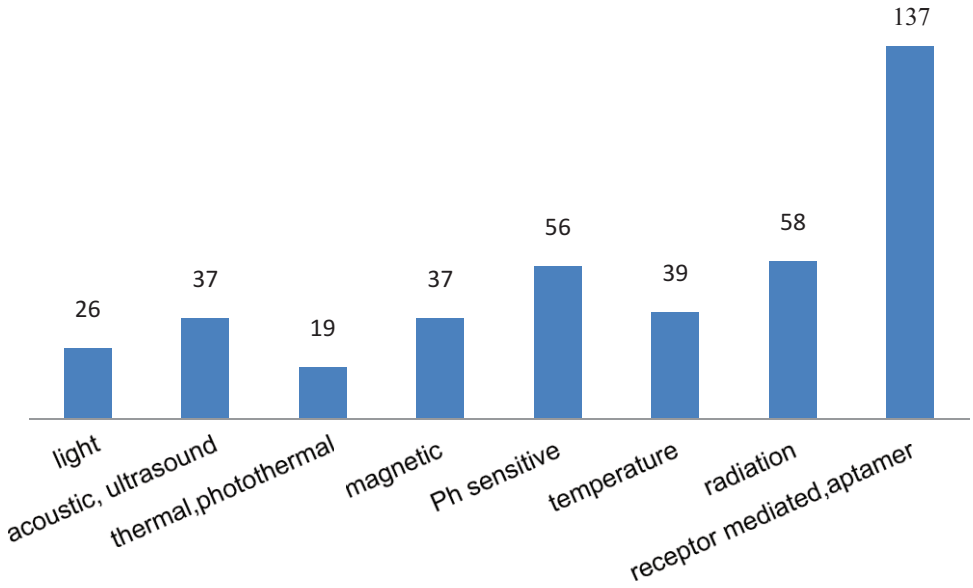

Fig. 25.4 Patent distribution on the basis of various stimuli

used for treating hypoxic tumors with nanoparticles used with photosensitizing agent.

Figure 25.5 represents the patent distribution according to the routes of administration of the drug particle. According to the represented analysis, the most commonly used route is parenteral, owing to the fact that the effects of the medication are much rapid and that it can be adminis-

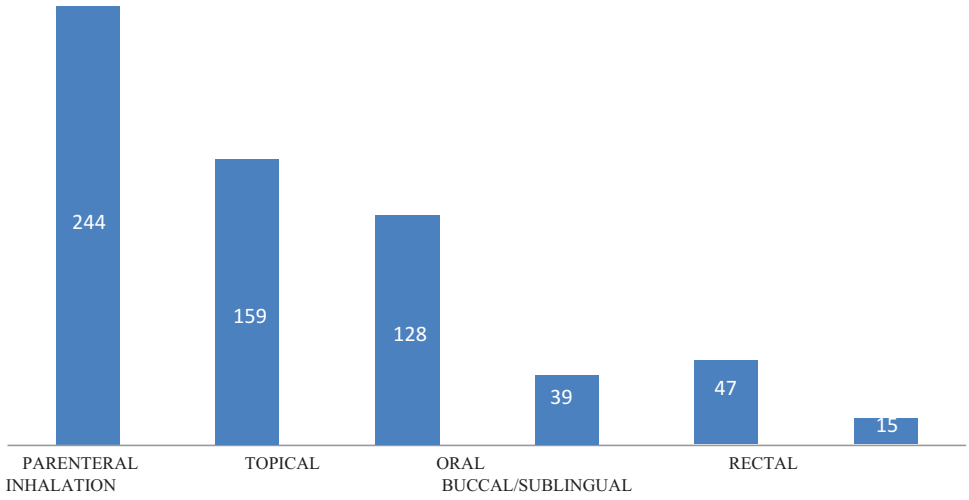

Fig. 25.5 Patent distribution on the basis of routes of administration

Fig. 25.6 Patent distribution on the basis of forms of delivery

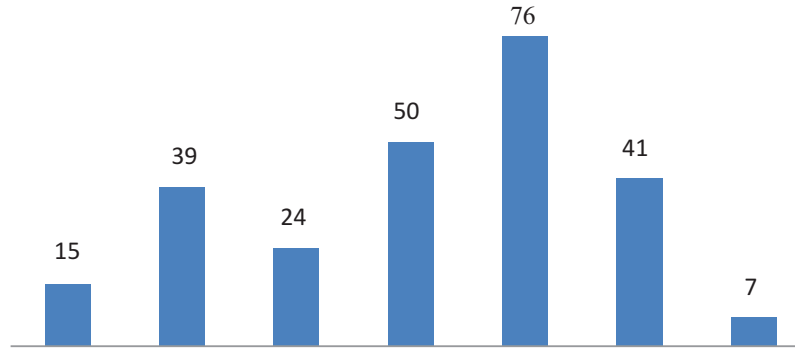

tered directly to the site. Following this trend, topical route is the second most important as this method of treatment is used to avoid systemic side effects when high doses are required at a localized area or as an alternative systemic administration route to avoid hepatic processing. For example, patent **US20130195983A1** talks about treating carcinoma and sarcoma classes of cancer by using the parenteral routes of action, more specifically the intravenous route.

Figure 25.6 depicts the patent distribution on the basis of form of delivery. Earlier known as lipid vesicles, the recent most popular form of delivery of the drugs is liposomes, as is evident from the graph. The exceptionally high use of liposomes accounts to the fact that they have high retention rates and excellent targeted sustained release. Following closely is the use of gels, mainly in rectal and oral formulations, as it is easy to administer over the affected area. For example, patent **CN100515497C** talks about liposomal drug delivery using nanoparticles to treat ovarian cancer conditions. Table 25.1 represents the different features of the mentioned routes of administration. The first-pass effect (mentioned in Table 25.1) is defined as phenomenon of drug metabolism whereby the concentration of a drug is greatly reduced before it reaches the systemic circulation (Fig. 25.7).

Nanoparticles as drug delivery systems enable unique approaches for cancer treatment. Nanoparticles are often used to deliver drugs, especially those that are highly toxic, directly to cancer cells. For example, patent **CN100515497C**

Table 25.1 Delivery routes and their properties

S. no.	Delivery route	Preferred forms of delivery	Type of effect	Bioavailability	Absorption
1	Oral	Tablets, capsules, gels	Systemic	5–100%	First-pass effect
2	Parenteral	Aqueous solutions, aerosols	Systemic	75–100%	Rapid effect
3	Buccal/ sublingual	Tablets	Systemic	5–100%	First-pass effect
4	Rectal	Aqueous solutions, cream, gel	Local	30–100%	50% first-pass effect
5	Topical	Creams, gel, aerosol, aqueous solution	Local	80–100%	Sustained effect
6	Inhalation	Aerosol sprays	Systemic, local	5–100%	Rapid effect

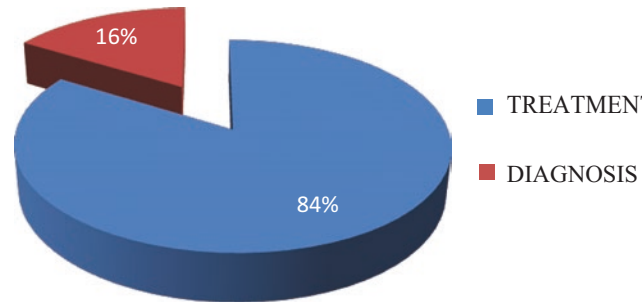

Fig. 25.7 Purpose of drug delivery

uses liposomal drug delivery systems to treat ovarian cancer. More recently developed nanoparticles are demonstrating the potential sophistication of these delivery systems by incorporating multifunctional capabilities and targeting strategies, in an effort to increase the efficacy of these systems against the most difficult challenges in cancer treatment, including drug resistance and metastatic disease. Another example is **WO2010003232A1**, which discloses the therapeutic action of drugs using nanoparticles to typically treat breast cancer forms. For diagnosing the cancer types and to detect the disease, different types of diagnostic methods are used, which include MRI, tomography, imaging, and CAT scan. Microbeam radiation therapy (MRT) can be enhanced by the prior administration of gadolinium-based nanoparticles to the patient. The nanoparticles also improve contrast in magnetic resonance imaging (MRI) permitting localization of the tumor. For example, patent **WO2005021501A1** directly refers the therapeutic and the diagnostic methods for the renal function monitoring analysis.

Figure 25.8 comprises the patent distribution trends relating the five broad classifications of cancer types. Most widely treated cancer is carcinoma, which contributes the highest ratio of patents as analyzed from the above graph. Carcinoma class includes the most common type of cancers occurring in humans and can be cured using the technology implying nanoparticles, while sarcoma cancers, related to bone and the connective tissues, are a very complex category and are difficult to treat using any technique. Hence, sarcoma class of cancers are least curable using nanoparticles as drug delivery methods. Table 25.2 classifies the different types of cancers and explains those giving relevant examples from the patent analysis (Fig. 25.9).

Imaging *An MRI (or magnetic resonance imaging)* scan is a radiology technique that uses magnetism, radio waves, and a computer to

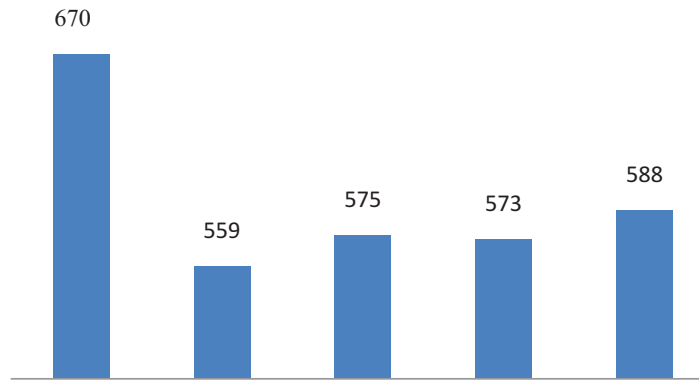

Fig. 25.8 Patent distribution on the basis of various cancer types

produce images of body structures. Example – patent **US20100183504A1** reveals a method that detects diseased cancer cell types using MRI techniques.

Ultrasonic imaging – Ultrasonic imaging is a mature medical technology. It accounts for one in four imaging studies and this proportion is increasing.

Computed Tomography A CT scan may be used to make sure a procedure is done correctly. For example, the doctor may use CT to guide a needle during a tissue biopsy or to guide the proper placement of a needle to drain an abscess. For example, **US20070031337A1** shows the use of gold nanoparticles, which bind to a specific receptor site and thus are used for tomography purposes.

Magnetic Resonance Spectroscopy (MRS) MR spectroscopy is conducted on the same machine as conventional MRI (see magnetic resonance imaging). The MRI scan uses a powerful magnet, radio waves, and a computer to create detailed images. Spectroscopy is a series of tests that are added to the MRI scan of your brain or spine to measure the chemical metabolism of a suspected tumor.

Figure 25.10 depicts the patent distribution trends according to their diagnostic applications. The most widely used applications include primarily imaging techniques. Nanoparticle types like manganese oxide particles are used as contrasting agent in MRI scan thus, accounting to its wide application. Apart from MRI scanning, the nanoparticles, especially gold, are used as optical resonance factor for tomography.

Some Important Trends in Technology Heads

This section includes trends in relation to the nanoparticle type and various other technology heads. Here, trends have been shown to signify the growing demand of a particular type of nanoparticle and what is the percentage focus with respect to other technology heads.

Polymer-Based Nanoparticle

Figure 25.11 shows the exponentially increase in use of polymer-based nanoparticle for the targeted drug delivery to cancerous cells, and there are certain combinations of polymer-based nanoparticles with other technology heads that are generally preferred. For example, the analysis shows that a more preferred form of delivery for polymer-based nanoparticle is gel due to its high absorption and high gel strength.

Gold Nanoparticle

Figure 25.12 shows the exponential increase in use of gold nanoparticles over the recent years, for the targeted drug delivery to cancerous cells.

Recent Patents:

- **US 20050256360 A1** – patent on gold nanoparticles for anti-epidermal growth factor

Table 25.2 Various cancer types with relevant patent examples

S. no.	Cancer types	Definition	Example
1	Carcinoma	Cancers that begin in the skin or in tissues that line or cover internal organs fall under this class	**EP1796683A1** depicts the method, compositions, and administration of calcium chelators to treat carcinoma
2	Lymphoma and myeloma	Cancers that begin in the cells of the immune system are referred in this category	Patent **US20120195961A1** has its claims based upon the use of spinosyn compositions for treating solid tumors, a lymphoma type of blood cancer, in humans
3	Leukemia	Leukemia refers to the cancer that starts in blood-forming tissue such as the bone marrow and causes a large number of abnormal blood cells to be produced and enter the blood	In patent **US20120039995A1** an arsenic compound is being used for treating the leukemia type of blood cancer
4	Sarcoma	Cancer that begins in the bone, cartilage, fat, muscle, blood vessels, or other connective or supportive tissue comes under this category of cancer	Patent **WO2013082535A2** with an oligo-receptor binding ability is useful for treating the sarcoma group of cancer
5	Central nervous system (CNS) cancer	Cancers that begin in the tissues of the brain and spinal cord, nervous disorders, and childhood disorder and thus the subsequent occurrence of brain cancer are called CNS class of cancer	Nanoparticles using oral and parenteral routes of drug administration are used as claimed by patent **EP1682152A2** to treat the brain cancer forms

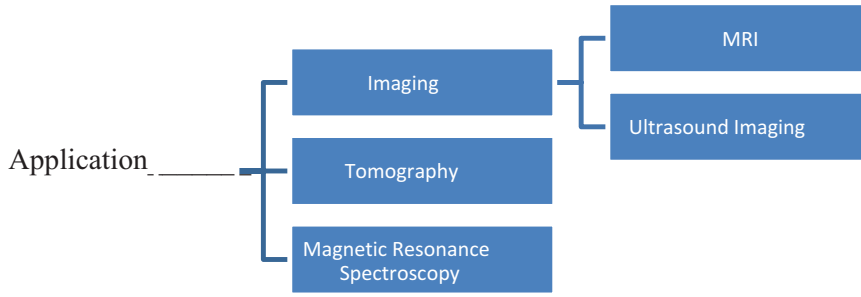

Fig. 25.9 Various diagnostic applications

receptor (EGFr) with active targeting and radiosensitization effect used for radiotherapy.

- **US 20100034735 A1** – patent on gold nanoparticles for cysteamine (AET) and thioglucose (Glu) with active targeting and radiosensitization effect used for radiotherapy.
- **WO 2009091597 A2** – patent on gold nanoshells for polyethylene glycol SHPEG with passive targeting; LPSR used for thermo-radiotherapy.
- **US20060034925** – patent on PLGA nanoparticles for bioadhesive coating with active targeting; drug delivery used for chemotherapy.
- **WO2000074658A1** – patent on polyacrylates, polymethacrylates, and polycyanolacrylates for Tween 80 with active targeting; drug delivery used for chemotherapy.

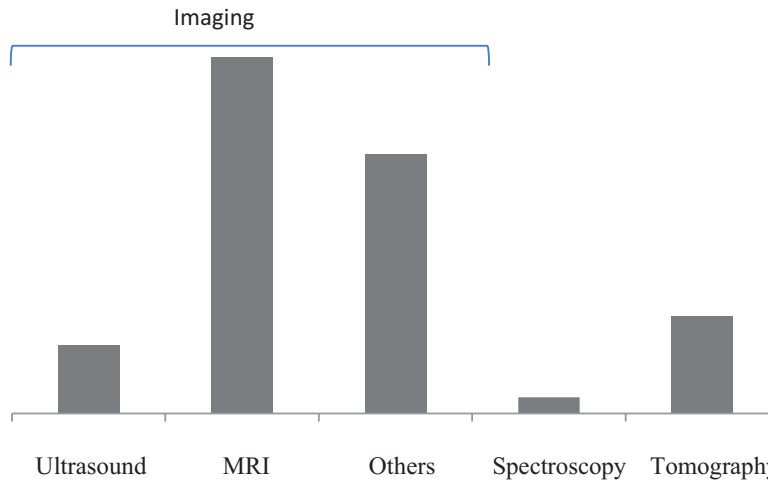

Fig. 25.10 Patent distribution on the basis of applications

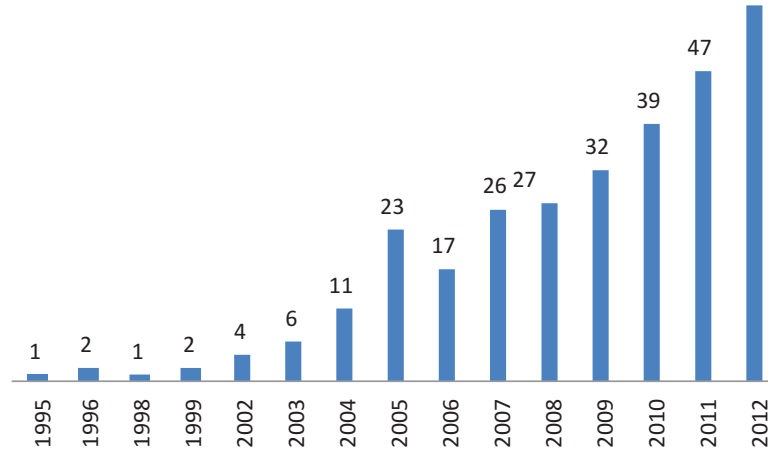

Fig. 25.11 Patent distribution trend of polymer-based nanoparticle type

- **WO2011088456** – patent on PEI and a polynucleotide for encoding p53 glucose/polyethyleneglycol (PEG) with active targeting; drug delivery used for chemotherapy.
- **EP1206251A1** – patent on derivatized isobutyl cyanoacrylate (IBCA) nanocapsules with folate with active targeting; drug delivery used for chemotherapy.
- **US 20100137206 A1** – patent on micelles as targeting peptide (sequence RGD4C) with active targeting; drug delivery used for chemotherapy.
- **US 7229973 B2** – patent on micelles as folate with active targeting; drug delivery used for chemotherapy.
- **US6090955** – patent on liposome with active targeting; drug delivery used for chemotherapy.
- **WO2001034130A1** – patent on liposome with active targeting; drug delivery used for chemotherapy.
- **US 20020127224A1** – patent on DdSe quantum dot coated with ZnS with tumor blood vessel antigen with light-emitting particles; photosensitizer activation used for photodynamic therapy.
- **US 20110237862 A1** – patent on quantum dots with iron oxide (Fe3O4), magnetic oxide nanoparticle coated with a silica (SiO2) shell and linked with CdSe/ZnS quantum dot with radiofrequency absorber used for radiofrequency ablation.
- **US20130183354** – patent on carbon nanotubes with human annexin V with active targeting, which emits heat when absorbed energy is used for thermal ablation.

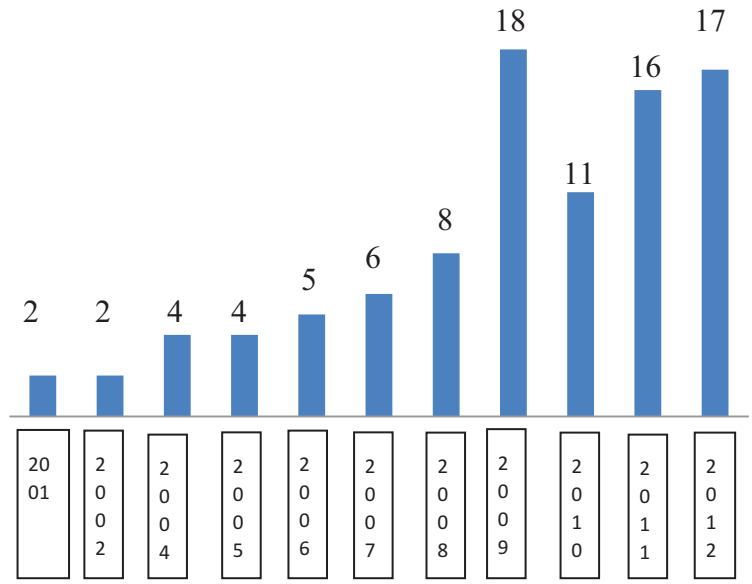

Fig. 25.12 Patent distribution trend of gold nanoparticle type

- **WO 2008082374 A2** – patent on carbon nanotubes which emit heat when absorbed energy is used as therapeutic nanobomb.

References

Cai W, Chen X. Nanoplatforms for targeted molecular imaging in living subjects. Small. 2007;3:1840–54.

Compositions and methods for modified dendrimer nanoparticle vaccine delivery. US201562222515P.

Dang Y, Zhang Y, Fan L, Chen H, Roco MC. Trends in worldwide nanotechnology patent applications: 1991 to 2008. J Nanopart Res. 2010;12:687–706.

Hosen SM. Pharmaceutical nanotechnology- a short review. 2015. https://doi.org/10.13140/RG.2.1.1432.7523.

Jeevanandam J, Barhoum A, Chan YS, Dufresne A, Danquah MK. Review on nanoparticles and nanostructured materials: history, sources, toxicity and regulations. Beilstein J Nanotechnol. 2018;9:1050–74. Published 2018 Apr 3. https://doi.org/10.3762/bjnano.9.98.

Miele E, Spinelli GP, Miele E, Tomao F, Tomao S. Albumin-bound formulation of paclitaxel (Abraxane ABI-007) in the treatment of breast cancer. Int J Nanomedicine. 2009;4:99–105. https://doi.org/10.2147/ijn.s3061.

Mody MR. Cancer nanotechnology: recent trends and developments. Int J Med Update. 2011;6(1):3–7.

Patra JK, Das G, Fraceto LF, et al. Nano based drug delivery systems: recent developments and future prospects. J Nanobiotechnol. 2018;16:71. https://doi.org/10.1186/s12951-018-0392-8.

Ranjan S, Dasgupta N. Nanoscience in food and agriculture: Springer. ISBN 978-3-319-39303-2; 2016. https://doi.org/10.1007/978-3-319-39303-2.

Sekhon B. Nanotechnology in agri-food production: an overview. Nanotechnol Sci Appl. 2014;7:31–53. https://doi.org/10.2147/NSA.S39406.

Shi J, Votruba AR, Farokhzad OC, Langer R. Nanotechnology in drug delivery and tissue engineering: from discovery to applications. Nano Lett. 2010;10(9):3223–30. https://doi.org/10.1021/nl102184c.

Singh N. Nanotechnology innovations, industrial applications and patents. Environ Chem Lett. 2017;15:185–91. https://doi.org/10.1007/s10311-017-0612-8.

Sokolov K, Follen M, Aaron J. Real time vital optical imaging of precancer using anti-epidermal growth factor receptor antibodies conjugated to gold nanoparticles. Cancer Res. 2003;63:1999–2004.

Tanaka T, Shiramoto S, Miyashita M, Fujishima Y, Kaneo Y. Tumor targeting based on the effect of enhanced permeability and retention and mechanism of receptor-mediated endocytosis. Int J Pharm. 2004;277:39–61.

Ventola CL. Progress in nanomedicine: approved and investigational nanodrugs. Pharm Ther. 2017;42(12):742–55.

Wang Y, Shurong M, xi Z. A synergistic combination therapy with paclitaxel and doxorubicin loaded micellar nanoparticles. Colloids Surf B: Biointerfaces. 2014;116:41–8.

www.lexxinnova.com. Nanoparticles smart drug delivery system for cancer

Zhao CY, Cheng R, Yang Z, Tian ZM. Nanotechnology for Cancer therapy based on chemotherapy. Molecules. 2018;23(4):826. Published 2018 Apr 4. https://doi.org/10.3390/molecules23040826.

Part VII

Injectable Nanosystems

26

Injectable Nanosystems and Inherent Nanoparticulate-Serum Interactions

Mershen Govender, Sunaina Indermun, Pradeep Kumar, Yahya E. Choonara, and Viness Pillay

Abstract

The development of nanoparticulate systems has been shown to be highly effective in the advancement of pharmaceutical drug delivery technology. The use of these systems, however, has been shown to have significant physical and chemical effects on blood constituents, especially when delivered via intravenous injection. These effects have been shown to impact not only the individual blood constituents and their physiological roles but also the efficacy of the nanoparticulate formulation as well. Numerous studies have therefore focused on the impacts of nanoparticulate delivery on blood and have detailed the modifications undertaken to ensure hemocompatibility. This chapter will therefore focus on the interactions between nanoparticulate delivery systems and blood constituents upon delivery, the effect of these interactions and the newer research that has been performed to overcome the known issues of nanoparticle blood compatibility.

M. Govender · S. Indermun · P. Kumar
Y. E. Choonara · V. Pillay (✉)
Wits Advanced Drug Delivery Platform Research Unit, Department of Pharmacy and Pharmacology, School of Therapeutic Sciences, Faculty of Health Sciences, University of the Witwatersrand, Johannesburg, Gauteng, South Africa
e-mail: viness.pillay@wits.ac.za

Keywords

Nanoparticulate system · Injectable delivery · Serum-Protein interactions · Hemocompatibility · Blood coagulation

1 Introduction

Nanosystems have been widely developed over the past few decades for their enhanced drug delivery applications. These systems, while effective, however, do exert an inherent effect on the physiological environment upon administration. Injectable systems which deliver drug directly to system circulation instantaneously come into physical contact with blood constituents. These include blood cells, platelets, and proteins, each of which have a different interaction upon contact with nanosystems (Fig. 26.1) (De La Cruz et al. 2017).

The interaction that occurs upon administration of nanosystems is dependent largely on the properties of the drug delivery system with the size, surface charge, and properties and morphology having a significant impact on the viability and functionality of the respective blood constituents. With these interactions, research has focused on the hemocompatibility of drugs as a significant component of nanoparticle development. This has resulted in significant modifica-

J. K. Patel, Y. V. Pathak (eds.), *Emerging Technologies for Nanoparticle Manufacturing*,
https://doi.org/10.1007/978-3-030-50703-9_26

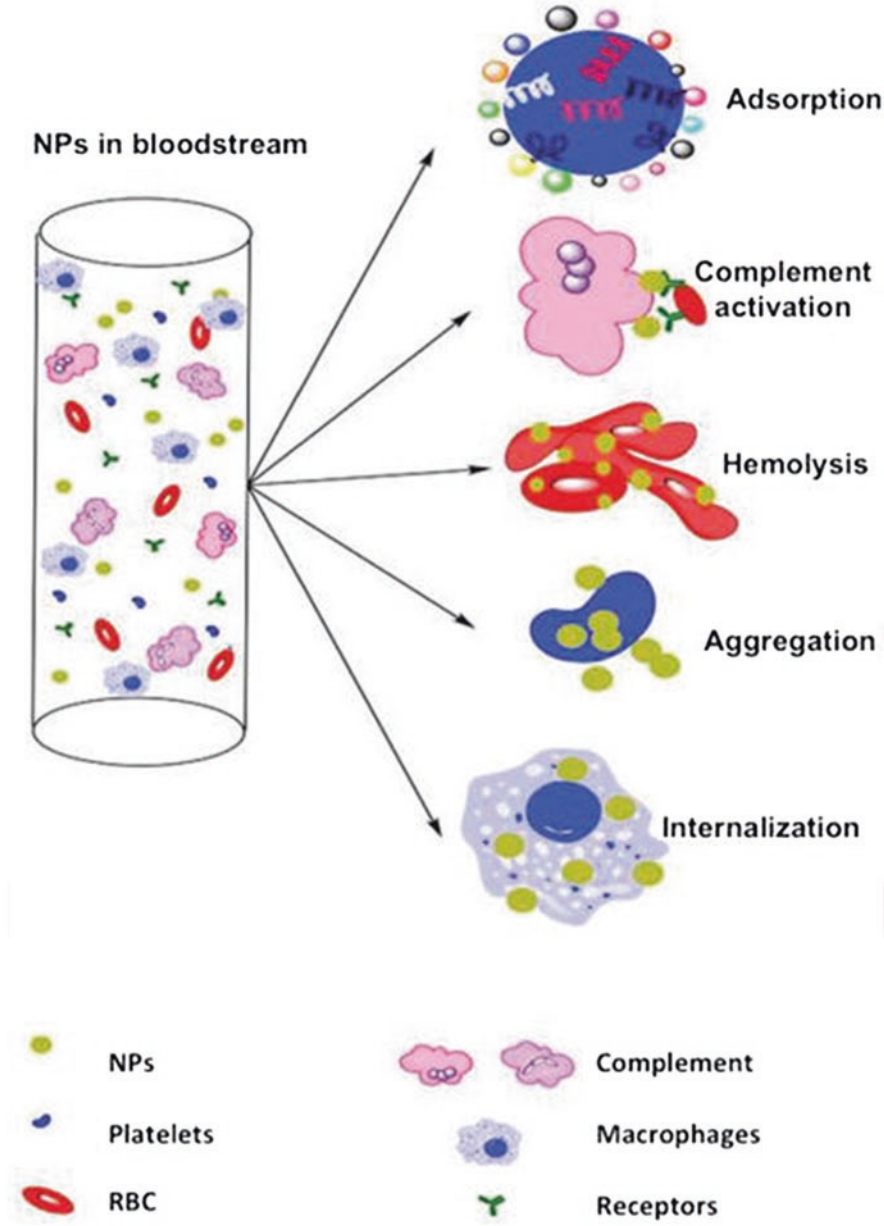

Fig. 26.1 Interaction of nanoparticles with bloodstream components and physiological effects. (Reproduced from De La Cruz et al. (2017) © 2017 The Author(s) Licensee IntechOpen)

tions to the developed particles to ensure that limited side effects occur upon administration.

With the need for the development of hemocompatible nanoparticles devoid of significant nanoparticle-serum constituent interactions, research has further used these interactions for the advancement of patient treatment through the development of systems such as platelet aggregates or immune enhancers (Gu 2018). These systems using innovative technologies have been shown to successfully utilize physiological processes to enhance nanoparticle efficacy.

This chapter will therefore focus on the impact of nanoparticulate delivery, primarily through the

intravenous route, on serum constituent efficacy, viability, and functionality. These constituents which include serum proteins, platelets, red blood cells, and immune cells interact with nanoparticulate in various ways, each with a potential physiological impact (De La Cruz et al. 2017; Zolnik et al. 2010; Gamucci et al. 2014). Research that has utilized these interactions for the advancement of therapeutic treatment has also been highlighted and discussed.

2 Interaction Between Nanoparticulate Systems and Serum Proteins

Numerous articles have been published highlighting the hemocompatibility of developed injectable nanoparticulate drug delivery systems. Research has shown that the physical interaction between nanoparticles and serum proteins often results in the development of the protein corona, which occurs when ionic-charged nanoparticles interact with the colloidal surface of serum proteins forming a biomolecular adsorption layer (De La Cruz et al. 2017; Abstiens et al. 2019). This protein corona consists of both soft and hard layers formed around the nanoparticle surface instantly upon administration of the nanoparticles due to interactions between the serum proteins and nanoparticles and is a result of London dispersion, Coulomb forces, p–p stacking, hydrogen-bonds and hydrophobic interactions. Particle properties such as particle size, surface curvature, charge, hydrophobicity, and topography have also been recognized to determine the kinetic degree and identity of the protein corona formation (Abstiens et al. 2019). The effect of the protein corona formation is significant as conformational changes of the protein adsorbed onto the surface of nanoparticles may result in new epitope exposure as well as functional and affinity changes (Parveen et al. 2017; Zhang et al. 2019; Liu et al. 2020). Due to these changes, variations of biological function may occur and as a result may cause potential biological injury. In order to assess the conformational changes, various spectroscopy techniques are generally employed as highlighted in Fig. 26.2.

A study undertaken by Abstiens et al. (Abstiens et al. 2019) investigated the interaction of functionalized polymeric nanoparticles with varying hydrophobicity and surface charge on serum proteins with emphasis on cargo leaching and colloidal stability from the nanoparticles. The results of this study detailed that the developed zwitterionic nanoparticles were least affected by the protein corona development as compared to the polymeric colloids functionalized with uncharged methoxy groups or negatively charged carboxylate groups. The reason given for this result was that the zwitterionic nanoparticles provide only a limited probability for serum proteins to interact via hydrophobic or electrostatic forces. The study also determined that positively charged nanoparticles have a greater interaction with serum proteins when compared to the other nanoparticles evaluated. This resulted in a decreased colloidal stability and increased leaching of drug from the nanoparticle core.

The protein corona furthermore has significant impacts on the cellular environment within the body. The degree of these effects however varies greatly from insignificant to apoptosis of the respective cell. The comprehensive review of the impact of the formed protein corona and its impact of nanoparticles and cells can be found in Table 26.1.

3 Interaction Between Nanosystems and Serum Blood Cells

Interactions between delivered nanosystems and serum blood cells are important to determine that unwanted side effects associated with blood cell changes do not occur. Various studies have been undertaken to investigate the effects of prepared nano-formulations on serum blood cells. One such study was undertaken by Bruckman et al. (Bruckman et al. 2014) and detailed the hemocompatibility of virus nanorods and nanospheres in mice serum specifically with hemolysis and blood coagulation (Fig. 26.3). The PEGylated tobacco mosaic nanosystems administered intra-

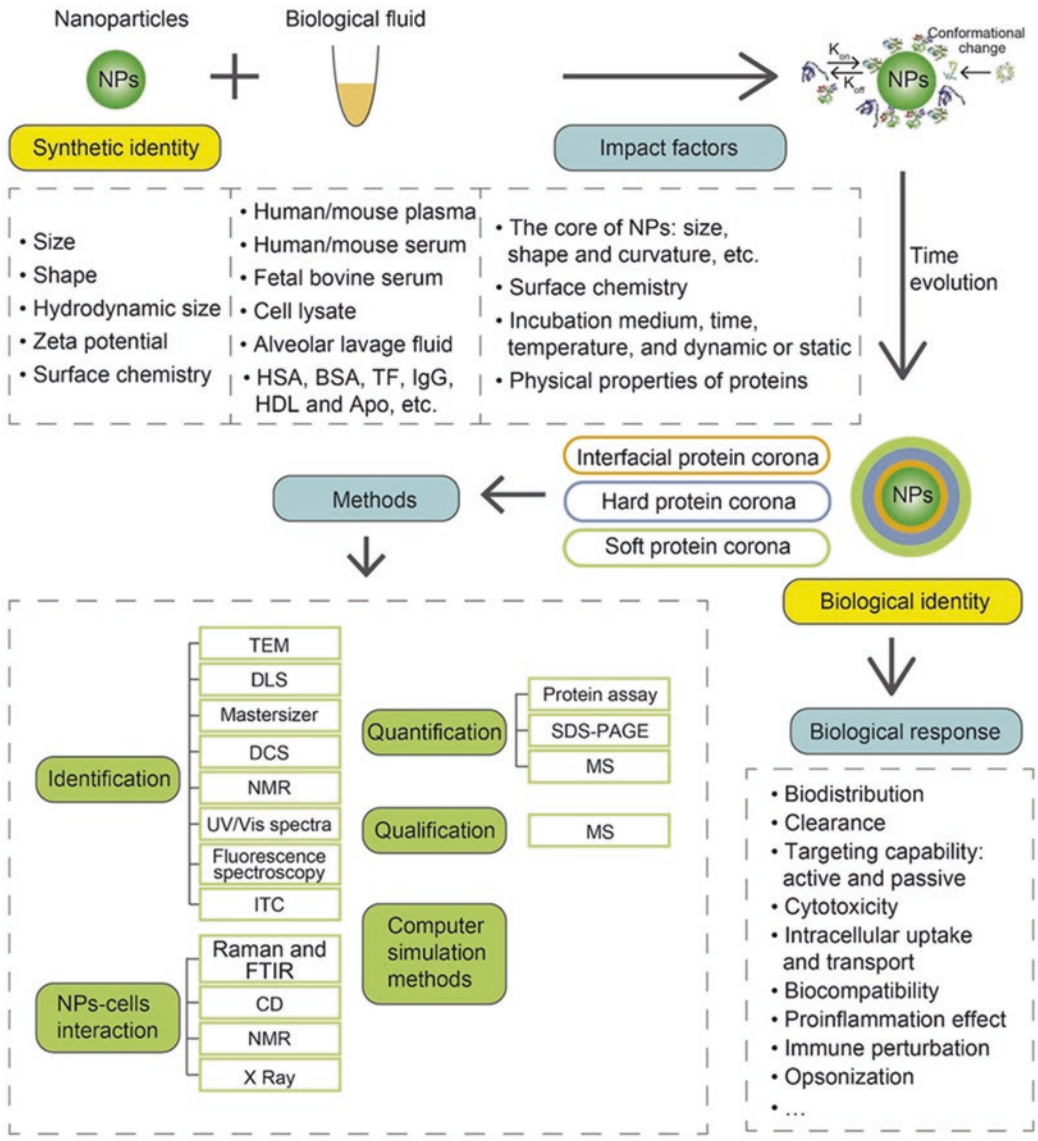

Fig. 26.2 The experimental workflow of protein corona and impact factors. *TEM* Transmission electron microscope, *DLS* Dynamic light scattering, *DCS* Differential centrifugation sedimentation, *NMR* Nuclear magnetic resonance, *ITC* Isothermal titration calorimetry, *FTIR* Fourier transform infrared, *CD* circular dichroism, *MS* Mass spectrometry. (Reproduced with permission from Liu et al. (2020) © 2019 Elsevier Ltd)

venously were determined to have minimal effects on red blood cell integrity and blood coagulation. While the properties of the developed systems in this study were shown to have positive results with regard to hemocompatibility, this study highlights the importance of evaluating the effects of nanosystems on blood cell properties and integrity.

Another study undertaken by Li and coworkers (LiH-C et al. 2013) investigated the hemocompatibility effects of monocrystalline nanodiamonds (NDs). The hemolytic ability was assessed in human red blood cells (RBCs). It was found that there was no RBC destruction irrespective of particle size (35–500 nm) and that the particles lacked thrombogenic activity.

Table 26.1 The impact of protein corona on the interaction between nanoparticles and cells

Type of protein corona	Nanoparticles	Size by TEM (nm)	Cell type	Level of cellular uptake	Level of cytotoxicity/type of immunotoxicity
DMEM with 10% FBS	Ag-CIT NPs	15 ± 3	NIH-3 T3	Up	Apoptosis
HSA	Ag-PVP NPs Ag-CIT NPs	20	SH-SY5Y HepG2	Down Down	Up Up
HSA	Ag-CIT NPs	20 110	HEK	Down Down	–
	Ag-SiO_2 NPs	20 120		ns ns	
IgG	Ag-CIT NPs	20 110	Down Down		
	Ag-SiO_2 NPs	20 120	Up Ns		
Tf	Ag-CIT NPs	20 110	Down Down		
	Ag-SiO_2 NPs	20 120	ns ns		
BSA	Ag-CIT NPs	20	RAECs	Down	ER stress
HDL				Down	ER stress
FBS				Down	ER stress
HSA BSA HDL	Ag-CIT NPs	20	RLECs and RAECs	Down	Cell activation; inducing IL-6 expression
10% FBS	Ag-CIT NPs 20 Ag-PVP NPs	20 110 20 110	RAW264.7	Up Up Up ns	Down Down Down Down
BSA	Ag-CIT NPs	20 110		Up Up	Down ns
	Ag-PVP NPs	20 110		Down ns	Down ns
Fibrinogen	Ag-PAA NPs	5	THP-1	–	Pro-inflammatory effect
Clusterin	Ag NPs	10	dTHP-1	Down	–
	SiO_2 NPs	70			
10% HS	SiO_2 NPs	50	M1 macrophages M2 macrophages	Down Down	–
10% heat-inactivated HS			M1 macrophages M2 macrophages	Block Block	
HAS			M1 macrophages M2 macrophages	Block Block	
10% FBS	SiO2 NPs	12 and 50	A549 and RAW264.7	Up	Down
Murine lung tissue fluid (TGF-b1)	SiO2 NPs	100	A549 cells	–	Epithelial-mesenchymal transition (EMT)
55% HP	BPEI-AuNPs LA-AuNPs PEG-AuNPs	40	HUVEC	Down Down no	Down Down Down

(continued)

Table 26.1 (continued)

Type of protein corona	Nanoparticles	Size by TEM (nm)	Cell type	Level of cellular uptake	Level of cytotoxicity/type of immunotoxicity
HAS	BPEI-AuNPs LA-AuNPs PEG-AuNPs	40 and 80		Up Down Uo	Down Down Down
DMEM with 10% FBS	PEG-Au NPs	5, 20, and 50	RAW 264.7 HepG2	Down	–
HS	PS-COOH NPs PS-NH_2 NPs	100	3D HepG2 cells	Up	–
FBS	PS-COOH NPs	40	A549	Down	–
HS	PS-COOH NPs	50	hMSCs	Ns	–
Human ApoA-4				Down	
Human ApoC-3				Down	
Human AntIII				Ns	
THRB				Ns	
VTN				Ns	
ApoH				Up	
SP-A	CH-mNPs	110–180	Murine AMs	Up	–
BSA	PMO-mNPs PL-mNPs			Down	
FCS	PEI-SPIO NPs	182 by DLS	hBMECs	Down	
BSA	Fe3O4 NPs	20	HeLa cells	Down	Down
BTf				Down	Down
Big				Down	Down
BFG				Down	Down
FBS	MHA NPs	14 × 2	MC3T3-E1 cells	–	Cell proliferation
Tf	FePt-COOH	5.6	HeLa cells	Down	–
HAS	NPs			Down	
BSA	GO NPs	250.63 ± 9.76	A549 HEK 293	Down Up	–
FBS	CdS NPs	30	NR8383 cells	Down	Apoptosis
HP	BP QDs	5	dTHP-1	Up	Pro-inflammatory effect Immune perturbation
FBS	PM2.5	–	HLFs	–	Aberrant proliferation

FBS, fetal bovine serum; HS, human serum; HSA, human serum albumin; Apo, apolipoprotein; Ant, antithrombin; THRB, coagulation factors prothrombin; VTN, vitronectin; SP-A, surfactant protein-A; BSA, bovine serum albumin; FCS, fetal calf serum; Tf, transferrin; BFG, bovine fibrinogen; HDL, high-density lipoprotein; HP, human plasma; TGFb1, transforming growth factor-b1. CIT, citrate; PS, polystyrene; CH, chitosan; mNPs, magnetite NPs; PMO, poly-maleic-oleic acid; PL, phosphatidylcholine; PEI, polyethylenimine; SPIO, superparamagnetic iron oxide; BPEI, branched polyethylenimine; LA, lipoic acid; PEG, polyethyleneglycol; GO NPs, gelatin-oleic NPs; PV, polyvinylpyrrolidone; PAA, poly(acrylic acid); BP QDs, black phosphorus quantum dots; MHA, magnetic hydroxyapatite; NIH-3 T3 cells, mouse embryonic fibroblast; hMSCs, human mesenchymal stem cells; AMs, alveolar macrophages; hBMECs, human brain microvascular endothelial cells; HeLa cells, human cervix carcinoma cells; HepG2 cells, human hepatocellular liver carcinoma cell line; A549 cells, lung carcinoma cells; HPTCs, human proximal tubule cells; HUVECs, human umbilical vein endothelial cells; RAW 264.7, mouse leukemia cells of monocyte macrophage; HEK 293, human embryonic kidney cells; SH-SY5Y, human neuroblastoma cells; RAECs, rat aortic endothelial cells; RLECs, rat lung epithelial; dTHP-1, differentiated human leukemic monocyte; NR8383 cells, rat lung macrophage line; HLFs, human lung fibroblasts; MC3T3-E1 cells, mouse embryonic osteoblast precursor cells

Ns: no significant effect

Adapted with permission from Liu et al. (2020)© 2019 Elsevier Ltd

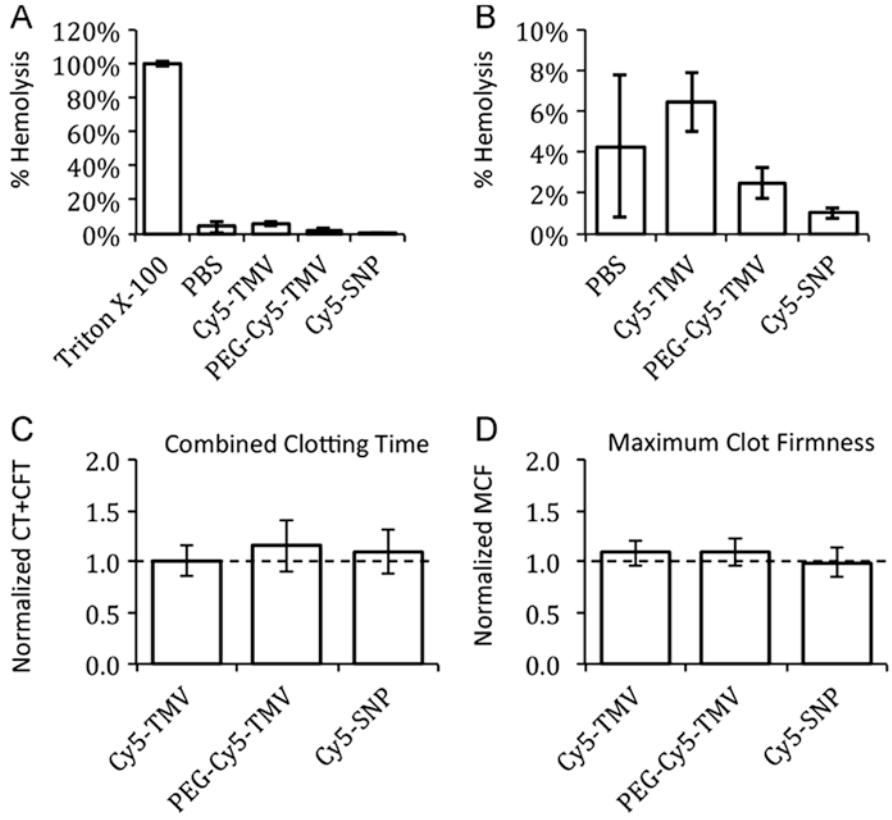

Fig. 26.3 Blood biocompatibility assays. (**a**) Red blood cell (RBC) hemolysis assay. (**b**) Zoomed in RBC hemolysis assay showing Cy5-TMV, PEG-Cy5-TMV, and Cy5-SNP do not lyse RBCs. Effect of Cy5-TMV, PEG-Cy5-TMV, and Cy5-SNP on (**c**) clotting (normalized to saline control) and (**d**) maximum clot firmness (MCF), measured in rotational thromboelastometry (ROTEM). There were no significant changes in the combined clotting time (CTþCFT) and maximum clot firmness compared to the saline control (dotted line). Error bars represent S.D. (Reproduced with permission from Bruckman et al. (2014) © 2013 Elsevier Inc)

Synthesized through high-pressure-high-temperature (HPHT) methods, the NDs were found to also be non-cytotoxic on human primary endothelial cells. The inflammatory cytokine levels (IL-1b and IL-6) were not found to be significantly elevated after intravenous injection into FVB mice.

Other studies that prepared hemocompatible nanosystems included the study undertaken by Palazzo and co-workers (Palazzo et al. 2019) who developed injectable liposome (Lipo-E4) and drug-in-cyclodextrin-in-liposome (DCL-E4) formulations for the delivery of estetrol (E4) for the treatment of neonatal hypoxic-ischemic encephalopathy (HIE). This estradiol metabolite was encapsulated in the formulation to enhance blood-brain barrier (BBB) permeation. In vitro tests were conducted on endothelial (EAhy926, HUVEC), neuronal, (Neuro2a) and BBB model cells (hCMEC/D3) and the hemocompatibility was assessed. The formulation displayed good hemocompatibility and no cellular toxicity. In addition, the protein corona formed was approximately 8 nm in size, and no hemolytic effect was observed highlighting a protein interaction but no significant effect on red blood cells. Azmi and co-workers (Azmi et al. 2016) also fabricated internally self-assembled "somes" or nanoparticles from a binary lipid system consisting of citrem and soy phosphatidylcholine. A range of lyotropic lamellar and non-lamellar liquid crystalline nanodispersions displayed increased hemocom-

patibility and a lack of late stage complement activation upon interaction with serum constituents.

Modification of the prepared nanosystems has also been determined to have a significant effect on hemocompatibility upon administration. Once such study by Datta and co-workers (Datta et al. 2017) was undertaken on the in vitro characteristics of titanium dioxide (TiO_2) nanoparticles. The nanoparticles were studied for their biocompatibility effects on human serum albumin, hepatocellular carcinoma (HepG2) cell line, and erythrocytes. The nanoparticles were functionalized with hydroxyl (hydroxylated (OH-TiO_2) titania), amine (aminosilane (NH2-TiO_2)), or thiol (mercaptosilane (SH-TiO_2)) moieties and the respective influence on nanoparticle toxicity and protein binding investigated. The hemolytic ability of the nanoparticles was found to be reduced by the functionalized nanoparticles, and the nanoparticles functionalized with amine moieties were found to significantly enhance hemocompatibility. Dose-dependent cytotoxicity was also observed from both the pristine and functionalized nanoparticles. Cell viability was further found to be increased when the nanoparticles were functionalized with the aminosilane or mercaptosilane moieties.

Lin and co-workers (Lin et al. 2019), by studying the effects of positively charged pH-responsive micelles on blood, proposed a biomimetic phosphorylcholine strategy to enhance the hemocompatibility of these types of nanoparticles (Fig. 26.4). The nanoparticles were designed to be able to form self-assembling biomimetic phosphorylcholine micelles from amphiphilic copolymers containing varying umbers of tertiary amino groups. The phosphorylcholine functioned to protect the positive charges induced by the amino groups and thereby improve hemocompatibility. No significant effect was demonstrated on the RBCs, platelet activation, and coagulation.

An additional study undertaken by Singh and co-workers (Singh et al. 2018) utilized 1,3β-glucan as an outer shell to paclitaxel-loaded chitosan nanoparticles (1,3β-Cs-PTX-NPs) for the chemotherapeutic treatment of malignant glioblastoma. The ligand-based targeting delivery system was evaluated in vitro in glioma stem cell line (C6) and a glioma cancer cell line (LN-18) where the nanoparticles displayed a higher cellular uptake and internalization in the C6 line as well as a higher in vitro efficacy against both cell lines. The study also evaluated the hemolytic potential of the 1,3β-Cs-PTX-NP formulation in RBCs from mice blood and was found to be significantly reduced as compared to paclitaxel thereby allowing for intravenous delivery. Moreover, extended release of paclitaxel was established, leading to the non-specific systemic toxicity of paclitaxel. Wang and co-workers (Wang et al. 2019) further synthesized a series of poly (N-isopropylacrylamide) (PNIPA)/layered double hydroxides (LDHs)/nano-hydroxyapatite (nano-HA) hydrogels. At 33 °C, the PNIPA/LDHs/HA composite hydrogels exhibited reversible sol-gel behavior. Hemolysis was assessed using human whole blood, and the gels were found to display a hemolysis percentage of ~1%. An additional study by Xu and co-workers (Xu et al. 2019) developed a multifunctional nucleic acid delivery nanosystem (TP-Gd/miRNA-ColIV) for thoracic aortic dissection (TAD) treatment. The nanosystem successfully delivered miR-145 to prevent TAD deterioration. Moreover, the system was found to display good blood compatibility and be nontoxic to organs.

4 Interaction Between Nanosystems and the Blood Coagulation System

The effect of nanoparticulate delivery on blood clotting has been highlighted previously to be significant in the prevention of unwanted side effects (Fröhlich 2016). These effects are as a result of the numerous cascading of signals that occur upon the physical adhering interaction between the platelets and the nanoparticle structure leading to fibrin cross-linking and clot formation. This can be of significance due to potential formation of potentially deadly thrombi which can lead to strokes or other cerebrovascular accidents (De La Cruz et al. 2017). The study of

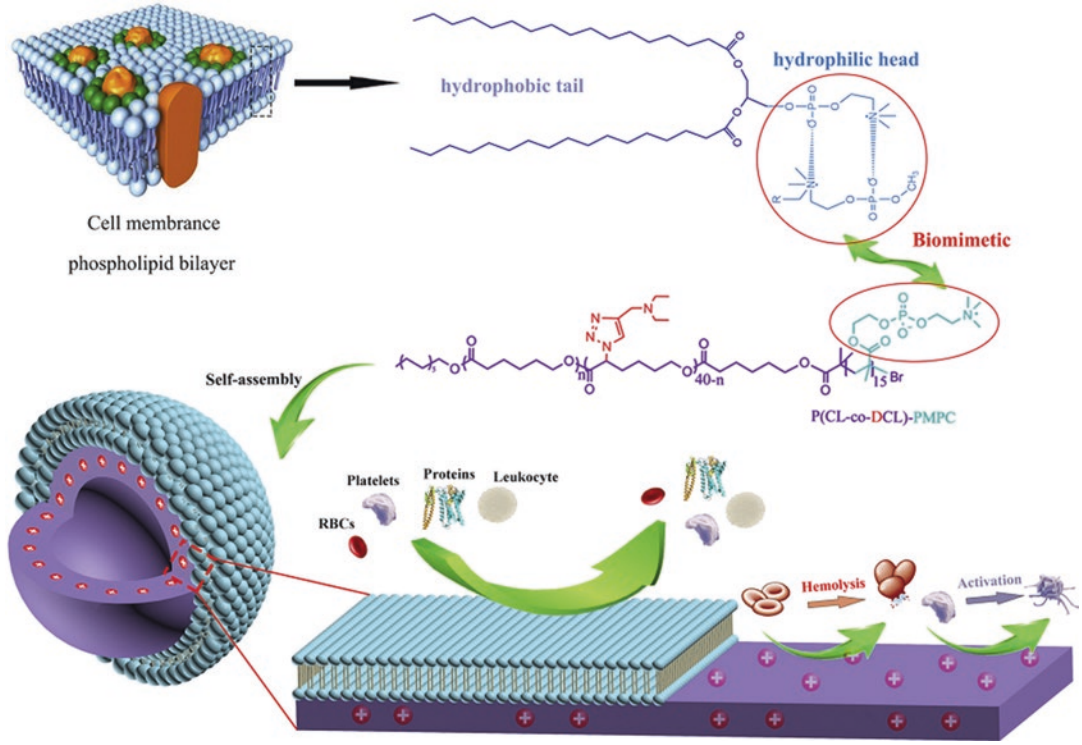

Fig. 26.4 Schematic illustration of the hemocompatibility of the micelles. (Reproduced with permission from Lin et al. (2019) © 2019 Elsevier B.V)

the effect of nanoparticle delivery on the coagulation system is therefore highly warranted and required.

The use of this interaction however can be advantageous as it allows for the controlling or modification of clotting functionality of the human body to exert required effects. In a study by Rajabi and co-workers (Rajabi et al. 2020), a nanocomposite hydrogel was fabricated for its potential as a sealant in surgical applications. This adhesive hydrogel contained thiolated gelatin (Gel-SH), gelatine methacrylate (GelMA), and polydopamine functionalized Laponite® (PD-LAP) which imparted an enhanced blood compatibility, blood clotting ability (2.25 min), and tissue adhesive strength to the nanocomposite gel (Fig. 26.5). In vitro cytocompatibility tests using L929 fibroblast cells revealed that after 5 days of various hydrogel culture, higher cell viability was demonstrated. The results also revealed a clotting time of more than 72% when in comparison to other tested sealants. The nanogel was found to be non-hemolytic with a hemolysis ratio of less than 5%.

Also, in the field of hydrogels, Zhao and coworkers (Zhao et al. 2018) developed injectable cryogels for hemorrhage and wound healing applications. The antibacterial conductive nanocomposite gels were composed of carbon nanotubes and glycidyl methacrylate functionalized quaternized chitosan. The hemostatic performance of the gels was assessed in mouse liver injury and mouse-tail amputation models by evaluating the bleeding and hemostatic times, whereby excellent hemostatic effects were observed. Additionally, the positive hemostatic effects were evaluated in the rabbit liver defect lethal non-compressible hemorrhage and standardized circular liver bleeding models. Results of these analyses revealed that the gels were found to also exhibit shape memory and wound healing properties. When evaluated against conventional hemostatic methods, the cryogels were also found to display superiority and a higher

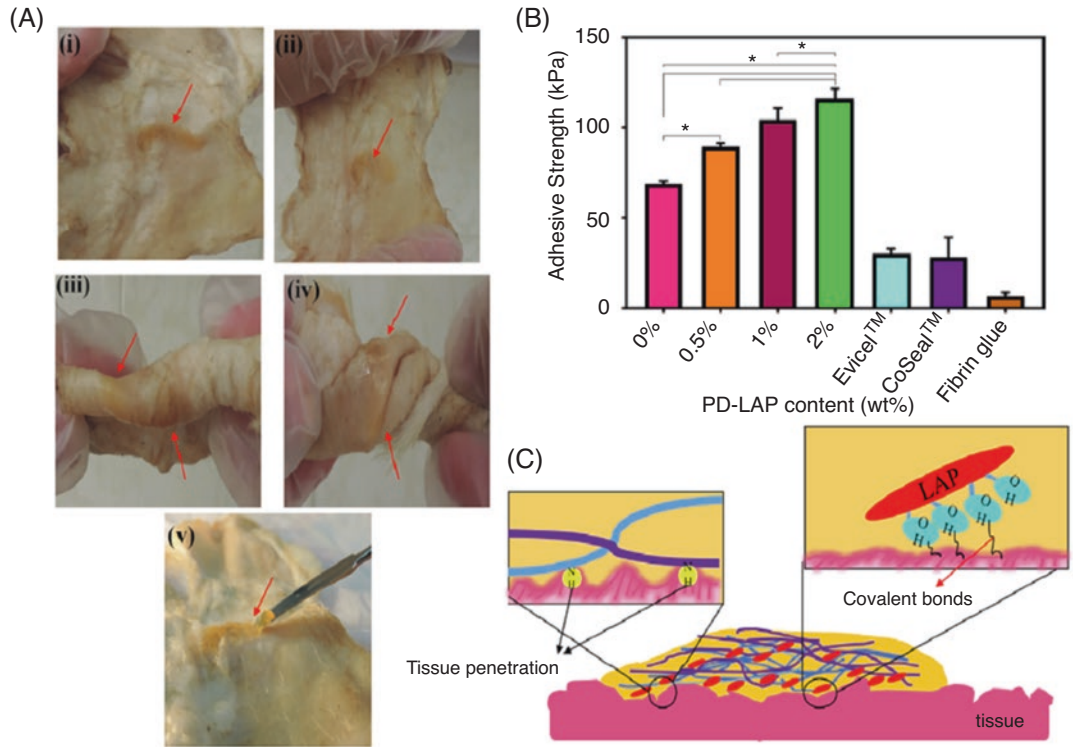

Fig. 26.5 Adhesive properties of nanocomposite hydrogels: (**a**) Photographs of gel-1% PD-LAP hydrogel adhered to sheepskin under (i) normal condition and under (ii) tensile, (iii) torsion, and (iv) twist deformation, confirming the high adhesion strength. (v) The nanocomposite hydrogels removed completely from the skin, demonstrating their highly cohesive strength. (**b**) Adhesive strength changes of nanocomposite hydrogels as a function of PD-LAP content. The adhesion strength of hydrogels was compared with the results of three commercial glues, with the data shown as means ± SD ($n = 3$) (*: $P < 0.05$). (**c**) Schematic representation of tissue penetration and new covalent bonds between tissue and nanocomposite hydrogels. (Reproduced with permission from Rajabi et al. (2020) ©2019 Elsevier Inc)

blood cell and platelet adhesion as well as activation and appreciable blood-clotting ability. Furthermore, the cryogels displayed excellent cytocompatibility and were found to be non-cytotoxic.

5 Nanoparticle Effects on Other Blood Constituents

The effects of nanoparticle interactions with serum constituents also extend beyond proteins, platelets, and red blood cells to include peripheral mononuclear cells such as lymphocytes, monocytes, natural killer cells, and granulocytes (De La Cruz et al. 2017). This is due to the administered nanoparticles often first being picked up by the phagocytic cells of the immune system which may lead to undesirable effects such as immunostimulation or immunosuppression. Further effects could also include inflammatory or autoimmune disorders or increases in the host's susceptibility to infections and cancer (Zolnik et al. 2010; Gamucci et al. 2014).

Additional interactions have also been noted previously to have a significant impact on the functionality of and communication between immune cells. This is due to the impact on exosomes which function in cell-to-cell communication (De La Cruz et al. 2017; Andersson-Willman et al. 2012). Research undertaken by Andersson-Willman et al.

(Andersson-Willman et al. 2012) noted the effects of TiO_2 and ZnO nanoparticles on dendritic cells, lymphocytes, and exosome production at sub-toxic concentrations. The results of this study detailed that the viability of the analyzed primary human peripheral blood mononuclear cells was not affected by the tested concentrations (1 to 100 μg/mL). However, a dose-dependent increase in cell death and caspase activity in monocyte-derived dendritic cells to ZnO was observed, which was not seen with the TiO_2 nanoparticles. The ZnO nanoparticles further induced a downregulation of FcγRIII (CD16) expression on NK cells noting that at the tested concentrations of ZnO nanoparticles, an effect on FcγR-mediated immune responses may occur.

These immune cells which can be induced through interaction with nanoparticles can further result in inflammation. Research has shown that the inflammatory response occurring as a result of administration of a drug delivery system is due to cytokine release. The properties of the number of different cytokines induced can be correlated with the surface charge of the particles delivered with highest number being for cationic micelles (13 cytokines) with zwitterionic (seven cytokines), neutral (three cytokines), and anionic micelles (one cytokine) significantly lower (Elsabahy and Wooley 2015). Cross-linking and encapsulation of the nanoparticles were also noted to significantly decrease the number of cytokines induced (Ferrari et al. 2018).

Research undertaken by Heidegger et al. (Heidegger et al. 2016) detailed the effects of mesoporous silica nanoparticles on immune cells (macrophages, lymphocytes, leukocytes). Results of this study detailed that the silica nanoparticles displayed minimal surface expression of activation markers and release of pro-inflammatory cytokines. Additionally, when the mesoporous silica nanoparticles were capped with a pH-responsive polymer and loaded with the Toll-like receptor 7 agonist R848, the immune-activating drug, a significant immune response was displayed.

6 Conclusion

Nanoparticulate delivery has considerably advanced the treatment of physiological conditions through enhancement of drug release, site targeting, and minimizing of drug dosing and side effects. The effects of these nanoparticles on serum constituents, however, are a significant parameter that has to be considered before the developed nanoparticles can be effectively used in patients. This will ultimately ensure that the nanosystem exerts the required properties intended with its administration.

References

Abstiens K, Figueroa SM, Gregoritza M, Goepferich AM. Interaction of functionalized nanoparticles with serum proteins and its impact on colloidal stability and cargo leaching. Soft Matter. 2019;15:709.

Andersson-Willman B, Gehrmann U, Cansu Z, Buerki-Thurnherr T, Krug HF, Gabrielsson S, Scheynius A. Effects of subtoxic concentrations of TiO_2 and ZnO nanoparticles on human lymphocytes, dendritic cells and exosome production. Toxicol Appl Pharm. 2012;264:94–103.

Azmi IDM, Wibroe PP, Wu L-P, Kazem AI, Amenitsch H, Moghimi SM, Yaghmur A. A structurally diverse library of safe-by-design citrem-phospholipid lamellar and non-lamellar liquid crystalline nano-assemblies. J Control Release. 2016;239:1–9.

Bruckman MA, Randolph LN, VanMeter A, Hern S, Shoffstall AJ, Taurog RE, Steinmetz NF. Biodistribution, pharmacokinetics and blood compatibility of native and PEGylated tobacco mosaic virus nano-rods and-spheres in mice. Virology. 2014;449:163–73.

Datta A, Dasgupta S, Mukherjee S. Modifications of nano-titania surface for *in vitro* evaluations of hemolysis, cytotoxicity, and nonspecific protein binding. Nanopart Res. 2017;19:142.

De La Cruz GG, Rodríguez-Fragoso P, Reyes-Esparza J, Rodríguez-López A, Gómez-Cansino R, Rodriguez-Fragoso L. Interaction of nanoparticles with blood components and associated pathophysiological effects. In: Gomes AC, Sarria MP, editors. Unraveling the safety profile of nanoscale particles and materials - from biomedical to environmental applications: IntechOpen; 2017. https://doi.org/10.5772/intechopen.69386.

Elsabahy M, Wooley KL. Data mining as a guide for the construction of crosslinked nanoparticles with low immunotoxicity via controlling polymerchemistry

and supramolecular assembly. Acc Chem Res. 2015;48(6):1620–30.

Ferrari R, Sponchioni M, Morbidellia M, Moscatelli D. Polymer nanoparticles for the intravenous delivery of anticancer drugs: the checkpoints on the road from the synthesis to clinical translation. Nanoscale. 2018;10:22701.

Fröhlich E. Action of nanoparticles on platelet activation and plasmatic coagulation. Curr Med Chem. 2016;23:408–30.

Gamucci O, Bertero A, Gagliardi M, Bardi G. Biomedical nanoparticles: overview of their surface immune-compatibility. Coatings. 2014;4:139–59.

Gu L. Tailored silica Nanomaterials for immunotherapy. ACS Cent Sci. 2018;4:527–9.

Heidegger S, Gößl D, Schmidt A, Niedermayer S, Argyo C, Endres S, Bein T, Bourquin C. Immune response to functionalized mesoporous silica nanoparticles for targeted drug delivery. Nanoscale. 2016;2

LiH-C HF-J, Chen C-P, Chang M-Y, PCH H, Chen C-C, Hung S-U, WuC-C CH-C. The hemocompatibility of oxidized diamond nanocrystals for biomedical applications. Sci Rep. 2013;3:3044.

Lin H, Wang Q, Zhong R, Li Z, Zhao W, Chen Y, Tian M, Luo X. Biomimetic phosphorylcholine strategy to improve the hemocompatibility of pH-responsive micelles containing tertiary amino groups. Colloids Surf B Biointerfaces. 2019;184:110545.

Liu N, Tang M, Ding J. The interaction between nanoparticles-protein corona complex and cells and its toxic effect on cells. Chemosphere. 2020;245:125624.

Palazzo C, Laloy J, Delvigne A-S, Nys G, Fillet M, Dogne J-M, Pequeu C, Foidart J-M, Evrard B, Piel G. Development of injectable liposomes and drug-in-cyclodextrin-in-liposome formulations encapsulating estetrol to prevent cerebral ischemia of premature babies. Eur J Pharm Biopharm. 2019;127:52–9.

Parveen R, Shamsi TN, Fatima S. Nanoparticles-protein interaction: role in protein aggregation and clinical implications. Int J Biol Macromol. 2017;94:386–95.

Rajabi N, Kharaziha M, Emadi R, Zarrabi A, Mokhtari H, Salehi S. An adhesive and injectable nanocomposite hydrogel of thiolated gelatin/gelatin methacrylate/Laponite® as a potential surgical sealant. J Colloid Interface Sci. 2020;564:155–69.

Singh PK, Srivastava AK, Dev A, Kaundal B, Choudhury SR, Karmakar S. 1, 3β-Glucan anchored, paclitaxel loaded chitosan nanocarrier endows enhanced hemocompatibility with efficient anti-glioblastoma stem cells therapy. Carbohydr Polym. 2018;180:365–75.

Wang S, Zhang Z, Dong L, Waterhouse GIN, Zhang Q, Li L. A remarkable thermosensitive hydrogel cross-linked by two inorganic nanoparticles with opposite charges. J Colloid Interface Sci. 2019;538:530–40.

Xu C, Zhang Y, Xu K, Nie J-J, Yu B, Li S, Cheng G, Li Y, Du J, Xu F-J. Multifunctional cationic nanosystems for nucleic acid therapy of thoracic aortic dissection. Nat Commun. 2019;10:3184.

Zhang T, Tang M, Yao Y, Ma Y, Pu Y. MWCNT interactions with protein: surface-induced changes in protein adsorption and the impact of protein corona on cellular uptake and cytotoxicity. Int J Nanomedicine. 2019;14:993–1009.

Zhao X, Guo B, Wu H, Liang Y, Ma PX. Injectable antibacterial conductive nanocomposite cryogels with rapid shape recovery for noncompressible hemorrhage and wound healing. Nat Commun. 2018;9:2784.

Zolnik BS, González-Fernández A, Sadrieh N, Dobrovolskaia MA. Nanoparticles and the immune system. Endocrinology. 2010;151(2):458–65.

Part VIII

Future Directions and Challenges

Current Challenges and Future Directions in Nanomedicine

27

Snigdha Das Mandal, Surjyanarayan Mandal, Yashwant V. Pathak, and Jayvadan K. Patel

Abstract

Nanomedicine research describes the medical application of nanotechnology and nanoparticle-based drug delivery systems for the treatment of cancer over the past two decades. Nanomedicine is basically a product of a newer scientific technology known as nanotechnology. Nanotechnology is a multidisciplinary scientific field that transforms the pattern of detecting diseases in the human body and also treating the damage. Nanomedicine applies to highly specific medical involvements for the prevention, diagnosis and treatment of various diseases. This developing discipline of nanomedicine brings active pharmaceutical agent and nanotechnology together in order to alter the therapies as well as improve the existing treatment procedures. These nanomedicines are capable of overcoming the biological barriers in the human body to improve the way to deliver the incorporated drug compounds to specific tissues and organs at a predetermined rate. More precisely, nanomedicines have been observed to modify the cellular and tissue uptake of therapeutic compounds and hence improve the biodistribution of compounds to target sites in vivo. In nanomedicine, the active biomolecules and their formulations are manipulated to produce nanostructures of pharmaceuticals of the same size so as to produce predetermined beneficial effect in human beings. These nanomedicines produce an excellent solution for early non-faulty diagnosis of diseases and hence will enhance the treatment of cancer, diabetes, Alzheimer's, Parkinson's and cardiovascular diseases. Nanomedicines have demonstrated several significant therapeutic advantages of biomolecules, however the beneficial clinical translation of these nanotechnology-based biomolecules have not progressed as expected. Hence, in this chapter, current understanding of nanoformulations of bioactives has been exemplified and the challenges are being addressed.

Keywords

Nanomedicine · Nanotechnology · Targeting · Bioactives · Biodistribution · Barriers

S. D. Mandal (✉)
Department of Pharmacy, Parul University, Vadodara, Gujarat, India

S. Mandal
R&D Head, AGIO Pharmaceuticals Ltd, Bhosari, Maharashtra, India

Y. V. Pathak
College of Pharmacy, University of South Florida Health, Tampa, FL, USA

J. K. Patel
Nootan Pharmacy College, Sankalchand Patel University, Visnagar, Gujarat, India

J. K. Patel, Y. V. Pathak (eds.), *Emerging Technologies for Nanoparticle Manufacturing*,
https://doi.org/10.1007/978-3-030-50703-9_27

1 Introduction

In recent years, nanotechnology has been increasingly applied to the area of medicine, which is defined as nanomedicine, as a new independent field of life sciences. Nanomedicines for their application in medical field mainly range from the utilization of the nanomaterials for development of nano-systems and biological devices to nano-electronic biosensors and other biological machines. Nanotechnology through nanoparticle-based drug delivery systems basically is emerged as very promising means of treating cancer (Ross et al. 2004). Furthermore, in the last few years, this nanotechnology is getting a great deal of attention due to its tremendous potential in disease diagnostics, monitoring and the treatment. Scientists around the globe from academics and companies are increasing their focus in this globally accepted area.

Nanomedicine is moving in many new directions. Firstly, in tissue engineering, it has been revealed that nanostructure in advanced biomaterials is highly important for how materials interact with the biological interface (Anwarul et al. 2018). Another example includes micro- and nanostructured chip systems for highly sensitive diagnostics, e.g. for detection of disease markers in blood (Shi et al. 2010). The field is progressing at an unbelievable speed, and there is no doubt that many new technologies will be introduced that provide better disease diagnostics and treatments for the benefit of the patients and society in the years to come. Even so, there are also certain challenges that the field faces at a fundamental level. Common to perhaps all technology developments within the field is a poor understanding of the complex interaction between the artificial materials we are developing and the biological environment they are placed in. This lack of understanding is at protein, cellular and whole organism level (Ross et al. 2004; Anwarul et al. 2018). It is clear that surface chemistry, nanoscale to macroscale morphology and material softness are parameters that all affect the biological behaviour of the technologies we are trying to develop, but our ability to understand and map these effects needs to be improved further over the next decades. This point is exemplified by discussing the current understanding of nanoparticle-based drug delivery systems for intravenous administration and their medical application. However, several debates, controversies as well as brainstorming sessions exist among academicians, medicine practitioners and industrial scientists in defining nanomedicines. Several regulatory agencies across the globe have put their views and defined nanotechnology and nanomedicines in various ways. As per the US Food and Drug Administration (USFDA), nanotechnology is the technology which allows scientists to create, explore and manipulate materials measured in nanometres (billionths of a metre) and those materials may differ in terms of their physical, chemical and biological inherent properties. The National Institutes of Health (NIH) in its 'National Institutes of Health Roadmap for Medical Research in Nanomedicine programme' defined nanomedicines as highly specific medical intercessions at the molecular level for curing disease or repairing damaged tissues, such as bone, muscle, other tissues or nerve. Further, Forward Look Nanomedicine programme of the European Science Foundation has comprehensively defined nanomedicine as a medicine which utilises the nano-sized tools, generally under the size of 1000 nm, for understanding the complexity of involved pathophysiology of disease followed by its diagnosis, prevention as well as treatment. The vital objective of nanotechnology and nanomedicines is to improve the quality of living life. Since the last few decades, nanomedicines have come out as the most interesting but promising and much investigated technique in the area of novel drug delivery and diagnostics. This is clear from the fact that a number of promising nanomedicine candidates are approved by different regulatory authorities across the globe like advanced drug delivery, imaging and diagnosis and/or regenerative medicines.

2 Current Challenges

Nanomedicine is expected to provide new breakthroughs to fight several incurable diseases, but for this, a genuine global effort is required to convert the laboratory innovation effectively to their clinical counterparts for the betterment of the human beings. Nanomedicines like nanotherapeutics and nanopharmaceuticals could achieve these important aspects of therapy like diagnosis, improve targeted therapies, reduce side effects and enhance therapeutic monitoring. These advantages will definitely improve the quality of life and be helpful in maximizing the cost-effectiveness of health care. Although nanomedicine has the potential advantages to overcome biological barriers, effectively deliver hydrophobic active entities and preferentially target the sites of infection, the field of nanomedicine is still at its early stage. Most of the nanomedicine research or inventions are still limited to the laboratory phase, and only a relatively small number of nanoparticle-based medicines have been approved for clinical use because of numerous challenges and hurdles at different stages of development (Shi et al. 2010). The first FDA-approved nano-drug formulation is Doxil® in 1995, which can prolong drug circulation time and avoid the RES due to involvement of PEGylation technique. The key feature of this nano-formulation is its stability followed by its ability to release accurate amount of the drug, i.e. doxorubicin at the tumour site (Anwarul et al. 2018; Shi et al. 2010). From 1995 to 2017, more than 50 nanopharmaceuticals have received FDA approval and are currently available for clinical use. The attractiveness of nanomedicine lies in their unique characteristics of three-dimensional assemblance with multiple nanoscale components. At the same time, due to its several complexities, nanomedicine product requires a careful design and engineering, strict characterization of physicochemical properties and validated manufacturing process for reproducible scale-up in order to achieve a consistent product with relatively stable physicochemical characteristics and pharmacological profiles. The safety and regulatory issues of nanomedicine need additional considerations compared with conventional medicines. So, it becomes an important aspect to review and summarise the challenges and limitations during the development followed by commercialization of nanomedicine products as well as to discuss the potential solutions to accelerate the growth of this important field.

Successfully translating nanomedicine from pre-clinical proof of concept to demonstration of therapeutic value in the clinic is still challenging; several obstacles have been identified as top scientific hurdles in bringing nano-engineered products to patients.

2.1 Biological Barriers and Drug Targeting

In order for the drugs to successfully reach the microenvironment of disease sites, nano-based formulation helps them to cross multiple biological barriers (Fig. 27.1).

For example, nanoparticles for oral delivery need to have high stability in the gastrointestinal tract, the ability to penetrate intestinal epithelium and the ability to keep the high systemic bioavailability of drugs after crossing several barriers. Compared with most of the small molecules delivered orally, intravenous administration (IV) is adopted as the only efficient route for delivering of large drug molecule proteins, peptides and polynucleotides. After systemic injection, drugs in circulation still have to overcome various biological barriers to reach their microtargets. The blood-brain barrier (BBB) plays major obstacle for treating the central nervous system diseases, i.e., it forbids almost 99% large and hydrophilic moieties to enter the brain and cerebrospinal fluid and hence brain targeting delivery suffers. There are various possible pathways by which drug-loaded nanoparticles or solute molecules move across the BBB, as shown in Fig. 27.2.

Another most important challenge the formulators encounter is to deliver nanomedicine containing therapeutic agents into solid tumours. Although tumour vasculature is highly heterogeneous in distribution and more permeable in some places, large areas of tumours with high

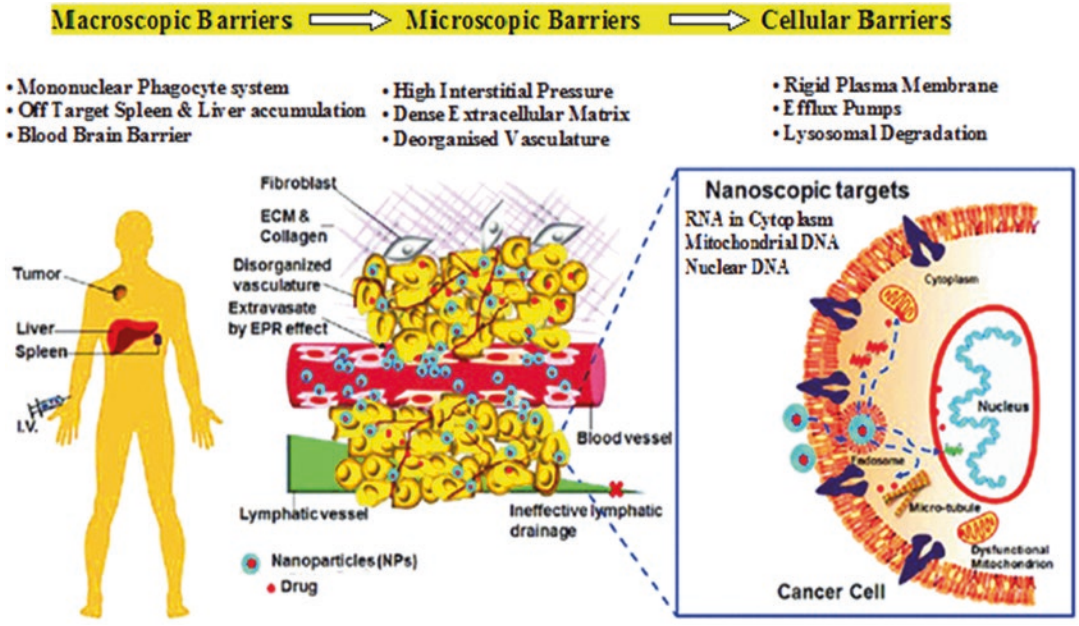

Fig. 27.1 Multiple barriers for nano-formulation

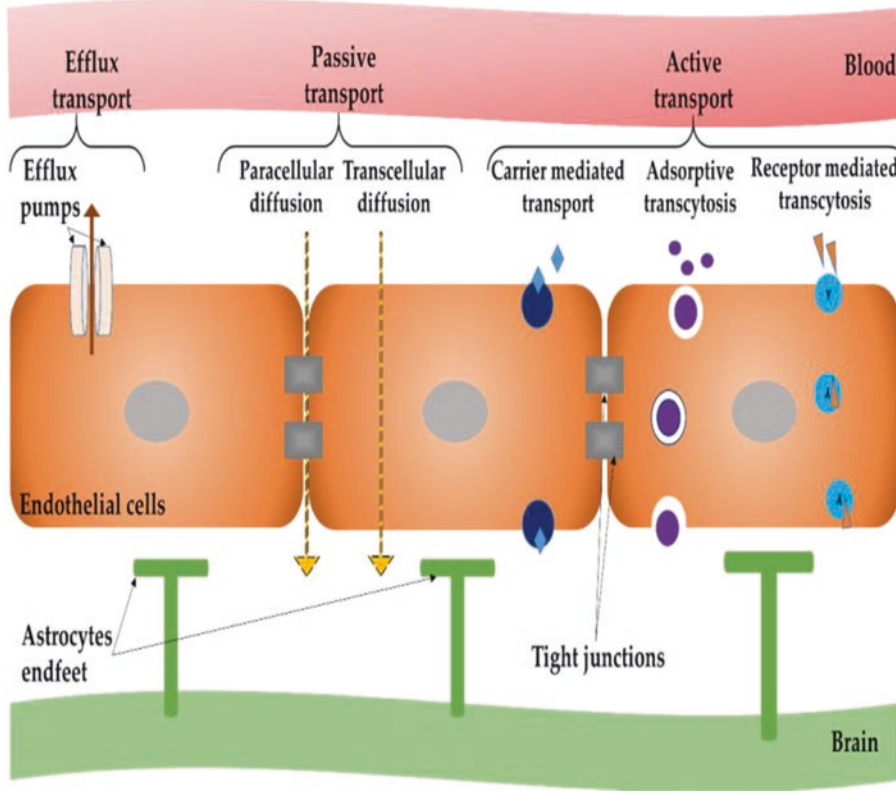

Fig. 27.2 Various pathways through which drug-loaded nanoparticles cross the BBB

cancer cell density and dense tumour stroma are still poorly perfused which further hinder the drug distribution in tumours. In tumour, impaired lymphatic drainage further increases the interstitial fluid pressure (IFP) which further adds another significant barrier to drug delivery and is considered as one of the main factors responsible for reduction in extravasation and transvascular transport of drugs despite the leaky tumour microvasculature and thus restrain the transport of molecules into interstitial space of tumour. Several nanoparticle-based delivery strategies like liposome, polymer micelle and peptide or protein nanoparticles are investigated thoroughly for their capability to deliver drugs.

Tumour vasculature is very leaky and highly permeable, and due to lack of proper lymphatic drainage, the enhanced permeability and retention (EPR) effect develops the accumulation of nanoparticles passively. The macromolecules further accumulated in the tumour microenvironment, and hence tumour drug delivery through EPR noticeably improved. The first marketed nanomedicines were pegylated liposomal formulation containing doxorubicin (Doxil®/Caelyx®) and paclitaxel (Abraxane®). The key issue of this passively targeted nanomedicine is controlling of the pharmacokinetics and biodistribution of nanoparticles by modulating its physicochemical properties. Although passive absorption process has some advantages, but active transport process can reduce the systemic drug exposure by utilizing the active biological transporters. The drugs are effectively targeted to the site of action and hence increases efficacy of the drug.

The active targeting nanoparticles have organized structures that facilitate the incorporation of various targeting active moieties like small molecular ligands for receptors, peptides, proteins, antibodies and oligonucleotides. It can reduce off-target organ toxicities by effectively delivering drugs to the target sites and hence facilitating cellular uptake of encapsulated therapeutic agents (Maeda 2001). Usually the ligands or monoclonal antibodies targeting to the surface receptors overexpressed by cancer cells, such as transferrin receptor (TfR), folate receptor (FR) and epidermal growth factor receptor (EGFR), decorate the surface of nanoparticles to increase cellular internalization of the reagents through endocytosis and improve the efficacy of systemic anticancer therapy (Allen 2002). Additionally, nanoparticles enable the uniform transport of large, biologically active molecules incorporating with protein transduction domain (PTD) and cell penetrating peptides (CPPs); otherwise they cannot effectively enter cancer cells (Maeda 2001; Allen 2002). Moreover, another possible target of nanomedicine is tumour endothelial cells. The cyclic as well as linear derivatives of oligopeptides RGD (Arg-Gly-Asp) bind to the integrins α2β3, αvb3 and α5β1, which provide a tumour penetrating function to the nano-formulations like liposomes and other nanoparticles. With RGD modification, nanoparticles deliver cytotoxic reagents to tumour tissue and achieve significant antitumour effects. The active targeting depends on the affinity and efficacy of a target and its specific ligand. Besides, it is very important to optimize the density of targeting ligands per nanocarrier to achieve not only high targeting efficiency but also to ensure an optimal internalization.

2.2 Analysis and Characterization of Nano-formulations

In comparison with the conventional pharmaceutical formulations, nanomedicine is a complex alternative consisting of other different components which rather serve to a specific function. So, identifying and characterizing those excipients along with active ingredient is very much essential and for this purpose more sophisticated, and appropriate analytical testing methods are required to characterize as well as quantify each formulation component. Furthermore, the interactions between these components and with the active ingredient/s including both physicochemical properties and biological behaviours are also to be investigated. So, it now becomes a challenge for the formulators to develop nanomedicine not only for its technical aspect but also the regulatory perspective. In general, the most important physicochemical features of nanomed-

icine are structure, particle size, size distribution, surface properties, surface charge, porosity and overall stability which are rather difficult to characterize in the developed nanomedicine products because of their changeable properties. Taking polydispersity (PD) as an example, it is an important parameter relating to the heterogeneity in terms of size, shape or mass of particles. So, if the developed nanomedicine formulations have the same average size but with different PD, it may lead to noticeable changes in the fate of the formulations like drug release rate, biocompatibility, stability and in vivo behaviours including their targeting properties and toxicity. Another problem the formulator usually encounters is stability characterization of nanomedicine. Biodegradable and biocompatible lipids and polymers have been widely used for the development of nanomedicine products due to their excellent physicochemical features. But this biodegradable property of these materials will also change due to the involvement of processing parameters like temperature, pH, etc. which in turn alter the properties of nanomedicine products during the storage either in the solutions or even in a lyophilized powder form. So, it is important to improve quality assessment of those biodegradable materials through validated and reproducible standards. In vivo biodistribution is another frequent issue of the nanocarriers over time. After administration in vivo, nanomedicines would reach biological fluids and may interact with biomolecules (e.g. proteins) or biological fluids (e.g. blood serum), which could significantly alter their physicochemical properties such as size, aggregation or agglomeration, and release profile and alter the function of nanomedicine in biological systems. It is indispensable to characterize completely the nanomedicine products under clinically relevant environments using in vitro and in vivo models in order to establish in vivo-in vitro correlation.

Nowadays although pictorial biodistribution of nanoparticle as well as their accumulation in bio-models can be obtained by using fluorescence or radiolabelling method, still it is very hard to assess the mass-balance information which is important in order to account the full administered dose and also to ensure safety and hence toxicity. Furthermore, the radiolabelling and fluorescence emitters are conjugated chemically to one of the formulation compositions of nanoparticles, which is not always stable in the internal environment and easily degraded. Therefore, it may lead to unreliable as well as variable results by tracing the degraded fluorescence or radiolabelling moiety instead of the drug or the nanoparticle as a whole. Additionally, it may be predicted that the distribution pattern of this chemically modified nanoparticles may be different in comparison with the same nanoparticles without radiolabelled or fluorescence modification. Last but not least, nanomedicine with more than one composition and the ability to carry and deliver multiple therapeutic and imaging agents may require individual tracking.

Thus, various characterization methods including the quantification of active and inactive ingredients along with the impurities, measurement of particle size and size distribution with light scattering, surface charge determination, imaging of nanoparticles by microscopy and new advanced techniques specifically to characterize the in vivo behaviours of nanoparticle are very much essential to ensure and establish that the developed nanomedicine formulations have all the desired properties for the intended therapeutic effect and reproducible efficacy with minimum side effects.

2.3 Scale-Up and Manufacturing

The most challenging problem in the development of pharmaceuticals is controlling key parameters along with the stability on a batch-to-batch basis and its applicability. Small-scale processes of nanomedicines may achieve reproducibility with well-characterized nanoparticles and their preclinical as well as clinical study results may be up to acceptable level. But in large-scale production, the physicochemical processes of the nanomaterial are found difficult to control, which in turn lead to batch-to-batch variations and failure in preclinical and early clinical studies. Most of the nano-formulations

including nanoparticles are three-dimensional complex products with specific components. Due to these multicomponent systems along with their special arrangement, the control over manufacturing process is very challenging. All of these factors make the manufacturing and scale-up of nanomedicine difficult. The first FDA-approved nanomedical therapeutics Doxil® also suffered the same issue which subsequently had to be suspended in November 2011 because of its manufacturing and sterility issues. The shortages of Doxil® were until 2014, and a different manufacturing method for Doxil® was adopted which subsequently increased the cost of medication. Properly identifying the components and understanding their interactions in the early development are required to ensure reproducibility of the product during the larger-scale 'manufacturing. In general, there are two preparation methods for nanoparticles like 'top-down' and 'bottom-up' approaches. Top-down methods manufacture nano-entities by grinding the larger particles using the milling technique, while bottom-up methods arrange and rearrange the smaller components into functional assemblies like monomer polymerization, etc. (Ferrari 2005). Several techniques like high-speed or high-pressure homogenization, sonication, milling, cross-linking, emulsification, organic solvent evaporation, centrifugation, filtration and lyophilization are always employed for manufacturing of nanomedical formulation. It becomes an important factor to select the suitable approaches and processing parameters in order to scale up the nanomedicines. These parameters may involve the molar ratio of nanomaterials, active ingredients, the excipients and the targeting moieties, the type of organic solvent and emulsifier/cross-linker/stabilizer, pressure, operating temperature and pH (Ferrari 2005). Choosing and considering the incorrect conditions could lead to altering the chemical structure of the therapeutic reagents and unpredictable impurities. Particularly, it is quite feasible enough to change chemical structure and its conformation of macromolecules like peptide and protein, by cross-linking, degradation, denaturation and coagulation. Hence the manufacturing of nanomedicine is not that simple, rather a well-defined, precise, validated production steps with strict control of quality imparting parameters are required. The relatively high raw material cost along with the need for sophisticated equipments and multistep production process also become hurdles for the manufacturing and scale-up of nanomedicine, which makes the production of nanotherapeutics very expensive. Therefore, in order to compensate the high developmental and manufacturing costs on nanomedicine products, the clinical effectiveness of nanomedicine drugs is more demanded than conventional available therapeutics. These factors may deter pharmaceutical companies from carrying out the large-scale production of nano-formulations.

2.4 Pharmacology and Safety Challenges

Physical as well as chemical characteristics of nanomedicine remarkably influence the pharmacological benefits as well as the safety profiles. Even in small changes composition and subtle alteration in the final manufactured products could result in significant changes in pharmacology and toxicity of nanomedicine (Couvreur and Vauthier 2006). The basic requirement to achieve the desired pharmacological profile of a successful pharmaceutical including nanomedicine is to design pharmacokinetic parameter of the formulation. Moreover, most of the researcher and pharmaceutical companies use the standard criteria of drug molecule to the assessment of nanomedicine. This is because active entities of small molecular size normally diffuse through biological barriers more readily, and hence at equilibrium the drug concentration in the blood is maintained to achieve the target tissue levels. Furthermore, the measurement of drug concentration in the plasma becomes an important criterion to determine PK and hence the fate of any pharmaceutical formulation. However, if this methodology is applied to nanomedicine, it cannot be presumed to be accurate and could be intrinsically flawed. Accordingly, different PK approaches with different indications are required

for different nanomedicines. For example, instead of the standard method to quantify the drug behaviour in plasma, the pharmacological parameters at the specific target site could be more relevant to evaluate and accesses the therapeutic action of nanomedicine products and the reproducibility as well. Furthermore, the bioequivalence of nanotechnology-based pharmaceutical products could be used to evaluate their effectiveness as well as to address toxicity issues for human health. The nanoscale size of nanomedicine products can simulate the intracellular biomolecules like polysaccharide, protein and enzyme involved in cell signalling, which may lead to unfavourable biological interactions. The nanotoxicology is an independent field of research now, and numerous data relating to the toxicity of different nanoparticles are available. On the other hand, the toxicity of nanomaterials remains difficult to evaluate, especially its long-term toxicity as because the classical drug toxicity assay determination for these nanomedicines may be inadequate. And there is no standard list of required tests. Thus, the search for advanced complementary assays along with the standard criterion for toxicity evaluation of products of nanomedicine becomes emergent. There are multiple properties, such as size, shape, surface charge, surface area, porosity or hydrophobicity, which affect the performance of nanomedicine drug and nanoproducts at the nano-bio interface. Thus, every nanomedicine product may have their own different issues and, hence, require particular and different evaluations. The term toxicity in pharmaceutical industry usually refers to chronic toxicity and acute toxicity. Chronic toxicity is a time-consuming study, and analyzing these chronic toxicity data is more demanding. Due to the unavailability of suitable animal model, immunotoxicity sometimes cannot readily carry over from in vitro testing to humans. On the other hand, acute toxicity generally includes haemolysis, oxidative stress, inflammation, impaired mitochondrial function or complement activation. Nanoparticles themselves and the biologics such as proteins, peptides, antibody fragments and nucleic acids in nanoparticles can serve as antigen sources that can provoke the immune response. The immunogenicity of nanoparticles can also be affected by their physicochemical properties, such as size, charge, solubility, surface characteristics and hydrophobicity.

2.5 Regulatory Challenges

Although the USFDA and European Medicines Agency (EMA) approved a number of nanomedicinal products for cancer therapy, there are not specifically implemented guidelines for drug products containing these kinds of materials by the FDA, EMA and by other regulatory bodies yet. The lack of information in the examination of nanomedicine products or nanomedicine therapeutics can only make regulatory decisions based on individual benefit and risk assessment (Jain 1994). As such the regulatory process is time-consuming and requires a high-level expert in innovative technologies, which may result in regulatory delays. Furthermore, regulatory issues are vital for the development of cutting-edge technologies to quantify or characterize and also to monitor the quality of nanomedicine products besides clinical trials and the approval process. Hence, there is an urgent requirement for elaborated regulatory guidelines for characterization and quality control as well as accessing the safety issue of nanomedicine products (Jain 1994). However, the definitions, guidelines and cooperation in this area are gradually established and improved. FDA has released the guidance for industry for nano-formulations, FDA-Regulated Product, in June 2014, in which nanomaterials are defined as engineered materials with dimension between 1 nm and 100 nm. The FDA and European Technology Platform on Nanomedicine (ETPN) further intend to work together with the Nanotechnology Characterization Laboratory (NCL) and European Nano-Characterization Laboratory (EUNCL), respectively, to promote the regulatory pints for characterizing nanomedicine products. The vital demand for regulatory agencies in nanomedicine therapeutics is to refine and standardize requirements for the approval of safe nanomedicine products. Along with the above controls and reviews, more advanced and multifunctional tools need to be developed to

characterize the complexity so that the approval process of nanomedicines could be improved.

3 Future Direction of Nanomedicines

Recently, the research on the application of nanomedicine is much more overvalued with huge number of patents and published research articles. However, the factual potential of this novel technology could only be measured by the approval of regulatory authorities followed by the genuine acceptance of the public around the globe. Both these factors, i.e. regulatory approval and public acceptance, play very significant role for the commercial success of nanomedicines. According to a recent research, the nanomedicine industry is treasured worth more than $150 billion worldwide. Further, it was speculated that the nanomedicine market especially related to anticancer products would grow more than 15% over a couple of years; it was further estimated that in the time to come, nanomedicine specially central nervous system products as well as anticancer products will dominate the market by contributing almost 40% revenue.

Nanotechnology is now in the floor to change the scale and methods of vascular imaging and drug delivery inside the biological system. The NIH (National Institutes of Health) Roadmap's 'Nanomedicine Initiatives' predicts that nanotechnologies will provide more medical benefits within the next 10 years. This includes the advancement of laboratory-based nanoscale diagnostic and drug discovery devices such as microchip devices, nanopore sequencing, etc. The National Cancer Institute has also similar programmes, i.e. production of nano-based multifunctional entities which can not only diagnose and deliver therapeutic agents but also monitor the progress of cancer treatment. These include engineering and designing of targeted contrast agents that improve the resolution of cancer cells to the single cell level along with the nanodevices capable of detailing the biological and evolutionary range of the multiple cancer cells which make up a tumour within an individual. Thus, nanocarriers may furnish the complete potential of nanotechnology in targeted imaging and drug delivery in vivo condition by correlating the physicochemical and physiological processes. So, a complex interaction begins for a nanovehicle and its microenvironment, for example, carrier stability; intra- and extracellular drug release rates in different pathological conditions; interaction with biological environment, such as opsonization; and other huddles like anatomical, physiological, immunological or biochemical en route to the desired target site and tissue-specific receptor expression and escape routes from the vasculature. Characteristically, the carrier design and their targeting strategies may vary in relation to the type, developmental stage and location of the disease. Further, the toxicity issues are very well-known concern, but are generally ignored. Therefore, it is very much essential that fundamental research shall be carried out to address these issues if application of these nanotechnologies is to be achieved. The future of nanomedicine will depend on the rational of development of several materials for designing the nanotechnology and sophisticated tools based around an efficient and thorough understanding of biological processes rather than forcing applications for some materials currently in vogue.

References

Allen TM. Ligand-targeted therapeutics in anticancer therapy. Nat Rev Cancer. 2002;2:750–63.

Anwarul H, Mahboob M, Adnan M, et al. Nanoparticles in tissue engineering: applications, challenges and prospects. Int J Nanomedicine. 2018;13:5637–55.

Couvreur P, Vauthier C. Nanotechnology: intelligent design to treat complex disease. Pharm Res. 2006;23:1417–50.

Ferrari M. Cancer nanotechnology: opportunities and challenges. Nat Rev Cancer. 2005;5:161–71.

Jain RK. Barriers to drug delivery in solid tumors. Sci Am. 1994;271:58–65.

Maeda H. The enhanced permeability and retention (EPR) effect in tumor vasculature: the key role of tumor-selective macromolecular drug targeting. Adv Enzym Regul. 2001;41:189–207.

Ross JS, Schenkein DP, Pietrusko R, et al. Targeted therapies for cancer. Am J Clin Pathol. 2004;122:598–609.

Shi J, Votruba AR, Farokhzad OC, et al. Nanotechnology in drug delivery and tissue engineering: from discovery to applications. Nano Lett. 2010;10:3223–30.

Index

J. K. Patel, Y. V. Pathak (eds.), *Emerging Technologies for Nanoparticle Manufacturing*,
https://doi.org/10.1007/978-3-030-50703-9

K